frontiers
RESEARCH TOPICS

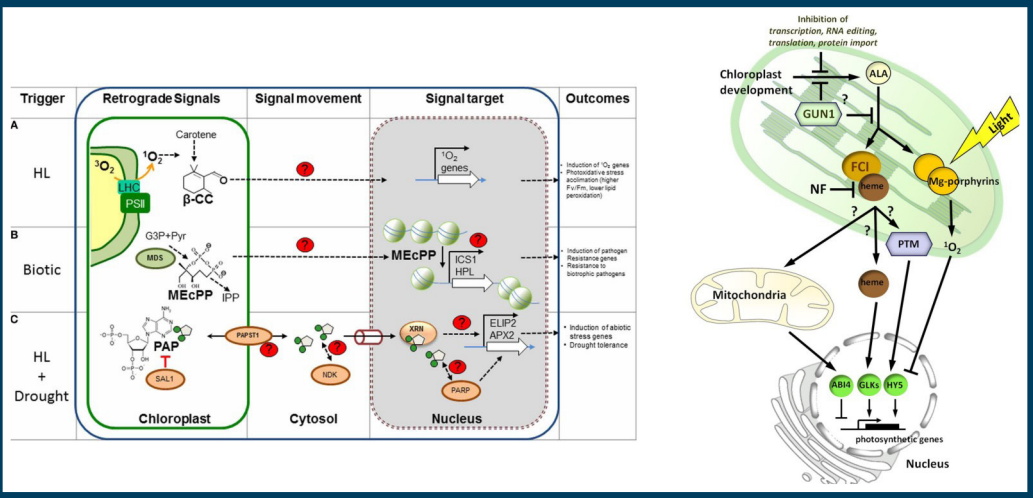

RETROGRADE SIGNALING IN PLANTS

Topic Editors
Dario Leister and Tatjana Kleine

frontiers in
PLANT SCIENCE

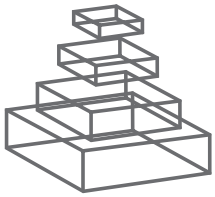

frontiers

FRONTIERS COPYRIGHT STATEMENT

© Copyright 2007-2013
Frontiers Media SA.
All rights reserved.

All content included on this site, such as text, graphics, logos, button icons, images, video/audio clips, downloads, data compilations and software, is the property of or is licensed to Frontiers Media SA ("Frontiers") or its licensees and/or subcontractors. The copyright in the text of individual articles is the property of their respective authors, subject to a license granted to Frontiers.

The compilation of articles constituting this e-book, as well as the compilation of all content on this site is the exclusive property of Frontiers. For the conditions for downloading and copying of e-books from Frontiers' website, please see the Terms for Website Use.

Images and graphics not forming part of user-contributed materials may not be downloaded or copied without permission.

Individual articles may be downloaded and reproduced in accordance with the principles of the CC-BY licence subject to any copyright or other notices. They may not be re-sold as an e-book.

As author or other contributor you grant a CC-BY licence to others to reproduce your articles, including any graphics and third-party materials supplied by you, in accordance with the Conditions for Website Use and subject to any copyright notices which you include in connection with your articles and materials.

All copyright, and all rights therein, are protected by national and international copyright laws.

The above represents a summary only. For the full conditions see the Conditions for Authors and the Conditions for Website Use.

ISSN 1664-8714
ISBN 978-2-88919-167-3
DOI 10.3389/978-2-88919-167-3

ABOUT FRONTIERS

Frontiers is more than just an open-access publisher of scholarly articles: it is a pioneering approach to the world of academia, radically improving the way scholarly research is managed. The grand vision of Frontiers is a world where all people have an equal opportunity to seek, share and generate knowledge. Frontiers provides immediate and permanent online open access to all its publications, but this alone is not enough to realize our grand goals.

FRONTIERS JOURNAL SERIES

The Frontiers Journal Series is a multi-tier and interdisciplinary set of open-access, online journals, promising a paradigm shift from the current review, selection and dissemination processes in academic publishing.
All Frontiers journals are driven by researchers for researchers; therefore, they constitute a service to the scholarly community. At the same time, the Frontiers Journal Series operates on a revolutionary invention, the tiered publishing system, initially addressing specific communities of scholars, and gradually climbing up to broader public understanding, thus serving the interests of the lay society, too.

DEDICATION TO QUALITY

Each Frontiers article is a landmark of the highest quality, thanks to genuinely collaborative interactions between authors and review editors, who include some of the world's best academicians. Research must be certified by peers before entering a stream of knowledge that may eventually reach the public - and shape society; therefore, Frontiers only applies the most rigorous and unbiased reviews.
Frontiers revolutionizes research publishing by freely delivering the most outstanding research, evaluated with no bias from both the academic and social point of view.
By applying the most advanced information technologies, Frontiers is catapulting scholarly publishing into a new generation.

WHAT ARE FRONTIERS RESEARCH TOPICS?

Frontiers Research Topics are very popular trademarks of the Frontiers Journals Series: they are collections of at least ten articles, all centered on a particular subject. With their unique mix of varied contributions from Original Research to Review Articles, Frontiers Research Topics unify the most influential researchers, the latest key findings and historical advances in a hot research area!
Find out more on how to host your own Frontiers Research Topic or contribute to one as an author by contacting the Frontiers Editorial Office: researchtopics@frontiersin.org

RETROGRADE SIGNALING INPLANTS

Topic Editors:
Dario Leister, Ludwig-Maximilians-University Munich, Germany
Tatjana Kleine, Ludwig-Maximilians-University Munich, Germany

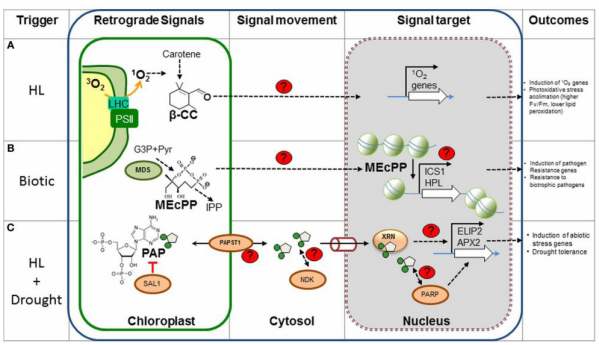

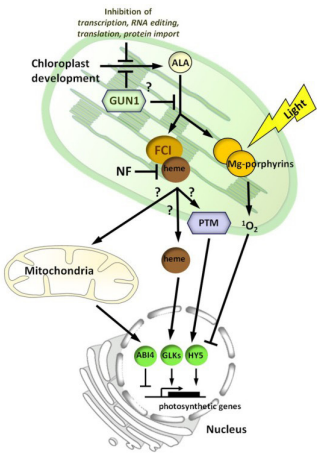

Changes in the developmental or metabolic state of chloroplasts or mitochondria can have profound effects on other cellular compartments and involve massive changes in the transcript profiles of nuclear genes. The concept of retrograde signalling posits that signals originating from chloroplasts or mitochondria modulate nuclear gene expression. Put simply, it claims that signalling factors are generated in the organelles, exported from the organelles, traverse the cytosol, and act in the nucleus. Pertinent signals are thought to derive from various sources, including among others the tetrapyrrole pathway, organellar gene expression, reactive oxygen species, or the redox state of the organelle. Recent studies have cast doubt on whether each of the candidate signalling molecules is genuine. Moreover, the unambiguous experimental verification of a signalling molecule is principally a difficult task to undertake. Therefore, despite some decades of research our

understanding of organellar signalling mechanisms remains limited. Thus, we want to discuss in this Frontiers Research Topic collection how future research should enable us to provide an integrated view of organellar-nucleus signalling and how this phenomenon can be addressed under physiologically relevant conditions and at multiple levels. Moreover, we want to provide an overview on the set of tentative signalling pathways and molecules and their potential interaction with each other, including "established" signals as well as very recent findings. In particular, we invite critical views on organelle-to-nucleus signalling and want to stimulate a discussion what experimental prerequisites are necessary and sufficient to define a plastid signal and what role different physiological conditions play in organelle-to-nucleus signalling and vice versa.

Table of Contents

frontiers in
PLANT SCIENCE

EDITORIAL
published: 12 March 2013
doi: 10.3389/fpls.2013.00045

Retrograde signals galore

Tatjana Kleine and Dario Leister*

Plant Molecular Biology (Botany), Department Biology I, Ludwig Maximilians University, Munich, Germany
**Correspondence: leister@lmu.de*

Edited by:
Steven Huber, United States Department of Agriculture, USA

Reviewed by:
Steven Huber, United States Department of Agriculture, USA

The term "retrograde signaling" refers to the concept that signals originating from chloroplasts or mitochondria can modulate nuclear gene expression (NGE). The evolutionary establishment of the complex mechanisms underlying retrograde signaling is likely to have required a long time period (reviewed in: Tanaka and Hanaoka, 2012). The initial notion, proposed almost 30 years ago, that a single plastid signal might regulate the expression of nuclear genes involved in plastid biogenesis (Oelmüller and Mohr, 1986) has since expanded to accommodate the insight that multiple signals are produced by plastids (Gray et al., 2003). While the ultimate effects of retrograde signaling on NGE have now been clearly defined, many aspects of the initiation and transmission of the signals, and their mode of action, remain unresolved, are a matter of speculation (Estavillo et al., 2012), or are controversial (Kleine et al., 2009). Relevant signals are thought to derive from various sources, including (1) reactive oxygen species (ROS), (2) the reduction/oxidation (redox) state of the organelle, (3) organellar gene expression (OGE), and (4) the tetrapyrrole pathway, and in the present volume Estavillo et al. (2012) describe "brand-new" retrograde signaling pathways involving (5) metabolites—particularly 3′-phosphoadenosine 5′-phosphate (PAP) and methylerythritol cyclodiphosphate (MEcPP)—and (6) a carotenoid derivative (β-cyclocitral [β-CC]).

The collection of Original Research (all conducted with the model plant *Arabidopsis thaliana*), Hypothesis and Theory, Mini Review, Review, and Perspective articles assembled for this Research Topic reflects not only the progress made in characterizing the four "classical" signal sources, but also highlights alternative interpretations of how information transfer from chloroplasts and mitochondria might be mediated and how the activities of these two organelles might be coordinated with that of the nucleus. Taken together, the contributions suggest a framework for future research in the retrograde signaling field.

PROGRESS IN ROS-ASSOCIATED SIGNALING

Photosynthetic organisms must continuously cope with ROS, such as singlet oxygen ($^1O_2$), the superoxide anion radical (O^{2-}), the hydroxyl radical ($OH^{\cdot}$), and hydrogen peroxide (H_2O_2), more especially when exposed to stresses (Apel and Hirt, 2004). Shapiguzov et al. (2012) summarize evidence for the influence of extracellular and chloroplastic ROS production on NGE and describe the routes by which such signals might reach the nucleus. However, the extent to which the precise chemical nature of ROS and their cellular compartment of origin may contribute to the multiplicity of responses that occur in plants is still unknown. Vestergaard et al. (2012) model intracellular H_2O_2 signaling via diffusion using a H_2O_2 signal originating at the plasma membrane and spreading through the plant cytosol. These authors conclude that, although diffusion-mediated signaling is theoretically possible, it is unlikely to work in practice, since it requires a much faster rate of enzymatic degradation and a much lower cellular background concentration of H_2O_2 than are observed experimentally. Plants overexpressing peroxisomal glycolate oxidase (GO) in plastids (GO plants) can be exploited to study the effects of plastid-generated H_2O_2 (Fahnenstich et al., 2008). In GO plants, genes that respond strongly to an induced, abrupt rise in levels of plastid-generated H_2O_2 encode proteins involved in the regulation of anthocyanin biosynthesis, as well as transcription factors and their interacting partners that affect development (Balazadeh et al., 2012).

Partial exposure of low light-adapted plants to excess light results in systemic acclimation to excess excitation energy and the attendant photo-oxidative stress in unexposed leaves (Karpinski et al., 1999). Gordon et al. (2012) show that transient changes in light intensity imprint a "memory" of the event that facilitates subsequent acclimation responses. Acclimation to high light (HL) is induced within minutes, and repeated exposure to short-term HL results in acclimation of the exposed tissue and that of emerging and young leaves (but not older leaves) to HL and oxidative stress. The double mutant *adg1-1 tpt-2*, which is defective in the small subunit of the ADP-glucose pyrophosphorylase (ADGase; a key enzyme in the starch biosynthetic pathway) and the triose phosphate/phosphate translocator (TPT; the major interface for the distribution of photoassimilates between the chloroplast and the cytosol), shows impaired acclimation to HL, resulting in impairments of the diurnal pattern of photoassimilate export from the chloroplast (Heinrichs et al., 2012). The rescue of this double mutant by exogenously supplied sugars provides evidence that chloroplasts are capable of directly sensing the carbohydrate status, and it raises the question whether retrograde signaling is actually necessary for sugar-mediated acclimation processes (Heinrichs et al., 2012).

One target of ROS- and redox-mediated retrograde signals is the gene for stromal ascorbate peroxidase (sAPX), which is involved in the chloroplast antioxidant defence system (Oelze et al., 2012). Here, it is shown that the transcription factor ANAC089 is localized to the trans-Golgi network and the ER, and is released upon treatment with reducing agents and targeted to the nucleus to bind to the *sAPX* promoter. Thus, ANAC089 might function in a negative retrograde signaling loop, lowering *sAPX* expression if the cell encounters highly reducing conditions (Klein et al., 2012).

PROGRESS IN REDOX-ASSOCIATED SIGNALING

Redox signals from photosynthesis itself report functional disturbances in photosynthesis. Their relation to the environment, potential transduction pathways to the nucleus and their impact on NGE are reviewed by Pfalz et al. (2012). Based on a review of the literature and of publicly available expression data, Tikkanen et al. (2012) postulate that changes in redox homeostasis at the thylakoid membrane, governed by thylakoid protein kinase STN7, reprogram the entire regulatory network in the cell. This idea underlines the need to consider retrograde signaling as part of a broader cellular network, instead of viewing it as a set of separate pathways (Estavillo et al., 2012). Hüner et al. (2012) focus on specific examples of acclimation to excess irradiance and temperature to illustrate how excitation pressure sensed within the chloroplast governs both local and remote molecular events that affect phenotypic plasticity. Further complexity in the major signaling pathways arises from their multiple interdependencies. Indeed, a genetic approach has revealed that signals related to the thylakoid redox state are also fed into the OGE-dependent retrograde pathway to modulate NGE and adjust the abundance of chloroplast proteins (Tadini et al., 2012). Lepistö et al. (2012) discuss evidence showing interaction of retrograde with light signaling pathways. Moreover, they present a hypothesis which proposes that heterogeneity in the plastid population can give rise to elaboration of distinct retrograde signals, based on NGE analysis of a mutant containing both photosynthetically active and non-photosynthetic plastids in a single mesophyll cell.

A valuable tool for the dissection of redox-dependent retrograde signaling is the *immutans* mutant, in which a lack of plastid terminal oxidase (PTOX) causes the formation of white and green sectors. The report by Foudree et al. (2012) provides an update on PTOX, the mechanism of *immutans* variegation, and discusses findings pertaining to compensatory mechanisms in the mutant.

Remarkably, the cofactors that supply many of the major post-translational modifications are either central metabolites or redox-active compounds. Hartl and Finkemeier (2012) evaluate the potential of phosphorylation, lysine acetylation, and glutathionylation not only to regulate organellar processes by modifying metabolic enzymes, but also to influence NGE. The retrograde signal transduction network might also encompass the dynamic, redox-dependent formation of microcompartments, as proposed by Wojtera-Kwiczor et al. (2012). Their experiments suggest redox-dependent binding of the glycolytic enzymes cytosolic glyceraldehyde-3-phosphate dehydrogenase and aldolase to the outer mitochondrial membrane and also to F-actin.

PROGRESS IN TETRAPYRROLE-ASSOCIATED SIGNALING

How exactly tetrapyrrole biosynthesis is associated with retrograde signaling and alters NGE remains elusive. Because of its central role as the rate-limiting step in tetrapyrrole biosynthesis, Czarnecki et al. (2012) chose to focus on the role of 5-aminolevulinic acid (ALA) biosynthesis in modulating NGE. These authors have investigated (1) ALA synthesis in the *genomes uncoupled* (*gun*) mutants *gun1-gun4* that show uncoupling of NGE from the physiological state of chloroplasts and assessed (2) the impact of post-translationally down-regulated ALA synthesis in gabaculine-treated seedlings and the *gun4-1* mutant by global transcriptome analysis. Another model postulates that a specific heme pool generated by flux through ferrochelatase I serves as a signal source (Woodson et al., 2011). Terry and Smith (2013) propose that this heme-related signal is the primary positive signal during chloroplast biogenesis. In addition to this positive signal, aberrant chloroplast development may produce a negative signal due to accumulation of unbound chlorophyll biosynthesis intermediates, such as photo-excited Mg-porphyrins, which generate $^1O_2$. Accordingly, the tetrapyrrole pathway may provide both positive and inhibitory signals to control NGE.

MITOCHONDRIA AND CHLOROPLAST CROSSTALK

Yet another level of complexity in organelle-nucleus crosstalk exists in photosynthetic eukaryotes because of the additional interactions between mitochondria and chloroplasts. Current evidence suggesting that the transcription factor ABA INSENSITIVE4 (ABI4) is important for both chloroplast and mitochondrial retrograde signaling pathways is presented by León et al. (2012). Van Aken and Whelan (2012) have analysed 27 microarray data sets relating to perturbations of chloroplast and mitochondrial function. Their results indicate that WRKY transcription factors play an important role in coordinating signaling from both organelles. Furthermore, new marker genes have been identified that respond specifically to mitochondrial and/or chloroplast dysfunction.

DUAL LOCALIZED PROTEINS AS COMMUNICATORS

Proteins that are found both in the energy-producing organelles and the nucleus are excellent candidates for communicating information between these compartments. WHIRLY1 is such a protein, since it can be translocated from chloroplasts to the nucleus (Isemer et al., 2012b). Here, Isemer et al. (2012a) show that plastid-located WHIRLY1 enhances the responsiveness of seeds toward ABA even when ABA is supplied exogenously.

Duchêne and Giegé (2012) review the identified instances of proteins that are found both in mitochondria and the nucleus, most of which seem to be related to gene expression regulation, and propose that some of them might act as retrograde signaling proteins for mitochondrial biogenesis. Further proteins involved in OGE and, presumably, NGE are proteins of the mitochondrial Transcription tERmination Factor (mTERF) family. Thus, mTERFs represent ideal candidates for coordination of the expression of organelle and nuclear genomes (Kleine, 2012).

OUTLOOK

Many research efforts have focused on dissecting retrograde signaling pathways using biochemical and genetic approaches. In addition, metabolomics and systems biology have great potential to promote hypothesis generation and help dissect signaling networks in an unbiased fashion. Here, Caldana et al. (2012) outline and discuss recent advances in elucidating retrograde signaling molecules and pathways, with an emphasis on metabolomics- and systems biology-driven approaches.

The concept of retrograde signaling posits that signaling factors are generated in the organelles, are exported from the organelles, traverse the cytosol, and act in the nucleus.

This notion is critically discussed by Leister (2012), highlighting the alternative scenario of a signaling factor that is actively exported from the organelle, such that NGE could be altered without changing the total concentration of the signaling molecule. Furthermore, the possibility must be considered that the signaling molecules generated in the organelle and the factors that trigger NGE are not necessarily identical. Finally, Estavillo et al. (2012) outline missing links or future areas of research that need to be addressed if we wish to gain a comprehensive understanding of plant intracellular signaling networks.

REFERENCES

Apel, K., and Hirt, H. (2004). Reactive oxygen species: metabolism, oxidative stress, and signal transduction. *Annu. Rev. Plant Biol.* 55, 373–399.

Balazadeh, S., Jaspert, N., Arif, M., Mueller-Röber, B., and Maurino, V. G. (2012). Expression of ROS-responsive genes and transcription factors after metabolic formation of H_2O_2 in chloroplasts. *Front. Plant Sci.* 3:234. doi: 10.3389/fpls.2012.00234

Caldana, C., Fernie, A. R., Willmitzer, L., and Steinhauser, D. (2012). Unraveling retrograde signaling pathways: finding candidate signaling molecules via metabolomics and systems biology driven approaches. *Front. Plant Sci.* 3:267. doi: 10.3389/fpls.2012.00267

Czarnecki, O., Gläßer, C., Chen, J. G., Mayer, K. F., and Grimm, B. (2012). Evidence for a contribution of ALA synthesis to plastid-to-nucleus signaling. *Front. Plant Sci.* 3:236. doi: 10.3389/fpls.2012.00236

Duchêne, A. M., and Giegé, P. (2012). Dual localized mitochondrial and nuclear proteins as gene expression regulators in plants? *Front. Plant Sci.* 3:221. doi: 10.3389/fpls.2012.00221

Estavillo, G. M., Chan, K. X., Phua, S. Y., and Pogson, B. J. (2012). Reconsidering the nature and mode of action of metabolite retrograde signals from the chloroplast. *Front. Plant Sci.* 3:300. doi: 10.3389/fpls.2012.00300

Fahnenstich, H., Scarpeci, T. E., Valle, E. M., Flügge, U. I., and Maurino, V. G. (2008). Generation of hydrogen peroxide in chloroplasts of Arabidopsis overexpressing glycolate oxidase as an inducible system to study oxidative stress. *Plant Physiol.* 148, 719–729.

Foudree, A., Putarjunan, A., Kambakam, S., Nolan, T., Fussell, J., Pogorelko, G., et al. (2012). The mechanism of variegation in *immutans* provides insight into chloroplast biogenesis. *Front. Plant Sci.* 3:260. doi: 10.3389/fpls.2012.00260

Gordon, M. J., Carmody, M., Albrecht, V., and Pogson, B. (2012). Systemic and local responses to repeated HL stress-induced retrograde signaling in Arabidopsis. *Front. Plant Sci.* 3:303. doi: 10.3389/fpls.2012.00303

Gray, J. C., Sullivan, J. A., Wang, J. H., Jerome, C. A., and Maclean, D. (2003). Coordination of plastid and nuclear gene expression. *Philos. Trans. R. Soc. Lond. B Biol. Sci.* 358, 135–144. discussion: 144–145.

Hartl, M., and Finkemeier, I. (2012). Plant mitochondrial retrograde signaling: post-translational modifications enter the stage. *Front. Plant Sci.* 3:253. doi: 10.3389/fpls.2012.00253

Heinrichs, L., Schmitz, J., Flügge, U. I., and Häusler, R. E. (2012). The mysterious rescue of *adg1-1/tpt-2* – an *Arabidopsis thaliana* double mutant impaired in acclimation to high light – by exogenously supplied sugars. *Front. Plant Sci.* 3:265. doi: 10.3389/fpls.2012.00265

Hüner, N. P., Bode, R., Dahal, K., Hollis, L., Rosso, D., Krol, M., et al. (2012). Chloroplast redox imbalance governs phenotypic plasticity: the "grand design of photosynthesis" revisited. *Front. Plant Sci.* 3:255. doi: 10.3389/fpls.2012.00255

Isemer, R., Krause, K., Grabe, N., Kitahata, N., Asami, T., and Krupinska, K. (2012a). Plastid located WHIRLY1 enhances the responsiveness of Arabidopsis seedlings toward abscisic acid. *Front. Plant Sci.* 3:283. doi: 10.3389/fpls.2012.00283

Isemer, R., Mulisch, M., Schafer, A., Kirchner, S., Koop, H. U., and Krupinska, K. (2012b). Recombinant Whirly1 translocates from transplastomic chloroplasts to the nucleus. *FEBS Lett.* 586, 85–88.

Karpinski, S., Reynolds, H., Karpinska, B., Wingsle, G., Creissen, G., and Mullineaux, P. (1999). Systemic signaling and acclimation in response to excess excitation energy in Arabidopsis. *Science* 284, 654–657.

Klein, P., Seidel, T., Stöcker, B., and Dietz, K. J. (2012). The membrane-tethered transcription factor ANAC089 serves as redox-dependent suppressor of stromal ascorbate peroxidase gene expression. *Front. Plant Sci.* 3:247. doi: 10.3389/fpls.2012.00247

Kleine, T. (2012). *Arabidopsis thaliana* mTERF proteins: evolution and functional classification. *Front. Plant Sci.* 3:233. doi: 10.3389/fpls.2012.00233

Kleine, T., Voigt, C., and Leister, D. (2009). Plastid signalling to the nucleus: messengers still lost in the mists? *Trends Genet.* 25, 185–192.

Leister, D. (2012). Retrograde signaling in plants: from simple to complex scenarios. *Front. Plant Sci.* 3:135. doi: 10.3389/fpls.2012.00135

León, P., Gregorio, J., and Cordoba, E. (2012). ABI4 and its role in chloroplast retrograde communication. *Front. Plant Sci.* 3:304. doi: 10.3389/fpls.2012.00304

Lepistö, A., Toivola, J., Nikkanen, L., and Rintamäki, E. (2012). Retrograde signaling from functionally heterogeneous plastids. *Front. Plant Sci.* 3:286. doi: 10.3389/fpls.2012.00286

Oelmüller, R., and Mohr, H. (1986). Photooxidative destruction of chloroplasts and its consequences for expression of nuclear genes. *Planta* 167, 106–113.

Oelze, M. L., Vogel, M. O., Alsharafa, K., Kahmann, U., Viehhauser, A., Maurino, V. G., et al. (2012). Efficient acclimation of the chloroplast antioxidant defence of *Arabidopsis thaliana* leaves in response to a 10- or 100-fold light increment and the possible involvement of retrograde signals. *J. Exp. Bot.* 63, 1297–1313.

Pfalz, J., Liebers, M., Hirth, M., Grübler, B., Holtzegel, U., Schröter, Y., et al. (2012). Environmental control of plant nuclear gene expression by chloroplast redox signals. *Front. Plant Sci.* 3:257. doi: 10.3389/fpls.2012.00257

Shapiguzov, A., Vainonen, J. P., Wrzaczek, M., and Kangasjärvi, J. (2012). ROS-talk – how the apoplast, the chloroplast, and the nucleus get the message through. *Front. Plant Sci.* 3:292. doi: 10.3389/fpls.2012.00292

Tadini, L., Romani, I., Pribil, M., Jahns, P., Leister, D., and Pesaresi, P. (2012). Thylakoid redox signals are integrated into organellar-gene-expression-dependent retrograde signaling in the *prors1-1* mutant. *Front. Plant Sci.* 3:282. doi: 10.3389/fpls.2012.00282

Tanaka, K., and Hanaoka, M. (2012). The early days of plastid retrograde signaling with respect to replication and transcription. *Front. Plant Sci.* 3:301. doi: 10.3389/fpls.2012.00301

Terry, M. J., and Smith, A. G. (2013). A model for tetrapyrrole synthesis as the primary mechanism for plastid-to-nucleus signaling during chloroplast biogenesis. *Front. Plant Sci.* 4:14. doi: 10.3389/fpls.2013.00014

Tikkanen, M., Gollan, P. J., Suorsa, M., Kangasjärvi, S., and Aro, E. M. (2012). STN7 operates in retrograde signaling through controlling redox balance in the electron transfer chain. *Front. Plant Sci.* 3:277. doi: 10.3389/fpls.2012.00277

Van Aken, O., and Whelan, J. (2012). Comparison of transcriptional changes to chloroplast and mitochondrial perturbations reveals common and specific responses in Arabidopsis. *Front. Plant Sci.* 3:281. doi: 10.3389/fpls.2012.00281

Vestergaard, C. L., Flyvbjerg, H., and Møller, I. M. (2012). Intracellular signaling by diffusion: can waves of hydrogen peroxide transmit intracellular information in plant cells? *Front. Plant Sci.* 3:295. doi: 10.3389/fpls.2012.00295

Wojtera-Kwiczor, J., Gross, F., Leffers, H. M., Kang, M., Schneider, M., and Scheibe, R. (2012). Transfer of a redox-signal through the cytosol by redox-dependent microcompartmentation of glycolytic enzymes at mitochondria and actin cytoskeleton. *Front. Plant Sci.* 3:284. doi: 10.3389/fpls.2012.00284

Woodson, J. D., Perez-Ruiz, J. M., and Chory, J. (2011). Heme synthesis by plastid ferrochelatase I regulates nuclear gene expression in plants. *Curr. Biol.* 21, 897–903.

Received: 19 February 2013; accepted: 22 February 2013; published online: 12 March 2013.

Citation: Kleine T and Leister D (2013) Retrograde signals galore. Front. Plant Sci. 4:45. doi: 10.3389/fpls.2013.00045

This article was submitted to Frontiers in Plant Physiology, a specialty of Frontiers in Plant Science.

Copyright © 2013 Kleine and Leister. This is an open-access article distributed under the terms of the Creative Commons Attribution License, which permits use, distribution and reproduction in other forums, provided the original authors and source are credited and subject to any copyright notices concerning any third-party graphics etc.

frontiers in
PLANT SCIENCE

HYPOTHESIS AND THEORY ARTICLE
published: 03 January 2013
doi: 10.3389/fpls.2012.00301

The early days of plastid retrograde signaling with respect to replication and transcription

***Kan Tanaka*[1]* and *Mitsumasa Hanaoka*[2]**

[1] *Chemical Resources Laboratory, Tokyo Institute of Technology, Yokohama, Japan*
[2] *Graduate School of Horticulture, Chiba University, Matsudo, Japan*

Edited by:
Dario Leister, Ludwig-Maximilians-University Munich, Germany

Reviewed by:
David M. Rhoads, University of Arizona, USA
Bernhard Grimm, Humboldt University Berlin, Germany
Stefan Hortensteiner, University of Zurich, Switzerland

***Correspondence:**
Kan Tanaka, Chemical Resources Laboratory, Tokyo Institute of Technology, 29-R1-4259 Nagatsuta, Midori-ku, Yokohama 226-8503, Japan.
e-mail: kntanaka@res.titech.ac.jp

The plastid signal was originally defined as a pathway that informs the nucleus of the chloroplast status and results in the modulation of expression of nuclear-encoded plastid protein genes. However, the transfer of chloroplast genes into the nuclear genome is a prerequisite in this scheme, although it should not have been established during the very early phase of chloroplast evolution. We recently demonstrated in a primitive red alga that the plastid-derived Mg-protoporphyrin IX activates nuclear DNA replication (NDR) through the stabilization of a G1 cyclin, which coordinates the timing of organelle and NDR. This mechanism apparently does not involve any transcriptional regulation in the nucleus, and could have been established prior to gene transfer events. However, a retrograde signal mediating light-responsive gene expression may have been established alongside gene transfer, because essential light sensing and regulatory systems were originally incorporated into plant cells by the photosynthetic endosymbiont. In this short article, we discuss the origins, early days and evolution of the plastid retrograde signal(s).

Keywords: cell cycle, checkpoint, chloroplast, DNA replication, nuclear gene transfer, retrograde signal, tetrapyrrole, transcription

INTRODUCTION

Eukaryotic cells contain various organelles, and continuous monitoring of and responding to their status are critical functions of the nucleus for managing cell integrity. Thus, eukaryotic cells have evolved intricate signaling mechanisms from the nucleus to organelles as well as from organelles to the nucleus (Woodson and Chory, 2008). Among such organelles, mitochondria and chloroplasts originated from symbioses with ancient bacteria, and show particular complexity in their structure and related signaling processes. Most notably, they contain their own genomes that were inherited from the ancestral bacteria, and concomitantly, bacterial-type gene expression and other cellular machineries are present in each organelle, independent of the nuclear system (Barbrook et al., 2010). These points discriminate these organelles from others, and this article mainly deals with chloroplasts.

Since the majority of chloroplast proteins are encoded by the nuclear genome and targeted into chloroplasts after translation in the cytoplasm (Bock and Timmis, 2008), communication in the nucleus-to-organelle direction is easily understandable (anterograde signaling). However, organelle-to-nucleus signaling, named retrograde signaling, has been the subject of controversy despite decades of research. In plant cells, changes in organelle condition such as oxidative damage or redox status have been known to modulate nuclear gene expression (Apel and Hirt, 2004; Pfannschmidt et al., 2009). Thus, genetic and other cell biological approaches have been used to clarify the relevant signaling pathway, and a number of genetic and metabolic components, as well as multiple signaling pathways, have been identified (Inaba et al., 2011). However, it should be noted that most of this research has been concentrated on the pathways modulating nuclear gene expression, and the non-transcriptional aspects of retrograde signaling have not been extensively examined thus far. We recently proposed that in a primitive red alga, a plastid-derived tetrapyrrole signal works to coordinate organelle DNA replication (ODR) and nuclear DNA replication (NDR), independent of transcriptional regulation in the nucleus (Kanesaki et al., 2009; Kobayashi et al., 2009, 2011). Here, we discuss early days of plastid retrograde signaling from the standpoint of its origin and evolution.

COORDINATION OF DNA REPLICATION IN PLANT CELLS

In plant cells, three independent organelles – chloroplasts, mitochondria, and the nucleus – each contain their own genome. While only one nucleus is usually present in a cell, dozens of chloroplasts and mitochondria are found in most land plant cells. The proliferation cycle of plant cells is defined based on the S and M phases, which correspond to NDR and cell division, respectively, as in other eukaryotic cells. Similarly, chloroplasts and mitochondria proliferate by replication of their own genomes and subsequent division, and are inherited by daughter cells through division of the cytoplasm. However, abundantly present chloroplasts and mitochondria asynchronously proliferate throughout the cell cycle phases of higher plant cells (Birky, 2001), and not only division but also fusion is frequently observed for mitochondria (Logan, 2006, 2010). Thus, the interrelationship between the cell cycle and the organelle proliferation cycles remains unclear in plant cells.

Microscopic analyses of ODR and NDR during leaf and root development have shown that ODR is extensively activated during the early phase of the development of these organs, while NDR appears to occur after the ODR activation phase (Sakai et al., 2004). These observations indicate that ODR is not strictly co-regulated with NDR, but has some flexible links to NDR by

unknown signaling mechanisms. In addition, a recent report strongly suggested links between the chloroplasts' developmental status and NDR during leaf development; Andriankaja et al. (2012) reported that differentiation of the chloroplast photosynthetic machinery is important for cell cycle arrest and the onset of endoreduplication and cell expansion during leaf development in *Arabidopsis*. The authors suggested that some retrograde signal from chloroplasts might be deeply involved in the cell cycle phase transition.

Organelle DNA replication precedes NDR in plant cells; this tendency is most evident in unicellular red algae of Cyanidiales such as *Cyanidium caldarium* and *Cyanidioschyzon merolae*, which contain only one chloroplast and one mitochondrion per cell. In these cells, ODR in the chloroplast and mitochondria occurs after the onset of the cell cycle, and NDR always occurs after ODR. Particularly unique among the unicellular red alga, *Cyanidioschyzon merolae* performs binary fission, and the division of each organelle occurs only once in a cell cycle (Suzuki et al., 1994). In addition, complete genome sequences of the nucleus, chloroplast, and mitochondrion are now available (Ohta et al., 1998, 2003; Matsuzaki et al., 2004), and tools for molecular genetic analyses have been extensively developed in *Cyanidioschyzon merolae* (Ohnuma et al., 2008, 2009; Imamura et al., 2010). We thus analyzed the interconnection between ODR and NDR using this model cell system. As the results have already been published in two papers (Kobayashi et al., 2009, 2011), we only summarize the main points here:

Under dark conditions, the cell cycle of *Cyanidioschyzon merolae* is arrested at the G1 phase. Initiation of the S phase requires activation of a cyclin/cdk protein kinase complex, Cyclin1/CDKA, but Cyclin1 is continuously recognized by an F-box protein (Fbx3) of ubiquitin ligase in darkness, which results in ubiquitination and degradation of Cyclin1 by proteasome and prevention of NDR. Light illumination activates the cell cycle and prompts entry into the S phase, however, it is ODR not NDR that is primarily activated by the light. Activation of ODR somehow results in accumulation of Mg-protoporphyrin IX (Mg-ProtoIX) very likely in the cytosol, and subsequent interaction of Mg-ProtoIX with Fbx3 prevents the ubiquitination and degradation of Cyclin1, which results in Cyclin1 accumulation, Cyclin1/CDKA activation, and finally NDR activation. In this working model, Mg-ProtoIX is produced only in the chloroplast, and thus can be considered a *bona fide* retrograde plastid signal. In the case of nuclear gene expression control, Mg-ProtoIX has long been suggested as a plastid retrograde signal (Nott et al., 2006). However, recent reports in the field of plastid retrograde signaling have denied the specific role of Mg-ProtoIX in the nuclear transcriptional regulation of vascular plants (Mochizuki et al., 2008; Moulin et al., 2008). In any case, the involvement of the tetrapyrrole biosynthetic pathway itself is likely, and it is intriguing to consider why these compounds are critical to interorganellar communication.

Prior to endosymbiosis, the cell cycle of the host eukaryote was probably non-phototrophic and likely driven by the usual Cyclin/CDK system that is unrelated to the external light conditions for photosynthesis. However, the cyanobacterial endosymbiont must have required light for proliferation. Thus, the endosymbiont of the early photosynthetic eukaryote was likely to be lost under dark conditions, unless some mechanism to couple the host–symbiont proliferation cycles evolved (**Figure 1**). The mechanism for the ODR–NDR coupling described above requires basically only one specific protein, Fbx3, to be established as an additional cytoplasmic component. Providing that the evolution of Fbx3 adequately explains the chloroplast-to-nucleus DNA replication coupling, this mechanism could have been established at a very early phase of chloroplast evolution because of its extreme simplicity. In addition, it should be noted that this mechanism does not require any gene transfer events from the chloroplast to the nucleus. Since the well-known plastid retrograde signals are related to the transcriptional regulation of nuclear genes encoding chloroplast-targeted proteins, gene transfer events are prerequisite for their existence. The establishment of endosymbiosis would have been prior to such gene transfer events, and our recent findings may have supported the stabilization of the transition states. A similar coupling mechanism has also been suggested to be present in vascular plant cells (Kobayashi et al., 2009), again indicating its common and early origin during plant evolution.

LIGHT-RESPONSIVE TRANSCRIPTIONAL REGULATION IN THE NUCLEUS

The significance of the coordination of nuclear and chloroplast DNA replication, which could have been established during very early stages of chloroplast evolution after the endosymbiotic event, is described above. In addition to DNA replication, along with gene transfer from the chloroplast to the nuclear genome, light-dependent expression of genetic information should also be coordinated between the nucleus and chloroplasts to enable suitable stoichiometry of gene products that are encoded in separate genomes (Goldschmidt-Clermont, 1998; Woodson and Chory, 2008). In vascular plants, it has been speculated that such coordination could be mediated by bi-directional (anterograde and retrograde) signaling pathways (Pogson et al., 2008; Barajas-López et al., 2012), and additionally, various types of photoreceptors as well as light signaling modules are well-known to regulate the light-dependent expression of a set of nuclear genes (Jiao et al., 2007). However, it is very difficult to imagine how and when this coordination and/or light regulation of nuclear gene expression could have been established in the course of chloroplast evolution after the endosymbiosis with an ancient cyanobacterial cell.

Before endosymbiosis, an ancient eukaryotic cell with a nucleus and mitochondria should have some, but not so highly complicated light-responsive regulation of gene expression because it was unnecessary to respond to the light environment as a non-photosynthetic organism. Conversely, cyanobacteria, which require oxygenic photosynthesis for their survival, should have a set of photosensory and photoregulatory mechanisms. Just after endosymbiosis, during the early stages of chloroplast evolution, light-responsive gene expression derived from cyanobacteria must have been completed inside the chloroplast (symbiont), and the regulation of nuclear gene expression should have been irrespective of the light conditions. However, mutual coordination of various cellular parameters, including metabolic fluxes, must have become crucial between the chloroplast and the host cell (**Figure 2**). In addition, gene transfer from the chloroplast to the nuclear genome has gradually occurred. Therefore, in a later phase

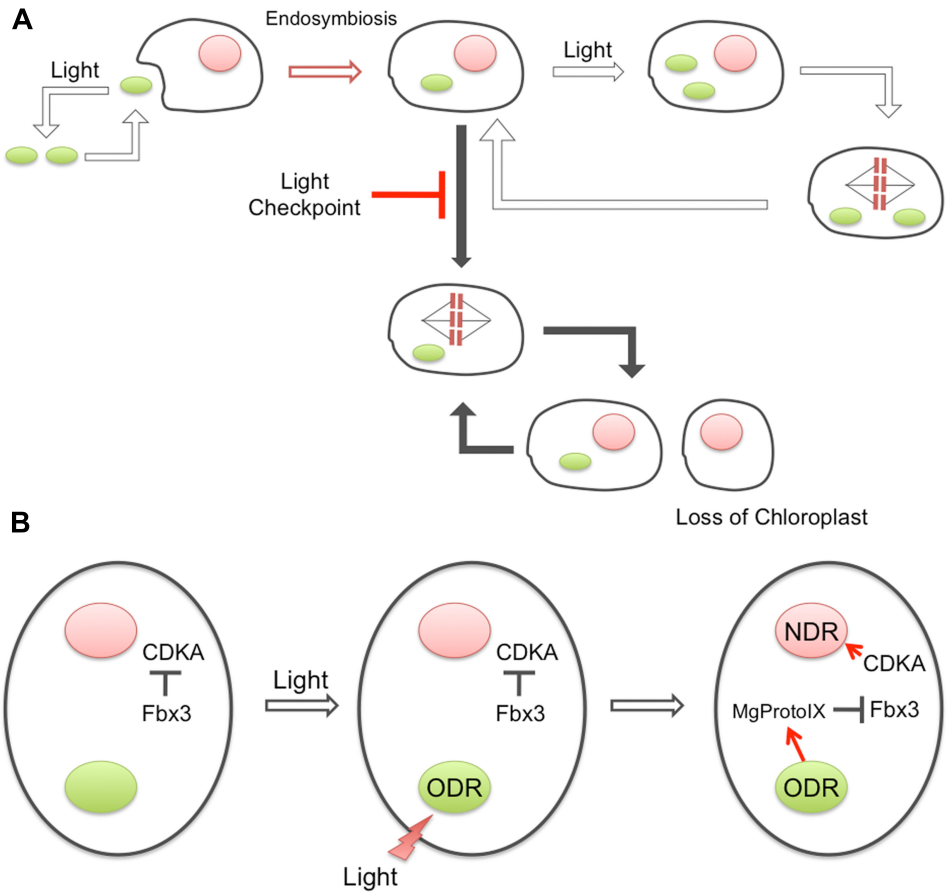

FIGURE 1 | Evolution of the coupling between ODR and NDR. (A) Prior to endosymbiosis, the ancestral cyanobacteria were living phototrophically and dependent on light, while the host eukaryotic cells were proliferating independent of light conditions. After the engulfment, the primitive chloroplast would have required light for proliferation, while the host did not. Therefore, the uniquely acquired chloroplast may have been lost if the host cell could proliferate in the dark. A newly evolved checkpoint system, "light checkpoint" in the figure, prevented host proliferation in the dark to maintain the endosymbiotic association. **(B)** Architecture of the light checkpoint. Under dark conditions, an F-box component of E3-ubiquitin ligase, Fbx3, recognizes Cyclin1, resulting in ubiquitination and prompt degradation. Cyclin1 is the cyclin that forms a complex with CDKA and activates NDR, and thus, degradation of Cyclin1 prevents NDR in the dark. Light illumination somehow activates ODR and results in the accumulation of Mg-ProtoIX in the cytosol. Interaction of Mg-ProtoIX with Fbx3 prevents the ubiquitination of Cyclin1 and induces the activation of CDKA and NDR.

of chloroplast evolution, light signals should have become transmitted into the nucleus to establish light-responsive coordinated gene expression as a photosynthetic eukaryote. During the subsequent evolution, plant-type photoreceptors and light signaling pathways were likely established.

Recently, we hypothesized a primitive mechanism for light response, as well as light regulation of nuclear gene expression, based on the analysis of a primitive red alga, *Cyanidioschyzon merolae*. Light-dependent transcriptional induction in the nucleus has been shown to occur in *Cyanidioschyzon merolae* (Fujiwara et al., 2009). However, no typical plant-specific photoreceptors (phytochromes and phototropins) were encoded in the *Cyanidioschyzon merolae* genome (Matsuzaki et al., 2004), although a group of cryptochrome-like genes are found (Asimgil and Kavakli, 2012). These lines of evidence suggest that a part of the photosensing in *Cyanidioschyzon merolae* occurs inside the chloroplast and thus light signal(s) could be transmitted into the nucleus by some retrograde mechanisms. As a candidate mediator for chloroplast-to-nucleus signaling in vascular plant cells, Mg-ProtoIX (which has already been mentioned in the previous section as a possible regulator for coordination of DNA replication between nuclear and organelle genomes) was examined to determine whether it could also regulate nuclear gene expression in *Cyanidioschyzon merolae*. As is consistent with recent negative reports for this signaling molecule (Mochizuki et al., 2008; Moulin et al., 2008), we could not obtain any experimental evidence supporting this hypothesis (Kanesaki et al., 2009). These observations also suggest the presence of another, presumably more primitive but fundamental, signaling pathway in *Cyanidioschyzon merolae*, which can transduce light signals into the nucleus (Kanesaki et al., 2012).

In bacteria, fungi, and plants, it is well-known that two-component regulatory systems are involved in the sensing of, and regulatory responses to, various environmental stimuli. This system is normally composed of sensory histidine kinases (HKs) that perceive environmental signals and response regulators required

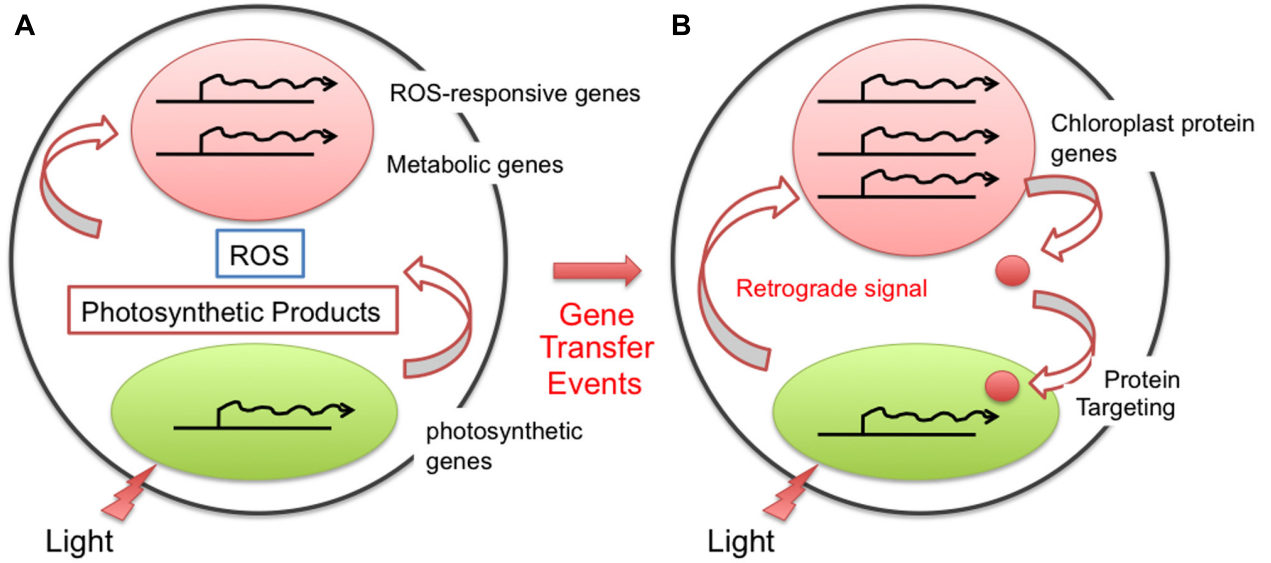

FIGURE 2 | Evolution of the chloroplast retrograde signal for nuclear transcriptional regulation. After endosymbiosis, the chloroplast performed photosynthesis, generating photosynthetic metabolites as well as reactive oxygen species (ROS). The ability to sense and respond to these compounds in the cytoplasm should have been present even prior to the gene transfer event, and thus the nucleus was likely able to cope with them without any specific evolution **(A)**. After the gene transfer event from the chloroplast to the nucleus, the location of the gene and its function differentiated. To modulate the function and amount of the gene product properly, the cell evolved a regulatory loop through a specific retrograde signaling pathway **(B)**.

for output regulation such as transcriptional regulation (Jung et al., 2012). There are genes for one histidine kinase (CmHIK) and two response regulators (Ycf27 and Ycf29) in the *Cyanidioschyzon merolae* nuclear and chloroplast genomes, respectively (Ohta et al., 2003; Matsuzaki et al., 2004). They are possibly involved in light-responsive transcriptional regulation in chloroplasts because their orthologous factors in cyanobacteria are considered to be required for light responses (Ashby and Mullineaux, 1999; Ashby et al., 2002). Since these factors and systems are not conserved in the chloroplasts of vascular plants, it is natural to consider that *Cyanidioschyzon merolae* has a more chloroplast-autonomous signaling mechanism, especially in response to light. This could represent a primitive style of light response during the course of chloroplast evolution. As mentioned above, the transcription of most nuclear genes is also regulated in a light-dependent manner in *Cyanidioschyzon merolae*. Thus, in the early days of chloroplast evolution, we hypothesize that a chloroplast photosensory mechanism(s), such as the two-component system inherited from cyanobacteria, might also have been responsible for light-dependent nuclear transcription via an unidentified chloroplast-to-nucleus retrograde signaling pathway(s). The establishment of a complex coordination mechanism for nuclear and organelle gene expression in response to light environments likely required a long time period. However, light-dependent nuclear transcription itself might have evolved alongside gene transfer to the nucleus. This retrograde signal(s) could be partly derived from chloroplast photosensory components including the two-component system, as well as an event of photosynthetic electron transfer. In any case, during early phases of chloroplast evolution, we expect that the development of fundamental crosstalk between the nucleus (host) and the chloroplast (symbiont) was essential to effectively respond to light environments, and to coordinate DNA replication and transcription of both genomes.

ACKNOWLEDGMENTS

This work was supported in part by Grants-in-Aid (24117505, 24770037 to Mitsumasa Hanaoka and 23120505, 24248061 to Kan Tanaka), and a Special Coordination Fund for Promoting Science and Technology (Mitsumasa Hanaoka), from the Ministry of Education, Culture, Sports, Science and Technology of Japan, or Japan Society for the Promotion of Science, the Sumitomo Foundation (Mitsumasa Hanaoka), and the Cooperative Research Program of "Network Joint Research Center for Materials and Devices" (Kan Tanaka and Mitsumasa Hanaoka).

REFERENCES

Andriankaja, F., Dhondt, S., De Bodt, S., Vanhaeren, H., Coppens, F., De Milde, L., et al. (2012). Exit from proliferation during leaf development in *Arabidopsis thaliana*: a not-so-gradual process. *Dev. Cell* 22, 64–78.

Apel, K., and Hirt, H. (2004). Reactive oxygen species: metabolism, oxidative stress, and signal transduction. *Annu. Rev. Plant Biol.* 55, 373–399.

Ashby, M. K., and Mullineaux, C. W. (1999). Cyanobacterial ycf27 gene products regulate energy transfer from phycobilisomes to photosystems I and II. *FEMS Microbiol. Lett.* 181, 253–260.

Ashby, M. K., Houmard, J., and Mullineaux, C. W. (2002). The ycf27 genes from cyanobacteria and eukaryotic algae: distribution and implications for chloroplast evolution. *FEMS Microbiol. Lett.* 214, 25–30.

Asimgil, H., and Kavakli, I. H. (2012). Purification and characterization of five members of photolyase/cryptochrome family from *Cyanidioschyzon merolae*. *Plant Sci.* 185–186, 190–198.

Barajas-López, J. D., Blanco, N. E., and Strand, A. (2012). Plastid-to-nucleus communication, signals controlling the running of the plant cell. *Biochim. Biophys. Acta* doi: 10.1016/j.bbamcr.2012.06.020 [Epub ahead of print].

Barbrook, A. C., Howe, C. J., Kurniawan, D. P., and Tarr, S. J. (2010). Organization and expression of organellar genomes. *Philos. Trans. R. Soc. Lond. B Biol. Sci.* 365, 785–797.

Birky, C. W. Jr. (2001). The inheritance of genes in mitochondria and chloroplasts: laws, mechanisms, and models. *Annu. Rev. Genet.* 35, 125–148.

Bock, R., and Timmis, J. N. (2008). Reconstructing evolution: gene transfer from plastids to the nucleus. *Bioessays* 30, 556–566.

Fujiwara, T., Misumi, O., Tashiro, K., Yoshida, Y., Nishida, K., Yagisawa, F., et al. (2009). Periodic gene expression patterns during the highly synchronized cell nucleus and organelle division cycles in the unicellular red alga *Cyanidioschyzon merolae*. *DNA Res.* 16, 59–72.

Goldschmidt-Clermont, M. (1998). Coordination of nuclear and chloroplast gene expression in plant cells. *Int. Rev. Cytol.* 177, 115–180.

Imamura, S., Terashita, M., Ohnuma, M., Maruyama, S., Minoda, A., Weber, A. P., et al. (2010). Nitrate assimilatory genes and their transcriptional regulation in a unicellular red alga *Cyanidioschyzon merolae*: genetic evidence for nitrite reduction by a sulfite reductase-like enzyme. *Plant Cell Physiol.* 51, 707–717.

Inaba, T., Yazu, F., Ito-Inaba, Y., Kakizaki, T., and Nakayama, K. (2011). Retrograde signaling pathway from plastid to nucleus. *Int. Rev. Cell Mol. Biol.* 290, 167–204.

Jiao, Y., Lau, O. S., and Deng, X. W. (2007). Light-regulated transcriptional networks in higher plants. *Nat. Rev. Genet.* 8, 217–230.

Jung, K., Fried, L., Behr, S., and Heermann, R. (2012). Histidine kinases and response regulators in networks. *Curr. Opin. Microbiol.* 15, 118–124.

Kanesaki, Y., Imamura, S., Minoda, A., and Tanaka, K. (2012). External light conditions and internal cell cycle phases coordinate accumulation of chloroplast and mitochondrial transcripts in the red alga *Cyanidioschyzon merolae*. *DNA Res.* 19, 289–303.

Kanesaki, Y., Kobayashi, Y., Hanaoka, M., and Tanaka, K. (2009). Mg-protoporphyrin IX signaling in *Cyanidioschyzon merolae*: multiple pathways may involve the retrograde signaling in plant cells. *Plant Signal. Behav.* 4, 1190–1192.

Kobayashi, Y., Imamura, S., Hanaoka, M., and Tanaka, K. (2011). A tetrapyrrole-regulated ubiquitin ligase controls algal nuclear DNA replication. *Nat. Cell Biol.* 13, 483–487.

Kobayashi, Y., Kanesaki, Y., Tanaka, A., Kuroiwa, H., Kuroiwa, T., and Tanaka, K. (2009). Tetrapyrrole signal as a cell-cycle coordinator from organelle to nuclear DNA replication in plant cells. *Proc. Natl. Acad. Sci. U.S.A.* 106, 803–807.

Logan, D. C. (2006). Plant mitochondrial dynamics. *Biochim. Biophys. Acta* 1763, 430–441.

Logan, D. C. (2010). The dynamic plant chondriome. *Semin. Cell Dev. Biol.* 21, 550–557.

Matsuzaki, M., Misumi, O., Shin-I, T., Maruyama, S., Takahara, M., Miyagishima, S. Y., et al. (2004). Genome sequence of the ultrasmall unicellular red alga *Cyanidioschyzon merolae* 10D. *Nature* 428, 653–657.

Mochizuki, N., Tanaka, R., Tanaka, A., Masuda, T., and Nagatani, A. (2008). The steady-state level of Mg-protoporphyrin IX is not a determinant of plastid-to-nucleus signaling in *Arabidopsis*. *Proc. Natl. Acad. Sci. U.S.A.* 105, 15184–15189.

Moulin, M., McCormac, A. C., Terry, M. J., and Smith, A. G. (2008). Tetrapyrrole profiling in *Arabidopsis* seedlings reveals that retrograde plastid nuclear signaling is not due to Mg-protoporphyrin IX accumulation. *Proc. Natl. Acad. Sci. U.S.A.* 105, 15178–15183.

Nott, A., Jung, H. S., Koussevitzky, S., and Chory, J. (2006). Plastid-to-nucleus retrograde signaling. *Annu. Rev. Plant Biol.* 57, 739–759.

Ohnuma, M., Misumi, O., Fujiwara, T., Watanabe, S., Tanaka, K., and Kuroiwa, T. (2009). Transient gene suppression in a red alga, *Cyanidioschyzon merolae* 10D. *Protoplasma* 236, 107–112.

Ohnuma, M., Yokoyama, T., Inouye, T., Sekine, Y., and Tanaka, K. (2008). Polyethylene glycol (PEG)-mediated transient gene expression in a red alga, *Cyanidioschyzon merolae* 10D. *Plant Cell Physiol.* 49, 117–120.

Ohta, N., Matsuzaki, M., Misumi, O., Miyagishima, S. Y., Nozaki, H., Tanaka, K., et al. (2003). Complete sequence and analysis of the plastid genome of the unicellular red alga *Cyanidioschyzon merolae*. *DNA Res.* 10, 67–77.

Ohta, N., Sato, N., and Kuroiwa, T. (1998). Structure and organization of the mitochondrial genome of the unicellular red alga *Cyanidioschyzon merolae* deduced from the complete nucleotide sequence. *Nucleic Acids Res.* 26, 5190–5198.

Pfannschmidt, T., Bräutigam, K., Wagner, R., Dietzel, L., Schröter, Y., Steiner, S., et al. (2009). Potential regulation of gene expression in photosynthetic cells by redox and energy state: approaches towards better understanding. *Ann. Bot.* 103, 599–607.

Pogson, B. J., Woo, N. S., Förster, B., and Small, I. D. (2008). Plastid signalling to the nucleus and beyond. *Trends Plant Sci.* 13, 602–609.

Sakai, A., Takano, H., and Kuroiwa, T. (2004). Organelle nuclei in higher plants: structure, composition, function, and evolution. *Int. Rev. Cytol.* 238, 59–118.

Suzuki, K., Ehara, T., Osafune, T., Kuroiwa, H., Kawano, S., and Kuroiwa, T. (1994). Behavior of mitochondria, chloroplasts and their nuclei during the mitotic cycle in the ultramicroalga *Cyanidioschyzon merolae*. *Eur. J. Cell Biol.* 63, 280–288.

Woodson, J. D., and Chory, J. (2008). Coordination of gene expression between organellar and nuclear genomes. *Nat. Rev. Genet.* 9, 383–395.

Conflict of Interest Statement: The authors declare that the research was conducted in the absence of any commercial or financial relationships that could be construed as a potential conflict of interest.

Received: 15 September 2012; accepted: 14 December 2012; published online: 03 January 2013.

Citation: Tanaka K and Hanaoka M (2013) The early days of plastid retrograde signaling with respect to replication and transcription. Front. Plant Sci. ***3****:301. doi: 10.3389/fpls.2012.00301*

This article was submitted to Frontiers in Plant Physiology, a specialty of Frontiers in Plant Science.

Copyright © 2013 Tanaka and Hanaoka. This is an open-access article distributed under the terms of the Creative Commons Attribution License, which permits use, distribution and reproduction in other forums, provided the original authors and source are credited and subject to any copyright notices concerning any third-party graphics etc.

frontiers in
PLANT SCIENCE

HYPOTHESIS AND THEORY ARTICLE
published: 04 January 2013
doi: 10.3389/fpls.2012.00300

Reconsidering the nature and mode of action of metabolite retrograde signals from the chloroplast

Gonzalo M. Estavillo, Kai Xun Chan, Su Yin Phua and Barry J. Pogson*

ARC Centre of Excellence in Plant Energy Biology, Research School of Biology, The Australian National University, Canberra, ACT, Australia

Edited by:
Dario Leister,
Ludwig-Maximilians-University Munich, Germany

Reviewed by:
Tatjana Kleine,
Ludwig-Maximilians-Universität München, Germany
Michel Havaux, Commissariat à l'Energie Atomique et aux Energies Alternatives, France

***Correspondence:**
Barry J. Pogson, ARC Centre of Excellence in Plant Energy of Biology, Research School of Biology, The Australian National University, Canberra, ACT 0200, Australia.
e-mail: barry.pogson@anu.edu.au

Plant organelles produce retrograde signals to alter nuclear gene expression in order to coordinate their biogenesis, maintain homeostasis, or optimize their performance under adverse conditions. Many signals of different chemical nature have been described in the past decades, including chlorophyll intermediates, reactive oxygen species (ROS), and adenosine derivatives. While the effects of retrograde signaling on gene expression are well understood, the initiation and transport of the signals and their mode of action have either not been resolved, or are a matter of speculation. Moreover, retrograde signaling should be considered as part of a broader cellular network, instead of as separate pathways, required to adjust to changing physiologically relevant conditions. Here we summarize current plastid retrograde signaling models in plants, with a focus on new signaling pathways, SAL1-PAP, methylerythritol cyclodiphosphate (MEcPP), and β-cyclocitral (β-CC), and outline missing links or future areas of research that we believe need to be addressed to have a better understanding of plant intracellular signaling networks.

Keywords: retrograde signaling, metabolite, drought, high light, gene regulation, 3′-phosphoadenosine 5′-phosphate, methylerythritol cyclodiphosphate, β-cyclocitral

INTRODUCTION

Chloroplasts originated from free-living cyanobacteria that were engulfed by the eukaryotic cell ancestor (Delwiche, 1999). This endosymbiotic event resulted in the transfer of thousands of genes from the cyanobacterial plastid ancestor into the nuclear genome of the host (Goksoyr, 1967; Martin et al., 2002). As a result of this gene transfer, the stoichiometry of nuclear and chloroplastic encoded polypeptides functioning in the plastids requires the coordination of both genomes. One such regulatory mechanism, called anterograde signaling, entails the coordination of plastid gene expression (PGE) by nuclear encoded proteins (Woodson and Chory, 2008). The reverse mechanism, or retrograde signaling, requires the transfer of signals from the plastids to the nucleus to regulate the expression of genes encoding both plastid-localized (Strand et al., 2003) and other proteins involved in many cellular processes (op den Camp et al., 2003; Koussevitzky et al., 2007; Pesaresi et al., 2009).

The biogenesis and functioning of plant organelles are coordinated with nuclear gene expression. Early stages of chloroplast development require the establishment of "biogenic" signals to coordinate the production of photosynthetic complexes and membranes (Oelmuller et al., 1986; Pogson et al., 2008). On the other hand, "operational" signals are important for the normal functioning of chloroplasts in mature plants (Pogson et al., 2008). Mature chloroplasts can act as environmental sensors as adverse environmental conditions such as high light (HL) and drought can cause energy imbalances leading to oxidative stress that will impair organellar and cellular function (Wilson et al., 2006). As a result, nuclear and plastidic gene regulation is required to reach homeostasis.

The first evidence that chloroplasts can regulate nuclear gene expression was obtained in the *albostrians* barley mutants deficient in plastid ribosomes (Bradbeer et al., 1979) and in Brassica plants treated with spectinomycin, an inhibitor of organelle protein synthesis (Zubko and Day, 1998). In both cases, bleached leaves were produced with decreased amount of nuclear encoded chloroplast proteins. These observations lead to the proposal that perturbation in plastidic processes give rise to plastid products, or signals that can control cytosolic protein translation.

Since then, different types of retrograde signaling pathways, depending on the trigger sources and signals, have been reported. One signaling pathway is associated with tetrapyrrole biosynthesis intermediates, like Mg-ProtoporphyrinIX (Mg-ProtoIX) (Strand et al., 2003) and haem (Woodson et al., 2011). A second type is initiated by changes in redox potential at the electron transport chain (Fey et al., 2005; Pfannschmidt et al., 2009). The production of reactive oxygen species (ROS), such as hydrogen peroxide (H_2O_2) and singlet oxygen ($^1O_2^-$) by excess oxidative power is a third mechanism that can trigger specific changes in nuclear gene expression (Apel and Hirt, 2004; Galvez-Valdivieso and Mullineaux, 2010; Suzuki et al., 2012). Finally, there is a type of retrograde signaling associated with PGE (Bradbeer et al., 1979; Nott et al., 2006).

The "classical," or linear, model of retrograde signaling describes that specific signals produced in the organelles by different developmental and environmental cues are able to move into the nucleus where they elicit specific gene regulation. Although there is a good understanding of some of the triggers, the nature, and the final outcomes related to gene expression for some of these proposed retrograde signals, some of the signals are still

debated or their mechanism of actions poorly understood. This *Perspectives* article presents a synopsis of the current knowledge of metabolite plant retrograde signals with a focus on the recent reports of novel signals. We also attempt to identify missing gaps in current models and provide suggestions for future directions of research. Readers are referenced to pertinent reviews for further details regarding other signaling pathways (Apel and Hirt, 2004; Pogson et al., 2008; Woodson and Chory, 2008; Galvez-Valdivieso and Mullineaux, 2010; Pfannschmidt, 2010; Barajas-López et al., 2012).

CLASSICAL RETROGRADE SIGNALS: CHLOROPHYLL PRECURSORS

Classical retrograde signals in plants generally involved artificially stressing the plant cells by treating the plants with the herbicide norflurazon (NF), which is an inhibitor of carotenoid biosynthesis that can perturb chloroplast development (Foudree et al., 2010). A mutant screen for altered expression of the nuclear genes encoding plastidic proteins during chloroplast development gene led to the discovery of the *GENOMES UNCOUPLED* (*GUN*) mutants (Susek et al., 1993). *gun* mutants are defective in the chloroplast-to-nucleus signal transduction that represses the expression of photosynthesis-associated nuclear genes (PhANG) genes such as *Light Harvesting Complex b (LHCB)* during perturbations of chloroplast development by NF.

At least two intermediates in the synthesis of photosynthetic pigments can act as plastidic signals to regulate nuclear gene expression. Treatment of wild type plants with NF not only inhibits the expression of the PhANG (Susek et al., 1993) but concomitantly induces 15-fold the levels of Mg-ProtoIX, the first committed precursor of chlorophyll. Genetic inhibition of Mg-ProtoIX production, such as in the *gun2* and *gun5* mutants (Mochizuki et al., 2001), which are defective in tetrapyrrole biosynthetic enzymes, results in misregulation of 70 out of 182 genes normally down-regulated in NF-treated wild type plants (Strand et al., 2003). Moreover, pharmacological approaches to accumulate Mg-ProtoIX, either by increasing its amount in the *gun2* and *gun5* mutants, or by feeding it to wild type plants, strongly support the hypothesis that Mg-ProtoIX is required for chloroplast-to-nucleus communication during early plant development (Strand et al., 2003; Kindgren et al., 2012).

Haem is a product of tetrapyrrole biosynthesis that acts as a positive retrograde signal from plastids in algae (von Gromoff et al., 2008). Evidence that haem could also be a potential signal in higher plants came from over expression of the *Ferrochelatase 1* (*FC*) gene in the gain-of-function *gun1-6D* mutant. FC1 over expression leads to the accumulation of PhANGs in the presence of NF (Woodson et al., 2011). This "*gun*" phenotype can be rescued pharmacologically by decreasing the FC activity with Fe^{2+} chelator dipyridyl (DP). This response seems to be specific to the activity of FC1, as over expression of the other chloroplast-localized FC2 did not increase PhANG expression. Unexpectedly, and unlike Mg-ProtoIX, a reduction in total haem, rather than accumulation, occurs in the FC1 OX, and wild type plants after NF treatment (Woodson et al., 2011). This finding is in agreement with the ineffectiveness of haem feeding in seedlings to silence *LHCB* (Strand et al., 2003), but is in contrast with the effect of hemin (a more stable Fe substitute), which promoted global changes in gene expression in *Chlamydomonas* (von Gromoff et al., 2008; Voss et al., 2011). It is proposed that FC1 acts on specific chloroplastic haem pool, which can act as a positive retrograde signal exported from the chloroplasts (Woodson et al., 2011). Although haem can be exported from isolated chloroplasts (Thomas and Weinstein, 1990), the actual transport mechanism is unknown. The fact that there is no correlation between free haem levels and the *gun* phenotype indicates that the signaling haem may be bound to specific targets (Espinas et al., 2012). A possible scenario is that haem interacts with cytosolic or nuclear factors, such as in yeast (Zhang and Hach, 1999) or with haem-binding proteins to regulate gene expression. However, more work is required to identify downstream targets of haem and their mode of action.

Although initial evidence indicate that Mg-ProtoIX accumulates under oxidative stress in the cytosol and represses PhANG expression (Strand et al., 2003; Ankele et al., 2007; Pontier et al., 2007), some findings suggest a lack of correlation between the metabolite levels and gene expression (Gadjieva et al., 2005; Mochizuki et al., 2008; Moulin et al., 2008; Kakizaki et al., 2009; Zhang et al., 2012). Interestingly, another recent finding shows that oxidative stress induced by NF can induce transient accumulation of tetrapyrroles with concomitant repression of *Lhcb* in adult plants (Zhang et al., 2011). The contradictory results could be explained by differences in experimental conditions or technical issues related to the quantification of tetrapyrroles.

Mg-ProtoIX accumulation specifically inhibits the expression of genes harboring the CUF1 (G-Box) *cis*-element (Strand et al., 2003). Two alternative models have been proposed whereby an increase of Mg-ProtoIX promotes either the release of a transcriptional activator or the binding of a repressor (Gray, 2003; Strand et al., 2003). While the potential for Mg-ProtoIX to move into the cytosol has been actively debated, recently more details of a possible mechanism of action mechanism have been described. Mg-ProtoIX was found to bind to the cytosolic heat shock 90-type protein (HSP90) and inhibit the ATPase activity of HSP90 *in vitro* (Kindgren et al., 2012). Feeding and genetic experiments confirmed that the *gun* phenotype triggered by oxidative stress is partially suppressed when HSP90 is silenced and that it requires the action of *Long Hypocotyl 5* (*HY5*) (Kindgren et al., 2012). Interestingly, HY5 binds to the promoter of photosynthetic genes (Lee et al., 2007). This type of signaling mechanism is analogous to that in yeast, where haem can interact with the complex HAP1-HSPs (Hon et al., 2001; Lee et al., 2002), which regulates proteins required for aerobic growth and oxidative damage control (Zhang and Hach, 1999). However, no direct interaction between HSP90 and HY5 has been reported yet in plants.

NOVEL RETROGRADE SIGNALING PATHWAYS

Despite a paucity of discovery of retrograde signals in the last decade, several signaling pathways have been recently proposed in the past 12 months. These novel signals include products of secondary metabolism (Estavillo et al., 2011; Xiao et al., 2012), oxidation products of carotenoids (Ramel et al., 2012), and dual localized proteins (Sun et al., 2011; Isemer et al., 2012) (**Figure 1**). These findings indicate that many metabolic pathways can act as

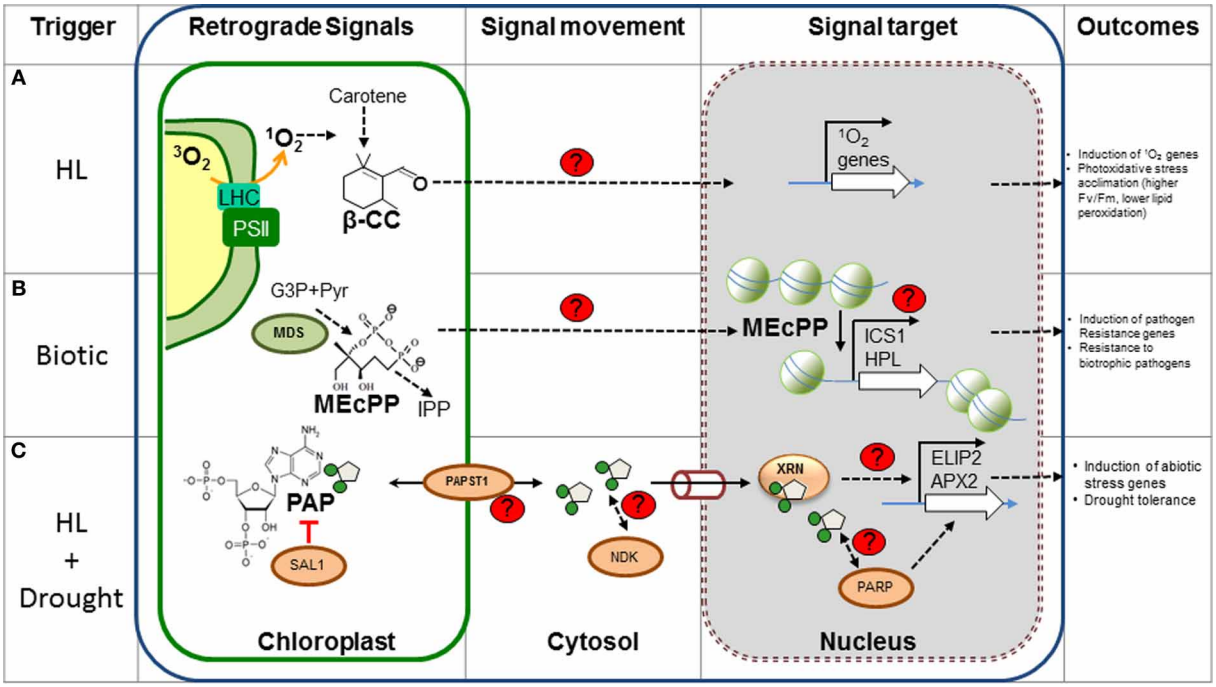

FIGURE 1 | New metabolic retrograde signaling pathways. The different components of recently discovered plant retrograde signaling pathways are shown. **(A)** β-CC is most likely produced by oxidation of carotenes by $^1O_2$ in the chloroplast and could diffuse through the membrane into the cytosol. Feeding β-CC results in the up-regulation of genes involved in stress responses, particularly those triggered by $^1O_2$. It is speculated that the electrophilic carbonyl group could react with electron donors, such as sulfhydryl groups; however, the actual targets and mode of action are unknown. **(B)** MEcPP, an intermediary of isoprenoid precursors, is produced by MDS in the plastidic MEP pathway. MEcPP over accumulating mutants present high levels of SA and are resistant to biotrophic pathogens. MEcPP regulates the expression of the *HPL* and *ICS1* gene, with concomitant production of SA. Although the transport and action mechanism are unknown, MEcPP could promote chromatin reorganization and induction of transcription of target genes. **(C)** PAP levels are catabolically regulated by SAL1 in the chloroplast and PAP transport is probably mediated by PAPST1. Cytosolic PAP could diffuse to the nucleus via the pores (cylinder) where it inhibits nuclear *XRNs* and affects gene regulation of stress inducible genes (i.e., *APX2* and *ELIP2*). This mechanism is thought to play a role during drought, as PAP levels increase 30-fold. Other potential PAP targets (Nucleotide diphosphate kinase, NDK, and poly (ADP-ribose) polymerase, PARP, proteins) may mediate other aspects of signaling. The control mechanism of gene regulation by the XRNs proteins is a matter of investigation. Red lines, inhibition; black arrows, induction or activation; proteins involved in the signaling are indicated as ovals. Unknown components, processes or targets are indicated with red "?" or with dashed arrows. β-CC, β-cyclocitral; MEP, Methylerythritol phosphate pathway; MEcPP, methylerythritol cyclodiphosphate; MDS, MEcPP synthase; IPP, isopentenyl diphosphate; G3P, glyceraldehyde 3-phosphate; SA, salicylic acid; HL, high light. Figure adapted from Xiao et al. (2012) and Estavillo et al. (2011).

potential sources of chloroplastic signals during different developmental stages of the plant or upon different stress responses. More importantly, unlike the previously discovered signals during artificial conditions, these new signals were identified during physiologically relevant stress responses like drought or HL. These new discoveries further support the concept that chloroplasts can indeed act as environmental sensors.

THE PHOSPHONUCLEOTIDE THAT ACTS AS RETROGRADE SIGNAL DURING HIGH LIGHT AND DROUGHT STRESS

The dinucleotide 3′-phosphoadenosine 5′-phosphate (PAP) is a novel metabolite discovered to play a role as a plastid signal during drought and HL stress in Arabidopsis (Estavillo et al., 2011). PAP accumulates in plants lacking the phosphatase SAL1/FRY1, which degrades PAP into adenosine monophosphate (AMP) and phosphate (Chen et al., 2011; Estavillo et al., 2011). PAP is also increased by up to 30 fold in wild type plants during drought (Estavillo et al., 2011) and exhibits a smaller increase in response to HL. The *sal1* mutants present up-regulation of 35% of the HL stress inducible genes, including *Ascorbate Peroxidase 2 (APX2)* and *Early Light Induced Protein 2 (ELIP2)*, altered metabolome and 50% increased survival under water limiting conditions (Rossel et al., 2006; Wilson et al., 2009). PAP is produced as a byproduct of sulfonation reactions catalysed by cytosolic sulfo transferases (SOTs), whereby sulphate is transferred from 3′-phosphoadenosine 5′-phosphosulfate (PAPS) to several metabolic substrates (Klein and Papenbrock, 2004). PAP levels are regulated by the dual localized SAL1 protein in both chloroplasts and mitochondria. Evidence that PAP can move between the chloroplast and nucleus was obtained by complementing PAP levels and *APX2* expression in *sal1* mutants with a SAL1 transgene targeted to the nucleus or chloroplast (Estavillo et al., 2011). Furthermore, a PAPS/PAP chloroplastic antiporter has now been reported that will facilitate exchange of PAP between the chloroplast and cytosol (Gigolashvili, 2012).

PAP most likely regulates gene expression by altering RNA metabolism mediated by 5–3′ exoribonucleases (XRNs). There

are three XRNs in Arabidopsis; two encode the nuclear-localized XRN2 and XRN3 and are homologues of yeast Xrn2p/Rat1p. XRN2 and XRN3 act on uncapped RNAs like the excised hairpin loops in precursor miRNA transcripts (Kastenmayer and Green, 2000). The third gene, XRN4, encodes for a cytosolic XRN (homologous to yeast Xrn2p) that targets the resulting 3′ cleavage products of miRNA targets (Kastenmayer and Green, 2000; Souret et al., 2004). *SAL1* and nuclear *XRN* mutants share similar morphological phenotypes (Gy et al., 2007), have improved drought tolerance and more than 50% of altered genes are co-regulated (Estavillo et al., 2011). Additionally, PAP can inhibit yeast XRN activity (Dichtl et al., 1997; van Dijk et al., 2011) and transcriptional regulation by HL of *ELIP2* and *APX2* genes is similar in Arabidopsis *sal1* mutants (Estavillo et al., 2011). The mechanism by which XRNs modulate specific transcripts, such as *APX2* during stress (i.e., impact on RNA post-transcriptional regulation, "degradome," etc.) is unknown and merits further research.

ISOPRENOID PRECURSOR MEDIATES ABIOTIC STRESS GENE REGULATION

A genetic screening for the constitutive expression of the stress inducible nuclear gene encoding the plastid-localized hydroxyperoxidase lyase (HPL) identified the isoprenoid precursor methylerythritol cyclodiphosphate (MEcPP) as a potential signal from the chloroplast (Xiao et al., 2012). MEcPP is converted to hydroxymethylbutenyl diphosphate (HMBPP) by 1-hydroxy-2-methyl-2-(E)-butenyl-4-diphosphate synthase (HDS) during the production of universal isoprenoid precursors by the methylerithrytol phosphate (MEP) pathway in plastids (Rodríguez-Concepción, 2006). The mutant *ceh1* (*constitutively expressing HPL 1*) accumulates MEcPP and *HPL* transcript, with up-regulation of salicylic acid (SA) production, and that of the *ICS1* (encoding a SA-biosynthetic enzyme) transcript. This results in *ceh1* mutants being more resistant to infection by *Pseudomonas syringae*, a biotrophic pathogen. Targeted silencing of all the enzymes in the MEP pathway indicates that only the accumulation of MEcPP is responsible for SA accumulation and induction of *HPL*. Moreover, feeding experiments demonstrates that MEcPP can directly regulate *HPL*. Thus, it seems that unlike the mechanism mediated by chlorophyll precursors where the flux through the pathway is important for retrograde signaling (Woodson et al., 2011), the induction of *HPL* is specifically triggered by MEcPP, and not by other intermediaries of the MEP pathway. Finally, the accumulation of MEcPP is also induced by wounding and HL stress with concomitant up-regulation of the *HPL* gene.

Strong evidence supports the hypothesis that MEcPP is an operational signal, and like PAP, demonstrates that mature chloroplasts can respond to external perturbations under physiologically relevant conditions. The gene response to MEcPP is specific and it does not involve regulation of PhANGs (Xiao et al., 2012). Comparative global gene expression analysis between *ceh1* relative to wild type is needed to determine the extent of the signaling cascade by MEcPP and potential overlaps with other retrograde networks. Interestingly, oxidative stress in bacterial cultures induced MEcPP production (Ostrovsky et al., 1998) and MEcPP has been involved with the disruption of the interaction between chlamydial histone-like proteins and DNA. This would suggest that MEcPP could affect chromatin remodeling and gene expression (Grieshaber et al., 2006). However, direct evidence for MEcPP movement and its mechanism of action in plants is still lacking and deserves further investigation.

A VOLATILE RETROGRADE SIGNAL

Carotenoids are considered to be one of the first lines of defense against $^1O_2$ produced by the triplet excited chlorophyll during HL stress. Direct measurement of $^1O_2$ and its regulated genes, indicates that production of $^1O_2$ is one of the early responses to HL stress in Arabidopsis (González-Pérez et al., 2011; Ramel et al., 2012). Excess $^1O_2$ under this condition leads to the production of oxidation products of carotenes. One of them, the volatile β-cyclocitral (β-CC), accumulates more than 1.5-fold after 1 h of stress treatment, which is accompanied by the induction of $^1O_2$ stress-responsive genes (Ramel et al., 2012). More significantly, increasing doses of this volatile compound induces the up-regulation of $^1O_2$, but not of H_2O_2, responsive genes. Microarray data also shows a striking specificity and similarity between gene expression profiles of β-CC plants and the *flu* mutant, which accumulates protochlorophyllide and presents a constitutive production of genes involved in oxidative stress by $^1O_2$ (op den Camp et al., 2003). Finally, incubation of plants with β-CC prior to HL and cold stress prevented accumulation of lipid peroxidation and deterioration of PSII photochemical efficiency in a dose dependent manner, suggesting that β-CC increases photoxidative damage tolerance mechanisms. β-CC is a volatile short-chain compound, making diffusion a possible way of distribution from the place of origin to other parts of the cell. A likely action mechanism for β-CC is by reacting with sulfhydryl groups of proteins but more work is required to identify the target proteins and mode of action. Finally, it is possible that β-CC is a signal intermediate of the cascade triggered by $^1O_2$ that relays the information to the cytosol.

MOBILE PROTEINS

The signals described above could be considered as metabolite signals, which in some instances are capable of moving out from the organelle to regulate nuclear gene expression. However, two examples of chloroplast-localized transcription factors (TF) that translocate to the nucleus and alter gene expression under specific conditions have been recently described. Arguably, metabolite signals that could be modulated by specific proteins better fit in the "signal" category (Leister, 2012), but identification of the existence of the mobile TF involved in retrograde signaling confirms the complexity of the mechanisms required to regulate nuclear gene expression.

The chloroplast envelope-bound PTM (PHD type transcription factor with transmembrane domains) is involved in retrograde signal pathways that regulate PhANGs expression under different types of stress conditions (Sun et al., 2011). The plant homeodomain (PHD) specifically binds methylated histones (H3K4me3) to promote transcription of downstream genes (De La Paz Sanchez and Gutierrez, 2009). Under normal

conditions, PTM resides in the outer membrane of the chloroplast. However, a shorter version of PTM protein lacking the transmembrane domain can be found in the nucleus after stress treatment with NF, lincomycin and HL. Stress conditions induce proteolytic cleavage of the full length protein and its translocation to the nucleus. Interestingly, the *ptm* mutant has reduced expression of *ABI4* and displays a *gun* phenotype (i.e., de-repression of *LHCB* in the presence of NF) similar to that of *gun1*, and *abi4* during HL treatment. The involvement of PTM in the same pathway as *GUN1* and *ABI4* was confirmed by analyses of the corresponding double mutants. Interestingly, the levels of H3K4m3 methylation in the *ABI4* promoter increased with the same stress treatments activating the PTM-dependent transcription of the *ABI4* gene. An unexpected observation was the lack of constitutive repression of *LHCB* in the absence of NF in plant expressing soluble PTM. Although this may indicate that additional GUN1 mediated signals may be required, this work demonstrates that PTM mediates several retrograde signaling pathways.

Another mobile protein that could potentially be involved in retrograde signaling is Whirly1 protein (Isemer et al., 2012). Arabidopsis Whirly proteins (AtWhy1 and 3) are required for plastid genome stability (Marechal et al., 2009) and the barley homologue interacts with intron-containing plastidic RNA (Melonek et al., 2010). The barley Whirly 1 (HvWhy1) protein is dual localized to both chloroplast and mitochondria (Grabowski et al., 2008) with the same molecular weight for both forms. Unlike PTM, the AtWhirly1 protein of the same molecular weight was found in both chloroplasts and nucleus of the same cell. It was recently shown that recombinant AtWhirly1 can move from chloroplasts to the nucleus by transformation of tobacco plastids with a HA-AtWhirly1 fusion protein (Isemer et al., 2012). This clever approach demonstrated that HA-AtWhirly1 protein can translocate from the plastid to the nucleus via an unknown mechanism. Although pathogenesis related genes are up-regulated in the transgenic lines (Isemer et al., 2012), suggesting the possible involvement of Whirly1 in retrograde signaling during pathogen attack, the movement mechanism of Whirly [i.e., via stromules, diffusion, transport (Krause et al., 2012)], and gene targets have to be further investigated.

DISSECTING SIGNALING PATHWAYS

It is relatively easy to envision a linear type of mechanism whereby the available pool of signal interacts with target proteins to regulate gene expression (Estavillo et al., 2011; Kindgren et al., 2011; Xiao et al., 2012). The other option is that one signal can target many proteins or regulate the expression of many genes involved in different pathways. Rather than a linear succession of events, this would represent an intricate network which could provide more subtle levels of regulation under different and specific conditions (Leister, 2012). We outline some of the approaches utilized to discover new retrograde signaling pathways and components (**Table 1**).

TRIGGERING AND MOVEMENT OF THE SIGNAL

Unlike the case of photosynthetic derived signals, it is less clear how the different triggers are sensed in most retrograde signaling pathways. For example, how is the protease mediated cleavage of PTM regulated by HL (Sun et al., 2011), or the accumulation and transport of PAP induced by drought and HL (Estavillo et al., 2011)? These are difficult questions to address as they may involve the interaction of many different signaling networks.

The movement of the signal between organelles is a key feature of a metabolite, or protein capable of conveying information into the nucleus. Passive diffusion and active transport are the two most likely scenarios depending on the type of signal. However, monitoring this movement can be technically challenging. Analytical methods for metabolic profiling, such as cell fractionation in conjunction with non-aqueous fractionation, GC/MS- and LC/MS-based, and HPLC, or confocal microscopy for specific signals can be attempted. For instance, the observation that Mg-ProtoIX can accumulate in both chloroplast and cytosol suggests that this metabolite can be exported from site of origin, which may result in the repression of photosynthetic genes under stress (Ankele et al., 2007; Zhang et al., 2011). However, such approaches may be too harsh for labile signals or may not be possible due to cross-contamination of organelles (Estavillo et al., 2011; Woodson et al., 2011).

An alternative to direct measurements of the signal is the use of genetic approaches. Genetically encoded biosensors specific for putative signals, such as those developed for sugars

Table 1 | Investigation of retrograde signaling pathways.

1. **Signal sensing**
   - Triggers for retrograde signals are not always clear
   - What are the actual "stress sensors"?
2. **Signal movement**
   - Confirmation of the movement: modulators targeted to specific compartments (Estavillo et al., 2011); genetically encoded biosensor; non-aqueous fractionation protocol coupled to MS.
   - Identification of transporters (Gigolashvili, 2012) and study of their regulation in mutant plants or under different stress conditions.
3. **Signal targets and elucidating mechanisms of action.**
   - Affinity chromatography coupled to proteomic analyses (Kindgren et al., 2011).
   - Revertant screenings (Wagner et al., 2004; Šimková et al., 2012).
   - Global changes in gene expression during fluctuating conditions (Brautigam et al., 2009; Voss et al., 2011).
   - Investigation of epigenetic control during retrograde signal (Sun et al., 2011).
4. **Elucidating cross talk between signaling pathways**
   - Comparison of global gene expression between different signaling mutants or under different triggering conditions (Schwarzländer et al., 2012)
   - Study of epistasis (i.e., multiple mutants).
5. **Developing new systems for signal discovery**.
   - Identification of new signals triggered by real physiological conditions or changing environments, like drought, light intensity and quality (Chan et al., 2010).
   - Genetic screens

Table indicating potential fields of research in retrograde signaling (1–5), and suggested approaches. Some examples are cited.

and hormones (Frommer et al., 2009), could be used to measure the dynamics of the signal movement in different compartments. In a similar approach, the levels of the signal can be manipulated by targeting "sensors," or "modulator" proteins to specific compartments and monitoring the changes in phenotypes. For example, targeting of a PAP degrading enzyme to the nucleus complements the molecular and morphological phenotype of *sal1* mutants, supporting the hypothesis that PAP moves in between organelles (Estavillo et al., 2011). Clearly, multiple lines of evidence are required to understand signal movement.

Identification of transporters that regulate the flux of the signal from the plastid into the cytosol is critical for understanding a signal transduction pathway. Although some of the proposed signals, like β-CC, could freely diffuse from the site of origin (Ramel et al., 2012), movement of others, like the highly charged PAP, or tetrapyrrole intermediates must necessitate specific transporters. There is good evidence that haem can leave intact chloroplasts (Thomas and Weinstein, 1990) and that Mg-ProtoIX can be found in the cytoplasm under stress conditions (Ankele et al., 2007). Although a couple of transport mechanisms have been proposed for Mg-ProtoIX (Moller et al., 2001; Larkin et al., 2003; Ankele et al., 2007), no chloroplast transporter has been described for haem. Very recently, co-expression analyses of genes related to glucosinolate metabolism lead to identification of PAPS transporter 1 (PAPST1), a transporter belonging to the mitochondrial carrier family that localizes to both the thylakoid, and plastid envelope (Gigolashvili, 2012). PAPST1 can transport ADP/ATP or PAPS /ATP, or PAP in an antiport manner *in vitro*. It still remains unclear whether this transporter plays any role in the PAP signaling pathway, especially during abiotic stress. Modulation of the transporter activity could be a major point of flux control, as also considered elsewhere (Leister, 2012).

HUNTING FOR SIGNALING MECHANISMS AND COMPONENTS

Affinity chromatography against putative signals coupled to proteomic analyses is a logical approach to dissect the components of the retrograde signaling pathways. This strategy rendered a large number of proteins associated to oxidative stress that bound to Mg-ProtoIX covalently linked gel matrix (Kindgren et al., 2011). This led to the proposal that a regulatory complex composed of HSP90 and Mg-ProtoIX could mediate gene expression (Kindgren et al., 2012). However, results can be misleading by non-specific interaction and proper controls and other additional lines of evidence are required (i.e., mutant analyses of potential targets, etc.).

Some of the retrograde mechanisms have been identified using inducible reporter genes, a common strategy for dissecting signaling pathways (Susek et al., 1993; Rossel et al., 2006; Estavillo et al., 2011). Another strategy to dissect new signaling components in order to understand mechanism of action is by performing reverse genetic screens of known signaling mutants (Šimková et al., 2012). However, the associated phenotypic screening can be misleading due to the potential pleiotropic effects of the signals. Additionally, study of co-regulated genes in a pathway can lead to the discovery of newer components (Gigolashvili, 2012).

CROSS-TALK BETWEEN PATHWAYS: LINEAR OR "ONE SIGNAL, MANY TARGETS"?

Although the general view of retrograde metabolic signals is that of the "classical" model, where one signal acts through a rather linear pathway, it is likely that a "one signal, many targets" scenario is more common than anticipated, especially when considering metabolites that could bind to proteins. For example, 60% of genes misregulated in the SAL1 mutant *alx8* mutant do not seem to be affected by XRNs (Estavillo et al., 2011). This implicates that additional PAP targets exist in plants that may be important in controlling gene expression during stress. In fact, in plants and other organisms PAP can bind to other proteins, such as SOTs (Klaassen and Boles, 1997), nucleoside diphosphate kinase (Schneider et al., 1998) and poly(ADP-ribose) polymerase 1 (Toledano et al., 2012).

There are several recent examples of some classical retrograde signals converging with other networks such as light signaling (Ruckle and Larkin, 2009), plant immune signaling (Nomura et al., 2012), transition from cell proliferation to cell expansion (Andriankaja et al., 2012), cold acclimation (Crosatti et al., 2012), and ABA signaling (Koussevitzky et al., 2007) to name a few. It would be interesting to investigate whether the newer metabolic signals interact with other pathways (such as stomata regulation) that could be modulated by ABA, which levels increase upon HL, or drought stress.

CONCLUDING REMARKS

Several new metabolite retrograde signals have been recently proposed (Estavillo et al., 2011; Ramel et al., 2012; Xiao et al., 2012). New knowledge about the mechanism of other signaling pathways has also been gained (Fischer et al., 2012; Kindgren et al., 2012; Maruta et al., 2012; Šimková et al., 2012). Yet, none of the pathways are complete and for some transport or movement has yet to be demonstrated. Consequently, signal sensing and modulation is an important area of research. Additional efforts in analytical techniques for signal quantification and movement are critical for assessing the true "signal" nature of a metabolite. The fact that two new signaling pathways involve post-transcriptional regulation (Estavillo et al., 2011) and histone modifications (Sun et al., 2011) open an unexplored area for research: are there other cases of chloroplast-to-nucleus regulation where these types of gene regulation occur? The combination of deep sequencing technologies with the traditional reporter gene screen and multiple mutant approaches (including revertants) can give a more detailed picture of specific and overlapping networks for gene regulation. Finally, the development of new experimental conditions (i.e., controlled drought, finer manipulation of light quality and intensity) and technologies (i.e., biosensors, phenomics, revertant screening, and proteomics) will be instrumental in the discovery of new, true signaling components.

ACKNOWLEDGMENTS

This work was funded by the Australian Research Council Centre of Excellence in Plant Energy of Biology (CE0561495), an ARC Linkage Grant (LP110200257), an Australian Commonwealth International Postgraduate Research Scholarship for Kai Xun Chan, and an the Australian National University PhD Merit Scholarship for Su Yin Phua.

REFERENCES

Andriankaja, M., Dhondt, S., De bodt, S., Vanhaeren, H., Coppens, F., De milde, L., et al. (2012). Exit from proliferation during leaf development in *Arabidopsis thaliana*: a not-so-gradual process. *Dev. Cell* 22, 64–78.

Ankele, E., Kindgren, P., Pesquet, E., and Strand, A. (2007). *In vivo* visualization of Mg-protoporphyrinIX, a coordinator of photosynthetic gene expression in the nucleus and the chloroplast. *Plant Cell* 19, 1964–1979.

Apel, K., and Hirt, H. (2004). Reactive oxygen species: metabolism, oxidative stress, and signal transduction. *Annu. Rev. Plant Biol.* 55, 373–399.

Barajas-López, J. D. D., Blanco, N. E., and Strand, Å. (2012). Plastid-to-nucleus communication, signals controlling the running of the plant cell. *Biochim. Biophys. Acta.* doi: 10.1016/j.bbamcr.2012.06.020. [Epub ahead of print].

Bradbeer, J. W., Atkinson, Y. E., Borner, T., and Hagemann, R. (1979). Cytoplasmic synthesis of plastid polypeptides may be controlled by plastid-synthesized Rna. *Nature* 279, 816–817.

Brautigam, K., Dietzel, L., Kleine, T., Stroher, E., Wormuth, D., Dietz, K. J., et al. (2009). Dynamic plastid redox signals integrate gene expression and metabolism to induce distinct metabolic states in photosynthetic acclimation in Arabidopsis. *Plant Cell* 21, 2715–2732.

Chan, K. X., Crisp, P. A., Estavillo, G. M., and Pogson, B. J. (2010). Chloroplast-to-nucleus communication: current knowledge, experimental strategies and relationship to drought stress signaling. *Plant Signal. Behav.* 5, 1–8.

Chen, H., Zhang, B., Hicks, L. M., and Xiong, L. (2011). A nucleotide metabolite controls stress-responsive gene expression and plant development. *PLoS ONE* 6:e26661. doi: 10.1371/journal.pone.0026661

Crosatti, C., Rizza, F., Badeck, F. W., Mazzucotelli, E., and Cattivelli, L. (2012). Harden the chloroplast to protect the plant. *Physiol. Plant.* 147, 55–63.

De La Paz Sanchez, M., and Gutierrez, C. (2009). Arabidopsis ORC1 is a PHD-containing H3K4me3 effector that regulates transcription. *Proc. Natl. Acad. Sci. U.S.A.* 106, 2065–2070.

Delwiche, C. F. (1999). Tracing the thread of plastid diversity through the tapestry of life. *Am. Nat.* 154, S164–S177.

Dichtl, B., Stevens, A., and Tollervey, D. (1997). Lithium toxicity in yeast is due to the inhibition of RNA processing enzymes. *EMBO J.* 16, 7184–7195.

Espinas, N. A., Kobayashi, K., Takahashi, S., Mochizuki, N., and Masuda, T. (2012). Evaluation of unbound free heme in plant cells by differential acetone extraction. *Plant Cell Physiol.* 53, 1344–1354.

Estavillo, G. M., Crisp, P. A., Pornsiriwong, W., Wirtz, M., Collinge, D., Carrie, C., et al. (2011). Evidence for a SAL1-PAP chloroplast retrograde pathway that functions in drought and high light signaling in Arabidopsis. *Plant Cell* 23, 3992–4012.

Fey, V., Wagner, R., Brautigam, K., Wirtz, M., Hell, R., Dietzmann, A., et al. (2005). Retrograde plastid redox signals in the expression of nuclear genes for chloroplast proteins of *Arabidopsis thaliana*. *J. Biol. Chem.* 280, 5318–5328.

Fischer, B. B., Ledford, H. K., Wakao, S., Huang, S. G., Casero, D., Pellegrini, M., et al. (2012). SINGLET OXYGEN RESISTANT 1 links reactive electrophile signaling to singlet oxygen acclimation in *Chlamydomonas reinhardtii*. *Proc. Natl. Acad. Sci. U.S.A.* 109, E1302–E1311.

Foudree, A., Aluru, M., and Rodermel, S. (2010). PDS activity acts as a rheostat of retrograde signaling during early chloroplast biogenesis. *Plant Signal. Behav.* 5, 1629–1632.

Frommer, W. B., Davidson, M. W., and Campbell, R. E. (2009). Genetically encoded biosensors based on engineered fluorescent proteins. *Chem. Soc. Rev.* 38, 2833–2841.

Gadjieva, R., Axelsson, E., Olsson, U., and Hansson, M. (2005). Analysis of gun phenotype in barley magnesium chelatase and Mg-protoporphyrin IX monomethyl ester cyclase mutants. *Plant Physiol. Biochem.* 43, 901–908.

Galvez-Valdivieso, G., and Mullineaux, P. M. (2010). The role of reactive oxygen species in signalling from chloroplasts to the nucleus. *Physiol. Plant.* 138, 430–439.

Gigolashvili, T. (2012). Much more than a thylakoid ADP/ATP carrier–enlightening a role of TAAC in plastidic phosphoadenosine 50-phosphosulfate (PAPS) supply to the cytosol. *Plant Cell* 21, 1813.

Goksoyr, J. (1967). Evolution of eucaryotic cells. *Nature* 214, 1161.

González-Pérez, S., Gutiérrez, J., García-García, F., Osuna, D., Dopazo, J., Lorenzo, Ó., et al. (2011). Early transcriptional defense responses in Arabidopsis cell suspension culture under high-light conditions. *Plant Physiol.* 156, 1439–1456.

Grabowski, E., Miao, Y., Mulisch, M., and Krupinska, K. (2008). Single-stranded DNA-binding protein Whirly1 in barley leaves is located in plastids and the nucleus of the same cell. *Plant Physiol.* 147, 1800–1804.

Gray, J. C. (2003). Chloroplast-to-nucleus signalling: a role for Mg-protoporphyrin. *Trends Genet.* 19, 526–529.

Grieshaber, N. A., Sager, J. B., Dooley, C. A., Hayes, S. F., and Hackstadt, T. (2006). Regulation of the *Chlamydia trachomatis* histone H1-Like protein Hc2 is IspE dependent and IhtA independent. *J. Bacteriol.* 188, 5289–5292.

Gy, I., Gasciolli, V., Lauressergues, D., Morel, J.-B., Gombert, J., Proux, F., et al. (2007). Arabidopsis FIERY1, XRN2, and XRN3 are endogenous RNA silencing suppressors. *Plant Cell* 19, 3451–3461.

Hon, T., Lee, H. C., Hach, A., Johnson, J. L., Craig, E. A., Erdjument-Bromage, H., et al. (2001). The Hsp70-Ydj1 molecular chaperone represses the activity of the heme activator protein Hap1 in the absence of heme. *Mol. Cell. Biol.* 21, 7923–7932.

Isemer, R., Mulisch, M., Schäfer, A., Kirchner, S., Koop, H.-U., and Krupinska, K. (2012). Recombinant Whirly1 translocates from transplastomic chloroplasts to the nucleus. *FEBS Lett.* 586, 85–88.

Kakizaki, T., Matsumura, H., Nakayama, K., Che, F.-S., Terauchi, R., and Inaba, T. (2009). Coordination of plastid protein import and nuclear gene expression by plastid-to-nucleus retrograde signaling. *Plant Physiol.* 151, 1339–1353.

Kastenmayer, J. P., and Green, P. J. (2000). Novel features of the XRN-family in Arabidopsis: evidence that AtXRN4, one of several orthologs of nuclear Xrn2p/Rat1p, functions in the cytoplasm. *Proc. Natl. Acad. Sci. U.S.A.* 97, 13985–13990.

Kindgren, P., Eriksson, M.-J., Benedict, C., Mohapatra, A., Gough, S. P., Hansson, M., et al. (2011). A novel proteomic approach reveals a role for Mg-protoporphyrin IX in response to oxidative stress. *Physiol. Plant.* 141, 310–320.

Kindgren, P., Norén, L., Barajas López, J. D. D., Shaikhali, J., and Strand, Å. (2012). Interplay between Heat Shock Protein 90 and HY5 controls PhANG expression in response to the GUN5 plastid signal. *Mol. Plant* 5, 901–913.

Klaassen, C., and Boles, J. (1997). Sulfation and sulfotransferases 5: the importance of 3'- phosphoadenosine 5'-phosphosulfate (PAPS) in the regulation of sulfation. *FASEB J.* 11, 404–418.

Klein, M., and Papenbrock, J. (2004). The multi-protein family of Arabidopsis sulphotransferases and their relatives in other plant species. *J. Exp. Bot.* 55, 1809–1820.

Koussevitzky, S., Nott, A., Mockler, T. C., Hong, F., Sachetto-Martins, G., Surpin, M., et al. (2007). Signals from chloroplasts converge to regulate nuclear gene expression. *Science* 316, 715–719.

Krause, K., Oetke, S., and Krupinska, K. (2012). Dual targeting and retrograde translocation: regulators of plant nuclear gene expression can be sequestered by plastids. *Int. J. Mol. Sci.* 13, 11085–11101.

Larkin, R. M., Alonso, J. M., Ecker, J. R., and Chory, J. (2003). GUN4, a regulator of chlorophyll synthesis and intracellular signaling. *Science* 299, 902–906.

Lee, H. C., Hon, T., and Zhang, L. (2002). The molecular chaperone Hsp90 mediates heme activation of the yeast transcriptional activator Hap1. *J. Biol. Chem.* 277, 7430–7437.

Lee, J., He, K., Stolc, V., Lee, H., Figueroa, P., Gao, Y., et al. (2007). Analysis of transcription factor HY5 genomic binding sites revealed its hierarchical role in light regulation of development. *Plant Cell* 19, 731–749.

Leister, D. (2012). Retrograde signalling in plants: from simple to complex scenarios. *Front. Plant Sci.* 3:135. doi: 10.3389/fpls.2012.00135

Marechal, A., Parent, J.-S., Veronneau-Lafortune, F., Joyeux, A., Lang, B. F., and Brisson, N. (2009). Whirly proteins maintain plastid genome stability in Arabidopsis. *Proc. Natl. Acad. Sci. U.S.A.* 106, 14693–14698.

Martin, W., Rujan, T., Richly, E., Hansen, A., Cornelsen, S., Lins, T., et al. (2002). Evolutionary analysis of Arabidopsis, cyanobacterial, and chloroplast genomes reveals plastid phylogeny and thousands of

cyanobacterial genes in the nucleus. 99, 12246–12251.

Maruta, T., Noshi, M., Tanouchi, A., Tamoi, M., Yabuta, Y., Yoshimura, K., et al. (2012). H2O2-triggered retrograde signaling from chloroplasts to nucleus plays specific role in response to stress. *J. Biol. Chem.* 287, 11717–11729.

Melonek, J., Mulisch, M., Schmitz-Linneweber, C., Grabowski, E., Hensel, G., and Krupinska, K. (2010). Whirly1 in chloroplasts associates with intron containing RNAs and rarely co-localizes with nucleoids. *Planta* 232, 471–481.

Mochizuki, N., Brusslan, J. A., Larkin, R., Nagatani, A., and Chory, J. (2001). Arabidopsis genomes uncoupled 5 (GUN5) mutant reveals the involvement of Mg-chelatase H subunit in plastid-to-nucleus signal transduction. *Proc. Natl. Acad. Sci. U.S.A.* 98, 2053–2058.

Mochizuki, N., Tanaka, R., Tanaka, A., Masuda, T., and Nagatani, A. (2008). The steady-state level of Mg-protoporphyrin IX is not a determinant of plastid-to-nucleus signaling in Arabidopsis. *Proc. Natl. Acad. Sci. U.S.A.* 105, 15184–15189.

Moller, S. G., Kunkel, T., and Chua, N. H. (2001). A plastidic ABC protein involved in intercompartmental communication of light signaling. *Genes Dev.* 15, 90–103.

Moulin, M., McCormac, A. C., Terry, M. J., and Smith, A. G. (2008). Tetrapyrrole profiling in Arabidopsis seedlings reveals that retrograde plastid nuclear signaling is not due to Mg-protoporphyrin IX accumulation. *Proc. Natl. Acad. Sci. U.S.A.* 105, 15178–15183.

Nomura, H., Komori, T., Uemura, S., Kanda, Y., Shimotani, K., Nakai, K., et al. (2012). Chloroplast-mediated activation of plant immune signalling in Arabidopsis. *Nat. Commun.* 3:926. doi: 10.1038/ncomms1926

Nott, A., Jung, H.-S., Koussevitzky, S., and Chory, J. (2006). Plastid-to-nucleus retrograde signaling. *Annu. Rev. Plant Biol.* 57, 739–759.

Oelmuller, R., Levitan, I., Bergfeld, R., Rajasekhar, V. K., and Mohr, H. (1986). Expression of nuclear genes as affected by treatments acting on the plastids. *Planta* 168, 482–492.

op den Camp, R. G. L., Przybyla, D., Ochsenbein, C., Laloi, C., Kim, C., Danon, A., et al. (2003). Rapid induction of distinct stress responses after the release of singlet oxygen in Arabidopsis. *Plant Cell* 15, 2320–2332.

Ostrovsky, D., Diomina, G., Lysak, E., Matveeva, E., Ogrel, O., and Trutko, S. (1998). Effect of oxidative stress on the biosynthesis of 2-C-methyl-d-erythritol-2, 4-cyclopyrophosphate and isoprenoids by several bacterial strains. *Arch. Microbiol.* 171, 69–72.

Pesaresi, P., Hertle, A., Pribil, M., Kleine, T., Wagner, R., Strissel, H., et al. (2009). Arabidopsis STN7 kinase provides a link between short- and long-term photosynthetic acclimation. *Plant Cell* 21, 2402–2423.

Pfannschmidt, T. (2010). Plastidial retrograde signalling a true plastid factor or just metabolite signatures? *Trends Plant Sci.* 15, 427–435.

Pfannschmidt, T., Bräutigam, K., Wagner, R., Dietzel, L., Schröter, Y., Steiner, S., et al. (2009). Potential regulation of gene expression in photosynthetic cells by redox and energy state: approaches towards better understanding. *Ann. Bot.* 103, 599–607.

Pogson, B. J., Woo, N. S., Förster, B., and Small, I. D. (2008). Plastid signalling to the nucleus and beyond. *Trends Plant Sci.* 13, 602–609.

Pontier, D., Albrieux, C., Joyard, J., Lagrange, T., and Block, M. A. (2007). Knock-out of the magnesium protoporphyrin IX methyltransferase gene in Arabidopsis. *J. Biol. Chem.* 282, 2297–2304.

Ramel, F., Birtic, S., Ginies, C., Soubigou-Taconnat, L., Triantaphylidès, C., and Havaux, M. (2012). Carotenoid oxidation products are stress signals that mediate gene responses to singlet oxygen in plants. *Proc. Natl. Acad. Sci. U.S.A.* 109, 5535–5540.

Rodríguez-Concepción, M. (2006). Early steps in isoprenoid biosynthesis: multilevel regulation of the supply of common precursors in plant cells. *Phytochem. Rev.* 5, 1–15.

Rossel, J. B., Walter, P. B., Hendrickson, L., Chow, W. S., Poole, A., Mullineaux, P. M., et al. (2006). A mutation affecting ASCORBATE PEROXIDASE 2 gene expression reveals a link between responses to high light and drought tolerance. *Plant Cell Environ.* 29, 269–281.

Ruckle, M. E., and Larkin, R. M. (2009). Plastid signals that affect photomorphogenesis in *Arabidopsis thaliana* are dependent on GENOMES UNCOUPLED 1 and cryptochrome 1. *New Phytol.* 182, 367–379.

Schneider, B., Xu, Y. W., Janin, J., Véron, M., and Deville-Bonne, D. (1998). 3′-Phosphorylated nucleotides are tight binding inhibitors of nucleoside diphosphate kinase activity. *J. Biol. Chem.* 273, 28773–28778.

Schwarzländer, M., König, A.-C., Sweetlove, L. J., and Finkemeier, I. (2012). The impact of impaired mitochondrial function on retrograde signalling: a meta-analysis of transcriptomic responses. *J. Exp. Bot.* 63, 1735–1750.

Šimková, K., Moreau, F., Pawlak, P., Vriet, C., Baruah, A., Alexandre, C., et al. (2012). Integration of stress-related and reactive oxygen species-mediated signals by Topoisomerase VI in *Arabidopsis thaliana*. *Proc. Natl. Acad. Sci. U.S.A.* 109, 16360–16365.

Souret, F. F., Kastenmayer, J. P., and Green, P. J. (2004). AtXRN4 Degrades mRNA in Arabidopsis and its substrates include selected miRNA targets. *Mol. Cell* 15, 173–183.

Strand, A., Asami, T., Alonso, J., Ecker, J. R., and Chory, J. (2003). Chloroplast to nucleus communication triggered by accumulation of Mg-protoporphyrinIX. *Nature* 421, 79–83.

Sun, X., Feng, P., Xu, X., Guo, H., Ma, J., Chi, W., et al. (2011). A chloroplast envelope-bound PHD transcription factor mediates chloroplast signals to the nucleus. *Nat. Commun.* 2:477. doi: 10.1038/ncomms1486

Susek, R. E., Ausubel, F. M., and Chory, J. (1993). Signal transduction mutants of Arabidopsis uncouple nuclear CAB and RBCS gene expression from chloroplast development. *Cell* 74, 787–799.

Suzuki, N., Koussevitzky, S., Mittler, R. O. N., and Miller, G. (2012). ROS and redox signalling in the response of plants to abiotic stress. *Plant Cell Environ.* 35, 259–270.

Thomas, J., and Weinstein, J. D. (1990). Measurement of heme efflux and heme content in isolated developing chloroplasts. *Plant Physiol.* 94, 1414–1423.

Toledano, E., Ogryzko, V., Danchin, A., Ladant, D., and Mechold, U. (2012). 3′-5′ phosphoadenosine phosphate is an inhibitor of PARP-1 and a potential mediator of the lithium-dependent inhibition of PARP-1 *in vivo*. *Biochem. J.* 443, 485–490.

van Dijk, E. L., Chen, C. L., D'Aubenton-Carafa,Y.,Gourvennec, S., Kwapisz, M., Roche, V., et al. (2011). XUTs are a class of Xrn1-sensitive antisense regulatory non-coding RNA in yeast. *Nature* 475, 114–117.

von Gromoff, E. D., Alawady, A., Meinecke, L., Grimm, B., and Beck, C. F. (2008). Heme, a plastid-derived regulator of nuclear gene expression in chlamydomonas. *Plant Cell* 20, 552–567.

Voss, B., Meinecke, L., Kurz, T., Al-Babili, S., Beck, C. F., and Hess, W. R. (2011). Hemin and magnesium-protoporphyrin IX induce global changes in gene expression in *Chlamydomonas reinhardtii*. *Plant Physiol.* 155, 892–905.

Wagner, D., Przybyla, D., op den Camp, R., Kim, C., Landgraf, F., Lee, K. P., et al. (2004). The genetic basis of singlet oxygen–induced stress responses of *Arabidopsis thaliana*. *Science* 306, 1183–1185.

Wilson, K. E., Ivanov, A. G., Öquist, G., Grodzinski, B., Sarhan, F., and Huner, N. P. A. (2006). Energy balance, organellar redox status, and acclimation to environmental stress. *Can. J. Bot.* 84, 1355–1370.

Wilson, P. B., Estavillo, G. M., Field, K. J., Pornsiriwong, W., Carroll, A. J., Howell, K. A., et al. (2009). The nucleotidase/phosphatase SAL1 is a negative regulator of drought tolerance in Arabidopsis. *Plant J.* 58, 299–317.

Woodson, J. D., and Chory, J. (2008). Coordination of gene expression between organellar and nuclear genomes. *Nat. Rev. Genet.* 9, 383–395.

Woodson J. D., Perez-Ruiz J. M., and Chory, J. (2011). Heme synthesis by plastid ferrochelatase i regulates nuclear gene expression in plants. *Curr. Biol.* 21, 897–903.

Xiao, Y., Savchenko, T., Baidoo, E. E., Chehab, W. E., Hayden D. M., Tolstikov V., et al. (2012). Retrograde signaling by the plastidial metabolite MEcPP regulates expression of nuclear stress-response genes. *Cell* 149, 1525–1535.

Zhang, L., and Hach, A. (1999). Molecular mechanism of heme signaling in yeast: the transcriptional activator Hap1 serves as the key

mediator. *Cell. Mol. Life Sci.* 56, 415–426.

Zhang, N.-H., Zhao, Y., Liang, H.-G., Sun, J.-Y., and Du, L.-F. (2012). A new *gun* mutant of oilseed rape with a reduced porphyrin flux through Mg-chelatase. *Acta Physiol. Plant.* doi: 10.1007/s11738-012-1049-0

Zhang, Z.-W., Yuan, S., Feng, H., Xu, F., Cheng, J., Shang, J., et al. (2011). Transient accumulation of Mg-protoporphyrin IX regulates expression of PhANGs– New evidence for the signaling role of tetrapyrroles in mature Arabidopsis plants. *J. Plant Physiol.* 168, 714–721.

Zubko, M. K., and Day, A. (1998). Stable albinism induced without mutagenesis: a model for ribosome-free plastid inheritance. *Plant J.* 15, 265–271.

Conflict of Interest Statement: The authors declare that the research was conducted in the absence of any commercial or financial relationships that could be construed as a potential conflict of interest.

Received: 30 October 2012; accepted: 12 December 2012; published online: 04 January 2013.

Citation: Estavillo GM, Chan KX, Phua SY and Pogson BJ (2013) Reconsidering the nature and mode of action of metabolite retrograde signals from the chloroplast. Front. Plant Sci. ***3****:300. doi: 10.3389/fpls.2012.00300*

This article was submitted to Frontiers in Plant Physiology, a specialty of Frontiers in Plant Science.

Copyright © 2013 Estavillo, Chan, Phua and Pogson. This is an open-access article distributed under the terms of the **Creative Commons Attribution License**, *which permits use, distribution and reproduction in other forums, provided the original authors and source are credited and subject to any copyright notices concerning any third-party graphics etc.*

frontiers in
PLANT SCIENCE

REVIEW ARTICLE
published: 27 December 2012
doi: 10.3389/fpls.2012.00292

ROS-talk – how the apoplast, the chloroplast, and the nucleus get the message through

Alexey Shapiguzov, Julia P. Vainonen, Michael Wrzaczek and Jaakko Kangasjärvi*

Division of Plant Biology, Department of Biosciences, University of Helsinki, Helsinki, Finland

Edited by:
Dario Leister, Ludwig Maximilian University of Munich, Germany

Reviewed by:
Daniel Hofius, Swedish University of Agricultural Sciences, Sweden
Markus Wirtz, Centre for Organismal Studies, Germany
Veronica G. Maurino, Heinrich-Heine-University Düsseldorf, Germany

***Correspondence:**
Jaakko Kangasjärvi, Division of Plant Biology, Department of Biosciences, University of Helsinki, Viikinkaari 1, P.O. Box 65, FIN-00014 Helsinki, Finland.
e-mail: jaakko.kangasjarvi@helsinki.fi

The production of reactive oxygen species (ROS) in different plant subcellular compartments is the hallmark of the response to many stress stimuli and developmental cues. The past two decades have seen a transition from regarding ROS as exclusively cytotoxic agents to being considered as reactive compounds which participate in elaborate signaling networks connecting various aspects of plant life. We have now arrived at a stage where it has become increasingly difficult to disregard the communication between different types and pools of ROS. Production of ROS in the extracellular space, the apoplast, can influence their generation in the chloroplast and both can regulate nuclear gene expression. In spite of existing information on these signaling events, we can still barely grasp the mechanisms of ROS signaling and communication between the organelles. In this review, we summarize evidence that supports the mutual influence of extracellular and chloroplastic ROS production on nuclear gene regulation and how this interaction might occur. We also reflect on how, and *via* which routes signals might reach the nucleus where they are ultimately integrated for transcriptional reprogramming. New ideas and approaches will be needed in the future to address the pressing questions of how ROS as signaling molecules can participate in the coordination of stress adaptation and development and how they are involved in the chatter of the organelles.

Keywords: ROS signaling, apoplast, chloroplasts, retrograde signaling, *Arabidopsis thaliana*

INTRODUCTION

During their life plants face a vast set of environmental challenges: extreme changes in ambient illumination, temperature, and humidity, differences in soil salinity, attack by pathogens and herbivores, mechanical wounding, etc. To withstand all these challenges, plants have developed a repertoire of signaling pathways that is unparalleled in its complexity among living organisms. Signaling through plant hormones (Vanstraelen and Benková, 2012), cell surface receptors (Geldner and Robatzek, 2008), and light perception by plastids and photoreceptors (Kami et al., 2010) are integrated in the cell to eventually reprogram gene expression and metabolism and shape strategic decisions on plant stress response and development (Jaillais and Chory, 2010).

A critical role in this signal integration and decision-making is played by a class of reactive forms of the molecular oxygen, collectively referred to as reactive oxygen species (ROS; Murphy et al., 2011; Kangasjärvi et al., 2012). ROS, including singlet oxygen ($^1O_2$), superoxide ($O_2^{\bullet -}$), hydrogen peroxide (H_2O_2), and hydroxyl radical ($^{\bullet}OH$) are unavoidable by-products of aerobic metabolism (Imlay, 2003, 2008; Ogilby, 2010) which have traditionally been regarded mainly as damaging cytotoxic agents. In line with this view, life has developed a plethora of ROS scavenging systems including the low-molecular weight compounds ascorbic acid and glutathione (Foyer and Noctor, 2011) as well as different classes of antioxidant enzymes (Apel and Hirt, 2004). During the recent years, however, a new concept has emerged where ROS play important signaling roles during development and stress responses, and controlled production of ROS acts as a signal. ROS are generated in many compartments of plant cells. Whereas the "ROS landscape" of the animal cell is dominated by mitochondria as the main source of ROS (Marchi et al., 2012), the role of these organelles in ROS production in plants is more subtle (Dutilleul et al., 2003; Suzuki et al., 2012) and is not addressed in this review. Apart from mitochondria, ROS are produced in the chloroplasts, the peroxisomes, and the apoplast, as well as in less commonly known locations, the nucleus and the endoplasmic reticulum (Overmyer et al., 2003; Ashtamker et al., 2007; Foyer and Noctor, 2009; Jaspers and Kangasjärvi, 2010; Mazars et al., 2010). Yet uncharacterized signaling networks between the organelles that employ ROS as second messengers have recently raised considerable interest (**Figure 1**). For example, ROS that are produced in the chloroplast have been implicated as intermediates in retrograde signaling from chloroplast to nucleus during acclimation of photosynthesis (Nott et al., 2006; Galvez-Valdivieso and Mullineaux, 2010). Intriguingly, however, it has recently been realized that the role of this signaling goes beyond optimization of photosynthesis: chloroplastic ROS production and photosynthetic functions are also regulated by cues that are perceived in the cell wall, frequently referred to as the extracellular space or the apoplast (Padmanabhan and Dinesh-Kumar, 2010). Thus, the *sensu stricto* retrograde signaling (from chloroplast to nucleus) can also be regarded as a part of a larger network where apoplastic signals induce the generation of ROS in the chloroplast, which in turn leads to regulation of nuclear gene expression by several still uncharacterized, but at least partially chloroplast-derived, ROS-dependent retrograde signals.

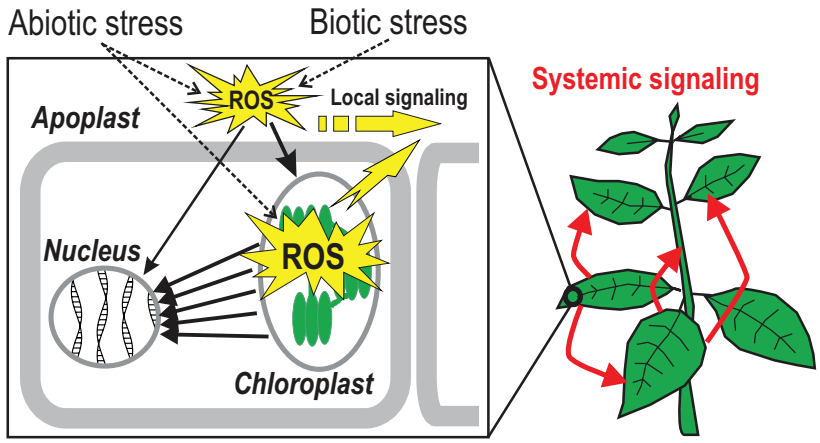

FIGURE 1 | Reactive oxygen species (ROS)-talk in plant cells. Biotic and abiotic stimuli lead to the generation of ROS in the apoplast which is subsequently communicated to the inside of the cell where the signal leads to an increase in chloroplastic ROS production. The chloroplast can further amplify the signal and transmit it to the nucleus *via* various cytosolic signaling networks. Apoplastic ROS signaling can also reach the nucleus through cytosolic pathways directly. Yellow arrows demonstrate intracellular transmission of apoplastic and chloroplastic ROS-induced signals where they connect neighboring cells (local signaling) or participate in long-distance ("systemic") signaling throughout the plant (red arrows).

ROS IN THE APOPLAST

Likely candidates involved in the apoplast-to-chloroplast signaling are ROS produced in the cell wall. Their accumulation in response to different abiotic and biotic stimuli during the so-called apoplastic "oxidative burst" depends on several classes of enzymes, including cell wall peroxidases (Bindschedler et al., 2006) and plasma membrane NADPH oxidases (**Figure 2**; Torres et al., 2002; Suzuki et al., 2011). The latter enzymes, commonly known as respiratory burst oxidase homologs (Rboh) are transmembrane flavoproteins that oxidize cytoplasmic NADPH, translocate electrons across plasma membrane and reduce extracellular ambient (triplet) oxygen to yield $O_2^{\bullet-}$ in the cell wall. Due to its charge, this short-lived ROS is unable to passively cross the lipid bilayer and remains in the apoplast, where it is rapidly converted into another species, H_2O_2, either spontaneously or in a reaction catalyzed by the superoxide dismutase (SOD; Browning et al., 2012). The functions of plant NADPH oxidases stretch beyond stress responses and include roles in development (Sagi and Fluhr, 2006; Takeda et al., 2008), in sodium transport in the xylem sap (Jiang et al., 2012), and intriguingly also in long-distance ("systemic") ROS signaling (Miller et al., 2009). In Arabidopsis wounding, heat stress, high light, and increased salinity result in RbohD-dependent systemic spread of the oxidative burst along the rosette leaves. The signal is triggered by intracellular Ca^{2+} spiking at the wounding site. It is propelled by accumulation of ROS in the apoplast and by – still unidentified – symplastic signals, one of which might be ROS production in chloroplasts: results by Joo et al. (2005) suggest that chloroplastic ROS is required for intercellular ROS signaling. This ROS "wave" travels across an Arabidopsis rosette at a rate of approximately 8 cm per minute (Miller et al., 2009). Taken together, the currently available data suggests different roles for ROS in strictly localized signaling events but also in systemic signaling.

We have obtained a good understanding of the processes in which apoplastic ROS are involved, but how they are perceived by plant cells remains unclear. It is not known how the signal is transmitted to the cytoplasm, the chloroplasts and eventually the nucleus and what are the interactions between the different subcellular compartments. The possibility of $O_2^{\bullet-}$ itself being the mediator of downstream signaling would require superoxide-specific extracellular receptors or anion channels in the direct vicinity to the site of $O_2^{\bullet-}$ production (Browning et al., 2012). Anion channels have been shown to mediate superoxide import in mammalian cells (Hawkins et al., 2007) thereby linking extracellular and intracellular ROS signaling. Analogous systems in plants have so far not been identified. Unlike superoxide, the H_2O_2 molecule is relatively stable (with a half-life of ~1 ms) under physiological conditions and in many respects resembles a molecule of water. Its dipole moment, similar to that of H_2O, limits passive diffusion of H_2O_2 through biological membranes. Possible candidates for the import of apoplastic H_2O_2 are aquaporins (**Figure 2**), a ubiquitous family of channel proteins that has undergone an extensive expansion in vascular plants (Zardoya, 2005; Soto et al., 2012). Recent studies have identified several aquaporins as specific H_2O_2 transporters in Arabidopsis (Bienert et al., 2007; Dynowski et al., 2008; Hooijmaijers et al., 2012). However, further research is required to assess the role of H_2O_2 transport during the oxidative burst. In addition to transport across membranes, $O_2^{\bullet-}$ and H_2O_2 may be sensed by a number of apoplastic compounds. Oxidation of extracellular pools of glutathione and ascorbic acid might play a role in transmitting the redox signal to the cytosol (Destro et al., 2011; Foyer and Noctor, 2011; Noctor et al., 2012). ROS can also be perceived by the apoplastic proteins and/or plasma membrane-localized receptors through redox modification of their cysteine residues (**Figure 2**). Those putative receptors or other sensory systems for extracellular ROS in plants have so far remained elusive, but for example, several classes of receptor-like protein kinases (RLKs) with cysteine-rich extracellular domains (most notably the CYSTEINE-RICH RLKs, CRKs) have been suggested to be

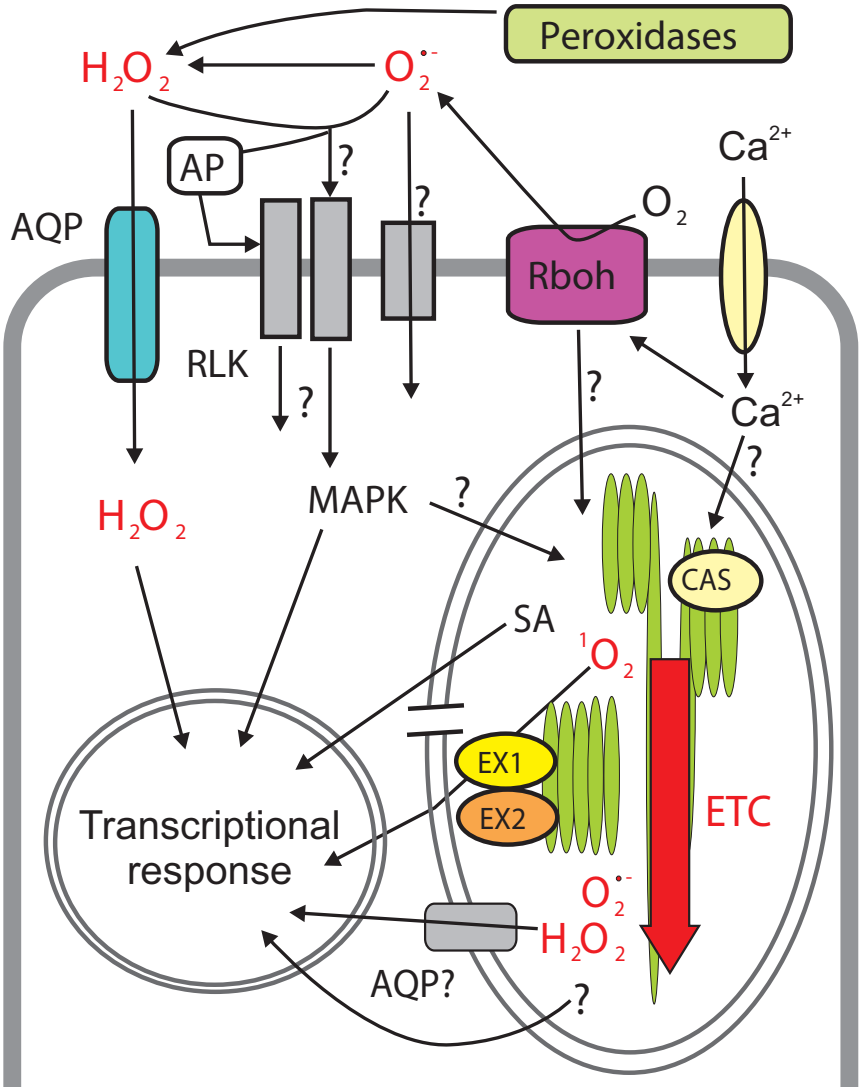

FIGURE 2 | Reactive oxygen species (ROS) signaling networks connecting apoplast, chloroplast and nucleus. Apoplastic ROS are produced by extracellular peroxidases (hydrogen peroxide; H_2O_2) and plasma membrane-bound NADPH oxidases, Rboh. Superoxide ($O_2^{\bullet-}$) is then converted to H_2O_2. H_2O_2 (and possibly $O_2^{\bullet-}$) might enter the cell through plasma membrane channels (aquaporins, AQP) and/or react with extracellular (apoplastic protein, AP) or transmembrane sensor proteins (e.g., receptor-like kinases, RLKs) ultimately resulting in changes in gene expression through intracellular signaling pathways, involving, for example, MAPKs (mitogen-activated protein kinases). Extracellular ROS production is sensed *via* yet unknown mechanisms in the chloroplast where ROS generation by the electron transfer chain (ETC) subsequently increases. Singlet oxygen ($^1O_2$) and $O_2^{\bullet-}/H_2O_2$ are produced in different domains of ETC. Elevated ROS inside the chloroplast results in transcriptional reprogramming through identified (e.g., EXECUTER1/2, EX1/EX2, rupture of chloroplast envelope) and unknown components of the retrograde signaling but also through hormone signaling, e.g., increased production of the stress hormone salicylic acid (SA). Channel proteins (AQP) might also allow ROS leak from the chloroplast to the cytoplasm. Calcium (Ca^{2+}) is involved in the regulation of ROS production in the apoplast and the chloroplast. In the latter case it acts through the sensory protein CALCIUM-SENSING RECEPTOR (CAS) but the mechanisms are still unclear.

involved in ROS perception (Shiu and Bleecker, 2003; Wrzaczek et al., 2010).

FROM BEYOND TO HERE, SIGNALS FROM THE EXTRACELLULAR SPACE

What happens in the plant cell after an extracellular oxidative burst has been triggered? A connection of apoplastic and chloroplastic ROS into common signaling networks during the plant stress response is evident in various model systems and processes (Joo et al., 2005; Vahisalu et al., 2010), although it is mechanistically still largely unexplained. The results suggest that the apoplastic ROS signal is transduced to the chloroplasts, where a secondary ROS production is initiated. This signal transmission might use cytosolic signaling components. Also, the location of chloroplasts close to the plasma membrane might facilitate direct communication between the two organelles. Thus, the chloroplast can act as

an "amplifier," or "execute" the signal received from the apoplast (**Figure 1**).

One of the examples of such a role of chloroplasts is the plant immune response to pathogens that is accompanied by a bi-phasic accumulation of ROS. The first phase occurs within tens of minutes from the onset of infection. It is mostly apoplastic and is tightly linked to NADPH oxidase activity (**Figure 2**). The second increase in ROS production happens several hours after the pathogen attack (Lamb and Dixon, 1997; Jones and Dangl, 2006). During this stage of response the infected cells might undergo programmed cell death (PCD) leading to the collapse of the infected tissue and, in the case of biotrophic pathogens, to suppression of pathogen growth. This specialized form of pathogen-triggered PCD is a part of the hypersensitive response (HR). Different subcellular compartments including apoplast, chloroplasts, mitochondria, and peroxisomes contribute to ROS production during HR, but a growing amount of evidence suggests a crucial role for the chloroplast in this process (Yao and Greenberg, 2006; Liu et al., 2007; Zurbriggen et al., 2009, 2010). Silencing of the chloroplast redox proteins peroxiredoxin and NADPH-dependent thioredoxin reductase C that scavenge chloroplastic H_2O_2 led to spreading PCD in response to application of coronatine, a phytotoxin with structural similarity to jasmonic acid produced by several pathogenic strains of *Pseudomonas* (Ishiga et al., 2012). The involvement of chloroplasts in plant immunity is further supported by the observation that the pathogen resistance of plants differs between light and dark (Roden and Ingle, 2009) and by the fact that several bacterial and viral elicitors interact with chloroplast-targeted proteins or are imported into chloroplasts (Padmanabhan and Dinesh-Kumar, 2010). Thus, not only the apoplast and the cytosol, but also the chloroplasts are strategic battlefields during the defense against pathogens (Padmanabhan and Dinesh-Kumar, 2010).

Chloroplast-generated ROS are not only involved in initiating and promoting cell death during the HR, but also in the up-regulation of defense-related genes, down-regulation of photosynthesis genes and even in limiting the spread of the cell death (Straus et al., 2010). For example, a significant portion of the genes induced by artificial metabolic overproduction of H_2O_2 *via* expression of glyoxylate oxidase in the chloroplasts (Balazadeh et al., 2012), are also induced by chitin, a well-known elicitor of the apoplastic oxidative burst and downstream pathogen defense responses. Similarly, silencing of thylakoid ascorbate peroxidase (tAPX) led to an increase in H_2O_2 production and to activation of defense responses (Maruta et al., 2012), including the accumulation of the stress hormone salicylic acid (SA), a central mediator of plant pathogen defense. These examples underline that H_2O_2 accumulation in the chloroplast and the related retrograde signaling are involved in the activation of defense genes during responses to pathogens.

CHLOROPLASTS AS THE PET PEEVE OF THE PLANT CELL

Why does the plant cell involve the chloroplast, the major site of energy production and biosynthesis in stress responses? One explanation is that photosynthesizing chloroplasts continuously produce ROS due to numerous electron transfer reactions in the presence of oxygen (Foyer and Noctor, 2003; Asada, 2006). Hence, in the photosynthesizing plant tissues chloroplasts are able to produce the most massive pools of ROS among different subcellular compartments.

Generation of ROS in the chloroplasts depends on multiple aspects of chloroplast physiology including photosynthesis, gene expression, chlorophyll (tetrapyrrole) biosynthesis, and hormonal control (Asada, 2006; Sierla et al., 2012). For example, the production of $O_2^{\bullet-}/H_2O_2$ by photosystem I (PS I) varies according to changing photosynthetic electron transfer and CO_2 fixation rate. Extracellular stimuli, such as recognition of bacterial components by the plasma membrane receptors, can rapidly regulate chloroplastic functions. During plant–pathogen interactions the cues perceived in the apoplast trigger MAPK cascades (**Figure 2**) and result in fast down-regulation of photosynthetic genes and accumulation of H_2O_2 in chloroplasts that is necessary for initiation of HR-mediated cell death (Liu et al., 2007). Another example is the transient decrease in the ability of PS II to dissipate excessive light energy as heat *via* non-photochemical quenching (NPQ) at an early stage of pathogen recognition. This decrease in NPQ makes chloroplasts more predisposed to the production of ROS, which might be a priming mechanism for chloroplast ROS signaling at later stages of immune response (Göhre et al., 2012). Several chloroplastic redox hubs, including the plastoquinone as well as the glutathione pools and the thioredoxin system, provide not only dynamic local regulation of photosynthesis, but also might communicate the chloroplast redox status to the cytosol (Marty et al., 2009; Bashandy et al., 2010; Foyer and Noctor, 2011; Noctor et al., 2012; Rochaix, 2012). For example, the redox state of plastoquinone, a component of photosynthetic electron transfer chain, is monitored through the thylakoid-associated protein kinase STATE TRANSITION 7 (STN7). STN7-dependent phosphorylation of chloroplast proteins leads on the one hand to optimization of photosynthesis in response to changing light conditions (*via* the reversible reallocation of light-harvesting antennae called state transitions) and on the other hand to a retrograde signal (Bonardi et al., 2005; Rochaix, 2012). Another chloroplast protein kinase, CHLOROPLAST SENSOR KINASE (CSK), couples plastoquinone redox state to the regulation of chloroplast gene expression (Puthiyaveetil et al., 2012). The *soldat8* mutation in the chloroplastic RNA polymerase *SIGMA SUBUNIT 6* (*SIG6*) gene increases the tolerance of seedlings to $^1O_2$ (Coll et al., 2009), which links chloroplast transcriptional control to the ROS signaling. The RNA-binding chloroplast protein GENOMES UNCOUPLED 1 (GUN1) is implicated both in chloroplast translation and tetrapyrrole biosynthesis and is somehow involved in retrograde signaling (Czarnecki et al., 2011; Woodson et al., 2012). GUN1, and one of the key components of tetrapyrrole biosynthesis, the ChlH subunit of magnesium chelatase, are also involved in abscisic acid signaling (Shen et al., 2006; Koussevitzky et al., 2007; Cutler et al., 2010; Shang et al., 2010). The heme, the product of a side branch of tetrapyrrole biosynthesis, exits chloroplasts to be used as a cofactor by numerous hemoproteins in the cell and to provide positive feedback on transcription of nuclear genes that encode chlorophyll-binding proteins of chloroplasts (Nott et al., 2006; Woodson et al., 2011, 2012; Czarnecki and Grimm, 2012). The disturbance of the cell affects the delicate physiological equilibrium of the chloroplasts resulting in elevated ROS production.

CHLOROPLASTIC ROS AS SIGNALS

Plant cells have over the course of evolution learned to use chloroplastic ROS for signaling purposes. Several studies have demonstrated a central role for the highly reactive singlet oxygen ($^1O_2$) as a chloroplastic signal involved in the regulation of plant cell death. PS II and its light-harvesting antennae produce $^1O_2$ when light-excited chlorophylls adopt the rare triplet state and then reduce triplet oxygen (Krieger-Liszkay et al., 2008). Production of $^1O_2$ is enhanced when the light-excited electrons cannot escape PS II chlorophylls because the downstream components of electron transfer chain (mainly the plastoquinone pool) are already over-reduced, a situation typical of excessive illumination. $^1O_2$ readily reacts with lipids, proteins, and pigments and is rapidly quenched by water, which makes its diffusion distance from the site of production shortest among all ROS (Asada, 2006). For that reason $^1O_2$ is unlikely to leave the chloroplasts, but several products of $^1O_2$-dependent lipid or carotenoid oxidation, including oxylipins (op den Camp et al., 2003; Przybyla et al., 2008) and volatile β-cyclocitral (Ramel et al., 2012), are suspected to act as the $^1O_2$-dependent retrograde signal.

The Arabidopsis *flu* mutant (Meskauskiene et al., 2001) has been used as a genetic tool to identify $^1O_2$-responsive genes and to dissect signaling pathways triggered by $^1O_2$ production in chloroplasts. The chloroplast-localized FLU protein inhibits one of the early enzymes of tetrapyrrole biosynthesis. *Flu* seedlings are unable to control the biosynthetic pathway through negative feedback and accumulate the chlorophyll precursor protochlorophyllide in the dark. Being transferred to light, the seedlings bleach and die due to the massive generation of $^1O_2$ in their chloroplasts. This death is primarily caused by a profound reprogramming of nuclear transcription rather than by mere chemical toxicity of $^1O_2$ (op den Camp et al., 2003). In addition, shortly after the exposure of *flu* seedlings to light, their chloroplasts rupture releasing the soluble stroma into the cytosol – this resembles the leakage of mitochondrial proteins to the cytosol during the mitochondria-triggered PCD. Two homologous chloroplast proteins EXECUTER1 and EXECUTER2 (**Figure 2**) conserved in higher plants are involved in this process, although their exact role is unknown (Wagner et al., 2004; Lee et al., 2007; Kim et al., 2012). It should be noted that although $^1O_2$-dependent PCD is significantly exacerbated in *flu*, it is not confined to the mutant but is also observed in wild-type Arabidopsis under severe light stress (Kim et al., 2012). The sensory and signaling systems involved in the transmission of the chloroplastic $^1O_2$-dependent signal to nucleus have not been identified, but it has been suggested that nuclear topoisomerase VI could act as an integrator of $^1O_2$-dependent signal in regulating nuclear gene expression (Šimková et al., 2012).

Apart from triggering PCD, the transcriptional reprogramming of *flu* induces many genes of stress response and leads to rapid accumulation of SA, inducing a defense pathway characteristic of plant reaction to pathogens or wounding (Ochsenbein et al., 2006; Lee et al., 2007). One of the mechanisms triggering this pathway exploits the calcium-sensing protein CAS localized to chloroplast thylakoids (**Figure 2**). Regulation of CAS activity is linked to the state of photosynthetic electron transfer chain. CAS has earlier been shown to be involved in high light acclimation of the green alga *Chlamydomonas reinhardtii* (Petroutsos et al., 2011) and it is phosphorylated by the thylakoid protein kinase STN8 (Vainonen et al., 2008), a paralog of STN7, which suggests a link between the CAS activity and the redox state of the plastoquinone pool. However, CAS is not only involved in light-dependent retrograde signaling: also various abiotic or biotic stress stimuli activate CAS through a yet unknown mechanism. This activation leads to reallocation of Ca^{2+} ions within the chloroplast and to accumulation of $^1O_2$, which, in turn, initiates defense responses through an unidentified retrograde signal (Nomura et al., 2012). Thus, CAS appears to act in the $^1O_2$-dependent retrograde signaling pathway discussed above.

Another source of ROS in chloroplasts is PS I. Its electron-donor side generates $O_2^{\bullet-}$ that is scavenged by chloroplast SOD to form H_2O_2 (Asada, 2006). H_2O_2, in turn, is reduced to water by a number of enzymes including ascorbate peroxidase (APX), peroxiredoxin, and glutathione peroxidase. H_2O_2 produced in chloroplasts gives rise to retrograde signals. The signaling is not well understood and might be a combination of passive diffusion of H_2O_2 with indirect pathways including hormonal (abscisic acid) signaling (Mullineaux and Karpinski, 2002; Galvez-Valdivieso and Mullineaux, 2010). The possibility of H_2O_2 leakage from chloroplasts is supported by the fact that a knockout of cytosolic APX1 leads to hypersensitivity of the photosynthetic apparatus to light stress (Davletova et al., 2005). Diffusion of H_2O_2 from chloroplasts has also been demonstrated *in vitro* (Mubarakshina et al., 2010). Aquaporins in the chloroplast envelope (**Figure 2**) seem to be involved in this H_2O_2 leakage (Borisova et al., 2012), but how the aquaporins are regulated is unknown. In any case, H_2O_2 itself is not likely to be the retrograde signaling substance that directly affects nuclear gene expression. More probably, it is sensed by compartment-specific redox-sensitive components, which mediate the signal to the nucleus (Sierla et al., 2012). Oxidized proteins or peptides have been suggested as one of the possible downstream mediators of such H_2O_2 signaling (Wrzaczek et al., 2009; Møller and Sweetlove, 2010).

THE FRUSTRATING COMPLEXITY OF ROS RESPONSES

One of the most frequently employed tools to investigate the role of $O_2^{\bullet-}$ in the chloroplast is the herbicide methyl viologen (MV; also known as paraquat). MV accelerates the production of $O_2^{\bullet-}$ by PS I and inhibits APX, leading to the accumulation of H_2O_2 in MV-treated plants (Mano et al., 2001). Comparison of the transcriptional responses to $^1O_2$ and H_2O_2 using the *flu* mutant and the plants treated with MV demonstrated the specific and to a large extent antagonistic effect of these two chloroplastic ROS on gene expression (op den Camp et al., 2003; Gadjev et al., 2006; Laloi et al., 2007). Interestingly, the transcriptional response to apoplastic H_2O_2 produced during oxidative burst has little similarity to the effect of either chloroplastic $O_2^{\bullet-}$/H_2O_2 or chloroplastic $^1O_2$ (Gadjev et al., 2006; Miller et al., 2009; Petrov et al., 2012; Sierla et al., 2012). This illustrates a remarkable specificity of cellular responses to different types and subcellular sources of ROS production. This also demonstrates the complexity of ROS signaling and raises the question of the mechanisms responsible for such specificity.

Clustering results of microarray experiments involving ROS production in different subcellular compartments reveals distinct

temporal signatures. For example, the gene expression profiles 4 h after elicitation with flg22 (a 22-amino acid fragment of the bacterial flagellar protein flagellin, which induces an apoplastic oxidative burst *via* the activation of NADPH oxidase) have similarities to the profiles induced by ozone, while 12 h after flg22 treatment the expression profile resembled that of chloroplastic ROS production induced by MV (Sierla et al., 2012). Ozone triggers generation of ROS in the apoplast, which leads to subsequent chloroplastic ROS production and transcriptional up-regulation of 25 (out of 44) Arabidopsis *CRK* genes, but the activation profile of these genes differs from that induced by high light (Wrzaczek et al., 2010). Thus, both temporal and spatial aspects appear to be involved in determining the specificity of ROS. In addition, the outcome is most likely dictated by the specific combinations of ROS ($O_2^{\bullet -}$, H_2O_2, or $^1O_2$). It is unlikely that, for example, merely a change in the cytoplasmic redox state could carry the information about the subcellular source of H_2O_2. Therefore, as proposed (Møller and Sweetlove, 2010), the signal transduction would require specific and distinct sensory systems for the different ROS in diverse subcellular compartments.

The involvement of chloroplasts in plant systemic signaling has also started to emerge recently (Joo et al., 2005; Szechyñska-Hebda et al., 2010). Excessive illumination of Arabidopsis rosettes resulted in the propagation of an electric signal as measured by changes in plasma membrane potential of bundle sheath cells of leaf central veins. The signal was systemic, i.e., it also spread over the shaded leaves of the entire rosette. It correlated with transients of H_2O_2 concentration and was altered in the mutant deficient in cytosolic APX2. Besides, the signal was deregulated by the inhibitors of photosynthetic electron transfer and blocked by a Ca^{2+} channel inhibitor. These observations suggest that information on light conditions perceived by the chloroplast photosynthetic apparatus is communicated to the cell, most likely through ROS production, and then propagated along the plant in a Ca^{2+}-channel dependent way (Szechyñska-Hebda et al., 2010). The possible integration of this pathway with a systemic NADPH oxidase-dependent signal (Miller et al., 2009) is the subject of further research.

The high focused localization of ROS signaling events raises the issue of organelle spatial organization inside the cell. Stromules, the transient protrusions of organellar surfaces that are known to be induced by stress, could be one of the mediators of this focused organellar cross-talk (Leister, 2012). Besides, all organelles move and dynamically associate with each other, and the role of this movement in stress response starts to be recognized (Suzuki et al., 2012). For example, the bacterial elicitor harpin leads to HR accompanied by redistribution of mesophyll cell chloroplasts in tobacco (Boccara et al., 2007). During the last 15 years the laws of organellar movement have started to be revealed, but the consequences of dynamic physical proximity and contact between the organelles are unknown (Suetsugu et al., 2010; Sakai and Haga, 2012). Recent studies demonstrate impairment of stress reactions in the Arabidopsis mutants which are unable to move chloroplasts in response to light stimuli or to dock them to the plasma membrane (Schmidt von Braun and Schleiff, 2008; Goh et al., 2009; Oliver et al., 2009; Lehmann et al., 2011).

CONCLUDING REMARKS

Research performed over the last two decades has made it clear that ROS signaling connects events that take place in very different subcellular locations, most importantly (but not limited to) the apoplast, the chloroplast, and the nucleus. To achieve the elaborate and fine-tuned responses to biotic and abiotic stimuli that we observe on transcriptional, biochemical, and physiological level, intense and strictly controlled communication between the subcellular "crime scenes" must take place. While some components of this information exchange have been proposed, we still lack a thorough understanding on how the apoplast, the chloroplast, and the nucleus keep in touch. It will be perhaps one of the major challenges of ROS research in plants to understand ROS-induced signaling pathways between different organelles. Once we find out which components transmit information under specific conditions, we will be able to generate an integrated view of ROS signaling and its role in environmental adaptation.

ACKNOWLEDGMENTS

Research in the Plant Stress group of Professor Jaakko Kangasjärvi is supported by Biocentrum Helsinki, the Academy of Finland, the University of Helsinki, and the ERA-PG.

REFERENCES

Apel, K., and Hirt, H. (2004). Reactive oxygen species: metabolism, oxidative stress, and signal transduction. *Annu. Rev. Plant Biol.* 55, 373–399.

Asada, K. (2006). Production and scavenging of reactive oxygen species in chloroplasts and their functions. *Plant Physiol.* 141, 391–396.

Ashtamker, C., Kiss, V., Sagi, M., Davydov, O., and Fluhr, R. (2007). Diverse subcellular locations of cryptogein-induced reactive oxygen species production in tobacco Bright Yellow-2 cells. *Plant Physiol.* 143, 1817–1826.

Balazadeh, S., Jaspert, N., Arif, M., Mueller-Roeber, B. and Maurino, V. G. (2012). Expression of ROS-responsive genes and transcription factors after metabolic formation of H_2O_2 in chloroplasts. *Front. Plant Sci.* 3:234. doi: 10.3389/fpls.2012.00234

Bashandy, T., Guilleminot, J., Vernoux, T., Caparros-Ruiz, D., Ljung, K., Meyer, Y., et al. (2010). Interplay between the NADP-linked thioredoxin and glutathione systems in *Arabidopsis* auxin signaling. *Plant Cell* 22, 376–391.

Bienert, G. P., Møller, A. L., Kristiansen, K. A., Schulz, A., Møller, I. M., Schjoerring, J. K., et al. (2007). Specific aquaporins facilitate the diffusion of hydrogen peroxide across membranes. *J. Biol. Chem.* 282, 1183–1192.

Bindschedler, L. V., Dewdney, J., Blee, K. A., Stone, J. M., Asai, T., Plotnikov, J., et al. (2006). Peroxidase-dependent apoplastic oxidative burst in Arabidopsis required for pathogen resistance. *Plant J.* 47, 851–863.

Boccara, M., Schwartz, W., Guiot, E., Vidal, G., De Paepe, R., Dubois, A., et al. (2007). Early chloroplastic alterations analysed by optical coherence tomography during a harpin-induced hypersensitive response. *Plant J.* 50, 338–346.

Bonardi, V., Pesaresi, P., Becker, T., Schleiff, E., Wagner, R., Pfannschmidt, T., et al. (2005). Photosystem II core phosphorylation and photosynthetic acclimation require two different protein kinases. *Nature* 437, 1179–1182.

Borisova, M. M., Kozuleva, M. A., Rudenko, N. N., Naydov, I. A., Klenina, I. B., and Ivanov, B. N. (2012). Photosynthetic electron flow to oxygen and diffusion of hydrogen peroxide through the chloroplast envelope via aquaporins. *Biochim. Biophys. Acta* 1817, 1314–1321.

Browning, E. A., Chatterjee, S., and Fisher, A. B. (2012). Stop the flow: a paradigm for cell signaling mediated by reactive oxygen species in the pulmonary endothelium. *Annu. Rev. Physiol.* 74, 403–424.

Coll, N. S., Danon, A., Meurer, J., Cho, W. K., and Apel, K. (2009). Characterization of *soldat8*, a suppressor of singlet oxygen-induced cell death in *Arabidopsis* seedlings. *Plant Cell Physiol.* 50, 707–718.

Cutler, S. R., Rodriguez, P. L., Finkelstein, R. R., and Abrams, S. R. (2010). Abscisic acid: emergence of a core signaling network. *Annu. Rev. Plant Biol.* 61, 651–679.

Czarnecki, O., and Grimm, B. (2012). Post-translational control of tetrapyrrole biosynthesis in plants, algae, and cyanobacteria. *J. Exp. Bot.* 63, 1675–1687.

Czarnecki, O., Hedtke, B., Melzer, M., Rothbart, M., Richter, A., Schröter, Y., et al. (2011). An *Arabidopsis* GluTR binding protein mediates spatial separation of 5-aminolevulinic acid synthesis in chloroplasts. *Plant Cell* 23, 4476–4491.

Davletova, S., Rizhsky, L., Liang, H., Shengqiang, Z., Oliver, D. J., Coutu, J., et al. (2005). Cytosolic ascorbate peroxidase 1 is a central component of the reactive oxygen gene network of Arabidopsis. *Plant Cell* 17, 268–281.

Destro, T., Prasad, D., Martignago, D., Bernet, I. L., Trentin, A. R., Renu, I. K., et al. (2011). Compensatory expression and substrate inducibility of γ-glutamyl transferase GGT2 isoform in *Arabidopsis thaliana*. *J. Exp. Bot.* 62, 805–814.

Dutilleul, C., Garmier, M., Noctor, G., Mathieu, C. D., Chétrit, P., Foyer, C. H., et al. (2003). Leaf mitochondria modulate whole cell redox homeostasis, set antioxidant capacity, and determine stress resistance throughaltered signaling and diurnal regulation. *Plant Cell* 15, 1212–1226.

Dynowski, M., Schaaf, G., Loque, D., Moran, O., and Ludewig, U. (2008). Plant plasma membrane water channels conduct the signalling molecule H_2O_2. *Biochem. J.* 414, 53–61.

Foyer, C. H., and Noctor, G. (2003). Redox sensing and signalling associated with reactive oxygen in chloroplasts, peroxisomes and mitochondria. *Physiol. Plant* 119, 355–364.

Foyer, C. H., and Noctor, G. (2009). Redox regulation in photosynthetic organisms: signaling, acclimation, and practical implications. *Antioxid. Redox Signal.* 11, 861–905.

Foyer, C. H., and Noctor, G. (2011). Ascorbate and glutathione: the heart of the redox hub. *Plant Physiol.* 155, 2–18.

Gadjev, I., Vanderauwera, S., Gechev, T. S., Laloi, C., Minkov, I. N., Shulaev, V., et al. (2006). Transcriptomic footprints disclose specificity of reactive oxygen species signaling in Arabidopsis. *Plant Physiol.* 141, 436–445.

Galvez-Valdivieso, G., and Mullineaux, P. M. (2010). The role of reactive oxygen species in signalling from chloroplasts to the nucleus. *Physiol. Plant* 138, 430–439.

Geldner, N., and Robatzek, S. (2008). Plant receptors go endosomal: a moving view on signal transduction. *Plant Physiol.* 147, 1565–1574.

Goh, C. H., Jang, S., Jung, S., Kim, H. S., Kang, H. G., Park, Y. I., et al. (2009). Rice *phot1a* mutation reduces plant growth by affecting photosynthetic responses to light during early seedling growth. *Plant Mol. Biol.* 69, 605–619.

Göhre, V., Jones, A. M., Sklenáø, J., Robatzek, S., and Weber, A. P. (2012). Molecular crosstalk between PAMP-triggered immunity and photosynthesis. *Mol. Plant Microbe Interact.* 25, 1083–1092.

Hawkins, B. J., Madesh, M., Kirkpatrick, C. J., and Fisher, A. B. (2007). Superoxide flux in endothelial cells via the chloride channel-3 mediates intracellular signaling. *Mol. Biol. Cell* 18, 2002–2012.

Hooijmaijers, C., Rhee, J. Y., Kwak, K. J., Chung, G. C., Horie, T., Katsuhara, M., et al. (2012). Hydrogen peroxide permeability of plasma membrane aquaporins of *Arabidopsis thaliana*. *J. Plant Res.* 125, 147–153.

Imlay, J. A. (2003). Pathways of oxidative damage. *Annu. Rev. Microbiol.* 57, 395–418.

Imlay, J. A. (2008). Cellular defenses against superoxide and hydrogen peroxide. *Annu. Rev. Biochem.* 77, 755–776.

Ishiga, Y., Ishiga, T., Wangdi, T., Mysore, K. S., and Uppalapati, S. R. (2012). NTRC and chloroplast-generated reactive oxygen species regulate *Pseudomonas syringae* pv. *tomato* disease development in tomato and *Arabidopsis*. *Mol. Plant Microbe Interact.* 25, 294–306.

Jaillais, Y., and Chory, J. (2010). Unraveling the paradoxes of plant hormone signaling integration. *Nat. Struct. Mol. Biol.* 17, 642–645.

Jaspers, P., and Kangasjärvi, J. (2010). Reactive oxygen species in abiotic stress signaling. *Physiol. Plant* 138, 405–413.

Jiang, C., Belfield, E. J., Mithani, A., Visscher, A., Ragoussis, J., Mott, R., et al. (2012). ROS-mediated vascular homeostatic control of root-to-shoot soil Na delivery in Arabidopsis. *EMBO J.* 31, 4359–4370.

Jones, J. D. G., and Dangl, J. L. (2006). The plant immune system. *Nature* 444, 323–329.

Joo, J. H., Wang, S., Chen, J. G., Jones, A. M., and Fedoroff, N. V. (2005). Different signaling and cell death roles of heterotrimeric G protein α and β subunits in the Arabidopsis oxidative stress response to ozone. *Plant Cell* 17, 957–970.

Kami, C., Lorrain, S., Hornitschek, P., and Fankhauser, C. (2010). Light-regulated plant growth and development. *Curr. Top. Dev. Biol.* 91, 29–66.

Kangasjärvi, S., Neukermans, J., Li, S., Aro, E. M., and Noctor, G. (2012). Photosynthesis, photorespiration, and light signalling in defence responses. *J. Exp. Bot.* 63, 1619–1636.

Kim, C., Meskauskiene, R., Zhang, S., Lee, K. P., Lakshmanan Ashok, M., Blajecka, K., et al. (2012). Chloroplasts of *Arabidopsis* are the source and a primary target of a plant-specific programmed cell death signaling pathway. *Plant Cell* 24, 3026–3039.

Koussevitzky, S., Nott, A., Mockler, T. C., Hong, F., Sachetto-Martins, G., Surpin, M., et al. (2007). Signals from chloroplasts converge to regulate nuclear gene expression. *Science* 316, 715–719.

Krieger-Liszkay, A., Fufezan, C., and Trebst, A. (2008). Singlet oxygen production in photosystem II and related protection mechanism. *Photosynth. Res.* 98, 551–564.

Laloi, C., Stachowiak, M., Pers-Kamczyc, E., Warzych, E., Murgia, I., and Apel, K. (2007). Cross-talk between singlet oxygen- and hydrogen peroxide-dependent signaling of stress responses in *Arabidopsis thaliana*. *Proc. Natl. Acad. Sci. U.S.A.* 104, 672–677.

Lamb, C., and Dixon, R. A. (1997). The oxidative burst in plant disease resistance. *Annu. Rev. Plant Physiol. Plant Mol. Biol.* 48, 251–275.

Lee, K. P., Kim, C., Landgraf, F., and Apel, K. (2007). EXECUTER1- and EXECUTER2-dependent transfer of stress-related signals from the plastid to the nucleus of *Arabidopsis thaliana*. *Proc. Natl. Acad. Sci. U.S.A.* 104, 10270–10275.

Lehmann, P., Nöthen, J., Schmidt von Braun, S., Bohnsack, M. T., Mirus, O., and Schleiff, E. (2011). Transitions of gene expression induced by short-term blue light. *Plant Biol.* 13, 349–361.

Leister, D. (2012). Retrograde signaling in plants: from simple to complex scenarios. *Front. Plant Sci.* 3:135. doi: 10.3389/fpls.2012.00135.

Liu, Y., Ren, D., Pike, S., Pallardy, S., Gassmann, W., and Zhang, S. (2007). Chloroplast-generated reactive oxygen species are involved in hypersensitive response-like cell death mediated by a mitogen-activated protein kinase cascade. *Plant J.* 51, 941–954.

Mano, J., Ohno, C., Domae, Y., and Asada, K. (2001). Chloroplastic ascorbate peroxidase is the primary target of methylviologen-induced photooxidative stress in spinach leaves: its relevance to monodehydroascorbate radical detected with *in vivo* ESR. *Biochim. Biophys. Acta* 1504, 275–287.

Marchi, S., Giorgi, C., Suski, J. M., Agnoletto, C., Bononi, A., Bonora, M., et al. (2012). Mitochondria-ros crosstalk in the control of cell death and aging. *J. Signal Transduct.* 2012, 329635.

Marty, L., Siala, W., Schwarzländer, M., Fricker, M. D., Wirtz, M., Sweetlove, L. J., et al. (2009). The NADPH-dependent thioredoxin system constitutes a functional backup for cytosolic glutathione reductase in *Arabidopsis*. *Proc. Natl. Acad. Sci. U.S.A.* 106, 9109–9114.

Maruta, T., Noshi, M., Tanouchi, A., Tamoi, M., Yabuta, Y., Yoshimura, K., et al. (2012). H_2O_2-triggered retrograde signaling from chloroplasts to nucleus plays specific role in response to stress. *J. Biol. Chem.* 287, 11717–11729.

Mazars, C., Thuleau, P., Lamotte, O., and Bourque, S. (2010). Cross-talk between ROS and calcium in regulation of nuclear activities. *Mol. Plant* 3, 706–718.

Meskauskiene, R., Nater, M., Goslings, D., Kessler, F., op den Camp, R., and Apel, K. (2001). FLU: a negative regulator of chlorophyll biosynthesis in *Arabidopsis thaliana*. *Proc. Natl. Acad. Sci. U.S.A.* 98, 12826–12831.

Miller, G., Schlauch, K., Tam, R., Cortes, D., Torres, M. A., Shulaev, V., et al. (2009). The plant NADPH oxidase RBOHD mediates rapid systemic signaling in response to diverse stimuli. *Sci. Signal.* 2, ra45.

Mubarakshina, M. M., Ivanov, B. N., Naydov, I. A., Hillier, W., Badger, M. R., and Krieger-Liszkay, A. (2010). Production and diffusion of chloroplastic H_2O_2 and its implication to signalling. *J. Exp. Bot.* 61, 3577–3587.

Mullineaux, P., and Karpinski, S. (2002). Signal transduction in response to excess light: getting out of the chloroplast. *Curr. Opin. Plant Biol.* 5, 43–48.

Murphy, M. P., Holmgren, A., Larsson, N. G., Halliwell, B., Chang, C. J., Kalyanaraman, B., et al. (2011). Unraveling the biological roles of reactive oxygen species. *Cell Metab.* 13, 361–366.

Møller, I. M., and Sweetlove, L. J. (2010). ROS signalling – specificity

is required. *Trends Plant Sci.* 15, 370–374.

Noctor, G., Mhamdi, A., Chaouch, S., Han, Y., Neukermans, J., Marquez-Garcia, B., et al. (2012). Glutathione in plants: an integrated overview. *Plant Cell Environ.* 35, 454–484.

Nomura, H., Komori, T., Uemura, S., Kanda, Y., Shimotani, K., Nakai, K., et al. (2012). Chloroplast-mediated activation of plant immune signalling in *Arabidopsis*. *Nat. Commun.* 3, 926.

Nott, A., Jung, H. -S., Koussevitzky, S., and Chory, J. (2006). Plastid-to-nucleus retrograde signaling. *Annu. Rev. Plant Biol.* 57, 739–759.

Ochsenbein, C., Przybyla, D., Danon, A., Landgraf, F., Göbel, C., Imboden, A., et al. (2006). The role of *EDS1* (enhanced disease susceptibility) during singlet oxygen-mediated stress responses of Arabidopsis. *Plant J.* 47, 445–456.

Ogilby, P. R. (2010). Singlet oxygen: there is indeed something new under the sun. *Chem. Soc. Rev.* 39, 3181–3209.

Oliver, J. P., Castro, A., Gaggero, C., Cascón, T., Schmelz, E. A., Castresana, C., et al. (2009). *Pythium* infection activates conserved plant defense responses in mosses. *Planta* 230, 569–579.

op den Camp, R. G. L., Przybyla, D., Ochsenbein, C., Laloi, C., Kim, C. H., Danon, A., et al. (2003). Rapid induction of distinct stress responses after the release of singlet oxygen in Arabidopsis. *Plant Cell* 15, 2320–2332.

Overmyer, K., Brosché, M., and Kangasjärvi, J. (2003). Reactive oxygen species and hormonal control of cell death. *Trends Plant Sci.* 8, 335–342.

Padmanabhan, M. S., and Dinesh-Kumar, S. P. (2010). All hands on deck – the role of chloroplasts, endoplasmic reticulum, and the nucleus in driving plant innate immunity. *Mol. Plant Microbe Interact.* 23, 1368–1380.

Petroutsos, D., Busch, A., Janssen, I., Trompelt, K., Bergner, S. V., Weinl, S., et al. (2011). The chloroplast calcium sensor CAS is required for photoacclimation in *Chlamydomonas reinhardtii*. *Plant Cell* 23, 2950–2963.

Petrov, V., Vermeirssen, V., De Clercq, I., Van Breusegem, F., Minkov, I., Vandepoele, K., et al. (2012). Identification of *cis*-regulatory elements specific for different types of reactive oxygen species in *Arabidopsis thaliana*. *Gene* 499, 52–60.

Przybyla, D., Göbel, C., Imboden, A., Hamberg, M., Feussner, I., and Apel, K. (2008). Enzymatic, but not non-enzymatic, $^1O_2$-mediated peroxidation of polyunsaturated fatty acids forms part of the EXECUTER1-dependent stress response program in the *flu* mutant of *Arabidopsis thaliana*. *Plant J.* 54, 236–248.

Puthiyaveetil, S., Ibrahim, I. M., and Allen, J. F. (2012). Oxidation-reduction signalling components in regulatory pathways of state transitions and photosystem stoichiometry adjustment in chloroplasts. *Plant Cell Environ.* 35, 347–359.

Ramel, F., Birtic, S., Ginies, C., Soubigou-Taconnat, L., Triantaphylidès, C., and Havaux, M. (2012). Carotenoid oxidation products are stress signals that mediate gene responses to singlet oxygen in plants. *Proc. Natl. Acad. Sci. U.S.A.* 109, 5535–5540.

Rochaix, J.-D. (2012). Regulation of photosynthetic electron transport. *Biochim. Biophys. Acta* 180, 375–383.

Roden, L. C., and Ingle, R. A. (2009). Lights, rhythms, infection: the role of light and the circadian clock in determining the outcome of plant–pathogen interactions. *Plant Cell* 21, 2546–2552.

Sagi, M., and Fluhr, R. (2006). Production of reactive oxygen species by plant NADPH oxidases. *Plant Physiol.* 141, 336–340.

Sakai, T., and Haga, K. (2012). Molecular genetic analysis of phototropism in Arabidopsis. *Plant Cell Physiol.* 53, 1517–1534.

Schmidt von Braun, S., and Schleiff, E. (2008). The chloroplast outer membrane protein CHUP1 interacts with actin and profilin. *Planta* 227, 1151–1159.

Shang, Y., Yan, L., Liu, Z. Q., Cao, Z., Mei, C., Xin, Q., et al. (2010). The Mg-chelatase H subunit of *Arabidopsis* antagonizes a group of WRKY transcription repressors to relieve ABA-responsive genes of inhibition. *Plant Cell* 22, 1909–1935.

Shen, Y.-Y., Wang, X.-F., Wu, F.-Q., Du, S.-Y., Cao, Z., Shang, Y., et al. (2006). The Mg-chelatase H subunit is an abscisic acid receptor. *Nature* 443, 823–826.

Shiu, S. H., and Bleecker, A. B. (2003). Expansion of the receptor-like kinase/Pelle gene family and receptor-like proteins in Arabidopsis. *Plant Physiol.* 132, 530–543.

Sierla, M., Rahikainen, M., Salojärvi, J., Kangasjärvi, J. and Kangasjärvi, S. (2012). Apoplastic and chloroplastic redox signaling networks in plant stress responses. *Antioxid. Redox Signal.* doi: 10.1089/ars.2012.5016 [Epub ahead of print].

Šimková, K., Moreau, F., Pawlak, P., Vriet, C., Baruah, A., Alexandre, C., et al. (2012). Integration of stress-related and reactive oxygen species-mediated signals by Topoisomerase VI in *Arabidopsis thaliana*. *Proc. Natl. Acad. Sci. U.S.A.* 109, 16360–16365.

Soto, G., Alleva, K., Amodeo, G., Muschietti, J., and Ayub, N. D. (2012). New insight into the evolution of aquaporins from flowering plants and vertebrates: orthologous identification and functional transfer is possible. *Gene* 503, 165–176.

Straus, M. R., Rietz, S., Ver Loren van Themaat, E., Bartsch, M., and Parker, J. E. (2010). Salicylic acid antagonism of EDS1-driven cell death is important for immune and oxidative stress responses in Arabidopsis. *Plant J.* 62, 628–640.

Suetsugu, N., Dolja, V. V., and Wada, M. (2010). Why have chloroplasts developed a unique motility system? *Plant Signal. Behav.* 5, 1190–1196.

Suzuki, N., Koussevitzky, S., Mittler, R., and Miller, G. (2012). ROS and redox signalling in the response of plants to abiotic stress. *Plant Cell Environ.* 35, 259–270.

Suzuki, N., Miller, G., Morales, J., Shulaev, V., Torres, M. A., and Mittler, R. (2011). Respiratory burst oxidases: the engines of ROS signaling. *Curr. Opin. Plant Biol.* 14, 691–699.

Szechyńska-Hebda, M., Kruk, J., Górecka, M., Karpińska, B., and Karpiński, S. (2010). Evidence for light wavelength-specific photoelectrophysiological signaling and memory of excess light episodes in *Arabidopsis*. *Plant Cell* 22, 2201–2218.

Takeda, S., Gapper, C., Kaya, H., Bell, E., Kuchitsu, K., and Dolan, L. (2008). Local positive feedback regulation determines cell shape in root hair cells. *Science* 319, 1241–1244.

Torres, M. A., Dangl, J. L., and Jones, J. D. G. (2002). *Arabidopsis* gp91^{phox} homologues *AtrbohD* and *AtrbohF* are required for accumulation of reactive oxygen intermediates in the plant defense response. *Proc. Natl. Acad. Sci. U.S.A.* 99, 517–522.

Vahisalu, T., Puzõrjova, I., Brosché, M., Valk, E., Lepiku, M., Moldau, H., et al. (2010). Ozone-triggered rapid stomatal response involves the production of reactive oxygen species, and is controlled by SLAC1 and OST1. *Plant J.* 62, 442–453.

Vainonen, J. P., Sakuragi, Y., Stael, S., Tikkanen, M., Allahverdiyeva, Y., Paakkarinen, V., et al. (2008). Light regulation of CaS, a novel phosphoprotein in the thylakoid membrane of *Arabidopsis thaliana*. *FEBS J.* 275, 1767–1777.

Vanstraelen, M., and Benková, E. (2012). Hormonal interactions in the regulation of plant development. *Annu. Rev. Cell Dev. Biol.* 28, 463–487.

Wagner, D., Przybyla, D., op den Camp, R., Kim, C., Landgraf, F., Lee, K. P., et al. (2004). The genetic basis of singlet oxygen-induced stress responses of *Arabidopsis thaliana*. *Science* 306, 1183–1185.

Woodson, J. D., Perez-Ruiz, J. M., and Chory, J. (2011). Heme synthesis by plastid ferrochelatase I regulates nuclear gene expression in plants. *Curr. Biol.* 21, 897–903.

Woodson, J. D., Perez-Ruiz, J. M., Schmitz, R. J., Ecker, J. R. and Chory, J. (2012). Sigma factor mediated plastid retrograde signals control nuclear gene expression. *Plant J.* doi: 10.1111/tpj.12011 [Epub ahead of print]

Wrzaczek, M., Brosché, M., Kollist, H., and Kangasjärvi, J. (2009). *Arabidopsis* GRI is involved in the regulation of cell death induced by extracellular ROS. *Proc. Natl. Acad. Sci. U.S.A.* 106, 5412–5417.

Wrzaczek, M., Brosché, M., Salojärvi, J., Kangasjärvi, S., Idänheimo, N., Mersmann, S., et al. (2010). Transcriptional regulation of the CRK/DUF26 group of Receptor-like protein kinases by ozone and plant hormones in Arabidopsis. *BMC Plant Biol.* 10:95. doi: 10.1186/1471-2229-10-95.

Yao, N., and Greenberg, J. T. (2006). Arabidopsis ACCELERATED CELL DEATH2 modulates programmed cell death. *Plant Cell* 18, 397–411.

Zardoya, R. (2005). Phylogeny and evolution of the major intrinsic protein family. *Biol. Cell* 97, 397–414.

Zurbriggen, M. D., Carrillo, N., and Hajirezaei, M. R. (2010). ROS signaling in the hypersensitive response: when, where and what for? *Plant Signal. Behav.* 5, 393–396.

Zurbriggen, M. D., Carrillo, N., Tognetti, V. B., Melzer, M., Peisker, M., Hause, B., et al. (2009). Chloroplast-generated reactive oxygen species play a major role in localized cell death during the non-host interaction between tobacco and *Xanthomonas campestris* pv. *vesicatoria*. *Plant J.* 60, 962–973.

Conflict of Interest Statement: The authors declare that the research was conducted in the absence of any commercial or financial relationships that could be construed as a potential conflict of interest.

Received: 19 October 2012; accepted: 07 December 2012; published online: 27 December 2012.

Citation: Shapiguzov A, Vainonen JP, Wrzaczek M and Kangasjärvi J (2012) ROS-talk – how the apoplast, the chloroplast, and the nucleus get the message through. Front. Plant Sci. ***3****:292. doi: 10.3389/fpls.2012.00292*
This article was submitted to Frontiers in Plant Physiology, a specialty of Frontiers in Plant Science.

Copyright © 2012 Shapiguzov, Vainonen, Wrzaczek and Kangasjärvi. This is an open-access article distributed under the terms of the Creative Commons Attribution License, which permits use, distribution and reproduction in other forums, provided the original authors and source are credited and subject to any copyright notices concerning any third-party graphics etc.

frontiers in
PLANT SCIENCE

ORIGINAL RESEARCH ARTICLE
published: 31 December 2012
doi: 10.3389/fpls.2012.00295

Intracellular signaling by diffusion: can waves of hydrogen peroxide transmit intracellular information in plant cells?

Christian Lyngby Vestergaard*[1], *Henrik Flyvbjerg*[1] and *Ian Max Møller*[2]

[1] Department of Micro- and Nanotechnology, Technical University of Denmark, Kongens Lyngby, Denmark
[2] Department of Molecular Biology and Genetics, Science and Technology, Aarhus University, Slagelse, Denmark

Edited by:
Tatjana Kleine, Ludwig-Maximilians-Universität München, Germany

Reviewed by:
Eva Hideg, University of Pecs, Hungary
Ronny Straube, Max Planck Institute for Dynamics of Complex Technical Systems, Germany

***Correspondence:**
Ian Max Møller, Department of Molecular Biology and Genetics, Science and Technology, Aarhus University, Forsøgsvej 1, DK-4200 Slagelse, Denmark.
e-mail: ian.max.moller@agrsci.dk

Amplitude- and frequency-modulated waves of Ca^{2+} ions transmit information inside cells. Reactive Oxygen Species (ROS), specifically hydrogen peroxide, have been proposed to have a similar role in plant cells. We consider the feasibility of such an intracellular communication system in view of the physical and biochemical conditions in plant cells. As model system, we use a H_2O_2 signal originating at the plasma membrane (PM) and spreading through the cytosol. We consider two maximally simple types of signals, isolated pulses and harmonic oscillations. First we consider the basic limits on such signals as regards signal origin, frequency, amplitude, and distance. Then we establish the impact of ROS-removing enzymes on the ability of H_2O_2 to transmit signals. Finally, we consider to what extent cytoplasmic streaming distorts signals. This modeling allows us to predict the conditions under which diffusion-mediated signaling is possible. We show that purely diffusive transmission of intracellular information by H_2O_2 over a distance of 1 μm (typical distance between organelles, which may function as relay stations) is possible at frequencies well above 1 Hz, which is the highest frequency observed experimentally. This allows both frequency and amplitude modulation of the signal. Signaling over a distance of 10 μm (typical distance between the PM and the nucleus) may be possible, but requires high signal amplitudes or, equivalently, a very low detection threshold. Furthermore, at this longer distance a high rate of enzymatic degradation is required to make signaling at frequencies above 0.1 Hz possible. In either case, cytoplasmic streaming does not seriously disturb signals. We conclude that although purely diffusion-mediated signaling without relaying stations is theoretically possible, it is unlikely to work in practice, since it requires a much faster enzymatic degradation and a much lower cellular background concentration of H_2O_2 than observed experimentally.

Keywords: diffusion, hydrogen peroxide, modeling, intracellular signaling, waves

INTRODUCTION

It has long been clear that hydrogen peroxide is involved in signaling in plant cells, and a variety of mechanisms have been proposed for the information transmission (Neill et al., 2002). In a meta-analysis of gene expression induced by a range of localized stress in *Arabidopsis* leaves, Gadjev et al. (2006) showed that all, or almost all, localized stress treatments activated a large group of genes, which they named *general oxidative stress response markers*. However, each treatment regulated a unique group of genes, indicating that origin-specific signals were transmitted within the cell. This demonstrates a fundamental signaling phenomenon, which could be operating in any organs, in any cell type in response to any environmental condition.

We have proposed that oxidized peptides are better suited for transmitting specific information to the nucleus than hydrogen peroxide, the most likely signaling molecule in the Reactive Oxygen Species (ROS) family (Møller and Sweetlove, 2010). In that analysis, we concluded that the combination of cytoplasmic streaming and hydrogen peroxide degradation would make signaling via waves of hydrogen peroxide difficult, but the conclusion was not based on any mathematical modeling. More recently, Mittler et al. (2011) proposed that "the ROS signal itself carries within it a decoded (Note: the authors must have meant "encoded" here) message, much like calcium signals that have specific oscillation patterns within defined cellular locations. The specific features of the signal (amplitude, frequency, and/or localization) could then be perceived and decoded by specialized mechanisms to trigger specific gene expression patterns."

We here consider to what extent intracellular hydrogen peroxide signaling via diffusion is possible, given the physical and biochemical conditions in the cytosol of plant cells. The proposed mechanism is similar to signaling in plant cells by calcium ions, where typically an external stimulus – an invading organism or a nearby cell – causes an influx of calcium ions across the plasma membrane (PM). These calcium ions diffuse through the cytosol to cause the release of calcium ions – either directly or indirectly via inositol triphosphate – from intracellular stores, typically the endoplasmic reticulum, which therefore acts as a relay station to maintain/amplify the signal. When release at the PM ceases, possibly via a negative feedback effect of the calcium ions, recovery

occurs as calcium ions are pumped out of the cell or into intracellular stores. The calcium ion signal is received and decoded, e.g., by transcription factors, to change gene expression (Berridge, 1993; Parekh, 2011).

Here the cytoplasm (cytosol plus organelles) acts as an excitable medium, a non-linear dynamical system, and has the capacity to propagate a pulse, while it cannot support the passing of another pulse until it has had time to recover (known as the refractory time). The amplitude and propagation speed of the pulse is affected by the buffering capacity of the cytosol and molecular crowding (Jafri and Keizer, 1995; Dargan and Parker, 2003; Falcke, 2003; Mironova and Mironov, 2008).

When plant cells, e.g., detect an invading organism at the cell wall, one of a cell's first responses is the recruitment of NADPH oxidase to the PM adjacent to the invasion site and the initiation of superoxide formation and ultimately hydrogen peroxide formation immediately outside the PM. The hydrogen peroxide can enter the cell via aquaporins in the PM (Bienert et al., 2007) and the cell *could* produce an amplitude- and/or frequency-modulated signal by synchronized modulation of the opening state of the aquaporin molecules in a membrane patch via phosphorylation/dephosphorylation (Maurel et al., 2009). We here address the *propagation* of such a signal, without which such a signal would make no sense.

We note that the presence of relaying stations in the cytosol is a prerequisite for calcium-mediated signaling in animal cells. We further note that no such relaying stations for H_2O_2 have been found in plant cells. We consequently consider how a diffusion-mediated signal propagates from the PM across the cytosol to the nucleus in a plant cell in the *absence* of relaying stations, and we investigate whether and when the signal can be delivered to the nucleus by diffusion alone.

We break the problem into its constituent parts and analyze it by starting with the simplest possible model, adding parts (and thus complexity) one at a time.

METHODS – THEORY AND MODELING

This section contains derivations of the theoretical description of diffusion-mediated signaling on which the results presented in Section "Results" are based. A list of the symbols used in the modeling is presented in **Table 1**.

THE DIFFUSION EQUATION

The dynamics of the concentration c of a species of diffusing molecules is described by the diffusion equation

$$\frac{\partial c}{\partial t}(\mathbf{r}, t) = D\nabla^2 c(\mathbf{r}, t), \tag{1}$$

where $\mathbf{r} = (x, y, z)$ denotes the position in space, t parameterizes time, and ∇^2 is the Laplace operator,

$$\nabla^2 = \frac{\partial^2}{\partial x^2} + \frac{\partial^2}{\partial y^2} + \frac{\partial^2}{\partial z^2}. \tag{2}$$

INSTANTANEOUS POINT-LIKE EMITTER, THE FUNDAMENTAL SOLUTION

Consider a point-like emitter which emits an instantaneous pulse of n_0 molecules at time $t = 0$. The concentration that is measured at a given distance $r = \sqrt{x^2 + y^2 + z^2}$ from the point of emission after a time t has elapsed, is then

$$G(\mathbf{r}, t) = \frac{n_0}{(4\pi Dt)^{\frac{3}{2}}} e^{-\frac{r^2}{4Dt}}, \tag{3}$$

which is the *fundamental solution* (http://en.wikipedia.org/wiki/Fundamental_solution, 2012-11-25) of the diffusion equation (Eq. 1).

EMISSION FROM A SINGLE CHANNEL IN A FLAT MEMBRANE

We next consider a single water channel in an infinite, flat impermeable membrane. We refer to this geometry as the *open geometry*. An aquaporin is less than 10 nm wide and is therefore effectively point-size compared to the distances over which the signal is transmitted (1–10 μm). We assume that the channel lets an instantaneous pulse of n_0 molecules cross the membrane. The geometry is the same as above except for the membrane, which restricts the molecules to one half of space. The concentration in that half is hence twice that given in Eq. 3,

$$c_0(\mathbf{r}, t) = \frac{2n_0}{(4\pi Dt)^{\frac{3}{2}}} e^{-\frac{r^2}{4Dt}}. \tag{4}$$

Equation 4 is the fundamental solution of the diffusion equation in the open geometry with its closed boundary condition at the membrane at $x = 0$,

$$\frac{\partial c_0\left((0, y, z), t\right)}{\partial x} = 0. \tag{5}$$

SYNCHRONIZED EMISSION FROM ALL CHANNELS IN AN AREA ON THE MEMBRANE

Now assume that channels are distributed evenly over the cell membrane. We denote by ρ_a the surface density of these channels. If in an area of size $a \times a$ all of these emit simultaneously, then the emitted signal can be found by adding up the concentrations from all emitters in that area, using c_0 for each emitter. That is, we find the concentration as the convolution of the fundamental solution (Eq. 4) with the constant density profile over the emission area.

$$c(\mathbf{r}, t) = \int_{-\frac{a}{2}}^{\frac{a}{2}} \int_{-\frac{a}{2}}^{\frac{a}{2}} \frac{2n_0\rho_a}{(4\pi Dt)^{\frac{3}{2}}} e^{-\frac{x^2+(y-y')^2+(z-z')^2}{4Dt}} dy'\, dz'. \tag{6}$$

At a point on the x-axis a distance x from the membrane – i.e., on the normal through the center $[(y, z) = (0, 0)]$ of the area containing channels (**Figure 1A**) – the measured concentration after emission is thus

$$c(x, t) = \frac{N_0}{\sqrt{\pi Dt}} e^{-\frac{x^2}{4Dt}} \operatorname{erf}\left(\frac{a}{4\sqrt{Dt}}\right)^2, \tag{7}$$

where $N_0 = \rho_a n_0$ and erf denotes the *error function*,

$$\operatorname{erf}(x) = \frac{2}{\sqrt{\pi}} \int_0^x e^{-s^2} ds. \tag{8}$$

Table 1 | List of symbols used in the mathematical modeling.

Parameter	Explanation	Parameter	Explanation
D	Diffusion coefficient	Δt	Time-interval during which the emitters (aquaporins) in the membrane stay open during the emission of a short pulse
∇^2	Laplace operator, $\nabla^2 = \frac{\partial^2}{\partial x^2} + \frac{\partial^2}{\partial y^2} + \frac{\partial^2}{\partial z^2}$	t_D	Characteristic diffusion time
$\mathbf{r}$	Vector describing the coordinates of a point in 3D space relative to the center of the source	$c_{\max}$	Peak concentration of the signal measured at the target
x	Distance from the source along the direction perpendicular to the cell membrane on which the source is located	c_{trough}	Maximal concentration at which a consecutive signal can be detected after emission of an initial signal
t	Time after emission of a signal	α	Ratio between c_{trough} and $c_{\max}$. Defined here to be either 1/10 or 1/100
G	Fundamental solution to the diffusion equation	$t_{\max}$	Time after emission at which the peak concentration is achieved
n_0	Amount of H_2O_2 molecules emitted by a single channel during a single pulse	t_{ref}	Refraction time. Defined as the point in time when the concentration reaches c_{trough}
ρ_a	Density of emitters (aquaporins) in the area on the membrane which constitutes the source	f	Frequency of signal emission
a	Linear dimension of the source (area $= a \times a$)	$V_{\max}$	Maximal enzymatic degradation rate
L	Length of the cell (in the closed geometry)	K_{m}	Michaelis constant
erf	The error function, $erf(x) = \frac{2}{\sqrt{\Pi}} \int_0^x e^{-s^2} ds$	v	Flow speed in a cytoplasmic stream
erfc	The complementary error function, $\text{erfc}(x) = 1 - \text{erf}(x)$	d	Width of a cytoplasmic stream
j_0	Amplitude of the flux over the membrane	Pe	Péclet number, which quantifies the relative importance of a flow compared to diffusion, $\text{Pe} = vd/D$

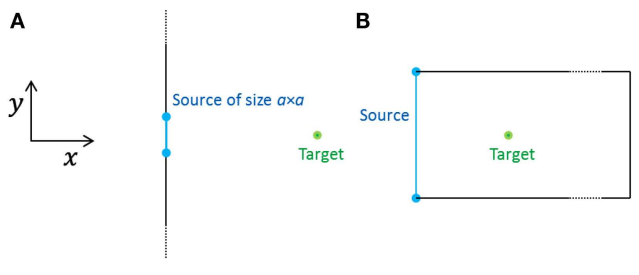

FIGURE 1 | Geometries of the two models considered, seen from above (the *z*-direction points out of the plane). (A) Open geometry: a square source emits into an infinite half-space. The target is situated at a distance x from the center of the source. **(B)** Closed geometry: the source fills the whole end-wall of a cell and the target is situated at a distance x from the center of the end-wall. All the cell walls are closed boundaries.

Note that when we are far enough away from the source (approximately when x is larger than a), the signal looks the same no matter what the source looks like; the forms of signals from different emission areas are very similar, the only difference is the scale, which is determined by the total number of molecules emitted. The same similarity of signals occurs even close to the emission area at late times, when the initial shapes of all signals have disappeared by diffusion and all signals are described by Eq. 4 (albeit with different amplitudes). This also means that the specific shape of the emission area is not important. Signals emitted from a square, circular, or differently shaped areas all look alike as long as the dimensions of the areas are roughly the same.

OPEN AND CLOSED GEOMETRIES

For simplicity, we have assumed above that the dimensions of the cell are much larger than a, the linear extent of the area emitting the signal, i.e., the cell is effectively infinitely large (**Figure 1A**). We refer to this case as the *open geometry*, because most of the cell membrane is absent, effectively, being too far away to matter in the diffusive dynamics of concentrations of signaling molecules. In the Results section, **Figures 3–7** present results for this geometry.

We shall see below that for the signal to be detectable at the target ($\sim$10 μm from the source), the area of emission must be of the same order ($\sim$10 μm $\times$ 10 μm) as the dimension of an epidermal cell ($\sim$10 μm $\times$ 20 μm $\times$ 100 μm). In an extreme example, the whole end-wall (10 μm $\times$ 20 μm) of the cell emits a synchronized signal and the cell walls act as closed (reflecting) boundaries (**Figure 1B**). Because of the closed boundary conditions the concentration inside the cell does not depend on the y- and z-coordinates and this geometry is mathematically equivalent to a point source emitting in one dimension. Then the concentration measured at time t after emission only depends on the distance in the x-direction from the source and on the length L of the cell, e.g., $L = 100$ μm. It is calculated using the *method of images* (Griffiths,

1999) and is

$$c(x,t) = \sum_{m=-\infty}^{\infty} \frac{N_0}{\sqrt{\pi D t}} e^{-\frac{(x-2mL)^2}{4Dt}}. \quad (9)$$

In the Section "Results," **Figures 8–12** present results from such a closed system. Note that while the sum in Eq. 9 in principle is infinite, only a few terms with values of m near 0 contribute in practice.

REFRACTORY TIME

The refractory time t_{ref} is the time it takes, after detection of a pulse signal, for the concentration in a given point to drop to a sufficiently low value to allow detection of a new pulse signal. We define this threshold concentration to be some fraction α of the peak concentration $c_{\max}$ attained at that point in consequence of an emitted signal, the *trough/peak ratio*. This peak concentration occurs at $t_{\max}$ by definition of this time. In the simplest possible case of the point source, this time is equal to the diffusion time, defined as $t_D = x^2/(6D)$ in three dimensions. In the simple case of an open geometry, one arrives at the same result, approximately, in cases where the target is further from the source than the size of the emission area. This approximation improves with distance from the source. In a closed geometry, $t_{\max}$ is approximately equal to $x^2/(2D)$, which is the diffusion time in one dimension. In general $t_{\max}$ must be found numerically.

The refractory time is found as the solution to the equation

$$c(x, t_{ref}) = \alpha c(x, t_{\max}), \quad (10)$$

and is

$$t_{ref} = -\frac{t_D}{W\left(-\frac{\alpha^{\frac{2}{3}}}{e}\right)} \quad (11)$$

in the simple cases of a point source as well as for an open geometry resembling a point source. Here W is the *Lambert-W function*, defined implicitly by $W(x)e^{W}(x) = x$.

SHORT PULSE SIGNAL

An instantaneous pulse is a mathematical abstraction, which is easy to work with, but which does not exist in reality, since an instantaneous emission of a signal of some amplitude N_0 would imply an infinite flux over the membrane. Instead, the channels stay open for a duration Δt during which a flux j_0 passes through, giving a total signal amplitude of $N_0 = j_0 \Delta t$. In the geometry described by Eq. 7, we cannot solve the diffusion equation analytically, and we must solve the diffusion equation (Eq. 1) numerically. This is done using *Comsol Multiphysics*, a finite element solver for physics and engineering applications.

However, for short times after emission, in the closed geometry or close to the source in the open geometry (i.e., in a point located at a distance from the source which is much smaller than the spatial extent of the source), the system is mathematically equivalent to that of a point source emitting in one dimension. Furthermore, at long times or far from the source in the open geometry, the system is equivalent to that of a point source emitter in three dimensions. Both these cases can be solved analytically. In the 1D case, for times $t \leq \Delta t$, the solution is

$$c_{t\leq\Delta t}(x,t) = \frac{j_0}{D}\left[\sqrt{\frac{4Dt}{\pi}} e^{-\frac{x^2}{4Dt}} - x \operatorname{erfc}\left(\frac{x}{\sqrt{4Dt}}\right)\right] \quad (12)$$

where erfc is the *complementary error function*, $\operatorname{erfc} = 1 - \operatorname{erf}$. For $t > \Delta t$, the solution is

$$c_{t>\Delta t}(x,t) = c_{t\leq\Delta t}(x,t) - c_{t\leq\Delta t}(x, t-\Delta t). \quad (13)$$

In the 3D case, the concentration measured at a distance x from the source along a line perpendicular to the membrane is for $t \leq \Delta t$,

$$c_{t\leq\Delta t}(x,t) = \frac{j_0}{2\pi D x} \operatorname{erfc}\left(\frac{x}{\sqrt{4Dt}}\right), \quad (14)$$

and for $t > \Delta t$,

$$c_{t>\Delta t}(x,t) = c_{t\leq\Delta t}(x,t) - c_{t\leq\Delta t}(x, t-\Delta t). \quad (15)$$

Figure 3 illustrates these analytical results. As long as Δt is approximately equal to or shorter than the characteristic diffusion time of an instantaneous pulse, the signal does not differ significantly from that of an instantaneous pulse. We refer to a signal of this type as a *short pulse signal*.

IS THE FLUX OVER THE MEMBRANE CONSTANT?

As far as we know, H_2O_2 is mainly transported over the membrane by aquaporins. These are passive channels, so the concentration inside the membrane cannot exceed the concentration c_{out} outside the membrane. Furthermore, if the concentration inside the membrane approaches the outside concentration, the flux will diminish.

The maximal concentration on the inside of the membrane is found at time Δt and is (from Eq. 12)

$$c(0, \Delta t) = j_0 \sqrt{\frac{4\Delta t}{D\pi}}. \quad (16)$$

This means that j_0 must be much smaller than $\sqrt{\pi D/4\Delta t}\, c_{\text{out}}$, or equivalently $\Delta t \ll \frac{\pi D c_{\text{out}}^2}{4 j_0^2}$ for the flux to stay constant during the time that the channels are open.

DEGRADATION OF H_2O_2

Hydrogen peroxide is degraded by enzymes inside the cell. We assume Michaelis–Menten kinetics. Then the evolution of the concentration is described by the reaction-diffusion equation

$$\frac{\partial c}{\partial t}(\mathbf{r},t) = -\frac{V_{\max} c(\mathbf{r},t)}{K_{\text{m}} + c(\mathbf{r},t)} + D\nabla^2 c(\mathbf{r},t). \quad (17)$$

The reaction-diffusion equation is non-linear, and no known analytical solution exists. We solve the equation numerically using *Comsol*.

HARMONICALLY OSCILLATING SIGNAL

We also consider a harmonically oscillating signal in the closed geometry, that is, a harmonically oscillating flux over the end membrane ($x = 0$) of the cell. This is described mathematically by the boundary condition

$$\frac{\partial c}{\partial x}(0,t) = \frac{j_0}{D}(1 - \cos\ 2\pi f t), \tag{18}$$

where j_0 is the average flux and f is the frequency of the signal. We solve the diffusion equation with degradation (Eq. 17) in one dimension numerically using *Comsol* with the boundary condition given by Eq. 18 at $x = 0$ and a closed boundary at $x = 100\,\mu$m.

CYTOPLASMIC STREAMING

We investigate the effect that cytoplasmic streaming may have on signaling. A cytoplasmic stream can be modeled as a roughly cylindrical stream of infinite extent in the open geometry (**Figure 2A**). If a signaling molecule diffuses into this stream, it will be translated in the direction of the stream with a speed approximately equal to the average speed v found in a cross-section of the stream until the molecule diffuses out of the stream again. As **Figure 2A** shows, molecules can circumvent the stream and many will reach the target without having crossed the stream. Those whose do cross it will spend an amount of time in the stream which is on the order of the characteristic diffusion time,

$$t_D = \frac{d^2}{4D} \tag{19}$$

where d is the width of the stream or the distance between the source and the target, whichever is smaller. During this time, a particle in the stream is translated a distance

$$\Delta y = \frac{v d^2}{4D} = \frac{Pe}{4} d \tag{20}$$

in the direction of the stream (the y-direction). Here Pe is the *Péclet number*. In biological cells Pe is typically much smaller than one.

Since d is smaller than the distance from the source to the target, Δy is negligible compared to the source-target distance if Pe is smaller than one. Thus, as long as Pe is smaller than one, the effect of cytoplasmic streams is negligible.

EXTREME EXAMPLE: AN INFINITE CYTOPLASMIC STREAM

In the previous subsection, we showed that cytoplasmic streaming has a negligible effect on signal transmission via diffusion in plant cells, by using an order-of-magnitude argument. The present subsection provides a more rigorous proof. It is rather equation-heavy and can be skipped.

We consider a cytoplasmic stream which fills the entire inside of the "cell" in the open geometry, moving with velocity v everywhere (**Figure 2B**). This is an extreme case; it is not physically realistic, but any realistic stream will do less transport of signaling molecules. So if we can show that this stream only has negligible effect on the signal measured at the target, then we know that a more realistic cytoplasmic stream, smaller and roughly cylindrical, e.g., has an even smaller effect.

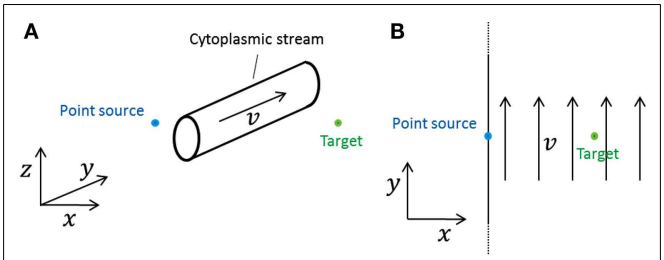

FIGURE 2 | Model systems considered for investigating the effect of cytoplasmic streams. In both cases a point source emits into a cell which is of effectively infinite size (open geometry). **(A)** A roughly cylindrical cytoplasmic stream of effectively infinite extent along the y-axis and of diameter d is situated between the source and the target. The direction of the stream is perpendicular to the line between source and target. **(B)** A cytoplasmic stream fills up the entire cell. The direction of the stream is perpendicular to the line between source and target.

At time t after emission of a short pulse signal from a point-like emitter located at $(x,y,z) = (0,0,0)$, the concentration at the point $\mathbf{r}$ inside this cell is equal to

$$c(\mathbf{r},t) = \frac{2n_0}{(4\pi D t)^{\frac{3}{2}}} e^{-\frac{x^2+(y-vt)^2+z^2}{4Dt}}. \tag{21}$$

The time $t_{\max}$ when the concentration reaches its peak at the point $\mathbf{r}$, is found by setting the derivative of Eq. 21 to zero and solving for t. This gives

$$t_{\max} = \frac{r}{v}\zeta, \tag{22}$$

where

$$\zeta = \sqrt{\left(\frac{3}{Pe}\right)^2 + 1} - \frac{3}{Pe} \tag{23}$$

and Pe is defined in Eq. 20. Measured at a distance x from the source and perpendicular to the stream $(y, z) = (0, 0)$, the peak signal is then

$$c_{\max}(x) = \frac{e^{-\frac{Pe(1+\zeta^2)}{4\zeta}}}{\left(\frac{4\pi D x \zeta}{v}\right)^{\frac{3}{2}}}. \tag{24}$$

This should be compared to the peak signal in the absence of a cytoplasmic stream,

$$c_{0,\max}(x) = \frac{e^{-\frac{3}{2}}}{\left(\frac{2\pi r^2}{3}\right)^{\frac{3}{2}}}. \tag{25}$$

Thus, the cytoplasmic stream decreases the peak concentration by a factor of

$$\frac{c_{\max}(x)}{c_{0,\max}(x)} = \left(\frac{Pe}{6\zeta}\right)^{\frac{3}{2}} e^{\frac{3}{2} - \frac{Pe(1+\zeta^2)}{4\zeta}}. \tag{26}$$

Even for a Péclet number of one, corresponding to a stream speed of 100 $\mu m\,s^{-1}$ (the highest reported in literature) and a source-target distance of 10 μm (the longest considered), this factor is equal to 0.96. The cytoplasmic stream only decreases the peak signal by 4% in this extreme case. Furthermore, in this case the time at which the peak concentration is measured is 0.97 times t_D, the time at which the peak concentration is measured in the absence of cytoplasmic streaming. So we can conclude that the effect of cytoplasmic streaming on the signal is completely negligible in more realistic, less extreme, scenarios.

TYPICAL BIOLOGICAL PARAMETER VALUES

The values of the various parameters introduced above and the way they influence the hydrogen peroxide signal, will be treated stepwise in the Results section. **Table 2** shows typical values of these parameters.

RESULTS

Two properties of the emitted signal determine whether it can be detected at the target: (i) the *peak concentration*, c_{max}, of the signaling molecules, which needs to be higher than the minimal detectable concentration, c_{detect}, and (ii) the *refractory time* of the signal, which is the time one must wait between emission of signals for successive signals to be discernible. We defined this period as the time it takes for the concentration at the target to drop to say 1/10 (or, alternatively, to 1/100) of its maximal concentration. Exactly to what fraction of its peak that the signal must drop to before a new signal can be discerned is unknown and probably varies between cells. We therefore discuss results for both the relatively low and high arbitrarily chosen peak/trough ratios of 10 and 100.

If we assume that the resting concentration of H_2O_2 in the cytosol is 0.1 μM (by analogy with free calcium ions in cells) and that the peak concentration must at least be ten times higher than this to be detected, then the minimal detectable concentration at the target is 1 μM for a peak/trough ratio of 10 and 10 μM for a peak/trough ratio of 100.

MAXIMAL FLUX OVER THE CELL MEMBRANE

H_2O_2 crosses the PM through aquaporins. The maximal flux through a single aquaporin channel is on the order of 10^9 molecules $channel^{-1}\,s^{-1}$ (Jensen and Mouritsen, 2006) while the number of channels per μm^2 is on the order of 30 (Li et al., 2011). This gives a maximal flux per μm^2 of 3×10^{10} molecules $\mu m^{-2}\,s^{-1}$, or in units of moles: 5×10^{-14} mol $\mu m^{-2} s^{-1}$. If we assume that the aquaporins allow H_2O_2 and water molecules to pass with rates proportional to their respective concentrations and we further assume that the

Table 2 | Parameters used in the modeling.

Parameter	Interval studied	Comment and/or reference
Diffusion coefficient	$D = 10^{-9}\,m^2\,s^{-1} = 10^3\,\mu m^2\,s^{-1}$	For diffusion in aqueous buffer $D = 1.7 \times 10^{-9}\,m^2 s^{-1}$ (van Stroe-Biezen et al., 1993); molecular crowding decreases D by approx. 20–50% (Straube and Ridgway, 2009)
Frequency	0.01–1 Hz	Assumed to lie in the same range as for Ca^{2+} (Jaffe, 1993)
Distance from source to target	1–10 μm	Typical cellular distances
Size of area on PM emitting synchronized pulse	Single channel – 10 $\mu m \times 10\,\mu m$	Relevant cellular dimensions
Assumed peak/trough ratio required to transmit signal	10–100-fold	
Minimal detection concentration	1–100 μM	Lower boundary is ten times the min. Ca^{2+} concentration measured in animal cells (Alberts et al., 1994); upper boundary is at the lower end of the average concentration measured in plant cells (Møller et al., 2007)
Maximal flux through a membrane channel	10^9 molecules s^{-1} $channel^{-1} = 1.7 \times 10^{-15}$ mol s^{-1} $channel^{-1}$	Total flux for both water and H_2O_2
Channel density	$\rho_a = 30$ channel μm^{-2}	Li et al. (2011)
Maximal H_2O_2 flux per μm^2	10^{-16} mol $\mu m^{-2} s^{-1}$	Calculated using the maximal flux and the channel density and assuming no selectivity of the channels
Maximal degradation rate	$V_{max} = 1$–100 $\mu M\,s^{-1}$	Lowest level estimated from Bonifacio et al. (2011)
Michaelis constant	20 μM for H_2O_2, values in the range 2–200 μM are considered	20 μM is the average for ascorbate peroxidases reviewed in Raven (2003)
Cytoplasmic streaming speed	1–100 $\mu m\,s^{-1}$	Goldstein et al. (2008)
Cytoplasmic stream width	1–10 μm	Kristiansen et al. (2009)

concentrations outside the PM are 100 mM for H_2O_2 (very high) and 55 M for water (standard), then the maximal flux of H_2O_2 over the cell membrane is 10^{-16} mol μm^{-2} s^{-1}.

A prerequisite for attaining this maximal flux is that the concentration of H_2O_2 outside the membrane is much higher than the concentration inside, since the aquaporins are passive channels. This is, however, always the case in practice, since even if we let the channel stay completely open for 1 s, the concentration will maximally reach 4 mM inside the cell.

SHORT PULSE SIGNAL

A signal is emitted at the PM by opening the aquaporins for a while. We first consider signals consisting of short pulses. All other types of signals can be constructed by adding short pulses and they are the type of signal, which allows the fastest frequency modulation. A short pulse is obtained by fast opening and closing of the channels in the membrane. For mathematical convenience this can be idealized to an instantaneous pulse where the channels are opened and closed infinitely fast and the flux over the membrane is infinite during this infinitesimal time-interval.

Increasing the time the channels stay open naturally increases the signal amplitude. At long times after emission, there is a simple proportionality between the time the channels stay open (and thus the total signal) and the concentration measured at the target; as with the different emission areas the curves describing the concentration all collapse to the same on curve (**Figure 3**), except for a scaling factor determined by the total amount of H_2O_2 emitted. That is, at sufficiently long times the curves become equal except for a scaling factor.

For times shortly after the emission of the signal, it is another story. Longer opening time flattens out the peak of the concentration, and the peak concentration, relative to the concentration measured at long times, is decreased. This in turn increases the refractory time.

When we consider a target that is 1 μm away, the signal can be considered a short pulse as long as the time during which the aquaporins stay open is approximately 1 ms or shorter, since its relative amplitude does not differ significantly from that of an instantaneous pulse (**Figure 3A**). The maximal amount of H_2O_2 that can be released in a single short pulse per unit area, i.e., the maximal amplitude of a short pulse signal, is then 10^{-19} mol μm^{-2}. At a distance of 10 μm, the signal can be considered a short pulse, if the aquaporins stay open for approximately 10 ms or less (**Figure 3B**), i.e., the maximal amplitude of such a short pulse is 10^{-18} mol μm^{-2}. Here, where the source-target distance (10 μm) is comparable to the dimensions of the source (10 μm × 10 μm), we also see that the signal received at the target is well approximated by the analytical solution for a point source (**Figure 3B**).

THE SIZE OF THE EMISSION AREA

The size of the activated area on the PM, the area creating the synchronized signal, may vary depending on, e.g., what caused the signal. This gives different signals. We consider emission area sizes ranging from a single channel to 100 μm^2: (i) a single channel, (ii) 1 μm × 1 μm (a small patch), and (iii) 10 μm × 10 μm (a large patch extending over a major fraction of one side of a plant cell).

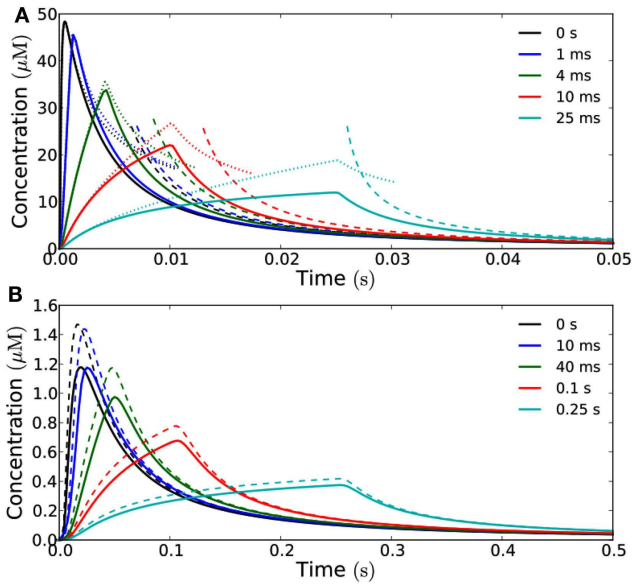

FIGURE 3 | How opening time of the channels influence the signal received at the target. Concentration as a function of time measured at a distance of 1 μm **(A)** and 10 μm **(B)** from a square emission patch of size 10 μm × 10 μm in the open geometry. The curves have been rescaled such that they correspond to the same total signal, i.e., the flux is adjusted such that the total amount of H_2O_2 emitted is the same for the different opening times and equal to 10^{-19} mol μm^{-2}. The time-interval in which the channels stay open is varied between 0 and 25 ms **(A)** and 0 and 0.25 s **(B)**. Solid curves represent exact results for a 10 μm × 10 μm area obtained from Comsol simulations while dashed lines represent analytical results for a point source. **(A)** Dotted lines represent the analytical (1D) solution for an infinite source area. Note how the exact results agree well with the analytical solutions for an infinite source for short times, since we are so close to the source that it effectively feels infinite at this short time-scale. At long times the analytical solutions corresponding to emission from a point source agree well with the exact results and all the curves collapse on the same curve. The diffusion time t_D of a signal emitted in an instantaneous pulse is equal to 1 ms. **(B)** At a distance of 10 μm from the source, the exact results are well approximated by the analytical solution for a point source emitter. The peak signal from a point source is slightly higher than from the 10 μm × 10 μm area since the initial point source signal is more concentrated. However, the curves are qualitatively similar and they all collapse to the same curve at long times as in **(A)**. The diffusion time t_D for an instantaneous pulse signal is here equal to 25 ms.

Varying the area of the patch from where molecules are emitted, affects the total amplitude of the signal, if other parameters are kept constant (**Figure 4**). Furthermore, a larger emission area means slower decay, i.e., longer refractory time (**Figures 5** and **6**).

For a signal emitted by a single channel, it is clear that we would need a very high initial signal amplitude to be able to detect the signal, even as close as 1 μm away. If we assume that the resting concentration of H_2O_2 is 0.1 μM and that we can detect the signal at a concentration 10-fold higher than this, we need a signal twenty times larger than what a single channel can emit in a short pulse, to be able to detect the signal from a single channel at 1 μm from the source. Thus, in the following we will only consider emission from sources of size 1 μm × 1 μm and 10 μm × 10 μm.

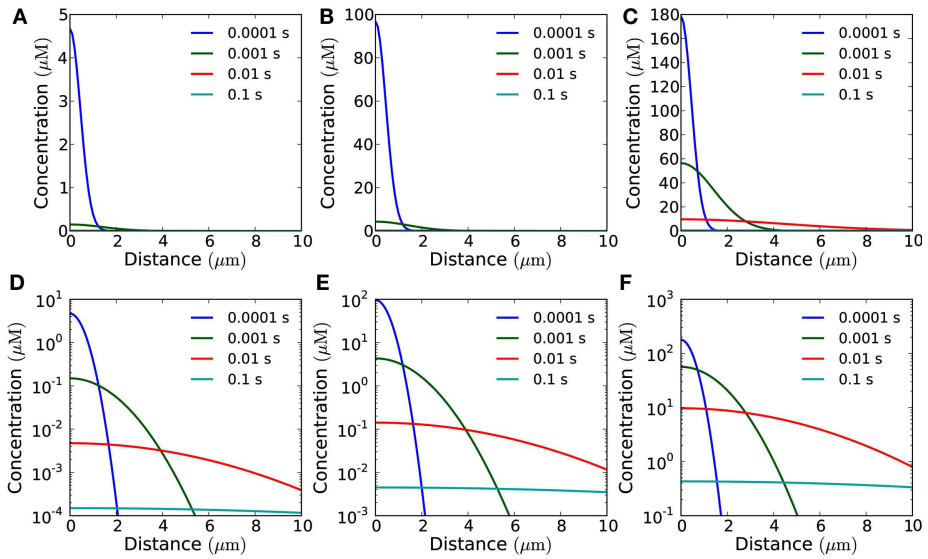

FIGURE 4 | Concentration of H_2O_2 as a function of distance from the membrane in the open geometry. Snapshots of the concentration profile at different points in time after emission of a single pulse of 10^{-19} mol μm^{-2} from areas of varying size: **(A)** for a single channel; **(B)** for an area of 1 μm × 1 μm (containing 30 channels); **(C)** for an area of 10 μm × 10 μm (3,000 channels). **(D–F)** Same plots as in **(A–C)** shown with logarithmic *y*-axis.

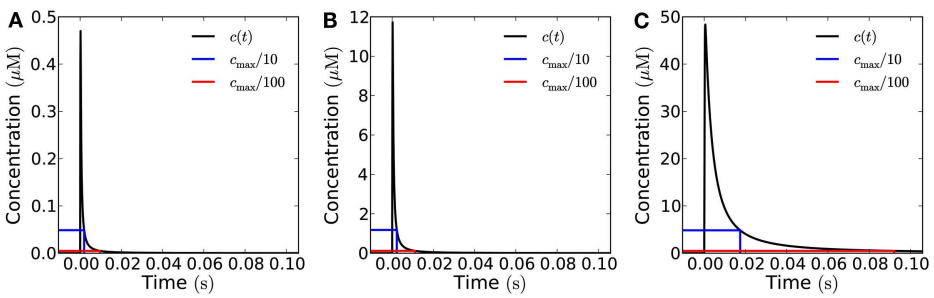

FIGURE 5 | Influence of the emission area on the measured signal at a target 1 μm from the source in the open geometry. Concentration of H_2O_2 as a function of time at a distance of 1 μm from the source after emission of a single pulse of 10^{-19} mol μm^{-2} from areas of varying size. The blue (red) lines mark 1/10th (1/100th) of the peak concentration and the time at which it is obtained. **(A)** for a single channel (signal: 3×10^{-21} mol) the refractory times are 1.9 and 9.6 ms depending on whether the peak/trough ratio is 10 or 100, respectively. **(B)** For a 1 μm × 1 μm area (30 channels, total signal: 10^{-19} mol), refractory times: 2.3 and 11 ms. **(C)** For a 10 μm × 10 μm area (3000 channels, total signal: 10^{-17} mol), refractory times: 19 and 100 ms. Note that the signal from a 1 μm × 1 μm area **(B)** and a point emitter **(A)** are almost identical when measured at a distance of 1 μm. This is also reflected in the refraction times.

DISTANCE FROM THE SOURCE

The refractory time does not depend on the signal amplitude, but depends highly on distance from the source and emission patch size (**Figures 5** and **6**). Increasing the distance between the source and the target increases the refractory time and, additionally, drastically decreases the amplitude of the signal (**Figures 5** and **6**). In the open geometry the main obstacle to signaling is the difficulty of attaining a peak concentration at the target which is sufficiently high to be detected.

At a distance of 1 μm (**Figure 5**), emission of a pulse of 10^{-19} mol μm^{-2} from an area of 1 μm × 1 μm (total signal is 10^{-19} mol) creates a detectable signal with a refractory time of 2.3 ms for a peak/trough ratio of 10 (11 ms for a ratio of 100), indicating that in the open geometry frequencies of up to 500 Hz are feasible even without enzymatic degradation of H_2O_2. When the area is larger, 10 μm × 10 μm (total signal: 10^{-17} mol), the signal is considerably stronger, but the refractory time increases to 19 ms (100 ms for a peak/trough ratio of 100), indicating that here frequencies up to 50 Hz are possible.

With distance, the wave broadens, thereby increasing the refractory time. At a distance of 10 μm (**Figure 6**), only an emission from the largest area considered (10 μm × 10 μm) is detectable, even if the detection limit is as low as 1 μM. Here the refractory time is 0.22 s for a peak/trough ratio of 10 (1.1 s for a ratio of 100), indicating that signaling with frequencies up to 5 Hz is feasible.

In general, as long as the distance between the target and the source is greater than or equal to the dimensions of the area of emission, the signal is well approximated by the signal

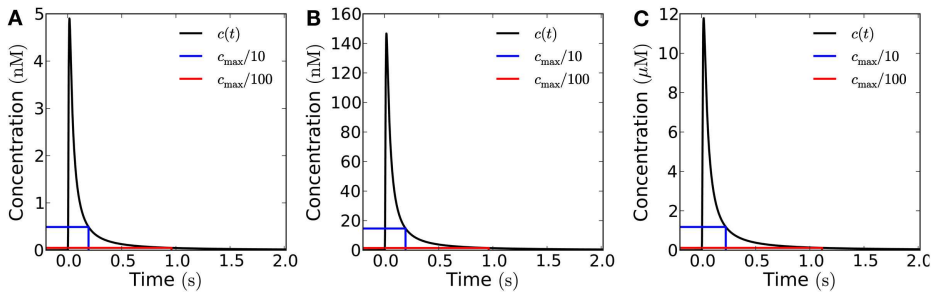

FIGURE 6 | Influence of the emission area on the measured signal at a target 10 μm from the source. Concentration of H_2O_2 as a function of time at a distance of 10 μm from the source after emission of a single instantaneous pulse of 10^{-18} mol μm^{-2} H_2O_2 from areas of varying size in the open geometry. The blue (red) lines mark 1/10th (1/100th) of the peak concentration and the time at which it is obtained. **(A)** For a single channel (signal: 3×10^{-20} mol) the refractory times are 0.19 and 0.96 s depending on whether the peak/trough ratio is 10 or 100, respectively. **(B)** For a 1 μm × 1 μm area (total signal: 10^{-18} mol), refractory times: 0.19 and 0.96 s. **(C)** For a 10 μm × 10 μm area (total signal: 10^{-16} mol), refractory times: 0.22 and 1.1 s. The time after signal emission where the concentration has dropped to 1/10 and 1/100 of its maximal value, are marked by vertical lines. All the three curves look almost identical except for the scale factor, i.e., the signals in **(B,C)** are practically indistinguishable from that of a point source **(A)**. Comparison of the refraction times in the three cases also shows this.

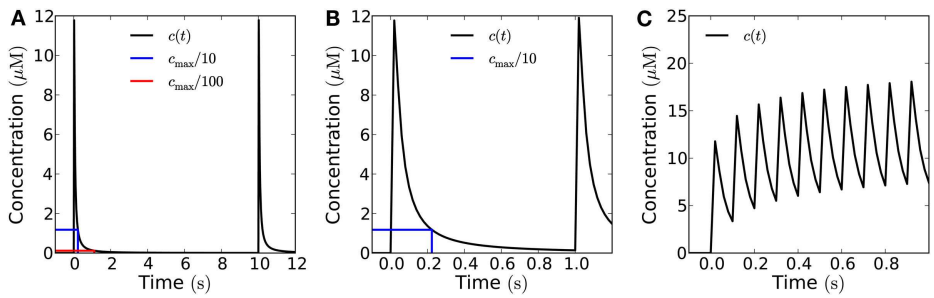

FIGURE 7 | Recorded signal at a distance of 10 μm from emitter of a train of pulses in the open geometry. The individual pulse amplitude is 10^{-18} mol μm^{-2} emitted from a 10 μm × 10 μm area (total individual signal: 10^{-16} mol). The blue (red) lines mark 1/10th (1/100th) of the peak concentration and the time at which it is obtained. **(A)** For an emission frequency of 0.1 Hz both a 10-fold and a 100-fold decrease of the signal is easily detected between emission of signals. **(B)** For an emission frequency of 1 Hz, a 100-fold difference is no longer obtained, the concentration only has time to decrease by a factor of 85 before the arrival of a new signal. **(C)** For an emission frequency of 10 Hz, only a maximal peak/bottom ratio of around two is seen at the target.

from a point source (compare **Figures 5A,B** and **6A–C**) and the refractory times are given approximately by the analytical result for a point emitter (Eq. 11). In this case, for a source-target distance of 1 μm, the refractory times for the signal to reach 1/10th and 1/100th of its peak value for a point source are 1.9 and 9.6 ms respectively. For a source-target distance of 10 μm, the refractory times for a point source are 0.19 and 0.96 s.

SIGNALING WITH TRAINS OF SHORT PULSES

Figure 7 shows what a train of short pulses emitted from a 10 μm × 10 μm area looks like at a distance of 10 μm from the source. At a low frequency, say 0.1 Hz, the H_2O_2 concentration has time to return to the resting level (**Figure 7A**), at 1 Hz, the level does not quite return to 1/100th of the peak value since the refractory time is 1.1 ms (**Figure 7B**), and at a frequency of 10 Hz there is a build-up of H_2O_2 and only a twofold difference between peak and trough, insufficient for the signal to be deciphered (**Figure 7C**).

FINITE CELL SIZE AND REMOVAL OF H_2O_2

We have until now assumed that the cell is so large that there is no effect of cell walls on the distribution of H_2O_2, except from the wall through which it enters the cell. In reality, and especially when we look at repeated pulses and other cases of continuous signaling, H_2O_2 will build-up in the cytosol and thereby prevent further signaling, unless it is removed.

We consider a closed geometry in which the signal is emitted from the whole end-wall of the cell, e.g., an area of 10 μm × 20 μm. This is the most restricted geometry that one can imagine, i.e., it complements the open geometry treated above and thereby delimits the range of possible phenomena. This is the geometry in which one can have the highest signal amplitudes, but on the other hand also the longest refractory times.

If no H_2O_2 is removed or degraded, signaling over 10 μm is not possible since the cell fills up with H_2O_2 and the concentration settles at a constant value throughout the cell of approximately 20% of c_{peak} as measured at 10 μm from the source. However, there are several mechanisms by which H_2O_2 can be removed – transport

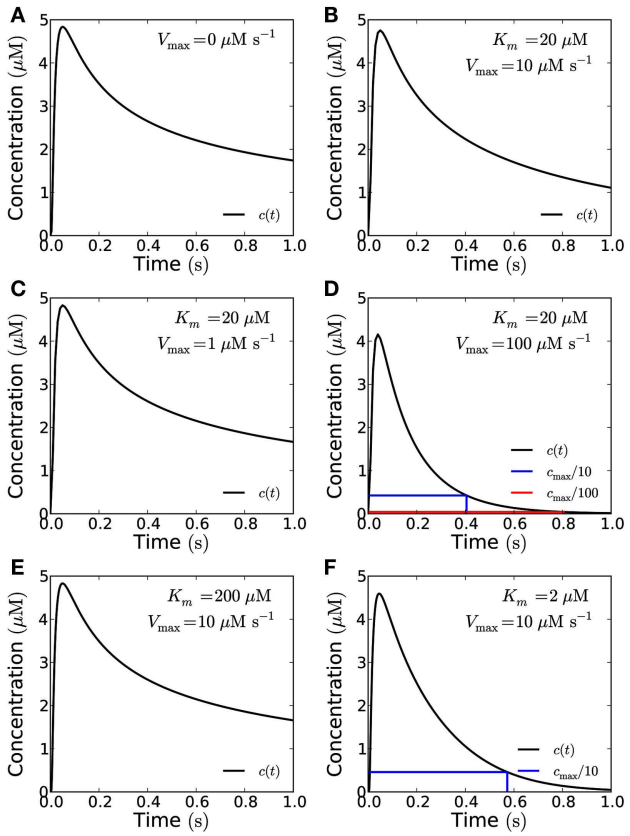

FIGURE 8 | The effect of enzymatic degradation of H_2O_2 on a short pulse signal. The signal is recorded at a distance of 10 μm from the source in the closed geometry. Enzymatic degradation of H_2O_2 reduces the refractory time, but does not significantly reduce the peak concentration. A signal of amplitude 10^{-19} mol μm^{-2} is emitted from the whole end-wall (10 μm × 20 μm area, total signal: 2×10^{-17} mol) of a 100 μm long cell and measured at a distance of 10 μm. H_2O_2 is reflected by the sides of the cell. **(A)** No degradation. **(B)** For degradation with $V_{max} = 10\,\mu M\,s^{-1}$ and $K_m = 20\,\mu M$. **(C)** $V_{max} = 1\,\mu M\,s^{-1}$ and $K_m = 20\,\mu M$. **(D)** $V_{max} = 100\,\mu M\,s^{-1}$ and $K_m = 20\,\mu M$. Here the refraction times are 0.4 s and 0.8 for 1/10th (blue lines) and 1/100th (red lines) of the peak concentration c_{max}. **(E)** For $K_m = 200\,\mu M$ and $V_{max} = 10\,\mu M\,s^{-1}$. **(F)** $K_m = 2\,\mu M$ and $V_{max} = 10\,\mu M\ s^{-1}$. Here the refraction time to reach 1/10th of the peak concentration is 0.57 s. The effect of lowering (raising) K_m is qualitatively equivalent to the effect of raising (lowering) V_{max}.

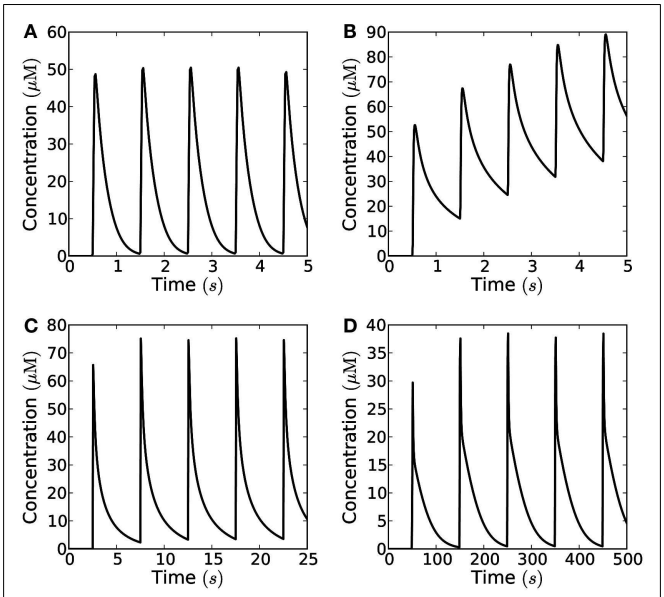

FIGURE 9 | Frequency-modulated signals consisting of short pulses. The range of frequencies at which signaling is possible in the closed geometry, depends strongly on the maximal degradation rate of H_2O_2. Concentration measured at 10 μm distance from an area of 10 μm × 10 μm, which emits short pulses; the signaling molecules are enzymatically degraded in a reaction with $K_m = 20\,\mu M$ and $V_{max} = 1-100\,\mu M\,s^{-1}$, the amount of H_2O_2 released by each pulse is $N_0 = 10^{-18}$ mol μm^{-2}. **(A)** For fast degradation ($V_{max} = 100\,\mu M\,s^{-1}$) high frequency ($f = 1$ Hz) and high amplitude signaling is possible; **(B)** for an intermediate degradation rate ($V_{max} = 10\,\mu M\,s^{-1}$) signaling is not possible at the highest frequencies (i.e., $f = 1$ Hz), since the signal's refractory time is too long; **(C)** at frequencies lower than 0.2 Hz signaling is possible for $V_{max} = 10\,\mu M\,s^{-1}$; **(D)** For slow degradation ($V_{max} = 1\,\mu M\,s^{-1}$) only low frequency signaling is possible ($f = 0.01$ Hz).

out of the cell or into organelles, chemical reactions, and enzymatic reactions. We cannot evaluate the magnitude of the former two and if transport out of the cell is passive it will counter the effect of the cell walls to some extent, i.e., the system will be described by the open geometry or some intermediary between the closed and open geometries. So here we will let H_2O_2 removal consist entirely of enzymatic degradation to analyze how H_2O_2 removal affects signaling. The cytosol contains several enzymes capable of removing hydrogen peroxide, e.g., ascorbate peroxidase. When we include removal of H_2O_2 by Michaelis–Menten kinetics in the model, we see that signaling over 10 μm becomes possible at frequencies up to 2.5 Hz (for a peak/trough ratio of 10) when the removal rate is $100\,\mu M\,s^{-1}$ (**Figures 8D** and **9A**). At a much lower removal rate ($1\,\mu M\,s^{-1}$) only signaling at rates up to 0.06 Hz is possible (for a peak/trough ratio of 10, 0.01 Hz for a ratio of 100, **Figure 8C**). Since the diffusion of H_2O_2 is fast on intracellular length scales, degradation does not affect the maximal concentration of H_2O_2 much (**Figure 8**), though it significantly decreases the refractory time. At an intermediate removal rate ($10\,\mu M\,s^{-1}$), similar to the one reported by Bonifacio et al. (2011) signaling at 0.2 Hz is possible (**Figures 9B,C**). In all cases peak concentrations of 50 μM at the target can be reached.

The Michaelis constant K_m may change as well, i.e., due to molecular crowding (see Effect of Molecular Crowding). We have considered a ten-fold increase or decrease in K_m (i.e., to 200 or 2 μM) and see that the effect of an increase in K_m is qualitatively the same as the effect of a corresponding decrease of V_{max} and *vice versa* (**Figures 8E,F**).

Frequencies, amplitudes, and background H_2O_2 concentrations, which make signaling possible are listed in **Tables 3** and **4**.

HARMONICALLY OSCILLATING SIGNAL

Thanks to the late French physicist Joseph Fourier (the inventor of Fourier analysis), we know that any signal can be constructed as a sum of harmonic functions, i.e., sines and cosines. This type of signal is complimentary to the short pulse, since it is

Table 3 | Possible parameter values for signaling over a distance of 1 μm using short pulses (open geometry).

Parameter	Approx. max. value	Comments
Frequency	500 Hz	For $c_{max}/c_{trough} = 10$
	90 Hz	For $c_{max}/c_{trough} = 100$
Amplitude	10–50 μM	For a 1 ms pulse and depending on the size of the emission area (1–100 μm^2)
	20–250 μM	For a 10 ms pulse; here the max. frequency is decreased by a factor two
Maximum background concentration	5–25 μM	For a 10 ms pulse and $c_{max}/c_{trough} = 10$

Table 4 | Possible parameter values for signaling over a distance of 10 μm using short pulses (closed geometry).

Parameter	Approx. max. value	Comments
Frequency	1–2 Hz	For $V_{max} = 100\,\mu M\,s^{-1}$, depending on c_{max}/c_{trough}
	0.2 Hz	For $V_{max} = 10\,\mu M\,s^{-1}$
	0.01 Hz	For $V_{max} = 1\,\mu M\,s^{-1}$
Amplitude	50 μM	For 10 ms pulses
	500 μM	For 0.1 s pulses, only possible for $V_{max} = 100\,\mu M\,s^{-1}$, and a max. frequency of 0.5 Hz
Maximum background concentration	5 μM	For 10 ms pulses and $c_{max}/c_{trough} = 10$

regulated gradually, whereas the short pulse is regulated by an abrupt open/close mechanism. The manner in which such a signal propagates thus gives us a new angle on the problem of signal transmission. This angle is the natural one to use in an investigation of the propagation of pulse trains, because a harmonic signal is the simplest possible periodic pulse train as seen from a mathematical point of view, and because more complicated pulse trains can be viewed as super-positions of these simple ones for analytical purposes. That is the essence of Fourier analysis. Add to this that harmonic signals are the carrier waves for signals encoded by frequency modulation.

While the non-linear kinetics of the Michaelis–Menten degradation term prevents us from solving the kinetic equation using Fourier analysis, that analysis still applies to the emitted signal. It is the interactions of different Fourier components of the propagating signal in the degradation term that bars Fourier analysis.

Figure 10 shows what a signal with a harmonic source looks like throughout the cell at different points in the emission cycle, i.e., snapshots of the concentration profile at different points in time. No spatial wave-like pattern is seen. This is a signature feature of diffusive transport in a non-excitable medium. This is because signal propagation is only driven by concentration gradients and the concentration of signaling molecules thus always will be highest at the source. The wave-pattern is only seen in the time-domain, e.g., when we follow the concentration in a single point over time (**Figure 11**). To see spatial wave-patterns in diffusion-mediated signaling a non-linear, excitable medium is required.

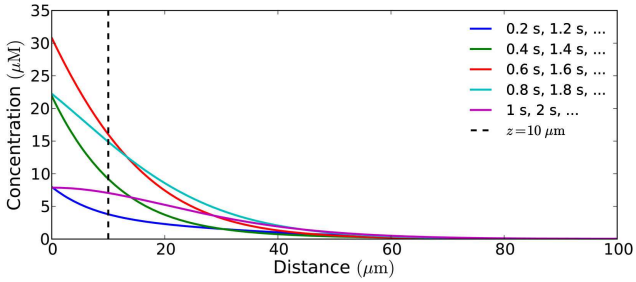

FIGURE 10 | Snapshots of the concentration profile in a cell of length 100 μm (closed geometry) of a signal from a harmonically (sinusoidal) emitting source, taken at different times in the emission cycle. No wave-like pattern is seen. This is a signature feature of signal propagation by diffusion. The wave is only in the time-domain and can be seen if one continuously monitors the concentration of H_2O_2 at a given distance, e.g., at 10 μm from the source. The period of the flux is 1 Hz, its amplitude is 10^{-18} mol $\mu m^{-2} s^{-1}$, and V_{max} is 100 $\mu M\,s^{-1}$.

Though harmonic signals in theory allow much higher signaling amplitudes, they are limited by the refractory time, and the possible peak concentrations are lower for harmonic signals than for short pulse at similar frequencies (**Figure 11**; **Table 5**). **Figures 12A,B** shows possible signaling frequencies as a function of V_{max} for signaling using short pulses (**Figure 12A**) and a harmonically oscillating flux (**Figure 12B**).

EFFECT OF MOLECULAR CROWDING

Molecular crowding effectively lowers the diffusion coefficient of a molecular species in the cytosol compared to its value in water. For calcium ions in animal cells, this effect is of the order of 20–50% (Straube and Ridgway, 2009). We have assumed a similar effect on the diffusion coefficient of H_2O_2 in plant cells, lowering the diffusion coefficient of H_2O_2 from 1,700 $\mu m^2\,s^{-1}$ (van Stroe-Biezen et al., 1993) to 1,000 $\mu m^2\,s^{-1}$. Excluding the effect of degradation, a twofold increase of the diffusion coefficient will simply decrease the characteristic diffusion time and refractory times by a factor two, but will not influence signal amplitudes; an increase of the diffusion coefficient diminishes the influence of degradation, since it reduces the time-scale of signaling.

Molecular crowding may also affect the binding rates and rates of catalysis of enzymes and thus change K_m and V_{max} (Zhou et al., 2008). A change of the rate of catalysis changes both K_m and V_{max} in the same direction, which means that these two effects largely cancel each other in this case (**Figure 8**). A change in the association rate between signaling molecules and the degradation enzymes only affects K_m and will thus to a larger extent affect reaction kinetics. The effect of crowding varies highly for different enzymes (Norris and Malys, 2011) and is unknown for enzymes degrading H_2O_2 in plant cells. So we have considered a wide range of possible values for K_m (2–200 μM, **Figure 8**).

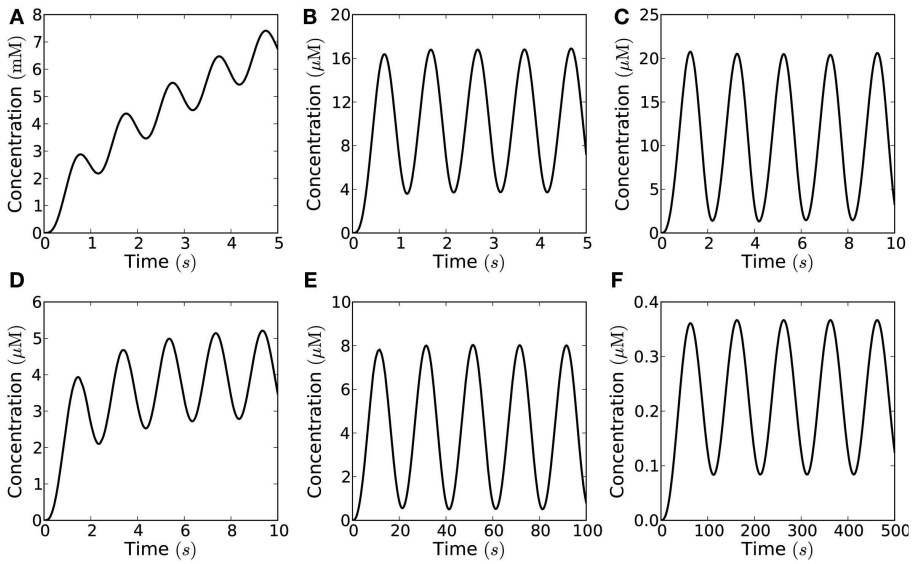

FIGURE 11 | Harmonically oscillating signals in theory allows much higher signaling amplitude than short pulses. However, in practice the amplitude needs to be limited to allow signaling at relevant frequencies, thus harmonic signals actually allow a lower signaling amplitude than short pulses at similar frequencies. Concentration measured at a distance of 10 μm from the emission area of 10 μm × 10 μm in the closed geometry, which emits a harmonic (sinusoidal) flux with amplitude j_0 and frequency $f = 1-0.01$ Hz; the signaling molecules are enzymatically degraded in a reaction with $K_m = 20\,\mu M$ and $V_{max} = 1-100\,\mu M\,s^{-1}$. **(A)** Even for maximal degradation rate ($V_{max} = 100\,\mu M\,s^{-1}$) the maximal flux of 10^{-16} mol $\mu m^{-2} s^{-1}$ is so high that the concentration of molecules build-up over time and no signaling is possible; **(B)** for a lower flux of 10^{-18} mol $\mu m^{-2} s^{-1}$ the concentration no longer builds up over time, but fast signaling is still not possible ($f = 1$ Hz) due to the long refractory time; **(C)** for a lower frequency ($f = 0.5$ Hz) signaling is possible (with $c_{max}/c_{trough} = 10$); **(D)** if the degradation rate is lower ($V_{max} = 10\,\mu M\,s^{-1}$) signaling at 0.5 Hz is no longer possible; **(E)** the frequency must be lowered accordingly to allow signaling ($f = 0.05$ Hz); **(F)** for a degradation rate of $1\,\mu M\,s^{-1}$ no signaling is possible, even with the lowest relevant frequencies ($f = 0.01$ Hz) and at very low amplitude ($j_0 = 10^{-21}$ mol $\mu m^{-2} s^{-1}$).

Table 5 | Possible parameter values for signaling over a distance of 10 μm using harmonic signals (closed geometry).

Parameter	Approx. max. value	Comments
Frequency	0.5 Hz	For $V_{max} = 100\,\mu M\,s^{-1}$
	0.05 Hz	For $V_{max} = 10\,\mu M\,s^{-1}$
	<0.01 Hz	For $V_{max} = 1\,\mu M\,s^{-1}$
Amplitude	10–20 μM	For $V_{max} = 100\,\mu M\,s^{-1}$ and $f = 0.5$ Hz. Can be higher for lower frequencies; lower V_{max} implies lower amplitude
Maximum background concentration	1–2 μM	For $c_{max}/c_{trough} = 10$ and depending on V_{max}

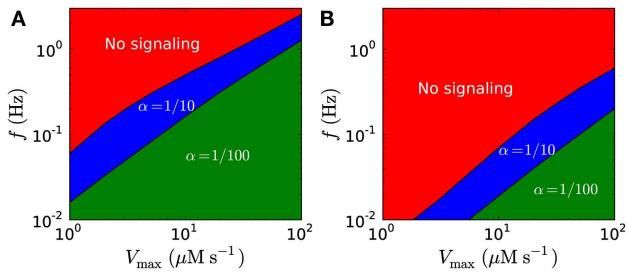

FIGURE 12 | Possible signaling frequencies *f* in the closed geometry as a function of V_{max}. Shown for trough/peak ratios of $\alpha = 1/10$ (blue) and $\alpha = 1/100$ (green). **(A)** Possible frequencies for short pulse signaling. **(B)** Possible frequencies for harmonic signaling. Higher frequencies are obtainable for short pulse signaling than for harmonic signaling. In both **(A,B)**, the signal detection threshold is 1 μM for $\alpha = 1/10$ and 10 μM for $\alpha = 1/100$, and K_m is 20 μM.

EFFECT OF CYTOPLASMIC STREAMING

Finally, we have investigated what effect cytoplasmic streaming may have on signaling. We have considered a roughly cylindrical cytoplasmic stream in between the source and the target (**Figure 2A**). A simple order-of-magnitude argument showed that the influence of the stream is negligible if the Péclet number is on the order of one or smaller. Here the Péclet number is defined as the ratio between the stream's width times the stream velocity and the diffusion coefficient. Considering the maximal stream speed reported in the literature, $v = 100\,\mu m$ (Goldstein et al., 2008; **Table 2**), and considering a stream which is as wide as the largest distance between the source and the target, 10 μm, we get a Péclet number of one. This means that even in this extreme case, cytoplasmic streaming does not significantly disturb signaling.

Thus, cytoplasmic streaming does not hinder intracellular signaling by diffusion, since the diffusion coefficient is so large compared to typical values of the cytoplasmic stream width and speed (**Table 2**). On the contrary, it lowers the refractory time, because the stream has a stronger delaying effect on the signal molecules that arrive late at the target than it has on the early arrivers, due to

the former spending more time in the stream than the latter. The net effect is a sharper profile of concentration plotted against time, similar to the situation in which signal molecules are degraded.

DISCUSSION

Our modeling shows that diffusion-mediated frequency- and amplitude-modulated signaling with H_2O_2 over distances of up to 10 μm is possible if we assume that the detection limit is low (on the order of 1 μM), the synchronized emission area is large (**Figures 6** and **8**), the flux over the membrane is high, and the removal rate is high (**Figures 8** and **9**). Under these conditions, signaling with a frequency of up to 2 Hz at 10 μm is possible with amplitudes up to 50 μM (**Figures 8**, **9**, and **12A**; **Table 4**).

The effect of enzymatic degradation of H_2O_2 is the opposite of what was proposed by Møller and Sweetlove (2010). Instead of making signaling difficult, a high rate of H_2O_2 degradation is actually a prerequisite for signaling as it reduces the refractory time (**Figures 7–9** and **11**). Other possible removal mechanisms are uptake into organelles and/or transport out of the cell, neither of which has been described for plant cells and both of which have the same overall effect as degradation, in as much as they would reduce the refractory time. The rate of H_2O_2 removal is a parameter that the plant cell may modulate to accommodate a wider range of signaling frequencies.

Also contrary to what was proposed by Møller and Sweetlove (2010), cytoplasmic streaming does not distort the H_2O_2 signal too much, because cytoplasmic stream speeds are slow compared to diffusion over the short cellular distances that are relevant.

The maximal amount of H_2O_2 emitted in a pulse at the PM depends on the density of aquaporins able to transport H_2O_2 as well as on the flux per channel in the opened state. The density of aquaporins has been estimated to be 30 molecules per μm^2 (Li et al., 2011) and the flux per channel is assumed to be 10^9 molecules s^{-1} (Jensen and Mouritsen, 2006). The channel density in the PM is probably a parameter that the plant needs to be able to regulate in response to long-term changes in the water supply. The question is how many of the molecules passing through the aquaporins are H_2O_2 and how many are water. We assumed no selectivity, but there could be some, which would alter the maximal possible flux. We assumed an external concentration of 100 mM H_2O_2 and that could well be an overestimate. We also assumed that all the aquaporins in the PM can transport H_2O_2, which is probably not the case (Bienert et al., 2007; Maurel et al., 2009). Thus, it is possible that the maximum flux possible across the PM turns out to be a limiting factor for H_2O_2 signaling by diffusion.

Opening times for the synchronized channels down to 1 ms were considered and were required for emission of short pulses over a distance of 1 μm (**Figure 3A**). Since opening of aquaporins is regulated by reversible phosphorylation/dephosphorylation, this would require that the protein kinase and phosphatase involved can complete their work in considerably less than 1 ms. We do not know whether this is possible.

An alternative to signaling by short pulses is H_2O_2 signals that resemble harmonic oscillations, which allow for longer opening/closing times for the PM aquaporins that produce these signals. However, in order to produce an harmonic oscillation, it is required that channel closing starts just as the maximal opening state has been achieved, and that may be more difficult to imagine in terms of enzyme kinetics. In this connection, it is interesting that a theoretical study has shown that aquaporin opening may also be voltage gated (Hub et al., 2010). Furthermore, while harmonically oscillating signals are able to create higher signal amplitudes since the channels stay open longer than for short pulse signaling (**Figure 11**) they have longer refraction times and only allow for signaling at much lower frequencies (**Figures 11** and **12B**).

The concentration of H_2O_2 in plant tissues has been reported to be in the micromolar to low millimolar range and usually higher under stress conditions, assuming an even distribution in all cells and cell parts including the vacuole (Halliwell and Gutteridge, 2007; Møller et al., 2007; and references therein). However, the observation that the ROS probe CM-H_2DCFDA [(5-(and-6) chloromethyl-2',7' dichlorodihydrofluorescein diacetate] does not give a signal in the vacuole (Bienert et al., 2007) may indicate that the vacuole contains little H_2O_2, which in turn indicates that the concentration in the rest of the cell, where signaling occurs, is even higher. We assume that the vast majority of this H_2O_2 is free (not bound), i.e., we assume the opposite of what is the case for Ca^{2+} for which the concentration of free cytosolic ions is three orders of magnitude lower than the total tissue content, due mainly to binding and sequestering inside organelles (e.g., Jafri and Keizer, 1995).

If H_2O_2 signaling via diffusion with resting levels below 1 μM is a general phenomenon, the waves would indeed have to contain very high peak concentrations in order to give a tissue average hundreds or thousands of times above the resting level. As we have demonstrated, that is very likely not the case, unless relaying stations exist. At higher resting levels in the cytosol for H_2O_2, the flux across the PM would become limiting and so would enzymatic degradation. In other words, the relatively high average levels of H_2O_2 observed to be present in plant tissues makes it highly improbable that information is transmitted via diffusing H_2O_2, unless relaying stations exist in the cytoplasm.

The tissue concentrations of H_2O_2 referred to above are, of course, averages and probably differ considerably between cell types. If we take a C3 leaf in the light, the photosynthetically active cells, such as the palisade cells, would have a massive turnover of ROS in the chloroplasts and in the peroxisomes as a result of photorespiration (Foyer and Noctor, 2003) and probably a relatively high cytosolic ROS concentration. In contrast, the leaf epidermal cells, which in many species contain no chloroplasts, would be expected to have a ROS concentration much lower than the average for the leaf. The epidermal cells are also often the first cells to confront invading pathogens, where ROS production is an early response, so it may be significant that it is also in these cells that the transmission of information from the PM by ROS diffusion would be more likely to take place because of a lower background concentration of H_2O_2.

It is a common observation that the cellular ROS production increases in plants in response to stress (Apel and Hirt, 2004). In non-photosynthetic cells, the presence of the mitochondrial alternative oxidase in the mitochondria is very important for keeping the cellular ROS level low, probably because it lowers the reduction level of the electron transport components that are responsible for mitochondrial ROS production (Maxwell et al., 1999; Møller,

2001). Consistent with this, the alternative oxidase is often induced by stress treatments (Gadjev et al., 2006) presumably to prevent the rise in ROS levels. It follows that ROS signaling is likely to occur in unstressed non-photosynthetic cells.

Relaying stations, such as the endoplasmic reticulum and the vacuole (Berridge, 1993; McAinsh and Hetherington, 1998; Stael et al., 2012), make up an important component in Ca^{2+}signaling, but none has been identified for hydrogen peroxide in plant cells. In animal cells, mitochondria are possible relaying stations (Zhou et al., 2010) for superoxide signaling, which may or may not work for plant mitochondria, given that the properties essential for the mechanism are not well described for plant mitochondria (Møller, 2001; Reape and McCabe, 2008).

In plant cells, mitochondria, peroxisomes, and plastids are potential relaying stations for H_2O_2 signaling, as they are known to produce ROS (Møller, 2001; Foyer and Noctor, 2003; Apel and Hirt, 2004). In fact, recently it was observed that the membrane potential of individual mitochondria oscillates *in vivo* as well as *in vitro* with pulse intervals of 5–50 s (i.e., frequencies of 0.02–0.2 Hz) and that this oscillation was affected by the redox state of the mitochondria (Schwarzländer et al., 2012). This could be an indication of a signaling network possibly involving ROS.

Even if H_2O_2 signaling by frequency- and amplitude-modulated waves occurs, we have little idea of how these signals are decoded. H_2O_2 is able to regulate genes as demonstrated in bacteria. A general trend in this regulation is that it involves the oxidation of a transcription factor thereby affecting its DNA-binding affinity (Lee and Helmann, 2006; Imlay, 2008). Whether such a system can decode a frequency- or amplitude-modulated signal is not known.

ACKNOWLEDGMENTS

This study was supported by grant 10-085228 from the Danish Council for Independent Research – Natural Sciences to Ian Max Møller.

REFERENCES

Alberts, B., Bray, D., Lewis, J., Raff, M., Roberts, K., and Watson, J. D. (1994). *Molecular Biology of the Cell*, 3rd Edn. New York, NY: Garland, 743–744.

Apel, K., and Hirt, H. (2004). Reactive oxygen species: metabolism, oxidative stress, and signal transduction. *Annu. Rev. Plant Biol.* 55, 373–399.

Berridge, M. J. (1993). Inositol triphosphate and calcium signaling. *Nature* 361, 315–325.

Bienert, G. P., Møller, A. L. B., Kristiansen, K. A., Schulz, A., Møller, I. M., Schjoerring, J. K., et al. (2007). Specific aquaporins facilitate the diffusion of hydrogen peroxide across membranes. *J. Biol. Chem.* 282, 1183–1192.

Bonifacio, A., Martins, M. O., Ribeiro, C. W., Fontenele, A. V., Carvalho, F. E. L., Margis-Pinheiro, M., et al. (2011). Role of peroxidases in the compensation of cytosolic peroxidase known down in rice plants under abiotic stress. *Plant Cell Environ.* 34, 1705–1722.

Dargan, S. L., and Parker, I. (2003). Buffer kinetics shape the spatiotemporal patterns of IP3-evoked Ca^{2+} signals. *J. Physiol.* 553.3, 775–788.

Falcke, M. (2003). Buffers and oscillations in intracellular Ca^{2+} dynamics. *Biophys. J.* 84, 28–41.

Foyer, C. H., and Noctor, G. (2003). Redox sensing and signaling associated with reactive oxygen in chloroplasts, peroxisomes and mitochondria. *Physiol. Plant.* 119, 355–364.

Gadjev, I., Vanderauwera, S., Gechev, T. S., Laloi, C., Minkov, I. N., Shulaev, V., et al. (2006). Transcriptomic footprints disclose specificity of reactive oxygen species signaling in Arabidopsis. *Plant Physiol.* 141, 436–445.

Goldstein, R. E., Tuval, I., and van de Meent, J.-W. (2008). Microfluidics of cytoplasmic streaming and its implications for intracellular transport. *Proc. Natl. Acad. Sci. U.S.A.* 105, 3663–3667.

Griffiths, D. J. (1999). *Introduction to Electrodynamics*, 3rd Edn. New Jersey: Prentice-Hall.

Halliwell, B., and Gutteridge, J. M. C. (2007). *Free Radicals in Biology and Medicine*. Oxford: Oxford University Press.

Hub, J. S., Aponte-Santamaría, C., Grubmüller, H., and de Groot, B. L. (2010). Voltage-regulated water flux through aquaporin channels in silico. *Biophys. J.* 99, L97–L99.

Imlay, J. A. (2008). Cellular defenses against superoxide and hydrogen peroxide. *Annu. Rev. Biochem.* 77, 755–776.

Jaffe, L. F. (1993). Classes and mechanisms of calcium waves. *Cell Calcium* 14, 736–745.

Jafri, M. S., and Keizer, J. (1995). On the roles of Ca^{2+} diffusion, Ca^{2+} buffers, and the endoplasmic reticulum in IP3-induced Ca^{2+} waves. *Biophys. J.* 69, 2139–2153.

Jensen, M. Ø., and Mouritsen, O. G. (2006). Single-channel water permeabilities of *Escherichia coli* aquaporins AqpZ and GlpF. *Biophys. J.* 90, 2270–2284.

Kristiansen, K. A., Jensen, P.-E., Møller, I. M., and Schulz, A. (2009). Technical focus: monitoring reactive oxygen species formation and localization in living cells by use of the fluorescent probe CM-H2DCFDA and confocal laser microscopy. *Physiol. Plant.* 136, 369–384.

Lee, J. W., and Helmann, J. D. (2006). The PerR transcription factor senses H2O2 by metal-catalysed histidine oxidation. *Nature* 440, 363–367.

Li, X., Wang, X., Yang, Y., Li, R., He, Q., Fang, X., et al. (2011). Single-molecule analysis of PIP2; 1 dynamics and partitioning reveals multiple modes of Arabidopsis plasma membrane aquaporin regulation. *Plant Cell* 23, 3780–3797.

Maurel, C., Sontoni, V., Luu, D.-T., Wudick, M. M., and Verdoucq, L. (2009). The cellular dynamics of plant aquaporin expression and functions. *Curr. Opin. Plant Biol.* 12, 690–698.

Maxwell, D. P., Wang, Y., and McIntosh, L. (1999). The alternative oxidase lowers mitochondrial reactive oxygen production in plant cells. *Proc. Natl. Acad. Sci. U.S.A.* 96, 8271–8276.

McAinsh, M. R., and Hetherington, A. M. (1998). Encoding specificity in Ca^{2+} signaling systems. *Trends Plant Sci.* 3, 32–36.

Mironova, L. A., and Mironov, S. L. (2008). Approximate analytical time-dependent solutions to describe large-amplitude local calcium transients in the presence of buffers. *Biophys. J.* 94, 349–358.

Mittler, R., Vanderauwera, S., Suzuki, N., Miller, G., Tognetti, V. B., Vandepoele, K., et al. (2011). ROS signaling – the new wave. *Trends Plant Sci.* 16, 300–309.

Møller, I. M. (2001). Plant mitochondria and oxidative stress. Electron transport, NADPH turnover and metabolism of reactive oxygen species. *Annu. Rev. Plant Physiol. Plant Mol. Biol.* 52, 561–591.

Møller, I. M., Jensen, P. E., and Hansson, A. (2007). Oxidative modifications to cellular components in plants. *Annu. Rev. Plant Biol.* 58, 459–481.

Møller, I. M., and Sweetlove, L. J. (2010). ROS signaling – specificity is required. *Trends Plant Sci.* 15, 370–374.

Neill, S., Desikan, R., and Hancock, J. (2002). Hydrogen peroxide signaling. *Curr. Opin. Plant Biol.* 5, 388–395.

Norris, M. G. S., and Malys, N. (2011). What is the true enzyme kinetics in the biological system? An investigation of macromolecular crowding effect upon enzyme kinetics of glucose-6-phosphate dehydrogenase. *Biochem. Biophys. Res. Commun.* 405, 388–392.

Parekh, A. B. (2011). Decoding cytosolic Ca^{2+} oscillations. *Trends Biochem. Sci.* 36, 78–87.

Raven, E. L. (2003). Understanding functional diversity and substrate specificity in haem peroxidases: what can we learn from ascorbate peroxidase? *Nat. Prod. Rep.* 20, 367–381.

Reape, T. J., and McCabe, P. F. (2008). Apoptotic-like programmed cell death in plants. *New Phytol.* 180, 13–26.

Schwarzländer, M., Logan, D. C., Johnston, I. G., Jones, N. S., Meyer, A. J., Fricker, M. D., et al. (2012). Pulsing of membrane potential in individual mitochondria: a stress-induced mechanism to regulate respiratory bioenergetics in Arabidopsis. *Plant Cell* 24, 1188–1201.

Stael, S., Wurzinger, B., Mair, A., Mehlmer, N., Vothknecht, U. C., and Teige, M. (2012). Plant organellar calcium signaling: an emerging field. *J. Exp. Bot.* 63, 1525–1542.

Straube, R., and Ridgway, D. (2009). Investigating the effects of molecular crowding on Ca^{2+} diffusion using a particle-based simulation model. *Chaos* 19, 037110.

van Stroe-Biezen, S. A. M., Everaerts, F. M., Janssen, L. J. J., and Tacken, R. A. (1993). Diffusion coefficients of oxygen, hydrogen peroxide and glucose in a hydrogel. *Anal. Chim. Acta* 273, 553–560.

Zhou, H., Rivas, G., and Minton, A. P. (2008). Macromolecular crowding and confinement: biochemical, biophysical , and potential physiological consequences. *Annu. Rev. Biophys.* 37, 375–397.

Zhou, L., Aon, M. A., Almas, T., Cortassa, S., Winslow, R. L., and O'Rourke, B. (2010). A reaction-diffusion model of ROS-induced ROS release in a mitochondrial network. *PLoS Comput. Biol.* 6:e1000657. doi:10.1371/journal.pcbi.1000657

Conflict of Interest Statement: The authors declare that the research was conducted in the absence of any commercial or financial relationships that could be construed as a potential conflict of interest.

Received: 18 September 2012; accepted: 10 December 2012; published online: 31 December 2012.

Citation: Vestergaard CL, Flyvbjerg H and Møller IM (2012) Intracellular signaling by diffusion: can waves of hydrogen peroxide transmit intracellular information in plant cells? Front. Plant Sci. ***3****:295. doi: 10.3389/fpls.2012.00295*

This article was submitted to Frontiers in Plant Physiology, a specialty of Frontiers in Plant Science.

Copyright © 2012 Vestergaard, Flyvbjerg and Møller. This is an open-access article distributed under the terms of the Creative Commons Attribution License, which permits use, distribution and reproduction in other forums, provided the original authors and source are credited and subject to any copyright notices concerning any third-party graphics etc.

frontiers in
PLANT SCIENCE

ORIGINAL RESEARCH ARTICLE
published: 01 November 2012
doi: 10.3389/fpls.2012.00234

Expression of ROS-responsive genes and transcription factors after metabolic formation of H_2O_2 in chloroplasts

Salma Balazadeh[1†], Nils Jaspert[2†], Muhammad Arif[1], Bernd Mueller-Roeber[1] and Veronica G. Maurino[2]*

[1] Institute of Biochemistry and Biology, University of Potsdam, Potsdam, Germany
[2] Plant Molecular Physiology and Biotechnology, Center of Excellence on Plant Sciences, Heinrich-Heine-University, Düsseldorf, Germany

Edited by:
Dario Leister,
Ludwig-Maximilians-University
Munich, Germany

Reviewed by:
Ian M. Møller, Aarhus University, Denmark
Jaakko Kangasjärvi, University of Helsinki, Finland
Haya Friedman, Volcani Center, ARO, Israel

***Correspondence:**
Veronica G. Maurino, Entwicklungs- und Molekularbiologie der Pflanzen, Heinrich-Heine-Universität, Universitätsstraße 1, 40225 Düsseldorf, Germany.
e-mail: veronica.maurino@uni-duesseldorf.de

† These authors equally contributed to this work.

Glycolate oxidase (GO) catalyses the oxidation of glycolate to glyoxylate, thereby consuming O_2 and producing H_2O_2. In this work, *Arabidopsis thaliana* plants expressing GO in the chloroplasts (GO plants) were used to assess the expressional behavior of reactive oxygen species (ROS)-responsive genes and transcription factors (TFs) after metabolic induction of H_2O_2 formation in chloroplasts. In this organelle, GO uses the glycolate derived from the oxygenase activity of RubisCO. Here, to identify genes responding to an abrupt production of H_2O_2 in chloroplasts we used quantitative real-time PCR (qRT-PCR) to test the expression of 187 ROS-responsive genes and 1880 TFs after transferring GO and wild-type (WT) plants grown at high CO_2 levels to ambient CO_2 concentration. Our data revealed coordinated expression changes of genes of specific functional networks 0.5 h after metabolic induction of H_2O_2 production in GO plants, including the induction of indole glucosinolate and camalexin biosynthesis genes. Comparative analysis using available microarray data suggests that signals for the induction of these genes through H_2O_2 may originate in the chloroplast. The TF profiling indicated an up-regulation in GO plants of a group of genes involved in the regulation of proanthocyanidin and anthocyanin biosynthesis. Moreover, the upregulation of expression of TF and TF-interacting proteins affecting development (e.g., cell division, stem branching, flowering time, flower development) would impact growth and reproductive capacity, resulting in altered development under conditions that promote the formation of H_2O_2.

Keywords: glycolate oxidase, H_2O_2, ROS-responsive genes, transcription factors

INTRODUCTION

Photosynthetic organisms are confronted with reactive oxygen species (ROS), such as singlet oxygen ($^1O_2$), the superoxide anion radical (O_2^-), the hydroxyl radical (OH·), and hydrogen peroxide (H_2O_2), which may cause oxidative stress and damage to important biological molecules (Apel and Hirt, 2004; Møller et al., 2007). Plants in their natural environments are often exposed to sudden increases in light intensity, which results in the absorption of excitation energy in excess of that required for metabolism. In chloroplasts, when absorbed energy is in excess at photosystem II (PSII), O_2^- is produced during the Mehler reaction by Fd-NADPH oxidase at PSI and is dismutated by superoxide dismutase (SOD) to H_2O_2 (Ort and Baker, 2002; Asada, 2006). The photorespiratory pathway consumes photosynthetic reducing energy and produces H_2O_2 in the peroxisomes through the action of glycolate oxidase (GO) (Maurino and Peterhansel, 2010). H_2O_2 is also produced during a variety of different reactions under stress conditions, often through the detoxification of $^1O_2$ and O_2^-. The generated H_2O_2 is scavenged by different antioxidant/enzyme reactions: the ascorbate and glutathione cycles, ascorbate peroxidase (APX), catalase, and peroxiredoxin (PRX) (Tripathi et al., 2009).

ROS generated in the chloroplast have been implicated as triggers of signaling pathways that influence expression of nuclear-encoded genes, which may initiate responses such as cell death or acclimation depending on the degree of the stress (Karpinski et al., 1999; Fryer et al., 2003; Op den Camp et al., 2003; Danon et al., 2005). H_2O_2 can take part in signaling acting as messenger either directly (e.g., by reversibly modifying critical thiol groups in target proteins; Neill et al., 2002) or by using an oxidized product as a secondary messenger (Møller et al., 2007). The H_2O_2-scavenging enzymes APX and dehydroascorbate reductase (DHAR) may act as highly efficient initiators of oxidative signaling by generating transient bursts of reduced glutathione. This in consequence triggers glutaredoxin-mediated protein oxidation (Neill et al., 2002). Crosstalk between redox pools of different cellular compartments, possibly transmitted by a redox shift in cellular components, has also been suggested to be important for control of the expression of nuclear genes (Baier and Dietz, 2005; Leister, 2005). A generalized model of H_2O_2 signal transduction pathways suggests that H_2O_2 may also directly oxidize transcription factors (TFs) in either the cytosol or the nucleus. Alternatively, H_2O_2-mediated activation of a signaling protein such as a protein kinase may activate TFs (Mittler

et al., 2004; Miao et al., 2007). TFs would interact with cognate H_2O_2-response elements in target gene promoters thereby modulating gene expression (Foyer and Noctor, 2005). Recently, Møller and Sweetlove (2010) put forward the hypothesis that H_2O_2 itself is unlikely to be the signaling molecule that selectively regulates nuclear-encoded chloroplastic genes but rather that oxidized peptides deriving from proteolysis of oxidized proteins would act as second messengers during retrograde ROS signaling. On the other hand, using spin trapping EPR spectroscopy in addition to chemical assays (employing Amplex Red reagent), Mubarakshina et al. (2010) showed that 5% of the H_2O_2 produced inside chloroplasts at high light intensities can actually be detected outside the organelles. This process may involve the pass of H_2O_2 through aquaporins (Bienert et al., 2007) and might be sufficient to trigger signaling processes outside the chloroplasts.

Desikan et al. (2001) showed that approximately 1% of the transcriptome was altered in H_2O_2-treated *Arabidopsis thaliana* (*A. thaliana*) cell cultures. Although H_2O_2-responsive promoters have been identified (Desikan et al., 2001), specific H_2O_2-regulatory DNA sequences and their cognate TFs have not been isolated and characterized. In more recent studies genes involved in H_2O_2 signal transduction have been identified or proposed, including mitogen-activated protein kinases (MAPKs), various TFs of e.g., the NAC, ZAT, and WRKY families, miRNAs and others (Van Breusegem et al., 2008; Li et al., 2011; Petrov and Van Breusegem, 2012). Moreover, using genome-wide analysis of catalase deficient *A. thaliana*, H_2O_2 was inferred to regulate the expression of genes encoding specific small heat shock proteins, several TFs and candidate regulatory proteins (Vandenabeele et al., 2004; Vanderauwera et al., 2005).

To date, it is not known to which extent the chemical specificity of the ROS and the cellular compartment of their release may contribute to the multiplicity of responses that occur in plants. A major challenge is to dissect the genetic networks that control ROS signaling and to assess specific and common responses toward different types of ROS signals. To this end, the molecular, biochemical and physiological responses of *A. thaliana* to elevated *in planta* levels of H_2O_2 were and are being investigated in various types of model systems including mutants altered in the ROS scavenging machinery (Maurino and Flügge, 2008). However, the analysis of dynamic physiological processes using (knock-out) mutants may not always be straightforward, especially when compensatory cellular mechanisms are induced. With respect to ROS-related mutants, changing the balance of scavenging enzymes may induce compensatory mechanisms such that signaling and oxidative damage effects may not be easily separated. Moreover, invasive experimental setups like the application of oxidative stress-causing agents may induce a non-specific oxidative stress that acts throughout the cell and triggers additional responses that may complicate the analysis of ROS signal transduction pathways (Maurino and Flügge, 2008). We have recently developed a tool to functionally dissect the action of plastid-generated H_2O_2, using plants overexpressing GO in plastids (GO plants; Fahnenstich et al., 2008). During photosynthesis, the oxygenase activity of ribulose 1,5-bisphosphate carboxylase/oxygenase (RubisCO) produces glycolate 2-phosphate within the chloroplasts, which is then dephosphorylated to glycolate by phosphoglycolate phosphatase (Maurino and Peterhansel, 2010). In GO plants, glycolate is oxidized to glyoxylate by the plastidic GO, with the parallel production of H_2O_2. When growing under moderate photon fluxes and ambient CO_2 concentration (photorespiratory conditions) the GO plants remain smaller than the wild type, presenting a reduced rosette diameter and yellowish leaves due to H_2O_2 accumulation (Fahnenstich et al., 2008). In contrast, in non-photorespiratory conditions (e.g., at high CO_2 concentration) the oxygenase activity of RubisCO is abolished and thus, the metabolic flux through GO is suppressed, allowing GO plants to grow like wild type (Fahnenstich et al., 2008). Transferring GO plants from high to ambient CO_2 concentration specifically induces H_2O_2 formation in the chloroplasts (Fahnenstich et al., 2008). These properties permit the modulation of plastidic produced H_2O_2 levels by changing light intensity and/or CO_2 levels (Maurino and Flügge, 2008). Moreover, H_2O_2 is specifically generated without a concomitant accumulation of superoxide or singlet oxygen, which are common precursors of H_2O_2 during ROS generation in chloroplasts. A similar experimental set-up was employed in previous studies using catalase null mutants in which the production of peroxisomal H_2O_2 is induced by changing the conditions of plant growth from non-photorespiratory to photorespiratory conditions (e.g., high light intensity) (Dat et al., 2000; Vandenabeele et al., 2004; Vanderauwera et al., 2005). The metabolic production of H_2O_2 may avoid the pleiotropic effects discussed above but it cannot be ruled out that ROS-unrelated pleiotropic reactions may occur in both approaches due to abrupt changes in CO_2 level or light intensity.

In this work we attempted to identify genes strongly responding to an abrupt production of H_2O_2 in chloroplasts of *A. thaliana*. To this end we tested the expressional changes of 187 nuclear-encoded ROS-responsive genes and 1880 TFs, using quantitative real-time (qRT)-PCR (Czechowski et al., 2004; Balazadeh et al., 2008; Wu et al., 2012) upon transfer of high CO_2-grown GO and wild-type (WT) plants to ambient CO_2 concentration. Our data revealed a rapid and coordinated expression response of ROS-affected genes of specific functional networks in GO including an early induction of indole glucosinolate and camalexin biosynthesis genes and an up-regulation of a group of genes involved in the regulation of proanthocyanidin and anthocyanin biosynthesis. Moreover, the upregulation of expression of TF and TF-interacting proteins affecting development (e.g., cell division, stem branching, flowering time, flower development) would impact growth and reproductive capacity, resulting in altered development under conditions that promote the formation of H_2O_2.

MATERIALS AND METHODS

PLANT MATERIAL

Arabidopsis thaliana (L.) Heynh. ecotype Columbia-0 (Col-0, wild-type) constitutively expressing glycolate oxidase (GO, At3g14420) in the plastids (GO plants) under the cauliflower mosaic virus 35S promoter were generated in our previous work (Fahnenstich et al., 2008). In these plants to direct the expression of GO to the chloroplats the stromal targeting presequence from

Arabidopsis thaliana phosphoglucomutase (At5g51820) was used (Fahnenstich et al., 2008). WT and GO transgenic plants were grown in pots containing 3 parts of soil (Gebr. Patzer KG, Sinntal-Jossa, Germany) and one part of vermiculite (Basalt Feuerfest, Linz, Austria) under a 16 h-light/8 h-dark regime at photosynthetically active photon flux densities (PPFD) of 75 μmol quanta m^{-2} s^{-1} at 22°C day/18°C night temperatures and a CO_2 concentration of 3000 ppm. After 3 weeks of growth plants were transferred to ambient CO_2 concentration (380 ppm) and the same PPFD. Whole rosettes were harvested at different time points after transfer, immediately frozen in liquid nitrogen and stored at −80°C until use for RNA isolation and H_2O_2 measurements.

ISOLATION OF RNA AND REAL-TIME PCR ANALYSIS

For the large-scale qRT-PCR analysis, total RNA was extracted from 100 mg leaves (fresh weight) using RNeasy Plant Mini kit (Qiagen, Valencia, USA) according to the manufacturer's protocol. DNAse I digestion was performed on 20–30 μg of total RNA using TURBO DNase Kit (Ambion, Cambridgeshire, UK) according to manufacturer's instructions. RNA integrity was checked on 1% (w/v) agarose gels and concentration measured with a Nanodrop ND-1000 spectrophotometer before and after DNAse treatment. Absence of genomic DNA was confirmed subsequently by quantitative PCR using primers that amplify an intron sequence of the gene At5g65080 (forward 5′-TTTTTTGCCCCCTTCGAATC-3′ and reverse 5′-ATCTTCCGCCACCACATTGTAC-3′). First-strand cDNA was synthesized from 8 μg to 10 μg of total RNA using RevertAid™ First Strand cDNA Synthesis Kit (Fermentas, St. Leon-Rot, Germany) following the manufacturer's protocol. The efficiency of cDNA synthesis was estimated by qRT-PCR using two different primer sets annealing to the 5′ and 3′ ends, respectively, of a control gene (At3g26650, *GAPDH*, glyceraldehyde-3-phosphate dehydrogenase). Primer sequences were as follows: for GAPDH3′, forward 5′-TTGGTGACAACAGGTCAAGCA-3′ and reverse 5′-AAACTTGTCGCTCAATGCAATC-3′; for GAPDH5′, forward 5′-TCTCGATCTCAATTTCGCAAAA-3′ and reverse 5′-CGAAACCGTTGATTCCGATTC-3′. Transcript levels of each gene were normalized to *ACTIN2* (At3g18780) transcript abundance (forward 5′-TCCCTCAGCACATTCCAGCAGAT-3′ and reverse 5′-AACGATTCCTGGACCTGCCTCATC-3′). A total of 187 ROS-responsive genes (Wu et al., 2012) and 1880 TFs (Czechowski et al., 2004; Balazadeh et al., 2008) were analyzed by qRT-PCR as previously described (Caldana et al., 2007; Balazadeh et al., 2008). PCR reactions were run on an ABI PRISM 7900HT sequence detection system (Applied Biosystems, Darmstadt, Germany), and amplification products were visualized using SYBR Green (Applied Biosystems).

H_2O_2 MEASUREMENTS

Levels of H_2O_2 were determined using the Amplex® Red Technology (Life Technologies, Darmstadt, Germany) following the manufacturer's instructions. Amplex Red (N-acetyl-3,7-dihydroxyphenoxazine) reacts with H_2O_2 in the presence of horseradish peroxidase and forms the fluorescent product resorufin. For the determinations, 100 mg leaves (fresh weight) were ground in liquid nitrogen into a fine powder and resuspended with 0.15 mL extraction buffer prepared as indicated by the manufacturer. This suspension was centrifuged at 4°C at 13,000 rpm for 15 min. Five μL of the supernatant, 45 μL distilled water and 50 μL of Amplex® Red solution were added to a microtitre plate. After 30 min incubation in the dark fluorescence was measured by excitation at 560 nm and emission reads at 590 nm. A calibration curve was established with known H_2O_2 concentrations.

GENE EXPRESSION NETWORK ANALYSIS

The two genes that were most strongly induced under photorespiratory conditions in GO plants at the 0.5 and 6 h time points (At3g02840 and At1g17180, respectively) were used as baits to identify globally coexpressed genes using the ATTED-II database (http://atted.jp), which allows evaluating genes that are coexpressed under five experimental conditions (tissue, abiotic stress, biotic stress, hormones, and light conditions) (Obayashi et al., 2009).

RESULTS AND DISCUSSION

INDUCTION OF H_2O_2 FORMATION IN GO PLANTS

The production of H_2O_2 in leaves of plants overexpressing GO in the plastids (Fahnenstich et al., 2008) was analyzed after activation of photorespiration by transferring high CO_2-grown plants to ambient-CO_2 conditions. As shown in **Table 1**, higher levels of H_2O_2 were determined in GO than in WT plants at 0.5 and 4 h after transfer while GO and WT plants maintained under non-photorespiratory conditions (3000 ppm CO_2) showed similar H_2O_2 levels at both time points (**Table 1**). Note, that as the measurements were performed using whole-leaf extracts the expected differences in chloroplastic H_2O_2 levels between GO and WT plants under photorespiratory condition may be higher than determined here.

EXPRESSION PROFILING OF ROS MARKER GENES IN GO AND WILD-TYPE PLANTS AFTER THE INDUCTION OF H_2O_2 FORMATION IN CHLOROPLASTS

To study the impact of an abrupt production of H_2O_2 in chloroplasts on nuclear gene expression, we analyzed transcript level changes of 187 ROS-responsive genes using a previously established qRT-PCR platform (detailed in Wu et al., 2012). The genes

Table 1 | Levels of H_2O_2 measured in whole rosettes (μmol/g FW) after shifting high CO_2-grown wild-type and GO plants to ambient CO_2 concentration for 0.5 and 4 h.

	0.5 h		4 h	
	High CO_2	Ambient CO_2	High CO_2	Ambient CO_2
WT	2.4 ± 0.2	2.3 ± 0.2	2.5 ± 0.4	2.7 ± 0.1
GO	2.5 ± 0.3	3.0 ± 0.3	2.6 ± 0.2	**3.4 ± 0.0**

Samples from control plants maintained in high CO_2 were processed in parallel. Values indicate the mean ± SE of three independent samples and those set in bold face indicate significant differences to the corresponding wild-type value calculated by Student's t-test ($P < 0.05$). WT, wild type.

included in the platform were chosen from published reports and our own experiments and represent four different groups that were already shown to be rapidly induced by (1) superoxide radical (O_2^-; 18 genes), (2) singlet oxygen ($^1O_2$; 22 genes), (3) H_2O_2 (53 genes), or (4) different types of ROS (general ROS-responsive genes; 94 in total).

Gene expression was analyzed in whole rosettes of 3-week-old WT and GO plants at 0.5, 4, 6, and 12 h after shifting high-CO_2-grown plants (non-photorespiratory condition) to ambient CO_2 concentration (photorespiratory condition). Expression profiling was performed in two biological replicates and log-fold change (log2 FC) ratios of expression changes were calculated for GO and WT plants by comparing gene expression levels before and after the CO_2 concentration shift. A total of 131 genes were expressed in all examined samples (**Table A1** in Appendix). The remaining 56 genes did not yield detectable PCR amplicons, indicating no or marginal expression under our experimental conditions.

Considering a 3-fold expression difference cut-off, 120 genes displayed differential expression in GO and/or WT plants upon transfer from high to ambient CO_2 concentration; the vast majority of the affected genes (116 in total) were up-regulated, and only four genes were down-regulated (**Figure 1**, **Table A1** in Appendix). Most noticeably, expression of 58 genes was induced in GO plants already within 0.5 h after the transfer to ambient CO_2 condition, whilst only a single gene was induced in the wild type at the same time point (**Figure 1**). Importantly, however, many genes showed also high expression in the wild type at later time points after the CO_2 concentration shift, but the expressional changes were in most cases more pronounced in GO than WT plants (**Figure 1**, and section "Early Induction of Indole Glucosinolate and Camalexin Biosynthesis Genes in GO Plants"). Thus, our data indicate that similar sets of ROS-responsive genes responded to the CO_2 shift in GO and WT plants; however, the dynamics of the transcriptional responses were clearly different in the two types of plants, being faster and more prominent in the GO plants.

EARLY INDUCTION OF INDOLE GLUCOSINOLATE AND CAMALEXIN BIOSYNTHESIS GENES IN GO PLANTS

To identify transcripts responsive to metabolically produced H_2O_2 we focused our analysis on the 0.5- and 6-h time points. Genes were considered differentially expressed when the fold change was more than 3-fold ($\log_2 \geq 1.56$).

At 0.5 h after shifting plants to ambient CO_2 concentration, 58 of the 131 expressed genes were induced in GO plants by more than 3-fold, whilst in the wild type the expression change was less than 3-fold, suggesting that these genes participate in early signaling steps triggered by the production of H_2O_2 under photorespiratory conditions (**Table 2**). After 6 h, seven of these genes showed WT levels of expression (below 3-fold), while 29 were further overexpressed only in GO (**Table 2**). Although at 6 h after transfer to ambient CO_2 the expression fold-change (FC) of the remaining 22 genes was higher than 3 in both, GO and WT plants, the expression change between GO and WT (FC_{GO}/FC_{WT}) was higher than 2 for 16 of these genes (**Table 2**), indicating that their higher expression in GO plants was triggered by the elevated levels of H_2O_2.

Later responding genes, which were affected only after 6 h under photorespiratory conditions, were also identified. From the 23 genes that showed an expression change of above 3-fold in GO, 13 were only induced in GO, while 10 genes were induced in both, GO and WT. The FC ratio in GO and WT (FC_{GO}/FC_{WT}) was above 2 for the 10 genes (**Table 3**), indicating that their expression in GO plants is controlled by the higher levels of H_2O_2, similar to the early-responsive genes.

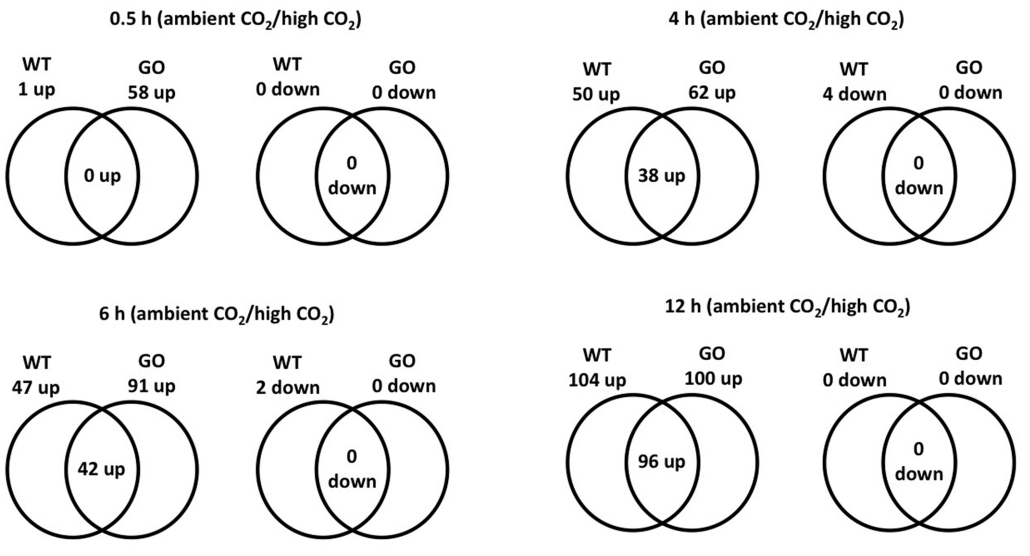

FIGURE 1 | Venn diagram of the number of ROS-responsive genes differentially expressed in wild-type and GO plants at different time points (0.5, 4, 6, and 12 h) after the transfer of plants grown at high CO_2 concentration (3000 ppm) to ambient CO_2 concentration (380 ppm).

Table 2 | ROS-responsive genes (58 in total) the expression of which was enhanced by more than 3-fold in GO plants 0.5 h after shifting plants grown at high CO_2 concentration (3000 ppm) to ambient CO_2 concentration (380 ppm).

AGI	0.5 h			6 h			Annotation
	FC_{WT}	FC_{GO}	FC_{GO}/FC_{WT}	FC_{WT}	FC_{GO}	FC_{GO}/FC_{WT}	
UP-REGULATED IN GO AT 0.5 H							
At1g69890	1.3	15.9	**12.0**	1.2	2.2	1.8	Protein of unknown function
At2g40000*	0.9	10.2	**11.2**	1.6	2.1	1.3	Ortholog of sugar beet HS1 PRO-1 2 (HSPRO2)
At2g18210	1.0	8.4	**8.2**	1.1	2.9	**2.6**	Protein of unknown function
At1g18570	1.2	6.8	**5.7**	0.7	2.5	**3.6**	Myb-type transcription factor (HIG1/MYB51)
At1g21100	1.6	6.9	**4.2**	0.7	1.5	**2.2**	Indole glucosinolate O-methyltransferase (IGMT1)
At5g64310	1.2	3.8	**3.1**	3.1	1.1	0.4	Arabinogalactan protein (AGP1C) of unknown function
At5g28630	1.4	4.0	**2.9**	0.3	0.4	1.5	Protein of unknown function
UP-REGULATED IN GO AT 0.5 H AND 6 H CHANGE IN GENE EXPRESSION IN WT AT 6 H < 3							
At3g02840*	1.1	79.3	**71.2**	2.9	65.4	**22.8**	Putative U-box-type E3 ubiquitin ligase
At2g37430*	0.9	53.3	**62.7**	1.9	190.8	**100.9**	C2H2 and C2HC zinc fingers superfamily protein (ZAT11)
At1g05575*	1.5	45.6	**29.9**	0.6	4.3	**6.8**	Protein of unknown function
At2g38470	1.4	31.5	**22.3**	1.8	7.5	**4.3**	WRKY-type transcription factor (WRKY33)
At4g17490	1.5	21.5	**14.7**	1.3	6.9	**5.2**	Ethylene-responsive element binding factor (ERF6)
At5g47230	1.3	17.4	**13.8**	1.5	4.4	**3.0**	Ethylene-responsive element binding factor (ERF5)
At1g66060	1.3	17.5	**13.2**	2.7	5.1	1.9	Protein of unknown function
At2g32030	1.3	16.4	**12.2**	1.9	24.5	**12.9**	Putative GNAT-type N-acetyltransferase
At2g26530*	1.2	13.3	**10.7**	2.1	5.4	**2.5**	Protein of unknown function; AR781
At1g21120	1.0	9.9	**10.3**	0.7	15.9	**22.1**	Indole glucosinolate O-methyltransferase (IGMT2)
At1g35210	1.1	11.2	**10.2**	2.9	14.4	**4.9**	Protein of unknown function
At3g55980*	1.4	14.3	**10.1**	1.2	4.0	**3.3**	Salt-inducible zinc finger 1, SZF1 (C3H47)
At2g33710	1.0	7.5	**7.7**	0.8	12.6	**15.0**	Putative ERF-type transcription factor
At2g25735*	1.8	10.8	**5.9**	0.6	3.2	**5.7**	Protein of unknown function
At5g54490	1.5	7.8	**5.3**	1.5	4.1	**2.8**	PBP1, Pinoid Binding Protein 1
At1g19020*	1.8	9.3	**5.1**	1.9	27.7	**14.5**	Protein of unknown function
At5g51190	1.4	6.8	**4.9**	1.8	5.0	**2.7**	Putative ERF-type transcription factor
At3g02800*	1.1	5.0	**4.5**	1.2	4.1	**3.4**	Tyrosine phosphatase (ATPFA-DSP3)
At5g64905	1.4	6.0	**4.4**	2.1	33.0	**16.0**	Putative peptide elicitor Pep3 precursor protein (ProPep3)
At1g76600*	1.4	5.8	**4.3**	1.7	11.0	**6.3**	Protein of unknown function
At3g23230	2.2	9.4	**4.2**	2.3	17.1	**7.5**	Putative ERF-type transcription factor (ERF98)
At1g59590	1.3	5.2	**4.1**	1.4	5.2	**3.8**	Zinc finger protein (ZCF37) of unknown function
At4g18880*	1.6	6.5	**4.0**	1.9	4.6	**2.4**	Heat stress-type transcription factor (HsfA4a/HSF21)
At2g41640	1.1	4.0	**3.7**	2.2	6.0	**2.7**	Protein of unknown function
At1g28190*	1.1	3.9	**3.5**	2.4	5.6	**2.3**	Protein of unknown function
At5g57220	2.8	9.1	**3.3**	1.3	6.9	**5.2**	Cytochrome P450 monooxygenase (CYP81F2)
At1g26380*	1.2	3.4	**3.0**	2.1	39.0	**18.9**	UDP-N-acetylmuramate dehydrogenase of unknown function
At2g31945	1.3	3.5	**2.7**	2.3	5.1	**2.2**	Protein of unknown function
At4g11280	1.5	3.0	**2.0**	1.4	5.9	**4.3**	1-Aminocyclopropane-1-carboxylate synthase (ACS6)
CHANGE IN GENE EXPRESSION IN WT AT 6 H > 3							
At1g80840	1.1	38.0	**35.4**	5.5	56.4	**10.3**	WRKY-type transcription factor (WRKY40)
At5g04340*	0.8	27.5	**32.6**	7.3	8.6	**1.2**	C2H2-zinc-finger-TF (C1-2iD-04) of unknown function
At2g22880	1.7	50.8	**29.4**	6.2	28.1	**4.5**	Protein of unknown function
At1g27730	1.1	30.1	**26.8**	6.0	28.0	**4.7**	C2H2-zinc-finger-TF (ZAT10/STZ)
At5g27420	1.2	32.7	**26.3**	3.0	15.0	**5.0**	Putative ubiquitin ligase, ATL subfamily (ATL31)
At1g61340	1.5	24.3	**16.3**	6.6	10.5	1.6	ATFBS1. F-Box stress induced 1 of unknown function
At5g59820	1.0	14.3	**14.1**	4.6	61.7	**13.5**	C2H2-zinc-finger-TF (ZAT12)
At5g24110*	1.0	13.3	**13.8**	3.3	91.2	**28.0**	WRKY-type transcription factor (WRKY30)
At4g24570	1.4	18.8	**13.6**	3.6	3.3	0.9	Dicarboxylate carrier (DIC2)

(Continued)

Table 2 | Continued

AGI	0.5 h			6 h			Annotation
	FC_{WT}	FC_{GO}	FC_{GO}/FC_{WT}	FC_{WT}	FC_{GO}	FC_{GO}/FC_{WT}	
At3g10930	1.7	19.0	**11.5**	8.5	38.8	**4.6**	Protein of unknown function
At3g25250*	1.5	17.3	**11.4**	11.1	153.6	**13.8**	Putative protein kinase (AGC2/OXI1)
At4g39670*	1.3	14.3	**10.7**	31.7	184.9	**5.8**	Sphingosine transfer protein; accelerated death 11 (ACD11)
At1g77450*	0.8	7.3	**9.5**	5.6	6.9	1.2	NAC-type transcription factor (ANAC032)
At1g72520	1.7	15.7	**9.3**	4.8	9.7	**2.0**	Lipoxygenase (LOX4)
At3g48650	1.9	14.8	**7.6**	6.2	7.4	1.2	14a-related protein of unknown function
At4g21390	1.8	13.0	**7.0**	6.5	28.9	**4.4**	Putative S-domain-type receptor protein kinase
At5g63790*	0.8	5.4	**7.0**	3.1	11.1	**3.6**	NAC-type transcription factor (ANAC102)
At4g37370	1.4	7.0	**5.0**	2.8	67.5	**24.1**	Cytochrome P450 monooxygenase (CYP81D8)
At1g63720	1.5	5.0	**3.2**	3.1	6.1	1.9	Hydroxyproline-rich glycoprotein family protein
At2g18690	1.5	4.4	**3.0**	6.6	24.7	**3.7**	Protein of unknown function
At1g05340*	1.2	3.4	**2.7**	4.3	7.9	1.8	Protein of unknown function
At1g57630	1.4	3.4	**2.4**	20.2	36.0	1.8	Protein of unknown function

Genes are listed according to the difference of the expression change between GO and wild-type (WT) plants (FC_{GO}/FC_{WT}) at 0.5 h. FC_{GO}/FC_{WT} values higher than 2 are shown in bold face. AGI: gene identification number given by the Arabidopsis Genome Initiative. Genes also induced in catalase loss-of function mutants are highlighted with an asterisk (*) (Inzé et al., 2012). Genes included in the same gene coexpression network of At3g02840 (putative U-box-type E3 ubiquitin ligase) are highlighted in bold face (http://atted.jp; Obayashi et al., 2009). The gene annotation was retrieved from TAIR (http://arabidopsis.org/index.jsp).

The most highly up-regulated gene in GO plants at 0.5 h after induction of H_2O_2 production was At3g02840 (encoding a putative U-box-type E3 ubiquitin ligase, known to respond immediately-early to fungal elicitation) (**Table 2**). We used the ATTED-II database (http://atted.jp; Obayashi et al., 2009) to discover genes coexpressed with At3g02840 and observed that 45 of the 58 genes induced at 0.5 h after induction of H_2O_2 production cluster together (**Table 2**), indicating that metabolically produced H_2O_2 in GO plants induces the coordinate expression of functionally related genes. A similar analysis using the most highly expressed gene at 6 h after induction of H_2O_2 production (At1g17180, encoding glutathione S-transferase Tau 25) indicated that another group of eight genes are coordinately expressed in GO plants at this later time point (**Table 3**).

Recently, Inzé et al. (2012) listed the 85 most strongly H_2O_2-responsive genes in catalase loss-of-function mutants shifted from low- to high-light conditions, where H_2O_2 is produced in peroxisomes by the action of photorespiratory GOs. Interestingly, 23 of the 81 genes, which changed their expression in the GO plants were also differentially expressed in catalase loss-of-function mutants (**Tables 2** and **3**), indicating that they respond to enhanced levels of H_2O_2 independent of the site of its generation; the remaining genes may then represent candidates preferentially responsive to H_2O_2 produced in chloroplasts. Many of the genes up-regulated in GO plants encode proteins or TFs of currently unknown specific functions. Interestingly, however, several of the early-responsive genes are involved in tryptophan-derived biosynthesis of the phytoanticipins camalexin and indole glucosinolates, i.e., secondary metabolites that have antifungal and insect-deterring functions (Kliebenstein et al., 2001; Bednarek et al., 2009). These genes encode (1) the transcription factor WRKY33 (At2g38470), which is involved in controlling camalexin biosynthesis (Birkenbihl et al., 2012); (2) the Myb-type transcription factor HIG1/MYB51 (At1g18570) involved in the positive regulation of indole glucosinolate biosynthesis by activating several target genes (Gigolashvili et al., 2007); (3) the O-methyltransferases IGMT1 (At1g21100) and IGMT2 (At1g21120), which catalyze the transfer of a methyl group to the hydroxy indole glucosinolate hydroxyindol-3-ylmethylglucosinolate (4 and 1OH-I3M, respectively) to form methoxyindol-3-ylmethylglucosinolate (4 and 1MO-I3M, respectively) (Pfalz et al., 2011); and (4) cytochrome P450 monooxygenase CYP81F2 (At5g57220), that is essential for the pathogen-induced accumulation of 4-methoxyindol-3-ylmethylglucosinolate (4MI3G) (Bednarek et al., 2009). Our data thus show the early induction of indole glucosinolate and camalexin biosynthesis genes in GO plants after metabolic formation of H_2O_2 through the activation of genes encoding enzymes involved in intermediate metabolite conversions and of TFs that act on several target genes of these biosynthetic pathways.

TRANSCRIPTION FACTOR PROFILING

To understand the potential effects of overexpression of GO in chloroplasts on the nuclear transcriptional program, we next broadened our analysis by testing the expression of 1880 TFs using a highly sensitive quantitative real-time PCR (qRT-PCR) platform (Czechowski et al., 2004; Balazadeh et al., 2008). Considering the data obtained from the profiling of the ROS-responsive genes, we analyzed the expression at 0.5 h after induction of H_2O_2 production to capture the early-responsive TFs. Expression profiling was performed in two biological replicates and log-fold change (log2 FC) ratios of expression changes were calculated for GO and WT plants by comparing gene expression levels before and after the transfer of plants grown at high CO_2 to ambient CO_2.

Table 3 | ROS-responsive genes (23 in total) the expression of which was enhanced more than 3-fold in GO plants 6 h after shifting plants grown at high CO_2 concentration to ambient CO_2 concentration.

AGI	0.5 h			6 h			Annotation
	FC_{WT}	FC_{GO}	FC_{GO}/FC_{WT}	FC_{WT}	FC_{GO}	FC_{GO}/FC_{WT}	
UP-REGULATED IN GO AT 6 H CHANGE IN GENE EXPRESSION IN WT < 3							
At1g26420	1.5	1.6	1.1	2.4	17.6	**7.3**	Putative reticuline dehydrogenase
At2g15480	1.0	2.8	**2.8**	1.2	7.2	**6.0**	UDP-dependent glycosyl transferase (UGT73B5)
At1g10040	1.2	1.8	1.5	2.1	10.4	**5.0**	Putative hydrolase
At2g29490	0.7	1.9	**2.8**	2.3	10.4	**4.5**	Tau glutathione S-transferase (GSTU1)
At5g46080	1.1	1.9	1.8	1.2	3.7	**3.1**	Putative protein kinase
At1g80820	1.2	1.5	1.3	2.5	7.8	**3.1**	Cinnamoyl CoA reductase, involved in lignin biosynthesis
At3g09410	1.2	0.8	0.7	1.2	3.2	**2.7**	Putative pectin acetylesterase
At2g29500*	1.0	1.1	1.2	1.5	3.8	**2.5**	HSP20-type protein (HSP17.6B-CI); unknown function
At4g22530*	1.3	0.8	0.7	2.4	5.9	**2.4**	Putative methyltransferase
At4g15975	1.7	1.3	0.7	1.6	3.7	**2.4**	Putative ubiquitin ligase (RRE4/ATL17)
At2g38340	1.0	0.7	0.7	2.7	6.1	**2.2**	Putative AP2-type transcription factor (DREB2E)
At3g13790	1.3	1.3	1.1	2.5	5.0	**2.0**	Putative cell wall invertase (CwINV1)
At1g76070	1.2	2.6	**2.2**	1.6	3.3	**2.0**	Protein of unknown function
CHANGE IN GENE EXPRESSION IN WT > 3							
At1g17180	0.6	0.9	1.4	7.5	104.0	**13.8**	Tau glutathione S-transferase (GSTU25)
At1g15520	1.2	0.8	0.7	12.4	111.9	**9.0**	ABC transporter (ABCG40/PDR12)
At1g17170	1.0	1.3	1.4	5.7	40.4	**7.0**	Tau glutathione S-transferase (GSTU24)
At1g74360	1.0	2.2	**2.2**	4.2	14.2	**3.4**	Putative LRR-type receptor protein kinase
At2g38250*	1.2	1.7	1.4	4.4	13.7	**3.1**	Putative trihelix-type transcription factor
At5g51060	1.3	1.0	0.7	14.4	44.0	**3.1**	Respiratory burst oxidase homolog (AtRBOHC/RHD2)
At5g20230	1.5	2.8	1.8	9.9	28.3	**2.9**	Senescence associated gene (BCB/SAG14)
At2g41380	1.1	1.2	1.1	9.6	21.2	**2.2**	Putative S-adenosyl-L-methionine-dependent methyltransferase
At1g13340	1.0	2.1	**2.0**	3.4	6.8	**2.0**	Protein of unknown function
At5g48850	1.1	0.8	0.7	3.3	7.4	**2.2**	Protein of unknown function (ATSDI1)

Genes are listed according to the difference of the expression change between GO and wild-type (WT) plants (FC_{GO}/FC_{WT}) at 6 h. FC_{GO}/FC_{WT} values higher than 2 are shown in bold face. AGI: gene identification number given by the Arabidopsis Genome Initiative. Genes also induced in catalase loss-of function mutants are highlighted with an asterisk (*) (Inzé et al., 2012). Genes included in the same gene coexpression network of At1g17180 (GSTU25) are highlighted in bold face (http://atted.jp; Obayashi et al., 2009). The gene annotation was retrieved from TAIR (http://arabidopsis.org/index.jsp).

TFs most strongly responding to H_2O_2 were identified by comparing their expression FC in GO and WT plants. A TF was considered differentially expressed when the FC in GO was more than 3-fold ($\log_2 \geq 1.56$) and less than 2-fold in the wild type ($\log_2 \geq 1.0$) (**Table 4**). Analysis of transcript profiles revealed that the expression of 1449 genes, representing 77% of all TF genes tested, could be detected (**Table A2** in Appendix). The remaining 23% (431 of the 1880 TFs) did not yield detectable PCR amplicons, indicating no or very weak expression in the tested material.

At 0.5 h after shifting plants to ambient CO_2 concentration, 78 of the 1449 genes were induced by more than 3-fold in GO plants, whereas in WT plants the expression changes of the same genes were less than 2-fold (**Table 4**). Using published data the involvement/participation of the TFs in specific biological processes (**Table 4**) could be assessed, which allowed the classification of the TFs into five functional groups (FG) enriched with specific gene ontology categories (**Figure 2**). FG1 contains TFs involved in the regulation of proanthocyanidin and anthocyanin biosynthesis (**Table 4** and **Figure 2**). The TFs TT8 and MYB75 affecting the gene expression of dihydroflavonol 4-reductase (Debeaujon et al., 2003) are included in this FG. FG2 contains TFs affecting developmental processes like lateral root formation (GATA23), flowering (FD1, ANAC089, TEM2 and SNZ), shoot branching (MYB2 and BRC2), senescence (ANAC092/ORE1) and cell division (ANAC068 and HAT4) (**Table 4** and **Figure 2**). The activation of these TFs in GO plants would result in altered growth and flowering (see below and Fahnenstich et al., 2008). FG3 includes TFs and TF-interacting proteins negatively regulating jasmonate (JA) signaling (*JAZ7*, *JAZ8*, *JAZ9*, *JAZ10*, *WRKY50*, and *WRKY51*; Chico et al., 2008; Staswick, 2009; Gao et al., 2011) (**Table 4** and **Figure 2**). JAZ proteins bind directly to the key transcription factor MYC2 and thereby prevent JA-dependent gene transcription (Chini et al., 2007; Pauwels et al., 2010). At the same time *JAZ* genes are rapidly induced by JA and some are MYC2-regulated. This feedback loop regulation would provide a rapid on and off switch of the pathway involving JA. Transcriptional activation of *JAZ* genes was found to occur in response to several biotic

Table 4 | Transcription factors the expression of which was enhanced by more than 3-fold in GO plants, but less than 2-fold in wild-type plants 0.5 h after shifting plants grown at high CO_2 concentration to ambient CO_2 concentration.

AGI	0.5 h after transfer to ambient CO_2			Gene family	Annotation	Function	FG
	FC_{WT}	FC_{GO}	FC_{GO}/FC_{WT}				
At5g19790	0.2	26.9	176.5	AP2/EREBP	RAP2.11	Modulates response to low potassium	4
At5g56200	0.1	14.5	169.0	C2H2	C1-4iB-01	Unknown function	5
At5g32460	1.3	123.7	92.9	B3	B3	Unknown function	5
At4g09820	0.8	34.4	45.5	bHLH	TT8	Regulation of proanthocyanidin and anthocyanin biosynthesis; affects dihydroflavonol 4-reductase gene expression.	1
At2g37430	1.9	80.4	43.3	C2H2	ZAT11	Unknown function	5
At1g48150	0.1	3.6	38.9	MADS	AGL74	Unknown function	5
At2g34600	0.4	8.4	24.1	ZIM	JAZ7	Jasmonate signaling; cambium regulator	3
At3g07260	0.8	19.0	22.7	FHA		Unknown function	5
At1g66380	1.9	40.0	21.6	MYB	MYB114	Regulates later steps of anthocyanin biosynthesis	1
At1g27730	1.8	36.3	20.5	C2H2	ZAT10/STZ	Involved in plant defense responses	4
At1g56650	0.6	12.1	20.1	MYB	MYB75	Involved in anthocyanin metabolism; regulates dihydroflavonol reductase expression	1
At5g37415	0.5	8.8	17.6	MADS	AGL105	Unknown function	5
At3g53340	0.4	6.5	17.5	CCAAT-HAP3	NF-YB10	Unknown function	5
At4g00250	0.4	6.3	16.8	GeBP	–	Indirect regulation of cytokinin response genes	2
At5g26930	0.7	9.6	13.5	C2C2(Zn)GATA	GATA-23	Controls lateral root founder cell specification	2
At4g26930	0.4	4.6	13.0	MYB	MYB97	Unknown function	5
At1g48000	1.3	13.8	11.1	MYB	MYB112	Unknown function	5
At5g51190	1.9	18.5	9.9	AP2/EREBP	–	Unknown function	5
At5g43540	0.4	3.2	8.8	C2H2	C1-1iAf-03	Unknown function	5
At3g55980	1.9	15.7	8.4	C3H	SZF1	Regulates salt stress responses	4
At1g74080	0.5	4.0	8.3	MYB	MYB122	Activator of the indole glucosinolate biosynthesis	4
At1g68880	0.6	5.1	8.1	bZIP	bZIP8	Unknown function	5
At4g35900	1.0	7.5	8.0	bZIP	bZIP14/FD-1	Required for regulation of flowering	2
At1g30135	0.8	5.9	7.6	ZIM	JAZ8	Represses jasmonate-regulated growth and defense responses	3
At4g01350	0.6	4.6	7.5	CHP-rich	–	Intracellular signal transduction, oxidation-reduction process, response to chitin	4
At1g43160	1.2	8.8	7.5	AP2/EREBP	RAP2.6	Regulation of development	2
At5g26170	0.8	6.3	7.5	WRKY	WRKY50	Repression of jasmonate-mediated signaling	3
At1g29280	0.8	5.5	7.2	WRKY	WRKY65	Unknown function	5
At1g75540	0.8	5.2	6.8	C2C2(Zn)CO	STH2	Positive regulation of photomorphogenesis	4
At2g33710	1.9	11.4	5.9	AP2/EREBP	ERF112	Unknown function	5
At3g01600	0.6	3.6	5.8	NAC	ANAC044	Unknown function	5
At5g27050	1.4	8.2	5.7	MADS	AGL101	Unknown function	5
At5g01380	0.9	5.3	5.7	Trihelix	–	Unknown function	5
At1g65130	1.2	6.4	5.5	C2H2	C2-1iB-03	Unknown function	5
At5g23260	1.0	5.4	5.4	MADS	AGL32/TT16	Regulates proanthocyanidin biosynthesis	1
At3g11580	0.9	4.6	5.4	ABI3/VP1	AP2/B3-like	Seed development	2
At3g56770	0.8	4.5	5.3	bHLH	–	Unknown function	5
At1g65110	0.6	3.2	5.1	C2H2	C2-1iB-01	Unknown function	5
At2g47190	1.2	6.0	4.9	MYB	MYB2	Inhibits cytokinin-mediated branching at late stages of development	2
At5g52260	1.0	4.7	4.8	MYB	MYB19	Unknown function	5
At5g39610	1.1	5.5	4.8	NAC	ANAC092/ORE1	Regulator of leaf senescence	2
At4g18880	1.6	7.4	4.6	HSF	HsfA4a/HSF21	Unknown function	5

(Continued)

Table 4 | Continued

AGI	0.5 h after transfer to ambient CO_2			Gene family	Annotation	Function	FG
	FC_{WT}	FC_{GO}	FC_{GO}/FC_{WT}				
At4g37610	1.1	4.8	4.3	TAZ	BTB5	Unknown function	5
At1g18960	1.3	5.4	4.3	MYB	–	Unknown function	5
At5g02470	0.8	3.2	4.0	E2F/DP	DPA	Endoreduplication control	2
At5g26880	1.0	3.8	3.9	MADS	AGL26	Unknown function	5
At1g68800	0.9	3.5	3.8	TCP	TCP12/BRC2	Prevents axillary bud development and outgrowth	2
At5g07500	1.9	7.0	3.7	C3H	C3H54	Required for heart-stage embryo formation	2
At4g01540	1.3	4.2	3.4	NAC	ANAC068	Mediates cytokinin signaling during cell division	2
At5g51780	1.6	5.4	3.3	bHLH	–	Unknown function	5
At2g42150	1.1	3.5	3.2	BD	–	Unknown function	5
At5g13220	1.1	3.4	3.2	ZIM	JAZ10/TIFY9	Jasmonate signaling repressor	3
At5g22290	1.2	3.8	3.1	NAC	ANAC089	Negative regulator of floral initiation	2
At2g13150	1.0	3.1	3.1	bZIP	bZIP31	Unknown function	5
At1g70700	1.1	3.3	3.0	ZIM	JAZ9	Jasmonate signaling repressor	3
At5g62320	1.2	3.5	3.0	MYB	MYB99	Unknown function	5
At4g39070	1.2	3.5	2.9	C2C2(Zn)CO	DBB2	Unknown function	5
At2g30250	1.6	4.4	2.8	WRKY	WRKY25	Involved in response to various abiotic stresses	4
At5g64810	1.7	4.8	2.8	WRKY	WRKY51	Repression of jasmonate-mediated signaling	3
At3g05800	1.9	5.3	2.7	bHLH	AIF1	Involved in brassinosteroid signaling	4
At3g01970	1.4	3.8	2.6	WRKY	WRKY45	Unknown function	5
At1g75490	1.7	4.4	2.7	AP2/EREBP	DREB2D	Unknown function	5
At1g68840	1.2	3.1	2.5	AP2/EREBP	RAV2/TEM2	Repressor of flowering	2
At1g79180	1.4	3.3	2.5	MYB	MYB63	Activates secondary wall biosynthesis	2
At4g09460	1.7	3.6	2.2	MYB	MYB8	Unknown function	5
At1g66600	1.4	3.0	2.1	WRKY	WRKY63	Involved in the regulation of responses to ABA and drought stress	4
At2g43500	1.5	3.1	2.1	NIN-like	–	Unknown function	5
At4g01520	1.8	3.7	2.0	NAC	ANAC067	Unknown function	5
At1g21000	1.6	3.2	2.0	PLATZ	–	Unknown function	5
At3g27810	1.7	3.4	2.0	MYB	MYB21	Petal and stamen development	2
At5g67300	1.6	3.1	1.9	MYB	MYB44	Regulates ethylene signaling	4
At2g39250	1.7	3.1	1.8	AP2/EREBP	SNZ	Represses flowering	2
At4g16780	1.7	3.1	1.8	HB	HB2/HAT4	Involved in cell expansion and cell proliferation	2
At4g24240	1.8	3.2	1.8	WRKY	WRKY7	Involved in plant defense responses	4
At4g01930	1.8	3.1	1.7	BPC/BRR	–	Unknown function	5
At5g62020	1.8	3.1	1.7	HSF	HsfB2a/HSF6	Unknown function	5
At2g43000	1.9	3.2	1.7	NAC	JUB1/ANAC042	Regulates camalexin biosynthesis and longevity	4
At4g17785	1.9	3.2	1.6	MYB	MYB39	Unknown function	5

Genes are listed according to the difference of the expression change between GO and wild-type (WT) plants (FC_{GO}/FC_{WT}). AGI: gene identification number given by the Arabidopsis Genome Initiative. A function was described for a gene when its involvement in a biological process/function was experimentally backed up as described in PubMed (www.ncbi.nlm.nih.gov/pubmed) or TAIR (http://arabidopsis.org/index.jsp). FG: functional group.

and abiotic challenges (Yan et al., 2007). JAZ proteins would also exert their effects on post-wound inhibition of vegetative growth in *A. thaliana* (Yan et al., 2007) and as repressors of necrosis and/or programmed cell death during development in tobacco (Oh et al., 2012). In GO plants, the action of *JAZ* genes together with those of FG2 would impact growth and reproductive capacity, resulting in altered development under conditions that promote the formation of H_2O_2. FG4 includes TFs with diverse functions in plant defense and signaling, e.g., activators of tryptophan-derived biosynthesis of camalexin (JUB1/ANAC042) and indole glucosinolates (MYB122), as well as regulators of photomorphogenesis (STH2) (**Table 4** and **Figure 2**). The early activation of camalexin and indole glucosinolate biosynthesis was also observed in the analysis performed with the ROS-responsive gene platform (**Table 1**). Finally, FG5 includes TFs with currently unknown functions (**Table 4** and **Figure 2**).

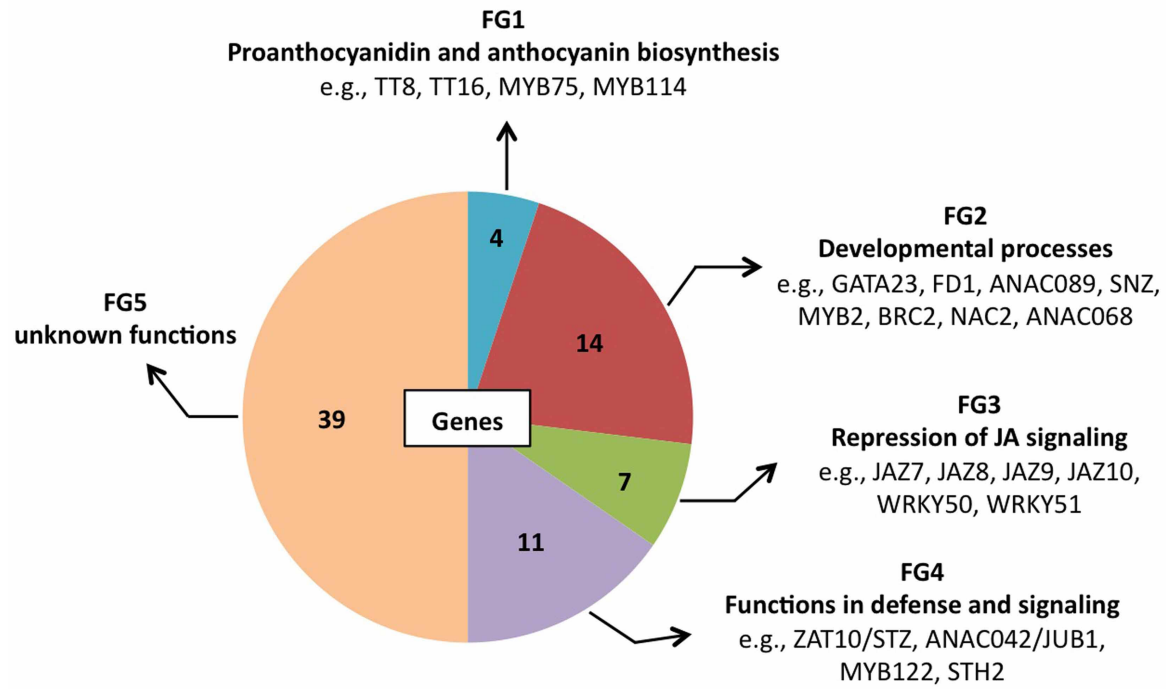

FIGURE 2 | Pie chart representation of the five functional groups (FG) of early H_2O_2-responsive TFs in GO plants. FG5 includes genes for which a distinct biological function has not been reported yet.

Table 5 | Transcription factors the expression of which was reduced by more than 3-fold in GO plants 0.5 h after shifting plants grown at high CO_2 concentration to ambient CO_2 concentration.

AGI	0.5 h after transfer to ambient CO_2			Gene family	Annotation	Function
	FC_{WT}	FC_{GO}	FC_{WT}/FC_{GO}			
At3g02310	47.1	0.12	380.8	MADS	SEP2/AGL4	Flower and ovule development
At3g13850	2.0	0.02	129.5	AS2 (LOB) I	ASL30/LBD22	Unknown function
At4g00260	21.6	0.23	92.1	B3	MEE45	Maternal effect embryo arrest 45
At4g27330	2.4	0.03	78.6	NZZ	NZZ/SPL	Controls stamen identity
At1g54760	11.6	0.31	37.6	MADS	AGL85	Unknown function
At3g60460	4.6	0.26	17.9	MYB	DUO1	Plays essential role in sperm cell specification
At2g45650	3.4	0.20	17.3	MADS	AGL6/RSB1	Involved in axillary bud formation; control of flowering time and lateral organ development
At5g26950	2.0	0.17	12.2	MADS	AGL93	Unknown function
At3g15170	1.9	0.16	11.9	NAC	ANAC054/CUC1	Shoot apical meristem formation and auxin-mediated lateral root formation; formation of organ boundary
At5g58280	0.8	0.15	5.3	B3	–	Unknown function
At5g15800	1.0	0.21	5.0	MADS	SEP1/AGL2	Involved in flower and ovule development
At3g56660	1.3	0.26	5.0	bZIP	bZIP49	Unknown function
At5g23000	0.6	0.18	3.3	MYB	MYB37/RAX1	Regulates axillary meristem formation; earliest spatial marker for future axillary meristems

Genes are listed according to the difference of the expression change between wild-type (WT) and GO plants (FC_{WT}/FC_{GO}). A function was described for a gene when its involvement in a biological process/function was experimentally backed up as described in PubMed (www.ncbi.nlm.nih.gov/pubmed) or TAIR (http://arabidopsis.org/index.jsp).

The analysis of the transcript profiles at 0.5 h after induction of H_2O_2 production in GO plants (**Table A2** in Appendix) also revealed a group of 13 genes that are down-regulated in GO relative to WT plants (**Table 5**). The function of five of these genes is currently unknown, but interestingly, the remaining eight genes positively control developmental processes. The down-regulation of expression of these TFs in GO plants together with the up-regulation of expression of TFs negatively affecting development (see FG2, **Table 3**) would act in concert to arrest growth and especially to delay the transition from the vegetative to the reproductive phase. Consistently, our previous results showed that GO plants growing under photorespiratory conditions are smaller than WT plants, presenting a reduced rosette diameter and a delay in flowering time (Fahnenstich et al., 2008).

CONCLUDING REMARKS

The metabolic induction of H_2O_2 formation in chloroplasts of GO plants under photorespiratory conditions triggered a faster and more prominent transcriptional response of ROS-responsive genes in these plants than in wild type. The changes of the transcriptional activities observed in GO plants early after induction of H_2O_2 production in chloroplasts suggest the establishment of responses that resemble those occurring at early times after wounding or herbivore attack, where H_2O_2 is also produced (Orozco-Cardenas and Ryan, 1999). These responses include (1) the retardation of development, which in part would be linked to JA signaling, and (2) the production of the phytoanticipins indole glucosinolates and camalexin. As in the case of herbivore attack, the retardation of development such as reductions in growth and reproduction observed in GO plants could be regarded as a strategy to allow more resource allocation to support defense and tolerance responses (Zavala and Baldwin, 2006). The data also suggest that signals for the early induction of indole glucosinolate and camalexin biosynthesis genes in GO plants through H_2O_2 may originate in chloroplasts as these genes showed no modified expression in catalase loss-of-function mutants (Inzé et al., 2012).

ACKNOWLEDGMENTS

Financial support was provided by the Deutsche Forschungsgemeinschaft (DFG) through grant MA 2379/11-1 to Veronica G. Maurino, and through grant MU 1199/14-1 (FOR 948) to Bernd Mueller-Roeber.

REFERENCES

Apel, K., and Hirt, H. (2004). Reactive oxygen species: metabolism, oxidative stress, and signal transduction. *Annu. Rev. Plant Biol.* 55, 373–399.

Asada, K. (2006). Production and scavenging of reactive oxygen species in chloroplasts and their fuction. *Plant Physiol.* 141, 391–396.

Baier, M., and Dietz, K.-J. (2005). Chloroplasts as source and target of cellular redox regulation: a discussion on chloroplast redox signals in context of plant physiology. *J. Exp. Bot.* 56, 1449–1462.

Balazadeh, S., Riaño-Pachón, D. M., and Mueller-Roeber, B. (2008). Transcription factors regulating leaf senescence in *Arabidopsis thaliana*. *Plant Biol.* 1, 63–75.

Bednarek, P., Pislewska-Bednarek, M., Svatos, A., Schneider, B., Doubsky, J., Mansurova, M., et al. (2009). A glucosinolate metabolism pathway in living plant cells mediates broad-spectrum antifungal defense. *Science* 323, 101–106.

Bienert, G. P., Møller, A. L., Kristiansen, K. A., Schulz, A., Møller, I. M., Schjoerring, J. K., et al. (2007). Specific aquaporins facilitate the diffusion of hydrogen peroxide across membranes. *J. Biol. Chem.* 282, 1183–1192.

Birkenbihl, R. P., Diezel, C., and Somssich, I. E. (2012). Arabidopsis WRKY33 is a key transcriptional regulator of hormonal and metabolic responses toward *Botrytis cinerea* infection. *Plant Physiol.* 159, 266–285.

Caldana, C., Scheible, W. R., Mueller-Roeber, B., and Ruzicic, S. (2007). A quantitative RT-PCR platform for high-throughput expression profiling of 2500 rice transcription factors. *Plant Meth.* 3, 7.

Chico, J. M., Chini, A., Fonseca, S., and Solano, R. (2008). JAZ repressors set the rhythm in jasmonate signaling. *Curr. Opin. Plant Biol.* 11, 486–494.

Chini, A., Fonseca, S., Fernandez, G., Adie, B., Chico, J. M., Lorenzo, O., et al. (2007). The JAZ family of repressors is the missing link in jasmonate signalling. *Nature* 448, 666–671.

Czechowski, T., Bari, R. P., Stitt, M., Scheible, W. R., and Udvardi, M. K. (2004). Real-time RT-PCR profiling of over 1400 Arabidopsis transcription factors: unprecedented sensitivity reveals novel root- and shoot-specific genes. *Plant J.* 38, 366–379.

Dat, J., Vandenabeele, S., Vranová, E., Van Montagu, M., Inzé, D., and Van Breusegem, F. (2000). Dual action of the active oxygen species during plant stress responses. *Cell Mol. Life Sci.* 57, 779–795.

Danon, A., Miersch, O., Felix, G., Camp, R. G., and Apel, K. (2005). Concurrent activation of cell death-regulating signalling pathways by singlet oxygen in *Arabidopsis thaliana*. *Plant J.* 41, 68–80.

Debeaujon, I., Nesi, N., Perez, P., Devic, M., Grandjean, O., Caboche, M., et al. (2003). Proanthocyanidin-accumulating cells in Arabidopsis testa: regulation of differentiation and role in seed development. *Plant Cell* 15, 2514–2531.

Desikan, R., Mackerness, S., Hancock, and Neill, S. J. (2001). Regulation of the Arabidopsis transcriptome by oxidative stress. *Plant Physiol.* 127, 159–172.

Fahnenstich, H., Scarpeci, T. E., Valle, E. M., Flügge, U. I., and Maurino, V. G. (2008). Generation of H_2O_2 in chloroplasts of *Arabidopsis thaliana* overexpressing glycolate oxidase as an inducible system to study oxidative stress. *Plant Physiol.* 148, 719–729.

Foyer, C. H., and Noctor, G. (2005). Redox homeostasis and antioxidant signaling: a metabolic interface between stress perception and physiological responses. *Plant Cell* 17, 1866–1875.

Fryer, M. J., Ball, L., Oxborough, K., Karpinski, S., Mullineaux, P. M., and Baker, N. R. (2003). Control of ascorbate peroxidase 2 expression by hydrogen peroxide and leaf water status during excess light stress reveals a functional organisation of Arabidopsis leaves. *Plant J.* 33, 691–705.

Gao, Z., Chung, E. H., Eitas, T. K., and Dangl, J. L. (2011). Plant intracellular innate immune receptor Resistance to *Pseudomonas syringae pv.* maculicola 1 (RPM1) is activated at, and functions on, the plasma membrane. *Proc. Natl. Acad. Sci. U.S.A.* 108, 8915.

Gigolashvili, T., Yatusevich, R., Berger, B., Müller, C., and Flügge, U. I. (2007). The R2R3-MYB transcription factor HAG1/MYB28 is a regulator of methionine-derived glucosinolate biosynthesis in *Arabidopsis thaliana*. *Plant J.* 51, 247–261.

Inzé, A., Vanderauwera, S., Hoeberichts, F. A., Vandorpe, M., Van Gaever, T., and Van Breusegem, F. (2012). A subcellular localization compendium of hydrogen peroxide-induced proteins. *Plant Cell Environ.* 35, 308–320.

Karpinski, S., Reynoldsm, H., Karpinska, B., Wingsle, G., Creissen, G., and Mullineaux, P. (1999). Systemic signalling and acclimation in response to excess excitation energy in Arabidopsis. *Science* 23, 654–657.

Kliebenstein, D. J., Kroymann, J., Brown, P., Figuth, A., Pedersen, D., Gershenzon, J., et al. (2001). Genetic control of natural variation in Arabidopsis glucosinolate accumulation. *Plant Physiol.* 126, 811–825.

Leister, D. (2005). Genomics-based dissection of the cross-talk of chloropalsts with the nucleus and mitochondria in Arabidopsis. *Gene* 354, 110–116.

Li, T., Li, H., Zhang, Y. X., and Liu, J. Y. (2011). Identification and analysis of seven H_2O_2-responsive miRNAs and 32 new miRNAs in the seedlings of rice (*Oryza sativa* L. ssp. indica). *Nucleic Acids Res.* 39, 2821–2833.

Maurino, V. G., and Flügge, U. I. (2008). Experimental systems to assess the effects of reactive oxygen

species in plant tissues. *Plant Signal. Behav.* 3, 919–924.

Maurino, V. G., and Peterhansel, C. (2010). Photorespiration: current status and approaches for metabolic engineering. *Curr. Opin. Plant Biol.* 13, 248–255.

Miao, Y., Laun, T. M., Smykowski, A., and Zentgraf, U. (2007). Arabidopsis MEKK1 can take a short cut: it can directly interact with senescence-related WRKY53 transcription factor on the protein level and can bind to its promoter. *Plant Mol. Biol.* 65, 63–76.

Mittler, R., Vandeerauwera, S., Gollery, M., and Van Breusegem, F. (2004). Reactive oxygen gene network of plants. *Trends Plant Sci.* 9, 490–498.

Møller, I. M., Jensen, P. E., and Hansson, A. (2007). Oxidative modifications to cellular components in plants. *Ann. Rev. Plant Biol.* 58, 459–481.

Møller, I. M., and Sweetlove, L. J. (2010). ROS signalling-specificity is required. *Trends Plant Sci.* 15, 370–374.

Mubarakshina, M. M., Ivanov, B. N., Naydov, I. A., Hillier, W., Badger, M. R., and Krieger-Liszkay, A. (2010). Production and diffusion of chloroplastic H_2O_2 and its implication to signalling. *J. Exp. Bot.* 61, 3577–3587.

Neill, S., Desikan, R., and Hancock, J. (2002). Hydrogen peroxide signaling. *Curr. Opin. Plant Biol.* 5, 388–395.

Obayashi, T., Hayashi, S., Saeki, M., Ohta, H., and Kinoshita, K. (2009). ATTED-II provides coexpressed gene networks for Arabidopsis. *Nucleic Acids Res.* 37, 987–991.

Oh, Y., Baldwin, I. T., and Gális, I. (2012). NaJAZh regulates a subset of defense responses against herbivores and spontaneous leaf necrosis in *Nicotiana attenuata* plants. *Plant Physiol.* 159, 769–788.

Op den Camp, R. G. L., Przybyla, D., Ochsenbein, C., Laloi, C., Kim, C., Danon, A., et al. (2003). Rapid induction of distinct stress responses after the release of singlet oxygen in Arabidopsis. *Plant Cell* 15, 2320–2332.

Orozco-Cardenas, M., and Ryan, C. A. (1999). Hydrogen peroxide is generated systemically in plant leaves by wounding and systemin via the octadecanoid pathway. *Proc. Natl. Acad. Sci. U.S.A.* 96, 6553–6557.

Ort, D. R., and Baker, N. R. (2002). A photoprotective role for O_2 as an alternative electron sink in photosynthesis? *Curr. Opin. Plant Biol.* 5, 193–198.

Pauwels, L., Barbero, G. F., Geerinck, J., Tilleman, S., Grunewald, W., Perez, A. C., et al. (2010). NINJA connects the co-repressor TOPLESS to jasmonate signalling. *Nature* 464, 788–791.

Petrov, V. D., and Van Breusegem, F. (2012). Hydrogen peroxide—a central hub for information flow in plant cells. *AoB Plants*. 2012, pls014. doi: 10.1093/aobpla/pls014

Pfalz, M., Mikkelsen, M. D., Bednarek, P., Olsen, C. E., Halkier, B. A., and Kroymann, J. (2011). Metabolic engineering in *Nicotiana benthamiana* reveals key enzyme functions in Arabidopsis indole glucosinolate modification. *Plant Cell* 23, 716–729.

Staswick, P. E. (2009). The tryptophan conjugates of jasmonic and indole-3-acetic acids are endogenous auxin inhibitors. *Plant Physiol.* 150, 1310–1321.

Tripathi, B. N., Bhatt, I., and Dietz, K. J. (2009). Peroxiredoxins: a less studied component of hydrogen peroxide detoxification in photosynthetic organisms. *Protoplasma* 235, 3–15.

Van Breusegem, F., Bailey-Serres, J., and Mittler, R. (2008). Unraveling the tapestry of networks involving reactive oxygen species in plants. *Plant Physiol.* 147, 978–984.

Vandenabeele, S., Vanderauwera, S., Vuylsteke, M., Rombauts, S., Langebartels, C., Seidlitz, H. K., et al. (2004). Catalase deficiency drastically affects gene expression induced by high light in *Arabidopsis thaliana*. *Plant J.* 39, 45–58.

Vanderauwera, S., Zimmermann, P., Rombauts, S., Vandenabeele, S., Langebartels, C., Gruissem, W., et al. (2005). Genome-wide analysis of hydrogen peroxide-regulated gene expression in Arabidopsis reveals a high light-induced transcriptional cluster involved in anthocyanin biosynthesis. *Plant Physiol.* 139, 806–821.

Wu, A., Allu, A. D., Garapati, P., Siddiqui, H., Dortay, H., Zanor, M.-I., et al. (2012). JUNGBRUNNEN1, a reactive oxygen species-responsive NAC transcription factor, regulates longevity in Arabidopsis. *Plant Cell* 24, 482–506.

Yan, Y., Stolz, S., Chetelat, A., Reymond, P., Pagni, M., Dubugnon, L., et al. (2007). A downstream mediator in the growth repression limb of the jasmonate pathway. *Plant Cell* 19, 2470–2483.

Zavala, J. A., and Baldwin, I. T. (2006). Jasmonic acid signalling and herbivore resistance traits constrain regrowth after herbivore attack in *Nicotiana attenuata*. *Plant Cell Environ.* 29, 1751–1760.

Conflict of Interest Statement: The authors declare that the research was conducted in the absence of any commercial or financial relationships that could be construed as a potential conflict of interest.

Received: 17 August 2012; accepted: 01 October 2012; published online: 01 November 2012.

Citation: Balazadeh S, Jaspert N, Arif M, Mueller-Roeber B and Maurino VG (2012) Expression of ROS-responsive genes and transcription factors after metabolic formation of H_2O_2 in chloroplasts. Front. Plant Sci. ***3****:234. doi: 10.3389/fpls.2012.00234*

This article was submitted to Frontiers in Plant Physiology, a specialty of Frontiers in Plant Science.

Copyright © 2012 Balazadeh, Jaspert, Arif, Mueller-Roeber and Maurino. This is an open-access article distributed under the terms of the Creative Commons Attribution License, which permits use, distribution and reproduction in other forums, provided the original authors and source are credited and subject to any copyright notices concerning any third-party graphics etc.

APPENDIX

Table A1 | Expression profile of 131 ROS-responsive genes in wild-type (WT) and GO plants after transferring seedlings to ambient CO_2 concentration.

AGI	log2 FCh							
	0.5 h WT	0.5 h GO	4 h WT	4 h GO	6 h WT	6 h GO	12 h WT	12 h GO
At1g02450	1.64	0.53	2.04	1.21	4.35	2.28	4.78	2.50
At1g05340	0.31	1.77	1.81	2.40	2.10	2.98	6.07	4.71
At1g05575	0.61	5.51	−1.36	1.90	−0.65	2.11	3.67	2.46
At1g10040	0.21	0.85	1.27	1.05	1.06	3.38	4.88	3.04
At1g13340	0.07	1.07	1.64	1.37	1.78	2.77	3.92	3.92
At1g14040	0.20	0.05	0.37	−0.24	0.42	0.28	1.54	0.51
At1g14200	−0.37	−0.58	−0.20	−1.26	0.38	0.52	1.92	1.20
At1g15520	0.22	−0.24	4.12	3.10	3.64	6.81	8.06	5.72
At1g16030	0.34	−0.29	0.11	0.71	0.18	0.13	0.95	0.22
At1g17170	−0.06	0.39	2.44	2.31	2.52	5.34	8.73	7.58
At1g17180	−0.65	−0.18	2.77	2.79	2.91	6.70	8.30	6.36
At1g18570	0.26	2.76	−1.48	−0.37	−0.53	1.33	3.99	2.48
At1g19020	0.87	3.21	0.34	1.88	0.93	4.79	6.83	5.94
At1g21100	0.72	2.78	−1.31	0.21	−0.56	0.61	1.18	1.88
At1g21120	−0.06	3.31	0.51	1.19	−0.47	3.99	4.94	3.88
At1g22400	0.08	−0.51	−0.53	−0.80	0.23	0.31	2.96	2.64
At1g26380	0.20	1.78	0.44	1.10	1.04	5.28	6.15	5.05
At1g26420	0.62	0.69	0.20	1.21	1.26	4.14	5.88	5.17
At1g27730	0.17	4.91	2.63	3.85	2.58	4.81	4.55	4.42
At1g28190	0.13	1.95	0.88	1.70	1.28	2.49	4.54	3.45
At1g35210	0.12	3.48	1.42	2.99	1.56	3.85	4.89	3.67
At1g35230	0.86	1.16	3.10	3.56	4.79	5.14	5.71	4.79
At1g53540	1.07	−0.58	3.69	2.64	1.84	0.61	3.25	2.09
At1g54050	−0.32	−0.27	1.45	0.96	0.99	0.38	−0.94	−0.35
At1g57630	0.50	1.78	3.52	3.63	4.34	5.17	7.31	5.93
At1g59590	0.34	2.37	−0.49	1.78	0.45	2.38	4.38	3.47
At1g61340	0.58	4.60	3.49	4.09	2.73	3.39	3.14	2.37
At1g61820	1.12	−0.18	0.36	−0.31	0.44	1.35	0.67	−0.26
At1g62300	0.81	1.45	1.78	2.26	2.80	3.71	4.75	4.20
At1g63720	0.63	2.31	1.45	1.89	1.65	2.61	4.47	3.77
At1g66060	0.40	4.13	0.65	1.31	1.45	2.35	3.48	3.19
At1g69890	0.40	3.99	−0.98	0.72	0.30	1.17	2.46	1.52
At1g72520	0.76	3.97	2.97	2.83	2.25	3.28	2.90	2.46
At1g73010	−1.19	−0.41	3.01	0.07	2.30	0.83	0.28	−0.72
At1g74310	−0.20	0.23	0.36	−1.58	−0.38	−0.02	0.93	0.89
At1g74360	−0.03	1.13	1.65	1.64	2.06	3.83	4.91	4.33
At1g74590	0.04	−0.20	0.60	0.27	0.58	0.26	2.51	1.39
At1g76070	0.21	1.38	0.63	1.49	0.71	1.72	2.85	2.14
At1g76600	0.44	2.54	0.51	2.42	0.81	3.45	5.35	4.45
At1g77450	−0.38	2.87	3.24	2.02	2.49	2.79	3.49	2.98
At1g80820	0.21	0.59	2.97	2.05	1.34	2.97	2.65	2.13
At1g80840	0.10	5.25	1.19	3.41	2.45	5.82	7.28	6.96
At2g15480	0.00	1.47	0.06	0.79	0.25	2.84	5.35	4.25
At2g18210	0.05	3.07	0.43	0.96	0.17	1.55	0.61	0.22
At2g18690	0.59	2.15	2.04	2.34	2.73	4.62	6.05	5.59
At2g20560	−0.17	0.21	0.92	−0.31	−0.15	0.05	2.15	1.16
At2g22470	0.09	−0.19	2.37	1.46	2.77	1.30	1.04	1.13

(Continued)

Table A1 | Continued

AGI	log2 FCh							
	0.5 h WT	0.5 h GO	4 h WT	4 h GO	6 h WT	6 h GO	12 h WT	12 h GO
At2g22880	0.79	5.67	1.97	3.69	2.64	4.81	4.38	4.64
At2g24540	0.42	1.13	8.22	7.56	4.97	5.63	0.77	2.64
At2g25735	0.86	3.43	−2.23	0.62	−0.84	1.68	3.57	3.00
At2g26150	−0.59	−0.02	1.64	−0.56	0.65	−0.58	2.39	1.80
At2g26530	0.32	3.73	0.82	3.15	1.07	2.42	2.44	2.12
At2g29490	−0.54	0.94	2.15	1.53	1.22	3.38	4.92	4.77
At2g29500	−0.04	0.17	1.43	1.02	0.63	1.94	0.96	1.79
At2g31945	0.40	1.82	1.06	1.22	1.17	2.34	1.79	2.25
At2g32030	0.42	4.03	0.48	2.74	0.93	4.61	5.56	4.93
At2g32120	0.46	0.37	−0.52	−0.09	−0.06	−0.86	−0.30	0.07
At2g33710	−0.04	2.90	−0.19	1.56	−0.25	3.66	3.87	3.13
At2g37430	−0.23	5.74	1.35	4.97	0.92	7.58	5.62	5.59
At2g38250	0.25	0.77	1.49	2.30	2.15	3.77	5.55	4.43
At2g38340	−0.07	−0.61	1.12	1.13	1.44	2.60	6.22	4.70
At2g38470	0.50	4.98	0.67	2.14	0.82	2.92	4.44	3.37
At2g40000	−0.14	3.35	−0.11	0.23	0.71	1.09	1.44	1.20
At2g41380	0.19	0.27	2.95	2.64	3.26	4.41	5.92	4.88
At2g41640	0.12	2.02	0.91	1.01	1.17	2.59	2.84	2.49
At2g43820	0.50	−0.11	−1.38	−0.24	0.09	0.68	3.02	3.05
At2g47000	0.15	0.22	0.59	2.57	0.55	4.43	7.60	6.33
At3g02800	0.14	2.31	0.32	0.24	0.24	2.02	2.39	2.03
At3g02840	0.16	6.31	2.03	3.30	1.52	6.03	5.78	4.98
At3g09270	0.63	0.34	1.67	1.09	0.99	0.59	3.57	2.16
At3g09350	−0.39	−0.12	1.10	−0.76	0.47	0.18	3.05	1.71
At3g09410	0.28	−0.27	0.22	0.81	0.22	1.66	1.46	−0.32
At3g10320	−0.36	0.84	2.31	1.49	3.05	2.85	6.78	3.90
At3g10930	0.72	4.25	1.97	3.89	3.08	5.28	7.56	5.90
At3g11840	1.19	1.22	1.67	0.87	0.88	1.81	3.81	2.49
At3g12580	1.37	−1.54	2.02	−0.52	−0.04	0.17	3.40	3.04
At3g13790	0.33	0.40	1.26	1.25	1.30	2.33	3.74	4.00
At3g15950	0.61	0.49	−0.10	0.56	−0.48	−0.36	0.16	−1.29
At3g16530	0.75	1.15	−0.28	0.06	−1.28	0.54	4.65	1.65
At3g17690	0.46	−0.81	3.25	1.73	2.59	2.74	6.04	3.25
At3g23230	1.17	3.23	0.32	0.93	1.19	4.09	5.32	4.06
At3g24500	−0.21	−0.49	0.36	−1.09	−0.42	−0.04	1.97	0.95
At3g25250	0.60	4.11	3.64	5.31	3.47	7.26	8.67	7.12
At3g26830	0.15	1.47	2.83	1.84	2.11	6.03	9.59	7.36
At3g28210	0.46	0.60	1.23	2.06	1.51	1.83	3.96	3.45
At3g46230	0.47	−0.41	2.47	2.16	1.53	0.83	1.95	1.24
At3g48650	0.96	3.89	1.28	2.32	2.62	2.89	4.03	4.23
At3g49580	−0.33	0.23	0.36	1.50	1.69	2.34	−0.07	0.17
At3g53230	0.98	−0.30	1.79	0.98	2.59	1.30	3.39	2.56
At3g55980	0.51	3.84	−0.17	0.94	0.26	1.99	3.60	2.75
At4g11280	0.62	1.59	0.86	1.13	0.45	2.56	4.27	3.03
At4g12400	0.07	−0.19	0.03	−0.76	−0.78	−0.16	1.54	0.28
At4g15975	0.79	0.36	−0.56	1.46	0.64	1.89	2.25	1.54
At4g17490	0.54	4.42	−0.53	2.52	0.41	2.78	3.29	2.20
At4g18880	0.71	2.71	0.86	2.34	0.92	2.21	3.85	2.85
At4g21390	0.88	3.70	2.50	3.44	2.71	4.86	4.60	4.41
At4g21990	−0.31	0.65	1.41	0.59	0.41	1.39	1.54	0.92

(Continued)

Table A1 | Continued

AGI	log2 FCh							
	0.5 h WT	0.5 h GO	4 h WT	4 h GO	6 h WT	6 h GO	12 h WT	12 h GO
At4g22530	0.38	−0.24	0.47	1.22	1.28	2.57	5.23	3.65
At4g24160	0.26	0.81	0.44	0.42	0.93	1.16	2.30	1.45
At4g24380	0.35	1.30	1.66	2.38	1.72	1.98	1.16	1.32
At4g24570	0.47	4.23	0.83	1.58	1.84	1.74	3.07	2.49
At4g37370	0.49	2.81	1.93	3.87	1.49	6.08	7.75	6.09
At4g39670	0.42	3.84	4.90	4.92	4.99	7.53	7.85	7.52
At5g04340	−0.25	4.78	3.28	3.13	2.87	3.10	5.35	4.22
At5g05730	0.52	0.78	1.40	2.23	0.49	1.27	2.95	1.99
At5g12020	0.23	−0.51	5.32	2.84	4.18	2.59	3.09	4.15
At5g12030	−0.18	0.07	3.39	1.03	1.22	1.97	2.90	3.00
At5g14700	0.19	1.14	2.48	2.11	1.59	1.74	1.49	0.80
At5g14730	0.43	0.40	−2.54	0.66	−1.85	1.42	3.48	2.00
At5g20230	0.60	1.47	2.40	3.33	3.30	4.82	6.06	5.41
At5g24110	−0.06	3.73	3.44	2.57	1.70	6.51	5.79	5.52
At5g25450	0.56	0.10	0.28	0.71	−0.36	0.63	3.48	1.90
At5g26220	0.28	−0.92	3.63	3.72	3.07	3.70	1.03	2.45
At5g27420	0.31	5.03	1.59	2.62	1.58	3.90	5.10	4.47
At5g28630	0.49	2.02	−2.90	−1.34	−1.83	−1.21	0.61	−0.72
At5g35320	−0.22	−0.13	0.67	−0.22	0.35	0.34	1.39	0.90
At5g46080	0.08	0.91	0.12	0.83	0.24	1.88	2.22	1.80
At5g47230	0.33	4.12	−0.05	2.21	0.55	2.13	3.61	2.44
At5g48570	0.33	−0.17	0.75	−0.27	−0.33	0.15	1.24	0.09
At5g48850	0.08	−0.39	1.07	1.52	1.74	2.90	−0.01	−0.41
At5g51060	0.40	−0.06	3.50	1.86	3.84	5.46	3.43	3.85
At5g51190	0.48	2.77	0.08	2.40	0.88	2.31	3.88	2.30
At5g51440	0.34	−0.29	0.65	1.16	−0.44	3.85	7.36	6.33
At5g52640	0.06	−0.18	0.96	−0.98	0.22	1.21	2.80	2.26
At5g54490	0.56	2.96	0.57	2.85	0.59	2.05	4.01	3.20
At5g57220	1.48	3.18	−1.68	0.44	−1.37	2.76	4.81	3.61
At5g59820	0.03	3.84	2.65	4.19	2.19	5.95	5.87	4.99
At5g63790	−0.37	2.42	1.55	1.69	1.63	3.47	3.56	3.23
At5g64310	0.29	1.92	1.58	1.13	1.61	0.13	0.53	0.54
At5g64510	−0.16	0.22	1.38	0.09	0.88	0.80	1.18	1.12
At5g64905	0.44	2.58	1.89	2.56	1.04	5.04	6.27	4.05

Numbers indicate log2 fold-change (FCh) expression ratio of genes after transferring plants to ambient CO_2 concentration compared to high CO_2 concentration. Values are means of two biological replicates.

Table A2 | Numbers indicate log2 fold-change (FCh) expression ratio of genes after transferring plants to ambient CO_2 concentration compared to high CO_2 concentration.

AGI	Gene family	log2 FCh	
		0.5 h WT	0.5 h GO
At1g01030	ABI3/VP1	0.74	0.97
At3g16280	AP2/EREBP	0.34	0.49
At3g16770	AP2/EREBP	0.28	0.61
At2g30470	ABI3/VP1	−0.01	−0.02
At3g20310	AP2/EREBP	0.82	0.98
At2g36080	ABI3/VP1	0.53	1.08
At2g46870	ABI3/VP1	−0.03	−0.16
At3g11580	ABI3/VP1	−0.23	2.19
At3g23230	AP2/EREBP	1.28	4.67
At3g25730	AP2/EREBP	0.05	0.61
At3g61970	ABI3/VP1	−0.11	0.10
At3g25890	AP2/EREBP	0.18	0.54
At4g01500	ABI3/VP1	0.92	0.50
At3g50260	AP2/EREBP	4.28	4.54
At4g21550	ABI3/VP1	−1.81	−3.72
At3g54320	AP2/EREBP	0.63	0.32
At5g60450	ARF	0.02	−0.28
At3g18990	B3	−0.02	0.53
At5g62000	ARF	0.38	0.47
At3g46770	B3	−1.55	0.31
At1g04880	ARID	0.01	−0.59
At3g53310	B3	−0.46	0.31
At1g20910	ARID	0.22	0.32
At4g00260	B3	4.43	−2.09
At4g01580	B3	−0.21	0.06
At1g76110	ARID	0.00	0.43
At1g76510	ARID	0.03	0.81
At4g31620	B3	1.67	−0.99
At2g46040	ARID	0.14	0.29
At3g13350	ARID	−0.31	0.31
At3g43240	ARID	−0.01	0.03
At4g31650	B3	−0.28	−0.17
At4g32010	ABI3/VP1	0.36	0.21
At5g06250	ABI3/VP1	−0.53	−0.16
At3g57600	AP2/EREBP	0.24	0.25
At1g14510	Alfin	0.10	0.17
At3g60490	AP2/EREBP	0.06	1.23
At2g02470	Alfin	0.29	0.45
At3g61630	AP2/EREBP	0.68	0.94
At3g11200	Alfin	−0.15	0.33
At4g06746	AP2/EREBP	1.76	3.06
At3g42790	Alfin	−0.01	0.42
At4g11140	AP2/EREBP	−0.16	−0.03
At5g05610	Alfin	0.10	0.51
At4g13040	AP2/EREBP	0.29	0.88
At5g20510	Alfin	−0.54	0.10
At5g26210	Alfin	−0.11	0.58
At4g16750	AP2/EREBP	−0.56	1.55
At1g01250	AP2/EREBP	−0.28	0.58
At4g17490	AP2/EREBP	4.25	5.93
At1g03800	AP2/EREBP	1.34	0.43
At4g17500	AP2/EREBP	1.21	2.79
At1g07900	AS2 (LOB) I	1.44	2.66
At1g16530	AS2 (LOB) I	1.40	0.91
At4g33280	B3	0.70	0.00
At1g31320	AS2 (LOB) I	0.77	0.35
At4g34400	B3	2.13	−0.37
At1g65620	AS2 (LOB) I	0.21	0.09
At5g18000	B3	−1.97	−0.43
At5g18090	B3	−0.20	−0.09
At5g32460	B3	0.41	6.95
At2g19820	AS2 (LOB) I	0.64	1.07
At5g58280	B3	−0.34	−2.35
At2g28500	AS2 (LOB) I	2.53	4.01
At5g60130	B3	−1.04	0.36
At5g60140	B3	0.34	0.37
At2g30340	AS2 (LOB) I	0.19	0.81
At1g06160	AP2/EREBP	−0.34	1.14
At4g23750	AP2/EREBP	0.75	0.56
At4g25470	AP2/EREBP	6.18	6.85
At1g12630	AP2/EREBP	−0.01	0.40
At4g25480	AP2/EREBP	6.17	5.68
At1g12890	AP2/EREBP	1.89	2.51
At4g27950	AP2/EREBP	0.73	−0.08
At1g13260	AP2/EREBP	0.63	1.06
At4g28140	AP2/EREBP	5.79	8.83
At4g31060	AP2/EREBP	−0.16	−0.16
At1g16060	AP2/EREBP	0.22	0.42
At4g32800	AP2/EREBP	−0.09	0.94
At1g19210	AP2/EREBP	3.96	4.18
At4g34410	AP2/EREBP	6.02	8.13
At1g21910	AP2/EREBP	−0.50	0.27
At4g36900	AP2/EREBP	0.31	1.15
At1g22190	AP2/EREBP	5.46	2.69
At4g36920	AP2/EREBP	−0.12	0.06
At1g22810	AP2/EREBP	6.10	7.03
At4g37750	AP2/EREBP	0.16	0.01
At1g01260	bHLH	0.40	0.98
At2g40470	AS2 (LOB) I	−0.03	1.14
At1g02340	bHLH	−0.38	0.48
At1g03040	bHLH	0.05	0.42
At1g05805	bHLH	0.26	0.69
At1g06150	bHLH	0.09	−0.14
At2g45420	AS2 (LOB) I	−0.51	1.14
At1g06170	bHLH	−0.71	0.30
At1g09250	bHLH	−0.08	0.96
At3g11090	AS2 (LOB) I	−0.12	0.14
At1g09530	bHLH	0.01	0.32

(Continued)

Table A2 | Continued

AGI	Gene family	log2 FCh	
		0.5 h WT	0.5 h GO
At3g13850	AS2 (LOB) I	1.00	−6.02
At1g10120	bHLH	−0.24	−0.09
At3g26620	AS2 (LOB) I	0.44	1.02
At1g10610	bHLH	−0.31	−0.23
At3g27650	AS2 (LOB) I	−0.85	0.20
At1g12860	bHLH	−0.38	0.00
At1g22985	AP2/EREBP	−0.01	0.73
At4g39780	AP2/EREBP	1.31	1.31
At5g05410	AP2/EREBP	2.04	2.95
At1g25560	AP2/EREBP	−0.64	0.28
At5g07580	AP2/EREBP	−1.35	−0.87
At5g10510	AP2/EREBP	0.85	−0.42
At1g28360	AP2/EREBP	1.36	0.70
At5g11190	AP2/EREBP	−0.20	0.55
At1g28370	AP2/EREBP	4.77	6.09
At5g11590	AP2/EREBP	0.72	1.28
At1g33760	AP2/EREBP	2.49	3.60
At5g13330	AP2/EREBP	0.32	0.69
At1g36060	AP2/EREBP	1.26	0.20
At5g13910	AP2/EREBP	−0.26	−0.89
At1g43160	AP2/EREBP	0.23	3.13
At1g44830	AP2/EREBP	−2.15	−0.73
At1g46768	AP2/EREBP	1.17	1.07
At3g27940	AS2 (LOB) I	−0.16	0.39
At1g18400	bHLH	−0.34	0.85
At1g22490	bHLH	0.09	0.48
At3g50510	AS2 (LOB) I	−0.42	−0.90
At4g00210	AS2 (LOB) I	−0.04	−0.62
At1g26260	bHLH	0.27	0.61
At4g00220	AS2 (LOB) I	0.19	0.64
At1g27660	bHLH	−0.17	0.58
At4g22700	AS2 (LOB) I	2.94	6.51
At1g29950	bHLH	−0.04	0.21
At5g63090	AS2 (LOB) I	−0.61	1.16
At1g31050	bHLH	−0.13	0.66
At1g32640	bHLH	1.91	2.86
At1g35460	bHLH	0.12	0.70
At5g19790	AP2/EREBP	−2.72	4.75
At1g50640	AP2/EREBP	1.59	1.23
At5g25190	AP2/EREBP	0.01	0.99
At5g25390	AP2/EREBP	−1.43	1.04
At5g25810	AP2/EREBP	−0.56	0.18
At1g53170	AP2/EREBP	2.63	3.00
At1g53910	AP2/EREBP	0.13	0.61
At5g44210	AP2/EREBP	1.55	1.59
At5g47220	AP2/EREBP	1.15	2.75
At1g63040	AP2/EREBP	1.40	1.52
At5g47230	AP2/EREBP	4.34	4.94
At1g64380	AP2/EREBP	4.20	4.16
At1g68550	AP2/EREBP	0.10	−0.13

(Continued)

Table A2 | Continued

AGI	Gene family	log2 FCh	
		0.5 h WT	0.5 h GO
At5g51190	AP2/EREBP	0.91	4.21
At1g68840	AP2/EREBP	0.32	1.62
At1g43770	bHLH	−0.44	0.19
At3g02550	AS2 (LOB) II	0.40	−0.76
At3g49940	AS2 (LOB) II	1.10	1.64
At1g51070	bHLH	0.12	0.63
At4g37540	AS2 (LOB) II	0.47	1.39
At1g51140	bHLH	−0.08	0.61
At5g67420	AS2 (LOB) II	1.15	1.20
At1g59640	bHLH	0.02	−0.10
At1g04100	Aux/IAA	−0.74	0.52
At1g04240	Aux/IAA	−0.77	0.28
At1g62975	bHLH	0.22	0.71
At1g04250	Aux/IAA	−0.33	0.99
At1g63650	bHLH	−0.09	0.44
At1g04550	Aux/IAA	0.18	0.50
At1g15050	Aux/IAA	0.46	0.92
At1g68240	bHLH	0.35	0.59
At1g15580	Aux/IAA	0.12	1.26
At1g68810	bHLH	−0.02	0.74
At1g51950	Aux/IAA	−0.20	0.45
At1g68920	bHLH	−0.18	0.15
At1g71130	AP2/EREBP	−0.06	0.73
At5g52020	AP2/EREBP	1.59	2.60
At5g53290	AP2/EREBP	0.94	−0.17
At1g71520	AP2/EREBP	3.60	5.02
At5g57390	AP2/EREBP	0.39	0.17
At1g72360	AP2/EREBP	−0.55	0.43
At5g60120	AP2/EREBP	0.40	0.42
At5g61590	AP2/EREBP	−2.96	−1.76
At1g74930	AP2/EREBP	4.49	4.80
At5g61600	AP2/EREBP	2.71	3.70
At1g75490	AP2/EREBP	0.73	2.15
At5g61890	AP2/EREBP	1.25	1.22
At1g77200	AP2/EREBP	−0.98	0.45
At5g64750	AP2/EREBP	2.48	2.27
At1g77640	AP2/EREBP	0.09	−0.48
At5g65130	AP2/EREBP	0.56	0.64
At1g78080	AP2/EREBP	2.43	2.50
At5g65510	AP2/EREBP	−0.63	−1.49
At1g79700	AP2/EREBP	−0.22	0.66
At1g52830	Aux/IAA	−0.12	0.08
At1g69010	bHLH	0.15	0.79
At1g80390	Aux/IAA	1.08	1.72
At2g01200	Aux/IAA	0.54	1.25
At1g72210	bHLH	1.02	−0.58
At2g22670	Aux/IAA	0.01	0.19
At1g73830	bHLH	−1.22	−0.72
At2g33310	Aux/IAA	0.04	0.16
At2g46990	Aux/IAA	0.07	1.22

(Continued)

Table A2 | Continued

AGI	Gene family	log2 FCh	
		0.5 h WT	0.5 h GO
At3g04730	Aux/IAA	−0.10	0.48
At3g15540	Aux/IAA	−0.25	0.47
At2g18300	bHLH	−0.68	0.05
At3g16500	Aux/IAA	0.10	0.71
At2g20095	bHLH	−0.12	−0.12
At3g17600	Aux/IAA	−0.27	1.57
At2g20180	bHLH	−0.53	−0.23
At3g23030	Aux/IAA	0.77	1.53
At3g23050	Aux/IAA	−0.39	0.82
At5g67180	AP2/EREBP	−0.23	−0.32
At2g20880	AP2/EREBP	5.11	7.22
At5g67190	AP2/EREBP	0.53	1.47
At2g22200	AP2/EREBP	2.28	3.07
At1g19220	ARF	0.14	−0.07
At2g23340	AP2/EREBP	0.86	0.80
At1g19850	ARF	0.49	−0.37
At2g25820	AP2/EREBP	0.00	1.42
At1g30330	ARF	−0.01	0.08
At2g28550	AP2/EREBP	0.34	0.56
At2g31230	AP2/EREBP	0.80	1.51
At2g33710	AP2/EREBP	0.95	3.51
At2g35700	AP2/EREBP	0.17	0.93
At2g38340	AP2/EREBP	0.45	−0.20
At2g39250	AP2/EREBP	0.76	1.64
At3g62100	Aux/IAA	0.32	0.57
At2g22770	bHLH	−0.12	0.93
At4g14550	Aux/IAA	−0.28	0.76
At2g24260	bHLH	0.79	0.38
At4g14560	Aux/IAA	0.83	1.05
At2g27230	bHLH	−0.04	0.21
At4g28640	Aux/IAA	−0.11	0.17
At2g28160	bHLH	−0.42	0.10
At4g29080	Aux/IAA	−0.18	0.62
At4g32280	Aux/IAA	−1.14	0.38
At5g25890	Aux/IAA	0.21	1.03
At2g31220	bHLH	−0.84	−0.45
At5g43700	Aux/IAA	−0.45	0.70
At2g31280	bHLH	0.10	0.00
At5g65670	Aux/IAA	−0.05	0.63
At2g40200	bHLH	−0.23	−0.03
At1g16640	B3	0.06	0.46
At2g41130	bHLH	0.08	1.11
At2g41240	bHLH	−0.57	−0.87
At1g59750	ARF	0.07	0.03
At2g41710	AP2/EREBP	0.18	0.38
At2g28350	ARF	−0.62	−0.35
At2g44840	AP2/EREBP	3.55	6.34
At2g33860	ARF	0.69	−1.21
At2g44940	AP2/EREBP	−1.71	0.13
At2g46530	ARF	0.16	0.35

(Continued)

Table A2 | Continued

AGI	Gene family	log2 FCh	
		0.5 h WT	0.5 h GO
At2g46310	AP2/EREBP	0.82	0.82
At3g61830	ARF	0.10	0.06
At2g47520	AP2/EREBP	0.66	0.34
At4g23980	ARF	0.23	0.39
At3g11020	AP2/EREBP	2.08	1.74
At4g30080	ARF	−0.25	0.49
At3g14230	AP2/EREBP	−0.02	0.72
At3g15210	AP2/EREBP	3.50	4.06
At5g37020	ARF	0.16	0.28
At1g49480	B3	−0.09	0.45
At2g42280	bHLH	0.28	0.96
At2g42300	bHLH	−0.56	−0.31
At2g24650	B3	−0.39	−0.14
At2g43010	bHLH	−0.31	0.16
At2g24680	B3	−0.08	−0.28
At2g43140	bHLH	0.57	−0.38
At2g24690	B3	−0.13	0.18
At2g46510	bHLH	0.71	1.44
At2g24700	B3	0.73	−1.17
At2g46810	bHLH	−0.30	0.56
At2g35310	B3	−0.37	−1.10
At2g46970	bHLH	−0.05	0.23
At3g06160	B3	−0.09	−0.37
At2g47270	bHLH	2.01	2.21
At3g06220	B3	0.29	−1.37
At3g05800	bHLH	0.95	2.40
At3g06120	bHLH	−0.05	0.15
At3g18960	B3	−7.62	−0.50
At3g06590	bHLH	−0.13	0.39
At3g07340	bHLH	−0.64	−0.30
At1g03970	bZIP	0.13	0.69
At3g17100	bHLH	−0.45	0.12
At1g06070	bZIP	0.42	0.19
At3g19500	bHLH	−0.26	1.20
At1g06850	bZIP	−0.43	−0.02
At3g19860	bHLH	0.41	0.25
At3g20640	bHLH	0.33	0.92
At1g13600	bZIP	−1.07	0.97
At3g21330	bHLH	0.35	0.61
At1g19490	bZIP	0.84	0.90
At3g22100	bHLH	1.18	3.16
At1g22070	bZIP	−0.40	0.67
At3g23210	bHLH	0.99	0.86
At1g32150	bZIP	0.47	0.72
At3g23690	bHLH	−0.16	0.26
At3g24140	bHLH	0.40	0.37
At3g25710	bHLH	0.75	0.89
At1g43700	bZIP	−0.04	0.56
At2g24790	C2C2(Zn) CO-like	0.18	0.97
At1g65110	C2H2	−0.67	1.69

(Continued)

Table A2 | Continued

AGI	Gene family	log2 FCh	
		0.5 h WT	0.5 h GO
At2g31380	C2C2(Zn) CO-like	0.59	0.81
At2g33500	C2C2(Zn) CO-like	0.11	0.65
At1g01930	C2H2	0.09	0.61
At2g47890	C2C2(Zn) CO-like	1.09	0.50
At1g02030	C2H2	0.55	0.82
At1g02040	C2H2	−0.50	0.39
At3g07650	C2C2(Zn) CO-like	0.87	1.08
At1g03840	C2H2	−0.66	−0.15
At3g21150	C2C2(Zn) CO-like	2.51	2.93
At1g04445	C2H2	2.53	0.68
At3g21880	C2C2(Zn) CO-like	2.16	2.79
At1g04990	C2H2	0.57	0.90
At3g21890	C2C2(Zn) CO-like	2.59	3.55
At1g08290	C2H2	0.59	0.38
At1g11490	C2H2	−0.51	0.33
At3g26744	bHLH	0.13	0.20
At1g45249	bZIP	0.80	1.01
At3g47640	bHLH	0.72	0.61
At1g49720	bZIP	0.49	0.83
At1g58110	bZIP	0.45	0.86
At3g56220	bHLH	−1.25	0.07
At1g68640	bZIP	−1.16	0.31
At3g56770	bHLH	−0.24	2.17
At1g68880	bZIP	−0.67	2.34
At3g56970	bHLH	0.11	0.05
At1g75390	bZIP	−0.43	−0.27
At3g56980	bHLH	0.00	−1.18
At1g77920	bZIP	−0.42	1.26
At3g57800	bHLH	−0.13	0.19
At2g04038	bZIP	−0.54	−0.49
At3g59060	bHLH	0.26	0.45
At3g61950	bHLH	−0.02	−0.58
At3g62090	bHLH	−1.46	1.29
At2g13150	bZIP	0.01	1.62
At4g27310	C2C2(Zn) CO-like	0.45	0.48
At4g38960	C2C2(Zn) CO-like	0.48	1.05
At1g14580	C2H2	2.14	0.20
At4g39070	C2C2(Zn) CO-like	0.25	1.79
At1g24625	C2H2	−0.61	0.31
At5g15840	C2C2(Zn) CO-like	0.78	0.61
At1g24630	C2H2	−0.54	0.33
At5g15850	C2C2(Zn) CO-like	0.53	1.05
At1g25250	C2H2	0.37	0.91
At5g24930	C2C2(Zn) CO-like	0.28	0.89
At1g26590	C2H2	−1.62	0.50
At5g48250	C2C2(Zn) CO-like	−0.69	0.48
At1g26610	C2H2	0.12	1.22
At5g54470	C2C2(Zn) CO-like	1.52	1.54
At1g27730	C2H2	0.82	5.18
At5g57660	C2C2(Zn) CO-like	0.19	0.82

(Continued)

Table A2 | Continued

AGI	Gene family	log2 FCh	
		0.5 h WT	0.5 h GO
At1g07640	C2C2(Zn) DOF	0.08	−0.17
At1g29600	C2H2	0.08	−0.17
At1g30970	C2H2	0.68	−0.31
At1g26790	C2C2(Zn) DOF	3.01	−0.64
At1g34370	C2H2	0.69	0.88
At4g00050	bHLH	0.72	0.13
At2g16770	bZIP	−0.20	0.52
At2g17770	bZIP	0.58	−0.17
At4g00480	bHLH	−0.33	0.45
At2g18160	bZIP	−0.71	−0.12
At4g00870	bHLH	0.28	−0.84
At2g21230	bZIP	−0.06	0.48
At4g01460	bHLH	0.42	0.87
At4g02590	bHLH	0.46	0.34
At2g22850	bZIP	0.04	0.88
At4g05170	bHLH	−0.31	0.75
At2g31370	bZIP	−0.02	0.42
At4g09180	bHLH	−0.09	0.20
At4g09820	bHLH	−0.41	5.10
At2g35530	bZIP	0.91	0.48
At4g14410	bHLH	0.02	0.67
At2g36270	bZIP	1.10	−1.17
At4g16430	bHLH	0.11	0.77
At2g40620	bZIP	0.26	0.07
At4g17880	bHLH	−0.77	0.12
At2g40950	bZIP	0.28	0.42
At1g28310	C2C2(Zn) DOF	−0.03	0.26
At1g29160	C2C2(Zn) DOF	0.11	0.40
At1g43850	C2H2	0.68	0.58
At1g43860	C2H2	−0.09	0.69
At1g47655	C2C2(Zn) DOF	0.24	0.22
At1g47860	C2H2	0.41	0.36
At1g51700	C2C2(Zn) DOF	1.89	2.29
At1g64620	C2C2(Zn) DOF	0.58	0.47
At1g55110	C2H2	1.08	1.07
At1g69570	C2C2(Zn) DOF	−0.38	0.90
At1g65120	C2H2	0.37	0.81
At2g28510	C2C2(Zn) DOF	0.91	0.81
At1g65130	C2H2	0.21	2.67
At2g28810	C2C2(Zn) DOF	0.55	0.14
At1g66140	C2H2	−0.06	0.25
At2g34140	C2C2(Zn) DOF	−0.27	0.52
At1g67030	C2H2	0.79	0.65
At2g37590	C2C2(Zn) DOF	0.52	0.87
At1g68130	C2H2	0.45	0.38
At2g46590	C2C2(Zn) DOF	−0.20	0.11
At1g68360	C2H2	−0.13	0.27
At4g20970	bHLH	−0.07	0.90
At2g41070	bZIP	0.53	0.53
At2g42380	bZIP	−0.86	0.03

(Continued)

Table A2 | Continued

AGI	Gene family	log2 FCh	
		0.5 h WT	0.5 h GO
At2g46270	bZIP	1.20	1.64
At3g10800	bZIP	0.40	0.74
At4g25410	bHLH	−0.12	0.27
At3g12250	bZIP	0.20	0.05
At4g28790	bHLH	−0.73	0.03
At3g17609	bZIP	0.95	1.16
At3g19290	bZIP	0.69	0.77
At4g29100	bHLH	0.23	0.41
At4g29930	bHLH	0.81	1.31
At4g30180	bHLH	−0.72	1.33
At3g51960	bZIP	0.19	0.90
At4g30980	bHLH	1.72	0.14
At3g54620	bZIP	0.29	0.62
At3g21270	C2C2(Zn) DOF	−0.33	0.48
At1g68480	C2H2	1.49	−0.70
At3g45610	C2C2(Zn) DOF	0.40	0.68
At1g72050	C2H2	0.28	0.53
At3g47500	C2C2(Zn) DOF	0.49	0.62
At1g75710	C2H2	0.00	0.15
At3g50410	C2C2(Zn) DOF	−0.05	0.48
At3g52440	C2C2(Zn) DOF	1.88	5.20
At2g01940	C2H2	−0.65	0.35
At3g55370	C2C2(Zn) DOF	0.29	0.63
At2g02070	C2H2	1.78	0.18
At3g61850	C2C2(Zn) DOF	−0.38	0.07
At2g02080	C2H2	0.73	0.09
At4g00940	C2C2(Zn) DOF	−0.37	0.42
At2g24500	C2H2	0.08	0.74
At3g56660	bZIP	0.37	−1.96
At4g34530	bHLH	0.09	0.38
At3g56850	bZIP	0.60	0.69
At4g36060	bHLH	0.04	0.50
At3g58120	bZIP	−1.52	−0.95
At4g36540	bHLH	−0.04	0.55
At3g62420	bZIP	−0.33	0.61
At4g36930	bHLH	0.44	−0.33
At4g01120	bZIP	0.23	0.87
At4g02640	bZIP	−0.01	0.50
At4g34000	bZIP	1.11	1.02
At5g01310	bHLH	0.43	0.70
At4g34590	bZIP	−0.18	0.39
At4g35040	bZIP	−0.47	0.57
At5g08130	bHLH	1.02	0.38
At4g35900	bZIP	−0.08	2.91
At5g09460	bHLH	−0.34	0.36
At4g36730	bZIP	0.26	0.51
At4g37730	bZIP	0.45	0.62
At4g24060	C2C2(Zn) DOF	−0.08	0.64
At2g26940	C2H2	0.02	0.88
At4g38000	C2C2(Zn) DOF	−0.99	1.49
At2g27100	C2H2	0.54	−0.21
At5g02460	C2C2(Zn) DOF	0.21	0.68
At5g39660	C2C2(Zn) DOF	0.40	1.33
At2g28200	C2H2	0.07	0.17
At5g60200	C2C2(Zn) DOF	0.27	0.77
At2g28710	C2H2	−0.51	0.59
At5g60850	C2C2(Zn) DOF	0.19	0.86
At2g29660	C2H2	−0.46	0.39
At5g62430	C2C2(Zn) DOF	0.67	1.18
At2g32930	C2H2	1.70	0.92
At5g62940	C2C2(Zn) DOF	0.06	0.71
At2g36480	C2H2	1.21	0.13
At5g65590	C2C2(Zn) DOF	−0.42	1.18
At2g36930	C2H2	0.44	0.09
At5g66940	C2C2(Zn) DOF	−0.38	−0.49
At2g37430	C2H2	0.89	6.33
At1g08000	C2C2(Zn) GATA	0.96	0.62
At1g08010	C2C2(Zn) GATA	1.05	0.41
At2g41940	C2H2	−0.76	−0.76
At5g10570	bHLH	−0.02	0.94
At4g38900	bZIP	0.12	0.61
At5g15160	bHLH	−0.19	0.27
At5g04840	bZIP	−0.06	0.25
At5g38860	bHLH	−0.35	0.30
At5g06950	bZIP	−3.42	0.81
At5g39860	bHLH	0.12	0.52
At5g06960	bZIP	−0.07	0.40
At5g41315	bHLH	1.22	1.01
At5g10030	bZIP	0.35	0.31
At5g46690	bHLH	−0.39	−0.34
At5g11260	bZIP	0.99	1.14
At5g46760	bHLH	−0.05	0.14
At5g15830	bZIP	−0.61	0.39
At5g46830	bHLH	−1.47	0.32
At5g24800	bZIP	0.20	1.07
At5g48560	bHLH	0.03	0.29
At5g28770	bZIP	−0.12	0.14
At1g51600	C2C2(Zn) GATA	0.23	0.85
At2g18380	C2C2(Zn) GATA	0.38	0.38
At2g45120	C2H2	0.20	0.28
At2g28340	C2C2(Zn) GATA	0.97	−0.02
At2g45050	C2C2(Zn) GATA	−0.39	0.90
At3g01460	C2H2	1.21	0.34
At3g06740	C2C2(Zn) GATA	−1.20	−0.64
At3g02790	C2H2	0.01	0.28
At3g16870	C2C2(Zn) GATA	0.02	−0.47
At3g02830	C2H2	0.22	0.54
At3g05760	C2H2	0.05	0.63
At3g21175	C2C2(Zn) GATA	0.07	0.55
At3g24050	C2C2(Zn) GATA	0.60	0.45

(Continued)

Table A2 | Continued

AGI	Gene family	log2 FCh	
		0.5 h WT	0.5 h GO
At3g10470	C2H2	0.41	−0.30
At3g13810	C2H2	0.29	1.00
At3g50870	C2C2(Zn) GATA	0.44	−0.02
At3g14740	C2H2	0.23	0.41
At3g51080	C2C2(Zn) GATA	0.43	0.39
At3g19580	C2H2	2.44	2.95
At5g50010	bHLH	−0.53	0.99
At5g50915	bHLH	0.50	1.15
At5g51780	bHLH	0.72	2.43
At5g44080	bZIP	0.05	0.31
At5g51790	bHLH	−0.57	0.21
At5g49450	bZIP	−0.04	1.02
At5g60830	bZIP	2.50	1.55
At5g54680	bHLH	0.45	0.44
At5g65210	bZIP	−0.10	0.17
At5g56960	bHLH	2.39	3.26
At1g19350	BZR	0.89	0.72
At5g57150	bHLH	0.27	0.55
At1g75080	BZR	1.20	0.95
At1g78700	BZR	1.74	0.50
At5g61270	bHLH	0.44	0.46
At3g50750	BZR	−0.10	0.34
At5g62610	bHLH	0.28	0.85
At4g18890	BZR	0.53	0.42
At5g64340	bHLH	−0.31	−0.18
At4g36780	BZR	0.65	0.53
At3g54810	C2C2(Zn) GATA	−0.02	−0.20
At3g60530	C2C2(Zn) GATA	−0.45	0.31
At4g17570	C2C2(Zn) GATA	−0.05	0.49
At4g24470	C2C2(Zn) GATA	0.48	0.09
At4g26150	C2C2(Zn) GATA	0.65	0.37
At3g44750	C2H2	0.06	0.23
At4g32890	C2C2(Zn) GATA	0.18	−0.17
At3g45260	C2H2	−0.02	0.11
At4g34680	C2C2(Zn) GATA	0.23	0.40
At4g36240	C2C2(Zn) GATA	0.02	0.26
At3g46080	C2H2	1.17	3.27
At4g36620	C2C2(Zn) GATA	0.51	0.01
At3g46090	C2H2	2.29	3.65
At5g25830	C2C2(Zn) GATA	−0.11	−0.10
At3g47890	C2H2	−0.01	0.20
At5g26930	C2C2(Zn) GATA	−0.49	3.26
At3g49930	C2H2	0.75	0.06
At5g47140	C2C2(Zn) GATA	0.04	0.70
At3g50700	C2H2	−0.32	1.30
At5g65320	bHLH	−0.83	−0.16
At1g06040	C2C2(Zn) CO-like	0.05	0.86
At5g65640	bHLH	0.04	0.79
At1g25440	C2C2(Zn) CO-like	−0.45	0.31
At5g67060	bHLH	−0.44	0.21

(Continued)

Table A2 | Continued

AGI	Gene family	log2 FCh	
		0.5 h WT	0.5 h GO
At1g28050	C2C2(Zn) CO-like	−0.09	1.01
At5g67110	bHLH	0.27	−0.20
At1g49130	C2C2(Zn) CO-like	−0.17	1.01
At1g14685	BPC/BRR	0.13	0.32
At1g68120	BPC/BRR	0.25	0.02
At1g68190	C2C2(Zn) CO-like	−0.39	0.54
At2g21240	BPC/BRR	−0.01	0.58
At1g68520	C2C2(Zn) CO-like	−0.58	0.18
At2g35550	BPC/BRR	0.12	0.92
At1g73870	C2C2(Zn) CO-like	0.59	0.68
At4g01930	BPC/BRR	0.85	1.64
At1g75540	C2C2(Zn) CO-like	−0.40	2.37
At1g78600	C2C2(Zn) CO-like	0.62	0.33
At5g42520	BPC/BRR	0.34	0.40
At2g21320	C2C2(Zn) CO-like	−0.09	0.69
At5g49300	C2C2(Zn) GATA	−0.24	1.01
At3g53600	C2H2	2.47	3.37
At5g56860	C2C2(Zn) GATA	−0.18	0.00
At5g66320	C2C2(Zn) GATA	2.87	0.64
At3g57480	C2H2	0.08	0.73
At1g08465	C2C2(Zn) YABBY	−0.20	0.56
At3g57670	C2H2	0.41	0.16
At3g58070	C2H2	0.09	1.07
At3g60580	C2H2	−0.19	0.51
At2g26580	C2C2(Zn) YABBY	0.37	0.81
At3g62240	C2H2	1.63	0.15
At2g45190	C2C2(Zn) YABBY	0.77	0.16
At4g02670	C2H2	0.69	0.56
At4g00180	C2C2(Zn) YABBY	0.58	0.26
At4g12240	C2H2	−0.34	0.18
At1g13400	C2H2	−0.19	−0.76
At4g15420	C2H2	0.12	0.83
At4g16610	C2H2	0.00	0.90
At4g17810	C2H2	−0.51	0.32
At3g14020	CCAAT-HAP2	1.21	0.92
At4g25610	C2H2	0.40	−0.74
At3g20910	CCAAT-HAP2	0.32	0.82
At5g06510	CCAAT-HAP2	0.02	−0.06
At4g27240	C2H2	−0.26	−0.11
At5g12840	CCAAT-HAP2	0.72	0.84
At4g31420	C2H2	−0.12	0.80
At2g13570	CCAAT-HAP3	−0.16	0.24
At2g27470	CCAAT-HAP3	0.09	−0.03
At5g01160	C2H2	0.90	0.52
At2g37060	CCAAT-HAP3	0.13	0.74
At2g38880	CCAAT-HAP3	0.42	0.78
At5g03150	C2H2	0.34	−0.17
At1g52150	HB	1.63	−0.43
At3g46640	GARP-G2-like	−0.17	−0.95
At1g62360	HB	−2.54	−1.92

(Continued)

Table A2 | Continued

AGI	Gene family	log2 FCh	
		0.5 h WT	0.5 h GO
At1g62990	HB	0.07	0.92
At4g13640	GARP-G2-like	0.27	0.30
At1g69780	HB	−0.93	0.70
At1g70920	HB	0.28	1.29
At4g28610	GARP-G2-like	0.50	0.62
At1g73360	HB	−0.50	0.20
At4g37180	GARP-G2-like	0.53	1.36
At1g75410	HB	0.09	0.62
At5g05090	GARP-G2-like	−0.21	0.30
At5g06800	GARP-G2-like	0.46	0.73
At1g79840	HB	−0.06	0.26
At5g16560	GARP-G2-like	−0.68	−0.18
At2g01430	HB	0.89	−0.31
At5g03510	C2H2	−0.33	−0.01
At3g53340	CCAAT-HAP3	−1.44	2.69
At5g03740	C2H2	0.13	0.28
At4g14540	CCAAT-HAP3	−0.19	0.56
At5g04340	C2H2	3.93	5.44
At5g47640	CCAAT-HAP3	0.91	1.44
At5g04390	C2H2	−0.65	−1.44
At5g47670	CCAAT-HAP3	0.54	−0.21
At1g07980	CCAAT-HAP5	−0.06	0.39
At1g08970	CCAAT-HAP5	0.23	0.74
At5g06650	C2H2	0.41	−0.09
At1g54830	CCAAT-HAP5	0.67	0.82
At5g09740	C2H2	0.15	0.51
At1g56170	CCAAT-HAP5	0.58	0.90
At5g10970	C2H2	−1.15	−0.37
At3g12480	CCAAT-HAP5	0.65	0.46
At3g48590	CCAAT-HAP5	0.52	0.54
At5g14140	C2H2	−0.05	1.09
At5g27910	CCAAT-HAP5	−1.06	1.11
At5g38140	CCAAT-HAP5	−0.17	−0.05
At5g18240	GARP-G2-like	0.09	0.67
At5g29000	GARP-G2-like	0.10	0.92
At2g02540	HB	0.05	0.06
At5g42630	GARP-G2-like	−1.15	0.23
At2g16400	HB	0.65	0.56
At5g44190	GARP-G2-like	0.01	0.22
At5g45580	GARP-G2-like	−0.96	0.18
At2g18550	HB	−1.44	1.14
At5g59570	GARP-G2-like	0.60	0.87
At2g22430	HB	1.79	1.63
At2g22800	HB	0.69	0.49
At1g44810	GeBP	−0.70	0.32
At2g23760	HB	0.03	0.55
At1g61730	GeBP	0.28	0.49
At2g27990	HB	−1.10	0.32
At2g28610	HB	−0.64	0.68
At2g25650	GeBP	−0.03	0.63

(Continued)

Table A2 | Continued

AGI	Gene family	log2 FCh	
		0.5 h WT	0.5 h GO
At5g16470	C2H2	−0.01	0.53
At5g43250	CCAAT-HAP5	−0.08	0.78
At5g16540	C2H2	0.15	0.85
At5g50470	CCAAT-HAP5	1.23	0.96
At5g18550	C2H2	1.57	0.12
At5g50480	CCAAT-HAP5	1.61	0.40
At5g63470	CCAAT-HAP5	−0.08	0.94
At5g25160	C2H2	−1.33	−0.40
At5g26610	C2H2	0.09	0.31
At4g01350	CHP-rich	−0.70	2.21
At5g37890	C2H2	0.30	0.61
At5g39550	C2H2	0.42	0.01
At2g20110	CPP(Zn)	0.14	−0.03
At3g04850	CPP(Zn)	−0.01	0.08
At5g40710	C2H2	−0.13	0.95
At3g16160	CPP(Zn)	−0.23	0.67
At2g36340	GeBP	−0.40	0.23
At3g04930	GeBP	0.10	0.87
At2g34710	HB	1.04	0.32
At4g00250	GeBP	−1.42	2.65
At2g35940	HB	0.53	0.95
At4g00270	GeBP	0.08	1.08
At2g36610	HB	−3.29	1.15
At4g00270	GeBP	−0.40	0.57
At2g44910	HB	−0.16	−0.13
At4g00390	GeBP	0.62	1.34
At2g46680	HB	1.05	1.08
At3g01220	HB	0.78	1.01
At3g01470	HB	0.33	0.28
At4g25210	GeBP	0.14	0.80
At5g14280	GeBP	0.06	0.25
At3g03660	HB	0.86	0.97
At5g28040	GeBP	0.49	0.46
At3g11260	HB	0.27	−0.71
At5g28040	GeBP	0.46	0.71
At3g18010	HB	0.78	1.05
At3g22760	CPP(Zn)	−0.35	0.13
At5g43170	C2H2	0.48	1.24
At3g22780	CPP(Zn)	0.13	0.19
At5g43540	C2H2	−1.44	1.69
At4g14770	CPP(Zn)	0.27	0.00
At5g44160	C2H2	0.35	0.50
At4g29000	CPP(Zn)	0.27	0.47
At5g25790	CPP(Zn)	0.21	1.24
At5g52010	C2H2	0.11	0.44
At1g47870	E2F/DP	0.33	0.46
At2g36010	E2F/DP	0.62	0.57
At3g01330	E2F/DP	−0.37	−0.25
At5g54630	C2H2	−0.29	0.21
At3g48160	E2F/DP	−0.08	0.23

(Continued)

Table A2 | Continued

AGI	Gene family	log2 FCh	
		0.5 h WT	0.5 h GO
At5g56200	C2H2	−3.54	3.86
At5g02470	E2F/DP	−0.34	1.65
At5g57520	C2H2	−1.45	−0.52
At5g03415	E2F/DP	0.41	0.22
At5g59820	C2H2	1.49	4.74
At5g14960	E2F/DP	1.08	0.27
At1g05055	General Transcription	0.47	0.27
At3g19510	HB	−0.08	0.11
At4g26170	General Transcription	−0.18	0.70
At3g49530	HB	1.86	2.55
At1g01160	GIF	0.22	0.35
At4g00850	GIF	0.69	1.16
At5g28640	GIF	−0.23	0.13
At1g07520	GRAS	1.57	2.32
At3g56560	HB	1.09	2.02
At1g07530	GRAS	0.23	0.71
At3g60390	HB	0.53	1.21
At1g14920	GRAS	0.18	−0.11
At3g61150	HB	0.73	0.72
At1g21450	GRAS	0.23	1.07
At3g61890	HB	1.26	1.68
At1g50420	GRAS	0.21	0.69
At1g50600	GRAS	0.17	0.95
At4g00730	HB	0.50	0.57
At5g60470	C2H2	−0.13	1.25
At5g22220	E2F/DP	0.47	0.72
At1g73730	EIL	1.23	0.52
At5g63280	C2H2	−0.03	0.21
At2g27050	EIL	−0.16	0.35
At5g64610	C2H2	−0.18	0.52
At3g20770	EIL	0.08	0.88
At5g66730	C2H2	0.28	0.22
At5g67450	C2H2	2.15	3.36
At1g32360	C3H	0.19	0.70
At1g60700	FHA	−0.01	0.07
At1g68200	C3H	0.27	0.51
At2g19810	C3H	0.75	1.30
At3g07220	FHA	0.37	0.45
At2g25900	C3H	−0.44	0.97
At3g07260	FHA	−0.25	4.25
At2g35430	C3H	0.11	0.74
At3g54350	FHA	0.28	0.42
At1g55580	GRAS	−0.24	−1.77
At4g01520	HB	0.88	1.90
At1g63100	GRAS	−0.14	−0.04
At4g01550	HB	−0.43	1.47
At1g66350	GRAS	−0.06	0.34
At4g02560	HB	0.48	0.40
At2g01570	GRAS	0.21	0.34
At4g03250	HB	0.32	0.63

(Continued)

Table A2 | Continued

AGI	Gene family	log2 FCh	
		0.5 h WT	0.5 h GO
At2g04890	GRAS	−0.18	0.67
At4g04890	HB	0.38	0.19
At2g37650	GRAS	0.28	0.40
At2g45160	GRAS	0.09	0.04
At4g16780	HB	0.80	1.65
At3g03450	GRAS	−0.19	0.08
At4g17460	HB	−1.60	−0.47
At3g13840	GRAS	0.16	1.57
At3g46600	GRAS	1.92	2.71
At4g21750	HB	0.60	0.64
At3g49950	GRAS	0.50	−0.70
At2g40140	C3H	3.19	3.95
At2g41900	C3H	0.16	0.46
At1g67710	GARP-ARR-B	−0.71	0.17
At3g06410	C3H	0.98	0.96
At2g01760	GARP-ARR-B	−0.85	0.18
At3g12130	C3H	0.44	0.68
At2g25180	GARP-ARR-B	0.26	−0.07
At3g12680	C3H	0.33	0.26
At3g16857	GARP-ARR-B	0.16	−0.01
At3g19360	C3H	0.64	0.38
At3g48440	C3H	0.68	0.39
At4g16110	GARP-ARR-B	−0.01	0.37
At3g51120	C3H	−0.03	0.35
At4g31920	GARP-ARR-B	−0.21	0.10
At3g55980	C3H	0.90	3.97
At5g07210	GARP-ARR-B	1.57	0.85
At4g00305	C3H	0.46	0.93
At4g01020	C3H	0.93	0.40
At4g29190	C3H	0.72	1.36
At1g13300	GARP-G2-like	1.44	0.56
At3g50650	GRAS	0.15	−0.27
At4g29940	HB	0.07	0.46
At3g54220	GRAS	0.61	0.37
At4g32040	HB	0.01	0.84
At3g60630	GRAS	0.16	0.50
At4g32880	HB	1.66	0.24
At4g00150	GRAS	0.57	0.58
At4g32980	HB	−0.66	0.12
At4g08250	GRAS	2.11	2.28
At4g34610	HB	0.27	0.20
At4g17230	GRAS	4.77	2.92
At4g35550	HB	0.22	0.40
At4g36710	GRAS	0.22	0.75
At4g37650	GRAS	0.29	0.47
At4g36870	HB	0.11	0.05
At5g17490	GRAS	0.26	1.26
At4g37790	HB	1.19	1.58
At5g41920	GRAS	0.10	0.47
At4g40060	HB	−0.01	0.70

(Continued)

Table A2 | Continued

AGI	Gene family	log2 FCh	
		0.5 h WT	0.5 h GO
At5g48150	GRAS	0.42	0.67
At5g02030	HB	0.12	0.55
At5g52510	GRAS	0.08	0.98
At5g03790	HB	−0.21	0.18
At5g06420	C3H	−0.39	0.04
At1g14600	GARP-G2-like	0.32	0.97
At5g06770	C3H	0.55	0.30
At1g25550	GARP-G2-like	1.12	1.73
At5g07060	C3H	0.17	1.35
At1g32240	GARP-G2-like	0.08	0.67
At5g07500	C3H	0.91	2.80
At1g49560	GARP-G2-like	−0.29	0.60
At5g12850	C3H	1.02	0.22
At1g68670	GARP-G2-like	0.47	1.19
At5g44260	C3H	−0.37	−0.47
At1g69580	GARP-G2-like	0.03	0.48
At5g58620	C3H	1.06	1.15
At1g79430	GARP-G2-like	0.39	0.03
At4g16150	CAMTA	0.23	1.05
At2g01060	GARP-G2-like	0.56	0.68
At1g67310	CAMTA	0.52	0.74
At2g02060	GARP-G2-like	0.25	0.47
At1g67910	CAMTA	0.33	0.68
At2g03500	GARP-G2-like	0.93	−0.19
At2g22300	CAMTA	0.44	1.20
At2g20400	GARP-G2-like	0.26	0.40
At2g22900	CAMTA	−0.41	0.60
At2g20570	GARP-G2-like	0.51	0.46
At5g59450	GRAS	1.21	1.78
At5g66770	GRAS	−0.12	−0.01
At5g06710	HB	0.66	0.31
At2g06200	GRF	−1.16	−1.07
At5g11060	HB	0.00	0.76
At2g22840	GRF	0.20	−0.25
At5g11270	HB	0.13	0.33
At2g36400	GRF	0.03	0.56
At5g15150	HB	−1.34	−0.12
At2g45480	GRF	−0.05	−0.23
At3g13960	GRF	0.16	0.03
At3g52910	GRF	−0.03	0.64
At5g19520	HB	−1.33	1.17
At4g24150	GRF	0.35	0.22
At5g25220	HB	0.55	1.12
At4g37740	GRF	0.97	−0.01
At5g53660	GRF	−1.00	1.00
At5g46880	HB	1.22	0.16
At1g05230	HB	0.28	0.17
At5g60690	HB	0.21	0.33
At3g16940	CAMTA	1.12	1.06
At2g38300	GARP-G2-like	0.10	0.95

(Continued)

Table A2 | Continued

AGI	Gene family	log2 FCh	
		0.5 h WT	0.5 h GO
At5g09410	CAMTA	0.51	0.60
At2g40260	GARP-G2-like	0.10	0.09
At5g64220	CAMTA	0.29	0.82
At2g40970	GARP-G2-like	0.23	0.85
At5g08190	CCAAT-DR1	0.01	0.22
At5g23090	CCAAT-DR1	−0.08	0.65
At3g04030	GARP-G2-like	0.06	−0.23
At1g17590	CCAAT-HAP2	0.04	0.59
At3g04450	GARP-G2-like	−0.09	0.61
At1g30500	CCAAT-HAP2	0.08	0.60
At3g10760	GARP-G2-like	−0.58	−0.19
At1g54160	CCAAT-HAP2	0.71	−0.27
At3g12730	GARP-G2-like	0.35	−0.04
At1g72830	CCAAT-HAP2	−0.59	0.48
At3g13040	GARP-G2-like	−0.06	0.79
At2g34720	CCAAT-HAP2	0.51	0.77
At3g05690	CCAAT-HAP2	0.08	−0.43
At3g24120	GARP-G2-like	0.25	0.59
At1g17920	HB	−0.71	−0.02
At1g20693	HMG	0.09	0.62
At1g19700	HB	0.25	0.60
At1g20696	HMG	0.12	0.51
At1g20700	HB	0.24	0.40
At2g17560	HMG	0.01	0.52
At2g34450	HMG	0.28	0.23
At1g23380	HB	−0.88	1.05
At3g28730	HMG	0.80	0.27
At1g26960	HB	−0.45	1.02
At3g51880	HMG	0.10	0.53
At1g27050	HB	0.49	0.55
At4g11080	HMG	−0.35	0.29
At1g28420	HB	−0.31	0.62
At4g23800	HMG	0.21	−0.23
At1g30490	HB	0.09	−0.23
At4g35570	HMG	0.18	0.53
At5g23420	HMG	0.00	0.63
At1g46480	HB	−0.16	0.19
At5g56780	HRT-like	−0.12	0.31
At1g32330	HSF	0.43	0.53
At1g46264	HSF	−0.15	−0.27
At1g67970	HSF	1.40	2.26
At3g54340	MADS	−0.63	−1.55
At1g74250	HSF	0.02	0.25
At3g57230	MADS	0.04	0.67
At1g77570	HSF	0.15	1.19
At3g57390	MADS	−0.14	0.40
At2g26150	HSF	0.06	0.46
At3g58780	MADS	−0.13	0.61
At3g02990	HSF	0.97	1.27
At3g24520	HSF	2.41	2.91

(Continued)

Table A2 | Continued

AGI	Gene family	log2 FCh	
		0.5 h WT	0.5 h GO
At4g11250	MADS	3.71	2.40
At5g02320	MYB	0.03	0.74
At5g03780	MYB	−0.17	0.43
At1g73410	MYB	0.81	−0.27
At5g04110	MYB	0.04	0.24
At1g74080	MYB	−1.03	2.02
At5g06100	MYB	0.33	0.38
At1g74430	MYB	−0.15	1.02
At5g06110	MYB	0.30	0.61
At1g74650	MYB	−0.10	0.98
At5g07690	MYB	−0.55	0.45
At1g79180	MYB	0.43	1.73
At5g07700	MYB	−0.27	0.92
At2g02820	MYB	−0.09	0.79
At5g10280	MYB	0.85	0.40
At2g03470	MYB	−0.26	0.94
At5g11510	MYB	0.34	0.01
At3g51910	HSF	0.45	0.79
At4g11880	MADS	−1.34	0.22
At4g18960	MADS	−0.27	−0.42
At4g11660	HSF	0.41	0.50
At4g22950	MADS	−0.32	−0.37
At4g13980	HSF	−0.12	−0.47
At4g24540	MADS	0.11	0.42
At4g17600	HSF	0.15	0.65
At4g36590	MADS	−1.41	1.10
At4g17750	HSF	0.42	0.38
At4g37940	MADS	−0.17	1.43
At4g18880	HSF	0.70	2.89
At5g10140	MADS	−1.26	0.83
At4g36990	HSF	0.06	1.02
At5g13790	MADS	−0.09	0.52
At5g03720	HSF	0.69	1.22
At5g15800	MADS	0.06	−2.27
At5g16820	HSF	0.53	0.95
At5g20240	MADS	−1.28	−3.08
At2g16720	MYB	0.32	1.27
At5g14750	MYB	−1.85	0.49
At2g23290	MYB	−1.90	−1.21
At5g15310	MYB	0.05	0.29
At5g16600	MYB	0.75	0.84
At5g16770	MYB	0.76	−0.23
At5g17800	MYB	−0.71	−0.65
At2g31180	MYB	−0.09	1.35
At5g18620	MYB	0.93	−1.05
At5g23000	MYB	−0.74	−2.44
At2g33610	MYB	−0.16	0.22
At5g23650	MYB	0.40	−0.73
At2g36890	MYB	−0.40	1.54
At5g26660	MYB	−0.40	1.47
At2g36960	MYB	0.12	0.37
At5g35550	MYB	−0.24	−0.93
At2g37630	MYB	1.40	0.21
At5g43840	HSF	1.08	1.36
At5g23260	MADS	0.00	2.43
At5g45710	HSF	0.21	0.73
At5g26630	MADS	−0.68	0.91
At5g62020	HSF	0.86	1.65
At1g08620	JUMONJI	0.44	0.43
At5g26870	MADS	−0.06	1.91
At1g30810	JUMONJI	0.82	0.40
At5g26950	MADS	1.01	−2.59
At5g27050	MADS	0.51	3.03
At5g27070	MADS	−0.01	1.39
At2g38950	JUMONJI	0.36	0.45
At3g20810	JUMONJI	1.48	0.30
At3g48430	JUMONJI	0.64	0.46
At5g27580	MADS	0.09	−0.58
At2g39880	MYB	−0.19	−0.40
At5g40330	MYB	0.07	0.38
At2g42150	MYB	0.15	1.82
At2g44430	MYB	0.23	0.22
At5g40360	MYB	1.31	0.44
At2g47190	MYB	0.30	2.58
At2g47210	MYB	0.52	0.58
At5g41020	MYB	0.10	0.26
At2g47460	MYB	−1.20	1.24
At5g45420	MYB	−0.21	0.71
At2g47620	MYB	−0.10	0.15
At5g47290	MYB	2.40	1.34
At3g01140	MYB	−0.14	0.93
At5g49330	MYB	0.40	0.53
At3g01530	MYB	1.43	1.13
At5g52260	MYB	−0.05	2.22
At3g05380	MYB	0.92	−0.13
At5g52600	MYB	−1.74	−1.43
At3g06490	MYB	−2.33	1.21
At5g54230	MYB	−0.96	−1.03
At5g04240	JUMONJI	−0.05	0.65
At5g46910	JUMONJI	0.88	1.37
At5g37415	MADS	−1.00	3.14
At5g63080	JUMONJI	−0.08	0.56
At1g01780	LIM	0.92	0.41
At1g10200	LIM	0.03	0.71
At2g39900	LIM	−0.17	0.21
At2g45800	LIM	0.19	0.84
At3g55770	LIM	−0.45	0.57
At5g48670	MADS	−0.47	0.54
At4g32551	LUG	0.14	0.39
At5g49420	MADS	0.51	0.07

(Continued)

Table A2 | Continued

AGI	Gene family	log2 FCh	
		0.5 h WT	0.5 h GO
At5g65070	MADS	−0.07	0.94
At5g51860	MADS	1.09	0.89
At3g08500	MYB	−0.72	−0.10
At5g55020	MYB	2.33	5.47
At3g09370	MYB	0.32	0.47
At3g10113	MYB	−0.54	−0.73
At3g11440	MYB	0.67	0.76
At5g60890	MYB	0.94	1.21
At3g11450	MYB	−0.14	1.07
At5g61420	MYB	−0.22	0.34
At3g12560	MYB	0.20	0.13
At5g62320	MYB	0.21	1.80
At5g62470	MYB	1.39	2.19
At3g12820	MYB	−0.50	−0.05
At5g65230	MYB	0.79	1.02
At3g13540	MYB	0.80	1.04
At5g67300	MYB	0.70	1.61
At1g18750	MADS	0.75	0.66
At1g22590	MADS	0.89	0.28
At5g60440	MADS	−0.25	0.00
At1g24260	MADS	−0.54	−0.31
At5g60910	MADS	0.69	0.02
At5g62165	MADS	−1.47	−1.31
At1g28450	MADS	−1.54	1.09
At5g65050	MADS	0.05	0.25
At1g28460	MADS	−0.17	1.43
At5g65060	MADS	0.51	0.20
At1g29960	MADS	−0.15	0.61
At5g65080	MADS	0.62	−0.97
At2g42680	MBF1	−0.05	0.84
At3g24500	MBF1	−0.19	0.35
At3g15320	MYB	−0.12	0.63
At1g01060	MYB-related	0.19	0.95
At3g18100	MYB	0.27	0.44
At1g01380	MYB-related	−0.22	0.91
At3g23250	MYB	2.02	4.29
At1g01520	MYB-related	1.62	1.67
At1g09770	MYB-related	0.41	0.38
At3g27220	MYB	−1.04	−0.13
At1g15720	MYB-related	0.34	0.39
At1g17460	MYB-related	0.71	0.61
At3g27810	MYB	0.79	1.76
At3g27920	MYB	0.15	0.47
At1g18330	MYB-related	−0.49	−0.63
At1g19000	MYB-related	−0.21	1.13
At3g28910	MYB	0.20	0.99
At1g49950	MYB-related	−0.08	0.73
At1g70000	MYB-related	−0.29	0.22
At1g71030	MYB-related	−0.27	0.77
At1g33070	MADS	0.19	1.12
At3g58680	MBF1	0.11	0.85
At1g47760	MADS	−0.02	0.30
At1g06180	MYB	0.39	0.55
At1g48150	MADS	−3.43	1.85
At1g06910	MYB	0.95	1.06
At1g54760	MADS	3.53	−1.70
At1g59810	MADS	−0.54	0.67
At1g08810	MYB	−0.22	0.30
At1g09540	MYB	2.23	1.43
At1g09710	MYB	0.83	−1.33
At1g13880	MYB	−0.17	0.99
At1g14350	MYB	0.09	0.63
At1g16490	MYB	−0.25	0.85
At1g17950	MYB	0.48	0.55
At3g46130	MYB	−0.32	−0.09
At1g72650	MYB-related	−0.27	0.56
At3g47600	MYB	0.27	0.89
At1g72740	MYB-related	0.41	0.92
At3g47680	MYB	0.34	0.06
At1g74840	MYB-related	0.11	0.96
At3g48920	MYB	2.56	2.79
At1g75250	MYB-related	0.57	0.81
At3g49690	MYB	0.14	0.48
At2g21650	MYB-related	0.06	0.47
At3g50060	MYB	0.62	1.24
At3g52250	MYB	0.16	0.70
At2g30420	MYB-related	0.31	−0.02
At2g38090	MYB-related	−0.26	0.52
At3g55730	MYB	−0.11	0.52
At2g46410	MYB-related	−0.19	0.79
At3g57980	MYB	0.10	0.08
At2g46830	MYB-related	0.09	0.65
At3g60460	MYB	2.21	−1.95
At3g09600	MYB-related	0.08	0.46
At3g61250	MYB	−0.69	−0.17
At1g18570	MYB	1.43	3.26
At1g69540	MADS	0.14	0.11
At1g18710	MYB	1.17	2.64
At1g71692	MADS	−0.65	1.13
At1g18960	MYB	0.33	2.42
At1g19510	MYB	0.08	0.54
At1g77080	MADS	−0.16	0.37
At1g21700	MYB	0.00	0.32
At1g22640	MYB	0.33	1.00
At2g03060	MADS	1.28	0.51
At1g26580	MYB	−0.08	0.26
At2g03710	MADS	−0.02	0.89
At2g14210	MADS	0.85	−0.08
At2g22540	MADS	−0.03	0.50
At3g10590	MYB-related	−1.36	0.27

(Continued)

Table A2 | Continued

AGI	Gene family	log2 FCh	
		0.5 h WT	0.5 h GO
At3g11280	MYB-related	−0.04	0.62
At4g01680	MYB	−0.95	0.94
At3g16350	MYB-related	1.18	0.64
At4g01980	MYB	1.15	−0.75
At3g24870	MYB-related	−0.34	0.16
At4g05100	MYB	1.03	2.63
At3g49850	MYB-related	−0.32	0.38
At4g09460	MYB	0.75	1.86
At4g01060	MYB-related	−0.77	0.32
At4g12350	MYB	1.00	0.22
At4g01280	MYB-related	0.45	0.96
At4g16420	MYB	0.12	0.48
At4g11400	MYB-related	0.16	0.67
At4g36570	MYB-related	−0.93	0.12
At4g17785	MYB	0.95	1.66
At4g39250	MYB-related	1.23	−0.59
At5g01200	MYB-related	−0.30	0.17
At1g48000	MYB	0.32	3.79
At1g49010	MYB	0.04	−0.22
At2g26880	MADS	1.64	0.81
At1g56650	MYB	−0.73	3.60
At2g28700	MADS	−1.04	1.44
At1g57560	MYB	0.14	1.31
At2g34440	MADS	0.35	0.09
At1g58220	MYB	0.97	0.51
At1g63910	MYB	0.06	−0.06
At2g42830	MADS	−2.35	−1.26
At1g66230	MYB	−0.64	0.17
At2g45650	MADS	1.77	−2.34
At2g45660	MADS	0.07	0.45
At1g66380	MYB	0.89	5.32
At3g02310	MADS	5.56	−3.02
At1g66390	MYB	0.04	−0.20
At4g21440	MYB	1.72	2.48
At5g02840	MYB-related	−0.12	0.57
At4g22680	MYB	0.57	1.29
At5g04760	MYB-related	0.64	1.18
At5g05790	MYB-related	−0.26	0.39
At4g26930	MYB	−1.50	2.20
At5g08520	MYB-related	0.58	−0.03
At4g28110	MYB	1.18	2.55
At5g17300	MYB-related	0.42	1.05
At4g32730	MYB	0.83	0.08
At5g37260	MYB-related	2.68	3.28
At4g34990	MYB	0.24	0.09
At5g52660	MYB-related	0.73	1.50
At4g37260	MYB	0.31	1.47
At5g53200	MYB-related	0.34	0.57
At5g56840	MYB-related	−0.33	0.62
At4g38620	MYB	0.41	0.47

(Continued)

Table A2 | Continued

AGI	Gene family	log2 FCh	
		0.5 h WT	0.5 h GO
At5g58900	MYB-related	0.09	0.41
At5g47370	NAC	0.73	0.99
At5g67580	MYB-related	−0.17	0.60
At1g01010	NAC	0.48	1.17
At5g53950	NAC	1.56	−1.00
At1g01720	NAC	2.88	2.70
At5g53980	NAC	0.30	−0.46
At5g56620	NAC	0.93	1.00
At1g02220	NAC	−0.30	0.77
At5g59340	HB	2.22	1.42
At5g61430	NAC	0.49	−0.05
At5g62380	NAC	0.14	0.82
At5g63790	NAC	1.41	3.14
At1g12260	NAC	9.20	0.96
At5g64060	NAC	−0.12	−0.11
At5g64530	NAC	0.08	1.20
At1g19790	SRS	−0.88	−0.17
At2g18120	SRS	0.43	0.73
At1g66600	WRKY	0.53	1.60
At2g21400	SRS	−0.27	1.28
At1g69310	WRKY	0.63	0.51
At3g54430	SRS	−0.14	0.26
At1g69810	WRKY	0.89	1.49
At4g36260	SRS	0.33	0.12
At5g12330	SRS	−2.00	0.13
At1g80840	WRKY	1.49	6.06
At5g33210	SRS	0.21	0.79
At2g03340	WRKY	0.12	0.13
At5g66350	SRS	−0.18	0.07
At2g04880	WRKY	0.04	0.72
At1g05690	TAZ	−0.02	0.84
At1g25580	NAC	0.08	0.68
At5g65310	NAC	−0.10	0.20
At5g66300	NAC	0.03	0.77
At1g28470	NAC	−0.82	0.54
At1g32510	NAC	0.43	0.42
At5g39690	NAM	1.18	1.50
At5g50820	NAM	0.53	0.50
At1g32870	NAC	0.38	0.81
At1g33060	NAC	0.16	0.31
At1g20640	NIN-like	0.52	−0.06
At1g34180	NAC	0.22	0.15
At1g64530	NIN-like	0.25	0.25
At1g34190	NAC	0.11	0.92
At1g74480	NIN-like	−2.56	1.54
At1g52880	NAC	−0.10	0.56
At1g76350	NIN-like	−0.30	0.48
At1g52890	NAC	2.82	3.69
At2g17150	NIN-like	0.82	−0.12
At4g37610	TAZ	0.17	2.27

(Continued)

Table A2 | Continued

AGI	Gene family	log2 FCh	
		0.5 h WT	0.5 h GO
At2g23320	WRKY	2.07	3.14
At5g63160	TAZ	2.00	2.10
At2g24570	WRKY	0.55	0.82
At5g67480	TAZ	−0.44	1.05
At2g25000	WRKY	−0.33	0.07
At1g30210	TCP	−0.05	0.41
At2g30250	WRKY	0.63	2.13
At1g35560	TCP	0.03	0.91
At2g30590	WRKY	−0.44	0.40
At1g53230	TCP	0.24	0.83
At1g58100	TCP	0.14	0.37
At2g37260	WRKY	−0.50	0.63
At1g67260	TCP	−2.70	−0.70
At2g38470	WRKY	1.50	5.33
At1g68800	TCP	−0.10	1.83
At2g40740	WRKY	0.70	−0.15
At1g69690	TCP	−0.80	0.28
At2g40750	WRKY	0.49	0.37
At1g72010	TCP	0.43	0.61
At2g44745	WRKY	−1.08	0.27
At2g31070	TCP	0.01	0.02
At1g54330	NAC	−0.82	0.42
At2g43500	NIN-like	0.60	1.64
At1g56010	NAC	−0.50	0.39
At2g43500	NIN-like	0.46	0.49
At3g59580	NIN-like	−0.41	0.14
At4g24020	NIN-like	0.79	0.45
At4g35270	NIN-like	0.54	0.54
At4g35590	NIN-like	0.71	0.81
At1g62700	NAC	0.10	1.52
At1g64105	NAC	−0.07	0.47
At1g65910	NAC	0.50	0.67
At4g27330	NZZ	1.25	−5.05
At2g37000	TCP	0.43	0.10
At2g46400	WRKY	1.44	4.82
At2g45680	TCP	−0.06	−0.07
At2g47260	WRKY	0.30	0.53
At3g02150	TCP	−0.14	1.23
At3g01080	WRKY	−0.10	1.38
At3g15030	TCP	−0.20	−0.06
At3g01970	WRKY	0.53	1.93
At3g04670	WRKY	−0.07	0.62
At3g27010	TCP	0.50	1.13
At3g56400	WRKY	0.86	1.42
At3g58710	WRKY	0.79	0.92
At3g47620	TCP	0.33	0.89
At4g18390	TCP	0.17	0.44
At4g01250	WRKY	2.23	2.87
At5g08070	TCP	0.09	0.22
At4g01720	WRKY	2.13	1.22

(Continued)

Table A2 | Continued

AGI	Gene family	log2 FCh	
		0.5 h WT	0.5 h GO
At5g08330	TCP	−0.52	−0.21
At4g04450	WRKY	0.96	−0.24
At5g23280	TCP	−0.67	0.09
At1g69490	NAC	2.94	4.59
At1g71930	NAC	0.51	0.16
At5g35770	Orphan (SAP)	−2.53	−1.58
At1g76420	NAC	−3.79	−0.14
At1g14410	PBF-2-like(Whirly)	0.60	0.20
At1g77450	NAC	2.40	2.71
At1g71260	PBF-2-like(Whirly)	0.05	0.22
At2g02740	PBF-2-like(Whirly)	0.00	0.35
At2g02450	NAC	0.98	1.08
At1g05380	PHD finger	0.18	0.22
At2g36720	PHD finger	0.04	0.40
At2g18060	NAC	0.14	−0.31
At3g14980	PHD finger	−0.05	0.09
At2g24430	NAC	2.76	2.38
At3g53680	PHD finger	0.29	0.79
At2g27300	NAC	−0.16	1.23
At4g14920	PHD finger	0.70	0.50
At2g33480	NAC	−1.81	0.06
At5g12400	PHD finger	0.91	0.58
At2g43000	NAC	0.92	1.67
At5g22260	PHD finger	4.59	0.75
At5g41030	TCP	0.84	1.27
At4g12020	WRKY	0.71	0.40
At5g51910	TCP	−0.29	0.09
At4g18170	WRKY	1.99	3.02
At5g60970	TCP	0.14	0.27
At1g13450	Trihelix	0.07	0.60
At4g23550	WRKY	−0.28	−0.03
At1g21200	Trihelix	−0.14	0.45
At4g23810	WRKY	3.77	4.73
At4g24240	WRKY	0.88	1.69
At1g31310	Trihelix	0.89	0.55
At1g33240	Trihelix	−0.65	−0.47
At4g26640	WRKY	1.45	−0.24
At1g54060	Trihelix	−0.26	0.43
At4g30935	WRKY	0.11	0.42
At1g76880	Trihelix	0.98	0.08
At4g31550	WRKY	2.07	2.38
At1g76890	Trihelix	−0.54	−0.10
At4g31800	WRKY	1.41	2.71
At2g33550	Trihelix	0.61	0.52
At4g39410	WRKY	−0.03	0.99
At5g35210	PHD finger	0.07	0.70
At3g01600	NAC	−0.70	1.83
At3g03200	NAC	−2.55	0.74
At5g58610	PHD finger	−1.39	−1.08
At3g04060	NAC	0.37	0.02

(Continued)

Table A2 | Continued

AGI	Gene family	log2 FCh	
		0.5 h WT	0.5 h GO
At3g04070	NAC	−0.45	0.76
At1g21000	PLATZ	0.65	1.67
At1g31040	PLATZ	−1.87	0.25
At3g04420	NAC	−0.17	0.64
At1g32700	PLATZ	−0.16	1.10
At1g43000	PLATZ	2.53	3.44
At3g10480	NAC	0.88	0.14
At1g76590	PLATZ	1.42	1.77
At3g10490	NAC	0.81	0.07
At2g27930	PLATZ	1.89	1.39
At3g10500	NAC	0.26	0.94
At3g60670	PLATZ	−0.09	0.31
At3g15170	NAC	0.95	−2.63
At4g17900	PLATZ	1.01	1.84
At2g35640	Trihelix	2.40	2.93
At5g01900	WRKY	1.78	5.60
At2g38250	Trihelix	0.84	0.37
At5g07100	WRKY	2.13	1.12
At2g44730	Trihelix	0.14	0.61
At3g01560	Trihelix	1.10	0.47
At5g22570	WRKY	0.59	1.16
At3g10040	Trihelix	−1.27	−0.35
At5g24110	WRKY	1.46	4.27
At3g11100	Trihelix	−0.20	0.44
At5g26170	WRKY	−0.25	2.65
At3g14180	Trihelix	0.07	0.81
At5g28650	WRKY	−0.01	−0.61
At3g19020	Trihelix	1.43	1.18
At3g24490	Trihelix	−0.22	0.42
At5g43290	WRKY	0.27	0.87
At3g24860	Trihelix	−0.07	0.35
At5g45050	WRKY	0.37	0.28
At3g25990	Trihelix	0.10	0.31
At5g45270	WRKY	0.76	0.96
At3g15500	NAC	2.51	3.62
At5g46710	PLATZ	1.85	2.23
At3g15510	NAC	0.51	0.57
At3g17730	NAC	0.40	1.19
At4g02020	Polycomb Group (PcG)	0.28	0.50
At3g29035	NAC	−0.40	1.40
At4g16845	Polycomb Group (PcG)	−0.08	0.09
At5g51230	Polycomb Group (PcG)	0.26	0.22
At3g27700	RRM-containing	0.52	0.78
At4g01540	NAC	0.33	2.07
At3g47120	RRM-containing	0.11	0.39
At4g27410	NAC	1.65	3.18
At2g37120	S1Fa-like	−1.00	0.63
At4g28500	NAC	−0.19	−0.07
At3g53370	S1Fa-like	0.11	0.66
At4g28530	NAC	−0.38	0.93

(Continued)

Table A2 | Continued

AGI	Gene family	log2 FCh	
		0.5 h WT	0.5 h GO
At1g02065	SBP	0.44	−0.72
At3g54390	Trihelix	−0.39	−0.11
At5g46350	WRKY	0.26	1.24
At3g58630	Trihelix	0.00	0.16
At5g49520	WRKY	1.74	2.73
At4g17050	Trihelix	−0.24	0.41
At5g52830	WRKY	0.93	1.22
At4g31270	Trihelix	−0.37	0.59
At5g56270	WRKY	−0.06	−0.03
At5g01380	Trihelix	−0.10	2.40
At5g64810	WRKY	0.78	2.26
At5g03680	Trihelix	−0.41	0.87
At1g14440	ZF-HD	−0.18	−0.17
At5g05550	Trihelix	−0.01	0.38
At1g14687	ZF-HD	0.06	0.36
At5g14540	Trihelix	3.11	0.00
At5g28300	Trihelix	−0.18	−0.58
At1g74660	ZF-HD	−0.26	0.00
At5g38560	Trihelix	0.48	0.69
At1g75240	ZF-HD	−0.45	−0.13
At5g47660	Trihelix	0.02	0.15
At2g02540	ZF-HD	−0.10	0.60
At5g63430	Trihelix	0.35	0.47
At2g18350	ZF-HD	0.34	0.27
At4g35580	NAC	0.59	0.36
At1g20980	SBP	0.39	0.60
At4g36160	NAC	0.08	1.12
At1g27360	SBP	0.91	0.64
At5g04400	NAC	1.31	1.79
At1g27370	SBP	0.56	0.01
At5g04410	NAC	0.21	0.52
At1g53160	SBP	−0.51	−0.46
At5g07680	NAC	−0.71	−0.44
At1g69170	SBP	−0.24	0.19
At5g08790	NAC	1.56	1.81
At2g33810	SBP	−0.01	0.12
At5g09330	NAC	0.76	0.34
At2g42200	SBP	−0.45	−0.37
At5g13180	NAC	−0.45	0.17
At2g47070	SBP	0.22	0.60
At5g14000	NAC	−0.57	−0.15
At3g15270	SBP	−0.51	−0.35
At3g57920	SBP	0.27	−0.36
At5g17260	NAC	0.22	0.79
At3g60030	SBP	0.22	0.30
At5g18270	NAC	0.31	0.84
At5g18830	SBP	0.04	0.26
At1g16070	TUB	−0.19	−0.25
At3g28920	ZF-HD	0.06	0.23
At1g25280	TUB	0.80	0.36

(Continued)

Table A2 | Continued

AGI	Gene family	log2 FCh	
		0.5 h WT	0.5 h GO
At3g50890	ZF-HD	−0.47	−0.58
At4g24660	ZF-HD	−0.36	−0.01
At1g47270	TUB	0.35	0.68
At5g15210	ZF-HD	−0.12	0.01
At5g39760	ZF-HD	0.84	0.07
At5g42780	ZF-HD	−0.17	−0.33
At1g76900	TUB	1.50	0.46
At2g18280	TUB	0.19	0.55
At5g65410	ZF-HD	1.11	0.15
At2g47900	TUB	1.25	0.11
At1g17380	ZIM	1.91	3.30
At3g06380	TUB	−0.02	0.64
At1g19180	ZIM	2.60	4.54
At5g18680	TUB	−0.10	0.44
At1g30135	ZIM	−0.37	2.56
At1g48500	ZIM	1.18	0.17
At5g18300	NAC	−0.83	−0.13
At5g43270	SBP	−0.64	−0.77
At5g22290	NAC	0.28	1.92
At5g50570	SBP	0.26	1.42
At5g22380	NAC	3.76	4.76
At5g50670	SBP	0.30	0.91
At5g24590	NAC	1.15	1.53
At1g05830	SET-domain	0.18	−0.06
At5g39610	NAC	0.19	2.46
At2g31650	SET-domain	0.27	0.57
At5g39820	NAC	1.91	0.05
At4g27910	SET-domain	0.29	0.60
At5g41410	NAC	0.08	−0.03
At4g30860	SET-domain	−0.13	0.71
At5g09790	SET-domain	0.48	0.50
At5g24330	SET-domain	−0.05	0.27
At5g46590	NAC	0.08	1.50
At5g53430	SET-domain	0.30	0.17
At4g28190	ULT	−0.26	0.02
At1g70700	ZIM	0.14	1.73
At1g28520	VOZ	0.32	0.75
At1g72450	ZIM	−0.27	1.16
At2g42400	VOZ	0.24	0.44
At1g74950	ZIM	0.27	0.93
At2g34600	ZIM	−1.53	3.07
At3g17860	ZIM	0.10	1.25
At1g29280	WRKY	−0.40	2.45
At3g43440	ZIM	0.15	0.16
At1g29860	WRKY	−0.16	1.03
At4g14713	ZIM	0.94	−0.11
At4g14720	ZIM	−0.01	0.21
At4g32570	ZIM	0.50	0.50
At1g62300	WRKY	2.04	2.08
At5g13220	ZIM	0.10	1.75
At5g20900	ZIM	0.22	1.13

Values are means of two biological replicates.

frontiers in
PLANT SCIENCE

ORIGINAL RESEARCH ARTICLE
published: 17 January 2013
doi: 10.3389/fpls.2012.00303

Systemic and local responses to repeated HL stress-induced retrograde signaling in *Arabidopsis*

Matthew J. Gordon, Melanie Carmody, Verónica Albrecht and Barry Pogson*

School of Biochemistry and Molecular Biology, Australian Research Council Centre of Excellence in Plant Energy Biology, Australian National University, Canberra, ACT, Australia

Edited by:
Dario Leister, Ludwig-Maximilians-University Munich, Germany

Reviewed by:
Thomas Pfannschmidt, Friedrich-Schiller-University Jena, Germany
Saijaliisa Kangasjärvi, University of Turku, Finland

***Correspondence:**
Barry Pogson, School of Biochemistry and Molecular Biology, Australian Research Council Centre of Excellence in Plant Energy Biology, Australian National University, Canberra, ACT 0200, Australia.
e-mail: barry.pogson@anu.edu.au

Chloroplasts of leaves under high light stress initiate signals to the nuclei of both exposed and distal leaves in order to acclimate against the potential threat of oxidative damage: a process known as high light systemic acquired acclimation (HL SAA). This study explores the nature of HL SAA, synergistic interactions with other environmental stresses, and the impact of repeated HL stress on the acclimation response of exposed and distal leaves. This necessitated the development of novel experimental systems to investigate the initiation, perception, and response to HL SAA. These systems were used to investigate the HL SAA response by monitoring the induction of mRNA in distal leaves not exposed to the HL stress. Acclimation to HL is induced within minutes and the response is proportionally dependent on the quality and quantity of light. HL SAA treatments in conjunction with variations in temperature and humidity reveal HL SAA is influenced by fluctuations in humidity. These treatments also result in changes in auxin accumulation and auxin-responsive genes. A key question in retrograde signaling is the extent to which transient changes in light intensity result in a "memory" of the event leading to acclimation responses. Repeated exposure to short term HL resulted in acclimation of the exposed tissue and that of emerging and young leaves (but not older leaves) to HL and oxidative stress.

Keywords: systemic acquired acclimation, high light, photoprotection, retrograde signaling, oxidative stress

INTRODUCTION

Acclimation to changes in the environment is required for optimal plant performance under adverse conditions. Factors such as light, temperature, drought, mineral concentrations, and biotic infection are all capable of causing extensive damage to plants as well as inducing short and long term acclimation responses (Stitt and Hurry, 2002; Durrant and Dong, 2004; Bartels and Sunkar, 2005; Atkin et al., 2006; Gorsuch et al., 2010; Biswal et al., 2011). High light (HL) causes damage to DNA, proteins, and lipids, including components of the photosynthetic apparatus (Kalbin et al., 2001; Takahashi and Badger, 2011). Exposure to prolonged periods of HL increases the generation of reactive oxygen species (ROS) and alters the redox state of photosynthetic components such as the electron carrier, plastoquinone (Karpinski et al., 1997; Asada, 2006). These components provide important retrograde signals that communicate the chloroplast status to the nucleus proving important information to drive transcriptional activation of defense systems (Pogson et al., 2008; Ramel et al., 2012). Recently, evidence for novel HL retrograde signals including the SAL1-PAP pathway and an oxidative by-product of beta-carotene has been published (Estavillo et al., 2011; Ramel et al., 2012).

Chloroplastic and retrograde signaling in response to HL induces (1) pathways that allow for the dissipation of excess energy; (2) systems that detoxify the harmful by-products of HL; and (3) mechanisms that reduce the amount of light absorbed by the plant. Plants have also evolved different mechanisms that facilitate the dissipation of accumulated excess energy absorbed under HL conditions, including chlororespiration, cyclic electron flow (CEF), photorespiration, and non-photochemical quenching (NPQ; Rumeau et al., 2007; Bauwe et al., 2010; de Bianchi et al., 2010; Johnson, 2011). Depending on light conditions, NPQ can account for 50% or more of the absorbed energy (Demmig-Adams et al., 1996) and thus is one of the main avenues for excess energy dissipation under HL exposure. On the other hand, to detoxify accumulating ROS plants can also use enzymes or plant pigments to convert ROS into more benign molecules. Superoxide dismutase (SOD) and ascorbate peroxidase (APX) are responsible for directly detoxifying ROS, superoxide ($o_2^{\bullet -}$), and hydrogen peroxide (H_2O_2), respectively. In contrast, plant pigments such as carotenoids and tocopherols remove ROS via chemical and physical quenching (Conn et al., 1991; Kobayashi and Della Penna, 2008).

From dawn till sunset plants are subjected to varying light intensities due to the angle of the sun and transient shade from clouds, leaves, and neighboring plants. Living in such an environment creates "hot spots" of solar energy that have the potential to cause extensive local photo-oxidative damage to plants. Moreover, such hotspots can trigger rapid acclimation in tissues directly experiencing high irradiance stress, and in distal tissues still under partial shade (i.e., leaves that do not experience HL stress). Acclimation of metabolism in distal leaves occurs as a result of a 15- to 60-min short term HL exposure, termed high light systemic acquired acclimation (HL SAA), in which HL stressed tissues of individual plants communicate to the distal parts of the plant

initiating stress acclimation. Even though research over that last decade has significantly progressed the understanding of HL SAA many unknowns still exist in regards to the identity of the retrograde signal(s) and the acclimation processes which they govern. Also unclear is the exact nature of the synergistic relationships between different stresses, how they affect the initiation of HL SAA and subsequent acclimation processes against multiple stresses (Koussevitzky et al., 2007; Mullineaux and Baker, 2010).

By exposing 1/3 of the *Arabidopsis* rosette to non-specific HL, research has shown that SAA seems to be tightly regulated by retrograde signals initiated through changes in photosynthesis during HL stress, specifically changes to the PQ pool redox state and ROS production (Karpinski et al., 1997; Rossel et al., 2007; Muhlenbock et al., 2008). H_2O_2 accumulates rapidly under HL and remains a likely signaling candidate as H_2O_2-signaling components have been implicated in triggering HL SAA (Mateo et al., 2004; Muhlenbock et al., 2008; Miller et al., 2009) and are associated with inducing defense responses under both abiotic and biotic stress (Vanderauwera et al., 2005; Miller et al., 2007, 2010; Muhlenbock et al., 2008). Additionally, recent publications suggest the involvement of light-wavelength-specific electrochemical and memory-based signaling systems influenced by both calcium-mediated signaling and glutathione (GSH; Karpinski and Szechynska-Hebda, 2010; Szechynska-Hebda et al., 2010). Nonetheless, specific components and connections between these different processes, particularly from a temporal perspective, remain to be clarified.

Microarray data shows that distal protective mechanisms in response to short term non-specific HL exposure in 1/3 of the *Arabidopsis* rosette are controlled by the transcriptional regulation of many HL-, ROS-, pathogen infection-, hormone-, and drought-responsive genes (Mullineaux et al., 2000; Rossel et al., 2007; Muhlenbock et al., 2008). Among these genes are transcripts responsible for ROS detoxification and signal transduction such as zinc finger transcription factors (ZAT), APXs, and pathogenesis-related proteins (PRs). The induction of these transcripts and subsequent acclimation is known to impart enhanced tolerance to two distinct types of stress: pathogen infection and HL oxidative stress (Rossel et al., 2007; Muhlenbock et al., 2008; Szechynska-Hebda et al., 2010). The relationship between HL SAA, the transcriptional activation of these many genes, their role in specific HL signaling, and acclimation processes however remains less clear.

In addition to short term transient HL SAA the growth of young, unstressed developing leaves can be altered by changing the environment in which the mature leaves are maintained. This process of developmentally linked long term acclimation allows plants to exhibit further phenotypic changes to improve performance of new tissue to that which the mature leaves were exposed; whether through differences in irradiance, CO_2, or temperature (Yano and Terashima, 2001; Coupe et al., 2006; Gorsuch et al., 2010). These modifications to new leaves include modifying leaf structure, growth rates, leaf and palisade tissue thickness, epidermal cell shape and size, as well as chloroplast number and density in the developing leaves (Lake et al., 2001; Yano and Terashima, 2001; Thomas et al., 2004; Coupe et al., 2006; Miyazawa et al., 2006; Araya et al., 2008; Jiang et al., 2011; Woo et al., 2011). Even though the exact mechanisms and signaling processes from mature leaves to meristems remain elusive there is evidence suggesting the possible involvement of retrograde signaling components such as ROS, the redox status of the PQ pool, other plant hormones, or microRNAs (Yano and Terashima, 2001; Thomas et al., 2004; Coupe et al., 2006; Jiang et al., 2011).

Many questions persist in regards to the mechanisms controlling short term HL SAA, the synergistic relationships with other stresses, and its role in acclimation processes that occur during a single day and over longer periods of time (several days). This is a study in two parts, firstly, the investigation of how light and environmental conditions affect HL SAA and secondly, the study of repeated HL treatments on signaling in exposed and distal mature leaves. This was achieved through (1) the development of a novel treatment system to further characterize the short term HL SAA gene activation in existing tissues under varying ambient qualities such as the duration of treatment, light intensity, temperature, and relative humidity (RH), as well as to determine the spatial distribution of oxidative stress tolerance across the rosette; (2) investigation of whether and how repeated, transient, and localized HL treatments can alter acclimation responses within existing mature leaves.

MATERIALS AND METHODS

GROWTH CONDITIONS AND LIGHT EXPERIMENTS

For all experiments *Arabidopsis thaliana* (Col-0) plants were cultivated in soil under a 12-h photoperiod of $150 \pm 25\,\mu$mol photons $m^{-2}\,s^{-1}$, $23/22 \pm 2$°C day/night temperatures, and $70 \pm 10\%$ day/night RH. All HL treatments utilized a new light emitting diode (LED)-array system and mature (approximately 4 weeks old) *Arabidopsis* plants. *Arabidopsis* leaf position for tissue collection were counted according to *Arabidopsis* phyllotaxy (Jurgens, 2001).

The HL SAA LED-array system consisted of nine white Luxeon III star LEDs (Lumileds Lighting)[1] controlled by current limiters and focusing lenses which produced a light spot with 1 cm radius (Karpinski et al., 1999; Rossel et al., 2007; Muhlenbock et al., 2008; Szechynska-Hebda et al., 2010). For initial HL treatments, HL LED-array validation and HL SAA transcriptional analysis, individual leaves of nine plants were simultaneously exposed to HL ($1500 \pm 50\,\mu$mol photons $m^{-2}\,s^{-1}$) or to LL conditions ($40 \pm 25\,\mu$mol photons $m^{-2}\,s^{-1}$). Subsequently, HL, control, and distal tissues from three treated individual plants were pooled to yield three "biological" replicates per tissue, immediately frozen in liquid N_2, and stored at −80°C. During analysis of environmental effects on HL SAA, plants were subjected to: HL exposure ($1500 \pm 50\,\mu$mol photons $m^{-2}\,s^{-1}$) for either 5, 30, 60, and 120 min; varied irradiances of 250, 500, 1000, or $1500 \pm 50\,\mu$mol photons $m^{-2}\,s^{-1}$ for 60 min. Light quality treatments were performed with white, ultra violet A (400 nm), blue (460 nm), green (515 nm), yellow (600 nm), red (680 nm), and far-red (720 nm) specific light. The wavelength and irradiance of the specialized LEDs (Roithner LaserTechnik, Vienna, Austria) was verified by a spectrophotometer (**Figure 1**). For the repeated medium-term treatments, mature *Arabidopsis* plants were either subjected to HL array treatment

[1]http://www.philipslumileds.com/

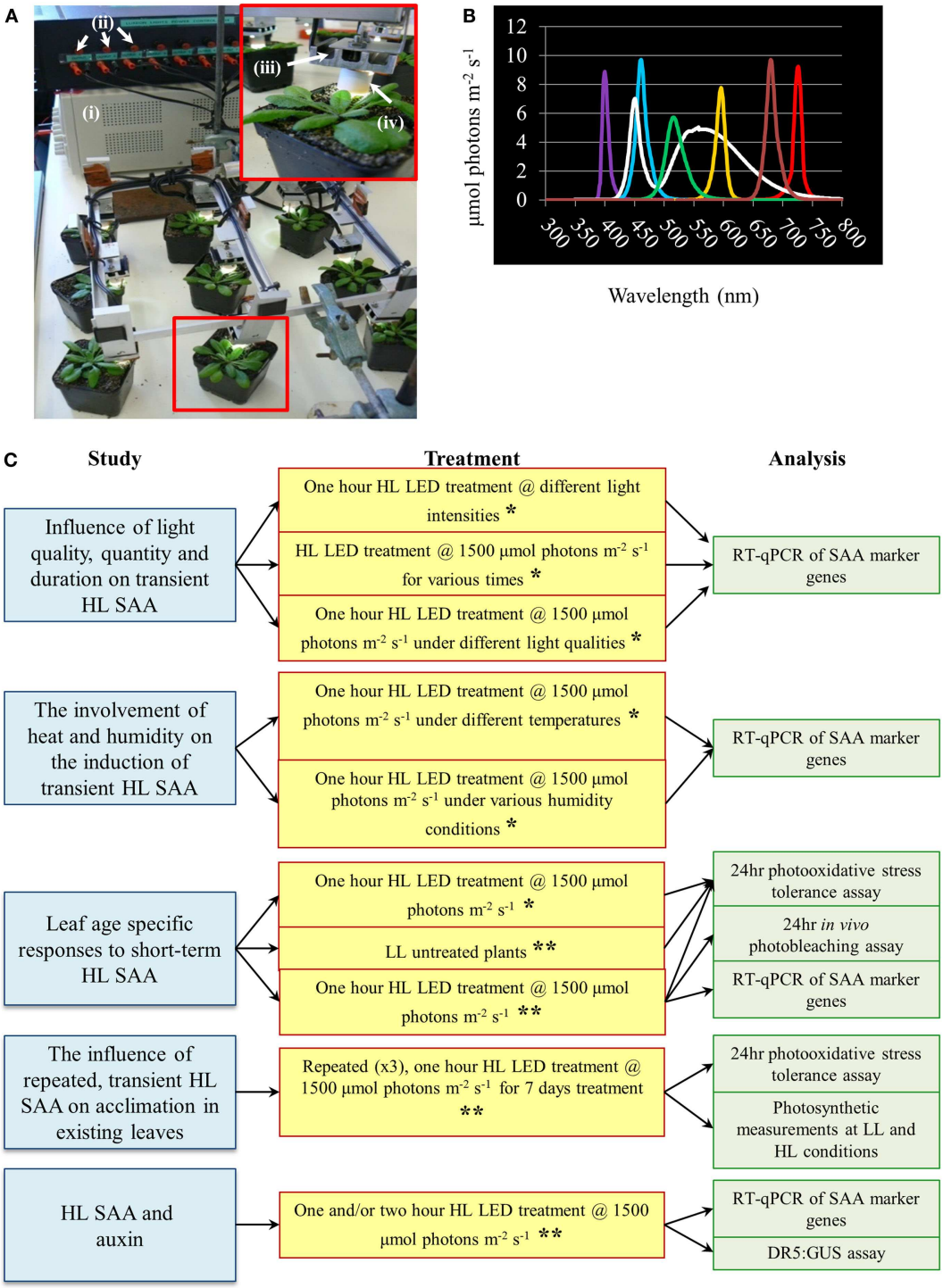

FIGURE 1 | High light systemic acquired acclimation-array, spectral output of specific LEDs and schematic overview of experiments conducted throughout the research article. (A) HL LED-array. Inset depicts a close-up image of a single treated *Arabidopsis* plant. Components of the HL LED-array include (i) power supply, (ii) current limiters for each LED, (iii) individual movable LED stage with heat sink, and (iv) light focusing lens. **(B)** Measured irradiance spectra from colored LEDs, $n = 3$. **(C)** Schematic diagram of the main areas of study, light treatments, and methods of analysis conducted throughout the research article. For all light treatment mature plants of approximately 4 weeks old grown under normal light conditions as detailed in Section "Materials and Methods" are used. For more detail on each individual treatment and analysis refer to Section "Materials and Methods." *Experiment conducted irrespective of leaf position. **Experiment conducted taking leaf position in to account.

($1500 \pm 50\,\mu$mol photons $m^{-2}\,s^{-1}$) three times a day for 60 min (separated by 120 min), for eight consecutive days, or remained untreated in the same growth environment.

All variable humidity and temperature specific HL SAA treatments were performed in a controlled environment chamber (Conviron S10H, Conviron, Ltd., Winnipeg, MB, Canada). Plants were subjected to either HL LED-array exposure ($1500 \pm 50\,\mu$mol photons $m^{-2}s^{-1}$) under varied humidity levels (30, 55, and 90% RH) at 21°C or at increasing temperatures (21, 28, and 32°C) at 55% RH.

RT-qPCR ANALYSIS

For gene transcript analysis, RNA was extracted from frozen samples using an RNeasy Plant Mini Kit (Qiagen, Ltd.) as instructed by the manufacturer's instructions. RNA was converted to cDNA using SuperScript III Reverse Transcriptase (Invitrogen), and RT-qPCR performed using a LightCycler 480 (Roche) with either the LightCycler Universal ProbeLibrary or Sybr green specified by the manufacturer's instructions. The LightCycler 480 software application (Roche; version 1.5.0) was used to determine crossing-point values for each reaction, amplification efficiency of each primer set, validation of each reaction, and relative expression values obtained as described (Pfaffl, 2001). For initial RT-qPCR experiments and primer validation target transcript levels were normalized to both reference genes, *CYCLOPHILIN 5 (CYP5)* and *PROTEIN PHOSPHATASE 2A (PP2A)*. In subsequent experiments target transcript level were normalized to one of the aforementioned reference genes. List of primers are outlined in **Table 2**. Statistical significance of results was tested by conducting paired student *t*-tests (between LL controls and other samples) and one-way analyses of variance (ANOVA) on all samples using the scientific statistical analysis program, SigmaPlot12 (Systat Software, Inc.). Least significant difference (LSD) *post hoc* tests were used where one-way ANOVAs indicated significant differences between factors.

IN VITRO AND *IN VIVO* STRESS TOLERANCE ASSAYS AND PHOTOSYNTHETIC MEASUREMENTS

The *in vitro* photo-oxidative stress tolerance assay was performed after short term HL SAA treatments and at the end of the 8-day period of the repeated, HL SAA study, using a method adapted from Rossel et al. (2007). Leaf disks from each of the treated plants were removed and floated (abaxial side down) on 0.5 M H_2O_2 in a clear 200 µL 96-well plate. The leaf disks were then exposed to HL ($1500 \pm 50\,\mu$mol photons $m^{-2}\,s^{-1}$) for 60 min and moved to LL growth conditions for 24 h while remaining in H_2O_2 solution, during which time photographs were taken periodically every 2 h to determine the extent of bleaching of the leaves. Analysis of the photos was performed using ImageJ[2] and Microsoft Excel (Microsoft, Washington, USA). The percentage of healthy (green), and bleached (white) tissue in each leaf disk was calculated and compared over time.

Plants subjected to the *in vivo* HL-stress tolerance assay were exposed to the HL spot treatment (leaf 4 @ $1000 \pm 50\,\mu$mol photons $m^{-2}\,s^{-1}$) for 60 min or remained untreated under LL growth conditions. Following the initial HL SAA treatment, treated and untreated whole plants were placed in a controlled growth environment chamber (Conviron S10H, Conviron, Ltd., Winnipeg, MB, Canada) under HL growth conditions for 24 h ($1500 \pm 25\,\mu$mol photons $m^{-2}\,s^{-1}$, $23/22 \pm 2$°C). Plants remained well watered for the duration of the 24-h treatment. During the 24-h HL treatment photographs were taken periodically to assess the first appearance photobleaching.

Chlorophyll fluorescence measurements were taken during the repeated, HL SAA study using an IMAGING-PAM chlorophyll fluorometer and analyzed with the ImagingWin software application (Walz, Effeltrich, Germany) as described (Krause and Weis, 1991; Oxborough, 2004; Baker, 2008). Tissue was sampled from existing mature tissues, as well as from the treated leaf as outlined in the transient HL SAA experiments.

MICROARRAY DATA COMPARISON AND TRANSCRIPT ANALYSIS

Microarray data from Rossel et al. (2007) was directly compared to six different studies of auxin microarray experiments (Sawa et al., 2002; Zhao et al., 2003; Redman et al., 2004; Overvoorde et al., 2005; Nemhauser et al., 2006; Lee et al., 2009). Only gene transcripts that demonstrated significant changes in gene expression (as determined in each respective article) were considered in this comparison. The functional characterization was based on gene ontology (GO) descriptions available on TAIR 10 (2012). As all transcripts had numerous GO descriptions, preference was given to auxin-related or stress networks.

AUXIN DETECTION USING DR5:GUS TRANSGENICS

DR5:GUS transgenic lines were provided by Dr. Christopher Cazzonelli (ANU). Mature *DR5:GUS* transgenic plants were either treated with LL conditions ($40 \pm 25\,\mu$mol photons $m^{-2}\,s^{-1}$), or with HL spot ($1500 \pm 50\,\mu$mol photons $m^{-2}\,s^{-1}$) for 60 or 120 min. GUS staining and localization was performed using a modified version of the GUS visualization assay (Stomp, 1992). Each plant was divided into separate 2 ml microfuge tubes.

RESULTS

TRANSCRIPTIONAL REGULATION OF GENES SPECIFIC TO HL SAA

A new HL SAA LED-array system was developed to enable repeated exposure of a leaf without altering the growth conditions of other leaves (**Figure 1**). This treatment applied a spot of light in the absence of heat and shading, facilitating a more environmentally relevant and specific test of HL-induced SAA compared to previous light treatment methods (Karpinski et al., 1999; Rossel et al., 2007; Muhlenbock et al., 2008; Szechynska-Hebda et al., 2010). Due to the specific nature of the treatment it also allows differentiation between retrograde signals derived from other stresses and solely HL.

It was necessary to validate the new method given the differences in light regimes between this and previous HL and HL SAA treatments. Thus, a detailed analysis of transcript changes in response to HL spot treatment of numerous genes involved in a range of plant processes from light signaling to ROS metabolism was performed. This provided (1) a greater understanding of the genetic regulation of HL retrograde responses governing the initiation and perpetuation of SAA; (2) identification of SAA marker

[2]http://rsbweb.nih.gov/ij/

genes that could be used in this study for an efficient quantification of HL SAA activation under different treatment regimes; and (3) identification of genes which are specifically induced in distal leaves, but not exposed leaves, which may give novel insight into the mechanisms or role of HL SAA in *Arabidopsis*.

For this analysis, genes were selected based on one of two factors: if they were reported to be involved in HL or SAA in previous studies (Karpinski et al., 1999; Mullineaux et al., 2000; Rossel et al., 2002, 2007); and according to their relative importance and involvement in light and stress signaling pathways in *Arabidopsis* (Rapp and Mullet, 1991; Yamaguchi-Shinozaki and Shinozaki, 1993; Braam et al., 1997; Hutin et al., 2003; Barrero et al., 2006; Lee et al., 2007; Zhu et al., 2010). Over 45 transcripts induced in both HL and distal leaf tissue, as well as genes reported to be induced in distal, but not HL-exposed leaves, were chosen for confirmation with RT-qPCR (**Table 1**). The vast majority of genes reported to be induced by HL SAA in microarrays and other experiments when a 1/3 of the rosette is exposed to HL were confirmed to be induced by the single spot of the HL LED-array system. However, all except one of the reported SAA specific inducible genes were also induced in the exposed tissue. The single gene that exhibited distal-specific expression, *Gretchen Hagen 3.3* (*GH3.3*; **Table 1**), encodes an enzyme involved in maintaining auxin homeostasis by auxin conjugation with amino acids (Staswick et al., 2005), which will be addressed later in this manuscript. *REDOX RESPONSIVE FACTOR 1* (*RRTF1*) and *ZAT10* were selected as marker genes for HL SAA in subsequent experiments as both transcripts exhibited strong, relatively consistent transcript induction under short term HL spot treatment.

INFLUENCE OF LIGHT QUALITY, QUANTITY, AND DURATION ON TRANSIENT HL SAA

Light intensity, quality, and duration of exposure all influence the generation of retrograde signals that in turn influence and activate different developmental and acclimation responses of treated tissues (Franklin and Whitelam, 2004; Li et al., 2009). Thus a series of experiments was conducted to explore the relationship between specific light qualities and specific HL SAA (**Figure 1C**). SAA induction was analyzed in plants treated with HL for 5, 30, 60, and 120 min, respectively. Both *ZAT10* and *RRTF1* transcript levels increased significantly within 5 min in both HL-treated and distal tissues and remained elevated for at least 60 min (**Figures 2A,B**), largely confirming earlier findings using different HL systems. However, after 2 h of HL exposure, transcript levels declined to pre-HL levels in both treated and distal tissues. Even though both SAA marker genes exhibit significant gene induction within 5 min (fourfold), RRTF1 mRNA accumulation was highest after 60 min (60-fold). Since treatment for 60 min showed the maximal increase in both marker genes, this treatment time was applied for all subsequent analyses.

Previous studies analyzed SAA-induced gene expression using relatively high, and ultimately damaging, light intensities in the order of 1500 μmol photons m^{-2} s^{-1} (Karpinski et al., 1999; Rossel et al., 2007; Muhlenbock et al., 2008). With such elevated light intensities to what extent this reflected severe photo-oxidative stress or changes in the electron transport rate and redox poise could not be evaluated. Consequently, 60 min HL LED-array treatments were performed on *Arabidopsis* plants at different light intensities (250, 500, 1000, and 1500 μmol photons m^{-2} s^{-1}, respectively). *RRTF1* and *ZAT10* were induced at already relatively small changes in light intensity (**Figures 2C,D**). Significantly, treatment with 250 μmol photons m^{-2} s^{-1} was sufficient to significantly increase mRNA-levels for both genes in HL-treated and distal tissues. As the light intensity increased, *RRTF1* transcript levels in both HL and distal tissues increased proportionally. In contrast, *ZAT10* showed a relatively small but significant increase in gene expression in both HL-treated and distal tissues under light intensities lower than 1500 μmol photons m^{-2} s^{-1}.

Light quality (wavelength) also plays an important role in HL response, acclimation, and plant developmental processes (Li et al., 2009). The HL-specific SAA response to different wavelengths was investigated using colored LEDs. The white LEDs exhibited two maximum peaks of emission (460, 570 nm). Each colored LED had a single specific peak of wavelength irradiance, namely: UVA (400 nm), blue (460 nm), green (515 nm), yellow (600 nm), red (680 nm), and far-red (720 nm; **Figure 1**). The relative expression levels of *RRTF1* and *ZAT10* were analyzed after HL treatment under the different light qualities using various statistical tests: independent *t*-tests for each time point, and LSD *post hoc* tests from one-way ANOVA combining all tissue-light treatment combinations. As expected, independent samples *t*-tests for each light quality treatment showed white light caused the most statistically significant SAA gene induction, followed by blue light, while UVA, yellow, and red light had less prominent induction of both *ZAT10* and *RRTF1*(**Figures 2E,F**). LSD tests from one-way ANOVA reveal that for both *RRTF1* and *ZAT10* white light caused the most prominent SAA gene induction ($P < 0.05$). Under blue light *RRTF1* also shows significant induction in comparison to the majority of the other light treatments ($P < 0.05$). On the other hand the significance of transcriptional changes of *ZAT10* between different light qualities becomes less apparent due to small relative fold changes and experimental variance. The results clearly demonstrate that the degree of HL SAA induction of the marker genes is wavelength-dependent.

THE INVOLVEMENT OF HEAT AND HUMIDITY ON THE INDUCTION OF TRANSIENT HL SAA

High light stress in a natural environment rarely occurs without changes in temperature and humidity, both of which are also powerful inducers of separate retrograde signaling and acclimation defense responses (Fryer et al., 2003; Zhou et al., 2004; Allakhverdiev et al., 2008). Consequently, we investigated the effect of heat and humidity in the induction of HL SAA. Relative transcript levels were normalized to LL at 21˚C for each temperature (**Figure 3A**). Both *RRTF1* and *ZAT10* transcript levels increased after HL exposure in both treated and distal tissues under all analyzed temperatures. Interestingly, expression of *RRTF1* at 28˚C was already increased in untreated LL plants compared to LL 21˚C. In contrast, at 32˚C *RRTF1* showed a significant reduction of transcript levels in all tissues. At the same time, *ZAT10* exhibited a slightly more linear response to HL SAA and heat. The results demonstrate that while the ambient temperature has a significant effect on the induction of HL SAA marker genes HL SAA still occurs at elevated temperatures.

Table 1 | Analysis of gene transcript abundance after 60 min HL LED-array treatment.

Gene locus	Annotation (TAIR10)	HL mRNA fold change	Standard error	DL mRNA fold change	Standard error	*Ref**
AT1G43160	*RAP2.6*	**2395**	1606	**450.4**	253.1	*ii*
AT4G15210	*ATBETA AMY*	**1090.3**	277.3	**85.7**	9.9	*i, iii*
AT3G22840	*ELIP1*	**79.1**	8	**7.3**	1.7	*ii*
AT4G34410	*RRTF1*	**68.9**	13.8	**28.2**	5	*iii*
AT5G20230	*BCB*	**39.8**	7.3	**65.8**	17.5	*iii*
AT4G28140	*Unknown (F26K10.20)*	**34.8**	6.8	**10.4**	2.5	*iii*
AT1G52890	*ANACO19*	**31.6**	12.6	**10.5**	0.8	*iii*
AT3G63060	*EDL3*	**29.5**	6.7	**4.9**	0.5	*iii*
AT1G12610	*DDF1*	**21.2**	3.9	**10.3**	3.1	*iii*
AT5G05410	*DREB2A*	**15.5**	1.5	**4.2**	0.6	*i, ii*
AT1G02400	*DTA1*	**12.2**	1.7	**9**	2.6	*iii*
AT1G28370	*ERF11*	**10**	4	**8.3**	2.2	*iii*
AT5G59820	*ZAT12*	**9.9**	1.4	**11.2**	0.4	*i*
AT5G04340	*ZAT6*	**9.3**	3	**3.8**	0.3	*iii*
AT1G01480	*ACS2*	**8.6**	0.8	**7.1**	1.7	*iii*
AT5G67300	*MYB44*	**8.4**	0.4	**4.9**	1.7	*iii*
AT2G42360	*Putative zinc finger protein*	**8.2**	2.6	**4.5**	1.2	*iii*
AT1G27730	*ZAT10*	**7.6**	0.8	**6.2**	1.9	*i*
AT1G21550	*Put. calcium binding protein*	**6.6**	0.9	**3.7**	0.4	*iii*
AT2G38870	*PR6-like*	**5.9**	2.5	**8.7**	3.2	*iii*
AT4G18170	*WRKY28*	**5.5**	0.5	**4.3**	0.4	*iii*
AT3G46660	*UGT76E12*	**5.4**	1.2	**2.2**	0.4	*iii*
AT5G47220	*ERF2*	**5.2**	1.6	**6.5**	1.4	*iii*
AT3G14440	*NCED3*	**3.8**	0.4	**4.3**	1.4	*ii*
AT2G35980	*NHL10*	**3.8**	0.9	**2.2**	0.3	*iii*
AT4G35090	*CAT2*	**3.3**	0.4	**2.5**	0.2	*i*
AT4G21680	*NRT1.8*	**2.6**	0.4	**3.6**	0.4	*iii*
AT5G50760	*Unknown (MFB16.16)*	**2.2**	0.1	**2.8**	0.5	*iii*
AT2G23170	*GH3.3*	**1.3**	0.5	**6.2**	0.9	*iii*
AT2G47730	*GST6*	**2.6**	0.3	**2.12**	0.2	*ii*
AT5G57560	*TCH4*	**2.2**	0.2	**2.1**	0.3	*ii*
AT5G52310	*RD29a*	**2**	0.5	**1.9**	0.2	*ii*
AT3G09640	*APX2*	**258.5**	234.2	**1.2**	0.6	*ii*
AT4G14690	*ELIP2*	**100.5**	18.4	**0.7**	0.1	*ii*
AT1G67090	*RBCS1A*	**2.2**	0.1	**1.1**	0.7	*ii*
AT2G22470	*AGP2*	**1.9**	0.2	**1.6**	0.2	*iii*
AT1G17170	*GST24*	**1.8**	0.6	**0.9**	0.1	*iii*
AT2G31570	*GPX2*	**1.7**	0.4	**1.2**	0.2	*i*
AT1G05680	*UGT74E2*	**1.4**	0.1	**0.9**	0.2	*iii*
AT1G29910	*LHCB1.2*	**1.3**	0.1	**1.4**	0.2	*ii*
AT2G27030	*CAM5*	**1.1**	0.1	**1.1**	0	*ii*
AT4G33630	*EX1*	**1.1**	0.1	**1.4**	0.1	*ii*
AT3G57260	*PR2*	**0.7**	0.4	**0.8**	0.3	*ii*

References used for gene selection: i. Karpinski et al. (1999), Mullineaux et al. (2000), Rossel et al. (2007), Rossel et al. (2002), ii. Rapp and Mullet (1991), Yamaguchi-Shinozaki and Shinozaki (1993), Braam et al. (1997), Hutin et al. (2003), Barrero et al. (2006), Lee et al. (2007), Zhu et al. (2010), iii Rossel et al. (2007).
Bold indicates gene fold change.

To assess the role of humidity in the induction of HL SAA, different humidity levels were used (30, 55, and 90% RH). Normalizing transcript levels of HL spot exposed plants to LL 90% RH revealed that humidity directly affects the induction of HL SAA. Even though independent samples *t*-tests for each treatment show statistically significant differences between LL samples at 90% humidity, LSD tests on one-way ANOVAs on all sample groups reveal that the difference between the expression of both marker genes under lower levels of humidity in LL and DL tissues is not statistically disparate ($P > 0.05$; **Figure 3B**). This is especially

Table 2 | Real-time RT-PCR primers and Universal ProbeLibrary probes (Roche) used for quantitative transcript analysis.

Target sequence anotation	Gene locus	Universal Probe Library probe		Primer sequences
ACS2	AT1G01480	80	F	CGACGACTTTACGAGGATGG
			R	GCTCGGAGAAGAGGTGAGTG
AGP2	AT2G22470	15	F	GGTTGCTTCTCCTCCTCAGA
			R	TGGAGTTAATCCAGCGGAAG
ANOCO19	AT1G52890	143	F	CAACAACGGTACTTCGTCCA
			R	TTGTCGATCTCTTGATGAAACG
APX2	AT3G09640	10	F	TCATCCTGGTAGACTGGACAAA
			R	CACATCTCTTAGATGATCCACACC
ATBETA AMY	AT4G15210	115	F	CCCGTTTACGTTATGCTTCC
			R	ACGTTTAAGCTGCGTTTCAAG
BCB	AT5G20230	3	F	GTAGGCGACGAGCTCGAAT
			R	TTCTGATACAACTGCCACATCA
CAM5	AT2G27030	103	F	TGTCAAAGTTATGATGGCAAAGA
			R	GAATTGCTACTACGCTTTGCTG
CAT2	AT4G35090	25	F	TCTGGTGCTCCTGTATGGAA
			R	TGGTAATCCTCAAGAAGGATAGGA
CYCLO	AT2G29960	103	F	GGCAGTTCCTAAAACTGCAGAA
			R	TTCCCTTGTAGTGTAGAGGTTTCC
DDF1	AT1G12610	12	F	CGGAGATGAGGCCTAAGAAG
			R	TGCCTCTGTAAACTGGGTGA
DREB2A	AT5G05410	121	F	GATTTTCAAATTTCGTCCCCTA
			R	TGTTCTGTTTCTATCTCCACTCTGA
DTA1	AT1G02400	141	F	TCATGATGATCCTTTCAAGTTCAG
			R	CCAAATCTCTAACCGTGCGTA
EDL3	AT3G63060	28	F	ATTGTCCGGCGAAGATCC
			R	CAGAAGAACATGAGTTTCGCTAAC
ELIP1	AT3G22840	126	F	GCACAAAGTTTAGCGACTTGC
			R	CGCAACGAATCCAACCAT
ELIP2	AT4G14690	101	F	CCACCACAAATGCCACAG
			R	GCAAATCTCCAAACTTCGTACTC
ERF11	AT1G28370	82	F	CGTCAAAACCAACGAAGGTAA
			R	ACGTCCCCATGGTCTCTTC
ERF2	AT5G47220	82	F	TTACGGAGACGGCAGTGAA
			R	AATTTCCCCCACGGTCTCT
EX1	AT4G33630	116	F	AGAAAGAGAAGAAGATTTCTGTCAAGA
			R	ATTTTGTCAAACCCGACAGC
GH3.3	AT2G23170	148	F	CATCACAGAGTTCCTCACAAGC
			R	GTCGGTCCATGTCTTCATCA
GH3.5	AT4G27260	148	F	CATCTCTGAGTTCCTCACAAGC
			R	GGAACGAACTGGCTCATCA
GPX2	AT2G31570	91	F	CCTGATGGCAAGGTCTTACAG
			R	GCAGTTTGAATGTCCTTCTCG
GST6	AT2G47730	15	F	AAGCAAGAGGCCCACCTT
			R	TCTTGACTCGAAAAGCGTCA
GST24	AT1G17170	12	F	AGACTTGGCCCGACAATAAC
			R	TCCTTCTCGCCGTAACATTC
LHCB1.2	AT1G29910	110	F	CCCATTGGGTCTTGCTACC
			R	CCGTTCTTGAGCTCCTTCAC
MYB44	AT5G67300	98	F	ACCTTCCGTTGAGCTTTTCA
			R	AGGAAGCGGTAGCACAACAG
NCED3	AT3G14440	22	F	TCGTCGTGATAGGGTCCTG
			R	TTCTCGTCAGACTCGTTGAAAA

(Continued)

Table 2 | Continued

Target sequence anotation	Gene locus	Universal Probe Library probe		Primer sequences
NHL10	AT2G35980	24	F	GCCTTCTACGGTCCATCAGT
			R	GTGCCCACGTCGGTAGTAG
NRT1.8	AT4G21680	47	F	TGTGCACCATGAAGAGTTGAA
			R	TGTAACAATAGCAGCTCTATCCAAG
PIN3	AT1G70940	59	F	TCTTGGAATGGCAATGTTTAGTT
			R	CTAACCGCCATGGCAAAC
PIN4	AT2G01420	159	F	TGCCCAAAATATTACAACAATCC
			R	TGGGTTGAAGTGCCATGA
PIN7	AT1G23080	159	F	TGGGCTCTTGTTGCTTTCA
			R	TCACCCAAACTGAACATTGC
PP2A	AT1G13320	29	F	GACCGGAGCAACTAGGAC
			R	AAAACTTGGTAACTTTTCCAGCA
PR2	AT3G57260	111	F	GCTTAGCCTCACCACCAATG
			R	CCCGTAGCATACTCCGATTT
PR6-like	AT2G38870	155	F	GACGAGTCGTGGTTGGTTAGT
			R	AACTTTAGGCATCAGTAACACAGAAA
Putative calcium binding protein	AT1G21550	63	F	GATGTGTTGGAACGGCTAGG
			R	CATTCTCCCACAATCCCAAG
Putative zinc finger protein	AT2G42360	35	F	AAACCAGGCTGAACTTGACTG
			R	CCGGGGATACAACTGTTTTG
RAP2.6	AT1G43160	140	F	GGACGATGGGTCATAAGAGAGA
			R	TGAGCTTTCACATTCTTTAGTCACA
RBCS1A	AT1G67090	8	F	CGCTCCTTTCAACGGACTTA
			R	AGTAATGTCGTTGTTAGCCTTGC
RD29a	AT5G52310	69	F	ACGTCGAGACCCCGATAAC
			R	CAATCTCCGGTACTCCTCCA
RRTF1	AT4G34410	68	F	TCGGGTATGCATTATCCTAACA
			R	AAGCTCTTGCTCCGGTGA
TCH4	AT5G57560	6	F	GCTCAACAAAGGATGAGATGG
			R	CCTCTTCGCATCCGTACAAT
UGT76E12	AT3G46660	138	F	TCTTTGGTTACCACTCTCTAACAAGA
			R	CTCTTCGTCACAACATGTGAATC
UGT74E2	AT1G05680	29	F	TGTGTGGAAGGTTGGGGTA
			R	TCTTCTCTTCTCACAAACCCATC
Unknown (F26K10.20)	AT4G28140	143	F	TCGTCCTAAACCCTATTTCCAA
			R	AAAGGGAAAGCCTCTAACGAA
Unknown (MFB16.16)	AT5G50760	152	F	CAAAAGGAAAGCCGAAGAAA
			R	GGACCAACGTAAACCGTGAA
WRKY28	AT4G18170	70	F	AGGACGGCAGCTTATACTAACG
			R	CACTTTGTCCATATCCATAATCCA
ZAT6	AT5G04340	8	F	CTCGCGACGGAGATAGAAAC
			R	AAGCAGAGGAGGTGAAGACG
ZAT10	AT1G27730	31	F	GGACAAAGGGTAAGCGATCTAA
			R	AGAAGCATGAGGCAAAAAGC
ZAT12	AT5G59820	103	F	CCCACGGTGACTACGTTGA
			R	TCAAATTGTCCACCATCCCTA

apparent at 30% RH, where the ability to induce distal expression of both *RRTF1* and *ZAT10* is almost abolished. Therefore, both humidity and temperature have an impact on the induction of HL SAA in distal leaves; with low humidity largely abolishing HL SAA compared to untreated, low humidity exposed plants.

LEAF AGE SPECIFIC RESPONSES TO SHORT TERM HL SAA

In a prior study, treating 1/3 of the rosette with HL for 60 min increased the tolerance to H_2O_2-mediated bleaching of leaf disks (Rossel et al., 2007). The new treatment system however exposes a much smaller area of a single leaf with HL,

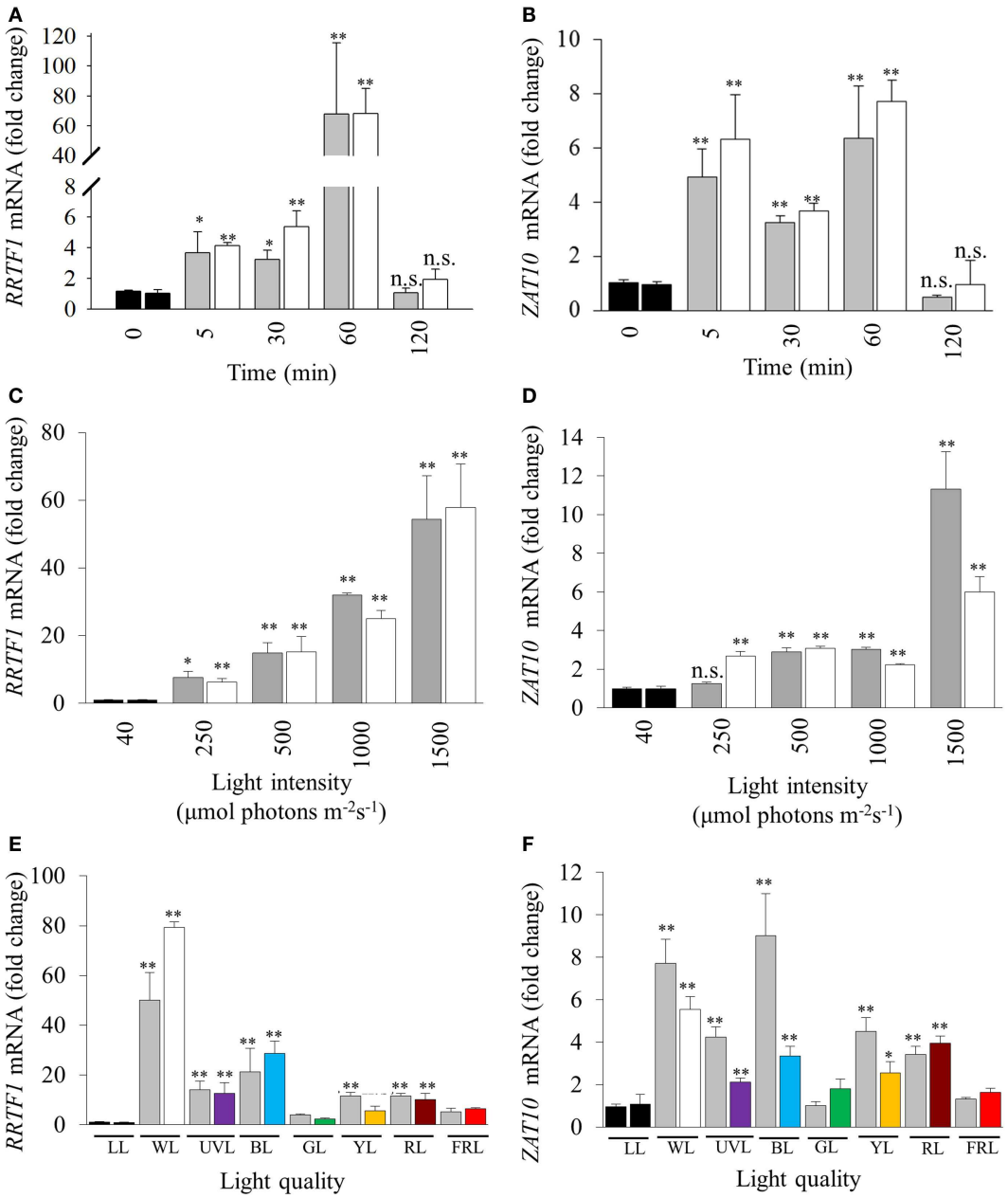

FIGURE 2 | Influence of duration, intensity, and quality of HL on SAA-mediated gene expression. (A), **(C)**, and **(E)** *RRTF1*; **(B)**, **(D)**, and **(F)** *ZAT10*. LL (black bars, 40 ± 25 µmol photons $m^{-2}s^{-1}$), HL-treated leaves (white, 1500 ± 50 µmol photons $m^{-2}s^{-1}$), and distal leaves (grey). **(A,B)** Duration of HL (1500 µmol photons m^{-2} s^{-1}) treatments after 0, 5, 30, 60, 120 min; **(C,D)** 60 min HL at 250, 500, 1000, and 1500 ± 50 µmol photons $m^{-2}s^{-1}$; **(E,F)** 60 min HL (1500 µmol photons m^{-2} s^{-1}) using LEDs of different light qualities: LL control plants (black, LL), distal (grey), white HL (WL), ultra violet light (UVL), blue (BL), green (GL), yellow (YL), red (RL), and far-red (FRL). For each sample $n = 6$, $*p < 0.005$, $**p < 0.001$, n.s., not significant, error bars indicate standard error. LSD *post hoc* tests from one-way ANOVAs show that for both *RRTF1* and *ZAT10* plants under white and blue light LED treatments caused the significant SAA gene induction ($P < 0.05$). For spectral details, Section "Materials and Methods" and **Figure 1**.

and thus a preliminary investigation into whether this has an impact on the HL SAA physiological response was assessed. The capacity of plant tissues to resist oxidative damage was measured by conducting an *in vitro* photo-oxidative stress tolerance assay which determines the degree of bleaching in response to HL and exogenous H_2O_2 (Förster et al., 2005; Rossel et al., 2007). As described in the Section "Materials and Methods" this assay uses HL and H_2O_2 as powerful reducing agents to extenuate and rapidly cause oxidative damage to plant tissues, thus inducing pigment bleaching. The extent and the rate at which bleaching occurs can thus be used to estimate the extent of photo-oxidative stress tolerance in plant tissues. However,

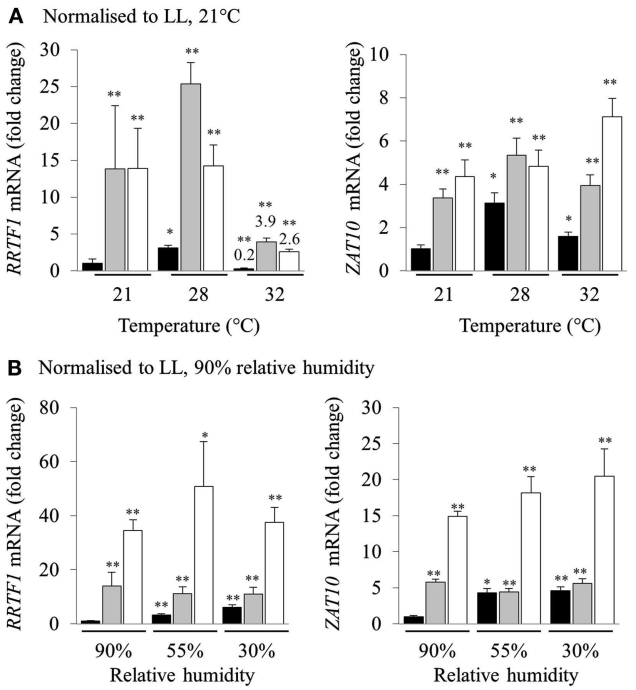

FIGURE 3 | Analysis of RRTF1 and *ZAT10* transcripts under 21, 28, and 32°C and 90, 55, and 30% relative humidity during HL SAA. LL control (black), HL (white), and distal (grey). In **(A)** the data are normalized to LL 21°C, for each sample, for **(B)** the data are normalized to LL 90% relative humidity, for each sample $n = 6$, $*p < 0.005$, $**p < 0.001$, n.s., not significant, error bars indicate standard error. LSD *post hoc* tests from one-way ANOVAs show that for both *RRTF1* and *ZAT10* plants under 55 and 30% humidity LED treatments the differences between LL and DL tissues is not statistically significant ($P > 0.05$).

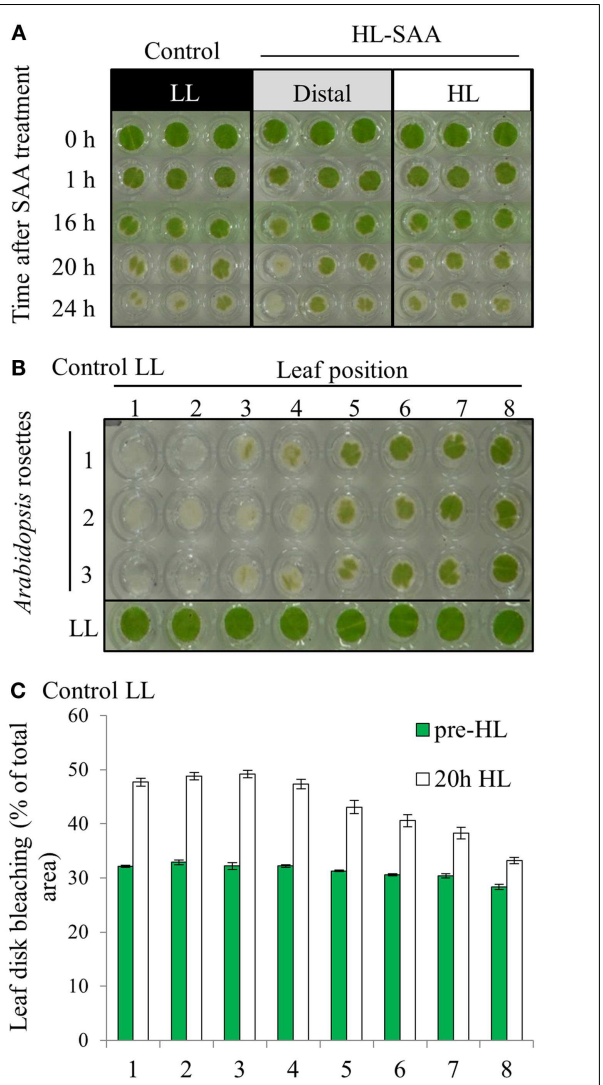

FIGURE 4 | *In vitro* photo-oxidative tolerance of leaf disks during HL SAA and control LL conditions. (A) Representative image of leaf disks sampled from LL (black), HL spot treated leaves (white), and distal leaves (gray). **(B)** Leaf disk assay of basal resistance to photo-oxidative stress across the *Arabidopsis* rosette in leaves under control LL growth conditions. **(C)** Analysis of **(B)** using ImageJ software to distinguish between bleached (white) and unbleached (green) tissues. Plants were either treated to HL spot treatment or remained under LL condition, as explained in Section "Material and Methods." Following treatment leaf disks were floated on H_2O_2 (0.5 M) in a 96-well plate, HL-treated for 60 mins, then returned to 150 μmol photons m^{-2} s^{-1} for 24 h. Photographs were taken throughout the 24-h period, experiment was performed in triplicate, $n = 3$.

variability between replicates was greater than variability between treatments (**Figure 4A**).

The variability between leaf disks was hypothesized to be a result of sampling leaves at different developmental stages. Indeed, an *in vitro* oxidative stress tolerance assay investigating leaf positional effects across an *Arabidopsis* rosette under normal LL growth conditions indicated basal leaf age-dependent tolerance in younger leaves (**Figures 4B,C**). Consequently, leaf age-dependent HL SAA transcriptional responses in the exposed and adjacent leaves were measured. Mature, fully expanded leaf 6 (**Figures 5A–C**) or 5 (**Figures 5D,E**) were also exposed to the HL LED-array, and the distal response quantified in two ways: tissue was either sampled from within the same leaf, immediately above (younger) and below (older; **Figures 5B,C**), or sampled only from the three younger leaves (**Figures 5D,E**). Independent samples *t*-tests for each leaf show statistically significant induction of the two marker genes in all treated tissues compared to LL controls (**Figures 5B–E**). More specifically, LSD tests on one-way ANOVAs combining all tissues show significant differences between leaf 5 and 7 when leaf 6 is treated with HL ($P < 0.05$; **Figures 5B,C**) and also between leaf 5, 6, and 8 when leaf 5 is treated ($P < 0.05$; **Figures 5D,E**). Thus revealing that in general, distal tissue within the treated leaf, or immediately adjacent, had comparable accumulation of transcripts to the exposed leaf, whereas transcript levels then decreased consistently in progressively younger leaves.

Based on the results of **Figures 4** and **5**, oxidative stress tolerance was investigated using the *in vitro* photo-oxidative tolerance assay taking leaf position into account (**Figure 6A**). Leaf 4 was treated with HL spot, leaf disks sampled from all leaves and the assay performed as described in Section "Materials and Methods." Results

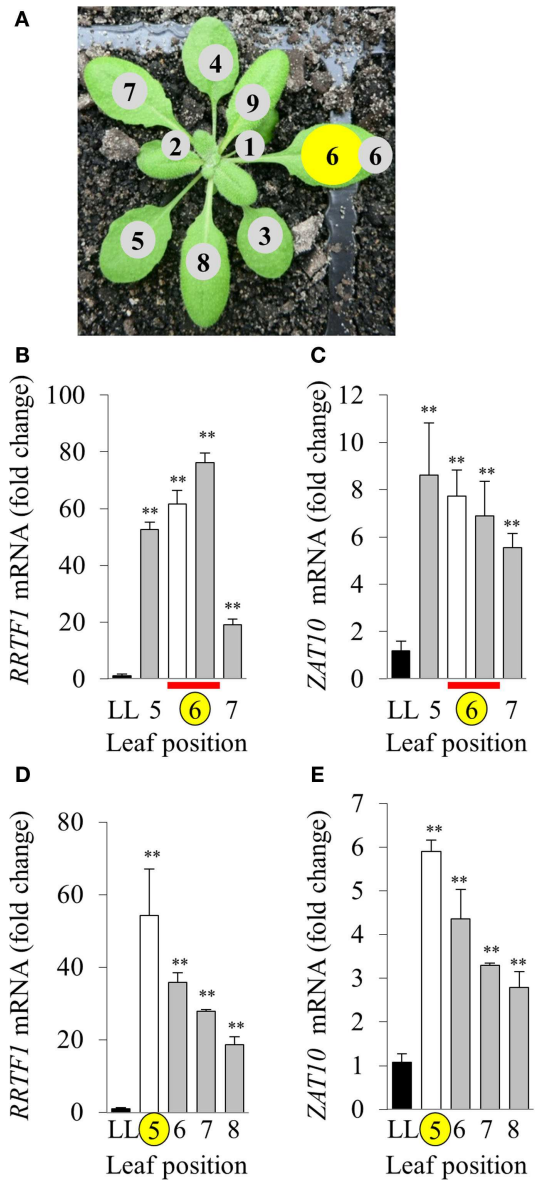

FIGURE 5 | Leaf position-dependent analysis of RRTF1 and *ZAT10* transcript abundance during HL SAA. (A) Representative image of leaf positions on the *Arabidopsis* rosette, where leaf position 6 is HL-treated (yellow). **(B,C)** HL and distal tissue sampled from leaf 6, distal from leaf positions 5 and 7, where LL control (black), HL (white), and distal (grey) leaves, HL and distal sampled from same leaf (red bar), HL-treated (yellow circle). **(D,E)** HL-treated leaf position 5, distal leaves 6, 7, and 8. $*p < 0.005$, $**p < 0.001$, n.s., not significant, error bars indicate standard error. $n = 6$. For both *RRTF1* and *ZAT10* LSD *post hoc* tests on one-way ANOVAs show significant differences between Leaf 5 and 7 when leaf 6 is treated with HL **(B,C)** and also between leaf 5, 6, and 8 when leaf 5 is treated [**(D,E)**; $P < 0.05$].

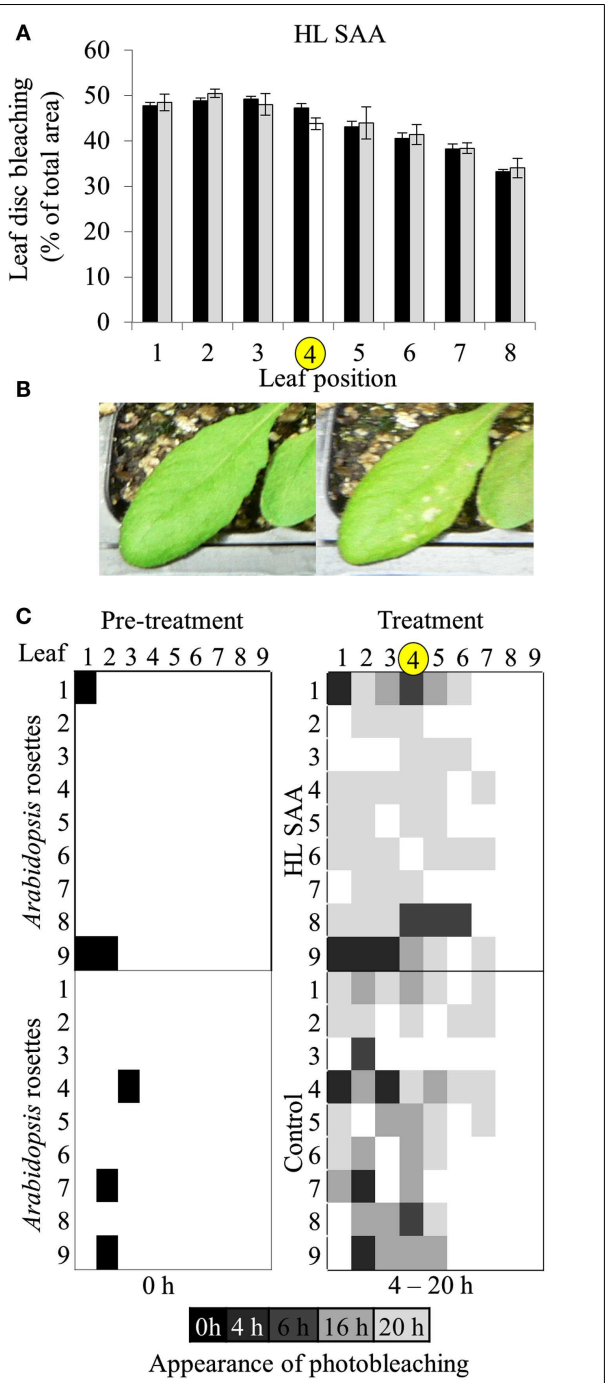

FIGURE 6 | Leaf position-dependent oxidative stress tolerance during HL SAA. (A) *In vitro* photo-oxidative stress tolerance leaf disk assay, *Arabidopsis* plants were either HL SAA treated at leaf position 4 (white bar, yellow circle) or remained untreated (black). Leaf disks were then taken from all leaves, including distal (gray), floated on H_2O_2, and assayed as in **Figure 5**. Photographs of the leaf disks taken after 20 h and were analyzed using ImageJ software to calculate the percentage of healthy and bleached tissue, $n = 3$. **(B)** First signs of photobleaching during the *in vivo* assay. **(C)** *In vivo* temporal assay of photobleaching development based on leaf position comparing HL SAA treated (top panels) and non-acclimated control plants (lower panels), $n = 9$.

from this *in vitro* assay did not indicate any substantial difference in photobleaching development between HL SAA acclimated and non-acclimated plants; however, there was a general trend of increased oxidative tolerance in younger tissues (**Figure 6A**).

Age-dependent HL SAA was then investigated *in vivo* by determining the first appearance of photobleaching in intact leaves subject to continuous HL after the HL spot treatment. This treatment was used to determine whether there is a specific spatial and age-dependent pattern of the onset of photobleaching as a result of HL SAA. *Arabidopsis* plants were either treated with HL SAA or left non-acclimated. The entire rosette was then subjected to 20 h HL and appearance of photobleaching recorded after 0, 4, 6, 16, and 20 h (**Figures 6B,C**). In both treated and untreated plants there was less and a slower rate of induction of bleaching in younger leaves. Interestingly, the temporal aspect of this assay revealed a slight difference between HL SAA acclimated and control, non-acclimated plants in that most HL SAA plants developed photobleaching at 20 h, whereas photobleaching in control plants appeared more rapidly and sporadically across the rosette under HL (indicated by increased number of darker shaded boxes). The temporal aspect of this assay indicates that HL SAA may be responsible for the coordinated acclimation of leaves across the rosette that could confer resistance to stress within the duration of a natural day length.

THE INFLUENCE OF REPEATED, TRANSIENT HL SAA ON ACCLIMATION IN EXISTING LEAVES

As plants exposed to short term HL SAA treatments failed to generate a strong acclimation response, we hypothesized that repetitive treatments are required to generate stronger acclimation responses. Under long term HL conditions systemic signaling from mature leaves influences the development of new, emerging tissues mediating changes in leaf structure and thickness, chloroplast prevalence, and growth rates (Coupe et al., 2006; Araya et al., 2008; Jiang et al., 2011). However, how existing leaves respond to repeated, short term HL spot treatments in distal and exposed leaves is unknown. Plants were subject to three, 1 h HL spot treatments per day for 8 days (**Figure 7**). Interestingly, analysis of HL SAA treated plants showed that the exposed leaf (6) and young emerging leaves (11+) of the HL-treated plants exhibited a statistically significant increased tolerance to oxidative stress after repeated, transient stress than their respective LL controls (**Figure 7**). By contrast, leaves 3–5 and 7–10 showed no significant difference between the respective HL-treated and non-treated tissues.

To determine if the acclimation response to repeated 1 h HL treatments was also reflected in changes to photosynthesis and photoinhibition, two photosynthetic parameters, ϕ_{PSII} (**Figure 8**) and NPQ (**Figure 9**), were measured at the end of the 8-day treatment. The measurements were undertaken at both 150 and 500 μmol photons m^{-2} s^{-1}. Under both light intensities, all leaves from HL-exposed and untreated plants exhibited relatively similar ϕ_{PSII} values (**Figure 8**), except for leaf 6 of the HL-exposed plants, which had slightly increased levels of ϕ_{PSII}. On the other hand, NPQ was markedly higher in the exposed leaf 6 and significantly higher in distal (HL SAA) tissue than in controls for the younger leaves (**Figure 9**). These observations indicate that repeated transient HL SAA treatments result in long term acclimation to HL in both exposed and distal leaves.

HL SAA AND AUXIN

Our initial analysis of different HL SAA marker transcript levels demonstrated specific distal expression of *GH3.3* (**Table 1**), an

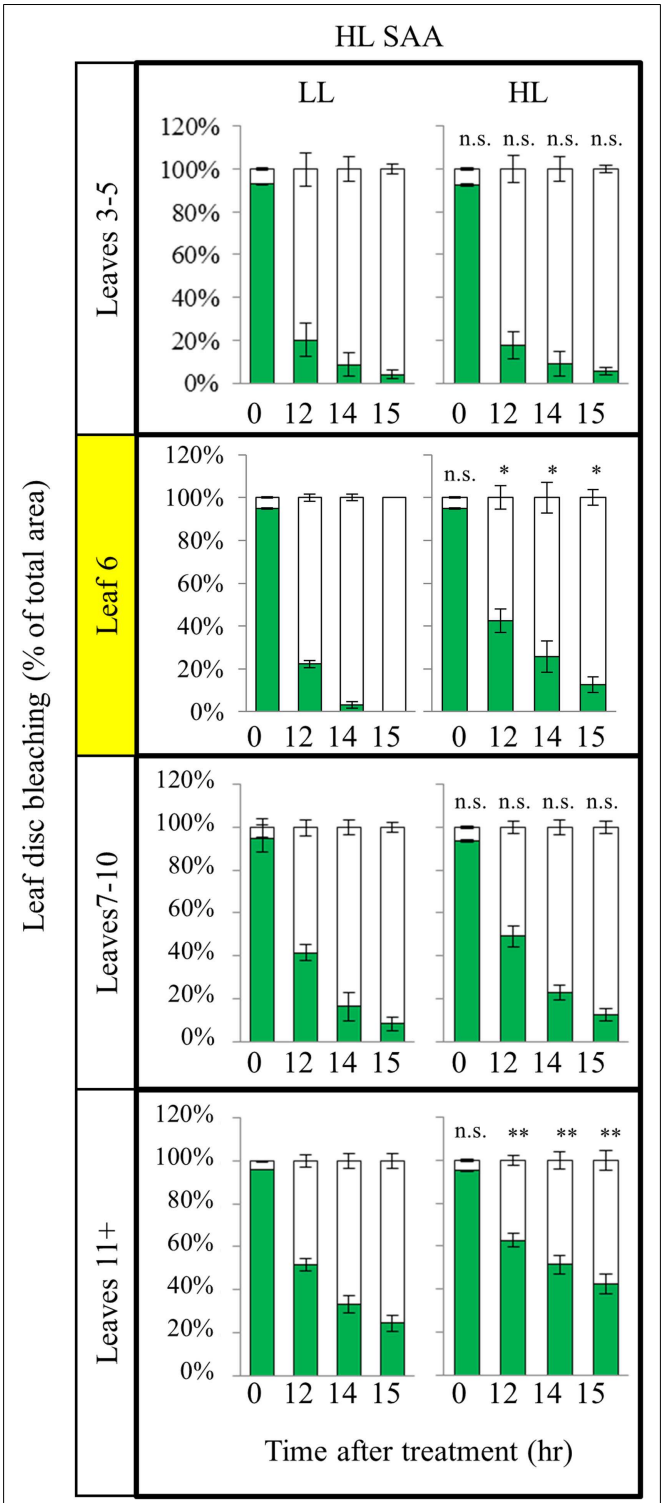

FIGURE 7 | *In vitro* photo-oxidative stress tolerance assay of repeated, transient HL SAA. *Arabidopsis* plants were either HL SAA treated for 60 min three times a day for 8 days (HL) or remained untreated (LL). Leaf disks were then taken from all leaves, floated on H_2O_2 and assayed as in **Figure 5**. Photographs were analyzed using ImageJ software, as in **Figure 5**, to calculate the percentage of healthy (green) and bleached (white) tissue. Pairwise *t*-tests were performed comparing the extent of bleaching between LL samples and the respective HL-treated leaves, $n = 3$.

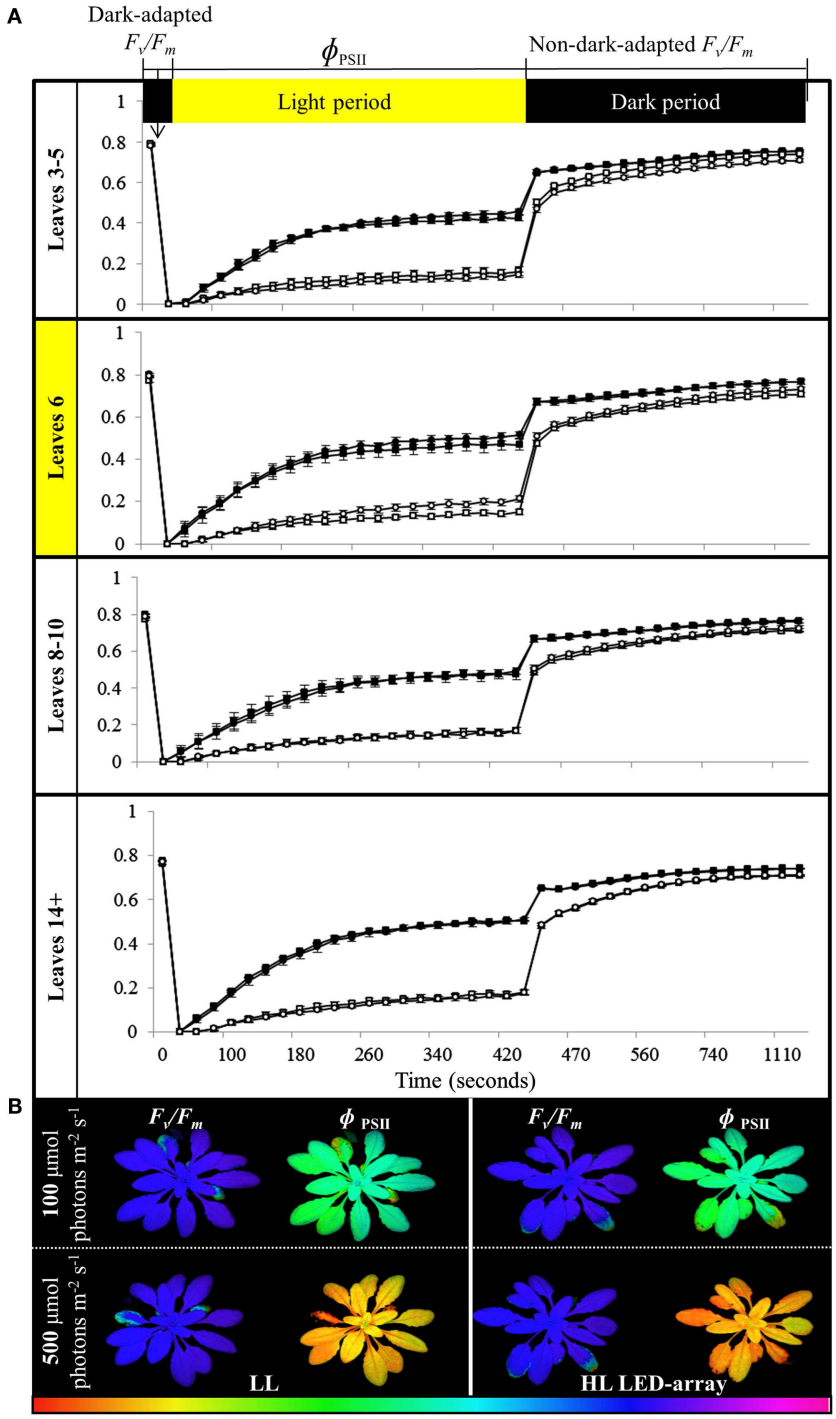

FIGURE 8 | Comparison of photoinhibition and recovery in plants after the repeated, transient HL SAA acclimation experiment exposed to 150 and 500 µmol photons m^{-2} s^{-1}. Treated plants were subjected to three separate 1 h HL LED-spot treatments per day for 8 days prior to measurement. **(A)** F_v/F_m and ϕ_{PSII} measurements of both HL LED-array treated (circle) and untreated plants (square) subsequently exposed to either 150 (closed symbol) or 500 µmol photons $m^{-2}s^{-1}$ (open symbol) and dark for the indicated time are shown. The leaf position is indicated. The entire experiment was performed in triplicate, one representative is shown for which $n = 3$. **(B)** A representative false colour image of F_v/F_m and ϕ_{PSII} (measured at 420 s) from HL LED-array exposed (HL) and untreated (LL) plants under 100 and 500 µmol photons $m^{-2}s^{-1}$. The colored scale bar represents the corresponding value of ϕ_{PSII} or F_v/F_m, increasing in value from left (red) to right (pink).

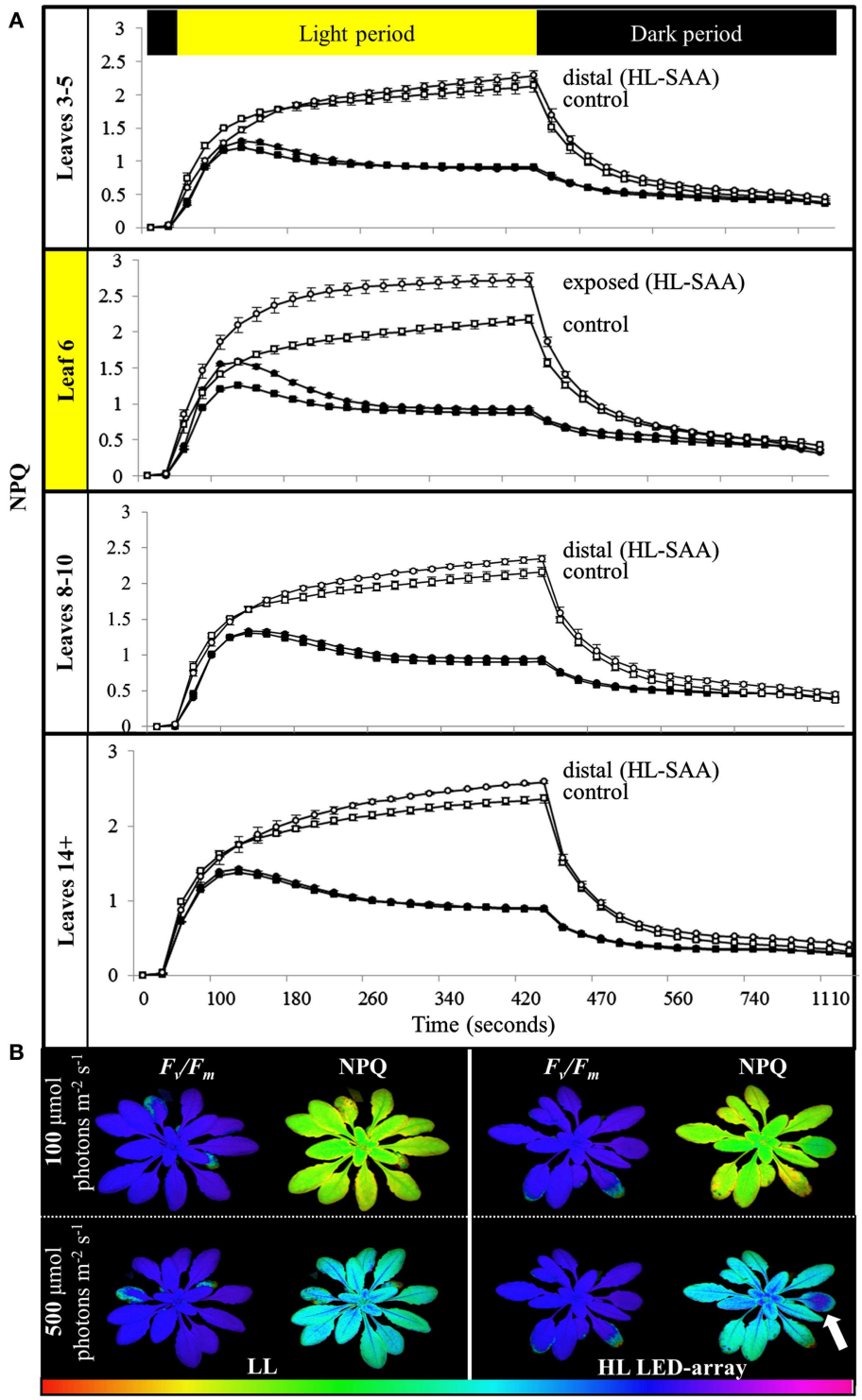

FIGURE 9 | Non-photochemical quenching induction and relaxation in plants after repeated, transient HL SAA. Treated plants were subjected to three separate 1 h HL LED-spot treatments per day for 8 days prior to measurement. **(A)** NPQ measurements of both HL LED-array treated (circle) and control plants (square) subsequently exposed to either 150 (closed symbol) or 500 µmol photons $m^{-2}s^{-1}$ (open symbol) and dark for the indicated time are shown. The leaf position is indicated. The entire experiment was performed in triplicate, one representative is shown for which $n = 3$. **(B)** A representative false color image of NPQ (measured at 420 s) from HL LED-array exposed (HL) and untreated (LL) plants under 100 and 500 µmol photons $m^{-2}s^{-1}$. The colored scale bar represents the corresponding value of NPQ increasing in value from left (red) to right (pink). The circle of dark blue on the treated leaf six is indicated with an arrow.

important gene in regulating auxin homeostasis (Staswick et al., 2005). This may indicate connections between HL SAA and developmental processes mediated by auxin. To determine the influence of HL SAA on auxin-regulated transcripts, we compared the genes that exhibited significant changes in the distal leaves of HL SAA plants (Rossel et al., 2007) with data from six different auxin treatment studies (Sawa et al., 2002; Zhao et al., 2003; Redman et al., 2004; Overvoorde et al., 2005; Nemhauser et al., 2006; Lee et al., 2009). The analysis revealed that a subset of 123 (out of 602) SAA transcripts were co-expressed with auxin-responsive genes (total of 1188; **Figure 10**; **Table 2**). This was a significantly higher overlap of genes than expected by random chance (two-sample *z*-statistic = 15.6, equivalent $p = 0.01$). Using GO annotation (TAIR 10, 2012) it became evident that the co-expressed genes in both HL SAA and two or more auxin treatment experiments exhibited a large proportion of genes involved in either auxin-related (29%) or plant stress processes (29%).

The connection between HL SAA and auxin was further investigated by analyzing the expression of auxin-responsive genes and the spatial distribution of auxin. Five transcripts were chosen (*GH3.3*, *GH3.5*, *PIN-FORMED3 (PIN3)*, *PIN4*, and *PIN7*). After the LED-spot treatment, independent samples *t*-tests show that both *GH3* transcripts exhibited statistically significant induction in the distal leaves (**Figures 11A,B**). The induced expression of the *GH3* transcripts is also specifically limited to that of the distal tissues, as LSD tests on one-way ANOVAs combining all tissues show significant differences between LL, DL, and HL-treated tissues ($P < 0.05$). Whereas *PIN4* and *PIN7* were down-regulated in HL and distal tissues and *PIN3* exhibited no significant changes in transcript levels (**Figures 11C–E**). Auxin distribution was inferred by using the auxin-responsive DR5:GUS transgene. Under LL, plants exhibited typical *DR5:GUS* staining, mainly localized to the leaf borders, hydathodes, and main vascular tissues (**Figure 11F**). In contrast, after HL spot treatment the distal leaves showed increased distribution of *DR5:GUS* in secondary vasculature and mesophyll cells (**Figure 11F**).

DISCUSSION

In this study we shed light on the processes which govern the initiation of HL SAA and retrograde signaling and provided evidence for acclimation in treated and young, distal leaves that include changes to photo-oxidative stress tolerance, NPQ, and auxin-responsive gene expression in response to repeated 1 h HL treatments.

HL SAA TRANSCRIPTIONAL RESPONSE AND SIGNAL INITIATION

Different lengths of HL treatment revealed that the induction of HL-responsive genes is abolished after 120 min, even under light stress (**Figures 2A,B**), highlighting the transient nature of the response to short term HL treatments. HL SAA induction was also proportional to light intensity (**Figures 2C,D**), suggesting a direct relationship between HL SAA signaling and retrograde signaling derived from photosynthesis in the HL-treated leaf. This hypothesis is supported by previous studies which have shown that pre-treatment with the photosynthetic inhibitor, 3-(3,4-dichlorophenyl)-1,1-dimethylurea (DCMU) was able to attenuate the SAA induction of two well-known marker genes *APX1* and *APX2* (Muhlenbock et al., 2008; Szechynska-Hebda et al., 2010). However, given the disparate nature of the HL treatment systems and marker genes used in this study, further DCMU treatments with our system would have to be conducted to support this theory. We demonstrated that the signal was initiated at low increases in light intensity, not just in response to severe stress of more than 10× of normal growth light as used in earlier studies (Karpinski et al., 1999; Mateo et al., 2004; Rossel et al., 2007; Muhlenbock et al., 2008; Miller et al., 2009; Szechynska-Hebda et al., 2010). Furthermore, the induction of these transcripts in distal tissues using a small area of applied light at moderate intensity indicates that the signaling of HL stress is not an average integration of shade and light signals generated across the plant, but a response to HL in a specific portion of a single leaf.

UVA, blue, yellow and red light-exposed plants exhibited significant systemic induction of *ZAT10* and *RRTF1* transcripts (**Figures 2E,F**), however the increase in mRNA under these conditions is a fraction of the observed response under white HL (**Figure 2C**). This may reflect the impact of the specific wavelengths on the rate of photosynthesis in the treated leaf (McCree, 1972), but would require additional photosynthetic measurements for confirmation. That is, while the intensity was the same for all treatments as in this study ($1500 \pm 50\,\mu mol\ photons\ m^{-2}\ s^{-1}$), the narrow wavelength would result in a lower overall total photosynthetic available radiation (PAR) available for capture by chlorophylls and carotenoids. Interestingly, for both UVA and blue light the lack of systemic response is in despite of an observed strong physiological photobleaching response in the treated tissue (data not shown). This indicates the presence of separate retrograde signaling systems which activate HL SAA independent from those that govern blue light responses and photodamage acclimation responses (Franklin and Whitelam, 2004; Suetsugu and Wada, 2007; Takahashi et al., 2010; Lehmann et al., 2011). This is further supported by the observation that the white LEDs do not produce any UV spectra yet exhibit the highest induction of HL SAA and that HL SAA induction occurs at intensities as low as $250\,\mu mol\ photons\ m^{-2}s^{-1}$. Such intensities are unlikely to even induce the xanthophyll cycle as zeaxanthin typically accumulates in response to $400\,\mu mol\ photons\ m^{-2}s^{-1}$ and above (Demmig-Adams et al., 1989). Thus, the induction at $250\,\mu mol\ photons\ m^{-2}s^{-1}$ indicates that changes in photosynthetic parameters and subsequent retrograde signals initiate HL SAA, not oxidative stress and damage, although the latter may contribute to the intensity of the response at higher light intensities.

Interestingly, blue light treatments resulted in increased transcript induction for both *RRTF1* and *ZAT10* compared to the other wavelengths (**Figures 2E,F**). This may be attributed to the known role of blue light in multiple acclimation responses (Liscum and Briggs, 1995; Folta and Spalding, 2001; Jarillo et al., 2001; Danon et al., 2006; Matsuda et al., 2008). Contrary to this hypothesis, it was shown that under HL the systemic induction of *APX1* and *APX2* exhibit no apparent attenuation and dependency of blue light perception via cryptochrome photoreceptors in double mutants *cry1*/*cry2* (Szechynska-Hebda et al., 2010). The discrepancy between the analyses and results presented in this study highlight the complexity of HL SAA and possible involvement of different retrograde signals including ROS and

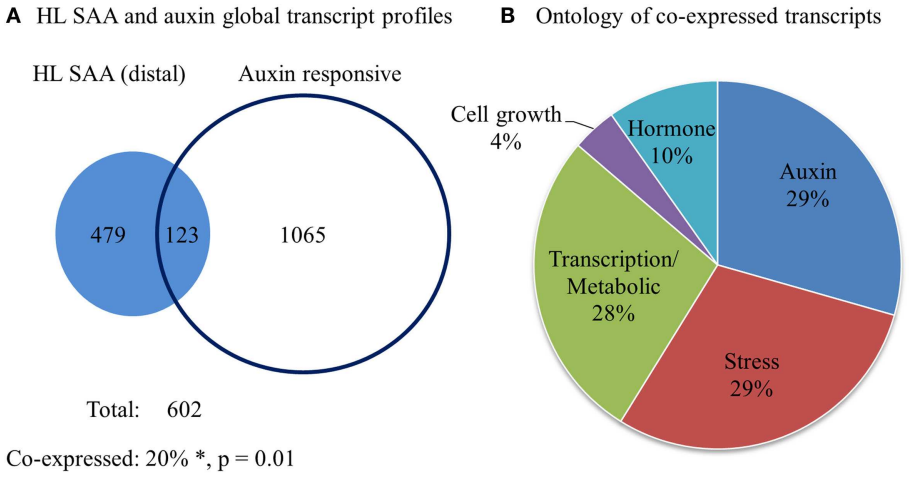

FIGURE 10 | Comparative analysis of HL SAA (distal) and auxin-responsive genes. (A) Venn diagram of all transcripts that exhibit significant co-expression between 60 min HL SAA treatment microarray data (Rossel et al., 2007) and at least two of the following auxin arrays (Sawa et al., 2002; Zhao et al., 2003; Redman et al., 2004; Overvoorde et al., 2005; Nemhauser et al., 2006; Lee et al., 2009). *The percentage of co-expressed genes is greater than would be expected by chance by a two-sample *z*-statistic (equals 15.6, equivalent $p = 0.01$). **(B)** GO annotation (TAIR 10, 2012) of co-expressed genes between HL SAA and two or more auxin treatment experiments.

photosynthesis-mediated signaling pathways. Two major forms of ROS, H_2O_2 and $^1O_2$, trigger different transcriptional responses including induction of *ZAT10* and *RRTF1*, respectively (op den Camp et al., 2003; Gadjev et al., 2006). Under HL SAA the downstream transcriptional regulation of *APX* isoforms may be influenced by both H_2O_2-derived and blue light $^1O_2$-derived signaling and be dependent on how these different ROS signaling pathways interact.

THE INFLUENCE OF TEMPERATURE AND HUMIDITY ON HL SAA

Even though heat exposure is able to cause photoinhibition (Allakhverdiev et al., 2008; Sainz et al., 2010) and to be synergistic to photo-oxidative stress (Rossel et al., 2002; Mittler, 2006), our study reveals that moderate heat stress does not influence HL SAA induction. That is, the increase in induction of *RRTF1* and *ZAT10* in distal leaves was similar at all analyzed temperatures (**Figure 3**), although at 32˚C there was a suppression of *RRTF1* transcripts relative to 21˚C in all three tissues, including the control.

In contrast to increased temperatures lower RH levels proportionally inhibited HL SAA induction in distal leaves (normalized to LL 90% RH; **Figure 3B**). This is surprising as 70% of HL inducible genes are also induced by drought stress and there are common regulators of both pathways that alter the expression of *ZAT10* and *APX2*, such as *SAL1* (Kimura et al., 2003; Wilson et al., 2009; Estavillo et al., 2011). Furthermore, low humidity is already known to induce *APX2* (Karpinski et al., 1997; Fryer et al., 2003; Hetherington and Woodward, 2003; Szechynska-Hebda et al., 2010); that is if anything a synergistic or additive effect of low RH and HL may have been expected. Yet, there was no additive induction in distal leaves at lower RH. This either reflects an epistatic effect, or the lower RH impairs the propagation of the SAA signal to distal leaves. With respect to epistasis, as noted above, both drought and HL have similar impacts on ABA induction and expression of genes such as *APX2* and *ZAT10* (Rossel et al., 2006) and it could be low RH and HL SAA act via the same pathway. Contradictory to this, there is an additive increase in gene expression in HL-treated leaves at low RH (**Figure 3B**). Furthermore, the drought and HL stress signaling SAL1 mutant, *alx8*, also retains the additive increase in *APX2* and *ELIP2* gene expression under drought and light stress (Rossel et al., 2006; Estavillo et al., 2011). This suggests that the loss of HL SAA induction under low RH is more consistent with impaired propagation than epistasis. This is intriguing as HL SAA acts via the vasculature, but most likely not in the xylem as it is observed in upper and lower leaves (**Figure 5**). Proposed SAA signals include ROS and electrochemical gradients, none of which are directly impacted by changes in transpiration. How exactly low RH impacts HL SAA signaling still needs further investigation.

THE RESPONSE TO REPEATED, SHORT TERM, LOCALIZED HL

To date, the study of acclimation processes and function of HL SAA has been restricted to evaluation of the immediate adaptation responses to one or several hours of HL (Rossel et al., 2007; Muhlenbock et al., 2008; Szechynska-Hebda et al., 2010). However, our study demonstrates that the single application of a highly localized signal did not result in any observable distal acclimation *in vitro* beyond the transcriptional changes (**Figures 4–6**). This is in contrast to earlier reports using 1/3 rosette HL treatment that resulted in distal acclimatory changes with respect to H_2O_2 tolerance and NPQ (Karpinski et al., 1999; Rossel et al., 2007; Szechynska-Hebda et al., 2010). Significantly, repeated, short term applications of the HL spot treatment over 8 days resulted in enhanced tolerance to H_2O_2 and elevated NPQ capacity compared to LL controls (**Figures 7–9**). Key to these observations was that the acclimatory response was increased in younger leaves as they had lower levels of *RRTF1* and *ZAT10* mRNA accumulation (**Figure 7**), and higher basal resistance to H_2O_2 bleaching compared to LL control plants (**Figure 5**). Younger leaf tissues are already described to exhibit increased resistance to numerous other stress conditions

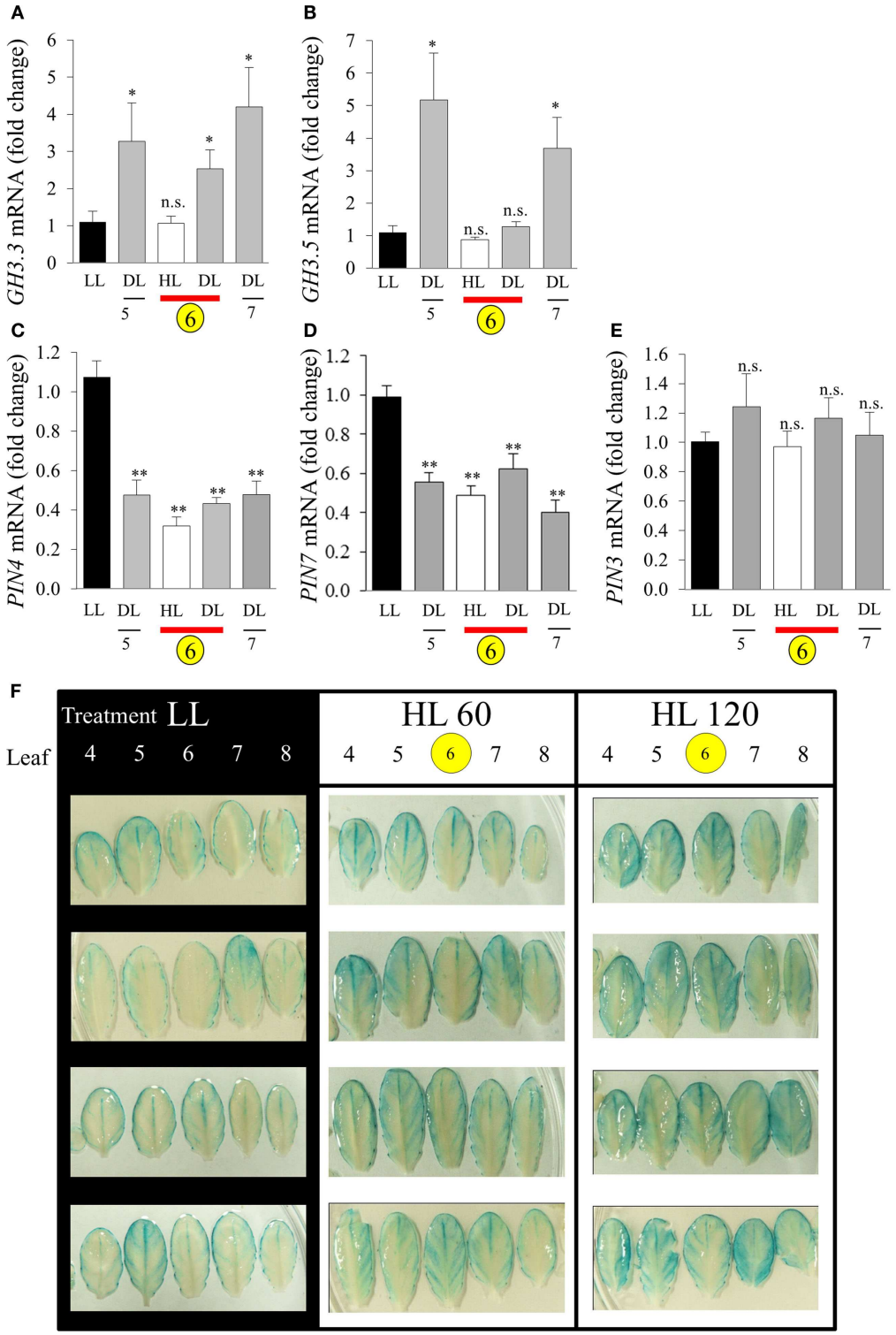

FIGURE 11 | Analysis of *GH3* and *PIN* transcript accumulation during HL SAA. Relative transcript levels of **(A)** *GH3.3*, **(B)** *GH3.5*, **(C)** *PIN4*, **(D)** PIN7, and **(E)** *PIN3* after the HL SAA treatment of leaf 6 (yellow circle). Distal tissue was sampled from leaves 5, 6, and 7 (grey), distal tissue was also sampled from within the HL-treated leaf (red bar), **(F)** Localization and distribution of auxin visualized by DR5:GUS after HL SAA. Representative images from four different plants showing leaves 4–8 (left to right) from *DR5:GUS* transgenics following illumination with either LL conditions ($40 \pm 25\,\mu$mol photons $m^{-2}s^{-1}$), HL LED-array treatment of leaf 6 ($1500 \pm 50\,\mu$mol photons $m^{-2}s^{-1}$) for either 60 (HL 60), or 120 min (HL 120). Pairwise *t*-tests were performed comparing the transcript levels in HL and DL samples with those of LL samples yielding *p*-values as shown Error bars indicate standard error, for each sample type, $n = 6$, $*p < 0.05$, $**p < 0.001$, n.s., not significant. $n = 8$ Per leaf for two independent auxin experiments.

including salt, drought, temperature, and ROS (Takagi et al., 2003; Jung, 2004; Muhlenbock et al., 2008; Hajlaoui et al., 2010; Yoon et al., 2011). The processes governing their acclimation in response to stress, however, are unclear (Takagi et al., 2003; Jung, 2004; Yoon et al., 2011).

Auxin is a well-established regulator of many plant processes including organ patterning, root and shoot architecture, vascular development, growth, and tropic responses (Benjamins and Scheres, 2008; Zhao, 2010). Our study describes how HL SAA is able to regulate distal-specific auxin-related gene transcription as well as free auxin distribution (Aloni et al., 2003) in both HL-treated and distal tissues (**Figure 11**). The *GH3.3* and *GH3.5* were exclusively expressed in distal tissue in response to HL SAA (**Figure 11**) and are from a class of proteins directly responsible for the maintenance of auxin homeostasis (Staswick et al., 2005). Over-expression of *GH3.5* alters the balance between free and conjugated auxin enhancing tolerance to pathogen infection and abiotic stresses such as drought, salinity, and temperature (Park et al., 2007; Zhang et al., 2007). Even though *GH3.3* is induced under pathogen infection its role in plant stress is relatively undefined (González-Lamothe et al., 2012). The proposed integration between auxin, oxidative stress, and ROS was reviewed recently (Tognetti et al., 2012). Auxin is capable of influencing ROS homeostasis by regulating proteins involved in ROS detoxification, including transcription regulators, the DELLA proteins and the ROS detoxifying enzymes, glutathione *S*-transferases (Laskowski et al., 2002; Paponov et al., 2008). Conversely, ROS produced under various stress conditions greatly influences auxin biosynthesis, metabolism, transport, and signal transduction pathways in exposed tissues (Tognetti et al., 2012). It is now evident that distal tissues of plants subjected to repeated HL spot treatments may exhibit similar changes in auxin-mediated processes.

In conclusion localized HL treatments and repeated, localized HL treatments initiate retrograde signals that lead to transcriptional and acclimatory responses in both treated and distal tissue. However, a single 1 h HL spot treatment is not sufficient to alter the acclimation response in distal tissues. HL SAA requires either a 1/3 of the rosette to be treated (Rossel et al., 2007), or a single leaf to be repeatedly subject to 1 h HL treatments. Questions remain as to whether the response to repeated HL SAA is at the cellular or subcellular level? What is the nature of the memory of repeated HL, is it for example due to changes in chromatin? Is the response reversible and does auxin contribute directly to the acclimation response? Why do young and old leaves respond differently to HL SAA? The nature of the signal and the respective roles of auxin and oxidative stress responsive genes in HL SAA from a temporal perspective, all require further investigation.

REFERENCES

Allakhverdiev, S., Kreslavski, V., Klimov, V., Los, D., Carpentier, R., and Mohanty, P. (2008). Heat stress: an overview of molecular responses in photosynthesis. *Photosyn. Res.* 98, 541–550.

Aloni, R., Schwalm, K., Langhans, M., and Ullrich, C. I. (2003). Gradual shifts in sites of free-auxin production during leaf-primordium development and their role in vascular differentiation and leaf morphogenesis in Arabidopsis. *Planta* 216, 841–853.

Araya, T., Noguchi, K., and Terashima, I. (2008). Manipulation of light and CO2 environments of the primary leaves of bean (Phaseolus vulgaris L.) affects photosynthesis in both the primary and the first trifoliate leaves: involvement of systemic regulation. *Plant Cell Environ.* 31, 50–61.

Asada, K. (2006). Production and scavenging of reactive oxygen species in chloroplasts and their functions. *Plant Physiol.* 141, 391–396.

Atkin, O. K., Loveys, B. R., Atkinson, L. J., and Pons, T. L. (2006). Phenotypic plasticity and growth temperature: understanding interspecific variability. *J. Exp. Bot.* 57, 267–281.

Baker, N. R. (2008). Chlorophyll fluorescence: a probe of photosynthesis in vivo. *Annu. Rev. Plant Biol.* 59, 89–113.

Barrero, J. M., Rodriguez, P. L., Quesada, V., Piqueras, P., Ponce, M. R., and Micol, J. L. (2006). Both abscisic acid (ABA)-dependent and ABA-independent pathways govern the induction of NCED3, AAO3 and ABA1 in response to salt stress. *Plant Cell Environ.* 29, 2000–2008.

Bartels, D., and Sunkar, R. (2005). Drought and salt tolerance in plants. *CRC Crit. Rev. Plant Sci.* 24, 23–58.

Bauwe, H., Hagemann, M., and Fernie, A. R. (2010). Photorespiration: players, partners and origin. *Trends Plant Sci.* 15, 330–336.

Benjamins, R., and Scheres, B. (2008). Auxin: the looping star in plant development. *Annu Rev Plant Biol.* 59, 443–465.

Biswal, B., Joshi, P. N., Raval, M. K., and Biswal, U. C. (2011). Photosynthesis, a global sensor of environmental stress in green plants: stress signalling and adaptation. *Curr. Sci.* 101, 47–56.

Braam, J., Sistrunk, M. L., Polisensky, D. H., Xu, W., Purugganan, M. M., Antosiewicz, D. M., et al. (1997). Plant responses to environmental stress: regulation and functions of the Arabidopsis TCH genes. *Planta* 203, S35–S41.

Conn, P. F., Schalch, W., and Truscott, T. G. (1991). The singlet oxygen and carotenoid interaction. *J. Photochem. Photobiol. B Biol.* 11, 41–47.

Coupe, S. A., Palmer, B. G., Lake, J. A., Overy, S. A., Oxborough, K., Woodward, F. I., et al. (2006). Systemic signalling of environmental cues in Arabidopsis leaves. *J. Exp. Bot.* 57, 329–341.

Danon, A., Sánchez Coll, N., and Apel, K. (2006). Cryptochrome-1-dependent execution of programmed cell death induced by singlet oxygen in Arabidopsis thaliana. *Proc. Natl. Acad. Sci. U.S.A.* 103, 17036–17041.

de Bianchi, S., Ballottari, M., Dall'Osto, L., and Bassi, R. (2010). Regulation of plant light harvesting by thermal dissipation of excess energy. *Biochem. Soc. Trans.* 38, 651–660.

Demmig-Adams, B., Adams, W. W. III, Barker, D. H., Logan, B. A., Bowling, D. R., and Verhoeven, A. S. (1996). Using chlorophyll fluorescence to assess the fraction of absorbed light allocated to thermal dissipation of excess excitation. *Physiol Plant* 98, 253–264.

Demmig-Adams, B., Winter, K., Kruger, A., and Czygan, F. (1989). "Light stress and photoprotection related to the carotenoid zeaxanthin in higher plants," in *Photosynthesis. Plant Biology*, Vol. 8, ed. W. R. Briggs (New York: Alan R. Liss, Inc.), 375–391.

Durrant, W. E., and Dong, X. (2004). Systemic acquired resistance. *Annu. Rev. Phytopathol.* 42, 185–209.

Estavillo, G. M., Crisp, P. A., Pornsiriwong, W., Wirtz, M., Collinge, D., Carrie, C., et al. (2011). Evidence for a SAL1-PAP chloroplast retrograde pathway that functions in drought and high light signaling in Arabidopsis. *Plant Cell* 23, 3992–4012.

Folta, K. M., and Spalding, E. P. (2001). Unexpected roles for cryptochrome 2 and phototropin revealed by high-resolution analysis of blue light-mediated hypocotyl growth inhibition. *Plant J.* 26, 471–478.

Förster, B., Osmond, C. B., and Pogson, B. J. (2005). Improved survival of very high light and oxidative stress is conferred by spontaneous gain-of-function mutations in Chlamydomonas. *Biochim. Biophys. Acta* 1709, 45–57.

Franklin, K. A., and Whitelam, G. C. (2004). Light signals, phytochromes and cross-talk with other environmental cues. *J. Exp. Bot.* 55, 271–276.

Fryer, M. J., Ball, L., Oxborough, K., Karpinski, S., Mullineaux, P. M., and Baker, N. R. (2003). Control of ascorbate peroxidase 2 expression by hydrogen peroxide and leaf water status during excess light stress reveals a functional organisation of Arabidopsis leaves. *Plant J.* 33, 691–705.

Gadjev, I., Vanderauwera, S., Gechev, T. S., Laloi, C., Minkov, I. N., Shulaev, V., et al. (2006). Transcriptomic footprints disclose specificity of reactive oxygen species signaling in Arabidopsis. *Plant Physiol.* 141, 436–445.

González-Lamothe, R., El Oirdi, M., Brisson, N., and Bouarab, K. (2012). The conjugated auxin indole-3-acetic acid-aspartic acid promotes plant disease development. *Plant Cell.* 24, 762–777.

Gorsuch, P. A., Sargeant, A. W., Penfield, S. D., Quick, W. P., and Atkin, O. K. (2010). Systemic low temperature signaling in Arabidopsis. *Plant Cell Physiol.* 51, 1488–1498.

Hajlaoui, H., Ayeb, N. E., Garrec, J. P., and Denden, M. (2010). Differential effects of salt stress on osmotic adjustment and solutes allocation on the basis of root and leaf tissue senescence of two silage maize (Zea mays L.) varieties. *Ind. Crops Prod.* 31, 122–130.

Hetherington, A. M., and Woodward, F. I. (2003). The role of stomata in sensing and driving environmental change. *Nature* 424, 901–908.

Hutin, C., Nussaume, L., Moise, N., Moya, I., Kloppstech, K., and Havaux, M. (2003). Early light-induced proteins protect Arabidopsis from photooxidative stress. *Proc. Natl. Acad. Sci. U.S.A.* 100, 4921–4926.

Jarillo, J. A., Gabrys, H., Capel, J., Alonso, J. M., Ecker, J. R., and Cashmore, A. R. (2001). Phototropin-related NPL1 controls chloroplast relocation induced by blue light. *Nature* 410, 952–954.

Jiang, C. D., Wang, X., Gao, H. Y., Shi, L., and Chow, W. S. (2011). Systemic regulation of leaf anatomical structure, photosynthetic performance, and high-light tolerance in sorghum. *Plant Physiol.* 155, 1416–1424.

Johnson, G. N. (2011). Physiology of PSI cyclic electron transport in higher plants. *Biochim. Biophys. Acta* 1807, 384–389.

Jung, S. Y. (2004). Variation in antioxidant metabolism of young and mature leaves of Arabidopsis thaliana subjected to drought. *Plant Sci.* 166, 459–466.

Jurgens, G. (2001). Apical-basal pattern formation in Arabidopsis embryogenesis. *EMBO J.* 20, 3609–3616.

Kalbin, G., Hidema, J., Brosche, M., Kumagai, T., Bornman, J. F., and Strid, A. (2001). UV-B-induced DNA damage and expression of defence genes under UV-B stress: tissue-specific molecular marker analysis in leaves. *Plant Cell Environ.* 24, 983–990.

Karpinski, S., Escobar, C., Karpinska, B., Creissen, G., and Mullineaux, P. M. (1997). Photosynthetic electron transport regulates the expression of cytosolic ascorbate peroxidase genes in Arabidopsis during excess light stress. *Plant Cell* 9, 627–640.

Karpinski, S., Reynolds, H., Karpinska, B., Wingsle, G., Creissen, G., and Mullineaux, P. (1999). Systemic signaling and acclimation in response to excess excitation energy in Arabidopsis. *Science* 284, 654–657.

Karpinski, S., and Szechynska-Hebda, M. (2010). Secret life of plants: from memory to intelligence. *Plant Signal. Behav.* 5, 1391–1394.

Kimura, M., Yamamoto, Y. Y., Seki, M., Sakurai, T., Sato, M., Abe, T., et al. (2003). Identification of Arabidopsis genes regulated by high light-stress using cDNA microarray. *Photochem. Photobiol.* 77, 226–233.

Kobayashi, N., and Della Penna, D. (2008). Tocopherol metabolism, oxidation and recycling under high light stress in Arabidopsis. *Plant J.* 55, 607–618.

Koussevitzky, S., Nott, A., Mockler, T. C., Hong, F., Sachetto-Martins, G., Surpin, M., et al. (2007). Signals from chloroplasts converge to regulate nuclear gene expression. *Science* 316, 715–719.

Krause, G. H., and Weis, E. (1991). Chlorophyll fluorescence and photosynthesis – the basics. *Annu. Rev. Plant Physiol. Plant Mol. Biol.* 42, 313–349.

Lake, J. A., Quick, W. P., Beerling, D. J., and Woodward, F. I. (2001). Plant development – signals from mature to new leaves. *Nature* 411, 154–154.

Laskowski, M. J., Dreher, K. A., Gehring, M. A., Abel, S., Gensler, A. L., and Sussex, I. M. (2002). FQR1, a novel primary auxin-response gene, encodes a flavin mononucleotide-binding quinone reductase. *Plant Physiol.* 128, 578–590.

Lee, D. J., Park, J. W., Lee, H. W., and Kim, J. (2009). Genome-wide analysis of the auxin-responsive transcriptome downstream of iaa1 and its expression analysis reveal the diversity and complexity of auxin-regulated gene expression. *J. Exp. Bot.* 60, 3935–3957.

Lee, K. P., Kim, C., Landgraf, F., and Apel, K. (2007). EXECUTER1- and EXECUTER2-dependent transfer of stress-related signals from the plastid to the nucleus of Arabidopsis thaliana. *Proc. Natl. Acad. Sci. U.S.A.* 104, 10270–10275.

Lehmann, P., Nöthen, J., Schmidt Von Braun, S., Bohnsack, M. T., Mirus, O., and Schleiff, E. (2011). Transitions of gene expression induced by short-term blue light. *Plant Biol.* 13, 349–361.

Li, Z. R., Wakao, S., Fischer, B. B., and Niyogi, K. K. (2009). Sensing and responding to excess light. *Annu. Rev. Plant Biol.* 60, 239–260.

Liscum, E., and Briggs, W. R. (1995). Mutations in the NPH1 locus of Arabidopsis disrupt the perception of phototropic stimuli. *Plant Cell* 7, 473–485.

Mateo, A., Mühlenbock, P., Rustérucci, C., Chang, C. C.-C., Miszalski, Z., Karpinska, B., et al. (2004). LESION SIMULATING DISEASE 1 is required for acclimation to conditions that promote excess excitation energy. *Plant Physiol.* 136, 2818–2830.

Matsuda, R., Ohashi-Kaneko, K., Fujiwara, K., and Kurata, K. (2008). Effects of blue light deficiency on acclimation of light energy partitioning in PSII and CO2 assimilation capacity to high irradiance in spinach leaves. *Plant Cell Physiol.* 49, 664–670.

McCree, K. J. (1972). Action spectrum, absorbance and the quantum yield of photosynthesis in crop plants. *Agr. Meteorol.* 9, 191–216.

Miller, G., Schlauch, K., Tam, R., Cortes, D., Torres, M. A., Shulaev, V., et al. (2009). The plant NADPH oxidase RBOHD mediates rapid systemic signaling in response to diverse stimuli. *Sci. Signal.* 2, A26–A35.

Miller, G., Suzuki, N., Ciftci-Yilmaz, S., and Mittler, R. (2010). Reactive oxygen species homeostasis and signalling during drought and salinity stresses. *Plant Cell Environ.* 33, 453–467.

Miller, G., Suzuki, N., Rizhsky, L., Hegie, A., Koussevitzky, S., and Mittler, R. (2007). Double mutants deficient in cytosolic and thylakoid ascorbate peroxidase reveal a complex mode of interaction between reactive oxygen species, plant development, and response to abiotic stresses. *Plant Physiol.* 144, 1777–1785.

Mittler, R. (2006). Abiotic stress, the field environment and stress combination. *Trends Plant Sci.* 11, 15–19.

Miyazawa, S. I., Livingston, N. J., and Turpin, D. H. (2006). Stomatal development in new leaves is related to the stomatal conductance of mature leaves in poplar (Populus trichocarpaxP-deltoides). *J. Exp. Bot.* 57, 373–380.

Muhlenbock, P., Szechynska-Hebda, M., Plaszczyca, M., Baudo, M., Mateo, A., Mullineaux, P. M., et al. (2008). Chloroplast signaling and LESION SIMULATING DISEASE1 regulate crosstalk between light acclimation and immunity in Arabidopsis. *Plant Cell* 20, 2339–2356.

Mullineaux, P., Ball, L., Escobar, C., Karpinska, B., Creissen, G., and Karpinski, S. (2000). Are diverse signalling pathways integrated in the regulation of Arabidopsis antioxidant defence gene expression in response to excess excitation energy? *Philos. Trans. R. Soc. Lond. B Biol. Sci.* 355, 1531–1540.

Mullineaux, P. M., and Baker, N. R. (2010). Oxidative stress: antagonistic signaling for acclimation or cell death? *Plant Physiol.* 154, 521–525.

Nemhauser, J. L., Hong, F. X., and Chory, J. (2006). Different plant hormones regulate similar processes through largely nonoverlapping transcriptional responses. *Cell* 126, 467–475.

op den Camp, R., Przybyla, D., Ochsenbein, C., Laloi, C., Kim, C., Danon, A., et al. (2003). Rapid induction of distinct stress responses after release of singlet oxygen in Arabidopsis. *Plant Cell* 15, 2320–2332.

Overvoorde, P. J., Okushima, Y., Alonso, J. M., Chan, A., Chang, C., Ecker, J. R., et al. (2005). Functional Genomic Analysis of the AUXIN/INDOLE-3-ACETIC ACID Gene Family Members in Arabidopsis thaliana. *Plant Cell* 17, 3282–3300.

Oxborough, K. (2004). Imaging of chlorophyll a fluorescence: theoretical and practical aspects of an emerging technique for the monitoring of photosynthetic performance. *J. Exp. Bot.* 55, 1195–1205.

Paponov, I. A., Paponov, M., Teale, W., Menges, M., Chakrabortee, S., Murray, J. A. H., et al. (2008). Comprehensive transcriptome analysis of auxin responses in Arabidopsis. *Mol. Plant* 1, 321–337.

Park, J. E., Park, J. Y., Kim, Y. S., Staswick, P. E., Jeon, J., Yun, J., et al. (2007). GH3-mediated auxin homeostasis links growth regulation with stress adaptation response in Arabidopsis. *J. Biol. Chem.* 282, 10036–10046.

Pfaffl, M. W. (2001). A new mathematical model for relative quantification in real-time RT-PCR. *Nucleic Acids Res.* 29, e45.

Pogson, B. J., Woo, N. S., Förster, B., and Small, I. D. (2008). Plastid signalling to the nucleus and beyond. *Trends Plant Sci.* 13, 602–609.

Ramel, F., Birtic, S., Ginies, C., Soubigou-Taconnat, L., Triantaphylidès, C., and Havaux, M. (2012). Carotenoid oxidation products are stress signals that mediate gene responses to singlet oxygen in plants. *Proc. Natl. Acad. Sci. U.S.A.* 109, 5535–5540.

Rapp, J. C., and Mullet, J. E. (1991). Chloroplast transcription is required to express the nuclear genes rbcS and cab. Plastid DNA copy number is

regulated independently. *Plant Mol. Biol.* 17, 813–823.

Redman, J., Haas, B., Tanimoto, G., and Town, C. (2004). Development and evaluation of an Arabidopsis whole genome Affymetrix probe array. *Plant J.* 38, 545–561.

Rossel, J., Walter, P., Hendrickson, L., Chow, W., Poole, A., Mullineaux, P., et al. (2006). A mutation affecting ascorbate peroxidase 2 gene expression reveals a link between responses to high light and drought tolerance. *Plant Cell Environ.* 29, 269–281.

Rossel, J. B., Wilson, I. W., and Pogson, B. J. (2002). Global changes in gene expression in response to high light in Arabidopsis. *Plant Physiol.* 130, 1109–1120.

Rossel, J. B., Wilson, P. B., Hussain, D., Woo, N. S., Gordon, M. J., Mewett, O. P., et al. (2007). Systemic and intracellular responses to photooxidative stress in Arabidopsis. *Plant Cell* 19, 4091–4110.

Rumeau, D., Peltier, G., and Cournac, L. (2007). Chlororespiration and cyclic electron flow around PSI during photosynthesis and plant stress response. *Plant Cell Environ.* 30, 1041–1051.

Sainz, M., Diaz, P., Monza, J., and Borsani, O. (2010). Heat stress results in loss of chloroplast Cu/Zn superoxide dismutase and increased damage to photosystem II in combined drought-heat stressed Lotus japonicus. *Physiol Plant* 140, 46–56.

Sawa, S., Ohgishi, M., Goda, H., Higuchi, K., Shimada, Y., Yoshida, S., et al. (2002). The HAT2 gene, a member of the HD-Zip gene family, isolated as an auxin inducible gene by DNA microarray screening, affects auxin response in Arabidopsis. *Plant J.* 32, 1011–1022.

Staswick, P. E., Serban, B., Rowe, M., Tiryaki, I., Maldonado, M. T., Maldonado, M. C., et al. (2005). Characterization of an Arabidopsis enzyme family that conjugates amino acids to indole-3-acetic acid. *Plant Cell* 17, 616–627.

Stitt, M., and Hurry, V. (2002). A plant for all seasons: alterations in photosynthetic carbon metabolism during cold acclimation in Arabidopsis. *Curr. Opin. Plant Biol.* 5, 199–206.

Stomp, A. M. (1992). "Histochemical localization of b-glucuronidase," in *GUS Protocols: Using the GUS Gene as a Reporter of Gene Expression*, ed. S. R. Gallagher (San Diego, CA: Academic Press), 103–113.

Suetsugu, N., and Wada, M. (2007). Chloroplast photorelocation movement mediated by phototropin family proteins in green plants. *Biol. Chem.* 388, 927–935.

Szechynska-Hebda, M., Kruk, J., Gorecka, M., Karpinska, B., and Karpinski, S. (2010). Evidence for light wavelength-specific photoelectrophysiological signaling and memory of excess light episodes in Arabidopsis. *Plant Cell* 22, 2201–2218.

Takagi, T., Nakamura, M., Hayashi, H., Inatsugi, R., Yano, R., and Nishida, I. (2003). The leaf-order-dependent enhancement of freezing tolerance in cold-acclimated Arabidopsis rosettes is not correlated with the transcript levels of the cold-inducible transcription factors of CBF/DREB1. *Plant Cell Physiol.* 44, 922–931.

Takahashi, S., and Badger, M. R. (2011). Photoprotection in plants: a new light on photosystem II damage. *Trends Plant Sci.* 16, 53–60.

Takahashi, S., Milward, S. E., Yamori, W., Evans, J. R., Hillier, W., and Badger, M. R. (2010). The solar action spectrum of photosystem II damage. *Plant Physiol.* 153, 988–993.

Thomas, P. W., Woodward, F. I., and Quick, W. P. (2004). Systemic irradiance signalling in tobacco. *New Phytol.* 161, 193–198.

Tognetti, V. B., Muhlenbock, P., and Van Breusegem, F. (2012). Stress homeostasis – the redox and auxin perspective. *Plant Cell Environ.* 35, 321–333.

Vanderauwera, S., Zimmermann, P., Rombauts, S., Vandenabeele, S., Langebartels, C., Gruissem, W., et al. (2005). Genome-wide analysis of hydrogen peroxide-regulated gene expression in Arabidopsis reveals a high light-induced transcriptional cluster involved in anthocyanin biosynthesis. *Plant Physiol.* 139, 806–821.

Wilson, P. B., Estavillo, G. M., Field, K. J., Pornsiriwong, W., Carroll, A. J., Howell, K. A., et al. (2009). The nucleotidase/phosphatase SAL1 is a negative regulator of drought tolerance in Arabidopsis. *Plant J.* 58, 299–317.

Woo, N. S., Gordon, M. J., Graham, S. R., Rossel, J. B., Badger, M. R., and Pogson, B. J. (2011). A mutation in the purine biosynthetic enzyme ATASE2 impacts high light signalling and acclimation responses in green and chlorotic sectors of Arabidopsis leaves. *Funct. Plant Biol.* 38, 401–419.

Yamaguchi-Shinozaki, K., and Shinozaki, K. (1993). Characterization of the expression of a desiccation-responsive rd29 gene of Arabidopsis thaliana and analysis of its promoter in transgenic plants. *Mol. Gen. Genet.* 236, 331–340.

Yano, S., and Terashima, I. (2001). Separate localization of light signal perception for sun or shade type chloroplast and palisade tissue differentiation in Chenopodium album. *Plant Cell Physiol.* 42, 1303–1310.

Yoon, J. Y., Shin, J. S., Shin, D. Y., Hyun, K. H., Burgos, N. R., Lee, S., et al. (2011). Tolerance to paraquat-mediated oxidative and environmental stresses in squash (Cucurbita spp.) leaves of various ages. *Pestic. Biochem. Physiol.* 99, 65–76.

Zhang, Z., Li, Q., Li, Z., Staswick, P. E., Wang, M., Zhu, Y., et al. (2007). Dual regulation role of GH3.5 in salicylic acid and auxin signaling during Arabidopsis-Pseudomonas syringae interaction. *Plant Physiol.* 145, 450–464.

Zhao, Y., Dai, X., Blackwell, H. E., Schreiber, S. L., and Chory, J. (2003). SIR1, an upstream component in auxin signaling identified by chemical genetics. *Science* 301, 1107–1110.

Zhao, Y. D. (2010). "Auxin biosynthesis and its role in plant development," in *Annual Review of Plant Biology*, Vol. 61, eds S. Merchant, W. R. Briggs, and D. Ort. (Palo Alto: Annual Reviews), 49–64.

Zhou, F., Menke, F. L. H., Yoshioka, K., Moder, W., Shirano, Y., and Klessig, D. F. (2004). High humidity suppresses ssi4-mediated cell death and disease resistance upstream of MAP kinase activation, H2O2 production and defense gene expression. *Plant J.* 39, 920–932.

Zhu, Q., Zhang, J., Gao, X., Tong, J., Xiao, L., Li, W., et al. (2010). The Arabidopsis AP2/ERF transcription factor RAP2.6 participates in ABA, salt and osmotic stress responses. *Gene* 457, 1–12.

Conflict of Interest Statement: The authors declare that the research was conducted in the absence of any commercial or financial relationships that could be construed as a potential conflict of interest.

Received: 30 October 2012; accepted: 16 December 2012; published online: 17 January 2013.

Citation: Gordon MJ, Carmody M, Albrecht V and Pogson B (2013) Systemic and local responses to repeated HL stress-induced retrograde signaling in Arabidopsis. Front. Plant Sci. ***3****:303. doi: 10.3389/fpls.2012.00303*

This article was submitted to Frontiers in Plant Physiology, a specialty of Frontiers in Plant Science.

Copyright © 2013 Gordon, Carmody, Albrecht and Pogson. This is an open-access article distributed under the terms of the Creative Commons Attribution License, which permits use, distribution and reproduction in other forums, provided the original authors and source are credited and subject to any copyright notices concerning any third-party graphics etc.

frontiers in
PLANT SCIENCE

ORIGINAL RESEARCH ARTICLE
published: 30 November 2012
doi: 10.3389/fpls.2012.00265

The mysterious rescue of *adg1-1/tpt-2* – an *Arabidopsis thaliana* double mutant impaired in acclimation to high light – by exogenously supplied sugars

Luisa Heinrichs, Jessica Schmitz, Ulf-Ingo Flügge and Rainer E. Häusler*

Department of Botany II, Cologne Biocenter, University of Cologne, Cologne, Germany

Edited by:
Tatjana Kleine, Ludwig-Maximilians-Universität München, Germany

Reviewed by:
Alisdair Fernie, Max Planck Institute for Plant Physiology, Germany
Peter Geigenberger, Ludwig-Maximilians-Universität München, Germany

***Correspondence:**
Rainer E. Häusler, Department of Botany II, Cologne Biocenter, University of Cologne, Zülpicherstr. 47b, 50674 Cologne, Germany.
e-mail: rainer.haeusler@uni-koeln.de

An *Arabidopsis thaliana* double mutant (*adg1-1/tpt-2*) defective in the day- and night-path of photoassimilate export from the chloroplast due to a knockout in the triose phosphate/phosphate translocator (TPT; *tpt-2*) and a lack of starch [mutation in ADP glucose pyrophosphorylase (AGPase); *adg1-1*] exhibits severe growth retardation, a decrease in the photosynthetic capacity, and a high chlorophyll fluorescence (HCF) phenotype under high light conditions. These phenotypes could be rescued when the plants were grown on sucrose (Suc) or glucose (Glc). Here we address the question whether Glc-sensing hexokinase1 (HXK1) defective in the *Glc insensitive 2* (*gin2-1*) mutant is involved in the sugar-dependent rescue of *adg1-1/tpt-2*. Triple mutants defective in the TPT, AGPase, and HXK1 (*adg1-1/tpt-2/gin2-1*) were established as homozygous lines and grown together with Col-*0* and Landsberg erecta (L*er*) wild-type plants, *gin2-1*, the *adg1-1/tpt-2* double mutant, and the *adg1-1/tpt-2/gpt2-1* triple mutant [additionally defective in the glucose 6-phosphate/phosphate translocator 2 (GPT2)] on agar in the presence or absence of 50 mM of each Glc, Suc, or fructose (Fru). The growth phenotype of the double mutant and both triple mutants could be rescued to a similar extent only by Glc and Suc, but not by Fru. All three sugars were capable of rescuing the HCF and photosynthesis phenotype, irrespectively of the presence or absence of HXK1. Quantitative RT-PCR analyses of sugar-responsive genes revealed that plastidial HXK (pHXK) was up-regulated in *adg1-1/tpt-2* plants grown on sugars, but showed no response in *adg1-1/tpt-2/gin2-1*. It appears likely that soluble sugars are directly taken up by the chloroplasts and enter further metabolism, which consumes ATP and NADPH from the photosynthetic light reaction and thereby rescues the photosynthesis phenotype of the double mutant. The implication of sugar turnover and probably signaling inside the chloroplasts for the concept of retrograde signaling is discussed.

Keywords: sugar signaling, photosynthesis, chlorophyll fluorescence, carbohydrate metabolism, chloroplasts

INTRODUCTION

Plants are exposed to a variety of environmental factors including stresses such as excessive light or drought. In order to survive even harsh conditions, plants have developed strategies to adapt to changing environmental conditions (Eberhard et al., 2008). The chloroplasts are particularly sensitive to the light intensity and the photosynthesis apparatus therein has to respond rapidly (short term response) or in the long term (acclimation) in order to adapt to changing light (Kleine et al., 2009).

Chloroplasts derive from cyanobacterial ancestors, but contain only a limited number of photosynthesis-related genes in their plastome, whereas the vast majority of chloroplast proteins are nuclear-encoded (Leister, 2003). Hence a constant communication between the chloroplasts and the nucleus is required to coordinate the expression of nuclear- and plastome-encoded photosynthesis genes and thus to adapt photosynthesis to the demand and to environmental cues. In order to describe this form of chloroplast to nucleus communication, the concept of retrograde signaling has been introduced (Beck, 2005; Koussevitzky et al., 2007; Kleine et al., 2009). Studies on mutant and wild-type plants revealed at least six possible signals chloroplasts might emit to trigger yet unknown signaling pathways or cascades. The list of these signals comprises (i) tetrapyrroles as intermediates of chlorophyll and heme biosynthesis (Surpin et al., 2002; Beck, 2005), (ii) chloroplast-generated redox signals (Pfannschmidt et al., 1999), (iii) reactive oxygen species (ROS; Kim et al., 2008; Foyer and Noctor, 2009; Miller et al., 2009; Triantaphylidès and Havaux, 2009), (iv) plastid gene expression (Ahlert et al., 2003), (v) the production of abscisic acid (ABA) as response to an enhanced xanthophyll cycle (Baier et al., 2004; Baier and Dietz, 2005), and chloroplast-derived metabolite signals including carbohydrates (Smeekens, 1998, 2000; Rolland et al., 2002, 2006; Bräutigam et al., 2009), which accumulate as a consequence of photosynthetic CO_2 assimilation.

In the light, photoassimilates are exported from the chloroplast stroma in form of triose phosphates (TP) mediated by the

TP/phosphate translocator (TPT; Fliege et al., 1978) in a strict counter exchange with inorganic phosphate (P_i). In contrast to this day-path, the night-path of photoassimilate export commences with the biosynthesis of transitory starch during the light period and its subsequent mobilization in the dark by β-amylase, debranching enzyme, and disproportionating enzyme 1 (DPE1; Zeeman et al., 2010). The resulting maltose and glucose (Glc) are exported by respective transporters of the inner envelope membrane (Weber et al., 2000; Niittylä et al., 2004; Weise et al., 2004) and can enter further metabolism. Maltose is converted to Glc and Glc1P by the action of cytosolic DPE2 (Lu and Sharkey, 2004, 2006) involving a heteroglycan (Fettke et al., 2008), cytosolic glucan phosphorylase (PSH2), and the phosphorylation of Glc by hexokinase. A disturbed day-path of photoassimilate export (i.e., diminished or lack of TPT activity) can be completely compensated by the night-path (Häusler et al., 1998; Schneider et al., 2002; Walters et al., 2004). A block in both paths can be brought about by a combined inhibition of TP export and starch biosynthesis [e.g., in the absence of ADP glucose pyrophosphorylase (ADG), the key enzyme of starch biosynthesis]. Two alleles of a double mutant defective in the TPT and ADG (*adg1-1/tpt-1*; Schneider et al., 2002; Häusler et al., 2009; and *adg1-1/tpt-2*; Schmitz et al., 2012) were still viable, albeit reduced in size. Moreover the double mutants exhibit a high chlorophyll a fluorescence (HCF) phenotype only when grown under high light (HL) condition. Low light (LL) grown plants were indistinguishable from the wild-type or the single mutants (Schmitz et al., 2012). The HCF phenotype is based on the accumulation of light harvesting complex proteins (LHCs) not associated with the core components of PSII or PSI. Biochemical analyses revealed that the *adg1-1/tpt-2* double mutant is deprived of soluble sugars and hence represents a plant suffering from carbohydrate starvation. Sugar depletion leads to an arrest of growth and a redirection of metabolism toward basic processes such as respiration based on amino acids and lipids rather than on glycolysis. Highly energy-consuming reactions such as protein biosynthesis are switched off (Yu, 1999; Contento et al., 2004; Bläsing et al., 2005; Ishizaki et al., 2005). Strikingly growth on sucrose or glucose not only rescued the growth retardation but also (at least partially) the HCF phenotype of the double mutant. This rescue was independent from the induction of a glucose 6-phosphate/phosphate translocator (GPT) as triple mutants, which lack *GPT2* expression could also be rescued by externally supplied sugars. *GPT2* expression responds strongly to elevated sugar levels, e.g., in low starch mutants such as *pgm1* (see MapMan; Thimm et al., 2004; Bläsing et al., 2005) or *adg1-1* (Kunz et al., 2010). Whilst the rescue of the growth phenotype of the *adg1-1/tpt-2* double mutant in the presence of externally supplied sugars can be partially explained by the provision of carbon skeletons as building blocks and energy supply, the rescue of the HCF phenotype remains obscure.

Glucose is capable of modulating the expression of nuclear-encoded PS genes (such as *LHC*s) by signaling pathways involving hexokinase1 (HXK1; Jang and Sheen, 1994; Jang et al., 1997; Smeekens, 1998; Xiao et al., 2000; Moore et al., 2003). The carbohydrate status of the mesophyll indirectly depends both on the rate of CO_2 assimilation and carbohydrate consumption (i.e., by export to the sinks). Hence, it is likely that the carbohydrate status is directly involved in acclimation of plants to the environment. Sugar sensing has been extensively studied in plants. A complex regulatory network has emerged integrating metabolic signals and environmental stimuli on the basis of the interaction of plant hormones such as abscisic acid (ABA), ethylene, or cytokinins and auxins (Rolland et al., 2006). In particular sugar and ABA sensing overlap to a large extent (Dekkers et al., 2008). The majority of studies on sugar and plant hormone interactions have been done during early seedling development (León and Sheen, 2003; Gibson, 2005). HXK1 defective in the *gin2* mutant appears to be the core component of plant Glc-sensing and signaling (Jang et al., 1997; Moore et al., 2003; Yanagisawa et al., 2003). HXK1 functions upstream of GIN1/ABA2 in the glucose signaling pathway (Zhou et al., 1998). Despite of the impaired glucose sensing *gin2* mutants accumulate wild-type like levels of sugar phosphates based on the residual activity of glucokinase. HXK activity has also been detected in the cytosol and associated with chloroplasts (Wiese et al., 1999) or mitochondria (Giege et al., 2003). However HXK1 can also translocate to the nucleus (Yanagisawa et al., 2003). Besides HXK1 and HXK2 which are localized outside of the chloroplasts, there is also evidence for the occurrence of a functional hexokinase in the plastid stroma (Karve et al., 2010), which has been proposed to be involved in plastid gene expression (Zhang et al., 2010). Apart from HXKs, plants contain several fructokinases, some of which might also be involved in sugar sensing (Pego and Smeekens, 2000). The *gin2* mutant, for instance, is still susceptible to fructose and sucrose (Rolland et al., 2006).

In this report we have addressed the question, whether the sugar-dependent rescue of the *adg1-1/tpt-2* growth and HCF phenotypes is mediated by the sugar sensing HXK1 defective in *gin2*. For this purpose a homozygous triple mutant defective in TPT, ADG, and HXK1 (*adg1-1/tpt-2/gin2*) has been generated and the effect of external Glc, Suc, and Fru supply on the growth, HCF phenotypes, and photosynthetic electron transport rate (ETR) has been studied. Our data suggest that HXK1 does not play a major role in the sugar-dependent rescue of the double mutant phenotypes.

MATERIALS AND METHODS

PLANT MATERIAL, GROWTH CONDITIONS, AND SAMPLING

Seeds of *Arabidopsis thaliana* ecotypes Col-*0*, and *Landsberg erecta* (L*er*) were obtained from the Nottingham Arabidopsis Stock Centre (NASC). In addition, the following mutant lines defective in the gene indicated were used: *gpt2-1* (At1g61800; Niewiadomski et al., 2005), *adg1-1* (At5g48300; Lin et al., 1988), and *gin2-1* (Moore et al., 2003) defective in HXK1 (At4g29130). The identification and isolation of the *tpt-2* mutant allele (At5g46110) and the establishment of *adg1-1/tpt-2* double mutants and *agd1-1/tpt-2/gpt2-1* triple mutants has been described elsewhere (Schmitz et al., 2012).

Plants were germinated and grown on sterile 1/2 Murashige–Skoog (MS) agar or on 1/2 MS agar supplemented with 50 mM of each Glc, Suc, or Fru for 3 weeks in a growth chamber at a light/dark cycle of 16 h/8 h, a day/night temperature of 22°C/18°C, and a photon flux density (PFD) of 300 $\mu mol\, m^{-2}\, s^{-1}$. As an osmotic control plants were also germinated and grown on 1/2 MS agar supplemented with 50 mM sorbitol.

For all further analyses 3-week-old plants were used. Photosynthesis measurements of dark-adapted plants were performed after the plants had been exposed to the light for 5 h. Similarly, plant material for starch and sugar determination or RNA extraction was harvested after 5 h in the light.

RNA EXTRACTION AND qRT-PCR

RNA was extracted according to Logemann et al. (1987). After treatment with DNA-free DNase (Ambion), oligo (dt)-primed cDNA of total RNA was synthesized using the BioScript reverse transcriptase (Bioline). The transcript abundance of *GPT2, LHCB1,* the genes encoding sedoheptulose 1,7-bisphosphatase (*SBP*), a nitrate reductase (*NR1*), and the plastidial HXK (*pHXK*) was analyzed by quantitative RT-PCR with the SYBR Green PCR Master Mix (Applied Biosystems) in combination with the 7300 Sequence Detection System (Applied Biosystems). Relative transcript amounts were quantified with the $\Delta\Delta C_t$ method (Ramakers et al., 2003). As a control *actin2* (*ACT2*, At3g18780) was used. The primers used in this study are listed in **Table 1**.

CARBOHYDRATE DETERMINATION

Starch and soluble sugars were isolated from frozen leaf material according to Lin et al. (1988) and determined with a coupled enzymatic assay (Stitt et al., 1989) in an InfiniTe 200 Pro plate reader (TECAN, Germany) in the absorbance mode.

IN VIVO DETERMINATION OF PHOTOSYSTEM II PERFORMANCE

Photosynthetic performance of PSII was determined by Chl *a* fluorescence measurements with the pulse amplitude modulation fluorometer Imaging-PAM (Walz, Effeltrich, Germany). The individual fluorescence parameters determined by the "saturation-pulse-method" are defined according to Schreiber et al. (1986). The photosynthetic ETR was calculated from the parameter ΦPSII as described by Genty et al. (1989). In order to compare maximum fluorescence (F_m) and ground fluorescence (F_o) directly between the different plant lines and conditions, care was taken that the distance between the surface of the leaf rosettes and the optics of the video camera as well as the settings of the PAM fluorometer were kept constant in all experiments.

Table 1 | Oligonucleotide primers used for the determination of T-DNA mutants by qRT-PCR.

AGI code	Name	Sequence 5′–3′
At3g18780	*ACT2* fwd	CTT GCA CCA AGC AGC ATC AA
	ACT2 rev	CCG ATC CAG ACA CTG TAC TTC CTT
At1g61800	*GPT2* fwd	TGC CCT CGG TGC TGC CAT TG
	GPT2 rev	TCCT CAC TGC TTC GCC TGT GAG T
At1g29920	*LHCB1* fwd	TTC CCT GGA GAC TAC GGA TG
	LHCB1 rev	CCC ACC TGC TTG GAT AAC T
At3g55800	*SBP* fwd	GTT CTC ACC AGG AAA CTT AAG AGC
	SBP rev	GGT GTA TCG CAG TGT GTA TTT CTC
At1g77760	*NR1* fwd	GAT GGG CTA GTA AGC ATA AGG AGA
	NR1 rev	ACA GCT TCA GTT ATA AAC CCG GTA
At1g47840	*pHXK* fwd	GAA TAT GAA TGC AAG GAG GAG AGT
	pHXK rev	CTT CTC CAG AAT TGC CAC TAT ACC

STATISTICAL EVALUATION OF EXPERIMENTAL DATA

The data are expressed as mean values ± standard error (SE) of the indicated number of independent measurements. Significant differences between more than two data sets were analyzed using single site ANOVA combined with the *post hoc* Tukey–Kramer test, which allows the comparison of unequal sample sizes and identifies those pairs of values, which are significantly different from each other (Ludbrook, 1998). For data plotting and fitting, SigmaPlot 10.0 for Windows (SPSS Inc.) was used. All statistical analyses are given in Supplementary Material.

RESULTS

GENERATION AND PROPERTIES OF HOMOZYGOUS *adg1-1/tpt-2/gin2-1* TRIPLE MUTANTS

The *gin2-1* mutant (Moore et al., 2003), which had been isolated from an EMS mutagenized *A. thaliana* population in the L*er* background, contains a translational stop codon after position 1296 downstream of the start codon leading to a non-functional protein. The identity of the mutant was confirmed by sequencing and by the response of seedlings to germinate and grow on high Glc concentrations (**Figures 1D,I,N**). The *gin2-1* mutant has been crossed to the *adg1-1/tpt-2* double mutant (Col-*0* background) and a homozygous triple mutant has been generated. Like *gin2-1*, seedlings of the *adg1-1/tpt-2/gin2-1* triple mutant were less sensitive to high Glc concentrations (**Figures 1E,J,O**), whereas both wild-type lines and the *adg1-1/tpt-2* double mutant showed a severe growth retardation (**Figures 1A–C,F–H,K–M**). Similar to the *adg1-1/tpt-2* double mutant, the *adg1-1/tpt-2/gin2-1* triple mutant was retarded in growth and dark-adapted plants exhibited a HCF phenotype (**Figure 2G**). There was no additional visible phenotype of the triple mutant compared to the double mutant, when plants were grown on soil or on MS agar plates in the absence of sugars.

THE ABSENCE OF HXK1 HAD ONLY LITTLE EFFECT ON THE SUGAR-DEPENDENT RESCUE OF THE GROWTH PHENOTYPE OF *adg1-1/tpt-2*

The retarded growth phenotype of the *adg1-1/tpt-2* double mutant could be rescued when the plants were grown on 50 mM Suc or Glc (Schmitz et al., 2012). The effect of Fru on plant growth and performance has not been investigated so far. Col-*0* and L*er* wild-type plants, *gin2-1*, *adg1-1/tpt-2*, and *adg1-1/tpt-2/gin2-1* were grown either on 1/2 MS agar (control) or on 1/2 MS agar supplemented with 50 mM each of Glc, Suc, and Fru. In addition we investigated the response of the *adg1-1/tpt-2/gpt-2* triple mutant toward growth on the individual sugars. This triple mutant lacks the activity of GPT2 (Kunz et al., 2010), which is inducible by increased levels of endogenous sugars (like in low starch mutants) or by exogenous sugar supply.

Col-*0* wild-type plants grown on Glc or Suc showed an about 40% increase in the total rosette area 21 days post germination. In contrast, Fru was ineffective in promoting vegetative growth (**Figure 2A**). Interestingly, the L*er* wild-type background lacked any promoting effect of Glc or Suc on the total rosette area (**Figure 2D**). Likewise in the *gin2-1* single mutant the promoting effect of Glc and Suc on vegetative growth was less pronounced and

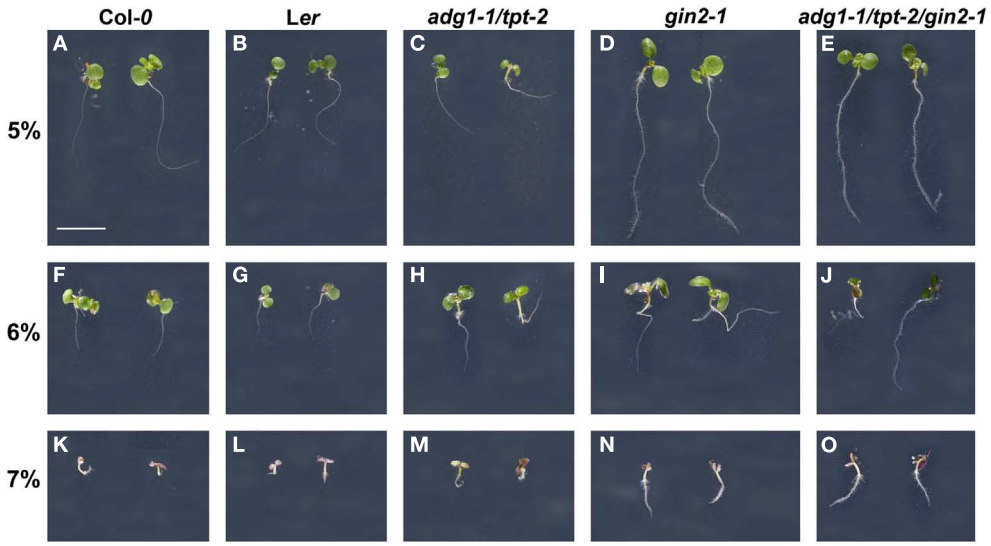

FIGURE 1 | Effect of 5–7% Glc on germination and seedling growth of Col-*0* (A,F,K) and L*er* (B,G,L) wild-type plants as well as on *adg1-1/tpt-2* (C,H,M), *gin2-1* (D,I,N), and the *adg1-1/tpt-2/gin2-1* triple mutant (E,J,O). The plants were grown for 11 days on 1/2 MS agar plates supplemented with 5% **(A–E)**, 6% **(F–J)**, or 7% **(K–O)** Glc at a PFD of 150 μmol m^{-2} s^{-1}. The bar in **(A)** represents 0.5 cm.

the presence of Fru resulted even in a substantial growth inhibition by more than 50% (**Figure 2E**).

The total rosette area of the *adg1-1/tpt-2* double mutant as well as the *adg1-1/tpt-2/gpt2-1* and *adg1-1/tpt-2/gin2-1* triple mutants was diminished by 60–70% in the absence of sugars compared to wild-type plants (**Figures 2B,C,F**). In all these lines growth on Glc or Suc, but not on Fru resulted in a substantial recovery in the total rosette area (**Figures 2B,C,F**). Moreover, there were some further qualitative and quantitative differences between the lines. Whereas growth on Glc and Suc fully restored the growth retardation of the *adg1-1/tpt-2* double mutant (**Figure 2B**), this effect was less pronounced with both sugars in the *adg1-1/tpt-2/gpt2-1* triple mutant (**Figure 2C**). Interestingly, growth on Glc completely restored the growth retardation of the *adg1-1/tpt-2/gin2-1* triple mutant (**Figure 2F**) to a level comparable to that of the *gin2-1* single mutant (**Figure 2E**). However, this rescue was significantly less pronounced compared to *adg1-1/tpt-2* grown on Glc, which probably reflects the lowered response toward both sugars observed in the L*er* background. Moreover, in the presence of Suc the *adg1-1/tpt-2/gin2-1* triple mutant even gained more than 50% of the total rosette area compared to the *gin2-1* single mutant grown in the absence of sugars (**Figures 2D,E**) and showed no significant difference to the *adg1-1/tpt-2* double mutant and the *adg1-1/tpt-2/gpt2-1* triple mutant grown on Suc. A statistical ANOVA analysis of differences in total rosette areas between the plants and treatments is provided in Table S1 in Supplementary Material.

THE RESCUE OF THE HCF PHENOTYPE AND OF PHOTOSYNTHETIC ETR IS INDEPENDENT FROM HXK1 IN THE *adg1-1/tpt-2* BACKGROUND

Similar to the growth phenotype, the HCF phenotype could be partially rescued when a*dg1-1/tpt-2, adg1-1/tpt-2/gpt2-1*, and *adg1-1/tpt-2/gin2-1* were grown on Glc and Suc (**Figure 2G**). Interestingly, although Fru failed to rescue the growth retardation or even inhibited growth in the background of L*er* and *gin2-1*, it caused some improvement of the HCF phenotype in the *adg1-1/tpt-2* double mutant and both the *adg1-1/tpt-2/gpt2-1* and *adg1-1/tpt-2/gin2-1* triple mutants. **Figure 2G** shows examples of false color images of maximum and ground Chl *a* fluorescence yield (i.e. F_m and F_o) as well as the F_v/F_m ratio of all lines grown on MS, Glc, Suc, or Fru obtained with the Imaging-PAM fluorometer.

From similar Chl *a* fluorescence images basic photosynthesis parameters were derived. The F_m and F_o values shown in **Figures 3A–F** refer to the mean F_m values of Col-*0* wild-type plants grown on MS agar plates in the absence of sugars (which was set to unity). The growth on Glc and Suc had no substantial effect on the F_m and F_o values of Col-*0* wild-type plants, whereas in the presence of Fru both F_m and F_o were diminished (**Figure 3A**). Such a Fru-dependent decrease in F_m and F_o was absent in the L*er* background (**Figure 3D**). Despite the differences in the relative F_m and F_o values, the F_v/F_m ratio of Col-*0* and L*er* remained unaffected by growth on sugars (**Figures 3G,J**). In the absence of externally supplied sugars, F_m and most pronounced F_o were substantially increased in the double mutant and both triple mutants (**Figures 3B,C,F**) resulting in a decrease in the F_v/F_m ratio from about 0.78 in the wild-type to below 0.4 (**Figures 3H,I,L**). The growth on all three individual sugars caused a substantial decrease in F_m and F_o and a recovery of the F_v/F_m ratio in the double and triple mutants. Strikingly F_m, F_o, and the F_v/F_m ratio of the *adg1-1/tpt-2/gin2-1* triple mutant responded similarly to growth on Glc, Suc, and Fru as a*dg1-1/tpt-2* and *adg1-1/tpt-2/gpt2-1* suggesting that the sugar-dependent rescue of the HCF phenotype occurs independently from HXK1 signaling. Moreover, the sugar-dependent recovery of F_m, F_o, and F_v/F_m is not a consequence of osmotic stress exerted on the plants in the presence of exogenously supplied sugars. In plants grown on 50 mM sorbitol (as an osmotic control), the F_v/F_m ratios in *adg1-1/tpt-2* and

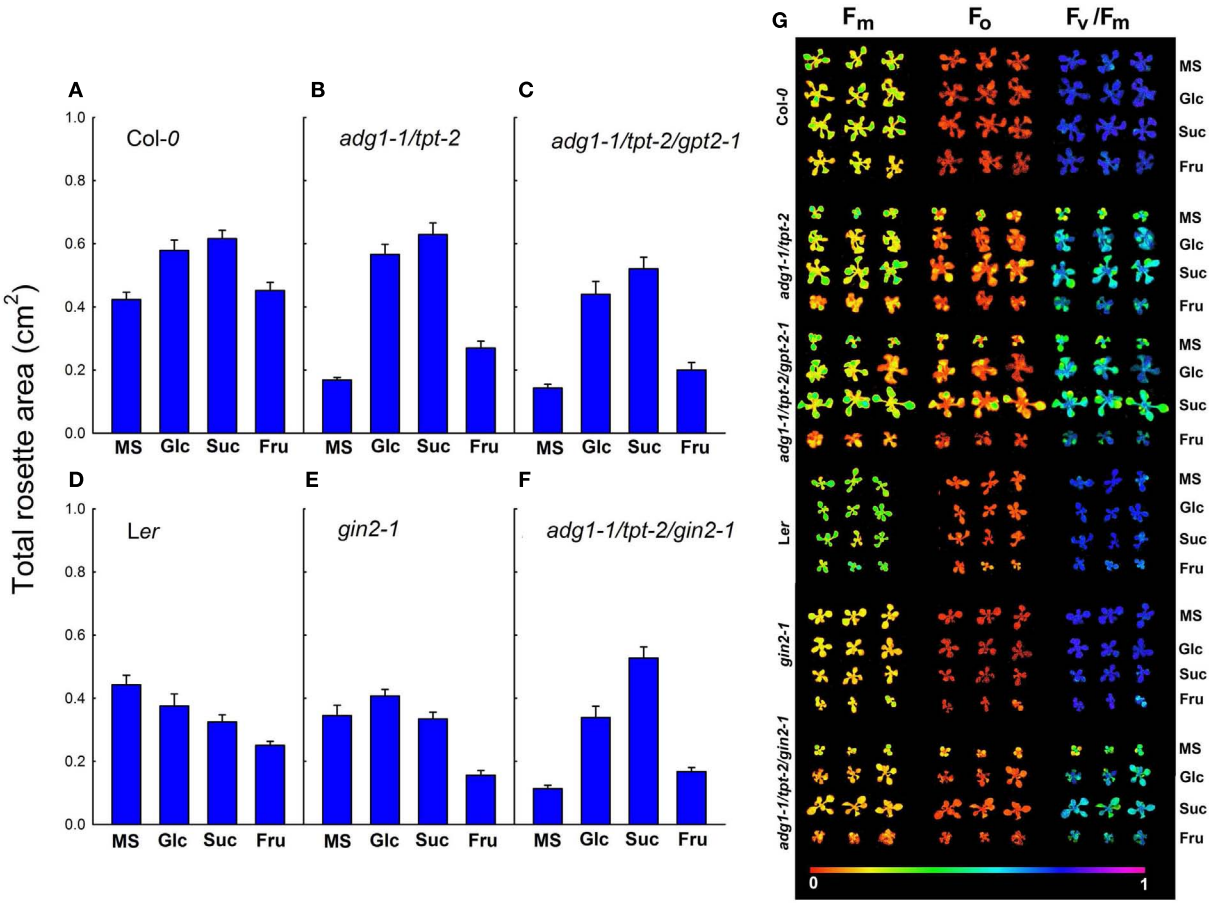

FIGURE 2 | Impact of sugar feeding on the total rosette area of Col-*0* (A), *adg1-1/tpt-2* (B), *adg1-1/tpt-2/gpt2*-1 (C), L*er* (D), *gin2-1* (E), and the *adg1-1/tpt-2/gin2-1* triple mutant (F). The data represent the mean ± SE were eight individual plants per line and treatment. Photosynthetic basic parameters (F_m, F_o, and the F_v/F_m ratio) of all lines comprised in **(A–F)** were measured with an Imaging-PAM fluorometer and are presented as false color images in response to external sugars **(G)**. The plants were grown for 3 weeks at a light/dark cycle of 16 h/8 h and a PDF of 300 μmol m^{-2} s^{-1}. The bar in **(G)** represents the numeric values of the false color images. The determination of the above parameters was conducted after 5 h in the light.

adg1-1/tpt-2/gin2-1 remained significantly below both wild-type lines and *gin2-1* (**Figure 4**). The statistical analysis of the data shown in **Figure 3** is given in Table S2 in Supplementary Material. The response of photosynthesis toward growth on different sugars was further analyzed by induction kinetics (**Figure 5**) and light response curves (**Figure 6**) of ETR.

In the Col-*0* background externally supplied sugars accelerated the establishment of steady state ETR (**Figure 4**). While, in the absence of sugars, the half time ($t_{1/2}$) to approach steady state was in the range of 80 s, $t_{1/2}$ was below 50 s in the presence of Glc, Suc, and Fru. Moreover, the steady state ETR was significantly higher in the presence of Glc and Suc, but not Fru, compared to the control plants grown on MS agar in the absence of sugars. In contrast to Col-*0*, externally supplied sugars showed neither a large effect on the $t_{1/2}$ nor on the maximum ETR in the L*er* background. However, steady state ETR was significantly lower when L*er* plants were grown on Fru compared to the un-fed control. For the *adg1-1/tpt-2* double mutant and the *adg1-1/tpt-2/gpt2-1* triple mutant the kinetics of ETR induction were very similar. In the absence of externally supplied sugars, the steady state ETR was significantly lower compared to the wild-type control, and the *adg1-1/tpt-2/gpt-2* triple mutant showed even a delay in the induction of ETR compared to the *adg1-1/tpt-2* double mutant. The steady state ETR in the presence of all three sugars recovered substantially in the *adg1-1/tpt-2* double and the *adg1-1/tpt-2/gpt2-1* triple mutant plants and approached values similar to the Col-*0* wild-type. However, in the presence of Suc the induction of ETR was slightly slower in *adg1-1/tpt-2/gpt2-1* compared to *adg1-1/tpt-2*. The lack of response of ETR induction to externally supplied sugars in the *gin2-1* mutant resembled that of the L*er* wild-type background, despite a delay in ETR induction in the presence of Suc. Like in L*er* the steady state ETR was slightly lower in *gin2-1* plants grown on Fru. Interestingly, the *adg1-1/tpt-2/gin2-1* triple mutant exhibited a pronounced delay in ETR induction in the absence of externally supplied sugars and the steady state ETR after 240 s in the light was significantly lower compared to the *adg1-1/tpt-2* double mutant or the *adg1-1/tpt-2/gpt2-1* triple mutant. Strikingly, the recovery of ETR with

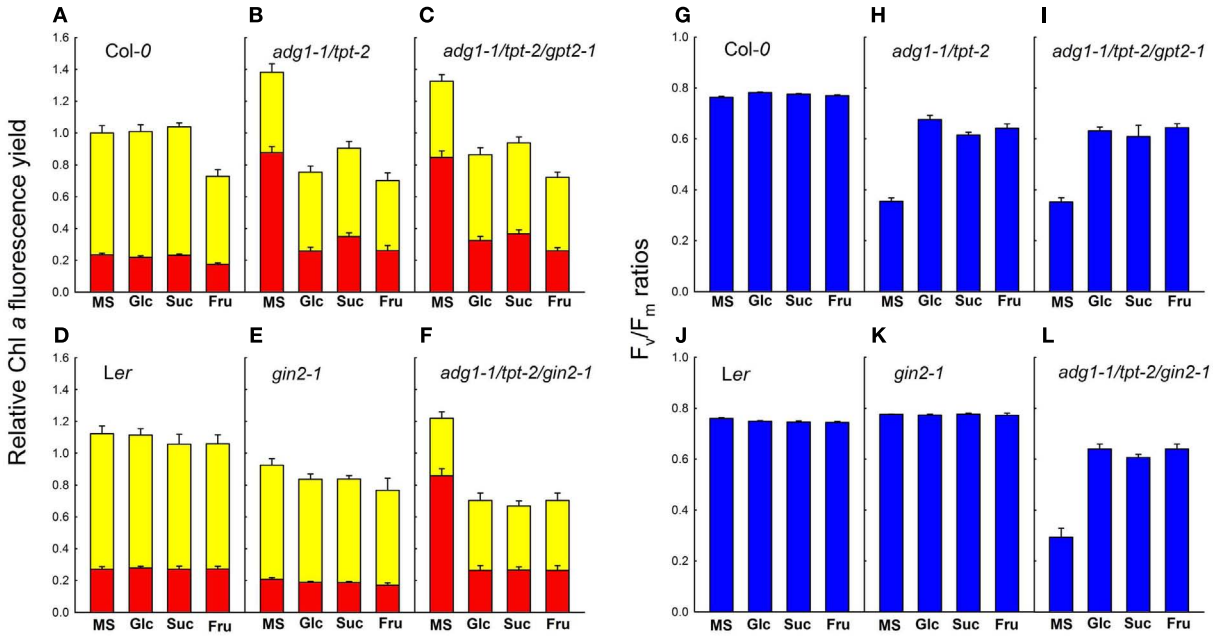

FIGURE 3 | Photosynthetic basic parameters of Col-*0* (A,G), *adg1-1/tpt-2* (B,H), *adg1-1/tpt-2/gpt2-1* (C,I), L*er* (D,J), *gin2-1* (E,K), and the *adg1-1/tpt-2/gin2-1* triple mutant (F,L) in response to the absence or presence of externally fed sugars. The relative Chl *a* fluorescence yield of F_m (yellow bars) and F_o (red bars) shown in **(A–F)** refers to the mean F_m value of Col-*0* plants grown on 1/2 MS agar (set to unity). The F_v/F_m ratios shown in **(G–L)** correspond to the F_m and F_o values in **(A–F)**. The data represent the mean ± SE of 10–20 individual plants per line and treatment. The plants were grown for 3 weeks, at a light/dark cycle of 16 h/8 h and a PDF of 300 μmol m^{-2} s^{-1}. Photosynthetic parameters were determined after 5 h in the light.

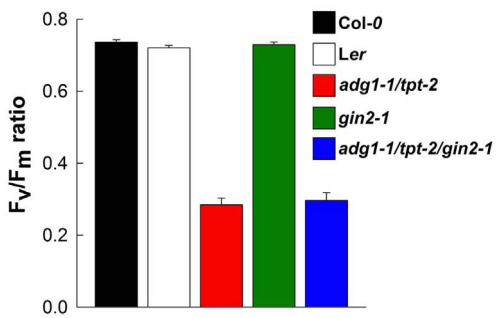

FIGURE 4 | Effect of growth on 50 mM sorbitol on the F_v/F_m ratios of 14-day-old Col-*0* (black bars) and L*er* (white bars) wild-type plants as well as *adg1-1/tpt-2* (red bars), *gin2-1* (green bars), and *adg1-1/tpt-2/gin2-1* (blue bars). The data are expressed as mean ± SE of between 5 and 10 individual measurements. An ANOVA/Tukey–Kramer analysis of the data sets revealed that the F_v/F_m ratio of *adg1-1/tpt-2* and *adg1-1/tpt-2/gin2-1* were significantly different ($P < 0.01$) from those of the other lines.

all three externally supplied sugars was significantly less pronounced in the *adg1-1/tpt-2/gin2-1* triple mutant compared to *adg1-1/tpt-2* and *adg1-1/tpt-2/gpt2-1*. Moreover, all three externally supplied sugars resulted in a similar level of ETR recovery in the *adg1-1/tpt-2/gin2-1* triple mutant. The statistical analysis of the data in **Figure 5** is given in Table S3 in Supplementary Material.

The light response curves of ETR (**Figure 6**) of all lines in this study resembled to some extent the induction kinetics of ETR (**Figure 5**). In the Col-*0* background, growth on Glc or Suc significantly promoted the maximum ETR at the highest PFD applied, whereas Fru had only little additional effect on maximum ETR. Likewise, there was no substantial effect of Glc and Suc on the light response curves of ETR in the L*er* background, while maximum ETR was slightly decreased in the presence of Fru. The light response curves of ETR determined for the *gin2-1* mutant resembled for all treatments those of the respective L*er* wild-type plants. In the absence of externally supplied sugars, maximum ETR was substantially inhibited in *adg1-1/tpt-2* and more so in *adg1-1/tpt-2/gpt2-1*. Strikingly, in the *adg1-1/tpt-2/gin2-1* triple mutant high PFDs inhibited ETR completely. The optimum ETR of about 18 μmol m^{-2} s^{-1} was attained at approximately 200 μmol m^{-2} s^{-1} and decreased with a further increase in the PDF. For the *adg1-1/tpt-2* double mutant, growth on Suc, and less pronounced on Glc and Fru, almost completely rescued ETR, which approached a similar level as in the un-fed wild-type (Col-*0*) control. Interestingly, all three sugars similarly promoted the light response of ETR in the *adg1-1/tpt-2/gpt2-1* triple mutant. As for the induction kinetics, the rescue of maximum ETR was significantly lower in the *adg1-1/tpt-2/gin2-1* triple mutant compared to *adg1-1/tpt-2* and *adg1-1/tpt-2/gpt2-1*. Similar to *adg1-1/tpt-2*, Suc rather than Glc or Fru had the most pronounced promoting effect on ETR recovery in *adg1-1/tpt-2/gin2-1*. A statistical analysis of the data in **Figure 6** is given in Table S4 in Supplementary Material.

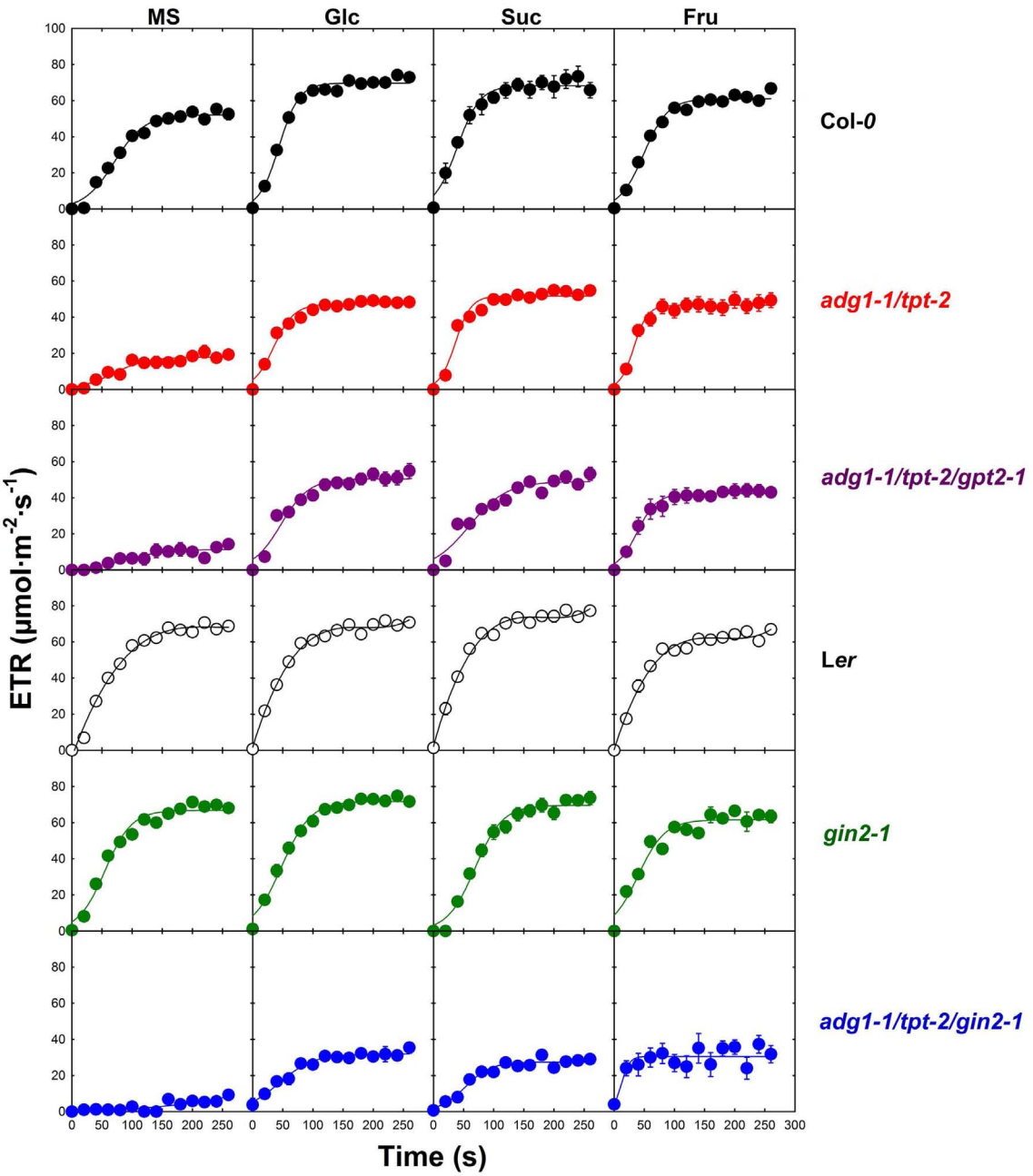

FIGURE 5 | Induction kinetics of photosynthetic electron transport (ETR) of Col-*0* (black symbols), *adg1-1/tpt-2* (red symbols), *adg1-1/tpt-2/gpt2-1* (purple symbols), L*er* (open symbols), *gin2-1* (green symbols), and the *adg1-1/tpt-2/gin2-1* triple mutant (blue symbols) in response to the absence or presence of externally fed sugars. The data represent the mean ± SE of 10–20 individual plants per line and treatment. The plants were grown for 3 weeks at a light/dark cycle of 16 h/8 h and a PDF of 300 µmol m^{-2} s^{-1}. ETR determinations were conducted after 5 h in the light.

ENDOGENOUS SUGAR CONTENTS IN WILD-TYPE AND MUTANT PLANTS REFLECT THE EXOGENOUS SUPPLY WITH CARBOHYDRATES

The rescue of the HCF and growth phenotype in *adg1-1/tpt-2* is largely independent from the presence or absence of HXK1. In contrast, ETR in the *adg1-1/tpt-2/gin2-1* triple mutant was significantly lower compared to *adg1-1/tpt-2* and *adg1-1/tpt-2/gpt2-1* grown on either of the three sugars. In order to further elucidate this observation, we analyzed the steady state contents of endogenous sugars and starch in leaves of mutant and wild-type plants (**Table 2**). The steady state levels of Glc, Suc, and Fru in MS-grown double mutant and both triple mutant plants were appreciably lower compared to both wild-type ecotypes. However, compared to growth on soil (Schmitz et al., 2012), endogenous carbohydrate contents in *adg1-1/tpt-2*

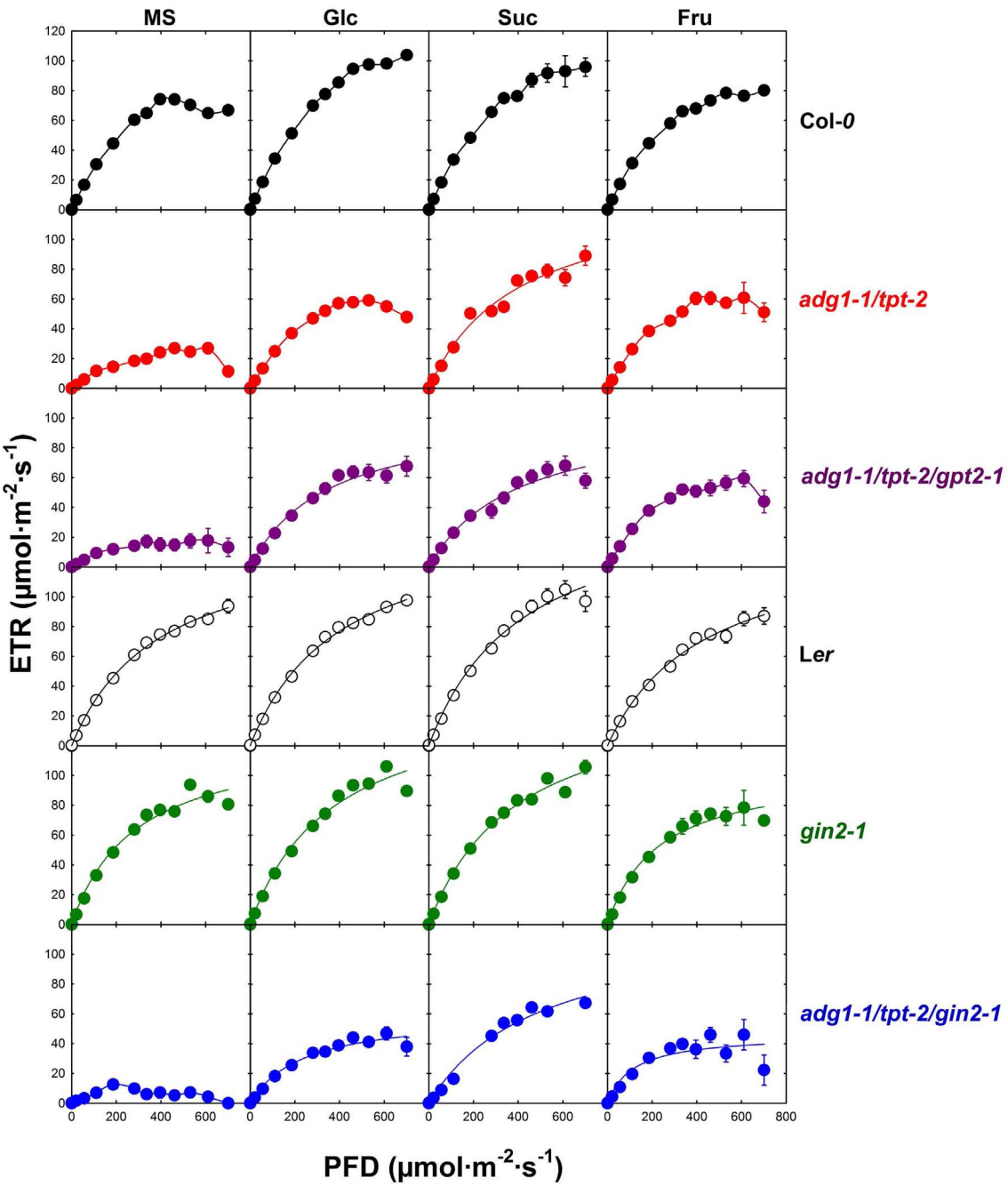

FIGURE 6 | Light dependency of photosynthetic electron transport (ETR) of Col-*0* (black symbols), *adg1-1/tpt-2* (red symbols), *adg1-1/tpt-2/gpt2*-1 (purple symbols), L*er* (open symbols), *gin2-1* (green symbols), and the *adg1-1/tpt-2/gin2-1* triple mutant (blue symbols) in response to the absence or presence of externally fed sugars. The data represent the mean ± SE of 10–20 individual plants per line and treatment. The plants were grown for 3 weeks, at a light/dark cycle of 16 h/8 h and a PDF of 300 µmol m^{-2} s^{-1}. ETR determinations were conducted after 5 h in the light.

were only moderately diminished. Hence, plants grown on agar appear to be less severely limited by endogenous carbohydrates.

For all lines, the steady state levels of those sugars the plants were grown upon, were significantly increased. While feeding of Glc and Fru particularly increased the respective levels of these sugars, the supply of Suc had a larger effect on the steady state contents of Glc and Fru rather than on Suc, reflecting the activities of various invertases, which are capable of converting Suc into the two monosaccharides Glc and Fru. In contrast, growth on Fru resulted in a significant decrease in Glc levels in L*er*, *gin2-1*, the *adg1-1/tpt-2* double mutant, and the *adg1-1/tpt-2/gin2-1*

Table 2 | Contents of soluble sugars and starch in rosette leaves of Col-*0*, *adg1-1/tpt-2*, *adg1-1/tpt-2/gpt2-1*, L*er*, *gin2-1*, and *adg1-1/tpt-2/gin2-1*.

Biotype	Treatment	Glc (μmol C6·g^{-1} FW)	Suc (μmol C6·g^{-1} FW)	Fru (μmol C6·g^{-1} FW)	Starch (μmol C6·g^{-1} FW)
Col-*0 (a)*	MS	6.59 ± 0.79	9.70 ± 0.63	2.45 ± 0.20	19.22 ± 2.48
	Glc	**17.64 ± 1.58**	10.19 ± 0.46	3.44 ± 0.35	39.36 ± 7.24
	Suc	19.56 ± 0.80	**13.44 ± 0.47**	8.74 ± 0.61	74.36 ± 8.22
	Fru	5.00 ± 1.43	5.43 ± 0.55	**10.92 ± 0.56**	57.93 ± 10.75
adg1-1/tpt-2 (b)	MS	4.20 ± 0.26	6.39 ± 0.37	1.10 ± 0.05	0.61 ± 0.14
	Glc	**13.89 ± 1.74**	5.56 ± 0.79	1.10 ± 0.21	0.49 ± 0.07
	Suc	12.31 ± 0.97	**11.75 ± 0.77**	6.05 ± 0.60	0.73 ± 0.05
	Fru	1.79 ± 0.14	4.18 ± 0.61	**24.02 ± 1.26**	0.42 ± 0.12
adg1-1/tpt-2/gpt2-1 (c)	MS	3.98 ± 0.39	4.72 ± 0.26	0.92 ± 0.08	1.01 ± 0.18
	Glc	**12.22 ± 0.40**	5.58 ± 0.21	1.28 ± 0.08	0.65 ± 0.09
	Suc	10.70 ± 0.72	**9.82 ± 0.23**	6.57 ± 0.30	0.60 ± 0.03
	Fru	3.18 ± 0.25	6.56 ± 0.77	**21.59 ± 1.11**	0.58 ± 0.20
L*er (d)*	MS	8.33 ± 0.21	5.27 ± 0.21	4.65 ± 0.37	26.14 ± 3.07
	Glc	**13.98 ± 1.22**	8.62 ± 0.34	7.46 ± 0.50	55.08 ± 8.37
	Suc	8.55 ± 3.98	**13.81 ± 6.52**	7.35 ± 0.33	324.96 ± 9.51
	Fru	2.69 ± 0.98	4.56 ± 0.21	**10.90 ± 1.40**	75.80 ± 11.21
gin2-1 (e)	MS	12.08 ± 0.14	12.15 ± 1.03	6.87 ± 0.11	66.22 ± 3.20
	Glc	**15.89 ± 0.88**	14.24 ± 1.63	8.67 ± 1.36	63.82 ± 14.73
	Suc	18.96 ± 0.66	**21.29 ± 2.26**	15.06 ± 0.65	145.67 ± 18.64
	Fru	5.15 ± 1.14	9.05 ± 1.45	**12.27 ± 2.50**	88.24 ± 23.09
adg1-1/tpt-2/gin2-1 (f)	MS	2.03 ± 0.44	5.12 ± 0.42	0.84 ± 0.13	0.06 ± 0.02
	Glc	**8.21 ± 2.39**	10.24 ± 0.78	3.21 ± 0.40	0.01 ± 0.00
	Suc	3.97 ± 0.86	**9.69 ± 0.90**	6.60 ± 1.48	0.00 ± 0.00
	Fru	0.50 ± 0.38	4.28 ± 0.47	**24.77 ± 4.52**	0.03 ± 0.00

The leaf samples were taken after 5 h in the light. The data represent the mean ± SE of three to six independent experiments. A detailed statistical analysis (ANOVA/Tukey–Kramer) of the data is contained in Table S5 in Supplementary Material. Bold numbers indicate the contents of those sugar species the plants were grown on.

triple mutants, whereas in Col-*0* and the *adg1-1/tpt-2/gpt2-1* triple mutant Glc levels were less affected.

A closer analysis of the steady state contents of individual sugars between the lines and the physiological effects exerted by their external supply (i.e., final rosette size of the plants or the recovery of photosynthesis parameters) revealed a heterogeneous picture. For instance, Fru failed to promote growth of the double mutant and both triple mutant plants. The steady state level of Fru in these lines was at least doubled compared to Col-*0* and L*er* or the *gin2-1* single mutant, suggesting that the turnover of Fru is slow compared to that of Suc or Glc. Hence, Fru is insufficient to rescue the mutants growth phenotype. Strikingly, the levels of Glc were significantly lower in double and triple mutants (particularly in *adg1-1/tpt-2/gin2-1*) when grown on Glc or Suc, compared to the respective wild-type or single mutant (i.e., *gin2-1*) control. Moreover, feeding of exogenous sugars promoted starch biosynthesis in both wild-type ecotypes and *gin2-1*. The most pronounced effect of external sugar-dependent starch biosynthesis has been observed in the L*er* background, in particular when the plants were grown on Suc. Starch contents in Suc-grown L*er* increased more than 10-fold compared to plants grown on MS. A significant (but less marked compared to L*er*) increase in starch contents was also evident for the *gin2-1* mutant grown on Suc. All three sugars had only little impact on the residual starch levels in the low starch background. Interestingly, residual starch in the a*dg1-1/tpt-2/gin2-1* triple mutant was barely detectable under all growth conditions. Hence, this triple mutant represents a true starch-free plant. A statistical analysis of the data in **Table 2** is given in Table S5 in Supplementary Material.

ETR IN THE *adg1-1/tpt-2*, *adg1-1/tpt-2/gpt-2*, AND *adg1-1/tpt-2/gin2-1* CORRELATES WITH THE CARBOHYDRATE STATUS IN THE MESOPHYLL

The most surprising outcome of our study was the observation that all three sugars were capable of rescuing not only the HCF phenotype of the double and triple mutants, but also ETR. In order to further elucidate this unexpected finding we plotted the steady state ETR of all lines in this study, obtained after the induction of photosynthesis (see **Figure 5**), against the average contents of Glc, Suc, and Fru (see **Table 2**). However, the plots shown in **Figures 7A–C** revealed only a poor correlation. The scattering of the data points appeared to be arbitrary and not linked to the contents of the individual sugars. Surprisingly, a plot of ETR vs. the sum of all soluble sugars resulted in an improved curve fit (**Figure 7D**). In a next step ETR was plotted against the sum of

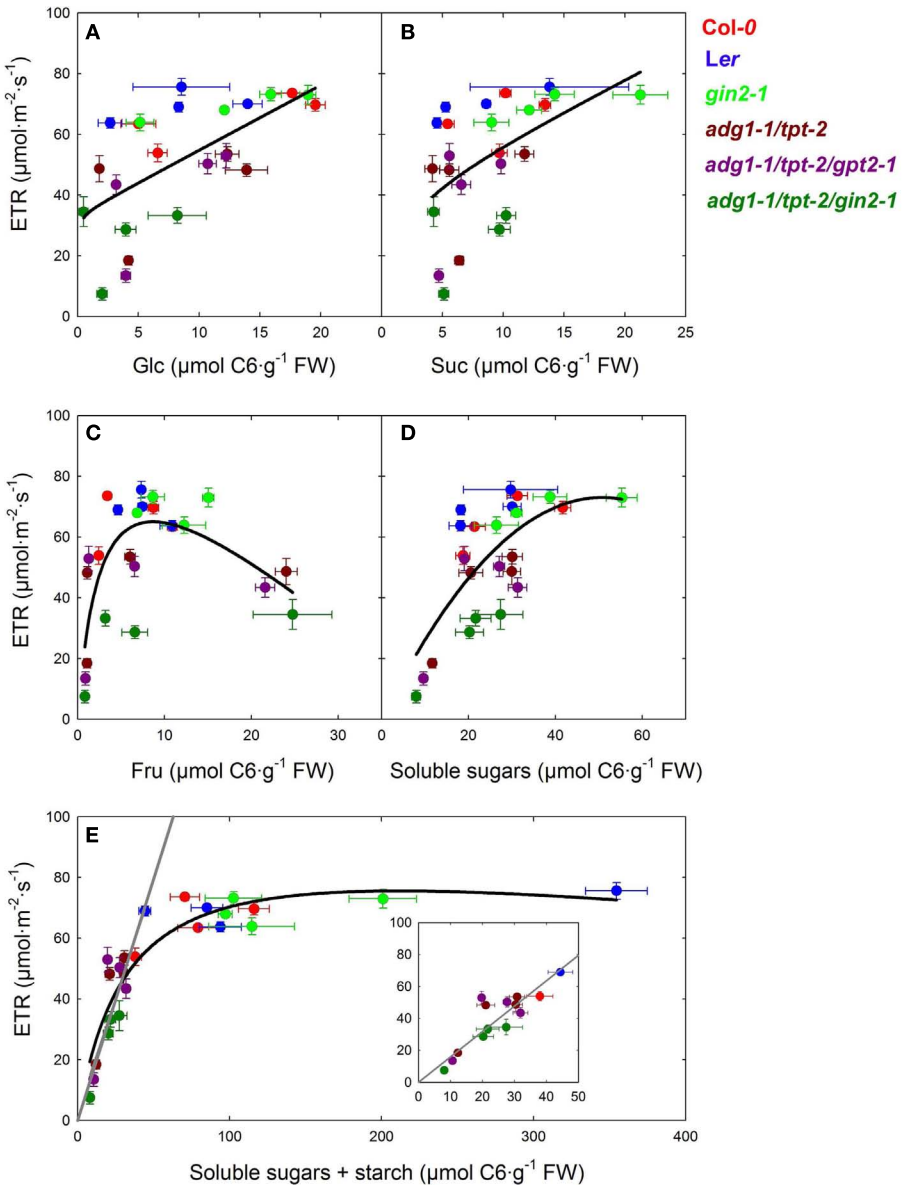

FIGURE 7 | Plots of photosynthetic ETR, obtained from steady state values in Figure 4, vs. the average content of Glc (A), Suc (B), and Fru (C) as well as the sum of contents of soluble sugars (D), and total carbohydrates, including starch (E). The black lines represent curve fits of the data points to single rectangular three parameter hyperbolas ($f = a{\cdot}x/[b + x] + c{\cdot}x$), whereas the gray lines derive from a linear regression analysis of all data points at total carbohydrate contents below 50 µmol C6·g^{-1} FW [see inset in **(E)**]. For the linear regression analysis a correlation coefficient of $R = 0.874$ was obtained. The individual plant lines are represented by different colors and are defined as Col-*0* (red), L*er* (blue), *gin2-1* (light green), *adg1-1/tpt-2* (dark red), *adg1-1/tpt-2/gpt2-1* (dark purple), and *adg1-1/tpt-2/gin2-1* (dark green).

the contents of all soluble sugars including the content of starch (expressed as C6 units). As might be expected, the ETR of all lines containing a substantial amount of starch clustered together at a constant average ETR of about 70 µmol m^{-2} s^{-1}. Interestingly, at a threshold well below 70 µmol C6·g^{-1}fw total carbohydrates, there was a linear correlation between ETR and the total carbohydrate content (**Figure 7E**). A regression analysis of all data below this threshold level resulted in a line with a correlation coefficient of $R = 0.874$. Similar curve fits were performed for the data deriving from the light dependency of ETR (**Figure 6**). Again, linear regression analyses of the data below the threshold level of total carbohydrates delivered a good linear correlation with *R*-values of up to 0.944 (not shown).

By plotting ETR against total carbohydrate contents we could separate plant lines containing sufficient amounts of starch from the low starch mutants. In the presence of starch, ETR appears to be independent from the total carbohydrate status of the mesophyll, whereas in mutants defective in the day- and night-path of

photoassimilate export from the chloroplasts ETR shows a direct correlation. Moreover, the moderate rescue of ETR observed in the *adg1-1/tpt-2/gin2-1* plants in the presence of externally supplied sugars would be consistent with lower contents of total carbohydrates in this line (compare **Table 2**) rather than with the defect in HXK1.

IMPACT OF GROWTH ON CARBOHYDRATES ON THE EXPRESSION OF SUGAR-RESPONSIVE GENES

It is well established that the supply of exogenous sugars suppresses the expression of photosynthesis-related genes (Smeekens, 1998; Xiao et al., 2000; Moore et al., 2003). HXK1 has been shown to be involved in the sugar-dependent suppression of *CAP1* (*LHCB1*) and for instance the gene encoding the Calvin Cycle enzyme *SBP*. In the *gin2-1* mutant, this sugar-dependent suppression of photosynthesis-related genes was largely abolished (Moore et al., 2003). Moreover, a nitrate reductase (*NR1*; Jang et al., 1997) and *GPT2* (e.g., Kunz et al., 2010; Schmitz et al., 2012) are induced in the presence of excess carbohydrates. Furthermore, there are indications that the gene encoding *pHXK* is also induced by exogenously supplied sugars (Zhang et al., 2010).

Here, we address the question, whether the sugar-dependent gene repression/induction is still operational in the double mutant background and whether *GPT2* and *pHXK* induction is mediated *via* HXK1-dependent signaling.

The expression level of *GPT2*, *LHCB1*, *SBP*, *NR1*, and *pHXK* has been determined in all lines (with the exception of *adg1-1/tpt-1/gpt2-1*) grown on the individual sugars compared to the MS control by qRT-PCR. The relative transcript abundance (log2 ratios) of the individual genes in the mutant and wild-type plants grown on Glc, Suc, or Fru have been compared to the MS control (i.e., in the absence of sugars; **Figure 8A**). Moreover, **Figure 8B** shows a detailed comparison of the relative transcript abundance between the individual lines in the absence or presence of Glc, Suc, and Fru in the growth medium.

Glucose 6-phosphate/phosphate translocator2 is only poorly expressed in photoautotrophic tissues (efp browser, http://bbc.botany.utoronto.ca/efp/; Winter et al., 2007; Kunz et al., 2010) and its expression was strongly induced in the Col-*0* background grown on Glc, Suc, or Fru (**Figure 8A**). Surprisingly in L*er* and *gin2-1*, the sugar-dependent induction of *GPT2* was less marked compared to Col-*0*. This diminished response to growth on exogenous sugars is probably due to the fact that in L*er* and *gin2-1* the basic expression level of *GPT2* was already increased compared to Col-*0* in the absence of sugars (**Figure 8B**). Strikingly, the sugar-dependent up-regulation of *GPT2* in the *adg1-1/tpt-2/gin2-1* triple mutant was not significantly different from the *adg1-1/tpt-2* double mutant, suggesting that HXK1 does not play a major role in the regulation of *GPT2* expression.

Light harvesting complex protein *B1* expression is supposed to be suppressed by sugars. Indeed in all lines, with the exception of *adg1-1/tpt-2/gin2-1*, growth on Glc moderately suppressed *LHCB1* expression, whereas growth on Suc and Fru resulted in an up-regulation of *LHCB1*. Surprisingly, the down-regulation of *LHCB1* in L*er* as a response toward growth on Glu was also present in *gin2-1* (**Figure 8A**). The only significant change in the Glc-response of *LHCB1* expression was observed between *adg1-1/tpt-2* (down-regulation of *LHCB1*) and *adg1-1/tpt-2/gin2-1* (no effect on *LHCB1* expression), suggesting that HXK1 might be involved in this response. Hence, the lack of difference between the Glc-response of *LHCB1* expression between L*er* and *gin2-1* would exclude an involvement of *HXK1*, whereas the de-suppression of *LHCB1* expression in *adg1-1/tpt-2/gin2-1* compared to *adg1-1/tpt-2* would support sensing and signaling by HXK1.

The relative transcript abundance of *SBP* delivered a heterogeneous picture (**Figure 8A**). It was slightly up-regulated in Col-*0* grown on Glc, but nearly unchanged in L*er* under the same conditions. The most prominent down-regulation of *SBP* expression was observed in *gin2-1* grown on Fru. Like for *LHCB1*, the down-regulation of *SBP* in the *adg1-1/tpt-2* double mutant grown of Glc was reverted in the *adg1-1/tpt-2/gin2-1* triple mutant.

In contrast to earlier observations *NR1* transcript abundance was decreased to a different extent in all lines grown on sugars compared to the MS-controls (**Figure 8A**). Strikingly, the sugar-dependent moderate suppression of *NR1* expression in the *adg1-1/tpt-2* double mutant was slightly relieved in the *adg1-1/tpt-2/gin2-1* triple mutant.

The relative transcript abundance of *pHXK* responded only moderately to the presence of sugars in the growth medium of Col-*0* and L*er* (**Figure 8A**). For Col-*0*, L*er*, and *gin2-1* the most pronounced effect on *pHXK* expression levels were apparent for plants grown on Fru. However, while growth in Fru resulted in a slight induction of *pHXK* in Col-*0*, the opposite was the case for L*er* and most pronounced for *gin2-1*. Most strikingly, *pHXK* expression was induced in *adg1-1/tpt-2* grown on either of the three sugars, whereas the induction of *pHXK* was appreciably diminished in the *adg1-1/tpt-2/gin2-1* triple mutant (**Figure 8A**). A statistical analysis of the data in **Figure 8** is given in Table S6 in Supplementary Material.

DISCUSSION

In this report we have addressed the question whether or not the carbohydrate-dependent rescue of the growth and HCF phenotype as well as of diminished photosynthetic ETR of *adg1-1/tpt-2* observed under HL-conditions is mediated by the sugar sensing HXK1 defective in the *gin2-1* mutant. For this purpose an *adg1-1/tpt-2/gin2-1* triple mutant has been generated and established as homozygous line. We compared the final size, photosynthetic performance, carbohydrate contents, and the expression of sugar-responsive genes of 21-day-old plants grown either on 1/2 MS agar in the absence or presence of 50 mM Glc, Suc, or Fru. In order to obtain a maximum degree of reproducibility, all photosynthesis measurements as well as the harvest of leaf material for further analyses, such as carbohydrate determinations or gene expression studies, were done approximately 5 h in the light.

The results of our experimental setup can be summarized as follows: (1) Growth on Glc and Suc, but not on Fru, could rescue the retarded growth phenotype of double and triple mutants defective in the day- and night-path of photoassimilate export from the chloroplast. The presence or absence of HXK1 does not exert any severe effect on the recovery of the final size of *adg1-1/tpt-2* plants grown on Glc or Suc (compare **Figure 2**). The lack of growth promoting effect of Fru is not understood, but might be

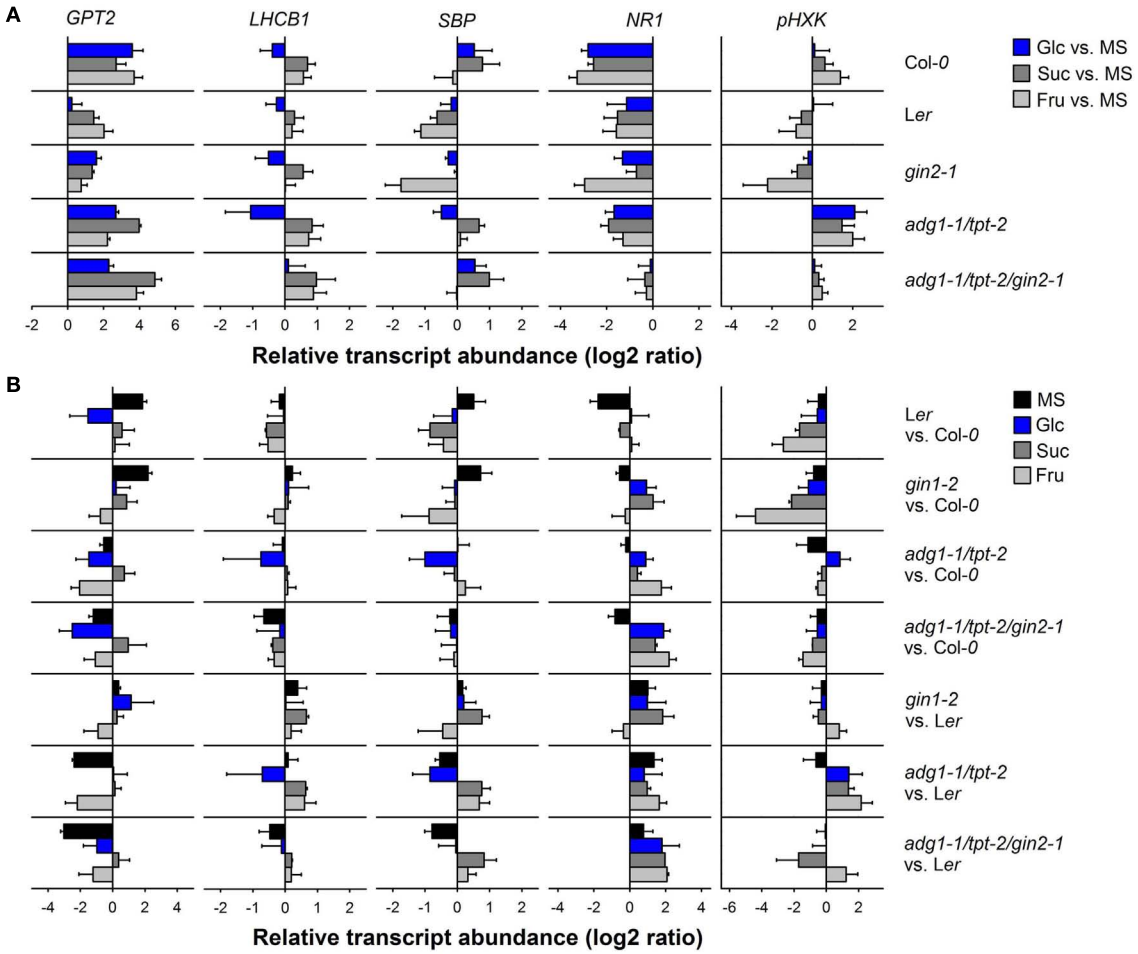

FIGURE 8 | Quantitative RT-PCR analyses of the relative transcript abundance of sugar-responsive genes (*GPT2, LHCB1, SBP, NR1, and pHXK*) in Col-*0*, L*er*, *gin2-1*, *adg1-1/tpt-2*, and a*dg1-1/tpt-2/gin2-1*. **(A)** The sugar-dependent regulation of the individual genes was assessed from their relative transcript abundance in plants grown on Glc (blue bars), Suc (gray bars), or Fru (light gray bars) compared to the MS control. The relative transcript abundance was expressed as log2 ratio. **(B)** Comparison of sugar-dependent gene regulation between the lines (i.e., referred to Col-*0* or L*er*) for plants grown on 1/2 MS (black bar), Glc (blue bars), Suc (gray bars), or Fru (light gray bars). The data represent the mean ± SE of two biological and at least four technical replicates. The determination of C_t values was considered independent for each control or treatment. For the assessment of log2 ratios a cross comparison between controls and treatments has been conducted resulting in $n = 4$ log2 ratios per treatment and biotype.

linked to product inhibition of invertases (Kingston-Smith et al., 1999). (2) Surprisingly all three sugars were capable of rescuing the HCF phenotype. Again, HXK1 is unlikely to play a prominent role in this rescue as *adg1-1/tpt-2/gin2-1* triple mutant plants showed an identical response as the double mutant (compare **Figure 3**). (3) Photosynthetic ETR in *adg1-1/tpt-2* and *adg1-1/tpt-2/gpt2-1* plants grown on either of the three sugars recovered almost to wild-type level. In contrast, this recovery was less pronounced in the *adg1-1/tpt-2/gin2-1* triple mutant, suggesting that the deficiency in HXK1 could have some impact on this diminished response of ETR (compare **Figures 5** and **6**). (4) Growth on individual sugars perturbed the steady state levels of endogenous soluble carbohydrates and starch to a different extent. For instance, growth on Glc had the most pronounced promoting effect on its own endogenous levels, whereas growth on Suc resulted only in a moderate increase in its own levels, but had a larger impact on the steady state contents of Glc and Fru, indicating a significant cleavage of Suc by various invertases. Moreover growth on Suc resulted in a dramatic increase in starch contents only in L*er* and to a lesser extent in the *gin2-1* mutant. Furthermore growth on Fru diminished the abundance of Glc and to some extend also of Suc in the different plant lines. In summary, the rescue of the HCF phenotype and ETR cannot be attributed to increased endogenous levels of individual sugars (compare **Table 2**), but it was directly correlated with the overall carbohydrate status of the mesophyll (compare **Figure 7**). This surprising observation deserves further attention in the future. (5) The expression profiles of genes known to be regulated by sugars delivered heterogeneous results in that they revealed only little response to the absence or presence of HXK1. It has to be considered that most expression studies involving *gin* mutants have been conducted at relatively high exogenously supplied Glc concentrations (2–6%) and/or in transient (i.e., 8–48 h)

feeding systems (e.g., Moore et al., 2003). The plants in our study have been grown on the individual sugars and could hence adapt to the constant supply with exogenous carbohydrates. Moreover, there were also ecotype-dependent differences in gene expression between Col-*0* and L*er*. For instance *GPT2* expression, which was induced in the presence of all three sugars in Col-*0*, remained almost unchanged in L*er* grown on Glc. Moreover, the expression level of *GPT2* was already appreciably higher in the L*er* compared to the Col-*0* background grown on 1/2 MS. The genome of the Col-*0* and L*er* ecotypes has been compared and a number of insdels (insertion deletions) discovered (Ziolkowski et al., 2009). L*er* for instance is a natural occurring *low level* β*-amylase* (*lba*) mutant, which is less sensitive to the sugar-induced expression of β-amylase (Mita et al., 1997). As β-amylase is the major enzyme for starch breakdown, the high levels of starch found in L*er* and *gin2-1* grown in Suc, might be explained by this deficiency. However, in the starch-free backgrounds of our study, a deficiency in the sugar-triggered induction of starch mobilizing enzymes appears to be less relevant. The most striking outcome of our expression analyses can be attributed to the sugar-dependent induction of *pHXK* in *adg1-1/tpt-2* and the lack of response in the *adg1-1/tpt-2/gin2-1* triple mutant (compare **Figure 8**).

VARIOUS PATHWAYS ARE INVOLVED IN SUGAR SENSING AND SIGNALING

In our approach, we investigated the impact of a deficiency in Glc-sensing HXK1 on the sugar-dependent rescue of the growth and photosynthesis phenotypes of *adg1-1/tpt-2*. Although HXK1 appears to play a central role in sugar sensing and signaling (Jang and Sheen, 1994; Moore et al., 2003; Cho et al., 2006, 2007), there are indications for numerous HXK1-independent sugar sensing and signaling mechanisms (Price et al., 2004; Rolland et al., 2006), also involving sensing of Suc (Rook et al., 1998; Vaughn et al., 2002) or Fru (Cho and Yoo, 2011; Li et al., 2012), components of the plasma membrane, like "regulator of G-protein signaling" (RGS; Chen and Jones, 2004), or sucrose non-fermenting related protein kinases (Snf1; Halford and Hey, 2009). Recently FRUCTOSE INSENSITIVE1 has been shown to act as a regulatory factor in Fru signaling and has been identified as cytosolic fructose 1,6-bisphosphatase (FbPase; Cho and Yoo, 2011). Like for the *gin* mutants the ability of mutant plants to overcome a developmental arrest in the presence of high Fru concentration (6%) was used as a screen. The diversity of various sugar sensing pathways and their interaction with hormonal signaling (Rolland et al., 2006) hamper the assessment of the sugar response in our system. Future work will also include the knockdown of further known components of carbohydrate sensing and signaling in the background of *adg1-1/tpt-2*.

CAN ANABOLIC PROCESSES WITHIN THE PLASTID STROMA BE FUELED BY IMPORTED CARBOHYDRATES?

Despite the presence of exogenously supplied sugars, the major constraints in the day- and night-path of carbohydrate export from the chloroplast are far away from being rescued in the double and triple mutants. In the absence of externally supplied sugars, the *adg1-1/tpt-2* double mutant presumably survives because of the alternative TP transport activity of the xylulose 5-phosphate/phosphate translocator (XPT, Eicks et al., 2002). Hence, the low ETR observed in *adg1-1/tpt-2* grown on soil or on 1/2 MS is the consequence of a limited capacity of this transporter to export TP for sucrose biosynthesis in the cytosol. Moreover, GPT2, which could export both Glc6P and TP, is not induced in *adg1-1/tpt-2* due to low endogenous sugar levels in the double mutant (compare **Figure 8B**). In contrast, when carbohydrates are supplied externally, the double and triple mutants gain biomass and the constraints in photosynthesis (i.e., ETR and the HCF phenotype) are almost completely rescued. However, biomass production requires not only carbon skeletons and energy, which can derive from glycolysis and subsequent respiration of exogenous supplied carbohydrates, but it also depends on the provision of specific compounds, such as fatty acids or certain amino acids (e.g., aromatic- or branched-chained amino acids). A number of anabolic pathways, such as *de novo* fatty acid biosynthesis (Ohlrogge et al., 1979; Ohlrogge and Jaworski, 1997), the production of aromatic- (Herrmann, 1995; Schmid and Amrhein, 1995; Herrmann and Weaver, 1999) or branched-chained amino acids (Schulze-Siebert et al., 1984) are confined to the plastid stroma. Furthermore, the biosynthesis of phytol as a part of Chl molecules and carotenoids depend on the mevalonate-independent way (DOXP/MEP) of isoprenoid biosynthesis, which is also located in the plastid stroma (Lichtenthaler, 1999). If these anabolic reactions in the stroma ceased, biomass production would collapse.

In principle, the chloroplasts should be able to use imported carbon for anabolic metabolic sequences and thereby consume energy and reducing power generated by the photosynthetic light reaction. Moreover, excessive stromal NADPH could also be exported to the cytosol via the malate valve (Scheibe et al., 2005; Taniguchi et al., 2005) and, depending on the concentration gradients, ATP could exit the chloroplast via the nucleoside triphosphate transporter (NTT; Haferkamp et al., 2011; Weber and Linka, 2011). However, in the presence of exogenously supplied sugars, energy and reducing equivalents could be provided by cytosolic glycolysis via substrate chain phosphorylation and subsequently by mitochondrial respiration.

For the import of carbon into the chloroplast, GPT2 would be a candidate, particularly as its expression is induced in the presence of elevated sugar levels. The import of cytosolic Glc6P deriving from the phosphorylation of Glc by HXK might be sufficient to drive anabolic processes within the chloroplast stroma. However, even in the absence of GPT2, ETR recovers in the *adg1-1/tpt-2/gpt-2* triple mutant when carbohydrates are supplied, ruling out a prominent function of carbon import into the chloroplast by GPT2. Furthermore, 3-phosphoglyceric acid (3-PGA), as an intermediate of cytosolic glycolysis, could be imported into the chloroplast by the TPT and/or the GPT. However, both functions are missing in the *adg1-1/tpt-2/gpt2-1* triple mutant. In contrast, although capable of transporting TP, the XPT cannot transport 3-PGA (Eicks et al., 2002). Finally phosphoenolpyruvate (PEP) or pyruvate produced in the final steps of glycolysis might enter the chloroplast via a PEP/phosphate translocator (PPT; Fischer et al., 1997) or a pyruvate transporter. For the latter, to date, only a Na-dependent transporter has been identified (Furumoto et al., 2011). The *A. thaliana* genome contains

two *PPT* genes, which are expressed in leaves, i.e., *PPT1* and *PPT2* (Knappe et al., 2003). PPT1, which is defective in the *chlorophyll a/b binding protein underexpressed1* (*cue1*) mutant (Streatfield et al., 1999) has been proposed to provide chloroplasts and non-green plastids with PEP as a precursor for the shikimate pathway. Chloroplasts and some non-green plastids are unable to provide PEP via plastidial glycolysis because of a lack of enolase (Prabhakar et al., 2009). Moreover, PEP can serve as substrate for *de novo* fatty acid biosynthesis and other anabolic pathways after conversion to pyruvate. Strikingly, an *A. thaliana* double mutants defective in both PPT1 and plastidial enolase was lethal (Prabhakar et al., 2010). PEP, besides of pyruvate, would be the only known products of glycolysis that might enter the chloroplast in the presence of exogenously supplied sugars.

It is, however, more likely that soluble sugars are directly taken up by the chloroplast, are converted to hexose-P by pHXK in the stroma and enter further metabolism. Strikingly, the expression of *pHXK* is appreciably induced in the *adg1-1/tpt-2* double mutant in the presence of sugars. Moreover, in the absence of HXK1 (i.e., in the *adg1-1/tpt-2/gin2-1* triple mutant) the induction of *pHXK* is much less pronounced compared to the double mutant (compare **Figure 8A**). Thus, a lowered rate of Glc6P production by pHXK would diminish energy and reducing equivalent consumption generated by the photosynthetic light reaction and thereby inhibits photosynthetic ETR. This scenario is consistent with an only moderate increase in ETR observed in the *adg1-1/tpt-2/gin2-1* mutant grown on sugars. Moreover, the most promoting effect on ETR in the *adg1-1/tpt-2/gin2-1* triple mutant has been achieved in plants grown on Suc (compare **Figure 6**), which could deliver double the amount of hexoses upon cleavage by invertases compared to Glc or Fru. Again, this observation indicates that ETR in the double and triple mutants is limited by carbon supply from the cytosol. It is tempting to speculate that CO_2 assimilation in *adg1-1/tpt-2* plants grown on sugars is reduced to a minimum, while the photosynthetic light reaction provides energy and reducing power for the metabolization of imported sugars. As both, Glc and Fru were equally effective in rescuing the photosynthesis phenotype of the double mutant, it would be required that at least both hexoses can enter the chloroplast. The uptake of a variety of soluble sugars into isolated spinach chloroplasts, including Glc, Fru, and even C4 sugars like arabinose, has been described more than three decades ago (Schäfer et al., 1977). However, the plastidial Glc transporter, which has been identified and characterized more than two decades later, does not seem to accept, e.g., Fru as a substrate (Weber et al., 2000). Provided that a yet unknown translocator is capable of transporting Fru along a concentration gradient, both hexoses might be sensed and further metabolized via pHXK (Zhang et al., 2010). There is further evidence for the occurrence of a plastidial invertase (Vargas et al., 2008), which could convert sucrose into Glc and Fru. However, so far no plastidial sucrose transporter has been identified. **Figure 9** illustrates the role of exogenously supplied sugars in the rescue of the *adg1-1/tpt-2* double mutant according to our hypothetical model. Please note, that uptake systems for Suc and Fru depicted in **Figure 9D** are merely speculative and lack any direct experimental proof.

IS RETROGRADE SIGNALING NECESSARY FOR SUGAR MEDIATED ACCLIMATION PROCESSES?

The concept of retrograde signaling presumes that certain signals generated within the chloroplasts are transmitted to the cytosol and trigger the expression or repression of nuclear-encoded genes required in the chloroplast. Exposure of LL-adapted plants to HL inevitably results in the temporary accumulation of carbohydrates in the mesophyll. Besides of the known sugar signaling pathways, there is increasing evidence that chloroplasts are capable of directly sensing the carbohydrate status in the cytosol. It has been demonstrated that pHXK of *A. thaliana* could act as a hexose sensor within the plastid stroma. Studies on plastidial gene expression (PGE) as a retrograde signal revealed that chloramphenicol or lincomycin treatment (i.e., to inhibit PGE specifically) combined with 3% Glc feeding repressed nuclear *LHCB* expression only in wild-type plants, but not in a mutant defective in *pHXK* (Zhang et al., 2010). Hence pHXK appears to work in concert with GENOME UNCOUPLED1 [GUN1, a chloroplast-located pentatricopeptide (PPR) protein] and ABA INSENSITIVE4 (ABI4, a sugar response transcription factor) in order to converge sugar and plastid derived PEG.

We could previously show that in HL-grown *adg1-1/tpt-2* plants the abundance of plastome- encoded PSII core components such as PsbB (CP47), PsbD (D2), PsbA (D1), and PsbC (CP43) were hardly detectable, whereas the abundance of PSII-associated LHCB proteins, as well as the oxygen evolving complex (OEC; PsbO), which are nuclear-encoded, remained unaffected (Schmitz et al., 2012). Considering that the day- and night-path of photoassimilate export from the chloroplast is blocked in the double mutant, this form of photoinhibition would be largely based on a diminished consumption of light reaction-derived reducing power and energy by the Calvin cycle. In contrast, low sugar contents in double mutant plants would keep the expression of nuclear-encoded, sugar-responsive photosynthesis genes, and the abundance of their respective products at a high level. Growth on Suc resulted in a recovery of D1 and D2 abundance and rescued the HCF phenotype (Schmitz et al., 2012). As the data in this report suggest, the sugar-dependent recovery of photosynthesis of *adg1-1/tpt-2* is most likely due to the uptake of soluble sugars into the chloroplasts and their further metabolization in the stroma, which consumes NADPH and ATP delivered by the photosynthetic light reaction and thereby counteracts photoinhibition. As for instance, apoplastic sugars would not be accessible to chloroplasts, a direct correlation between ETR and the overall carbohydrate status, as observed here, can only be brought about, when there are at least equal proportions of all soluble sugars in the various compartments of the mesophyll [i.e., the apoplast (cell wall and vacuole), the cytosol, the mitochondrial matrix, and the chloroplast stroma].

Assuming the presence of uptake systems for various sugars in the inner envelope of the chloroplasts, it is tempting to speculate that chloroplasts might be capable of sensing the carbohydrate status in the surrounding cytosol. In the *adg1-1/tpt-2* double mutant, the uptake of cytosolic sugars into the chloroplast can be indirectly detected by an increase in ETR (compare **Figures 6** and **7**). However, in wild-type plants a similar uptake of sugars into the chloroplasts as in *adg1-1/tpt-2* would not be accessible to detection

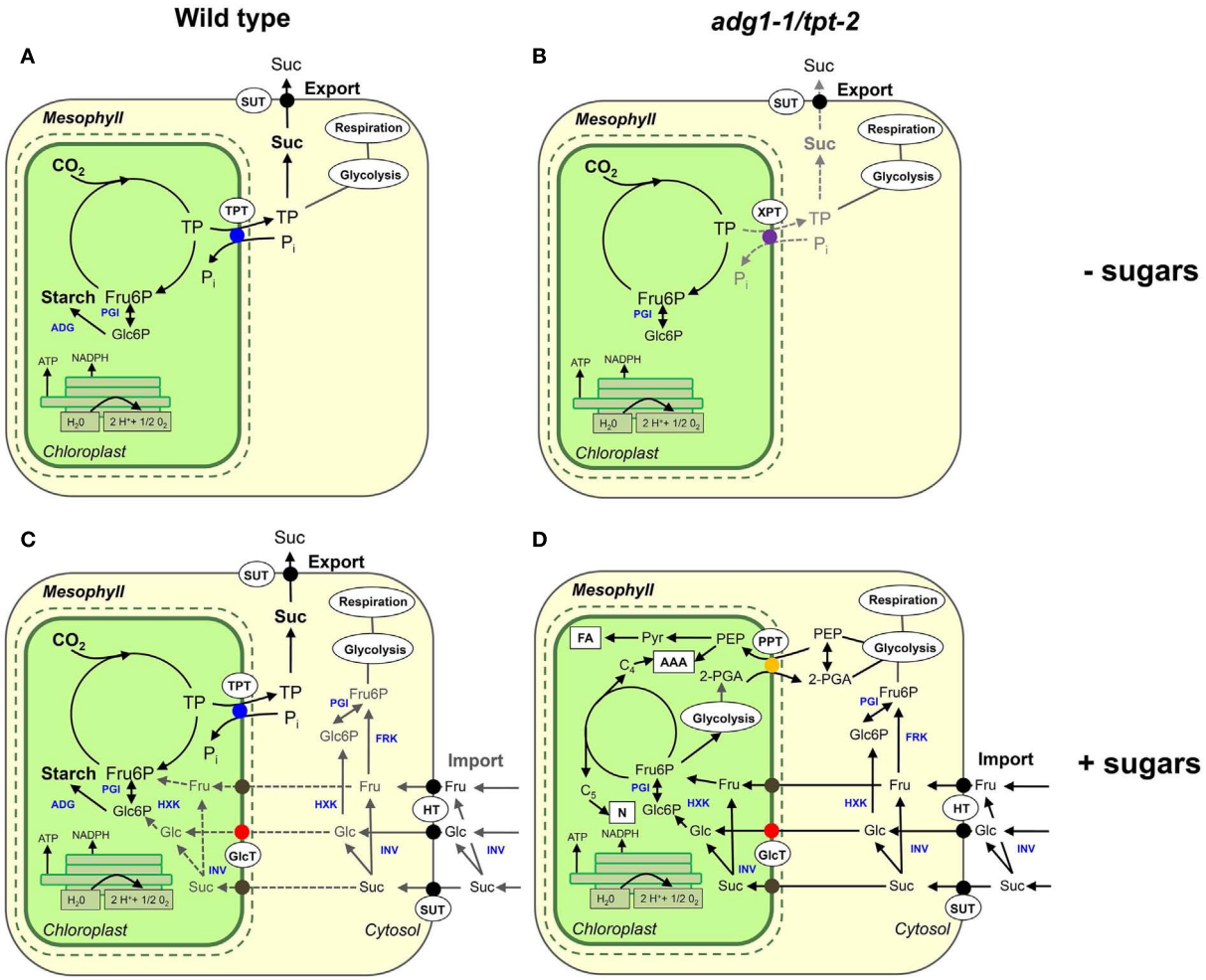

FIGURE 9 | Main metabolic paths of carbon metabolism in wild-type and *adg1-1/tpt-2* mutant plants in the absence or presence of exogenously supplied sugars during the light period. (A) Wild-type plants invest energy and reducing power deriving from the photosynthetic light reaction for CO_2 assimilation and the subsequent export of TP to support sucrose biosynthesis in the cytosol and its export *via* the phloem (day-path of assimilate export from the chloroplast). Simultaneously transitory starch is formed, which is degraded during the dark period (night-path of assimilate export from the chloroplast). **(B)** The *adg1-1/tpt-2* double mutant, defective in the day- and night-path survives because some TP can be exported via the XPT. The low rate of carbon export from the chloroplasts inhibits ETR and leads to photoinhibition under HL-conditions. **(C)** Chloroplasts of wild-type plants grown on exogenously supplied sugars can probably sense increased levels of cytosolic carbohydrates. The main route for NADPH and ATP consumption is still the Calvin cycle and starch biosynthesis. **(D)** According to our hypothesis, in the *adg1-1/tpt-2* double mutant externally supplied sugars are taken up by chloroplasts and used for anabolism within the stroma, probably involving 2-PGA/PEP exchange across the inner envelope membrane *via* a PPT (Fischer et al., 1997). Most likely CO_2 assimilation is reduced to a minimum. Additional abbreviation used here are defined as follows: AAA, aromatic amino acids; ADG, ADPglucose pyrophosphorylase; FA, fatty acids; FRK, fructokinase; GlcT, glucose transporter; HT, hexose transporter; HXK, hexokinase; INV, invertase; N, nucleotides; PGI, phosphoglucose isomerase; PPT, phosphoenolpyruvate/phosphate translocator; SUT, sucrose transporter; TPT, triose phosphate/phosphate translocator; XPT, xylulose 5-phosphate/phosphate translocator. For the sake of clarity, processes taking place in the vacuole or at the tonoplast membrane have been omitted. Please note that the flow of metabolism in **(D)** is purely hypothetical and not necessarily supported by experimental data (e.g., the import of Fru or Suc into the chloroplasts).

on a whole leave scale. ETR in wild-type plants is governed by the Calvin Cycle and the subsequent export of TP as well as the synthesis of transitory starch. Hence, the *adg1-1/tpt-2* double mutant can be considered as a test system for studying the impact of exogenous sugars on metabolism and sugar sensing in the chloroplast.

Provided that the cytosol, including the nucleus, and the chloroplasts are equipped with sugar sensors and signaling pathways that control the expression of plastome- and/or nuclear-encoded photosynthesis genes, both genomes might be regulated independently from each other on the basis of the response toward a varying carbohydrate status in the mesophyll. Such an autonomous sugar-based regulation of both genomes would also synchronize the response of chloroplasts that are at various physiological states.

CONCLUSION

Our data suggest that chloroplast can take up exogenously supplied sugars and use them as an alternative source for anabolic processes when the day- and night-path of photoassimilate export is blocked.

Moreover, in the *adg1-1/tpt-2* system a direct correlation of ETR with the carbohydrate status in the mesophyll exists, which poses the question, whether chloroplasts are capable of sensing the metabolic state in the cytosol. The data in this report scratch only at the surface and need to be supported by future experiments. Combined knockdowns of known plastidial carbohydrate consuming enzymes, such as pHXK and pINV, as well as plastidial sugar transporters (i.e., the glucose transporter) in the *adg1-1/tpt-2* and wild-type background are on the way. Moreover, the overexpression of a hexose-P phosphatase targeted to the chloroplasts should counteract the sugar-dependent rescue of ETR in the *adg1-1/tpt-2* background by a futile cycle at the site of pHXK. Future experiments will also focus on the transient feeding of various sugars at different concentrations and the assessment of their fate in metabolism by ^{13}C-flux measurements, combined with metabolome and transcriptome analyses.

ACKNOWLEDGMENTS

We thank the Deutsche Forschungsgemeinschaft for funding in the frame of the Research Unit 804 and Dr. Iris Finkemeier (LMU Munich) for the provision of the *gin2-1* mutant.

SUPPLEMENTARY MATERIAL

The Supplementary Material for this article can be found online at http://www.frontiersin.org/Plant_Physiology/10.3389/fpls.2012.00265/abstract

Table S1 | Statistical analysis (ANOVA/Tukey–Kramer) of total rosette areas of wild-type and mutant plants grown either an 1/2 MS (control) or on 50 mM each of Glc, Suc, or Fru (see Figure 2). (A) The rosette leaf areas of the individual lines were compared for each treatment (i.e., growth on MS, Glc, Suc, or Fru) and biotype. The biotypes are denoted, a = Col-0; b = *adg1-1/tpt-2*, c = *adg1-1/tpt-2/gpt2-1*, d = *Ler*, e = *gin2-1*, f = *adg1-1/tpt-2/gin2-1*. **(B)** The response of total rosette area toward the individual treatments was compared within each biotype with a = MS, b = Glc, c = Suc, d = Fru. The significance levels of $P < 0.05$ or $P < 0.01$ are indicated by light or dark blue colors.

Table S2 | Statistical analysis (ANOVA/Tukey–Kramer) of photosynthesis parameters (*Fm*, *Fo*, *Fv*/*Fm*) in rosette leaves of wild-type and mutant plants grown either on 1/2 MS (control) or on 50 mM each of Glc, Suc, or Fru (see Figure 3). (A) The photosynthesis parameters of the individual biotypes were compared for each treatment (i.e., growth on MS, Glc, Suc, or Fru) and line. The biotypes are denoted, a = Col-0; b = *adg1-1/tpt-2*, c = *adg1-1/tpt-2/gpt2-1*, d = *Ler*, e = *gin2-1*, f = *adg1-1/tpt-2/gin2-1*. **(B)** The response of photosynthesis parameters toward the individual treatments was compared within each biotype with a = MS; b = Glc, c = Suc, d = Fru. The significance levels of $P < 0.05$ or $P < 0.01$ are indicated by light or dark blue colors.

Table S3 | Statistical analysis (ANOVA/Tukey–Kramer) of maximum ETR after induction of photosynthesis in rosette leaves of wild-type and mutant plants grown either on MS (control) or on 50 mM each of Glc, Suc, or Fru (see Figure 3). (A) The ETR of the individual lines was compared for each treatment (i.e., growth on MS, Glc, Suc, or Fru) and line. The lines are denoted, a = Col-0; b = *adg1-1/tpt-2*, c = *adg1-1/tpt-2/gpt2-1*, d = *Ler*, e = *gin2-1*, f = *adg1-1/tpt-2/gin2-1*. **(B)** The response of ETR toward the individual treatments was compared within each line with a = MS; b = Glc, c = Suc, d = Fru. The significance levels of $P < 0.05$ or $P < 0.01$ are indicated by light or dark blue colors.

Table S4 | Statistical analysis (ANOVA/Tukey–Kramer) of ETR at three different PFDs taken from the light curves measured in rosette leaves of wild-type and mutant plants grown either on MS (control) or on 50 mM each of Glc, Suc, or Fru (see Figure 4). (A) The ETR of the individual lines was compared for each treatment (i.e., growth on MS, Glc, Suc, or Fru) and line. The lines are denoted, a = Col-0; b = *adg1-1/tpt-2*, c = *adg1-1/tpt-2/gpt2-1*, d = *Ler*, e = *gin2-1*, f = *adg1-1/tpt-2/gin2-1*. **(B)** The response of ETR toward the individual treatments was compared within each line with a = MS; b = Glc, c = Suc, d = Fru. The individual PFDs are given in parenthesis. The significance levels of $P < 0.05$ or $P < 0.01$ are indicated by light or dark blue colors.

Table S5 | Statistical analysis (ANOVA/Tukey–Kramer) of sugar and starch contents in rosette leaves of wild-type and mutant plants grown either on 1/2 MS (control) or on 50 mM each of Glc, Suc, or Fru (see Table 2). (A) The sugar and starch contents of the individual biotypes were compared for each treatment (i.e., growth on MS, Glc, Suc, or Fru) and line. The biotypes are denoted, a = Col-0; b = *adg1-1/tpt-2*, c = *adg1-1/tpt-2/gpt2-1*, d = *Ler*, e = *gin2-1*, f = *adg1-1/tpt-2/gin2-1*. **(B)** The response of sugar and starch contents toward the individual treatments was compared within each biotype with a = MS; b = Glc, c = Suc, d = Fru. The significance levels of $P < 0.05$ or $P < 0.01$ are indicated by light or dark blue colors.

Table S6 | Statistical analysis (ANOVA/Tukey–Kramer) of the relative transcript abundance (log2 ratio) of sugar-responsive genes in rosette leaves of wild-type and mutant plants grown either on 1/2 MS (control) or on 50 mM each of Glc, Suc, or Fru (see Figure 8). (A) The log2 ratios (±) the sugars indicated were compared between each biotype. The biotypes are denoted, a = Col-0; b = *Ler*, c = *adg1-1/tpt-2*, d = *gin2-1*, e = *adg1-1/tpt-2/gin2-1*. **(B)** Comparison of log2 ratios between the biotypes grown either on MS, Glc, Suc, or Fru. The biotypes compared with each other are denoted: a = *Ler* vs. Col-0; b = *adg1-1/tpt-2* vs. Col-0, c = *gin2-1* vs. Col-0, d = *adg1-1/tpt-2/gin2-1* vs. Col-0; e = *adg1-1/tpt-2* vs. *Ler*; f = *gin2-1* vs. *Ler*; g = *adg1-1/tpt-2/gin2-1* vs. *Ler*. The significance levels of $P < 0.05$ or $P < 0.01$ are indicated by light or dark blue colors.

REFERENCES

Ahlert, D., Ruf, S., and Bock, R. (2003). Plastid protein synthesis is required for plant development in tobacco. *Proc. Natl. Acad. Sci. U.S.A.* 100, 15730–15735.

Baier, M., and Dietz, K.-J. (2005). Chloroplasts as source and target of cellular redox regulation: a discussion on chloroplast redox signals in the context of plant physiology. *J. Exp. Bot.* 56, 1449–1462.

Baier, M., Ströher, E., and Dietz, K.-J. (2004). The acceptor availability at photosystem I and ABA control nuclear expression of 2-Cys peroxiredoxin-A in *Arabidopsis thaliana*. *Plant Cell Physiol.* 45, 997–1006.

Beck, C. F. (2005). Signaling pathways from the chloroplast to the nucleus. *Planta* 222, 743–756.

Bläsing, O. E., Gibon, Y., Günther, M., Höhne, M., Morcuende, R., Osuna, D., et al. (2005). Sugars and circadian regulation make major contributions to the global regulation of diurnal gene expression in Arabidopsis. *Plant Cell* 17, 3257–3281.

Bräutigam, K., Dietzel, L., Kleine, T., Ströher, E., Wormuth, D., Dietz, K.-J., et al. (2009). Dynamic plastid redox signals integrate gene expression and metabolism to induce distinct metabolic states in photosynthetic acclimation in Arabidopsis. *Plant Cell* 21, 2715–2732.

Chen, J. G., and Jones, A. M. (2004). AtRGS1 function in *Arabidopsis thaliana*. *Meth. Enzymol.* 389, 338–350.

Cho, Y. H., and Yoo, S. D. (2011). Signaling role of fructose mediated by FINS1/FBP in *Arabidopsis thaliana*. *PLoS Genet.* 7, e1001263. doi:10.1371/journal.pgen.1001263

Cho, Y. H., Yoo, S. D., and Sheen, J. (2006). Regulatory functions of nuclear hexokinase1 complex in glucose signaling. *Cell* 127, 579–589.

Cho, Y. H., Yoo, S. D., and Sheen, J. (2007). Glucose signaling through nuclear hexokinase1 complex in Arabidopsis. *Plant Signal. Behav.* 2, 123–124.

Contento, A. L., Kim, S. J., and Bassham, D. C. (2004). Transcriptome profiling of the response of Arabidopsis suspension culture cells to Suc starvation. *Plant Physiol.* 135, 2330–2347.

Dekkers, B. J., Schuurmans, J. A., and Smeekens, S. C. (2008). Interaction between sugar and abscisic acid signaling during early seedling development in Arabidopsis. *Plant Mol. Biol.* 67, 151–167.

Eberhard, S., Finazzi, G., and Wollman, F. A. (2008). The dynamics of photosynthesis. *Annu. Rev. Genet.* 42, 463–515.

Eicks, M., Maurino, V., Knappe, S., Flügge, U. I., and Fischer, K. (2002). The plastidic pentose phosphate translocator represents a link between the cytosolic and the plastidic pentose phosphate pathways in plants. *Plant Physiol.* 128, 512–522.

Fettke, J., Nunes-Nesi, A., Alpers, J., Szkop, M., Fernie, A. R., and Steup, M. (2008). Alterations in cytosolic glucose phosphate metabolism affect structural features and biochemical properties of starch-related heteroglycans. *Plant Physiol.* 148, 1614–1629.

Fischer, K., Kammerer, B., Gutensohn, M., Arbinger, B., Weber, A., Häusler, R. E., et al. (1997). A new class of plastidic phosphate translocators: a putative link between primary and secondary metabolism by the phosphoenolpyruvate/phosphate antiporter. *Plant Cell* 9, 453–462.

Fliege, R., Flügge, U. I., Werdan, K., and Heldt, H. W. (1978). Specific transport of inorganic phosphate, 3-phosphoglycerate and triosephosphates across the inner membrane of the envelope in spinach chloroplasts. *Biochim. Biophys. Acta* 502, 232–247.

Foyer, C. H., and Noctor, G. (2009). Redox regulation in photosynthetic organisms: signaling, acclimation, and practical implications. *Antioxid. Redox Signal.* 11, 861–905.

Furumoto, T., Yamaguchi, T., Ohshima-Ichie, Y., Nakamura, M., Tsuchida-Iwata, Y., Shimamura, M., et al. (2011). A plastidial sodium-dependent pyruvate transporter. *Nature* 476, 472–475.

Genty, B., Briantais, J. M., and Baker, N. R. (1989). The relationship between the quantum yield of photosynthetic transport and quenching of chlorophyll fluorescence. *Biochim. Biophys. Acta* 990, 87–92.

Gibson, S. I. (2005). Control of plant development and gene expression by sugar signaling. *Curr. Opin. Plant Biol.* 8, 93–102.

Giege, P., Heazlewood, J. L., Roessner-Tunali, U., Millar, A. H., Fernie, A. R., Leaver, C. J., et al. (2003). Enzymes of glycolysis are functionally associated with the mitochondrion in Arabidopsis cells. *Plant Cell* 15, 2140–2151.

Haferkamp, I., Fernie, A. R., and Neuhaus, H. E. (2011). Adenine nucleotide transport in plants: much more than a mitochondrial issue. *Trends Plant Sci.* 16, 507–515.

Halford, N. G., and Hey, S. J. (2009). Snf1-related protein kinases (SnRKs) act within an intricate network that links metabolic and stress signaling in plants. *Biochem. J.* 419, 247–259.

Häusler, R. E., Geimer, S., Kunz, H. H., Schmitz, J., Dörmann, P., Bell, K., et al. (2009). Chlororespiration and grana hyperstacking: how an Arabidopsis double mutant can survive despite defects in starch biosynthesis and daily carbon export from chloroplasts. *Plant Physiol.* 149, 515–533.

Häusler, R. E., Schlieben, N. H., Schulz, B., and Flügge, U. I. (1998). Compensation of decreased triosephosphate/phosphate translocator activity by accelerated starch turnover and glucose transport in transgenic tobacco. *Planta* 204, 366–376.

Herrmann, K. M. (1995). The shikimate pathway: early steps in the biosynthesis of aromatic compounds. *Plant Cell* 7, 907–919.

Herrmann, K. M., and Weaver, L. M. (1999). The shikimate pathway. *Annu. Rev. Plant Physiol. Plant Mol. Biol.* 50, 473–503.

Ishizaki, K., Larson, T. R., Schauer, N., Fernie, A. R., Graham, I. A., and Leaver, C. J. (2005). The critical role of Arabidopsis electron-transfer flavoprotein: ubiquinone oxidoreductase during dark-induced starvation. *Plant Cell* 17, 2587–2600.

Jang, J. C., León, P., Zhou, L., and Sheen, J. (1997). Hexokinase as a sugar sensor in higher plants. *Plant Cell* 9, 5–19.

Jang, J. C., and Sheen, J. (1994). Sugar sensing in higher plants. *Plant Cell* 6, 1665–1679.

Karve, R., Lauria, M., Virnig, A., Xia, X., Rauh, B. L., and Moore, B. (2010). Evolutionary lineages and functional diversification of plant hexokinases. *Mol. Plant* 3, 334–346.

Kim, C., Meskauskiene, R., Apel, K., and Laloi, C. (2008). No single way to understand singlet oxygen signaling in plants. *EMBO Rep.* 9, 435–439.

Kingston-Smith, A. H., Walker, R. P., and Pollock, C. J. (1999). Invertase in leaves: conundrum or control point? *J. Exp. Bot.* 50, 735–743.

Kleine, T., Voigt, C., and Leister, D. (2009). Plastid signaling to the nucleus: messengers still lost in the mists? *Trends Genet.* 25, 185–192.

Knappe, S., Löttgert, T., Schneider, A., Voll, L., Flügge, U. I., and Fischer, K. (2003). Characterization of two functional phosphoenolpyruvate/phosphate translocator (PPT) genes in Arabidopsis-AtPPT1 may be involved in the provision of signals for correct mesophyll development. *Plant J.* 36, 411–420.

Koussevitzky, S., Nott, A., Mockler, T. C., Hong, F., Sachetto-Martins, G., Surpin, M., et al. (2007). Signals from chloroplasts converge to regulate nuclear gene expression. *Science* 316, 715–719.

Kunz, H. H., Häusler, R. E., Fettke, J., Herbst, K., Niewiedomski, P., Gierth, M., et al. (2010). The role of plastidial glucose6-phosphate/phosphate translocators in vegetative tissues of *Arabidopsis thaliana* mutants impaired in starch biosynthesis. *Plant Biol.* 12(Suppl. 1), 115–128.

Leister, D. (2003). Chloroplast research in the genomic age. *Trends Genet.* 19, 47–56.

León, P., and Sheen, J. (2003). Sugar and hormone connections. *Trends Plant Sci.* 8, 110–116.

Li, Y., Li, L. L., Fan, R. C., Peng, C. C., Sun, H. L., Zhu, S. Y., et al. (2012). Arabidopsis sucrose transporter SUT4 interacts with cytochrome b5-2 to regulate seed germination in response to sucrose and glucose. *Mol. Plant* 5, 1029–1041.

Lichtenthaler, H. K. (1999). The 1-deoxy-D-xylulose-5-phosphate pathway of isoprenoid biosynthesis in plants. *Annu. Rev. Plant Physiol. Plant Mol. Biol.* 50, 47–65.

Lin, T. P., Caspar, T., Somerville, C., and Preiss, J. (1988). Isolation and characterization of a starchless mutant of *Arabidopsis thaliana* (L.) Heynh lacking ADPglucose pyrophosphorylase activity. *Plant Physiol.* 86, 1131–1135.

Logemann, J., Schell, J., and Willmitzer, L. (1987). Improved method for the isolation of RNA from plant tissues. *Anal. Biochem.* 163, 16–20.

Lu, Y., and Sharkey, T. D. (2004). The role of amylomaltase in maltose metabolism in the cytosol of photosynthetic cells. *Planta* 218, 466–473.

Lu, Y., and Sharkey, T. D. (2006). The importance of maltose in transitory starch breakdown. *Plant Cell Environ.* 29, 353–366.

Ludbrook, J. (1998). Multiple comparison procedures updated. *Clin. Exp. Pharmacol. Physiol.* 25, 1032–1037.

Miller, G., Suzuki, N., Ciftci-Yilmaz, S., and Mittler, R. (2009). Reactive oxygen species homeostasis and signaling during drought and salinity stresses. *Plant Cell Environ.* 33, 453–467.

Mita, S., Murano, N., Akaike, M., and Nakamura, K. (1997). Mutants of *Arabidopsis thaliana* with pleiotropic effects on the expression of the gene for β-amylase and on the accumulation of anthocyanin that are inducible by sugars. *Plant J.* 11, 841–851.

Moore, B., Zhou, L., Rolland, F., Hall, Q., Cheng, W. H., Liu, Y. X., et al. (2003). Role of the Arabidopsis glucose sensor HXK1 in nutrient, light, and hormonal signaling. *Science* 300, 332–336.

Niewiadomski, P., Knappe, S., Geimer, S., Fischer, K., Schulz, B., Unte, U. S., et al. (2005). The Arabidopsis plastidic glucose 6-phosphate/phosphate translocator GPT1 is essential for pollen maturation and embryo sac development. *Plant Cell* 17, 760–775.

Niittylä, T., Messerli, G., Trevisan, M., Chen, J., Smith, A. M., and Zeeman, S. C. (2004). A previously unknown maltose transporter essential for starch degradation in leaves. *Science* 303, 87–89.

Ohlrogge, J. B., and Jaworski, J. G. (1997). Regulation of fatty acid synthesis. *Annu. Rev. Plant Physiol. Plant Mol. Biol.* 48, 109–136.

Ohlrogge, J. B., Kuhn, D. N., and Stumpf, P. K. (1979). Subcellular localization of acyl carrier protein in leaf protoplasts of Spinacia-oleracea. *Proc. Natl. Acad. Sci. U.S.A.* 76, 1194–1198.

Pego, J. V., and Smeekens, S. C. (2000). Plant fructokinases: a sweet family get-together. *Trends Plant Sci.* 5, 531–516.

Pfannschmidt, T., Nilsson, A., and Allen, J. F. (1999). Photosynthetic control of chloroplast gene expression. *Nature* 397, 625–628.

Prabhakar, V., Löttgert, T., Geimer, S., Dörmann, P., Krüger, S., Vijayakumar, V., et al. (2010). Phosphoenolpyruvate provision to plastids is essential for gametophyte and sporophyte development in *Arabidopsis thaliana*. *Plant Cell* 22, 2594–2617.

Prabhakar, V., Löttgert, T., Gigolashvili, T., Bell, K., Flügge, U. I., and Häusler, R. E. (2009). Molecular and functional characterization of the plastid-localized phosphoenolpyruvate enolase (ENO1) from *Arabidopsis thaliana*. *FEBS Lett.* 583, 983–991.

Price, J., Laxmi, A., St Martin, S. K., and Jang, J. C. (2004). Global transcription profiling reveals multiple sugar signal transduction mechanisms in Arabidopsis. *Plant Cell* 16, 2128–2150.

Ramakers, C., Ruijter, J. M., Deprez, R. H. L., and Moorman, A. F. M. (2003). Assumption-free analysis of quantitative real-time polymerase chain

reaction (PCR) data. *Neurosci. Lett.* 339, 62–66.

Rolland, F., Baena-Gonzalez, E., and Sheen, J. (2006). Sugar sensing and signaling in plants: conserved and novel mechanisms. *Annu. Rev. Plant Biol.* 57, 675–709.

Rolland, F., Moore, B., and Sheen, J. (2002). Sugar sensing and signaling in plants. *Plant Cell* 14(Suppl.), 185–205.

Rook, F., Gerrits, N., Kortstee, A., van Kampen, M., Borrias, M., Weisbeek, P., et al. (1998). Sucrose-specific signaling represses translation of the Arabidopsis ATB2 bZIP transcription factor gene. *Plant J.* 15, 253–263.

Schäfer, G., Heber, U., and Heldt, H. W. (1977). Glucose transport into spinach chloroplasts. *Plant Physiol.* 60, 286–289.

Scheibe, R., Backhausen, J. E., and Emmerlich, V. (2005). Strategies to maintain redox homeostasis during photosynthesis under changing conditions. *J. Exp. Bot.* 56, 1481–1489.

Schmid, J., and Amrhein, N. (1995). Molecular organization of the shikimate pathway in higher plants. *Phytochemistry* 39, 737–749.

Schmitz, J., Schöttler, M. A., Krueger, S., Geimer, S., Schneider, A., Kleine, T., et al. (2012). Defects in leaf carbohydrate metabolism compromise acclimation to high light and lead to a high chlorophyll fluorescence phenotype in *Arabidopsis thaliana*. *BMC Plant Biol.* 12, 8. doi:10.1186/1471-2229-12-8

Schneider, A., Häusler, R. E., Kolukisaoglu, U., Kunze, R., van der Graaff, E., Schwacke, R., et al. (2002). An *Arabidopsis thaliana* knock-out mutant of the chloroplast triose phosphate/phosphate translocator is severely compromised only when starch synthesis, but not starch mobilisation is abolished. *Plant J.* 32, 685–699.

Schreiber, U., Schliwa, U., and Bilger, W. (1986). Continuous recording of photochemical and non-photochemical chlorophyll fluorescence quenching with a new type of modulation fluorometer. *Photosyn. Res.* 10, 51–62.

Schulze-Siebert, D., Heineke, D., Scharf, H., and Schultz, G. (1984). Pyruvate-derived amino-acids in spinach-chloroplasts – synthesis and regulation during photosynthetic carbon metabolism. *Plant Physiol.* 76, 465–471.

Smeekens, S. (1998). Sugar regulation of gene expression in plants. *Curr. Opin. Plant Biol.* 1, 230–234.

Smeekens, S. (2000). Sugar-induced signal transduction in plants. *Annu. Rev. Plant Physiol. Plant Mol. Biol.* 51, 49–81.

Stitt, M., Lilley, R. M. C., Gerhardt, R., and Heldt, H. (1989). Determination of metabolite levels in specific cells and subcellular compartments of plant leaves. *Meth. Enzymol.* 174, 518–552.

Streatfield, S. J., Weber, A., Kinsman, E. A., Häusler, R. E., Li, J., Post-Beittenmiller, D., et al. (1999). The phosphoenolpyruvate/phosphate translocator is required for phenolic metabolism, palisade cell development, and plastid-dependent nuclear gene expression. *Plant Cell* 11, 1609–1622.

Surpin, M., Larkin, R., and Chory, J. (2002). Signal transduction between the chloroplast and the nucleus. *Plant Cell* 14, 327–338.

Taniguchi, M., Nagasaki, J., and Tomita, Y. (2005). Does the malate valve prevent chloroplasts from excessive reducing power? *Plant Cell Physiol.* 46, 6–16.

Thimm, O., Bläsing, O., Gibon, Y., Nagel, A., Meyer, S., Krüger, P., et al. (2004). MAPMAN: a user-driven tool to display genomics data sets onto diagrams of metabolic pathways and other biological processes. *Plant J.* 37, 914–939.

Triantaphylidès, C., and Havaux, M. (2009). Singlet oxygen in plants: production, detoxification and signaling. *Trends Plant Sci.* 14, 219–228.

Vargas, W. A., Pontis, H. G., and Salerno, G. L. (2008). New insights on sucrose metabolism: evidence for an active A/N Inv in chloroplasts uncovers a novel component of the intracellular carbon trafficking. *Planta* 227, 795–807.

Vaughn, M. W., Harrington, G. N., and Bush, D. R. (2002). Sucrose-mediated transcriptional regulation of sucrose symporter activity in the phloem. *Proc. Natl. Acad. Sci. U.S.A.* 99, 10876–10880.

Walters, R. G., Ibrahim, D. G., Horton, P., and Kruger, N. J. (2004). A mutant of Arabidopsis lacking the triose-phosphate/phosphate translocator reveals metabolic regulation of starch breakdown in the light. *Plant Physiol.* 135, 891–906.

Weber, A., Servaites, J. C., Geiger, D. R., Kofler, H., Hille, D., Gröner, F., et al. (2000). Identification, purification and molecular cloning of a putative plastidic glucose translocator. *Plant Cell* 12, 787–801.

Weber, A. P. M., and Linka, N. (2011). Connecting the plastid: transporters of the plastid envelope and their role in linking plastidial with cytosolic metabolism. *Annu. Rev. Plant Biol.* 62, 53–77.

Weise, S. E., Weber, A. P., and Sharkey, T. D. (2004). Maltose is the major form of carbon exported from the chloroplast at night. *Planta* 218, 474–482.

Wiese, A., Gröner, F., Sonnewald, U., Deppner, H., Lerchl, J., Hebbeker, U., et al. (1999). Spinach hexokinase I is located in the outer envelope membrane of plastids. *FEBS Lett.* 461, 13–18.

Winter, D., Vinegar, B., Nahal, H., Ammar, R., Wilson, G. V., and Provart, N. J. (2007). An "Electronic Fluorescent Pictograph" browser for exploring and analyzing large-scale biological data sets. *PLoS ONE* 2, e718. doi:10.1371/journal.pone.0000718

Xiao, W., Sheen, J., and Jang, J. C. (2000). The role of hexokinase in plant sugar signal transduction and growth and development. *Plant Mol. Biol.* 44, 451–461.

Yanagisawa, S., Yoo, S. D., and Sheen, J. (2003). Differential regulation of EIN3 stability by glucose and ethylene signaling in plants. *Nature* 425, 521–525.

Yu, S. M. (1999). Cellular and genetic responses of plants to sugar starvation. *Plant Physiol.* 121, 687–693.

Zeeman, S. C., Kossmann, J., and Smith, A. M. (2010). Starch: its metabolism, evolution, and biotechnological modification in plants. *Annu. Rev. Plant Biol.* 61, 209–234.

Zhang, Z. W., Yuan, S., Xu, F., Yang, H., Zhang, N. H., Cheng, J., et al. (2010). The plastid hexokinase pHXK: a node of convergence for sugar and plastid signals in Arabidopsis. *FEBS Lett.* 584, 3573–3579.

Zhou, L., Jang, J. C., Jones, T. L., and Sheen, J. (1998). Glucose and ethylene signal transduction crosstalk revealed by an Arabidopsis glucose-insensitive mutant. *Proc. Natl. Acad. Sci. U.S.A.* 95, 10294–10299.

Ziolkowski, P. A., Koczyk, G., Galganski, L., and Sadowski, J. (2009). Genome sequence comparison of Col and Ler lines reveals the dynamic nature of Arabidopsis chromosomes. *Nucleic Acids Res.* 37, 3189–3201.

Conflict of Interest Statement: The authors declare that the research was conducted in the absence of any commercial or financial relationships that could be construed as a potential conflict of interest.

Received: 17 September 2012; accepted: 12 November 2012; published online: 30 November 2012.

Citation: Heinrichs L, Schmitz J, Flügge U-I and Häusler RE (2012) The mysterious rescue of adg1-1/tpt-2 – an Arabidopsis thaliana double mutant impaired in acclimation to high light – by exogenously supplied sugars. Front. Plant Sci. ***3****:265. doi: 10.3389/fpls.2012.00265*

This article was submitted to Frontiers in Plant Physiology, a specialty of Frontiers in Plant Science.

Copyright © 2012 Heinrichs, Schmitz, Flügge and Häusler. This is an open-access article distributed under the terms of the Creative Commons Attribution License, which permits use, distribution and reproduction in other forums, provided the original authors and source are credited and subject to any copyright notices concerning any third-party graphics etc.

frontiers in
PLANT SCIENCE

ORIGINAL RESEARCH ARTICLE
published: 09 November 2012
doi: 10.3389/fpls.2012.00247

The membrane-tethered transcription factor ANAC089 serves as redox-dependent suppressor of stromal ascorbate peroxidase gene expression

Peter Klein, Thorsten Seidel, Benedikt Stöcker and Karl-Josef Dietz*

Biochemistry and Physiology of Plants, W5-134, Faculty of Biology and CeBiTec, Bielefeld University, Bielefeld, Germany

Edited by:
Tatjana Kleine, Ludwig-Maximilians-Universität München, Germany

Reviewed by:
Wataru Sakamoto, Okayama University, Japan
Stanislaw Karpinski, Warsaw University of Life Sciences, Poland

***Correspondence:**
Karl-Josef Dietz, Biochemistry and Physiology of Plants, W5-134, Faculty of Biology and CeBiTec, Bielefeld University, 33501 Bielefeld, Germany.
e-mail: karl-josef.dietz@uni-bielefeld.de

The stromal ascorbate peroxidase (sAPX) functions as central element of the chloroplast antioxidant defense system. Its expression is under retrograde control of chloroplast signals including redox- and reactive oxygen species-linked cues. The sAPX promoter of *Arabidopsis thaliana* was dissected in transient reporter assays using mesophyll protoplasts. The study revealed regulatory elements up to −1868 upstream of the start codon. By yeast-one-hybrid screening, the transcription factor ANAC089 was identified to bind to the promoter fragment 2 (−1262 to −1646 bp upstream of translational initiation). Upon mutation of the *cis*-acting element CACG, binding of ANAC089 was abolished. Expression of a fused fluorescent protein version and comparison with known endomembrane markers localized ANAC089 to the *trans*-Golgi network and the ER. The transcription factor was released upon treatment with reducing agents and targeted to the nucleus. Transactivation assays using wild type and mutated versions of the promoter showed a partial suppression of reporter expression. The data indicate that ANAC089 functions in a negative retrograde loop, lowering sAPX expression if the cell encounters a highly reducing condition. This conclusion was supported by reciprocal transcript accumulation of ANAC089 and sAPX during acclimation to low, normal, and high light conditions.

Keywords: ascorbate peroxidase, gene expression, redox regulation, retrograde signaling, transcription factor

INTRODUCTION

Photosynthetic metabolism involves light driven electron transfer reactions, production of metabolic intermediates with high reducing potential and the generation of reactive oxygen species (ROS). The photosynthesizing chloroplast is equipped with an intricate redox sensory system, a multilayered antioxidant defense and diverse repair mechanisms to minimize ROS-dependent damage. On the one hand, appropriate sensing allows for using redox and ROS information to adjust photosynthetic metabolism and tune gene expression in the plastids but also in the nuclear genome by retrograde signal transfer from the chloroplast to the nucleus (Baier and Dietz, 2005). Pogson et al. (2008) distinguished retrograde signaling in developmental and operational control. Operational control coordinates nuclear gene expression with the actual needs of photosynthetic metabolism. Analyses of transcriptional dynamics in response to environmental or pharmacological perturbations and elaborated mutant screenings have allowed researchers to pinpoint to signaling cues triggering retrograde signaling in operational control (Leister, 2012). Accumulation of singlet oxygen, changes in redox state of intersystem electron transport chain, redox state of metabolites or proteins as for example thioredoxin downstream of photosystem I, intermediates of chlorophyll synthesis and hormone precursors such as for abscisic acid are linked to specific changes in transcript abundance of nuclear encoded chloroplast proteins (Pfannschmidt, 2010). While ROS generation in the illuminated chloroplast is mostly governed by primary light reactions and counteracted by mechanisms that quench excess excitation energy (Li et al., 2009), ROS are decomposed by high capacity antioxidant systems (Asada, 1999; Dietz et al., 2006).

Superoxide is dismutated by CuZn- and Fe-SOD, and hydrogen peroxide decomposed by thylakoid-bound and stromal ascorbate peroxidase (tAPX, sAPX; Nakano and Asada, 1981) or thiol-dependent peroxidases (Dietz, 2011). It has been estimated that thiol-dependent peroxidase activity reaches about 40% and ascorbate-dependent activity about 60% of total hydrogen peroxide decomposition activity in chloroplasts (Dietz et al., 2006). Both systems are prone to inhibition and thus are subjected to turnover, sAPX and tAPX in particular if ascorbate concentrations are low (Miyake and Asada, 1996). Their expression in the nucleus must be under retrograde control to cope with demand for antioxidant capacity (Oelze et al., 2012).

sAPX and tAPX are encoded by separate nuclear genes in *Arabidopsis thaliana*. Complete deletion of sAPX and tAPX is compensated in *A. thaliana* under regular growth conditions (Kangasjärvi et al., 2008). Symptoms of oxidative stress in these plants develop in stressful environment and in particular during early seedling development. *sAPX* and *tAPX* transcript levels

Abbreviations: 3-AT, 3-amino-1,2,4-triazol; DTT, dithiothreitol; CFP, (enhanced) cyan fluorescent protein; EMSA, electrophoretic mobility shift assay; FRET, Förster/fluorescence resonance energy transfer; MTTF, membrane-tethered transcription factors; ROS, reactive oxygen species; sAPX, stromal ascorbate peroxidase; SOD, superoxide dismutase; TF, transcription factor; YFP, (enhanced) yellow fluorescent protein.

are regulated in dependence on developmental state of the leaves (Pena-Ahumada et al., 2006) and environmental cues, such as light intensity (Oelze et al., 2012). After transfer of low or normal light acclimated *A. thaliana* to 100- or 10-fold higher light intensity, respectively, *sAPX*-mRNA levels start to increase after 30 min and reach a maximum at 3–6 h after transfer to high light (Oelze et al., 2012). In contrast to transcript regulation, sAPX and tAPX protein levels respond much less.

Signaling pathways often innervate transcription factors that modulate target gene expression in response to environmental stimuli (Golldack et al., 2011). However despite the importance of chloroplast ascorbate peroxidases in antioxidant defense, transcription factors involved in their regulation have not been described. Based on transcript regulation it can be assumed, that redox and ROS signals might be involved in regulating *tapx* and *sapx* gene expression. Transcriptome analyses have differentiated $O_2^{\cdot-}$/H_2O_2-dependent regulation from singlet oxygen-dependent regulation (op den Camp et al., 2003). *sAPX* was not among the significantly regulated transcripts responding to methylviologen or to illumination of protochlorophyllide accumulating *flu* mutants (op den Camp et al., 2003). Compensatory retrograde regulation is apparent from knock down lines of *A. thaliana* deficient in the alternative H_2O_2-detoxifying 2-Cys peroxiredoxin (Baier et al., 2000) where *sAPX* and *tAPX* transcripts were up-regulated, and in double knock out of tAPX and sAPX (Kangasjärvi et al., 2008) where 2-Cys peroxiredoxin protein levels were increased. Apparently there is a delicate feedback from the chloroplast antioxidant defense system to nuclear gene expression.

The aim of the study was to approach a better and mechanistic understanding of *sapx* gene expression regulation. The promoter was analyzed for regulatory regions. The transcription factor ANAC089 identified in a yeast-one-hybrid (Y1H) screening was subjected to a more detailed inspection for binding site and regulatory properties. The specific promoter region *sapx2*-1 proved to be responsive to oxidative versus reductive cues by ANAC089. The obtained data indicate a role of ANAC089 as repressor of sapx gene activity under highly reducing conditions where the need for sAPX expression or sAPX turnover might be low.

MATERIALS AND METHODS

PLANT GROWTH AND LIGHT TREATMENT

Arabidopsis thaliana was grown in a growth chamber at a photoperiod of 10 h with 80 µmol quanta m^{-2} s^{-1} and 21°C, and a dark phase of 14 h at 18°C, both at 50% relative humidity. The pots contained Spezialsubstrat (Stender AG, Schermbeck, Germany), Osmocote Start as fertilizer (Scotts Australia PTY Ltd, Bella Vista, Australia), and one tablet of Lizetan (Bayer, Leverkusen, Germany) per L soil. Three week old plants were either transferred to 8 µmol quanta m^{-2} s^{-1} (low light, L-light) or kept at 80 µmol quanta m^{-2} s^{-1} (normal light, N-light) for another 10 days. Then the 4.5 week old plants were exposed to high light (H-light, 800 µmol quanta m^{-2} s^{-1}) 1 h after onset of light (9 am). Control plants were kept in L- or N-light. At 3 p.m. complete rosettes of 4–12 plants from the four treatments were harvested, frozen in liquid nitrogen, and stored at −80°C until further processing.

TRANSCRIPT ANALYSIS

RNA isolation, cDNA synthesis, and semi-quantitative RT-PCR analysis were performed according to Wormuth et al. (2006) using primers as described in **Table 1**. Equal loading of cDNA was adjusted with *ACTIN2* amplificate. Annealing temperatures and amplification cycle numbers were optimized for each target transcript (Oelze et al., 2012).

GENERATION OF YEAST-ONE-HYBRID LIBRARY AND SCREENING

cDNA synthesis, construction of Y1H library and screening were performed using the Clontech Matchmaker system as described in Klein and Dietz (2010). To achieve a wide coverage of conditionally expressed transcripts, RNA was isolated from a set of differentially stress-treated *A. thaliana* seedlings. The treatments were as follows: (1) Control: 1 h at 120 µmol quanta m^{-2} s^{-1}; (2) combined oxidative and high light stress: 1 h at 5 mM H_2O_2 and 1140 µmol quanta m^{-2} s^{-1}; (3) drought stress and high light: 1 h drought and 1140 µmol quanta m^{-2} s^{-1}; (4) heat stress: 1 h at 40°C and 84 µmol quanta m^{-2} s^{-1}; (5) cold and darkness: 1 h at 4°C in darkness; (6) cold in light: 1 h at 4°C and 32 µmol quanta m^{-2} s^{-1}; (7) UV-illumination: 3 × UV for 10 s each with regeneration for 30 min at 120 µmol quanta m^{-2} s^{-1}; (8) dark-light transition: 1 h darkness followed by 30 min 120 µmol quanta m^{-2} s^{-1}; (9) high light: 1 h at about 1100 µmol quanta m^{-2} s^{-1}; and (10) low salt: 1 h at 5 mM NaCl and 1100 µmol quanta m^{-2} s^{-1}. The bait DNA sequence was cloned into the pHis2 vector using the *Sma*I and *Sac*I endonucleases, while the pGADT7-Rec2 was used as the prey vector. Both vectors were cotransformed into yeast strain Y187. Interaction between fusion protein and DNA-sequence was scored on SD medium supplemented with the appropriate amino acids, i.e., SD/-His/-Leu/-Trp. To suppress leaky His3 activity, 3-amino-1,2,4-triazol (3-AT) was added, for the promoter fragments

Table 1 | Oligonucleotide primers used for (a) cloning of the sAPX promotor fragments into the p35SYFP vector using *Bam*HI and *Nco*I restriction sites and (b) transcript analysis.

	Sequence
Promoter fragment	
sAPX-1-for	5′-AAAAAGGATCCTTTCGGACCTGGAGAG-3′
sAPX-2-for	5′-AAAAAGGATCCGCACGTCTAGTGAAAGATCC-3′
sAPX-2-mut-for	5′-AAAAAGGATCCGAAAATCTAGTGAAAGATCC-3′
sAPX-3-for	5′-AAAAAGGATCCTGTCAACCAAGTCGCCTTG-3′
sAPX-5-for	5′-AAAAAGGATCCCCCGTCACCATTACCATC-3′
sAPX-6-for	5′-AAAAAGGATCCCTCTATGGACTTTATTGG-3′
sAPX-rev	5′-AAAAACCCATGGTTCTGAGGGGTATAATAGTAAT-3′
Transcript analysis	
ANAC089-for	5′-ATGGACACGAAGGCGGTT-3′
ANAC089-DB-rev	5′-CAATCAGACGGGCTCCCTG-3′
sAPX-for	5′-ATGCTGCTAACGCTGGTCTT-3′
sAPX-rev	5′-CCTAACGTGTGAGCACCAGA-3′
Actin-2-for (At3g18780)	5′-TTGGTAGGCCAAGACATCAT-3′
Actin-2-rev	5′-GGAGCCTCGGTAAGAAGAAC-3′

sapx2-1 and *sapx2-1$_{mut}$*, the 3-AT concentration was adjusted to 15 mM.

AMPLIFICATION OF *sapx* PROMOTER FRAGMENTS

sapx (At4g08390) promoter fragments were amplified by polymerase chain reaction using the primers listed in **Table 1**. Amplification products were separated by agarose gel electrophoresis, eluted and used for cloning. For transient reporter assays they were fused to EYFP as described in Shaikhali et al. (2008). As reference construct, CFP was fused downstream of the p35S-promoter (Shaikhali et al., 2008). Correctness of constructs was confirmed by DNA sequencing (MWG Biotech, Eberswalde or CeBiTec, Bielefeld, Germany).

RECOMBINANT PRODUCTION OF ANAC089 PROTEIN AND ELECTROPHORETIC MOBILITY SHIFT ASSAY

The *anac089* coding sequence was amplified using forward (ANAC089-for: 5′-AAAAAAGGATCCATGGACACGAAGGCGGTTG-3′) and reverse primers (ANAC089-rev: 5′-AAAAACTCGAGTTCTAGATAAAACAACATTG-3′) and directionally cloned into pET28a vector using *Bam*HI and *Xho*I restriction sites. The vector was transformed into BL21 (DE3) pLysS *Escherichia coli* cells. Following inoculation with preculture the main culture was grown to OD = 0.6, induced with 400 μM isopropyl-β-D-thiogalactopyranoside and further incubated for 4 h. Cells were sedimented, frozen, and thawn, resuspended in lysis buffer (50 mM Na-phosphate buffer, pH 8, 300 mM NaCl, 10 mM imidazole, 1 mg/ml lysozyme), sonified, incubated and cell debris sedimented by centrifugation. The His_6-tagged ANAC089 protein was purified by Ni-nitrilotriacetic acid chromatography (Qiagen, Hilden, Germany). Following washing of loosely bound proteins, ANAC089 protein was eluted with elution buffer (50 mM Na-phosphate buffer, pH 8, 300 mM NaCl, 250 mM imidazole). Recombinant protein was dialyzed against 40 mM K-phosphate buffer, pH 7, using dialysis tubing with 10 kDa cutoff. Protein was quantified with BioRad reagent (BioRad Laboratories, München, Germany) with bovine serum albumin as standard. An electrophoretic mobility shift assay (EMSA) was performed with the DIG Gel Shift Kit (2nd generation, Roche, Mannheim, Germany): target DNA was the sAPX promoter fragment 2-1 at an amount of 8 ng per lane. As indicated unlabeled competitor DNA was added at 2 μg concentration and ANAC089 protein at 100 ng. An additional label free EMSA was performed as well. Here recombinant ANAC089 protein equivalent to 360 μM concentration was incubated with 25 ng promotor fragment *sapx-2* (or *sapx-2$_{mut}$*) in 20 μl EMSA buffer (100 mM HEPES, pH 7.5, 500 mM KCl, 25% glycerol, 5 mM dithiothreitol) at 22°C for 30 min. The assay mix was subsequently loaded on 4% agarose gels and the DNA separated by electrophoresis at 80 V. DNA was visualized by ethidium bromide staining and documented.

CONSTRUCTS FOR FLUORESCENCE MICROSCOPY

ANAC089 was fused to fluorescent proteins for various cell imaging experiments. In each case the enhanced variants of CFP and YFP (ECFP, EYFP) were used for the construction of the vectors. In the following, the short versions CFP and YFP are used in the text. In the transactivation analysis of **Figure 7**, mCherry was fused to ANAC089 (Seidel et al., 2010). The constructs were p35S:CFP:ANAC089, p35S:YFP:ANAC089, p35S:ANAC089:CFP, p35S:ANAC089:YFP, p35S:YFP:ANAC089:CFP, and p35S:mCherry:ANAC089. The cloning strategy included the insertion of the *anac089* gene upstream of the fluorophore gene into the p35S:CFP-NOST and the p35S:YFP-NOST vector using the ANAC089-for (5′-AAAAAAGGATCCAATGGACACGAAGGCGGTTG-3′) and ANAC089-rev (5′-AAAAAACCGGTTCTAGATAAAACAACATTGC-3′) primers for gene amplification. The *anac089* gene was then fused to the vector utilizing the *Bam*HI and *Age*I endonucleases. The p35S:CFP:ANAC089 and p35S:YFP:ANAC089 constructs were created using the ANAC089-for (5′-AAAAAGCGGCCGCATGGACACGAAGGCGGTT-3′) and ANAC089-rev (5′-AAAAAGAATTCTTATTCTAGATAAAACAACA-3′) primers for the gene amplification which was inserted into the vector using the *Not*I and *Eco*RI endonucleases. The generation of the p35S:YFP:ANAC089:CFP construct was performed in two steps. First the *anac089:cfp* hybrid gene was amplified using the p35S:ANAC089:CFP vector as DNA template. The ANAC089-for (5′-AAAAAAGCGGCCGCATGGACACGAAGGCGGTT-3′) and CFP-rev primer (5′-AAAAAGAATTCTTACTTGTACAGCTCGTC-3′) allowed to insert the amplified hybrid gene into the *Not*I and *Eco*RI restriction sites of the p35S:YFP-C vector, resulting in the p35S:YFP:ANAC089:CFP construct. The various p*sAPX*-YFP promoter fragments were generated using the primer combinations from **Table 1**. The deletion fragments were finally cloned into the pEYFP vector. Gos12 was cloned into 35S-CFP-Nost using the oligonucleotides Gos12-*Bam*HI-for (5′-AAAAGGATCCAATGACAGAATCGAGTCTGGAT-3′) and Gos12-*Age*I-rev (5′-AAAAACCGGTGATTTTGAGAGCCAGTAGATGAT-3′). Sar1 (Sar1-*Bam*HI-for 5′-AAAAGGATCCAATGTTCCTGGTGGATTGG-3′; Sar1-*Age*I-rev 5′-TTTTACCGGTCCGTCGATATATTGAGA-3′), and Clathrin light chain (ClathrinLC-*Bam*HI-for 5′-AAAAGGATCCAATGTCGTCAACCTTGAGC-3′; ClathrinLC-*Age*I-rev 5′-TTTTACCGGTCCCAACTTCTCTGTAAC-3′) were cloned into 35S-CFP-NosT and 35S-YFP-NosT using *Bam*HI and *Age*I restriction sites and plasma membrane ATPase AHA1 (AHA1-*Bam*HI-For 5′-AAAAGCGGCCGCATGTCAGGTCTCGAAGAT-3′; AHA1-*Eco*RI-rev 5′-TTTTTGAATTCTACACAGTGTAGTGATG-3′) was cloned into 35S-CFP-C and 35S-YFP-C, respectively, using *Not*I and *Eco*RI restriction sites. Emissions of fused fluorescent protein in cotransfection or transactivation experiments were quantified in the appropriate detector channel of the confocal laser scanning microscope as described in Shaikhali et al. (2008).

REDOX REGULATION OF THE sAPX PROMOTER

Protoplasts were prepared from At7 cell suspension culture of *A. thaliana* (Seidel et al., 2010). Five days after passage to new medium, cells were sedimented, washed in 50 ml 240 mM $CaCl_2$, digested and transfected with *sapx*:YFP promoter constructs as described in Seidel et al. (2004). After incubation at 26°C in darkness for 16 h the different batches were adjusted to the final H_2O_2 concentration of 5 mM and DTT of 10 mM, respectively, or left as controls and incubated for further 2 h in darkness at 26°C for 16 h. The relative YFP and CFP emission intensities were measured using the confocal laser scanning microscope (Leica SP2

Heidelberg, Germany). Finally, out of those three different samples the YFP/CFP was calculated.

CELL IMAGING OF SUBCELLULAR ANAC089 LOCALIZATION AND PROCESSING

Protoplasts prepared from the At7 cell suspension culture were transfected either with the construct combination 35S:ANAC089:CFP and 35S:ANAC089:YFP or 35S:CFP:ANAC089 and 35S:YFP:ANAC089. Homodimerization of ANAC089 *in vivo* was analyzed by Förster resonance energy transfer (FRET; Seidel et al., 2005). Fluorescence of single protoplasts was imaged with a confocal laser scanning microscope (Leica SP2, Heidelberg, Germany). Calculation of FRET efficiency was done as described in Seidel et al. (2005).

BIOINFORMATIC ANALYSIS OF PROMOTER SEQUENCES AND AMINO ACID SEQUENCES

sapx promoter sequences were searched for the presence of putative *cis*-elements with the program Matinspector[1]. The promoters of 27416 *A. thaliana* genes with a length of 3000 bp were downloaded from TAIR[2] and screened for the ATGCACGTC motif allowing for 1 bp mismatch with the program CLC Main Workbench[3]. Search for transcripts co-expressed with *sAPX* was performed using the online tool offered at http://www.arabidopsis.leeds.ac.uk/act/coexpanalyser.php. Cleavage site prediction of ANAC089 was performed with ProP1.0[4] and resulted in two hits, a peculiar Arg/Lys-specific site at amino acid position 163 and a second site at position 297 just close to the membrane spanning α-helix based on prediction from mammalian protease processing sites.

RESULTS

The promoter region of *sapx* was cloned as assumed full length or truncated form and fused to enhanced yellow fluorescent protein (YFP) as reporter gene. The selected *sapx1* DNA sequence started from −1868 bp upstream of the translational initiation site down to −1, *sapx3* from −1321 to −1, *sapx5* from −691 to −1 and *sapx6* from −263 to −1. At7-protoplasts were co-transfected with these EYFP reporter constructs simultaneously with a p35S:CFP construct as reference to correct for variable expression levels. The normalized ratios of YFP/CFP were calculated and plotted against the DNA fragment length (**Figure 1**). Transcriptional enhancers were present in all segments since reporter activity decreased with each truncation. H_2O_2 stimulated expression driven by each fragment significantly.

Since the data of **Figure 1** did not reveal a clear and restricted redox regulation site, the *sapx* promoter was fragmented into five overlapping segments (**Figure 2**) and used for a Y1H screening. 3-AT concentrations to suppress for leaky *His3*-expression without transactivator were adjusted for each construct and were within recommended concentration range for *sapx1* and *sapx2* with 15–20 mM, and already quite high for *sapx3* and *sapx4* (80 and

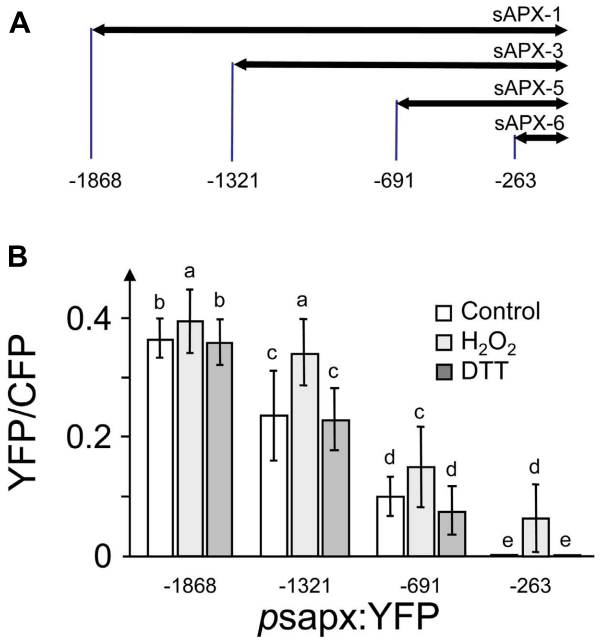

FIGURE 1 | Deletion fragments of the *sapx* promoter constructed for promoter activation assay in *A. thaliana* protoplasts. (A) Schematics of the *sapx* promoter fragments. **(B)** Expression of the YFP reporter gene fused downstream to the *sapx* promoter deletion fragments under control, oxidizing (5 mM H_2O_2) and reducing conditions (10 mM DTT) normalized to CFP accumulation under control of the 35S promoter. (1) Promoter fragment p*sapx1*; (2) promoter fragment p*sapx3*; (3) promoter fragment p*sapx5*; and (4) promoter fragment p*sapx6*. Intensities of CFP and YFP were quantified in the respective emission channels of the CLSM (Shaikhali et al., 2008). The results are means ± SD of 60–80 protoplasts. Different letters mark groups of significant difference with $p < 0.05$ (Student's *t*-test).

110 mM, respectively). The *sapx5* fragment remained leaky even at >120 mM 3-AT. This may explain why reliable and specific binding of promising candidates could not be observed for *sapx3* to *5*. Among the many positive clones only the gene encoding ANAC089 (At5g22290) which was identified as activator of *sapx2* fragment driven reporter expression in yeast appeared promising for further analysis. Retransformation of yeast cells with isolated bait and prey vectors reproduced the interaction between ANAC089 and *sapx2*. Bioinformatic analysis identified two potential binding sites for NAC transcription factors in *sapx2* (sequence position −1646 till −1431, original sequence: GCACGTCTAGTGAAAGATCC, mutated sequence: GAAAATCTAGTGAAAGATCC; second possible binding site was the motive CATCCC at −1627 till −1622). Subcloning confined the transactivation to the *sapx2-1* fragment of 216 bp length (**Figure 2B**, C1) and mutation of the upstream located CACG motif to AAAA (position −1645 to −1642) abolished transactivation of *HIS3* reporter in the *sapx2-1*$_{mut}$:*HIS3* reporter construct after cotransfection with ANAC089 (**Figure 2**, C3).

Analysis of the *in silico* translated cDNA allowed the identification of the N-terminal NAC domain and a putative C-terminal membrane anchor (**Figure 3A**). ANAC089 protein was recombinantly expressed in *E. coli* as His_6-tagged protein and purified by Ni-affinity chromatography (**Figure 3B**). Binding of

[1]http://www.genomatix.de

[2]ftp://ftp.arabidopsis.org

[3]http://www.clcbio.com/

[4]http://www.cbs.dtu.dk/services/ProP/

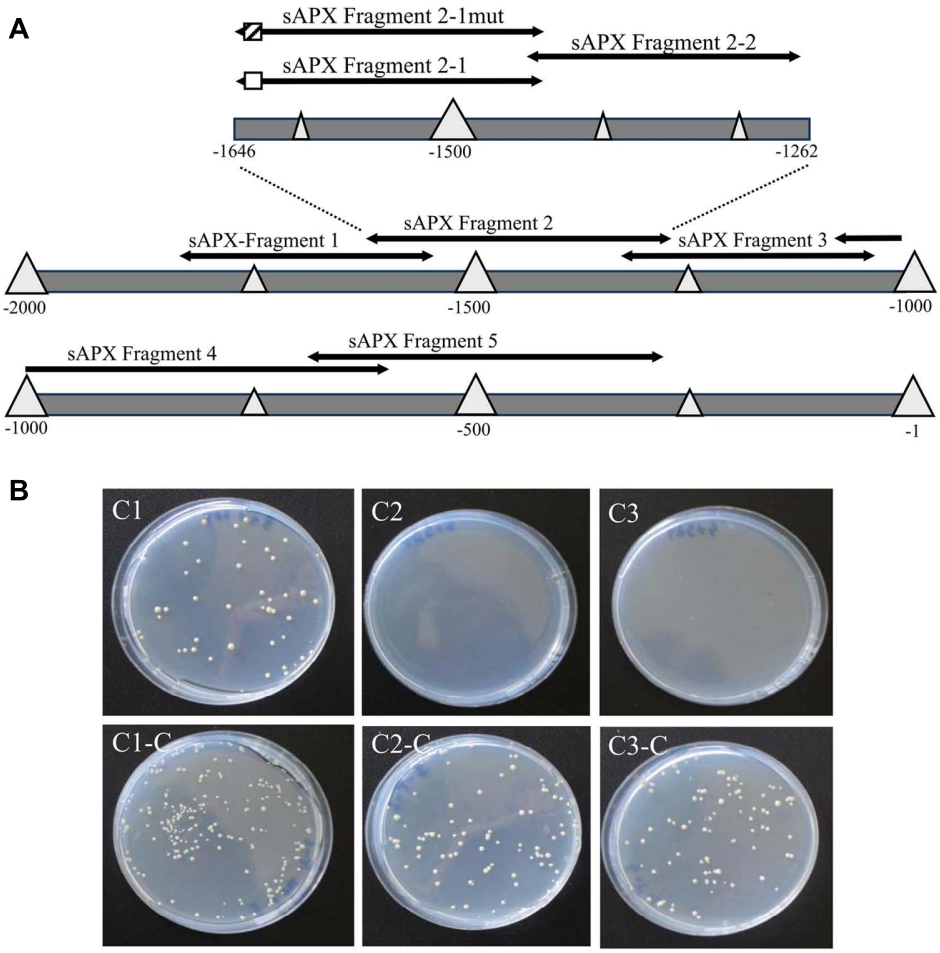

FIGURE 2 | Schematics of the promoter of *sapx* used for yeast-one-hybrid screening and binding to the specific *cis*-element. **(A)** Fragment p*sapx1* (−1563 to −1868 bp); p*sapx2* (−1262 to −1646 bp); p*sapx3* (−954 to −1321 bp); p*sapx4* (−609 to −1018 bp); p*sapx5* (−246 to −691 bp); p*sapx6* (−1 to −263 bp). Division of p*sapx2* for localization of the ANAC-binding *cis*-element: pHis2:*sapx2*-1/mut (−1432 bis −1646), pHis2:*sapx2*-2 (−1432 bis −1451). The potential target element for binding of ANAC089 is marked as hatched and the mutagenized region in white box. **(B)** Experimental identification of the binding site of ANAC089 within promoter segment pHis2:*sapx2* using the Y1H system on SD/-Trp/-His/-Leu/+3 AT selective medium (C1, C2, C3) and for control on SD/-Trp/-Leu selective medium (C1-C, C2-C, C3-C). (C1) p His2:*sapx2*-1; (C2) pHis2:*sapx2*-1mut; and (C3) p His2:*sapx2*-2. All cells grew under non-stringent selection showing their viability, while under stringent conditions only the cells grew that were harboring the wild type sapx2-1 fragment and expressing ANAC089.

His_6-ANAC089 to *sapx2-1* promoter fragment *in vitro* was studied using the EMSA (**Figure 3C**). A shift was seen upon addition ANAC089 protein and the shift was abolished upon addition of 250-fold excess competitor DNA. Mutation of the binding site abolished the ANAC089-dependent gel shift (not shown).

At7 protoplasts were transfected with constructs of p35S:ANAC089:CFP and p35S:ANAC089:YFP (**Figure 4**). Both constructs were co-expressed and the reporter fluorescence was observed in the plasma membrane and membrane vesicles (**Figures 4B,C**). Analysis for protein–protein interaction by FRET between the CFP- and YFP-fused ANAC089 revealed homooligomer formation (**Figure 4G**). FRET efficiency was significantly above the threshold which was defined as 10% from transfection results with free CFP and YFP (Seidel et al., 2005). FRET was higher if CFP and YFP were fused to the N-terminus of ANAC089. In this case, the fluorophore must have rested in the cytosol. Apparently, also the membrane-associated transcription factor is able to oligomerize. FRET between CFP:ANAC089 and YFP:ANAC089 was at about 28%, whereas the fusion the CFP and YFP fluorophores to the C-terminus of the ANAC089 resulted in 14% FRET efficiency, a value also above the threshold. Lower FRET might be explained by steric constraints, higher distance, or less stable interaction at the C-terminus of ANAC089 and cannot be distinguished by this *in vivo* method.

ABI5, a transcription factor with established localization in the nucleus (Lopez-Molina et al., 2003), was used as a control (**Figure 4F**) and accumulated at a site distinct to ANAC089. Analysis of the coding region with the program TMHMM Server v. 2.0 at http://www.cbs.dtu.dk/services/TMHMM-2.0/ allowed for the identification of a putative transmembrane domain at the C-terminus (**Figure 4H**, see also **Figure 3A**). ANAC089 has been reported before to be a member of a subgroup within the family of

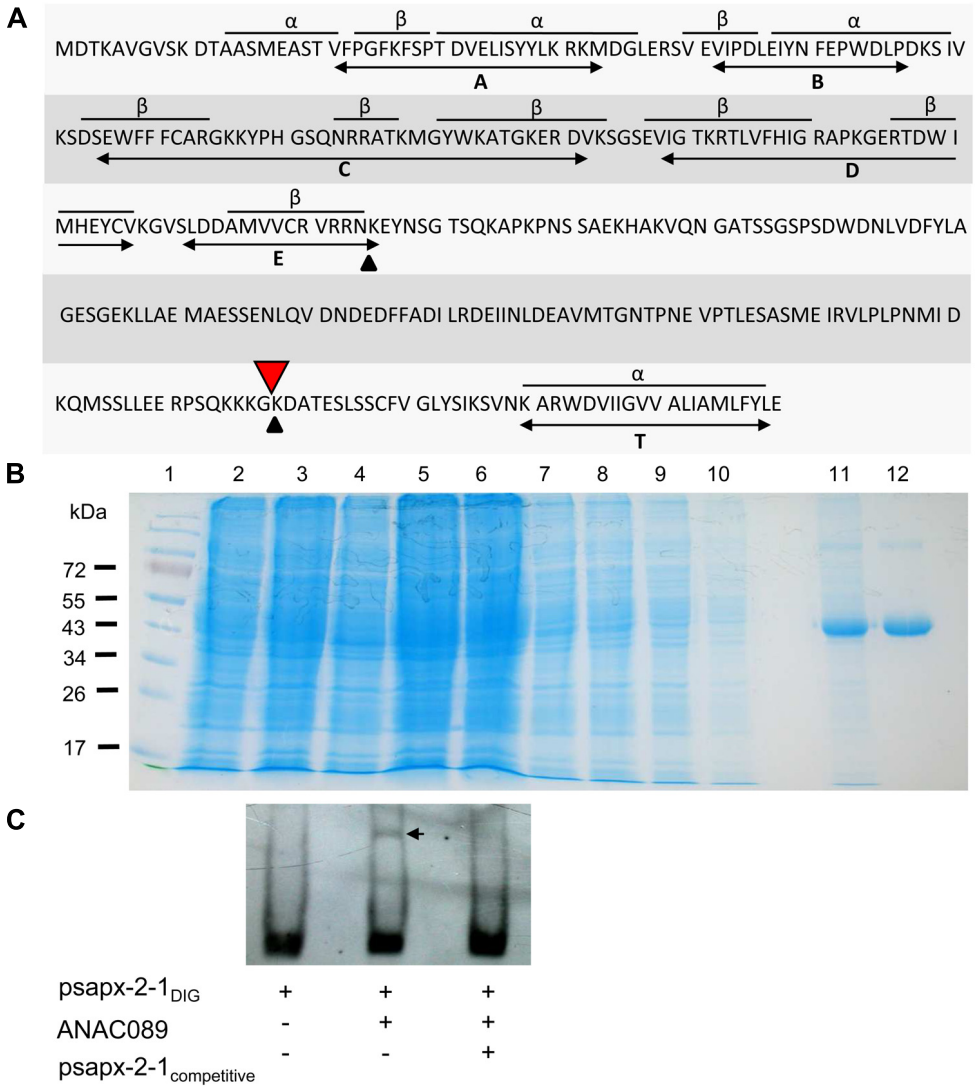

FIGURE 3 | Structure of ANAC089, generation of recombinant His_6-ANAC089 and EMSA. (A) Primary structure of the ANAC089 transcription factor. The N-terminal ANAC domain consists of three α-helices and eight β-sheets in conserved arrangement (A–E). The bioinformatically predicted transmembrane α-helix (T) of the ANAC089 protein is localized at amino acid position 319–339. Putative protein cleavage sites are indicated with arrows. His_6-ANAC089 was expressed in *E. coli* and purified by Ni-NTA affinity chromatography. **(B)** Heterologous expression and purification of His6-tagged ANAC089. The recombinant ANAC089 protein was expressed in BL21 (DE3) pLysS *E. coli* cells which were induced with 400 μM isopropyl-β-D-thiogalactopyranoside for 4 h. By SDS PAGE the time-dependent expression of the recombinant ANAC089 protein, as well as the purification process was analyzed. (1) Prestained protein ladder (Fermentas); (2) 0 h after IPTG induction; (3) 2 h after IPTG induction; (4) 4 h after IPTG induction; (5) cell extract; (6) cell pellet; (7–10) column wash fractions; (11) first fraction of ANAC089 elution; and (12) second fraction of ANAC089 elution. **(C)** Electrophoretic mobility shift assay: ANAC089 promoter fragment interaction *in vitro* using the DIG Gel Shift Kit (2nd generation, Roche). Verification of the specificity of ANAC089 binding to the *cis*-element within the sAPX promoter fragment 2-1. Promoter fragment psapx2-1 was loaded at 8 ng DNA. The amount of unlabeled competitor was 2 μg DNA. ANAC089 protein was added at 100 ng. The arrow head marks the shifted band.

NAC transcription factors which is tethered to membranes (Kim et al., 2007). Incubation of transfected protoplasts with dithiothreitol (10 mM) showed time-dependent release of ANAC089 from the membrane and translocation to the nucleus when the fluorophore was fused to the N-terminus of the transcription factor (**Figures 5A–F**). ANAC089 lacking the C-terminal membrane domain localized to the nucleus similar to the nuclear transcription factor ABI5 (**Figures 5G–I**). ANAC089 remained tethered to the membrane under oxidizing conditions established by addition of 10 mM H_2O_2 to the protoplast suspension (**Figures 5K–M**). The next experiment addressed the question whether the carboxyterminus rests at the peripheral membranes after cleavage. The protoplasts were transfected with the triple fusion construct YFP:ANAC089:CFP (**Figures 5N–P**). Following treatment with DTT, the released YFP:ANAC protein accumulated in the nucleus, while the CFP fused to the carboxyterminus of ANAC stayed at the membrane despite the reductive treatment of the protoplasts.

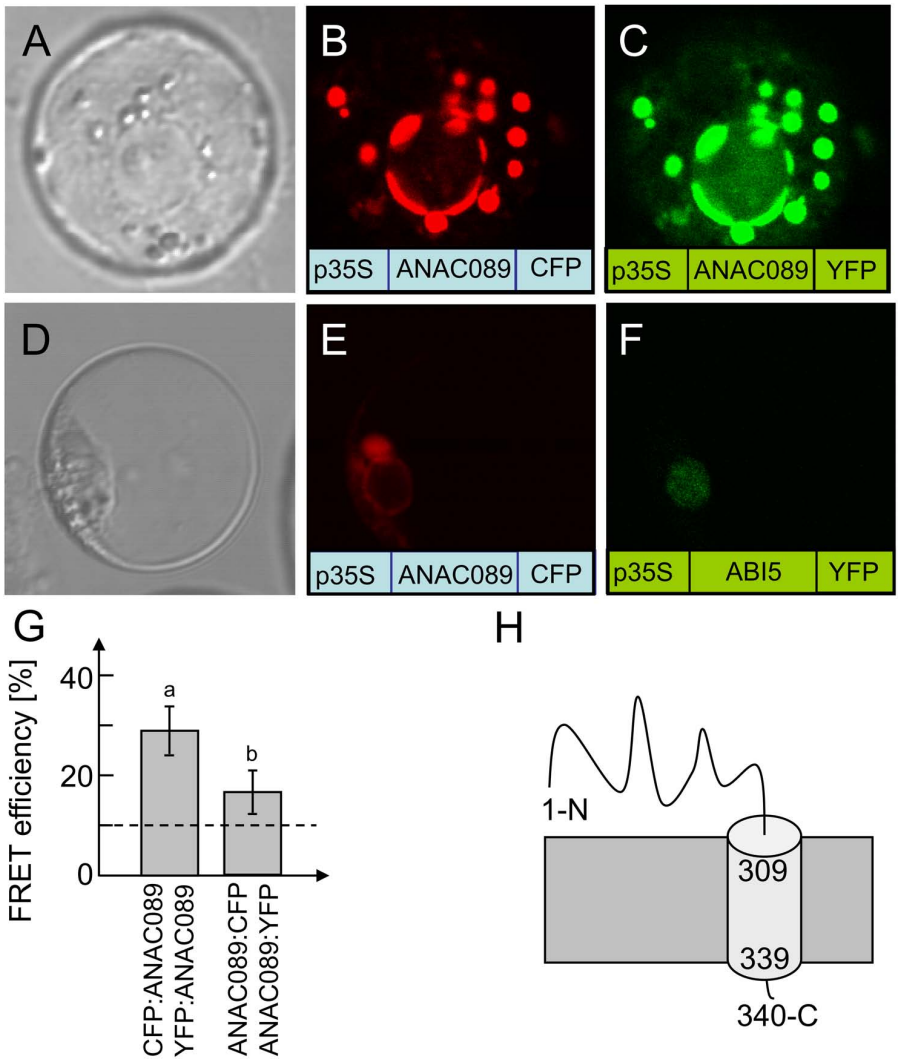

FIGURE 4 | Subcellular localization of ANAC089 in *A. thaliana* protoplasts. (A) Protoplast in bright field. Fluorescence image of a protoplast expressing the C-terminally CFP-tagged ANAC089 **(B)** or the C-terminally YFP-tagged ANAC089 **(C)**. Comparative localization of ANAC089 und ABI5 with C-terminally fused fluorophores in *A. thaliana* protoplasts. **(D)** Bright field control picture. **(E)** ANAC089-CFP-signal detected in vesicles, endoplasmic reticulum, and plasmamembrane. **(F)** ABI5-YFP-signal in cell nucleus. **(G)** Dimerization detection by FRET analysis: protoplasts were co-transfected with either CFP:ANAC089 and YFP:ANAC089:YFP (left column) or ANAC089:CFP and ANAC089:YFP (right). In both cases significant FRET above the threshold of co-expressed free CFP and YFP could be detected (mean ± SD, $n > 60$ protoplasts, three transfections). **(H)** Putative topology of ANAC089 in the membrane.

The membrane localization of the membrane-anchored ANAC089 was investigated in more detail in protoplasts co-transfected with a set of marker proteins for compartments of the secretory pathway (Uemura et al., 2004; Hanton et al., 2008; Neubert et al., 2008; Seidel et al., 2008; Hwang and Robinson, 2009; **Figure 6**). No co-localization was seen with the plasmamembrane H^+-ATPase and the Golgi SNARE Gos 12 (**Figures 6A–C,Q–S**), while VHA-e and Vma21a (**Figures 6G–I**) showed a high degree of co-localization with ANAC089, respectively (**Figures 6D–F**). All other marker proteins, the light chain of Clathrin (CLAT; **Figures 6K–M**) and Sar1 (**Figures 6N–P**) showed only partial co-localization. The data are consistent with a preferred localization of ANAC089 in the *trans*-Golgi network and in the ER.

The regulatory effect of ANAC089 on *sapx* gene expression was studied in transactivation assays (**Figure 7**). *A. thaliana* mesophyll protoplasts were transfected with (i) a reference constructs expressing CFP under the control of the 35S-promoter, (ii) the *yfp* gene placed under control of the *psap2-1* and *psap2-1*$_{mut}$ promoter sequences as transactivation reporter, and (iii) and the construct ANAC089:mCherry as transcriptional modifier. mCherry was fused to the C-terminus of the ANAC089 to check for expression of the *anac089*-gene in transfected protoplasts. The ratio of YFP to CFP was constant in protoplasts transfected with all combinations except for the cells containing the wild type *psap2-1* promoter and expressing ANAC089. Here a significant suppression of YFP reporter intensity by 25% was observed. This suppression was not

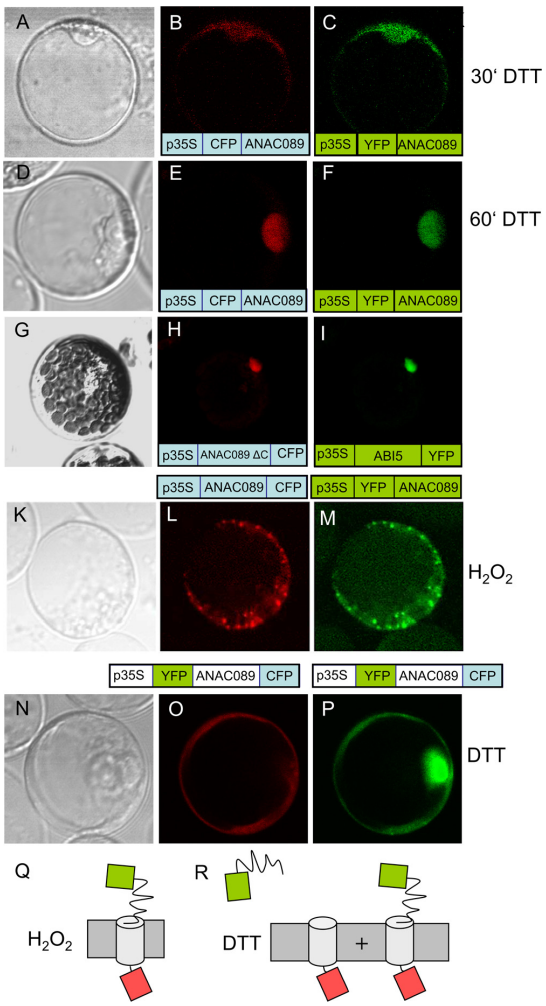

FIGURE 5 | Redox-dependent dynamics of ANAC089 localization. (A–F) Time-dependent localization of ANAC089 was documented following a treatment with dithiothreitol (10 mM DTT). Images were taken at $t = 30$ min **(A–C)** and $t = 60$ min **(D–F)**. **(A, D)** Bright field image. **(B, E)** Fluorescence signal of N-terminally fused CFP (ANAC089-CFP). **(C, F)** Fluorescence signal of N-terminally fused YFP (ANAC089-YFP). **(G–I)** Nuclear accumulation of ANAC089 lacking the transmembrane domain. Protoplasts were transformed with the 3′-truncated ANAC089 coding for a variant that lacks the C-terminal membrane domain (total remaining length 298 aa, see **Figure 3A**, red arrow). In parallel the protoplasts were transformed with ABI5 expression construct. Both fluorophore-fused proteins localized to the nucleus. **(K–M)** Localization of N-terminally fused fluorophores in response to H_2O_2. Protoplasts of *A. thaliana* were treated with 5 mM H_2O_2 for $t = 60$ min. **(K)** Bright field. **(L)** ANAC089:CFP-signal. **(M)** ANAC089:YFP-signal. **(N–P)** Translocation of ANAC089 to the nucleus following reductive activation with 10 mM DTT for 60 min. In this case a double fusion was used, namely YFP:ANAC089:CFP under control of the p35S. **(N)** Bright field image. **(O)** CFP signal of the membrane-associated domain. **(P)** YFP signal of the cleaved N-terminal domain of the ANAC089-YFP in the nucleus. The transfection experiments were repeated three times with 70–90% of the successfully transformed protoplasts showing the same result. **(Q,R)** Schematics of underlying model explaining release of YFP to the nucleus following cleavage: CFP in each case rests at the membrane due to its fusion to the membrane-residing helix. The N-terminally fused YFP also rests at the membrane under oxidizing conditions **(M)**, or is partially or fully released with time under reducing conditions which cause cleavage of the ANAC089 domain from the membrane anchor **(P)**.

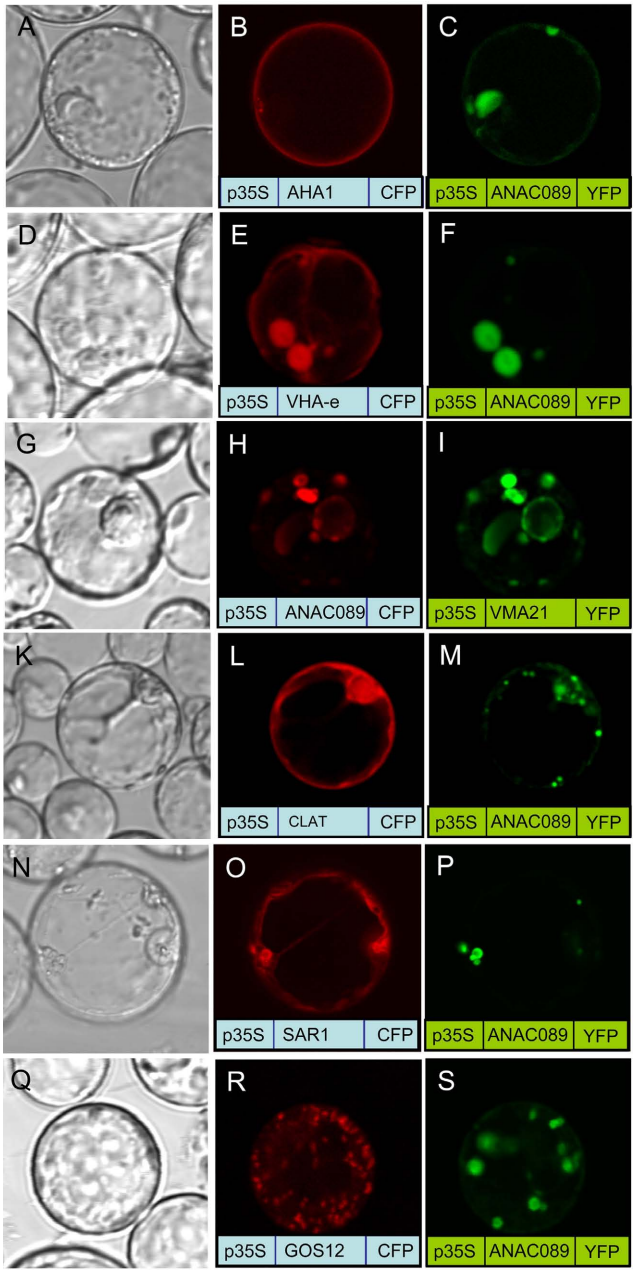

FIGURE 6 | Co-localization of fluorophore-fused ANAC089 with marker proteins. Protoplasts were co-transfected with ANAC089 fused to either CFP or YFP as indicated and a marker protein as follows: **(A–C)** AHA1, the plasmamembrane H^+-ATPase, **(D–F)** VHA-e, a subunit of the V_0 domain of V-ATPase that localizes to TGN/EE, **(G–I)** VMA21a, an ER-resident assembly factor of the V-ATPas, **(K–M)** Clathrin, the light chain of the clathrin coat, **(N–P)** Sar1, the small GTPase of COP II vesicle transport anterograde transport between ER and Golgi, and **(Q–S)** GOS12, a Golgi SNARE.

detected in protoplasts transfected with the mutated promoter proving the importance of the CACG-element in the suppressive regulation. The same suppressive effect was detected when using the full length *sapx* promoter in the absence or presence of co-expressed ANAC089 (**Figure 7B**).

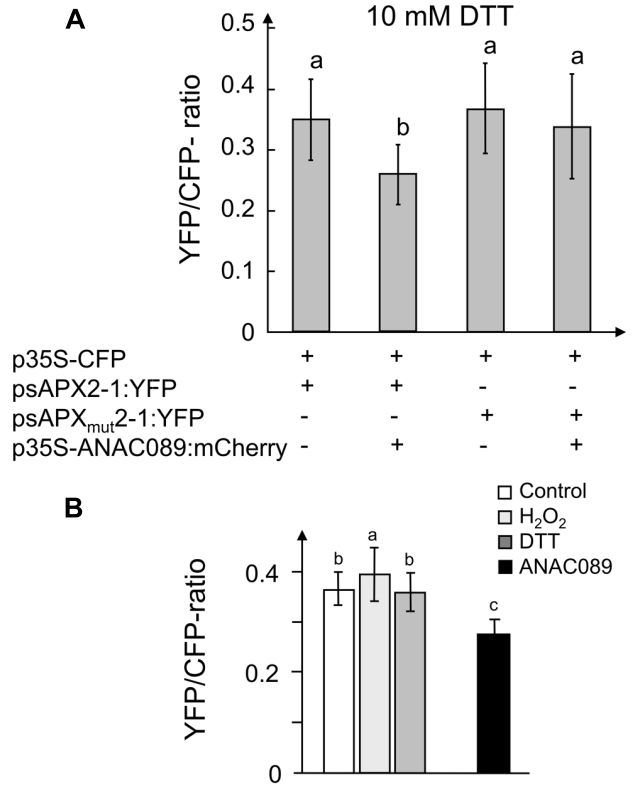

FIGURE 7 | Effect of overexpressed ANAC089 on reporter gene expression and confirmation of involved *cis*-element CACG. (A) (1st bar) Co-transformation of fragment p*sapx2*-1:YFP with 35S-CFP. (2nd bar) Co-transformation of p*sapx2*-1:YFP with 35S-ANAC089-mCherry and 35S-CFP. (3rd bar) Co-transformation of p*sapx2*-1mut:YFP with 35S-CFP. (4th bar) Co-transformation of p*sapx2*-1mut with 35S-ANAC089-mCherry and 35S-CFP. Prior to the measurement protoplasts were incubated with 10 mM DTT for 2 h. The result represent means ± SD from two experiments with a total $n > 30$ protoplasts per construct. **(B)** A similar effect was seen if the full length promoter (−1 to −1868) was used. The first three columns are as in **Figure 1** (expression in control, H_2O_2, or DTT-treated protoplasts), the set of three columns on the left hand side represent reporter strength under control conditions, in the presence of H_2O_2 and DTT, respectively, the fourth column shows the result with co-expressed p35S:ANAC089. The data are means ± SD from 68, 56, 56, 72, 74, and 83 protoplasts (from left to right column). Different letters indicate significant difference at $p < 0.05$ (Student's *t*-test).

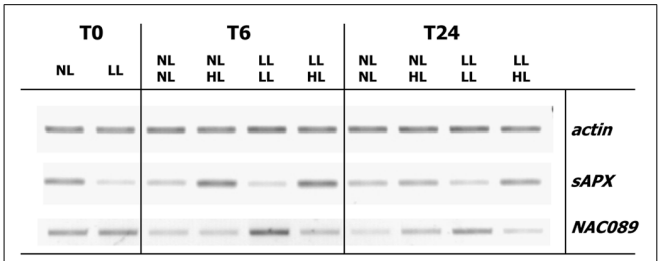

FIGURE 8 | Regulation of sAPX and ANAC089 transcript amounts in a light shift experiment. *A. thaliana* were grown for 3 weeks in normal light, either maintained under this condition for another 10 days (80 μmol quanta m^{-2} s^{-1}, N-light) or acclimated to very low light (8 μmol quanta·m^{-2} s^{-1}, L-light) for 10 days. The plants were transferred to high light (800 μmol quanta m^{-2} s^{-1}, H-light). Rosettes were harvested at $t = 0$, after 6 or 24 h. RNA was isolated and processed as described by Oelze et al. (2012). Semiquantitative RT-PCR was performed following cDNA synthesis. DNA products were separated by agarose gel electrophoresis and visualized by ethidium bromide staining. Band intensity indicates relative abundance of transcripts.

Finally the relationship between *anac089* and *sapx* gene expression was studied in *A. thaliana* rosettes subjected to a light shift treatment similar to the experiment described in Oelze et al. (2012). Plants fully acclimated to a shady growth condition for 10 days (8 μmol quanta·m^{-2} s^{-1}) or grown under normal growth conditions (80 μmol quanta·m^{-2} s^{-1}) were transferred to high light (800 μmol quanta·m^{-2} s^{-1}) for 6 h. This treatment is known to induce strong regulation of *sAPX* transcript amounts (Oelze et al., 2012). *sAPX* and *ANAC089* transcript amounts were semiquantified and normalized to *ACTIN2* transcript amounts (**Figure 8**). While *sAPX*-mRNA levels were higher in normal light grown plants than in low light acclimated ones, they increased upon transfer to high light. The response was stronger 6 h after transfer than after 24 h. *ANAC089* mRNA levels behaved in a roughly inverse manner. They were high when *sAPX* transcript levels were low and *vice versa*.

In the last step, the presence of the *cis*-element binding ANAC089 in sAPX promoter was searched in the whole *A. thaliana* genome. To this end the frequency of the putative ANAC *cis*-element ATGCACGTC identified by Matinspector with a score of 0.979 was investigated in the whole *A. thaliana* genome. The promoters of 27416 *A. thaliana* genes with a length of 3000 bp were downloaded from TAIR[5] and screened for the ATGCACGTC motif with the program CLC Main Workbench[6]. The fully conserved ATGCACGTC motif was found in 196 promoters, either in forward or reverse orientation. In 6903 promoters the motif was present with a single nucleotide exchange. *sAPX* co-expression was analyzed at http://www.arabidopsis.leeds.ac.uk/act/coexpanalyser.php and the 1400 most co-expressed genes were compared with the identified ANAC *cis*-element containing promoters. The obtained list contains candidate genes that might be partially co-regulated with sAPX based on the presence of the ATGCACGTC motif (**Table 2**). Among the genes containing the ATGCACGTC motif (one mismatch allowed) with a co-expression *p*-value > 0.5 are many candidates that show a functional link to stress acclimation and redox metabolism like glutathione reductase, flavonoid biosynthesis enzymes or mitochondrial function.

DISCUSSION

This work identified and describes the transcription factor ANAC089 as a negative regulator of *sapx* expression (**Figure 7**). The *A. thaliana* genome encodes close to 2,000 putative transcription factors (Iida et al., 2005). The plant-specific NAC transcription factor family comprises about 110 genes in *A. thaliana*. Their usually N-terminally conserved NAC domain of about 60 amino acids was first identified in the three representatives named NAM (no apical meristem), ATAF1/2 and CUC2 (cup shaped cotyledon;

[5]ftp://ftp.arabidopsis.org

[6]http://www.clcbio.com/

Table 2 | Bioinformatic identification of genes that carry the ATGCACGTC motif in their promoter and co-expressed with *sAPX*.

Identifier	*p*-value	*r*-value	Function
AT4G33520	0.628337	$8.9e^{-37}$	Metal-transporting P-type ATPase
AT3G29200	0.611953	$1.8e^{-34}$	Chorismate mutase, chloroplast (CM1)
AT3G55120	0.594613	$3.6e^{-32}$	Chalcone–flavanone isomerase
AT3G24170	0.592559	$6.6e^{-32}$	Glutathione reductase, putative
AT2G45440	0.585632	$4.9e^{-31}$	Dihydrodipicolinate synthase 2 (DHDPS2)
AT1G63290	0.569233	$4.8e^{-29}$	Ribulose-phosphate 3-epimerase, cytosolic, putative
AT4G16265	0.560068	$5.5e^{-28}$	DNA-directed RNA polymerase II, putative
AT1G18320	0.559598	$6.3e^{-28}$	Mitochondrial import inner membrane translocase subunit Tim17
AT3G17609	0.551960	$4.5e^{-27}$	bZIP transcription factor/HY5-like protein (HYH)
AT3G06680	0.544932	$2.7e^{-26}$	60S ribosomal protein L29 (RPL29B)
AT3G49180	0.530617	$8.8e^{-25}$	Transducin family protein/WD-40 repeat family
AT5G44160	0.528320	$1.5e^{-24}$	Zinc finger (C2H2 type) family protein
AT2G20450	0.523633	$4.5e^{-24}$	60S ribosomal protein L14 (RPL14A)
AT2G26380	0.522760	$5.6e^{-24}$	Disease resistance protein-related/LRR protein
AT5G59850	0.519257	$1.3e^{-23}$	40S ribosomal protein S15A
AT3G10530	0.519230	$1.3e^{-23}$	Transducin family protein/WD-40 repeat family
AT5G20600	0.514334	$3.8e^{-23}$	Expressed protein
AT5G50810	0.513390	$4.7e^{-23}$	Mitochondrial import inner membrane translocase TIM8
AT5G15910	0.512829	$5.4e^{-23}$	NAD(P)-dependent steroid dehydrogenase, related
AT2G23350	0.512790	$5.4e^{-23}$	Polyadenylate-binding protein, putative/PABP, putative
AT2G17270	0.510441	$9.2e^{-23}$	Mitochondrial substrate carrier family protein
AT4G36020	0.508859	$1.3e^{-22}$	Cold-shock DNA-binding family
AT1G60850	0.507399	$1.8e^{-22}$	DNA-directed RNA polymerase, putative

Following a genome-wide search with the ATGCACGTC motif, the hits were compared with the promoters of sAPX-co-regulated transcripts. The list gives the results with a p-value >0.5.

Jensen et al., 2010). The NAC domain contains the DNA binding domain, dimerization domain and nuclear localization sequence (Ernst et al., 2004). ANAC089 possesses all these features in its N-terminus.

NAC transcription factors have been shown to be involved in developmental processes, hormonal signaling and responses to abiotic and biotic stresses (Hu et al., 2010). Interestingly, several members of the NAC transcription factor family possess transmembrane anchors. They belong to the membrane-tethered transcription factors (MTTFs). The membrane-associated form is inactive by immobilization. Their proteolytic processing releases the functional TF. The transcript level of *NAC-MTTFs* often is up-regulated under conditions of abiotic stress or in the presence of hormones (Kim et al., 2006). Here it is shown that ANAC089 fusion protein localizes to vesicle-like structures and peripheral membranes. This is in line with the report by Li et al. (2010) showing similar localization. Upon its reductive release from the membrane ANAC089 localized to the nucleus (**Figure 5**). Thus our experiments provide evidence for a signaling cue that triggers its release and gives evidence for process dynamics. The almost exclusive nuclear localization after 60 min in this study was identical to images recorded after expressing a C-terminally truncated variant, ANAC089ΔC containing amino acids 1 to 310 (Li et al., 2010) and could be confirmed in our cell system after expressing a C-terminally truncated version of ANAC089 lacking the transmembrane domain. Our data indicate that a reductive stimulus is involved in release of the functional TF.

A critical element in the proposed signaling pathway is the protease that releases ANAC089 from the membrane. Conditional proteolysis which is hypothetical at present would allow for rapid transcriptional response to a changing environmental or developmental cue. Up to now, the molecular entities shedding the TFs from their membrane in plants are unknown. In the case of another NAC-MTTF named NTM1, the calpain inhibitor ALLN prevented cleavage from the membrane. Since ALLN specificity is not high, the precise nature of the involved protease remains to be established (Kim et al., 2006). The ANAC089 sequence contains two predicted cleavage sites; a peculiar Arg/Lys-specific site at amino acid position 163 (VVCRVRR|NK) with a high probability and a second site with lower score at position 297 (RPSQKKK|GK) just close to the membrane spanning α-helix based on mammalian protease processing sites (**Figure 3**). About 3% of all *A. thaliana* genes code for proteases (Garcia-Lorenzo et al., 2006) most of which have not been analyzed in any detail. The chloroplast serine

Deg1 protease is activated under reductive conditions. It is suggested to localize to the thylakoid membrane and contains many Cys residue, e.g., 10 Cys in *A. thaliana* (Ströher and Dietz, 2008). Deg proteases function as ATP-independent serine endopeptidases and are found in different organelles and the nucleolus (Deg9) but not in the cytosol or at the endomembranes (Schuhmann and Adamska, 2012). Thus they may serve as examples of principle but unlikely are involved in releasing ANAC089 from their endomembrane attachment site. Three *Arabidopsis* Cys proteases have been shown to be inhibited by binding to protein disulfide isomerase and activated *in vitro* after addition of DTT. The active Cys proteases are involved in cell type-specific programmed cell death in the endothelium of developing seeds (Ondzighi et al., 2008). Thus in addition to the more frequently described oxidative activation of proteases, the given examples reveal that reductive activation of specific proteases as hypothesized here occurs *in planta* as well. The cleavage sites in ANAC089 are predicted for serine proteases of the furin type which are also found in plants. In addition to redox-dependent activation of the protease by disulfide reduction or release from binding partners, a third type of redox regulation might be achieved by burying the cleavage domain of the substrate protein ANAC089 either by conformational changes or posttranslational modifications, e.g., by glutathionylation. ANAC089 contains four Cys residues which may be involved in such a mechanism (**Figure 3A**).

Recently, ANAC089 was linked to sugar sensing in a screen for fructose-insensitive *A. thaliana* mutants. One of the selected mutants *FSQ6* carries an *anac089* allele with premature translational stop in the third exon which enabled growth in the presence of 6.5% (w/v) fructose (Li et al., 2011). This C-terminally truncated ANAC089 in *FSQ6* lacks the membrane spanning helix, thus is not tethered to membranes and immediately translocates to the nucleus upon its synthesis. The expressed ANAC089 variant in *FSQ6* is considered as gain-of function mutation with constitutive ANAC089-dependent target gene expression (Li et al., 2011). Our results demonstrate release of the N-terminus of ANAC089 upon treatment with reductant (**Figure 5**). In their comprehensive search and cataloguing of NAC transcription factors in the rice and *A. thaliana* genomes Ooka et al. (2003) sorted ANAC089 in the group of OsNAC08-related NACs together with ANAC060 and ANAC040. Membrane-tethering of at least 13 ANACs was reported by Kim et al. (2007) the transcript levels of which were often up-regulated under cold, salinity, or heat stress. This contrasts expression of ANAC089. Its mRNA level was high at the end of the dark phase and under low light conditions (**Figure 8**) and down-regulated under high light. High light exposure of normal or low light grown plants imposes excess excitation energy stress and induces a profound transcriptional acclimation response (Khandelwal et al., 2008; Oelze et al., 2012 and unpublished). High light induces oxidative stress and ROS-related signaling (Bechtold et al., 2008). Thus *ANAC089* showed a regulation tentatively reciprocal to the ROS level.

First reports have described cues that lead to the release of membrane-tethered NAC transcription factor. Cytokinin-dependent signaling involves the membrane-anchored ANAC transcription factor NTM1 which regulates cell division (Kim et al., 2006). The MTTF-NAC (At3g49530) mediates part of the cold stress response. Cold temperatures lead to release of the functional NAC-TF from the plasmamembrane over a long time period between 0.5 and 15 h (Seo et al., 2010). In neither of these cases a biochemical cue could be proposed that triggers the shedding. Thus the here reported redox-dependent release offers a first mechanistic interpretation of the processing by intracellular redox signals.

ANAC089 has been shown to be expressed in cotyledons, germinating seedlings, in the vasculature of hypocotyls, roots, rosette and cauline leaves, but also in the interveinal region of the rosette leaves (Li et al., 2010). ANAC089 overexpression delayed flowering time possibly by affecting expression of flower regulatory genes such as CONSTANS (CO) and FLOWERING LOCUS T (FT) whose transcript was suppressed and FLOWERING LOCUS C (FLC) whose transcript accumulation was enhanced (Li et al., 2010). Apparently ANAC089 has multiple functions.

This study assigns an additional and novel role to ANAC089, namely in regulating the expression of sAPX, an important player of the chloroplast antioxidant system. The chloroplast antioxidant system in photosynthesizing cells is expressed at a high level under most conditions (Foyer and Noctor, 2005). This realizes a strong antioxidant defense in a variable environment. However leaves may encounter environmental conditions that prevent photosynthesis-related oxidative stress. Such a reduced state of the glutathione system (Noctor and Foyer, 1998) and the thiol-disulfide redox regulatory network (Dietz, 2008) are likely established if leaves are permanently shaded (Oelze et al., 2012). Then down-regulation of the defense system might save resources for other important synthetic activities. Shedding of ANAC089 from the cytosol-facing side of endomembranes by a thiol redox-regulated process may then allow for translocation of the released functional ANAC089-protein to the nucleus and will subsequently lower *sapx* gene expression. Comparing protein amounts and transcript levels in *A. thaliana* plants acclimated to low, normal, and high light indicates that low levels of *sAPX* transcript are sufficient to maintain high sAPX protein amounts under such conditions probably due to reduced turnover. Such a role of ANAC089 is tentatively supported by the antiparallel transcript regulation of *ANAC089* and *sAPX* in rosettes acclimated and maintained in low and normal light or subsequently transferred to high light (**Figure 8**). According to this scenario, ANAC089 functions in a negative retrograde loop, lowering sAPX expression if the cell encounters highly reducing conditions. In this case the retrograde signal would be a thiol-disulfide redox cue. The putative binding site ATGCACGTC of ANAC089 in the *sapx* promoter is present in many genes tentatively co-expressed with *sAPX*. It will be interesting to investigate the effect of ANAC089 on the expression of these candidate targets including *sapx* by use of transgenic *A. thaliana* lacking or overexpressing ANAC089.

ACKNOWLEDGMENTS

We gratefully acknowledge support by Prof. Margarete Baier (FU Berlin, Germany) in the very early phase of the project particularly in the Y1H-library construction. This work was conducted within the framework of the FOR804 on retrograde signaling (Di346) funded by the Deutsche Forschungsgemeinschaft.

REFERENCES

Asada, K. (1999). The water–water cycle in chloroplasts: scavenging of active oxygens and dissipation of excess photons. *Annu. Rev. Plant Physiol. Plant Mol. Biol.* 50, 601–639.

Baier, M., and Dietz, K. J. (2005). Chloroplasts as source and target of cellular redox regulation: a discussion on chloroplast redox signals in the context of plant physiology. *J. Exp. Bot.* 56, 1449–1462.

Baier, M., Noctor, G., Foyer, C. H., and Dietz, K. J. (2000). Antisense suppression of 2-Cys peroxiredoxin in *Arabidopsis thaliana* specifically enhances the activities and expression of enzymes associated with ascorbate metabolism, but not glutathione metabolism. *Plant Physiol.* 124, 823–832.

Bechtold, U., Richard, O., Zamboni, A., Gapper, C., Geisler, M., Pogson, B. J., et al. (2008). Impact of chloroplastic- and extracellular-sourced ROS on high light-responsive gene expression in *Arabidopsis*. *J. Exp. Bot.* 59, 121–133.

Dietz, K. J. (2008). Redox signal integration: from stimulus to networks and genes. *Physiol. Plant.* 133, 459–468.

Dietz, K. J. (2011). Peroxiredoxins in plants and cyanobacteria. *Antioxid. Redox Signal.* 15, 1129–1159.

Dietz, K. J., Jacob, S., Oelze, M. L., Laxa, M., Tognetti, V., de Miranda, S. M. N., et al. (2006). The function of peroxiredoxins in plant organelle redox metabolism. *J. Exp. Bot.* 57, 1697–1709.

Ernst, H. A., Olsen, A. N., Larsen, S., and Lo Leggio, L. (2004). Structure of the conserved domain of ANAC, a member of the NAC family of transcription factors. *EMBO Rep.* 5, 297–303.

Foyer, C. H., and Noctor, G. (2005). Oxidant and antioxidant signalling in plants: a re-evaluation of the concept of oxidative stress in a physiological context. *Plant Cell Physiol.* 28, 1056–1071.

Garcia-Lorenzo, M., Sjödin, A., Jansson, S., and Funk, C. (2006). Protease gene families in *Populus* and *Arabidopsis*. *BMC Plant Biol.* 6, 30. doi: 10.1186/1471-2229-6-30

Golldack, D., Lüking, I., and Yang, O. (2011). Plant tolerance to drought and salinity: stress regulating transcription factors and their functional significance in the cellular transcriptional network. *Plant Cell Rep.* 30, 1383–1391.

Hanton, S. L., Chatre, L., Matheson, L. A., Rossi, M., Held, M. A., and Brandizzi, F. (2008). Plant Sar1 isoforms with near-identical protein sequences exhibit different localizations and effects on secretion. *Plant Mol. Biol.* 67, 283–294.

Hu, R., Qi, G., Kong, Y., Kong, D., Gao, Q., and Zhou, G. (2010). Comprehensive analysis of NAC domain transcription factor gene family in *Populus trichocarpa*. *BMC Plant Biol.* 10, 145. doi: 10.1186/1471-2229-10-145

Hwang, I., and Robinson, D. G. (2009). Transport vesicle formation in plant cells. *Curr. Opin. Plant Biol.* 12, 660–669

Iida, K., Seki, M., Sakurai, T., Satou, M., Akiyama, K., Toyoda, T., et al. (2005). RARTF: database and tools for complete sets of *Arabidopsis* transcription factors. *DNA Res.* 12, 247–256.

Jensen, M. K., Kjaersgaard, T., Nielsen, M. M., Galberg, P., Petersen, K., O'Shea, C., et al. (2010). The *Arabidopsis thaliana* NAC transcription factor family: structure–function relationships and determinants of ANAC019 stress signalling. *Biochem. J.* 426, 183–196.

Kangasjärvi, S., Lepisto, A., Hannikainen, K., Piippo, M., Luomala, E. M., Aro, E. M., et al. (2008). Diverse roles for chloroplast stromal and thylakoid-bound ascorbate peroxidases in plant stress responses. *Biochem. J.* 412, 275–285.

Khandelwal, A., Elvitigala, T., Ghosh, B., and Quatrano, R. S. (2008). *Arabidopsis* transcriptome reveals control circuits regulating redox homeostasis and the role of an AP2 transcription factor. *Plant Physiol.* 148, 2050–2058.

Kim, S. Y., Kim, S. G., Kim, Y. S., Seo, P. J., Bae, M., Yoon, H. K., et al. (2007). Exploring membrane-associated NAC transcription factors in *Arabidopsis*: implications of membrane biology in genome regulation. *Nucleic Acid Res.* 35, 203–213.

Kim, Y. S., Kim, S. G., Park, J. E., Park, H. Y., Lim, M. H., Chua, N. H., et al. (2006). A membrane-bound NAC transcription factor regulates cell division in *Arabidopsis*. *Plant Cell* 18, 3132–3144.

Klein, P., and Dietz, K. J. (2010). Identification of DNA-binding proteins and protein–protein interactions by yeast one-hybrid and yeast two-hybrid screen. *Methods Mol. Biol.* 639, 171–192.

Leister, D. (2012). Retrograde signaling in plants: from simple to complex scenarios. *Front. Plant Sci.* 3: 135. doi: 10.3389/fpls.2012.00135

Li, J. Q., Zhang, J. A., Wang, X. C., and Chen, J. (2010). A membrane-tethered transcription factor ANAC089 negatively regulates floral initiation in *Arabidopsis thaliana*. *Sci. China Life Sci.* 53, 1299–1306.

Li, P., Wind, J. J., Shi, X., Zhang, H., Hanson, J., and Smeekens, S. C. (2011). Fructose sensitivity is suppressed in *Arabidopsis* by the transcription factor ANAC089 lacking the membrane-bound domain. *Proc. Natl. Acad. Sci. U.S.A.* 108, 3436–3441.

Li, Z. R., Wakao, S., Fischer, B. B., and Niyogi, K. K. (2009). Sensing and responding to excess light. *Annu. Rev. Plant Biol.* 60, 239–260.

Lopez-Molina, L., Mongrand, S., Kinoshita, N., and Chua, N.-H. (2003). AFP is a novel negative regulator of ABA signalling that promotes ABI5 protein degradation. *Genes Dev.* 17, 410–418.

Miyake, C., and Asada, K. (1996). Inactivation mechanism of ascorbate peroxidase at low concentrations of ascorbate; hydrogen peroxide decomposes compound I of ascorbate peroxidase. *Plant Cell Physiol.* 37, 423–430.

Nakano, Y., and Asada, K. (1981). Hydrogen peroxide is scavenged by ascorbate specific peroxidase in spinach chloroplasts. *Plant Cell Physiol.* 22, 867–880.

Neubert, C., Graham, L., Black-Maier, E. W., Liu, T. Y., Stierhof, Y. D., Seidel, T., et al. (2008). *Arabidopsis* has two functional orthologs of the yeast V-ATPase assembly factor Vma21p. *Traffic* 9, 1618–1628.

Noctor, G., and Foyer, C. H. (1998). Ascorbate and glutathione: keeping active oxygen under control. *Annu. Rev. Plant Physiol. Plant Mol. Biol.* 49, 249–279.

Oelze, M. L., Vogel, M. O., Alsharafa, K., Kahmann, U., Viehhauser, A., Maurino, V. G., et al. (2012). Efficient acclimation of the chloroplast antioxidant defence of *Arabidopsis thaliana* leaves in response to a 10- or 100-fold light increment and the possible involvement of retrograde signals. *J. Exp. Bot.* 63, 1297–1313.

Ondzighi, C. A., Christopher, D. A., Cho, E. J., Chang, S. C., and Staehelin, L. A. (2008). *Arabidopsis* protein disulfide isomerase-5 inhibits cysteine proteases during trafficking to vacuoles before programmed cell death of the endothelium in developing seeds. *Plant Cell* 20, 2205–2220.

Ooka, H., Satoh, K., Doi, K., Nagata, T., Otomo, Y., Murakami, K., et al. (2003). Comprehensive analysis of NAC family genes in *Oryza sativa* and *Arabidopsis thaliana*. *DNA Res.* 10, 239–247.

op den Camp, R. G. L., Przybyla, D., Ochsenbein, C., Laloi, C., Kim, C., Danon, A., et al. (2003). Rapid induction of distinct stress responses after the release of singlet oxygen in *Arabidopsis*. *Plant Cell* 15, 2320–2332.

Pena-Ahumada, A., Kahmann, U., Dietz, K. J., and Baier, M. (2006). Regulation of peroxiredoxin expression versus expression of Halliwell-Asada-Cycle enzymes during early seedling development of *Arabidopsis thaliana*. *Photosynth. Res.* 89, 99–112.

Pfannschmidt, T. (2010). Plastidial retrograde signaling – a true "plastid factor" or just metabolite signatures? *Trends Plant Sci.* 15, 427–435.

Pogson, B. J., Nick, S. W., Förster, B., and Small, I. (2008). Plastid signaling to the nucleus and beyond. *Trends Plant Sci.* 13, 602–609.

Schuhmann, H., and Adamska, I. (2012). Deg proteases and their role in protein quality control and processing in different subcellular compartments of the plant cell. *Physiol. Plant.* 145, 224–234.

Seidel, T., Golldack, D., and Dietz, K. J. (2005). Mapping of C-termini of V-ATPase subunits by in vivo-FRET measurements. *FEBS Lett.* 579, 4374–4382.

Seidel, T., Kluge, C., Hanitzsch, M., Ross, J., Sauer, M., Dietz, K. J., et al. (2004). Colocalization and FRET-analysis of subunits c and a of the vacuolar H+-ATPase in living plant cells. *J. Biotechnol.* 112, 165–175.

Seidel, T., Schnitzer, D., Golldack, D., and Dietz, K. J. (2008). Organelle-specific isoenzymes of plant V-ATPase as revealed by in vivo-FRET analysis. *BMC Cell Biol.* 9, 28. doi: 10.1186/1471-2121-9-28

Seidel, T., Seefeldt, B., Sauer, M., and Dietz, K. J. (2010) In vivo analysis of the 2-Cys peroxiredoxin oligomeric state by two-step FRET. *J. Biotechnol.* 149, 272–279.

Seo, P. J., Kim, M. J., Song, J. S., Kim, Y. S., Kim, H. J., and Park, C. M. (2010). Proteolytic processing of an *Arabidopsis* membrane-bound NAC transcription factor is triggered by cold-induced changes in membrane fluidity. *Biochem. J.* 427, 359–367.

Shaikhali, J., Heiber, I., Seidel, T., Ströher, E., Hiltscher, H., Birkmann, S., et al. (2008). The redox-sensitive transcription factor Rap2.4a controls nuclear expression of 2-Cys peroxiredoxin A and other chloroplast antioxidant enzymes. *BMC Plant Biol.* 8, 48. doi: 10.1186/1471-2229-8-48

Ströher, E., and Dietz, K. J. (2008). The dynamic thiol-disulphide redox proteome of the *Arabidopsis thaliana* chloroplast as revealed by differential

electrophoretic mobility. *Physiol. Plant.* 133, 566–583.

Uemura, T., Ueda, T., Ohniwa, R. L., Nakano, A., Takeyasu, K., and Sato, M. H. (2004). Systematic analysis of SNARE molecules in *Arabidopsis*: dissection of the post-Golgi Network in plant cells. *Cell Struct. Funct.* 29, 49–65

Wormuth, D., Baier, M., Kandlbinder, A., Scheibe, R., Hartung, W., and Dietz, K. J. (2006). Regulation of nuclear and chloroplast transcript levels by photosynthetic signals triggered through modified CO2 availability. *BMC Plant Biol.* 6, 15. doi: 10.1186/1471-2229-6-15

Conflict of Interest Statement: The authors declare that the research was conducted in the absence of any commercial or financial relationships that could be construed as a potential conflict of interest.

Received: 10 August 2012; paper pending published: 03 September 2012; accepted: 19 October 2012; published online: 09 November 2012.

Citation: Klein P, Seidel T, Stöcker B and Dietz K-J (2012) The membrane-tethered transcription factor ANAC089 serves as redox-dependent suppressor of stromal ascorbate peroxidase gene expression. Front. Plant Sci. ***3****:247. doi: 10.3389/fpls.2012.00247*

This article was submitted to Frontiers in Plant Physiology, a specialty of Frontiers in Plant Science.

Copyright © 2012 Klein, Seidel, Stöcker and Dietz. This is an open-access article distributed under the terms of the Creative Commons Attribution License, which permits use, distribution and reproduction in other forums, provided the original authors and source are credited and subject to any copyright notices concerning any third-party graphics etc.

frontiers in
PLANT SCIENCE

REVIEW ARTICLE
published: 19 November 2012
doi: 10.3389/fpls.2012.00257

Environmental control of plant nuclear gene expression by chloroplast redox signals

Jeannette Pfalz, Monique Liebers, Matthias Hirth, Björn Grübler, Ute Holtzegel, Yvonne Schröter, Lars Dietzel† and Thomas Pfannschmidt*†

Junior Research Group "Plant acclimation to environmental changes: Protein analysis by MS", Department of Plant Physiology, Institute of General Botany and Plant Physiology, Friedrich-Schiller-University Jena, Jena, Germany

Edited by:
Tatjana Kleine, Ludwig-Maximilians-Universität München, Germany

Reviewed by:
Norman Huner, University of Western Ontario, Canada
Conrad Mullineaux, Queen Mary, University of London, UK

****Correspondence:***
Thomas Pfannschmidt, Department of Plant Physiology, Institute of General Botany and Plant Physiology, Friedrich-Schiller-University Jena, Dornburger Str. 159, 07743 Jena, Germany.
e-mail: thomas.pfannschmidt@uni-jena.de

†Present address:
Lars Dietzel, Goethe-University Frankfurt, Frankfurt/Main, Germany
Thomas Pfannschmidt, Laboratoire de Physiologie Cellulaire et Végétale, CNRS/UJF/INRA/CEA Grenoble, Institut de Recherches en Technologies et Sciencesb pour le Vivant, Grenoble Cedex 9, France

Plant photosynthesis takes place in specialized cell organelles, the chloroplasts, which perform all essential steps of this process. The proteins involved in photosynthesis are encoded by genes located on the plastid and nuclear genomes. Proper function and regulation of light harvesting and energy fixation thus requires a tight coordination of the gene expression machineries in the two genetic compartments. This is achieved by a bi-directional exchange of information between nucleus and plastids. Signals emerging from plastids report the functional and developmental state of the organelle to the nucleus and initiate distinct nuclear gene expression profiles, which trigger responses that support or improve plastid functions. Recent research indicated that this signaling is absolutely essential for plant growth and development. Reduction/oxidation (redox) signals from photosynthesis are key players in this information network since they do report functional disturbances in photosynthesis, the primary energy source of plants. Such disturbances are caused by environmental fluctuations for instance in illumination, temperature, or water availability. These environmental changes affect the linear electron flow of photosynthesis and result in changes of the redox state of the components involved [e.g., the plastoquinone (PQ) pool] or coupled to it (e.g., the thioredoxin pool). Thus, the changes in redox state directly reflect the environmental impact and serve as immediate plastidial signals to the nucleus. The triggered responses range from counterbalancing reactions within the physiological range up to severe stress responses including cell death. This review focuses on physiological redox signals from photosynthetic electron transport (PET), their relation to the environment, potential transduction pathways to the nucleus and their impact on nuclear gene expression.

Keywords: photosynthetic acclimation, electron transport, redox signaling, gene expression, environmental sensing

INTRODUCTION

Plants are sessile and, therefore, cannot escape from unfavorable conditions in their environment. During evolution they developed a number of responses which help them to deal with varying and adverse environmental cues. These responses cover several time scales acting at the physiological level within minutes, at the developmental level within days and at the seasonal level within months. Most of these responses work at the molecular level including regulation of gene expression networks, adjustment of metabolic pathways, or nutrient allocation. One important sensing system of plants for changes in the environment is photosynthesis. Its unique combination of light-dependent light harvesting processes and temperature-dependent carbon fixation reactions makes it ideal for precise and rapid detection of abiotic environmental changes since for optimal photosynthesis both parts needs to work in a fine-tuned balance. Changes in temperature, light intensity or quality, or in the availability of water, CO_2, or nutrients may disturb this balance resulting in less efficient photosynthesis. In all cases the immediate effect is a change in photosynthetic electron flux which affects the reduction/oxidation (redox) state of the components involved in it. In many cases this change in redox state initiates acclimation responses which help the plant adapting the photosynthetic process to the changed environment (Anderson et al., 1995; Kanervo et al., 2005; Walters, 2005; Dietzel et al., 2008a; Eberhard et al., 2008). However, since photosynthesis is the ultimate source of energy for plants it is tightly connected with many other physiological and metabolic processes. The redox signals regulating photosynthesis, thus, lead to a systemic response also in non-photosynthetic processes. It is important to note that the type of response depends highly on strength and duration of the environmental disturbance and its effect on photosynthesis. In recent years laboratory experiments have uncovered a number of strategies how plants cope with the environment, but we are far away from understanding these responses under free-fluctuating conditions in nature which can vary in an unpredictable way. It

becomes increasingly clear that many redox signals occur at the same time or in varying combinations when observed under natural or variable experimental conditions. It is, therefore, reasonable to assume the action of redox signaling networks rather than that of single signaling pathways. Nevertheless, for building networks it is essential to understand the immediate molecular mechanisms initiated by a distinct redox signal. Thus, in future a combined strategy of experiments with a single changing parameter and experiments with two or more changing parameters will be required.

IMPORTANT OPERATIONAL REDOX SIGNALS FROM PHOTOSYNTHESIS

Photosynthesis, in simple terms, is the light-driven transfer of electrons and protons from water to $NADP^+$, the formation of ATP using the trans-thylakoidal proton gradient generated during this transfer and, subsequently, the use of these reduction and energy equivalents in the fixation of CO_2 to produce carbohydrates as chemical energy source for growth and development of the organism (Buchanan et al., 2002). This complex process contains many reduction and oxidation steps and, therefore, the components involved change their redox status depending on the efficiency of photosynthesis. Two of them, plastoquinone (PQ) and thioredoxin, are of special importance as they fulfil not only a function as redox-active molecules but also initiate signaling cascades which control molecular responses acclimating photosynthesis to the environment (Aro and Andersson, 2001; Foyer et al., 2012). This includes also the control of nuclear gene expression and, thus, represents an example for operational control in retrograde signaling (Pogson et al., 2008) which will be the focus of this review.

PQ is the intermediate electron carrier which connects photosystem (PS) II and the cytochrome (cyt) b_6f complex in the photosynthetic electron transport (PET) chain. This location makes this molecule pool very sensitive to any imbalance in the relative activities of PSII and PSI, especially since the PQ oxidation represents the slowest step in linear electron transport (Allen, 2004). Under conditions favoring PSII PSI becomes rate-limiting and the PQ pool receives more electrons from PSII than it can deliver to PSI resulting in a reduction of PQ. Under conditions favoring PSI the opposite situation is established and the pool becomes oxidized. These redox changes occur almost immediately and can be induced either physiologically by environmental changes or chemically by treatment with electron transport inhibitors (Pfannschmidt et al., 2009). DCMU irreversibly binds to the Q_B binding site of PSII and prevents any electron transport from PSII to subsequent acceptors resulting in oxidation of the PQ pool. DBMIB binds to the plastoquinol-oxidation site of the cyt b_6f complex resulting in PQ reduction (Trebst, 1980). It must be noted that DBMIB is a labile compound which becomes easily inactivated if not re-supplied. Furthermore it can loose its specificity since at high concentrations it also binds to the DCMU binding site. Experiments based on such inhibitor treatments, therefore, essentially require titration controls and must be checked for side effects (Pfannschmidt et al., 2009).

In photosynthesis the PQ redox state controls phosphorylation of light harvesting complex proteins of PSII (LHCII) and the relative allocation of the mobile antenna to the two PS. This short-term response (half-time ∼10 min) balances excitation energy distribution between the PSs (state transitions) and requires the action of the thylakoid-bound kinase STN7 (Rochaix, 2007). In the long-term (half-time 1–2 days) PQ redox state controls the adjustment of PS stoichiometry which requires a tight control of both plastid and nuclear encoded photosynthesis genes (Allen and Pfannschmidt, 2000). The latter requires the transduction of the PQ redox signal toward the nuclear compartment and represents an important plastidial signal.

Thioredoxins are a family of small proteins with a size of ∼12 kDa which possess a redox-active dithiol group in a conserved WCGPC amino acid motif (Schurmann and Buchanan, 2008). In *Arabidopsis* 44 different thioredoxins have been identified and a large number of them are active in the chloroplast (Meyer et al., 2005). These receive their electrons from PSI *via* the action of an enzyme called ferredoxin–thioredoxin oxidoreductase (FTR). In the dark thioredoxins are usually oxidized but become rapidly reduced upon illumination when the PET chain is activated. In their reduced state they are able to reduce regulatory thiol groups especially in the enzymes of the Calvin–Benson cycle and, by this means, control production of carbohydrates in the carbon reduction cycle of photosynthesis. They also functionally separate the reductive and oxidative pentose-phosphate pathway avoiding futile cycling of common substrates (Buchanan et al., 2002).

In recent years a number of additional thioredoxin targets have been identified for instance in the lumen (Buchanan and Balmer, 2005; Buchanan and Luan, 2005). Most recently a novel thioredoxin-like protein designated as TrxZ has been identified as subunit of the plastid RNA polymerase complex potentially linking redox regulation and plastid transcription (Arsova et al., 2010; Schroter et al., 2010). Inactivation of its gene in *Arabidopsis* creates an albino phenotype indicating that it cannot be replaced by any other thioredoxin, a property which is unique in this group of reductive proteins.

As an unavoidable side reaction of oxygenic photosynthesis reaction centres transfer electrons not only to their primary acceptors but also to molecular oxygen in their immediate surrounding generating reactive oxygen species (ROS) such as superoxide (mainly at PSI *via* ferredoxin) or singlet oxygen (mainly at PSII *via* triplett state chlorophylls) (Apel and Hirt, 2004). ROS induce oxidative damages to proteins or membrane lipids and, therefore, are harmful for all kinds of biological molecules including the photosynthetic apparatus itself (e.g., during photoinhibition). Plant cells and chloroplasts, therefore, possess a sophisticated antioxidant network consisting of reductive low-molecular weight components (glutathione, ascorbate, and α-tocopherol) (Szarka et al., 2012) as well as various enzymatic activities (superoxide dismutases, ascorbate peroxidises, peroxiredoxins, and glutaredoxins) (Dietz, 2011; Zaffagnini et al., 2012) which scavenge and detoxify ROS and a number of recently discovered reactive nitrogen species (NOS) such as nitric oxide (NO) (Navrot et al., 2011). However, ROS and NOS possess a dual role and act also as important signaling molecules in stress responses including pathogen defense and programmed cell death. This includes a number of redox-dependent protein modifications

such as glutathionylation or nitrosylation. This area of research is rapidly expanding and has been extensively reviewed elsewhere. This review will include only that work which is essential for understanding of physiological redox signals from the PQ and Trx pools and the reader interested in details of stress responses is referred to the reviews mentioned above and the references therein.

ENVIRONMENTAL INDUCTION OF PHOTOSYNTHETIC REDOX SIGNALS

The processes of light energy absorption, transfer within the antenna, and charge separation depend mainly on the biophysical properties of the reaction centres and their antenna structure. These processes are largely independent from ambient temperature; however, the amounts of photons absorbed and the efficiency of their transport are directly influenced by the quantity and the quality of the incident light (see also below). In addition, in natural habitats the illumination of plants is not constant but fluctuates within seconds and minutes, as well as daily and seasonal periods, having multiple effects on electron transport efficiency. In contrast, subsequent metabolic reaction such as the Calvin–Benson cycle, N- and S-reduction reactions or other plastid biosynthesis pathways are not directly affected by light but are strongly influenced by the environmental temperature as well as by availability of substrates, nutrients, carbon, or water. Nevertheless they require sufficient amounts of energy and reduction equivalents (i.e., ATP and $NADPH_2$) from the light reaction for optimal activity. Thus they are also dependent on the functionality of PET *via* its production of ATP and $NADPH_2$. On the other hand efficient PET is possible only if a sufficiently high concentration of final electron acceptors (i.e., $NADP^+$) is available. If metabolic activities and, thus, the use of ATP and $NADPH_2$ are down-regulated (for instance by low temperatures), the availability of these final acceptors can become limiting leading to a feedback restriction in electron transport efficiency. In conclusion, there exists a delicate balance between photosynthetic light reaction and subsequent metabolism leading to a mutual dependency which is largely determined by the residing environmental condition (**Figure 1**). This makes photosynthesis a very sensitive system for environmental changes in the surrounding of the plant

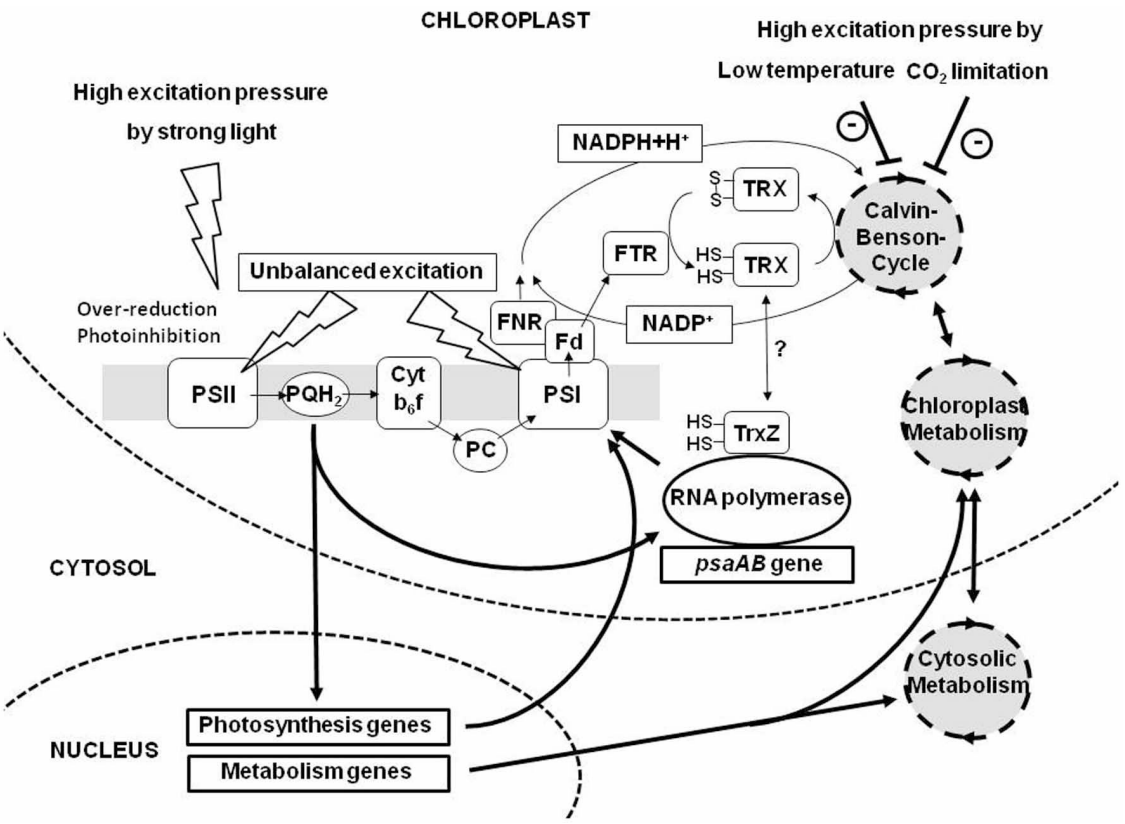

FIGURE 1 | Overview of environmental constraints affecting photosynthesis and redox-controlled gene expression events. Three major compartments of plant cells, chloroplast, cytosol, and nucleus are shown. The photosynthetic electron transport chain (consisting of the complexes PSII, Cyt b_6f complex, and PSI) and the coupled carbon fixation reactions are depicted schematically. Redox signals from the PQ pool (PQH2) and the thioredoxin system (TRX) are induced by changes in light, temperature, and CO_2 availability or combinations of these parameters. Electron transport and transfer of reducing power are indicated by thin black arrows. Redox signaling, metabolic interactions, and feedback regulation from gene expression are indicated by thick black arrows. Fd, ferredoxin; FNR, ferredoxin-NADP-oxidoreductase; FTR, ferredoxin-thioredoxin-oxidoreductase; PC, plastocyanin; *psaAB,* plastid genes for the apoproteins PsaA and PsaB of PSI (the main triggers of photosystem stoichiometry adjustment). For further details see text. How TrxZ is reduced and how it regulates the plastid RNA polymerase is unknown to date.

which are reflected by the reduction state of the electron transport chain, i.e., the PQ pool and the thioredoxin system.

Well known and characterized in this context are the influences of excitation pressure on PSII (**Figure 1**). Under conditions of high excitation pressure absorbed light energy exceeds the demands of the dark reaction leading to a reduction of the electron transport chain while under conditions of low excitation pressure the opposite occurs (Hüner et al., 1998). These two situations are, however, not unambiguous with respect to the inducing environmental condition. High excitation pressure can be induced by sudden and strong increases in light intensity resulting in the absorption of too much photons (Karpinski et al., 1997), but it can be also induced by much weaker light intensities when the efficiency of the dark reaction is strongly restricted by, e.g., a shift to low temperatures or low water availability (Ensminger et al., 2006). All situations will result in a reduced PQ pool and the increased formation of ROS (as well as a number of other signals not clearly defined yet) exacerbating a clear interpretation and understanding of results from experiments under free running conditions. Experimental set-ups, therefore, are usually designed in a way that only one environmental parameter is changed in a distinct manner to understand the respective signaling and the induced acclimation responses. Very common are variations in light intensity at a constant temperature, but also variations of temperature at a constant light intensity are useful to study the effects of excitation pressure (Hüner et al., 1998). Alternatively the redox state of the electron transport chain can be manipulated by growing plants under artificial light sources with varying light quality (Chow et al., 1990; Melis, 1991; Allen, 1992). This set-up uses the fact that the absorption maxima of PSII and PSI differ by 20 nm (680 versus 700 nm). In natural habitats a strong enrichment of far-red wave lengths occurs within a canopy or dense plant population due to selective absorption of blue and red wavelengths in the top leaf layer (Terashima and Hikosaka, 1995; Smith, 2000; Dietzel et al., 2008a). This leads to an overexcitation of PSI relative to PSII and to an imbalance in excitation energy distribution between the PSs (**Figure 1**) which is counteracted by state transitions or PS stoichiometry adjustment. Under laboratory conditions this effect can be mimicked with the use of special light sources which excite preferentially PSII or PSI leading to a reduction or oxidation of the electron transport chain. An advantage of this system is that it works in a weak intensity range (well below 50 μE photons) which largely avoids the formation of ROS and other stress related symptoms allowing to clearly separate low- and high-light effects on the electron transport chain (Mullineaux and Emlyn-Jones, 2005; Piippo et al., 2006; Wagner et al., 2008). It was shown in *Arabidopsis* that separate acclimation strategies to low and high-light conditions exist and that the plant is able to respond in quite different and distinct ways to these environmental signals (Bailey et al., 2001).

Knowledge obtained in such relatively simple experimental systems has been used to understand the much more complex situations in under realistic ecophysiological conditions. To this end recent studies investigated interactions of two or more parameters or the effects of permanently and/or freely fluctuating parameters to study the effects on the redox state of the electron transport chain and the corresponding acclimation responses (Kulheim et al., 2002; Frenkel et al., 2007; Tikkanen et al., 2010). Initial results strongly indicate that such variability in the environment creates a complex situation at the molecular level in the chloroplast which is difficult to interpret and to understand. Systems biology approaches in this field may help (see also below) as these have the power to integrate gene expression and metabolomics data (Bräutigam et al., 2009; Frenkel et al., 2009). However, bioinformatics and modeling needs to be further developed to be useful for future biological applications.

Finally, an important point which must be mentioned is that different species may respond in different ways in one and the same set-up simply because of their differing abilities, e.g., in the dissipation of excess excitation energy *via* non-photochemical quenching (NPQ). This process involves the action of the PsbS protein, a special member of the family of the light-harvesting complex proteins, and the activity of the xanthophyll cycle (Li et al., 2000; Niyogi et al., 2005). These contribute to a conformational change in the light harvesting complex of PSII under high light and the subsequent dissipation of absorbed excess light energy as heat counteracting the generation of ROS. The efficiency of NPQ, however, can be variable depending on the ecological specialization of the species (Demmig-Adams and Adams, 2006). Generalization from one species to other species, thus, is often difficult. However, comparative testing of various species or ecotypes in defined set-ups (now often called phenotyping) opens up the possibility to understand different ecological strategies of plant species and families which might help to engineer more stress-resistant or tolerant crops (Zhu et al., 2010). Development of a basic model with variable input and output parameters which puts redox signals into a framework of environmental acclimation responses in plants thus is highly desirable (Dietz and Pfannschmidt, 2011).

SIGNAL TRANSDUCTION OF CHLOROPLAST REDOX SIGNALS TOWARD THE NUCLEUS

The mechanisms by which redox signals from photosynthesis are transduced to the nucleus are largely not understood. Nevertheless, a number of proteins have been identified which are involved in the mediation of such signals at least within the plastid compartment.

The kinases STN7 and CSK1 are involved in the redox signaling from the PQ pool toward the plastid gene expression machinery which controls the adjustment of PS stoichiometry in response to long-term light quality shifts (Bonardi et al., 2005; Puthiyaveetil et al., 2008). Since PSs are composed also of nuclear encoded components this redox signaling requires a branch toward the nuclear compartment. Mutant analyses strongly suggest that the two signaling branches diverge at or directly after the STN7 kinase (Pesaresi et al., 2009). Further steps in this signaling cascade are unknown, but some experimental evidence exists that mediation of PQ redox signals both to plastid and nuclear gene expression machineries involve phosphorylation-dependent mechanisms (Escoubas et al., 1995; Steiner et al., 2009; Shimizu et al., 2010). As a theoretical possibility it has been discussed that PQ molecules from the thylakoid membrane system may also enter the envelope membrane of chloroplasts and directly signal the redox state to components associated or attached with

it (Pfannschmidt et al., 2003). Experimental data for this are, however, lacking.

The transduction of redox signals from the thioredoxin system is mainly restricted to the understanding of SH-group-mediated control of enzymatic activities in the metabolism while it is not clear how this affects plastid gene expression. Existence of a thiol-dependent signal affecting chloroplast transcription beside the phosphorylation cascade mentioned above could be shown in *in organello* run-on transcription experiments (Steiner et al., 2009) and potential candidates for its transmission are the RNA polymerase subunits PAP6/FLN1 and PAP10/TrxZ (Arsova et al., 2010; Steiner et al., 2011) (**Figure 1**). The molecular connections, however, still require extensive further investigation.

Stress-induced hydrogen peroxide has been discussed to diffuse directly to the cytosol as it is the most stable ROS which can easily pass membranes (Pfannschmidt, 2003; Foyer and Noctor, 2005; Dietzel et al., 2008b). In the cytosol it can interact with a number of potential mediators including MAP kinase cascades or *rimb* (redox imbalanced) components (Kovtun et al., 2000; Heiber et al., 2007) which control down-stream redox regulators such as Rcd1 or Rap2.4a that affect nuclear gene expression (Shaikhali et al., 2008). ROS pattern have been also discussed as long-distance signals transmitted from cell to cell through the complete plant (Mittler et al., 2011). This involves signaling of high-light stress from exposed to unexposed leaves in *Arabidopsis* (Karpinski et al., 1999) as well as induction of cell death by singlet oxygen from PSII (Meskauskiene et al., 2001; Kim et al., 2012). The latter response can be genetically suppressed by inactivation of the chloroplast-located proteins Executer 1 (Ex1) and 2 (Ex2) indicating a role of them in transmission of singlet oxygen signals (Wagner et al., 2004). How this works mechanistically and which functions are exerted by Ex1 and Ex2 is unknown to date. Gun1 (*genomes uncoupled 1*) is a penta-tricopeptide repeat (PPR) protein with still unknown function which is postulated to merge plastidial signals from gene expression and ROS sending it to the nucleus (Cottage et al., 2007; Koussevitzky et al., 2007). This might involve the action of PTM, an envelope-localized PhD transcription factor which has been postulated to be released from plastids upon receiving a plastidial signal (possibly by Gun1) (Sun et al., 2011). After release from the outer membrane by a yet unknown protease it enters the nucleus and controls the expression of the ABI4 (*abscisic acid insensitive 4*) transcription factor. Finally, an indirect way of ROS signaling has been postulated to work *via* the ROS-sensitive glutathione biosynthesis pathway (so far only in *Arabidopsis*) since it appears that the synthesizing enzymes GSH1 and 2 are localized to the chloroplast and the cytosol, respectively. This would require the transport of γ-glutamyl-cysteine out of the chloroplast in order to synthesize the complete glutathione molecule in response to the accumulation of ROS (Mullineaux and Rausch, 2005; Wachter et al., 2005).

In conclusion, the effective transmission of plastidial redox signals both generated within the physiological range and under stress conditions is elusive although a number of interesting working hypotheses exist. How these models relate to each other, therefore, is a matter of future research.

REDOX-INDUCED RESPONSE PATTERNS IN NUCLEAR GENE EXPRESSION

While the transmission of redox signals remained still elusive our understanding of the regulated target genes or gene groups has clearly improved in recent years. Initial evidence for effects of photosynthetic redox signals especially from the PQ pool on nuclear gene expression were obtained in unicellular algae (Escoubas et al., 1995; Maxwell et al., 1995) and, subsequently, also in vascular plants (Petracek et al., 1997; Pfannschmidt et al., 2001; Pursiheimo et al., 2001; Yang et al., 2001). This included changes in the transcript level, translation efficiency, or promoter usage. Typically, these set-ups used light treatments with combinations of electron transport inhibitors to affect the expression of nuclear encoded genes in model organisms like pea (Sullivan and Gray, 1999), tobacco (Pfannschmidt et al., 2001), or *Arabidopsis* (Fey et al., 2005). The favorite target gene in many cases was the Lhcb1 gene [encoding one major protein of the light-harvesting complex of PSII (LHCII)], the "classical" reporter for plastidial signaling since it displays a nicely regulated response pattern under different light treatments. In addition, also other photosynthesis-related genes were tested such as *PetE* (encoding plastocyanin), *Fed1* (encoding ferredoxin 1), or *Nia2* (encoding the cytosolic nitrate reductase) as well as the stress related *Apx2* gene (encoding the ascorbate peroxidase 2) (Karpinski et al., 1997; Petracek et al., 1997; Oswald et al., 2001; Sherameti et al., 2002). Nevertheless, all these reports must be regarded as pilot studies since they were restricted to a very small number of genes. Thus, they allowed the identification of signal origin and some regulation principles but were not representative for the response of specific gene groups such as photosynthesis associated nuclear genes (PhANGs) which are believed to be the primary target of plastidial signals.

With the successful sequencing of the *Arabidopsis* genome array technologies became available which allowed a genome-wide monitoring of nuclear gene expression changes in response to a variety of photosynthetic redox signals. This was first done with *Arabidopsis* plants which were subjected to a PQ reduction signal induced by a light quality shift from PSI- to PSII-light (Fey et al., 2005). In a parallel experiment plants were treated with the same light shift but the redox signal was blocked by the simultaneous application of DCMU. Redox controlled genes were identified by a comparison of the expression patterns in this set-up using a macroarray targeted to genes for proteins with predicted chloroplast location (Kurth et al., 2002). By this means 286 nuclear genes were identified to be under redox control. An additional inhibitor control, however, uncovered some unspecific side effect of the drug indicating that only 54 genes behaved in an "ideal" response pattern as expected if being under PQ redox control (Fey et al., 2005). Nevertheless, the number of regulated genes was unexpectedly high and not restricted to the expected target genes, i.e., PhANGs, but involved genes from all important gene groups such as gene regulation, signal transduction, or various biosynthetic pathways. In a different study *Arabidopsis* plants were subjected to light intensity and light quality shifts and the response pattern was detected with an array with around 8000 randomly selected *Arabidopsis* genes (Piippo et al., 2006). The general response was similar but it was concluded

that the responsible redox signal was initiated in the stroma of chloroplasts not in the PQ pool.

In a more recent study an extensive kinetic approach was chosen to obtain a detailed picture of the dynamics of redox signaling and the corresponding response patterns. To this end *Arabidopsis* plants were subjected to either a reduction or an oxidation signal by using light-quality shifts and samples were taken directly before and 0.5, 2, 8, and 48 h after the shift (Bräutigam et al., 2009). The subsequent gene expression profiling revealed a number of important observations: (1) It demonstrated that the gene expression changes occurred in a very quick and dynamic manner indicating that a single observation time point (as done usually) reveals only a small part of the redox regulated genes. (2) It confirmed that metabolisms genes are a major part of the responsive gene groups and that PhANGs indeed display a unique response pattern among all regulated gene groups (**Figure 1**). (3) It indicated that redox signals from the PQ pool and stromal redox components are simultaneously active and a novel model for cooperative redox signaling was deduced (Bräutigam et al., 2010) which resolved the contradicting conclusion from the earlier studies mentioned above (Fey et al., 2005; Piippo et al., 2006).

A recent study used a genetic approach for studying redox responsive genes in *Arabidopsis* mutants with defects in the genes *stn7*, *psad1*, or *psae1* (encoding the thylakoid kinase STN7 and the PSI subunits PsaE1 and PsaD1) which are all devoid of state transitions and disturbed in redox signals from the PQ pool (Pesaresi et al., 2009). Comparison of transcript profiles of greenhouse grown plants led to the identification of 56 genes which were regulated in the same manner in all three genotypes representing either potential targets for PQ redox signals or putative representatives for a compensation response. Since in this study Affymetrix full-genome arrays were used also genes for non-chloroplast located proteins could be detected which were 39 out of the identified 56 genes, indicating that plastidial redox signals also affect genes for components in compartments other than plastids (**Figure 1**). This extends the potential influence of plastidial signals to the entire cell, demonstrating that this type of regulation is important not only for the plastid itself but appears to be a general part of the cellular signaling network (see also next chapter).

In an attempt to obtain a more detailed picture of the redox regulation network in *Arabidopsis* a systems biology study performed a meta-analysis of the kinetic and genetic approaches described above supplemented with further data from literature and data bases (Yao et al., 2011). Two transcription factors, ARR10 and ATH1-B, were proposed to be hubs in the redox gene regulatory network while the major photomorphogenesis regulator HY5 was considered to be not specifically affected in its connectivity by light-quality shifts and, thus, being not a specific component of the redox signaling network.

In summary, the recent array approaches revealed a much more complex redox regulation network in plant cells than originally anticipated. Apparently, photosynthetic redox signals do not only adjust photosynthesis genes but also genes coding for metabolic enzymes, signal transduction components, and gene regulation factors. This indicates a major role for redox signals in the cellular signaling networks of plants.

RELATION OF REDOX- AND PHOTORECEPTOR-MEDIATED LIGHT RESPONSES

Light is not only an energy source for plants but also provides important information which regulates major developmental responses such as photomorphogenesis of seedlings, shade avoidance responses, phototropism, circadian rhythms, or flower induction as well as more physiological responses such as chloroplast movement or stomatal opening (Jiao et al., 2007). These responses are regulated by a battery of photoreceptors which detect wavelengths and fluency rates of incident light such as the red/far-red light detecting phytochrome family (Smith, 1995), the blue light detecting cryptochromes and phototropins (Briggs and Christie, 2002; Lin and Shalitin, 2003), or the recently discovered UV-B light receptor (Rizzini et al., 2011). All these light-receptors control specific down-stream regulators which affect nuclear gene expression (Jiao et al., 2007). Since the photosynthetic light reaction can be driven with the same wavelengths it, thus, appears possible that there exists a potential cross-talk between the photoreceptor-mediated signaling networks and light-induced redox signals from photosynthesis. This assumption was initially supported by the observation that light and plastidial signals (induced by norflurazon treatment) act at the same *cis*-elements in the promoters of nuclear photosynthesis genes *Lhcb1* and *RbcS* (Kusnetsov et al., 1996; Strand et al., 2003; Acevedo-Hernandez et al., 2005). However, photoreceptor mutants revealed fully functional photosynthetic acclimation responses (Walters et al., 1999; Fey et al., 2005) indicating that photoreceptors are neither required nor essential for redox-controlled adjustment processes in chloroplasts. On the other hand it could be shown that a number of newly isolated cryptochrome 1 alleles behaved like weak *gun* alleles and it has been hypothesized that Gun1-mediated plastidial signals remodel light-signaling networks by interaction with the basic photomorphogenesis regulators Hy5 (Ruckle et al., 2007). This apparent contradiction can be resolved by identifying the class of plastidial signals being active in this context. Norflurazon treatment and *gun* mutants characterize a distinct class of plastid signals defined as "biogenic control" which represent signaling events essential for the proper build-up of the plastidial compartment (Pogson et al., 2008) and which are decisive especially in the very early phases of chloroplast generation (Pogson and Albrecht, 2011). In contrast, redox signals from photosynthesis become active only after photomorphogenesis was successfully performed, thus representing the most prominent class of signals defined as "operational control" (Pogson et al., 2008). Therefore, it can be hypothesized that photoreceptor-mediated signaling is dominant in morphological programmes which generate new tissues while photosynthetic redox signals become important only in existing tissues which must be functionally adjusted to the environment (**Figure 2**). New observations, however, suggest that this categorization is not as clear as assumed here. Studies in variegation mutants of *Arabidopsis* could demonstrate that the degree of variegation directly and positively correlates with the intensity of excitation pressure on the growing plant (Rosso et al., 2009). Very recent studies of chloroplast

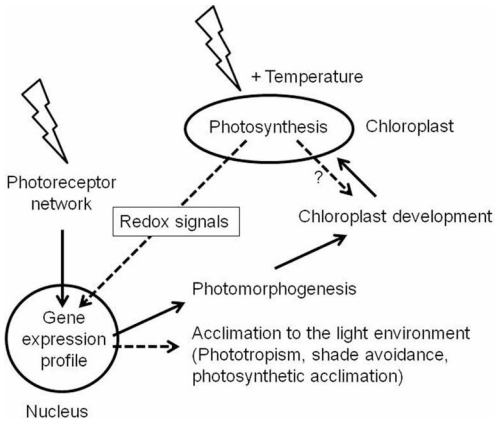

FIGURE 2 | Relation of photoreceptor- and photosynthesis-mediated light signaling. Light (indicated by flash arrows) is sensed by photoreceptors in germinating and growing seedlings. They initiate gene expression profiles in the nucleus which run the photomorphogenic programme. A central part of this programme is the build-up of chloroplasts and the photosynthetic apparatus. As soon as this is functional it serves as additional light and temperature sensing system which affects nuclear gene expression by redox signals. Potential redox signals affecting chloroplast biogenesis are indicated by a question mark. Photoreceptor - and photosynthesis-mediated signals (solid and hatched black arrows, respectively) are integrated in the nucleus and induce modifying programmes which acclimate plant growth and function to the residing environment. The interconnectivity of the respective gene expression profiles is largely unknown; however, it is assumed that photoreceptors are dominant regulators of plant development while photosynthetic redox signals preferentially control acclimation responses.

development in the shoot apex of *Arabidopsis* indicated that the fate of plastid development is determined in a very limited and small cell layer of the shoot apical meristem (Charuvi et al., 2012) providing a morphological indication that supports the likeliness of the excitation pressure model. Furthermore, other results suggest a link between plant resistance responses and plastids which might be light-mediated (Ballare et al., 2012). It appears that plastidial signals can modify plant defence responses although the molecular links are not understood yet (Karpinski et al., 2003; Kangasjarvi et al., 2012). The strong vertical light quality gradients within dense plant populations affect both the phytochrome system *via* the red to far-red ratio as well as the excitation energy distribution between the PSs. A parallel action of both signaling networks thus would be conceivable. Array data obtained in set-ups investigating light-quality regulated genes, however, uncovered only very small overlap between phytochrome- and redox-mediated transcript profiles (Bräutigam et al., 2009). This argues for a parallel rather than an interacting influence on nuclear gene expression; however, to provide final proof for this conclusion array experiments which directly address this specific question needs to be designed and performed.

In conclusion, we need more knowledge to understand how the two fundamental light-dependent signaling networks, controlled by photoreceptors and photosynthetic redox signals, are integrated to regulate nuclear gene expression. As another complication one also needs to consider the action of mitochondria, which are tightly connected to chloroplast function and redox state (Raghavendra and Padmasree, 2003). Future work needs to integrate communication pathways and metabolic interaction of the three different genetic compartments of plant cells in order to obtain a comprehensive view how they respond to environmental constraints in a coordinated manner (Pfannschmidt, 2010).

ACKNOWLEDGMENTS

Work of the authors was supported by grants from the Deutsche Forschungsgemeinschaft to Jeannette Pfalz, Thomas Pfannschmidt and the research group FOR 804 "Retrograde signaling in plants."

REFERENCES

Acevedo-Hernandez, G. J., Leon, P., and Herrera-Estrella, L. R. (2005). Sugar and ABA responsiveness of a minimal RBCS light-responsive unit is mediated by direct binding of ABI4. *Plant J.* 43, 506–519.

Allen, J. F. (1992). Protein phosphorylation in regulation of photosynthesis. *Biochim. Biophys. Acta* 1098, 275–335.

Allen, J. F. (2004). Cytochrome b(6)f: structure for signalling and vectorial metabolism. *Trends Plant Sci.* 9, 130–137.

Allen, J. F., and Pfannschmidt, T. (2000). Balancing the two photosystems: photosynthetic electron transfer governs transcription of reaction centre genes in chloroplasts. *Philos. Trans. R. Soc. Lond. B Biol. Sci.* 355, 1351–1357.

Anderson, J. M., Chow, W. S., and Park, Y.-I. (1995). The grand design of photosynthesis: acclimation of the photosynthetic apparatus to environmental cues. *Photosynth. Res.* 46, 129–139.

Apel, K., and Hirt, H. (2004). Reactive oxygen species: metabolism, oxidative stress, and signal transduction. *Annu. Rev. Plant Biol.* 55, 373–399.

Aro, E.-M., and Andersson, B. (2001). *Regulation of Photosynthesis*. Dordrecht: Kluwer Academic Publishers.

Arsova, B., Hoja, U., Wimmelbacher, M., Greiner, E., Ustun, S., Melzer, M., et al. (2010). Plastidial thioredoxin z interacts with two fructokinase-like proteins in a thiol-dependent manner: evidence for an essential role in chloroplast development in arabidopsis and *Nicotiana benthamiana*. *Plant Cell* 22, 1498–1515.

Bailey, S., Walters, R. G., Jansson, S., and Horton, P. (2001). Acclimation of *Arabidopsis thaliana* to the light environment: the existence of separate low light and high light responses. *Planta* 213, 794–801.

Ballare, C. L., Mazza, C. A., Austin, A. T., and Pierik, R. (2012). Canopy light and plant health. *Plant Physiol.* 160, 145–155.

Bonardi, V., Pesaresi, P., Becker, T., Schleiff, E., Wagner, R., Pfannschmidt, T., et al. (2005). Photosystem II core phosphorylation and photosynthetic acclimation require two different protein kinases. *Nature* 437, 1179–1182.

Bräutigam, K., Dietzel, L., Kleine, T., Ströher, E., Wormuth, D., Dietz, K. J., et al. (2009). Dynamic plastid redox signals integrate gene expression and metabolism to induce distinct metabolic states in photosynthetic acclimation in Arabidopsis. *Plant Cell* 21, 2715–2732.

Bräutigam, K., Dietzel, L., and Pfannschmidt, T. (2010). Hypothesis-a binary redox control mode as universal regulator of photosynthetic light acclimation. *Plant Signal. Behav.* 5, 81–85.

Briggs, W. R., and Christie, J. M. (2002). Phototropins 1 and 2: versatile plant blue-light receptors. *Trends Plant Sci.* 7, 204–210.

Buchanan, B. B., and Balmer, Y. (2005). Redox regulation: a broadening horizon. *Annu. Rev. Plant Biol.* 56, 187–220.

Buchanan, B. B., Gruissem, W., and Jones, R. L. (2002). *Biochemistry and Molecular Biology of Plants*. Somerset: John Wiley and Sons Inc.

Buchanan, B. B., and Luan, S. (2005). Redox regulation in the chloroplast thylakoid lumen: a new frontier in photosynthesis research. *J. Exp. Bot.* 56, 1439–1447.

Charuvi, D., Kiss, V., Nevo, R., Shimoni, E., Adam, Z., and Reich,

Z. (2012). Gain and loss of photosynthetic membranes during plastid differentiation in the shoot apex of arabidopsis. *Plant Cell* 24, 1143–1157.

Chow, W. S., Melis, A., and Anderson, J. M. (1990). Adjustments of photosystem stoichiometry in chloroplasts improve the quantum efficiency of photosynthesis. *Proc. Natl. Acad. Sci. U.S.A.* 87, 7502–7506.

Cottage, A. J., Mott, E. K., Wang, J. H., Sullivan, J. A., Maclean, D., Tran, L., et al. (2007). GUN1 (GENOMES UNCOUPLED1) encodes a pentatricopeptide repeat (PPR) protein involved in plastid protein synthesis-responsive retrograde signaling to the nucleus. *Photosynth. Res.* 91, 276.

Demmig-Adams, B., and Adams, W. W. 3rd. (2006). Photoprotection in an ecological context: the remarkable flexibility of thermal energy dissipation. *New Phytol.* 172, 11–21.

Dietz, K. J. (2011). Peroxiredoxins in plants and cyanobacteria. *Antioxid. Redox Signal.* 15, 1129–1159.

Dietz, K. J., and Pfannschmidt, T. (2011). Novel regulators in photosynthetic redox control of plant metabolism and gene expression. *Plant Physiol.* 155, 1477–1485.

Dietzel, L., Bräutigam, K., and Pfannschmidt, T. (2008a). Photosynthetic acclimation: state transitions and adjustment of photosystem stoichiometry - functional relationships between short-term and long-term light quality acclimation in plants. *FEBS J.* 275, 1080–1088.

Dietzel, L., Steiner, S., Schröter, Y., and Pfannschmidt, T. (2008b). *Plastid-To-Nucleus Communication in Plant Cells: Retrograde Signalling*. Berlin, Heidelberg: Springer.

Eberhard, S., Finazzi, G., and Wollman, F. A. (2008). The dynamics of photosynthesis. *Annu. Rev. Genet.* 42, 463–515.

Ensminger, I., Busch, F., and Huner, N. P. A. (2006). Photostasis and cold acclimation: sensing low temperature through photosynthesis. *Physiol. Plant.* 126, 28–44.

Escoubas, J. M., Lomas, M., Laroche, J., and Falkowski, P. G. (1995). Light-intensity regulation of cab gene-transcription is signaled by the redox state of the plastoquinone pool. *Proc. Natl. Acad. Sci. U.S.A.* 92, 10237–10241.

Fey, V., Wagner, R., Brautigam, K., Wirtz, M., Hell, R., Dietzmann, A., et al. (2005). Retrograde plastid redox signals in the expression of nuclear genes for chloroplast proteins of *Arabidopsis thaliana*. *J. Biol. Chem.* 280, 5318–5328.

Foyer, C. H., Neukermans, J., Queval, G., Noctor, G., and Harbinson, J. (2012). Photosynthetic control of electron transport and the regulation of gene expression. *J. Exp. Bot.* 63, 1637–1661.

Foyer, C. H., and Noctor, G. (2005). Redox homeostasis and antioxidant signaling: a metabolic interface between stress perception and physiological responses. *Plant Cell* 17, 1866–1875.

Frenkel, M., Bellafiore, S., Rochaix, J. D., and Jansson, S. (2007). Hierarchy amongst photosynthetic acclimation responses for plant fitness. *Physiol. Plant.* 129, 455–459.

Frenkel, M., Kulheim, C., Johansson Jankanpaa, H., Skogstrom, O., Dall'Osto, L., Agren, J., et al. (2009). Improper excess light dissipation in Arabidopsis results in a metabolic reprogramming. *BMC Plant Biol.* 9:12. doi: 10.1186/1471-2229-9-12

Heiber, I., Stroher, E., Raatz, B., Busse, I., Kahmann, U., Bevan, M. W., et al. (2007). The redox imbalanced mutants of arabidopsis differentiate signaling pathways for redox regulation of chloroplast antioxidant enzymes. *Plant Physiol.* 143, 1774–1788.

Hüner, N. P. A., Oquist, G., and Sarhan, F. (1998). Energy balance and acclimation to light and cold. *Trends Plant Sci.* 3, 224–230.

Jiao, Y. L., Lau, O. S., and Deng, X. W. (2007). Light-regulated transcriptional networks in higher plants. *Nat. Rev. Genet.* 8, 217–230.

Kanervo, E., Suorsa, M., and Aro, E. M. (2005). Functional flexibility and acclimation of the thylakoid membrane. *Photochem. Photobiol. Sci.* 4, 1072–1080.

Kangasjarvi, S., Neukermans, J., Li, S., Aro, E.-M., and Noctor, G. (2012). Photosynthesis, photorespiration, and light signalling in defence responses. *J. Exp. Bot.* 63, 1619–1636.

Karpinski, S., Escobar, C., Karpinska, B., Creissen, G., and Mullineaux, P. M. (1997). Photosynthetic electron transport regulates the expression of cytosolic ascorbate peroxidase genes in Arabidopsis during excess light stress. *Plant Cell* 9, 627–640.

Karpinski, S., Gabrys, H., Mateo, A., Karpinska, B., and Mullineaux, P. M. (2003). Light perception in plant disease defence signalling. *Curr. Opin. Plant Biol.* 6, 390–396.

Karpinski, S., Reynolds, H., Karpinska, B., Wingsle, G., Creissen, G., and Mullineaux, P. (1999). Systemic signaling and acclimation in response to excess excitation energy in Arabidopsis. *Science* 284, 654–657.

Kim, C., Meskauskiene, R., Zhang, S., Lee, K. P., Ashok, M. L., Blajecka, K., et al. (2012). Chloroplasts of Arabidopsis are the source and a primary target of a plant-specific programmed cell death signaling pathway. *Plant Cell* 24, 3026–3039.

Koussevitzky, S., Nott, A., Mockler, T. C., Hong, F., Sachetto-Martins, G., Surpin, M., et al. (2007). Signals from chloroplasts converge to regulate nuclear gene expression. *Science* 316, 715–719.

Kovtun, Y., Chiu, W. L., Tena, G., and Sheen, J. (2000). Functional analysis of oxidative stress-activated mitogen-activated protein kinase cascade in plants. *Proc. Natl. Acad. Sci. U.S.A.* 97, 2940–2945.

Kulheim, C., Agren, J., and Jansson, S. (2002). Rapid regulation of light harvesting and plant fitness in the field. *Science* 297, 91–93.

Kurth, J., Varotto, C., Pesaresi, P., Biehl, A., Richly, E., Salamini, F., et al. (2002). Gene-sequence-tag expression analyses of 1, 800 genes related to chloroplast functions. *Planta* 215, 101–109.

Kusnetsov, V., Bolle, C., Lubberstedt, T., Sopory, S., Herrmann, R. G., and Oelmuller, R. (1996). Evidence that the plastid signal and light operate via the same cis-acting elements in the promoters of nuclear genes for plastid proteins. *Mol. Gen. Genet.* 252, 631–639.

Li, X. P., Björkman, O., Shih, C., Grossman, A. R., Rosenquist, M., Jansson, S., et al. (2000). A pigment-binding protein essential for regulation of photosynthetic light-harvesting. *Nature* 403, 391–395.

Lin, C., and Shalitin, D. (2003). Cryptochrome structure and signal transduction. *Annu. Rev. Plant Biol.* 54, 469–496.

Maxwell, D. P., Laudenbach, D. E., and Huner, N. P. A. (1995). Redox regulation of light-harvesting complex-II and cab Messenger-RNA abundance in *Dunaliella salina*. *Plant Physiol.* 109, 787–795.

Melis, A. (1991). Dynamics of photosynthetic membrane composition and function. *Biochim. Biophys. Acta* 1058, 87–106.

Meskauskiene, R., Nater, M., Goslings, D., Kessler, F., Den Camp, R. O., and Apel, K. (2001). FLU: a negative regulator of chlorophyll biosynthesis in *Arabidopsis thaliana*. *Proc. Natl. Acad. Sci. U.S.A.* 98, 12826–12831.

Meyer, Y., Reichheld, J. P., and Vignols, F. (2005). Thioredoxins in Arabidopsis and other plants. *Photosynth. Res.* 86, 419–433.

Mittler, R., Vanderauwera, S., Suzuki, N., Miller, G., Tognetti, V. B., Vandepoele, K., et al. (2011). ROS signaling: the new wave? *Trends Plant Sci.* 16, 300–309.

Mullineaux, C. W., and Emlyn-Jones, D. (2005). State transitions: an example of acclimation to low-light stress. *J. Exp. Bot.* 56, 389–393.

Mullineaux, P. M., and Rausch, T. (2005). Glutathione, photosynthesis and the redox regulation of stress-responsive gene expression. *Photosynth. Res.* 86, 459–474.

Navrot, N., Finnie, C., Svensson, B., and Hägglund, P. (2011). Plant redox proteomics. *J. Proteomics* 74, 1450–1462.

Niyogi, K. K., Li, X. P., Rosenberg, V., and Jung, H. S. (2005). Is PsbS the site of non-photochemical quenching in photosynthesis? *J. Exp. Bot.* 56, 375–382.

Oswald, O., Martin, T., Dominy, P. J., and Graham, I. A. (2001). Plastid redox state and sugars: interactive regulators of nuclear-encoded photosynthetic gene expression. *Proc. Natl. Acad. Sci. U.S.A.* 98, 2047–2052.

Pesaresi, P., Hertle, A., Pribil, M., Kleine, T., Wagner, R., Strissel, H., et al. (2009). Arabidopsis STN7 kinase provides a link between short- and long-term photosynthetic acclimation. *Plant Cell* 21, 2402–2423.

Petracek, M. E., Dickey, L. F., Huber, S. C., and Thompson, W. F. (1997). Light-regulated changes in abundance and polyribosome association of ferredoxin mRNA are dependent on photosynthesis. *Plant Cell* 9, 2291–2300.

Pfannschmidt, T. (2003). Chloroplast redox signals: how photosynthesis controls its own genes. *Trends Plant Sci.* 8, 33–41.

Pfannschmidt, T. (2010). Plastidial retrograde signalling - a true "plastid factor" or just metabolite signatures? *Trends Plant Sci.* 15, 427–435.

Pfannschmidt, T., Brautigam, K., Wagner, R., Dietzel, L., Schroter, Y., Steiner, S., et al. (2009). Potential regulation of gene expression in photosynthetic cells by redox and energy state: approaches towards better understanding. *Ann. Bot.* 103, 599–607.

Pfannschmidt, T., Schutze, K., Brost, M., and Oelmuller, R. (2001). A novel mechanism of nuclear photosynthesis gene regulation by redox signals from the chloroplast

during photosystem stoichiometry adjustment. *J. Biol. Chem.* 276, 36125–36130.

Pfannschmidt, T., Schutze, K., Fey, V., Sherameti, I., and Oelmuller, R. (2003). Chloroplast redox control of nuclear gene expression - a new class of plastid signals in interorganellar communication. *Antioxid. Redox Signal.* 5, 95–101.

Piippo, M., Allahverdiyeva, Y., Paakkarinen, V., Suoranta, U. M., Battchikova, N., and Aro, E. M. (2006). Chloroplast-mediated regulation of nuclear genes in *Arabidopsis thaliana* in the absence of light stress. *Physiol. Genomics* 25, 142–152.

Pogson, B. J., and Albrecht, V. (2011). Genetic dissection of chloroplast biogenesis and development: an overview. *Plant Physiol.* 155, 1545–1551.

Pogson, B. J., Woo, N. S., Förster, B., and Small, I. D. (2008). Plastid signalling to the nucleus and beyond. *Trends Plant Sci.* 13, 602–609.

Pursiheimo, S., Mulo, P., Rintamaki, E., and Aro, E. M. (2001). Coregulation of light-harvesting complex II phosphorylation and lhcb mRNA accumulation in winter rye. *Plant J.* 26, 317–327.

Puthiyaveetil, S., Kavanagh, T. A., Cain, P., Sullivan, J. A., Newell, C. A., Gray, J. C., et al. (2008). The ancestral symbiont sensor kinase CSK links photosynthesis with gene expression in chloroplasts. *Proc. Natl. Acad. Sci. U.S.A.* 105, 10061–10066.

Raghavendra, A. S., and Padmasree, K. (2003). Beneficial interactions of mitochondrial metabolism with photosynthetic carbon assimilation. *Trends Plant Sci.* 8, 546–553.

Rizzini, L., Favory, J. J., Cloix, C., Faggionato, D., O'Hara, A., Kaiserli, E., et al. (2011). Perception of UV-B by the Arabidopsis UVR8 protein. *Science* 332, 103–106.

Rochaix, J. D. (2007). Role of thylakoid protein kinases in photosynthetic acclimation. *FEBS Lett.* 581, 2768–2775.

Rosso, D., Bode, R., Li, W. Z., Krol, M., Saccon, D., Wang, S., et al. (2009). photosynthetic redox imbalance governs leaf sectoring in the *Arabidopsis thaliana* variegation mutants immutans, spotty, var1, and var2. *Plant Cell* 21, 3473–3492.

Ruckle, M. E., Demarco, S. M., and Larkin, R. M. (2007). Plastid signals remodel light signaling networks and are essential for efficient chloroplast biogenesis in Arabidopsis. *Plant Cell* 19, 3944–3960.

Schroter, Y., Steiner, S., Matthai, K., and Pfannschmidt, T. (2010). Analysis of oligomeric protein complexes in the chloroplast sub-proteome of nucleic acid-binding proteins from mustard reveals potential redox regulators of plastid gene expression. *Proteomics* 10, 2191–2204.

Schurmann, P., and Buchanan, B. B. (2008). The ferredoxin/thioredoxin system of oxygenic photosynthesis. *Antioxid. Redox Signal.* 10, 1235–1273.

Shaikhali, J., Heiber, I., Seidel, T., Stroeher, E., Hiltscher, H., Birkmann, S., et al. (2008). The transcription factor Rap2.4a confers redox sensitivity to nuclear expression of chloroplast antioxidant enzymes. *BMC Plant Biol.* 8:48. doi: 10.1186/1471-2229-8-48

Sherameti, I., Sopory, S. K., Trebicka, A., Pfannschmidt, T., and Oelmuller, R. (2002). Photosynthetic electron transport determines nitrate reductase gene expression and activity in higher plants. *J. Biol. Chem.* 277, 46594–46600.

Shimizu, M., Kato, H., Ogawa, T., Kurachi, A., Nakagawa, Y., and Kobayashi, H. (2010). Sigma factor phosphorylation in the photosynthetic control of photosystem stoichiometry. *Proc. Natl. Acad. Sci. U.S.A.* 107, 10760–10764.

Smith, H. (1995). Physiological and ecological function within the phytochrome family. *Annu. Rev. Plant Physiol. Plant Mol. Biol.* 46, 289–315.

Smith, H. (2000). Phytochromes and light signal perception by plants-an emerging synthesis. *Nature* 407, 585–591.

Steiner, S., Dietzel, L., Schröter, Y., Fey, V., Wagner, R., and Pfannschmidt, T. (2009). The role of phosphorylation in redox regulation of photosynthesis genes psaA and psbA during photosynthetic acclimation of mustard. *Mol. Plant* 2, 416–429.

Steiner, S., Schröter, Y., Pfalz, J., and Pfannschmidt, T. (2011). Identification of essential subunits in the plastid-encoded RNA polymerase complex reveals building blocks for proper plastid development. *Plant Physiol.* 157, 1–13.

Strand, A., Asami, T., Alonso, J., Ecker, J. R., and Chory, J. (2003). Chloroplast to nucleus communication triggered by accumulation of Mg-protoporphyrinIX. *Nature* 421, 79–83.

Sullivan, J. A., and Gray, J. C. (1999). Plastid translation is required for the expression of nuclear photosynthesis genes in the dark and in roots of the pea lip1 mutant. *Plant Cell* 11, 901–910.

Sun, X., Feng, P., Xu, X., Guo, H., Ma, J., Chi, W., et al. (2011). A chloroplast envelope-bound PHD transcription factor mediates chloroplast signals to the nucleus. *Nat. Commun.* 2, 477.

Szarka, A., Tomaskovics, B., and Banhegyi, G. (2012). The ascorbate-glutathione-a-tocopherol triad in abiotic stress response. *Int. J. Mol. Sci.* 13, 4458–4483.

Terashima, I., and Hikosaka, K. (1995). Comparative ecophysiology of leaf and canopy photosynthesis. *Plant Cell Environ.* 18, 1111–1128.

Tikkanen, M., Grieco, M., Kangasjarvi, S., and Aro, E. M. (2010). Thylakoid protein phosphorylation in higher plant chloroplasts optimizes electron transfer under fluctuating light. *Plant Physiol.* 152, 723–735.

Trebst, A. (1980). Inhibitors in electron flow: tools for the functional and structural localization of carriers and energy conservation sites. *Methods Enzymol.* 69, 675–715.

Wachter, A., Wolf, S., Steininger, H., Bogs, J., and Rausch, T. (2005). Differential targeting of GSH1 and GSH2 is achieved by multiple transcription initiation: implications for the compartmentation of glutathione biosynthesis in the Brassicaceae. *Plant J.* 41, 15–30.

Wagner, D., Przybyla, D., Camp, R. O. D., Kim, C., Landgraf, F., Lee, K. P., et al. (2004). The genetic basis of singlet oxygen-induced stress responses of *Arabidopsis thaliana*. *Science* 306, 1183–1185.

Wagner, R., Dietzel, L., Bräutigam, K., Fischer, W., and Pfannschmidt, T. (2008). The long-term response to fluctuating light quality is an important and distinct light acclimation mechanism that supports survival of *Arabidopsis thaliana* under low light conditions. *Planta* 228, 573–587.

Walters, R. G. (2005). Towards an understanding of photosynthetic acclimation. *J. Exp. Bot.* 56, 435–447.

Walters, R. G., Rogers, J. J. M., Shephard, F., and Horton, P. (1999). Acclimation of *Arabidopsis thaliana* to the light environment: the role of photoreceptors. *Planta* 209, 517–527.

Yang, D. H., Andersson, B., Aro, E. M., and Ohad, I. (2001). The redox state of the plastoquinone pool controls the level of the light-harvesting chlorophyll a/b binding protein complex II (LHC II) during photoacclimation - Cytochrome b(6)f deficient *Lemna perpusilla* plants are locked in a state of high-light acclimation. *Photosynth. Res.* 68, 163–174.

Yao, C.-W., Hsu, B.-D., and Chen, B.-S. (2011). Constructing gene regulatory networks for long-term photosynthetic light acclimation in *Arabidopsis thaliana*. *BMC Bioinformatics* 12:335. doi: 10.1186/1471-2105-12-335

Zaffagnini, M., Bedhomme, M., Lemaire, S. D., and Trost, P. (2012). The emerging roles of protein glutathionylation in chloroplasts. *Plant Sci.* 185–186, 86–96.

Zhu, X.-G., Long, S. P., and Ort, D. R. (2010). Improving photosynthetic efficiency for greater yield. *Annu. Rev. Plant Biol.* 61, 235–261.

Conflict of Interest Statement: The authors declare that the research was conducted in the absence of any commercial or financial relationships that could be construed as a potential conflict of interest.

Received: 23 September 2012; accepted: 01 November 2012; published online: 19 November 2012.

*Citation: Pfalz J, Liebers M, Hirth M, Grübler B, Holtzegel U, Schröter Y, Dietzel L and Pfannschmidt T (2012) Environmental control of plant nuclear gene expression by chloroplast redox signals. Front. Plant Sci. **3**:257. doi: 10.3389/fpls.2012.00257*

This article was submitted to Frontiers in Plant Physiology, a specialty of Frontiers in Plant Science.

Copyright © 2012 Pfalz, Liebers, Hirth, Grübler, Holtzegel, Schröter, Dietzel and Pfannschmidt. This is an open-access article distributed under the terms of the Creative Commons Attribution License, which permits use, distribution and reproduction in other forums, provided the original authors and source are credited and subject to any copyright notices concerning any third-party graphics etc.

frontiers in
PLANT SCIENCE

REVIEW ARTICLE
published: 19 December 2012
doi: 10.3389/fpls.2012.00277

STN7 operates in retrograde signaling through controlling redox balance in the electron transfer chain

Mikko Tikkanen, Peter J. Gollan, Marjaana Suorsa, Saijaliisa Kangasjärvi and Eva-Mari Aro*

Molecular Plant Biology, Department of Biochemistry and Food Chemistry, University of Turku, Turku, Finland

Edited by:
Tatjana Kleine, Ludwig-Maximilians-Universität München, Germany

Reviewed by:
Paolo Pesaresi, Università Degli Studi di Milano, Italy
Takashi Shiina, Kyoto Prefectural University, Japan

****Correspondence:***
Eva-Mari Aro, Molecular Plant Biology, Department of Biochemistry and Food Chemistry, University of Turku, FIN–20014 Turku, Finland.
e-mail: evaaro@utu.fi

Phosphorylation of the major photosynthetic light harvesting antenna proteins by STN7 kinase balances excitation between PSII and PSI. Phosphorylation of such abundant proteins is unique, differing distinctively from conventional tasks of protein kinases in phosphorylation of low abundance proteins in signaling cascades. Excitation balance between PSII and PSI is critical for redox homeostasis between the plastoquinone and plastocyanin pools and PSI electron acceptors, determining the capacity of the thylakoid membrane to produce reactive oxygen species (ROS) that operate as signals relaying information between chloroplasts and other cellular compartments. STN7 has also been proposed to be a conventional signaling kinase, instigating the phosphorylation cascade required for coordinated expression of photosynthesis genes and assembly of the photosynthetic machinery. The absence of STN7 kinase, however, does not prevent plants from sensing redox imbalance and adjusting the stoichiometry of the photosynthetic machinery to restore redox homeostasis. This suggests that STN7 is not essential for signaling between the chloroplast and the nucleus. Here we discuss the evolution and functions of the STN7 and other thylakoid protein kinases and phosphatases, and the inherent difficulties in analyzing signaling cascades initiated from the photosynthetic machinery. Based on our analyses of literature and publicly available expression data, we conclude that STN7 exerts it signaling effect primarily by controlling chloroplast ROS homeostasis through maintaining steady-state phosphorylation of the light harvesting II proteins and the redox balance in the thylakoid membrane. ROS are important signaling molecules with a direct effect on the development of jasmonate, which in turn relays information out from the chloroplast. We propose that thylakoid membrane redox homeostasis, regulated by SNT7, sends cell-wide signals that reprogram the entire hormonal network in the cell.

Keywords: STN7, redox, thylakoid, retrograde signaling, reactive oxygen species, jasmonate biosynthesis and signaling

INTRODUCTION

Reversible protein phosphorylation modulates the cellular activity of target proteins by altering their chemical and structural characteristics, and is a ubiquitous mechanism for transmitting signals throughout the cell. Phosphorylation signal cascades usually involve the sequential phosphorylation and/or dephosphorylation of low abundance proteins including kinases, phosphatases, and protein receptors, culminating in the regulation of countless cellular metabolic processes. The reversible phosphorylation of several proteins in the plant thylakoid membrane is atypical, as these are among the most abundant membrane proteins in nature, and the physiological importance of this phenomenon is not yet fully understood. Phosphorylation of thylakoid proteins is known to play a role in coordinating the assembly and repair of the photosynthetic machinery, and in maintaining redox balance in the photosynthetic electron transfer chain (ETC) under changing environmental conditions. Membrane protein phosphorylation is also implicated in the transmission of retrograde signals from the thylakoid in response to the redox state of the intersystem ETC. This phosphorylation-mediated signal cascade has been suggested as a means of regulating the expression of chloroplast- and nuclear-encoded photosynthetic genes in response to environmental cues, hypothetically linking the operational status of the photosynthetic machinery with its assembly, repair, and acclimation according to environmental cues. The existence of such a retrograde mechanism remains hypothetical and any involvement of membrane phosphorylation, either directly or indirectly, is unclear.

At least 15 kinases and 10 phosphatases exist in higher plant chloroplasts (Bayer et al., 2012), but so far only the kinases STN7 (Bellafiore et al., 2005) and STN8 (Bonardi et al., 2005) and the phosphatases TAP38 (Pribil et al., 2010), also called PPH1 (Shapiguzov et al., 2010), and PBCP (Samol et al., 2012) have demonstrated their involvement in the heavy-duty phosphorylation of thylakoid proteins. The exploration of a possible retrograde signaling network involving thylakoid membrane phosphorylation has largely concentrated on the activities of these kinases and phosphatases, particularly on the biophysical characterizations of knockout mutants (Bellafiore et al., 2005; Bonardi et al., 2005;

Abbreviations: ETC, electron transfer chain; JA, jasmonic acid; LHC, light harvesting complex; LTR, long-term response; MeJA, methyl jasmonate; PC, plastocyanin; PQ, plastoquinone; PS, photosystem; ROS, reactive oxygen species.

Pribil et al., 2010; Shapiguzov et al., 2010; Tikkanen et al., 2010; Samol et al., 2012). However, deciphering the results of these experiments is often complex due to the primary roles of STN7, STN8, TAP38, and PBCP in maintaining redox homeostasis and proper assembly of thylakoid protein complexes, as well as the existence of multiple redox signaling pathways extending from the chloroplast. In this review we discuss the possible roles of membrane protein phosphorylation in retrograde signaling in the context of recent discoveries and common misconceptions in this field. The importance of STN7, STN8, TAP38, and PBCP in the photosynthesis, stress response, and plant development are examined in light of our *in silico* analysis of their expression and evolution in plants. Our analysis describes the far-reaching impact of thylakoid protein phosphorylation on cell signaling, plant growth, and stress response that arises from a primary role of the kinases/phosphatases in safeguarding photosynthetic redox homeostasis and production of reactive oxygen species (ROS).

THYLAKOID PROTEIN PHOSPHORYLATION; THE KNOWN AND THE UNKNOWN

The importance of reversible LHCII protein phosphorylation in inducing state transitions in the photosynthetic machinery is well known (Allen et al., 1981; Depege et al., 2003; Bellafiore et al., 2005; Pribil et al., 2010; Shapiguzov et al., 2010), but only recently it was established that the *steady-state* phosphorylation of PSII and LHCII proteins ensures balanced distribution of energy to both photosystems to control the redox status of the ETC (Grieco et al., 2012). The STN7 kinase is responsible for phosphorylation of LCHII proteins and, to a lesser extent, the PSII core proteins CP43, D1, and D2 (Bellafiore et al., 2005; Fristedt and Vener, 2011), while STN8 primarily targets the PSII core proteins (Bonardi et al., 2005; Vainonen et al., 2005) and exclusively phosphorylates the calcium signaling membrane protein Calcium Sensing Receptor (CAS; Vainonen et al., 2008). Dephosphorylation of LHCII proteins is carried out predominantly by the TAP38/PPH1 phosphatase (Pribil et al., 2010; Shapiguzov et al., 2010), while the PBCP phosphatase operates mainly in PSII core dephosphorylation (Samol et al., 2012); however, like the kinases, these two phosphatases also show some substrate overlap (Samol et al., 2012). STN7-mediated LHCII phosphorylation is required to provide sufficient excitation energy to PSI in order to maintain excitation and functional balance of PSII and PSI, which is especially important under low levels of white light, where the thermal dissipation of excitation energy is low and energy transfer from LHCII to the photosystems must be efficient (Finazzi et al., 2004; Tikkanen et al., 2010, 2011). In contrast, strong STN7- and STN8-dependent reversible phosphorylation of thylakoid proteins, induced by extreme changes in low-intensity light quality that preferentially excites either PSI (far red light) or PSII (red and blue light), distorts the excitation balance between PSII and PSI and leads to "state transitions."

In addition to its role in directly maintaining excitation balance within the photosynthetic system under white light conditions, the STN7 kinase itself is also implicated in retrograde signaling from the chloroplast to the nucleus in order to regulate the expression of nuclear-encoded photosynthetic proteins (Wagner et al., 2008; Bräutigam et al., 2009; Pesaresi et al., 2009, 2010; Leister, 2012). This so-called long-term response (LTR) occurs over a course of hours and days to readjust the stoichiometry of the components of the photosynthetic apparatus according to retrograde signals. STN7 in particular is anticipated to be an important instigator of redox-responsive retrograde signaling due to its redox-sensitive kinase activity (Pesaresi et al., 2009); however, the details of any such role and the identities of signaling intermediates are unknown. As such, the importance of STN7 and thylakoid phosphorylation for retrograde signaling remains speculative.

Analysis of *stn7* mutants in our lab shows that strong reduction of the intersystem ETC in the absence of STN7 leads to an increase in the PSI-to-PSII ratio during thylakoid membrane biogenesis (Tikkanen et al., 2006), which acts to restore the ETC redox balance and thus makes the *stn7* mutant behave like the wild type under constant growth condition (Tikkanen et al., 2006; Grieco et al., 2012). These results clearly show that *stn7* plants have the ability to monitor the redox balance of the ETC and can carry out retrograde signaling independently of any STN7-mediated phosphorylation. However, we did observe stunted growth and diminished relative amounts of PSI in *stn7* plants grown under normal growth light that was interrupted with high light peaks (Tikkanen et al., 2010), in line with the results obtained from plants that were treated with alternating 1 h of PSII and 1 h of PSI lights or with 1 h of 50 and 1 h of 240 μmol m^{-2} s^{-1} of light (Bellafiore et al., 2005), indicating that STN7 is required for effective retrograde signaling under these stressful conditions. As such, the possibility of a primary role for STN7 in phosphorylation-mediated retrograde signaling cannot be excluded, but the notion that STN7 *per se* is vital in this process appears to be untrue. This assertion challenges the *status quo* and is currently rather contentious, but the conclusion that STN7 is central to redox-induced LTR based on manipulation of the intersystem ETC in *stn7* mutants using of distinct light qualities (Bräutigam et al., 2009) may be misleading. The change in gene expression can be largely explained by the incapability of *stn7* to oxidize the ETC due to poor capture of photons by PSI in the absence of LHCII phosphorylation. Indeed, comparing *stn7* with various PSI subunit mutants that have functional STN7 kinase and LHCII phosphorylation, but are differently inhibited in the transfer of energy from P-LHCII to PSI, reveals varying levels of ETC redox unbalance that can easily account for the slight differences in the levels of gene expression, the majority of which follow a common trend among these mutants. It should also be noted that *stn7* grown in white light prior to treatment with PSI and PSII lights has corrected redox imbalance by increasing the amount of PSI complexes. However, these accumulated PSI centers become useless in PSII light, which is hardly absorbed by PSI, leading to ETC imbalance and altered redox signaling in *stn7*. Conversely, under far red light where LHCII is dephosphorylated in both WT and *stn7*, the abnormally high quantity of PSI in *stn7* is fully operational and efficiently oxidizes the ETC, again deviating the redox signaling of *stn7* from that of WT. It is important to recognize the difficulty in dissecting the effects of altered redox states in chloroplasts from those due the specific absence of STN7 in mutant plants, and these results must be interpreted carefully.

The main role of STN8-mediated phosphorylation of the PSII core proteins appears to involve the regulation of fluent turnover of PSII, although STN7 also takes part in this process (Vainonen et al.,

2005; Fristedt and Vener, 2011; Tikkanen and Aro, 2011). A further role of thylakoid protein phosphorylation exists in coordinating the assembly of the photosynthetic complexes. Phosphorylation of subunits in photosynthetic protein complexes contributes negative charges that are required for the correct structure of the machinery (Barber, 1980; Kruse et al., 1997), which is particularly important for fluent turnover of PSII under high light intensity (Tikkanen et al., 2008) and is also likely to play a part in prompt synthesis of the thylakoid protein complexes during rapid growth of new green tissues. The synthesis and assembly of the photosynthetic complexes proceed in a highly coordinated and stepwise process that is constantly regulated by dozens of proteins through feed-back mechanisms from previous assembly steps (Mulo et al., 2008). Tight regulation of this process is vital for synchronized nuclear and chloroplast gene expression, and to control the biosynthesis and membrane incorporation of chlorophyll-protein complexes, which are photosensitive and can produce damaging ROS. The activities of STN7, STN8, TAP38, and PBCP in regulating thylakoid phosphorylation positions them as important regulators of assembly of the photosynthetic machinery, and it follows that membrane signals will be altered in mutants lacking these kinases and/or phosphatases, further complicating the study of their direct involvement in retrograde signaling.

STN7 AND STN8 DOMAIN STRUCTURE AND EVOLUTION

Duplication of an ancestor serine/threonine kinase gave rise to STN7 and STN8, which share over 30% amino acid identity in *Arabidopsis*. Each conserves the characteristic serine/threonine-targeting kinase domain as well as a hydrophobic transmembrane region that is responsible for their localization in the thylakoid membrane (**Figure 1**). Unlike STN8, STN7 possesses a pair of cysteine residues situated on the N-terminal of the transmembrane domain that form a lumen-exposed disulfide bridge that is thought to modulate its kinase activity (Lemeille et al., 2009), while a unique C-terminal domain contains four sites of reversible phosphorylation which regulate the accumulation of STN7 in the membrane (Willig et al., 2011). STN8 is distinct from its paralog in its inclusion of a charged region close to the N-terminus of the kinase domain that does not appear in STN7. These characteristic features are well conserved in orthologs of STN7 and STN8 in other plants (discussed below), suggesting that the roles for the thylakoid kinases are conserved across the plant kingdom.

Duplicate kinase orthologs of STN7 and STN8 were identified in all members of the green plant lineage examined in this work, with the exception of the conifers that appear to lack an STN7 homolog (**Figure 2**). The existence of homologs in the green algae *Chlamydomonas reinhardtii* (called Stt7 and Stl1, respectively) and *Ostreococcus lucimarinus* but not in red algae or diatoms (Grouneva et al., 2012), indicate that duplication of the original serine/threonine kinase took place in the early stages of green plant evolution. Although they are relative outliers among plant serine-threonine kinases, the isolated kinase domain sequences of STN7 and STN8 show considerable homology to the B-type cyclin-dependent kinases (CDKB), which are plant-specific members of the eukaryotic CDKs that have diverged from other eukaryotic CDKs, operating to regulate gene expression and cell differentiation exclusively in plants (Corellou et al., 2005). The functional motifs required for cyclin-binding and regulation of CDKB kinase activity are not conserved in STN7 or STN8, however the possibility that the heritage of these thylakoid kinases lies in the regulation of cell cycling suggests their cellular influence may extend beyond dynamic reorganization of the thylakoid membrane to a broader role in cell signaling.

Single, well conserved STN7 and STN8 orthologs occur in higher plants, while additional duplications within this group were identified in lower plants (**Figure 2**). *STN7* duplication has occurred independently and relatively recently in the moss *Physcomitrella patens*, with both descendant genes contributing transcripts that encode typical STN7 proteins. Interestingly *P. patens* also contains duplicate *TAP38* genes, perhaps indicating

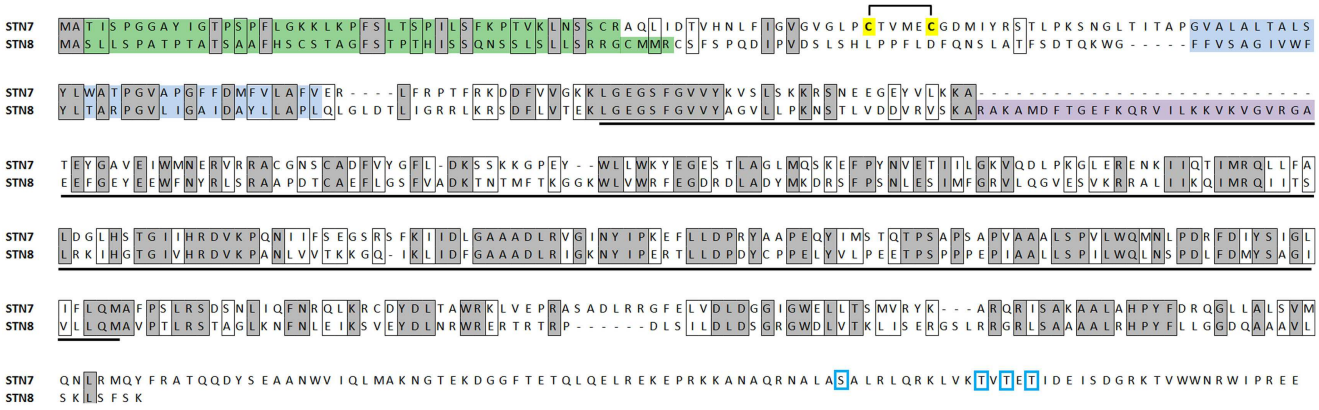

FIGURE 1 | Alignment of the amino acid sequences of STN7 (At1g68830) and STN8 (At5g01920) showing sites of identical (shaded, boxed) and similar (boxed) residues. The signal peptides (predicted using ChloroP software; http://www.cbs.dtu.dk/services/ChloroP/) are shown in green, transmembrane domains (predicted using TMHMM; http://www.cbs.dtu.dk/services/TMHMM/) are shown in blue, Ser/Thr kinase domains (detected using NCBI Conserved Domain Search; http://www.ncbi.nlm.nih.gov/Structure/cdd/wrpsb.cgi) are underlined in black. A hydrophilic sequence unique to SNT8 is shown in purple, disulfide bridge-forming cysteines in SNT7 are highlighted yellow and phosphorylated residues are boxed in blue.

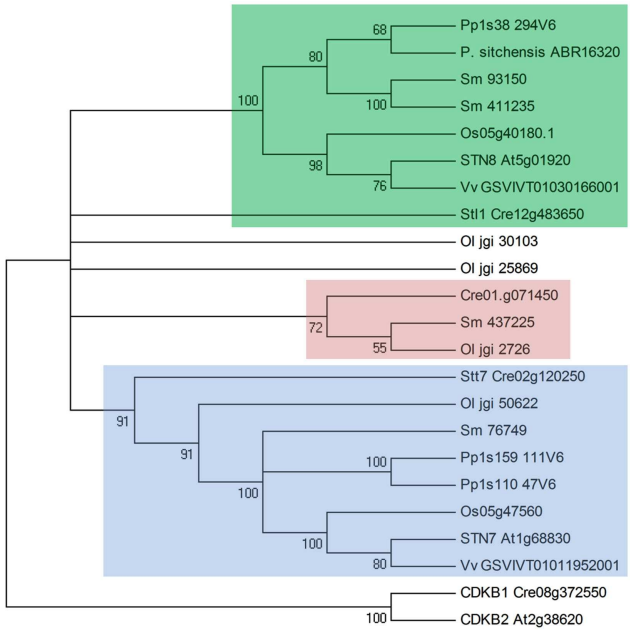

FIGURE 2 | Phylogenetic relationships between STN7, STN8, and their homologs among the green plant lineage. Shown is a condensed Neighbor-Joining tree constructed from amino acid sequences using Poisson correction in MEGA5. Numbers indicate bootstrapping values for branching points. STN7 and orthologs are highlighted blue, STN8 and orthologs are highlighted green, and predicted mitochondrial duplications within the gene family are highlighted red. Protein sequences were retrieved from the Phytozome, JGI, and NCBI GenBank genome databases, with gene identifiers shown for *Arabidopsis thaliana* (At), *Oryza sativa* (Os), *Vitis vinifera* (Vv), *Physcomitrella patens* (Pp), *Picea sitchensis* (*P. sitchensis*), *Selaginella moellendorffii* (Sm), *Chlamydomonas reinhardtii* (Cre), and *Ostreococcus lucimarinus* (Ol). Cyclin-dependent kinase B (CDKB) sequences were included as the nearest plant homologs to the STN7/STN8 kinases.

a development of two distinct antagonistic STN7/TAP38 systems regulating thylakoid membrane protein phosphorylation. The genome of the lycophyte *Selaginella moellendorffii* encodes two STN8-like kinases that are predicted to be chloroplast-localized, while *S. moellendorffii* and the algae *C. reinhardtii* and *O. lucimarinus* all contain duplications of STN7/STN8 genes that are predicted to be mitochondria-targeted and are not found in higher plants.

THYLAKOID MEMBRANE PROTEIN KINASE/PHOSPHATASE EXPRESSION ANALYSES USING MICROARRAY DATA; EXPRESSION DURING PLANT GROWTH AND DEVELOPMENT

We analyzed the expression levels of *STN7*, *STN8*, *TAP38*, and *PBCP* genes in green tissues of *Arabidopsis* Columbia-0 at different stages of plant development using publicly available microarray data (**Figure 3**). Comparison of these data revealed higher expression of all four genes in cotyledons than in vegetative rosettes, and also closely correlated expression of respective kinase-phosphatase pairs (STN7-TAP38 and STN8-PCBP), which is in line with their shared substrates and likely antagonistic roles. Strikingly, the developmental expression profiles show clear upregulation of *STN7* and *TAP38* transcripts in senescent leaves, while the expression of *STN8* and *PBCP* can be seen to decline sharply (**Figure 3**). An identical trend was observed in rice microarrays (not shown). We observed a clear upregulation of *STN7* expression in response to numerous abiotic and biotic stress conditions which, along with the relatively high *STN7/TAP38* expression during plant senescence, appears to be in conflict with the observation that LHCII phosphorylation is low under such conditions of acceptor side limited photosynthesis (Rintamäki et al., 2000; Pursiheimo et al., 2001; Hou et al., 2003). Furthermore, a decrease in LHCII protein content that would be expected to occur under these conditions would lead to degradation of STN7 (Lemeille et al., 2009; Willig et al., 2011). One explanation for *STN7* upregulation during stress and senescence may be to compensate for an unavoidable degree of stress-related inactivation or degradation of STN7 in an attempt to maintain sufficient cellular levels of the kinase. It may also be possible that STN7 performs an alternative role in these conditions. A low chlorophyll a/b ratio in the *stn7* mutant, shown to be independent of thylakoid protein stoichiometry (Tikkanen et al., 2006), suggests a role for STN7 in either chlorophyll a synthesis or chlorophyll b degradation. Interestingly, our microarray analysis showed correlation between the expression profiles of *STN7* and several genes directly involved in isoprenoid biosynthesis and/or degradation, supporting a role in regulating chlorophyll accumulation. A final possibility may be that STN7/TAP38 activity is involved in the controlled degradation of LCHII, a process that is tightly regulated to prevent untimely release of phytotoxic chlorophyll which generates ROS (Kariola et al., 2005). Notably, chlorophyll b detoxification involves initial conversion to chlorophyll a (Hortensteiner and Krautler, 2011), which could explain the low chlorophyll a/b ratio in *stn7* that may be attributed to an inability to process chlorophyll b in the mutant. Furthermore, chlorophyll degradation products are known to operate in ROS-mediated retrograde signaling during plant stress response, but many other ROS signaling pathways exist, explaining the acquisition of a compensatory signaling mechanism in *stn7* that nonetheless became insufficient or ineffective under highly stressful conditions. STN7 regulation of LHCII decomposition and chlorophyll degradation would be particularly relevant under stress and during senescence, but may also be a mechanism for retrograde regulation of gene expression that is constitutively activated throughout plant development in response to the redox condition of the thylakoid and consequently also of the chloroplast stroma.

Unlike *STN7* and *TAP38*, *STN8* and *PCPB* expression levels decreased during senescence and were unaffected by biotic and abiotic stresses. The expression profiles *STN8* and *PCPB* correlated with a large number of photosystem subunits and factors regulating the expression of plastid genes and other chloroplast development processes, suggesting a primary role in regulating the biogenesis and function of photosynthetic membranes. It is interesting to note that *STN8*/*PCPB* expression was consistent during early and later stages of vegetative growth, while *STN7*/*TAP38* expression appeared to be higher in developed rosettes. Preliminary results from our lab show that the steady-state levels of LHCII phosphorylation regulate formation of PSII-LHCII-PSI-LHCI megacomplexes that are an important factor in lateral heterogeneity

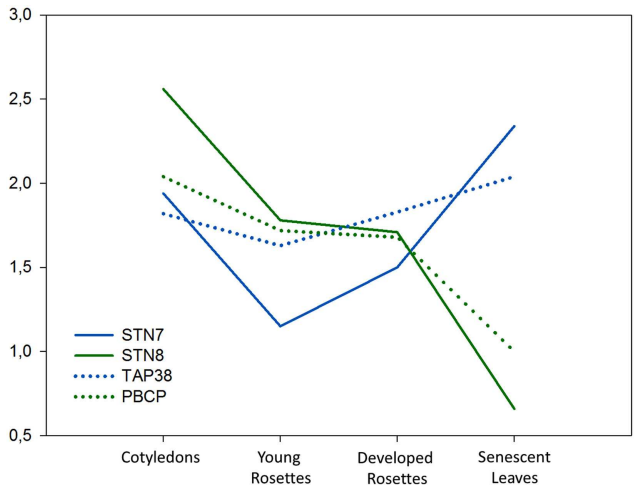

FIGURE 3 | Expression of *STN7, STN8, TAP38,* and *PBCP* in vegetative tissues during *Arabidopsis* development. Expression data were extracted from microarray data sets ATGE_1_A–C (cotyledons), ATGE_22_A–C (young rosettes), ATGE_24_A–C (developed rosettes), and ATGE_25_A–C (senescent leaves) which are available in NCBI GEO database (http://www.ncbi.nlm.nih.gov/geo/). These arrays were analyzed in the curated Bio-Array Resource database (http://bar.utoronto.ca/). Expression level >1 shows upregulation, <1 shows downregulation compared to the median level of *STN7*, *STN8*, *TAP38*, or *PBCP* expression in the AtGeneExpress database (set as 1).

of photosynthetic membranes (Rantala and Aro, unpublished), which occurs only at later stages of plant development. Strong expression of the thylakoid kinases and phosphatases, particularly STN8, in cotyledons may relate to their importance in assembly of PSII during early plant development. Additionally, they may be active in customizing the photosynthetic machinery for effective utilization of light energy during these early stages when the seedling is not capable of handling large amounts of reducing power. In light of this conceivably vital role during early plant development, it is puzzling that the *stn8* and *stn7/stn8* mutants lack any seedling phenotype compared to WT plants, although it is now clear that STN8 activity becomes important at moderate high light intensities (500–1,000 $\mu E\, m^{-2}\, s^{-1}$) that occur in nature but are lower than the light intensities commonly used in laboratory high light experiments. Interestingly, recent analysis of the *stn8* mutation in rice has described a stunted growth phenotype with severe problems in the degradation of damaged D1 protein (a congress poster and personal communication Choon-Hwan Lee and Krishna Nath).

REDOX STATE OF THYLAKOID ELECTRON TRANSFER CHAIN AFFECTS ROS SIGNALING IN PLANT STRESS RESPONSE

We analyzed gene expression using the microarrays of *stn7* and *psad* mutants (Ihnatowicz et al., 2004, 2008; Pesaresi et al., 2009) to explore the effects of interrupted redox balance, caused by over reduction of the ETC between PSII and PSI, on the expression of thylakoid membrane, Calvin cycle, and ROS-responsive genes (**Figure 4**). We compared the expression profile of the *stn7* kinase mutant to the expression profiles of other mutants and paid special attention to mutants with disturbed thylakoid redox balance (*psad*; Pesaresi et al., 2009) or those devoid of supposedly essential components of retrograde signaling. The "genomes uncoupled" (*gun*) mutants have been demonstrated to have inhibited chloroplast-to-nucleus signaling (Koussevitzky et al., 2007) and the "conditional fluorescence" (*flu*) mutant was included to elucidate chloroplast ROS-initiated and EXECUTER-protein-mediated signaling from the chloroplast (Meskauskiene et al., 2001; op den Camp et al., 2003; Lee et al., 2007). These microarray data demonstrated that the expression of photosynthetic light harvesting and Calvin cycle genes was hardly affected by changes in ETC redox balance in *stn7* and *psad*, which is in line with earlier results from our lab showing these genes to be regulated by stromal or metabolic cues resulting from normal photosynthetic activity rather than by membrane redox signals (Fey et al., 2005; Piippo et al., 2006). On the other hand, *stn7* and *psad* knockout have a strong effect on the expression of various ROS-responsive genes (discussed below). Furthermore the regulation of these genes was similar in both mutants (**Figure 4**), indicating that both generate similar retrograde signals due to their shared perturbation to thylakoid membrane redox homeostasis.

Increasing evidence suggests that photosynthetic electron transfer reactions elicit ROS signals that mediate key functions in both abiotic and biotic stress responses in plants (Kangasjärvi et al., 2012; Suzuki et al., 2012). Recently, Nomura et al. (2012) demonstrated that the thylakoid CAS protein is required for suppression of photosynthesis-related genes and upregulation of pathogenesis-related genes upon recognition of bacterial flagellin in the extra-cellular space. Analysis of microarray profiles further revealed that one third of the genes with reduced induction in *cas-1* mutants overlapped with genes induced by singlet oxygen ($^1O_2$) in the *flu* system. In *flu* mutants, dark-induced accumulation of chlorophyll intermediates causes a massive release of singlet oxygen upon re-illumination, inducing strong expression of a specific set of ROS-responsive genes (op den Camp et al., 2003; Laloi et al., 2007). Thus, among thylakoid-associated pathways, CAS is required for full elicitation of $^1O_2$-responsive gene expression changes under stress conditions, yet the role of CAS phosphorylation by STN8 in this process remains elusive.

To assess the capacities of *stn7* and *psad* mutant plants for generating ROS signals, we compared gene expression in these redox mutants with those in the *flu* mutant. Several genes that showed strongly upregulated expression in *flu* were strongly downregulated in the redox mutants, including the plasma membrane NADPH oxidase *RBOHD*, the mitochondrial alternative oxidase *AOX1a*, and the cytoplasmic thioredoxin *TRX5* (**Figure 4**), each of which mediates key functions in cellular redox signaling and is a major player in the regulation of plant immunity (Torres et al., 2002; Tada et al., 2008; Zhang et al., 2012). This apparently opposite regulation of ROS-induced gene expression in *stn7* and *psad* as compared to *flu* clearly demonstrates perturbed ROS signaling in the redox mutants. It is possible that altered PSI excitation due to ETC over reduction in *stn7* and *psad* (Pesaresi et al., 2009) limits the capacity to generate singlet oxygen that is normally produced by photosynthetic electron transfer, which may attenuate ROS signaling. Conceivably, alternative signaling pathways also contribute to the expression of ROS-responsive genes in the

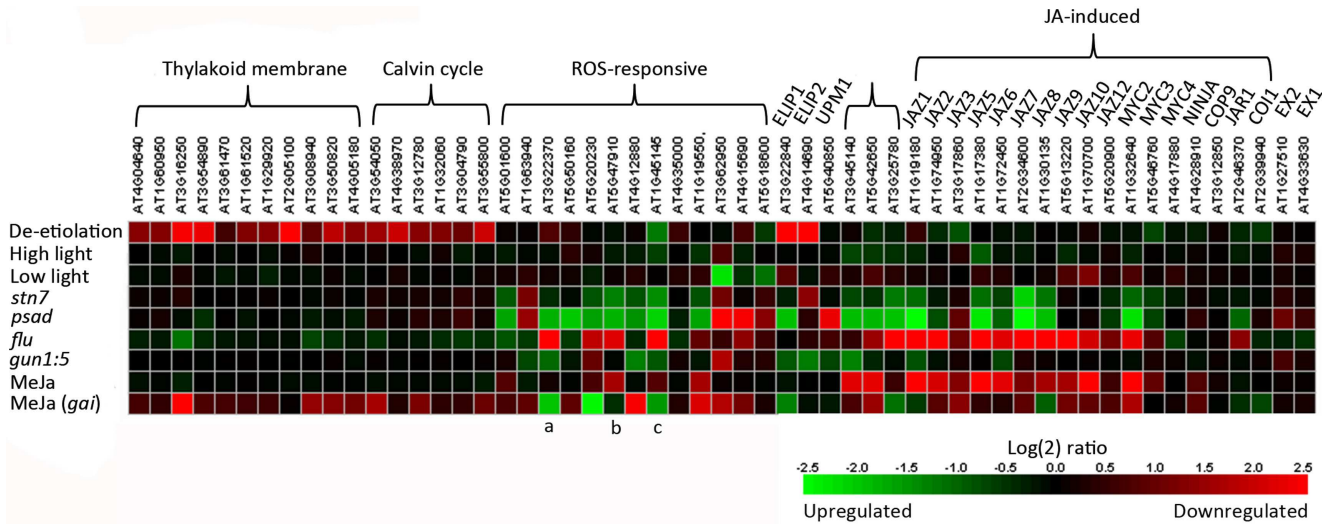

FIGURE 4 | Heat map comparing expression of relevant genes using microarray data available in the Genevestigator database (Hruz et al., 2008). Details of genes included can be found in Appendix. Light conditions shown are de-etiolation (120 min illumination of dark-adapted plants), high light treatment (120 min)/growth light, and low light (120 min)/growth light. Expression profiles of *stn7* (GEO ID: GSM399900 – 902) and *psad* (GEO ID: GSM99903 – 904) have interrupted thylakoid membrane redox balance, *flu* (GEO ID: GSM272987 – 988) constitutively produces singlet oxygen and *gun1:5* (GEO ID: GSM142773, 777, 779, 781) lacks chloroplast-to-nucleus signaling. Expression in methyl jasmonate (MeJa)-treated wildtype and giberellin-insensitive (*gai*) plants (Array Express ID: E-MEXP-883) is also shown. Specific ROS-responsive genes discussed in text are (a) AOX1a, (b) RbohD, and (c) TRX5.

nucleus. Indeed, both *stn7* and *psad* show upregulation of the gene encoding chloroplast antioxidant enzyme *MDAR6*, which is correspondingly downregulated in *flu*. These signaling effects may be related to H_2O_2, which has been shown to act antagonistically to singlet oxygen-dependent signals (Laloi et al., 2007).

NADPH oxidases are key enzymes that promote pathogen or ozone induced ROS burst in the apoplast (Kangasjärvi et al., 2005). The downregulation of *RBOHD* occurring in *stn7* and *psad* suggests that over reduction of the intersystem ETC leads to an inhibited capacity to mediate ROS signals that originate from both inside and outside the chloroplast. This may further explain the lack of any obvious ROS-related stress phenotype in the redox mutants *stn7* and *psad* that would typically arise from uncontrolled ROS signals between the chloroplast and the rest of the cell. More broadly, these findings clearly connect redox homeostasis in the thylakoid membrane, as maintained by regulated excitation energy transfer between PSI and PSII, with the transmission of ROS signals throughout the plant cell. These analyses also support the view that the redox condition of the thylakoid membrane that is sensitive to various environmental cues instigates a cell-wide response, rather than specifically regulating the expression of photosynthesis-related genes.

THE ROLE OF MEMBRANE PROTEIN PHOSPHORYLATION IN SIGNALING PATHWAYS WITHIN AND OUTSIDE OF THE CHLOROPLAST

Microarray data show that cell-wide ROS signaling is sensitive to the accumulation of reducing power in ETC and the inability to reduce PSI electron acceptors; however it remains unclear how these signals are transmitted from the thylakoid membrane to the nucleus. Our analysis of gene expression in *stn7* and *psad* with disrupted redox balance showed generally downregulated expression of genes directly involved in the biosynthesis and regulation of jasmonic acid (JA), while the same genes are upregulated in high light and strongly upregulated in *flu* (**Figure 4**). The JA signaling pathway is induced in the chloroplasts of plants subjected to high light, biotic or abiotic stress, or any factors that limit plant metabolism and/or generate surplus reducing power that exceeds the capacity of stromal metabolism. JA signaling leads to downsizing of photosynthetic pigment-protein complexes at the level of gene expression (**Figure 4**), in order to downregulate the photosynthetic activity and alleviate the pressure on the ETC in stressed plants. The response to JA is clear in the microarray data, showing photosynthetic and Calvin cycle genes to be slightly or moderately downregulated (see **Figure 4** and Appendix for details) during treatment with methyl jasmonate (MeJA), a derivative of JA. The same inhibitory effect on these genes is evident in the ROS-producing *flu* mutant, wherein the JA signaling pathway is clearly induced (**Figure 4**, Danon et al., 2005). JA synthesis enzymes and JA-induced genes encoding the MYC2 transcription factor and the "jasmonate-ZIM-domain" (JAZ) proteins are strongly downregulated in *stn7* and *psad*. This illustrates an absence of JA synthesis that occurs concomitantly with disturbed redox balance and inhibited ROS signaling in the redox mutants. Together these results suggest that JA, the biosynthesis of which is triggered by oxidation of thylakoid membrane fatty acids in the chloroplast, is a candidate for the missing intermediate in the redox-mediated signaling cascade. This aligns well with the observation that *RBOHD* is upregulated by JA treatment and downregulated in *psad* and *stn7* (**Figure 4**). ROS signals are transmitted from *flu* chloroplasts via

the plastid EXECUTER proteins (EX1 and EX2; Lee et al., 2007), both of which are downregulated in the *flu* microarray (−1.2- and −1.4-fold, respectively) and upregulated in *psad* (2.1- and 1.5-fold, respectively) and *stn7* (1.3- and 1.1-fold, respectively). Based on the findings described above, we suggest that the redox state of the thylakoid membrane determines ROS production, which in turn induces oxylipin signals that are transmitted by EXECUTERs out of the chloroplast (see **Figure 5**).

Based on these observations, one could expect that the down-regulation of JA signaling found in the *psad* and *stn7* mutants would lead to overexpression of the photosynthetic genes and enhanced growth of mutants. Indeed, the importance of JA signaling involves a role in balancing the stress response mechanisms with plant growth, to achieve optimum growth without compromising the stress tolerance. This occurs in collaboration between the JA and gibberellin (GA) signaling pathways (Yang et al., 2012). This cross-talk is clearly important for regulation of the expression of thylakoid membrane and Calvin cycle proteins, which are upregulated in MeJA-treated GA-insensitive (*gai*) mutant compared to MeJA-treated WT (**Figure 4**). The *stn7* mutant, however, grows normally, and the expression of photosynthetic genes is unchanged (**Figure 4**), suggesting that additional mechanisms can also regulate the expression of photosynthetic genes and/or compensate for interrupted JA synthesis. The *tap38* mutant, however, does grow faster than the WT under low light (Pribil et al., 2010). This phenotype could stem from a high level of LHCII

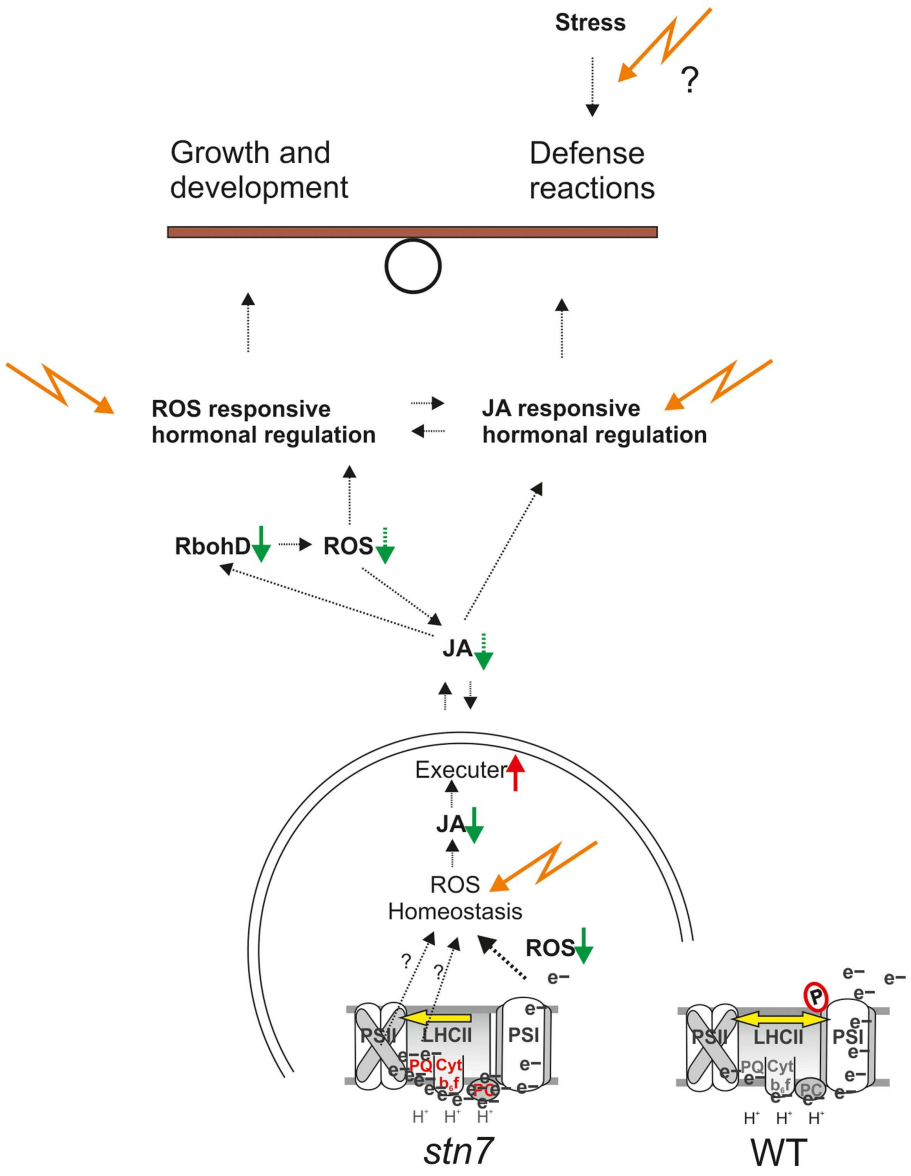

FIGURE 5 | A plant's allocation of resources to growth or defense responses is determined by a balance between growth-promoting and the defense-promoting signaling pathways. As illustrated in this model, we propose that regulation of the excitation energy distribution between PSII and PSI by thylakoid membrane protein phosphorylation controls cell signaling and systemic responses via ROS-induced, hormone-mediated signaling networks.

phosphorylation and the subsequent decrease in PSII excitation in *tap38*, which would result in an inability to efficiently reduce PSI electron acceptors and therefore lead to a highly oxidized ETC. In this respect *tap38*, *stn7*, and *psad* share dysfunctional PSI, and so it is likely that *tap38* would also have decreased JA signaling from the chloroplast. The difference lies in the ETC redox states, namely over-reduced in *stn7* and *psad* and over-oxidized in *tap38*, which could induce differing signaling cascades that may explain their different growth phenotypes. Unfortunately no large-scale gene expression data from the *tap38* mutant is currently available, but it may be hypothesized from the evidence provided in this work that the redox state of the PQ pool and the ROS status of PSI operate in relaying information from the chloroplast to the cellular signaling networks for the control of nuclear gene expression.

CONCLUDING REMARKS

An involvement of thylakoid kinases and phosphatases in regulating nuclear gene expression correlates with their relatedness to conventional signaling enzymes, and yet the unusually high concentration of phosphorylated proteins in photosynthetic membranes suggests an atypical function that may encompass a structure-dependent regulation of thylakoid activities. Our analysis indicates that a direct involvement of STN7 and membrane protein phosphorylation in signaling photosynthetic gene expression has been somewhat over-stated, and that retrograde signaling is more likely to be sensitive to the redox homeostasis of the membrane, which relies on the cooperative functioning of all photosynthetic components and their regulators. The mechanism for transmission of redox signals from the membrane to nucleus remains unclear; however, as illustrated in **Figure 5**, our results show that redox-sensitive production of ROS molecules is important for jasmonate synthesis in the chloroplast, and for hormone signaling in the wider cell.

In *stn7* and in other mutants with increased PSII function relative to PSI, such as *psad*, a decreased capacity the intersystem ETC is over-reduced while the PSI acceptor side is under-reduced, decreasing the capacity of PSI to produce H_2O_2 and possibly increasing $^1O_2$ production by PSII and LHCII, thereby modifying ROS homeostasis of the thylakoid membrane. The altered ROS homeostasis downregulates the jasmonate (JA) biosynthesis pathway and upregulates the EXECUTER (EX1 and EX2) proteins proposed to mediate emission of ROS signals from the chloroplast. We propose that the signaling molecules mediated by EX1 and EX2 proteins are jasmonates produced from thylakoid lipids according to the photosynthetic ROS status, by the enzymes that are strongly downregulated in *stn7* and *psad* (**Figure 4**). Disrupted ROS homeostasis and subsequent reduction in JA synthesis can explain the downregulation of the plasma membrane NADPH oxidase RbohD, a JA-responsive ROS-producing enzyme at the center of ROS- and hormone-mediated networks of plant defense response.

Reactive oxygen species signals impact hormone signaling pathways that operate at all levels of cellular metabolism, both through direct interaction and via JA. Under standard growth conditions, the effects of ETC redox imbalance on hormone regulation appear to be buffered or counteracted by overlapping and redundant signaling pathways. It is unknown, however, how these readjustments to redox imbalance may compromise a plant's ability to defend against plant pathogens, which is particularly relevant in the natural environment that presents continuous fluctuations in environmental conditions and an array of other abiotic and biotic stresses.

ACKNOWLEDGMENTS

The authors gratefully acknowledge funding by the Academy of Finland, project numbers 260094 (Mikko Tikkanen), 138703 (Marjaana Suorsa), CoE projects 118637 (Eva-Mari Aro), 218157 (Saijaliisa Kangasjärvi), and 130595 (Saijaliisa Kangasjärvi).

REFERENCES

Allen, J. F., Bennet, J., Steinback, K. E., and Arntzen, C. J. (1981). Chloroplast protein phosphorylation couples plastoquinone redox state to distribution of excitation energy between photosystems. *Nature* 291, 25–29.

Barber, J. (1980). Membrane surface charges and potentials in relation to photosynthesis. *Biochim. Biophys. Acta* 594, 253–308.

Bayer, R. G., Stael, S., Rocha, A. G., Mair, A., Vothknecht, U. C., and Teige, M. (2012). Chloroplast-localized protein kinases: a step forward towards a complete inventory. *J. Exp. Bot.* 63, 1713–1723.

Bellafiore, S., Barneche, F., Peltier, G., and Rochaix, J. D. (2005). State transitions and light adaptation require chloroplast thylakoid protein kinase STN7. *Nature* 433, 892–895.

Bonardi, V., Pesaresi, P., Becker, T., Schleiff, E., Wagner, R., Pfannschmidt, T., et al. (2005). Photosystem II core phosphorylation and photosynthetic acclimation require two different protein kinases. *Nature* 437, 1179–1182.

Bräutigam, K., Dietzel, L., Kleine, T., Stroher, E., Wormuth, D., Dietz, K. J., et al. (2009). Dynamic plastid redox signals integrate gene expression and metabolism to induce distinct metabolic states in photosynthetic acclimation in *Arabidopsis*. *Plant Cell* 21, 2715–2732.

Corellou, F., Camasses, A., Ligat, L., Peaucellier, G., and Bouget, F. Y. (2005). A typical regulation of a green lineage-specific B-type cyclin-dependent kinase. *Plant Physiol.* 138, 1627–1636.

Danon, A., Miersch, O., Felix, G., Camp, R. G., and Apel, K. (2005). Concurrent activation of cell death-regulating signaling pathways by singlet oxygen in *Arabidopsis thaliana*. *Plant J.* 41, 68–80.

Depege, N., Bellafiore, S., and Rochaix, J. D. (2003). Role of chloroplast protein kinase Stt7 in LHCII phosphorylation and state transition in *Chlamydomonas*. *Science* 299, 1572–1575.

Fey, V., Wagner, R., Bräutigam, K., Wirtz, M., Hell, R., Dietzmann, A., et al. (2005). Retrograde plastid redox signals in the expression of nuclear genes for chloroplast proteins of *Arabidopsis thaliana*. *J. Biol. Chem.* 280, 5318–5328.

Finazzi, G., Johnson, G. N., Dallosto, L., Joliot, P., Wollman, F. A., and Bassi, R. (2004). A zeaxanthin-independent nonphotochemical quenching mechanism localized in the photosystem II core complex. *Proc. Natl. Acad. Sci. U.S.A.* 101, 12375–12380.

Fristedt, R., and Vener, A. V. (2011). High light induced disassembly of photosystem II supercomplexes in *Arabidopsis* requires STN7-dependent phosphorylation of CP29. *PLoS ONE* 6:e24565. doi:10.1371/journal.pone.0024565

Grieco, M., Tikkanen, M., Paakkarinen, V., Kangasjärvi, S., and Aro, E. M. (2012). Steady-state phosphorylation of light-harvesting complex II proteins preserves Photosystem I under fluctuating white light. *Plant Physiol.* doi:10.1104/pp.112.206466

Grouneva, I., Gollan, P. J., Kangasjärvi, S., Suorsa, M., Tikkanen, M., and Aro, E. M. (2012). Phylogenetic viewpoints on regulation of light harvesting and electron transport in eukaryotic photosynthetic organisms. *Planta.* doi:10.1007/s00425-012-1744-5

Hortensteiner, S., and Krautler, B. (2011). Chlorophyll breakdown in higher plants. *Biochim. Biophys. Acta* 1807, 977–988.

Hou, C. X., Rintamäki, E., and Aro, E. M. (2003). Ascorbate-mediated LHCII protein phosphorylation – LHCII kinase regulation in light and in darkness. *Biochemistry* 42, 5828–5836.

Hruz, T., Laule, O., Szabo, G., Wessendorp, F., Bleuler, S., Oertle, L., et al. (2008). Genevestigator v3: a reference expression database for the meta-analysis of transcriptomes. *Adv. Bioinformatics* 2008, 420747.

Ihnatowicz, A., Pesaresi, P., Lohrig, K., Wolters, D., Muller, B., and Leister, D. (2008). Impaired photosystem I oxidation induces STN7-dependent phosphorylation of the light-harvesting complex I protein Lhca4 in *Arabidopsis thaliana*. *Planta* 227, 717–722.

Ihnatowicz, A., Pesaresi, P., Varotto, C., Richly, E., Schneider, A., Jahns, P., et al. (2004). Mutants for photosystem I subunit D of *Arabidopsis thaliana*: effects on photosynthesis, photosystem I stability and expression of nuclear genes for chloroplast functions. *Plant J.* 37, 839–852.

Kangasjärvi, J., Jaspers, P., and Kollist, H. (2005). Signalling and cell death in ozone-exposed plants. *Plant Cell Environ.* 28, 1021–1036.

Kangasjärvi, S., Neukermans, J., Li, S., Aro, E. M., and Noctor, G. (2012). Photosynthesis, photorespiration, and light signalling in defence responses. *J. Exp. Bot.* 63, 1619–1636.

Kariola, T., Brader, G., Li, J., and Palva, E. T. (2005). Chlorophyllase 1, a damage control enzyme, affects the balance between defense pathways in plants. *Plant Cell* 17, 282–294.

Koussevitzky, S., Nott, A., Mockler, T. C., Hong, F., Sachetto-Martins, G., Surpin, M., et al. (2007). Signals from chloroplasts converge to regulate nuclear gene expression. *Science* 316, 715–719.

Kruse, O., Zheleva, D., and Barber, J. (1997). Stabilization of photosystem two dimers by phosphorylation: implication for the regulation of the turnover of D1 protein. *FEBS Lett.* 408, 276–280.

Laloi, C., Stachowiak, M., Pers-Kamczyc, E., Warzych, E., Murgia, I., and Apel, K. (2007). Cross-talk between singlet oxygen- and hydrogen peroxide-dependent signaling of stress responses in *Arabidopsis thaliana*. *Proc. Natl. Acad. Sci. U.S.A.* 104, 672–677.

Lee, K. P., Kim, C., Landgraf, F., and Apel, K. (2007). EXECUTER1- and EXECUTER2-dependent transfer of stress-related signals from the plastid to the nucleus of *Arabidopsis thaliana*. *Proc. Natl. Acad. Sci. U.S.A.* 104, 10270–10275.

Leister, D. (2012). Retrograde signaling in plants: from simple to complex scenarios. *Front. Plant Sci.* 3:135. doi:10.3389/fpls.2012.00135

Lemeille, S., Willig, A., Depege-Fargeix, N., Delessert, C., Bassi, R., and Rochaix, J. D. (2009). Analysis of the chloroplast protein kinase Stt7 during state transitions. *PLoS Biol.* 7:e1000045. doi:10.1371/journal.pbio.1000045

Meskauskiene, R., Nater, M., Goslings, D., Kessler, F., Op den Camp, R., and Apel, K. (2001). FLU: a negative regulator of chlorophyll biosynthesis in *Arabidopsis thaliana*. *Proc. Natl. Acad. Sci. U.S.A.* 98, 12826–12831.

Mulo, P., Sirpiö, S., Suorsa, M., and Aro, E. M. (2008). Auxiliary proteins involved in the assembly and sustenance of photosystem II. *Photosyn. Res.* 98, 489–501.

Nomura, H., Komori, T., Uemura, S., Kanda, Y., Shimotani, K., Nakai, K., et al. (2012). Chloroplast-mediated activation of plant immune signalling in *Arabidopsis*. *Nat. Commun.* 3, 926.

op den Camp, R. G., Przybyla, D., Ochsenbein, C., Laloi, C., Kim, C., Danon, A., et al. (2003). Rapid induction of distinct stress responses after the release of singlet oxygen in *Arabidopsis*. *Plant Cell* 15, 2320–2332.

Pesaresi, P., Hertle, A., Pribi, M., Schneider, A., Kleine, T., and Leister, D. (2010). Optimizing photosynthesis under fluctuating light: the role of the *Arabidopsis* STN7 kinase. *Plant Signal. Behav.* 5, 21–25.

Pesaresi, P., Hertle, A., Pribil, M., Kleine, T., Wagner, R., Strissel, H., et al. (2009). *Arabidopsis* STN7 kinase provides a link between short- and long-term photosynthetic acclimation. *Plant Cell* 21, 2402–2423.

Piippo, M., Allahverdiyeva, Y., Paakkarinen, V., Suoranta, U. M., Battchikova, N., and Aro, E. M. (2006). Chloroplast-mediated regulation of nuclear genes in *Arabidopsis thaliana* in the absence of light stress. *Physiol. Genomics* 25, 142–152.

Pribil, M., Pesaresi, O., Hertle, A., Barbato, R., and Leister, D. (2010). Role of plastid protein phosphatase TAP38 in LHCII dephosphorylation and thylakoid electron flow. *PLoS Biol.* 8:e1000288. doi:10.1371/journal.pbio.1000288

Pursiheimo, S., Mulo, P., Rintamäki, E., and Aro, E. M. (2001). Coregulation of light-harvesting complex II phosphorylation and lhcb mRNA accumulation in winter rye. *Plant J.* 26, 317–327.

Rintamäki, E., Martinsuo, P., Pursiheimo, S., and Aro, E. M. (2000). Cooperative regulation of light-harvesting complex II phosphorylation via the plastoquinol and ferredoxin-thioredoxin system in chloroplasts. *Proc. Natl. Acad. Sci. U.S.A.* 97, 11644–11649.

Samol, I., Shapiguzov, A., Ingelsson, B., Fucile, G., Crevecoeur, M., Vener, A. V., et al. (2012). Identification of a photosystem II phosphatase involved in light acclimation in *Arabidopsis*. *Plant Cell* 24, 2596–2609.

Shapiguzov, A., Ingelsson, B., Samol, I., Andres, C., Kessler, F., Rochaix, J. D., et al. (2010). The PPH1 phosphatase is specifically involved in LHCII dephosphorylation and state transitions in *Arabidopsis*. *Proc. Natl. Acad. Sci. U.S.A.* 107, 4782–4787.

Suzuki, N., Koussevitzky, S., Mittler, R., and Miller, G. (2012). ROS and redox signalling in the response of plants to abiotic stress. *Plant Cell Environ.* 35, 259–270.

Tada, Y., Spoel, S. H., Pajerowska-Mukhtar, K., Mou, Z., Song, J., Wang, C., et al. (2008). Plant immunity requires conformational changes [corrected] of NPR1 via S-nitrosylation and thioredoxins. *Science* 321, 952–956.

Tikkanen, M., and Aro, E. M. (2011). Thylakoid protein phosphorylation in dynamic regulation of photosystem II in higher plants. *Biochim. Biophys. Acta* 1817, 232–238.

Tikkanen, M., Grieco, M., and Aro, E. M. (2011). Novel insights into plant light-harvesting complex II phosphorylation and 'state transitions.' *Trends Plant Sci.* 16, 126–131.

Tikkanen, M., Grieco, M., Kangasjarvi, S., and Aro, E. M. (2010). Thylakoid protein phosphorylation in higher plant chloroplasts optimizes electron transfer under fluctuating light. *Plant Physiol.* 152, 723–735.

Tikkanen, M., Nurmi, M., Kangasjärvi, S., and Aro, E. M. (2008). Core protein phosphorylation facilitates the repair of photodamaged photosystem II at high light. *Biochim. Biophys. Acta* 1777, 1432–1437.

Tikkanen, M., Piippo, M., Suorsa, M., Sirpiö, S., Mulo, P., Vainonen, J., et al. (2006). State transitions revisited-a buffering system for dynamic low light acclimation of *Arabidopsis*. *Plant Mol. Biol.* 62, 779–793.

Torres, M. A., Dangl, J. L., and Jones, J. D. (2002). *Arabidopsis* gp91phox homologues AtrbohD and AtrbohF are required for accumulation of reactive oxygen intermediates in the plant defense response. *Proc. Natl. Acad. Sci. U.S.A.* 99, 517–522.

Vainonen, J. P., Hansson, M., and Vener, A. V. (2005). STN8 protein kinase in *Arabidopsis thaliana* is specific in phosphorylation of photosystem II core proteins. *J. Biol. Chem.* 280, 33679–33686.

Vainonen, J. P., Sakuragi, Y., Stael, S., Tikkanen, M., Allahverdiyeva, Y., Paakkarinen, V., et al. (2008). Light regulation of CaS, a novel phosphoprotein in the thylakoid membrane of *Arabidopsis thaliana*. *FEBS J.* 275, 1767–1777.

Wagner, R., Dietzel, L., Brautigam, K., Fischer, W., and Pfannschmidt, T. (2008). The long-term response to fluctuating light quality is an important and distinct light acclimation mechanism that supports survival of *Arabidopsis thaliana* under low light conditions. *Planta* 228, 573–587.

Willig, A., Shapiguzov, A., Goldschmidt-Clermont, M., and Rochaix, J. D. (2011). The phosphorylation status of the chloroplast protein kinase STN7 of *Arabidopsis* affects its turnover. *Plant Physiol.* 157, 2102–2107.

Yang, D. L., Yao, J., Mei, C. S., Tong, X. H., Zeng, L. Z., Li, Q., et al. (2012). Plant hormone jasmonate prioritizes defense over growth by interfering with gibberellin signaling cascade. *Proc. Natl. Acad. Sci. U.S.A.* 109, E1192–E1200.

Zhang, L., Oh, Y., Li, H., Baldwin, I. T., and Galis, I. (2012). Alternative oxidase in resistance to biotic stresses: *Nicotiana attenuata* AOX contributes to resistance to a pathogen and a piercing-sucking insect but not manduca sexta larvae. *Plant Physiol.* 160, 1453–1467.

Conflict of Interest Statement: The authors declare that the research was conducted in the absence of any commercial or financial relationships that could be construed as a potential conflict of interest.

Received: 19 September 2012; accepted: 23 November 2012; published online: 19 December 2012.

*Citation: Tikkanen M, Gollan PJ, Suorsa M, Kangasjärvi S and Aro E-M (2012) STN7 operates in retrograde signaling through controlling redox balance in the electron transfer chain. Front. Plant Sci. **3**:277. doi: 10.3389/fpls.2012.00277*

This article was submitted to Frontiers in Plant Physiology, a specialty of Frontiers in Plant Science.

Copyright © 2012 Tikkanen, Gollan, Suorsa, Kangasjärvi and Aro. This is an open-access article distributed under the terms of the Creative Commons Attribution License, which permits use, distribution and reproduction in other forums, provided the original authors and source are credited and subject to any copyright notices concerning any third-party graphics etc.

APPENDIX

Function	Localization	AGI locus identifier	Description	Expression fold change	Treatment
Photosynthesis	Thylakoid membrane	At4g04640	ATP synthase subunit gamma	−1.11	MeJA
		At1g60950	Ferredoxin A	−1.02	
		At3g16250	Photosynthetic NDH subcomplex B3	−1.35	
		At3g54890	PSI light harvesting protein Lhca1	−1.06	
		At3g61470	PSI light harvesting protein Lhca2	−1.14	
		At1g61520	PSI light harvesting protein Lhca3	−1.06	
		At1g29930	PSII chlorophyll a/b-binding protein Lhcb1.3	−1.16	
		At2g05070	PSII chlorophyll a/b-binding protein Lhcb2.2	−1.47	
		At3g08940	PSII chlorophyll a/b-binding protein Lhcb4.2	−1.20	
		At3g50820	PsbO subunit of PSII oxygen-evolving complex	−1.24	
		At4g05180	PsbQ subunit of PSII oxygen-evolving complex	−1.02	
Calvin cycle	Chloroplast stroma	At3g54050	Fructose 1,6-bisphosphate phosphatase	−1.62	MeJA
		At4g38970	Fructose 1,6-bisphosphate aldolase	−1.08	
		At3g12780	Phosphoglycerate kinase	−1.08	
		At1g32060	Phosphoribulokinase	−1.28	
		At3g04790	Ribose 5-phosphate isomerase	−1.18	
		At3g55800	Sedoheptulose bisphosphatase	−1.14	
ROS-responsive	Chloroplast	At5g01600	Ferritin 1		
		At1g63940	Monodehydroascorbate reductase 6 (MDAR6)		
	Mitochondrion	At3g22370	Alternative oxidase 1a (AOX1a)		
		At5g50160	Ferric chelate reductase		
	Plasma membrane	At5g20230	Copper-binding protein/Senescence-associated gene 14 (SAG14)		
		At5g47910	Respiratory burst oxidase homolog D (RboHD)		
	Apoplast	At4g12880	Early nodulin-like protein 19 (ENODL19)		
	Cytoplasm	At1g45145	Thioredoxin 5		
		At4g35000	Ascorbate peroxidase 3		
		At1g19570	Dehydroascorbate reductase 1/5		
		At5g18600	Glutaredoxin-like protein		
	ER	At3g62950	Glutaredoxin (GRXC11)		
		At4g15690	Glutaredoxin (GRXS5)		
Chlorophyll-binding	Thylakoid Membrane	At3g22840	Early light-inducible protein 1 (ELIP1)		
		At4g14690	Early light-inducible protein 2 (ELIP2)		
Siroheme biosynthesis	Chloroplast	At5g40850	Uroporphyrin methyltransferase (UPM1)		
JA synthesis enzymes	Chloroplast	At3g45140	Lipoxygenase 2 (LOX2)		
		At5g42650	Allene oxide synthase		
		At3g25780	Allene oxide cyclize		
Negative regulation of JA-induced gene expression	Nucleus	At1g19180	Jasmonate ZIM-domain protein 1 (JAZ1)		
		At1g74950	Jasmonate ZIM-domain protein 2 (JAZ2)		
		At3g17860	Jasmonate ZIM-domain protein 3 (JAZ3)		
		At1g17380	Jasmonate ZIM-domain protein 5 (JAZ5)		
		At1g72450	Jasmonate ZIM-domain protein 6 (JAZ6)		
		At2g34600	Jasmonate ZIM-domain protein 7 (JAZ7)		
		At1g30135	Jasmonate ZIM-domain protein 8 (JAZ8)		
		At1g70700	Jasmonate ZIM-domain protein 9 (JAZ9)		
		At5g13220	Jasmonate ZIM-domain protein 10 (JAZ10)		
		At5g20900	Jasmonate ZIM-domain protein 12 (JAZ12)		
		At4g28910	Novel interactor of JAZ (NINJA)		

(Continued)

Continued

Function	Localization	AGI locus identifier	Description	Expression fold change	Treatment
Transcriptional activator of JA-responsive gene expression	Nucleus	At1g32640 At5g46760 At4g17880	MYC2 MYC3 MYC4		
JA signaling regulation	Cytoplasm/nucleus	At3g12850	Involved in COP9 signalosome complex		
Catalyzes JA-Ile synthesis, promotes JA signaling pathway	Cytoplasm	At2g46370	JA resistance1 (JAR1)		
Interacts with JAZ, required for JA-induced gene expression	Nucleus	At2g39940	Coronatine insensitive 1 (COI1)		
Relay of singlet oxygen-induced signal	Thylakoid Membrane	At4g33630 At1g27510	Executer1 (EX1) Executer2 (EX2)		

frontiers in
PLANT SCIENCE

REVIEW ARTICLE
published: 20 November 2012
doi: 10.3389/fpls.2012.00255

Chloroplast redox imbalance governs phenotypic plasticity: the "grand design of photosynthesis" revisited

Norman P. A. Hüner[1,2]*, Rainer Bode[1,2], Keshav Dahal[1,2†], Lauren Hollis[1,2], Dominic Rosso[1,2], Marianna Krol[1,2] and Alexander G. Ivanov[1,2]

[1] Department of Biology, Western University, London, ON, Canada
[2] The Biotron Centre for Experimental Climate Change Research, Western University, London, ON, Canada

Edited by:
Dario Leister,
Ludwig-Maximilians-University
Munich, Germany

Reviewed by:
Eva-Mari Aro, University of Turku,
Finland
Thomas Pfannschmidt,
Friedrich-Schiller-University Jena,
Germany

***Correspondence:**
Norman P. A. Hüner, Department of
Biology, Western University,
London, Canada N6A 5B7.
e-mail: nhuner@uwo.ca

†Present address:
Keshav Dahal, Department of Cell and
Systems Biology, University of
Toronto at Scarborough, 1265 Military
Trail, Scarborough, Canada M1C 1A4.

Sunlight, the ultimate energy source for life on our planet, enters the biosphere as a direct consequence of the evolution of photoautotrophy. Photoautotrophs must balance the light energy absorbed and trapped through extremely fast, temperature-insensitive photochemistry with energy consumed through much slower, temperature-dependent biochemistry and metabolism. The attainment of such a balance in cellular energy flow between chloroplasts, mitochondria and the cytosol is called photostasis. Photoautotrophs sense cellular energy imbalances through modulation of excitation pressure which is a measure of the relative redox state of Q_A, the first stable quinone electron acceptor of photosystem II reaction centers. High excitation pressure constitutes a potential stress condition that can be caused either by exposure to an irradiance that exceeds the capacity of C, N, and S assimilation to utilize the electrons generated from the absorbed energy or by low temperature or any stress that decreases the capacity of the metabolic pathways downstream of photochemistry to utilize photosynthetically generated reductants. The similarities and differences in the phenotypic responses between cyanobacteria, green algae, crop plants, and variegation mutants of *Arabidopsis thaliana* as a function of cold acclimation and photoacclimation are reconciled in terms of differential responses to excitation pressure and the predisposition of photoautotrophs to maintain photostasis. The various acclimation strategies associated with green algae and cyanobacteria versus winter cereals and *A. thaliana* are discussed in terms of retrograde regulation and the "grand design of photosynthesis" originally proposed by Arnon (1982).

Keywords: acclimation, excitation pressure, phenotype, photostasis, plasticity, redox sensing/signaling

INTRODUCTION

Evolution has harnessed sunlight as the energy source for life because it is cheap, abundant, available in a very predictable manner and present in seemingly inexhaustible quantities when measured on a biological time scale. In photoautotrophic eukaryotes, the integral, thylakoid membrane, chlorophyll-pigment-protein complexes associated with photosystem II (PSII) and photosystem I (PSI) absorb, convert, and trap this energy as electrons (**Figure 1**). Intersystem photosynthetic electron transport (PET) connects the two photosystems through coupled oxidation–reduction of the plastoquinone (PQ) pool, the Cytochrome b_6/f complex (Cyt b_6/f), and plastocyanin (PC). The net result of linear PET is the biosynthesis of reducing power in the form of NADPH and chemical energy in the form of ATP. Alternatively, electrons generated by PSI can be re-cycled through PSI cyclic PET which allows photosynthetic organisms to regulate ATP/NADPH ratios in the chloroplast (Shikanai, 2007; Johnson, 2011)

An astonishing characteristic of photosynthesis is that evolution has combined processes that exhibit extreme disparities in temperature sensitivities and rate constants that differ by at least 10 orders of magnitude (Hüner and Grodzinski, 2011). Consequently, photosynthetic organisms are predisposed to maintain a balance between the rates of light energy trapping through extremely fast (femtosecond to picosecond time scale) but temperature-insensitive photophysical and photochemical processes of light absorption, energy transfer, and charge separation that generates electrons within the photosynthetic reaction centers versus the much slower but very temperature-sensitive processes of C, N, and S-metabolism (**Figure 1**), and ultimately growth and development that utilize the photosynthetic reductants. To overcome this disparity in reaction rates and temperature sensitivity, non-photochemical quenching mechanisms (NPQ) have evolved to dissipate any excess energy not used in photosynthesis as heat either through antenna quenching via the xanthophyll cycle (Demmig-Adams and Adams, 1992; Horton et al., 1996, 2008; Demmig-Adams et al., 1999) and/or reaction center quenching through PSII charge recombination (Krause and Weis, 1991; Walters and Horton, 1993; Hüner et al., 2006) to protect the PSII reaction center from over-excitation and ensure survival in a fluctuating light environment (**Figure 1**). The balance between energy trapping versus energy utilization and/or dissipation is called photostasis.

Photostasis can be represented by the equation, $\sigma_{PSII} \cdot E_k = \tau^{-1}$ (Falkowski and Chen, 2003; Hüner et al., 2003) where σ_{PSII} is the effective absorption cross-section of PSII, E_k is the irradiance (I) at which the maximum photosynthetic quantum yield

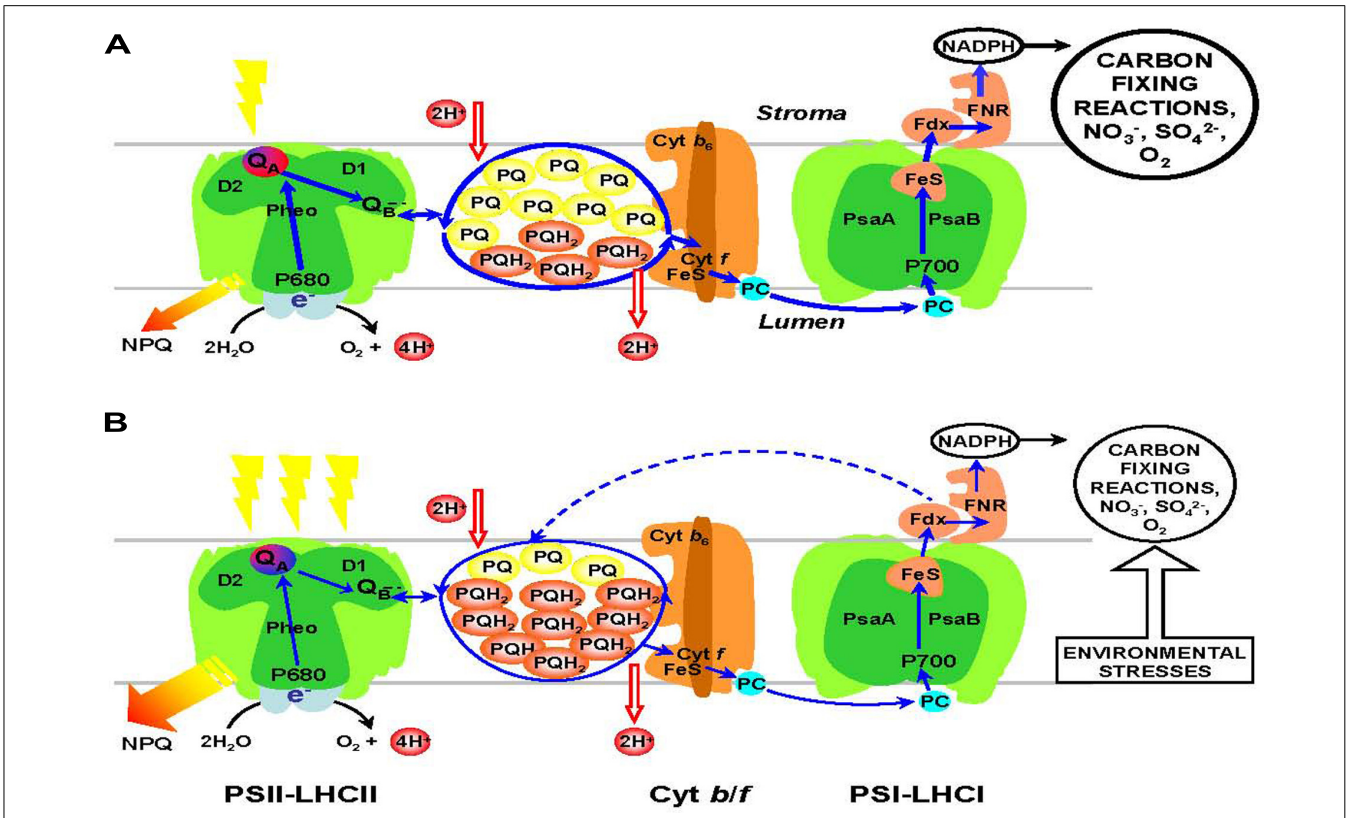

FIGURE 1 | General model of the photosynthetic electron transport chain. (A) Low excitation pressure conditions are indicated by a single yellow lighting bolt. Under these conditions, the PQ pool is largely in the oxidized state because the rate of photosynthetic electron transport plus NPQ match the rate of consumption of photosynthetic reductant, NADPH. Thick solid blue arrows indicate linear electron transport from photosystem II (PSII) to photosystem I (PSI) to reduce $NADP^+$ to NADPH which is consumed by C, N, and S metabolism. Energy dissipated as heat through NPQ is minimal. PQ, plastoquinone (yellow); PQH_2, plastoquinol (orange). **(B)** High excitation pressure conditions can be generated by either high light (3 lightning bolts) or by environmental stresses such as low temperature or nutrient stress which inhibit rates of metabolism. Under these conditions, the PQ pool is largely reduced to plastoquinol and energy dissipated through NPQ is increased. Consequently, rates of linear electron transport between PSII and PSI decrease (thin solid blue arrows) and enhance rates of PSI cyclic electron transport (broken blue arrow).

balances photosynthetic capacity and τ^{-1} is the turnover rate of metabolic sinks, such as the assimilation of C, N, or S and ultimately by growth and development, that consume photosynthetic electrons. The product $\sigma_{PSII} \cdot E_k$ is, by and large, insensitive to temperature in the biologically significant range (0–45°C) because it reflects the photophysical processes of light absorption and energy transfer within the light-harvesting antennae and core antennae pigment–protein complexes, which result in the induction of photochemistry and a charge separated state in the PSII reaction center. Although PSI absorbs light, its photochemical turnover rate is much higher than PSII and is normally not considered to be rate-limiting in PET (Ke, 2001) and therefore is not included in the equation for photostasis. In contrast, τ^{-1}, which reflects biochemical reactions that consume photosynthetically generated electrons, is very temperature-sensitive (Melis, 1998; Hüner et al., 2003; Ensminger et al., 2006; Wilson et al., 2006; McDonald et al., 2011).

High excitation pressure (HEP) is a consequence of an imbalance between energy trapped through photochemistry versus energy either utilized through biochemistry or dissipated through NPQ and will occur whenever $\sigma_{PSII} \cdot E_k > \tau^{-1}$ (Hüner et al., 2003; Ensminger et al., 2006; Wilson et al., 2006). Since the oxidation of plastoquinol (PQH_2) by the Cyt b_6/f complex is the rate-limiting step of intersystem PET (Haehnel, 1984), HEP results in an over-reduction of the PQ pool and the intersystem PET chain (**Figure 1**). This can be detected *in vivo* as an accumulation of closed PSII reaction centers and quantified by Chl a fluorescence as either 1-qP (Dietz et al., 1985; Hüner et al., 1998) or 1-qL (Hendrickson et al., 2004; Kramer et al., 2004; Baker, 2008) where qP and qL represent the photochemical quenching parameter (Schreiber et al., 1994; Baker, 2008). HEP occurs under any condition whereby $I > E_k$, and can be generated by many environmental conditions including exposure to high light (HL) or any combination of HL or low temperature (LT), nutrient limitation or water status. Thus, theoretically, the effects of acclimation to any of these stresses on the structure and function of the photosynthetic apparatus should mimic acclimation to high irradiance (Hüner et al., 1998, 2003; Ensminger et al., 2006; Wilson et al., 2006).

Photoautotrophs respond to growth and development under HEP by remodeling the structure and function of the photosynthetic apparatus to balance cellular energy flow and establish a new photostatic state. According to the equation for photostasis,

this can occur in the following ways: first, by enhancing sink capacity (τ^{-1}) through increased rates of energetically "useful" processes that consume photosynthetic reductants and fixed C such as respiration, N-assimilation and ultimately growth which results in increased biomass production. Alternatively, photostasis can be achieved by decreasing the efficiency of light absorption and trapping (σ_{PSII}) through energetically "wasteful" processes by either increasing rates of NPQ through stimulation of the xanthophyll cycle in the short-term (Demmig-Adams and Adams, 1992; Demmig-Adams et al., 1999) and/or reducing the physical size of the light-harvesting complex to decrease the probability of light absorption itself in the long-term (Hüner et al., 2003). However, the specific strategies employed to re-establish photostasis appear to be species-dependent and may result in alterations in the observable characteristics of an individual due to genotype versus environment interactions. Thus, a single genotype may exhibit variable phenotypes in response to changes in their environment. This is defined as phenotypic plasticity which reflects the integrated regulation of transcriptional, translational, and post-translational events with higher order processes associated with metabolism, growth, and photomorphogenesis. The latter is defined as the development of plant form and structure by light other than that utilized in photosynthesis. In contrast to photosynthesis, photomorphogenesis is regulated by specialized photoreceptors such as phytochrome and cryptochrome (Quail et al., 1995; Cashmore, 1997; Whitelam and Devlin, 1998). The focus of this review is on the role of light absorbed by the photosynthetic apparatus in governing phenotypic plasticity independent of photomorphogenesis. Fey et al. (2005) showed that redox signals from the photosynthetic apparatus can operate through retrograde signaling to affect nuclear gene expression independently of signaling through photoreceptors involved in photomorphogenesis. Furthermore, using various photomorphogenic mutants of *Arabidopsis thaliana*, Walters et al. (1999) showed that *Arabidopsis* mutants impaired in photomorphogenesis still retained the ability to adjust the structure and function of the photosynthetic apparatus in response to changes in growth irradiance. Thus, photoreceptors involved in photomorphogenesis are not required for the remodeling of the photosynthetic apparatus during the re-establishment of photostasis.

Energy sensing/signaling, retrograde regulation, and the molecular mechanisms that underlie phenotypic plasticity are complex, integrated cellular processes. Due to inherent restrictions with respect to length of this manuscript, we are not able to provide an exhaustive review of all pertinent published data in these areas of research. Rather, we focus on specific examples of acclimation to irradiance and temperature to illustrate how excitation pressure sensed within the chloroplast governs both local as well as distant molecular events to affect phenotypic plasticity.

REGULATION OF PHENOTYPIC PLASTICITY IN GREEN ALGAE AND CYANOBACTERIA

Growth and development of the green algae, *Dunaliella tertiolecta*, *D. salina*, and *Chlorella vulgaris*, under HL results in a typical yellow to yellow-green, HEP phenotype which is characterized by low Chl per cell and high ratios of Chl a/b ($\geq$10) compared to the typical green phenotype observed upon growth at low light (Sukenik et al., 1987; Escoubas et al., 1995; Maxwell et al., 1995a,b; Wilson and Hüner, 2000). Since the nuclear encoded LHCII polypeptides bind the bulk of the Chl in eukaryotic chloroplasts (Green et al., 2003), this HL phenotype reflects alterations in σ_{PSII}. Since the equivalent phenotype is generated by growth at LT and moderate irradiance which generates an excitation pressure comparable to the HL condition in *D. salina* and *Chlorella vulgaris* as well as the filamentous cyanobacterium, *Plectonema boryanum*, this phenotype is not a HL phenotype *per se* but rather should be considered a HEP phenotype (Maxwell et al., 1995a,b; Hüner et al., 1998, 2003; Miskiewicz et al., 2000, 2002; Wilson et al., 2003, 2006; Ensminger et al., 2006). The decrease in σ_{PSII} in response to growth at HEP can be reconciled, in part, by the fact that *Chlorella vulgaris* exhibits a limited capacity to adjust photosynthetic carbon metabolism (Savitch et al., 1996) and growth rates (Wilson and Hüner, 2000) in response to HL. Similar results have been reported for *P. boryanum* (Miskiewicz et al., 2000, 2002). Thus, neither of these photosynthetic microbes is able to adjust their sink capacity (τ^{-1}) sufficiently to balance the increased energy input due to HL. Thus, to survive under HL conditions, these organisms decrease σ_{PSII} by decreasing their efficiencies to harvest and trap light coupled with enhanced dissipation of absorbed excess light through NPQ. Similarly, LT inhibits growth due to thermodynamic constraints and to survive at LT, these organisms also decrease σ_{PSII} to compensate for the lower growth rates thus lower sink capacity (τ^{-1}) for a given irradiance (Miskiewicz et al., 2000; Wilson and Hüner, 2000). Thus, the phenotypic congruence between acclimation to either LT or HL in these unicellular organisms appears to be a consequence of limitations in their capacity to adjust sink capacity in response to changes in temperature and light which generates a comparable HEP condition.

Complementary chromatic adaptation (CCA) is a phenotypic change exhibited by cyanobacteria in response to changes in ambient light quality (Kehoe and Gutu, 2006; Gutu and Kehoe, 2012). CCA is an historical misnomer and is actually an acclimation response to changes in light color (Kehoe and Gutu, 2006). When the filamentous cyanobacterium, *Fremyella diplosiphon*, is grown under green light, this cyanobacterium exhibits a red pigmented phenotype whereas it exhibits a blue-green phenotype when grown under red light. This acclimation response to light color is completely reversible and reflects alterations in the major light-harvesting pigments, phycoerythrin and phycocyanin, associated with phycobilisomes (Gantt, 1994). The regulation of CCA appears to involve the integration of a phytochrome-type photoreceptor pathway that is sensitive to green and red light in addition to a pathway that is redox-sensitive and involves PET (Kehoe and Gutu, 2006).

Coordinated regulation of Chl biosynthesis, *Lhcb* transcript abundance as well as Lhcb polypeptide accumulation is likely an important characteristic of acclimation to HEP in green algae. However, retrograde regulation examined in a *gun4* mutant of *Chlamydomonas reinhardtii* indicates that down-regulation of *LHC* genes is governed post-transcriptionally with minimal transcriptional co-ordination (Formighieri et al., 2012). Chl b is required for the assembly and stabilization of LHCII (Thornber et al., 1994). Masuda et al. (2003) demonstrated that changes in

the levels of *CAO* transcripts, encoding the enzyme catalyzing the conversion of Chl a to Chl b, occur concomitantly with changes in *Lhcb* transcript abundance during acclimation to HL intensity in *D. salina* while the use of site specific inhibitors of the PET demonstrated that the redox state of the PQ pool regulates both *CAO* and *Lhcb* transcript abundance. This is consistent with previous work demonstrating the regulation of *Lhcb* transcription by the redox state of the PQ pool in *D. tertiolecta* during photoacclimation (Escoubas et al., 1995). These studies are consistent with acclimation to HEP in green algae since HL has the potential to create imbalances in energy flow (Hüner et al., 1998; Ensminger et al., 2006). The pale yellow-green pigmentation of algal cultures acclimated to HEP may reflect limitations at the level of Chl biosynthesis. Studies in *CAO* over-expressors in higher plants have indicated that changes in *CAO* transcription rates are sufficient to cause increases in the abundance of Lhcb polypeptides (Tanaka et al., 2001; Tanaka and Tanaka, 2007; Biswal et al., 2012) indicating that modulation of σ_{PSII} may occur through transcriptional regulation of Chl b biosynthesis. Similarly, levels of CAO have been correlated to Chl b abundance and LHCII antenna size in *D. salina* (Masuda et al., 2002). It is currently unclear whether retrograde signals originating from the redox state of the PQ pool during acclimation to HEP directly coordinate Chl biosynthesis and LHCII abundance in green algae through transcriptional regulation of nuclear-encoded *Lhcb* and *CAO* genes in parallel or indirectly through a regulatory mechanism involving modulation of Chl b biosynthesis at the level of transcriptional control of *CAO* expression.

The mechanisms underlying the signal transduction pathways associated with retrograde regulation between the chloroplast and the nucleus in plants and green algae remain equivocal. However, recent evidence supports the role of heme, Mg protoporphyrin IX, HSP70, and HSP90 as important components in the retrograde signaling pathway (Strand et al., 2003a; von Gromoff et al., 2008; Kindgren et al., 2012). In addition, important biochemical evidence for the involvement of a protein phosphorylation cascade has been reported for *D. salina* (Escoubas et al., 1995; Masuda et al., 2003). Protein kinase inhibitors prevented the induction of *Lhcb* and *CAO* expression during acclimation to low light intensity in *D. salina* (Masuda et al., 2003). Furthermore, *cis*-acting elements in the promoter region of algal *Lhcb* genes have been identified which are likely required for the plastidic redox regulation of nuclear gene expression (Escoubas et al., 1995; Chen et al., 2004). Furthermore, primary C and N metabolic pathways between chloroplasts and mitochondria and may also represent important communication pathways between these two organelles (Raghavendra et al., 1994; Gardestrom et al., 2002; Wilson et al., 2003). For example, inhibition of respiratory electron transport resulted in an increase in excitation pressure (Wilson et al., 2003) and decreased activation of Calvin cycle enzymes (Padmasree and Raghavendra, 2001). Furthermore, HEP stimulated the expression of the mitochondrial alternative oxidase (AOX; Rosso et al., 2009).

Does the generation of the yellow, HEP phenotype in *Chlorella vulgaris* represent a threshold response to varying excitation pressure? If so, one would expect a sigmoidal response for changes in Chl content, Chl a/b ratios and Lhcb content as a function of excitation pressure. This could be interpreted to indicate that the redox sensor(s) that respond to excitation pressure act as a "molecular on–off switch," that is, a minimum excitation pressure must be attained before nuclear encoded *Lhcb* genes are repressed by HEP through retrograde regulation. The proxies for phenotype included total Chl/cell and Lhcb content which exhibited a linear but negative relationship with increasing excitation pressure (Maxwell et al., 1995a,b; Wilson and Hüner, 2000). Concomitantly, Chl a/b ratios and xanthophyll cycle activity, and hence NPQ, also varied linearly but positively, as expected, as a function of increasing excitation pressure (Wilson and Hüner, 2000). Since all proxies for the phenotypic response of *Chlorella vulgaris* varied linearly as a function of excitation pressure, this indicates that the redox sensor(s) that govern the phenotypic response to excitation pressure in *Chlorella vulgaris* is not a "molecular on–off switch" but rather is analogous to a "molecular rheostat."

ROLE OF CBF TRANSCRIPTION FACTORS IN THE REGULATION OF PHENOTYPIC PLASTICITY IN TERRESTRIAL PLANTS

Brassica napus, winter cereals such wheat and rye grown at LTs exhibit a developmental shift from an elongated to a dwarf growth habit (Gray et al., 1997; Dahal et al., 2012a,b). However, the biomass of the dwarf plants are equal to or higher than the plants which exhibit the elongated phenotype due to a combination of increased leaf thickness, increased cytoplasmic volume coupled with decreased water content with no change in the total number of leaves (Hüner et al., 1984; Krol et al., 1984; Boese and Hüner, 1990; Strand et al., 1999; Gorsuch et al., 2010; Dahal et al., 2012a,b). Previously, it was presumed that this dwarf growth habit was strictly a response to growth at LT and this phenotype was used to select for freezing tolerance (Levitt, 1980). However, growth at HL but warm temperatures generates a comparable dwarf growth habit as observed at LT. Thus, it was shown that this dwarf phenotype is, in fact, governed by excitation pressure rather than by LT (Gray et al., 1997; Hüner et al., 1998). In contrast to green algae, *Chlorella vulgaris* and *D. salina* and the cyanobacterium, *P. boryanum*, these cold acclimated winter cultivars maintain photostasis by matching a high efficiency for light absorption (σ_{PSII}) with an increased capacity for CO_2 assimilation (τ^{-1}) through the up-regulation of transcription and translation of genes coding for Rubisco and the regulatory enzymes of cytosolic sucrose and fructan biosynthesis (Savitch et al., 2000a; Stitt and Hurry, 2002; Strand et al., 2003b; Ensminger et al., 2006; Dahal et al., 2012a,b) coupled with enhanced rates for leaf carbon export (Leonardos et al., 2003) and the suppression of photorespiration (Savitch et al., 2000b). These results are consistent with the global analyses of the cold acclimated *A. thaliana* metabolome which indicate a major reprogramming of carbon metabolism relative to non-acclimated plants (Gray and Heath, 2005). As a result, energy use efficiency is enhanced because the dissipation of absorbed light energy through NPQ is kept to a minimum while absorbed light energy used for C-assimilation is maximized resulting in increased biomass accumulation (Hüner et al., 1998; Stitt and Hurry, 2002; Strand et al., 2003b; Ensminger et al., 2006; Dahal et al., 2012a,b). This not only maximizes the chemical energy stored and carbon pool available for the renewed growth and reproduction in the spring but the accumulation of photosynthetic end-products such as sucrose also provides

cryoprotectants to stabilize the cell membranes against freezing events during the winter (Stitt and Hurry, 2002).

What governs this complex, integrated phenomenon which appears to involve a system-wide change in morphology, physiology, and biochemistry of cold-tolerant crop plants? It has been suggested that cold- binding transcription factors/dehydration responsive element binding factors (CBFs/DREBs) control the phenotypic plasticity and freezing tolerance in cold-tolerant species (Jaglo-Ottosen et al., 1998; Liu et al., 1998; Kasuga et al., 1999; Gilmour et al., 2000, 2004; Savitch et al., 2005; Theocharis et al., 2012). Recently, we reported that the over-expression of a specific *CBF* in *Brassica napus*, *BnCBF17*, not only induces a dwarf phenotype but concomitantly enhances photosynthetic performance, the efficiency of energy conversion, water use efficiency, and biomass production comparable to that observed in cold acclimated *B. napus* (Savitch et al., 2005; Dahal et al., 2012a). We suggest that the transcription factor, *BnCBF17*, may be either a master regulator or certainly a central component which governs the regulation of plant architecture, photosynthetic capacity, and energy conversion efficiency of crops. In *Arabidopsis*, the protein kinases, KIN10/KIN11, act as a central integrator of transcription networks associated with plant carbon metabolism and energy balance (Baena-Gonzalez et al., 2007). CBFs may interact with KIN10/KIN11 to affect photosynthetic performance in response to excitation pressure. However, the governance of phenotypic plasticity and photosynthetic performance by CBFs/DREBs in winter cultivars must also be integrated with the process of vernalization (Amasino, 2004; Sung and Amasino, 2005; Trevaskis et al., 2007; Trevaskis, 2010). Thus, gene regulation by *CBFs* extends well beyond its traditional role in cold acclimation and freezing tolerance. As discussed in detail by Murchie et al. (2009), elucidation of the mechanisms which govern the dynamic nature of energy partitioning between energetically "useful processes" involved in C and N-assimilation for biomass and seed production versus apparently energetically "wasteful processes" such as the dissipation of absorbed light energy as heat through NPQ to optimize plant survival remains a major challenge in maximizing crop productivity. Modulation of *CBF* expression levels may provide important new insights into potential molecular and genetic approaches focused on the maintenance or even the enhancement of plant productivity under suboptimal growth conditions associated with climate change (Dahal et al., 2012a).

EXCITATION PRESSURE GOVERNS CHAOTIC LEAF VARIEGATION PATTERNS

The *A. thaliana* chaotic variegated mutant, *immutans* (*im*), displays unpredictable white and green sectoring patterns due to differential stability of thylakoid membranes during chloroplast biogenesis and are considered plastid autonomous (Rodermel, 2002; Yu et al., 2007). IMMUTANS (IM) is encoded by a single nuclear gene which is translated into a 35 kD thylakoid polypeptide where it functions as a plastid terminal oxidase (PTOX). Cloning and characterization of *IM* revealed that it is related to the mitochondrial inner membrane AOX (Carol et al., 1999; Wu et al., 1999; McDonald et al., 2011) which oxidizes ubiquinol and reduces molecular oxygen (Vanlerberghe and McIntosh, 1997). By analogy, it has been suggested that IM is induced under stress conditions and oxidizes PQH_2 and reduces O_2 to water (Carol et al., 1999; Wu et al., 1999; Carol and Kuntz, 2001; Rodermel, 2001; McDonald et al., 2011). Consequently, PTOX is considered to be the essential oxidase which participates in the chlororespiratory pathway (Cournac et al., 2000a,b). Recently, Fu et al. (2012) reported that AOX1a and AOX2 can functionally substitute for PTOX in the *immutans* mutant of *A. thaliana* and rescue the variegated phenotype. It is proposed that IM is not only essential for carotenoid biosynthesis and chlororespiration but it is also acts as a "safety valve" in the photoprotection of PSII (Niyogi, 1999; Cournac et al., 2000a,b; Rodermel, 2001; Joet et al., 2002; Peltier and Cournac, 2002).

Recently, we reported specific growth conditions that completely suppressed the variegated phenotype of *im* such that it exhibited an "all green" phenotype indistinguishable from the wild type (WT) even though neither *IM* expression nor IM accumulation was detected (Rosso et al., 2006). By exploiting this phenomenon and comparing *im* knockout plants with WT, as well as a 6× and 16× over-expressor of *IM*, we reported that in mature, fully expanded leaves of *A. thaliana*, IM (PTOX) cannot compete with $P700^+$ for PSII-generated electrons under optimal growth conditions. We concluded that under optimal growth conditions, PTOX cannot act as a simple "safety valve" in *A. thaliana* leaves exhibiting full photosynthetic competence (Rosso et al., 2006). Our conclusion is consistent with that of Heyno et al. (2009) who reported that over-expression of PTOX in tobacco induced rather than ameliorated oxidative stress. In contrast to these reports, there are numerous reports of specific abiotic stress conditions which induce the expression and accumulation of PTOX in alpine plant species (Streb et al., 2005), the halophile, *Thellungiella halophila* (Stepien and Johnson, 2009) as well as the marine cyanobacterium, *Synechococcus* WH8102 and marine green alga, *Ostreococcus* (Bailey et al., 2008; Cardol et al., 2008; Grossman et al., 2010). Furthermore, Baena-Gonzalez et al. (2003) reported that deletion of tobacco plastid *psbA* triggers an up-regulation of the thylakoid-associated NAD(P)H dehydrogenase complex as well as PTOX.

All oxygenic photoautotrophs exhibit the presence of IM (PTOX) in their genomes (McDonald et al., 2011). How can the apparent conflicting reports regarding the function of IM (PTOX) be reconciled? Meta-transcriptome analyses of PTOX indicated that PTOX expression is primarily developmentally regulated in *Arabidopsis* rather than by stress (Rosso et al., 2006). To address the role of IM (PTOX) in leaf development, we developed a sensitive, high resolution, non-destructive imaging technique by which we could quantify the extent of variegation as a function of time. This allowed us to quantify the effects of growth irradiance and temperature on the extent of variegation as a function of developmental time. Using this technique, we were able to show that the absence of IM is necessary but not sufficient to explain variegation in *A. thaliana*. In fact, the extent of variegation is governed by excitation pressure not only in *im* but also in the other *Arabidopsis* variegated mutants such as *spotty*, *var1*, and *var2* (Rosso et al., 2009). The biogenesis and assembly of thylakoid membranes requires tight co-ordination between the *de novo* synthesis of Chl and other pigments, lipids as well as chloroplast and nuclear encoded proteins (Eberhard et al., 2008; Sakamoto et al., 2008). This raises an

important developmental question as to how a photoautotroph mitigates the potential damaging effects of photo-oxidative stress during the biogenesis and assembly of its photosystems prior to the establishment of a fully functional photosynthetic apparatus. In WT plants, protection from photo-oxidative stress is provided through transient stimulation of non-photochemical dissipation of excess energy through the xanthophyll cycle (Demmig-Adams and Adams, 1992; Murchie et al., 2009) as shown during early greening in barley (Krol et al., 1999) as well as the induction of myriad plant oxidative stress genes including *AOX* (Aluru et al., 2009). However, *im* seedlings are unable to biosynthesize photoprotective carotenoids involved in the xanthophyll cycle (Wetzel et al., 1994). Although IM cannot compete with $P700^+$ for PSII-generated electrons in mature leaves that are photosynthetically competent (Rosso et al., 2006), its presence is essential to minimize excitation pressure and the potential for photo-oxidative damage during the very early stages in the assembly and biogenesis of the photosynthetic apparatus prior to the attainment of full photosynthetic competence (Rosso et al., 2006, 2009).

To account for the variable and unpredictable patterns of leaf variegation in *immutans*, we suggest the presence of a gradient of excitation pressure within the developing leaf primordia during light-dependent chloroplast biogenesis: the data indicate that if excitation pressure in a particular developing sector is lower than 0.2, chloroplast biogenesis proceeds normally and an "all green" sector(s) with a LEP phenotype will develop; however, if excitation pressure in a particular developing sector exceeds 0.2, thylakoid assembly and chloroplast biogenesis is inhibited and white sectors with a HEP phenotype will develop (Rosso et al., 2009). This implies a threshold-dependence for the sensor(s) that govern the HEP versus the LEP phenotype in *im* in response to changes in excitation pressure, and therefore, appear to act as "molecular on–off switches" in contrast to that observed for the regulation of the HEP phenotype in the green alga, *Chlorella vulgaris*.

There appears to be a consensus that PTOX not only acts as the terminal oxidase in the chlororespiratory pathway (Cournac et al., 2000a,b) but also acts an important alternative photosynthetic electron sink under any condition where PSI is acceptor-limited. Under these conditions, the induction of PTOX as an alternative, O_2-dependent pathway for photosynthetic electron flow would mitigate any PSI limitation and protect PSII from over-excitation by oxidizing PQH_2 and reducing O_2 to water (Grossman et al., 2010; McDonald et al., 2011). This is consistent with the recent results of Formighieri et al. (2012) who reported that a *gun4* mutant of *Chlamydomonas reinhardtii* exhibits a significant decrease in PSI/PSII ratios coupled with an increase in PTOX activity which may protect the *gun4* mutant from HEP under conditions where PSI levels may be limiting. In addition, the biogenesis and assembly of the photosynthetic apparatus appears to be coordinated with mitochondrial redox balance as indicated by the fact AOX expression is modulated by excitation pressure originating within the chloroplast (Rosso et al., 2009) indicating redox communication between chloroplasts and mitochondria.

Unlike photoacclimation or LT acclimation discussed above, chaotic leaf variegation in *A. thaliana* is a consequence of destabilization of the developing photosynthetic apparatus by excitation pressure during thylakoid membrane assembly and chloroplast biogenesis rather than an example of remodeling of the photosynthetic apparatus by adjusting either σ_{PSII} or τ^{-1}. The control of variegation in various *Arabidopsis* mutants represents an excellent example of how chloroplast redox sensing/signaling, through excitation pressure, mediates the interaction of the nuclear encoded *IMMUTANS* gene with its environment to affect chloroplast biogenesis, leaf development, and subsequent phenotype.

WHAT IS THE PRIMARY SITE(S) FOR SENSING CHLOROPLAST ENERGY IMBALANCE?

Research with cyanobacteria (Fujita, 1997), green algae (Escoubas et al., 1995; Maxwell et al., 1995a,b; Hüner et al., 1998; Wilson et al., 2003), and plants (Anderson et al., 1995; Pfannschmidt, 2003; Fey et al., 2005; Woodson and Chory, 2008; Brautigam et al., 2009; Pesaresi et al., 2009; Rochaix, 2011) indicates that a key component of redox sensing/signaling associated with the photosynthetic apparatus is the PQ pool, a mobile electron carrier that shuttles electrons from PSII to the Cyt b_6/f. This is based, in part, on experiments where the characteristic, yellow-green, HL phenotype of green algae brought about by photoacclimation, that is, acclimation to high irradiance, could be mimicked by chemically modulating the redox status of the intersystem PQ pool. This is traditionally accomplished by using minimal concentrations of the PET inhibitors, either 2,5-dibromo-3-methyl-6-isopropylbenzoquinone (DBMIB) or 3-(3′,4′-dichlorophenyl)-1,1-dimethylurea (DCMU; Escoubas et al., 1995; Pfannschmidt et al., 1999; Pfannschmidt, 2003; Wilson et al., 2003; Piippo et al., 2006). Since DBMIB inhibits the oxidation of PQH_2 by the Cyt b_6/f complex, PSII keeps the PQ pool reduced in the light. This induces the HL phenotype which is characterized by low Chl content per cell, high Chl a/b ratio (>10), accumulation of the carotenoid-binding protein (Cbr; Krol et al., 1997) but suppression of both *Lhcb2* expression and Lhcb2 accumulation through retrograde regulation of nuclear encoded genes by the chloroplast in *Chlorella vulgaris* and *D. salina*. Since this HL phenotype is also mimicked by growth of *Chlorella vulgaris* and *D. salina* at LT (Maxwell et al., 1995a,b; Wilson et al., 2006), we designate this as a HEP phenotype. In contrast, since DCMU prevents the exit of electrons from PSII reaction centers into the PQ pool, PSI is able to keep the PQ pool oxidized in the light. Under these conditions, cells exhibit a LEP phenotype characterized by a high Chl content per cell, low Chl a/b ratio (3.0–3.5), and high levels of *Lhcb2* expression and Lhcb2 accumulation (Escoubas et al., 1995; Maxwell et al., 1995a,b; Wilson et al., 2003). This LEP phenotype can also be generated by growth at either low irradiance or high temperature but moderate irradiance in *Chlorella vulgaris* (Maxwell et al., 1995a,b; Hüner et al., 1998; Wilson et al., 2003). Since Q_A, the first stable quinone electron acceptor within the PSII reaction center is considered to be in rapid equilibrium with the PQ pool of intersystem electron transport (Dietz et al., 1985; Schreiber et al., 1994; Maxwell et al., 1995a,b; Baker, 2008), we have assumed that the PQ pool is the primary redox sensor that governs changes in excitation pressure (Hüner et al., 1998, 2003, 2006; Oquist and Huner, 2003; Ensminger et al., 2006; Morgan-Kiss et al., 2006; Wilson et al., 2006; McDonald et al., 2011). However, our earlier report for the regulation of

HEP and LEP phenotypes in the filamentous cyanobacterium, *P. boryanum*, indicated that the PQ pool is probably not the major site from which redox signals emanate to control pigmented phenotype through modulation of the composition and structure of phycobilisomes in this cyanobacterium (Miskiewicz et al., 2000, 2002). This is consistent with the recent report by Piippo et al. (2006) who reported that the PQ pool is not the major redox sensor regulating photoacclimation in *A. thaliana* and that the primary redox signals probably emanate from the acceptor-side of PSI.

The assumption that the combination of DCMU and DBMIB identifies the redox state of the PQ pool as the primary site of chloroplast redox sensing/signaling ignores the potential contributions of other PET components to redox sensing/signaling. Indeed, recent research in *Arabidopsis* suggests that the redox state of ferredoxin (Fd), thioredoxins (Trx), and peroxiredoxins on the acceptor-side of PSI (Dietz, 2003, 2008; Dietz and Scheibe, 2004) as well as the generation of reactive oxygen species (ROS; Apel and Hirt, 2004; Wagner et al., 2004) may constitute a complex network of redox senors/signals involved in the retrograde pathway of communication from the chloroplast to the nucleus (Koussevitzky et al., 2007; Fernandez and Strand, 2008; Jung and Chory, 2010). In fact, Piippo et al. (2006) suggest that the reducing side of PSI may represent the major source of chloroplast redox signaling involved in retrograde regulation. Furthermore, PSII itself may also contribute to retrograde regulation of nuclear genes through the generation of singlet oxygen (Apel and Hirt, 2004; Wagner et al., 2004; Nott et al., 2006; Lee et al., 2007; Fernandez and Strand, 2008) and thus, may contribute to redox regulation by excitation pressure. Using a combination of inhibitors, uncouplers, and antimycin A, Chen et al. (2004) identified two different sensors involved in the retrograde signal transduction pathway in *D. salina*. The transthylakoid membrane potential (pmf) appeared to govern gene expression in response to changes in irradiance on a short time scale (<4 h), whereas on time scales of 8 h or longer, the redox state of the PQ pool appeared to become the more prominent sensor. Thus, the regulation of gene expression and phenotypic plasticity through excitation pressure in green algae must represent a complex interacting *intracellular* network of sensors and signal transduction pathways.

However, in terrestrial crop plants and *A. thaliana*, a similar complex, intracellular network must be integrated with an equally complex sensor/signal transduction pathway that extends over long distances from leaf chloroplasts to meristematic tissue such as the crown in cereals. This long distance sensor/signaling pathway must convey information regarding the redox status of the leaf chloroplasts to regulate meristematic cell division and differentiation and affect plant growth, development, and morphology (Gray et al., 1997). There is a growing body of evidence that the environment has a significant impact on cell development not only in leaves (Rosso et al., 2009) but also in roots (Tsukagoshi et al., 2010) as well as anthers (Kelliher and Walbot, 2012; Whipple, 2012) through modulation of cellular redox state. Furthermore, there is growing support in the literature that although hydrogen peroxide is a toxic molecule generated by various stress conditions in plants (Mittler et al., 2004), it is also an important molecule involved in systemic signaling and acclimation to excitation pressure in plants (Karpinski et al., 1999; Mullineaux et al., 2000; Fryer et al., 2003; Mullineaux et al., 2006; Geisler et al., 2006).

THE "GRAND DESIGN OF PHOTOSYNTHESIS"

Figure 2 represents a simplified model that attempts to summarize the central role of the photosynthetic apparatus as a major sensor of excitation pressure that is modulated by irradiance (sunlight) and LT (snowflake) in photoautotrophs. It is clearly established that the PET chain is an important source of redox signals involved in intracellular redox signaling. There appears to be a consensus that, within the PET chain, several potential redox sensors appear to exist including PSII, the PQ pool, the thylakoid proton motive force (pmf) as well as the acceptor-side of PSI. The latter would include the redox status of Fd, Trx, peroxiredoxins, H_2O_2, as well as metabolic intermediates of carbon metabolism. The acceptor-side of PSI appears to be a major site of redox sensing/signaling in the chloroplast. These sensors may contribute to varying extents and may act independently or in concert to initiate retrograde signaling to the nucleus to affect transcriptional regulation of nuclear photosynthetic genes. The end result of such retrograde redox sensing/signaling in response to changes in excitation pressure is the remodeling of the structure and function of the photosynthetic apparatus to re-establish photostasis.

In addition to intracellular retrograde redox sensing/signaling, redox signals from the chloroplast must be transmitted to various meristematic regions such as the crown tissue within winter cereals to affect plant morphology (e.g., dwarf phenotype). Consequently, this redox signaling pathway probably involves long distance transport via the plant vascular system. Possible components of this long distance signaling pathway may include but are not restricted to hormones, H_2O_2, and photosynthetic end-products such as sucrose. The rate of long distance transport from source to sink as well as sink activity reflected in rates of growth and development can, in turn, feedback regulate the extent of chloroplastic excitation pressure. Thus, we suggest that phenotypic plasticity governed by excitation pressure initially sensed in leaf chloroplasts is the result not only of local remodeling of the photosynthetic apparatus, but also the regulation of remote meristematic regions to affect plant morphology.

Thirty years ago, Arnon (1982) proposed the concept of a "grand design of photosynthesis" which was re-introduced by Anderson et al. (1995). Anderson et al. (1995) conclude that the "grand design of photosynthesis with exquisite regulation ensures that the responses of both photoreceptors and photosystems II and I, acting as their own light sensors, are inextricably linked with feedback metabolic responses from photosynthesis itself, which allow plants to respond to both sudden and sustained fluctuations in environmental cues." This notion has been supported either directly (Anderson et al., 1995; Hüner et al., 1998; Ensminger et al., 2006; Wilson et al., 2006; Pfannschmidt and Yang, 2012) or indirectly (Pfannschmidt, 2003; Fey et al., 2005; Murchie et al., 2009; Lepisto and Rintamaki, 2012). Although the precise nature of the redox sensors and signal transduction pathways associated with excitation pressure remain to be elucidated, we maintain that the data summarized in this review are consistent with the notion of a "grand design of photosynthesis." Consequently, we suggest that,

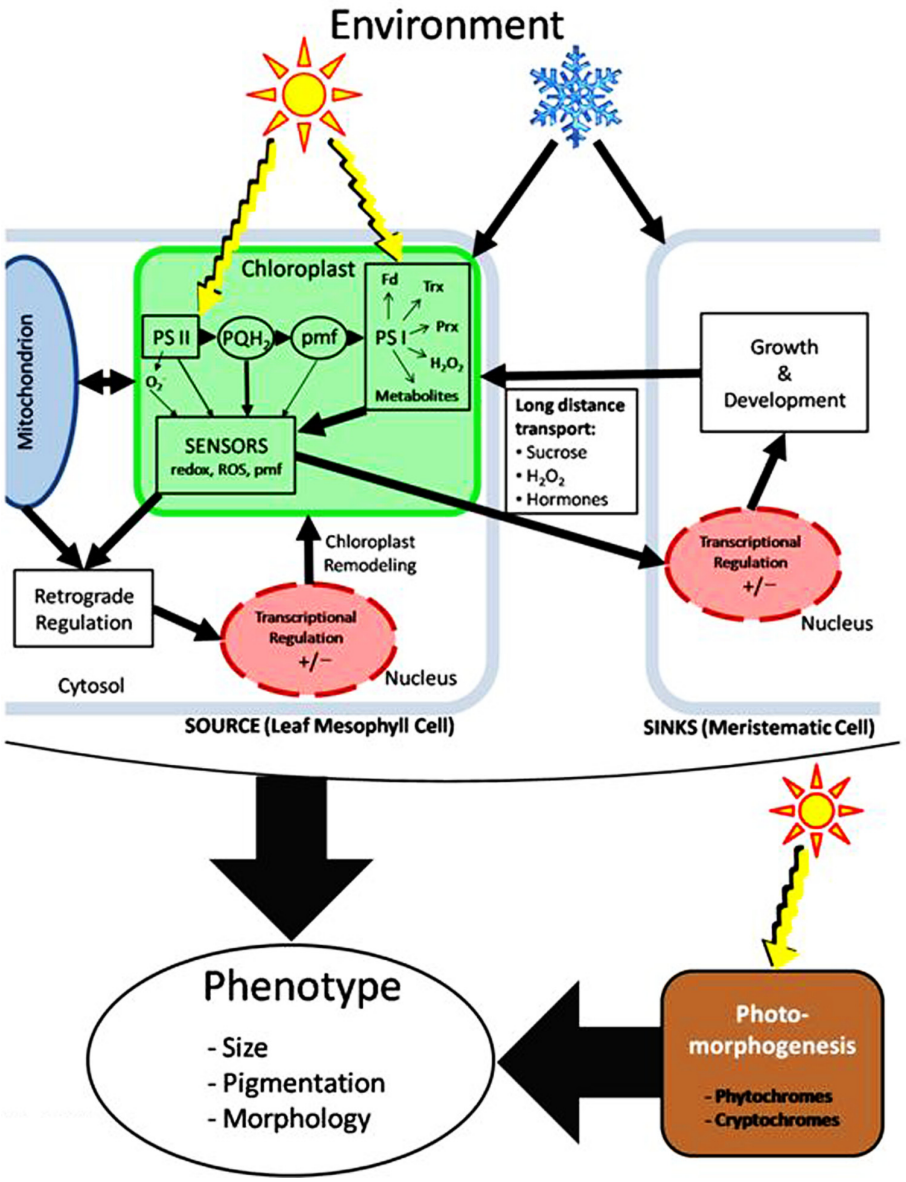

FIGURE 2 | A model illustrating the environmental regulation of phenotypic plasticity via chloroplast redox sensing coupled to both intracellular and long distance signal transduction. Light is the ultimate source of energy for photoautotrophs. Energy imbalances generated either by changes in high light (sun) or low temperature (snowflake) are sensed in the chloroplast by modulation of the redox state of the photosynthetic apparatus. Such redox information is exchanged between chloroplasts and mitochondria through carbon metabolism. Intracellular redox imbalances in chloroplasts and mitochondria are conveyed to the nucleus through retrograde regulation to affect remodeling of the photosynthetic apparatus to re-establish photostasis and energy balance. The remodeling of the photosynthetic apparatus may be reflected in changes phenotype exhibited as alterations in pigmentation in certain algae and cyanobacteria. In vascular plants, information regarding chloroplast redox imbalance is also conveyed to distant sinks such as meristematic regions of a plant to affect growth and development. This occurs through long distance signaling via the vascular system. Such information also contributes to the regulation of phenotypic plasticity reflected in changes in vascular plant morphology. In plants, distant sink limitations induced by low temperature can also be important in feedback regulation of energy balance in chloroplasts in source leaves. Thus, phenotypic plasticity is the result of the integration of both photosynthetic as well as photomorphogenic events. PSII, photosystem II; PSI, photosystem I; PQH_2, reduced plastoquinone; pmf, proton motive force; Fd, ferredoxin; Trx, thioredoxins; Prx, peroxiredoxins.

in addition to its traditional role as the energy transformer for the biosphere, the photosynthetic apparatus should also be considered a major energy sensor which is modulated by environmental cues and plays a major role in the regulation of phenotypic plasticity (**Figure 2**).

Although all photoautotrophs can sense changes in their environment through the modulation of excitation pressure, we suggest that it is source–sink relationships that ultimately modulate the extent of excitation pressure which then governs the observed phenotype of photoautotrophs during growth at

either HL or LT. Thus, photoautotrophs must integrate information regarding changes in light quality through photoreceptors with changes in light as an energy source through the redox state of the photosynthetic apparatus to affect plant growth and morphology (Anderson et al., 1995; Fryer et al., 2003; Lepisto and Rintamaki, 2012; **Figure 2**). Since sunlight represents the ultimate energy source for our biosphere, greater understanding of the role of the chloroplast as an energy sensor which governs energy partitioning and energy utilization efficiency as well as phenotypic plasticity will be essential for the maintenance or possibly even the enhancement of plant biomass for energy and crop productivity for food under suboptimal growth conditions associated with climate change (Murchie et al., 2009; Dahal et al., 2012a).

ACKNOWLEDGMENTS

NPAH acknowledges the financial support of the Natural Sciences and Engineering Research Council of Canada, the Canada Research Chairs Programme and the Canada Foundation for Innovation.

REFERENCES

Aluru, M. R., Zola, J., Foudree, A., and Rodermel, S. R. (2009). Chloroplast photooxidation-induced transcriptome reprogramming in *Arabidopsis* immutans white leaf sectors. *Plant Physiol.* 150, 904–923.

Amasino, R. (2004). Vernalization, competence, and the epigenetic memory of winter. *Plant Cell* 16, 2553–2559.

Anderson, J. M., Chow, W. S., and Park, Y.-I. (1995). The grand design of photosynthesis: acclimation of the photosynthetic apparatus to environmental cues. *Photosyn. Res.* 46, 129–139.

Apel, K., and Hirt, H. (2004). Reactive oxygen species: metabolism, oxidative stress, and signal transduction. *Ann. Rev. Plant Biol.* 55, 373–399.

Arnon, D. I. (1982). Sunlight, earth life: the grand design of photosynthesis. *Sciences* 22, 22–27.

Baena-Gonzalez, E., Allahverdiyeva, Y., Svab, Z., Maliga, P., Josse, E.-M., Kuntz, M., et al. (2003). Deletion of the tobacco plastid psbA gene triggers an upregulation of the thylakoid-associated NAD(P)H dehydrogenase complex and the plastid terminal oxidase (PTOX). *Plant J.* 35, 704–716.

Baena-Gonzalez, E., Rolland, F., Thevelein, J. M., and Sheen, J. (2007). A central integrator of transcription networks in plant stress and energy signalling. *Nature* 448, 938–942.

Bailey, S., Melis, A., Mackey, K. R. M., Cardol, P., Finazzi, G., van Dijken, G., et al. (2008). Alternative photosynthetic electron flow to oxygen in marine *Synechococcus*. *Biochim. Biophys. Acta* 1777, 269–276.

Baker, N. R. (2008). Chlorophyll fluorescence: a probe of photosynthesis in vivo. *Ann. Rev. Plant Biol.* 59, 89–113.

Biswal, A. K., Pattanayak, G. K., Pandey, S. S., Leelavathi, S., Reddy, V. S., Govindjee, X., et al. (2012). Light intensity-dependent modulation of chlorophyll b biosynthesis and photosynthesis by overexpression of chlorophyllide a oxygenase in tobacco. *Plant Physiol.* 159, 433–449.

Boese, S. R., and Hüner, N. P. A. (1990). Effect of growth temperature and temperature shifts on spinach leaf morphology and photosynthesis. *Plant Physiol.* 94, 1830–1836.

Brautigam, K., Dietzel, L., Kleine, T., Stroher, E., Wormuth. D., Dietz, K.-J., et al. (2009). Dynamic plastid redox signals integrate gene expression and metabolism to induce distinct metabolic states in photosynthetic acclimation in *Arabidopsis*. *Plant Cell* 21, 2715–2732.

Cardol, P., Bailleul, B., Rappaport, F., Derelle, E., Bacal, D., Breyton, C., et al. (2008). An original adaptation of photosynthesis in the marine green alga *Ostreococcus*. *Proc. Natl. Acad. Sci. U.S.A.* 105, 7881–7886.

Carol, P., and Kuntz, M. (2001). A plastid terminal oxidase comes to light: implications for carotenoid biosynthesis and chlororespiration. *Trends Plant Sci.* 6, 31–36.

Carol, P., Stevenson, D., Bisanz, C., Breitenbach, J., Sandmann, G., Mache, R., et al. (1999). Mutations in the *Arabidopsis* gene IMMUTANS cause a variegated phenotype by inactivating a chloroplast terminal oxidase associated with phytoene desaturation. *Plant Cell* 11, 57–68.

Cashmore, A. R. (1997). The cryptochrome family of photoreceptors. *Plant Cell Environ.* 20, 764–767.

Chen, Y.-B., Durnford, D. G., Koblizek, M., and Falkowski, P. G. (2004). Plastid regulation of Lhcb1 transcription in the chlorophyte alga *Dunaliella tertiolecta*. *Plant Physiol.* 136, 3737–3750.

Cournac, L., Josse, E. M., Joet, T., Rumeau, D, Redding, K., Kuntz, M., et al. (2000a). Flexibility in photosynthetic electron transport: a newly identified chloroplast oxidase involved in chlororespiration. *Philos. Trans. R. Soc. Lond. B Biol. Sci.* 355, 1447–1454.

Cournac, L., Redding, K., Ravanel, J., Rumeau, D., Josse, E. M., Kuntz, M., et al. (2000b). Electron flow between photosystem II and oxygen in chloroplasts of photosystem I-deficient algae is mediated by a quinol oxidase involved in chlororespiration. *J. Biol. Chem.* 275, 17256–17262.

Dahal, K., Gadapati W., Savitch, L. V., Singh, J., and Hüner, N. P. A. (2012a). Cold acclimation and BnCBF17-over-expression enhance photosynthetic performance and energy conversion efficiency during long-term growth of Brassica napus under elevated CO2 conditions. *Planta* 236, 1639–1652.

Dahal, K., Kane, K., Gadapati, W., Webb, E., Savitch, L. V., Singh, J., et al. (2012b). The effects of phenotypic plasticity on photosynthetic performance in winter rye, winter wheat and *Brassica napus*. *Physiol. Plant.* 144, 169–188.

Demmig-Adams, B., and Adams, W. W. III (1992). Photoprotection and other responses of plants to high light stress. *Ann. Rev. Plant Physiol. Plant Mol. Biol.* 43, 599–626.

Demmig-Adams, B., Adams W. W. III, Ebbert, V., and Logan, B. A. (1999). "Ecophysiology of the xanthophyll cycle", in *Advances in Photosynthesis. The Photochemistry of Carotenoids*, Vol. 8, eds H. A. Frank, A. J. Young, G. Britton, and R. J. Cogdell (Dordrecht: Kluwer Academic Publishers), 245–269.

Dietz, K.-J. (2003). Plant peroxiredoxins. *Ann. Rev. Plant Biol.* 54, 93–107.

Dietz, K.-J. (2008). Redox signal integration: from stimulus to networks and genes. *Physiol. Plant.* 133, 459–468.

Dietz, K.-J., and Scheibe, R. (2004). Redox regulation: an introduction. *Physiol. Plant.* 120, 1–3.

Dietz, K.-J., Schreiber, U., and Heber, U. (1985). The relationship between the redox state of QA and photosynthesis in leaves at various carbon-dioxide, oxygen and light regimes. *Planta* 166, 219–226.

Eberhard, S., Finazzi, G., and Wollman, F.-A. (2008). The dynamics of photosynthesis. *Ann. Rev. Genetics* 42, 463–515.

Ensminger, I., Busch, F., and Hüner, N. P. A. (2006). Photostasis and cold acclimation: sensing low temperature through photosynthesis. *Physiol. Plant.* 126, 28–44.

Escoubas, J.-M., Lomas, M., LaRoche, J., and Falkowski, P. G. (1995). Light intensity regulates cab gene transcription via the redox state of the plastoquinone pool in the green alga, *Dunaliella tertiolecta*. *Proc. Natl. Acad. Sci. U.S.A.* 92, 10237–10241.

Falkowski, P. G. and Chen, Y. -B. (2003). "Photoacclimation of light harvesting systems in eukaryotic algae", in *Advances in Photosynthesis and Respiration,* Vol. 13, *Light Harvesting Antennas in Photosynthesis,* eds. B. R. Green and W. W. Parson (Dordrecht: Kluwer Academic Publishers), 423–447.

Fernandez, A. P., and Strand, A. (2008). Retrograde signaling and plant stress: plastid signals initiate cellular stress responses. *Curr. Opin. Plant Biol.* 11, 509–513.

Fey, V., Wagner, R., Brautigam, K., and Pfannschmidt, T. (2005). Photosynthetic redox control of nuclear gene expression. *J. Exp. Bot.* 56, 1491–1498.

Formighieri, C., Ceol, M., Bonente, G., Rochaix, J.-D., and Bassi, R. (2012). Retrograde signaling and photoprotection in a gun4 mutant of *Chlamydomonas reinhardtii*. *Mol. Plant* doi: 10.1093/mp/sss051 [Epub ahead of print].

Fryer, M. J., Ball, L., Oxborough, K., Karpinski, S., Mullineaux, P. M., and Baker, N. R. (2003). Control of ascorbate peroxidase 2 expression by hydrogen peroxide and leaf water status during excess light stress reveals a functional organisation of *Arabidopsis* leaves. *Plant J.* 33, 691–705.

Fu, A., Liu, H., Yu, F., Kambakam, S., Luan, S., and Rodermel, S. (2012). Alternative oxidases (AOX1a and AOX2) can functionally substitute for plastid terminal oxidase in *Arabidopsis* chloroplasts. *Plant Cell* 24, 1579–1595.

Fujita, Y. (1997). A study on the dynamic features of photosystem stoichiometry – accomplishments and problems for future studies. *Photosyn. Res.* 53, 83–93.

Gantt, E. (1994) "Supramolecular membrane organization", in *Advances in Photosynthesis. Molecular Biology of Cyanobacteria*, Vol. 1, ed. D. A. Bryant (Dordrecht: Kluwer Academic Publishers), 119–138.

Gardestrom, P., Igamberdiev, A. U., and Raghavendra, A. S. (2002). "Mitochondrial functions in the light and significance to carbon-nitrogen interactions", in *Advances in Photosynthesis and Respiration. Photosynthetic Nitrogen Assimilation and Associated Carbon Respiratory Metabolism*, Vol. 12, eds. C. H. Foyer and G. Noctor (Dordrecht: Kluwer Academic Publishers), 151–172.

Geisler, M., Kleczkowski, L. A., and Karpinski, S. (2006). A universal algorithm for genome-wide in silicio identification of biologically significant gene promoter putative cis-regulatory-elements; identification of new elements for reactive oxygen species and sucrose signaling in *Arabidopsis. Plant J.* 45, 384–398.

Gilmour, S. J., Fowler, S. G., and Thomashow, M. F. (2004). *Arabidopsis* transcriptional activators CBF1, CBF2, and CBF3 have matching functional activities. *Plant Mol. Biol.* 54, 767–781.

Gilmour, S. J., Sebolt, A. M., Salazar, M. P., Everard, J. D., and Thomashow, M. F. (2000). Overexpression of the *Arabidopsis* CBF3 transcriptional activator mimics multiple biochemical changes associated with cold acclimation. *Plant Physiol.* 124, 1854–1865.

Gorsuch, P. A., Pandey, S., and Atkin, O. K. (2010). Temporal heterogeneity of cold acclimation phenotypes in *Arabidopsis* leaves. *Plant Cell Environ.* 33, 244–258.

Gray, G. R., Chauvin, L.-P., Sarhan, F., and Hüner, N. P. A. (1997). Cold acclimation and freezing tolerance (A complex interaction of light and temperature). *Plant Physiol.* 114, 467–474.

Gray, G. R., and Heath, D. (2005). A global reorganization of the metabolome in *Arabidopsis* during cold acclimation is revealed by metabolic fingerprinting. *Physiol. Plant.* 124, 236–248.

Green, B. R., Anderson, J. M., and Parson, W. W. (2003). "Photosynthetic membranes and their light harvesting antennas", in *Advances in Photosynthesis and Respiration,* Vol. 13, *Light Harvesting Antennas in Photosynthesis*, eds. B. R. Green and W. W. Parson (Dordrecht: Kluwer Academic Publishers), 1–28.

Grossman, A. R., Mackey, K. R. M., and Bailey, S. (2010). A perspective on photosynthesis in the oligotrophic oceans: hypothesis concerning alternative routes of electron flow. *J. Phycol.* 46, 629–634.

Gutu, A., and Kehoe, D. M. (2012). Emerging perspectives on the mechanisms, regulation, and distribution of light color acclimation in cyanobacteria. *Mol. Plant* 5, 1–13.

Haehnel, W. (1984). Photosynthetic electron transport in higher plants. *Ann. Rev. Plant Physiol.* 35, 659–693.

Hendrickson, L., Furbank, R. T., and Chow, W. S. (2004). A simple alternative approach to assessing the fate of absorbed light energy using chlorophyll fluorescence. *Photosyn. Res.* 82, 73–81.

Heyno, E., Gross, C.M., Laureau, C., Culcasi, M., Petrie, S. and Kreiger-Liszkay, A. (2009) Plastid alternative oxidase (PTOX) promotes oxidative stress when overexpressed in tobacco. *J. Biol. Chem.* 284, 31174–31180.

Horton, P., Johnson, M. P., Perez-Bueno, M. L., Kiss, A. Z., and Ruban, A. V. (2008). Photosynthetic acclimation: does the dynamic structure and macro-organisation of photosystem II in higher plant grana membranes regulate light harvesting states? *FEBS J.* 275, 1069–1079.

Horton, P., Ruban, A. V., and Walters, R. G. (1996). Regulation of light harvesting in green plants. *Ann. Rev. Plant Physiol. Plant Mol. Biol.* 47, 655–684.

Hüner, N. P. A., Elfman, B., Krol, M., and MacIntosh, A. (1984). Growth and development at cold hardening temperatures. Chloroplast ultrastructure, pigment content and composition. *Can. J. Bot.* 62, 53–60.

Hüner, N. P. A. and Grodzinski, B. (2011). "Photosynthesis and photoautotrophy" in *Comprehensive Biotechnology*, Vol. 1, ed. M. Moo-Young (Elsevier), 315–322.

Hüner, N. P. A., Ivanov, A. G., Sane, P. V., Pocock, T., Krol, M., Balseris, A., et al. (2006). "Photoprotection of Photosystem II: reaction centre quenching versus antenna quenching", in *Advances in Photosynthesis and Respiration*, Vol. 21, *Photoprotection, Gene Regulation and Environment*, eds. B. Demmig-Adams, W. W. Adams III, and A. K. Mattoo (Dordrecht: Springer), 155–173.

Hüner, N. P. A., Öquist, G., and Melis, A. (2003). "Photostasis in plants, green algae and cyanobacteria: the role of light harvesting antenna complexes", in *Advances in Photosynthesis and Respiration,* Vol. 13, *Light Harvesting Antennas in Photosynthesis*, eds. B. R. Green and W. W. (Dordrecht: Kluwer Academic Publishers), 401–421.

Hüner, N. P. A., Öquist, G., and Sarhan, F. (1998). Energy balance and acclimation to light and cold. *Trends Plant Sci.* 3, 224–230.

Jaglo-Ottosen, K. R., Gilmour, S. J., Zarka, D. G., Schabenberger, O., and Thomashow, M. F. (1998). *Arabidopsis* CBF1 overexpression induces COR genes and enhances freezing tolerance. *Science* 280, 104–106.

Joet, T., Cournac, L., Peltier, G., and Havaux, M. (2002). Cyclic electron flow around photosystem I in C3 plants. In vivo control by the redox state of chloroplasts and involvement of the NADH-dehydrogenase complex. *Plant Physiol.* 128, 760–769.

Johnson, G. N. (2011). PSI cyclic electron transport in higher plants. *Biochim. Biophys. Acta.* 1807, 906–911.

Jung, H.-S., and Chory, J. (2010). Signaling between chloroplasts and the nucleus: can a systems biology approach bring clarity to a complex and highly regulated pathway? *Plant Physiol.* 152, 453–459.

Karpinski, S., Reynolds, H., Karpinska, B., Wingsle, G., Creissen, G., and Mullineaux, P. (1999). Systemic signaling and acclimation in response to excess excitation energy in *Arabidopsis. Science* 284, 654–657.

Kasuga, M., Liu, Q., Miura, S., Yamaguchi-Shinozaki, K., and Shinozaki, K. (1999). Improving plant drought, salt, and freezing tolerance by gene transfer of a single stress-inducible transcription factor. *Nat. Biotechnol.* 17, 287–291.

Ke, B. (2001). "Photosystem I – introduction", in *Advances in Photosynthesis. Photobiochemistry and Photobiophysics*, Vol. 10, ed. Govindjee (Dordrecht: Kluwer Academic Publishers), 419–430.

Kehoe, D. M., and Gutu, A. (2006). Responding to color: the regulation of complementary chromatic adaptation. *Ann. Rev. Plant Biol.* 57, 127–150.

Kelliher, T., and Walbot, V. (2012). Hypoxia triggers meiotic fate acquisition in maize. *Science* 337, 345–348.

Kindgren, P., Noren, L., Barajas Lopez, J. dD., Shaikhali, J., and Strand, A. (2012). Interplay between HEAT SHOCK PROTEIN 90 and HY5 controls PhANG expression in response to the GUN5 plastid signal. *Mol. Plant* 5, 901–913.

Koussevitzky, S., Nott, A., Mockler, T. C., Hong, F., Sachetto-Martins, G., Surpin, M., et al. (2007). Signals from chloroplasts converge to regulate nuclear gene expression. *Science* 316, 715–719.

Kramer, D. M., Johnson, G., Kiirats, O., and Edwards, G. E. (2004). New fluorescence parameters for the determination of QA redox state and excitation energy fluxes. *Photosyn. Res.* 79, 209–218.

Krause, G. H., and Weis, E. (1991). Chlorophyll fluorescence and photosynthesis: the basics. *Ann. Rev. Plant Physiol. Plant Mol. Biol.* 42, 313–349.

Krol, M., Griffith, M., and Hüner, N. P. A. (1984). An appropriate physiological control for environmental temperature studies: comparative growth kinetics for winter rye. *Can. J. Bot.* 62, 1062–1068.

Krol, M., Ivanov, A. G., Jansson, S., Kloppstech, K., and Hüner, N. P. A. (1999). Greening under high light or cold temperature affects the level of xanthophyll-cycle pigments, early light-inducible proteins, and light-harvesting polypeptides in wild-type barley and the chlorina f2 mutant. *Plant Physiol.* 120, 193–203.

Krol, M., Maxwell, D. P., and Hüner, N. P. A. (1997). Exposure of *Dunaliella salina* to low temperature mimics the high light-induced accumulation of carotenoids and the carotenoid binding protein (Cbr). *Plant Cell Physiol.* 38, 213–216.

Lee, K. P., Kim, C., Landgraf, F., and Apel, K. (2007). EXECUTER1- and EXECUTER2-dependent transfer of stress-related signals from the plastid to the nucleus of *Arabidopsis thaliana. Proc. Natl. Acad. Sci. U.S.A.* 104, 10270–10275.

Leonardos, E. D., Savitch, L. V., Hüner, N. P. A., Öquist, G., and Grodzinski, B. (2003). Daily photosynthetic and C-export patterns in winter wheat leaves during cold stress and acclimation. *Physiol. Plant.* 117, 521–531.

Lepisto, A. and Rintamaki, E. (2012). Co-ordination of plastid and light signalling pathways upon development of *Arabidopsis* leaves under various photoperiods. *Mol. Plant.* 5, 799–816.

Levitt, J. (1980). *Responses of Plants to Environmental Stresses. Chilling, Freezing, and High Temperature Stresses*, Vol. I. New York: Academic Press.

Liu, Q., Kasuga, M., Sakuma, Y., Abe, H., Miura, S., Yamaguchi-Shinozaki, K., and Shinozaki, K. (1998). Two transcription factors, DREB1 and DREB2, with an EREBP/AP2 DNA

binding domain separate two cellular signal transduction pathways in drought- and low-temperature-responsive gene expression, respectively, in *Arabidopsis*. *Plant Cell* 10, 1391–1406.

Masuda, T., Polle, J. E. W., and Melis, A. (2002). Biosynthesis and distribution of chlorophyll among the photosystems during recovery of the green alga *Dunaliella salina* from irradiance stress. *Plant Physiol.* 128, 603–614.

Masuda, T., Tanaka, A., and Melis, A. (2003). Chlorophyll antenna size adjustments by irradiance in *Dunaliella salina* involve coordinate regulation of chlorophyll a oxygenase (CAO) and Lhcb gene expression. *Plant Mol. Biol.* 51, 757–771.

Maxwell, D. P., Falk, S., and Hüner, N. P. A. (1995a). Photosystem II excitation pressure and development of resistance to photoinhibition I. LHCII abundance and zeaxanthin content in *Chlorella vulgaris*. *Plant Physiol.* 107, 687–694.

Maxwell, D. P., Laudenbach, D. E., and Hüner, N. P. A. (1995b). Redox regulation of light-harvesting complex II and cab mRNA abundance in *Dunaliella salina*. *Plant Physiol.* 109, 787–795.

McDonald, A. E., Ivanov, A. G., Bode, R., Maxwell, D. P., Rodermel, S. R., and Hüner N. P. A. (2011). Flexibility in photosynthetic electron transport: the physiological role of plastoquinol terminal oxidase (PTOX). *Biochim.Biophys. Acta* 1807, 954–967.

Melis, A. (1998). "Photostasis in plants", in *Photostasis and Related Phenomena*, eds R. Williams and A. Thistle (New York: Plenum Press), 207–220.

Miskiewicz, E., Ivanov, A. G., and Hüner, N. P. A. (2002). Stoichiometry of the photosynthetic apparatus and phycobilisome structure of the cyanobacterium *Plectonema boryanum* UTEX 485 are regulated by both light and temperature. *Plant Physiol.* 130, 1414–1425.

Miskiewicz, E., Ivanov, A. G., Williams, J. P., Khan, M. U., Falk, S., and Hüner, N. P. A. (2000). Photosynthetic acclimation of the filamentous cyanobacterium, *Plectonema boryanum* UTEX 485, to temperature and light. *Plant Cell Physiol.* 41, 767–775.

Mittler, R., Vanderauwera, S., Gollery, M., and Van Breusegem, F. (2004). Reactive oxygen gene network of plants. *Trends Plant Sci.* 9, 490–498.

Morgan-Kiss, R. M., Priscu, J. C., Pocock, T., Gudynaite-Savitch, L., and Hüner, N. P. A. (2006). Adaptation and acclimation of photosynthetic microorganisms to permanently cold environments. *Microbiol. Mol. Biol. Rev.* 70, 222–252.

Mullineaux, P. M., Ball, L., Escobar, C., Karpinska, B., Creissen, G., and Karpinski, S. (2000). Are diverse signalling pathways integrated in the regulation of *Arabidopsis* antioxidant defence gene expression in response to excess excitation energy? *Philos. Trans. R. Soc. Lond. B Biol. Sci.* 355, 1531–1540.

Mullineaux, P. M., Karpinski, S., and Baker, N. R. (2006). Spatial dependence for hydrogen peroxide-directed signaling in light-stressed plants. *Plant Physiol.* 141, 346–350.

Murchie, E. H., Pinto, M., and Horton, P. (2009). Agriculture and the new challenges for photosynthesis research. *New Phytol.* 181, 532–552.

Niyogi, K. K. (1999). Photoprotection revisited: genetic and molecular approaches. *Ann. Rev. Plant Physiol. Plant Mol. Biol.* 50, 333–359.

Nott, A., Jung, H.-S., Koussevitzky, S., and Chory, J. (2006). Plastid-to-nucleus retrograde signaling. *Ann. Rev. Plant Biol.* 57, 739–759.

Öquist, G., and Huüner, N. P. A. (2003). Photosynthesis of overwintering evergreen plants. *Ann. Rev. Plant Biol.* 54, 329–355.

Padmasree, K., and Raghavendra, A. S. (2001). Consequence of restricted mitochondrial oxidative metabolism on photosynthetic carbon assimilation in mesophyll protoplasts: decrease in light activation of four chloroplastic enzymes. *Physiol. Plant.* 112, 582–588.

Peltier, G., and Cournac, L. (2002). Chlororespiration. *Ann. Rev. Plant Biol.* 53, 523–550.

Pesaresi, P., Hertle, A., Pribil, M., Kleine, T., Wagner, R., Strissel, H., et al. (2009). *Arabidopsis* STN7 kinase provides a link between short- and long-term photosynthetic acclimation. *Plant Cell* 21, 2402–2423.

Pfannschmidt, T. (2003). Chloroplast redox signals: how photosynthesis controls its own genes. *Trends Plant Sci.* 8, 33–41.

Pfannschmidt, T., Nilsson, A., and Allen, J. F. (1999). Photosynthetic control of chloroplast gene expression. *Nature* 397, 625–628.

Pfannschmidt, T. and Yang, C. (2012). The hidden function of photosynthesis: a sensing system for environmental conditions that regulates photoacclimation responses. *Protoplasma* 249, 125–136.

Piippo, M., Allahverdiyeva, Y., Paakkarinen, V., Suoranta, U.-M., Battchikova, N., and Aro, E.-M. (2006). Chloroplast-mediated regulation of nuclear genes in *Arabidopsis thaliana* in the absence of light stress. *Physiol. Genomics* 25, 142–152.

Quail, P. H., Boylan, M. T., Parks, B. M., Short, T. W., Xu, Y., and Wagner, D. (1995). Phytochromes: photosensory perception and signal transduction. *Science* 268, 675–680.

Raghavendra, A. S., Padmasree, K., and Saradadevi, K. (1994). Interdependence of photosynthesis and respiration in plant cells: interactions between chloroplasts and mitochondria. *Plant Sci.* 97, 1–14.

Rochaix, J. D. (2011). Regulation of photosynthetic electron transport. *Biochim. Biophys. Acta* 1807, 375–383.

Rodermel, S. (2001). Pathways of plastid-to-nucleus signaling. *Trends Plant Sci.* 6, 471–478.

Rodermel, S. (2002). "*Arabidopsis* variegation mutants." in *The Arabodopsis Book*, eds. C. R. Sommerville and E. M. Meyerowitz (American Society of Plant Biologists). Available at: http://www.bioone.org/pdfserv/i1543-8120-030-01-0001.pdf.

Rosso, D., Bode, R., Li, W., Krol, M., Saccon, D., Wang, S., et al. (2009). Photosynthetic redox imbalance governs leaf sectoring in the *Arabidopsis thaliana* variegation mutants immutans, spotty, var1, and var2. *Plant Cell* 21, 3473–3492.

Rosso, D., Ivanov, A. G., Fu, A., Geisler-Lee, J., Hendrickson, L., Geisler, M., et al. (2006). IMMUTANS does not act as a stress-induced safety valve in the protection of the photosynthetic apparatus of *Arabidopsis* during steady-state photosynthesis. *Plant Physiol.* 142, 574–585.

Sakamoto, W., Miyagishima, S.-Y. and Jarvis, P. (2008). "Chloroplast biogenesis: control of plastid development, protein import, division and inheritance," in *The Arabidopsis Book*, eds. C. R. Sommerville and E. M. Meyerowitz (American Society of Plant Biologists). Available at: http://www.bioone.org/pdfserv/i1543-8120-030-01-0001.pdf.

Savitch, L. V., Allard, G., Seki, M., Robert, L. S., Tinker, N. A., Hüner, N. P. A., et al. (2005). The effect of over-expression of two *Brassica* CBF/DREB1-Like transcription factors on photosynthetic capacity and freezing tolerance in *Brassica napus*. *Plant Cell Physiol.* 46, 1525–1539.

Savitch, L. V., Harney, T., and Hüner, N. P. A. (2000a). Sucrose metabolism in spring and winter wheat in response to high irradiance, cold stress and cold acclimation. *Physiol. Plant.* 108, 270–278.

Savitch, L. V., Massacci, A., Gray, G. R., and Hüner, N. P. A. (2000b). Acclimation to low temperature or high light mitigates sensitivity to photoinhibition: roles of the Calvin cycle and the Mehler reaction. *Aust. J. Plant Physiol.* 27, 253–264.

Savitch, L. V., Maxwell, D. P., and Hüner, N. P. A. (1996). Photosystem II excitation pressure and photosynthetic carbon metabolism in *Chlorella vulgaris*. *Plant Physiol.* 111, 127–136.

Schreiber, U., Bilger, W., and Neubauer, C. (1994). "Chlorophyll fluorescence as a nonintrusive indicator for rapid assessment of in vivo photosynthesis,"in *Ecophysiology of Photosynthesis*, eds E. D. Schulze and M. M. Caldwell (Berlin: Springer-Verlag), 49–70.

Shikanai, T. (2007). Cyclic electron transport around photosystem I: genetic approaches. *Ann. Rev. Plant Biol.* 58, 199–217.

Stepien, P., and Johnson, G. N. (2009). Contrasting responses of photosynthesis to salt stress in the glycophyte *Arabidopsis* and the halophyte *Thellungiella*: role of the plastid terminal oxidase as an alternative electron sink. *Plant Physiol.* 149, 1154–1165.

Stitt, M., and Hurry, V. (2002). A plant for all seasons: alterations in photosynthetic carbon metabolism during cold acclimation in *Arabidopsis*. *Curr. Opin. Plant Biol.* 5, 199–206.

Strand, A., Asami, T., Alonso, J., Ecker, J. R., and Chory, J. (2003a). Chloroplast to nucleus communication trigered by accumulation of Mg-protoporphyrin IX. *Nature* 421, 79–83.

Strand, A., Foyer, C. H., Gustafsson, P., Gardestrom, P., and Hurry, V. (2003b). Altering flux through the sucrose biosynthesis pathway in transgenic *Arabidopsis thaliana* modifies photosynthetic acclimation at low temperatures and the development of freezing tolerance. *Plant Cell Environ.* 26, 523–535.

Strand, A., Hurry, V., Henkes, S., Hüner, N. P. A., Gustafsson, P., Gardestrom, P., et al. (1999). Acclimation of *Arabidopsis* leaves developing at low temperatures. Increasing cytoplasmic volume accompanies increased activities of enzymes in the Calvin cycle and in the sucrose-biosynthesis pathway. *Plant Physiol.* 119, 1387–1397.

Streb, P., Josse, E.-M., Gallouet, E., Baptist, F., Kuntz, M., and Cornic, G. (2005). Evidence for alternative electron sinks to photosynthetic carbon assimilation in the high mountain plant species *Ranunculus glacialis*. *Plant Cell Environ.* 28, 1123–1135.

Sukenik, A., Wyman, K. D., Bennett, J., and Falkowski, P. G. (1987). A novel mechanism for regulating the excitation of photosystem II in a green alga. *Nature* 327, 704–707.

Sung, S., and Amasino, R. M. (2005). Remembering winter: toward a molecular understanding of vernalization. *Ann. Rev. Plant Biol.* 56, 491–508.

Tanaka, R., Koshino, Y., Sawa, S., Ishiguro, S., Okada, K., and Tanaka, A. (2001). Overexpression of chlorophyllide a oxygenase (CAO) enlarges the antenna size of photosystem II in *Arabidopsis thaliana*. *Plant J.* 26, 365–373.

Tanaka, R., and Tanaka, A. (2007). Tetrapyrrole biosynthesis in higher plants. *Ann. Rev. Plant Biol.* 58, 321–346.

Theocharis, A., Clemente, C., and Barka, E. A. (2012). Physiological and molecular changes in plants grown at low temperatures. *Planta* 235, 1091–1105.

Thornber, J. P., Cogdell, R. J., Chitnis, P., Morishige, D. T., Peter, G. F., Gomez, S. M., et al. (1994). "Antenna pigment–protein complexes of higher plants and purple bacteria," in *Advances in Molecular and Cell Biology*, Vol. 10, ed. J. Barber (London: JAI Press), 55–118.

Trevaskis, B. (2010). The central role of the VERNALIZATION1 gene in the vernalization response of cereals. *Funct. Plant Biol.* 37, 479–487.

Trevaskis, B., Hemming, M. N., Dennis, E. S., and Peacock, W. J. (2007). The molecular basis of vernalization-induced flowering in cereals. *Trends Plant Sci.* 12, 352–357.

Tsukagoshi, H., Busch, W., and Benfey, P. N. (2010). Transcriptional regulation of ROS controls transition from proliferation to differentiation in the root. *Cell* 143, 606–616.

Vanlerberghe, G. C., and McIntosh, L. (1997). Alternative oxidase: from gene to function. *Ann. Rev. Plant Physiol. Plant Mol. Biol.* 48, 703–734.

von Gromoff, E. D., Alawady, A., Meinecke, L., Grimm, B., and Beck, C. F. (2008). Heme, a plastid-derived regulator of nuclear gene expression in *Chlamydomonas*. *Plant Cell* 20, 552–567.

Wagner, D., Przybyla, D., op den Camp, R., Kim, C., Landgraf, F., Lee, K. P., et al. (2004). The genetic basis of singlet oxygen-induced stress responses of *Arabidopsis thaliana*. *Science* 306, 1183–1185.

Walters, R. G., and Horton, P. (1993). Theoretical assessment of alternative mechanisms for non-photochemical quenching of PSII fluorescence in barley leaves. *Photosyn. Res.* 36, 119–139.

Walters, R. G., Rogers, J. J. M., Shephard, F., and Horton, P. (1999). Acclimation of *Arabidopsis thaliana* to the light environment: the role of photoreceptors. *Planta* 209, 517–527.

Wetzel, C. M., Jiang, C. Z., Meehan, L. J., Voytas, E. F. and Rodermel, S. (1994). Nuclear-organelle interactions: the immutans variegation mutant of *Arabidopsis* is plastid autonomous and impaired in carotenoid biosynthesis. *Plant J.* 6, 161–175.

Whipple, C. (2012). Defining the plant germ line: nature or nuture? *Science* 337, 301–302.

Whitelam, G. C., and Devlin, P. F. (1998). Light Signalling in *Arabidopsis*. *Plant Physiol. Biochem.* 36, 125–133.

Wilson, K. E., and Hüner, N. P. A. (2000). The role of growth rate, redox-state of the plastoquinone pool and the trans-thylakoid ΔpH in photoacclimation of *Chlorella vulgaris* to growth irradiance and temperature. *Planta* 212, 93–102.

Wilson, K. E., Ivanov, A. G., Öquist, G., Grodzinski, B., Sarhan, F., and Hüner, N. P. A. (2006). Energy balance, organellar redox status and acclimation to environmental stress. *Can. J. Bot.* 84, 1355–1370.

Wilson, K. E., Krol, M., and Hüner, N. P. A. (2003). Temperature-induced greening of *Chlorella vulgaris*. The role of the cellular energy balance and zeaxanthin-dependent nonphotochemical quenching. *Planta* 217, 616 –627.

Woodson, J. D., and Chory, J. (2008). Coordination of gene expression between organellar and nuclear genomes. *Nat. Rev. Genet.* 9, 383–395.

Wu, D., Wright, D. A., Wetzel, C., Voytas, D. F., and Rodermel, S. (1999). The IMMUTANS variegation locus of *Arabidopsis* defines a mitochondrial alternative oxidase homolog that functions during early chloroplast biogenesis. *Plant Cell* 11, 43–56.

Yu, F., Fu, A., Aluru, M., Park, S., Xu, Y., Liu, H., et al. (2007). Variegation mutants and mechanisms of chloroplast biogenesis. *Plant Cell Environ.* 30, 350–365.

Conflict of Interest Statement: The authors declare that the research was conducted in the absence of any commercial or financial relationships that could be construed as a potential conflict of interest.

Received: 16 August 2012; accepted: 30 October 2012; published online: 20 November 2012.

*Citation: Hüner NPA, Bode R, Dahal K, Hollis L, Rosso D, Krol M and Ivanov AG (2012) Chloroplast redox imbalance governs phenotypic plasticity: the "grand design of photosynthesis" revisited. Front. Plant Sci. **3**:255. doi: 10.3389/fpls.2012.00255*

This article was submitted to Frontiers in Plant Physiology, a specialty of Frontiers in Plant Science.

Copyright © 2012 Hüner, Bode, Dahal, Hollis, Rosso, Krol and Ivanov. This is an open-access article distributed under the terms of the Creative Commons Attribution License, which permits use, distribution and reproduction in other forums, provided the original authors and source are credited and subject to any copyright notices concerning any third-party graphics etc.

frontiers in
PLANT SCIENCE

ORIGINAL RESEARCH ARTICLE
published: 27 December 2012
doi: 10.3389/fpls.2012.00282

Thylakoid redox signals are integrated into organellar-gene-expression-dependent retrograde signaling in the *prors1-1* mutant

***Luca Tadini*[1], *Isidora Romani*[1], *Mathias Pribil*[1], *Peter Jahns*[2], *Dario Leister*[1]* *and Paolo Pesaresi*[3]**

[1] *Plant Molecular Biology (Botany), Department Biology I, Ludwig-Maximilians-Universität München, Munich, Germany*
[2] *Plant Biochemistry, Heinrich-Heine-University Düsseldorf, Düsseldorf, Germany*
[3] *Dipartimento di Bioscienze, Università degli studi di Milano, Milan, Italy*

Edited by:
Tatjana Kleine, Ludwig-Maximilians-Universität München, Germany

Reviewed by:
Shan Lu, Nanjing University, China
Margarete Baier, FU Berlin, Germany

****Correspondence:***
Dario Leister, Plant Molecular Biology (Botany), Department Biology I, Ludwig-Maximilians-Universität München, Großhaderner Str. 2, D-82152 Planegg-Martinsried, Germany.
e-mail: leister@lmu.de

Perturbations in organellar gene expression (OGE) and the thylakoid redox state (TRS) activate retrograde signaling pathways that adaptively modify nuclear gene expression (NGE), according to developmental and metabolic needs. The *prors1-1* mutation in Arabidopsis down-regulates the expression of the nuclear gene *Prolyl-tRNA Synthetase1* (*PRORS1*) which acts in both plastids and mitochondria, thereby impairing protein synthesis in both organelles and triggering OGE-dependent retrograde signaling. Because the mutation also affects thylakoid electron transport, TRS-dependent signals may likewise have an impact on the changes in NGE observed in this genotype. In this study, we have investigated whether signals related to TRS are actually integrated into the OGE-dependent retrograde signaling pathway. To this end, the *chaos* mutation (for chlorophyll a/b binding protein harvesting-organelle specific), which shows a partial loss of PSII antennae proteins and thus a reduction in PSII light absorption capability, was introduced into the *prors1-1* mutant background. The resulting double mutant displayed a *prors1-1*-like reduction in plastid translation rate and a *chaos*-like decrease in PSII antenna size, whereas the hyper-reduction of the thylakoid electron transport chain, caused by the *prors1-1* mutation, was alleviated, as determined by monitoring chlorophyll (Chl) fluorescence and thylakoid phosphorylation. Interestingly, a substantial fraction of the nucleus-encoded photosynthesis genes down-regulated in the *prors1-1* mutant are expressed at nearly wild-type rates in *prors1-1 chaos* leaves, and this recovery is reflected in the steady-state levels of their protein products in the chloroplast. We therefore conclude that signals related to photosynthetic electron transport and TRS, and indirectly to carbohydrate metabolism and energy balance, are indeed fed into the OGE-dependent retrograde pathway to modulate NGE and adjust the abundance of chloroplast proteins.

Keywords: gene expression, organelle, translation, light, redox, retrograde signaling

INTRODUCTION

Several features link mitochondria and plastids within the plant cell. Both organelles maintain and express genetic information, conduct electron transport functions, and are metabolically interdependent (Woodson and Chory, 2008).

In addition, the majority of mitochondrial and plastid proteins are nucleus-encoded (Kleine et al., 2009a). Therefore, to ensure that the multiprotein complexes essential for photosynthesis and respiration are assembled correctly, the activities of both organelle types must be closely coordinated with that of the nuclear genome. Signals from the organelles to the nucleus are collectively referred as retrograde signals and can largely be grouped into two categories. (1) Biogenic control, i.e., developmental control of organelle biogenesis needs to be appropriately staged and the required subunits and cofactors need to be present in correct stoichiometry for accurate assembly; and (2) operational control, representing rapid adjustments that are made to energy metabolism in response to environmental and developmental constraints to maintain optimal production and both limit and repair damage induced by oxidative stress (reviewed in Leister, 2005; Pesaresi et al., 2007; Pogson et al., 2008; Woodson and Chory, 2008; Barajas-Lopez et al., in press). Given the complexity of organellar functions, a variety of interlinked retrograde pathways can be expected (Kleine et al., 2009b; Leister, 2012).

Several metabolites have been proposed to act as messenger molecules during retrograde signaling, including (1) tetrapyrroles (Mg-protoporphyrin IX or heme) (Strand et al., 2003; Woodson et al., 2011); (2) phosphonucleotide 3′-phosphoadenosine 5′-phosphate (PAP) (Estavillo et al., 2011); (3) β-cyclocitral (Ramel et al., 2012); and (4) methylerythritol cyclodiphosphate (MEcPP) (Xiao et al., 2012). Moreover, plastid retrograde signaling has also been associated with responses to perturbations in photosynthetic electron transport [changes in thylakoid and stromal redox state, accumulation of the reactive oxygen species (ROS) $^1O_2$ and H_2O_2 (reviewed in Apel and Hirt, 2004; Oelze et al., 2008)], as well as in organellar gene expression (OGE),

involving the pentatricopetide protein GUN1, abscisic acid (ABA) and the transcription factors PTM and ABI4 (Sullivan and Gray, 1999; Koussevitzky et al., 2007; Sun et al., 2011).

Recently, the role of Mg-protoporphyrin IX (Mg-ProtoIX) as a plastid signal has been questioned, since its accumulation following norflurazon treatment could not be correlated with changes in NGE (Mochizuki et al., 2008; Moulin et al., 2008). Consequently, it was suggested that either rapid changes in the flux through the tetrapyrrole pathway, or the accumulation of Mg-ProtoIX in a specific cellular compartment could be the origin of the plastid signal (Mochizuki et al., 2008; Moulin et al., 2008); however, these aspects deserve further investigations. Similarly, the role of ROS as classical retrograde signals is debated, because they are either probably too short-lived to reach the nucleus, as in the case of singlet oxygen $^1O_2$, or too unspecific (H_2O_2) to act as information carriers (Moller and Sweetlove, 2010).

Beside the uncertainty on messenger molecules, little is also known about the extent to which different signals can be integrated into common pathways. The first insights into signaling pathways that serve to integrate chloroplast and mitochondrial activities with NGE were obtained through the characterization of mutant alleles of *PRORS1* (*At5g52520*), an Arabidopsis gene coding for a prolyl-tRNA synthetase that is imported into both chloroplasts and mitochondria (Pesaresi et al., 2006). The leaky *prors1-1* mutant allele exhibited defects in photosynthesis due to the simultaneous impairment of translation in plastids and mitochondria. Concomitantly, a specific and marked drop in the levels of transcripts of nuclear genes for proteins involved in the light reactions of photosynthesis was observed, implying that the activity of the OGE-dependent retrograde signaling pathway was altered. To investigate the specific roles of protein synthesis in mitochondria and chloroplasts in regulating nuclear photosynthetic gene expression, Arabidopsis mutants altered in mRNA translation in either mitochondria (*mrpl11-1*) or plastids (*prpl11-1*) were isolated (Pesaresi et al., 2001, 2006). Comparison of the transcript profiles of *prors1-1*, *mrpl11-1*, and *prpl11-1* mutants and the double mutant *mrpl11-1 prpl11-1* showed that plastids and mitochondria generate signals which act synergistically to modulate nuclear photosynthetic gene expression.

In this study, we have investigated the extent to which signals related to photosynthetic electron transport contribute to the OGE-dependent retrograde signaling pathway, by introducing the *chaos* mutation (Klimyuk et al., 1999) into the *prors1-1* mutant background. In the *chaos* mutant, the *CAO* gene (*At2g47450*), which codes for the chloroplast recognition particle cpSRP43, is inactivated. CpSRP43 together with cpSRP54 form the chloroplast signal recognition particle complex (Keegstra and Cline, 1999), required for the integration of the PSII antenna proteins (Lhcb proteins) into the thylakoid membranes (Schuenemann et al., 1998; Amin et al., 1999; Klimyuk et al., 1999). Consequently, *chaos* plants are characterized by reduced PSII antenna size, as manifested by decreased Chl *b* and Lhcb protein contents, together with reduced levels of oxygen production and growth rate (Amin et al., 1999; Klimyuk et al., 1999). Moreover, the reduced light absorption is also associated with significantly lower foliar H_2O_2 levels than in wild type (WT), and is responsible for less photobleaching of leaves, lower induction of cytosolic ascorbate peroxidases, and lower degree of photoinhibition, indicating that *chaos* chloroplasts are maintained in a more oxidized state than WT (Klenell et al., 2005).

The *prors1-1 chaos* double mutant was compared with each single mutant in relation to rates of translation in plastids, photosynthetic performance, and NGE. The results obtained imply that signals related to photosynthetic electron transport, and indirectly to carbon metabolism and energy balance, can indeed be integrated into the OGE-dependent retrograde pathway.

MATERIALS AND METHODS

PLANT MATERIAL, PROPAGATION, AND GROWTH MEASUREMENTS

The *prors1-1* mutant allele and its detection by PCR are described in Pesaresi et al. (2006). In particular, the mutation is caused by a T-DNA insertion (*pAC106*) at −44 bp from the translation starting codon. The gene-specific primers prors1-sense (5′-AACCAAGCATGAGTTTCTCG-3′) and prors1-antisense (5′-ATCCGGAAAGAGGTCTGTTC-3′) were employed to detect the WT *PRORS1* allele; the T-DNA-specific primer T9697 (5′-CTCTTTCTTTTTCTCCATATTGACCAT-3′) and prors1-antisense were used to identify the *prors1-1* mutant allele. The *chaos* mutant used in this study was identified in a population mutagenized with the *En* transposon (Wisman et al., 1998) based on its photosynthetic performance and leaf pigment composition (Varotto et al., 2000). The mutant allele carries an *En* insertion (which is stable because of 249-bp deletion at the left border) at position +149 (relative to the start codon) in the single-exon gene *CAO*. The gene-specific primers cao-sense (5′-ATGCAAAAGGTCTTCTTGGC-3′) and cao-antisense (5′-CCTCTCTCGTCTTCCACTTC-3′) were employed in PCRs to detect the WT *CAO* allele; the *En*-specific primer EnR (5′-GAGCGTCGGTCCCCACACTTCTATAC-3′) and cao-antisense were used to identify the *chaos* mutant allele. The *prors1-1 chaos* double mutant was obtained by crossing *prors1-1* and *chaos* single mutants and PCR-genotyping F2 individuals. *Arabidopsis thaliana* Heynh. WT (Col-0) and mutant plants were grown under controlled growth chamber conditions as described (Pesaresi et al., 2009). The method used for growth measurement has been described before (Leister et al., 1999).

NUCLEIC ACID ANALYSIS

A. thaliana DNA was isolated as described (Ihnatowicz et al., 2004). For RNA analysis, total leaf RNA was extracted from fresh tissue using the TRIzol reagent (Invitrogen, Germany). Northern analysis was performed under stringent conditions, according to Sambrook and Russell (2001). Probes complementary to nuclear or chloroplast genes were used for the hybridization experiments. Primers used to amplify the probes are listed in **Table 1**. All probes used were cDNA fragments labeled with ^{32}P. Signals were quantified with a phosphoimager (Typhoon; GE Healthcare, Munich, Germany) using the program ImageQuant (version 1.2; Molecular Dynamics). For quantitative real-time PCR (qRT-PCR) analysis, 4 μg aliquots of total RNA, treated with DNase I (Roche Applied Science) for at least 30 min, were utilized for first-strand cDNA synthesis using iScript reverse transcriptase

Table 1 | Oligonucleotide sequences employed for gene expression analysis.

Gene	Sense primer	Antisense primer
psaB (ATCG00340)	GTATTGCTACCGCACATGAC	CCACGAAACTCTTGGTTTCC
psbA (ATCG00020)	CGGCCAAAATAACCGTGAGC	TATACAACGGCGGTCCTTATG
RbcL (ATCG00490)	CGTTGGAGAGACCGTTTCTT	CAAAGCCCAAAGTTGACTCC
RbcS (AT1G67090)	ATGGCTTCCTCTATGTTCTC	CGGTGCATCCGAACAATGGA
Lhca1(AT3G54890)	GTCAAGCCACTTACTTGGGA	GGGATAACAATATCGCCAATG
Lhca2(AT3G61470)	GAGTTCCTAACGAAGATCGG	AAGATTGTGGCGTGACCAGG
Lhca3(AT1G61520)	AGGCTGGTCTGATTCCAGCA	ACTTGAGGCTGGTCAAGACG
Lhca4(AT3G47470)	TGAGTGGTACGATGCTGGGA	GTGTTGTGCCATGGGTCAGA
Lhcb1(AT1G29910)	GACTTTCAGCTGATCCCGAG	CGGTCCCTTACCAGTGACAA
*Lhcb1(AT1G29910)**	AGAGTCGCAGGAAATGGG	AAGCCTCTGGGTCGGTAG
Lhcb2(AT2G05070)	GAGACATTCGCTAAGAACCG	CCAGTAACAATGGCTTGGAC
*Lhcb2(AT2G05070)**	GCTATCCAACAATCCTCCTTC	CCAGTTAAGTAAGACGGTGTG
Lhcb3(AT5G54270)	GGAGATGGGCAATGTTGGGA	TAGTTGCGAAAGCCCACGCA
*Lhcb3(AT5G54270)**	CCGTGTGGACTTCAAAGAACC	CGCCAACACCATCAAGACC
Lhcb4(AT3G08940)	AGCTAGTGGATGGATCATCT	CAGGAGGAAGAGAAGGTATC
PsaD1(AT4G02770)	AAGCCGCCGGGATCTTCAAC	CTAAGCCTTGTCCCCAAAGC
PsaE1(AT4G28750)	ATGGCGATGACGACAGCATC	TGTTGGTCGATATGTTGGCG
PsaF (AT1G31330)	GTTCGACAACTACGGGAAGT	CTTAGCAATGAGATCACCAT
PsaK (AT1G30380)	ATGGTCTTCG AGCCACCAAA	CGTTCAGGTGCATGAGAATA
PsaO (AT1G08380)	ATGGCAGCAACATTTGCAAC	GTAATCTTCAGTCCTGCCCT
PsbO2 (AT3G50820)	AGACGGAAGCGTGAAGTTCA	CAATCTGACCGTACCAAACC
PsbT2 (AT3G21055)	ATGGCGTCAATGACCATGAC	CAGTTACGGCATATCTTGGC
PsbX (AT2G06520)	ATGGCTTCTACCTCCGCGAT	TAGGTTCTCTTGACAGGGTC
Ferritin1(AT5G01600)	ATGGCCTCAAACGCACTCTC	ATGCCCTCTCTCTTCCTCAC
*Ferritin1(AT5G01600)**	TAAACGTTCACAAAGTGGCC	TAGAGGTCCAAGTCTAGTTC
AOX1(AT1G32350)	GGTTCTGAATGGAAGTGGAAC	GGAGCTGGAGCTTCCTTTAGT
*AOX1(AT1G32350)**	CCGCACTCTTCGACCGGTAC	GCTGAACCGTCCGGTTTAGT
2CPA (AT3G11630)	ATGGCGTCTGTTGCTTCTTC	TGCAAGGTGAGAGAACACAC
*2CPA (AT3G11630)**	CCGGATTTGCTCGACGCTCT	CAACTTCTCAAATTCTGAATGC
CAT1(AT1G20630)	CTTCTTTGACTGTCGGAACTC	CCAGTATCCTCCAGTTCTCC
*CAT1(AT1G20630)**	ACAACAGTGCAGACACACGC	AGCGCTTGAAGGACGAACCC
*ACTIN**	ACTACTGGTATTGTGTTGGACTC	CCCTTACGATTTCACGCTCTG

Asterisk indicates primer pairs employed for qRT-PCR analyses.

(Bio-Rad) according to the supplier's instructions. The qRT-PCR profiling was carried out on an iCycler iQ5 real-time PCR system (Bio-Rad), using the oligonucleotide sequences reported in **Table 1**. Actin was used as internal standard. Data from three biological and three technical replicates were analyzed with Bio-Rad iQ5 software (version 2.0).

PAGE AND IMMUNOBLOT ANALYSES

Leaves were harvested from plants at the 6-leaf rosette stage, and thylakoids were prepared as described (Bassi et al., 1985). For SDS-PAGE, thylakoid proteins isolated from equal amounts of leaf material (fresh weight) were fractionated on denaturing Tris-glycine SDS-PAGE gels (with 12% PA) and the protein content was stained with colloidal Coomassie blue (G 250).

For immunoblot analyses, total proteins were prepared from plants at the 6-leaf rosette stage (Martinez-Garcia et al., 1999), then fractionated by SDS-PAGE (on 12% polyacrylamide gels) (Schägger and von Jagow, 1987). Subsequently, proteins were transferred to poly(vinylidene difluoride) membranes (Ihnatowicz et al., 2004), and replicate filters were probed with appropriate antibodies. Signals were detected by enhanced chemiluminescence (GE Healthcare). Thylakoid protein phosphorylation was monitored with a phosphothreonine-specific antibody (Cell Signaling Technology) in total leaf protein extracts obtained from WT and mutant plants kept overnight in the dark and then exposed to light (80 μmol photons m^{-2} s^{-1}) for 4 h.

Coomassie-stained gels and immunoblots were scanned and quantified using ImageQuant (version 1.2; Molecular Dynamics).

In vivo TRANSLATION ASSAY

The *in vivo* translation assay was performed essentially as in Pesaresi (2011). Twelve leaf discs (4 cm in diameter) were incubated in a buffer containing 20 μg/ml cycloheximide, 1 mM K_2HPO_4–KH_2PO_4 (pH 6.3), and 0.1% (w/v) Tween-20 to block cytosolic translation. [^{35}S]methionine was added to the buffer (0.1 mCi/ml) and infiltrated into the discs under vacuum. Leaves

were exposed to light (20 μmol photons m^{-2} s^{-1}) and four leaf discs were collected at each time point (5, 15, and 30 min). Total proteins were extracted as described above and fractionated by Tris-glycine SDS-PAGE (12% PA). Signals were detected and quantified using the phosphoimager and the ImageQuant program as described above.

Chl FLUORESCENCE, OXYGEN EVOLUTION, AND PIGMENT ANALYSES

In vivo Chl a fluorescence of leaves was measured using the Dual-PAM-100 (Walz, Effeltrich, Germany) as described (Pesaresi et al., 2009). Five plants of each genotype were analyzed and average values plus standard deviations were calculated. Plants were first dark-adapted for 30 min and minimal fluorescence (F_0) was measured. Then pulses (0.8 s) of saturating white light (5000 μmol photons m^{-2} s^{-1}) were used to determine the maximum fluorescence (F_M), and the ratio $(F_M - F_0)/F_M = F_V/F_M$ (maximum quantum yield of PSII) was calculated. An 8-min exposure to actinic red light (37 μmol photons m^{-2} s^{-1}) served to drive electron transport between PSII and PSI at steady state. In particular, the employed routine allowed to measure the steady-state fluorescence (F_S) and the maximum fluorescence after light adaptation ($F_{M'}$) (saturation pulse, 0.8 s, 5000 μmol photons m^{-2} s^{-1}) every 20 s. The ratio $(F_{M'} - F_S)/F_{M'}$ gives the effective quantum yield of PSII (Φ_{II}),while the excitation pressure parameter 1-qL reflects the size of the reduced fraction of Q_A. The coefficient of photochemical quenching, qL, was calculated as $(F_{M'} - F_S)/(F_{M'} - F_{0'}) \times F_{0'}/F_S$ (Kramer et al., 2004), with $F_{0'}$ being the minimum fluorescence after removal of the illumination. A 2-min dark period was also employed to monitor the recovery to the maximum quantum yield of PSII.

In vivo Chl a fluorescence of whole plants was recorded using an imaging Chl fluorometer (Imaging PAM; Walz, Germany). Dark-adapted plants were exposed to a pulsed, blue measuring beam (1 Hz, intensity 4; F_0) and a saturating light flash (intensity 4) to obtain F_V/F_M. A 10-min exposure to actinic light (80 μmol photons m^{-2} s^{-1}) was then used to calculate Φ_{II} at the steady state.

Rates of oxygen evolution from leaf discs were measured with a Clark-type oxygen electrode (Hansatech Instruments Ltd.) as described by Havaux and Devaud (1994). In particular, measurements were performed at saturating CO_2 concentration by employing a bicarbonate/carbonate buffer. The light limited rates of photosynthetic O_2 evolution were measured at 80 μmol photons m^{-2} s^{-1}. Pigments were analyzed by reversed-phase HPLC (Farber et al., 1997).

RESULTS

LIGHT ABSORPTION AND OXYGEN EVOLUTION ARE REDUCED IN *prors1-1 chaos* LEAVES

The double mutant *prors1-1 chaos* was generated as described in "Materials and Methods." Like the corresponding single mutants *prors1-1* and *chaos*, the *prors1-1 chaos* double mutant has pale-green cotyledons and leaves, and is smaller than WT plants of the same age (**Figure 1A**). Quantification of growth rates by non-invasive image analysis under growth chamber conditions showed that while *prors1-1* and *chaos* mutants were about 20 and 30% smaller, respectively, than WT plants at 4 weeks of age, the *prors1-1 chaos* double mutant displayed a size reduction of more than 50% relative to WT plants (**Figures 1A,B**). In addition, reductions in petiole length could be observed in *prors1-1*, *chaos* and, more markedly, in *prors1-1 chaos* mutants during the first stages of plant development, whereas such differences were less pronounced in adult plants (**Figure 1C**). Col-0, *prors1-1*, and *chaos* plants showed also a very similar number of leaves throughout the life cycle, whereas the leaf number was slightly decreased in *prors1-1 chaos* plants, particularly during the first 2 weeks after germination (**Figure 1D**).

Four-week-old WT and mutant plants were also subjected to Chl a fluorescence measurements to monitor photosynthetic performance (**Figure 2**). The data showed a lower maximum quantum yield of PSII (F_V/F_M) in *prors1-1*, whereas values higher than in WT were observed in *chaos* leaves. Accordingly, the *chaos* mutation was able to restore F_V/F_M to the WT level in *prors1-1 chaos* leaves (**Figures 2A,C**). When the Φ_{II} parameter, reflecting the effective quantum yield of PSII, was taken into account, it could be also observed that *prors1-1* plants showed reduced Φ_{II} values with respect to Col-0, whereas *chaos* and *prors1-1 chaos* values were even higher than those of WT leaves (**Figures 2B,C**). In agreement with these observations, a decrease in the degree of reduction of Q_A (the primary electron acceptor of PSII) and the plastoquinone (PQ) pool (measured as 1-qL; a parameter frequently used for an indirect estimation of the redox state of the PQ pool; Kramer et al., 2004; Jung et al., 2010) was observed in *chaos* and *prors1-1 chaos* leaves (**Figure 2D**), suggesting a reduced net electron injection into the thylakoid transport chain, caused by *chaos* mutation. This aspect was investigated further by measuring oxygen production with a Clark-type oxygen electrode under standard lighting conditions. The levels of oxygen production per unit of leaf area were always found to be lower in *chaos* and *prors1-1 chaos* leaves than in Col-0 or the *prors1-1* single mutant (*chaos*, 0.014 ± 0.002 μmol m^{-2} h^{-1}; *prors1-1 chaos*, 0.011 ± 0.003; *prors1-1*, 0.023 ± 0.004; Col-0, 0.029 ± 0.003).

To quantify the alteration in leaf coloration in *prors1-1*, *chaos,* and *prors1-1 chaos* plants, leaf pigments were analyzed by HPLC (**Table 2**). As expected, the total Chl content (Chl a+b) was reduced by about 57 and 66% in *chaos* and *prors1-1 chaos* leaves, respectively, and the Chl a/b ratio was 3.69 in *chaos* and 3.01 in *prors1-1 chaos* leaves, with respect to 2.71 in Col-0. In addition, carotenoids that bind specifically to PSII antenna proteins (Lhcb), such as neoxanthin (Nx), lutein (Lut), and the VAZ pool (violaxanthin + antheraxanthin + zeaxanthin) were markedly reduced in *chaos* and *prors1-1 chaos* mutants. In contrast, β-carotene, which associates with PSII-core proteins, showed only a marginal decrease in mutant leaves, confirming the specific decrease in levels of PSII antenna proteins in the mutants containing the *chaos* allele.

Taken together, the data indicate that, in the *prors1-1 chaos* double mutant, the reduction in the size of the PSII antenna caused by the *chaos* mutation, and the resulting decrease in the total amount of light absorbed, effectively counteracts the increase in thylakoid electron pressure due to *prors1-1*. Hence, the excessive reduction of the thylakoid electron transport chain

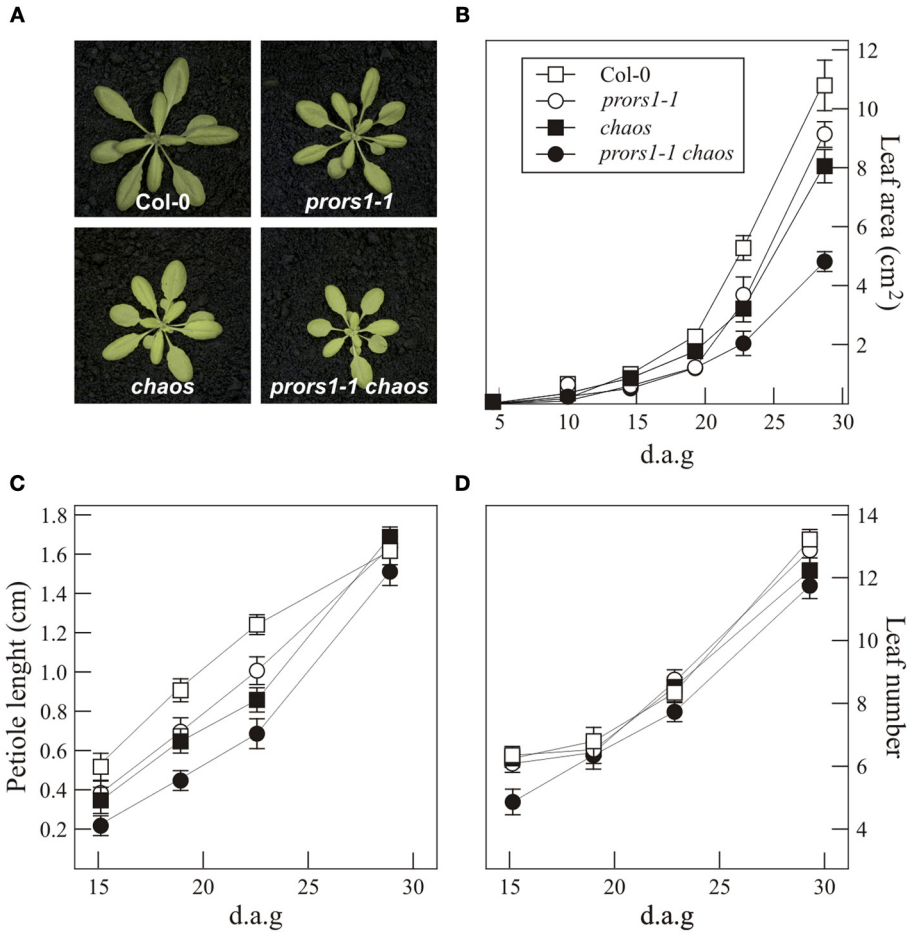

FIGURE 1 | Phenotypes of mutant (*prors1-1, chaos,* and *prors1-1 chaos*) and WT (Col-0) plants. (A) The different genotypes were grown for 4 weeks in the growth chamber. **(B)** The growth rates of the different genotypes were measured from 4 d to 28 d after germination (d.a.g.). **(C)** Petiole length was measured by monitoring the petiole of the fifth true leaf from 15 to 28 d.a.g. **(D)** The number of true leaves was determined during the period from 15 to 28 d.a.g. Each point reported in **(B)**, **(C)**, and **(D)** is based on the determination of average leaf area, petiole length and leaf number, respectively, in at least 12 individuals. Bars indicate standard deviations.

revealed by the increased 1-qL values in the *prors1-1* mutant is alleviated in *prors1-1 chaos* plants.

LEVELS OF LIGHT-HARVESTING COMPLEXES AND THYLAKOID PHOSPHORYLATION ARE REDUCED IN *prors1-1 chaos* LEAVES

To determine the effects of the combined action of the *chaos* and *prors1-1* mutations on thylakoid protein composition, membranes isolated from WT and mutant plants were fractionated by 1D SDS-PAGE (**Figure 3A**). As expected, densitometric analyses revealed a decrease of about 70% for the major light-harvesting complex of PSII (Lhcb1, Lhcb2, Lhcb3) in both *chaos* and *prors1-1 chaos* plants (**Table 3**). In addition, *prors1-1* and *prors1-1 chaos* thylakoids were characterized by a decrease in the α- and β-subunits of the ATPase complex by 47 and 56%, respectively. A more detailed picture of thylakoid protein composition in WT and mutant plants was obtained through immunoblot analysis (**Figure 3B**, **Table 3**). In particular, some PSII antenna proteins, such as Lhcb1, Lhcb2, and Lhcb6, showed similar reductions in both *chaos* and *prors1-1 chaos* thylakoids, whereas Lhca1 accumulation in *prors1-1 chaos* appeared to be the result of an additive effect of the two single mutations. Levels of most of the other subunits analyzed, including polypeptides from the PSI antenna (Lhca2), the PSII antenna (Lhcb5), the cores of PSI (PsaD and PsaF) and PSII (D1, CP43, and D2), and the oxygen-evolving complex (PsbQ), were higher (i.e., closer to WT-like levels) in *prors1-1 chaos* than in *prors1-1* thylakoids. No marked differences were observed between WT and mutant plants with respect to the accumulation of PsbO (a subunit of the oxygen-evolving complex), PsbS (subunit of PSII involved in non-photochemical quenching of Chl fluorescence) or the large subunit of RubisCO (RbcL).

The major decrease in PSII antenna proteins and the lower 1-qL values observed in *chaos* and *prors1-1 chaos* leaves imply that the thylakoid electron transport chain is more oxidized in these genotypes than in *prors1-1* plants. Because the level of thylakoid protein phosphorylation is directly linked to the reduction state of the PQ pool, immunoblot analysis using a phosphothreonine-specific antibody was carried out

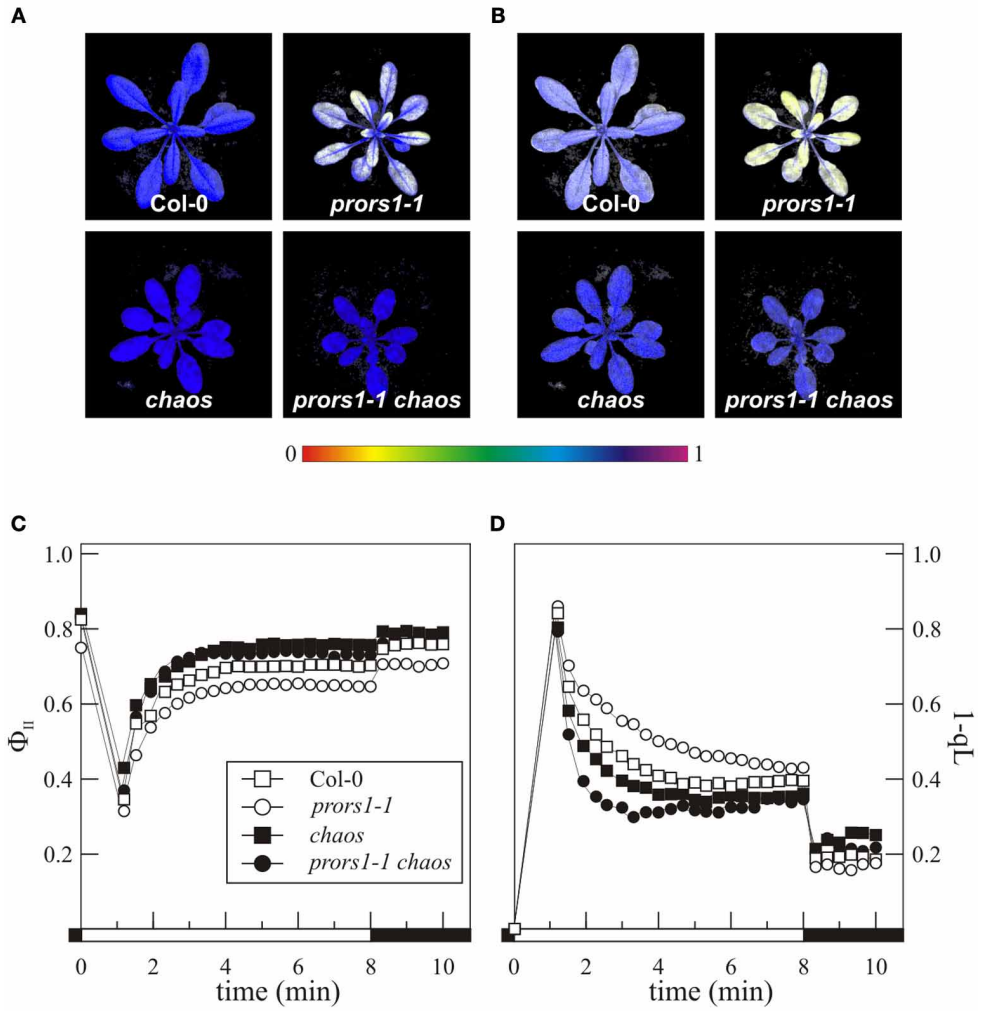

FIGURE 2 | Photosynthetic performance of mutant (*prors1-1, chaos,* and *prors1-1 chaos*) and WT (Col-0) plants. The photosynthetic parameters F_V/F_M **(A)** and Φ_{II} **(B)** were measured in the different genotypes, by employing an imaging Chl fluorometer, as described in "Materials and Methods." Signal intensities for F_V/F_M and Φ_{II} are indicated according to the color scale at the bottom of the panel. F_V/F_M (time 0), Φ_{II} **(C)** and 1-qL **(D)** were also measured using the Dual-PAM-100, as described in "Materials and Methods." Black bars indicate dark periods, and white bars light periods. Standard deviations were always below 10%.

Table 2 | Levels of leaf pigments in light-adapted mutant (*prors1-1, chaos,* and *prors1-1 chaos*) and WT (Col-0) plants at the 6-leaf rosette stage.

	Leaf pigment content (pmol/mg leaf)							
	Nx	**Lut**	**Chl b**	**Chl a**	**β-Car**	**VAZ**	**Chl a + b**	**Chl a/b**
Col-0	60 ± 5	197 ± 15	580 ± 34	1574 ± 54	211 ± 7	66 ± 5	2154 ± 53	2.71 ± 0.09
prors1-1	45 ± 3	154 ± 10	480 ± 28	1225 ± 71	121 ± 8	66 ± 1	1705 ± 68	2.55 ± 0.15
chaos	29 ± 1	103 ± 9	197 ± 6	728 ± 34	176 ± 7	34 ± 3	925 ± 40	3.69 ± 0.08
prors1-1 chaos	24 ± 3	92 ± 9	165 ± 12	497 ± 39	174 ± 10	43 ± 4	742 ± 61	3.01 ± 0.09

Leaf pigments were quantified by HPLC and are reported in pmol/mg leaf (fresh weight). Mean values ± SD are shown. Nx, neoxanthin; Lut, lutein; Chl b, chlorophyll b; Chl a, chlorophyll a; β-Car, β-carotene; VAZ, violaxanthin + antheraxanthin + zeaxanthin.

to investigate this further (**Figure 3C**). PSII-core proteins and LHCII phosphorylation were markedly increased in light-adapted *prors1-1* thylakoids, in particular when the reduced accumulation of these proteins in *prors1-1* plants (**Table 3**) is accounted for. On the other hand, a marked decrease of D1, D2, and CP43 phosphorylation was observed in light-adapted thylakoids isolated from *chaos* and *prors1-1 chaos* leaves. In the dark, only marginal levels of thylakoid protein

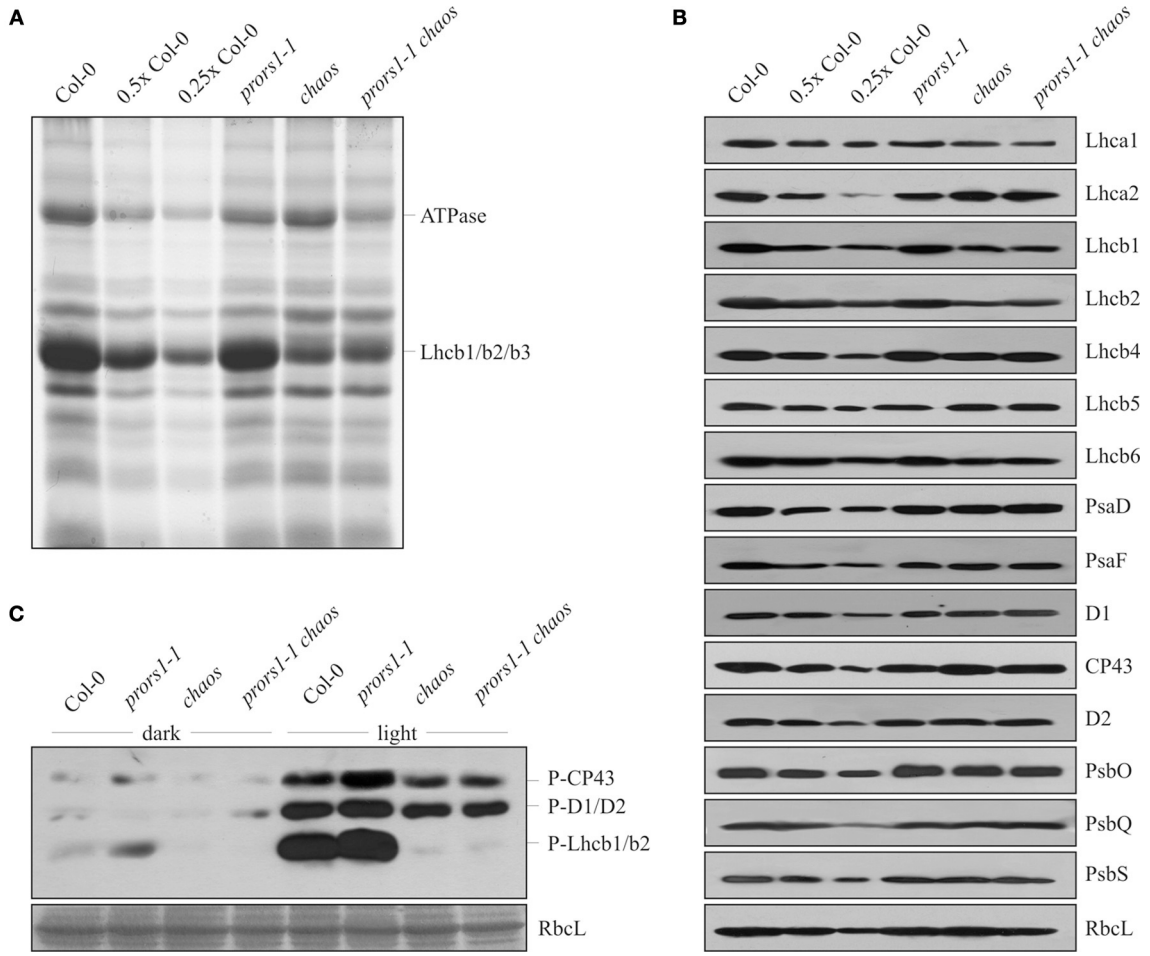

FIGURE 3 | 1D SDS-PAGE and immunoblot analysis of thylakoid proteins from WT (Col-0) and mutant (*prors1-1, chaos,* and *prors1-1 chaos*) leaves. (A) Thylakoid proteins isolated from equal amounts of leaf (fresh weight) were fractionated by SDS-PAGE and stained with Coomassie Brilliant blue. Band intensities were quantified by densitometric analyses (see "Materials and Methods"). **(B)** Identical amounts of total leaf proteins were fractionated by SDS-PAGEs as in **(A)**, transferred onto nylon filters and probed with antibodies raised against individual subunits of PSI (PsaD, PsaF), PSII (D1, CP43, D2, PsbO, PsbQ, PsbS), LHCI (Lhca1, Lhca2) and LHCII (Lhcb1, Lhcb2, Lhcb4, Lhcb5, Lhcb6), and the large subunit of RubisCO (RbcL). The lanes marked 0.5× Col-0 and 0.25× Col-0 were loaded with the indicated dilutions of the standard control sample. **(C)** Identical amounts of total proteins isolated from dark- and light-adapted plants were fractionated by SDS-PAGE as in **(A)**, blotted onto nylon filters and probed with a phosphothreonine (P-Thr)-specific antibody. A portion of the Coomassie Brilliant Blue-stained gel, corresponding to the RbcL migration region, was used to check for equal loading.

phosphorylation were detected in the different genetic backgrounds.

Thus, the polypeptide composition of *prors1-1 chaos* thylakoids seems to be influenced by two major factors. Additive effects of the two single mutations *prors1-1* and *chaos* seem to act on the abundance of Lhca1, Lhcb2, and the ATPase complex, while another group of photosynthetic proteins, the abundance of which is unaffected in the *chaos* mutant but decreased in *prors1* 1(e.g., D1, PsaF, PsbQ, Lhca2, Lhcb4, and Lhcb5), behaves in a WT-like manner in *prors1-1 chaos* plants. These findings indicate (1) that the increased excitation pressure in *prors1-1* thylakoids (revealed by the increase in the 1-qL value and in thylakoid phosphorylation) markedly affects the accumulation of certain photosynthetic proteins, and (2) that this effect can be attenuated by reducing PSII antenna size through the *chaos* mutation.

PLASTID PROTEIN SYNTHESIS IS UNAFFECTED BY THE *chaos* MUTATION

To determine whether the differences in thylakoid protein accumulation observed between *prors1-1* and *prors1-1 chaos* plants were due to *chaos*-dependent adaptive mechanisms that can modulate the translation process, plastid protein synthesis was investigated. To this end, the rate of incorporation of [^{35}S]methionine into plastid proteins in young leaves of WT and mutant (*prors1-1*, *chaos* and *prors1-1 chaos*) plants was monitored for 5, 15, and 30 min in the presence of light and inhibitors of cytoplasmic protein synthesis (**Figure 4**). Subsequently, total leaf proteins were extracted and fractionated by SDS-PAGE. In five independent experiments, the amounts of RbcL labeled in *prors1-1* and *prors1-1 chaos* plants were comparable, and equivalent to about 55% of WT levels. A marginal decrease in PSII-D1 signals was

Table 3 | Quantification of thylakoid (phospho)proteins in light-adapted mutant (*prors1-1, chaos,* and *prors1-1 chaos*) and WT (Col-0) plants.

Protein	*prors1-1*		*chaos*		*prors1-1 chaos*	
	1D-PAGE	Immunoblot	1D-PAGE	Immunoblot	1D-PAGE	Immunoblot
PsaD	nd	0.89 ± 0.07	nd	0.87 ± 0.08	nd	1.22 ± 0.06
PsaF	nd	0.78 ± 0.03	nd	1.12 ± 0.06	nd	1.25 ± 0.08
D1*	nd	0.61 ± 0.05	nd	0.96 ± 0.06	nd	1.23 ± 0.05
P-D1/D2	nd	1.67 ± 0.03	nd	0.52 ± 0.04	nd	0.64 ± 0.03
CP43*	nd	0.68 ± 0.05	nd	0.87 ± 0.06	nd	0.94 ± 0.08
P-CP43	nd	2.31 ± 0.06	nd	0.48 ± 0.03	nd	0.46 ± 0.03
D2*	nd	0.75 ± 0.07	nd	0.92 ± 0.06	nd	0.98 ± 0.07
PsbO	nd	1.12 ± 0.05	nd	0.97 ± 0.04	nd	1.09 ± 0.07
PsbQ	nd	0.77 ± 0.08	nd	0.91 ± 0.05	nd	1.12 ± 0.04
PsbS	nd	0.94 ± 0.05	nd	0.86 ± 0.07	nd	0.85 ± 0.08
Lhca1	nd	0.89 ± 0.05	nd	0.49 ± 0.05	nd	0.23 ± 0.06
Lhca2	nd	0.78 ± 0.03	nd	0.95 ± 0.03	nd	1.06 ± 0.08
Lhcb1/b2/b3	0.84 ± 0.05	$b1 = 0.85 \pm 0.06$; $b2 = 0.86 \pm 0.04$	0.31 ± 0.04	$b1 = 0.23 \pm 0.05$; $b2 = 0.32 \pm 0.04$	0.29 ± 0.03	$b1 = 0.28 \pm 0.04$; $b2 = 0.26 \pm 0.07$
P-Lhcb1/b2	nd	1.41 ± 0.09	nd	ns	nd	ns
Lhcb4	nd	1.12 ± 0.09	nd	0.79 ± 0.04	nd	0.94 ± 0.03
Lhcb5	nd	0.79 ± 0.04	nd	0.98 ± 0.06	nd	0.98 ± 0.06
Lhcb6	nd	0.81 ± 0.03	nd	0.24 ± 0.05	nd	0.33 ± 0.05
ATPase (α, β^*)	0.63 ± 0.03	nd	0.86 ± 0.05	nd	0.44 ± 0.05	nd
RbcL*	nd	0.91 ± 0.04	nd	0.98 ± 0.02	nd	0.85 ± 0.06

*WT levels are set to 100%. Average values were calculated from three independent 1D-PA gels and protein gel blots (see **Figure 3**). nd, not determined; ns, not significant.*

**Proteins encoded by plastid genes. P-, phosphorylated protein. Note that levels of thylakoid protein phosphorylation in the dark are not reported, since signals were barely detectable.*

also observed in these two mutants, whereas *chaos* plants behaved essentially like WT in this respect.

Taken together, these results exclude the possibility that the differences in thylakoid protein accumulation observed in *prors1-1* and *prors1-1 chaos* mutants result from differences in the rate of plastid protein synthesis. Therefore, the increased accumulation of plastid-encoded subunits in *prors1-1 chaos* (relative to *prors1-1*) leaves must be attributed to differences in post-translational events (including greater protein stability) associated with the lower level of oxidative damage incurred when light absorption and photosynthetic electron transport are less efficient. The nearly WT abundance of nucleus-encoded proteins observed in *prors1-1 chaos* thylakoids might be due to increases in transcription, translation, or protein stability, or any combination of these.

THE *chaos* MUTATION PARTIALLY SUPPRESSES THE OGE-DEPENDENT RETROGRADE SIGNALING PATHWAY

To assess the relative contribution of photosynthetic electron transport and the associated changes in TRS to the OGE-dependent signaling pathway, expression analyses of plastid and nuclear photosynthesis genes were conducted on WT and mutant plants. Probes for one plastid and nine nuclear genes encoding subunits of PSI and its antenna, one plastid and seven nuclear genes encoding subunits of PSII and its antenna, and for the plastid-encoded large subunit (RbcL) and the nucleus-encoded small subunit (RbcS) of RubisCO were hybridized to RNA gel blots loaded with total RNA from light-adapted leaves (**Figure 5A**). As expected, all nuclear photosynthesis genes were down-regulated in *prors1-1* plants, confirming the role of mitochondrial and plastid translation rate in triggering photosynthesis-related NGE (**Figure 5A**). However, in the *prors1-1 chaos* double mutant, 15 of the 17 nuclear photosynthesis genes analyzed were up-regulated relative to *prors1-1*. In particular, expression of *Lhca1*, *Lhca2*, *PsaE1*, *PsaF*, *PsaK*, *PsaO*, *Lhcb1*, *Lhcb2,* and *PsbX* in *prors1-1 chaos* leaves was identical to (and in the case of *PsbT2* even higher than) that in WT. The remaining genes (*PsaD1*, *Lhcb3*, *Lhcb4*, *PsbO2,* and *RbcS*) were derepressed in *prors1-1 chaos*, in some cases to levels similar to those seen in the *chaos* single mutant, but lower than in WT. Exceptions were represented by *Lhca3* and *Lhca4* genes, which were down-regulated in both *prors1-1* and *prors1-1 chaos* mutants. The limited capacity for light absorption caused by the *chaos* mutation also influences plastid gene expression, as shown by the marked drop in *psaA-B* expression in *chaos* and *prors1-1 chaos* mutants, whereas *psbA* and *RbcL* levels were almost unchanged in mutant plants.

Expression of genes involved in scavenging or preventing the formation of ROS was also investigated. The levels of transcripts of *Ferritin1*, mitochondrial alternative oxidase (*AOX1*), catalase (*CAT1*) and 2-Cys-peroxiredoxin-A (*2CPA*), expression of which has been reported to be stimulated by increases in ROS production, were only slightly altered in the mutant genotypes.

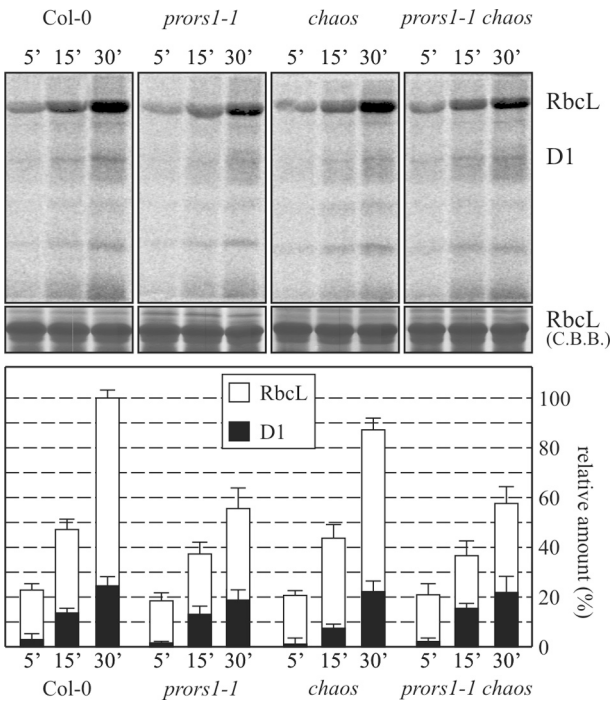

FIGURE 4 | Translational efficiency of chloroplast-encoded mRNAs in WT (Col-0) and mutant (*prors1-1, chaos,* and *prors1-1 chaos*) leaves. Leaves isolated from 6-leaf-rosette plants were pulse-labeled with [^{35}S]methionine under low-level illumination (20 μmol photons m^{-2} s^{-1}) for 5, 15, and 30 min in the presence of cycloheximide to inhibit cytosolic protein synthesis. Total leaf proteins were then isolated, fractionated by SDS-PAGE, and detected by autoradiography. A portion of the Coomassie Brilliant Blue (CBB)-stained gel, corresponding to the RbcL migration region, was employed as internal standard for data normalization. Levels of [^{35}S]methionine incorporation into RbcL and D1 proteins were quantified and are shown in the histogram. Values are averages of 5 independent experiments and were normalized to the maximal signal intensities obtained in WT leaves after 30 min labeling.

In order to validate the gene expression data obtained by Northern blot hybridizations, the expression of *Lhcb1*, *Lhcb2*, *Lhcb3*, *Ferritin1*, *AOX1*, *2CPA,* and *CAT1*, all of them belonging to large gene families, was also monitored by qRT-PCR analyses (**Figure 5B**). In this case too, *Lhcb* expression was specifically down-regulated in *prors1-1* leaves and derepressed in *prors1-1 chaos* plants. On the contrary, the expression of all the other genes remained unchanged between Col-0 and mutant leaves.

Taken together, the data clearly demonstrate that the OGE-dependent signaling pathway is tightly linked to photosynthetic electron transport and the associated TRS. In the *prors1-1 chaos* double mutant, the significant reduction in light absorption and oxygen evolution caused by the *chaos* mutation largely prevents the specific down-regulation of nuclear photosynthetic genes caused by the *prors1-1* mutation. Interestingly, this effect is likely to be caused by the altered redox state of the thylakoid electron transport chain (as shown by reduced levels of thylakoid protein phosphorylation and *psaA-B* operon expression), not by a burst of ROS production, as indicated by the limited changes in the expression of ROS-induced genes.

DISCUSSION

Attempts to distinguish between different retrograde signaling pathways have been hampered by difficulties in discriminating between primary and secondary effects caused by chemical inhibitors, and a comparative lack of genetic mutants that influence organellar function in a specific, well-defined manner (Leister, 2012; Barajas-Lopez et al., in press). In this study we have investigated the retrograde signaling pathway(s) active in *prors1-1* mutant plants, which exhibit perturbations in two chloroplast functions relevant for retrograde signaling: (1) a mild defect in protein synthesis in both mitochondria and chloroplasts; and (2) altered photosynthetic electron transport (this manuscript; Pesaresi et al., 2006).

DIMINISHED LIGHT ABSORPTION MITIGATES THE DEFECT IN PHOTOSYNTHETIC ELECTRON TRANSPORT IN *prors1-1* PLANTS

The excessively reduced state of the thylakoid electron transport chain observed in the *prors1-1* mutant, as indicated by increased thylakoid protein phosphorylation, reduced effective quantum yield of PSII, and increased 1-qL values, supports the notion that many alterations in plant cell metabolism directly or indirectly impinge on the redox state of photosynthetic electron transport components, making the photosynthetic apparatus a major sensor of physiological imbalances (Pfannschmidt and Yang, 2012). Therefore, changes in thylakoid excitation pressure may be associated with major modifications in gene expression at the organellar and nuclear levels. Here, we have specifically addressed this issue by introducing the *chaos* mutation into *prors1-1* plants. This mutation in the *CAO* gene reduces the size of the PSII antenna, thus mimicking a major adaptive mechanism that plants have evolved to protect themselves against the damaging effects of excess light energy (for a review see: Oelze et al., 2008). Down-regulation of the *CAO* gene, which codes for the cpSRP43 subunit involved in the insertion of Lhcb proteins into the thylakoids (Klimyuk et al., 1999), has actually been implicated in the system that remodels the photosynthetic machinery to safeguard against photo-oxidative stress (Klenell et al., 2005). And indeed, in *prors1-1 chaos* double mutant plants, the thylakoid electron transport chain is more highly oxidized, as indicated by the higher Φ_{II} and lower 1-qL values, as well as reduced O_2 production relative to *prors1-1* plants, and the concomitant reduction in thylakoid protein phosphorylation. These data support previous findings where *chaos* seedlings have been reported to be highly tolerant to photooxidative stress under both tightly controlled laboratory conditions and highly variable conditions in the field, and to mitigate the effects of the *lesion simulating disease 1* (*lsd1*) mutation (Mateo et al., 2004; Klenell et al., 2005). These effects are attributable to a decrease in light absorption resulting from the limited availability of proteins of the major light-harvesting complex of PSII caused by the *chaos* mutation. Immunoblot and pigment content analyses confirm that steady-state levels of Lhcb1, Lhcb2, Lhcb3, and the minor antenna Lhcb6 are markedly reduced in *chaos* and *prors1-1 chaos* mutants (this manuscript; Klimyuk et al., 1999). The observation that transcripts of the plastid *psaA-B* operon are less abundant in *chaos* and *prors1-1 chaos* leaves, but higher in *prors1-1* chloroplasts, than in WT supports the idea that the PQ pool is more oxidized

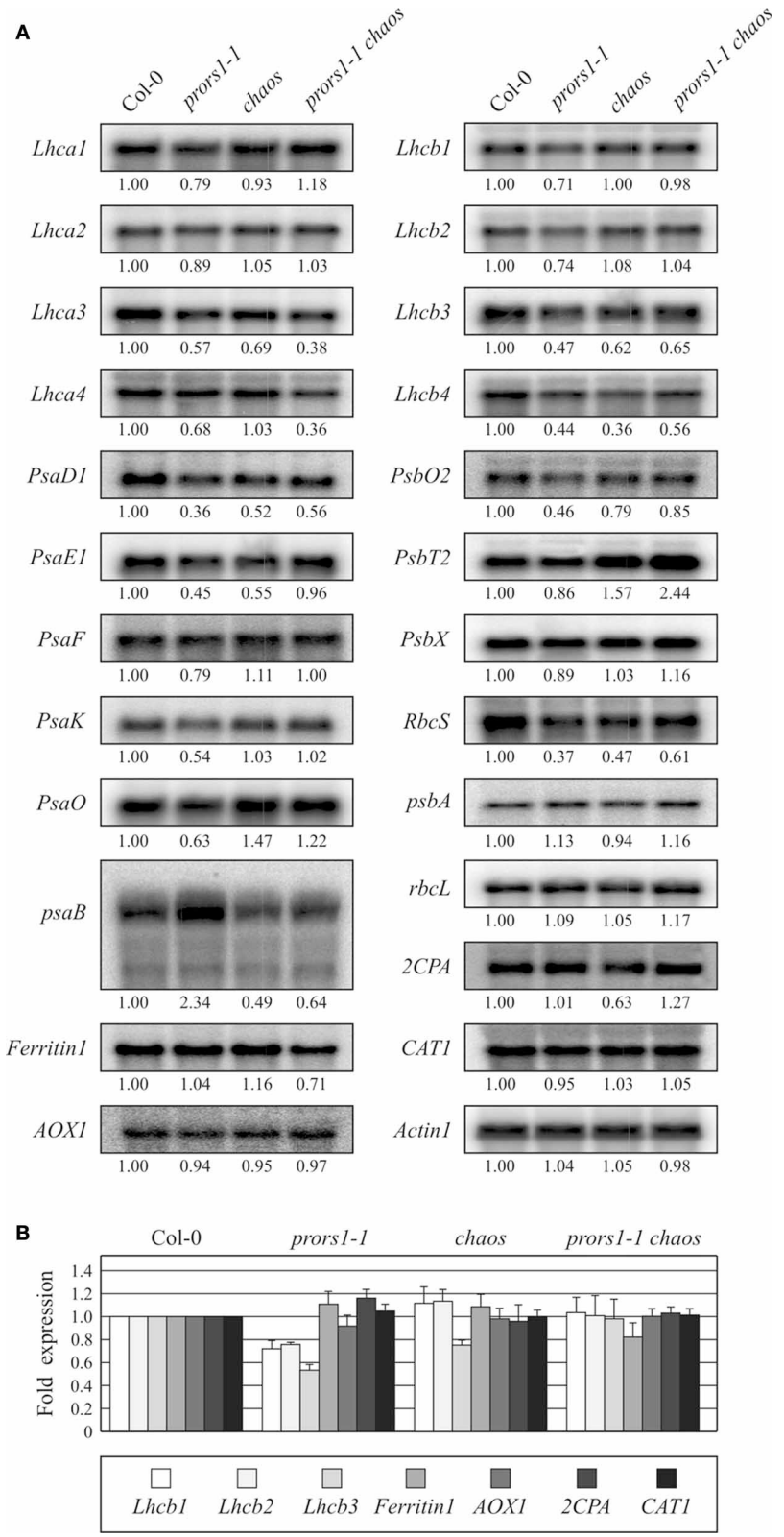

FIGURE 5 | Expression analysis of photosynthesis and antioxidant genes in WT (Col-0) and mutant (*prors1-1, chaos,* and *prors1-1 chaos*) leaves. **(A)** Twenty microgram samples of total RNA from light-adapted WT, *prors1-1*, *chaos,* and *prors1-1 chaos* mutant plants were size-fractionated by agarose gel electrophoresis, transferred to nitrocellulose filters and probed with cDNA fragments specific for transcripts encoding subunits of PSI (*Lhca1*, *-2*, *-3*, *-4*, *psaB*, *PsaD1*, *PsaE1*, *PsaF*, *PsaK*, *PsaO*), PSII (*Lhcb1*, *-2*, *-3*, *-4*, *psbA*, *PsbO2*, *(Continued)*

FIGURE 5 | Continued
PsbT2, *PsbX*) and Rubisco (*RbcS*, *RbcL*). Expression of nuclear genes encoding antioxidant enzymes, such as *Ferritin1*, *AOX1*, *2CPA*, CAT1, and *AOX1*, was also monitored. Three independent RNA gel-blot analyses were performed for each gene. Equal loading of RNA was checked by hybridization with *Actin1* specific probe. **(B)** Expression of genes belonging to multi-gene families, such as *Lhcb1*, *Lhcb2*, *Lhcb3*, *Ferritin1*, *AOX1*, *2CPA*, and *CAT1*, was also monitored by qRT-PCR as described in "Materials and Methods." Average values from three biological and three technical replicates are reported. Note that the expression level of each of the gene analyzed was normalized to 1 in Col-0 background. Bars indicate standard deviations.

in the presence of the *chaos* mutation, because expression of this operon is promoted by a reduced PQ pool (Pfannschmidt et al., 1999a,b; Allen and Pfannschmidt, 2000). Despite the partial reversal of the hyper-reduction of the thylakoid electron transport chain, the *prors1-1 chaos* plants showed a reduction of about 50% in growth rate relative to *prors1-1* single mutants under growth chamber conditions, most probably as a result of the constraints on O_2 evolution, and consequently on ATP and NADPH production.

LIGHT ABSORPTION AND THE INFLUENCE OF TRS ON THE OGE-DEPENDENT RETROGRADE PATHWAY

The alleviation of the hyper-reduction of the thylakoid electron transport chain caused by the *prors1-1* mutation, together with the persistence of the defect in protein synthesis in plastids and mitochondria, as demonstrated by *in vivo* labeling assays (see **Figure 4**), make *prors1-1 chaos* plants ideal material for distinguishing between OGE- and TRS-dependent retrograde signals. Analyses of nuclear genes which are down-regulated in *prors1-1* (this manuscript; Pesaresi et al., 2006), and form part of a dynamic inter-compartmental transcriptional network dedicated to adjusting the activity of organelles in response to the cellular energy state and environmental stress (Biehl et al., 2005; Leister et al., 2011), support the notion that TRS and OGE play important roles in retrograde signaling. The *prors1-1 chaos* plants show a general derepression of nuclear photosynthetic genes relative to the *prors1-1* mutant. More specifically, the genes affected could be divided into four major groups: (1) genes transcribed at higher levels than in WT (like *PsbT2*), (2) genes transcribed at WT levels (*Lhca1*, *Lhca2*, *PsaE1*, *PsaF*, *PsaK*, *PsaO*, *Lhcb1*, *Lhcb2*, and *PsbX*), (3) genes expressed at levels higher than in *prors1-1* but lower than in WT leaves (*PsaD1*, *Lhcb3*, *Lhcb4*, *PsbO2,* and *RbcS*), and (4) genes whose expression was not derepressed by the *chaos* mutation (*Lhca3* and *Lhca4*). Hence, in the *prors1-1 chaos* double mutant, the decrease in the TRS stimulus (caused by the *chaos* mutation) neutralizes some of the gene regulatory effects of the *prors1-1* mutation. This observation allows us to conclude that these genes are regulated by TRS (and possibly also indirectly by the chloroplast redox state and the associated carbon metabolism), or synergistically by TRS and OGE. Indeed, we would argue that TRS and OGE signals together contribute to retrograde signaling, although the degree to which their action is synergistic varies from gene to gene. Interestingly, the transcriptional derepression effect observed in *prors1-1 chaos* leaves is associated with increased accumulation of most of the corresponding gene products, indicating the physiological significance of this regulation of transcript abundance. Thus, with the major exception of proteins whose accumulation requires their cpSRP43-mediated, post-translational insertion into thylakoids (i.e., Lhcb subunits), the levels of other photosynthetic proteins analyzed were generally higher in the *prors1-1 chaos* double mutant than in *prors1-1*, and essentially identical to those seen in WT (see **Figure 2** and **Table 3**).

However, it should not be forgotten that the down-regulation of nuclear photosynthesis genes in *prors1-1* leaves persists even after dark adaptation, which would suggest that the OGE-dependent retrograde pathway is largely independent of light, and thus of photosynthesis and TRS (Pesaresi et al., 2006). However, this is more likely to be an example of "systemic acquired acclimation" (SAA), where plants retain a "memory" of stress conditions induced by environmental or, as in the case of *prors1-1*, genetic factors, which allows them to mount a more effective defence against further episodes of such a stress (Karpinski et al., in press). The phenomenon is triggered by systemic redox changes in the thylakoid electron transport chain, and it avoids the need for *prors1-1* plants to induce the response to excess excitation energy *de novo* every time a dark-to-light transition takes place, thus saving energy for other metabolic pathways.

Because changes in OGE inevitably affect TRS and may also result in ROS-mediated oxidative stress, TRS and/or ROS might contribute directly to OGE signaling. However, the fact that there is no change in the expression of genes involved in detoxifying ROS, such as *Ferritin1*, *2CPA*, *CAT1* and *AOX1*, argues against the possibility that the OGE signaling pathway is triggered by oxidative stress in *prors1-1* plants (this manuscript; Pesaresi et al., 2006). Nonetheless, an involvement of ROS, in particular of H_2O_2, in OGE signaling cannot be entirely ruled out, since studies of isolated thylakoid membranes and intact chloroplasts have shown that a fraction of the plastid-produced H_2O_2 reaches the cytosol even under low-light conditions, which argues that physiological levels of H_2O_2 may play a role in signaling (Bienert et al., 2007; Mubarakshina et al., 2010).

On the other hand, changes in photosynthetic electron transport and the associated alteration of the redox state of PQ pool and stromal compounds *per se*, cannot explain the coordinated down-regulation of nuclear photosynthesis gene expression observed in *prors1-1* leaves. This is because only the simultaneous impairment of mitochondrial and plastid OGE results in the down-regulation of most of the nuclear photosynthetic genes in this genotype (Pesaresi et al., 2006). Indeed, light-shift experiments in combination with DCMU treatments have demonstrated that only 54 nuclear Arabidopsis genes are under the direct control of the PQ redox state, and only two of these codes for components directly associated with photosynthesis (Fey et al., 2005). Moreover, the derepression of photosynthesis gene expression in *prors1-1 chaos* leaves is only partial (the accumulation of *Lhca3*, *Lhca4*, *PsaD1*, *Lhcb3*, *Lhcb4*, *PsbO2,* and

RbcS transcripts was not restored to WT levels), implying the existence of multiple signal sources in both plastids and mitochondria, which must be integrated to enable the re-orchestration of photosynthetic NGE.

Since, photosynthetic electron transport is responsible of synthesis of carbohydrates that, in turn, are consumed in mitochondria by respiration, sugars may be also regarded as signaling metabolites involved in retrograde communication (Baier and Dietz, 2005). Thus, increased levels of glucose or sucrose repress photosynthesis gene expression, by involving hexokinase that is critical for sensing and responding to hexose signals, intracellularly (Jang et al., 1997; Rolland et al., 2006). Moreover, ABA has been also proposed to play a role in retrograde signaling, due to the fact that ABA biosynthesis starts into the chloroplasts and that ABA is strictly interconnected with photosynthesis (Baier et al., 2004). As a matter of fact, recent findings have placed the transcription factor ABI4 at the crossroads between mitochondrial and chloroplast retrograde signaling pathways and perhaps as a convergence point for mitochondria-plastid-nucleus coordination (Giraud et al., 2008). Nevertheless, *prors1-1* plants appear to be able to maintain a memory of stress conditions, suggesting that also chromatin remodeling factors, and not only transcription factors, may have a prominent role in retrograde signaling.

ACKNOWLEDGMENTS

This work was supported by grants to Paolo Pesaresi from the Italian Ministry of Research (Special Fund for Basic Research, Grant No. PRIN 2008XB7774B) and to Dario Leister from the Deutsche Forschungsgemeinschaft (SFB-TR1, TP B8, and FOR 804). We thank Paul Hardy for critical reading of the manuscript.

REFERENCES

Allen, J. F., and Pfannschmidt, T. (2000). Balancing the two photosystems: photosynthetic electron transfer governs transcription of reaction centre genes in chloroplasts. *Philos. Trans. R. Soc. Lond. B Biol. Sci.* 355, 1351–1357.

Amin, P., Sy, D. A., Pilgrim, M. L., Parry, D. H., Nussaume, L., and Hoffman, N. E. (1999). Arabidopsis mutants lacking the 43- and 54-kilodalton subunits of the chloroplast signal recognition particle have distinct phenotypes. *Plant Physiol.* 121, 61–70.

Apel, K., and Hirt, H. (2004). Reactive oxygen species: metabolism, oxidative stress, and signal transduction. *Annu. Rev. Plant Biol.* 55, 373–399.

Baier, M., and Dietz, K. J. (2005). Chloroplasts as source and target of cellular redox regulation: a discussion on chloroplast redox signals in the context of plant physiology. *J. Exp. Bot.* 56, 1449–1462.

Baier, M., Stroher, E., and Dietz, K. J. (2004). The acceptor availability at photosystem I and ABA control nuclear expression of 2-Cys peroxiredoxin-A in *Arabidopsis thaliana*. *Plant Cell Physiol.* 45, 997–1006.

Barajas-Lopez, J. D., Blanco, N. E., and Strand, A. (in press). Plastid-to-nucleus communication, signals controlling the running of the plant cell. *Biochim. Biophys. Acta*. doi: 10.1016/j.bbr.2011.03.031

Bassi, R., Peruffo, A. D., Barbato, R., and Ghisi, R. (1985). Differences in chlorophyll-protein complexes and composition of polypeptides between thylakoids from bundle sheaths and mesophyll-cells in maize. *Eur. J. Biochem.* 146, 589–595.

Biehl, A., Richly, E., Noutsos, C., Salamini, F., and Leister, D. (2005). Analysis of 101 nuclear transcriptomes reveals 23 distinct regulons and their relationship to metabolism, chromosomal gene distribution and co-ordination of nuclear and plastid gene expression. *Gene* 344, 33–41.

Bienert, G. P., Moller, A. L., Kristiansen, K. A., Schulz, A., Moller, I. M., Schjoerring, J. K., et al. (2007). Specific aquaporins facilitate the diffusion of hydrogen peroxide across membranes. *Eur. J. Biochem.* 282, 1183–1192.

Estavillo, G. M., Crisp, P. A., Pornsiriwong, W., Wirtz, M., Collinge, D., Carrie, C., et al. (2011). Evidence for a SAL1-PAP chloroplast retrograde pathway that functions in drought and high light signaling in Arabidopsis. *Plant Cell* 23, 3992–4012.

Farber, A., Young, A. J., Ruban, A. V., Horton, P., and Jahns, P. (1997). Dynamics of xanthophyll-cycle activity in different antenna subcomplexes in the photosynthetic membranes of higher plants (the relationship between zeaxanthin conversion and nonphotochemical fluorescence quenching). *Plant Physiol.* 115, 1609–1618.

Fey, V., Wagner, R., Brautigam, K., Wirtz, M., Hell, R., Dietzmann, A., et al. (2005). Retrograde plastid redox signals in the expression of nuclear genes for chloroplast proteins of *Arabidopsis thaliana*. *J. Biol. Chem.* 280, 5318–5328.

Giraud, E., Ho, L. H., Clifton, R., Carroll, A., Estavillo, G., Tan, Y. F., et al. (2008). The absence of ALTERNATIVE OXIDASE1a in Arabidopsis results in acute sensitivity to combined light and drought stress. *Plant Physiol.* 147, 595–610.

Havaux, M., and Devaud, A. (1994). Photoinhibition of photosynthesis in chilled potato leaves is not correlated with a loss of photosystem-II activity – preferential inactivation of photosystem-I. *Photosynth. Res.* 40, 75–92.

Ihnatowicz, A., Pesaresi, P., Varotto, C., Richly, E., Schneider, A., Jahns, P., et al. (2004). Mutants for photosystem I subunit D of *Arabidopsis thaliana*: effects on photosynthesis, photosystem I stability and expression of nuclear genes for chloroplast functions. *Plant J.* 37, 839–852.

Jang, J. C., Leon, P., Zhou, L., and Sheen, J. (1997). Hexokinase as a sugar sensor in higher plants. *Plant Cell* 9, 5–19.

Jung, H. S., Okegawa, Y., Shih, P. M., Kellogg, E., Abdel-Ghany, S. E., Pilon, M., et al. (2010). *Arabidopsis thaliana* PGR7 encodes a conserved chloroplast protein that is necessary for efficient photosynthetic electron transport. *PloS ONE* 5:e11688. doi: 10.1371/journal.pone.0011688

Karpinski, S., Szechynska-Hebda, M., Wituszynska, W., and Burdiak, P. (in press). Light acclimation, retrograde signalling, cell death, and immune defences in plants. *Plant Cell Environ.* doi: 10.1111/pce.12018

Keegstra, K., and Cline, K. (1999). Protein import and routing systems of chloroplasts. *Plant Cell* 11, 557–570.

Kleine, T., Maier, U. G., and Leister, D. (2009a). DNA transfer from organelles to the nucleus: the idiosyncratic genetics of endosymbiosis. *Annu. Rev. Plant Biol.* 60, 115–138.

Kleine, T., Voigt, C., and Leister, D. (2009b). Plastid signalling to the nucleus: messengers still lost in the mists? *Trends Genet.* 25, 185–192.

Klenell, M., Morita, S., Tiemblo-Olmo, M., Muhlenbock, P., Karpinski, S., and Karpinska, B. (2005). Involvement of the chloroplast signal recognition particle cpSRP43 in acclimation to conditions promoting photooxidative stress in Arabidopsis. *Plant Cell Physiol.* 46, 118–129.

Klimyuk, V. I., Persello-Cartieaux, F., Havaux, M., Contard-David, P., Schuenemann, D., Meiherhoff, K., et al. (1999). A chromodomain protein encoded by the Arabidopsis *CAO* gene is a plant-specific component of the chloroplast signal recognition particle pathway that is involved in LHCP targeting. *Plant Cell* 11, 87–99.

Koussevitzky, S., Nott, A., Mockler, T. C., Hong, F., Sachetto-Martins, G., Surpin, M., et al. (2007). Signals from chloroplasts converge to regulate nuclear gene expression. *Science* 316, 715–719.

Kramer, D. M., Johnson, G., Kiirats, O., and Edwards, G. E. (2004). New fluorescence parameters for the determination of Q_A redox state and excitation energy fluxes. *Photosynth. Res.* 79, 209–218.

Leister, D. (2005). Origin, evolution and genetic effects of nuclear insertions of organelle DNA. *Trends Genet.* 21, 655–663.

Leister, D. (2012). Retrograde signaling in plants: from simple to complex scenarios. *Front. Plant Sci.* 3:135. doi: 10.3389/fpls.2012.00135

Leister, D., Varotto, C., Pesaresi, P., Niwergall, A., and Salamini, F. (1999). Large-scale evaluation of plant growth in *Arabidopsis thaliana* by non-invasive image analysis. *Plant Physiol. Biochem.* 37, 671–678.

Leister, D., Wang, X., Haberer, G., Mayer, K. F., and Kleine, T. (2011).

Intracompartmental and intercompartmental transcriptional networks coordinate the expression of genes for organellar functions. *Plant Physiol.* 157, 386–404.

Martinez-Garcia, J. F., Monte, E., and Quail, P. H. (1999). A simple, rapid and quantitative method for preparing Arabidopsis protein extracts for immunoblot analysis. *Plant J.* 20, 251–257.

Mateo, A., Muhlenbock, P., Rusterucci, C., Chang, C. C., Miszalski, Z., Karpinska, B., et al. (2004). *LESION SIMULATING DISEASE 1* is required for acclimation to conditions that promote excess excitation energy. *Plant Physiol.* 136, 2818–2830.

Mochizuki, N., Tanaka, R., Tanaka, A., Masuda, T., and Nagatani, A. (2008). The steady-state level of Mg-protoporphyrin IX is not a determinant of plastid-to-nucleus signaling in Arabidopsis. *Proc. Natl. Acad. Sci. U.S.A.* 105, 15184–15189.

Moller, I. M., and Sweetlove, L. J. (2010). ROS signalling–specificity is required. *Trends Plant Sci.* 15, 370–374.

Moulin, M., McCormac, A. C., Terry, M. J., and Smith, A. G. (2008). Tetrapyrrole profiling in Arabidopsis seedlings reveals that retrograde plastid nuclear signaling is not due to Mg-protoporphyrin IX accumulation. *Proc. Natl. Acad. Sci. U.S.A.* 105, 15178–15183.

Mubarakshina, M. M., Ivanov, B. N., Naydov, I. A., Hillier, W., Badger, M. R., and Krieger-Liszkay, A. (2010). Production and diffusion of chloroplastic H_2O_2 and its implication to signalling. *J. Exp. Bot.* 61, 3577–3587.

Oelze, M. L., Kandlbinder, A., and Dietz, K. J. (2008). Redox regulation and overreduction control in the photosynthesizing cell: complexity in redox regulatory networks. *Biochim. Biophys. Acta* 1780, 1261–1272.

Pesaresi, P. (2011). Studying translation in Arabidopsis chloroplasts. *Methods Mol. Biol.* 774, 209–224.

Pesaresi, P., Hertle, A., Pribil, M., Kleine, T., Wagner, R., Strissel, H., et al. (2009). Arabidopsis STN7 kinase provides a link between short- and long-term photosynthetic acclimation. *Plant Cell* 21, 2402–2423.

Pesaresi, P., Masiero, S., Eubel, H., Braun, H. P., Bhushan, S., Glaser, E., et al. (2006). Nuclear photosynthetic gene expression is synergistically modulated by rates of protein synthesis in chloroplasts and mitochondria. *Plant Cell* 18, 970–991.

Pesaresi, P., Schneider, A., Kleine, T., and Leister, D. (2007). Interorganellar communication. *Curr. Opin. Plant Biol.* 10, 600–606.

Pesaresi, P., Varotto, C., Meurer, J., Jahns, P., Salamini, F., and Leister, D. (2001). Knock-out of the plastid ribosomal protein L11 in Arabidopsis: effects on mRNA translation and photosynthesis. *Plant J.* 27, 179–189.

Pfannschmidt, T., Nilsson, A., and Allen, J. F. (1999a). Photosynthetic control of chloroplast gene expression. *Nature* 397, 625–628.

Pfannschmidt, T., Nilsson, A., Tullberg, A., Link, G., and Allen, J. F. (1999b). Direct transcriptional control of the chloroplast genes *psbA* and *psaAB* adjusts photosynthesis to light energy distribution in plants. *IUBMB Life* 48, 271–276.

Pfannschmidt, T., and Yang, C. (2012). The hidden function of photosynthesis: a sensing system for environmental conditions that regulates plant acclimation responses. *Protoplasma* 249 (Suppl. 2), 125–136.

Pogson, B. J., Woo, N. S., Forster, B., and Small, I. D. (2008). Plastid signalling to the nucleus and beyond. *Trends Plant Sci.* 13, 602–609.

Ramel, F., Birtic, S., Ginies, C., Soubigou-Taconnat, L., Triantaphylides, C., and Havaux, M. (2012). Carotenoid oxidation products are stress signals that mediate gene responses to singlet oxygen in plants. *Proc. Natl. Acad. Sci. U.S.A.* 109, 5535–5540.

Rolland, F., Baena-Gonzalez, E., and Sheen, J. (2006). Sugar sensing and signaling in plants: conserved and novel mechanisms. *Annu. Rev. Plant Biol.* 57, 675–709.

Sambrook, J., and Russell, D. W. (2001). *Molecular Cloning: A Laboratory Manual*. 3rd Edn. Cold Spring Harbor, NY: Cold Spring Harbor Laboratory Press.

Schägger, H., and von Jagow, G. (1987). Tricine-sodium dodecyl sulfate-polyacrylamide gel electrophoresis for the separation of proteins in the range from 1 to 100 kDa. *Anal. Biochem.* 166, 368–379.

Schuenemann, D., Gupta, S., Persello-Cartieaux, F., Klimyuk, V. I., Jones, J. D., Nussaume, L., et al. (1998). A novel signal recognition particle targets light-harvesting proteins to the thylakoid membranes. *Proc. Natl. Acad. Sci. U.S.A.* 95, 10312–10316.

Strand, A., Asami, T., Alonso, J., Ecker, J. R., and Chory, J. (2003). Chloroplast to nucleus communication triggered by accumulation of Mg-protoporphyrinIX. *Nature* 421, 79–83.

Sullivan, J. A., and Gray, J. C. (1999). Plastid translation is required for the expression of nuclear photosynthesis genes in the dark and in roots of the pea *lip1* mutant. *Plant Cell* 11, 901–910.

Sun, X., Feng, P., Xu, X., Guo, H., Ma, J., Chi, W., et al. (2011). A chloroplast envelope-bound PHD transcription factor mediates chloroplast signals to the nucleus. *Nat. Commun.* 2:477. doi: 10.1038/ncomms1486

Varotto, C., Pesaresi, P., Maiwald, D., Kurth, J., Salamini, F., and Leister, D. (2000). Identification of photosynthetic mutants of Arabidopsis by automatic screening for altered effective quantum yield of photosystem 2. *Photosynthetica* 38, 497–504.

Wisman, E., Hartmann, U., Sagasser, M., Baumann, E., Palme, K., Hahlbrock, K., et al. (1998). Knock-out mutants from an En-1 mutagenized *Arabidopsis thaliana* population generate phenylpropanoid biosynthesis phenotypes. *Proc. Natl. Acad. Sci. U.S.A.* 95, 12432–12437.

Woodson, J. D., and Chory, J. (2008). Coordination of gene expression between organellar and nuclear genomes. *Nat. Rev. Genet.* 9, 383–395.

Woodson, J. D., Perez-Ruiz, J. M., and Chory, J. (2011). Heme synthesis by plastid ferrochelatase I regulates nuclear gene expression in plants. *Curr. Biol.* 21, 897–903.

Xiao, Y., Savchenko, T., Baidoo, E. E., Chehab, W. E., Hayden, D. M., Tolstikov, V., et al. (2012). Retrograde signaling by the plastidial metabolite MEcPP regulates expression of nuclear stress-response genes. *Cell* 149, 1525–1535.

Conflict of Interest Statement: The authors declare that the research was conducted in the absence of any commercial or financial relationships that could be construed as a potential conflict of interest.

Received: 24 September 2012; accepted: 30 November 2012; published online: 27 December 2012.

Citation: Tadini L, Romani I, Pribil M, Jahns P, Leister D and Pesaresi P (2012) Thylakoid redox signals are integrated into organellar-gene-expression-dependent retrograde signaling in the prors1-1 mutant. Front. Plant Sci. ***3****:282. doi: 10.3389/fpls.2012.00282*

This article was submitted to Frontiers in Plant Physiology, a specialty of Frontiers in Plant Science.

Copyright © 2012 Tadini, Romani, Pribil, Jahns, Leister and Pesaresi. This is an open-access article distributed under the terms of the ***Creative Commons Attribution License****, which permits use, distribution and reproduction in other forums, provided the original authors and source are credited and subject to any copyright notices concerning any third-party graphics etc.*

frontiers in
PLANT SCIENCE

HYPOTHESIS AND THEORY ARTICLE
published: 19 December 2012
doi: 10.3389/fpls.2012.00286

Retrograde signaling from functionally heterogeneous plastids

Anna Lepistö, Jouni Toivola, Lauri Nikkanen and Eevi Rintamäki*

Molecular Plant Biology, Department of Biochemistry and Food Chemistry, University of Turku, Turku, Finland

Edited by:
Dario Leister,
Ludwig-Maximilians-Universität München, Germany

Reviewed by:
Peter Doermann, Universität Bonn, Germany
Dario Leister,
Ludwig-Maximilians-Universität München, Germany

****Correspondence:***
Eevi Rintamäki, Molecular Plant Biology, Department of Biochemistry and Food Chemistry, University of Turku, FIN-20014 Turku, Finland.
e-mail: evirin@utu.fi

Structural and functional components of chloroplast are encoded by genes localized both to nuclear and plastid genomes of plant cell. Development from etioplasts to chloroplasts is triggered by light receptors that activate the expression of photosynthesis-associated nuclear genes (PhaNGs). In addition to photoreceptor-mediated pathways, retrograde signals from the chloroplast to the nucleus activate or repress the expression of nuclear genes involved in acclimatory or stress responses in plant leaves. A plant mesophyll cell contains up to 100 chloroplasts that function autonomously, raising intriguing questions about homogeneity and coordination of retrograde signals transmitted from chloroplast to nucleus. We have previously demonstrated that the knockout of the chloroplast regulatory protein, chloroplast NADPH-dependent thioredoxin reductase (NTRC) leads to a heterogeneous population of chloroplasts with a range of different functional states. The heterogeneous chloroplast population activates both redox-dependent and undifferentiated plastid-generated retrograde signaling pathways in the mutant leaves. Transcriptome data from the *ntrc* knockout lines suggest that the induction of the redox-dependent signaling pathway depends on light conditions and leads to activation of stress-responsive gene expression. Analysis of mutants in different developmental stages allows to dissect signals from normal and anomalous chloroplasts. Thus, the signals derived from anomalous chloroplasts repress expression of PhaNGs as well as genes associated with light receptor signaling and differentiation of stomata, implying interaction between retrograde pathways and plant development. Analysis of the nuclear gene expression in mutants of retrograde signaling pathways in *ntrc* background would reveal the components that mediate signals generated from heterogeneous plastids to nucleus.

Keywords: light signaling, redox signals, nuclear gene expression, stress, differentiation, NTRC

INTRODUCTION

Light is the primary environmental factor controlling plant development and acclimation processes, regulating the entire life cycle of plants from seed germination to seed production (Sullivan and Deng, 2003). Light is perceived directly by blue (cryptochromes CRY, phototropins, and zeitlupe ZTL) and red light (phytochromes PHY) photoreceptors, which then activate signaling networks to initiate an array of light response processes such as photomorphogenesis, photoperiodic development, as well as acclimatory and protective modifications of plants. Light signals are also mediated by chloroplasts to control chloroplast biogenesis and acclimation to changes in light quality, quantity, and day length. Transcriptomics studies have demonstrated that between 5 and 25% of Arabidopsis (*Arabidopsis thaliana*) genes are light-regulated, depending on gene content in microarrays and experimental conditions (Jiao et al., 2007; Sharrock, 2008; Li et al., 2012). Recently, light receptor-dependent signaling pathways have been suggested to interact with chloroplast retrograde signaling pathways (Ruckle and Larkin, 2009). The mechanisms by which photoreceptor-dependent signals and chloroplast signals interact are not well understood. Here we review recent findings from the study of the light and retrograde signaling pathways and discuss evidence showing interaction of these signaling pathways. We also present a hypothesis proposing that a heterogeneous plastid population leads to formation of distinct retrograde signals from chloroplast to nucleus. The hypothesis is based on our analysis of nuclear gene expression in an Arabidopsis mutant containing both photosynthetically active chloroplasts and non-photosynthetic plastids in a single mesophyll cell.

LIGHT SIGNALING PATHWAYS IN THE CONTROL OF PHOTOSYNTHETIC DEVELOPMENT OF LEAF

Light receptors control leaf development in angiosperm species by regulating chloroplast biogenesis. Development of chloroplasts from etioplasts is triggered by light by two primary mechanisms. In the absence of light, nuclear repressor molecules such as constitutive photomorphogenic 1 (COP1) and phytochrome-interacting factors (PIFs) cause degradation of positive light regulators that would activate the expression of light-responsive genes, thereby suppressing light-induced processes and maintaining etiolation-specific processes (see the reviews by Bae and Choi, 2008; Bu et al., 2011; Li et al., 2012). Upon illumination, light-activated phytochromes and cryptochromes move from cytoplasm to the nucleus and drive photomorphogenetic development of seedlings by removing repressors from the nucleus and by enhancing the expression of the positive light regulators like HY5 (long hypocotyl

5), and Golden 2-likes (GLKs) proteins (Nagy and Schäfer, 2002; Bae and Choi, 2008; Waters et al., 2009; Bu et al., 2011). The removal of COP1 from the nucleus also stabilizes the positive regulators (Bae and Choi, 2008) which, in turn, activate the transcription of genes involved in chloroplast development, cell division, and plant growth. Expression of light-induced genes was recently found also to be regulated by epigenetic factors (Li et al., 2012). In angiosperms, chlorophyll is synthesized exclusively in light because the reduction of protochlorophyllide to chlorophyllide is energized by photons absorbed by protochlorophyllide bound to the protochlorophyllide oxidoreductase (POR) enzyme (Reinbothe et al., 1996).

Besides light receptor-driven signaling networks, retrograde signals from chloroplast and mitochondria to the nucleus impact seedling development and plant acclimation to environmental cues (Larkin and Ruckle, 2008; Pogson et al., 2008; Woodson and Chory, 2008; Kleine et al., 2009; Inaba, 2010; Jung and Chory, 2010; Barajas-López et al., 2012; Leister, 2012). Retrograde signals can activate or repress nuclear gene expression, depending on the genes and processes dissected. Several sources of retrograde signals in chloroplast have been identified during last decades, including altered production of tetrapyrrole biosynthesis intermediates, defective expression of plastid genes, production of reactive oxygen species (ROS) in plastids, and the redox state of thylakoid electron transfer components (PET; Pfannschmidt et al., 1999; Sullivan and Gray, 1999; Pursiheimo et al., 2001; Strand et al., 2003; Piippo et al., 2006; Pesaresi et al., 2007; Kim et al., 2008; Muhlenbock et al., 2008; Foyer and Noctor, 2009; Lepistö and Rintamäki, 2012). Redox components at the acceptor side of photosystem I (PSI) also initiate retrograde signals that modify nuclear gene expression (Pursiheimo et al., 2001; Piippo et al., 2006).

The routes of retrograde signal transmission within the chloroplast, through the cytoplasm and eventually to the nucleus are still fairly unknown, although some components of the signaling pathway have been identified. A genetic screen for potential signaling molecules identified a number of *gun* (*genomes uncoupled*) mutants in which the nuclear gene expression was unresponsive to plastid signals (Mochizuki et al., 2001). This approach identified the *GUN1* gene encoding a chloroplast pentatricopeptide repeat-containing protein (Koussevitzky et al., 2007). GUN1 has been described as a "switchboard" inside a chloroplast that can receive signals from tetrapyrrole intermediates, chloroplast translation machinery (Koussevitzky et al., 2007; Woodson and Chory, 2008; Cottage et al., 2010), and from the redox state of PET (Inaba, 2010; Sun et al., 2011). Chloroplast proteins EXECUTER 1 and 2 (EX1, EX2) are components of a $^1O_2$-dependent retrograde signaling route that controls cell death in plants (Wagner et al., 2004; Kim et al., 2008). Recently, highly promising candidates mediating the signal from chloroplast to nucleus has been identified. Phosphoadenosine phosphate (PAP) has been suggested to carry information from chloroplast to nucleus (Estavillo et al., 2011). PAP accumulates in chloroplast in response to drought and high light and moves to nucleus, in which it activates the expression of stress-related genes (Estavillo et al., 2011). Sun et al. (2011) also identified a promising candidate for a mediator of retrograde signal from chloroplast envelope to nucleus. The homeodomain transcription factor PTM is attached to the chloroplast envelope. Following a signal from the chloroplast, a peptide is cleaved from the N-terminus of PTM and the peptide translocates to the nucleus where it activates expression of *ABI4*, a nuclear AP2-type transcription factor. ABI4 was previously shown to act downstream of GUN1 in the plastid-derived signaling pathway and to repress the expression of photosynthetic genes by binding to CCAC motif upstream of light-responsive genes (Koussevitzky et al., 2007). Another nuclear transcription factor, GLK2, has been proposed to act downstream from chloroplast retrograde signaling. GLK1 and GLK2 control chloroplast biogenesis and acclimation of a plant to light intensity by preferentially activating the expression of genes in chlorophyll biosynthesis and light-harvesting complexes (Waters et al., 2009). The expression of both *GLK*s genes is regulated by phytochromes (Tepperman et al., 2006), while the expression of GLK2 also responds to plastid-derived signals (Waters et al., 2009).

ACCLIMATION OF THE PHOTOSYNTHETIC STRUCTURES TO LIGHT INTENSITY AND TO THE LENGTH OF DIURNAL PHOTOPERIOD

Plants adjust leaf cell morphology and chloroplast ultrastructure according to incident light conditions in order to coordinate absorption of solar energy with the capacity for carbon assimilation. This light acclimation involves adjustments to the photosynthetic apparatus, such as changes in photosystem stoichiometry and the size of light-harvesting antennae, as well as modulation of stromal enzyme activities and antioxidant production (Walters and Horton, 1995; Vanderauwera et al., 2005; Bartoli et al., 2006; Li et al., 2009). Several reports suggest that the light signal triggering the modification of photosynthetic traits is perceived in chloroplast rather than mediated by cytoplasmic light receptors (Pfannschmidt et al., 1999; Pursiheimo et al., 2001; Piippo et al., 2006; Muhlenbock et al., 2008; Bräutigam et al., 2009; Foyer and Noctor, 2009).

In addition to light intensity, the length of the diurnal photoperiod influences on the development of leaf structure and composition of chloroplasts. We have shown that Arabidopsis plants grown under identical light intensities in either short or long photoperiods show both structural and photosynthetic characteristics typical of shade or sun plants, respectively (Lepistö et al., 2009; Lepistö and Rintamäki, 2012). The characteristics modified by the length of the photoperiod include the density of stomata in leaf epidermis, respiration and CO_2 assimilation capacity, the ultrastructure of chloroplast, and the chlorophyll a/b ratio in thylakoid membranes (Lepistö et al., 2009; Lepistö and Rintamäki, 2012). Thus, the modifications of photosynthetic traits induced by photoperiod length resemble light intensity acclimation strategies. Acclimation of chloroplast ultrastructure to light intensity is largely controlled by chloroplast signals, whereas light receptor signaling associated with the circadian clock regulates the photoperiodic development in plants. The signaling cascade controlling photoperiodic development consists of complex network of multiple, functionally-redundant regulators within a circadian clock (for recent reviews, see Turck et al., 2008; Harmer, 2009; Imaizumi, 2010; Song et al., 2010). The circadian clock is entrained to a 24-h cycle by photoperiodic signals transmitted

from photoreceptors, and while the light-regulated mechanisms of resetting the clock are still not clear, expression of components of transcriptional feedback loops within the circadian clock is known to be regulated by light (Imaizumi, 2010; Song et al., 2010). Importantly, interaction between the circadian clock and light receptors is complex, since the circadian clock also controls the adaptation of light signaling pathways to the light/dark cycles (Li et al., 2012). Whether signals generated in chloroplasts also regulate the photoperiodic development of photosynthetic structures in leaves, and whether these signaling pathways are independent or interconnected with guiding leaf differentiation under various light regimes, are interesting questions that remain to be answered.

MUTATION IN CHLOROPLAST COMPONENTS AS A TOOL TO DISSECT CHLOROPLAST-TO-NUCLEUS RETROGRADE SIGNALING

Chloroplast retrograde signaling pathways have largely been investigated by dissecting nuclear gene expression in the *gun* mutants (Mochizuki et al., 2001). In these studies, norflurazon (NF) and lincomycin treatments that induce bleaching of seedlings have been used to generate signals from non-functional plastids (Mochizuki et al., 2001, 2008; Strand et al., 2003; Moulin et al., 2008; Cottage et al., 2010). It is likely, however, that these harsh treatments induce secondary modifications in nuclear gene expression that confound interpretation of the experimental data. On the other hand, mutating chloroplast proteins to impair chloroplast function without inducing plastid bleaching is also an approach to investigate chloroplast retrograde signaling pathways. Some chloroplast mutants exhibiting conditional phenotype that appear only under specific circumstances (Yu et al., 2007; Kim et al., 2008; Sirpiö et al., 2008; Lepistö et al., 2009; Rosso et al., 2009; Tikkanen et al., 2010) can also be used to dissect signaling pathways.

We have employed an Arabidopsis mutant lacking the nuclear-encoded chloroplast regulatory protein, chloroplast NADPH-dependent thioredoxin reductase (NTRC) to dissect chloroplast retrograde signaling pathway. NTRC is a member of chloroplast thioredoxin family (Serrato et al., 2004). Redox-active cysteines in thioredoxins are used to reduce disulfide bridges in target proteins. NTRC knockout mutants (*ntrc*) have reduced growth and decreased chlorophyll content (Perez-Ruiz et al., 2006; Lepistö et al., 2009), indicating that it is an important component of the chloroplast redox network. NTRC has been shown to regulate the activities of chloroplast proteins involved in ROS scavenging, and in the synthesis of chlorophyll, starch, and aromatic amino acids (Perez-Ruiz et al., 2006; Stenbaek et al., 2008; Kirchsteiger et al., 2009; Lepistö et al., 2009; Michalska et al., 2009; Pulido et al., 2010). Intriguingly, *ntrc* mutants possess both normal chloroplasts and irregularly differentiated plastids in a single mesophyll cell (**Figure 1**; Lepistö and Rintamäki, 2012). Some of the chloroplasts in *ntrc* are elongated and possess anomalous terminal appendages (Lepistö, 2011). The mesophyll cells of *ntrc* lines also contain small plastid-like organelles with poorly developed thylakoid membranes (**Figure 1**; Lepistö and Rintamäki, 2012), suggesting that NTRC controls early steps of chloroplast differentiation.

The phenotype of the *ntrc* mutant depends on light conditions (Perez-Ruiz et al., 2006; Lepistö et al., 2009), and is most pronounced when plants are grown under short photoperiods (**Figure 1**), especially under high light. On the other hand, low light and long photoperiods reduce growth defects in *ntrc* lines. In comparison to wild-type, 60 and 90% retardation of the *ntrc* biomass was recorded under long and short photoperiod, respectively (Lepistö et al., 2009). The anomalous *ntrc* chloroplasts were present in seedlings as well as in young developing and mature leaves grown under all light conditions studied (**Figure 1**; Lepistö, 2011), suggesting that generally slow growth of *ntrc* plants is primarily due to the defects in chloroplast differentiation in the absence of NTRC. It is likely, however, that the further reduced growth rate under short photoperiods is caused by imbalance in starch metabolism that is more severe in *ntrc* mutants grown under a shorter photoperiod (Lepistö, 2011). Defective starch metabolism (Kirchsteiger et al., 2009; Lepistö, 2011) impaired the utilization of light energy for carbon fixation in *ntrc* lines acclimated to short photoperiod, thereby increasing the reduced state of the components in PET. Accordingly, *ntrc* leaf grown under short photoperiod suffered from chronic photoinhibition of PSII in growth light (Lepistö et al., 2009).

TWO MODELS FOR RETROGRADE SIGNALING PATHWAYS IN *ntrc* KNOCKOUT LINES

The *ntrc* lines are valuable in dissecting different aspects of chloroplast-to-nucleus retrograde signaling pathways by (i) showing how heterogeneous population of plastids in a single cell influences the quantity, quality, and complexity of chloroplast signals and (ii) facilitating the study of conditionally induced retrograde signals in chloroplast. Genome-wide transcript profiling of *ntrc* lines revealed two gene expression clusters in mutant plants (**Figure 2**; Lepistö et al., 2009). The first cluster contained genes that were repressed in *ntrc* independently of photoperiod length and leaf age, including photosynthetic genes, light signaling genes, and the genes regulating the stomatal density in leaf epidermis (cluster 1 in **Figure 2**). The hypocotyl of *ntrc* lines has a weakened response to far-red and low fluence-rate blue light (Lepistö et al., 2009) that is coincident with the repression of the CRY2 gene and a component of the far-red light signaling pathway, respectively (**Figure 2**). Furthermore, the *ntrc* lines also have reduced ability to control the stomatal density under light conditions in which the differentiation of epidermal cells to guard cells is reduced in wild-type leaves (Lepistö et al., 2009). Accordingly, the expression of the genes encoding the repressors of the development of stomatal guard cells (SDD1 and EPF1) is significantly reduced in *ntrc* lines (**Figure 2**). Another 60 genes were also repressed in *ntrc* lines independently of the age or growth light conditions (Lepistö et al., 2009). Half of these repressed genes encode unknown proteins or proteins with putative domains, while the rest of the repressed genes cannot be categorized to any specific functional groups or linked to visible *ntrc* phenotype.

Because NTRC is a chloroplast-localized protein, the down-regulation of cluster 1 genes is likely due to a signal from *ntrc* chloroplast to nucleus. These results show that this repressive chloroplast signal not only down-regulates photosynthetic genes, but also controls processes linked to photosynthetic function

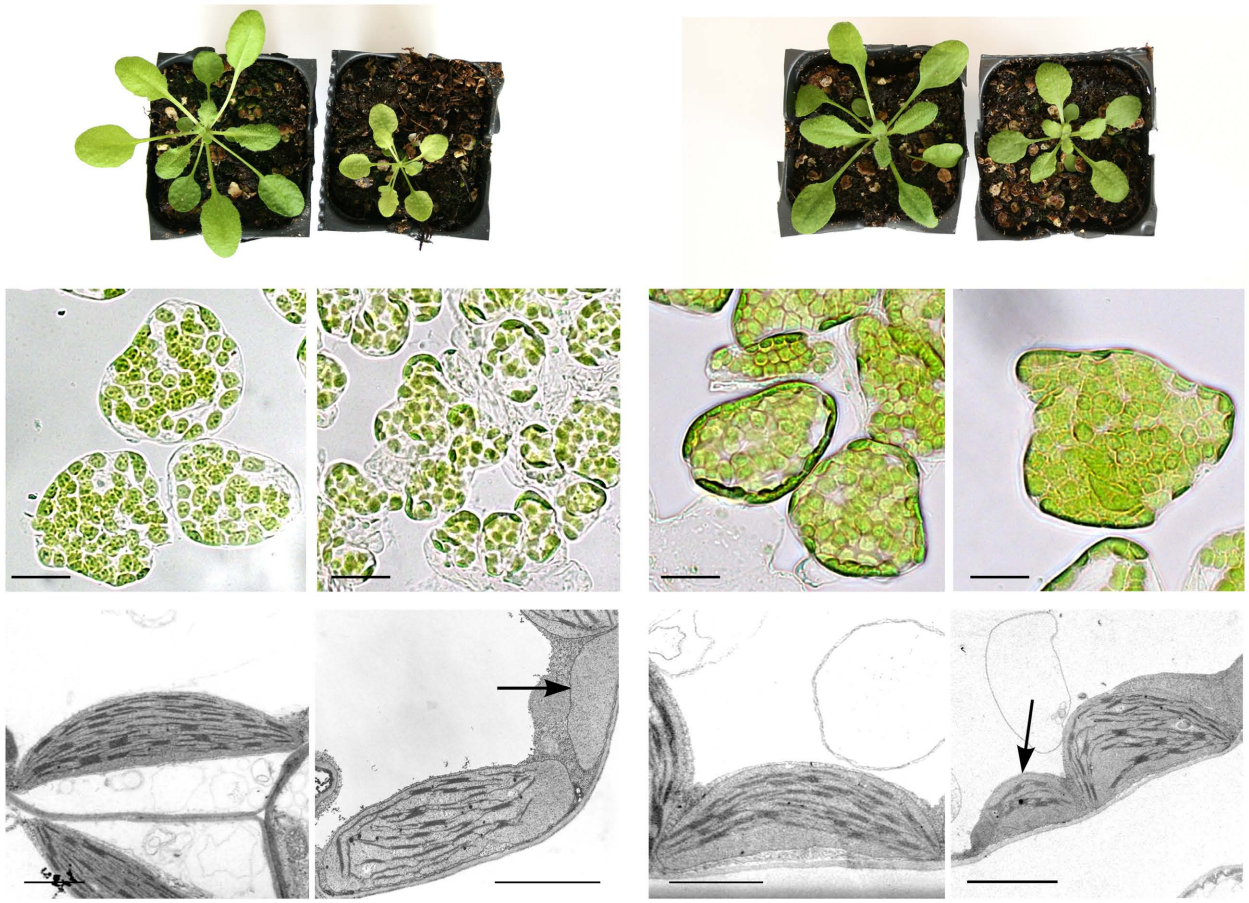

FIGURE 1 | Rosette phenotypes, bright field images, and electron micrographs of the mesophyll cells in wild-type and *ntrc* line. The plants were grown under short (SD) and long (LD) photoperiod of 8 h and 16 h light, respectively. Plastid-like organelles with poorly developed thylakoid membranes are indicated by arrows. Scale bars: 20 μm in light microscope images and 2 μm in electron micrographs, respectively.

such as stomatal differentiation. Furthermore, down-regulation of genes responsive to far-red light and low fluence-rate blue light, along with the long hypocotyl phenotype in the mutant, indicate that the chloroplast signal in *ntrc* interacts with signaling pathways controlled by light receptors.

The second cluster contained genes that were conditionally up-regulated in mature leaves of *ntrc* plants (cluster 2 in **Figure 2**), with stronger expression levels coinciding with a stronger *ntrc* mutant phenotype. The cluster 2 includes genes of chlorophyll synthesis that are strongly light-regulated (Matsumoto et al., 2004). In addition, cluster 2 genes encode enzymes in the photorespiration pathway, as well as chloroplast proteases and several heat shock proteins that are involved in stress responses (**Figure 2**). Another 30 genes (Lepistö et al., 2009) show expression profile similar to cluster 2 genes in **Figure 2**. Interestingly, cluster 2 genes were not up-regulated in young *ntrc* seedlings indicating that the regulatory signal generated from the chloroplast may arise from long-term modifications of chloroplast metabolism.

Light conditions have a different effect on the expression of the clusters 1 and 2 genes in *ntrc* lines, suggesting that retrograde signals initiate at different sources. Can these signals be identified and how are they transduced from chloroplasts to the nucleus? Repression of cluster 1 gene expression resembles the expression pattern of genes in treatments abolishing plastid function or plastid gene expression (Sullivan and Gray, 1999; Strand et al., 2003; Koussevitzky et al., 2007; Ruckle et al., 2007; Mochizuki et al., 2008). This retrograde signal is therefore likely to be a result of poorly differentiated anomalous chloroplasts in *ntrc* mesophyll cells (**Figure 1**). We hypothesize that the poorly differentiated small plastids arise from asymmetric division of a chloroplast in an expanding *ntrc* leaf (Lepistö, 2011). The irregular division may result in unequal distribution of resources between daughter plastids that impairs the development of the smaller plastid. Anomalous chloroplasts are present in *ntrc* cotyledons and leaves grown under various light conditions and the abundance even rises in expanded leaves (**Table 1**). However, cluster 1 genes were equally down-regulated in seedlings and mature leaves of *ntrc*, and their repressed expression was unrelated to the severity of the mutant phenotype, indicating that the regulation of cluster 1 genes does not depend on the abundance of anomalous

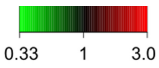

		GO cellular component	AGI code
CLUSTER 1 GENES			
PhaNGs	FZL; Thylakoid membrane organization-like	chloroplast	AT1G03160
	LHCB1.4	chloroplast	AT2G34430
	LHCB1.5	chloroplast	AT2G34420
	LHCB2.2	chloroplast	AT2G05070
	LHCB3	chloroplast	AT5G54270
	RuBisCO small subunit 1A	chloroplast	AT1G67090
Light signalling-related genes	CRY2; Cryptochrome 2		AT1G04400
	FRS3; Far1-related sequence 3		AT2G27110
Stomatal development	SDD1; Stomatal density and distribution	secretion	AT1G04110
	EPF1; Epidermal patterning factor 1	secretion	AT2G20875
CLUSTER 2 GENES			
Tetrapyrrole biosynthesis	HEMA1; glutamyl-tRNA reductase	chloroplast	AT1G58290
	GUN5; Genomes uncoupled 5	chloroplast	AT5G13630
Photorespiration	CAT2; Catalase 2	peroxisome	AT4G35090
	GGT1; Alanine-2-oxoglutarate aminotransferase1	peroxisome	AT1G23310
	HPR; Hydroxypyruvate reductase	peroxisome	AT1G68010
	SHM1; Serine hydroxymethyltransferase 1	mitochondrion	AT4G37930
	CDCP1; glycine decarboxylase P-protein 1	mitochondrion	AT4G33010
	FdGOGAT; Fd-dependent glutamate synthase 1	chloroplast	AT5G04140
Proteases	ATPREP1/ATZNMP; Zinc metalloprotease pitrilysin subfamily A	chloroplast / mitochondria	AT3G19170
	CLPC1; Clp protease, Heat shock protein 93-V	chloroplast	AT5G50920
	TPP2; Tripeptidyl peptidase II	chloroplast	AT4G20850
	SPP; Stromal processing peptidase	chloroplast	AT5G42390
Heat shock proteins + stress responses	HSP70; Heat shock protein 70		AT3G12580
	HSP81-3; Heat shock protein 81-3	secretion	AT5G56010
	HSP70-3, Heat shock cognate 70 kDa protein 3		AT3G09440
	HSP81-1; Heat shock protein 81-1		AT5G52640
	HSP17.6-CII; 17.6 kDa class II heat shock protein		AT5G12020
	AT-HSP17.6A; Heat shock protein 17.6A		AT5G12030
	BIP; Luminal binding protein	secretion	AT5G42020
	GPX7; Glutathione peroxidase	chloroplast	AT4G31870
	RCD1; Radical-induced cell death 1		AT1G32230

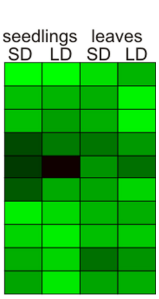

FIGURE 2 | Differentially expressed cluster 1 and cluster 2 genes in *ntrc* relative to wild-type *Arabidopsis* in 10-d-old seedlings and rosette leaves. The plants were grown under short (SD) and long (LD) photoperiod of 8 and 16 h light, respectively. Values are the means ± SEM of three independent biological replicates. For standard errors, *p*-values and for a complete list of differentially expressed genes (see Lepistö et al., 2009, Supplemental Table S2 online; www.plantphysiol.org). Copyright American Society of Plant Biologists.

Table 1 | The leaf width, the area of palisade mesophyll cells, and the number of chloroplasts in Col-0 and *ntrc* grown under short day (SD) and long day (LD) condition.

Growth conditions and age		Leaf number	Leaf width (mm)	Palisade mesophyll cell area (μm^2)	Chloroplasts per palisade mesophyll cell transection	Chloroplasts per 100 μm^2 of palisade cell area	Chloroplasts per 100 μm^2 of palisade cell area (% of Col-0)
SD,	Col-0	1	2.9 ± 0.2	358 ± 12	7.5 ± 0.2	2.09	
10 days	*ntrc*	1	1.7 ± 0.3	199 ± 8	4.4 ± 0.2	2.21	105%
SD,	Col-0	7	9.4 ± 1.3	1008 ± 40	9.9 ± 0.2	0.98	
4 weeks	*ntrc*	7	4.7 ± 0.3	684 ± 29	4.9 ± 0.2	0.72	73%
SD,	Col-0	12	11.2 ± 0.9	771 ± 32	9.7 ± 0.3	1.28	
6 weeks	*ntrc*	12	7.2 ± 1.2	857 ± 33	6.8 ± 0.2	0.79	61%
LD,	Col-0	6	9.4 ± 1.9	1564 ± 60	10.3 ± 0.3	0.66	
3 weeks	*ntrc*	6	7.2 ± 0.6	1788 ± 72	10.1 ± 0.3	0.56	84%

Data are determined from light microscope cross-sections of leaf (see Lepistö and Rintamäki, 2012). The parameters measured for SD plants with different age indicate that in comparison to wild-type the relative proportion of chloroplasts with differentiated thylakoids decreases as the ntrc palisade cell and leaf expands. The decrease likely depends on the accumulation of small plastids with poorly developed thylakoids in ntrc cells, which are not visible in light microscope cross-sections of leaf. Data are presented as means ± SEM of 30 cells in four independent experiments (leaf width, palisade mesophyll cell area, and chloroplast number per mesophyll cell).

chloroplasts. This suggests that the regulatory effect is independent of the strength of retrograde signals that are emitted from these plastids. The plastid signal is probably detected by a downstream signaling component inside the chloroplast or in the envelope, which relays the information through the cytoplasm to the nucleus (see the scenario in Figures 1C and 2 in Leister, 2012), where a nuclear component of the signaling cascade activates expression of the repressor, which in turn controls the expression of target genes (**Figure 3A**). The chloroplast retrograde signaling pathway recruiting GUN1 and/or PTM fulfills the criteria for retrograde signaling pathway repressing the cluster 1 genes in *ntrc* (**Figure 3A**). Both signaling components have shown to act down-stream to chloroplast signal and up-stream to ABI4, a repressor of light-induced genes. The knockout lines of *gun1* and *ptm* under standard growth conditions are indistinguishable from wild-type (Mochizuki et al., 2001; Sun et al., 2011). Testing the nuclear gene expression in *ntrc* mutants in *gun* and *ptm* backgrounds under various light conditions would reveal whether GUN1 and/or PTM mediates a signal generated from an anomalous *ntrc* plastid to nucleus.

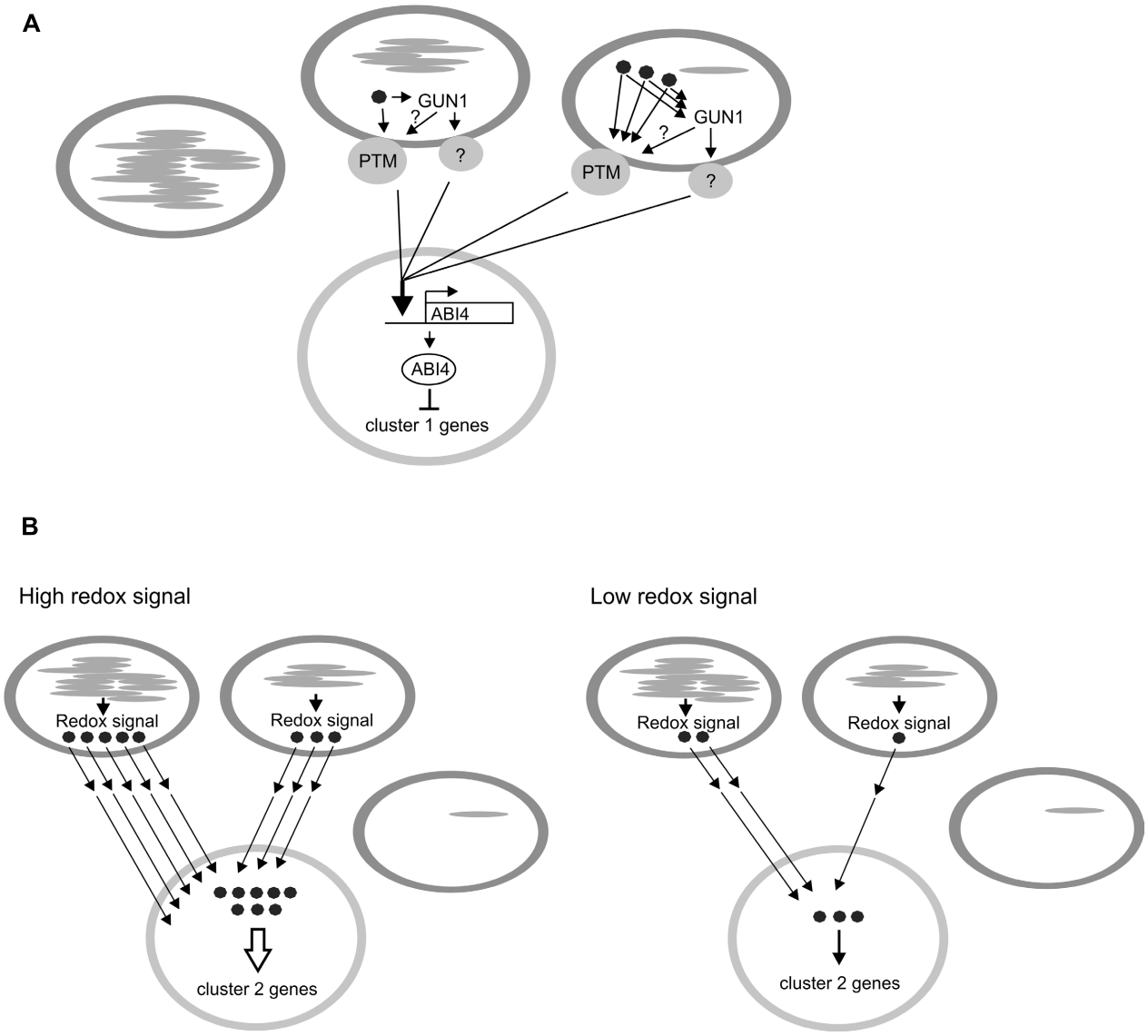

FIGURE 3 | Models for the plastid-to-nucleus retrograde signaling pathway initiated from plastids in *ntrc* mesophyll cell. (A) Signal (●) derived from anomalous plastids in *ntrc* leaves. This signal is mediated by GUN1 and/or PTM to nucleus, where the N-terminal fragment of PTM induces the *ABI4* expression. ABI4, in turn, represses the expression of cluster 1 genes (**Figure 2**). The expression level of cluster 1 genes does not correlate with the abundance of the signal originally generated in the plastids. **(B)** Redox-dependent retrograde signaling pathway in *ntrc* mesophyll cell. Redox signal (●) is conditionally generated in *ntrc* chloroplast containing functional thylakoids. The abundance of the signal is high in chloroplasts with low capacity to utilize absorbed light energy in carbon fixation. The signal exits from chloroplast and interacts with the downstream component(s) in cytosol or in nucleus, where the expression of cluster 2 genes is activated. For details, see the text.

We propose that the expression of the cluster 2 genes in *ntrc* is regulated by a different signaling pathway than the one described for cluster 1 genes. The transcript levels of the up-regulated cluster 2 genes in *ntrc* lines were positively correlated with the severity of the mutant phenotype. The short photoperiod that induced the strongest mutant phenotype in *ntrc* also significantly enhanced photoinhibition of PSII in mutant *ntrc* leaves (Lepistö et al., 2009). The short photoperiod also caused a severe imbalance in starch metabolism (Lepistö, 2011) that decreases the utilization of light energy and consequentially increases the redox status of chloroplasts (Lepistö et al., 2009). Thus, the signal activating the expression of cluster 2 genes in mature *ntrc* chloroplast may arise from reduced components of the electron transfer chain, likely from the plastoquinone pool or from the acceptor side of PSI (Pfannschmidt et al., 1999; Pursiheimo et al., 2001; Piippo et al., 2006; Pesaresi et al., 2007; Bräutigam et al., 2009; Barajas-López et al., 2012). This redox signal activates expression of genes involved in stress responses, such as heat shock proteins and chloroplast proteases. Photorespiratory genes also respond to this redox signal, likely because photorespiration has been proposed to protect chloroplasts against over-reduction by dissipating excess light energy that cannot be utilized in photosynthetic carbon metabolism (Kozaki and Takeba, 1996). Cluster 2 genes are only slightly up-regulated in *ntrc* plants acclimated to a long photoperiod because of fewer redox signals are produced in the photosynthetically active chloroplasts with less attenuated starch metabolism (**Figure 3B**; Lepistö, 2011).

Expression of *HEMA1* and *GUN5*, members of the most important light-regulated gene cluster in tetrapyrrole synthesis (Matsumoto et al., 2004), was also conditionally up-regulated in *ntrc* leaves (**Figure 2**). Heme and intermediates of chlorophyll biosynthesis are thought to act as signaling molecules in the chloroplast-derived signaling pathway (Strand et al., 2003; Woodson et al., 2011). In comparison to wild-type, *ntrc* lines accumulated higher amount of the chlorophyll biosynthesis intermediate magnesium protoporphyrin IX (Mg-Proto; Stenbaek et al., 2008). Therefore, tetrapyrrole biosynthesis intermediates may mediate and/or strengthen the redox signal generated by light reactions in *ntrc* lines. Tetrapyrrole intermediates are reported to generate signals repressing photosynthesis-associated nuclear genes (PhaNG) expression (Woodson and Chory, 2008; Inaba, 2010), but this has been subsequently challenged (Mochizuki et al., 2008; Moulin et al., 2008). On the other hand, Mg-Proto and heme have been shown to stimulate *HSP70* and *HEMA* gene expression in *Chlamydomonas* (Vasileuskaya et al., 2004; von Gromoff et al., 2006, 2008), which resembles the response observed in *ntrc* leaves. The heme- and Mg-Proto-dependent signaling cascade in *Chlamydomonas* differs significantly from the GUN1-mediated pathway (von Gromoff et al., 2008), suggesting that this signaling route is GUN1-independent, although nuclear factor(s) involved in heme- or Mg-Proto-dependent signaling are not known (von Gromoff et al., 2008). With respect to the signal characteristic, conditionally induced retrograde signal in *ntrc* leaves (**Figure 3B**) resembles the passive diffusion transport mechanism described by Leister (2012) in Figure 1C. In this scenario, the chloroplast signal migrates from the chloroplast to the cytoplasm and/or to the nucleus, in which the expression level of cluster 2 genes depends on the concentration of signaling molecule (**Figure 3B**). To find components of this signaling pathway, *ntrc* lines can be transformed with a reporter gene fused to the promoter of cluster 2 genes and subsequently mutagenizing these transgenic lines by ethyl methane sulfonate (EMS). Mutants that no longer respond to the conditional chloroplast signal would potentially contain mutations in signaling components of this pathway.

ACKNOWLEDGMENTS

This work was supported by the Academy of Finland (project numbers 127819 and 130192), Finnish Graduate School in Plant Biology and Turku University Foundation. We thank the personnel of the Laboratory of Electron Microscopy at the Medical faculty of the University of Turku, Leena Salminen for sample preparation and Markus Peurla for assistance with the microscope. We also thank Dr. Peter Gollan for critical reading of the manuscript.

REFERENCES

Bae, G., and Choi, G. (2008). Decoding of light signals by plant phytochromes and their interacting proteins. *Annu. Rev. Plant Biol.* 59, 281–311.

Barajas-López, J. de D., Blanco, N. E., and Strand, Å. (2012). Plastid-to-nucleus communication, signals controlling the running of the plant cell. *Biochim. Biophys. Acta.* doi: 10.1016/j.bbamcr.2012.06.020 [Epub ahead of print].

Bartoli, C. G., Yu, J., Gomez, F., Fernandez, L., McIntosh, L., and Foyer, C. H. (2006). Inter- relationships between light and respiration in the control of ascorbic acid synthesis and accumulation in *Arabidopsis thaliana* leaves. *J. Exp. Bot.* 57, 1621–1631.

Bräutigam, K., Dietzel, L., Kleine, T., Stroher, E., Wormuth, D., Dietz, K.-J., et al. (2009). Dynamic plastid redox signals integrate gene expression and metabolism to induce distinct metabolic states in photosynthetic acclimation in Arabidopsis. *Plant Cell* 21, 2715–2732.

Bu, Q., Castillon, A., Chen, F., Zhu, L., and Huq, E. (2011). Dimerization and blue light regulation of PIF1 interacting bHLH proteins in Arabidopsis. *Plant Mol. Biol.* 77, 501–511.

Cottage, A., Mott, E. K., Kempster, J. A., and Gray, J. C. (2010). The Arabidopsis plastid-signalling mutant gun1 (genomes uncoupled1) shows altered sensitivity to sucrose and abscisic acid and alterations in early seedling development. *J. Exp. Bot.* 61, 3773–3786.

Estavillo, G. M., Crisp, P. A., Pornsiriwong, W., Wirtz, M., Collinge, D., Carrie, C., et al. (2011). Evidence for a SAL1-PAP chloroplast retrograde pathway that functions in drought and high light signaling in Arabidopsis. *Plant Cell* 23, 3992–4012.

Foyer, C. H., and Noctor, G. (2009). Redox regulation in photosynthetic organisms, signaling, acclimation, and practical implications. *Antioxid. Redox Signal.* 11, 861–905.

Harmer, S. L. (2009). The circadian system in higher plants. *Annu. Rev. Plant Biol.* 60, 357–377.

Imaizumi, T. (2010). Arabidopsis circadian clock and photoperiodism: time to think about location. *Curr. Opin. Plant Biol.* 13, 83–89.

Inaba, T. (2010). Bilateral communication between plastid and the nucleus: plastid protein import and plastid-to-nucleus retrograde signaling. *Biosci. Biotechnol. Biochem.* 74, 471–476.

Jiao, Y., Lau, O. S., and Deng, X. W. (2007). Light-regulated transcriptional networks in higher plants. *Nat. Rev. Genet.* 8, 217–230.

Jung, H. S., and Chory, J. (2010). Signaling between chloroplasts and the nucleus, can a systems biology approach bring clarity to a complex and highly regulated pathway? *Plant Physiol.* 152, 453–459.

Kim, C., Meskauskiene, R., Apel, K., and Laloi, C. (2008). No single way to understand singlet oxygen signalling in plants. *EMBO Rep.* 9, 435–439.

Kirchsteiger, K., Pulido, P., Gonzalez, M., and Cejudo, F. J. (2009). NADPH thioredoxin reductase C controls the redox status of chloroplast 2-Cys peroxiredoxins in *Arabidopsis thaliana*. *Mol. Plant* 2, 298–307.

Kleine, T., Voigt, C., and Leister, D. (2009). Plastid signalling to the

nucleus: messengers still lost in the mists? *Trends Genet.* 25, 185–192.

Koussevitzky, S., Nott, A., Mockler, T. C., Hong, F., Sachetto-Martins, G., Surpin, M., et al. (2007). Signals from chloroplasts converge to regulate nuclear gene expression. *Science* 316, 715–719.

Kozaki, A., and Takeba, G. (1996). Photorespiration protects C3 plants from photooxidation. *Nature* 384, 557–560.

Larkin, R. M., and Ruckle, M. E. (2008). Integration of light and plastid signals. *Curr. Opin. Plant Biol.* 11, 593–599.

Leister, D. (2012). Retrograde signaling in plants: from simple to complex scenarios. *Front. Plant Sci.* 3:135. doi: 10.3389/fpls.2012.00135

Lepistö, A. (2011). *NADPH-dependent Thioredoxin System in Regulation of Chloroplast Functions.* PhD thesis, University of Turku, Turku. Available at: http://urn.fi/URN:ISBN:978-951-29-4695-2

Lepistö, A., Kangasjärvi, S., Luomala, E.-M., Brader, G., Sipari, N., Keränen, M., et al. (2009). Chloroplast NADPH-thioredoxin reductase interacts with photoperiodic development in Arabidopsis. *Plant Physiol.* 149, 1261–1276.

Lepistö, A., and Rintamäki, E. (2012). Coordination of plastid and light signaling pathways upon development of Arabidopsis leaves under various photoperiods. *Mol. Plant* 5, 799–816.

Li, J., Terzaghi, W., and Deng, X. W. (2012). Genomic basis for light control of plant development. *Protein Cell* 3, 106–116.

Li, Z., Wakao, S., Fischer, B. B., and Niyogi, K. K. (2009). Sensing and responding to excess light. *Annu. Rev. Plant Biol.* 60, 239–260.

Matsumoto, F., Obayashi, T., Sasaki-Sekimoto, Y., Ohta, H., Takamiya, K., and Masuda, T. (2004). Gene expression profiling of the tetrapyrrole metabolic pathway in Arabidopsis with a mini-array system. *Plant Physiol.* 135, 2379–2391.

Michalska, J., Zauber, H., Buchanan, B. B., Cejudo, F. J., and Geigenberger, P. (2009). NTRC links built-in thioredoxin to light and sucrose in regulating starch synthesis in chloroplasts and amyloplasts. *Proc. Natl. Acad. Sci. U.S.A.* 106, 9908–9913.

Mochizuki, N., Brusslan, J. A., Larkin, R., Nagatani, A., and Chory, J. (2001). Arabidopsis genomes uncoupled 5 (GUN5) mutant reveals the involvement of Mg-chelatase H subunit in plastid-to-nucleus signal transduction. *Proc. Natl. Acad. Sci. U.S.A.* 98, 2053–2058.

Mochizuki, N., Tanaka, R., Tanaka, A., Masuda, T., and Nagatani, A. (2008). The steady- state level of Mg-protoporphyrin IX is not a determinant of plastid-to-nucleus signaling in Arabidopsis. *Proc. Natl. Acad. Sci. U.S.A.* 105, 15184–15189.

Moulin, M., McCormac, A. C., Terry, M. J., and Smith, A. G. (2008). Tetrapyrrole profiling in Arabidopsis seedlings reveals that retrograde plastid nuclear signaling is not due to Mg-protoporphyrin IX accumulation. *Proc. Natl. Acad. Sci. U.S.A.* 105, 15178–15183.

Muhlenbock, P., Szechynska-Hebda, M., Plaszczyca, M., Baudo, M., Mateo, A., Mullineaux, P. M., et al. (2008). Chloroplast signaling and LESION SIMULATING DISEASE1 regulate crosstalk between light acclimation and immunity in Arabidopsis. *Plant Cell* 20, 2339–2356.

Nagy, F., and Schäfer, E. (2002). Phytochromes control photomorphogenesis by differentially regulated, interacting signaling pathways in higher plants. *Annu. Rev. Plant Biol.* 53, 329–355.

Perez-Ruiz, J. M., Spinola, M. C., Kirchsteiger, K., Moreno, J., Sahrawy, M., and Cejudo, F. J. (2006). Rice NTRC is a high-efficiency redox system for chloroplast protection against oxidative damage. *Plant Cell* 18, 2356–2368.

Pesaresi, P., Schneider, A., Kleine, T., and Leister, D. (2007). Interorganellar communication. *Curr. Opin. Plant Biol.* 10, 600–606.

Pfannschmidt, T., Nilsson, A., Tullberg, A., Link, G., and Allen, J. F. (1999). Direct transcriptional control of the chloroplast genes psbA and psaAB adjusts photosynthesis to light energy distribution in plants. *IUBMB Life* 48, 271–276.

Piippo, M., Allahverdiyeva, Y., Paakkarinen, V., Suoranta, U., Battchikova, N., and Aro, E.- M. (2006). Chloroplast-mediated regulation of nuclear genes in *Arabidopsis thaliana* in the absence of light stress. *Physiol. Genomics* 25, 142–152.

Pogson, B. J., Woo, N. S., Forster, B., and Small, I. D. (2008). Plastid signalling to the nucleus and beyond. *Trends Plant Sci.* 13, 602–609.

Pulido, P., Spinola, M. C., Kirchsteiger, K., Guinea, M., Pascual, M. B., Sahrawy, M., et al. (2010). Functional analysis of the pathways for 2-Cys peroxiredoxin reduction in *Arabidopsis thaliana* chloroplasts. *J. Exp. Bot.* 61, 4043–4054.

Pursiheimo, S., Mulo, P., Rintamäki, E., and Aro, E.-M. (2001). Coregulation of light-harvesting complex II phosphorylation and lhcb mRNA accumulation in winter rye. *Plant J.* 26, 317–327.

Reinbothe, S., Reinbothe, C., Lebedev, N., and Apel, K. (1996). PORA and PORB, two light-dependent protochlorophyllide-reducing enzymes of angiosperm chlorophyll biosynthesis. *Plant Cell* 8, 763–769.

Rosso, D., Bode, R., Li, W., Krol, M., Saccon, D., Wang, S., et al. (2009). Photosynthetic redox imbalance governs leaf sectoring in the *Arabidopsis thaliana* variegation mutants immutans, spotty, var1, and var2. *Plant Cell* 21, 3473–3492.

Ruckle, M. E., DeMarco, S. M., and Larkin, R. M. (2007). Plastid signals remodel light signaling networks and are essential for efficient chloroplast biogenesis in Arabidopsis. *Plant Cell* 19, 3944–3960.

Ruckle, M. E., and Larkin, R. M. (2009). Plastid signals that affect photomorphogenesis in *Arabidopsis thaliana* are dependent on GENOMES UNCOUPLED 1 and cryptochrome 1. *New Phytol.*182, 367–379.

Serrato, A. J., Perez-Ruiz, J. M., Spinola, M. C., and Cejudo, F. J. (2004). A novel NADPH thioredoxin reductase, localized in the chloroplast, which deficiency causes hypersensitivity to abiotic stress in *Arabidopsis thaliana*. *J. Biol. Chem.* 279, 43821–43827.

Sharrock, R. A. (2008). The phytochrome red/far-red photoreceptor superfamily. *Genome Biol.* 9, 230.

Sirpiö, S., Khrouchtchova, A., Allahverdiyeva, Y., Hansson, M., Fristedt, R., Vener, A. V., et al. (2008). AtCYP38 ensures early biogenesis, correct assembly and sustenance of photosystem II. *Plant J.* 55, 639–651.

Song, Y. H., Ito, S., and Imaizumi, T. (2010). Similarities in the circadian clock and photoperiodism in plants. *Curr. Opin. Plant Biol.* 13, 594–603.

Stenbaek, A., Hansson, A., Wulff, R. P., Hansson, M., Dietz, K.-J., and Jensen, P. E. (2008). NADPH-dependent thioredoxin reductase and 2-Cys peroxiredoxins are needed for the protection of Mg-protoporphyrin monomethyl ester cyclase. *FEBS Lett.* 582, 2773–2778.

Strand, Å., Asami, T., Alonso, J., Ecker, J. R., and Chory, J. (2003). Chloroplast to nucleus communication triggered by accumulation of Mg-protoporphyrinIX. *Nature* 421, 79–83.

Sullivan, J. A., and Deng, X. W. (2003). From seed to seed, the role of photoreceptors in Arabidopsis development. *Dev. Biol.* 260, 289–297.

Sullivan, J. A., and Gray, J. C. (1999). Plastid translation is required for the expression of nuclear photosynthetic genes in the dark and in roots of the pea lip1 mutant. *Plant Cell* 11, 901–910.

Sun, X., Feng, P., Xu, X., Guo, H., Ma, J., Chi, W., et al. (2011). A chloroplast envelope-bound PHD transcription factor mediates chloroplast signals to the nucleus. *Nat. Commun.* 2, 477.

Tepperman, J. M., Hwang, Y. S., and Quail, P. H. (2006). phyA dominates in transduction of red-light signals to rapidly responding genes at the initiation of Arabidopsis seedling de-etiolation. *Plant J.* 48, 728–742.

Tikkanen, M., Grieco, M., Kangasjärvi, S., and Aro, E.-M. (2010). Thylakoid protein phosphorylation in higher plant chloroplasts optimizes electron transfer under fluctuating light. *Plant Physiol.* 152, 723–735.

Turck, F., Fornara, F., and Coupland, G. (2008). Regulation and identity of florigen: FLOWERING LOCUS T moves center stage. *Annu. Rev. Plant Biol.* 59, 573–594.

Vanderauwera, S., Zimmermann, P., Rombauts, S., Vandenabeele, S., Langebartels, C., Gruissem, W., et al. (2005). Genome-wide analysis of hydrogen peroxide-regulated gene expression in Arabidopsis reveals a high light- induced transcriptional cluster involved in anthocyanin biosynthesis. *Plant Physiol.* 139, 806–821.

Vasileuskaya, Z., Oster, U., and Beck, C. F. (2004). Involvement of tetrapyrroles in inter- organellar signaling in plants and algae. *Photosynth. Res.* 82, 289–299.

von Gromoff, E. D., Alawady, A., Meinecke, L., Grimm, B., and Beck, C. F. (2008). Heme, a plastid-derived regulator of nuclear gene expression in *Chlamydomonas*. *Plant Cell* 20, 552–567.

von Gromoff, E. D., Schroda, M., Oster, U., and Beck, C. F. (2006). Identification of a plastid response element that acts as an enhancer within the *Chlamydomonas* HSP70A promoter. *Nucleic Acids Res.* 34, 4767–4779.

Wagner, D., Przybyla, D., Op den Camp, R., Kim, C., Landgraf, F., Lee, K. P., et al. (2004). The genetic basis of singlet oxygen-induced stress responses of *Arabidopsis thaliana*. *Science* 306, 1183–1185.

Walters, R. G., and Horton, P. (1995). Acclimation of *Arabidopsis thaliana* to the light environment: changes in composition of the photosynthetic apparatus. *Planta* 195, 248–256.

Waters, M. T., Wang, P., Korkaric, M., Capper, R. G., Saunders, N. J., and

Langdale, J. A. (2009). GLK transcription factors coordinate expression of the photosynthetic apparatus in Arabidopsis. *Plant Cell* 21, 1109–1128.

Woodson, J. D., and Chory, J. (2008). Coordination of gene expression between organellar and nuclear genomes. *Nat. Rev. Genet.* 9, 383–395.

Woodson, J. D., Perez-Ruiz, J. M., and Chory, J. (2011). Heme synthesis by plastid ferrochelatase I regulates nuclear gene expression in plants. *Curr. Biol.* 21, 897–903.

Yu, F., Fu, A., Aluru, M., Park, S., Xu, Y., Liu, H., et al. (2007). Variegation mutants and mechanisms of chloroplast biogenesis. *Plant Cell Environ.* 30, 350–365.

Conflict of Interest Statement: The authors declare that the research was conducted in the absence of any commercial or financial relationships that could be construed as a potential conflict of interest.

Received: 06 September 2012; accepted: 03 December 2012; published online: 19 December 2012.

Citation: Lepistö A, Toivola J, Nikkanen L and Rintamäki E (2012) Retrograde signaling from functionally heterogeneous plastids. Front. Plant Sci. 3:286. doi: 10.3389/fpls.2012.00286

This article was submitted to Frontiers in Plant Physiology, a specialty of Frontiers in Plant Science.

Copyright © 2012 Lepistö, Toivola, Nikkanen and Rintamäki. This is an open-access article distributed under the terms of the Creative Commons Attribution License, which permits use, distribution and reproduction in other forums, provided the original authors and source are credited and subject to any copyright notices concerning any third-party graphics etc.

frontiers in
PLANT SCIENCE

REVIEW ARTICLE
published: 27 November 2012
doi: 10.3389/fpls.2012.00260

The mechanism of variegation in *immutans* provides insight into chloroplast biogenesis

Andrew Foudree, Aarthi Putarjunan, Sekhar Kambakam, Trevor Nolan, Jenna Fussell, Gennady Pogorelko and Steve Rodermel*

Department of Genetics, Development, and Cell Biology, Iowa State University, Ames, IA, USA

Edited by:
Tatjana Kleine, Ludwig-Maximilians-Universität München, Germany

Reviewed by:
Toshiharu Shikanai, Kyoto University, Japan
Ko Noguchi, The University of Tokyo, Japan

***Correspondence:**
Steve Rodermel, Department of Genetics, Development, and Cell Biology, Iowa State University, 457 Bessey Hall, Ames, IA 50011, USA. e-mail: rodermel@iastate.edu

The *immutans* (*im*) variegation mutant of *Arabidopsis* has green and white-sectored leaves due to the absence of fully functional plastid terminal oxidase (PTOX), a plastoquinol oxidase in thylakoid membranes. PTOX appears to be at the nexus of a growing number of biochemical pathways in the plastid, including carotenoid biosynthesis, PSI cyclic electron flow, and chlororespiration. During the early steps of chloroplast biogenesis, PTOX serves as an alternate electron sink and is a prime determinant of the redox poise of the developing photosynthetic apparatus. Whereas a lack of PTOX causes the formation of photooxidized plastids in the white sectors of *im*, compensating mechanisms allow the green sectors to escape the effects of the mutation. This manuscript provides an update on PTOX, the mechanism of *im* variegation, and findings about *im* compensatory mechanisms.

Keywords: IMMUTANS, PTOX, variegation, chloroplast, photosynthesis, carotenoids, chloroplast biogenesis, retrograde signaling

INTRODUCTION

Variegation mutants provide an excellent system to explore the mechanisms of chloroplast biogenesis and the nature of communication between the nucleus-cytoplasm, chloroplast, and mitochondrion (Rodermel, 2001; Yu et al., 2007). The leaves of these mutants contain green and chlorotic (white, yellow) sectors that arise as a consequence of mutations in nuclear or organelle genes (Tilney-Bassett, 1975). Whereas cells in the green sectors have morphologically normal chloroplasts, cells in the chlorotic sectors contain pigment-deficient plastids with abnormal membrane structures (Aluru et al., 2001). One common mechanism of variegation involves the induction of defective chloroplasts (or mitochondria) by mutations in nuclear genes that code for organelle proteins. In some cases the green and white cells have different genotypes. For example, transposable element activity can inactivate a gene required for normal chloroplast function in some cells (chlorotic cells) while excision can reconstitute gene function (green cells). In other cases of variegation, the two types of cells have the same (mutant) genotype, indicating that the gene product is required in some, but not all cells of the mutant. This raises the question of how the green cells escape this requirement. Is there a compensating activity? Our operating hypothesis is that answers to this question will provide insight into mechanisms of variegation, as well as into pathways and regulatory networks of chloroplast biogenesis.

The past decade has witnessed a growing interest in the use of variegation mutants to address fundamental questions in photosynthesis and chloroplast biogenesis (Yu et al., 2007; Liu et al., 2010). Yet, mechanisms of variegation are still poorly understood. Here we focus on the mechanism of variegation in *immutans* (*im*), which defines the gene for plastid terminal oxidase (PTOX), a versatile quinol oxidase in plastid membranes. Early studies led to the notion that this mechanism involves the attainment of a threshold by developing plastids (the threshold hypothesis). In this manuscript, we review the underlying assumptions and experiments in support of this hypothesis and discuss approaches and studies that have been used to gain insight into factors that compensate for a lack of PTOX.

IMMUTANS

The *im* variegation mutant is one of the oldest *Arabidopsis* mutants, reported independently by Rédei and Röbbelen in the 1960's (Rédei, 1963; Röbbelen, 1968). Cells in the green sectors of *im* have morphologically normal chloroplasts, whereas cells in the white sectors are heteroplastidic and contain abnormal plastids that lack pigments and organized lamellae, as well as rare, normal-appearing chloroplasts (Wetzel et al., 1994). The extent of white sector formation in *im* is promoted by high light and low temperature (Rédei, 1963, 1967; Röbbelen, 1968; Wetzel et al., 1994; Rosso et al., 2009). HPLC analyses showed that the white sectors accumulate the colorless C_{40} carotenoid intermediate, phytoene, indicating that *im* is impaired in the activity of phytoene desaturase (PDS), the enzyme which converts phytoene to zeta-carotene (Wetzel et al., 1994). All the steps of carotenogenesis take place in the plastid and are mediated by nuclear-encoded enzymes that are imported into the organelle post-translationally, and PDS mediates an early step of the pathway (DellaPenna and Pogson, 2006). An inhibition of PDS activity would thus result in lack of accumulation of downstream, colored (photoprotective) carotenoids, and under high light conditions, would be anticipated to give rise to white, photooxidized plastids. A defect of this sort is consistent with the light-sensitivity of *im*; as in other carotenoid mutants, the higher the light intensity, the greater the extent of photooxidation (white sector formation) (Oelmüller, 1989; Mayfield and Taylor, 2005). The presence of normal-appearing chloroplasts in *im*, on the other hand, suggests that some plastids are able to bypass the

requirement for the *IM* gene product, likely because of compensating activities that make them less susceptible to photooxidation early in their development.

PTOX FUNCTION

IMMUTANS was cloned in *Arabidopsis* by both map-based methods (Wu et al., 1999) and T-DNA tagging (Carol et al., 1999). The gene product (IM) was discovered to be a plastid membrane protein that is distantly related (37% amino acid similarity) to alternative oxidase (AOX), a mitochondrial inner membrane protein which functions in the alternative (cyanide-resistant) pathway of respiration, where it transfers electrons from ubiquinol to molecular oxygen (Wu et al., 1999). Central among its physiological functions, AOX is an important sensor of cellular redox balance (Giraud et al., 2008; McDonald, 2008). Similar to AOX, IM has quinol oxidase activity *in vivo* and *in vitro* and, consequently, it has been designated PTOX (Joët et al., 2002; Josse et al., 2003). PTOX is found in some cyanophages, which might serve as vectors for transfer of PTOX among cyanobacteria, but otherwise appears to be limited to oxygenic photosynthetic prokaryotes and eukaryotes, where it is found in all lineages (McDonald et al., 2011). *IM* is generally present as a single copy gene, although two copies are found in some cyanobacteria, red algae and green algae (Wang et al., 2009; Houille-Vernes et al., 2011). In chloroplasts, PTOX is bound to the stromal lamellae of thylakoids and is modeled as an interfacial membrane protein whose active site faces the stroma (Berthold et al., 2000; Joët et al., 2002; Lennon et al., 2003). It does not appear to be present in chloroplast envelope membranes.

Several functions have been ascribed to PTOX. The phytoene-accumulation phenotype of *im* led to the suggestion that PTOX serves as the terminal oxidase of an oxygen-dependent redox pathway that desaturates phytoene (Beyer et al., 1989; Mayer et al., 1990, 1992; Hugueney et al., 1992; Schulz et al., 1993; Nievelstein et al., 1995; Norris et al., 1995; Al-Babili et al., 1996). This pathway is thought to involve transfer of electrons from phytoene to plastoquinone (PQ) via PDS, forming ζ-carotene and plastoquinol (PQH_2), and from PQH_2 to molecular oxygen via PTOX, forming water and PQ (Carol et al., 1999; Wu et al., 1999; Rosso et al., 2009). Thylakoids of developing *im* plastids have over-reduced PQ pools (Rosso et al., 2009), and according to this pathway, the accumulation of phytoene in *im* can be explained by a decreased supply of PQ available to PDS, as suggested by Okegawa et al. (2010), and/or because electron transfer from phytoene into an over-reduced PQ pool is not energetically favorable (Rochaix, 2011). In addition to the phytoene-accumulation phenotype of mutants that lack PTOX (*im* in *Arabidopsis* and the orthologous *ghost* mutant in tomato) (Wetzel et al., 1994; Josse et al., 2000; Barr et al., 2004; Shahbazi et al., 2007), an involvement of PTOX in carotenogenesis is suggested by the close coordination between PTOX expression and carotenoid production in a number of systems, perhaps most strikingly in chromoplasts during the ripening of tomato, citrus, and pepper fruit (Josse et al., 2000; Barr et al., 2004). Another noteworthy example is the upregulation of PTOX expression in etiolated seedlings of *Arabidopsis* treated with paclobutrazol (PAC), an inhibitor of gibberellin biosynthesis; PAC causes an increase in carotenoid production (Rodríguez-Villalón et al., 2009).

It might be noted that all the enzymes of carotenogenesis are present in chloroplast envelopes, with the exception of PDS which is also found in thylakoids (Joyard et al., 2009). The involvement of PTOX in carotenogenesis is therefore puzzling given its apparent exclusive location in thylakoids (Lennon et al., 2003). This suggests that carotenoid intermediates are trafficked between the envelope and thylakoids, perhaps via vesicles, by connections between the envelope and thylakoids, or by carrier proteins (Adam et al., 2011; Ngaki et al., 2012). There might also be PTOX-independent mechanisms of plastoquinol oxidation in envelopes, such as PQH_2 autooxidation (Khorobrykh and Ivanov, 2002), the activity of another plastoquinol oxidase (Buchel and Garab, 1995; Lajko et al., 1997; Joët et al., 2002), or perhaps a plastoquinol peroxidase (Casano et al., 2000; Rumeau et al., 2007).

IM mRNAs are ubiquitously expressed in *Arabidopsis*, and the anatomies of various plastid types are affected in *im* (Aluru et al., 2001), as well as in tomato *ghost* (Josse et al., 2000; Barr et al., 2004). However, a positive correlation between *IM* mRNA levels and carotenoid accumulation does not always hold, and *IM* is expressed highly in some tissues with low carotenoid accumulation (Aluru et al., 2001). Considered together, these observations argue that the role of PTOX in plastid metabolism is not limited to carotenogenesis. In fact, since its discovery over 13 years ago, it has become apparent that PTOX resides at the nexus of a growing number of redox pathways in the plastid. For instance, *in vitro* and *in vivo* studies have demonstrated that PTOX is the terminal oxidase of chlororespiration (non-photochemical reduction of the PQ pool) (Peltier and Cournac, 2002; Rumeau et al., 2007). Chlororespiration involves the transfer of electrons from NAD(P)H (and/or Ferredoxin) to PQ via a thylakoid NAD(P)H dehydrogenase (NDH) complex, and from PQH_2 to molecular oxygen via PTOX (Peng et al., 2012). One purpose of chlororespiration is to help poise the redox state of the PQ pool during cyclic electron flow (CEF) around PSI (Trouillard et al., 2012). In addition to chlororespiration, PTOX mediates chromorespiration, the analogous process in chromoplasts (Josse et al., 2000; Barr et al., 2004; Rodrigo et al., 2004; Shahbazi et al., 2007).

Safety valves are photoprotective mechanisms that dissipate excess photons and electrons (Niyogi, 2000). They include non-photochemical quenching mechanisms and alternative electron acceptors that prevent over-reduction of photosynthetic electron carriers, thereby protecting PSI and PSII from photodamage (Aro et al., 1993; Allahverdiyeva et al., 2005). Soon after its discovery, Niyogi (2000) proposed that PTOX-mediated electron flow from PQH_2 to O_2 might act as a safety valve. Early support for this hypothesis came from studies showing that the green leaf sectors of *im* have morphological, biochemical, and molecular adaptations similar to plants acclimated to growth in high light, even when grown in permissive (low light) conditions (Aluru et al., 2001). Early studies also showed that *IM* mRNAs and proteins are significantly upregulated in high light conditions in antisense mutants of tobacco that lack both ascorbate peroxidase and catalase (Rizhsky et al., 2002). A number of experiments have since supported the safety valve hypothesis in systems as diverse as the alpine species *Ranunculus glacialis* and *Soldanella alpina* (Streb et al., 2005; Laureau et al., 2011); oat exposed to heat and high light (Quiles, 2006); mature green leaves and green fruit of the tomato *ghost* mutant

subjected to high light stress (Shahbazi et al., 2007); wild species of *Brassica fruticulosa* versus the agricultural species *Brassica oleracea* adapted to both heat and high light (Díaz et al., 2007); the salt-stressed halophyte *Thellungiella* (Stepien and Johnson, 2009); and cold-acclimated Lodgepole pine (Savitch et al., 2010).

In addition to altered expression in response to environmental factors, PTOX is upregulated in various photosynthetic mutants, including the *gun4* mutant of *Chlamydomonas* and the tobacco *rbcL* and *psbA* deletion mutants. The *gun4* mutants lack GUN4, a regulatory subunit of Mg-chelatase, and enhanced PTOX activities in these mutants were suggested to play a physiological role in decreasing PSII excitation pressures (Formighieri et al., 2012). The *rbcL* mutants lack Rubisco and consequently two major electron sinks, CO_2 fixation and photorespiration; it was proposed that elevated PTOX levels in these mutants reduce oxidative pressure on both PSI and PSII (Allahverdiyeva et al., 2005). In the *psbA* mutants, which lack the D1 protein of PSII, it was hypothesized that enhanced PTOX levels primarily support increased carotenoid production as a way to quench singlet oxygen generated by free LHCII accumulation in the mutant (Baena-González et al., 2003). Despite the growing number of examples of PTOX upregulation, *cis* and *trans* regulatory factors have yet to be reported.

The demonstration that PTOX serves as a safety valve in a particular system is not straightforward and must rely on more than gene expression data, since there are many ways of preventing over-reduction of the electron transport chain, such as upregulation of downstream electron sinks, as found in some cold-tolerant plants, or upregulation of the Mehler reaction (e.g., Gray et al., 1997; Savitch et al., 2000); alterations in PTOX expression might be a secondary effect. There are also some cases where PTOX does not act as a safety valve. For example, overexpression of *Arabidopsis* PTOX does not impart increased resistance to photoinhibition in mature tobacco leaves (Joët et al., 2002), nor does it regulate the redox state of the PQ pool during steady state photosynthesis in *Arabidopsis* (Rosso et al., 2006). These findings are consistent with the observation that the steady state flux of electrons through PTOX is relatively minor – estimated to be <2% of the flux through the photosynthetic electron transport chain (PETC) (Ort and Baker, 2002). On the other hand, these same studies showed that PTOX is important in preventing over-reduction of PSII acceptors during dark to light transients (Joët et al., 2002), and that it protects against PSI photoinhibition (Rosso et al., 2006). The latter has been confirmed in recent experiments showing that PTOX acts as a safety valve in *Arabidopsis* under stress conditions of low temperature and high light, where it protects against both PSII and PSI photoinhibition (Ivanov et al., 2012).

In this context it is important to note that in contrast to PSII, where there are a number of photochemical and non-photochemical mechanisms to avoid over-reduction of PSII acceptors, the repertoire is rather more limited for PSI and includes, most prominently, the water–water cycle (reviewed in Rumeau et al., 2007). PTOX might thus turn out to be an important mechanism to reduce electron pressure on PSI, as during stress when NADPH/ATP ratios are high and CEF around PSI is activated; in concert with NDH, PTOX might serve to poise the redox state of intersystem carriers by recycling electrons to PQ. This might also be the case during chloroplast biogenesis when it has been demonstrated that PTOX is a central regulator of thylakoid redox and PSII excitation pressure (Rosso et al., 2009).

Although not within the scope of this review, it might be mentioned that the functions described for PTOX in cyanobacteria and eukaryotic algae are similar to those in higher plants (reviewed by McDonald et al., 2011). These include carotenogenesis and response to diverse environmental stresses, such as high light, temperature, salt, iron, and phosphate deprivation (Moseley et al., 2006; Bailey et al., 2008; Wang et al., 2009). One difference is that cyanobacterial respiratory and PETCs share some components, which offers the possibility of PTOX control of both activities.

In summary, there is growing evidence that PTOX is a versatile terminal oxidase in chloroplast metabolism and that its primary physiological role varies from taxon to taxon. This might not be surprising, since PTOX is only one element of a large network of factors involved in stress tolerance, pigment biosynthesis, and photosynthetic control (regulation of ATP/NADPH ratios) (Kramer and Evans, 2011; Foyer et al., 2012). In such a network, it might be anticipated that the relative importance of a given element varies according to developmental and/or physiological context. For instance, PTOX might turn out to play a more significant regulatory role in PSI cyclic electron transport in bundle sheath cells of C4 plants than in mesophyll cells of C3 plants; in contrast to C3 plants, cyclic electron transport is a key regulator of ATP synthesis during C4 photosynthesis (Rumeau et al., 2007; Foyer et al., 2012). Given the ubiquity of PTOX expression, it might also be predicted that novel functions will be found for PTOX, especially in non-green plastids. A schematic diagram of PTOX in thylakoids is shown in **Figure 1**.

MECHANISM OF VARIEGATION: THE THRESHOLD HYPOTHESIS

STUDIES USING MATURE LEAVES

Nearly all molecular and biochemical studies on *im* have been conducted using fully expanded rosette leaves; for comparative studies, green versus white sectors have been obtained by dissection or via fluorescence-activated cell sorting (FACS) (Wetzel et al., 1994; Meehan et al., 1996; Aluru et al., 2009). Alternatively, all-green *im* leaves have been produced by altering light conditions during early seedling development (Rosso et al., 2009).

The notion that *im* variegation is due to a *threshold* came from two sets of observations. The first was that the white sectors of *im* are heteroplastidic, indicating that *im* behaves in a plastid autonomous manner, i.e., plastid phenotypes within a cell are determined independently in the *im* background. The second was that intermediate plastid phenotypes are not seen; plastids in the green sectors look similar to one another, as do abnormal plastids in the white sectors (**Figure 2**). Taken together with the finding that the white (but not green) sectors accumulate phytoene, the first iteration of the *threshold hypothesis* held that plastid phenotype in *im* is determined by the attainment of a threshold of PDS activity during chloroplast biogenesis: developing plastids with above-threshold activities are able to produce enough downstream, photoprotective carotenoids to form normal-appearing chloroplasts (green sectors), whereas plastids with below-threshold PDS activities are deficient in colored carotenoid production and susceptible to photooxidation (white plastids and sectors) (Wetzel et al., 1994;

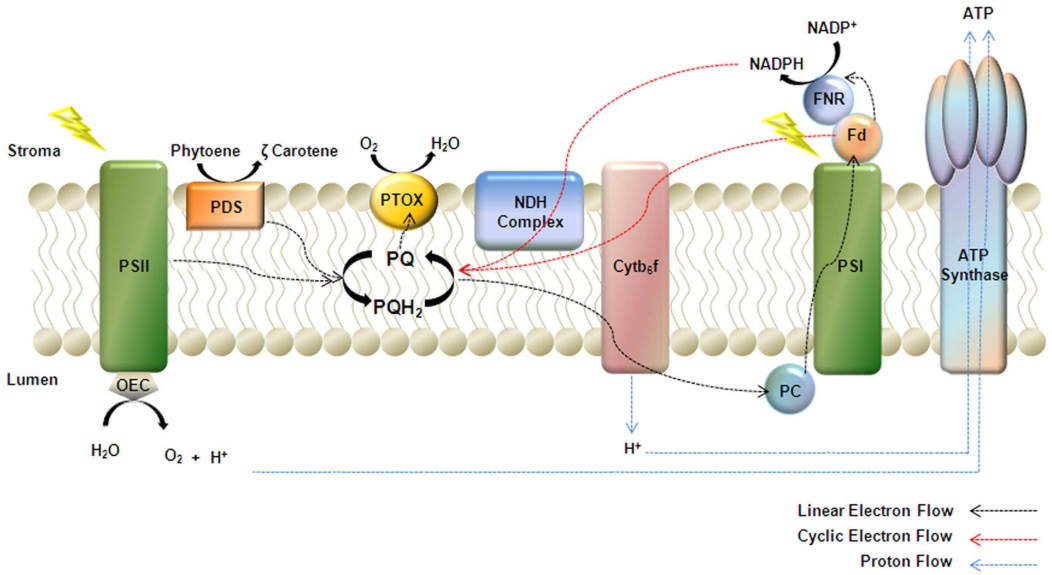

FIGURE 1 | Model of PTOX as a cofactor of phytoene desaturase (PDS). PTOX is a plastoquinol terminal oxidase that regulates the redox state of the plastoquinone pool (PQ) during early chloroplast biogenesis. Electrons from linear electron flow, cyclic electron flow mediated by either NDH or the Fd dependent PGR5 pathway, and the desaturation of phytoene, feed into the PQ pool. PTOX plays a pivotal role in transferring electrons from the PQ pool to molecular oxygen thus keeping the pool oxidized.

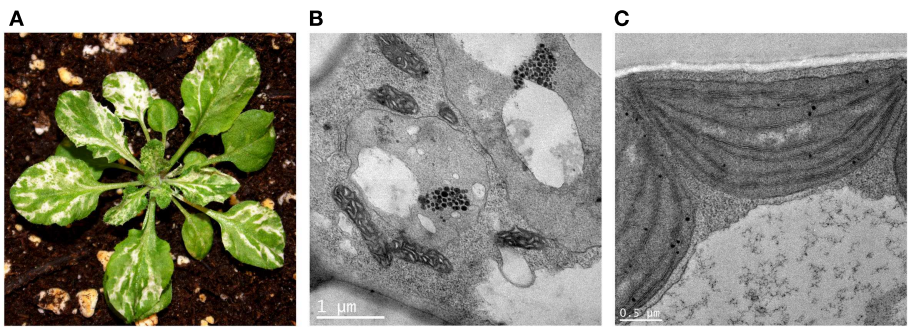

FIGURE 2 | Ultrastructural analysis of *immutans* (A). A representative *immutans* plant grown at 22°C under continuous illumination for 7 days at 5 µmol photons $m^{-2}s^{-1}$ followed by 3 weeks at 100 µmol photons $m^{-2}s^{-1}$. **(B)** Representative plastids from an *im* white sector. The plastids lack organized lamellar structures and contain vacuoles and numerous plastoglobules. **(C)** Representative chloroplast from an *im* green sector.

Wetzel and Rodermel, 1998). This hypothesis was later refined after *IM* was cloned and its function was defined (described in greater detail later).

Chloroplast biogenesis involves the differentiation of a small number of proplastids in the shoot apical meristem into chloroplasts early in leaf primordial development (Mullet, 1988). This process is accompanied by several rounds of plastid division (Robertson et al., 1995; Pyke and López-Juez, 1999). In C3 plants like *Arabidopsis*, leaf expansion along the proximal-distal axis results from cell divisions at the base of the leaf, while cell divisions at the center of the leaf and extending outward cause lateral expansion (Pyke et al., 1991; Van Lijsebettens and Clarke, 1998). Hence, the oldest chloroplasts are present in cells at the tips and margins of the leaf, whereas the youngest ones are found in cells at the base of the leaf and at the midveins. Although plastid number depends on cell size (Possingham and Lawrence, 1983), a typical *Arabidopsis* meristem cell contains a dozen or so proplastids whereas a mesophyll cell contains from 100 to 120 mature chloroplasts (Mullet, 1988; Pyke and López-Juez, 1999). The numbers of plastids in *im* green and white sectors have not yet been reported.

Wetzel et al. (1994) performed light-shift experiments to determine when PTOX activity is first required following germination. These studies showed that cotyledon pigmentation (all-green, all-white, or variegated) is influenced by the intensity of light (low or high) perceived between 0 and 24 h after seed coat breakage; the intensity perceived before or after this interval did not matter. During this period, proplastids differentiate into chloroplasts within the developing cotyledon (Mansfield and Briarty, 1996).

This indicates that PTOX plays a crucial role in early chloroplast biogenesis.

We have recently exploited confocal microscopy to visualize *im* variegation during leaf primordia development. **Figure 3** shows the red autofluorescence from chloroplasts in cells of wild type and *im* leaf primordia; each primordium is located between the two cotyledons. The figure dramatically illustrates that *im* cotyledons and primordia have fewer chloroplasts than wild type, and that *im* variegation develops very early in leaf development.

STUDIES USING GREENING AS A MODEL SYSTEM

Etioplasts in dark-grown angiosperm seedlings have prolamellar bodies (PLB) that contain abundant ternary complexes of protochlorophyllide (PChlide), PChlide reductase (POR), and NADPH (Solymosi and Schoefs, 2010). Upon exposure to light, PChlide is converted to chlorophyllide (Chlide) and the membranes of the PLB disperse to form thylakoids and organized grana (Adam et al., 2011). Most of the protein components of the photosynthetic apparatus are present in etioplasts, and hence de-etiolation (greening) primarily involves the coordinated synthesis and assembly of pigments and pigment-binding proteins to form functional electron transport chains (von Zychlinski et al., 2005; Blomqvist et al., 2008; Kanervo et al., 2008). Photosynthetic competence is attained in *Arabidopsis* ∼5 h after light induction at 22°C and 100 μmol photons $m^{-2}s^{-1}$ (Rosso et al., 2009).

Using *Arabidopsis* de-etiolation as a model system, Hüner's group found that white sector formation in *im* is positively correlated with elevated excitation pressures during early greening, irrespective of whether excitation pressures are modulated by light and/or temperature (Rosso et al., 2009). Excitation pressure is a relative measure of the reduction state of Q_A, the first stable electron acceptor of PSII (Dietz et al., 1985; Hüner et al., 1998), and is measured by chlorophyll *a* fluorometry (Krause and Weis, 1991). The elevated excitation pressures in *im* were accompanied by delayed biogenesis of the thylakoid membrane, as monitored by the abundance of protein markers of chloroplast development (Rosso et al., 2009). Given these considerations, our current working model of *im* variegation assumes that above-threshold excitation pressures predispose developing plastids to photooxidation, whereas *im* plastids with below-threshold excitation pressures have the capacity to develop into normal chloroplasts. This model is based on the twin notions of plastid autonomy and plastid heterogeneity. We surmise that excitation pressures vary from plastid-to-plastid in the developing leaf primordium because of intrinsic differences in plastid biochemistry caused, for example, by gradients in the leaf, sometimes steep, of light and of determinants of light capture, and use (Smith et al., 1997), including cell-specific circadian rhythms that dictate reactive oxygen species (ROS) scavenging capacities (Velez-Ramirez et al., 2011). Such heterogeneity appears to be widespread and has recently been reported in species as diverse as trees (Solymosi et al., 2012). One advantage of this model is that it can account for the phytoene-accumulation phenotype of *im*, as well as for the ultrastructural defects of *im* white plastids. For instance, one of the primary targets of over-reduction might be membrane biogenesis since a prominent effect of ROS formation is lipid peroxidation of polyunsaturated fatty acids (Møller et al., 2007). A lack of plastid galactolipids coupled with a lack of stabilizing carotenoids might impede membrane formation, giving rise to the large vesicles seen in *im* white plastids (**Figure 2**).

In summary, our current model of *im* variegation proposes that the pattern of green/white sectoring is a reflection of the pattern of leaf development in C3 plants, coupled with a heterogeneity in plastid-to-plastid excitation pressure during early cell and plastid development, i.e., the chaotic sectoring in the mature leaf is established in the leaf primordium. Recent support for the threshold hypothesis has come from the *altered APX2 expression 13* (*alx13*) variegation mutant of *Arabidopsis* (Woo et al., 2011).

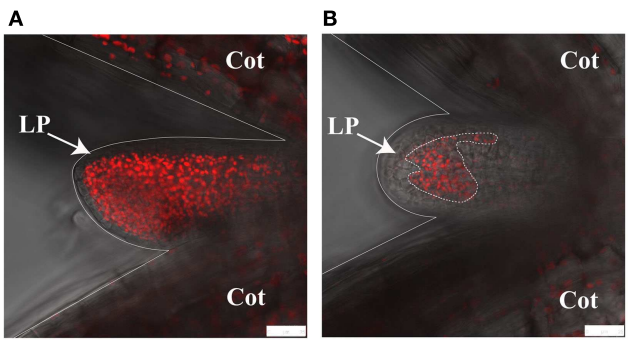

FIGURE 3 | Confocal microscopy of leaf primordia. The images show first leaf primordia (LP) and flanking cotyledons (Cot) from wild type **(A)** and *immutans* **(B)**. Images were captured by taking a confocal image of autofluorescence (red) and overlaying it with a non-confocal transmitted light image (gray). Plants were grown at 22°C under continuous illumination for 3 days at 5 μmol photons $m^{-2}s^{-1}$ followed by 2 days at a light intensity 100 μmol photons $m^{-2}s^{-1}$. White scale bars represent 25 μm.

COMPENSATING FACTORS

Because the green sectors of *im* contain morphologically normal chloroplasts, we have proposed that they arise from plastids that escape the effects of the *im/im* mutation early in chloroplast biogenesis, presumably by the action of compensating factors that affect excitation pressure thresholds, directly or indirectly. Two approaches have been used to gain insight into these factors: (1) molecular characterization of green versus white *im* sectors; and (2) identification and characterization of second-site suppressors of *im* variegation. These approaches will be summarized briefly.

HOW DO THE GREEN AND WHITE SECTORS OF *im* DIFFER?

The green leaf sectors of *im* have higher photosynthetic rates than wild type leaves, monitored either by rates of O_2 evolution or $^{14}CO_2$ uptake (Aluru et al., 2001, 2007). They also have elevated chl *a/b* ratios and enhanced chlorophyll amounts; FACS analyses have revealed these increases are due to elevated chloroplast numbers (per unit volume) rather than to enhanced amounts of chlorophyll per chloroplast (Meehan et al., 1996). Accompanying these changes, the anatomies of the green leaf sectors are reminiscent of leaves adapted to growth in high light conditions, e.g., they are thicker than normal due to enlarged air spaces, mesophyll cells, and epidermal cells (Aluru et al., 2001). On the other hand, the white leaf sectors have a normal thickness, but their palisade cells fail to expand. This perturbation is consistent with an impairment

in retrograde signaling that regulates leaf developmental programming (Rodermel, 2001; López-Juez, 2009; Ruckle and Larkin, 2009). We have made a similar proposal to explain reduced fruit size and disruptions in pericarp tissue morphogenesis in the tomato *ghost* mutant (Barr et al., 2004).

Consistent with elevated rates of photosynthesis, the green leaf sectors have increased Rubisco and sucrose phosphate synthase (SPS) activities, enhanced starch and sucrose pool sizes, and an altered pattern of carbohydrate partitioning that favors sucrose over starch (Aluru et al., 2007). By contrast, the white sectors accumulate low levels of sucrose and have increased acid invertase activities. These observations suggest that sucrose moves along a gradient from the green to the white cells, where it is hydrolyzed and used for growth. It is therefore possible that photosynthetic rates in the green sectors are controlled, in part, by sink demand, and that the elevation of photosynthetic rates in the green sectors is part of a growth strategy to compensate for reductions in total source tissue (Aluru et al., 2007).

Global transcriptomics experiments have revealed that some of the differences between the green and white *im* sectors are likely due to alterations in transcript abundance (Aluru et al., 2009). In particular, genes for photosynthesis and photosynthesis-related processes are repressed in *im* white tissues, while genes for sucrose catabolism, transport, mitochondrial electron transport, and fermentation are induced. This suggests that energy is derived via aerobic and anaerobic metabolism of imported sugar in the *im* white cells, in accord with findings from the biochemical studies, discussed above. The profiling studies also showed that oxidative stress response genes are generally induced in both the green and white *im* tissues, but that some stress genes are significantly more upregulated in the green than white sectors. These genes are targets for investigation as potential compensating factors.

SECOND-SITE SUPPRESSORS OF *im* VARIEGATION

The above studies have been conducted with mature leaves, and although they have provided valuable information about *im*, they are limited in their usefulness regarding information about the primary lesion in *im* because they describe developmental, physiological, and biochemical states that represent long term adaptations to the lack of PTOX in the leaf. They do not provide information about the primary alterations that occur when the mutation first becomes active during chloroplast biogenesis and when compensating mechanisms might first come into play.

Given that all alleles of *im* isolated to date are null (Carol et al., 1999; Wu et al., 1999), an attractive strategy to identify compensating factors is to take advantage of *Arabidopsis* genetics to characterize second-site suppressors of *im* variegation, i.e., second-site mutations that reverse the *im* defect, generating all-green plants. These factors would be anticipated to define elements and/or processes that are able to substitute for or bypass the requirement for PTOX activity during chloroplast biogenesis. One advantage of using a genetic approach to identify these factors is that the early stages of chloroplast development are difficult to access by other approaches (biochemistry, molecular biology). Presumably, compensating factors that are active during early chloroplast biogenesis would permit the desaturation reactions of carotenogenesis to occur in a PTOX-independent manner under high light conditions, e.g., by other oxidases or by PTOX-independent pathways of PQH_2 re-oxidation coupled to PDS (discussed earlier). Shahbazi et al. (2007) provided early support for this idea on the basis of experiments showing that phytoene did not accumulate following exposure of mature green leaf or fruit tissues of the *ghost* mutant to high light: carotenoid synthesis occurred normally in the absence of PTOX. Later in chloroplast development we assume that compensating factors include elements of the PETC downstream of the PQ pool that are capable of oxidizing plastoquinol, thus obviating the need for PTOX.

In this context, it might be noted that early studies showing an O_2 requirement for PDS activity were based on *in vitro* systems from non-photosynthetic chromoplasts (Beyer et al., 1989; Mayer et al., 1990). Interestingly, an "oxidoreductase fraction" was proposed to act as an intermediate between PDS and O_2 in these systems (Beyer et al., 1989). We suggest that this O_2 requirement reflects a need for PTOX activity in the absence of compensating factors, such as photosynthetic electron transport. This would be consistent with the general conclusion that PTOX is required for carotenogenesis during chloroplast biogenesis and stress, but not during steady state photosynthesis (Rosso et al., 2006, 2009).

AOX2 and AOX1a suppressors

To identify *im* suppressors, we have conducted EMS and activation-tagging mutagenesis of *im* and screened for mutant plants with a non-variegated phenotype. Molecular characterization of one suppressor line (designated *ATG791*) has been reported (Fu et al., 2012). This line is all-green and, surprisingly, carries an activation-tagged (overexpressed) version of mitochondrial AOX2. *Arabidopsis* contains five members of the AOX gene family, all of which are thought to be exclusively mitochondrial in location (AOX1a-d and AOX2); AOX2 is a low abundance, seed-specific member of this family (Saisho et al., 1997, 2001; Clifton et al., 2006; Winter et al., 2007; Polidoros et al., 2009).

We found that AOX2 is targeted to chloroplast thylakoids of *ATG791*, where its activity replaces that of PTOX in the desaturation steps of carotenogenesis, i.e., it rescues the phytoene-accumulation defect of *im*, restoring carotenoid biosynthesis to normal. This restoration is accompanied by a normalization of excitation pressures, suggesting that the two processes are linked (Fu et al., 2012). It is therefore likely that elevated carotenoids in the suppressor lines are directly responsible for rescue of the variegation phenotype, and hence for recovery of the capacity to undergo normal chloroplast biogenesis. Results similar to *ATG791* were obtained when AOX2 was overexpressed using the CaMV 35S promoter, or when *AOX1a* – the most highly and ubiquitously expressed member of the *Arabidopsis* AOX gene family, was re-engineered to target the plastid; overexpressed AOX1a is found exclusively in mitochondria (Clifton et al., 2006; Winter et al., 2007; Polidoros et al., 2009). In both cases, the *im*-induced defects in phytoene-accumulation and chloroplast biogenesis were reversed.

Further experiments with the AOX2 and AOX1a overexpression lines showed that chloroplast-localized AOX2, but not AOX1a, formed monomers and dimers in the thylakoid membrane, reminiscent of AOX regulation in mitochondrial inner membranes. In addition, both proteins accumulated as higher molecular weight complexes in thylakoids, though these complexes differed in size

and number between the two lines. Interestingly, photosynthetic activities, as monitored by chlorophyll fluorescence, were not generally perturbed in the overexpression lines, nor was growth altered. This suggests that the presence of AOX1a and AOX2 complexes in thylakoids does not significantly perturb steady state photosynthesis, at least under non-stress conditions. Our operating assumption is that the suppressor lines define novel electron transport paths in the chloroplast.

AOX2 has previously been localized to mitochondria (Saisho et al., 2001), and because it was imported into chloroplasts using its own transit peptide in the *AOX2* overexpression lines, as well as in transient expression assays, our current working hypothesis is that AOX2 is a dual-targeted protein that functions in plastids to supplement PTOX activity during the early events of chloroplast biogenesis. Although the idea that AOX2 is normally an *im*-compensating activity needs further confirmation, the ability of AOX1a to substitute for PTOX in the correct physiological and developmental contexts is a dramatic example of the capacity of a mitochondrial protein to replace the function of a chloroplast protein, and illustrates the plasticity of the photosynthetic apparatus. This is all the more remarkable given the striking differences in regulation, substrate-specificity (ubiquinol in mitochondria versus plastoquinol in plastids) and phylogenetic distance between AOX and PTOX (McDonald et al., 2011; Fu et al., 2012). It will therefore be of great interest to explore further how chloroplast AOX1a and AOX2 mediate redox reactions during photosynthesis.

pgr5 and crr2–2 suppressors

Shikanai's group has long been studying mechanisms of PSI cyclic electron transport, a process that contributes to ΔpH formation across the thylakoid, but not to NAD(P)H accumulation, thus providing a way of manipulating ATP/NAD(P)H ratios (Shikanai, 2007). Okegawa et al. (2010) reported that two mutants perturbed in this process – *crr2-2* (*chlororespiratory reduction*) (Hashimoto et al., 2003) and *pgr5* (*proton gradient regulation 5*) (Munekage et al., 2002) are able to suppress *im* variegation. The *pgr5* mutant is defective in electron transport, has a reduced ΔpH, an over-reduced stroma (a decreased ATP/NADPH), an oxidized $P700^+$, and a loss of qE (Munekage et al., 2002; DalCorso et al., 2008; Okegawa et al., 2008). The *crr2-2* mutant, on the other hand, is defective in NDH activity due to aberrant expression of the plastid *ndhB* gene (Hashimoto et al., 2003); it has photosynthetic characteristics similar to *pgr5* (Okegawa et al., 2010). Neither of these mutants has a chloroplast development phenotype (Munekage et al., 2004).

Okegawa et al. (2010) assumed that *crr2-2* and *pgr5* define separate pathways of PSI cyclic electron transport, and given this assumption, the goal of their experiments was to examine genetic interactions between these pathways and PTOX, all of which share the PQ pool. The observation that loss of either one of these pathways (in *crr2-2* or *pgr5*) or both (in *crr2-2/pgr5*) is able to suppress *im* variegation can be explained by reduced excitation pressures during early chloroplast development, due to a decreased flux of electrons into the PQ pool. The converse suppression by *im* of the photosynthetic defects in *crr2-2* and *pgr5* is more problematic to explain, but might be due to altered ATP/NADPH ratios and activation of the water–water cycle in an *im* background (Okegawa et al., 2010).

One factor complicating an understanding of the mechanism of *im* suppression in these studies is that considerable controversy surrounds the function of PGR5 (reviewed in Kramer and Evans, 2011). The only agreement seems to be that PGR5 plays a role in fluctuating light conditions (Tikkanen et al., 2010). Although further studies will be needed to define the interactions between PTOX, PGR5, and NDH, it is clear from the present data that interactions occur between these three components very early in chloroplast development. All three are also present in etioplasts (Aluru et al., 2001; Long et al., 2008; Peng et al., 2008), perhaps to help poise the PQ pool for photosynthesis.

In summary, suppressor analysis holds great promise as a tool to understand the function of PTOX and mechanisms of compensation that occur in its absence. The data in this paper high light the significance of *im* suppressor analysis for understanding pathways and interactions that mediate early chloroplast development, and they include the identification of novel proteins (AOX2) and pathways (PSI cyclic electron transport).

ACKNOWLEDGMENTS

We extend our thanks to Margaret Carter of the Iowa State Image Analysis Facility. Additionally, we thank Dr. Harry Horner and Tracey Pepper of the Iowa State Microscopy and NanoImaging Facility. This work was supported by funding to Steve Rodermel from the Chemical Sciences, Geosciences, and Biosciences Division, U.S. Department of Energy (DE-FG02-94ER20147).

REFERENCES

Adam, Z., Charuvi, D., Tsabari, O., Knopf, R. R., and Reich, Z. (2011). Biogenesis of thylakoid networks in angiosperms: knowns and unknowns. *Plant Mol. Biol.* 76, 221–234.

Al-Babili, S., Lintig, J. V., Haubruck, H., and Beyer, P. (1996). A novel, soluble form of phytoene desaturase from *Narcissus pseudonarcissus* chromoplasts is Hsp70-complexed and competent for flavination, membrane association and enzymatic activation. *Plant J.* 9, 601–612.

Allahverdiyeva, Y., Mamedov, F., Mäenpää, P., Vass, I., and Aro, E. M. (2005). Modulation of photosynthetic electron transport in the absence of terminal electron acceptors: characterization of the *rbcL* deletion mutant of tobacco. *Biochim. Biophys. Acta* 1709, 69–83.

Aluru, M. R., Bae, H., Wu, D., and Rodermel, S. R. (2001). The *Arabidopsis immutans* mutation affects plastid differentiation and the morphogenesis of white and green sectors in variegated plants. *Plant Physiol.* 127, 67–77.

Aluru, M. R., Stessman, D., Spalding, M. H., and Rodermel, S. R. (2007). Alterations in photosynthesis in *Arabidopsis* lacking IMMUTANS, a chloroplast terminal oxidase. *Photosyn. Res.* 91, 11–23.

Aluru, M. R., Zola, J., Foudree, A., and Rodermel, S. R. (2009). Chloroplast photooxidation-induced transcriptome reprogramming in *Arabidopsis immutans* white leaf sectors. *Plant Physiol.* 150, 904–923.

Aro, E. M., Virgin, I., and Andersson, B. (1993). Photoinhibition of photosystem II: inactivation, protein damage and turnover. *Biochim. Biophys. Acta* 1143, 113–134.

Baena-González, E., Allahverdiyeva, Y., Svab, Z., Maliga, P., Josse, E. M., Kuntz, M., et al. (2003). Deletion of the tobacco plastid *psbA* gene triggers an upregulation of the thylakoid-associated NAD(P)H dehydrogenase complex and the plastid terminal oxidase (PTOX). *Plant J.* 35, 704–716.

Bailey, S., Melis, A., Mackey, K. R. M., Cardol, P., Finazzi, G., van Dijken, G., et al. (2008). Alternative photosynthetic electron flow to oxygen in marine *Synechococcus*. *Biochim. Biophys. Acta* 1777, 269–276.

Barr, J., White, W. S., Chen, L., Bae, H., and Rodermel, S. (2004). The GHOST terminal oxidase regulates developmental programming in tomato fruit. *Plant Cell Environ.* 27, 840–852.

Berthold, D. A., Andersson, M. E., and Nordlund, P. (2000). New insight into the structure and function of the alternative oxidase. *Biochim. Biophys. Acta* 1460, 241–254.

Beyer, P., Mayer, M., and Kleinig, H. (1989). Molecular oxygen and the state of geometric isomerism of intermediates are essential in the carotene desaturation and cyclization reactions in daffodil chromoplasts. *Eur. J. Biochem.* 184, 141–150.

Blomqvist, L. A., Ryberg, M., and Sundqvist, C. (2008). Proteomic analysis of highly purified prolamellar bodies reveals their significance in chloroplast development. *Photosyn. Res.* 96, 37–50.

Buchel, C., and Garab, G. (1995). Evidence for the operation of a cyanide-sensitive oxidase in chlororespiration in the thylakoids of the chlorophyll *c*-containing alga *Pleurochloris meiringensis* (Xanthophyceae). *Planta* 197, 69–75.

Carol, P., Stevenson, D., Bisanz, C., Breitenbach, J., Sandmann, G., Mache, R., et al. (1999). Mutations in the *Arabidopsis* gene IMMUTANS cause a variegated phenotype by inactivating a chloroplast terminal oxidase associated with phytoene desaturation. *Plant Cell* 11, 57–68.

Casano, L. M., Zapata, J. M., Martin, M., and Sabater, B. (2000). Chlororespiration and poising of cyclic electron transport. *J. Biol. Chem.* 275, 942–948.

Clifton, R., Millar, A. H., and Whelan, J. (2006). Alternative oxidases in *Arabidopsis*: a comparative analysis of differential expression in the gene family provides new insights into function of nonphosphorylating bypasses. *Biochim. Biophys. Acta* 1757, 730–741.

DalCorso, G., Pesaresi, P., Masiero, S., Aseeva, E., Schunemann, D., Finazzi, G., et al. (2008). A complex containing PGRL1 and PGR5 is involved in the switch between linear and cyclic electron flow in *Arabidopsis*. *Cell* 132, 273–285.

DellaPenna, D., and Pogson, B. J. (2006). Vitamin synthesis in plants: tocopherols and carotenoids. *Annu. Rev. Plant Biol.* 57, 711–738.

Díaz, M., De Haro, V., Munoz, R., and Quiles, M. J. (2007). Chlororespiration is involved in the adaptation of *Brassica* plants to heat and high light intensity. *Plant Cell Environ.* 30, 1578–1585.

Dietz, K. J., Schreiber, U., and Heber, U. (1985). The relationship between the redox state of Q_A and photosynthesis in leaves at various carbon-dioxide, oxygen and light regimes. *Planta* 166, 219–226.

Formighieri, C., Ceol, M., Bonente, G., Rochaix, J. D., and Bassi, R. (2012). Retrograde signaling and photoprotection in a gun4 mutant of Chlamydomonas reinhardtii. *Mol. Plant.* doi:10.1093/mp/sss051

Foyer, C. H., Neukermans, J., Queval, G., Noctor, G., and Harbinson, J. (2012). Photosynthetic control of electron transport and the regulation of gene expression. *J. Exp. Bot.* 63, 1637–1661.

Fu, A., Liu, H., Yu, F., Kambakam, S., Luan, S., and Rodermel, S. (2012). Alternative oxidases (AOX1a and AOX2) can functionally substitute for plastid terminal oxidase in *Arabidopsis* chloroplasts. *Plant Cell* 24, 1579–1595.

Giraud, E., Ho, L. H., Clifton, R., Carroll, A., Estavillo, G., Tan, Y. F., et al. (2008). The absence of ALTERNATIVE OXIDASE1a in *Arabidopsis* results in acute sensitivity to combined light and drought stress. *Plant Physiol.* 147, 595–610.

Gray, G. R., Chauvin, L. P., Sarhan, F., and Huner, N. P. A. (1997). Cold acclimation and freezing tolerance. A complex interaction of light and temperature. *Plant Physiol.* 114, 467–474.

Hashimoto, M., Endo, T., Peltier, G., Tasaka, M., and Shikanai, T. (2003). A nucleus-encoded factor, CRR2, is essential for the expression of chloroplast *ndhB* in *Arabidopsis*. *Plant J.* 36, 541–549.

Houille-Vernes, L., Rappaport, F., Wollman, F.-A., Alric, J., and Johnson, X. (2011). Plastid terminal oxidase 2 (PTOX2) is the major oxidase involved in chlororespiration in *Chlamydomonas*. *Proc. Natl. Acad. Sci. U.S.A.* 108, 20820–20825.

Hugueney, P., Römer, S., Kuntz, M., and Camara, B. (1992). Characterization and molecular cloning of a flavoprotein catalyzing the synthesis of phytofluene, and zeta-carotene in *Capsicum* chromoplasts. *Eur. J. Biochem.* 209, 399–407.

Hüner, N. P. A., Öquist, G., and Sarhan, F. (1998). Energy balance and acclimation to light and cold. *Trends Plant Sci.* 3, 224–230.

Ivanov, A. G., Rosso, D., Savitch, L. V., Stachula, P., Rosembert, M., Oquist, G., et al. (2012). Implications of alternative electron sinks in increased resistance of PSII and PSI photochemistry to high light stress in cold-acclimated *Arabidopsis thaliana*. *Photosyn. Res.* 113, 191–206.

Joët, T., Genty, B., Josse, E. M., Kuntz, M., Cournac, L., and Peltier, G. (2002). Involvement of a plastid terminal oxidase in plastoquinone oxidation as evidenced by expression of the *Arabidopsis thaliana* enzyme in tobacco. *J. Biol. Chem.* 277, 31623–31630.

Josse, E. M., Alcaraz, J.-P., Labouré, A. M., and Kuntz, M. (2003). In vitro characterization of a plastid terminal oxidase (PTOX). *Eur. J. Biochem.* 270, 3787–3794.

Josse, E. M., Simkin, A. J., Gaffé, J., Labouré, A. M., Kuntz, M., and Carol, P. (2000). A plastid terminal oxidase associated with carotenoid desaturation during chromoplast differentiation. *Plant Physiol.* 123, 1427–1436.

Joyard, J., Ferro, M., Masselon, C., Seigneurin-Berny, D., Salvi, D., Garin, J., et al. (2009). Chloroplast proteomics and the compartmentation of plastidial isoprenoid biosynthetic pathways. *Mol. Plant* 2, 1154–1180.

Kanervo, E., Singh, M., Suorsa, M., Paakkarinen, V., Aro, E., Battchikova, N., et al. (2008). Expression of protein complexes and individual proteins upon transition of etioplasts to chloroplasts in pea (*Pisum sativum*). *Plant Cell Physiol.* 49, 396–410.

Khorobrykh, S. A., and Ivanov, B. N. (2002). Oxygen reduction in a plastoquinone pool of isolated pea thylakoids. *Photosyn. Res.* 71, 209–219.

Kramer, D. M., and Evans, J. R. (2011). The importance of energy balance in improving photosynthetic productivity. *Plant Physiol.* 155, 70–78.

Krause, G. H., and Weis, E. (1991). Chlorophyll fluorescence and photosynthesis: the basics. *Annu. Rev. Plant Physiol. Plant Mol. Biol.* 42, 313–349.

Lajko, F., Kadioglu, A., Borbely, G., and Garab, G. (1997). Competition between the photosynthetic and the (chloro)respiratory electron transport chains in cyanobacteria, green algae and higher plants. Effect of heat stress. *Photosynthetica* 33, 217–226.

Laureau, C., Bligny, R., and Streb, P. (2011). The significance of glutathione for photoprotection at contrasting temperatures in the alpine plant species *Soldanella alpina* and *Ranunculus glacialis*. *Physiol. Plant* 143, 246–260.

Lennon, A. M., Prommeenate, P., and Nixon, P. J. (2003). Location, expression and orientation of the putative chlororespiratory enzymes, Ndh and IMMUTANS, in higher-plant plastids. *Planta* 218, 254–260.

Liu, X., Yu, F., and Rodermel, S. (2010). *Arabidopsis* chloroplast FtsH, *var2* and suppressors of *var2* leaf variegation: a review. *J. Integr. Plant Biol.* 52, 750–761.

Long, T. A., Okegawa, Y., Shikanai, T., Schmidt, G. W., and Covert, S. F. (2008). Conserved role of proton gradient regulation 5 in the regulation of PSI cyclic electron transport. *Planta* 228, 907–918.

López-Juez, E. (2009). Steering the solar panel: plastids influence development. *New Phytol.* 182, 287–290.

Mansfield, S. G., and Briarty, L. G. (1996). The dynamics of seedling and cotyledon cell development in *Arabidopsis thaliana* during reserve mobilization. *Int. J. Plant Sci.* 157, 280–295.

Mayer, M. P., Beyer, P., and Kleinig, H. (1990). Quinone compounds are able to replace molecular oxygen as terminal electron acceptor in phytoene desaturation in chromoplasts of *Narcissus pseudonarcissus* L. *Eur. J. Biochem.* 191, 359–363.

Mayer, M. P., Nievelstein, V., and Beyer, P. (1992). Purification and characterization of a NADPH dependent oxidoreductase from chromoplasts of *Narcissus pseudonarcissus*: a redox-mediator possibly involved in carotene desaturation. *Plant Physiol. Biochem.* 30, 389–398.

Mayfield, S. P., and Taylor, W. C. (2005). Carotenoid-deficient maize seedlings fail to accumulate light-harvesting chlorophyll *a/b* binding protein (LHCP) mRNA. *Eur. J. Biochem.* 144, 79–84.

McDonald, A. E. (2008). Alternative oxidase: an inter-kingdom perspective on the function and regulation of this broadly distributed "cyanide-resistant" terminal oxidase. *Funct. Plant Biol.* 35, 535–552.

McDonald, A. E., Ivanov, A. G., Bode, R., Maxwell, D. P., Rodermel, S. R., and Hüner, N. P. A. (2011). Flexibility in photosynthetic electron transport: the physiological role of plastoquinol terminal oxidase (PTOX). *Biochim. Biophys. Acta* 1807, 954–967.

Meehan, L., Harkins, K., Chory, J., and Rodermel, S. (1996). Lhcb transcription is coordinated with cell size and chlorophyll accumulation. Studies on fluorescence-activated, cell-sorter-purified single cells from wild-type and *immutans Arabidopsis thaliana*. *Plant Physiol.* 112, 953–963.

Møller, I. M., Jensen, P. E., and Hansson, A. (2007). Oxidative modifications

to cellular components in plants. *Annu. Rev. Plant Biol.* 58, 459–481.

Moseley, J. L., Chang, C. W., and Grossman, A. R. (2006). Genome-based approaches to understanding phosphorus deprivation responses and PSR1 control in *Chlamydomonas reinhardtii*. *Eukaryot. Cell* 5, 26–44.

Mullet, J. E. (1988). Chloroplast development and gene expression. *Annu. Rev. Plant Physiol. Plant Mol. Biol.* 39, 475–502.

Munekage, Y., Hashimoto, M., Miyake, C., Tomizawa, K., Endo, T., Tasaka, M., et al. (2004). Cyclic electron flow around photosystem I is essential for photosynthesis. *Nature* 429, 579–582.

Munekage, Y., Hojo, M., Meurer, J., Endo, T., Tasaka, M., and Shikanai, T. (2002). PGR5 is involved in cyclic electron flow around photosystem I and is essential for photoprotection in *Arabidopsis*. *Cell* 110, 361–371.

Ngaki, M. N., Louie, G. V., Philippe, R. N., Manning, G., Pojer, F., Bowman, M. E., et al. (2012). Evolution of the chalcone isomerase fold from fatty acid-binding to stereospecific enzyme. *Nature* 485, 53–533.

Nievelstein, V., Vandekerckhove, J., Tadros, M. H., von Lintig, J., Nitschke, W., and Beyer, P. (1995). Carotene desaturation is linked to a respiratory redox pathway in *Narcissus pseudonarcissus* chromoplast membranes: involvement of a 23-kDa oxygen-evolving-complex-like protein. *Eur. J. Biochem.* 233, 864–872.

Niyogi, K. K. (2000). Safety valves for photosynthesis. *Curr. Opin. Plant Biol.* 3, 455–460.

Norris, S. R., Barrette, T. R., and DellaPenna, D. (1995). Genetic dissection of carotenoid synthesis in *Arabidopsis* defines plastoquinone as an essential component of phytoene desaturation. *Plant Cell* 7, 2139–2149.

Oelmüller, R. (1989). Photooxidative destruction of chloroplasts and its effect on nuclear gene expression and extraplastidic enzyme levels. *Photochem. Photobiol.* 49, 229–239.

Okegawa, Y., Kagawa, Y., Kobayashi, Y., and Shikanai, T. (2008). Characterization of factors affecting the activity of photosystem I cyclic electron transport in chloroplasts. *Plant Cell Physiol.* 49, 825–834.

Okegawa, Y., Kobayashi, Y., and Shikanai, T. (2010). Physiological links among alternative electron transport pathways that reduce and oxidize plastoquinone in *Arabidopsis*. *Plant J.* 63, 458–468.

Ort, D. R., and Baker, N. R. (2002). A photoprotective role for O_2 as an alternative electron sink in photosynthesis? *Curr. Opin. Plant Biol.* 5, 193–198.

Peltier, G., and Cournac, L. (2002). Chlororespiration. *Annu. Rev. Plant Biol.* 53, 523–550.

Peng, L., Fukao, Y., Fujiwara, M., and Shikanai, T. (2012). Multistep assembly of chloroplast NADH dehydrogenase-like subcomplex A requires several nucleus-encoded proteins, including CRR41 and CRR42, in *Arabidopsis*. *Plant Cell* 24, 202–214.

Peng, L., Shimizu, H., and Shikanai, T. (2008). The chloroplast NAD(P)H dehydrogenase complex interacts with photosystem I in *Arabidopsis*. *J. Biol. Chem.* 283, 34873–34879.

Polidoros, A. N., Mylona, P. V., and Arnholdt-Schmitt, B. (2009). AOX gene structure, transcript variation and expression in plants. *Physiol. Plant* 137, 342–354.

Possingham, J. V., and Lawrence, M. E. (1983). Controls to plastid division. *Int. Rev. Cytol.* 84, 1–56.

Pyke, K., and López-Juez, E. (1999). Cellular differentiation and leaf morphogenesis in *Arabidopsis*. *CRC Crit. Rev. Plant Sci.* 18, 527–546.

Pyke, K. A., Marrison, J. L., and Leech, R. M. (1991). Temporal and spatial development of the cells of the expanding first leaf of *Arabidopsis thaliana* (L.) Heynh. *J. Exp. Bot.* 42, 1407–1416.

Quiles, M. J. (2006). Stimulation of chlororespiration by heat and high light intensity in oat plants. *Plant Cell Environ.* 29, 1463–1470.

Rédei, G. P. (1963). Somatic instability caused by a cysteine-sensitive gene in *Arabidopsis*. *Science* 139, 767–769.

Rédei, G. P. (1967). Biochemical aspects of a genetically determined variegation in *Arabidopsis*. *Genetics* 56, 431–443.

Rizhsky, L., Hallak-Herr, E., Van Breusegem, F., Rachmilevitch, S., Barr, J. E., Rodermel, S., et al. (2002). Double antisense plants lacking ascorbate peroxidase and catalase are less sensitive to oxidative stress than single antisense plants lacking ascorbate peroxidase or catalase. *Plant J.* 32, 329–342.

Röbbelen, G. (1968). Genbedingte Rotlicht-Empfindlichkeit der Chloroplastendifferenzierung bei *Arabidopsis*. *Planta* 80, 237–254.

Robertson, E. J., Pyke, K. A., and Leech, R. M. (1995). *arc6*, An extreme chloroplast division mutant of *Arabidopsis*, also alters proplastid proliferation and morphology in shoot and root apices. *J. Cell Sci.* 108, 2937–2944.

Rochaix, J. D. (2011). Regulation of photosynthetic electron transport. *Biochim. Biophys. Acta* 1807, 878–886.

Rodermel, S. R. (2001). Pathways of plastid-to-nucleus signaling. *Trends Plant Sci.* 6, 471–478.

Rodrigo, M. J., Marcos, J. F., and Zacarias, L. (2004). Biochemical and molecular analysis of carotenoid biosynthesis in flavedo of orange (*Citrus sinensis* L.) during fruit development and maturation. *J. Agric. Food Chem.* 52, 6724–6731.

Rodríguez-Villalón, A., Gas, E., and Rodríguez-Concepción, M. (2009). Phytoene synthase activity controls the biosynthesis of carotenoids and the supply of their metabolic precursors in dark-grown *Arabidopsis* seedlings. *Plant J.* 60, 424–435.

Rosso, D., Bode, R., Li, W., Krol, M., Saccon, D., Wang, S., et al. (2009). Photosynthetic redox imbalance governs leaf sectoring in the *Arabidopsis thaliana* variegation mutants *immutans, spotty, var1* and *var2*. *Plant Cell* 21, 3473–3492.

Rosso, D., Ivanov, A. G., Fu, A., Geisler-Lee, J., Hendrickson, L., Geisler, M., et al. (2006). IMMUTANS does not act as a stress-induced safety valve in the protection of the photosynthetic apparatus of *Arabidopsis* during steady-state photosynthesis. *Plant Physiol.* 142, 574–585.

Ruckle, M. E., and Larkin, R. M. (2009). Plastid signals that affect photomorphogenesis in *Arabidopsis thaliana* are dependent on GENOMES UNCOUPLED 1 and cryptochrome 1. *New Phytol.* 182, 367–379.

Rumeau, D., Peltier, G., and Cournac, L. (2007). Chlororespiration and cyclic electron flow around PSI during photosynthesis and plant stress response. *Plant Cell Environ.* 30, 1041–1051.

Saisho, D., Nakazono, M., Lee, K. H., Tsutsumi, N., Akita, S., and Hirai, A. (2001). The gene for alternative oxidase-2 (AOX2) from *Arabidopsis thaliana* consists of five exons unlike other AOX genes and is transcribed at an early stage during germination. *Genes Genet. Syst.* 76, 89–97.

Saisho, D., Nambara, E., Naito, S., Tsutsumi, N., Hirai, A., and Nakazono, M. (1997). Characterization of the gene family for alternative oxidase from *Arabidopsis thaliana*. *Plant Mol. Biol.* 35, 585–596.

Savitch, L. V., Ivanov, A. G., Krol, M. K., Sprott, D. P., Oquist, G., and Huner, N. P. A. (2010). Regulation of energy partitioning and alternative electron transport pathways during cold acclimation of Lodgepole pine is oxygen dependent. *Plant Cell Physiol.* 51, 1555–1570.

Savitch, L. V., Massacci, A., Gray, G. R., and Huner, N. P. A. (2000). Acclimation to low temperature or high light mitigates sensitivity to photoinhibition: roles of the Calvin cycle and the Mehler reaction. *Aust. J. Plant Physiol.* 27, 253–264.

Schulz, A., Ort, O., Beyer, P., and Kleinig, H. (1993). SC-0051, a 2-benzoylcyclohexane-1,3-dione bleaching herbicide, is a potent inhibitor of the enzyme p-hydroxyphenylpyruvate dioxygenase. *FEBS Lett.* 318, 162–166.

Shahbazi, M., Gilbert, M., Labouré, A. M., and Kuntz, M. (2007). Dual role of the plastid terminal oxidase in tomato. *Plant Physiol.* 145, 691–702.

Shikanai, T. (2007). Cyclic electron transport around photosystem I: genetic approaches. *Annu. Rev. Plant Biol.* 58, 199–217.

Smith, W. K., Vogelmann, T. C., DeLucia, E. H., Bell, D. T., and Shepherd, K. A. (1997). Leaf form and photosynthesis: do leaf structure and orientation interact to regulate internal light and carbon dioxide? *Bioscience* 47, 785–793.

Solymosi, K., Morandi, D., Bóka, K., Böddi, B., and Schoefs, B. (2012). High biological variability of plastids, photosynthetic pigments and pigment forms of leaf primordia in buds. *Planta* 235, 1035–1049.

Solymosi, K., and Schoefs, B. (2010). Etioplast and etio-chloroplast formation under natural conditions: the dark side of chlorophyll biosynthesis in angiosperms. *Photosyn. Res.* 105, 143–166.

Stepien, P., and Johnson, G. N. (2009). Contrasting responses of photosynthesis to salt stress in the glycophyte *Arabidopsis* and the halophyte *Thellungiella*: role of the plastid terminal oxidase as an alternative electron sink. *Plant Physiol.* 149, 1154–1165.

Streb, P., Josse, E. M., Gallouët, E., Baptist, F., Kuntz, M., and Cornic, G. (2005). Evidence for alternative electron sinks to photosynthetic carbon assimilation in the high mountain plant species *Ranunculus glacialis*. *Plant Cell Environ.* 28, 1123–1135.

Tikkanen, M., Grieco, M., Kangasjarvi, S., and Aro, E. M. (2010). Thylakoid protein phosphorylation in higher plant chloroplasts optimizes electron transfer under fluctuating light. *Plant Physiol.* 152, 723–735.

Tilney-Bassett, R. A. E. (1975). "Genetics of variegated plants," in *Genetics and Biogenesis of Mitochondria and Chloroplasts*, eds C. W. Birky, P. S. Perlman, and T. J. Byers (Columbus, OH: Ohio State University Press), 268–308.

Trouillard, M., Shahbazi, M., Moyet, L., Rappaport, F., Joliot, P., Kuntz, M., et al. (2012). Kinetic properties and physiological role of the plastoquinone terminal oxidase (PTOX) in a vascular plant. *Biochim. Biophys. Acta* 1817, 2140–2148.

Van Lijsebettens, M., and Clarke, J. (1998). Leaf development in *Arabidopsis*. *Plant Physiol. Biochem.* 36, 47–60.

Velez-Ramirez, A. I., van Ieperen, W., Vreugdenhil, D., and Millenaar, F. F. (2011). Plants under continuous light. *Trends Plant Sci.* 16, 310–318.

von Zychlinski, A., Kleffmann, T., Krishnamurthy, N., Sjolander, K., Baginsky, S., and Gruissem, W. (2005). Proteome analysis of the rice etioplast. *Mol. Cell. Proteomics* 4, 1072–1084.

Wang, J., Sommerfeld, M., and Hu, Q. (2009). Occurrence and environmental stress responses of two plastid terminal oxidases in *Haematococcus pluvialis* (Chlorophyceae). *Planta* 230, 191–203.

Wetzel, C. M., Jiang, C. Z., Meehan, L. J., Voytas, D. F., and Rodermel, S. R. (1994). Nuclear-organelle interactions: the *immutans* variegation mutant of *Arabidopsis* is plastid autonomous and impaired in carotenoid biosynthesis. *Plant J.* 6, 161–175.

Wetzel, C. M., and Rodermel, S. (1998). Regulation of phytoene desaturase expression is independent of leaf pigment content in *Arabidopsis thaliana*. *Plant Mol. Biol.* 37, 1045–1053.

Winter, D., Vinegar, B., Nahal, H., Ammar, R., Wilson, G. V., and Provart, N. J. (2007). An "electronic fluorescent pictograph" browser for exploring and analyzing large-scale biological data sets. *PLoS ONE* 8, e718. doi:10.1371/journal.pone.0000718

Woo, N. S., Gordon, M. J., Graham, S. R., Rossel, J. B., Badger, M. R., and Pogson, B. J. (2011). A mutation in the purine biosynthetic enzyme ATASE2 impacts high light signalling and acclimation responses in green and chlorotic sectors of *Arabidopsis* leaves. *Funct. Plant Biol.* 38, 401–419.

Wu, D., Wright, D. A., Wetzel, C., Voytas, D. F., and Rodermel, S. (1999). The IMMUTANS variegation locus of *Arabidopsis* defines a mitochondrial alternative oxidase homolog that functions during early chloroplast biogenesis. *Plant Cell* 11, 43–55.

Yu, F., Fu, A., Aluru, M., Park, S., Xu, Y., Liu, H., et al. (2007). Variegation mutants and mechanisms of chloroplast biogenesis. *Plant Cell Environ.* 30, 350–365.

Conflict of Interest Statement: The authors declare that the research was conducted in the absence of any commercial or financial relationships that could be construed as a potential conflict of interest.

Received: 21 September 2012; accepted: 06 November 2012; published online: 27 November 2012.

Citation: Foudree A, Putarjunan A, Kambakam S, Nolan T, Fussell J, Pogorelko G and Rodermel S (2012) The mechanism of variegation in immutans provides insight into chloroplast biogenesis. Front. Plant Sci. ***3****:260. doi: 10.3389/fpls.2012.00260*

This article was submitted to Frontiers in Plant Physiology, a specialty of Frontiers in Plant Science.

Copyright © 2012 Foudree, Putarjunan, Kambakam, Nolan, Fussell, Pogorelko and Rodermel. This is an open-access article distributed under the terms of the Creative Commons Attribution License, which permits use, distribution and reproduction in other forums, provided the original authors and source are credited and subject to any copyright notices concerning any third-party graphics etc.

frontiers in
PLANT SCIENCE

PERSPECTIVE ARTICLE
published: 12 November 2012
doi: 10.3389/fpls.2012.00253

Plant mitochondrial retrograde signaling: post-translational modifications enter the stage

Markus Hartl and Iris Finkemeier*

Department Biology I, Ludwig Maximilians University Munich, Planegg-Martinsried, Germany

Edited by:
Dario Leister, Ludwig Maximilians University Munich, Germany

Reviewed by:
Steven Huber, United States Department of Agriculture - Agricultural Research Service, USA
Ian Max Møller, Aarhus University, Denmark

***Correspondence:**
Iris Finkemeier, Department Biology I, Ludwig Maximilians University Munich, Grosshaderner Strasse 2-4, 82152 Planegg-Martinsried, Germany.
e-mail: i.finkemeier@lmu.de

Beside their central function in respiration plant mitochondria play important roles in diverse processes such as redox homeostasis, provision of precursor molecules for essential biosynthetic pathways, and programmed cell death. These different functions require the organelle to communicate with the rest of the cell by perceiving, transducing, and emitting signals. As the vast majority of mitochondrial proteins are encoded in the nuclear genome, changes in mitochondrial status must be fed back to the nucleus to coordinate gene expression accordingly, a process termed retrograde signaling. However, the nature of these signaling pathways in plants and their underlying signaling molecules – or indirect metabolite or redox signals – are not completely resolved. We explore the potential of different post-translational modifications (PTMs) to contribute to mitochondrial retrograde signaling. Remarkably, the substrates used for modifying proteins in many major PTMs are either central metabolites or redox-active compounds, as for example ATP, acetyl-CoA, NAD^+, and glutathione. This suggests that the metabolic status of organelles and of the cell in general could be indirectly gaged by the enzymes catalyzing the various PTMs. We examine the evidence supporting this hypothesis with regard to three major PTMs, namely phosphorylation, lysine acetylation, and glutathionylation and assess their potential to regulate not only organellar processes by modifying metabolic enzymes but also to influence nuclear gene expression.

Keywords: plants, mitochondria, retrograde signaling, post-translational modifications, metabolites

INTRODUCTION

Plant mitochondria are central hubs in the conversion of energy and redox homeostasis and are connected to metabolic pathways from different subcellular compartments. Hence, mitochondria are ideally placed to act as sensors of the energetic and metabolic status of the plant cell (Sweetlove et al., 2007; Millar et al., 2011). Perturbations of the cellular energy status can lead to a reconfiguration of mitochondrial activities which in turn have profound effects on other cellular compartments, including major changes in nuclear gene expression (NGE) and photosynthetic activity (Rhoads, 2011; Schwarzländer et al., 2012). Changes in NGE which are triggered by signals derived from metabolic perturbations in organelles are termed retrograde responses (RRs) and are considered important means of tuning anterograde regulation to retain metabolic plasticity (Rhoads, 2011). However, so far the well understood RRs were uncovered mainly in yeast and animals, whereas in plants conclusive evidence for the exact nature of particular retrograde signals and their transduction is largely lacking. This holds especially true for mitochondrial RR (MRR) for which so far only putative signaling candidates and one downstream transcription factor (ABI4) could be identified (Gray et al., 2004; Giraud et al., 2009). The difficulties in elucidating the nature of RR might originate in their possible complexity. Recently, Leister (2012) defined characteristics of retrograde signals and theoretically explored different scenarios of how single and multiple retrograde signals could transduce information to the nucleus in an isolated or coordinated fashion.

In general two types of retrograde signals can be distinguished (**Figure 1**):

1. Primary or direct retrograde signals are generated in the organelle and either passively diffuse or are actively transported to the nucleus, where they modulate NGE. Primary retrograde signals are therefore most likely metabolic intermediates generated from metabolic pathways in the respective organelles.
2. Secondary or indirect signals are activated by primary signals inside or outside the organelle, and travel to the nucleus or activate a cascade of signaling events that eventually alter NGE.

Post-translational modifications (PTMs) are ideally suited for signal integration and thus present a likely mechanism to transduce indirect retrograde signals. PTMs such as phosphorylation have key roles in signal transduction and amplification of cytosolic signaling cascades. It is therefore conceivable that primary mitochondrial signals could generate secondary signals (Møller and Sweetlove, 2010) or activate signal transduction cascades that traverse the cytosol. Here, we discuss evidence that PTMs connected to mitochondrial energy and redox metabolism occurring both outside and inside mitochondria are potential key players in transducing indirect MRR signals. We propose that recent technological advances in high resolution mass-spectrometry and sample preparation will allow wide and largely unbiased screens for mitochondrial PTMs and their dynamics (Witze et al., 2007;

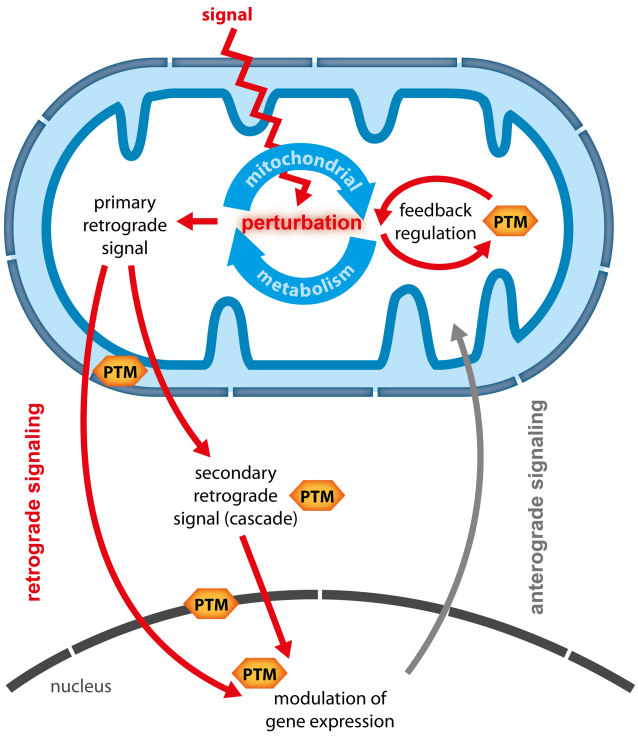

FIGURE 1 | Potential functions of PTMs in mitochondrial retrograde signaling. When an external signal or stress causes perturbations in mitochondrial metabolism several responses are possible and PTMs could contribute on multiple levels. (1) Mitochondrial metabolism is adapted via feedback regulation, during which PTM catalyzing enzymes could alter enzymatic activity in response to changes in metabolic status. (2) Metabolic intermediates are generated as primary retrograde signals, which either travel directly to the nucleus, or which are perceived at the mitochondrial boundary or in the cytosol and then translated into secondary signals or signaling cascades. PTMs are likely to be involved in the generation and transduction of such secondary signals. Moreover, PTMs could transduce signals across the inner mitochondrial or the nuclear membrane. In the nucleus PTMs of histones, transcription factors or transcriptional complexes could translate mitochondria-derived signals into specific changes in gene expression.

Choudhary and Mann, 2010). Such PTM-based analyses could help to elucidate the black box of MRR and to reveal some of its signaling components.

POST-TRANSLATIONAL MODIFICATIONS – LIGHT IN THE BLACK BOX OF MITOCHONDRIAL SIGNALING?

Post-translational modifications provide a powerful mechanism to rapidly and temporarily alter protein functions and locations in the cell, and they are also capable of providing information to regulatory proteins by creating docking sites for PTM-recognition domains (Deribe et al., 2010). PTMs which are dynamic, rapid, and reversible are suitable to direct transient changes in cellular metabolism and signaling. Intriguingly, the substrates of several major PTM-modifying enzymes are either central metabolites or redox-active compounds, as for example ATP, acetyl-CoA, NAD^+, and glutathione, which suggests that the activity of these enzymes could be directly coupled to the energy status or redox status of the organelle.

PHOSPHORYLATION

Although a few phosphorylation-regulated mitochondrial enzymes are well established, such as the pyruvate dehydrogenase (Gemel and Randall, 1992), only recently the regulatory role of phosphorylation in mitochondrial signal processing and metabolic regulation has begun to emerge (Pagliarini and Dixon, 2006; Ito et al., 2007; Juszczuk et al., 2007; Foster et al., 2009). There are indications that all major kinase signaling pathways in mammals can target the mitochondrion and influence mitochondrial function (Horbinski and Chu, 2005; Pagliarini and Dixon, 2006). Recent publications describe 77 phosphoproteins in mitochondria from human muscle cells and 181 phosphoproteins from murine cardiac mitochondria (Deng et al., 2011; Zhao et al., 2011). However, despite remarkable efforts merely 22 phosphoproteins are reported for *Arabidopsis* (Ito et al., 2009) and 14, mostly different, phosphoproteins for potato (Bykova et al., 2003). It is very likely that mitochondrial status and signaling varies with tissue and environmental conditions, which could explain why putative phosphoproteins remained undetected in studies concentrating on cell cultures or particular tissues. Similar to the fragmentary mitochondrial phosphoproteome, the available data describing mitochondrial protein kinases and phosphatases in plants is scarce (Heazlewood et al., 2004; Juszczuk et al., 2007). Several kinases and phosphatases attached to the outer mitochondrial membrane have recently been identified, but their possible role in mitochondrial signaling remains to be explored (Duncan et al., 2011; Sun et al., 2012). A large-scale yeast two-hybrid screen for interactors of mitogen-activated protein kinases (MAPKs) in rice indicates that these kinases could phosphorylate mitochondrial proteins (Singh et al., 2012). Lundquist et al. (2012) suggested that the so far largely neglected ABC1K protein kinase family could further fill the gap of mitochondrial kinases but clearly more experimental work will be necessary.

The points mentioned above indicate that phosphorylation might influence mitochondrial function but whether it could also influence MRR remains an open question. First evidence that plant MRR is indeed partially regulated via phosphorylation comes from the observation that the citrate-dependent induction of the mitochondrial alternative oxidase can be inhibited by the protein kinase inhibitor staurosporine (Djajanegara et al., 2002). Furthermore, Takahashi et al. (2003) demonstrated that spermine-induced functional changes in tobacco mitochondria trigger a MAPK-cascade and activate specific hypersensitive response genes. However, both pathways were not further explored yet.

Mitochondrial signals could activate phosphorylation-dependent signaling cascades inside or outside the organelle, which transduce MRR. Strong support for the existence of such a mechanism was found in yeast, where the "RTG-dependent pathway" represents one of the best-studied MRR. It has been shown that perturbations of mitochondrial functions in yeast result in lowered mitochondrial membrane potentials, eliciting a kinase-based response that regulates the phosphorylation status and translocation of specific TFs to the nucleus (Liu and Butow, 2006; Jazwinski, 2012). Candidates for phosphorylation-dependent signaling involved in MRR in plants are SNF1-related kinases (SnRKs), with the cytosolic SnRK1 in particular, and the target of rapamycin (TOR) protein kinases. SnRK1 and TOR

belong to different evolutionary conserved families of protein kinases, which likely function as master regulators and sensors of energy and nutrient metabolism during growth and development as well as under energy-depleting stress conditions (Polge and Thomas, 2007; Baena-González and Sheen, 2008; Dobrenel et al., 2011; Ghillebert et al., 2011; Ren et al., 2011; Xiong and Sheen, 2012). Although some important modulators of SnRK1- and TOR-activity have been described the main metabolic signals that activate these kinases remain unknown (Baena-González and Sheen, 2008; Ghillebert et al., 2011; Xiong and Sheen, 2012). Interestingly, there is an overlap in regulated transcripts between SnRK1-mediated responses and specific conditions of mitochondrial dysfunction (Schwarzländer et al., 2012) and it will be interesting to ascertain whether SnRK1 integrates metabolic signals from mitochondria, thus contributing to MRR. In yeast and mammals TOR signaling is vital for the maintenance of mitochondrial respiration and it is involved in the MRR (Schieke and Finkel, 2006). For example mammalian TOR (mTOR) interacts with PGC1α (Cunningham et al., 2007), a transcriptional activator regulating mitochondrial biogenesis and activity. Recent results in *Arabidopsis* suggest that TOR could have a similar function in plants but the exact mechanisms remain to be discovered (Leiber et al., 2010; Xiong and Sheen, 2012).

LYSINE ACETYLATION

Acetylation of the ε-amino group of lysine residues on proteins has recently emerged as a major PTM of proteins that has the potential to rival the regulatory role of phosphorylation (Choudhary et al., 2009; Norvell and McMahon, 2010). For a long time the research on lysine acetylation of proteins has concentrated almost exclusively on histones and transcriptional regulation. However, lysine acetylation of non-histone proteins was confirmed to be a widespread PTM in prokaryotes and eukaryotes that has profound regulatory effects on various metabolic and developmental processes (Close et al., 2010; Xing and Poirier, 2012). From a number of studies it became evident that lysine acetylation is involved in energy-homeostasis and regulation of carbon-flux, by directly altering NGE or the activities of key metabolic enzymes, such as glyceraldehyde 3-phosphate dehydrogenase and isocitrate dehydrogenase in *Salmonella enterica* (Wang et al., 2010), or mammalian mitochondrial acetyl-CoA-synthetase 2 (Hallows et al., 2006; Schwer et al., 2006). Furthermore, Kim et al. (2006) demonstrated that lysine acetylation patterns varied depending on nutritional status. Anderson and Hirschey (2012) estimated 35% of all mammalian mitochondrial proteins to have at least one acetylation site, and found pathways involved in the generation of energy, fatty acid metabolism, sugar metabolism, and amino acid metabolism to be significantly enriched in acetylated proteins. Important progress has also been made in identifying lysine-acetylated non-histone proteins in *Arabidopsis* (Finkemeier et al., 2011; Wu et al., 2011). These two studies describe a total number of 125 proteins to be lysine-acetylated in *Arabidopsis*, with cytochrome c representing the only mitochondrial protein. Only six common proteins were identified in both studies (Xing and Poirier, 2012), which suggests that the overall coverage was fairly low and that more extensive screens are likely to identify a much larger number of lysine-acetylated proteins in plants.

The huge potential of lysine acetylation acting as a metabolic sensor and regulator lies in the chemistry of the enzymes that catalyze this PTM. Lysine acetyltransferases (KATs) transfer the acetyl-moiety from acetyl-CoA to the target proteins. This suggests that the availability of the central metabolic intermediate acetyl-CoA or the acetyl-CoA/CoA ratio could be directly gaged by KATs (Xing and Poirier, 2012). As acetyl-CoA occurs in the cytosol and in organelles but cannot freely diffuse through membranes it has to be synthesized and metabolized independently in each compartment, which makes it a good indicator of local carbon status (Oliver et al., 2009). In *Arabidopsis* at least 12 KATs were identified by sequence homology and a number of them has been described to influence various developmental processes via acetylation of histones (Pandey et al., 2002; Earley et al., 2007; Servet et al., 2010). Information on KATs that acetylate non-histone proteins outside the nucleus is largely lacking. Only one mitochondrially localized KAT has been identified that acetylates lysine-residues of proteins belonging to the respiratory electron transport chain (ETC; Scott et al., 2012). It is well conceivable that there are other classes of KATs that remain to be discovered (Anderson and Hirschey, 2012).

In contrast, much more evidence is available for the reverse reaction catalyzed by lysine deacetylases (KDACs), in particular the KDAC class III of the so-called sirtuins (for "silent information regulation 2 homolog"). Sirtuins differ from the other three classes of deacetylases in their dependence on NAD^+ as substrate and the release of *O*-acetyl-ribose and nicotinamide (NAM) as by-products of the deacetylation. The NAD^+/NADH ratio reflects the energy status of a cell and several studies found that starvation conditions activate sirtuins in yeast and mammals, leading to transcriptional and metabolic adaptation via the deacetylation of histones, TFs, and metabolic enzymes (Zhong and Mostoslavsky, 2011; Houtkooper et al., 2012). These observations led to the hypothesis that protein acetylation could serve as a central switch between oxidative and fermentative metabolism, with acetyl-CoA, NAD^+, KATs, and NAD^+-dependent KDACs as key players (Guarente, 2011; Xing and Poirier, 2012). Although direct evidence is missing, such a model would allow the integration of MRR (Verdin et al., 2010). For example the activity of PGC1α (see above) is modulated by reversible acetylation through the KAT GCN5 and sirtuin 1 (SIRT1), depending on cellular acetyl-CoA and NAD^+ status (Canto and Auwerx, 2009). Furthermore, SIRT3 is regarded to be the major mitochondrial deacetylase in mammals with many targets involved in mitochondrial metabolism. This includes central enzymes as for example complex I, II, and III of the ETC, isocitrate dehydrogenases and glutamate dehydrogenase in the TCA-cycle, mitochondrial acetyl-CoA-synthetase, and long-chain acyl-CoA dehydrogenase, which is involved in fatty acid oxidation (Anderson and Hirschey, 2012; Houtkooper et al., 2012). From these observations a common model has emerged suggesting that under starvation conditions SIRT3 is activated by increased NAD^+ levels, stimulating oxidative metabolism and ATP-production (Zhong and Mostoslavsky, 2011). Changes in the cytosolic AMP/ATP ratio could be perceived by the AMP-activated protein kinase (AMPK, a homolog of SnRK1 mentioned above), which promotes catabolism and inactivates energy-consuming pathways (Verdin et al., 2010). Although the AMPK plant homolog SnRK1 is not allosterically regulated by the AMP/ATP ratio (Ghillebert et al.,

2011) it is intimately linked with cellular carbon status. Consequently, a sirtuin-dependent metabolic regulatory pathway seems possible in plants. The *Arabidopsis* genome encodes for two sirtuin genes, of which one (AtSRT2) comes in seven different splice-forms. However, the subcellular localization and the possible functions in metabolic regulation remain to be determined. Apart from sirtuins *Arabidopsis* expresses at least 16 KDACs of other classes, the functions of which have just started to be unraveled (Pandey et al., 2002; Hollender and Liu, 2008). While some of them were confirmed to deacetylate histones in the nucleus to regulate developmental processes (e.g., HDA6; Wu et al., 2008; Yu et al., 2011), others, like HDA5, HDA8, and HDA14, were found to be expressed in the cytosol, chloroplasts, or mitochondria and seem to be involved in the acetylation of non-histone proteins, as for example α-tubulin in the case of HDA14 (Alinsug et al., 2012; Tran et al., 2012). The dependence on central metabolites as co-substrates and the potential to directly and reversibly influence NGE and enzymatic activities makes lysine acetylation a promising candidate for regulating plant metabolism on multiple levels including MRR.

PTMs CONNECTED TO MITOCHONDRIAL REDOX STATE

Reactive oxygen species (ROS) are continuously produced as by-products of respiratory metabolism. Their production is increased under conditions of high matrix NADH/NAD^+ ratios or when the ubiquinone pool is highly reduced in conjunction with a high membrane potential (Møller, 2001; Murphy, 2009). Hence, the mitochondrial redox state is intimately linked to mitochondrial energy metabolism, and is defined by the balance of ROS produced by metabolic processes and the availability of NADPH as reducing equivalent to sustain the antioxidant system. The mitochondrial antioxidant defense system has a key role in the detoxification of peroxides and thus is a prime target to affect redox signaling. PTMs on plant mitochondrial antioxidant enzymes have not yet been studied in detail, but phosphorylation sites of antioxidant enzymes have been identified in several studies and are awaiting further functional characterization (Nakagami et al., 2010).

Oxidative PTMs of proteins that arise from increased ROS production in mitochondria can either be irreversible or reversible. The chemistry of oxidative modifications on proteins is quite complex and their full potential is not explored yet. The best-characterized irreversible protein oxidation in mitochondria is carbonylation, which is regarded as an indicator of oxidative damage to the cell (Møller et al., 2011). The iron-sulfur cluster of the TCA-cycle enzyme aconitase for example is particularly prone to oxidative inactivation, which might activate MRR in plants by increasing mitochondrial citrate levels (Gray et al., 2004; Rhoads and Subbaiah, 2007). Reversible oxidative modifications only occur at cysteine and methionine residues of proteins, which can be reversed by sulfiredoxins (in case of cysteine sulfinic acids), thioredoxins (TRXs; in case of disulfides), glutaredoxins (GRXs; in case of disulfides and glutathione-mixed disulfides) and methionine sulfoxide reductases (in case of methionine sulfoxides). Disulfides formed during cysteine oxidation play important roles in regulating enzyme activities and protein functions in diverse metabolic processes as well as in transcriptional regulation and signaling in plants and animals (Foyer and Noctor, 2009; Konig et al., 2012; Murphy, 2012). In the matrix of plant mitochondria 50 TRX-linked proteins and 18 GRX-linked proteins have been identified from various metabolic processes (Balmer et al., 2004; Rouhier et al., 2005). However, the *in vivo* confirmation of the functional regulation of plant mitochondrial metabolism by TRXs and GRXs is still lacking. The plant mitochondrial disulphide proteome was further assessed in a study using diagonal gel electrophoresis (Winger et al., 2007), identifying 21 proteins from major metabolic pathways which form either inter- or intramolecular disulfides under oxidizing conditions. Catalytic cysteines are important for the activities of many enzymes involved in metabolism (e.g., cysteine proteases, ubiquitin ligases, and peroxidases) and signaling (e.g., tyrosine phosphatases). *S*-Glutathionylation is a reversible PTM of cysteine, which is regarded as mechanism to protect redox-active cysteines from irreversible inactivation beside its role in redox signaling (Gallogly and Mieyal, 2007). Both glycine decarboxylase, a key enzyme in the photorespiratory pathway, as well as galactonolactone dehydrogenase, a major enzyme in ascorbate synthesis, were inactivated by glutathionylation in plant mitochondria (Leferink et al., 2009; Palmieri et al., 2010). Hence, glutathionylation could play a role in the temporary protection of these metabolic enzymes under conditions of oxidative stress. Metabolic changes resulting from inhibitions of these enzymes could then play a role in MRR. Irreversibly inactivated proteins can be degraded in all mitochondrial subcompartments (Fischer et al., 2012). Recent work in *C. elegans* demonstrated that the mitochondrial peptide exporter HAF-1 is required for MRR (Haynes et al., 2010). Møller and Sweetlove (2010) suggested that oxidatively modified peptides in particular could convey specific information to regulate oxidative stress-induced MRR in plants. Novel proteomic approaches using bifunctional thiol-specific alkylation reagents coupled to an epitope tag, or to a fluorescent or isotope-label will provide useful tools to further explore the functional significance of the mitochondrial redox proteome and its putative role in regulating MRR in plants (Held and Gibson, 2012).

FUTURE DIRECTIONS

A recent in-depth bioinformatics analysis estimated the plant mitochondrial proteome to contain about 2500 proteins (Cui et al., 2011). Many of these proteins will contain multiple PTMs of different types, which will consequently alter protein functions or even localization of proteins within the mitochondria. When thinking of the role of PTMs in signaling, primarily the classical phosphorylation-based MAPK-cascades come to mind, which are often initiated by receptor kinases. However, it is also conceivable that different types of PTMs could be series-connected or could interact in a codified crosstalk. A recent *in silico* study demonstrated that lysine acetylation sites have a great potential to affect nearby phosphorylation, methylation, and ubiquitination sites (Lu et al., 2011). Such a crosstalk was indeed observed in an *in vivo* study using the genome-reduced bacterium *Mycoplasma pneumoniae* (van Noort et al., 2012). Deletion of the only two protein kinases and a unique protein phosphatase modulated lysine acetylation patterns, while in return deletion of the only two KATs had an impact on protein phosphorylation. Hence, many scenarios are conceivable that include phosphorylation-based signaling cascades regulated by various types of PTMs. Just

as conceivable is the inverse scenario, having, phosphorylation or lysine acetylation regulating the activity of metabolic enzymes which would affect metabolic signaling. Such a complex PTM-based crosstalk is for example demonstrated in the regulation of the activity of the mitochondrial manganese superoxide dismutase (MnSOD). MnSOD is responsible for the decomposition of superoxide to hydrogen peroxide in the mitochondrial matrix. The activity of MnSOD can be modified by several PTMs including phosphorylation, lysine acetylation, and tyrosine nitration in mammals (Yamakura et al., 1998; Hopper et al., 2006; Ozden et al., 2011), while phosphorylation, carbonylation, and oxidative degradation of MnSOD have been observed in plants (Sweetlove et al., 2002; Kristensen et al., 2004; Juszczuk et al., 2007). Removal of phosphorylation and lysine acetylation from MnSOD were both shown to increase its activity, however, these occur under different physiological conditions (Finley and Haigis, 2009; Foster et al., 2009; Fukai and Ushio-Fukai, 2011; Ozden et al., 2011). Hence both modifications are probably connected in a codified crosstalk and will impact on mitochondrial redox signaling.

Several key questions will need to be answered in future research to fully understand the complexity and regulation of the mitochondrial proteome in dependence on environmental or metabolic cues: (1) Do different PTMs identified on the same proteins occur at the same time and if not what is their sequential arrangement?, (2) What is the physiological role of the different PTMs with regard to protein function?, and (3) Do different PTMs influence each other? To investigate these questions in detail and to further explore the role of PTMs in MRR, sophisticated proteomic analyses will be necessary that allow a time-resolved and in-depth inventory of the mitochondrial proteome and its modifications under conditions that trigger MRR. Furthermore, shot-gun proteomics approaches that analyze fractionated whole cell proteomes rather than sub-proteomes from isolated organelles might be more suitable for such type of analysis. Mitochondrial isolation procedures often take several hours and can have broad impacts on mitochondrial PTMs such as oxidative modifications. Several examples of PTM-based regulation of central mitochondrial proteins in animals demonstrate the need for further dissection of the functions of PTMs in plant mitochondrial signaling. Furthermore, autotrophic plant tissues differ fundamentally from animal heterotrophic tissues in terms of energy production, consumption, and homeostasis, and it is most likely that novel plant-specific regulatory mechanisms will be identified.

ACKNOWLEDGMENTS

We apologize to all colleagues whose work could not be cited due to space restrictions. This work was supported by the Deutsche Forschungsgemeinschaft, Germany (Emmy Noether Programme FI-1655/1-1 and Research Unit 804).

REFERENCES

Alinsug, M. V., Chen, F. F., Luo, M., Tai, R., Jiang, L., and Wu, K. (2012). Subcellular localization of class II HDAs in *Arabidopsis thaliana*: nucleocytoplasmic shuttling of HDA15 is driven by light. *PLoS ONE* 7, e30846. doi: 10.1371/journal.pone.0030846

Anderson, K. A., and Hirschey, M. D. (2012). Mitochondrial protein acetylation regulates metabolism. *Essays Biochem.* 52, 23–35.

Baena-González, E., and Sheen, J. (2008). Convergent energy and stress signaling. *Trends Plant Sci.* 13, 474–482.

Balmer, Y., Vensel, W. H., Tanaka, C. K., Hurkman, W. J., Gelhaye, E., Rouhier, N., et al. (2004). Thioredoxin links redox to the regulation of fundamental processes of plant mitochondria. *Proc. Natl. Acad. Sci. U.S.A.* 101, 2642–2647.

Bykova, N. V., Egsgaard, H., and Møller, I. M. (2003). Identification of 14 new phosphoproteins involved in important plant mitochondrial processes. *FEBS Lett.* 540, 141–146.

Canto, C., and Auwerx, J. (2009). PGC-1alpha, SIRT1 and AMPK, an energy sensing network that controls energy expenditure. *Curr. Opin. Lipidol.* 20, 98–105.

Choudhary, C., Kumar, C., Gnad, F., Nielsen, M. L., Rehman, M., Walther, T. C., et al. (2009). Lysine acetylation targets protein complexes and co-regulates major cellular functions. *Science* 325, 834–840.

Choudhary, C., and Mann, M. (2010). Decoding signalling networks by mass spectrometry-based proteomics. *Nat. Rev. Mol Cell Biol.* 11, 427–439.

Close, P., Creppe, C., Gillard, M., Ladang, A., Chapelle, J.-P., Nguyen, L., et al. (2010). The emerging role of lysine acetylation of non-nuclear proteins. *Cell. Mol. Life Sci.* 67, 1255–1264.

Cui, J., Liu, J., Li, Y., and Shi, T. (2011). Integrative Identification of *Arabidopsis* mitochondrial proteome and its function exploitation through protein interaction network. *PLoS ONE* 6, e16022. doi: 10.1371/journal.pone.0016022

Cunningham, J. T., Rodgers, J. T., Arlow, D. H., Vazquez, F., Mootha, V. K., and Puigserver, P. (2007). mTOR controls mitochondrial oxidative function through a YY1–PGC-1[agr] transcriptional complex. *Nature* 450, 736–740.

Deng, N., Zhang, J., Zong, C., Wang, Y., Lu, H., Yang, P., et al. (2011). Phosphoproteome analysis reveals regulatory sites in major pathways of cardiac mitochondria. *Mol. Cell. Proteomics* 10, M110.000117.

Deribe, Y. L., Pawson, T., and Dikic, I. (2010). Post-translational modifications in signal integration. *Nat. Struct. Mol. Biol.* 17, 666–672.

Djajanegara, I., Finnegan, P. M., Mathieu, C., Mccabe, T., Whelan, J., and Day, D. A. (2002). Regulation of alternative oxidase gene expression in soybean. *Plant Mol. Biol.* 50, 735–742.

Dobrenel, T., Marchive, C., Sormani, R., Moreau, M., Mozzo, M., Montane, M. H., et al. (2011). Regulation of plant growth and metabolism by the TOR kinase. *Biochem. Soc. Trans.* 39, 477–481.

Duncan, O., Taylor, N. L., Carrie, C., Eubel, H., Kubiszewski-Jakubiak, S., Zhang, B., et al. (2011). Multiple lines of evidence localize signaling, morphology, and lipid biosynthesis machinery to the mitochondrial outer membrane of *Arabidopsis*. *Plant Physiol.* 157, 1093–1113.

Earley, K. W., Shook, M. S., Brower-Toland, B., Hicks, L., and Pikaard, C. S. (2007). In vitro specificities of *Arabidopsis* co-activator histone acetyltransferases: implications for histone hyperacetylation in gene activation. *Plant J.* 52, 615–626.

Finkemeier, I., Laxa, M., Miguet, L., Howden, A., and Sweetlove, L. (2011). Proteins of diverse function and subcellular location are lysine-acetylated in *Arabidopsis*. *Plant Physiol.* 155, 1779–1790.

Finley, L. W., and Haigis, M. C. (2009). The coordination of nuclear and mitochondrial communication during aging and calorie restriction. *Ageing Res. Rev.* 8, 173–188.

Fischer, F., Hamann, A., and Osiewacz, H. D. (2012). Mitochondrial quality control: an integrated network of pathways. *Trends Biochem. Sci.* 37, 284–292.

Foster, D. B., Van Eyk, J. E., Marbán, E., and O'Rourke, B. (2009). Redox signaling and protein phosphorylation in mitochondria: progress and prospects. *J. Bioenerg. Biomembr.* 41, 159–168.

Foyer, C. H., and Noctor, G. (2009). Redox regulation in photosynthetic organisms: signaling, acclimation, and practical implications. *Antioxid. Redox. Signal.* 11, 861–905.

Fukai, T., and Ushio-Fukai, M. (2011). Superoxide dismutases: role in redox signaling, vascular function, and diseases. *Antioxid. Redox. Signal.* 15, 1583–1606.

Gallogly, M. M., and Mieyal, J. J. (2007). Mechanisms of reversible protein glutathionylation in redox signaling and oxidative stress. *Curr. Opin. Pharmacol.* 7, 381–391.

Gemel, J., and Randall, D. D. (1992). Light regulation of leaf mitochondrial pyruvate dehydrogenase complex: role of photorespiratory carbon metabolism. *Plant Physiol.* 100, 908–914.

Ghillebert, R., Swinnen, E., Wen, J., Vandesteene, L., Ramon, M., Norga, K., et al. (2011). The

AMPK/SNF1/SnRK1 fuel gauge and energy regulator: structure, function and regulation. *FEBS J.* 278, 3978–3990.

Giraud, E., Van Aken, O., Ho, L. H. M., and Whelan, J. (2009). The transcription factor ABI4 is a regulator of mitochondrial retrograde expression of ALTERNATIVE OXIDASE1a. *Plant Physiol.* 150, 1286–1296.

Gray, G. R., Maxwell, D. P., Villarimo, A. R., and Mcintosh, L. (2004). Mitochondria/nuclear signaling of alternative oxidase gene expression occurs through distinct pathways involving organic acids and reactive oxygen species. *Plant Cell Rep.* 23, 497–503.

Guarente, L. (2011). The logic linking protein acetylation and metabolism. *Cell metab.* 14, 151–153.

Hallows, W. C., Lee, S., and Denu, J. M. (2006). Sirtuins deacetylate and activate mammalian acetyl-CoA synthetases. *Proc. Natl. Acad. Sci. U.S.A.* 103, 10230–10235.

Haynes, C. M., Yang, Y., Blais, S. P., Neubert, T. A., and Ron, D. (2010). The matrix peptide exporter HAF-1 signals a mitochondrial UPR by activating the transcription factor ZC376.7 in *C. elegans. Mol. Cell* 37, 529–540.

Heazlewood, J. L., Tonti-Filippini, J. S., Gout, A. M., Day, D. A., Whelan, J., and Millar, A. H. (2004). Experimental analysis of the *Arabidopsis* mitochondrial proteome highlights signaling and regulatory components, provides assessment of targeting prediction programs, and indicates plant-specific mitochondrial proteins. *Plant Cell* 16, 241.

Held, J. M., and Gibson, B. W. (2012). Regulatory control or oxidative damage? Proteomic approaches to interrogate the role of cysteine oxidation status in biological processes. *Mol. Cell. Proteomics* 11, R111.013037.

Hollender, C., and Liu, Z. (2008). Histone deacetylase genes in *Arabidopsis* development. *J. Integr. Plant Biol.* 50, 875–885.

Hopper, R. K., Carroll, S., Aponte, A. M., Johnson, D. T., French, S., Shen, R. F., et al. (2006). Mitochondrial matrix phosphoproteome: effect of extra mitochondrial calcium. *Biochemistry* 45, 2524–2536.

Horbinski, C., and Chu, C. T. (2005). Kinase signaling cascades in the mitochondrion: a matter of life or death. *Free Radic. Biol. Med.* 38, 2–11.

Houtkooper, R. H., Pirinen, E., and Auwerx, J. (2012). Sirtuins as regulators of metabolism and healthspan. *Nat. Rev. Mol. Cell Biol.* 13, 225–238.

Ito, J., Heazlewood, J. L., and Millar, A. H. (2007). The plant mitochondrial proteome and the challenge of defining the posttranslational modifications responsible for signalling and stress effects on respiratory functions. *Physiol. Plant.* 129, 207–224.

Ito, J., Taylor, N. L., Castleden, I., Weckwerth, W., Millar, A. H., and Heazlewood, J. L. (2009). A survey of the *Arabidopsis thaliana* mitochondrial phosphoproteome. *Proteomics* 9, 4229–4240.

Jazwinski, S. M. (2012). The retrograde response: when mitochondrial quality control is not enough. *Biochim. Biophys. Acta* doi: 10.1016/j.bbamcr.2012.02.010 [Epub ahead of print]

Juszczuk, I. M., Bykova, N. V., and Møller, I. M. (2007). Protein phosphorylation in plant mitochondria. *Physiol. Plant.* 129, 90–103.

Kim, S. C., Sprung, R., Chen, Y., Xu, Y., Ball, H., Pei, J., et al. (2006). Substrate and functional diversity of lysine acetylation revealed by a proteomics survey. *Mol. Cell* 23, 607–618.

Konig, J., Muthuramalingam, M., and Dietz, K. J. (2012). Mechanisms and dynamics in the thiol/disulfide redox regulatory network: transmitters, sensors and targets. *Curr. Opin. Plant Biol* 15, 261–268.

Kristensen, B. K., Askerlund, P., Bykova, N. V., Egsgaard, H., and Moller, I. M. (2004). Identification of oxidised proteins in the matrix of rice leaf mitochondria by immunoprecipitation and two-dimensional liquid chromatography-tandem mass spectrometry. *Phytochemistry* 65, 1839–1851.

Leferink, N. G., Van Duijn, E., Barendregt, A., Heck, A. J., and Van Berkel, W. J. (2009). Galactonolactone dehydrogenase requires a redox-sensitive thiol for optimal production of vitamin C. *Plant Physiol.* 150, 596–605.

Leiber, R.-M., John, F., Verhertbruggen, Y., Diet, A., Knox, J. P., and Ringli, C. (2010). The TOR pathway modulates the structure of cell walls in *Arabidopsis. Plant Cell* 22, 1898–1908.

Leister, D. (2012). Retrograde signaling in plants: from simple to complex scenarios. *Front. Plant Sci.* 3:135. doi: 10.3389/fpls.2012.00135

Liu, Z., and Butow, R. A. (2006). Mitochondrial retrograde signaling. *Annu. Rev. Genet.* 40, 159–185.

Lu, Z., Cheng, Z., Zhao, Y., and Volchenboum, S. L. (2011). Bioinformatic analysis and post-translational modification crosstalk prediction of lysine acetylation. *PLoS ONE* 6, e28228. doi: 10.1371/journal.pone.0028228

Lundquist, P. K., Davis, J. I., and Van Wijk, K. J. (2012). ABC1K atypical kinases in plants: filling the organellar kinase void. *Trends Plant Sci.* 17, 546–555.

Millar, A. H., Whelan, J., Soole, K. L., and Day, D. A. (2011). Organization and regulation of mitochondrial respiration in plants. *Annu. Rev. Plant Biol.* 62, 79–104.

Møller, I. M. (2001). Plant mitochondria and oxidative stress: electron transport, NADPH turnover, and metabolism of reactive oxygen species. *Annu. Rev. Plant Physiol. Plant Mol. Biol.* 52, 561–591.

Møller, I. M., Rogowska-Wrzesinska, A., and Rao, R. S. (2011). Protein carbonylation and metal-catalyzed protein oxidation in a cellular perspective. *J. Proteomics* 74, 2228–2242.

Møller, I. M., and Sweetlove, L. J. (2010). ROS signalling – specificity is required. *Trends Plant Sci.* 15, 370–374.

Murphy, M. P. (2009). How mitochondria produce reactive oxygen species. *Biochem. J.* 417, 1–13.

Murphy, M. P. (2012). Mitochondrial thiols in antioxidant protection and redox signaling: distinct roles for glutathionylation and other thiol modifications. *Antioxid. Redox. Signal.* 16, 476–495.

Nakagami, H., Sugiyama, N., Mochida, K., Daudi, A., Yoshida, Y., Toyoda, T., et al. (2010). Large-scale comparative phosphoproteomics identifies conserved phosphorylation sites in plants. *Plant Physiol.* 153, 1161–1174.

Norvell, A., and McMmahon, S. B. (2010). Rise of the Rival. *Science* 327, 964–965.

Oliver, D. J., Nikolau, B. J., and Wurtele, E. S. (2009). Acetyl-CoA—life at the metabolic nexus. *Plant Sci.* 176, 597–601.

Ozden, O., Park, S. H., Kim, H. S., Jiang, H., Coleman, M. C., Spitz, D. R., et al. (2011). Acetylation of MnSOD directs enzymatic activity responding to cellular nutrient status or oxidative stress. *Aging (Albany NY)* 3, 102–107.

Pagliarini, D. J., and Dixon, J. E. (2006). Mitochondrial modulation: reversible phosphorylation takes center stage? *Trends Biochem. Sci.* 31, 26–34.

Palmieri, M. C., Lindermayr, C., Bauwe, H., Steinhauser, C., and Durner, J. (2010). Regulation of plant glycine decarboxylase by s-nitrosylation and glutathionylation. *Plant Physiol.* 152, 1514–1528.

Pandey, R., Müller, A., Napoli, C., Selinger, D., Pikaard, C. S., Richards, E., et al. (2002). Analysis of histone acetyltransferase and histone deacetylase families of *Arabidopsis thaliana* suggests functional diversification of chromatin modification among multicellular eukaryotes. *Nucleic Acids Res.* 30, 5036–5055.

Polge, C., and Thomas, M. (2007). SNF1/AMPK/SnRK1 kinases, global regulators at the heart of energy control? *Trends Plant Sci.* 12, 20–28.

Ren, M., Qiu, S., Venglat, P., Xiang, D., Feng, L., Selvaraj, G., et al. (2011). Target of rapamycin regulates development and ribosomal RNA expression through kinase domain in *Arabidopsis. Plant Physiol.* 155, 1367–1382.

Rhoads, D. M. (2011). "Plant mitochondrial retrograde regulation," in *Plant Mitochondria*, ed. F. Kempken (New York: Springer), 411–437.

Rhoads, D. M., and Subbaiah, C. C. (2007). Mitochondrial retrograde regulation in plants. *Mitochondrion* 7, 177–194.

Rouhier, N., Villarejo, A., Srivastava, M., Gelhaye, E., Keech, O., Droux, M., et al. (2005). Identification of plant glutaredoxin targets. *Antioxid. Redox. Signal.* 7, 919–929.

Schieke, S. M., and Finkel, T. (2006). Mitochondrial signaling, TOR, and life span. *Biol. Chem.* 387, 1357.

Schwarzländer, M., König, A. C., Sweetlove, L. J., and Finkemeier, I. (2012). The impact of impaired mitochondrial function on retrograde signalling: a meta-analysis of transcriptomic responses. *J. Exp. Bot.* 63, 1735–1750.

Schwer, B., Bunkenborg, J., Verdin, R. O., Andersen, J. S., and Verdin, E. (2006). Reversible lysine acetylation controls the activity of the mitochondrial enzyme acetyl-CoA synthetase 2. *Proc. Natl. Acad. Sci. U.S.A.* 103, 10224–10229.

Scott, I., Webster, B. R., Li, J. H., and Sack, M. N. (2012). Identification of a molecular component of the mitochondrial acetyltransferase programme: a novel role for GCN5L1. *Biochem. J.* 443, 655–661.

Servet, C., Conde E Silva, N., Zhou, D.-X., and Conde, N. (2010). Histone acetyltransferase AtGCN5/HAG1 is a versatile regulator of developmental and inducible gene expression in *Arabidopsis. Mol. Plant* 3, 670–677.

Singh, R., Lee, M.-O., Lee, J.-E., Choi, J., Park, J. H., Kim, E. H., et al. (2012). Rice mitogen-activated protein kinase interactome analysis using the yeast two-hybrid system. *Plant Physiol.* 160, 477–487.

Sun, F., Carrie, C., Law, S., Murcha, M. W., Zhang, R., Law, Y. S., et al. (2012). AtPAP2 is a tail-anchored protein in the outer membrane of

chloroplasts and mitochondria. *Plant Signal. Behav.* 7, 927–932.
Sweetlove, L. J., Fait, A., Nunes-Nesi, A., Williams, T., and Fernie, A. R. (2007). The mitochondrion: an integration point of cellular metabolism and signalling. *Crit. Rev. Plant Sci.* 26, 17–43.
Sweetlove, L. J., Heazlewood, J. L., Herald, V., Holtzapffel, R., Day, D. A., Leaver, C. J., et al. (2002). The impact of oxidative stress on *Arabidopsis* mitochondria. *Plant J.* 32, 891–904.
Takahashi, Y., Berberich, T., Miyazaki, A., Seo, S., Ohashi, Y., and Kusano, T. (2003). Spermine signalling in tobacco: activation of mitogen-activated protein kinases by spermine is mediated through mitochondrial dysfunction. *Plant J.* 36, 820–829.
Tran, H. T., Nimick, M., Uhrig, G., Templeton, G., Morrice, N., Gourlay, R., et al. (2012). *Arabidopsis thaliana* histone deacetylase 14 (HDA14) is an α-tubulin deacetylase that associates with PP2a and enriches in the microtubule fraction with the putative histone acetyltransferase ELP3. *Plant J.* 71, 263–272.
van Noort, V., Seebacher, J., Bader, S., Mohammed, S., Vonkova, I., Betts, M. J., et al. (2012). Cross-talk between phosphorylation and lysine acetylation in a genome-reduced bacterium. *Mol. Syst. Biol.* 8, 571.
Verdin, E., Hirschey, M. D., Finley, L. W. S., and Haigis, M. C. (2010). Sirtuin regulation of mitochondria: energy production, apoptosis, and signaling. *Trends Biochem. Sci.* 35, 669–675.
Wang, Q., Zhang, Y., Yang, C., Xiong, H., Lin, Y., Yao, J., et al. (2010). Acetylation of metabolic enzymes coordinates carbon source utilization and metabolic flux. *Science* 327, 1004–1007.
Winger, A. M., Taylor, N. L., Heazlewood, J. L., Day, D. A., and Millar, A. H. (2007). Identification of intra- and intermolecular disulphide bonding in the plant mitochondrial proteome by diagonal gel electrophoresis. *Proteomics* 7, 4158–4170.
Witze, E. S., Old, W. M., Resing, K. A., and Ahn, N. G. (2007). Mapping protein post-translational modifications with mass spectrometry. *Nat. Methods* 4, 798–806.
Wu, K., Zhang, L., Zhou, C., Yu, C.-W., and Chaikam, V. (2008). HDA6 is required for jasmonate response, senescence and flowering in *Arabidopsis*. *J. Exp. Bot.* 59, 225–234.
Wu, X., Oh, M.-H., Schwarz, E., Larue, C. T., Sivaguru, M., Imai, B. S., et al. (2011). Lysine acetylation is a widespread protein modification for diverse proteins in *Arabidopsis*. *Plant Physiol.* 155, 1769–1778.
Xing, S., and Poirier, Y. (2012). The protein acetylome and the regulation of metabolism. *Trends Plant Sci.* 1–8.
Xiong, Y., and Sheen, J. (2012). Rapamycin and glucose-target of rapamycin (TOR) protein signaling in plants. *J. Biol. Chem.* 287, 2836–2842.
Yamakura, F., Taka, H., Fujimura, T., and Murayama, K. (1998). Inactivation of human manganese-superoxide dismutase by peroxynitrite is caused by exclusive nitration of tyrosine 34 to 3-nitrotyrosine. *J. Biol. Chem.* 273, 14085–14089.
Yu, C.-W., Liu, X., Luo, M., Chen, C., Lin, X., Tian, G., et al. (2011). HISTONE DEACETYLASE6 interacts with FLOWERING LOCUS D and regulates flowering in *Arabidopsis*. *Plant Physiol.* 156, 173–184.
Zhao, X., León, I. R., Bak, S., Mogensen, M., Wrzesinski, K., Højlund, K., et al. (2011). Phosphoproteome analysis of functional mitochondria isolated from resting human muscle reveals extensive phosphorylation of inner membrane protein complexes and enzymes. *Mol. Cell. Proteomics* 10, M110.000299.
Zhong, L., and Mostoslavsky, R. (2011). Fine tuning our cellular factories: sirtuins in mitochondrial biology. *Cell Metab.* 13, 621–626.

Conflict of Interest Statement: The authors declare that the research was conducted in the absence of any commercial or financial relationships that could be construed as a potential conflict of interest.

Received: 23 September 2012; accepted: 22 October 2012; published online: 12 November 2012.
*Citation: Hartl M and Finkemeier I (2012) Plant mitochondrial retrograde signaling: post-translational modifications enter the stage. Front. Plant Sci. **3**:253. doi: 10.3389/fpls.2012.00253*
This article was submitted to Frontiers in Plant Physiology, a specialty of Frontiers in Plant Science.
Copyright © 2012 Hartl and Finkemeier. This is an open-access article distributed under the terms of the Creative Commons Attribution License, which permits use, distribution and reproduction in other forums, provided the original authors and source are credited and subject to any copyright notices concerning any third-party graphics etc.

frontiers in
PLANT SCIENCE

ORIGINAL RESEARCH ARTICLE
published: 09 January 2013
doi: 10.3389/fpls.2012.00284

Transfer of a redox-signal through the cytosol by redox-dependent microcompartmentation of glycolytic enzymes at mitochondria and actin cytoskeleton

Joanna Wojtera-Kwiczor†, Felicitas Groß, Hans-Martin Leffers, Minhee Kang, Markus Schneider and Renate Scheibe*

Department of Plant Physiology, Faculty of Biology and Chemistry, University of Osnabrueck, Osnabrueck, Germany

Edited by:
Dario Leister,
Ludwig-Maximilians-University Munich, Germany

Reviewed by:
Zhong-Nan Yang, Shanghai Normal University, China
Rainer E. Häusler, Univertity Cologne, Germany

***Correspondence:**
Renate Scheibe, Department of Plant Physiology, Faculty of Biology and Chemistry, University of Osnabrueck, D-49069 Osnabrueck, Germany.
e-mail: scheibe@biologie.uni-osnabrueck.de

†Present address:
Joanna Wojtera-Kwiczor, Biochemistry Department, Institute of Molecular Biology and Biotechnology, Faculty of Biology, A. Mickiewicz University in Poznan, Umultowska St. 89, 61-614 Poznan, Poland.

The cytosolic glyceraldehyde-3-phosphate dehydrogenase (GAPDH, EC 1.2.1.12, GapC) plays an important role in glycolysis by providing the cell with ATP and NADH. Interestingly, despite its glycolytic function in the cytosol, GAPDH was reported to possess additional non-glycolytic activities, correlating with its nuclear, or cytoskeletal localization in animal cells. In transiently transformed mesophyll protoplasts from *Arabidopsis thaliana* colocalization and interaction of the glycolytic enzymes with the mitochondria and with the actin cytoskeleton was visualized by confocal laser scanning microscopy (cLSM) using fluorescent protein fusions and by bimolecular fluorescence complementation, respectively. Yeast two-hybrid screens, dot-blot overlay assays, and co-sedimentation assays were used to identify potential protein–protein interactions between two cytosolic GAPDH isoforms (GapC1, At3g04120; GapC2, At1g13440) from *A. thaliana* with the neighboring glycolytic enzyme, fructose 1,6-bisphosphate aldolase (FBA6, At2g36460), the mitochondrial porin (VDAC3; At5g15090), and actin *in vitro*. From these experiments, a mitochondrial association is suggested for both glycolytic enzymes, GAPDH and aldolase, which appear to bind to the outer mitochondrial membrane, in a redox-dependent manner. In addition, both glycolytic enzymes were found to bind to F-actin in co-sedimentation assays, and lead to bundling of purified rabbit actin, as visualized by cLSM. Actin-binding and bundling occurred reversibly under oxidizing conditions. We speculate that such dynamic formation of microcompartments is part of a redox-dependent retrograde signal transduction network for adaptation upon oxidative stress.

Keywords: actin cytoskeleton, colocalization, glycolytic enzymes, microcompartmentation, mitochondria, redox-dependent binding, redox-signaling, VDAC

INTRODUCTION

The glycolytic pathway consists of 10 enzymes that catalyze the reversible oxidation of glucose to pyruvate with generation of ATP and a reductant (NADH), and provides pyruvate for plant mitochondrial respiration. Glycolysis supplies also carbon skeletons for other biosynthetic processes, such as synthesis of fatty acids, nucleic acids, isoprenoids, and amino acids, being therefore important in actively growing autotrophic tissues. Moreover, glycolysis becomes a crucial player in many biochemical adaptations to environmental stresses such as nutrient limitation, osmotic stress, drought, hypoxia, anaerobiosis, and cold/freezing, as well as during seed germination (Plaxton, 1996). Since these aspects are crucial for plant development and growth, there has to be a multi-faceted regulation of glycolysis in plants. In particular, the posttranslational modifications of plant glycolytic enzymes may be of key importance upon oxidative/nitrosative stress (Dixon et al., 2005; Lindermayr et al., 2005), since S-nitrosylation of the *Arabidopsis* GAPDH, for instance, was shown to inhibit its activity in a reversible manner (Lindermayr et al., 2005). Similar effects were demonstrated for the GSSG- and GSNO-treated recombinant cytosolic GAPDH (Holtgrefe et al., 2008), and for cytosolic aldolase from *Arabidopsis thaliana* (van der Linde et al., 2011), as well as for the S-glutathionylated triose-phosphate isomerase (Ito et al., 2003). Nuclear localization was also reported for the glycolytic isoenzymes from the cytosol (Hameister et al., 2007; Holtgrefe et al., 2008; van der Linde et al., 2011).

Another regulatory aspect influencing the glycolytic pathway seems to be its spatial organization in the plant cell (Fernie et al., 2004). Change of the cellular microenvironment may trigger new effects, i.e., transient protein–protein interactions, formation of a metabolon, protein association with certain subcellular structures, such as organelle membranes or cytoskeletal lattice,

Abbreviations: ACT, actin; BiFC, bimolecular fluorescence complementation; CFP, cyan fluorescent protein; cLSM, confocal laser scanning microscopy; diamide, azodicarboxylic acid bis(dimethylamide); DTT, dithiotreitol; ER, endoplasmatic reticulum; FBA, cytosolic fructose 1,6-bisphosphate aldolase; GapC/GAPDH, cytosolic NAD-dependent glyceraldehyde-3-phosphate dehydrogenase; GFP, green fluorescent protein; GSH/GSSG/GSNO, reduced/oxidized glutathione/nitrosoglutathione; HXK, hexokinase; OMM, outer mitochondrial membrane; PM, plasma membrane; VDAC, voltage-dependent anion channel; YFP, yellow fluorescent protein.

or translocation to other subcellular compartments. Observations made mainly in animal cells, and only recently in plants, gave hints for variable subcellular localizations of certain glycolytic enzymes that were classically considered as a soluble system of proteins. A long list of glycolytic enzymes associated with the cytoskeleton in animal cells accumulated over the past decades (Walsh et al., 1980, 1989; Somers et al., 1990; Schindler et al., 2001; Schmitz and Bereiter-Hahn, 2002), but the cytoskeleton-association phenomenon has been reported for plant glycolytic enzymes only in the last years (Azama et al., 2003; Holtgräwe et al., 2005; Balasubramanian et al., 2007).

In our previous observations, the *Arabidopsis* mesophyll cells, transiently expressing a GFP-fusion with GapC and aldolase isoforms, respectively, were found not only to exhibit cytosolic and nuclear fluorescent signals (Holtgrefe et al., 2008; van der Linde et al., 2011), but signals also occurred as foci-like structures of yet unknown nature. Moreover, in our earlier work, a mitochondrial porin, VDAC1a, had been identified as a putative binding partner in a yeast two-hybrid screen of a maize seedling cDNA library (Holtgräwe et al., 2005). Hence, in the light of recent reports on possible mitochondrial microcompartmentation of several glycolytic enzymes (Giegé et al., 2003; Holtgräwe et al., 2005; Kim et al., 2006; Balasubramanian et al., 2007; Damari-Weissler et al., 2007; Graham et al., 2007), the observed fluorescent GapC1 and GapC2 foci were further analyzed in the context of their association with organelles and cytoskeleton. Therefore, Bimolecular Fluorescence Complementation (BiFC), the "one-on-one" version of the yeast two-hybrid assay, dot-blot overlay assays, and co-sedimentation assays with F-actin were applied to test the possible interactions between both *Arabidopsis* GapC isoforms, aldolase, VDAC3, and the actin cytoskeleton. Considering the glycolytic enzymes, it became a challenge to reveal their spatial organization, since it seems to play a regulatory role (Fernie et al., 2004). However, little is known about factors influencing the dynamic microcompartmentation of glycolytic enzymes *in planta* (Graham et al., 2007). Transient changes are possibly triggered by redox-changes occurring in the cytosol, when the cells are exposed to stress. They might serve as a signal, leading to reorganization of the cytosol, and finally to changed cellular functions and acclimation. The *in vitro* studies presented here were performed in order to test redox-dependency of the protein–protein interactions between glycolytic enzymes, actin cytoskeleton and the outer mitochondrial membrane (OMM) through VDAC.

EXPERIMENTAL PROCEDURES

ISOLATION OF MESOPHYLL PROTOPLASTS FROM *A. THALIANA* PLANTS

Mesophyll protoplasts isolated from of *A. thaliana* plants (ecotype Columbia) were used for *in vivo* labeling of the subcellular structures and organelles, such as Golgi apparatus, nucleus, actin cytoskeleton, and mitochondria, as well as visualization of subcellular localization of proteins fused to CFP, GFP, or YFP. Protoplasts were isolated from leaves of 5- to 6-week-old wild-type *A. thaliana* plants, according to Seidel et al. (2004), with some modifications (Voss et al., 2008).

VISUALIZATION OF FLUORESCENCE-TAGGED PROTEINS IN TRANSIENTLY TRANSFORMED PROTOPLASTS FROM *A. THALIANA*

The glycolytic enzymes were expressed in *Arabidopsis* protoplasts from the pGFP-2 vector as a C-terminal fusion with the Green Fluorescent Protein (pGFP GapC1 and pGFP GapC2), under control of the constitutive CaMV 35S promoter (Kost et al., 1998). Similar experiments were carried out with vectors encoding GapC isoforms as CFP fusions, based on the p-35S-CFP-NosT vector, which was kindly provided by Thorsten Seidel (University of Bielefeld, Germany). A chimera of the mCherry protein with a transmembrane domain of a rat α-2,6-sialyl-transferase, which is a mammalian, Golgi-targeted glycosylation enzyme (Saint-Jore et al., 2002), was used in order to visualize Golgi apparatus in the plant cell. This construct was obtained from Ekkehard Neuhaus (TU Kaiserslautern, Germany). Visualization of actin microfilaments in plant cells was performed using a vector encoding tdTomato: AtFim1 ABD2, kindly provided by Takumi Higaki (University of Tokyo, Japan; Sano et al., 2005). It consists of the second actin-binding domain (ABD2) of the fimbrin-like protein from *A. thaliana* (AtFim1), fused with tdTomato (Shaner et al., 2004). Plant mitochondria were visualized by staining mesophyll protoplasts with the MitoTracker® Orange CMTMRos (Molecular Probes/Invitrogen, Karlsruhe, Germany).

The protein–protein interactions between the glycolytic enzymes, GapC and aldolase, with VDAC3, were investigated by means of the BiFC technique (BiFC or split YFP; Hu et al., 2002). Appropriate vectors, pUC-SPYNE and pUC-SPYCE (Walter et al., 2004) obtained from Prof. Jörg Kudla (University of Muenster), were used to design constructs expressing the respective proteins. Fusions of aldolase (FBA6, At2g36460), VDAC3 (At5g15090), or GapC1 and GapC2 with the N-terminal or the C-terminal half of the YFP are described as X:YFP^{N} or X:YFP^{C}, respectively. Combination of plasmids, pUC-SPYNE-bZip63 and pUC-SPYCE-bZip63, coding for an YFP-fusion with the transcription factor bZip63, was used as a positive control in the BiFC assay. Homodimerization of this protein was already demonstrated to occur in the plant nucleus (Walter et al., 2004).

The transiently transformed protoplasts incubated between 8 and 16 h, were stained with 50 nM MitoTracker® Orange CMTMRos for 15 min at RT, in the dark, prior to imaging. Afterwards, the sample was centrifuged for 1 min at 100 × *g*, and the resulting pellet was resuspended with 1 ml W5 solution. The plant cells were immediately observed using the cLSM 510 META (Carl Zeiss, Göttingen, Germany). CFP and autofluorescence of chlorophyll were visualized with excitation at 458 nm and emission at 480–520 and 650–710 nm, respectively. GFP and autofluorescence of chlorophyll were visualized with excitation at 488 nm and emission at 500–530 nm and 650–710 nm, respectively. YFP and autofluorescence of chlorophyll were visualized with excitation at 514 nm and emission at 535–590 nm and 650–704 nm (detected with META Detector), respectively.

When observed with stained mitochondria, GFP and autofluorescence of chlorophyll were visualized with excitation at 488 nm and emission at 500–530 nm and 650–704 nm, respectively, whereas MitoTracker® Orange was excited with 543 nm and emitted at 565–615 nm. The same settings were used for the

combination with GFP, when actin cytoskeleton was additionally visualized. In case, when YFP was expressed in *Arabidopsis* protoplasts along with stained mitochondria, YFP was visualized with excitation at 514 nm and emission at 522–533 nm, whereas MitoTracker® Orange was excited with 543 nm and emitted at 565–597 nm, both detected with META Detector, respectively.

YEAST TWO-HYBRID SCREEN WITH GapC1 AND 2 AS BAITS, AND "ONE-ON-ONE" ASSAYS

The two isoforms of GAPDH from *A. thaliana* (GapC1, At3g04120) and GapC2, At1g13440) were applied as baits in the two-hybrid screen of the cDNA library for positive protein–protein interactions, according to Kolonin et al. (2000) with small modifications. The cDNA library from *A. thaliana* suspension cell culture was obtained from Prof. Koncz, University of Bonn (Nemeth et al., 1998). Screens were performed according to manufacturer's instructions (The Matchmaker Two-Hybrid Library Construction and Screening Kit, Clontech). As further confirmation of the interactions found in the DNA-library screen, the putatively positive interactions were tested in a "one-on-one" assay. For this aim, the haploid AH109 strain provides all needed reporter genes (HIS3, ADE2, MEL1), so that it could be cotransformed with both vectors encoding the investigated bait and prey proteins. The positively transformed yeast colonies, with two replicates in each case, were tested for activation of the reporter genes ADE2, HIS3, MEL1 by "drop test" on selective media lacking tryptophane, leucine, and histidine (SD/TDO). For strong protein–protein interaction, medium was additionally lacking adenine (SD/QDO/X-α-Gal). In case of control experiments, yeast cells were transformed with a combination of the investigated partner and empty bait (pGBKT7) or prey vector (pGADT7).

CO-SEDIMENTATION ASSAY

Since plant and animal actin are highly conserved in sequence (88% identity), co-sedimentation experiments were performed with commercially available rabbit muscle actin (>99% pure) that was purchased from Cytoskeleton (Denver, CO, USA). Actin was purified by a polymerization/depolymerization cycle prior to usage. In order to exclude the possibility to capture soluble enzymes during polymerization without specific binding, the polymerization step was performed prior to the addition of the soluble enzymes.

G-actin was prepared in low-salt buffer (LSB; 5 mM Tris-HCl pH 7.6, 0.2 mM $CaCl_2$, 0.2 mM ATP, 0.15 mM NAD) by incubation of rabbit muscle actin for 30 min on ice, buffer change over Pierce Desalting Spin Columns (Rockford, USA) and ultracentrifugation at 100,000 × *g* for 1 h at 4°C. G-actin was polymerized upon addition of 1x polymerization inducer [PI; 50x stock: 250 mM Tris-HCl (pH 7.6), 100 mM $MgCl_2$, 50 mM ATP, 7.5 mM NAD, 2 M KCl] at a protein concentration of 0.4 mg/ml in LSB. Aldolase (FBA6, At2g36460) GAPDH (GapC1; At3g04120), and BSA (negative control) were also adjusted to a protein concentration of 0.4 mg/ml with 1x assay buffer [50x stock: 250 mM Tris-HCl (pH 7.6), 100 mM $MgCl_2$, 50 mM ATP, 7.5 mM NAD]. F-actin and the glycolytic protein/s were mixed with a 1:1 ratio on a protein basis, and redox reagents (final concentrations: diamide + GSH: each 1 mM, GSSG: 5 mM, GSNO: 0.5 mM, H_2O_2 + GSH: each 0.5 mM) were added. The mixtures were incubated at 22°C for 30 min. Then DTT_{red} (final concentration 10 mM) was added to one part of the mixtures, followed by incubation for 5 min at 22°C. Then supernatant and pellet were separated by ultracentrifugation at 100,000 × *g* for 1 h at 22°C. Both fractions were analyzed by SDS-PAGE (10%) and subsequent staining of the gels with Coomassie Brilliant Blue R.

IN VITRO VISUALIZATION OF ACTIN

Samples of F-actin together with GapC1, aldolase, or both enzymes were prepared as described for the co-sedimentation assay. Then DTT_{red} (10 mM final concentration) was added to the mixtures for another incubation at 22°C for 5 min and stained with phalloidin labeled with tetramethylrhodamine B isothiocyanate (Sigma-Aldrich; final concentration 70 nM). Fluorescence was visualized by cLSM (510 META, Zeiss, Jena, Germany) using the Plan-Apochromat 63x/1,4 Oil DIC objective. Picture calculation and processing were done with the LSM Image Browser (Zeiss, Jena, Germany).

DOT-BLOT OVERLAY ASSAY WITH CROSSLINKING

Overlay dot-blot analyses were performed with recombinant GAPDH; GapC1, At3g04120, VDAC3 (At5g150910) reconstituted into liposomes, purified F-actin, G-actin (from rabbit muscle, Sigma-Aldrich), and BSA as a negative control. In the case of VDAC3, TOM40, and empty liposomes were used as negative controls. The proteins (each 2 μg) were dripped onto nitrocellulose membranes and air-dried. The membranes were blocked with 6% BSA in TBS-T (50 mM Tris-HCl, 150 mM NaCl, and 0.2% Tween 20, pH 8) for 1 h and washed. Membranes were then incubated with 100 μg/ml recombinant cytosolic fructose 1,6-bisphosphate aldolase (FBA6, At2g36460) in the presence of 10 mM DTT, 0.1 mM GSNO, 5 mM GSSG, 1 mM diamide plus 1 mM GSH or 0.5 mM H_2O_2 plus 0.5 mM GSH, or VDAC3 in liposomes, respectively, for 1 h at room temperature and finally washed. For crosslinking, the membranes were treated with 0.115% glutaraldehyde in 20 mM HEPES buffer (pH 7.5) for 5 min at 37°C and washed (Migneault et al., 2004). Immunodetection was achieved with polyclonal antibody against maize aldolase (1:10,000) or against VDAC1 (1:5000, Agrisera, Sweden) for 1 h at room temperature and color development using goat anti-rabbit IgG conjugated with alkaline phosphatase (1:5000; BioRad, Munich) using BCIP/NBT as substrates, or the second antiserum conjugated with horseradish peroxidase (1:3000, BioRad, Munich) using ECL (iNtRON Biotechnol., Korea) as substrate.

For the dot-blot analyses, VDAC3 was synthesized in a cell-free system (RTSTM 100 Wheat Germ CECF, 5PRIME, Hamburg, Germany) and separated from the reaction mix via reconstitution into liposomes in the presence of 80 mM nonanoyl-*N*-methylglucamide (MEGA 9). The reconstitution of VDAC3 into liposomes was verified by a Nycodenz® density gradient flotation assay of the proteoliposomes. The dot-blot assay was performed as described above in the presence and the absence of 10 mM DTT.

HOMOLOGY MODELING OF 3D-STRUCTURES

The three-dimensional structures of the proteins were generated using the homology modeling mode of the SWISS-model

workspace (Bordoli et al., 2009). The template structures for the homology modeling of the *A. thaliana* proteins were selected in accordance with the protein structures which were used by Forlemu et al. (2011). For the comparison of the amino acids which were identified by Forlemu et al. (2011) and Ouporov et al. (1999) to be involved in the ionic interaction, a multiple sequence alignment was performed.

RESULTS

IN VIVO COLOCALIZATION OF GAPC WITH MITOCHONDRIA

Apart from the even cytosolic distribution and the occasional nuclear localization of the GFP-fused GapC1, GapC2, and aldolase, reported previously (Holtgrefe et al., 2008; van der Linde et al., 2011), fluorescent signals appeared in a non-homogeneous distribution as locally accumulated foci of GapC2:GFP and GapC1:GFP/CFP in the cytosol of the transformed protoplasts (**Figures 1A,B**). The GapC-containing structures emitted intense fluorescence that in many cases was much stronger than the cytosolically distributed GFP-fused enzyme, which was frequently observed. The diffuse cytosolic signal was therefore not imaged in certain cases, due to down-regulation of the detector in the cLSM 510 META (**Figure 1**, GapC2:GFP). The cytosolic aggregates of GapC:GFP seemed to vary with regard of their size, shape, and amount. A higher magnification resulted in a better resolution of the foci-like spots, showing their branched constitution in several cases (**Figure 1B**, magnified GapC2:GFP) and suggested that these fluorescent structures, formed by GapC:GFP isoforms, could be associated with certain organelles.

Interestingly, the presence of At1g13440- and At3g04120-encoded GapC in the secretory pathways was predicted using the ARAMEMNON database (data not shown) and was reported by Santoni et al. (1998) and Marmagne et al. (2004), who both identified GapC in the PM protein fraction from *Arabidopsis*. In addition to PM, vacuole, endoplasmic reticulum (ER),

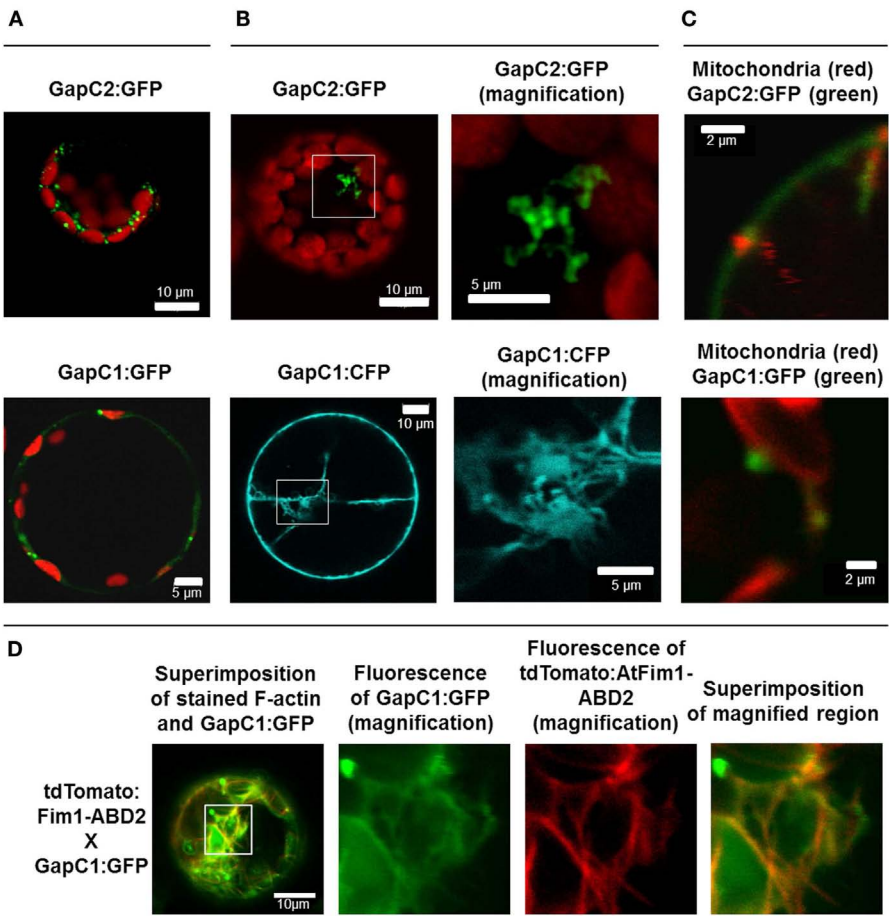

FIGURE 1 | Manifold localization patterns of the GAPDH isoforms. GFP- and CFP fusions of the two isoforms of GAPDH (GapC1 and GapC2) were transiently expressed in the protoplasts, isolated from leaves of 6-week-old plants of *A. thaliana*. **(A)** Superimposition of chlorophyll autofluorescence and locally accumulated GFP-fusions of the two isoforms. **(B)** GFP- and CFP-fluorescence from the GapC1 and GapC2 fusions, respectively. On the right hand side, magnifications are shown of relevant parts. **(C)** Colocalization of GFP-fused GapC1 and GapC2 with MitoTracker-stained mitochondria. **(A–C)**. Pictures in the last lane present the magnified areas indicated in the overlays. Images in the YFP and MitoTracker channel were taken in the frame mode, both channels separately which caused a short time delay between the red and green channel, due to respective dichroic mirror settings. **(D)** Protoplasts were transformed with GapC1:GFP (green) and tdTomato:Fim1ABD2 (red). The fotos in the panels 2, 3, and 4 show the magnification of the boxed area in foto 1. All images were taken with the confocal Laser Scanning Microscope LSM 510 META, Zeiss.

and the Golgi apparatus constitute the major components of the plant secretory system (Brandizzi et al., 2004). In this context, the fraction of manifold, small GapC:GFP foci, resembling plant Golgi apparatus, was tested for colocalization with Golgi stacks using a chimera of the mCherry protein with a transmembrane domain of a rat α-2,6 sialyl-transferase (Saint-Jore et al., 2002). However, no colocalization of signals emitted by GapC:GFP foci and by the Golgi apparatus could be detected (data not shown).

GapC-organelle association was then tested with the mitochondria dye MitoTracker® Orange. Fluorescence-intensity profiles of the signals emitted by both GFP-fusion GapC and MitoTracker® Orange enabled a colocalization analysis, which indicated that some of the smaller foci of GapC:GFP were associated with mitochondria (**Figure 1C**; **Figures A1** and **A2** in Appendix), whereas the bigger branched structures were never close to these organelles (data not shown).

GapC isoforms can also form cytoplasmic strands when expressed transiently as CFP fusions that might be correlated with cytoskeleton (**Figure 1B**, lower pictures, **Figure A3** in Appendix). When fluorescent fusion of tdTomato with the actin-binding domain ABD2 of fimbrin (AtFim1) was applied for staining actin filaments, an additional peak for tdTomato, that appeared within the GFP-emission range, was noticed in protoplasts that were transiently expressing GapC1:GFP (**Figure 1D**; **Figure A4** in Appendix). Therefore, the analysis of cytoskeletal association of GapC isoforms had to be modified. During microscopic imaging with cLSM 510 META it turned out that, by down-regulation of the detector, the bleeding-through artifacts could be removed, allowing visualization of the stronger GapC1:GFP foci only, with respect to the stained actin cytoskeleton. This approach enabled the observation of the punctuate signals emitted by GFP-fusion GapC, and showed that the clusters might move between actin fibrils, but their direct association with stained actin filaments was not obvious (**Figure 2**).

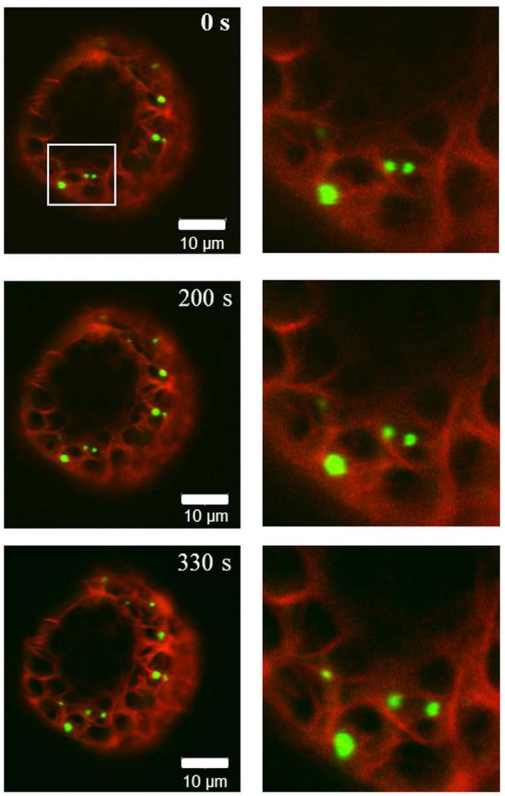

FIGURE 2 | Time-lapse images of GapC1:GFP aggregates with respect to the actin cytoskeleton. Time-lapse images of the GAPDH aggregates in relation to the actin cytoskeleton show GapC1:GFP aggregates moving along actin fibers (depicted with white frames). Images were taken after the indicated times. Actin filaments are stained with tdTomato:AtFim1 ABD2 (red). The GapC1:GFP foci are displayed in green. Scale bar: 10 µm. The images were taken with the Confocal Laser Scanning Microscope LSM 510 META, Zeiss.

PROTEIN–PROTEIN INTERACTION PARTNERS OF GAPC IN THE YEAST-2-HYBRID SYSTEM

Identification of new interaction partners of GapC by a yeast two-hybrid screen of a cDNA library could elucidate its variable subcellular localization and novel "moonlighting" features, which have been suggested for the animal counterpart (for review see: Sirover, 1999, and Sirover, 2005). Such approach might also help to reveal, why this cytosolic enzyme can localize to different subcellular structures, such as nucleus (Holtgrefe et al., 2008), or possibly with the OMM, which has been recently observed (Giegé et al., 2003; Graham et al., 2007), and what we follow in this study. Here, a yeast two-hybrid screen of the cDNA library from *A. thaliana* was performed. Among 42 putative interaction partners of the GapC2, four cDNA coding for the voltage-dependent anion channel VDAC3 (At5g15090), a porin from the OMM, and 11 GapC clones could be identified. The presence of yeast colonies expressing GapC1 and GapC2 protein on SD/QDO/X-α-Gal is a hint to suggest positive, but weaker interactions between subunits of different GapC isoforms, which form not only homo-, but also heterooligomers. A yeast two-hybrid screen with GapC1 as bait protein revealed 16 protein–protein interaction partners of this isoform. Among them, 13 sequences were full-length clones encoding VDAC3 (At5g15090).

Both isoforms, GapC1 and GapC2, and VDAC3 were applied in an additional set of "one-on-one" yeast two-hybrid assays, in order to retest the specificity of these associations. The colonies containing hybrid GapC isoforms fused with the GAL4-BD domain, and VDAC3 fused with the GAL4-AD domain grew under high-stringency conditions, confirming the positive interaction found in the yeast two-hybrid screen (**Figure 3**). With help of control vectors, it was surprisingly shown that autoactivation of all reporter genes took place in the case of VDAC3-AD (expressed from the pACT2 or pGADT7 vector), cotransfected with an empty vector pGBKT7 or pGBKT7-LamC. The appropriate yeast colonies grew on SD/TDO and additionally on SD/QDO/X-α-Gal. This unspecific autoactivation of reporter genes seemed to be a property of VDAC3-AD, which was not the case for the VDAC3-BD, expressed from pGBKT7 under a truncated ADH1 promoter (**Figure 3**). However, it also did not interact with any of the GapC isoforms. The initially identified VDAC3-AD and GapC-BD interaction

Bait	Prey	SD/TDO	SD/QDO + X-α-Gal
p53	RecT		
GapC2	*VDAC3*		
GapC1	*VDAC3*		
GapC2	GapC2		
GapC1	GapC2		
GapC1	GapC1		
GapC2	GapC1		
GapC2	-		
GapC1	-		
-	GapC2		
-	GapC1		
-	*VDAC3 in pACT2*		
-	*VDAC3*		
LamC	*VDAC3*		
VDAC3	-		
VDAC3	GapC2		
VDAC3	GapC1		

FIGURE 3 | Yeast 2-hybrid "one-on-one" assays between GapC isoforms, aldolase, and VDAC3. Putatively positive interactions had been identified in the yeast two-hybrid screen of the cDNA library from *A. thaliana*. Here, to retest these findings, the haploid yeast strain AH109 was cotransformed with constructs, expressing bait, or prey proteins, as indicated in the table. Serial dilution of the appropriate overnight yeast culture was dropped onto selective media to demonstrate the stringency of binding between proteins. Colonies growing on SD/Leu$^-$, Trp$^-$ were successfully transformed with both vectors, encoding the investigated proteins. Growth on SD/TDO and SD/QDO/X-α-Gal is a sign of positive interactions. Italics indicate false positive results due to autoactivation by VDAC3 when used as a prey.

could therefore not be confirmed, due to the autoactivating property of VDAC3-AD. Excluding the effect of autoactivation by only using VDAC3 as a bait, the interaction with aldolase was also tested. Surprisingly, only a weak interaction of aldolase with itself when forming an homooligomer was found. Its interactions with GapC1 and 2, or with VDAC3 were negative in this assay (data not shown).

BIMOLECULAR FLUORESCENCE COMPLEMENTATION APPROACH TO TEST THE *IN VIVO* INTERACTION OF GAPC AND ALDOLASE WITH MITOCHONDRIAL PORIN

Split YFP fusions of GapC isoforms and VDAC3 were expressed in *Arabidopsis* protoplasts, with the aim to verify their putatively direct interaction *in planta*, which was found in the yeast two-hybrid screen, but appeared to be false positive in the "one-on-one assay" (**Figure 3**). In both combinations of YFP fusions, fluorescent signals could be detected in protoplasts. Some of the fluorescent foci were colocalized with mitochondria (**Figure 4A**), but other observed signals, reflecting interaction between GapC and porin, did not overlap with the organelles stained with MitoTracker® Orange (**Figure 4B**), which was also the case for GapC:GFP (**Figure 1**, **Figures A1** and **A2** in Appendix).

Previous screening of the cDNA library from hypoxic seedlings of *Zea mays*, as well as a dot-blot overlay assay had demonstrated binding of the cytosolic isoform of maize fructose 1,6-bisphosphate aldolase to the mitochondrial porin, VDAC1a (Holtgräwe et al., 2005). It was therefore tempting to look also at this interaction *in vivo*, in *Arabidopsis* protoplasts, that enabled the expression of aldolase fused to the N-terminal (FBA:YFP^N), and VDAC3 fused to the C-terminal half of the YFP (VDAC3:YFP^C). Indeed, fluorescent signals occurred in a locally accumulated form. Additional staining of mitochondria confirmed the location of the fluorescent foci next to these organelles (**Figure 4C**). No signals were observed, however, when vectors encoding aldolase fused to the C-terminal (FBA:YFP^C), and VDAC3 fused to the N-terminal half of the YFP (VDAC3:YFP^N) were used. Therefore, sterical factors may determine whether the direct binding of aldolase to VDAC3 can occur. This localization pattern was not detected in the negative controls (**Figure A5** in Appendix). When an empty pUC-SPYNE vector and GapC1, GapC2, or FBA6, fused to the C-terminal halves of the YFP, were used, positive BiFC signals that were homogeneously distributed in the cytoplasm or even localized in the nucleus, were surprisingly found in several protoplasts. An identical, cytosolic localization pattern was observed also in the *Arabidopsis* protoplasts expressing split YFP-fused GapC1 and/or GapC2, reflecting the homo- and heterooligomerization of its subunits, respectively (data not shown). Beside this cytosolic compartmentation, FBA6 and GapC interacted also in a locally accumulated way, in some cases close to the stained mitochondria (**Figures 4D,E**), which correlated with the microscopic observations regarding potential mitochondrial association of GapC:GFP (**Figures 1** and **2**; **Figure A1** in Appendix). With respect to the negative controls that were false positive, the cytosolic, YFP-like fluorescent signals are not easily distinguishable from the false positive interaction. These putatively positive results may be unspecific and the homogeneous distribution of interacting glycolytic enzymes could be artifactual. The irreversible nature of the association between the two YFP fragments, especially when they are overexpressed or documented after a longer period of the transient expression, namely over 24 h, may be the reason for the false positive signals (Zhong et al., 2008).

IN VITRO INTERACTIONS BETWEEN GAPDH, ALDOLASE, RABBIT ACTIN, AND VDAC AND THEIR REDOX-DEPENDENCE

From the above described experimental approaches that are frequently used to study protein–protein interactions, no uniform picture could be drawn as to the *in vivo* binding of soluble glycolytic enzymes to cellular structures. This is probably due to the fact that the cellular state and the actual microenvironment of the interacting partners cannot easily be controlled. Unknown cellular factors, such as posttranslational modifications, another protein required for this interaction or a redox-signal coming from the mitochondrial matrix or from the chloroplasts could play a

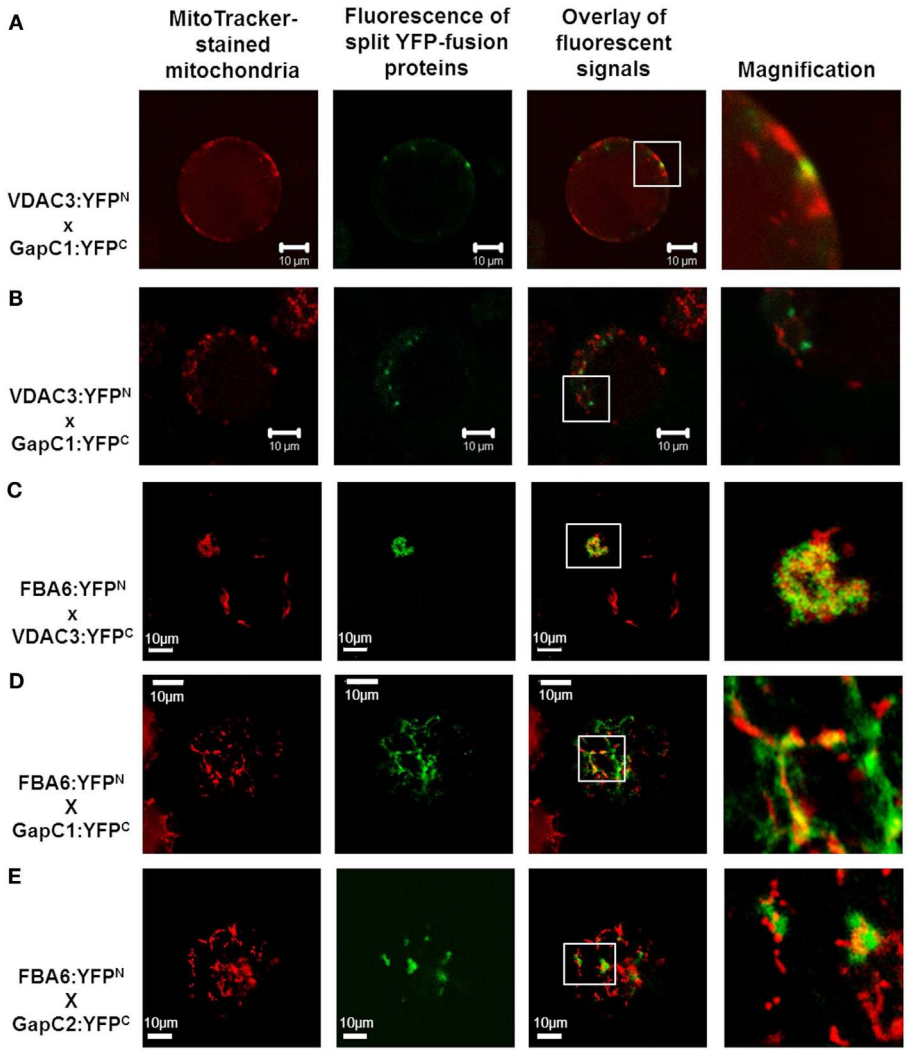

FIGURE 4 | Colocalization of aldolase (FBA6) and GapC with mitochondria. Vectors encoding the investigated proteins were cotransformed in protoplasts, isolated from leaves of *A. thaliana* plants. The fluorescent signals from GapC1 interacting with VDAC3 **(A,B)**, FBA6, and VDAC3 **(C)**, as well as FBA6 with GapC1 or GapC2 **(D,E)**, fused with N- or C-terminal halves of YFP, respectively, were tested for mitochondrial localization by staining the cells with 50 nM MitoTracker® Orange CMTMRos (Molecular Probes).

crucial role for all observations made in *in vivo* systems such as isolated protoplasts, or in yeast cells where the tested interactions take place in the nucleus. In order to study the redox-dependence of the observed interactions under defined conditions, various *in vitro* assays were performed with the purified recombinant proteins.

Co-sedimentation assays with rabbit F-actin and the glycolytic enzymes

Incubation of F-actin with recombinant plant aldolase and GapC1 under reducing conditions and subsequent centrifugation resulted in a pellet fraction containing only actin and no glycolytic enzymes as can be seen from the SDS-PAGE analysis after ultracentrifugation (**Figure 5**, control). In contrast, incubation under various different oxidizing conditions resulted in the appearance of a certain portion of GapC and/or aldolase in the pellet fractions, diamide and GSSG treatment yielding mainly aldolase in the pellet, while GSNO resulted in GapC associating with F-actin. Subsequent reduction of an aliquot reversed the binding completely (**Figure 5**). Both, aldolase and GapC were also added separately to the F-actin preparation, yielding the same results as were obtained with both enzymes present simultaneously (data not shown).

Bundling assays with rabbit actin stained with phalloidin-rhodamin

Bundle-like structures, formed by stained rabbit F-actin, were detected only under oxidizing conditions in the simultaneous presence of the glycolytic enzymes (**Figure 6**, left column), or of each of the enzymes alone (data not shown). The bundle structures disappeared when the sample was reduced subsequently with DTT (**Figure 6**, right column). When the enzymes were added in the presence of DTT, the same picture was apparent

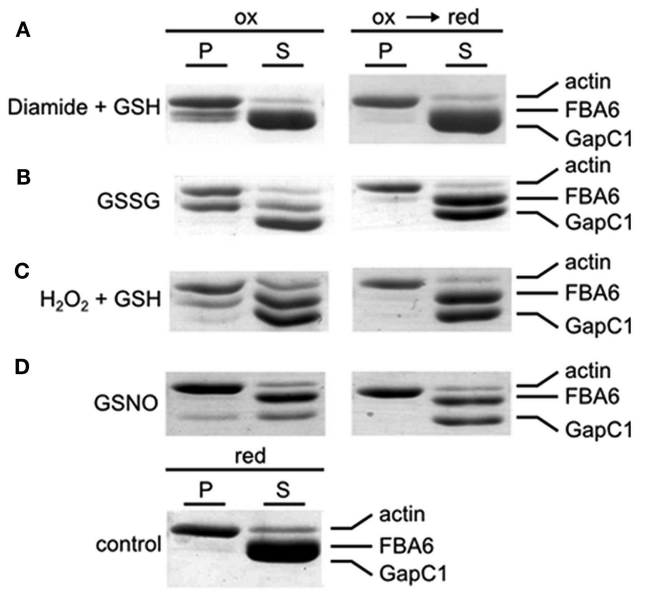

FIGURE 5 | Co-sedimentation assay with F-actin, GAPDH, and aldolase under oxidizing and reducing conditions. Samples with rabbit F-actin, FBA6, and GapC1 were first oxidized with the specific redox reagents **(A)** Diamide + GSH (each 0.5 mM); **(B)** GSSG (5 mM); **(C)** H_2O_2 + GSH (each 0.5 mM); **(D)** GSNO (0.5 mM) with a following reduction by DTT_{red} (10 mM). The control sample with F-actin, FBA6, and GapC1 was only incubated with DTT_{red} (10 mM). The mixtures were then centrifugated at 100,000 × *g* for 1 h. Supernatant (S) and pellet (P) were separated for analysis by SDS-PAGE and the gels were stained with Coomassie Brilliant blue.

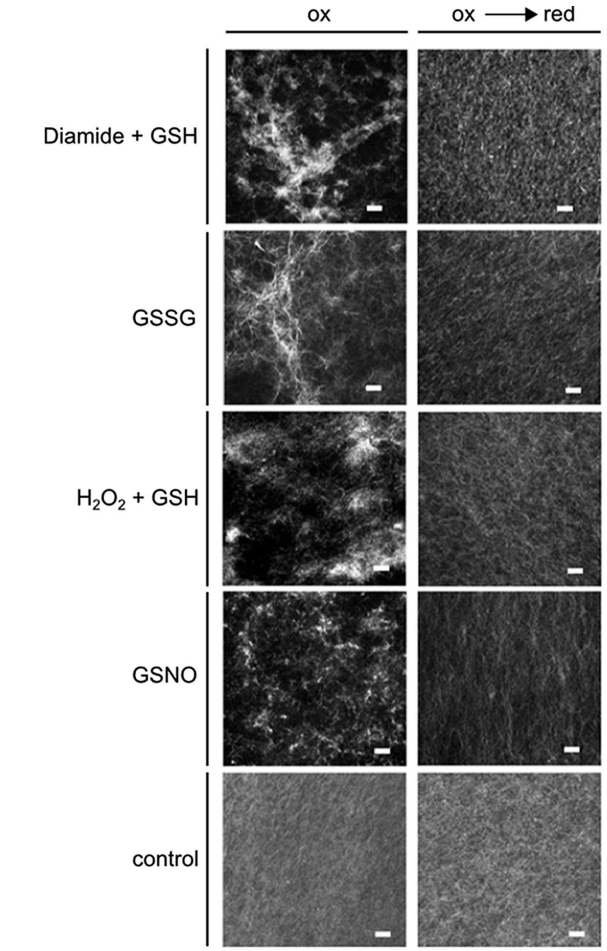

FIGURE 6 | Effect of redox-state on F-actin bundling activity of GapC and aldolase. Samples with rabbit F-actin, aldolase, and GapC1 were first oxidized with the specific redox reagents: diamide + GSH (each 0.5 mM); GSSG (5 mM); H_2O_2 + GSH (each 0.5 mM); GSNO (0.5 mM) followed by a reduction step with DTT_{red} (10 mM). Subsequently, the samples were stained with rhodamine-labeled phalloidin (70 nM) and fluorescence was visualized by cLSM. The control experiment represents an incubation of F-actin with BSA incubated with diamide + GSH, and the subsequent reduction with DTT. Scale bar: 10 μm.

as with subsequent reduction of the previously oxidized sample (data not shown). In case, when only DTT was present without any enzymes added, there was no formation of bundles visible either (data not shown). In a control experiment, no glycolytic enzyme, but BSA was present instead, both under oxidizing and subsequent reducing conditions, and no bundle structures were visible under both conditions (**Figure 6**, lowest row). Although in these experiments it is not possible to detect any bound proteins, the bundling activity of the glycolytic enzymes became apparent, due to the changed appearance of the actin structure, as visualized by microscopy. Taken together, these experiments indicate that the glycolytic enzymes might act as bundling agents, but in a reversible manner only under oxidizing conditions.

Dot-blot overlay confirms redox-dependent binding of the glycolytic enzymes to F-actin and mitochondrial porin

Redox-dependent binding of aldolase to F-actin, G-actin, and GapC1 under oxidizing conditions as observed in the co-sedimentation assays (**Figure 5**) was confirmed by the dot-blot overlay assay. Under all oxidizing conditions, a positive reaction was observed except with BSA that was used as a negative control. In the final immunodecoration any aldolase that had bound to a spotted protein could be detected (**Figure 7**). Glutathionylation, as well as nitrosylation resulted in binding of aldolase to F-actin, but also to GapC with a similar affinity. The interaction between G-actin and the modified FBA6 was much weaker than with the filamentous protein. Reduction prevented any binding of the added aldolase, only the formation of a homomeric oligomer of aldolase took place also under reducing conditions as apparent after immunostaining (**Figure 7A**, left lane).

The regulation of the direct binding of FBA6 and GapC to VDAC3 found in protoplasts was verified by means of a dot-blot overlay approach. Under oxidizing conditions the binding of aldolase to VDAC3 could be detected by immunodecoration with antibody against aldolase (**Figure 7B**). Similarly, a positive signal was also observed when oxidized GapC was overlaid with VDAC3 and immunodecorated with anti-VDAC antibody (**Figure 7C**). These positive reactions were not observed with the empty liposomes and TOM40 or with BSA, which were used as negative

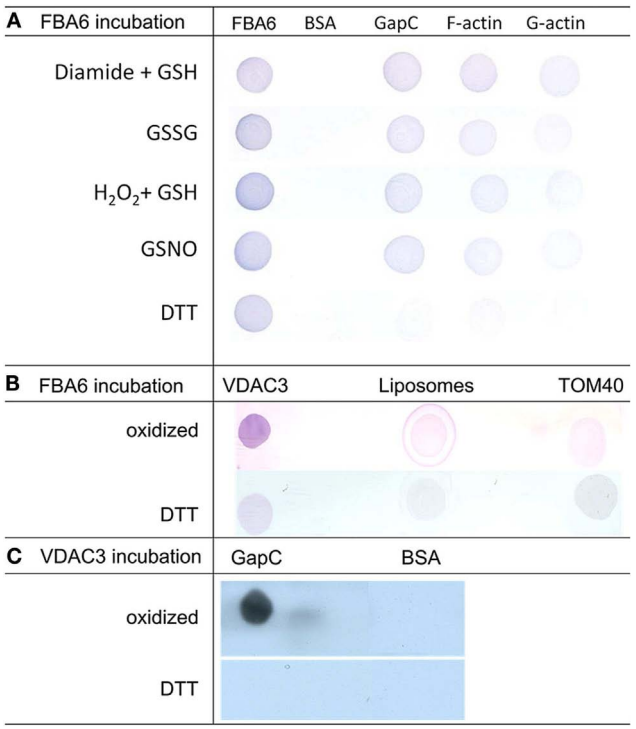

FIGURE 7 | Analysis redox-dependent binding of aldolase to GAPDH, actin and VDAC3 by Far Western blotting. (A) Aldolase (FBA6; At2g36460), GAPDH (GapC1; At3g04120), G-actin, rabbit F-actin, and bovine serum albumin (BSA) as negative control (2 μg each) were applied onto a nitrocellulose membrane, overlaid with 100 μg/ml aldolase in the presence of 10 mM DTT, 0.1 mM GSNO, 5 mM GSSG, 1 mM diamide plus, 1 mM GSH, or 0.5 mM H_2O_2 plus 0.5 mM GSH, and probed with polyclonal antibody against maize aldolase as described in Section Experimental Procedures. **(B)** VDAC3 (At5g15090) reconstituted into liposomes was applied onto a nitrocellulose membrane, overlaid with 100 μg/ml aldolase in the presence of 10 mM DTT and without reductant (oxidized). Empty liposomes and TOM40 were used as controls, immunological detection of bound aldolase was as in **(A)**. **(C)**. GapC and BSA as a control were applied to the membrane, which was overlaid with VDAC3 in liposomes. Detection was with anti-VDAC1 serum and the HRP-conjugated second antiserum using ECL as a substrate as described in Section Experimental Procedures.

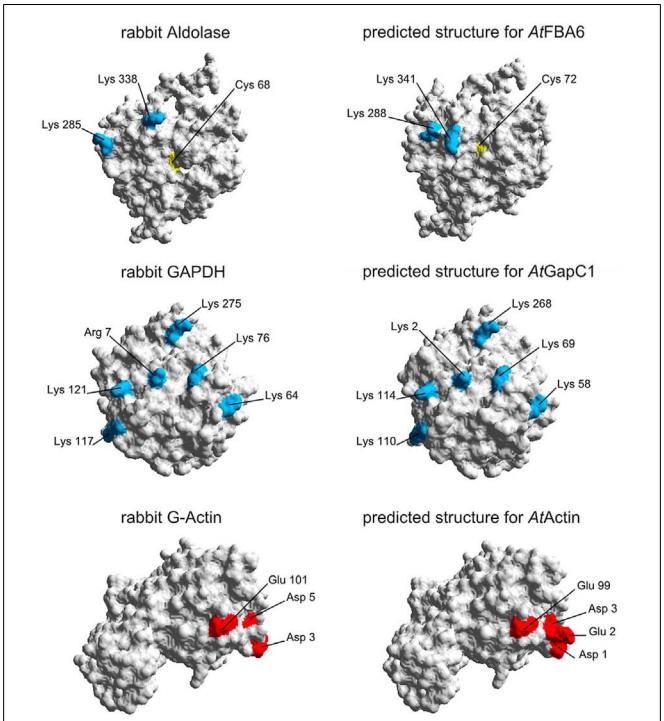

FIGURE 8 | Homology modeling of 3D-structures of aldolase, GAPDH, and actin. On the left hand side, the proteins from rabbit as used by Forlemu et al. (2011) are shown. The corresponding *Arabidopsis* proteins on the right hand side were modeled with SWISS-MODEL as described in Section Experimental Procedures. By using the Swiss-Pdb Viewer 4.0.4, the molecular surface of the generated protein models was calculated and the conserved amino acids which are necessary for the protein–protein interaction are colored: Positively charged amino acids are blue, negatively charged amino acids are red. Cysteines are shown in yellow.

controls in this assay. Reduction prevented any binding of the glycolytic enzymes to the porin.

HOMOLOGY MODELING OF ACTIN-BINDING

There is evidence from earlier work on the animal model that actin-binding sites contain amino-acid motifs with clustered charged residues, namely Asp and Glu, as well as Lys and Arg (Forlemu et al., 2011). It is obvious from the comparison with the animal counterparts that the positions of the positively and negatively charged residues on the surface of the proteins, which are implicated to be involved in the binding, are rather conserved, as are these proteins altogether (**Figure 8**). From the side view that is depicted to demonstrate the relative positions of these charged residues, it is not possible to locate surface Cys residues that have been shown to be subject to redox-modifications. However, it can be imagined that even distant molecular changes upon redox-modification of these residues can allosterically affect the binding sites by changing the charge distribution in the critical surface area.

DISCUSSION

BINDING OF GLYCOLYTIC ENZYMES TO MITOCHONDRIA

It appears to be a general phenomenon for cytoplasmic, metabolic proteins that organize into extensive physical structures upon nutrient depletion. Such functional foci formation may enhance substrate channeling and metabolite flux control, and decrease the free diffusion of intermediates (Ovadi and Saks, 2004). Moreover, a spatial or functional organization of metabolic pathways into complexes could flexibly assemble or disassemble upon demand of the cell. The enzyme–enzyme interactions may evoke locally high substrate concentrations and, in consequence, an enhanced transfer or metabolic channeling of intermediates from one active site of an enzyme to another (Ovadi and Srere, 1996). GFP-fused Ade4, a purine biosynthetic enzyme, expressed in yeast, formed foci in the absence of adenine and occurred in a diffused form when adenine was added (Narayanaswamy et al., 2009). The authors reported also on glutamine synthetase (Gln1) foci that cycled reversibly in the absence and presence of glucose. Such metabolon formation

may also regulate competition between branched pathways for common metabolites, coordinate the activities of pathways with shared enzymes or intermediates, and sequester reactive or toxic molecules (Winkel, 2004). The observed dynamic association of FBA6-GapC complexes with mitochondria may respond to the respiration demands of the organelles, as suggested by Giegé et al. (2003). The authors proposed that attachment of the glycolytic reaction sequence to the outside of mitochondria may ensure the provision of a localized supply of pyruvate, in order to directly support mitochondrial respiration. Graham et al. (2007) demonstrated an evidence for physiological dependency for mitochondrial association of the glycolytic pathway. With the exception of hexokinase, the partitioning of all the glycolytic enzymes to the isolated *Arabidopsis* and potato tuber mitochondria decreased upon KCN treatment, which inhibits Complex IV of the mitochondrial respiratory chain. Stimulation of respiration with CCCP (carbonyl cyanide m-chlorophenylhydrazone), which uncouples the mitochondrial electron transport from ATP synthesis, led to an increase in the association of glycolytic enzymes with these organelles. A similar result was shown by Garmier et al. (2008) who reported on GAPDH (At3g04120) and aldolase (At3g52930) which, among several proteins analyzed with DIGE, decreased their abundance in isolated mitochondria following their treatment with rotenone, the inhibitor of Complex I of the mitochondrial respiratory chain. Our findings support therefore the concept of dynamic compartmentation of glycolytic metabolons, which in turn could enable a faster response of plant metabolism to environmental and physiological changes, reflected by variation in the cytosolic redox status.

Using GapC1 and GapC2 as baits in the yeast two-hybrid screen of the cDNA library from *Arabidopsis* suspension cell cultures gave initial hints for a direct association of these enzymes with the OMM via At5g15090-encoded VDAC3. This result was in good agreement with Graham et al. (2007), who succeeded in purifying GAPDH (At1g13440) and, in addition, the At5g15090-encoded VDAC as aldolase-interaction partners in a pull-down assay with the aldolase antibody. The authors suggested that GapC can attach at the surface of mitochondria directly via VDAC or indirectly, through an interaction with aldolase. Voltage-dependent anion channel (VDAC) is a porin-type β-barrel diffusion pore, located in the OMM (Clausen et al., 2004). This channel is functionally highly conserved among vertebrates, invertebrates, fungi, and plants, but the conservation is not as evident in the primary sequence, as it is in the secondary structure deduced from that sequence (Song and Colombini, 1996; Colombini, 2004). Our identification of VDAC3 as a GapC-interaction partner in the yeast two-hybrid screen and its confirmation *in vivo* via split YFP seemed to support the idea of a direct mitochondrial localization of GapC. Surprisingly, subsequent "one-on-one" yeast two-hybrid assays, where a single yeast strain (AH109) was cotransformed with two constructs encoding bait (GapC) and prey proteins (VDAC3), shed new light on the putative interaction. Due to the autoactivation of all reporter genes by the VDAC3, the interaction between GapC isoforms and the OMM porin emerged as a so-called false positive result (**Figure 3**). This could be caused by lack of certain posttranslational modifications in yeast cells or misfolding of the plant fusion protein that potentially may alter activity or binding of the investigated proteins. Therefore, it is often proposed to switch from the tested AD- to BD-fusion protein (Solmaz, 2003). According to the manufacturer, the pGADT7 vector runs expression of fusion proteins under a strong, full-length ADH1 promoter, in contrast to pACT2 or pGBKT7. This could lead to a high level of the VDAC3-AD fusion protein in the yeast cell and its autoactivating property. Interestingly, VDAC3 expressed from pACT2 also seemed to behave unspecifically in the described experiment, although the ADH1 promoter in this vector is truncated. The autoactivation property could be possibly explained by improper folding of this hydrophobic membrane protein under certain conditions prevailing in the yeast nucleoplasm.

THE ROLE OF VDAC-BINDING PROTEINS IN INTEGRATING METABOLISM AND CELLULAR FUNCTIONS

Holtgräwe et al. (2005) screened the cDNA library from hypoxic seedlings of *Zea mays* with the cytosolic isoform of maize aldolase and isolated the mitochondrial porin VDAC1a. The authors supported these findings by a dot-blot overlay assay, suggesting an interaction of the glycolytic enzyme with mitochondria via membrane porins. With a similar approach we found that the *in vitro* interaction of FBA6 or GapC with VDAC3 is stronger, when the glycolytic enzymes are not reduced with DTT (**Figure 7**). In plants, GAPDH appears to possess a general role in stress perception due to its reactive thiol, thus possibly functioning as a sensor for increased H_2O_2 levels (Hancock et al., 2006). The mitochondrial binding of aldolase or GapC seems therefore to be redox-dependent and connected to stresses that result in redox imbalance and generation of ROS and RNS in plant cells (see Leister, 2012). Previously, oxidative modifications and concomitant inactivation of both glycolytic enzymes had been demonstrated in *in vitro* experiments (Holtgrefe et al., 2008; van der Linde et al., 2011). Through association to the mitochondrial porin in their less active or even inactive form, the glycolytic enzymes might play an alternative function by carrying a redox-signal from cytosol to mitochondria and thus possibly initiating alternative responses, in extreme cases even cell death. In this context, it is noteworthy that the interaction of GAPDH with VDAC had been shown to be inhibited by DTT treatment in human cell lines (Tarze et al., 2007). In yeast, a central role of VDAC in transducing the cellular redox-state to the nucleus has been suggested (Galganska et al., 2010). In mammals, physical binding of GAPDH to VDAC1 was suggested to induce mitochondrial membrane permeabilization and apoptosis (Tarze et al., 2007). The association of the glycolytic enzymes with mitochondrial VDAC might well be connected with initial events during induction of programmed cell death (PCD).

VDAC facilitates metabolite exchange between the organelle and the cytosol, with higher affinity to organic anions, due to its highly conducting state, referred to as the open state (Colombini, 2004). VDAC is permeable to Ca^{2+} and regulated by different ligands, such as glutamate, ATP, or NADH (Colombini, 2004; Yehezkel et al., 2006), or by interacting proteins, such as actin (Xu et al., 2001), tubulin (Rostovtseva et al., 2008),

or hexokinase (HXK; Kim et al., 2006; Balasubramanian et al., 2007). It also plays an active role in apoptosis by suppressing the release of apoptogenic factors into the cytosol, such as cytochrome *c* (Blachly-Dyson and Forte, 2001; Arzoine et al., 2009). It was demonstrated in mammalian cell lines that hexokinase can inhibit apoptosis by binding to VDAC (Azoulay-Zohar et al., 2004). Moreover, the respective cytoplasmic domains that are required for interaction with hexokinase and are involved in protection against cell death via inhibiting release of cytochrome *c*, were also found in the VDAC protein (Abu-Hamad et al., 2008). In *Arabidopsis* plants, interruption of hexokinase function activated PCD, whereas overexpression of predominantly mitochondria-associated HXK1 and HXK2 conferred enhanced resistance against H_2O_2 and α-picolinic acid (Kim et al., 2006). Interestingly, it was shown recently that not abiotic stress, such as drought, cold, salinity, but only bacterial pathogen infection leads to up-regulation of the expression level of four *Arabidopsis* VDACs (Lee et al., 2009). It becomes obvious that the VDAC-binding proteins are responsible for integration of plant metabolism and cellular functions, which might be also the case for aldolase and GapC.

REDOX-DEPEDENT BINDING OF GLYCOLYTIC ENZYMES TO THE ACTIN CYTOSKELETON *IN VITRO*

Plants generate a series of signaling molecules, that may act in controlling processes such as growth, development, response to biotic and abiotic environmental stimuli, and PCD. These molecules are Reactive Oxygen Species (ROS), for instance, which result from a turnover of oxygen by cells of aerobic organisms, but in excess may cause damage to membrane lipids, DNA and proteins (Klatt and Lamas, 2000). ROS include singlet oxygen, H_2O_2, superoxide and hydroxyl radicals that remain under control, as long as the cellular antioxidant mechanisms comprising the radical-scavenging enzymes or redox-active compounds, such as the cysteine-containing tripeptide glutathione (GSH) and ascorbate, are functional (for review see: Foyer and Noctor, 2011). The cellular redox status depends on the ratio of the oxoidized and reduced forms of an intracellular pool of redox molecules, mainly GSH. Usually, GSH is present in millimolar concentrations and in up to 100-fold excess over GSSG. The oxidation of only a small amount of GSH to GSSG may dramatically change this ratio and, in consequence, the redox status of the cell. This, in turn, may evoke protein mixed disulfide formation or even protein degradation (Klatt and Lamas, 2000). In the cytoplasm, there are many redox-sensitive proteins that form transient disulfide bonds while catalyzing the reduction of thiol groups (Cumming et al., 2004). Glutaredoxins use the abundant GSH to reduce disulfide bonds via a thiol-disulfide interchange. The reduced thioredoxins belong to the second group of antioxidant enzymes that bind to substrate proteins containing a disulfide bond, while a dithiol-disulfide exchange reaction occurs, in which the active site cysteine residues of thioredoxin are oxidized, whereas the cysteine residues in the substrate protein are reduced (Cumming et al., 2004). In a situation, when the cellular redox homeostasis, i.e., the balance between prooxidants and antioxidants, is altered because of excessive production of ROS and/or impairment of cellular antioxidant mechanisms, cytosolic cysteine residues may become susceptible to oxidation. Under non-stressed conditions, disulfide bond formation occurs primarily in the oxidizing environment of the ER in eukaryotic cells, and in chloroplasts upon darkening.

Along with ROS, Reactive Nitrogen Species (RNS) are also produced in plant cells. While the role of NO as a signaling molecule is better understood, less information is available on other RNS, but it is well known, that analogous damage due to RNS during the nitrosative stress may take place in the plant cell upon high salinity, for instance (Valderrama et al., 2007). *S*-nitrosylation of plant proteins was demonstrated by treating extracts from *Arabidopsis* cell suspension cultures with the NO-donor *S*-nitrosoglutathione (GSNO) and by exposure of plants to gaseous NO (Lindermayr et al., 2005). Among over 50 *S*-nitrosylated proteins, stress-related, redox-related, signaling/regulating, cytoskeleton, as well as metabolic proteins were detected in both approaches. With respect to the present study, interesting *S*-nitrosothionylated targets were tubulin α and β, actin isoform ACT2/7, and the glycolytic enzymes GAPDH, aldolase, triose-P isomerase, phosphoglycerate kinase, and enolase. Interestingly, S-glutathionylation of both GapC isoforms, as well as aldolase, enolase, sucrose synthase, and cytoskeletal components – ACT2/7, tubulin α and β – were also shown to occur in *Arabidopsis* suspension cultures upon treatment with the oxidant tert-butylhydroperoxide (Dixon et al., 2005). NO is assumed to play a role in signaling also in plants (Moreau et al., 2010). Moreover, NO signaling has been proposed to involve posttranslational modification of cytoskeletal elements in many plant stress response and developmental processes (Yemets et al., 2011). The experimental increase of NO levels in cells of maize roots was shown to reversibly impact the actin cytoskeleton assembly and its organization (Kasprowicz et al., 2009). ROS signals were also implicated in actin reorganization and PCD in pollen tubes during self-incompatibility response (Wilkins et al., 2011). NO is also known as a multi-faceted signaling molecule that acts in many cellular processes, such as stomatal closure, seed germination, root development, senescence, flowering time, activation of defense-related genes, and hypersensitive cell death (Wang et al., 2006).

Posttranslational modifications are of great interest for the protein–protein interaction events. Hara et al. (2005), for instance, demonstrated that before human GAPDH reaches the nucleus, it undergoes *S*-nitrosylation, which triggers its interaction with Siah1 and enables the nuclear translocation of GAPDH. In response to environmental fluctuations and stressors, the complex regulation of metabolic enzymes may function through posttranslational modifications that can affect enzymatic activity, intracellular localization, protein–protein interactions, and stability (Huber and Hardin, 2004). Therefore, a new issue of stress-induced covalent modifications of the enzyme appear to be crucial for the microcompartmentation events that are involved in the regulation of many cellular processes, in particular in pathophysiology (Marozkina and Gaston, 2012). Interestingly, NO might have also impact on the actin protein directly or on actin-binding proteins (Kasprowicz et al., 2009). In fact, upon nitrosylation with GSNO, GapC was found in a pellet of filamentous rabbit actin, but when it was reduced with DTT, it did not interact with F-actin

and remained soluble (**Figure 5**, fourth lane). Under these conditions, FBA6 was not interacting with F-actin, as if there were a competition for a binding site at F-actin. Moreover, nitrosylated, as well as glutathionylated GapC and FBA6 together caused bundling of actin filaments that was reversible upon reduction (**Figure 6**). The incorporation of NO, as well as glutathione upon formation of a mixed disulfide could be shown for *Arabidopsis* GapC (Holtgrefe et al., 2008) and aldolase (van der Linde et al., 2011). The reactive cysteine residues in the active site of both *Arabidopsis* GapC1 and GapC2 isoforms were shown by Holtgrefe et al. (2008) as susceptible to thiol modification and oxidation. A similar bahaviour was described for cytosolic aldolase isoforms (van der Linde et al., 2011). The addition of GSSG and GSNO was shown to inactivate these enzymes, and this inactivation was fully or at least partially reversible upon addition of DTT. These results indicate that GapC and aldolase might overtake a new role as actin bundling proteins in their inactive form. Since Schmitz and Bereiter-Hahn (2002) did not find any correlation in cytoskeletal association of human GAPDH in presence and absence of NO, they proposed that the association of GAPDH to stress fibers in human cells deprived of serum is unlikely to have a general function, such as to create a glycolytic microcompartment or to allow an enhanced glycolytic flux via metabolic channeling (Knull and Walsh, 1992; Al-Habori, 1995; Masters, 1996). Instead, Schmitz and Bereiter-Hahn (2002) suggested that the cytoskeletal association of GAPDH upon serum depletion might serve initiating cytoskeletal rearrangements during apoptosis, which is induced by prolonged serum withdrawal. In plants, there is also evidence that rearrangement of the cytoskeleton is actively involved in signaling the need for PCD, not only as a consequence of this event occurring under stress and during development (for review see: Smertenko and Franklin-Tong, 2011). A binding and bundling function is conceivable for *Arabidopsis* GapC and aldolase upon oxidizing conditions, occurring when plants are exposed to biotic or abiotic stress. Regulation of the cytoskeletal reorganization upon binding of GapC and aldolase in plants remains to be elucidated in future investigations.

ACTIN-BINDING REGION IN ALDOLASE AND GAPDH

The actin-binding sites of aldolase and GAPDH have been investigated in the animal model using peptide binding and site-directed mutagenesis (Humphreys et al., 1986; O'Reilly and Clarke, 1993; Wang et al., 1996), as well as by a Brownian Dynamics approach which underlines the ionic nature of these interactions (Forlemu et al., 2011). It seems indeed that the contact sites of the interactions carry a high number of charged amino acids, which occur in clusters over the whole sequences of actin (mainly negatively charged Glu and Asp residues), aldolase (Lys residues at the C-terminus), and GAPDH (both positively and negatively charged Lys, Glu, and Asp residues highly accumulating in the N-terminal half of the sequence; Forlemu et al., 2011). Since actin and the glycolytic enzymes are highly conserved in all organisms, the same pattern of charge distribution at largely conserved positions is apparent in the *Arabidopsis* homologs (**Figure 8**). Therefore, it can be assumed that binding of aldolase and GapC1 in *Arabidopsis* takes place in a similar manner. Taking into account the Cys modifications that lead to inactivation of cytosolic aldolase (van der Linde et al., 2011) and GAPDH (Holtgrefe et al., 2008), the intensity of the interaction might well be influenced, resulting in the differential binding properties described here. The S-glutathionylation of Cys-374 (Dalle-Donne et al., 2003) and the disulfide formation between Cys-285 and Cys-374 of actin (Farah and Amberg, 2007) have been implicated in being an essential part of oxidative stress sensing in human and yeast cells, respectively. In proteomic analyses to identify potentially *S*-nitrosylated plant proteins, among many others also GAPDH, aldolase, and actin were identified (Lindermayr et al., 2005). The importance of posttranslational modifications to carefully orchestrate protein–protein interactions in larger protein ensembles, by influencing the strength of the interactions within a functional module, has been put forward by Stein et al. (2009). Such dynamic interactions are of particular importance in transient microcompartments, as occurring in signaling processes, e.g., initiated by NO (Marozkina and Gaston, 2012). Future work with mutated protein constructs, with either Cys residues or charges modified in the critical regions of the proteins, will allow to study the effect of changed surface properties on the affinities *in vitro* and *in vivo*.

PREDICTIONS FROM DATABASES

Many databases are available with results from analyses with respect to putative protein–protein interactions in all organisms. A recent attempt has been made to compile all this information concerning the cellular networks for *A. thaliana* in one single database, thus combining knowledge coming from many different, experimental approaches, by creating the interactive web tool ANAP (*Arabidopsis* Network Analysis Pipeline; Wang et al., 2012) and similar databases. ANAP compiles more than 200,000 interaction pairs from the various sources, whereby a large number of the interactions are assumed from coexpression data. Only in some of the cases, biochemical investigations have followed up such putative interactions. From this database, we have extracted information concerning the candidates in focus in the present study (**Table 1**). Not in all cases interactions were found for the identical isoforms, then also some closely related isoforms are included

Table 1 | Predicted and experimentally verified interactions between aldolase, GAPDH, actin and VDAC.

	ACT8	FBA4	FBA6	GapC1	VDAC1	VDAC2	VDAC3
ACT8			A	A	A		
FBA4			B, C, D	B, C			
FBA6	A	B, C, D		A, B, C	A	A	A
GapC1	A	B, C	A, B, C		A	A	A
VDAC1	A		A	A		A	A, C, E
VDAC2			A	A	A		
VDAC3			A	A	A, C, E		

The ANAP network analysis tool was used to compile evidences for interactions deduced from various types of experiments or setups. A, Coexpression; B, Inferred by curator; C, Interologs mapping; D, Phylogenetic profile; E, Predicted text mining. The gray background indicates interaction partners confirmed experimentally in this work.

into the table. But the overall picture underlines the interactions between aldolase, GAPDH, VDAC, and actin investigated here. Data from databases (source for evidence is specified by the letters A–E) in combination with our experimental *in vivo* and *in vitro* findings (shaded in gray) suggest a model, where the transient formation of a contact between mitochondria (via VDAC) and the actin cytoskeleton is achieved by interactions with the glycolytic enzymes aldolase and GAPDH. The dynamic rearrangement in the cytosol is thought to occur upon redox-changes as part of a signal transduction chain.

CONCLUSIONS AND FUTURE PERSPECTIVES

Actin dynamics and redox-changes are involved in many stress and developmental processes (for review see: Yemets et al., 2011). Therefore, the restructuring of the actin cytoskeleton, association of VDAC-binding proteins at mitochondria, possibly leading to changed functions, such as induction of PCD, and the transfer of the glycolytic enzymes to the nucleus, are potential steps in a complex signal transduction network (for review see: Scheibe and Dietz, 2012). The term "moonlighting" reflects the phenomenon of independent, non-catalytic functions that a well known catalytic protein may possess additionally, due to separate functional domains (Moore, 2004). These multiple functions could be attained as a consequence of changes in the cellular localization of a protein, its expression by different cell types, its oligomeric state, or the cellular concentration of a ligand, substrate, cofactor or product (Jeffery, 1999). Novel unexpected features and variable subcellular locations have already been revealed for the mammalian GAPDH (Hara et al., 2006; Sirover, 2011; Tristan et al., 2011). In plants, the phenomenon of moonlighting functions of the glycolytic enzymes is yet to be investigated in more detail. As redox-changes are now discovered to occur – at least transiently – in all cell compartments in all organisms, any redox-challenge imposed on the cell can be transformed into a specific thiol modification pattern, finally leading to the required response and to acclimation (Spadaro et al., 2010). It is, however, likely that this dynamic level of regulation, as suggested here by the observations *in vivo* and *in vitro*, is even more important in photoautotrophic organisms where the conditions fluctuate dramatically (Potters et al., 2010; Scheibe and Dietz, 2012). In view of this fact, our study aims at the understanding of a dynamic protein interaction network that might be involved in retrograde redox-signal processing.

ACKNOWLEDGMENTS

This work was performed within the SFB 944 "Physiology and dynamics of cellular microcompartments" and previously within the framework of Graduate College 612 "Molecular Physiology: Interactions between Cellular Nanostructures", both financially supported by the Deutsche Forschungsgemeinschaft. The authors thank Ekkehard Neuhaus (Technical University Kaiserslautern, Germany) for his kind gift of a chimera of the mCherry protein with a transmembrane domain of rat α-2,6-sialyl-transferase. They also greatly appreciate Jörg Kudla's (University of Münster, Germany) donation of pUC-SPYNE, pUC-SPYCE, pUC-SPYNE-bZip63, and pUC-SPYCE-bZip63 vectors. The authors thank the members of the Richard Wagner group (University of Osnabrueck, Germany) for the donation of the pIVEX plasmids, the TOM40 protein and for advice. The work of various students is also acknowledged, namely of Christina Wunrau, Nora Gutsche, Ellen Voskors, Thomas Albers, Jan-Peter Heinen, Frauke Adamla.

REFERENCES

Abu-Hamad, S., Zaid, H., Israelson, A., Nahon, E., and Shoshan-Barmatz, V. (2008). Hexokinase-I protection against apoptotic cell death is mediated via interaction with the voltage-dependent anion channel-1: mapping the site of binding. *J. Biol. Chem.* 283, 13482–13490.

Al-Habori, M. (1995). Microcompartmentation, metabolic channelling and carbohydrate metabolism. *Int. J. Biochem. Cell Biol.* 27, 123–132.

Arzoine, L., Zilberberg, N., Ben-Romano, R., and Shoshan-Barmatz, V. (2009). Voltage-dependent anion channel 1-based peptides interact with hexokinase to prevent its anti-apoptotic activity. *J. Biol. Chem.* 284, 3946–3955.

Azama, K., Abe, S., Sugimoto, H., and Davies, E. (2003). Lysine-containing proteins in maize endosperm: a major contribution from cytoskeleton-associated carbohydrate-metabolizing enzymes. *Planta* 217, 628–638.

Azoulay-Zohar, H., Israelson, A., Abu-Hamad, S., and Shoshan-Barmatz, V. (2004). In self-defence: hexokinase promotes voltage-dependent anion channel closure and prevents mitochondria-mediated apoptotic cell death. *Biochem. J.* 377, 347–355.

Balasubramanian, R., Karve, A., Kandasamy, M., Meagher, R. B., and Moore, B. (2007). A role for F-actin in hexokinase-mediated glucose signaling. *Plant Physiol.* 145, 1423–1434.

Blachly-Dyson, E., and Forte, M. (2001). VDAC channels. *IUBMB Life* 52, 113–118.

Bordoli, L., Kiefer, F., Arnold, K., Benkert, P., Battey, J., and Schwede, T. (2009). Protein structure homology modeling using SWISS-MODEL workspace. *Nat. Protoc.* 4, 1–13.

Brandizzi, F., Irons, S. L., Johansen, J., Kotzer, A., and Neumann, U. (2004). GFP is the way to glow: bioimaging of the plant endomembrane system. *J. Microsc.* 214, 138–158.

Clausen, C., Ilkavets, I., Thomson, R., Philippar, K., Vojta, A., Möhlmann, T., et al. (2004). Intracellular localization of VDAC proteins in plants. *Planta* 220, 30–37.

Colombini, M. (2004). VDAC: the channel at the interface between mitochondria and the cytosol. *Mol. Cell. Biochem.* 256–257, 107–115.

Cumming, R. C., Andon, N. L., Haynes, P. A., Park, M., Fischer, W. H., and Schubert, D. (2004). Protein disulfide bond formation in the cytoplasm during oxidative stress. *J. Biol. Chem.* 279, 21749–21758.

Dalle-Donne, I., Giustarini, D., Rossi, R., Colombo, R., and Milzani, A. (2003). Reversible S-glutathionylation of Cys374 regulates actin filament formation by inducing structural changes in the actin molecule. *Free Radic. Biol. Med.* 34, 23–32.

Damari-Weissler, H., Ginzburg, A., Gidoni, D., Mett, A., Krassovskaya, I., Weber, A. P. M., et al. (2007). Spinach SoHXK1 is a mitochondria-associated hexokinase. *Planta* 226, 1053–1058.

Dixon, D. P., Skipsey, M., Grundy, N. M., and Edwards, R. (2005). Stress-induced protein S-glutathionylation in *Arabidopsis*. *Plant Physiol.* 138, 2233–2244.

Farah, M. E., and Amberg, D. C. (2007). Conserved actin cysteine residues are oxidative stress sensors that can regulate cell death in yeast. *Mol. Biol. Cell* 18, 1359–1365.

Fernie, A. R., Carrari, F., and Sweetlove, L. J. (2004). Respiratory metabolism: glycolysis, the TCA cycle and mitochondrial electron transport. *Curr. Opin. Plant Biol.* 7, 254–261.

Forlemu, N. Y., Njabon, E. N., Carlson, K. L., Schmidt, E. S., Waingeh, V. F., and Thomasson, K. A. (2011). Ionic strength dependence of F-actin and glycolytic enzyme associations: a Brownian dynamics simulations approach. *Proteins* 79, 2813–2827.

Foyer, C. H., and Noctor, G. (2011). Ascorbate and glutathione: the heart of the redox hub. *Plant Physiol.* 155, 2–18.

Galganska, H., Karachitos, A., Wojtkowska, M., Stobienia, O., Budzinska, M., and Kmita, H. (2010). Communication between mitochondria and nucleus: putative role of VDAC in reduction/oxidation mechanism. *Biochim. Biophys. Acta* 1797, 1276–1280.

Garmier, M., Carroll, A. J., Delannoy, E., Vallet, C., Day, D. A., Small, I. D., et al. (2008). Complex I dysfunction redirects cellular and mitochondrial metabolism in *Arabidopsis*. *Plant Physiol.* 148, 1324–1341.

Giegé, P., Heazlewood, J. L., Roessner-Tunali, U., Millar, A. H., Fernie, A. R., Leaver, C. J., et al. (2003). Enzymes of glycolysis are functionally associated with the mitochondrion in *Arabidopsis* cells. *Plant Cell* 15, 2140–2151.

Graham, J. W. A., Williams, T. C. R., Morgan, M., Fernie, A. R., Ratcliffe, R. G., and Sweetlove, L. J. (2007). Glycolytic enzymes associate dynamically with mitochondria in response to respiratory demand and support substrate channeling. *Plant Cell* 19, 3723–3738.

Hameister, S., Becker, B., Holtgrefe, S., Strodtkötter, I., Linke, V., Backhausen, J. E., et al. (2007). Transcriptional regulation of NADP-dependent malate dehydrogenase: comparative genetics and identification of DNA-binding proteins. *J. Mol. Evol.* 65, 437–455.

Hancock, J., Desikan, R., Harrison, J., Bright, J., Hooley, R., and Neill, S. (2006). Doing the unexpected: proteins involved in hydrogen peroxide perception. *J. Exp. Bot.* 57, 1711–1718.

Hara, M. R., Agrawal, N., Kim, S. F., Cascio, M. B., Fujimuro, M., Ozeki, Y., et al. (2005). *S*-nitrosylated GAPDH initiates apoptotic cell death by nuclear translocation following Siah1 binding. *Nat. Cell Biol.* 7, 665–674.

Hara, M. R., Cascio, M. B., and Sawa, A. (2006). GAPDH as a sensor of NO stress. *Biochim. Biophys. Acta* 1762, 502–509.

Holtgräwe, D., Scholz, A., Altmann, B., and Scheibe, R. (2005). Cytoskeleton-associated, carbohydrate-metabolizing enzymes in maize identified by yeast two-hybrid-screening. *Physiol. Plant.* 125, 141–156.

Holtgrefe, S., Gohlke, J., Starmann, J., Druce, S., Klocke, S., Altmann, B., et al. (2008). Regulation of plant cytosolic glyceraldehyde 3-phosphate dehydrogenase isoforms by thiol modifications. *Physiol. Plant.* 133, 211–228.

Hu, C. D., Chinenov, Y., and Kerppola, T. K. (2002). Visualization of interactions among bZIP and Rel family proteins in living cells using bimolecular fluorescence complementation. *Mol. Cell* 9, 789–798.

Huber, S. C., and Hardin, S. C. (2004). Numerous posttranslational modifications provide opportunities for the intricate regulation of metabolic enzymes at multiple levels. *Curr. Opin. Plant Biol.* 7, 318–322.

Humphreys, L., Reid, S., and Masters, C. (1986). Studies on the topographical localization of the binding sites for substrate and for actin on the enzymes, glyceraldehydephosphate dehydrogenase and phosphofructokinase. *Int. J. Biochem.* 18, 445–451.

Ito, H., Iwabuchi, M., and Ogawa, K. (2003). The sugar-metabolic enzymes aldolase and triosephosphate isomerase are targets of glutathionylation in *Arabidopsis thaliana*: detection using biotinylated glutathione. *Plant Cell Physiol.* 44, 655–660.

Jeffery, C. J. (1999). Moonlighting proteins. *TIBS* 24, 8–11.

Kasprowicz, A., Szuba, A., Volkmann, D., Baluska, F., and Wojtaszek, P. (2009). Nitric oxide modulates dynamic actin cytoskeleton and vesicle trafficking in a cell type-specific manner in root apices. *J. Exp. Bot.* 60, 1605–1617.

Kim, M., Lim, J. H., Ahn, C. S., Park, K., Kim, G. T., Kim, W. T., et al. (2006). Mitochondria-associated hexokinases play a role in the control of programmed cell death in *Nicotiana benthamiana*. *Plant Cell* 18, 2341–2355.

Klatt, P., and Lamas, S. (2000). Regulation of protein function by S-glutathiolation in response to oxidative and nitrosative stress. *Eur. J. Biochem.* 267, 4928–4944.

Knull, H. R., and Walsh, J. L. (1992). Association of glycolytic enzymes with the cytoskeleton. *Curr. Top. Cell. Regul.* 33, 15–30.

Kolonin, M. G., Zhong, J., and Finley, R. L. (2000). Interaction mating methods in two-hybrid system. *Meth. Enzymol.* 328, 26–46.

Kost, B., Spielhofer, P., and Chua, N.-H. (1998). A GFP-mouse talin fusion protein labels plant actin filaments in vivo and visualizes the actin cytoskeleton in growing pollen tubes. *Plant J.* 16, 393–401.

Lee, S. M., Hoang, M. H. T., Han, H. J., Kim, H. S., Lee, K., Kim, K. E., et al. (2009). Pathogen inducible voltage-dependent anion channel (AtVDAC) isoforms are localized to mitochondria membrane in *Arabidopsis*. *Mol. Cells* 27, 321–327.

Leister, D. (2012). Retrograde signaling in plants: from simple to complex scenarios. *Front. Plant Sci.* 3:135. doi:10.3389/fpls.2012.00135

Lindermayr, C., Saalbach, G., and Durner, J. (2005). Proteomic identification of S-nitrosylated proteins in *Arabidopsis*. *Plant Physiol.* 137, 921–930.

Marmagne, A., Rouet, M.-A., Ferro, M., Rolland, N., Alcon, C., Joyard, J., et al. (2004). Identification of new intrinsic proteins in *Arabidopsis* plasma membrane proteome. *Mol. Cell. Proteomics* 3.7, 675–691.

Marozkina, N. V., and Gaston, B. (2012). *S*-Nitrosylation signaling regulates cellular protein interactions. *Biochim. Biophys. Acta* 1820, 722–729.

Masters, J. (1996). "On the role of the cytoskeleton in metabolic compartmentation," in *The Cytoskeleton: Role in Cell Physiology*, Vol. 2, eds J. Hesketh and I. Pryme (Greenwich: JAI Press Inc.), 1–30.

Migneault, I., Dartiguenave, D., Bertrand, M. J., and Waldron, K. C. (2004). Glutaraldehyde: behavior in aqueous solution, reaction with proteins, and application to enzyme crosslinking. *BioTechniques* 37, 790–802.

Moore, B. D. (2004). Bifunctional and moonlighting enzymes: lighting the way to regulatory control. *Trends Plant Sci.* 9, 221–228.

Moreau, M., Lindermayr, C., Durner, J., and Klessig, D. F. (2010). NO synthesis and signaling in plants – where do we stand? *Physiol. Plant.* 138, 372–383.

Narayanaswamy, R., Levy, M., Tsechansky, M., Stovall, G. M., O'Connell, J. D., Mirrielees, J., et al. (2009). Widespread reorganization of meta-bolic enzymes into reversible assemblies upon nutrient starvation. *Proc. Natl. Acad. Sci. U.S.A.* 106, 10147–10152.

Nemeth, K., Salchert, K., Putnoky, P., Bhalerao, R., Koncz-Kalman, Z., Stankovic-Stangeland, B., et al. (1998). Pleiotropic control of glucose and hormone responses by PRL1 an nuclear WD protein in *Arabidopsis*. *Genes Dev.* 12, 3059–3073.

O'Reilly, G., and Clarke, F. (1993). Identification of an actin binding region in aldolase. *FEBS Lett.* 321, 69–72.

Ouporov, I. V., Knull, H. R., and Thomasson, K. A. (1999). Brownian dynamics simulations of interactions between aldolase and G- or F-actin. *Biophys. J.* 76, 17–27.

Ovadi, J., and Saks, V. (2004). On the origin of intracellular compartmentation and organized metabolic systems. *Mol. Cell. Biochem.* 256–257, 5–12.

Ovadi, J., and Srere, P. A. (1996). Metabolic consequences of enzyme interactions. *Cell Biochem. Funct.* 14, 249–258.

Plaxton, W. C. (1996). The organization and regulation of plant glycolysis. *Annu. Rev. Plant Physiol. Plant Mol. Biol.* 47, 185–214.

Potters, G., Horemans, N., and Jansen, M. A. K. (2010). The cellular redox state in plant stress biology – a charging concept. *Plant Physiol. Biochem.* 48, 292–300.

Rostovtseva, T. K., Sheldon, K. L., Hassanzadeh, E., Monge, C., Saks, V., Bezrukov, S. M., et al. (2008). Tubulin binding blocks mitochondrial voltage-dependent anion channel and regulates respiration. *Proc. Natl. Acad. Sci. U.S.A.* 105, 18746–18751.

Saint-Jore, C. M., Evins, J., Batoko, H., Brandizzi, F., Moore, I., and Hawes, C. (2002). Redistribution of membrane proteins between the Golgi apparatus and endoplasmic reticulum in plants is reversible and not dependent on cytoskeletal networks. *Plant J.* 29, 661–678.

Sano, T., Higaki, T., Oda, Y., Hayashi, T., and Hasezawa, S. (2005). Appearance of actin microfilament "twin peaks" in mitosis and their function in cell plate formation, as visualized in tobacco BY-2 cells expressing GFP-fimbrin. *Plant J.* 44, 595–605.

Santoni, V., Rouquie, D., Doumas, P., Mansion, M., Boutry, M., Degand, H., et al. (1998). Use of a proteome strategy for tagging proteins present at the plasma membrane. *Plant J.* 16, 633–641.

Scheibe, R., and Dietz, K.-J. (2012). Reduction-oxidation network for flexible adjustment of cellular metabolism in photoautotrophic cells. *Plant Cell Environ.* 35, 202–216.

Schindler, R., Weichselsdorfer, E., Wagner, O., and Bereiter-Hahn, J. (2001). Aldolase-localization in cultured cells: cell-type and substrate-specific regulation of cytoskeletal associations. *Biochem. Cell Biol.* 79, 719–728.

Schmitz, H. D., and Bereiter-Hahn, J. (2002). Glyceraldehyde-3-phosphate dehydrogenase associates with actin filaments in serum deprived NIH 3T3 cells only. *Cell Biol. Int.* 26, 155–164.

Seidel, T., Kluge, C., Hanitzsch, M., Ross, J., Sauer, M., Dietz, K.-J., et al. (2004). Colocalization and FRET-analysis of subunits c and a of the vacuolar H+-ATPase inliving plant cells. *J. Biotechnol.* 112, 165–175.

Shaner, N. C., Campbell, R. E., Steinbach, P. A., Giepmans, B. N.,

Palmer, A. E., and Tsien, R. Y. (2004). Improved monomeric red, orange and yellow fluorescent proteins derived from Discosoma sp. red fluorescent protein. *Nat. Biotechnol.* 22, 1567–1572.

Sirover, M. A. (1999). New insights into an old protein: the functional diversity of mammalian glyceraldehyde-3-phosphate dehydrogenase. *Biochim. Biophys. Acta* 1432, 159–184.

Sirover, M. A. (2005). New nuclear functions of the glycolytic protein, glyceraldehyde-3-phosphate dehydrogenase, in mammalian cells. *J. Cell. Biochem.* 95, 45–52.

Sirover, M. A. (2011). On the functional diversity of glyceraldehyde-3-phosphate dehydrogenase: biochemical mechanisms and regulatory control. *Biochim. Biophys. Acta* 1810, 741–751.

Smertenko, A., and Franklin-Tong, V. E. (2011). Organisation and regulation of the cytoskeleton in plant programmed cell death. *Cell Death Differ.* 18, 1263–1270.

Solmaz, S. (2003). Yeast two hybrid assay: a fishing tale. *BioTeach. J.* 1, 81–87.

Somers, M., Engelborghs, Y., and Baert, J. (1990). Analysis of the binding of glyceraldehyde-3-phosphate dehy-drogenase to microtubules, the mechanism of bundle formation and the linkage effect. *Eur. J. Biochem.* 193, 437–444.

Song, J., and Colombini, M. (1996). Indications of a common folding pattern for VDAC channels from all sources. *J. Bioenerg. Biomembr.* 28, 153–161.

Spadaro, D., Yun, B.-W., Spoel, S. H., Chu, C., Wang, Y.-Q., and Loake, G. J. (2010). The redox switch: dynamic regulation of protein function by cysteine modifications. *Physiol. Plant.* 138, 360–371.

Stein, A., Pache, R. A., Bernadó, P., Pons, M., and Aloy, P. (2009). Dynamic interactions of proteins in complex networks: a more structured view. *FEBS J.* 276, 5390–5405.

Tarze, A., Deniaud, A., Le Bras, M., Maillier, E., Molle, D., Larochette, N., et al. (2007). GAPDH, a novel regulator of the pro-apoptotic mitochondrial membrane permeabilization. *Oncogene* 26, 2606–2620.

Tristan, C., Shahani, N., Sedlak, T. W., and Sawa, A. (2011). The diverse functions of GAPDH: Views from different subcellular compartments. *Cell. Signal.* 23, 317–323.

Valderrama, R., Corpas, F. J., Carreras, A., Fernandez-Ocana, A., Chaki, M., Luque, F., et al. (2007). Nitrosative stress in plants. *FEBS Lett.* 581, 453–461.

van der Linde, K., Gutsche, N., Leffers, H.-M., Lindermayr, C., Müller, B., Holtgrefe, S., et al. (2011). Regulation of plant cytosolic aldolase functions by redox-modifications. *Plant Physiol. Biochem.* 49, 946–957.

Voss, I., Koelmann, M., Wojtera, J., Holtgrefe, S., Kitzmann, C., Backhausen, J. E., et al. (2008). Knockout of major leaf ferredoxin reveals new redox-regulatory adaptations in *Arabidopsis thaliana*. *Physiol. Plant.* 133, 584–598.

Walsh, J. L., Keith, T. J., and Knull, H. R. (1989). Glycolytic enzyme interactions with tubulin and microtubules. *Biochim. Biophys. Acta* 999, 64–70.

Walsh, T. P., Winzor, D. J., Clarke, F. M., Masters, C. J., and Morton, D. J. (1980). Binding of aldolase to actin-containing filaments. Evidence of interaction with the regulatory proteins of skeletal muscle. *Biochem. J.* 186, 89–98.

Walter, M., Chaban, C., Schütze, K., Batistic, O., Weckerman, K., Näke, C., et al. (2004). Visualization of protein interactions in living plant cells using bimolecular fluorescence complementation. *Plant J.* 40, 428–438.

Wang, C., Marshall, A., Zhang, D., and Wilson, Z. A. (2012). ANAP: An integrated knowledge base for *Arabidopsis* protein interaction network analysis. *Plant Physiol.* 158, 1523–1533.

Wang, J., Morris, A. J., Tolan, D. R., and Pagliaro, L. (1996). The molecular nature of the F-actin binding activity of aldolase revealed with site-directed mutants. *J. Biol. Chem.* 271, 6861–6865.

Wang, Y., Yun, B. W., Kwon, E., Hong, J. K., Yoon, J., and Loake, G. J. (2006). S-Nitrosylation: an emerging redox-based post-translational modification in plants. *J. Exp. Bot.* 57, 1777–1784.

Wilkins, K. A., Bancroft, J., Bosch, M., Ings, J., Smirnoff, N., and Franklin-Tong, V. E. (2011). Reactive oxygen species and nitric oxide mediate actin reorganization and programmed cell death in the self-incompatibility response of Papaver. *Plant Physiol.* 156, 404–416.

Winkel, B. S. (2004). Metabolic channeling in plants. *Annu. Rev. Plant Biol.* 55, 85–107.

Xu, X., Forbes, J. G., and Colombini, M. (2001). Actin modulates the gating of Neurospora crassa VDAC. *J. Membr. Biol.* 180, 73–81.

Yehezkel, G., Hadad, N., Zaid, H., Sivan, S., and Shoshan-Barmatz, V. (2006). Nucleotide-binding sites in the voltage-dependent anion channel: characterization and localization. *J. Biol. Chem.* 281, 5938–5946.

Yemets, A. I., Krasylenko, Y. A., Lytvyn, D. I., Sheremet, Y. A., and Blume, Y. B. (2011). Nitric oxide signalling via cytoskeleton in plants. *Plant Sci.* 181, 545–554.

Zhong, S., Lin, Z., and Grierson, D. (2008). Tomato ethylene receptor–CTR interactions: visualization of NEVER-RIPE interactions with multiple CTRs at the endoplasmic reticulum. *J. Exp. Bot.* 59, 965–972.

Conflict of Interest Statement: The authors declare that the research was conducted in the absence of any commercial or financial relationships that could be construed as a potential conflict of interest.

Received: 12 September 2012; accepted: 30 November 2012; published online: 09 January 2013.

*Citation: Wojtera-Kwiczor J, Groß F, Leffers H-M, Kang M, Schneider M and Scheibe R (2013) Transfer of a redox-signal through the cytosol by redox-dependent microcompartmentation of glycolytic enzymes at mitochondria and actin cytoskeleton. Front. Plant Sci. **3**:284. doi: 10.3389/fpls.2012.00284*

This article was submitted to Frontiers in Plant Physiology, a specialty of Frontiers in Plant Science.

Copyright © 2013 Wojtera-Kwiczor, Groß, Leffers, Kang, Schneider and Scheibe. This is an open-access article distributed under the terms of the Creative Commons Attribution License, which permits use, distribution and reproduction in other forums, provided the original authors and source are credited and subject to any copyright notices concerning any third-party graphics etc.

APPENDIX

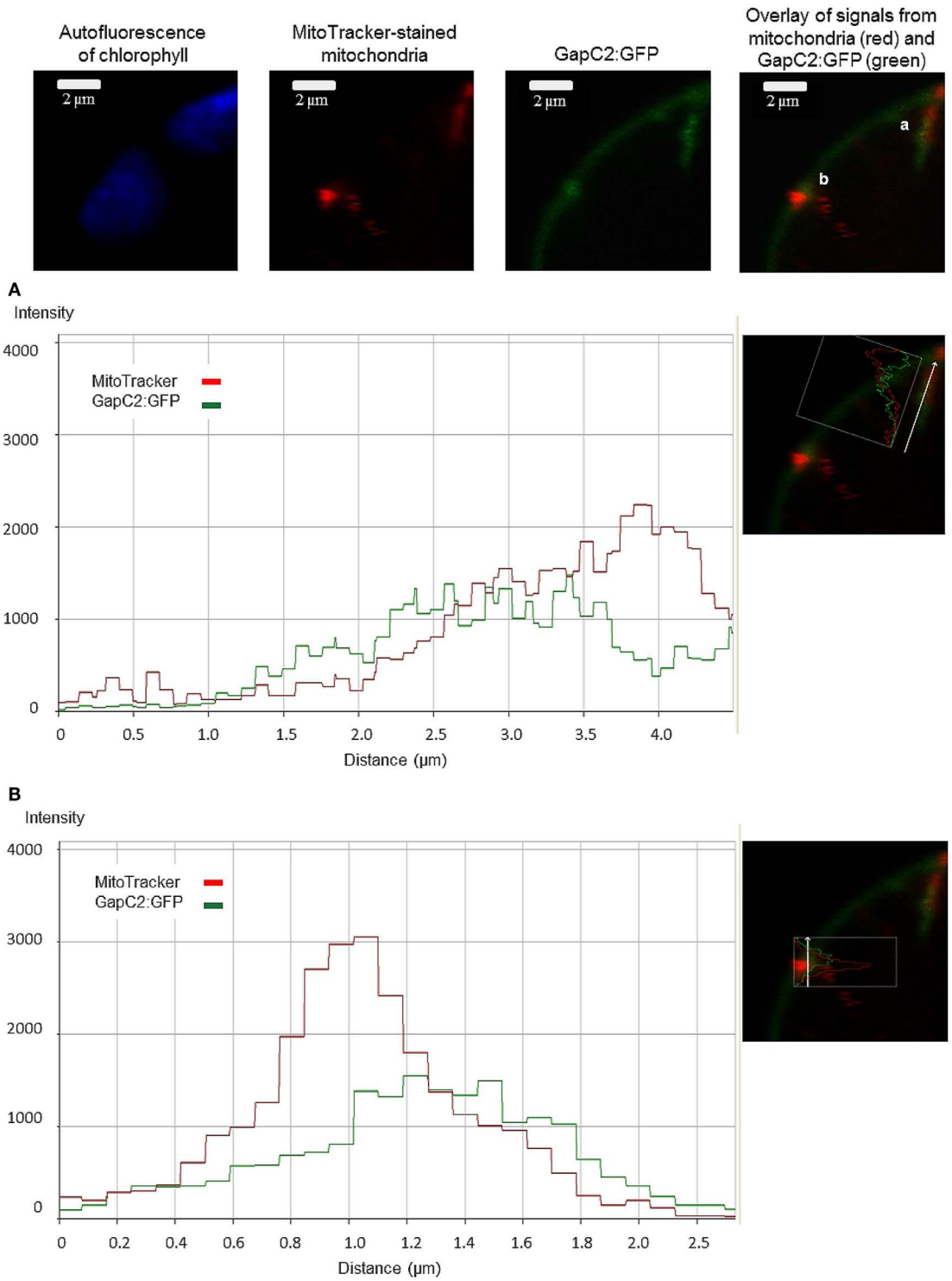

FIGURE A1 | Colocalization analysis of GAPDH (GapC2) with mitochondria. The magnified section of the protoplast expressing GapC2:GFP displays regions of a possible association of the glycolytic enzyme with the mitochondrion, stained with 50 nM MitoTracker® Orange CMTMRos (Molecular Probes). The diagrams show the colocalization analysis using fluorescence-intensity profiles of both fluorescent signals **(A,B)**.

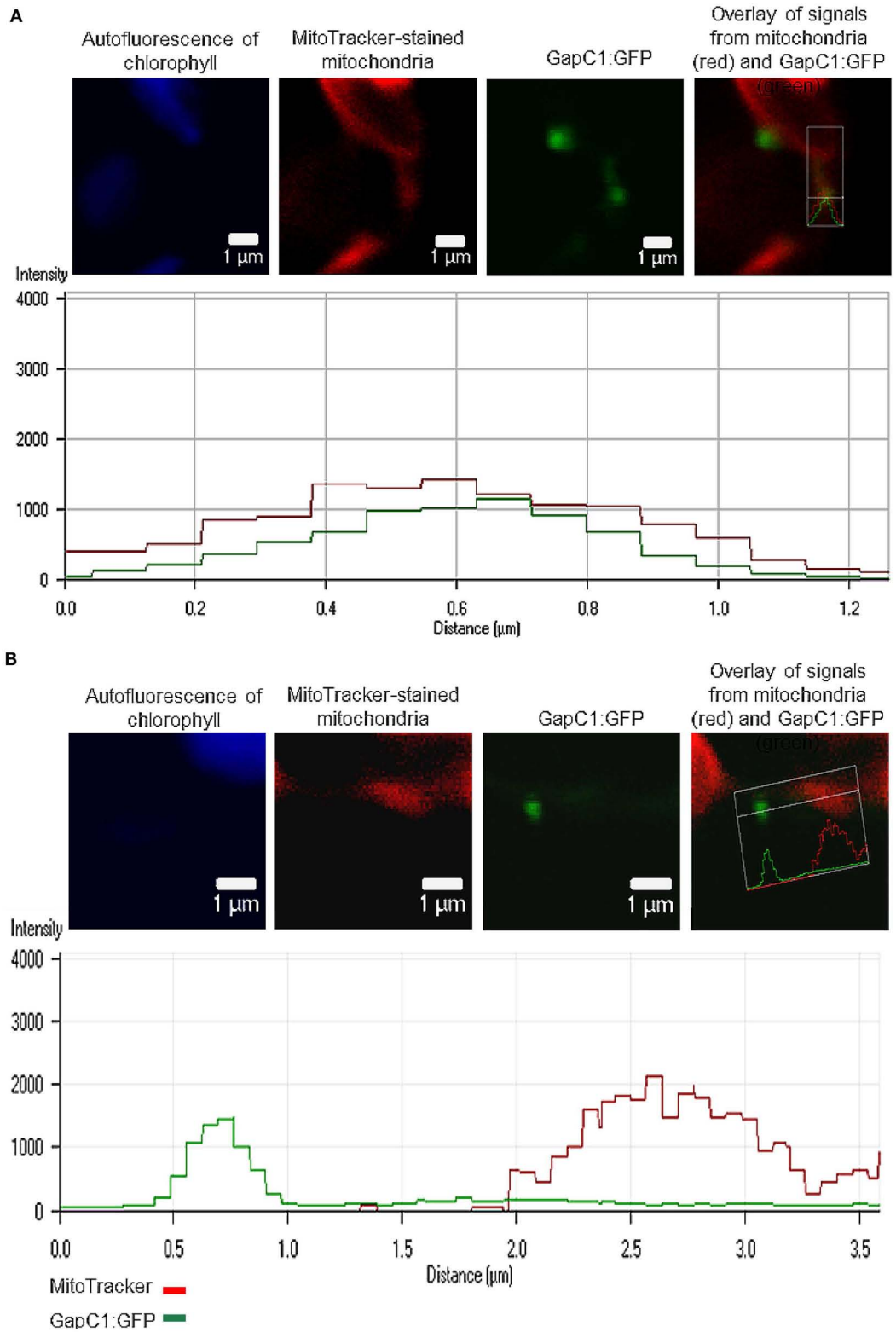

FIGURE A2 | Occasional colocalization of GAPDH (GapC1) with mitochondria. GapC1:GFP was transiently expressed in the protoplasts, isolated from Arabidopsis plants. Mitochondria were stained using 50 nMMitoTracker® Orange CMTMRos (Molecular Probes). Two regions of interest (ROI), depicted with a white frame, were magnified in order to perform a colocalization analysis by means of a fluorescence-intensity profile. One ROI displays a possible association of the glycolytic enzyme with mitochondrion **(A)**, whereas the other ROI shows no mitochondria association at the moment of visualization **(B)**.

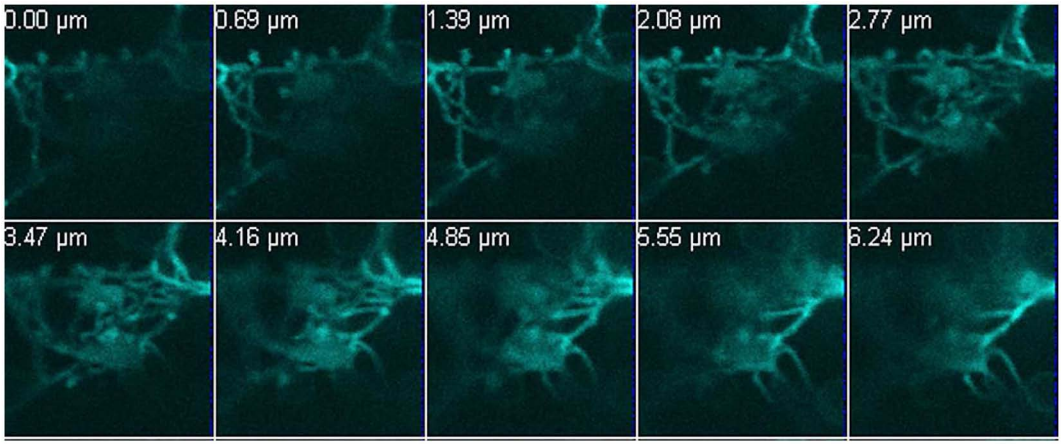

FIGURE A3 | A network formed by the fluorescently labelled GAPDH. A 13-µm deep Z-stack was performed to demonstrate the filamentous structures of GapC1:CFP in three dimensions in the examined protoplast. The appropriate scale bar is included in the **Figure 1**. The images were taken with the Confocal Laser Scanning Microscope LSM 510 META, Zeiss.

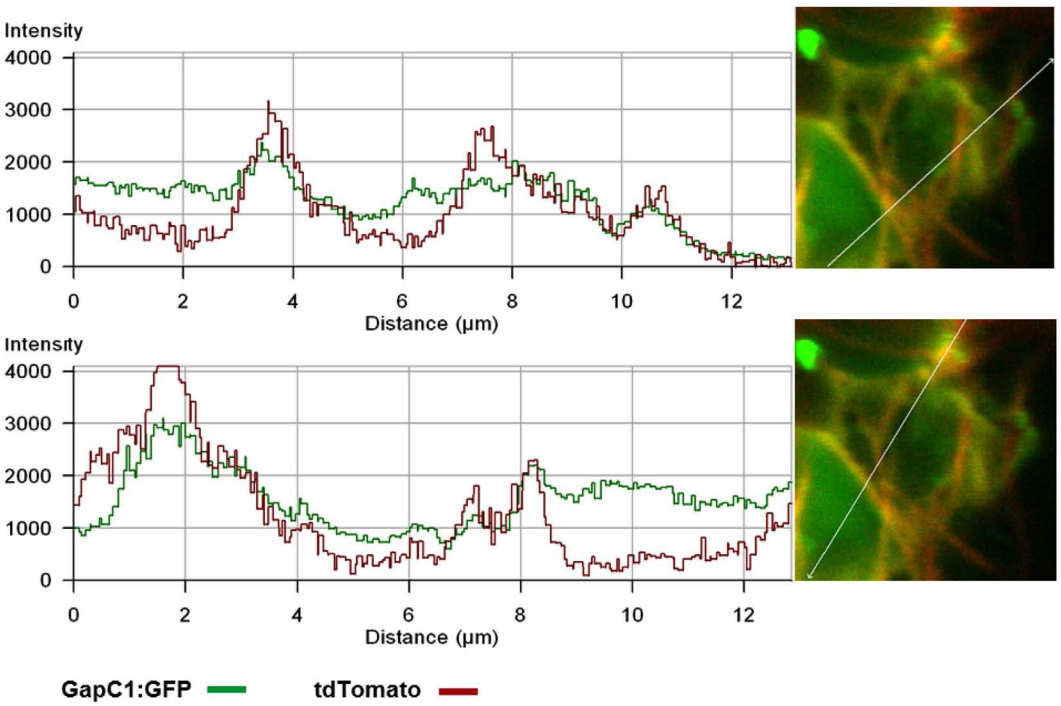

FIGURE A4 | Overlap of fluorescence emission from tdTomato-Fimbrin and GapC-GFP. Fluorescent signals of GapC1:GFP and F-actin, stained with tdTomato:AtFim1-ABD2, were analyzed with the fluorescence-intensity profile. The GapC1:GFP protein seems to bind the stained actin filaments in the plant cell, since the plotted fluorescent signals partially cover the same regions along a distance of approximately 12 µm. The diagram was performed with the Zeiss LSM 5 software.

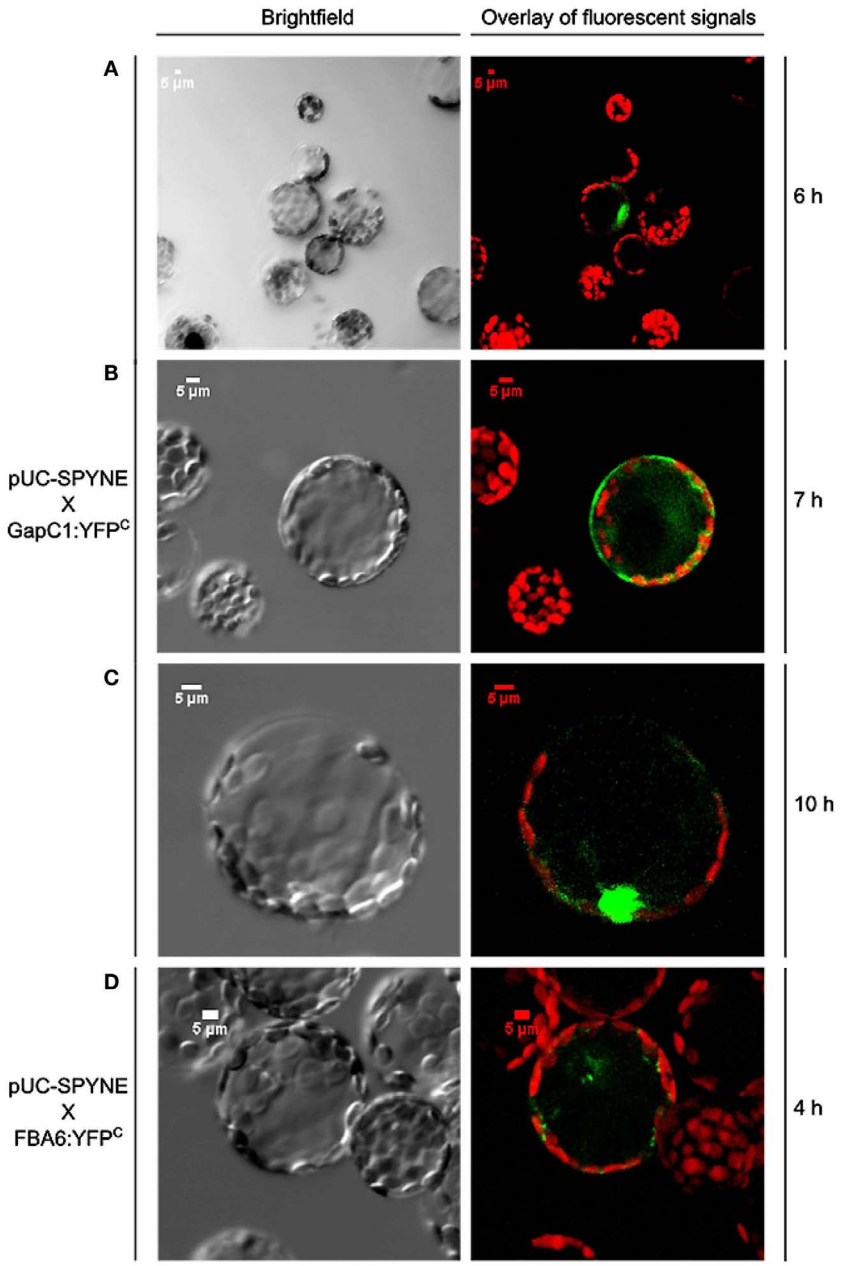

FIGURE A5 | Negative controls for BiFC experiments analyzing any colocalization of aldolase (FBA6) and GapC1. Vectors encoding the investigated proteins were cotransformed in protoplasts, isolated from leaves of A. thaliana plants. **(A-C)** is a time course of the expression of the empty vector with only the N-terminal half of YFP and GapC1 fused with the C-terminal half of YFP. In **(D)**, the same is shown for FBA6 after 4 h.

frontiers in
PLANT SCIENCE

ORIGINAL RESEARCH ARTICLE
published: 29 October 2012
doi: 10.3389/fpls.2012.00236

Evidence for a contribution of ALA synthesis to plastid-to-nucleus signaling

***Olaf Czarnecki*[1,2], *Christine Gläßer*[3], *Jin-Gui Chen*[2], *Klaus F. X. Mayer*[3] *and Bernhard Grimm*[1]*

[1] Department of Plant Physiology, Institute of Biology, Humboldt-Universität zu Berlin, Berlin, Germany
[2] Plant Systems Biology, Biosciences Division, Oak Ridge National Laboratory, Oak Ridge, TN, USA
[3] Institute of Bioinformatics and Systems Biology, German Research Center for Environmental Health, Helmholtz Zentrum München, Neuherberg, Germany

Edited by:
Tatjana Kleine, Ludwig-Maximilians-Universität München, Germany

Reviewed by:
Guillaume Pilot, Virginia Tech, USA
Felix Kessler, University of Neuchâtel, Switzerland

***Correspondence:**
Bernhard Grimm, Department of Plant Physiology, Institute of Biology, Humboldt-Universität zu Berlin, Philippstraße 13, Building 12, D-10115 Berlin, Germany.
e-mail: bernhard.grimm@biologie.hu-berlin.de

The formation of 5-aminolevulinic acid (ALA) in tetrapyrrole biosynthesis is widely controlled by environmental and metabolic feedback cues that determine the influx into the entire metabolic path. Because of its central role as the rate-limiting step, we hypothesized a potential role of ALA biosynthesis in tetrapyrrole-mediated retrograde signaling and exploited the direct impact of ALA biosynthesis on nuclear gene expression (NGE) by using two different approaches. Firstly, the *Arabidopsis gun1*, *hy1* (*gun2*), *hy2* (*gun3*), *gun4* mutants showing uncoupled NGE from the physiological state of chloroplasts were thoroughly examined for regulatory modifications of ALA synthesis and transcriptional control in the nucleus. We found that reduced ALA-synthesizing capacity is common to analyzed *gun* mutants. Inhibition of ALA synthesis by gabaculine (GAB) that inactivates glutamate-1-semialdehyde aminotransferase and ALA feeding of wild-type and mutant seedlings corroborate the expression data of *gun* mutants. Transcript level of photosynthetic marker genes were enhanced in norflurazon (NF)-treated seedlings upon additional GAB treatment, while enhanced ALA amounts diminish these RNA levels in NF-treated wild-type in comparison to the solely NF-treated seedlings. Secondly, the impact of posttranslationally down-regulated ALA synthesis on NGE was investigated by global transcriptome analysis of GAB-treated *Arabidopsis* seedlings and the *gun4-1* mutant, which is also characterized by reduced ALA formation. A common set of significantly modulated genes was identified indicating ALA synthesis as a potential signal emitter. The over-represented gene ontology categories of genes with decreased or increased transcript abundance highlight a few biological processes and cellular functions, which are remarkably affected in response to plastid-localized ALA biosynthesis. These results support the hypothesis that ALA biosynthesis correlates with retrograde signaling-mediated control of NGE.

Keywords: ALA synthesis, retrograde signaling, gabaculine, *gun* mutants, microarray analysis

INTRODUCTION

Organellar genes translocated to the nucleus of host organisms during the process of evolution remain necessary for the function of organelles that now support important processes within their hosts. For example, several thousand nucleus-encoded proteins are required for chloroplast biogenesis, including the formation of complexes consisting of both nuclear and plastid-encoded subunits (Timmis et al., 2004). This bigenome-dependent assembly of functional protein complexes requires a finely tuned balance of anterograde and retrograde control. While anterograde control determines organellar metabolism and gene expression, nuclear gene expression (NGE) are under retrograde control responding to organelles. However, detailed knowledge about signaling molecules and pathways is still lacking (Papenbrock and Grimm, 2001; Brusslan and Peterson, 2002; Surpin et al., 2002; Gray et al., 2003; Pfannschmidt et al., 2003; Baier and Dietz, 2005; Beck and Grimm, 2006; Pogson et al., 2008; Kleine et al., 2009; Jung and Chory, 2010).

Physiological and genetic analyses of NGE modulation indicate that tetrapyrrole-mediated signaling may be an important mechanism for retrograde control over NGE. Down-regulation of individual enzymatic steps of tetrapyrrole biosynthesis (**Figure 1**), as a result of either gene silencing or enzyme inhibitors, has been shown to reduce the expression of a *LHCB* gene encoding a light-harvesting chlorophyll (Chl)-binding protein of photosystem II in a number of studies. For example, in initial experiments, the iron-chelating 2,2-dipyridyl was applied to light-exposed cultures of the green algae *Chlamydomonas reinhardtii*, resulting in accumulation of protoporphyrin IX (Proto) and Mg protoporphyrin IX monomethylester (MgProtoME) and, concomitantly, in reduced *LHCB* mRNA content (Johanningmeier and Howell, 1984). Later

Abbreviations: ALA, 5-aminolevulinic acid; Chl, chlorophyll; fw, fresh weight; GAB, gabaculine; GluTR, glutamyl tRNA reductase; GO, gene ontology; GSAT, glutamate 1-semialdehyde aminotransferase; MgProto, Mg protoporphyrin IX; MgProtoME, Mg protoporphyrin IX monomethylester; NF, norflurazon; NGE, nuclear gene expression; Pchlide, protochlorophyllide; PhANGs, photosynthesis-associated nuclear genes; POR, protochlorophyllide oxidoreductase; Proto, protoporphyrin IX; ROS, reactive oxygen species.

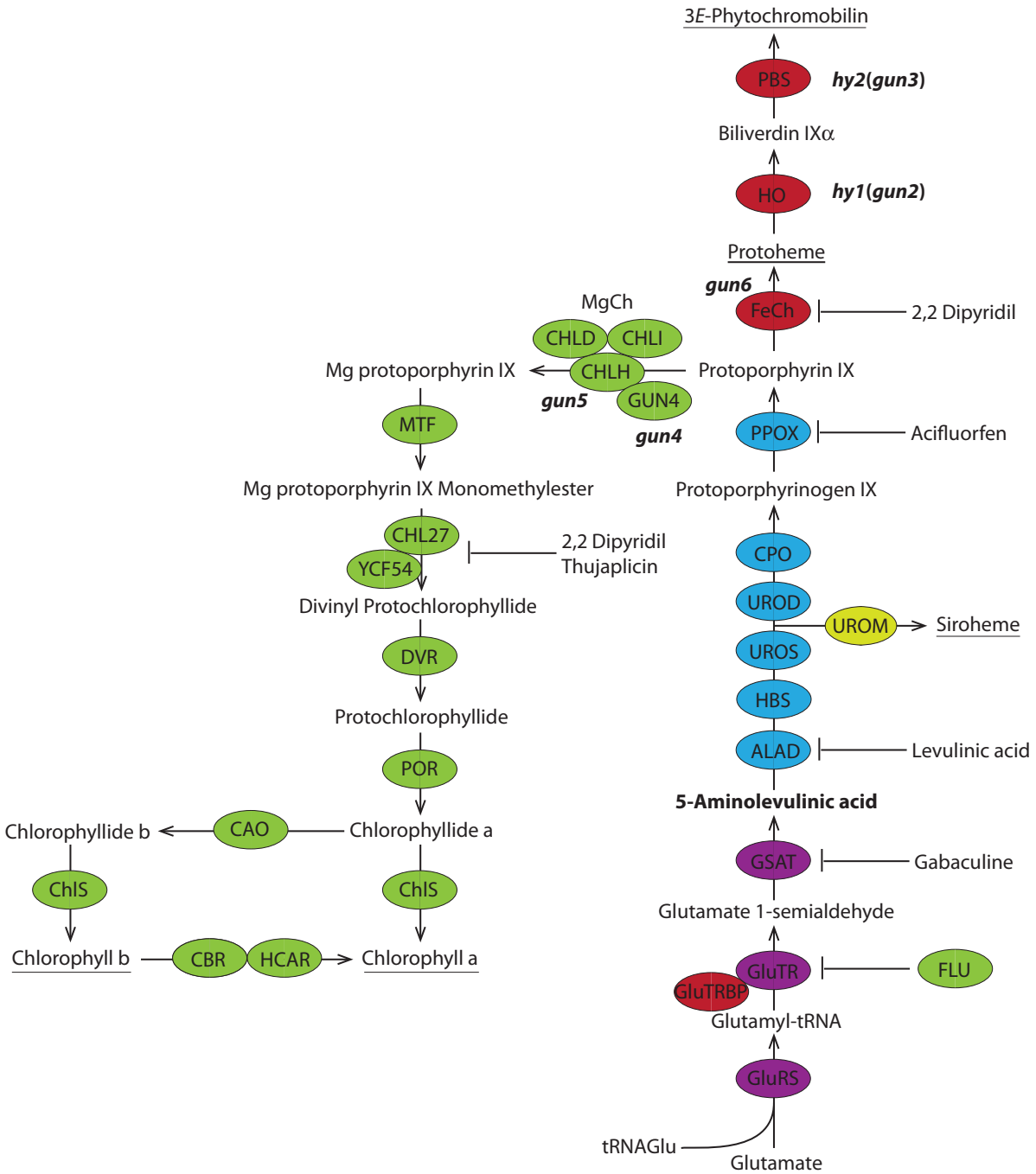

FIGURE 1 | Metabolic pathway of tetrapyrrole biosynthesis in plants. The color code comprise the five sections of the tetrapyrrole biosynthetic pathway: ALA synthesis purple, porphyrin synthesis blue, the Fe branch red, Mg branch green, siroheme synthesis yellow. The universal precursor of all tetrapyrroles 5-aminolevulinic acid (ALA) is synthesized from glutamate via a three-step reaction. ALA is further metabolized to protoporphyrin IX before the pathway branches into heme (and phytochromobilin) and chlorophyll biosynthesis. The ratio of chlorophyll a and b is balanced in the chlorophyll cycle. The end products of the pathway are underlined. Mutants of tetrapyrrole biosynthetic enzymes that play a role in plastid-to-nucleus signaling and inhibitors of certain enzymatic steps are shown. ALAD, ALA dehydratase; CAO, Chl a oxygenase; CBR, chlorophyll b reductase; ChlS, chlorophyll synthase; CPO, coproporphyrinogen III oxidase; DVR, divinyl protochlorophyllide reductase; FeCh, Fe chelatase; FLU, flourescent; GluRS, glutamyl-tRNA synthetase; GluTR, glutamyl-tRNA reductase; GluTRBP, GluTR binding protein; GSAT, glutamate-1-semialdehyde aminotransferase; HBS, hydroxymethylbilane synthase; HCAR, 7-hydroxymethyl chlorophyll a reductase; HO, heme oxygenase; MgCh, Mg chelatase; MTF, Mg protoporphyrin IX methyltransferase; PBS, phytochromobilin synthase; POR, light dependent NADPH-protochlorophyllide oxidoreductase; PPOX, protoporphyrinogen IX oxidase; UROD, uroporphyrinogen III decarboxylase; UROM, uroporphyrinogen III methyltransferase; UROS, uroporphyrinogen III synthase.

studies found increased levels of *LHCB* transcripts in dark-grown *C. reinhardtii* cultures fed with Mg porphyrin, as well as in *Chlamydomonas CHLH* and *CHLD* (**Figure 1**) deletion mutant strains where Mg porphyrin had accumulated, which underlines the correlation between Mg porphyrin-mediated signaling and NGE (Kropat et al., 1997; La Rocca et al., 2001; Vasileuskaya et al., 2004). The accumulation of MgProtoME in dark-incubated cress seedlings through inhibition by thujaplicin resulted in elevated *LHCB* mRNA content that was likely related to a metabolic response resembling light-induced control of nuclear genes for photosynthesis and plastid development (Oster et al., 1996). Last, inactivation of Mg chelatase, Mg protoporphyrin IX (MgProto) methyltransferase, and Chl synthase (**Figure 1**) resulted in altered expression of multiple nuclear-encoded genes in the tetrapyrrole biosynthesis in transgenic tobacco plants (Papenbrock et al., 2000b; Alawady and Grimm, 2005; Shalygo et al., 2009).

A mutant screen of *Arabidopsis* seedlings treated with norflurazon (NF), an inhibitor of carotenoid biosynthesis, identified components of retrograde signaling contributing to un-coupling of *LHCB* expression from chloroplast development (Susek et al., 1993). Four out of five *genomes uncoupled* (*gun*) mutants were reported to encode proteins involved in tetrapyrrole biosynthesis (**Figure 1**). *GUN2* and *GUN3,* encoding the heme oxygenase and the phytochromobilin synthase (Mochizuki et al., 2001), are allelic to *hy1* and *hy2*, respectively. The *Arabidopsis hy* mutants have been initially identified in mutant screens for deficits in light signaling (Chory et al., 1989). These mutants are phytochrome-deficient due to impaired synthesis of the chromophore phytochromobiline. *GUN4* encodes a regulator of Mg chelatase activity (Larkin et al., 2003; Peter and Grimm, 2009) and *GUN5* encodes the CHLH subunit of Mg chelatase (Mochizuki et al., 2001). *GUN1* encodes a plastid-localized protein of the pentatricopeptide-repeat protein family that acts independently of tetrapyrrole biosynthesis (Koussevitzky et al., 2007). Accumulation of MgProto was compared from wild-type, *gun5* and *gun2* and it has been proposed that due to its prevalence MgProto likely acts as a signaling molecule for the expression of *LHCB1* and other nuclear-encoded genes (Strand et al., 2003). However, in more recent studies, no clear correlation was shown between steady-state levels of MgProto and *LHCB* expression in NF-treated *Arabidopsis* seedlings. It was suggested that phenotypical differences between *gun* and wild-type seedlings, including *LHCB* expression, may be attributed to ROS-based retrograde signaling (Mochizuki et al., 2008; Moulin et al., 2008). In addition, transgenic plants overexpressing *FCI* encoding ferrochelatase I (**Figure 1**) show *gun*-like altered expression of photosynthesis-associated nuclear genes (PhANGs) highlighting heme as a potential signaling molecule in plastid-to-nucleus communication (Woodson et al., 2011).

Taken together, this evidence indicates that tetrapyrrole intermediates, such as Mg porphyrins, and endproducts, such as heme, are potential emitters of plastid-derived retrograde signals generated from tetrapyrrole metabolism. However, steady-state levels of tetrapyrrole metabolites and endproducts are also usually correlated with the synthesis of 5-aminolevulinic acid (ALA, **Figure 1**), which is the rate-limiting step of tetrapyrrole biosynthesis (Papenbrock et al., 2000a; Alawady and Grimm, 2005; Shalygo et al., 2009; Peter et al., 2010).

In cyanobacteria, algae and plants ALA is synthesized in a three-step reaction including activation of glutamate by binding to a plastid $tRNA^{Glu}$ followed by a reduction of glutamate to glutamate-1-semialdehyde catalyzed by glutamyl-tRNA reductase (GluTR) and a final transamination mediated by glutamate-1-semialdehyde aminotransferase (GSAT; **Figure 1**). Following synthesis, ALA is further processed in the branched pathway leading to the tetrapyrrole end products Chl, heme, siroheme, and phytochromobilin (**Figure 1**; Papenbrock and Grimm, 2001; Tanaka and Tanaka, 2007).

5-Aminolevulinic acid synthesis is controlled at the transcriptional and posttranslational level by changes in environment (e.g., light, temperature) and endogenous stimuli, such as hormonal and metabolic feedback regulation. Furthermore, several feedback-control mechanisms affect ALA biosynthesis on a posttranslational level. The negative regulator FLU binds to GluTR and mediates the suppression of ALA synthesis in the dark (Meskauskiene et al., 2001; Meskauskiene and Apel, 2002), most likely by interaction with protochlorophyllide oxidoreductase (POR) and in response to immediate accumulating Pchlide (Richter et al., 2010; Kauss et al., 2012). For example, the *Arabidopsis flu* mutant does not down-regulate GluTR activity, and accumulates Pchlide in darkness which subsequently generates singlet oxygen upon light exposure (Op den Camp et al., 2003).

Our aim was to examine the strong regulatory impact of ALA synthesis on tetrapyrrole biosynthesis, including its potential role in retrograde signal-mediated NGE derived from tetrapyrrole metabolism. We show that reduced ALA synthesis in *gun4-1* mutants, and inhibition of ALA synthesis by gabaculine (GAB) in wild-type *Arabidopsis* seedlings, lead to elevated transcript levels of photosynthetic genes if treated with NF. Taken together, these data support the idea that ALA-mediated retrograde signaling may modify NGE in *Arabidopsis* plants.

MATERIALS AND METHODS

PLANT GROWTH CONDITIONS

The *hy1* and *hy2* mutants of *Arabidopsis thaliana* L. originated from the ecotype Landsberg erecta (Ler-0) background (Chory et al., 1989), and *gun1-1* and *gun4-1* mutants (Col-0 background) were initially described in Susek et al. (1993) and Larkin et al. (2003), respectively. For analysis of etiolated, de-etiolated, and 7-day-old wild-type and mutant seedlings, seeds were surface-sterilized and plated onto 0.5× MS medium (Murashige and Skoog, 1962) supplemented with 1% (w/v) sucrose 0.8% (w/v) agar. After vernalization at 4°C for 2 days, plates and pots were transferred to a growth chamber with light intensity of 100–120 μmol photons m^{-2} s^{-1} at 22–23°C under a 12-h light/12-h dark regime. Etiolated seedlings were exposed to light for 2 h to synchronize germination before they were dark-incubated for 3 days. Ten micromolars of GAB (5-aminocyclohexa-1,3-diene-1-carboxylic acid) or 100 μM ALA or 1 μM NF were supplied to the MS medium as indicated in the results.

DETERMINATION OF ALA

5-Aminolevulinic acid content was measured using the method from Mauzerall and Granick (1956). Seedlings or leaves (100–200 mg fresh weight) were harvested 1 h after the start of

illumination and incubated in a buffer containing 50 mM Tris-HCl (pH 7.2) and 40 mM levulinate for 3 h at 22–23˚C and 100 μmol photons m^{-2} s^{-1}. Following the incubation, plant material was dried, weighed, and frozen in liquid nitrogen. Frozen samples were homogenized, resuspended in 20 mM K-phosphate buffer (pH 6.8) and centrifuged for 10 min at 16,000 × *g*. Four hundred microliters of the supernatant were mixed with 100 μl ethyl acetoacetate and boiled for 10 min at 100˚C. Samples were mixed with 500 μl modified Ehrlich's reagent (373 ml acetic acid, 90 ml 70% v/v perchloric acid, 1.55 g $HgCl_2$, 9.10 g 4-dimethylaminobenzaldehyde diluted to 500 ml with H_2O) and centrifuged for 5 min at 16,000 × *g*. Absorption was measured at 526, 553, and 720 nm and the ALA content of the samples was calculated using a standard curve generated by commercial ALA (Sigma–Aldrich Inc.).

DETERMINATION OF THE PCHLIDE CONTENT

Extraction of Pchlide was performed according to the protocol of Koski and Smith (1948). Etiolated *Arabidopsis* WT and mutant seedlings (100–300 mg fresh weight) were treated with steam for 2 min, ground in liquid nitrogen, and extracted three times in alkaline acetone (9 vol 100% acetone: 1 vol 0.1 N NH_4OH). After centrifugation at 16,000 × *g* for 10 min the supernatants were collected and Pchlide content was determined by fluorescence spectroscopy. Extracts were excited at 433 nm and fluorescence emission was recorded at 632–633 nm. For calibration, a Pchlide standard was extracted from 7-day-old etiolated barley leaves (Koski and Smith, 1948) and quantified using the Pchlide extinction coefficient in diethyl ether at 623 nm of 35,600 M^{-1} cm^{-1} (Dawson et al., 1986).

PIGMENT ANALYSIS

Chlorophyll and carotenoids were extracted from 100 mg (fresh weight) of seedlings or leaf material with 80% (v/v) acetone containing 10 μM potassium hydroxide. Supernatants of three extraction steps were combined and analyzed spectrophotometrically (Lichtenthaler, 1987; Czarnecki et al., 2011b).

QUANTITATIVE REAL-TIME PCR

Total RNA of seedlings was extracted using the Invisorb Spin Plant RNA Mini Kit (Invitek, Germany). A cDNA was reversely transcribed using 2 μg total RNA, oligo-dT_{18} Primer and RevertAid™M-MuLV Reverse Transcriptase (Fermentas) according to the manufacturer's instructions. Real-time PCR was performed using a StepOnePlus and SYBR Green PCR Master Mix (Applied Biosystems) containing ROX as internal control. For all PCRs the following cycling conditions were used: 10 min at 95˚C, 40 cycles of 15 s at 95˚C, and 60 s at 60˚C. Primers used are given in Table S1 in Supplementary Material. Calculation of expression levels in relation to *AtSAND* (At2g28390) or *AtACT2* (At3g18780) expression was performed using the $2^{-\Delta\Delta Ct}$ method according to Livak and Schmittgen (2001).

MICROARRAY HYBRIDIZATION AND DATA ANALYSIS

Microarray analysis was performed using the ATH1 *Arabidopsis* GeneChip. The quality control of RNA, preparation of biotinylated RNA, and hybridization was performed at KFB Regensburg[1] using the GeneChip®3′ IVT Express Kit and Affymetrix standard protocols. All microarray data reported here are described following MIAME guidelines and deposited in NCBI Gene Expression Omnibus (GEO) under the accession number GSE27704.

Normalization and differential expression

In order to analyze differential expression among the *Arabidopsis* wild-type Col-0 control, the wild-type seedlings treated with GAB, and the *gun4-1* mutant, microarray signal intensities were calculated from raw data by using robust multi-array average (RMA) expression measure (Irizarry et al., 2003). Subsequently, pairwise comparisons between all wild-type replicates and all GAB-treated replicates or all *gun4-1* replicates were performed to tag differentially expressed genes in treated or mutant seedlings. For this purpose, the LIMMA package (Smyth, 2004) in R/Bioconductor (Gentleman et al., 2004) was used with an empirical Bayes linear modeling approach. The obtained *P*-values for multiple testing were corrected according to Benjamini and Yekutieli (2001). Genes were considered to be significantly differentially expressed if their respective *P*-value was ≤ 0.05 and the log-fold change was either $<\log(2/3)$ or $>\log(3/2)$.

Heatmaps

A set of these differentially expressed genes was clustered according to their log-fold change using a *k*-means clustering approach in *R* (Hartigan and Wong, 1978; Ihaka and Gentleman, 1996). The expression of each gene in each cluster was depicted using a heatmap implemented in the *R* stats package. The scaling was based on rows, thus left at default, while the colors were set to an interpolation of blue and yellow. The genes being clustered in a Venn diagram were depicted alike.

Gene ontology-enrichment analysis

Gene ontology (GO)-enrichment analysis was performed using different algorithms: (i) a customized program was used for calculating over-represented GO terms (Ashburner et al., 2000) in a given set of genes. GO files (released 2010/05) were downloaded from the GO website[2], and GO annotations for *Arabidopsis* from the TAIR website[3] (release TAIR9). The subsequent calculation was based on hypergeometric distribution. The resulting *P*-value was corrected using the Bonferroni correction. GO terms with a probability of ≤ 0.05 were accepted as significant, whereas greater values lead to a rejection of a specific GO term. (ii) The program BiNGO 2.44 with Cytoscape 2.7 (Maere et al., 2005) was used together with the Amigo website[4]. A correction for false discovery rates was determined with BiNGO software using the method of Benjamini and Hochberg (1995).

Motif discovery

For motif discovery we used FIRE, Finding Informative Regulatory Elements (Elemento et al., 2007). Based on the concept of

[1] http://www.kfb-regensburg.de
[2] http://www.geneontology.org
[3] http://www.arabidopsis.org
[4] http://amigo.geneontology.org

mutual information, FIRE calculates putative *cis* elements in a set of genes using a database of promoter elements. Further, FIRE scores simple motif definitions in the form of *k*-mers, searching each combination for under- or over-representation in a defined set of genes. It is possible to define a set of genes using a continuous FIRE approach or using a pre-clustered set as discrete approach. For our analysis, we used a 2-kb upstream promoter annotation based on TAIR9. We further used FIRE in a continuous analysis with a standard robustness index threshold of 6, and with 3–10 *k*-mers.

STATISTICAL NOTE

All experiments were performed independently three to six times. In order to test the significant differences between calculated values, equality of variances was tested by a *F*-test followed by Student's *t*-test using a *P*-value of <0.05 as the threshold for significant difference.

RESULTS

ARABIDOPSIS GUN MUTANTS SHARE REDUCED ALA SYNTHESIS RATES

Inactivation of the expression of Mg chelatase, MgProto methyltransferase, and Chl synthase, enzymes in the Chl-synthesizing branch, results in diminished ALA-forming capacity (Papenbrock et al., 2000b; Alawady and Grimm, 2005; Shalygo et al., 2009). Since all but one known *Arabidopsis gun* mutants are also affected in genes related to tetrapyrrole biosynthesis (Nott et al., 2006), we collectively tested the *Arabidopsis gun1-1*, *hy1* (allelic to *gun2*), *hy2* (allelic to *gun3*), and *gun4-1* mutants for their *in vivo* ALA synthesis rate. Analysis of 7-day-old *hy1*, *hy2*, and *gun4-1* mutant seedlings revealed a severe reduction in ALA synthesis rate compared to their corresponding wild-types Ler-0 and Col-0 (**Figure 2**); ALA formation was also reduced in *gun1-1* seedlings. As a consequence of decreased ALA formation, the contents of Chl (a + b) and carotenoids were significantly reduced in 7-day-old *hy1*, *hy2*, *gun1-1*, and *gun4-1* seedlings compared with wild-type seedlings (**Table 1**).

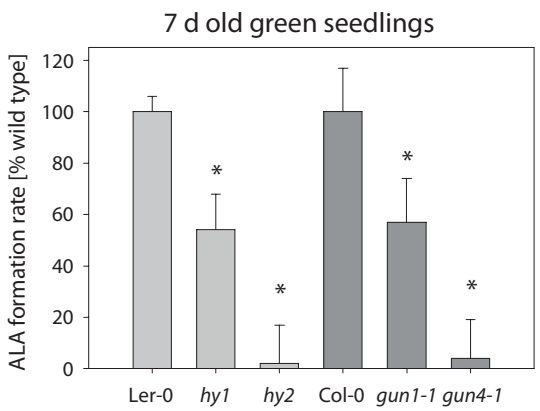

FIGURE 2 | ALA formation rate in four *Arabidopsis hy1, hy2, gun1-1,* and *gun4-1* mutants. The ALA formation rate was determined in the leaves of 7-day-old seedlings grown on 0.5× MS medium supplemented with 1% (w/v) sucrose and given in% of the corresponding wild-type Ler-0 (light gray, 11 pmol ALA mg fw^{-1} h^{-1}) or Col-0 (dark gray, 20 pmol ALA mg fw^{-1} h^{-1}), respectively. Data are means of at least three biological replica ± SD. * Indicates a significant difference from wild-type at a level of $P < 0.05$.

THE *GUN* PHENOTYPE COINCIDES WITH THE MODULATION OF ALA SYNTHESIS RATES

Application of 10 μM GAB was reported to diminish Chl accumulation by approximately 50% in de-etiolating barley leaves (Hill et al., 1985; Nair et al., 1990) based on the inhibition of GSAT activity (Grimm et al., 1991), though not affecting the GluTR and GSAT abundance (Demko et al., 2010). In *Arabidopsis* application of 10 μM GAB resulted in an 80% reduction of Chl a and b contents in treated seedlings compared to untreated, de-etiolating seedlings illuminated for 6 h as well as 6-day-old green seedlings (Figure S1A in Supplementary Material). The phenotype of the GAB-treated plants with low pigment contents was similar to the visible phenotype of the *Arabidopsis gun4-1* mutant (Figure S1B in Supplementary Material). Since *gun* mutants and GAB-treated seedlings share the reduced ALA synthesis rate, we were interested to prove whether *Arabidopsis* wild-type seedlings with GAB-inhibited ALA synthesis modulate expression of marker genes for plastid signaling similarly to *gun* mutants.

In parallel to GAB inhibition of ALA biosynthesis, we intended to modify reversely the endogenous pool of ALA by additional supply of ALA to seedlings. It was previously reported that feeding of etiolated seedlings with increasing amounts of ALA correlates with synchronously increasing levels of non-photoconvertible Pchlide (Armstrong et al., 1995). In order to raise the intracellular ALA pool without photo-oxidative risks we performed preliminary experiments to select the appropriate amounts of ALA. Application of ALA to etiolated *Arabidopsis* seedlings caused increasing Pchlide levels when young seedlings were fed with ALA at amounts greater than 50 μM. Application of 100 μM ALA resulted in four-time higher Pchlide levels in etiolated seedlings in the analyzed time period compared to untreated seedlings (Figure S2 in Supplementary Material; 1.0 ± 0.3 vs. 4.5 ± 1.3 pmol mg fw^{-1}). Light-grown seedlings fed with 100 μM ALA did not show visible photo-bleaching at the given light exposure (Figure S3 in Supplementary Material), though the addition of ALA at concentrations

Table 1 | Pigment content of 7-day-old *Arabidopsis hy1, hy2, gun1-1,* and *gun4-1* mutants and the corresponding wild-type seedlings Ler-0 and Col-0.

Line	Chl (a + b) (ng mg fw^{-1})	Carotenoids (ng mg fw^{-1})
Ler-0	172 ± 29	42 ± 5
hy1	102 ± 9*	32 ± 3
hy2	68 ± 15*	22 ± 6*
Col-0	207 ± 19	54 ± 5
gun1-1	114 ± 19*	36 ± 7*
gun4-1	64 ± 7*	22 ± 2*

*Given are means ± SD of three independent extractions. *, Indicates a significant difference from the wild-type ($P < 0.05$).*

greater than 250 μM generated a visible stress phenotype in illuminated *Arabidopsis* seedlings (at 100 μmol photons m^{-2} s^{-1}) that was likely due to elevated levels of photo-reactive tetrapyrrole intermediates.

Then, wild-type Col-0, *gun1-1* and *gun4-1* seedlings were subjected to 10 μM GAB or 100 μM ALA during germination and were incubated with NF to replicate experimental conditions that were applied to study the *gun* phenotype. Control and chemically treated wild-type and *gun* mutants were harvested either after 3-day-growth in darkness, 3 days in darkness followed by 1 day light exposure, or after 6 days growth in photoperiodic light (12 h, 100–120 μmol photons m^{-2} s^{-1}). The transcription levels of two photosynthesis genes, *AtLHCB1.2* and *AtRBSC*, were determined by qRT-PCR in these samples (**Figures 3** and **4**).

The analysis of the transcription levels of *AtLHCB1.2* and *AtRBSC* in wild-type Col-0, *gun1-1* and *gun4-1* seedlings subjected to 10 μM GAB during germination and incubated with NF revealed the following results: (i) Inhibition of carotenoid biosynthesis by NF treatment drastically lowered the transcript level in light-exposed, but not in etiolated seedlings (**Figures 3** and **4**). (ii) The *AtLHCB1.2* and *AtRBCS* expression of NF-treated and light-exposed *gun1-1* and *gun4-1* seedlings was de-repressed relative to that of wild-type Col-0 and confirmed the expected *gun* phenotype in our experimental approaches (**Figures 3** and **4**). (iii) Inhibition of ALA synthesis by GAB did not affect the expression of *AtLHCB1.2* and *AtRBCS* in etiolated, greening, or green seedlings, with the exception of slightly reduced expression levels of both genes in the wild-type Col-0 and *gun1-1* after 1 day of de-etiolation (**Figures 3B,E**). Six-day-old, green *gun1-1* seedlings showed elevated *AtLHCB1.2* expression in response to GAB (**Figure 3C**). (iv) GAB supply of NF-incubated *Arabidopsis* seedlings resulted in elevated *AtRBSC* and *AtLHCB1.2* expression levels compared to seedlings treated solely with NF. This counteracting effect of NF plus GAB vs. NF alone on elevated transcript contents was observed in the wild-type Col-0, but also in *gun1-1* and *gun4-1* in both 1 day illuminated (**Figures 3B,E**) and 6-day-old green seedlings (**Figures 3C,F**).

The analysis of *AtLHCB1.2* and *AtRBSC* transcription levels in wild-type Col-0, *gun1-1* and *gun4-1* seedlings subjected to 100 μM ALA during germination and incubated with NF revealed the following results: (v) ALA treatment reduced the *AtLHCB1.2* and *AtRBCS* transcript amounts of wild-type Col-0 seedlings in both light and darkness (**Figures 4A–C,E**). *Gun1-1* showed a compromised accumulation of transcripts of both genes in de-etiolating seedlings (**Figures 4B,E**), while *AtLHCB1.2* and *AtRBCS* transcript levels remained stable in ALA-fed *gun4-1* seedlings grown under all experimental conditions (**Figure 4**). (vi) Combined application of NF and ALA in light-exposed seedlings affected the two analyzed transcript contents even more negatively than the exclusive NF supply (**Figures 4B,C,F**).

Inhibition of ALA synthesis by GAB in NF-treated wild-type Col-0 led to the increased accumulation of both *AtLHCB1.2* and *AtRBCS* at rates that resembled the *gun* phenotype. The effects of GAB treatment were even more enhanced in the NF-treated *gun1-1* mutant, indicating additive acting mechanisms on NGE in *gun1-1*. However, in comparison with the wild-type Col-0, the modulation of *AtLHCB1.2* and *AtRBCS* transcript accumulation was less pronounced when GAB was added to the NF-treated *gun4-1* mutant (**Figure 3**).

In contrast to the results observed when GAB was added to inhibit ALA synthesis, ALA addition caused decreasing *AtLHCB1.2* and *AtRBSC* transcript levels in *Arabidopsis* wild-type Col-0 seedlings (**Figures 4B,E**). Since reduced *AtLHCB1.2* and *AtRBSC* transcript contents were also determined in etiolated seedlings, it can be excluded that photo-oxidative inhibition mainly caused the changes of NGE of photosynthetic genes (see also phenotypes displayed in Figure S3 in Supplementary Material). It is concluded that supply of low and non-phototoxic acting amounts of ALA in NF-treated and light-exposed seedlings abrogates the *gun* phenotype. Thus, regulatory consequences of the ALA synthesis rate and the endogenous ALA pool on NGE can be studied in both experimental approaches without the confounding side effects.

GLOBAL RESPONSE OF NGE TO INHIBITION OF ALA SYNTHESIS

After etiolated *Arabidopsis* Col-0 seedlings were illuminated, Chl contents increased from zero to 31 ± 3 ng Chl a and 12 ± 4 ng Chl b mg fw^{-1} within 6 h of illumination (Figure S4 in Supplementary Material). After 48 h, the contents of Chl a and b were elevated to 157 ± 17 and 44 ± 6 ng mg fw^{-1}, respectively. Carotenoid contents increased from 11 ± 1 in etiolated seedlings to 64 ± 6 ng mg fw^{-1} during 48 h of de-etiolation (Figure S4 in Supplementary Material). Since ALA synthesis is highly regulated and determines the amount of metabolites that are introduced into the branched metabolic pathway of tetrapyrrole biosynthesis, it is likely that the capacity of ALA synthesis has a strong impact on chloroplast biogenesis.

In continuation of our studies on the regulatory effect of ALA synthesis on NGE, we compared the transcriptome of developing *Arabidopsis* seedlings in response to inhibited ALA synthesis. An Affymetrix GeneChip (ATH1) microarray analysis was performed with RNA from 6 h light-exposed etiolated *Arabidopsis* seedlings incubated with or without 10 μM GAB. Moreover, in comparison to wild-type control we analyzed NGE of the 6 h light-exposed de-etiolating *gun4-1* mutants. The time point for the comparative transcriptome analysis was chosen since initial amounts of Chl accumulated upon illumination of etiolated seedlings (Figure S4 in Supplementary Materials). We decided on *gun4-1*, because the mutant shows posttranslational reduction of ALA synthesis without reduced expression of the ALA-forming enzymes (Peter and Grimm, 2009). We searched for early responsive genes upon inhibited ALA biosynthesis to minimize interference of pleiotropic effects of ALA deficiency (e.g., reduced photosynthetic capacity). Differentially expressed genes were identified in the transcriptome analysis with a P-value of ≤ 0.05 and a log-fold change of $<\log(2/3)$ or $>\log(3/2)$, respectively, compared to untreated *Arabidopsis* wild-type Col-0 seedlings (**Figure 5**; Data Sheet 2 in Supplementary Material). Comparison of the transcript profiles revealed that GAB treatment of developing *Arabidopsis* wild-type Col-0 seedlings resulted in the differential regulation of 325 genes representing approximately 1.5% of the entire *Arabidopsis* genome. Inhibited ALA synthesis resulted in the repression of 158 genes and the up-regulation of 167 genes. Compared to wild-type Col-0, *gun4-1* displayed 1536 mis-regulated genes (7.2% of the total ATH1 genome) at the same selected time point of 6 h of

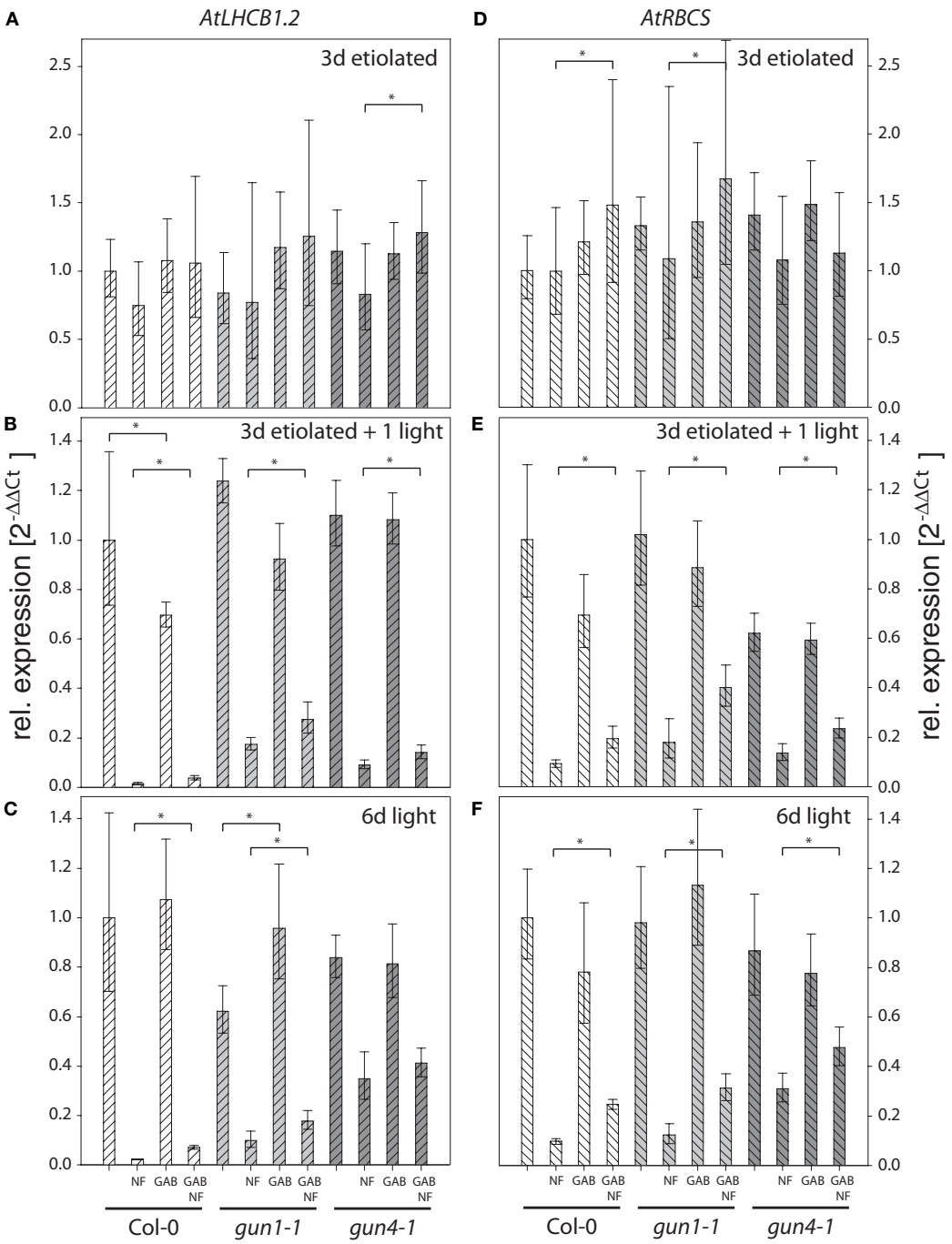

FIGURE 3 | Quantitative analysis of *AtLHCB1.2* (A–C) and *AtRBCS* (D–F) transcripts in *Arabidopsis* seedlings fed with gabaculine (GAB) and norflurazon (NF). Seedlings of *Arabidopsis* wild-type Col-0, *gun1-1*, and *gun4-1* mutants fed with or without 10 μM GAB and 1 μM NF were etiolated for 3 days **(A,D)**, etiolated for 3 days and subsequently illuminated for 1 day **(B,E)**, or germinated in photoperiodic light for 6 day **(C,F)**. *AtLHCB1.2* and *AtRBCS* expression levels were quantified by real-time PCR and calculated by the $2^{-\Delta\Delta Ct}$ method using *AtACT2* expression as standard. Expression data are compared to the untreated wild-type Col-0 and shown as means of at least three biological replicates ± SD. * Indicates a significant difference of pairs indicated by brackets at a level of $P < 0.05$. Tested were GAB-treated samples vs. untreated and GAB and NF treated vs. NF-treated samples within each genotype.

de-etiolation, whereas 993 and 543 genes showed a down- and up-regulated expression, respectively (**Figure 5**; Data Sheet 2 in Supplementary Material). However, a high number of genes were collectively down-regulated (119 genes) and up-regulated (88 genes) in GAB-treated and *gun4-1* seedlings (**Figure 5B**; Data Sheet 2 in Supplementary Material). The overlapping genes represented 12.5% of the differentially expressed genes (equals 207 combined genes out of the total amount of 1654 differentially regulated genes

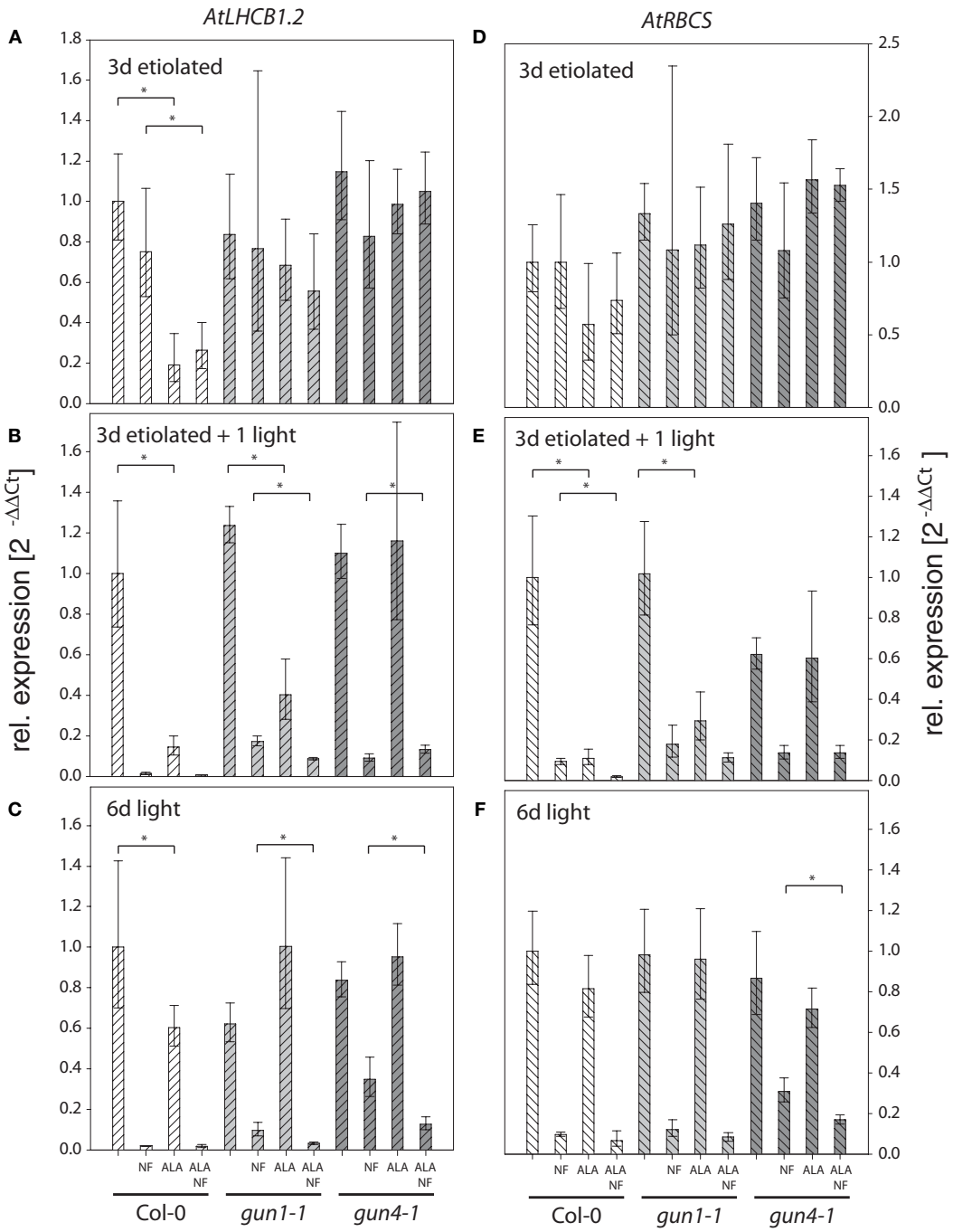

FIGURE 4 | Quantitative analysis of *AtLHCB1.2* (A–C) and *AtRBCS* (D–F) transcripts in *Arabidopsis* seedlings fed with 5-aminolevulinic acid (ALA) and norflurazon (NF). Seedlings of *Arabidopsis* wild-type Col-0, *gun1-1*, and *gun4-1* mutants fed with or without 100 μM ALA and 1 μM NF were etiolated for 3 days **(A,D)**, etiolated for 3 days and subsequently illuminated for 1 day **(B,E)**, or germinated in photoperiodic light for 6 days **(C,F)**. *AtLHCB1.2* and *AtRBCS* expression levels were quantified by real-time PCR and calculated by the $2^{-\Delta\Delta Ct}$ method using *AtACT2* expression as standard. Expression data are compared to the untreated wild-type Col-0 and shown as means of at least three biological replicates ± SD. * Indicates a significant difference of pairs indicated by brackets at a level of $P < 0.05$. Tested were ALA treated samples vs. untreated and ALA and NF treated vs. NF-treated samples within each genotype.

observed in both microarrays). Apart from two exceptions, all genes were congruently found to be either down- or up-regulated in both sets of seedlings with lower ALA synthesis (GAB-treated and the *gun4-1* seedlings) when compared with control seedlings (Data Sheet 2 in Suppmentary Material). **Tables 2** and **3** present the transcripts of the common set of genes in GAB-treated and

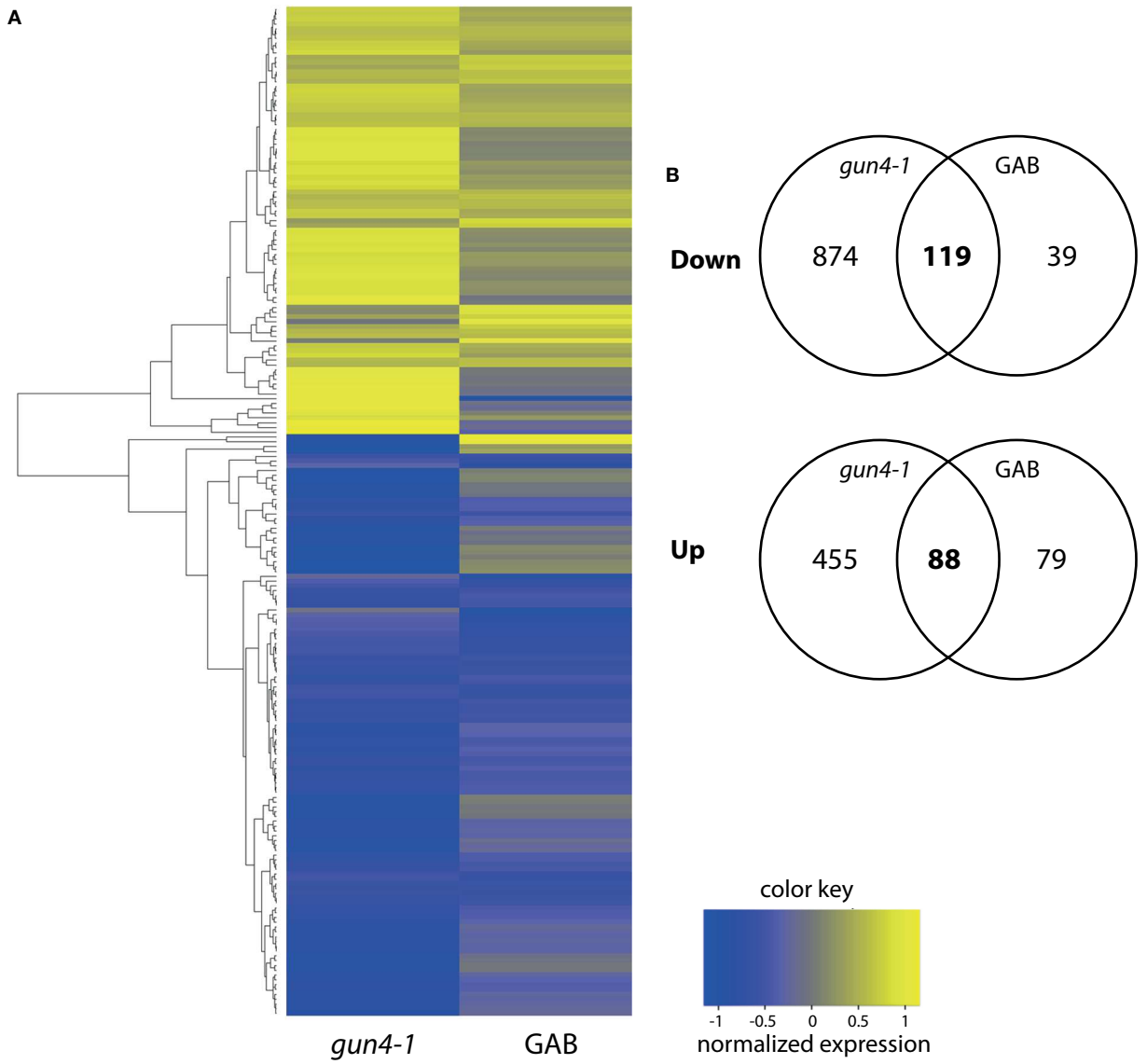

FIGURE 5 | (A) Heatmap analysis of differentially expressed genes in GAB-treated Arabidopsis wild-type Col-0 or *gun4-1* mutants 6 h after illumination of etiolated seedlings. All genes showing a fold change of <2/3 or >3/2 and a *P*-value of <0.05 in both conditions were analyzed. **(B)** Venn diagrams summarizing changes of transcript abundance in GAB-treated *Arabidopsis* wild-type Col-0 or *gun4-1* mutants 6 h after illumination of etiolated seedlings. The intersections of the circles represent the number of genes whose transcript abundance was decreased ("Down") or increased ("Up") in both compared to the untreated *Arabidopsis* wild-type Col-0.

gun4-1 seedlings in comparison to untreated wild-type seedlings with the greatest response to inhibition of ALA synthesis based on fold repression (≤0.5, **Table 2**) and fold induction (≥2, **Table 3**).

Transcriptomic comparisons showed that a high number of genes commonly affected by reduced ALA synthesis in GAB-treated *Arabidopsis* seedlings were also found in *gun4-1* mutants. Nearly 75% of the genes down-regulated in GAB-treated *Arabidopsis* seedlings were also down-regulated in *gun4-1*. These genes represent 12% of the 993 genes down-regulated in *gun4-1* (**Figure 5B**). Similarly, 53% of the genes up-regulated in GAB-treated seedlings were also up-regulated in *gun4-1*. These 88 genes represented 16% of the genes up-regulated in *gun4-1*. The results indicate a high number of identical genes identified in both transcriptomic comparisons, which are commonly affected by reduced ALA synthesis in GAB-treated *Arabidopsis* seedlings and *gun4-1*. This set of identical early responsive genes in both transcriptome analyses supports the view that besides the impaired Mg chelatase activity, *gun4-1* is also significantly compromised in ALA biosynthesis. Due to additional effects of GUN4 deficiency on other physiological processes, the transcriptome of *gun4-1* displayed a broader range of modulated genes.

Analysis of GO categories revealed an overrepresentation of transcripts encoding proteins involved in nuclear DNA replication within the cluster of genes being down-regulated in both

Table 2 | Listed are genes that showed a significantly ($P \leq 0.05$) decreased transcript abundance after 6 h of de-etiolation in response to inhibited ALA formation (GAB) and in the *gun4-1* mutant.

AGI number	GAB vs. Col-0 fold change	GAB vs. Col-0 *P*-value	*gun4-1* vs. Col-0 fold change	*gun4-1* vs. Col-0 *P*-value	SUBA localization	Description	qRT-PCR performed (see Table S2 in Supplementary Material)
At5g08030	0.247	0.000	0.249	0.000	Mito, Cp, ER, Nuc, Ex, Vac	Glycerophosphoryl diester phosphodiesterase	
At1g13650	0.273	0.000	0.381	0.000	Mito, Perox	Unknown protein	
At2g20570	0.300	0.000	0.351	0.000	Cyt	GPRI1 (GBF'S Pro-rich region-interacting factor 1)	Yes
At5g46690	0.345	0.000	0.344	0.000	Nuc	Beta HLH protein 71 (bHLH071)	
At1g61800	0.347	0.000	0.486	0.000	Cp, Mito, Ex, PM	Glucose-6-phosphate transmembrane transporter (GPT2)	Yes
At3g26960	0.372	0.000	0.288	0.000	Ex, ER, Nuc	Unknown protein	Yes
At5g55450	0.376	0.005	0.278	0.000	Ex, ER	Protease inhibitor	
At4g04610	0.385	0.019	0.166	0.000	Cp	APS reductase 1 (APR1)	Yes
At4g28250	0.387	0.003	0.182	0.000	Ex, ER, Vac	ATEXPB3 (Expansin B3)	Yes
At2g20750	0.407	0.000	0.176	0.000	Ex	ATEXPB1 (Expansin B1)	
At3g61820	0.414	0.000	0.344	0.000	Cp, Ex	Aspartyl protease family protein	Yes
At3g47380	0.431	0.005	0.465	0.002	Ex, Mito, ER, Nuc	Invertase/pectin methylesterase inhibitor	
At1g56650	0.439	0.000	0.355	0.000	Nuc	PAP1 (production of anthocyanin pigment 1); DNA binding/transcription factor	Yes
At5g45650	0.443	0.001	0.356	0.000	Mito, ER, Ex	Subtilase family protein	Yes
At1g24020	0.457	0.017	0.160	0.000	Cyt, Perox	MLP423 (MLP-like protein 423)	Yes
At3g59670	0.459	0.000	0.528	0.000	Nuc	Unknown protein	
At2g31270	0.460	0.000	0.645	0.005	Mito, Nuc, Cp	CDT1A (homolog of yeast CDT1 A); cyclin-dependent protein kinase	
At4g11460	0.468	0.014	0.271	0.000	Ex, ER, Nuc, Vac	Protein kinase family protein	
At4g34588	0.474	0.003	0.428	0.000	No data	CPuORF2 (conserved peptide upstream open reading frame 2)	
At4g34590	0.474	0.003	0.428	0.000	Nuc	GBF6 (G-BOX BINDING FACTOR 6)	Yes
At5g05960	0.477	0.014	0.170	0.000	ER, Ex	Protease inhibitor/seed storage/lipid transfer protein (LTP) family protein	
At4g28680	0.480	0.001	0.432	0.000	Cyt, Mit, ER	Putative tyrosine decarboxylase	
At3g05600	0.481	0.005	0.459	0.001	Cp, Perox, Cyt	Putative epoxide hydrolase	Yes
At4g39510	0.485	0.001	0.369	0.000	Mito, ER, Cyt, Ex, Nuc	CYP96A12; electron carrier/heme binding/iron ion binding/monooxygenase/oxygen binding	Yes
At1g66940	0.493	0.002	0.265	0.000	Ex, ER, Cyt, Ex	Protein kinase-related	Yes
At4g38950	0.500	0.004	0.393	0.000	Nuc	Kinesin motor family protein	Yes

*In contrast to the results shown in **Figure 5**, there are only transcripts listed with a fold change ≤0.5. Given are the fold changes, corresponding P-values, the putative subcellular localizations using the SUBA database (Heazlewood et al., 2007) and gene annotations based on the TAIR9 release of the Arabidopsis genome. (Cp, chloroplasts; Cyt, cytosol; ER, endoplasmic reticulum; Ex, extracellular; Mito, mitochondria; Nuc, nucleus; Perox, peroxisome; PM, plasma membrane; Vac, vacuole).*

Table 3 | Listed are genes that showed a significantly ($P \leq 0.05$) increased transcript abundance after 6 h of de-etiolation in response to inhibited ALA formation (GAB) and in the *gun4-1* mutant.

AGI number	GAB vs. Col-0 fold change	GAB vs. Col-0 *P*-value	*gun4-1* vs. Col-0 fold change	*gun4-1* vs. Col-0 *P*-value	SUBA localization	Description	qRT-PCR performed (see Table S2 in Supplementary Material)
At1g05560	4.010	0.000	2.057	0.000	Cp, Mito, Cyt	UDP-glucose:4-aminobenzoate acylglucosyltransferase (UGT75B1)	Yes
At1g22890	3.708	0.000	6.331	0.000	ER, Nuc, Cp	Unknown protein	Yes
At2g04040	3.267	0.001	3.156	0.000	PM, Ex, Vac	TX1; antiporter/multidrug efflux pump/multidrug transporter/transporter	
At3g22060	2.838	0.000	3.278	0.000	Ex, Vac	Receptor protein kinase-related	Yes
At2g19800	2.838	0.000	2.686	0.000	Cyt	MIOX2 (Myo-inositol oxygenase 2)	
At5g16980	2.773	0.000	1.635	0.011	Cyt, Mito, Cp	Putative NADP-dependent oxidoreductase	
At3g20340	2.728	0.000	1.903	0.001	Nuc	Down-regulated under photo-oxidative stress.	
At5g43450	2.722	0.000	3.317	0.000	Cyt, Nuc	Putative 2-oxoglutarate-dependent dioxygenase	
At3g47340	2.680	0.000	5.921	0.000	Cyt, Cp	ASN1 (glutamine-dependent asparagine synthase 1)	Yes
At1g05680	2.591	0.005	2.247	0.003	Mito, Cyt, Cp	UDP-glucoronosyl/UDP-glucosyl transferase	Yes
At5g16970	2.590	0.000	1.791	0.000		AT-AER (2-alkenal reductase)	
At3g28740	2.455	0.001	2.472	0.000	Mito, ER, Ex, PM	CYP81D1; electron carrier/heme binding/iron ion binding/monooxygenase/oxygen binding	Yes
At3g20270	2.445	0.011	2.036	0.012	Cp, Cyt, Ex	Lipid-binding serum glycoprotein family protein	
At2g17880	2.423	0.001	3.176	0.000	Cp, Mito, Nuc	Putative DNAJ heat shock protein	Yes
At1g35140	2.362	0.000	12.734	0.000	Ex	Phosphate induced 1 (PHI-1)	
At4g31870	2.340	0.002	2.257	0.001	Cp, Mito, Perox, Nuc	ATGPX7 (glutathione peroxidase 7)	Yes
At1g08630	2.307	0.001	8.617	0.000	Cp, Nuc, Cyt	THA1 (threonine aldolase 1)	Yes
At5g57560	2.218	0.000	6.492	0.000	Ex, Mito, Er	TCH4 (touch 4); hydrolase, acting on glycosyl bonds/xyloglucan:xyloglucosyl transferase	Yes
At5g06860	2.187	0.001	1.775	0.001	Ex	PGIP1 (polygalacturonase inhibiting protein 1)	
At2g29340	2.143	0.001	2.036	0.000	Cyt, Ex, ER	Short-chain dehydrogenase/reductase (SDR) family protein	Yes
At5g17300	2.069	0.001	2.115	0.000	Nuc	Myb family transcription factor	Yes
At4g15260	2.044	0.000	2.059	0.000	Cyt, Cp	UDP-glucoronosyl/UDP-glucosyl transferase	Yes
At5g20230	2.042	0.005	22.472	0.000	PM	ATBCB (blue-copper binding protein)	Yes
At5g14470	2.010	0.001	6.425	0.000	Cyt, Nuc	GHMP kinase-related	
At3g15760	2.005	0.001	2.027	0.000	Ex, Mito, Nuc, Cp	Unknown protein	Yes

In contrast to the results shown in ***Figure 5****, there are only transcripts listed with a fold change ≥2.0. Given are the fold changes, corresponding P-values, the putative subcellular localizations using the SUBA database (Heazlewood et al., 2007) and gene annotations based on the 9.0 release of the Arabidopsis genome. (Cp, chloroplasts; Cyt, cytosol; ER, endoplasmic reticulum; Ex, extracellular; Mito, mitochondria; Nuc, nucleus; Perox, peroxisome; PM, plasma membrane; Vac, vacuole).*

GAB-treated *Arabidopsis* wild-type Col-0 and *gun4-1* seedlings (**Figure 6A**). Within the cluster of up-regulated genes, neither cellular components nor functions were overrepresented. Genes encoding proteins responding to sucrose stimulus, oxidative stress, and the absence of light were overrepresented within the biological process category, whereas transcripts involved in posttranslational modification of proteins (disulfide bonds and glycosyl groups) were overrepresented in the molecular function category (**Figure 6B**). GO analyses extended to all differentially expressed transcripts additionally revealed that reduction of ALA synthesis in GAB-treated seedlings and in *gun4-1* mutants caused a reduced abundance of transcripts for sulfur metabolism (sulfate assimilation, sulfate reduction, and adenyl-sulfate reductase activity) at an early stage of development (Figure S5A in Supplementary Material). The significantly over-represented GO categories additionally identified in up-regulated transcripts were more diverse and include transcripts related to the circadian rhythm, redox homeostasis, auxin signaling, and tocopherol biosynthesis (Figure S5B in Supplementary Material).

It is remarkable that within the small set of 207 combined genes that differentially respond to two different mechanisms of inhibited ALA synthesis (**Figure 5B**), no genes were found which are involved in Chl biosynthesis and photosynthesis (**Tables 2** and **3**; Data Sheet 2 in Supplementary Material). We compared microarray data with transcripts levels obtained by qRT-PCR of two genes involved in ALA synthesis, *AtHEMA1* and *AtGluTRBP* (Czarnecki et al., 2011a) and other marker genes for chloroplast functions, e.g., *AtTOC159*, *AtELIP1*, *AtELIP2*, and *AtLHCB1.2* in 6 h de-etiolated GAB-treated wild-type and *gun4-1* seedlings. In both sets of seedlings the expression levels of these genes were not significantly altered in response to inhibition of ALA formation (**Figure 7**; Table S2 in Supplementary Material), except a 30–50% stimulated expression of *AtHEMA1* and *AtTOC159* in *gun4-1* compared to the control transcript levels of wild-type seedlings.

Screening of genomic sequences upstream of the transcription initiation region of differentially expressed genes in GAB-treated or *gun4-1 Arabidopsis* seedlings using FIRE analysis did not reveal an over-representation of a promoter motif in GAB-treated *Arabidopsis* seedlings. However, an I-box motif (5′-CTTATCC-3′) was overrepresented in three clusters representing transcripts with enhanced expression in *gun4-1* seedlings (**Figure 8**; Data Sheet 3 in Supplementary Material). Consistently, over-represented GO categories were identified within genes forming clusters with over-represented promoter motifs. The I-box motif found in clusters C1–C3 formed by genes over-expressed in *gun4-1* seedlings seems to be a promoter element of genes involved in sucrose and light stress, but also secondary metabolic systems, e.g., cell wall biosynthesis and defense reactions (**Table 4**).

Quality and robustness of expression data obtained by microarray analysis were validated by independent expression analysis of selected genes via qRT-PCR. Therefore, 36 genes up- or down-regulated in both *gun4-1* and GAB-treated wild-type seedlings were selected either by reason of the putative chloroplast localization of their encoded proteins, their function as transcription factor, or the strong alterations in the transcript abundance determined by the microarray analysis in comparison to control (Table S2 in Supplementary Material). Quantitative RT-PCR expression analysis was performed with de-etiolated seedlings after 6 and 24 h of illumination. The data of the global transcriptome analysis were confirmed in approximately 67% of the performed qRT-PCR reactions. Moreover, the majority of transcripts being mis-regulated in GAB-treated wild-type and *gun4-1* seedlings after 6 h of de-etiolation were also mis-regulated after 24 h of light exposure

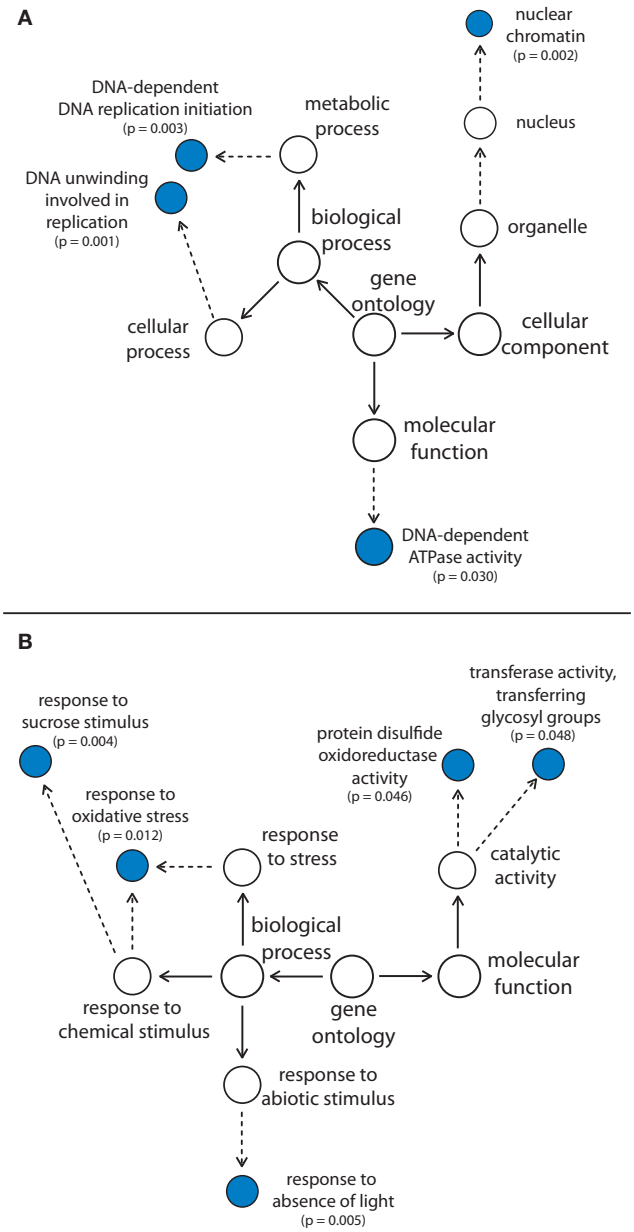

FIGURE 6 | Overrepresentation of gene ontology (GO) categories in genes showing decreased (A) and increased (B) transcript abundance in GAB-treated *Arabidopsis* wild-type Col-0 and *gun4-1* mutants 6 h after illumination of etiolated seedlings. The 119 or 88 genes, respectively, being differentially regulated in both GAB-treated and *gun4-1* seedlings, were analyzed for over-represented GO categories (*P*-value of <0.05). Dotted lines indicate intermediate categories that are not shown.

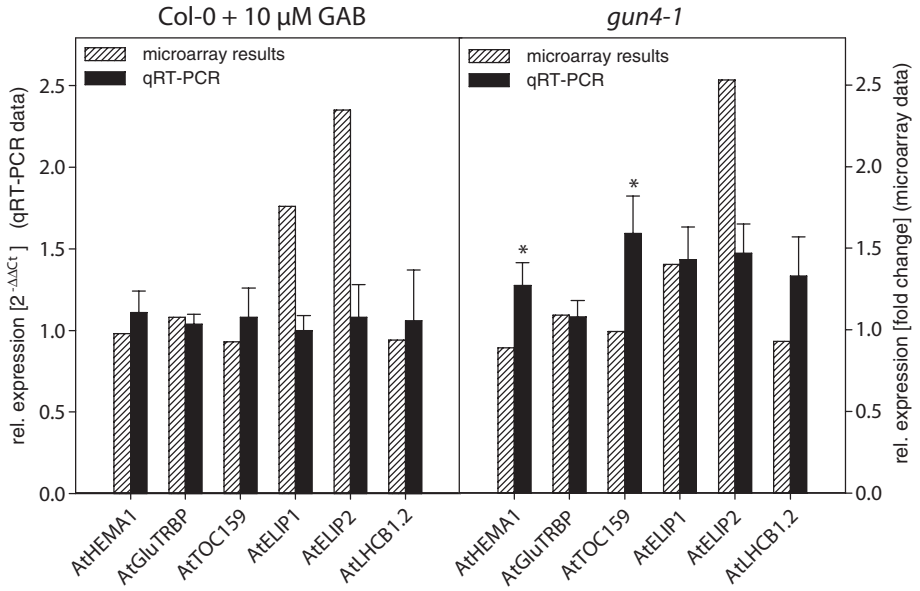

FIGURE 7 | Comparison of expression data obtained by microarray analysis and qRT-PCR. RNA from GAB-treated *Arabidopsis* wild-type seedlings and *gun4-1* mutant seedlings was extracted 6 h after light exposure of 3-day-old etiolated seedlings. In addition to microarray analysis, transcript abundance of a defined set of genes was determined by quantitative real-time PCR and calculated in relation to *AtSAND* expression compared to untreated *Arabidopsis* wild-type Col-0 seedlings [$2^{-\Delta\Delta Ct}$]. qRT-PCR data are shown as average ± SD of three biological replicates. * Indicates a significant difference from the untreated *Arabidopsis* wild-type Col-0 (*P*-value of <0.05).

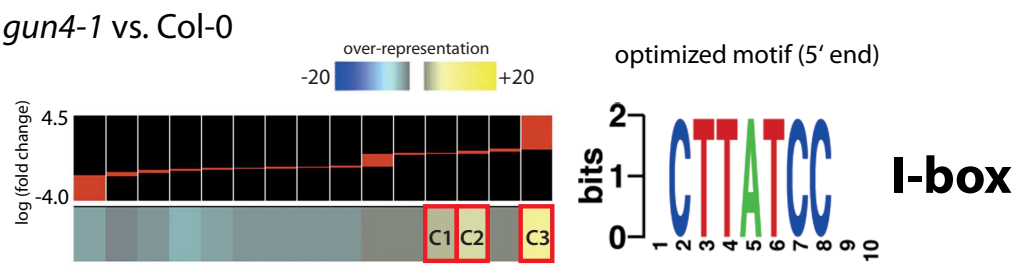

FIGURE 8 | Identification of informative promoter sequence motifs of regulated transcripts in *gun4-1* mutant seedlings compared to untreated *Arabidopsis* wild-type Col-0 seedlings. Columns on the left correspond to groups of genes clustered according to the similarity in their expression pattern [log (fold change)] within the microarray experiments. Clusters highlighted in red (C1, C2, and C3) show a significant over-representation of the specified motif. The sequence on the right represents the optimized motif and its name based on JASPAR, TRANSFAC, or PLACE. Names and descriptions of transcripts forming clusters C1–C3 were given in Data Sheet 3 in Supplementary Material.

(**Figure 9**; Table S2 in Supplementary Material). This confirmation revealed a robust data set created by microarray analysis of transcriptional changes in response to reduced ALA synthesis.

DISCUSSION

COMPROMISED ALA BIOSYNTHESIS IS A TRAIT OF *GUN* MUTANTS

By using GAB to reduce ALA formation we proved a role of ALA-synthesizing activity in plastid-to-nucleus communication and modulation of NGE. Transcript accumulation of *LHCB1.2* has been previously examined in NF-treated *Arabidopsis* seedlings to identify mutants affected in retrograde signaling (Susek et al., 1993). Four out of five initially identified *gun* mutants are perturbed in tetrapyrrole biosynthesis. We found that reduced ALA synthesis rates are a common metabolic trait of *gun1-1*, *hy1* (allelic to *gun2*), *hy2* (allelic to *gun3*), and *gun4-1* mutants (**Figure 2**). A lower ALA-synthesizing capacity has been previously reported for *gun4-1* (Peter and Grimm, 2009), and other transgenic lines with reduced expression of *CHLH*, *CHLI*, *CHLM*, and *CHLG* encoding either one of the three different Mg chelatase subunits, Mgproto methyltransferase, or Chl synthase, respectively (**Figure 1**; Papenbrock et al., 2000a,b; Alawady and Grimm, 2005; Shalygo et al., 2009). Mutants with deficiency in the synthesis of Mg chelatase subunits are considered to be phenotypically equivalent to the *gun5* mutant.

We added GAB to *Arabidopsis* wild-type seedlings to simulate reductions in ALA synthesis and changes in NGE of the *gun*

Table 4 | Cluster C1–C3 (Figure 8) showing significant over-represented specific motifs in mis-regulated genes of *gun4-1* mutants analyzed for overrepresentation of gene ontology (GO) categories.

Cluster	Domain (C, F, P)	*P*-value	GO category	Description
C1	F	0.014	GO:0016491	Oxidoreductase activity
C2	P	0.004	GO:0009743	Response to carbohydrate stimulus
		0.032	GO:0010200	Response to chitin
C3	C	0.037	GO:0044464	Cell part
	F	0.047	GO:0005199	Structural constituent of cell wall
		0.036	GO:0016762	Xyloglucan:xyloglucoyl transferase activity
	P	0.023	GO:0050832	Defense response to fungus
		0.006	GO:0009646	Response to absence of light
		0.026	GO:0010200	Response to chitin
		0.005	GO:0009744	Response to sucrose stimulus

The genes forming the respective clusters (Data Sheet 3 in Supplementary Material) were analyzed for over-represented GO categories ($P \leq 0.05$). Intermediate GO categories are omitted. C, cellular component; F, molecular function; P, biological process.

mutants. We showed that inhibition of ALA formation by GAB mimics the *gun* phenotype in NF-treated *Arabidopsis* wild-type seedlings and results in elevated transcript levels of the photosynthetic genes *LHCB1.2* and *RBCS* compared to the NF treatment without GAB addition (**Figure 3**). GAB addition had similar effects on NF-treated *gun1-1* and *gun4-1* seedlings (**Figure 3**). In contrast to NF-treated and light-exposed seedlings, the combined addition of NF and GAB did not influence the transcript levels of *LHCB1.2* and *RBCS* in etiolated *gun*-mutant and wild-type seedlings. The lack of an effect of GAB addition on NGE in etiolated seedlings is likely explained by a minimal ALA synthesis rate caused by FLU-mediated inactivation of GluTR (Meskauskiene et al., 2001; Meskauskiene and Apel, 2002; Richter et al., 2010; Kauss et al., 2012).

ADDITIONAL ALA SUPPLY AND ACCUMULATION OF PHOTOSYNTHETIC GENES

Since reduced ALA synthesis was shown to mimic a *gun* phenotype in wild-type seedlings, we then added low amounts of ALA to germinating *Arabidopsis gun1-1* and *gun4-1* seedlings to test if elevated ALA amounts suppress the *gun* phenotype. Additional supply of low amounts of ALA decreased the transcript levels of *LHCB1.2* and *RBCS* in both etiolated and illuminated wild-type seedlings. ALA feeding potentiated the NF-induced decrease of transcript contents of photosynthetic genes in greening and green wild-type and *gun1-1* seedlings. In contrast, elevated ALA pools in *gun4-1* resulted in less pronounced changes of NGE compared to both wild-type Col-0 and *gun1-1*, indicating that *gun4-1* is less sensitive to exogenously applied ALA (**Figure 4**).

It was previously reported that ALA feeding of etiolated *Arabidopsis* seedlings results in an increased *LHCB* promoter-driven GUS-activity (Lopez-Juez et al., 1999), whereas the same amount of exogenous ALA leads to suppressed *LHCB* expression in dark-incubated and light-exposed seedlings (Vinti et al., 2000). An inhibition of the light signaling-mediated induction of gene expression was proposed in both cases (Lopez-Juez et al., 1999; Vinti et al., 2000). We also observed the reduction in *LHCB* and *RBCS* mRNA levels in wild-type and *gun1-1* seedlings as a response to ALA feeding (**Figure 4**), but cannot confirm a stimulatory effect of ALA on *LHCB1.2* expression in etiolated seedlings. The difference might be explained with different concentrations of ALA used or different developmental states of the seedlings (3 vs. 7 days dark incubation).

As feeding of *Arabidopsis* wild-type, *gun1-1* and *gun4-1* mutants with exogenous ALA represses the *gun* phenotype under NF treatment (**Figure 4**), we suggest that the observed changes in expression of *LHCB1.2* and *RBCS* are either due to modification of ALA biosynthesis rates or the ALA pool. This is consistent with the observed changes in the accumulation of these mRNAs in response to applied NF and GAB (**Figure 3**). Considering the opposite effects of ALA supply and inhibition of ALA synthesis, a direct impact of ALA biosynthesis or the ALA steady-state level is proposed.

It is remarkable that transcript accumulation of the *LHCB1.2* and *RBCS* in the NF-treated *gun4-1* mutant showed a lower sensitivity to the addition of GAB and ALA. This favors the idea of GUN4 being a component of the mechanism translating the state of plastid ALA synthesis into a nuclear response. A role of GUN4 in posttranslational regulation of ALA formation has been previously proposed (Peter and Grimm, 2009). It is hypothesized that GUN4 stimulates ALA synthesis in light. This is supported by observations that *gun4* knock-out mutants cannot survive photoperiodic growth conditions and do not accumulate Chl under these conditions, but slowly green and grow under continuous dim light.

However, although we clearly show that GAB treatment mimics the *gun* phenotype in *Arabidopsis* wild-type seedlings and excess ALA represses the *gun* phenotype of NF-treated *gun* mutants, it should be kept in mind that NF generally is a very deleterious herbicide leading to a bleaching leaf phenotype initially caused by inhibition phytoene desaturase, an enzyme involved in carotenoid biosynthesis (Breitenbach et al., 2002). It was previously suggested that retrograde signals emitted by chloroplast destruction under NF treatment are heavily influenced by production of a complex ROS pattern that likely acts as a modulator of NGE itself (Op den Camp et al., 2003; Apel and Hirt, 2004; Kim et al., 2008; Moulin et al., 2008).

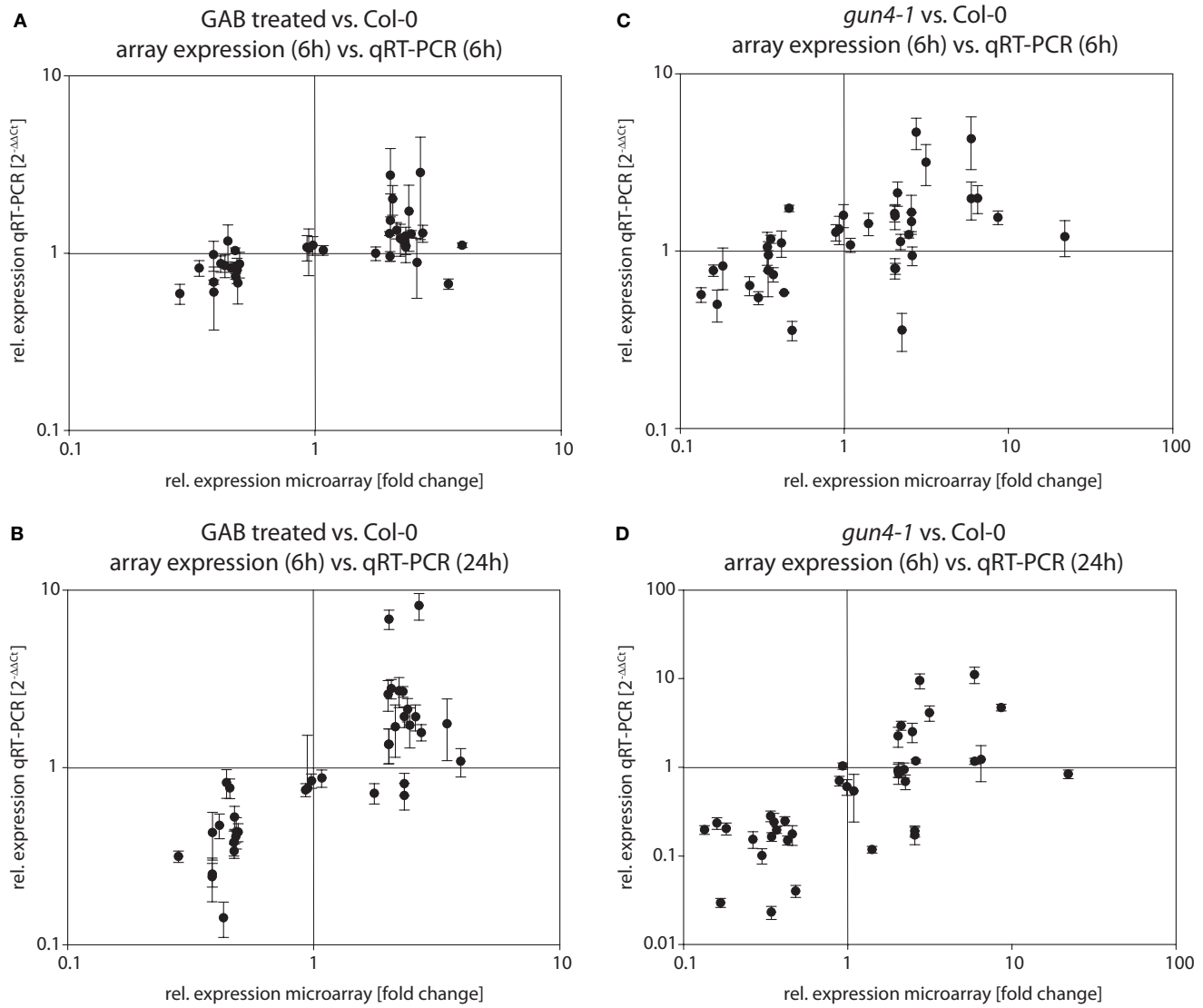

FIGURE 9 | Verification of microarray results via qRT-PCR. RNA from GAB-treated *Arabidopsis* wild-type seedlings **(A,B)** and *gun4-1* mutant seedlings **(C,D)** was extracted 6 h **(A,C)** and 24 h **(B,D)**, respectively, after light exposure. Transcript abundance of a defined set of genes (see **Tables 2** and **3** and Table S2 in Supplementary Material) was determined by quantitative real-time PCR and calculated as relative expression [$2^{-\Delta\Delta Ct}$] compared to untreated *Arabidopsis* wild-type Col-0 seedlings. Relative expressions obtained by qRT-PCR are plotted against relative expressions in microarray experiments (sampling 6 h after light exposure) in order to compare relative expressions in both experimental approaches.

Considering recently developed ideas that retrograde signaling is not necessarily the result of single and distinct emitted signal molecules but rather the result of continuously sensed metabolic and genetic activities in the organelles (Pogson et al., 2008; Kleine et al., 2009; Pfannschmidt, 2010), changes in NGE provoked by NF-induced inhibition of chloroplast development may not reflect signaling pathways under non-destructive or non-lethal conditions. In this context, it is an important observation that 6-day-old low light-exposed *gun* mutants do not display significantly increased *LHCB1.2* expression under NF treatment (Voigt et al., 2010). Moreover, the authors also found that under NF treatment *LHCB1.2* expression was not increased in several *Arabidopsis* T-DNA insertion mutants affected in genes of tetrapyrrole biosynthesis. In consequence, the appropriateness of PhANGs (e.g., *LHCB1.2*, *RBCS*, *CA*) may put into question as primary target genes of plastid signaling.

INHIBITION OF ALA BIOSYNTHESIS INDUCES CHANGES IN THE *ARABIDOPSIS* TRANSCRIPTOME

We intended to examine the hypothesis that reduced ALA formation instantaneously releases a retrograde signal and performed a transcriptome analysis to explore rapid changes in transcript profiles in response to lower ALA biosynthesis before other regulatory mechanisms of successive changes in tetrapyrrole biosynthesis and chloroplast biogenesis proceed (e.g., photosynthesis, redox poise, ROS). The microarray analysis with GAB-treated

seedlings and *gun4-1* seedlings revealed a common set of significantly up- and down-regulated genes in response to reduced ALA synthesis (**Figure 5**; **Tables 2** and **3**). In addition to previously proposed signaling derived from tetrapyrroles (Mochizuki et al., 2001; Strand et al., 2003; Woodson et al., 2011), this list of deregulated genes indicates the potential of ALA synthesis-derived retrograde signaling.

Kobayashi et al. (2009) opened the view on the interrelation between tetrapyrrole biosynthesis, function of tetrapyrrole intermediates, and the cell cycle process involved in DNA replication. The authors found a strong interdependence of plastid and mitochondrial DNA replication prior to nuclear DNA replication in the primitive red alga *Cyanidioschyzon merolae*. The coordination of nuclear DNA replication followed after the organellar replication was regulated through tetrapyrrole signaling contributing to organelle-nucleus communication. In this context it is remarkable to identify groups of over-represented GO categories among genes deregulated in seedlings with reduced ALA-synthesizing capacity that are involved in DNA replication and nuclear chromatin organization (**Figure 6A**). Moreover, the regulatory dependency of Mg porphyrins and plastid function of GUN1, a pentatricopeptide-repeat protein with the potential to bind nucleic acids implicates a regulatory link between tetrapyrrole biosynthesis and control of genes for DNA and RNA metabolism (Koussevitzky et al., 2007).

WHAT COMMENDS ALA SYNTHESIS TO BE A SIGNAL EMITTER FOR NGE?

Plastid signals have been proposed to convert multiple light signaling pathways controlling PhANGs (Ruckle et al., 2007). The over-representation of target genes reacting to abiotic stimuli and absence of light indicate a role of reduced ALA synthesis for modulation of light signaling networks (**Figure 6B**). It is conceivable that the metabolic pathway of Chl biosynthesis contributes to intracellular communication between chloroplast and nucleus in response to environmental and biological cues, such as abiotic stress and sucrose status to adjust the significant energy-converting processes of photosynthesis. In this context, the *cis*-element I-Box was found to be overrepresented in promoters of deregulated genes in *gun4-1* (**Figure 8**). On the other hand, among deregulated genes carrying an I-box in the promoter region genes responding to sucrose and light stress are overrepresented (**Table 4**). This finding is in agreement to previous results of I-Box-binding factors that are regulated by light, sugar sensing, and the circadian clock (Donald and Cashmore, 1990; Borello et al., 1993).

The compilation of up- and down-regulated genes identified in the transcriptomes of GAB-treated seedlings as well as *gun4-1* knock-down seedlings revealed a significant and representative set of identically regulated genes indicating that modified ALA biosynthesis and/or the ALA pool in plastids have an impact on NGE at early stages of plant development. Since the time point chosen in our comparative transcriptome analysis corresponded to the first detectable accumulation of Chl (Figure S4 in Supplementary Material) upon illumination of etiolated seedlings, it may be assumed that the described changes in NGE are primary effects in response to inhibited ALA formation. Moreover, typical marker genes for photosynthesis and chloroplast biogenesis are missing among these genes identified in both experimental approaches (**Figure 7**).

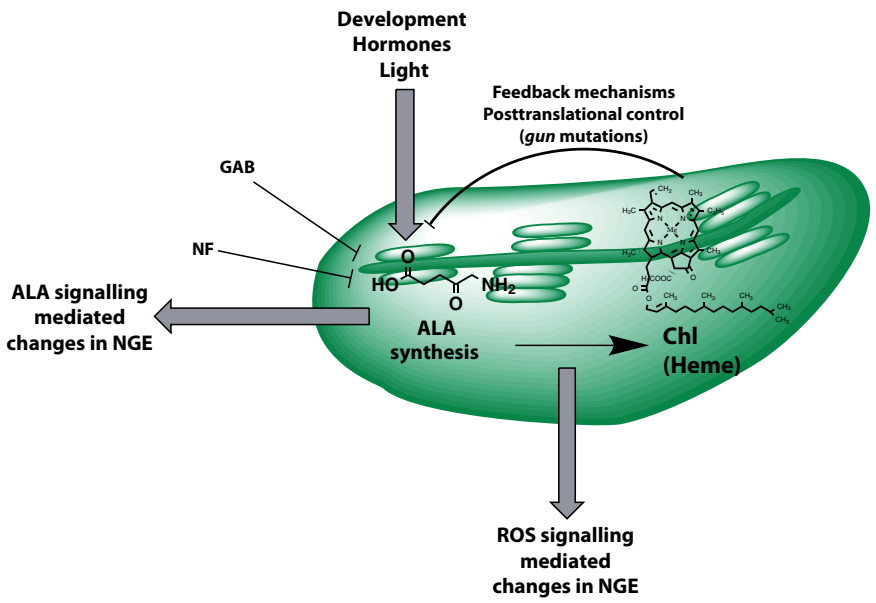

FIGURE 10 | Model summarizing control mechanisms that act on and are emitted from ALA biosynthesis. The contribution to plastid-derived retrograde signaling is highlighted. ALA formation is posttranslationally controlled by several known feedback mechanisms of the Chl and Mg branch of the pathway (e.g., heme, Mg chelatase assembly, GUN4) also reflecting the impact of the *gun2-gun5* mutations on ALA synthesis. Intermediates of the tetrapyrrole biosynthetic pathway (e.g., Mg Protoporphyrin IX) were discussed to be involved in signaling pathways and likely act via reactive oxygen species (ROS)-mediated changes in nuclear gene expression (NGE). Gabaculine (GAB) directly inhibits ALA formation resulting in changes of NGE at very early stages of chloroplast development. Norflurazon (NF) inhibits tetrapyrrole biosynthesis indirectly.

It can be concluded that our experimental setup allows an insight in the primary impact of modulated ALA biosynthesis on NGE. Consecutively, compromised tetrapyrrole biosynthesis will induce numerous regulatory adaptations to long-term perturbation of ALA biosynthesis, including modification of PhANGs expression and additional protective mechanisms against photo-oxidative damage (Op den Camp et al., 2003). This holds true for mutants with impaired tetrapyrrole biosynthesis, such as several *gun* mutants, which experience a reduced ALA synthesis followed by extenuated Chl contents. When NF-treated seedlings are short of carotenoids, Chl-binding proteins cannot be stabilized, free Chl accumulates and causes severe photo-oxidative damage in wild-type seedlings. It is suggested that reduced metabolic flow in the tetrapyrrole biosynthetic pathway will modify the potential risk of photo-oxidative stress. This is in agreement with biochemical and genetic investigations of NF-treated *gun* mutants which point to an integrative plastid signaling converging at least signals derived from tetrapyrrole biosynthesis, organellar gene expression, and abscisic acid signaling (Voigt et al., 2010).

We propose an extended concept of tetrapyrrole-mediated retrograde signaling that moves an ALA synthesis-dependent mechanism controlling NGE into focus (**Figure 10**). This model integrates changes in NGE of many mutants affected in tetrapyrrole biosynthesis (Mochizuki et al., 2001; Larkin et al., 2003; Woodson et al., 2011) and takes into account the deleterious properties of intermediates of the Mg branch of tetrapyrrole biosynthesis in plastid-to-nucleus communication (Mochizuki et al., 2008; Moulin et al., 2008; Kleine et al., 2009). This ALA-dependent signaling occurs apart from GUN1-mediated-signaling (Koussevitzky et al., 2007) since regulatory impact of feeding with ALA or GAB on *LHCB1.2* and *RBCS* expression acts additively to the *gun1-1* phenotype (**Figures 3** and **4**). Since we observed that ALA feeding did not suppress expression of *LHCB1.2* and *RCBS* in *gun4-1*, a function of GUN4 in the retrograde signaling pathway from ALA biosynthesis is suggested (**Figure 4**). Because multiple endogenous and environmental factors control the rate-limiting ALA synthesis and, thus, control the metabolic flow of tetrapyrrole intermediates for Chl and heme synthesis, retrograde signals emitted at the level of ALA formation are proposed to adjust the transcriptional machinery in the nucleus.

ACKNOWLEDGMENTS

The authors are grateful for financial support by the Deutsche Forschungsgemeinschaft (FOR 804 to Klaus F. X. Mayer and Bernhard Grimm). This work was also supported by the Office of Biological and Environmental Research in the Department of Energy (DOE) Office of Science for the BioEnergy Science Center (BESC). Oak Ridge National Laboratory is managed by UT-Battelle, LLC, for the U.S. Department of Energy under contract DE-AC05-00OR22725. The authors thank Georg Haberer for helpful discussion of microarray data and Colleen M. Iversen for a critical reading of the manuscript. The *hy1* and *hy2* mutants were kindly provided by Alison G. Smith (University of Cambridge, UK), the *gun1-1* mutant by Thomas Pfannschmidt (Friedrich Schiller University Jena, Germany), and the *gun 4-1* mutant by Joanne Chory (Salk Institute for Biological Studies, USA).

AUTHOR NOTE

The submitted manuscript has been authored by a contractor of the U.S. Government under contract DE-AC05-00OR22725. Accordingly, the U.S. Government retains a non-exclusive, royalty-free license to publish or reproduce the published form of this contribution, or allow others to do so, for U.S. Government purposes.

SUPPLEMENTARY MATERIAL

The Supplementary Material for this article can be found online at http://www.frontiersin.org/Plant_Physiology/10.3389/fpls.2012.00236/abstract

Table S1 | PCR Primers to amplify gene specific probes used for quantitative real-time PCR. Primers for *AtLHCB1.2*, and *AtRBCS* were taken from Mochizuki et al. (2008).

Table S2 | Verification of microarray results via qRT-PCR. RNA from GAB-treated *Arabidopsis* wild-type seedlings and *gun4-1* mutant seedlings was extracted 6 and 24 h, respectively, after light exposure. Transcript abundance of a defined set of genes was determined by quantitative real-time PCR and calculated as relative expression ($2^{-\Delta\Delta Ct}$) compared to untreated *Arabidopsis* wild-type Col-0 seedlings. qRT-PCR data are given as average ± SD of three biological replicates. Listed are relative expressions obtained by microarray experiments (sampling 6 h after light exposure) as well as qRT-PCR in order to compare relative expressions in both experimental approaches. Relative expressions of qRT-PCR data were calculated using *AtSAND* (for 6 h values) and *AtACT2* (for 24 h values) as reference. Bold: Relative transcript abundance in GAB-treated or *gun4-1* seedlings (determined by qRT-PCR) significantly differs from the untreated *Arabidopsis* wild-type Col-0 ($P < 0.05$).

Figure S1 | Pigment content (A) and phenotype (B) of *Arabidopsis* wild-type Col-0 seedlings, Col-0 seedlings treated with 10 μM gabaculine (GAB), and *gun4-1* mutant seedlings 6 h after de-etiolation or after 6 days growing on MS medium (control) or MS medium + 10 μM GAB. The contents of Chl a, Chl b, and Car of the untreated controls were 0.7 ± 0.2, 0.4 ± 0.2, and 2.6 ± 0.6 ng mg fw^{-1} 6 h after deetiolation and 172 ± 20, 44 ± 3, and 57 ± 5 ng mg fw^{-1} for 6 days old seedlings, respectively.

Figure S2 | Pchlide content of etiolated *Arabidopsis* Col-0 seedlings grown in liquid MS medium containing increasing concentrations of ALA. Surface sterilized seedlings were germinated and grown for 3 days in darkness under continuous shaking. Above an ALA concentration of 50 μM in the medium seedlings over-accumulate Pchlide.

Figure S3 | Phenotypes of *Arabidopsis* wild-type Col-0, *gun1-1*, and *gun4-1* treated with combinations of 1 μM norflurazon (NF), 10 μM gabaculine (GAB), and 100 μM ALA, respectively. Seedlings were grown on 0.5 MS medium supplemented with 1% (w/v) sucrose containing the indicated chemicals for 6 days under photoperiodic growth light (12 h light/12 h dark) at 100–120 μmol photons m^{-2} s^{-1}.

Figure S4 | Pigment accumulation during de-etiolation of 3-day-old etiolated *Arabidopsis* Col-0 seedlings. Given are means ± SD of three independent extractions.

Figure S5 | Overrepresentation of gene ontology (GO) categories in genes showing decreased (A) and increased (B) transcript abundance in GAB-treated *Arabidopsis* wild-type Col-0 and/or *gun4-1* mutants 6 h after illumination of etiolated seedlings. All 1032 genes being down-regulated **(A)** and 622 genes being upregulated **(B)** in both GAB treated and *gun4-1* seedlings, were analyzed for overrepresented GO categories (*P*-value of <0.05). Dotted lines indicate intermediate categories that are not shown. Calculation of overrepresented GO categories based on BiNGO 2.44.

REFERENCES

Alawady, A. E., and Grimm, B. (2005). Tobacco Mg protoporphyrin IX methyltransferase is involved in inverse activation of Mg porphyrin and protoheme synthesis. *Plant J.* 41, 282–290.

Apel, K., and Hirt, H. (2004). Reactive oxygen species: metabolism, oxidative stress, and signal transduction. *Annu. Rev. Plant Biol.* 55, 373–399.

Armstrong, G. A., Runge, S., Frick, G., Sperling, U., and Apel, K. (1995). Identification of NADPH:protochlorophyllide oxidoreductases A and B: a branched pathway for light-dependent chlorophyll biosynthesis in Arabidopsis thaliana. *Plant Physiol.* 108, 1505–1517.

Ashburner, M., Ball, C. A., Blake, J. A., Botstein, D., Butler, H., Cherry, J. M., et al. (2000). Gene Ontology: tool for the unification of biology. *Nat. Genet.* 25, 25–29.

Baier, M., and Dietz, K. J. (2005). Chloroplasts as source and target of cellular redox regulation: a discussion on chloroplast redox signals in the context of plant physiology. *J. Exp. Bot.* 56, 1449–1462.

Beck, C. F., and Grimm, B. (2006). "Involvement of tetrapyrroles in cellular regulation," in *Chlorophylls and Bacteriochlorophylls: Biochemistry, Biophysics, Functions and Applications*, eds B. Grimm, R. J. Porra, and W. Rudiger (Dordrecht: Springer), 223–235.

Benjamini, Y., and Hochberg, Y. (1995). Controlling the false discovery rate: a practical and powerful approach to multiple testing. *J. R. Stat. Soc. B* 57, 289–300.

Benjamini, Y., and Yekutieli, D. (2001). The control of the false discovery rate in multiple testing under dependency. *Ann. Stat.* 29, 1165–1188.

Borello, U., Ceccarelli, E., and Giuliano, G. (1993). Constitutive, light-responsive and circadian clock-responsive factors compete for the different l box elements in plant light-regulated promoters. *Plant J.* 4, 611–619.

Breitenbach, J., Boger, P., and Sandmann, G. (2002). Interaction of bleaching herbicides with the target enzyme zeta-carotene desaturase. *Pestic. Biochem. Physiol.* 73, 104–109.

Brusslan, J. A., and Peterson, M. P. (2002). Tetrapyrrole regulation of nuclear gene expression. *Photosyn. Res.* 71, 185–194.

Chory, J., Peto, C. A., Ashbaugh, M., Saganich, R., Pratt, L., and Ausubel, F. (1989). Different roles for phytochrome in etiolated and green plants deduced from characterization of Arabidopsis thaliana mutants. *Plant Cell* 1, 867–880.

Czarnecki, O., Hedtke, B., Melzer, M., Rothbart, M., Richter, A., Schroter, Y., et al. (2011a). An Arabidopsis GluTR binding protein mediates spatial separation of 5-aminolevulinic acid synthesis in chloroplasts. *Plant Cell* 23, 4476–4491.

Czarnecki, O., Peter, E., and Grimm, B. (2011b). "Methods for analysis of photosynthetic pigments and steady-state levels of intermediates of tetrapyrrole biosynthesis," in *Chloroplast Research in Arabidopsis: Methods and Protocols*, ed. P. R. Jarvis (Totowa: Humana Press), 357–385.

Dawson, R. C. M., Elliott, D. C., Elliot, W. H., and Jones, K. M. (1986). *Data for Biochemical Research*. New York: Oxford University Press.

Demko, V., Pavlovic, A., and Hudak, J. (2010). Gabaculine alters plastid development and differentially affects abundance of plastid-encoded DPOR and nuclear-encoded GluTR and FLU-like proteins in spruce cotyledons. *J. Plant Physiol.* 167, 693–700.

Donald, R. G., and Cashmore, A. R. (1990). Mutation of either G box or I box sequences profoundly affects expression from the Arabidopsis rbcS-1A promoter. *EMBO J.* 9, 1717–1726.

Elemento, O., Slonim, N., and Tavazoie, S. (2007). A universal framework for regulatory element discovery across all genomes and data types. *Mol. Cell* 28, 337–350.

Gentleman, R. C., Carey, V. J., Bates, D. M., Bolstad, B., Dettling, M., Dudoit, S., et al. (2004). Bioconductor: open software development for computational biology and bioinformatics. *Genet. Biol.* 5, R80.

Gray, J. C., Sullivan, J. A., Wang, J. H., Jerome, C. A., and Maclean, D. (2003). Coordination of plastid and nuclear gene expression. *Philos. Trans. R. Soc. Lond. B Biol. Sci.* 358, 135–144; discussion 144–135.

Grimm, B., Smith, A. J., Kannangara, C. G., and Smith, M. (1991). Gabaculine-resistant glutamate 1-semialdehyde aminotransferase of Synechococcus. Deletion of a tripeptide close to the NH2 terminus and internal amino acid substitution. *J. Biol. Chem.* 266, 12495–12501.

Hartigan, J. A., and Wong, M. A. (1978). A k-means clustering algorithm. *Appl. Stat.* 78, 100–108.

Heazlewood, J. L., Verboom, R. E., Tonti-Filippini, J., Small, I., and Millar, A. H. (2007). SUBA: the Arabidopsis subcellular database. *Nucleic Acids Res.* 35, D213–D218.

Hill, C. M., Pearson, S. A., Smith, A. J., and Rogers, L. J. (1985). Inhibition of chlorophyll synthesis in Hordeum vulgare by 3-amino 2,3-dihydrobenzoic acid (gabaculin). *Biosci. Rep.* 5, 775–781.

Ihaka, R., and Gentleman, R. (1996). R: A language for data analysis and graphics. *J. Comput. Graph. Stat.* 5, 299–314.

Irizarry, R. A., Hobbs, B., Collin, F., Beazer-Barclay, Y. D., Antonellis, K. J., Scherf, U., et al. (2003). Exploration, normalization, and summaries of high density oligonucleotide array probe level data. *Biostatistics* 4, 249–264.

Johanningmeier, U., and Howell, S. H. (1984). Regulation of light-harvesting chlorophyll-binding protein mRNA accumulation in Chlamydomonas reinhardi. Possible involvement of chlorophyll synthesis precursors. *J. Biol. Chem.* 259, 13541–13549.

Jung, H. S., and Chory, J. (2010). Signaling between chloroplasts and the nucleus: can a systems biology approach bring clarity to a complex and highly regulated pathway? *Plant Physiol.* 152, 453–459.

Kauss, D., Bischof, S., Steiner, S., Apel, K., and Meskauskiene, R. (2012). FLU, a negative feedback regulator of tetrapyrrole biosynthesis, is physically linked to the final steps of the Mg++-branch of this pathway. *FEBS Lett.* 586, 211–216.

Kim, C. H., Meskauskiene, R., Apel, K., and Laloi, C. (2008). No single way to understand singlet oxygen signalling in plants. *EMBO Rep.* 9, 435–439.

Kleine, T., Voigt, C., and Leister, D. (2009). Plastid signalling to the nucleus: messengers still lost in the mists? *Trends Genet.* 25, 185–192.

Kobayashi, Y., Kanesaki, Y., Tanaka, A., Kuroiwa, H., Kuroiwa, T., and Tanaka, K. (2009). Tetrapyrrole signal as a cell-cycle coordinator from organelle to nuclear DNA replication in plant cells. *Proc. Natl. Acad. Sci. U.S.A.* 106, 803–807.

Koski, V. M., and Smith, J. H. (1948). The isolation and spectral absorption properties of protochlorophyll from etiolated barley seedlings. *J. Am. Chem. Soc.* 70, 3558–3562.

Koussevitzky, S., Nott, A., Mockler, T. C., Hong, F., Sachetto-Martins, G., Surpin, M., et al. (2007). Signals from chloroplasts converge to regulate nuclear gene expression. *Science* 316, 715–719.

Kropat, J., Oster, U., Rudiger, W., and Beck, C. F. (1997). Chlorophyll precursors are signals of chloroplast origin involved in light induction of nuclear heat-shock genes. *Proc. Natl. Acad. Sci. U.S.A.* 94, 14168–14172.

La Rocca, N., Rascio, N., Oster, U., and Rudiger, W. (2001). Amitrole treatment of etiolated barley seedlings leads to deregulation of tetrapyrrole synthesis and to reduced expression of Lhc and RbcS genes. *Planta* 213, 101–108.

Larkin, R. M., Alonso, J. M., Ecker, J. R., and Chory, J. (2003). GUN4, a regulator of chlorophyll synthesis and intracellular signaling. *Science* 299, 902–906.

Lichtenthaler, H. K. (1987). Chlorophylls and carotenoids: pigments of photosynthetic membranes. *Meth. Enzymol.* 148, 350–382.

Livak, K. J., and Schmittgen, T. D. (2001). Analysis of relative gene expression data using real-time quantitative PCR and the 2(-Delta Delta C(T)) method. *Methods* 25, 402–408.

Lopez-Juez, E., Baynton, C. E., Page, A. M., Pyke, K. A., Robertson, S., and Vinti, G. (1999). "Multiple light and plastid signals control chloroplast development in Arabidopsis," in *Photosynthesis: Mechanisms and Effects*, ed. G. Garab (Dordrecht: Kluwer Academic Publishers), 2805–2808.

Maere, S., Heymans, K., and Kuiper, M. (2005). BiNGO: a cytoscape plugin to assess overrepresentation of gene ontology categories in biological networks. *Bioinformatics* 21, 3448–3449.

Mauzerall, D., and Granick, S. (1956). The occurrence and determination of delta-amino-levulinic acid and porphobilinogen in urine. *J. Biol. Chem.* 219, 435–446.

Meskauskiene, R., and Apel, K. (2002). Interaction of FLU, a negative regulator of tetrapyrrole biosynthesis, with the glutamyl-tRNA reductase requires the tetratricopeptide repeat domain of FLU. *FEBS Lett.* 532, 27–30.

Meskauskiene, R., Nater, M., Goslings, D., Kessler, F., Op Den Camp, R., and Apel, K. (2001). FLU: a negative regulator of chlorophyll biosynthesis in Arabidopsis thaliana. *Proc. Natl. Acad. Sci. U.S.A.* 98, 12826–12831.

Mochizuki, N., Brusslan, J. A., Larkin, R., Nagatani, A., and Chory, J. (2001). Arabidopsis genomes uncoupled 5 (GUN5) mutant reveals the involvement of Mg-chelatase H subunit in plastid-to-nucleus signal

transduction. *Proc. Natl. Acad. Sci. U.S.A.* 98, 2053–2058.

Mochizuki, N., Tanaka, R., Tanaka, A., Masuda, T., and Nagatani, A. (2008). The steady-state level of Mg-protoporphyrin IX is not a determinant of plastid-to-nucleus signaling in Arabidopsis. *Proc. Natl. Acad. Sci. U.S.A.* 105, 15184–15189.

Moulin, M., Mccormac, A. C., Terry, M. J., and Smith, A. G. (2008). Tetrapyrrole profiling in Arabidopsis seedlings reveals that retrograde plastid nuclear signaling is not due to Mg-protoporphyrin IX accumulation. *Proc. Natl. Acad. Sci. U.S.A.* 105, 15178–15183.

Murashige, T., and Skoog, F. (1962). A revised medium for rapid growth and bio assays with tobacco tissue cultures. *Physiol. Plant* 15, 473–497.

Nair, S. P., Kannangara, C. G., Harwood, J. L., and John, R. A. (1990). Inhibition studies on 5-aminolevulinate biosynthesis in Pisum sativum L. (Pea). *Biochem. Soc. Trans.* 18, 656–657.

Nott, A., Jung, H. S., Koussevitzky, S., and Chory, J. (2006). Plastid-to-nucleus retrograde signaling. *Annu. Rev. Plant Biol.* 57, 739–759.

Op den Camp, R. G., Przybyla, D., Ochsenbein, C., Laloi, C., Kim, C., Danon, A., et al. (2003). Rapid induction of distinct stress responses after the release of singlet oxygen in Arabidopsis. *Plant Cell* 15, 2320–2332.

Oster, U., Brunner, H., and Rudiger, W. (1996). The greening process in cress seedlings.5. Possible interference of chlorophyll precursors, accumulated after thujaplicin treatment, with light-regulated expression of Lhc genes. *J. Photochem. Photobiol. B Biol.* 36, 255–261.

Papenbrock, J., and Grimm, B. (2001). Regulatory network of tetrapyrrole biosynthesis – studies of intracellular signalling involved in metabolic and developmental control of plastids. *Planta* 213, 667–681.

Papenbrock, J., Mock, H. P., Tanaka, R., Kruse, E., and Grimm, B. (2000a). Role of magnesium chelatase activity in the early steps of the tetrapyrrole biosynthetic pathway. *Plant Physiol.* 122, 1161–1169.

Papenbrock, J., Pfundel, E., Mock, H. P., and Grimm, B. (2000b). Decreased and increased expression of the subunit CHL I diminishes Mg chelatase activity and reduces chlorophyll synthesis in transgenic tobacco plants. *Plant J.* 22, 155–164.

Peter, E., and Grimm, B. (2009). GUN4 is required for posttranslational control of plant tetrapyrrole biosynthesis. *Mol. Plant* 2, 1198–1210.

Peter, E., Rothbart, M., Oelze, M. L., Shalygo, N., Dietz, K. J., and Grimm, B. (2010). Mg protoporphyrin monomethylester cyclase deficiency and effects on the tetrapyrrole metabolism in different light conditions. *Plant Cell Physiol.* 51, 1229–1241.

Pfannschmidt, T. (2010). Plastidial retrograde signalling – a true "plastid factor" or just metabolite signatures? *Trends Plant Sci.* 15, 427–435.

Pfannschmidt, T., Schutze, K., Fey, V., Sherameti, I., and Oelmuller, R. (2003). Chloroplast redox control of nuclear gene expression – a new class of plastid signals in interorganellar communication. *Antioxid. Redox Signal.* 5, 95–101.

Pogson, B. J., Woo, N. S., Forster, B., and Small, I. D. (2008). Plastid signalling to the nucleus and beyond. *Trends Plant Sci.* 13, 602–609.

Richter, A., Peter, E., Pors, Y., Lorenzen, S., Grimm, B., and Czarnecki, O. (2010). Rapid dark repression of 5-aminolevulinic acid synthesis in green barley leaves. *Plant Cell Physiol.* 51, 670–681.

Ruckle, M. E., Demarco, S. M., and Larkin, R. M. (2007). Plastid signals remodel light signaling networks and are essential for efficient chloroplast biogenesis in Arabidopsis. *Plant Cell* 19, 3944–3960.

Shalygo, N., Czarnecki, O., Peter, E., and Grimm, B. (2009). Expression of chlorophyll synthase is also involved in feedback-control of chlorophyll biosynthesis. *Plant Mol. Biol.* 71, 425–436.

Smyth, G. K. (2004). Linear models and empirical Bayes methods for assessing differential expression in microarray experiments. *Stat. Appl. Genet. Mol. Biol.* 3, Article3.

Strand, A., Asami, T., Alonso, J., Ecker, J. R., and Chory, J. (2003). Chloroplast to nucleus communication triggered by accumulation of Mg-protoporphyrin IX. *Nature* 421, 79–83.

Surpin, M., Larkin, R. M., and Chory, J. (2002). Signal transduction between the chloroplast and the nucleus. *Plant Cell* 14(Suppl), S327–S338.

Susek, R. E., Ausubel, F. M., and Chory, J. (1993). Signal transduction mutants of Arabidopsis uncouple nuclear CAB and RBCS gene expression from chloroplast development. *Cell* 74, 787–799.

Tanaka, R., and Tanaka, A. (2007). Tetrapyrrole biosynthesis in higher plants. *Annu. Rev. Plant Biol.* 58, 321–346.

Timmis, J. N., Ayliffe, M. A., Huang, C. Y., and Martin, W. (2004). Endosymbiotic gene transfer: organelle genomes forge eukaryotic chromosomes. *Nat. Rev. Genet.* 5, 123–135.

Vasileuskaya, Z., Oster, U., and Beck, C. F. (2004). Involvement of tetrapyrroles in inter-organellar signaling in plants and algae. *Photosyn. Res.* 82, 289–299.

Vinti, G., Hills, A., Campbell, S., Bowyer, J. R., Mochizuki, N., Chory, J., et al. (2000). Interactions between hy1 and gun mutants of Arabidopsis, and their implications for plastid/nuclear signalling. *Plant J.* 24, 883–894.

Voigt, C., Oster, U., Bornke, F., Jahns, P., Dietz, K. J., Leister, D., et al. (2010). In-depth analysis of the distinctive effects of norflurazon implies that tetrapyrrole biosynthesis, organellar gene expression and ABA cooperate in the GUN-type of plastid signalling. *Physiol. Plant* 138, 503–519.

Woodson, J. D., Perez-Ruiz, J. M., and Chory, J. (2011). Heme synthesis by plastid ferrochelatase I regulates nuclear gene expression in plants. *Curr. Biol.* 21, 897–903.

Conflict of Interest Statement: The authors declare that the research was conducted in the absence of any commercial or financial relationships that could be construed as a potential conflict of interest.

Received: 14 August 2012; paper pending published: 06 September 2012; accepted: 03 October 2012; published online: 29 October 2012.

Citation: Czarnecki O, Gläßer C, Chen J-G, Mayer KFX and Grimm B (2012) Evidence for a contribution of ALA synthesis to plastid-to-nucleus signaling. Front. Plant Sci. ***3****:236. doi: 10.3389/fpls.2012.00236*

This article was submitted to Frontiers in Plant Physiology, a specialty of Frontiers in Plant Science.

Copyright © 2012 Czarnecki, Gläßer, Chen, Mayer and Grimm. This is an open-access article distributed under the terms of the Creative Commons Attribution License, which permits use, distribution and reproduction in other forums, provided the original authors and source are credited and subject to any copyright notices concerning any third-party graphics etc.

frontiers in
PLANT SCIENCE

HYPOTHESIS AND THEORY ARTICLE
published: 13 February 2013
doi: 10.3389/fpls.2013.00014

A model for tetrapyrrole synthesis as the primary mechanism for plastid-to-nucleus signaling during chloroplast biogenesis

Matthew J. Terry*[1,2] ***and Alison G. Smith*[3]**

[1] *Centre for Biological Sciences, University of Southampton, Southampton, UK*
[2] *Institute for Life Sciences, University of Southampton, Southampton, UK*
[3] *Department of Plant Sciences, University of Cambridge, Cambridge, UK*

Edited by:
Dario Leister, Ludwig-Maximilians-Universität München, Germany

Reviewed by:
Tatjana Kleine, Ludwig-Maximilians-Universität München, Germany
Paolo Pesaresi, Università degli Studi di Milano, Italy

****Correspondence:***
Matthew J. Terry, Centre for Biological Sciences, University of Southampton, Life Sciences Building 85, Highfield Campus, Southampton SO17 1BJ, UK.
e-mail: mjt@soton.ac.uk

Chloroplast biogenesis involves the co-ordinated expression of the chloroplast and nuclear genomes, requiring information to be sent from the developing chloroplasts to the nucleus. This is achieved through retrograde signaling pathways and can be demonstrated experimentally using the photobleaching herbicide, norflurazon, which in seedlings results in chloroplast damage and the reduced expression of many photosynthesis-related, nuclear genes. Genetic analysis of this pathway points to a major role for tetrapyrrole synthesis in retrograde signaling, as well as a strong interaction with light signaling pathways. Currently, the best model to explain the genetic data is that a specific heme pool generated by flux through ferrochelatase-1 functions as a positive signal to promote the expression of genes required for chloroplast development. We propose that this heme-related signal is the primary positive signal during chloroplast biogenesis, and that treatments and mutations affecting chloroplast transcription, RNA editing, translation, or protein import all impact on the synthesis and/or processing of this signal. A positive signal is consistent with the need to provide information on chloroplast status at all times. We further propose that GUN1 normally serves to restrict the production of the heme signal. In addition to a positive signal re-enforcing chloroplast development under normal conditions, aberrant chloroplast development may produce a negative signal due to accumulation of unbound chlorophyll biosynthesis intermediates, such as Mg-porphyrins. Under these conditions a rapid shut-down of tetrapyrrole synthesis is required. We propose that accumulation of these intermediates results in a rapid light-dependent inhibition of nuclear gene expression that is most likely mediated via singlet oxygen generated by photo-excitation of Mg-porphyrins. Thus, the tetrapyrrole pathway may provide both positive and inhibitory signals to control expression of nuclear genes.

Keywords: retrograde signaling, photomorphogenesis, heme, protochlorophyllide, chlorophyll, ferrochelatase, *gun* mutants, singlet oxygen

INTRODUCTION

Chloroplasts are essential organelles in plant cells, responsible for harvesting the majority of the Earth's energy obtained from the sun. Understanding chloroplast biogenesis is therefore both of great fundamental importance, and is essential in underpinning attempts to manipulate this process in the search for new sources of renewable energy. Chloroplasts evolved through the integration of free-living photosynthetic prokaryotic organisms into eukaryotic hosts, following an endosymbiotic relationship. However, the gene complement of these endosymbionts (encoding as many as 4500 proteins) has since been redistributed so that plant chloroplasts now encode genes for fewer than 100 proteins (Martin et al., 2002), with the remaining genes in the nucleus. As a consequence some 2000–3000 proteins are synthesized in the cytosol, and imported into the chloroplast (Gray et al., 2003; Zybailov et al., 2008; Jung and Chory, 2010). The regulation of chloroplast development and function therefore requires the co-ordination of both nuclear and chloroplast genomes.

There are two major groups of chloroplast-targeted proteins encoded by the nucleus: important components of the chloroplast genetic machinery, including one of the RNA polymerases and a large number of pentatricopeptide repeat (PPR) proteins involved in RNA processing; and the enzymes and other nucleus-encoded chloroplast proteins that comprise the components of the photosynthetic machinery. This latter group, referred to as "photosynthetic genes" (**Figure 1A**) are expressed in response to light via anterograde signaling pathways, which include those mediated by the phytochrome and cryptochrome families of photoreceptors (Waters and Langdale, 2009). Since many components of these signaling pathways are shared with other de-etiolation responses, considerable progress has been made recently in understanding light regulation of anterograde signaling (Leivar et al., 2009; Shin et al., 2009; Stephenson et al., 2009; Richter et al., 2010).

However, in any regulatory system information needs to travel in both directions, and chloroplasts are able to send information back to the nucleus to control expression of photosynthetic

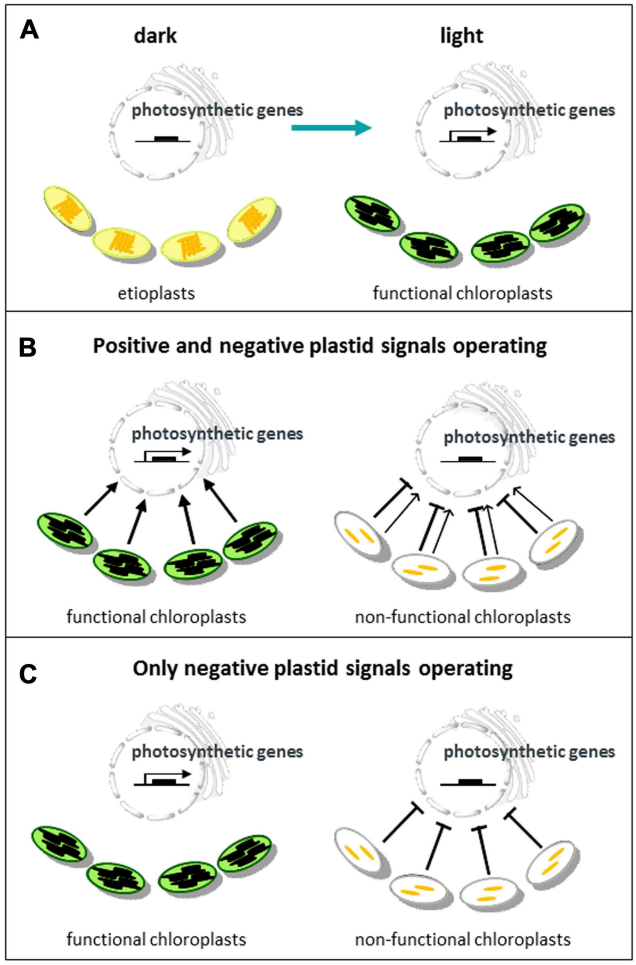

FIGURE 1 | Models for communication between plastids and the nucleus. (A) During chloroplast biogenesis light promotes the synthesis of many nuclear-encoded proteins required for the development of etioplasts into functional chloroplasts. **(B)** Under normal conditions a positive plastid signal provides information on the developmental status of the chloroplast and promotes nuclear gene expression. Chloroplast damage or loss of function leads to a reduction in the positive signal (in most conditions) and an additional inhibitory signal. **(C)** The alternative model in which only an inhibitory plastid signal resulting from chloroplast damage or loss of function provides information, but there is no feedback from the chloroplast to the nucleus under normal conditions.

genes via plastid-to-nucleus signaling (hereafter termed plastid signaling). In mature plants, chloroplasts can provide the nucleus with information about the environment that serves to optimize photosynthesis and other aspects of plant function such as the response to a variety of stresses. This type of plastid signaling has been defined as *operational control* (Pogson et al., 2008). This article, however, is concerned with *biogenic control*, i.e., signals that provide information about the developmental status of the chloroplast during the process of chloroplast biogenesis. Just as importantly these signals will also provide information on the number of developing chloroplasts that need to be provided with new proteins. Biogenic control has been studied primarily in de-etiolating seedlings, but may equally apply during the synthesis of new chloroplasts in the apical meristem. However, in addition to these developmental signals a young seedling is exposed to the same environmental cues as mature plants and extremes of light and temperature are likely to have even more severe effects at this stage of development. Therefore models of plastid signaling during biogenic control need to include integration of environmental information. So what would be the nature of such a signal? If a signal is required to provide information on the progression of chloroplast development then it makes sense that this signal is present throughout the developmental process. Only a positive plastid signal, as illustrated in **Figure 1B**, can provide this continuous information. An inhibitory signal that provides information about chloroplast damage should not be continuous – the only information potentially provided by a negative signal produced under normal conditions is its absence (**Figure 1C**). There is evidence in the early literature for a continuous plastid signal that permits expression of light-regulated genes (Oelmüller et al., 1986; Burgess and Taylor, 1988), and as we shall see such a model is now supported genetically (Woodson et al., 2011).

It is over 30 years since Bradbeer et al. (1979) first inferred that plants with abnormal chloroplasts showed reduced nuclear gene expression and thus that signals from the chloroplast were required for the expression of certain nuclear genes. However, despite remaining a highly active research area, our understanding of how chloroplasts signal to the nucleus has remained opaque (Pogson et al., 2008; Jung and Chory, 2010; Kleine et al., 2009; Pfannschmidt, 2010; Inaba et al., 2011; Leister, 2012). There are a number of reasons for this. Research on plastid signaling has been limited by the fact we have only isolated data sets utilizing different experimental systems. The use of different species, plastid treatments, seedling age, gene outputs etc., has contributed to confusion in the field that has hampered the development of robust and testable models for plastid signaling. A further complication is that the severity of treatments used invariably elicits a strong stress response that may mask signaling responses under normal physiological conditions, including the adjustment to mild stress conditions. These problems are particularly pertinent when trying to separate the role of plastid signaling during chloroplast biogenesis from that of mature chloroplasts. In this article we propose a model for plastid signaling during chloroplast biogenesis in which there are positive and negative plastid signals regulating nuclear gene expression. In doing this we have synthesized the available data to examine the role of tetrapyrrole synthesis in mediating both of these plastid signals.

JUST HOW MANY PLASTID SIGNALING MOLECULES ARE THERE?

Retrograde signaling was demonstrated in early experiments using plants with defective plastids, either as a result of mutation (Harpster et al., 1984) or the use of inhibitors of plastid translation or norflurazon (NF), a photobleaching herbicide that inhibits the carotenoid synthesis enzyme phytoene desaturase (Oelmüller et al., 1986). These experiments showed that plastid integrity was required for the expression of nuclear-encoded photosynthetic genes. Indeed, NF and the plastid translation inhibitor lincomycin (Lin) are still the standard experimental tools today

for demonstrating the requirement for functional chloroplasts to maintain nuclear gene expression during chloroplast biogenesis. NF treatment results in photo-oxidative damage of chloroplasts under white light due to unquenched triplet chlorophyll formation and leads to a catastrophic reduction in the expression of nearly 1000 nuclear genes (Strand et al., 2003; Koussevitzky et al., 2007; Moulin et al., 2008; Aluru et al., 2009). Lin treatment results in an even stronger response, with twice as many genes down-regulated (Cottage et al., 2008; Ruckle et al., 2012), provided that it is applied within 2–3 days of germination (Oelmüller et al., 1986; Gray et al., 2003).

Since the earliest observations the search has been on for the chloroplast-derived molecules that are affected by these treatments and thus could be signaling the nucleus to bring about changes in nuclear gene expression. There are now a range of candidate molecules in the literature (most recently reviewed by Leister, 2012), many of them coming to light quite recently. They can be categorized broadly into three separate classes of molecule:

PROTEINS

There are two proteins that have been shown recently to be translocated between plastids and the nucleus, suggesting they may be good candidates for mediating signaling between these compartments. Introduction of the gene for the transcriptional activator Whirly1 into tobacco chloroplast DNA resulted in synthesis of the protein in the chloroplast, but it was able to translocate to the nucleus to activate pathogen response genes (Isemer et al., 2012). In the second, the chloroplast envelope-bound plant homeodomain transcription factor (PTM) was shown to undergo proteolytic cleavage under conditions affecting plastid signaling, resulting in the accumulation of the amino terminal fragment in the nucleus (Sun et al., 2011). This PTM fragment targets the *ABI4* gene, activating its expression and, since ABI4 itself is implicated in plastid-dependent regulation of nuclear gene expression (Koussevitzky et al., 2007), this signaling mechanism looks very promising.

REACTIVE OXYGEN SPECIES

Reactive oxygen species (ROS) can be generated in the chloroplast through the action of photosynthesis with the superoxide anion radical and hydrogen peroxide produced from the reduction of oxygen at photosystem I (PSI) and singlet oxygen produced at PSII (Apel and Hirt, 2004). Accumulation of all three species has been shown to result in major changes in nuclear gene expression and thus convey information about the status of the chloroplast (op den Camp et al., 2003; Gadjev et al., 2006; Galvez-Valdivieso and Mullineaux, 2010).

METABOLITES

Several different classes of metabolites have the potential to be involved in chloroplast-to-nucleus communication. They are characterized by being synthesized in the chloroplast and then translocated into the cytosol or to other cellular compartments. Molecules such as amino acids, lipids, and reducing equivalents are exported from the chloroplast, and many hormones including the gibberellins, abscisic acid (ABA), jasmonate, and the strigolactones are at least partially synthesized in the chloroplast. One group of molecules that has been repeatedly implicated is the tetrapyrroles (discussed in more detail below). Heme, the phytochrome chromophore phytochromobilin, and chlorophyll breakdown products, are all known to leave the chloroplast and thus have the potential to modify cellular processes (Mochizuki et al., 2010). Other metabolites have also been shown recently to affect nuclear gene expression. The isoprenoid precursor methylerythritol cyclodiphosphate (MEcPP) was suggested as a plastid-derived signal regulating the nuclear gene *HPL* encoding the chloroplast-localized oxylipin biosynthesis enzyme hydroperoxide lyase (Xiao et al., 2012). Another example, is 3′-phosphoadenosine 5′-phosphate (PAP), which has been demonstrated to play a role as a chloroplast signal regulating a number of drought and high light-inducible genes, including *APX2* (Estavillo et al., 2011).

Can any of these signals result in the dramatic reduction in nuclear gene expression seen after severe treatments, such as with NF or Lin? One hypothesis is that there is not a single signal, and with so many chloroplast-derived metabolites able to influence nuclear gene expression, it is the combination of their effects – as metabolite signatures – that we observe as a plastid signal (Pfannschmidt, 2010). While this is a useful concept in our understanding of signal integration, it cannot account for the precipitous reduction in expression of many nuclear genes when chloroplast development is blocked. Such a proposal is also inconsistent with transcriptomic meta-analyses (Richly et al., 2003; Biehl et al., 2005). In these studies an analysis of the regulation of an almost complete gene set of nucleus-encoded chloroplast genes indicated that there was one master regulatory switch leading to the up- or down-regulation of a conserved group of genes and that this was tightly linked to mutations affecting the chloroplast (Richly et al., 2003). A more exhaustive follow-up study supported this idea, but was able to sub-divide gene classes further by function (Biehl et al., 2005), suggesting differential interaction with other signals. Regulation through the combined signaling of many metabolites might be expected to show a more complex gene expression profile. Since these studies were conducted with mature plants it suggests that a limited number of specific signals are also likely to be important during operational plastid signaling. However, signals such as MEcPP or PAP may reflect the response to changes in environmental conditions not tested for in these meta-analyses and could still contribute to a broad spectrum of signals involved in operational control, interacting with other signals such as those related to redox state (Dietz and Pfannschmidt, 2011). To drive the formation and development of chloroplasts during biogenesis it is more likely that a limited number of specific signals are required. And to understand this biogenic control we need to consider fully the genetic evidence available.

THE GENETICS OF PLASTID SIGNALING DURING CHLOROPLAST BIOGENESIS (*GENOMES UNCOUPLED* MUTANTS)

There are very many mutations and treatments affecting chloroplast function that lead to a reduction in the expression of nuclear

genes (discussed in more detail below). However, what we currently know about the pathways regulating chloroplast-to-nucleus communication during chloroplast biogenesis comes primarily from the isolation of *genomes uncoupled* (*gun*) mutants in which the expression of the nuclear gene *Lhcb* is maintained following chloroplast damage using NF treatment (Susek et al., 1993). To date, screening for this phenotype has generated mutants in two major categories: mutants affected in tetrapyrrole metabolism (Susek et al., 1993; Mochizuki et al., 2001; Larkin et al., 2003; Woodson et al., 2011) and mutants in light signaling components (Ruckle et al., 2007). Given the close association between light and plastid-signaling (Vinti et al., 2005; Larkin and Ruckle, 2008), and the primary role of light in regulating chloroplast development (Waters and Langdale, 2009), it is perhaps not surprising that a mutant lacking the blue-light photoreceptor cryptochrome 1 (CRY1) and the light signaling mutants *hy5* and *cop1* show altered response to chloroplast status (Ruckle et al., 2007). HY5 is a basic leucine zipper transcription factor that normally induces the expression of photosynthesis-related genes in response to phytochrome and cryptochrome signaling. However, it has been proposed that HY5 is converted to a negative regulator of photosynthetic genes after Lin treatment (Ruckle et al., 2007) when its function is dependent on the presence of another transcription factor ABI4 (Larkin and Ruckle, 2008). Consistent with this, *abi4* mutants also show a *gun* phenotype (Koussevitzky et al., 2007). Integration of light and plastid signaling responses at the genetic level supports earlier observations that the *cis*-regulatory elements mediating these responses appear to be common to both processes (Bolle et al., 1994; Kusnetsov et al., 1996; Puente et al., 1996; McCormac et al., 2001).

The original *gun* mutant screen isolated five mutants that retained partial expression of *Lhcb* after NF treatment. GUN1 is a PPR protein that binds nucleic acids (Susek et al., 1993; Koussevitzky et al., 2007) and is discussed later. The other four *gun* mutants were found to be mutated in tetrapyrrole synthesis genes: *GUN2*, *GUN3*, and *GUN5* encode heme oxygenase, phytochromobilin synthase, and the H subunit of Mg-chelatase (CHLH), respectively (**Figure 2**; Mochizuki et al., 2001), while GUN4 is a regulator of Mg-chelatase activity (Larkin et al., 2003). Subsequently it has been demonstrated that mutants lacking the D subunit (Strand et al., 2003) and both I subunits (Huang and Li, 2009) of Mg-chelatase also show a *gun* phenotype. Based on the characterization of these mutants and the apparent observation that the chlorophyll biosynthetic intermediate, Mg-protoporphyrin IX (Mg-proto), accumulated after NF treatment, it was proposed that Mg-proto acted as a mobile signal mediating chloroplast regulation of nuclear gene expression (Strand et al., 2003). However, this result has not been supported by further biochemical and genetic analysis in seedlings (Gadjieva et al., 2005; Mochizuki et al., 2008; Moulin et al., 2008; Voigt et al., 2010). In these experiments detailed measurements of Mg-proto and its methyl ester showed that there was no correlation between levels of these chlorophyll precursors and nuclear gene expression when Mg-proto levels were manipulated genetically (Mochizuki et al., 2008; Voigt et al., 2010) or using a range of growth conditions and treatments (Moulin et al., 2008). Moreover, a liquid chromatography-mass spectrometry approach was used to identify unambiguously the intermediates being measured, and no large accumulation of Mg-proto was observed under any condition, further supporting this conclusion (Moulin et al., 2008). These results also explained a previous observation that the *xantha-l* mutant of barley that accumulates Mg-proto did not show a reduction in nuclear gene expression (Gadjieva et al., 2005). Instead the identification of a dominant *gun* mutation (*gun6-1D*) that results in the overexpression of ferrochelatase-1 (FC1) has led to a model in which flux through a specific heme pool mediates plastid signaling (Woodson et al., 2011). This model provides an explanation for the phenotype of all the tetrapyrrole-related *gun* mutants in the tetrapyrrole pathway. As can be seen from **Figure 2**, blocking Mg-chelatase activity would be expected to direct protoporphyrin IX to heme synthesis (Cornah et al., 2003) thus increasing FC1 activity and heme levels. Similarly, inhibition of heme degradation in the *gun2* and *gun3* mutants would also be predicted to increase heme. Importantly, the simplest interpretation of the FC1-dependent *gun* phenotype is that it corresponds to the production of a positive signal promoting expression of nuclear-encoded chloroplast genes (**Figure 1B**) – the first such direct genetic evidence.

A HEME-MEDIATED POSITIVE PLASTID SIGNAL DURING CHLOROPLAST BIOGENESIS

The observation that the dominant *gun6* mutant had a *gun* phenotype was confirmed by overexpression of FC1 in wild-type plants. In contrast, overexpression of a second ferrochelatase isoform (FC2; **Figure 2**) did not result in this phenotype (Woodson et al., 2011). Moreover, a catalytically inactive FC1 was also unable to rescue nuclear gene expression, and the role of FC1 was dependent on flux through the pathway. These results indicate that it is the activity of FC1 that is crucial, and suggest that a specific FC1-derived pool of heme is functioning as a positive signal (or the precursor of such a signal) to promote expression of nuclear-encoded photosynthetic genes (Woodson et al., 2011). Furthermore, overexpression of FC1 can also rescue the loss of nuclear gene expression observed in a mutant lacking the SIG2 sigma factor involved in plastid-encoded RNA polymerase (PEP)-dependent plastid transcription (Woodson et al., 2013).

Does the model of a positive heme-related signal fit with all of the current data? Strand et al. (2003) originally reported that mutants in two trunk pathway enzymes, porphobilinogen deaminase (PBGD) and *lin2* lacking coproporphyrinogen oxidase (CPO; see **Figure 2**), showed a *gun* phenotype, as did treatment with the protoporphyrinogen oxidase (PPO) inhibitor S23142, results that would be inconsistent with heme as a positive regulator. In contrast, Woodson et al. (2011) reported that *lin2* did not show a *gun* phenotype, and that neither did the *hema1hema2* double mutant, defective in glutamyl-tRNA reductase, a key enzyme in the synthesis of the tetrapyrrole precursor 5-aminolevulinic acid (ALA), nor treatment with gabaculine, which inhibits the second ALA synthesis enzyme, glutamate semialdehyde aminomutase. Voigt et al. (2010) also failed to detect a *gun* phenotype for a range of mutants in enzymes in the trunk tetrapyrrole pathway between ALA and protoporphyrin IX. Clearly a consensus needs to be reached on the characterization of these mutants. Similarly, it is difficult to reconcile the observation that ALA feeding can inhibit

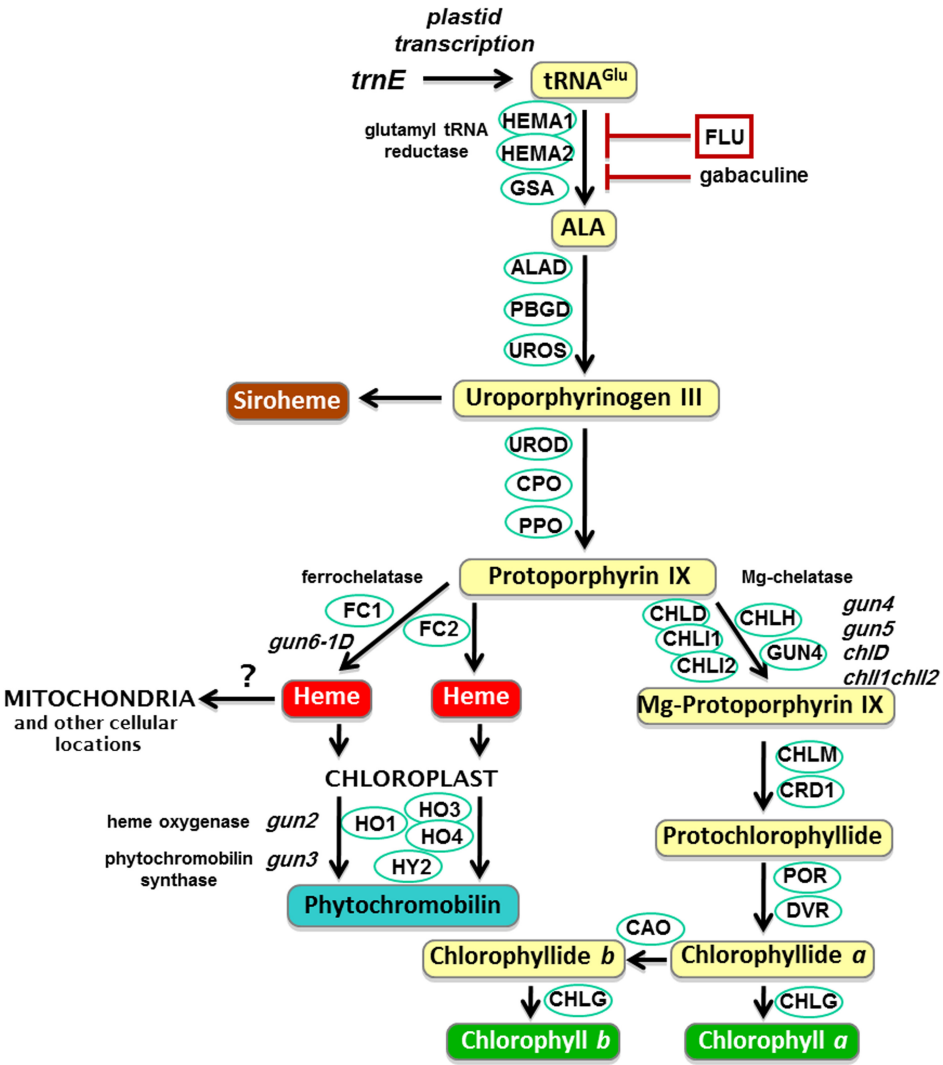

FIGURE 2 | The plant tetrapyrrole pathway with key enzymes and *gun* mutants. ALA, 5-aminolevulinic acid; HEMA, glutamyl-tRNA reductase; GSA, glutamate-1-semialdehyde 2,1-aminomutase; ALAD, 5-aminolevulinate dehydratase; PBGD, porphobilinogen deaminase; UROS, uroporphyrinogen III synthase; UROD, uroporphyrinogen III decarboxylase; CPO, coproporphyrinogen III oxidase; PPO, protoporphyrinogen IX oxidase; CHLH, Mg-chelatase H subunit; CHLI, Mg-chelatase I subunit; CHLD, Mg-chelatase D subunit; GUN4, regulator of Mg-chelatase; CHLM, Mg-proto IX methyltransferase; CRD1, Mg-proto IX monomethylester cyclase; POR, NADPH:protochlorophyllide oxidoreductase A, B and C; DVR, divinyl-protochlorophyllide reductase; CHLG, chlorophyll synthase; CAO, chlorophyllide *a* oxygenase; FC, ferrochelatase; HO, heme oxygenase; HY2, phytochromobilin synthase.

gene expression in dark (D) and far-red light (FR) grown seedlings (Vinti et al., 2000). A more recent study confirmed this result, but showed that ALA can rescue nuclear gene expression when the heme signal appears to be limiting, such as in the *sig2* mutant (Woodson et al., 2013). The demonstration that overexpression of protochlorophyllide oxidoreductase A and B (PORA and PORB) also causes a *gun* phenotype (McCormac and Terry, 2002) can most probably be explained by the extraordinary photo-oxidative buffering capacity of these proteins, which could have reduced the impact of the NF treatment. Alternatively, as POR overexpression also inhibits a proposed inhibitory pathway in the light (see later), this may have contributed to the observed phenotype on NF.

Another area that requires further resolution is the measurement of the proposed heme pool. Heme is present in plant cells bound covalently to c-type cytochromes, and non-covalently to b-type cytochromes and the vast majority of other hemoproteins, which include cytochromes P450, nitrate reductase, NADPH oxidases, peroxidases, and catalases (Cornah et al., 2003; Mochizuki et al., 2010). It is generally assumed that there is a pool of "free" heme that is either in transit between compartments, or associated with the site of synthesis, although since heme is very lipophilic it is unlikely to be in solution. It is this free-heme pool that is proposed to be involved in signaling, and it is likely to be small compared with total cellular heme. However, there is currently no satisfactory way of measuring free heme, nor even

confirming that it is present. Woodson et al. (2011) measured total non-covalently bound heme by acid-acetone extraction and a chemiluminescence-based detection method using reconstitution of horseradish peroxidase activity (Masuda and Takahashi, 2006), and found it was reduced after NF treatment, but not measurably increased in the *gun* mutants (with the exception of the heme oxygenase-deficient *gun2*). It is worth noting though, that *gun1* and *gun5* could both rescue heme levels in the *sig2* mutant background, which also had reduced heme (Woodson et al., 2013). The reduction in total non-covalently bound heme after a NF treatment (Woodson et al., 2011) is in agreement with an earlier acid extraction-based measurement (Kumar et al., 1999), but measurement of heme using alkali-acetone extraction and the same chemiluminescence-based detection assay produced the opposite result (Voigt et al., 2010). A more thorough analysis of this problem using a combination of different extraction methodologies suggests that a neutral-acetone extraction may give the best approximation of an unbound heme pool (Espinas et al., 2012). In this study, although total heme was reduced after NF treatment, an increase in an unbound free heme pool was observed, indicating that the method used by Voigt et al. (2010) more closely approximated to the measurement of an unbound heme pool. Nonetheless, how this information relates to a putative heme signal remains unclear. Any signal could be transient and may not accumulate at all, being instantly metabolized to a bilin for example. Certainly, there is no requirement for heme to be a mobile signal. Indeed, although heme is significantly less photo-toxic than Mg-proto, it is still a reactive molecule that interacts with other cellular components and thus any heme functioning as a signaling molecule is likely to be carefully chaperoned.

One potentially important aspect of the data of Woodson et al. (2011) is that an FC1-generated heme pool is associated with a requirement for non-photosynthetic heme. Both *FC1* and *HEMA2* show regulatory patterns inconsistent with a major role in photosynthesis (Ujwal et al., 2002; Nagai et al., 2007), and in fact are induced under stress conditions (Nagai et al., 2007; Moulin et al., 2008; Avin-Wittenberg et al., 2012). Following NF treatment neither gene was repressed, in stark contrast to all other tetrapyrrole synthesis genes except the mitochondrial *PPO2* (Moulin et al., 2008). Interestingly, nuclear gene expression on NF was rescued not only by overexpression of FCI, but also by HEMA2 (Woodson et al., 2011). It has long been speculated that there may be two spatially separated ALA pools providing tetrapyrroles for different purposes (Huang and Castelfranco, 1990), and recent data describing the discovery of a glutamyl-tRNA reductase binding protein (GBP) has put this suggestion back on the agenda (Czarnecki et al., 2011). In this case mutants lacking GBP showed differential inhibition of heme and chlorophyll synthesis, suggesting the possibility of a bifurcated pathway originating from ALA, although the model does not propose a simple separation of *HEMA1*- and *HEMA2*-encoded glutamyl-tRNA reductases. A more sophisticated model of tetrapyrrole synthesis may be needed to account for all the observations reported.

The close association between chloroplast and mitochondrial function has led to the integration of mitochondria into models for chloroplast-to-nucleus communication (Leister, 2005; Pfannschmidt, 2010). For example, in adult plants inhibition of chloroplast and mitochondrial translation had a synergistic effect on the down-regulation of nuclear-encoded chloroplast genes (Pesaresi et al., 2006). In the context of the current discussion it is interesting that mitochondria are a major sink for non-photosynthetic heme for the respiratory complexes. Heme is either made in the chloroplast and then transported to mitochondria, or possibly an earlier precursor is translocated, with the final two steps in heme synthesis taking place in the mitochondria (discussed in Mochizuki et al., 2010). It is tempting to speculate that an FC1-dependent positive plastid signal may require, at least in part, processing in mitochondria. Such a result might account for the synergistic effect of damaging both compartments (Pesaresi et al., 2006), while explaining why chloroplast damage can lead to a loss of gene expression when mitochondrial damage alone does not. The observation that mitochondrial-dependent up-regulation of *ALTERNATIVE OXIDASE1a* is mediated by ABI4 (Giraud et al., 2009), which is strongly implicated in plastid signaling (Koussevitzky et al., 2007), is also intriguing.

HEME AS A SIGNALING MOLECULE IN OTHER ORGANISMS

So how suitable is heme as a signaling molecule? In fact heme has been implicated in signaling in a wide range of systems and is well established as a signaling molecule in heterotrophic bacteria, fungi, and animals. In these systems, heme is either the only, or the major, tetrapyrrole molecule that is synthesized, and its role in regulating its own synthesis has been intensively investigated. Furthermore, it has also been shown that heme regulates cellular processes more generally, although the exact nature of its role as a regulator varies between organisms (Mense and Zhang, 2006; Furuyama et al., 2007). Nevertheless, evidence has emerged for conserved mechanisms of heme regulation that may be important in our understanding of heme signaling in plants.

In rhizobia and other α-proteobacteria, the iron response regulator (IRR) modulates the cellular response to available levels of iron including regulation of heme synthesis (Small et al., 2009). Under iron-deficiency IRR inhibits expression of the *hemB* gene encoding ALA dehydratase (ALAD; **Figure 2**), thus preventing accumulation of phototoxic heme biosynthesis intermediates. In *Bradyrhizobium japonicum* this is regulated by the conditional stability of IRR, which accumulates under iron-deficient conditions. In iron-replete conditions IRR is bound by ferrochelatase and is directly targeted for degradation by the heme product of this enzyme (Qi and O'Brian, 2002). Therefore in this system heme can act as a signaling molecule without accumulation as free heme. Under iron deficiency protoporphyrin IX accumulates, which promotes dissociation of ferrochelatase from IRR, thus preventing degradation. Deletion studies on IRR from *Bradyrhizobium* showed that it contained two heme binding sites: a heme-regulatory motif (HRM), which is characterized as containing a conserved Cys-Pro, and a second site with a His-xxx-His configuration that bind to ferric and ferrous heme, respectively (Yang et al., 2005a). Interestingly, other rhizobia only contain the His domain and in *Rhizobium leguminosarum* binding of heme to IRR does not affect stability, but instead prevents binding to regulatory promoter sequences (Singleton et al., 2010).

The HRM motif is critical for heme signaling in a wide variety of eukaryotic systems. The first recognition of the HRM came from the study of the mammalian enzyme 5-aminolevulinic acid synthase (ALAS), which in animals and yeast is responsible for the synthesis of ALA in a single step from succinyl coA and glycine (in contrast to the pathway from glutamate involving glutamyl-tRNA reductase and glutamate semialdehyde aminomutase found in plants, algae, and the majority of bacteria). In mammals there are two ALAS isoforms, both of which are targeted to the mitochondria via N-terminal targeting peptides that contain two copies of the HRM consensus sequence (Lathrop and Timko, 1993). Binding of heme to these two HRMs inhibits import of the ALAS precursors into mitochondria *in vitro* although additional factors were required to inhibit import of ALAS2 *in vivo* (Munakata et al., 2004). Another important example relevant to the current discussion comes from the yeast, *Saccharomyces cerevisiae.* In this case, the oxygen-dependent synthesis of heme, via the enzymes CPO and PPO (see **Figure 2**), initiates mitochondrial biogenesis as a result of heme-regulated expression of many nuclear genes (Zhang and Hach, 1999). This is achieved via heme activator protein 1 (HAP1), which contains seven HRMs, with heme binding affecting both the DNA binding and transcription-activation activities of HAP1 (Zhang and Guarente, 1995). Heme also affects nuclear gene transcription in mammals. An important mediator of this process is the basic leucine zipper protein Bach1, which contains six HRM motifs (Ogawa et al., 2001). Bach1 forms heterodimers with the Maf-related oncogene family to repress genes such as *HO-1* encoding heme oxygenase 1. In the presence of heme, Bach1 is ubiquitinated and degraded, leading to increased *HO-1* expression (Zenke-Kawasaki et al., 2007). As well as transcriptional effects, heme also modulates gene expression at the translational level. In rat reticulocytes, under heme-deficient conditions, a heme-regulated inhibitor, eIF2α kinase (HRI) phosphorylates eIF2α, preventing it from being recycled and thus protein synthesis is inhibited (Bauer et al., 2001). When heme is present, it can bind to HRI (which contains two HRMs) inactivating the kinase activity.

A more general role for heme as a signaling molecule has been established from the study of the circadian clock and how it interacts with metabolism. Heme biosynthesis is circadian-regulated and several components of the mammalian clock bind heme including PER2, NPAS2 (Kaasik and Lee, 2004; Yang et al., 2008), and Rev-erbα (Yin et al., 2007). This in turn regulates the ability of these factors to interact with nuclear transcription factors, thus influencing gene expression. In the case of PER2, heme-binding is via an HRM, but for NPAS2 and Rev-erbα, although the axial ligand is still cysteine, it is not within a classic HRM (Shimizu, 2012). Rev-erbα additionally utilizes a histidine as an axial ligand (Yin et al., 2007) and for NPAS2 the cysteine resides in a PAS domain (named after the proteins Per, ARNT, and Sim), a widely occurring domain that functions in binding a wide variety of small molecules (Henry and Crosson, 2011). Another broad role for heme regulation comes from the observation that a key miRNA processing enzyme in human cells, the RNA-binding protein DiGeorge critical region 8 (DGCR8) requires bound heme for activity (Faller et al., 2007). Since up to 30% of all human genes are regulated by miRNAs (Lewis et al., 2005), this indicates the scope for the influence of heme in these cells.

Are these mechanisms directly applicable to photosynthetic systems, where chlorophyll is the major tetrapyrrole synthesized? In addition to the evidence for a role for heme in plastid signaling in *Arabidopsis* (Woodson et al., 2011), heme has also been proposed (along with Mg-proto) as a signal in the green alga *Chlamydomonas reinhardtii* (von Gromoff et al., 2008). Analysis of the *Chlamydomonas* transcriptome showed that the expression of hundreds of genes was affected by heme, but only a few of these genes were associated with a photosynthetic function (Voss et al., 2011). The mechanism for this regulation is unknown and, although heme-binding proteins have been identified in plants (Takahashi et al., 2008; Mochizuki et al., 2010), classic HRM-containing regulators have not. In this context the recent identification of a heme regulatory protein in purple bacteria may be important (Yin et al., 2012). PpsR, which together with AppA mediates light and redox regulation of bacteriochlorophyll biosynthesis in *Rhodobacter sphaeroides*, shows modified DNA binding in response to heme, with heme binding mediated by an atypical HRM with a Cys-Ile motif (Yin et al., 2012). As PAS domains, which also function as heme-binding domains (Gilles-Gonzalez and Gonzalez, 2005), are widespread in plants, and with new regulatory heme-binding motifs being discovered, there is still plenty of potential for direct heme-regulatory mechanisms in plants.

THE HEME-MEDIATED SIGNAL IS THE PRIMARY PLASTID SIGNAL DURING CHLOROPLAST BIOGENESIS

If we accept that a heme-related signal is the leading candidate as a positive plastid signal based on the genetic evidence, then is this the only signal during chloroplast biogenesis? From the earliest studies it was established that inhibition of chloroplast translation resulted in an inhibition of nuclear gene expression (Oelmüller et al., 1986; Sullivan and Gray, 1999) and the interaction of the translational inhibitor Lin and NF with the *gun* mutants has led to the suggestion that whilst the two treatments both result in disrupted chloroplasts, they affect separate signaling pathways. This was most obviously demonstrated by the observation that inhibition of *Lhcb* expression after Lin treatment is rescued in the *gun1* mutant, but not in the *gun2–gun5* mutants (Gray et al., 2003; McCormac and Terry, 2004; Koussevitzky et al., 2007). Indeed, initial genetic (Mochizuki et al., 2001) and gene expression studies (Strand et al., 2003; McCormac and Terry, 2004) also suggested separate signaling pathways. For example, it was shown that loss of GUN5 had a stronger effect on expression of *Lhcb* than on *HEMA1*, but that this sensitivity was reversed in *gun1* (McCormac and Terry, 2004). However, recent experiments demonstrating that 89% of genes that are repressed by *gun1* are also repressed by *gun5,* and that strong alleles of *gun1* are epistatic to *gun5* (Koussevitzky et al., 2007), support the proposal that they do in fact reside in the same pathway, and that GUN1 plays a central role in all plastid signals including those defined by GUN2–5 (Koussevitzky et al., 2007). If this is the case, then the observation that *HEMA1* expression is fully rescued in a *gun1gun5* double mutant (McCormac and Terry, 2004) supports the idea that the heme signal is the primary, if not the only, positive plastid signal during chloroplast biogenesis.

There are actually many different treatments and mutations that affect chloroplast function and development and have an impact on nuclear gene expression (see Inaba et al., 2011 for a comprehensive list), and the consequences of these impairments have often been interpreted as defining independent signaling pathways. The expression of nucleus-encoded photosynthesis genes is blocked by conditions that inhibit early chloroplast development such as chloroplast transcription inhibitors (Rapp and Mullet, 1991) or mutations affecting transcription (*sig2*; Woodson et al., 2013), plastid RNA editing (Kakizaki et al., 2012), chloroplast protein synthesis (Hess et al., 1994; Pesaresi et al., 2006) or import of nucleus-encoded chloroplast proteins (*ppi2*; Kakizaki et al., 2009). In addition, various mutants with impaired chloroplast development such as the *cue* mutants of *Arabidopsis* also fall into this category (López-Juez et al., 1998; Vinti et al., 2005). It seems unnecessarily complex and therefore rather unlikely that inhibition of these processes each leads to an independent plastid signal, and the observation that *gun1* can rescue the plastid signaling response in *ppi2* (Kakizaki et al., 2009) and *sig2* (Woodson et al., 2013) as well as after Lin and NF treatments, supports the concept of a single primary pathway. We therefore propose that the simplest explanation for the effects of all of the treatments and mutations described above is that they compromise the production and/or processing of the positive heme-related signal.

A Mg-PORPHYRIN-DEPENDENT INHIBITORY PATHWAY DURING DEFECTIVE CHLOROPLAST DEVELOPMENT

Does a regulatory system in which there is a single positive signal provide the flexibility of regulation required for modulating such a complex and important process as chloroplast biogenesis? Perhaps more specifically if the signal is based on the synthesis of a tetrapyrrole, what happens when tetrapyrrole synthesis is in excess? Overaccumulation of tetrapyrroles has damaging photo-oxidative consequences for a seedling. This is most dramatically demonstrated in the *flu* mutant of *Arabidopsis* (Meskauskiene et al., 2001). FLU is a repressor of glutamyl-tRNA reductase activity and *flu* mutants therefore accumulate high levels of protochlorophyllide in the dark. On transfer to white light there is rapid production of singlet oxygen (op den Camp et al., 2003) resulting in severe tissue damage and seedling death (Wagner et al., 2004). A similar situation is observed in the block-of-greening response induced by a FR treatment prior to transfer to white light (Barnes et al., 1996). During the FR treatment phyA-dependent photoreceptor signaling pathways are activated, but photoconversion of protochlorophyllide by POR (**Figure 2**) does not proceed, resulting in the accumulation of protochlorophyllide at the same time as there is depletion of POR (Barnes et al., 1996; McCormac and Terry, 2002). Such an FR treatment can be lethal, but overexpression of PORA or PORB is able to rescue this response (Sperling et al., 1997). The advantage of this system is that the severity of the treatment can easily be adjusted by the length or fluence rate of the FR period and we have demonstrated that under conditions in which seedlings survive there is severe reduction in nuclear gene expression for photosynthesis-related genes (McCormac and Terry, 2002). Thus, under conditions in which ALA synthesis, and therefore all tetrapyrrole synthesis including a positive, heme-related signal is increased, there is inhibition of nuclear gene expression. This is strongly suggestive of an additional repressive signal. The generation of this signal is inhibited by overexpression of POR in the plastids as well as by the *gun5* mutant in which Mg-proto synthesis is impaired (McCormac and Terry, 2002, 2004). Consistent with it being a separate signal, down-regulation after a FR pre-treatment can be shown to be additive with inhibition of gene expression on NF (McCormac and Terry, 2002). Interestingly though, the FR-induced signal is exacerbated in a *gun1* mutant and inhibited by a simultaneous Lin treatment (McCormac and Terry, 2004).

A transcriptomic analysis of the effect of a FR pre-treatment on nuclear gene expression showed a strong overlap with a singlet oxygen-regulated gene set (McCormac and Terry, unpublished results). We therefore propose that the positive, inductive heme-related pathway is balanced by a repressive/inhibitory signaling pathway that is initiated by singlet oxygen generated via the accumulation of Mg-porphyrins and other chlorophyll precursors (**Figure 3**). This repressive signal may not have been observed in transcriptomic experiments using *flu,* which also accumulates Mg-porphyrins, as these studies used *flu* plants at the rosette stage (op den Camp et al., 2003). In contrast to the positive signal, which can be demonstrated to function in the dark (Sullivan and Gray, 1999; Woodson et al., 2013), the repressive signal is light-dependent, consistent with its role in protection from photo-oxidative damage. The primary aim of this repressive pathway is to shut-down tetrapyrrole synthesis (and chloroplast development) to prevent seedling lethality under conditions in which regulation of the tetrapyrrole pathway has been compromised. In this respect, the FR pre-treatment may be representative of seedling emergence under leaf litter, or by an extended dark period. Certainly mutants in light signaling pathways such as the *pif* mutants also show similar responses (Huq et al., 2004; Stephenson et al., 2009), and thus any perturbation of the light or developmental pathways regulating etioplast and early chloroplast development may need to be compensated for by a protective repressive signaling pathway. In this regard, it is interesting that the plant goes to great lengths to balance the synthesis of protochlorophyllide and POR through the combined action of light and hormone signaling pathways to optimize this de-etiolation response (Zhong et al., 2009; Cheminant et al., 2011).

THE ROLE OF GUN1

The development of a model in which two different tetrapyrrole-related pathways regulate the expression of photosynthesis-related genes might explain some of the observations in the literature that are difficult to reconcile with existing models. This includes the role of GUN1. Because the *gun1* mutant rescues plastid signaling under a wide range of conditions that reduce nuclear gene expression, including treatment with NF and Lin (Koussevitzky et al., 2007), or the *sig2* (Woodson et al., 2013), and *ppi2* (Kakizaki et al., 2009) mutations, models of GUN1 function have invariably placed it in a central integrating role *downstream* of these supposed signals. However, we suggest an alternative model that fits the existing data in which GUN1 functions *upstream* of the heme-related signal, as either a general repressor of chloroplast

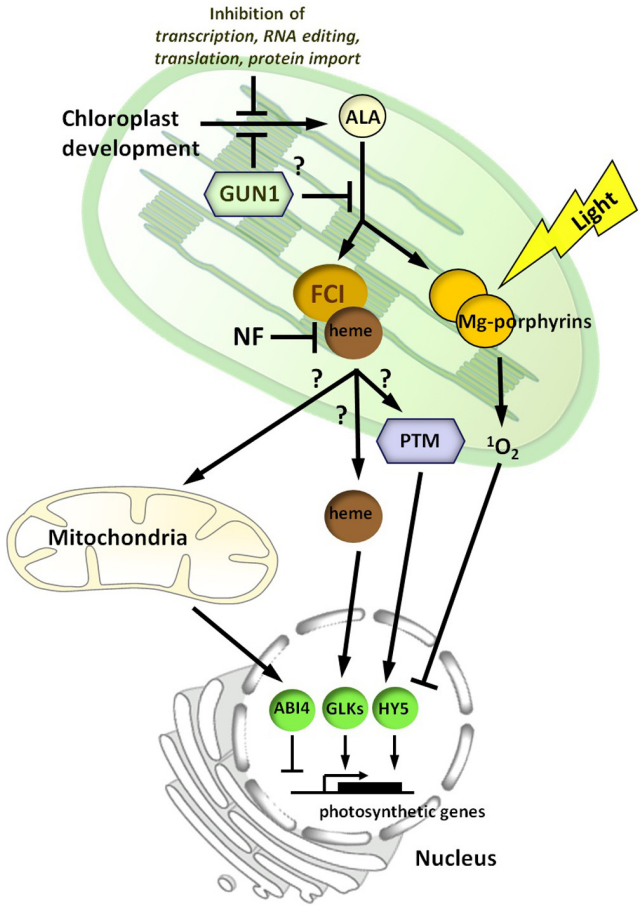

FIGURE 3 | A model for chloroplast to nucleus signaling during chloroplast biogenesis. In this model, there are two signaling pathways proposed. A *positive heme-related* signal, mediated by ferrochelatase 1 (FC1), whose production reflects the developmental status of the chloroplast. Inhibition of chloroplast development by norflurazon (NF) treatment blocks production or transmission of this signal. The heme-related signal may be heme itself or a heme metabolite, and is possibly conveyed via the mitochondria. The plant homeodomain transcription factor (PTM) is also a good signaling candidate and a number of other nuclear-localized transcription factors, including ABI4, HY5, and GLK1/2 have been implicated. GUN1 is proposed to repress chloroplast development or the synthesis of the signal before or after the synthesis of the rate-limiting intermediate 5-aminolevulinic acid (ALA). The environment can impact adversely on the positive signal through effects on chloroplast development. Under conditions in which this leads to excess accumulation of chlorophyll precursors, such as Mg-porphyrins, a second *inhibitory light-dependent* signal, mediated by singlet oxygen ($^1O_2$), represses photosynthetic and tetrapyrrole synthesis genes.

development or more specifically as a repressor of tetrapyrrole accumulation. Thus in a *gun1* mutant the positive heme-related signal would be enhanced. Indeed such an effect was observed on the reduced heme levels seen in *sig2* (Woodson et al., 2013). The extension of this argument is that *gun1* mutants would be expected to have an increased positive signal in the dark (as the repressive signal is light-dependent). This is observed in the *sig2* mutant (Woodson et al., 2013) and we have also reported that the expression of the plastid signal-responsive gene *HEMA1* is increased in the dark in *gun1* seedlings (McCormac and Terry, 2004). Finally, an increase in tetrapyrrole accumulation should also increase the strength of the inhibitory signal under appropriate conditions and *gun1* seedlings are more susceptible to loss of gene expression following a FR treatment (McCormac and Terry, 2004). The role of GUN1 as a repressor of chloroplast development would appear at first to be in contradiction to earlier studies suggesting it is required for chloroplast development (Mochizuki et al., 1996; Ruckle et al., 2007). This interpretation rests on the observation that *gun1* seedlings do not green normally in the light. However, we would argue that this inability to green is completely consistent with an elevated *HEMA1* expression and increased tetrapyrrole synthesis which would lead to an increased susceptibility to photobleaching on transfer to white light (Mochizuki et al., 1996; McCormac and Terry, 2004). In this respect the situation is very similar to the interpretation of the *pif3* mutant phenotype. In this case the inability to green on transfer to light was originally interpreted as PIF3 having a positive role in chloroplast development (Monte et al., 2004), but it was subsequently demonstrated that PIF3 functions to repress photosynthetic gene expression (Stephenson et al., 2009).

What might be the function of GUN1 in repressing chloroplast development or tetrapyrrole synthesis? GUN1 encodes a PPR protein (Koussevitzky et al., 2007). PPR proteins bind RNA and are involved in RNA metabolism, resulting in changes in plastid gene expression (Schmitz-Linneweber and Small, 2008). One obvious target for GUN1 might therefore be the plastid-transcribed $tRNA^{Glu}$, the substrate for glutamyl-tRNA reductase (**Figure 2**), the rate limiting step of tetrapyrrole synthesis. If the role of GUN1 was to control the availability of $tRNA^{Glu}$ for heme synthesis then its absence might lead to increased plastid signaling via increased substrate for FC1, and therefore a stronger heme signal under conditions when this is normally limited. The recent demonstration that the sigma factors SIG2 and SIG6 are both required for nuclear gene expression, $tRNA^{Glu}$ expression and heme synthesis, support this link (Woodson et al., 2013). However, although *gun1* could rescue the gene expression phenotype of *sig2* and *sig6* it did not do this through an increase in steady-state levels of $tRNA^{Glu}$ transcript (Woodson et al., 2013). Instead it is possible to speculate about other mechanisms of GUN1 function such as restricting access of $tRNA^{Glu}$ to glutamyl-tRNA reductase, rather than protein synthesis, or even selection between the glutamyl-tRNA reductase isoforms encoded by the *HEMA1* and *HEMA2* genes. Alternatively GUN1 may have a broader role in plastid RNA metabolism. Kakizaki et al. (2012) observed that many conditions that affect plastid signaling also affect RNA editing in plastids, although no differences in editing were seen in *gun1* for the two genes studied, *accD* and *rps14*. It has been noted that GUN1 shares considerable similarity with pTAC2 (Koussevitzky et al., 2007), which forms part of a transcriptionally active complex required for expression of PEP-transcribed genes (Pfalz et al., 2006). Interestingly, another component of this complex, pTAC12 (HEMERA), has dual chloroplast and nuclear localization (Chen et al., 2010), and plays an important role in light signaling (Galvão et al., 2012). Given the strong interaction between plastid and light signaling (Ruckle et al., 2007; Larkin and Ruckle, 2008), understanding the link

between PEP-mediated plastid transcription and light regulation of nuclear gene expression may also provide further clues about the role of GUN1.

In contrast to *gun1*, the *gun2–gun6* mutants cannot rescue conditions that block early chloroplast development. An explanation for this is that these mutations "protect" the loss of the heme signal by increasing heme synthesis at the expense of Mg-porphyrin or bilin production, but in treatments affecting the early stages of chloroplast development there is no signal to protect. Similarly, the model explains the rather unusual observation that, while Lin and NF treatments or FR treatment and NF are additive, Lin partially rescues a FR treatment response (McCormac and Terry, 2004). Our model would propose that because Lin treatment blocks chloroplast development it prevents Mg-porphyrin synthesis and the full expression of the inhibitory response. Moreover, it is possible that, since a singlet oxygen signal would be produced by excitation of tetrapyrroles including Mg-proto, the inhibitory pathway may account for some of the studies in which a correlation between Mg-proto accumulation and inhibition of nuclear gene expression has been observed (Strand et al., 2003; Pontier et al., 2007; Kindgren et al., 2011): the fact that both pathways are operating under some conditions and that individual genes show different sensitivities to treatments affecting them (McCormac and Terry, 2004) may also explain why this correlation is far from absolute (Mochizuki et al., 2008; Moulin et al., 2008; Voigt et al., 2010). The same argument could also account for some of the confusion about whether GUN1 and GUN2–GUN6 function in the same pathway (e.g., Vinti et al., 2000; Mochizuki et al., 2001; McCormac and Terry, 2004).

HOW DO TETRAPYRROLES SIGNAL TO THE NUCLEUS?

The most significant gap in our understanding of plastid signaling is the nature of the signal that moves from the plastid to influence nuclear gene expression, either by acting in the nucleus directly or via interaction with a cytoplasmic signaling pathway. It is possible that heme derived from FC1 can function as a mobile signal to interact directly with downstream components in the nucleus or cytoplasm. Heme is less photo-toxic than Mg-proto and thus is more suitable as a signaling molecule, but it would nevertheless need to be associated with one of the numerous heme-binding proteins recently identified, in order to be transported around the cell (Mochizuki et al., 2010). As shown in **Figure 3**, and discussed earlier, the mitochondria could also be a destination for at least some of this pool. However, there is no requirement for heme to leave the chloroplast: any signal could be passed on immediately. An obvious candidate would be a product of heme degradation such as a bilin (Terry et al., 2002), although in this case it might be expected that *gun2* (*hy1*) and *gun3* (*hy2*; **Figure 2**) would not have *gun* phenotypes. However, the fate of heme in plant cells is still poorly understood (Mochizuki et al., 2010) and a mobile heme signal cannot be ruled out. Alternatively, with many chloroplast and mitochondrial proteins requiring a heme cofactor to be functional there are many potential mechanisms by which a heme signal could be transduced. One interesting candidate that was identified recently is the chloroplast envelope-bound PTM protein (Sun et al., 2011). Mutants in *ptm* are also *gun* mutants, and it was demonstrated that PTM functions in the same pathway as GUN1 (Sun et al., 2011). As PTM is proposed to undergo proteolytic cleavage to give an amino terminal fragment that directly regulates *ABI4* expression, such a plastid-signaling pathway would be satisfyingly simple. ABI4 has already been identified as a downstream regulator of the GUN pathway (Koussevitzky et al., 2007), where it may function to integrate a number of additional signals regulating nucleus-encoded photosynthetic genes such as sucrose (Oswald et al., 2001), ABA (Koussevitzky et al., 2007), a mitochondrial signal (Giraud et al., 2009), and most recently a heat responsive retrograde signal (Yu et al., 2012). In addition, it has been proposed that ABI4 functions together with HY5 to mediate plastid signaling responses, thus integrating them into the light signaling network (Ruckle et al., 2007; Larkin and Ruckle, 2008). However, it is likely that other transcription factors are also involved in the positive or inhibitory pathways. Two important regulators of chloroplast development, GLK1 and GLK2, are certainly candidates for such a role (Kakizaki et al., 2009; Waters et al., 2009), as are the recently described *END* genes (Ruckle et al., 2012). Whether these targets serve as a convergence point between the positive and inhibitory pathways remains to be elucidated.

If the inhibitory signal is indeed singlet oxygen-mediated, as postulated above, it is possible that its signal transduction utilizes some of the same components identified for singlet oxygen-mediated stress responses in the *flu* mutant. These include the chloroplast proteins EXECUTER1 and EXECUTER2 (EX1 and EX2; Wagner et al., 2004; Lee et al., 2007), as well as a requirement for CRY1 in a singlet oxygen-mediated programmed cell death response (Danon et al., 2006). Interestingly, CRY1 also has been proposed to play a role in response to high irradiance stress (Kleine et al., 2007), and *cry1* mutants were identified as *gun* mutants (Ruckle et al., 2007). Singlet oxygen itself has a short half-life and any information contained in a singlet oxygen burst would need to be passed locally in the first instance. It has therefore been speculated that various lipid-related metabolites of singlet oxygen action may be involved in signaling. One particularly promising candidate is the β-carotene-derived oxidation product β-cyclocitral (Ramel et al., 2012). However, it should be emphasized that an inhibitory signal involved in regulation of chloroplast development may be quite distinct from that involved in the induction of stress signaling genes. For example, EX1- and EX2-dependent cell death responses require fully developed chloroplasts to be observed (Kim et al., 2012). In addition, given the observation that singlet oxygen and hydrogen peroxide signaling appear to be antagonistic (Laloi et al., 2007) it is tempting to speculate that the induction of nuclear gene expression by the positive heme-related signal is mediated by a low level of hydrogen peroxide. In this way biogenic control might mirror the effects later in development (operational control) in which a balance of singlet oxygen and hydrogen peroxide signaling, resulting from excitation of PSII and PSI, respectively, may be important in communicating changes in relative excitation to the nucleus in mature plants. There is already considerable evidence that hydrogen peroxide functions as a plastid signaling molecule in high light responses, and so might also make a suitable candidate for retrograde signaling during chloroplast development (Galvez-Valdivieso and Mullineaux, 2010).

CONCLUSION

In this article we have described a model for the role of chloroplast-localized tetrapyrrole synthesis in regulating nuclear gene expression. The model builds on the seminal work of the Chory laboratory in demonstrating genetically that a heme-related signal acts as a positive signal for chloroplast biogenesis (Woodson et al., 2011), but has a number of significant additions. The key features of the model are that: (i) all of the chloroplast treatments and mutants that are characterized as reducing nuclear gene expression do so by inhibiting the capacity of the chloroplast to make or process a heme-related signal; (ii) GUN1 acts early in this pathway to promote signal production, rather than late in pathway integrating many different signals; and (iii) an inhibitory signal derived from light excitation of Mg-porphyrins and other chlorophyll precursors serves to reduce tetrapyrrole synthesis and restrict chloroplast development under conditions in which these molecules are in dangerous excess. The model focuses on a single biological system, namely early seedling development in *Arabidopsis*, and thus should be easily testable and improved upon in many laboratories – once the central features of a model are defined and broadly accepted in one system, its significance across different systems can be assessed. The model focuses on what happens during biogenic control; however, a key question will be to determine the overlap between biogenic and operational control. Clearly the environment will have a major impact on early seedling development, but do developing chloroplasts sense these changes in a fundamentally different way?

There is increasing evidence that plastid signaling pathways are part of fundamental signaling networks that not only mediate the plant's response to stress, but also operate in a pre-stress environment to co-ordinate developmental and environmental cues. For example, mutations in EX1 and EX2 inhibit singlet oxygen signaling during embryogenesis, resulting in impaired chloroplast development in germinating seedlings. In this system, the stress hormone ABA promotes chloroplast development (Kim et al., 2009) perhaps because application of ABA results in a *gun* phenotype (Voigt et al., 2010). The developing theme is that mild stress responses mediated by chloroplasts function to protect plants from more severe stress later (Saini et al., 2011). Plastid signals are linked to both environmental stresses such as high light (Galvez-Valdivieso et al., 2009; Ramel et al., 2012), cold (Yoshida et al., 1998; Yang et al., 2005b), and drought (Miller et al., 2010; Estavillo et al., 2011) as well as a range of developmental responses (Yu et al., 2007; Ruckle and Larkin, 2009; Burch-Smith et al., 2011; Fleischmann et al., 2011). How these responses are integrated with the biogenic signals described here will be a critical next step in understanding how a seedling is able to become established in a potentially hostile environment.

ACKNOWLEDGMENTS

Research on plastid signaling in the authors' laboratories is supported by Biotechnology and Biological Sciences Research Council grants BB/J018139/1 and BB/J018694/1 to Matthew J. Terry and Alison G. Smith, respectively.

REFERENCES

Apel, K., and Hirt, H. (2004). Reactive oxygen species: metabolism, oxidative stress, and signal transduction. *Annu. Rev. Plant Biol.* 55, 373–399.

Aluru, M. R., Zola, J., Foudree, A., and Rodermel, S. R. (2009). Chloroplast photooxidation-induced transcriptome reprogramming in *Arabidopsis* immutans white leaf sectors. *Plant Physiol.* 150, 904–923.

Avin-Wittenberg, T., Tzin, V., Angelovici, R., Less, H., and Galili, G. (2012). Deciphering energy-associated gene networks operating in the response of *Arabidopsis* plants to stress and nutritional cues. *Plant J.* 70, 954–966.

Barnes, S. A., Nishizawa, N. K., Quaggio, R. B., Whitelam, G. C., and Chua, N.-H. (1996). Far-red light blocks greening of *Arabidopsis* seedlings via a phytochrome A-mediated change in plastid development. *Plant Cell* 8, 601–613.

Bauer, B. N., Rafie-Kolpin, M., Lu, L., Han, A., and Chen, J. J. (2001). Multiple autophosphorylation is essential for the formation of the active and stable homodimer of heme-regulated eIF2α kinase. *Biochemistry* 40, 11543–11551.

Biehl, A., Richly, E., Noutsos, C., Salamini, F., and Leister, D. (2005). Analysis of 101 nuclear transcriptomes reveals 23 distinct regulons and their relationship to metabolism, chromosomal gene distribution and co-ordination of nuclear and plastid gene expression. *Gene* 344, 33–41.

Bolle, C., Sopory, S., Lübberstedt, T., Klösgen, R. B., Herrmann, R. G., and Oelmüller, R. (1994). The role of plastids in the expression of nuclear genes for thylakoid proteins studied with chimeric β-glucuronidase gene fusions. *Plant Physiol.* 105, 1355–1364.

Bradbeer, J. W., Atkinson, Y. E., Börner, T., and Hagemann, R. (1979). Cytoplasmic synthesis of plastid polypeptides may be controlled by plastid-synthesized RNA. *Nature* 279, 816–817.

Burch-Smith, T. M., Brunkard, J. O., Choi, Y. G., and Zambryski, P. C. (2011). Organelle–nucleus cross-talk regulates plant intercellular communication via plasmodesmata. *Proc. Natl. Acad. Sci. U.S.A.* 108, 1451–1460.

Burgess, D. G., and Taylor, W. C. (1988). The chloroplast affects the transcription of a nuclear gene family. *Mol. Gen. Genet.* 214, 89–96.

Cheminant, S., Wild, M., Bouvier, F., Pelletier, S., Renou, J. P., Erhardt, M., et al. (2011). DELLAs regulate chlorophyll and carotenoid biosynthesis to prevent photooxidative damage during seedling deetiolation in *Arabidopsis*. *Plant Cell* 23, 1849–1860.

Chen, M., Galvao, R. M., Li, M., Burger, B., Bugea, J., Bolado, J., et al. (2010). *Arabidopsis* HEMERA/pTAC12 initiates photomorphogenesis by phytochromes. *Cell* 141, 1230–1240.

Cornah, J. E., Terry, M. J., and Smith, A. G. (2003). Green or red: what stops the traffic in the tetrapyrrole pathway? *Trends Plant Sci.* 8, 224–230.

Cottage, A. J., Mott, E. K., Wang, J.-H., Sullivan, J. A., MacLean, D., Tran, L., et al. (2008). "GUN1 (GENOMES UNCOUPLED1) encodes a pentatricopeptide repeat (PPR) protein involved in plastid protein synthesis-responsive retrograde signaling to the nucleus," in *Photosynthesis: Energy from the Sun. 14th International Congress on Photosynthesis*, ed. J. F. Allen, E. Gnatt, J. H. Golbeck, and B. Osmond (Dordrecht: Springer), 1201–1205.

Czarnecki, O., Hedtke, B., Melzer, M., Rothbart, M., Richter, A., Schroter, Y., et al. (2011). An *Arabidopsis* GluTR binding protein mediates spatial separation of 5-aminolevulinic acid synthesis in chloroplasts. *Plant Cell* 23, 4476–4491.

Danon, A., Coll, N. S., and Apel, K. (2006). Cryptochrome-1-dependent execution of programmed cell death induced by singlet oxygen in *Arabidopsis thaliana*. *Proc. Natl. Acad. Sci. U.S.A.* 103, 17036–17041.

Dietz, K. J., and Pfannschmidt, T. (2011). Novel regulators in photosynthetic redox control of plant metabolism and gene expression. *Plant Physiol.* 155, 1477–1485.

Espinas, N. A., Kobayashi, K., Takahashi, S., Mochizuki, N., and Masuda, T. (2012). Evaluation of unbound free heme in plant cells by differential acetone extraction. *Plant Cell Physiol.* 53, 1344–1354.

Estavillo, G. M., Crisp, P. A., Pornsiriwong, W., Wirtz, M., Collinge, D., Carrie, C., et al. (2011). Evidence for a SAL1-PAP chloroplast retrograde pathway that functions in drought and high light signaling in *Arabidopsis*. *Plant Cell* 23, 3992–4012.

Faller, M., Matsunaga, M., Yin, S., Loo, J. A., and Guo, F. (2007). Heme is involved in microRNA processing. *Nat. Struct. Mol. Biol.* 14, 23–29.

Fleischmann, T. T., Scharff, L. B., Alkatib, S., Hasdorf, S., Schottler, M. A., and Bock, R. (2011). Nonessential plastid-encoded ribosomal proteins in tobacco: a developmental role for plastid translation and implications for reductive genome evolution. *Plant Cell* 23, 3137–3155.

Furuyama, K., Kaneko, K., and Vargas, P. D. (2007). Heme as a magnificent molecule with multiple missions: heme determines its own fate and governs cellular homeostasis. *Tohoku J. Exp. Med.* 213, 1–16.

Gadjev, I., Vanderauwera, S., Gechev, T. S., Laloi, C., Minkov, I., Shuaev, V., et al. (2006). Transcriptomic footprints disclose specificity of reactive oxygen species signaling in *Arabidopsis*. *Plant Physiol.* 141, 436–445.

Gadjieva, R., Axelsson, E., Olsson, U., and Hansson, M. (2005). Analysis of gun phenotype in barley magnesium chelatase and Mg-protoporphyrin IX monomethyl ester cyclase mutants. *Plant Physiol. Biochem.* 43, 901–908.

Galvão, R. M., Li, M., Kothadia, S. M., Haskel, J. D., Decker, P. V., Van Buskirk, E. K., et al. (2012). Photoactivated phytochromes interact with HEMERA and promote its accumulation to establish photomorphogenesis in *Arabidopsis*. *Genes Dev.* 26, 1851–1863.

Galvez-Valdivieso, G., Fryer, M. J., Lawson, T., Slattery, K., Truman, W., Smirnoff, N., et al. (2009). The high light response in *Arabidopsis* involves ABA signaling between vascular and bundle sheath cells. *Plant Cell* 21, 2143–2162.

Galvez-Valdivieso, G., and Mullineaux, P. M. (2010). The role of reactive oxygen species in signaling from chloroplasts to the nucleus. *Physiol. Plant.* 138, 430–439.

Gilles-Gonzalez, M. A., and Gonzalez, G. (2005). Heme-based sensors: defining characteristics, recent developments, and regulatory hypotheses. *J. Inorg. Biochem.* 99, 1–22.

Giraud, E., Van Aken, O., Ho, L. H. M., and Whelan, J. (2009). The transcription factor ABI4 is a regulator of mitochondrial retrograde expression of ALTERNATIVE OXIDASE1a. *Plant Physiol.* 150, 1286–1296.

Gray, J. C., Sullivan, J. A., Wang, J.-H., Jerome, C. A., and Maclean, D. (2003). Coordination of plastid and nuclear gene expression. *Philos. Trans. R. Soc. Lond. B* 358, 135–145.

Harpster, M. H., Mayfield, S. P., and Taylor, W. C. (1984). Effects of pigment-deficient mutants on the accumulation of photosynthetic proteins in maize. *Plant Mol. Biol.* 3, 59–71.

Henry, J. T., and Crosson, S. (2011). Ligand-binding PAS domains in a genomic, cellular, and structural context. *Ann. Rev. Microbiol.* 65, 261–286.

Hess, W. R., Muller, A., Nagy, F., and Borner, T. (1994). Ribosome deficient plastids affect transcription of light-induced nuclear genes: genetic evidence for a plastid-derived signal. *Mol. Gen. Genet.* 242, 305–312.

Huang, L., and Castelfranco, P. A. (1990). Regulation of 5-aminolevulinic acid (ALA) synthesis in developing chloroplasts: III. Evidence for functional heterogeneity of the ALA pool. *Plant Physiol.* 92, 172–178.

Huang, Y.-S., and Li, H.-M. (2009). *Arabidopsis* CHLI2 can substitute for CHLI1. *Plant Physiol.* 150, 636–645.

Huq, E., Al-Sady, B., Hudson, M., Kim, C., Apel, K., and Quail, P. H. (2004). Phytochrome-interacting factor 1 is a critical bHLH regulator of chlorophyll biosynthesis. *Science* 305, 1937–1941.

Inaba, T., Yazu, F., Ito-Inaba, Y., Kakizaki, T., and Nakayama, K. (2011). Retrograde signaling pathway from plastid to nucleus. *Int. Rev. Cell Mol. Biol.* 290,167–204.

Isemer, R., Mulisch, M., Schäfer, A., Kirchner, S., Koop, H. U., and Krupinska, K. (2012). Recombinant Whirly1 translocates from transplastomic chloroplasts to the nucleus. *FEBS Lett.* 586, 85–88.

Jung, H. S., and Chory, J. (2010). Signaling between chloroplasts and the nucleus: can a systems biology approach bring clarity to a complex and highly regulated pathway? *Plant Physiol.* 152, 453–459.

Kakizaki, T., Matsumura, H., Nakayama, K., Che, F. S., Terauchi, R., and Inaba, T. (2009). Coordination of plastid protein import and nuclear gene expression by plastid-to-nucleus retrograde signaling. *Plant Physiol.* 151, 1339–1353.

Kakizaki, T., Yazu, F., Nakayama, K., Ito-Inaba, Y., and Inaba, T. (2012). Plastid signaling under multiple conditions is accompanied by a common defect in RNA editing in plastids. *J. Exp. Bot.* 63, 251–260.

Kaasik, K., and Lee, C. C. (2004). Reciprocal regulation of haem biosynthesis and the circadian clock in mammals. *Nature* 430, 467–471.

Kim, C., Lee, K. P., Baruah, A., Nater, M., Göbel, C., Feussner, I., et al. (2009). 1O2-mediated retrograde signaling during late embryogenesis predetermines plastid differentiation in seedlings by recruiting abscisic acid. *Proc. Natl. Acad. Sci. U.S.A.* 106, 9920–9924.

Kim, C., Meskauskiene, R., Zhang, S. R., Lee, K. P., Ashok, M. L., Blajecka, K., et al. (2012). Chloroplasts of *Arabidopsis* are the source and a primary target of a plant-specific programmed cell death signaling pathway. *Plant Cell* 24, 3026–3039.

Kindgren, P., Eriksson, M. J., Benedict, C., Mohapatra, A., Gough, S. P., Hansson, M., et al. (2011). A novel proteomic approach reveals a role for Mg-protoporphyrin IX in response to oxidative stress. *Physiol. Plant.* 141, 310–320.

Kleine, T., Kindgren, P., Benedict, C., Hendrickson, L., and Strand, A. (2007). Genome-wide gene expression analysis reveals a critical role for CRYPTOCHROME1 in the response of *Arabidopsis* to high irradiance. *Plant Physiol.* 144, 1391–1406.

Kleine, T., Voigt, C., and Leister, D. (2009). Plastid signaling to the nucleus: messengers still lost in the mists? *Trends Genet.* 25, 185–190.

Koussevitzky, S., Nott, A., Mockler, T. C., Hong, F., Sachetto-Martins, G., Surpin, M., et al. (2007). Signals from chloroplasts converge to regulate nuclear gene expression. *Science* 316, 715–719.

Kumar, M. A., Chaturvedia, S., and Söll, D. (1999). Selective inhibition of HEMA gene expression by photooxidation in *Arabidopsis thaliana*. *Phytochemistry* 51, 847–851.

Kusnetsov, V., Bolle, C., Lübberstedt, T., Sopory, S., Herrmann, R. G., and Oelmüller, R. (1996). Evidence that the plastid signal and light operate via the same cis-acting elements in the promoters of nuclear genes for plastid proteins. *Mol. Gen. Genet.* 252, 631–639.

Laloi, C., Stachowiak, M., Pers-Kamczyc, E., Warzych, E., Murgia, I., and Apel, K. (2007). Cross-talk between singlet oxygen- and hydrogen peroxide-dependent signaling of stress responses in *Arabidopsis thaliana*. *Proc. Natl. Acad. Sci. U.S.A.* 104, 672–677.

Larkin, R. M., Alonso, J. M., Ecker, J. R., and Chory, J. (2003). GUN4, a regulator of chlorophyll synthesis and intracellular signaling. *Science* 299, 902–906.

Larkin, R. M., and Ruckle, M. E. (2008). Integration of light and plastid signals. *Curr. Opin. Plant Biol.* 11, 593–599.

Lathrop, J. T., and Timko, M. P. (1993). Regulation by heme of mitochondrial protein transport through a conserved amino acid motif. *Science* 259, 522–525.

Lee, K. P., Kim, C., Landgraf, F., and Apel, K. (2007). EXECUTER1- and EXECUTER2-dependent transfer of stress-related signals from the plastid to the nucleus of *Arabidopsis thaliana*. *Proc. Natl. Acad. Sci. U.S.A.* 104, 10270–10275.

Leister, D. (2005). Genomics-based dissection of the cross-talk of chloroplasts with the nucleus and mitochondria in *Arabidopsis*. *Gene* 354, 110 – 116.

Leister, D. (2012). Retrograde signaling in plants: from simple to complex scenarios. *Front. Plant Sci.* 3:135. doi: 10.3389/fpls.2012.00135

Leivar, P., Tepperman, J. M., Monte, E., Calderon, R. H., Liu, T. L., and Quail, P. H. (2009). Definition of early transcriptional circuitry involved in light-induced reversal of PIF-imposed repression of photomorphogenesis in young *Arabidopsis* seedlings. *Plant Cell* 21, 3535–3553.

Lewis, B. P., Burge, C. B., and Bartel, D. P. (2005). Conserved seed pairing, often flanked by adenosines, indicates that thousands of human genes are microRNA targets. *Cell* 120, 15–20.

López-Juez, E., Jarvis, R. P., Takeuchi, A., Page, A. M., and Chory, J. (1998). New *Arabidopsis* cue mutants suggest a close connection between plastid- and phytochrome regulation of nuclear gene expression. *Plant Physiol.* 118, 803–815.

Martin, W., Rujan, T., Richly, E., Hansen, A., Cornelsen, S., Lins, T., et al. (2002). Evolutionary analysis of *Arabidopsis*, cyanobacterial, and chloroplast genomes reveals plastid phylogeny and thousands of cyanobacterial genes in the nucleus. *Proc. Natl. Acad. Sci. U.S.A.* 99, 12246–12251.

Masuda, T., and Takahashi, S. (2006). Chemiluminescent-based method for heme determination by reconstitution with horseradish peroxidase apo-enzyme. *Anal. Biochem.* 355, 307–309.

McCormac, A. C., Fischer, A., Kumar, A. M., Söll, D., and Terry, M. J. (2001). Regulation of HEMA1 expression by phytochrome and a plastid signal during de-etiolation in *Arabidopsis thaliana*. *Plant J.* 25, 549–561.

McCormac, A. C., and Terry, M. J. (2002). Loss of nuclear gene expression during the phytochrome A-mediated far-red block of greening response. *Plant Physiol.* 130, 402–414.

McCormac, A. C., and Terry, M. J. (2004). The nuclear genes Lhcb and HEMA1 are differentially sensitive to plastid signals and suggest distinct roles for the GUN1 and GUN5 plastid-signaling pathways during de-etiolation. *Plant J.* 40, 672–685.

Mense, S. M., and Zhang, L. (2006). Heme: a versatile signaling molecule controlling the activities of diverse

regulators ranging from transcription factors to MAP kinases. *Cell Res.* 16, 681–692.

Meskauskiene, R., Nater, M., Goslings, D., Kessler, F., op den Camp, R., and Apel, K. (2001). FLU: a negative regulator of chlorophyll biosynthesis in *Arabidopsis thaliana*. *Proc. Natl. Acad. Sci. U.S.A.* 98, 12826–12831.

Miller, G., Suzuki, N., Ciftci-Yilmaz, S., and Mittler, R. (2010). Reactive oxygen species homeostasis and signaling during drought and salinity stresses. *Plant Cell Environ.* 33, 453–467.

Mochizuki, N., Brusslan, J. A., Larkin, R., Nagatani, A., and Chory, J. (2001). *Arabidopsis* genomes uncoupled 5 (GUN5) mutant reveals the involvement of Mg-chelatase H subunit in plastid-to-nucleus signal transduction. *Proc. Natl. Acad. Sci. U.S.A.* 98, 2053–2058.

Mochizuki, N., Susek, R., and Chory, J. (1996). An intracellular signal transduction pathway between the chloroplast and nucleus is involved in de-etiolation. *Plant Physiol.* 112, 1465–1469.

Mochizuki, N., Tanaka, R., Grimm, B., Masuda, T., Moulin, M., Smith, A. G., et al. (2010). The cell biology of tetrapyrroles: a life and death struggle. *Trends Plant Sci.* 15, 488–498.

Mochizuki, N., Tanaka, R., Tanaka, A., Masuda, T., and Nagatani, A. (2008). The steady-state level of Mg-protoporphyrin IX is not a determinant of plastid-to-nucleus signaling in *Arabidopsis*. *Proc. Natl. Acad. Sci. U.S.A.* 105, 15184–15189.

Monte, E., Tepperman, J. M., Al-Sady, B., Kaczorowski, K. A., Alonso, J. M., Ecker, J. R., et al. (2004). The phytochrome-interacting transcription factor, PIF3, acts early, selectively, and positively in light-induced chloroplast development. *Proc. Natl. Acad. Sci. U.S.A.* 101, 16091–16098.

Moulin, M., McCormac, A. C., Terry, M. J., and Smith, A. G. (2008). Tetrapyrrole profiling in *Arabidopsis* seedlings reveals that retrograde plastid nuclear signaling is not due to Mg-protoporphyrin IX accumulation. *Proc. Natl. Acad. Sci. U.S.A.* 105, 15178–15183.

Munakata, H., Sun, J. Y., Yoshida, K., Nakatani, T., Honda, E., Hayakawa, S., et al. (2004). Role of the heme regulatory motif in the heme-mediated inhibition of mitochondrial import of 5-aminolevulinate synthase. *J. Biochem.* 136, 233–238.

Nagai, S., Koide, M., Takahashi, S., Kikuta, A., Aono, M., Sasaki-Sekimoto, Y., et al. (2007). Induction of isoforms of tetrapyrrole biosynthetic enzymes, AtHEMA2 and AtFC1, under stress conditions and their physiological functions in *Arabidopsis*. *Plant Physiol.* 144, 1039–1051.

Oelmüller, R., Levitan, I., Bergfeld, R., Rajasekhar, V., and Mohr, H. (1986). Expression of nuclear genes as affected by treatments acting on the plastids. *Planta* 168, 482–492

Ogawa, K., Sun, J., Taketani, S., Nakajima, O., Nishitani, C., Sassa, S., et al. (2001). Heme mediates derepression of Maf recognition element through direct binding to transcription repressor Bach1. *EMBO J.* 20, 2835–2843.

op den Camp, R. G. L., Przybyla, D., Ochsenbein, C., Laloi, C., Kim, C. H., Danon, A., et al. (2003). Rapid induction of distinct stress responses after the release of singlet oxygen in *Arabidopsis*. *Plant Cell* 15, 2320–2332.

Oswald, O., Martin, T., Dominy, P. J., and Graham, I. (2001). Plastid redox state and sugars: interactive regulators of nuclear-encoded photosynthetic gene expression. *Proc. Natl. Acad. Sci. U.S.A.* 98, 2047–2052.

Pesaresi, P., Masiero, S., Eubel, H., Braun, H. P., Bhushan, S., Glaser, E., et al. (2006). Nuclear photosynthesis gene expression is synergistically modulated by rates of protein synthesis in chloroplasts and mitochondria. *Plant Cell* 18, 970–991

Pfalz, J., Liere, K., Kandlbinder, A., Dietz, K.-J., and Oelmüller, R. (2006). pTAC2, -6, and -12 are components of the transcriptionally active plastid chromosome that are required for plastid gene expression. *Plant Cell* 18, 176–197.

Pfannschmidt, T. (2010). Plastidial retrograde signaling – a true "plastid factor" or just metabolite signatures? *Trends Plant Sci.* 15, 427–435.

Pogson, B. J., Woo, N. S., Förster, B., and Small, I. D. (2008). Plastid signaling to the nucleus and beyond. *Trends Plant Sci.* 13, 602–609.

Pontier, D., Albrieux, C., Joyard, J., Lagrange, T., and Block, M. A. (2007). Knock-out of the magnesium protoporphyrin IX methyltransferase gene in *Arabidopsis*: effects on chloroplast development and on chloroplast-to-nucleus signaling. *J. Biol. Chem.* 282, 2297–2304.

Puente, P., Wei, N., and Deng, X.-W. (1996). Combinatorial interplay of promoter elements constitutes the minimal determinants for light and developmental control of gene expression in *Arabidopsis*. *EMBO J.* 15, 3732–3743.

Qi, Z., and O'Brian, M. R. (2002). Interaction between the bacterial iron response regulator and ferrochelatase mediates genetic control of heme biosynthesis. *Mol. Cell* 9, 155–162.

Ramel, F., Birtic, S., Ginies, C., Soubigou-Taconnat, L., Triantaphylides, C., and Havaux, M. (2012). Carotenoid oxidation products are stress signals that mediate gene responses to singlet oxygen in plants. *Proc. Natl. Acad. Sci. U.S.A.* 109, 5535–5540.

Rapp, J. C., and Mullet, J. E. (1991). Chloroplast transcription is required to express the nuclear genes rbcS and cab. Plastid DNA copy number is regulated independently. *Plant Mol. Biol.* 17, 813–823.

Richly, E., Dietzmann, A., Biehl, A., Kurth, J., Laloi, C., Apel, K., et al. (2003). Covariations in the nuclear chloroplast transcriptome reveal a regulatory master-switch. *EMBO Rep.* 4, 491–498

Richter, R., Behringer, C., Müller,I. K., and Schwechheimer, C. (2010). The GATA-type transcription factors GNC and GNL/CGA1 repress gibberellin signaling downstream from DELLA proteins and PHYTOCHROME-INTERACTING FACTORS. *Genes Dev.* 24, 2093-2104

Ruckle, M. E., Burgoon, L. D., Lawrence, L. A., Sinkler, C. A., and Larkin, R. M. (2012). Plastids are major regulators of light signaling in *Arabidopsis*. *Plant Physiol.* 159, 366–390.

Ruckle, M. E., DeMarco, S. M., and Larkin, R. M. (2007). Plastid signals remodel light signaling networks and are essential for efficient chloroplast biogenesis in *Arabidopsis*. *Plant Cell* 19, 3944–3960.

Ruckle, M. E., and Larkin, R. M. (2009). Plastid signals that affect photomorphogenesis in *Arabidopsis thaliana* are dependent on GENOMES UNCOUPLED 1 and cryptochrome 1. *New Phytol.* 182, 367–379.

Saini, G., Meskauskiene, R., Pijacka, W., Roszak, P., Sjogren, L. L. E., Clarke, A. K., et al. (2011). 'Happy on norflurazon' (hon) mutations implicate perturbance of plastid homeostasis with activating stress acclimatization and changing nuclear gene expression in norflurazon- treated seedlings. *Plant J.* 65, 690–702.

Schmitz-Linneweber, C., and Small, I. (2008). Pentatricopeptide repeat proteins: A socket set for organelle gene expression. *Trends Plant Sci.* 13, 663–670.

Shimizu, T. (2012). Binding of cysteine thiolate to the Fe(III) heme complex is critical for the function of heme sensor proteins. *J. Inorg. Biochem.* 108, 171–177.

Shin, J., Kim, K., Kang, H., Zulfugarov, I. S., Bae, G., Lee, C. H., et al. (2009). Phytochromes promote seedling light responses by inhibiting four negatively-acting phytochrome-interacting factors. *Proc. Natl. Acad. Sci. U.S.A.* 106, 7660–7665.

Singleton, C., White, G. F., Todd, J. D., Marritt, S. J., Cheesman, M. R., Johnston, A. W. B., et al. (2010). Heme-responsive DNA binding by the global iron regulator Irr from *Rhizobium leguminosarum*. *J. Biol. Chem.* 285, 16023–16031.

Small, S. K., Puri, S., and O'Brian, M. R. (2009). Heme-dependent metalloregulation by the iron response regulator (Irr) protein in *Rhizobium* and other Alpha-proteobacteria. *Biometals* 22, 89–97.

Sperling, U., van Cleve, B., Frick, G., Apel, K., and Armstrong, G. A. (1997). Overexpression of light-dependent PORA or PORB in plants depleted of endogenous POR by far-red light enhances seedlings survival in white light and protects against photooxidative damage. *Plant J.* 12, 649–658.

Stephenson, P. G., Fankhauser, C., and Terry, M. J. (2009). PIF3 is a repressor of chloroplast development. *Proc. Natl. Acad. Sci. U.S.A.* 106, 7654–7659.

Strand, A., Asami, T., Alonso, J., Ecker, J. R., and Chory, J. (2003). Chloroplast to nucleus communication triggered by accumulation of Mg-protoporphyrin IX. *Nature* 421, 79–83.

Sullivan, J. A., and Gray, J. C. (1999). Plastid translation is required for the expression of nuclear photosynthesis genes in the dark and in roots of the pea lip 1 mutant. *Plant Cell* 11, 901–911.

Sun, X., Feng, P., Xu, X., Guo, H., Ma, J., Chi, W., et al. (2011). A chloroplast envelope-bound PHD transcription factor mediates chloroplast signals to the nucleus. *Nat. Commun.* 2, 477.

Susek, R. E., Ausubel, F. M., and Chory, J. (1993). Signal transduction mutants of *Arabidopsis* uncouple nuclear CAB and RBCS gene expression from chloroplast development. *Cell* 74, 787–799.

Takahashi, S., Ogawa, T., Inoue, K., and Masuda, T. (2008). Characterization of cytosolic tetrapyrrole-binding proteins in *Arabidopsis thaliana*. *Photochem. Photobiol. Sci.* 7, 1216–1224.

Terry, M. J., Linley, P. J., and Kohchi, T. (2002). Making light of it: the role of plant haem oxygenases in phytochrome chromophore synthesis. *Biochem. Soc. Trans.* 30, 604–609.

Ujwal, M. L., McCormac, A. C., Goulding, A., Kumar, A. M., Soll, D., and

Terry, M. J. (2002). Divergent regulation of the HEMA gene family encoding glutamyl-tRNA reductase in *Arabidopsis thaliana*: expression of HEMA2 is regulated by sugars, but is independent of light and plastid signaling. *Plant Mol. Biol.* 50, 83–91.

Vinti, G., Fourrier, N., Bowyer, J. R., and López-Juez, E. (2005). *Arabidopsis* cue mutants with defective plastids are impaired primarily in the photocontrol of expression of photosynthesis-associated nuclear genes. *Plant Mol. Biol.* 57, 343–357.

Vinti, G., Hills, A., Campbell, S., Bowyer, J. R., Mochizuki, N., Chory, J., et al. (2000). Interactions between hy1 and gun mutants of *Arabidopsis*, and their implications for plastid/nuclear signaling. *Plant J.* 24, 883–894.

Voigt, C., Oster, U., Börnke, F., Jahns, P., Dietz, K. J., Leister, D., et al. (2010). In-depth analysis of the distinctive effects of norflurazon implies that tetrapyrrole biosynthesis, organellar gene expression and ABA cooperate in the GUN-type of plastid signaling. *Physiol. Plant.* 138, 503–519.

von Gromoff, E. D., Alawady, A., Meinecke, L., Grimm, B., and Beck, C. F. (2008). Heme, a plastid-derived regulator of nuclear gene expression in *Chlamydomonas*. *Plant Cell* 20, 552–567.

Voss, B., Meinecke, L., Kurz, T., Al-Babili, S., Beck, C. F., and Hess, W. R. (2011). Hemin and Mg-Protoporphyrin IX induce global changes in gene expression in *Chlamydomonas reinhardtii*. *Plant Physiol.* 155, 892–905.

Wagner, D., Przybyla, D., Op den Camp, R., Kim, C., Landgraf, F., Lee, K. P., et al. (2004). The genetic basis of singlet oxygen-induced stress responses of *Arabidopsis thaliana*. *Science* 306, 1183–1185.

Waters, M. T., and Langdale, J. A. (2009). The making of a chloroplast. *EMBO J.* 28, 2861–2873.

Waters, M. T., Wang, P., Korkaric, M., Capper, R. G., Saunders, N. J., and Langdale, J. A. (2009). GLK transcription factors coordinate expression of the photosynthetic apparatus in *Arabidopsis*. *Plant Cell* 21, 1109–1128.

Woodson, J. D., Perez-Ruiz, J. M., and Chory, J. (2011). Heme synthesis by plastid ferrochelatase I regulates nuclear gene expression in plants. *Curr. Biol.* 21, 897–903.

Woodson, J. D., Perez-Ruiz, J. M., Schmitz, R. J., Ecker, J. R., and Chory, J. (2013). Sigma factor mediated plastid retrograde signals control nuclear gene expression. *Plant J.* 70, 1–13.

Xiao, Y., Savchenko, T., Baidoo, E. E. K., Chehab, W. E., Hayden, D. M., Tolstikov, V., et al. (2012). Retrograde signaling by the plastidial metabolite MEcPP regulates expression of nuclear stress-response genes. *Cell* 149, 1525–1535.

Yang, J., Ishimori, K., and O'Brian, M. R. (2005a). Two heme binding sites are involved in the regulated degradation of the bacterial iron response regulator (Irr) protein. *J. Biol. Chem.* 280, 7671–7676.

Yang, M.-T., Chen, S.-L., Lin, C.-Y., and Chen, Y.-M. (2005b). Chilling stress suppresses chloroplast development and nuclear gene expression in leaves of mung bean seedlings. *Planta* 221, 374–385.

Yang, J., Kim, K. D., Lucas, A., Drahos, K. E., Santos, C. S., Mury, S. P., et al. (2008). A novel heme-regulatory motif mediates heme-dependent degradation of the circadian factor period 2. *Mol. Cell. Biol.* 28, 4697–4711.

Yin, L., Dragnea, V., and Bauer, C. E. (2012). PpsR, a regulator of heme and bacteriochlorophyll biosynthesis, is a heme-sensing protein. *J. Biol. Chem.* 287, 13850–13858.

Yin, L., Wu, N., Curtin, J. C., Qatanani, M., Szwergold, N. R., Reid, R. A., et al. (2007). Rev-erb(, a heme sensor that coordinates metabolic and circadian pathways. *Science* 318, 1786–1789.

Yoshida, R., Sato, T., Kanno, A., and Kameya, T. (1998). Streptomycin mimics the cool temperature response in rice plants. *J. Exp. Bot.* 49, 221–227.

Yu, F., Fu, A., Aluru, M., Park, S., Xu, Y., Liu, H., et al. (2007). Variegation mutants and mechanisms of chloroplast biogenesis. *Plant Cell Environ.* 30, 350–365.

Yu, H.-D., Yang, X.-F., Chen, S.-T., Wang, Y.-T., Li, J.-K., Shen, Q., et al. (2012). Downregulation of chloroplast RPS1 negatively modulates nuclear heat-responsive expression of HsfA2 and its target genes in *Arabidopsis*. *PLoS Genet.* 8:e1002669. doi: 10.1371/journal.pgen.1002669

Zenke-Kawasaki, Y., Dohi, Y., Katoh, Y., Ikura, T., Ikura, M., Asahara, T., et al. (2007). Heme induces ubiquitination and degradation of the transcription factor Bach1. *Mol. Cell. Biol.* 27, 6962–6971.

Zhang, L., and Guarente, L. (1995). Heme binds to a short sequence that serves a regulatory function in diverse proteins. *EMBO J.* 14, 313–320.

Zhang, L., and Hach, A. (1999). Molecular mechanism of heme signaling in yeast: the transcriptional activator Hap1 serves as the key mediator. *Cell. Mol. Life Sci.* 56, 415–426.

Zhong, S., Zhao, M., Shi, T., Shi, H., An, F., Zhao, Q., et al. (2009). EIN3/EIL1 cooperate with PIF1 to prevent photo-oxidation and to promote greening of *Arabidopsis* seedlings. *Proc. Natl. Acad. Sci. U.S.A.* 106, 21431–21436.

Zybailov, B., Rutschow, H., Friso, G., Rudella, A., Emanuelsson, O., Sun, Q., et al. (2008). Sorting signals, N-terminal modifications and abundance of the chloroplast proteome. *PLoS ONE* 3:e1994. doi: 10.1371/journal.pone.0001994

Conflict of Interest Statement: The authors declare that the research was conducted in the absence of any commercial or financial relationships that could be construed as a potential conflict of interest.

Received: 26 December 2012; accepted: 20 January 2013; published online: 13 February 2013.

Citation: Terry MJ and Smith AG (2013) A model for tetrapyrrole synthesis as the primary mechanism for plastid-to-nucleus signaling during chloroplast biogenesis. Front. Plant Sci. ***4****:14. doi: 10.3389/fpls.2013.00014*

This article was submitted to Frontiers in Plant Physiology, a specialty of Frontiers in Plant Science.

Copyright © 2013 Terry and Smith. This is an open-access article distributed under the terms of the Creative Commons Attribution License, which permits use, distribution and reproduction in other forums, provided the original authors and source are credited and subject to any copyright notices concerning any third-party graphics etc.

frontiers in
PLANT SCIENCE

REVIEW ARTICLE
published: 10 January 2013
doi: 10.3389/fpls.2012.00304

ABI4 and its role in chloroplast retrograde communication

Patricia León*, Josefat Gregorio and Elizabeth Cordoba

Departamento de Biología Molecular de Plantas, Instituto de Biotecnología, Universidad Nacional Autónoma de México, Cuernavaca, Morelos, México

Edited by:
Dario Leister, Ludwig Maximilians University Munich, Germany

Reviewed by:
Iris Finkemeier, Ludwig Maximilians University Munich, Germany
Xuwu Sun, Institute of Botany, Chinese Academy of Sciences, China

****Correspondence:***
Patricia León, Departamento de Biología Molecular de Plantas, Instituto de Biotecnología, Universidad Nacional Autónoma de México, Avenida Universidad 2001, Colonia Chamilpa, Cuernavaca, Morelos 62210, México.
e-mail: patricia@ibt.unam.mx

The acquisition of plastids is a landmark event in plant evolution. The proper functionality of these organelles depends on strict and continuous communication between the plastids and the nucleus to precisely adjust gene expression in response to the organelle's requirements. Signals originating from the plastids impact the expression of a variety of nuclear genes, and this retrograde communication is essential to couple the nuclear expression of plastid-localized products with organelle gene expression and, ultimately, functionality. Major advances have been made in this field over the past few years with the characterization of independent retrograde signaling pathways and the identification of some of their components. One such factor is the nuclear transcriptional factor ABI4 (ABA-INSENTIVE 4). ABI4, together with the plastid PPR GUN1 protein, has been proposed to function as a node of convergence for multiple plastid retrograde signaling pathways. ABI4 is conserved among plants and also plays important roles in various critical developmental and metabolic processes. ABI4 is a versatile regulator that positively and negatively modulates the expression of many genes, including other transcriptional factors. However, its mode of action during plastid retrograde signaling is not fully understood. In this review, we describe the current evidence that supports the participation of ABI4 in different retrograde communication pathways. ABI4 is regulated at the transcriptional and post-transcriptional level. A known regulator of ABI4 includes the PTM transcription factor, which moves from the chloroplast to the nucleus. This transcription factor is a candidate for the transmission of retrograde signals between the plastid and ABI4.

Keywords: retrograde communication, ABI4, plastids, chloroplast, nuclear photosynthetic genes, signaling

The endosymbiotic acquisition of the chloroplast and mitochondria by eukaryotic cells are two of the most important events in the history of life on Earth (Margulis, 1971). Chloroplasts provide plants with autotrophic capacity, and their byproducts are the source of the majority of the carbon skeletons of all living organisms. Today, chloroplasts host not only the photosynthetic pathway but also other essential metabolic pathways, many of which are readily traced to prokaryotic ancestors (Gould et al., 2008). These include the synthesis of amino acids, fatty acids, and vitamins. Additionally, hormones and an enormous number of secondary metabolites, many of them important to humans, are also synthesized in plastids. Coevolution between the original endosymbiont and the plant cell has resulted in a heterogenous family of plastid types, each with specialized functions and all essential for plant survival (Neuhaus and Emes, 2000; Vothknecht and Westhoff, 2001).

The plastid genome encodes around 100 genes. Therefore, more than 95% of the proteins required for plastid function are encoded in the nucleus, and the corresponding proteins are imported into the organelle post-translationally. This latter step is achieved through a transit peptide present at the N-terminus that suffices for import into the organelles, found in the majority of nuclear-encoded plastid proteins (NEPPs; Li and Chiu, 2010). However, with the massive transfer of genes to the nucleus, the organelles lost autonomy and became dependent on the host. The nucleus gained control over the expression of the transferred genes and consequently over the plastid function and development in what is known as anterograde regulation.

In silico predictions based on the presence of putative transit peptides yield estimates of 2500–4500 NEPPs (Richly and Leister, 2004). Although the location of many of these proteins has not been experimentally proven, large-scale proteomics experiments (http://ppdb.tc.cornell.edu/) corroborate the complexity of the plastid proteome (Zybailov et al., 2008; Joyard et al., 2009). Moreover, these analyses elucidated proteomic differences between plastid types and within developmental stages, demonstrating that plastid protein composition is both complex and dynamic (Zybailov et al., 2008). A significant proportion of the proteins imported into plastids form macromolecular complexes (Olinares et al., 2010). Examples include complexes of the photosynthetic apparatus as well as those involved in organelle maintenance, such as ribosomes and DNA or RNA polymerases (Kovacs-Bogdan et al., 2010; Olinares et al., 2011). In many cases, these complexes consist of subunits that are encoded in both the nucleus and the plastid genomes, with functions that depend on proper stoichiometry. The process is further complicated by the requirement of some of these complexes for specific cofactors and the reorganization and replacement or repair of specific subunits under certain conditions (Rochaix, 2011; Janska et al., 2012). While it has been established that post-translational regulatory processes play an important role in this coordination (Rochaix, 2011), it is also clear that coordination between the nucleus and the organelle

at the level of gene expression is an essential element to ensuring proper organelle functionality. As was already mentioned, the nucleus regulates plastid gene expression through regulating NEPPs (Woodson and Chory, 2008; Stern et al., 2010). Nonetheless, retrograde mechanisms that permit the mitochondria and plastids to transmit their developmental and metabolic status to the nucleus have evolved, resulting in the modulation of nuclear gene expression in response to the needs of the organelle.

RETROGRADE REGULATION IS AN ESSENTIAL MECHANISM FOR ORGANELLE FUNCTIONALITY

Since the isolation of the *albostrians* (*Hordeum vulgare* cv. Haisa) mutant more than 30 years ago (Hedtke et al., 1999), data have accumulated that demonstrate the existence of multiple plastidial retrograde signaling pathways in response to specific developmental and metabolic cues of the plastids. In all cases, it is assumed that a signal(s) must exit the plastid to transmit information directly or indirectly to components in the nucleus to fine-tune nuclear gene expression. Different pathways have been defined based primarily on the regulated nuclear genes and the participating factors. Most of our present knowledge is based on studies from *Arabidopsis thaliana* using inhibitors and mutants that impair organelle development (Rapp and Mullet, 1991; Hedtke et al., 1999; Sullivan and Gray, 1999; Pesaresi et al., 2001; Nott et al., 2006; Woodson and Chory, 2008). In recent years, the diversity and complexity of signaling pathways have necessitated more dynamic consideration to enhance our understanding of these events (Leister, 2012). Advances in this field have been sizeable and are covered in detail in various reviews (Mullineaux and Karpinski, 2002; Nott et al., 2006; Pesaresi et al., 2007; Pogson et al., 2008; Woodson and Chory, 2008; Chan et al., 2010; Galvez-Valdivieso and Mullineaux, 2010; Inaba et al., 2011). The purpose of this review is to describe the recent identification of the factors that are recognized as important elements in regulating the expression of NEPPs in response to retrograde signals.

A common effect of all retrograde signaling pathways is the alteration of nuclear gene expression, and the available evidence indicates that these changes are, in most cases, at the level of transcription (Richly et al., 2003; Leister et al., 2011). An exception to this is a recently described pathway, referred to as PAP (3′-phosphoadenosine 5′-phosphate). PAP itself moves to the nucleus, acting as a true signal, and increases gene expression by inhibiting the activity of the nuclear 5′ to 3′ exoribonucleases (XRN2 and XRN3), which act as negative regulators of the high light and drought stress responses (Dichtl et al., 1997; Estavillo et al., 2011). This example illustrates the possibility that post-transcriptional regulators such as ribonucleases also participate in the reprogramming of nuclear expression caused by retrograde signals (Estavillo et al., 2011).

Early analyses of the retrograde chloroplast signaling pathways primarily monitored a few particular genes like *LHCB* and *RBCS* (Bradbeer et al., 1979; López-Juez, 2009). Identification of additional targets has been used to define distinctive retrograde pathways, their potential interactions and overlapping components, and the identification of candidate signaling molecules responsible for the changes in gene expression (Koussevitzky et al., 2007; Brautigam et al., 2009; Leister et al., 2011). Initial genomic studies from wild-type plants and mutants with altered retrograde signal responses, such as *genomes uncoupled* (*gun*), which no longer represses NEPPs in the presence of norflurazon, an inhibitor of carotenoid biosynthesis (Susek et al., 1993), demonstrated the coordination of many chloroplast genes following a two-state switch behavior (on or off). Based on these data, it was proposed that master switches existed for several retrograde responses (Richly et al., 2003). *Cis*-acting elements involved in abscisic acid (ABA) responses that are over-represented in the upstream regions of the *gun*-affected genes and known putative regulatory factors that may interact with these sequences have been identified (Niu et al., 2002; Koussevitzky et al., 2007). One such regulator is the ABA-INSENTIVE 4 (ABI4) transcription factor, which was predicted to be important in plastidic retrograde signaling pathways (Koussevitzky et al., 2007).

ABI4 IS A VERSATILE REGULATOR FOR MULTIPLE SIGNALING RESPONSES

The ABI4 protein belongs to the DREB A3 subgroup of a large family of plant-specific transcription factors known as AP2/EREBP (Sakuma et al., 2002). The *A. thaliana* genome encodes 147 AP2/EREBP members, and many of them are of particular interest because they are implicated in many signaling processes, including biotic and abiotic stress responses (Mizoi et al., 2012). In spite of the similarity between the AP2 DNA-binding domain with other members of the DREB A subgroup, ABI4 stands out as a unique member in the A3 clade based on its sequence (Dietz et al., 2010). Orthologs of ABI4 have been reported in maize and rice (Niu et al., 2002), and homologous sequences are found in many plant species, indicating that this factor is conserved in most plants. In *A. thaliana*, ABI4 is a unique gene, and this also appears to be true for other plants such as maize and rice.

Over the past decade, ABI4 has emerged as a central player in many signaling processes during plant development (**Figure 1**). The isolation of ABI4 in a screen for ABA-insensitive (*abi*) mutants was the first evidence linking this factor with ABA signaling (Finkelstein et al., 1998). Unlike wild-type plants, *abi4* mutants display resistance to the ABA inhibitory effect during germination and seedling and chloroplast development (**Figure 2A**). Additional *abi4* alleles were isolated in several screenings for mutants with altered responses to sugars (Arenas-Huertero et al., 2000; Huijser et al., 2000; Laby et al., 2001; Rook et al., 2001). The presence of high sugar levels triggers post-germinative seedling arrest (chloroplast and leaf development) in wild-type plants, but not in the *abi4* mutant (**Figure 2B**). ABI4 and hormones such as ABA and ethylene play an essential role in sugar perception during early seedling development (León and Sheen, 2003; Rolland et al., 2006; Rook et al., 2006a) and in the primary root (Cui et al., 2012). The developmental arrest in response to sugars only occurs during early developmental stages, similar to some of the retrograde chloroplast signaling responses (Dekkers et al., 2008). Sugars and ABA have been proposed to act as important signals during early development by directly controlling germination, photo-autotrophic development, the expression of photosynthetic genes (Baier and Dietz, 2005; Katagiri et al., 2005; Cottage et al., 2010; Lee et al., 2012) and even the initiation of plastid retrograde signaling (Koussevitzky et al., 2007). ABI4 also plays an important role in other

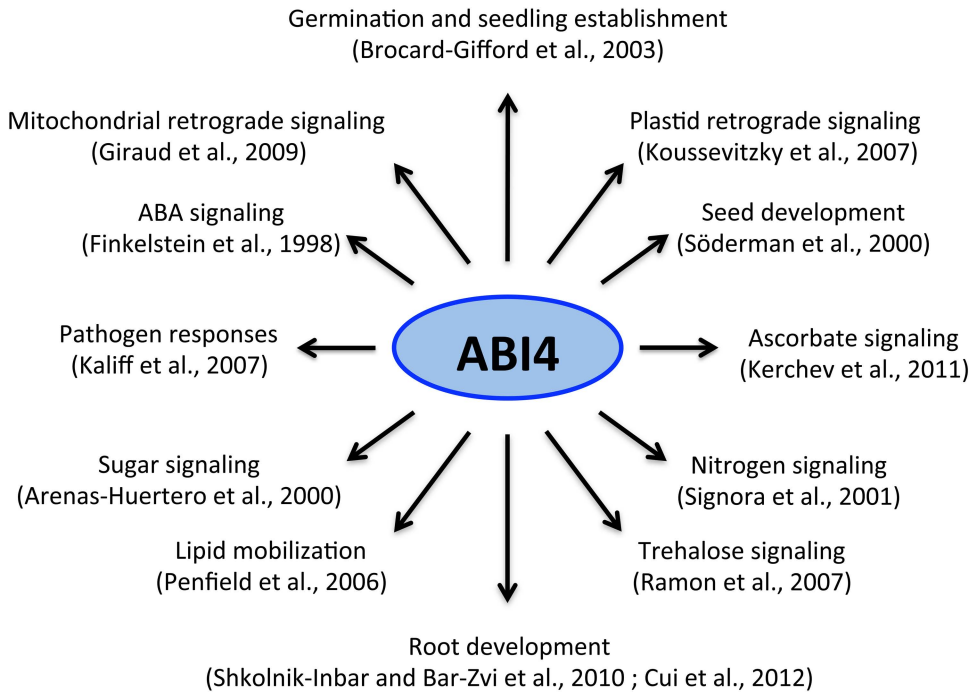

FIGURE 1 | ABI4 and its role in plant growth and development. ABI4 acts as a node of convergence of multiple signals that regulate different processes during plant development.

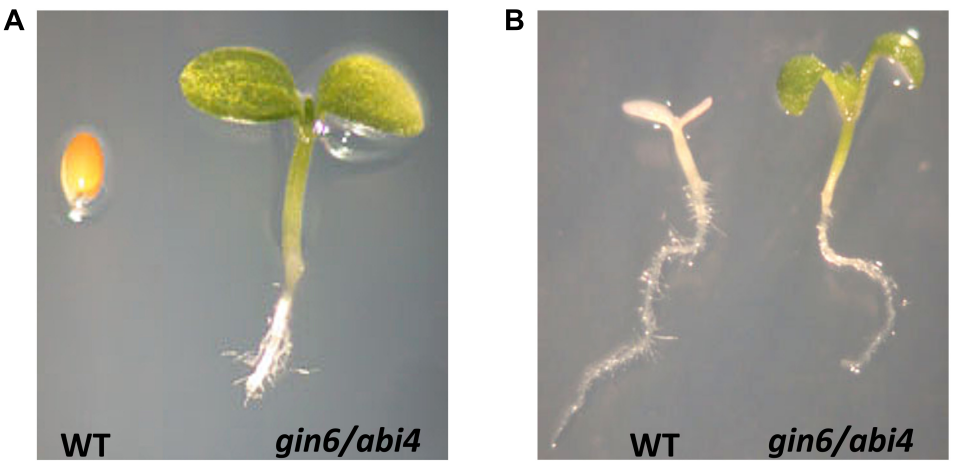

FIGURE 2 | ABI4 is required for ABA and sugar signaling. The *abi4/gin6* mutant plant is ABA-insensitive (*abi*) and glucose-insensitive (*gin*). *A. thaliana* wild-type plants are unable to grow in 5 μM of ABA, whereas the *abi4* mutant plant develops normally **(A)**. In media containing 6.5% glucose (Glc), the development of wild-type plants arrests, and they do not accumulate chlorophyll in contrast to the *abi4/gin6* mutant, which continues growing and displays a green phenotype and cotyledon expansion **(B)**.

plant functions including nitrogen signaling, lipid mobilization in the embryo, root growth, lateral root inhibition, and pathogen resistance (Signora et al., 2001; Jakab et al., 2005; Penfield et al., 2006; Kaliff et al., 2007; Shkolnik-Inbar and Bar-Zvi, 2010; Kerchev et al., 2011; Cui et al., 2012). Recent studies demonstrated that ABI4 is also required for redox responses in ascorbate-mediated signaling (Kerchev et al., 2011). These studies provided evidence of a close interaction between the redox and sugar signaling pathways (Foyer et al., 2012), which further supports the prominent role of ABI4 as a point of convergence for various signaling pathways (**Figure 1**).

For the purpose of this review, it is particularly interesting that the ABI4 transcription factor has been found to be important in chloroplast retrograde signaling pathways (see below) and in mitochondrial retrograde communication. The induction of the nuclear-encoded alternative oxidase gene (*AOX*) in response

to defects in electron transport chain inhibition by rotenone has been commonly used as a marker for mitochondrial retrograde signaling responses (Rhoads et al., 2006; Rhoads and Subbaiah, 2007). This induction is abolished in the *abi4* mutant during rotenone challenge (Giraud et al., 2009). ABI4 was demonstrated to bind directly to upstream elements of the *AOX* gene. These data indicate that ABI4 also plays a direct role in mitochondrial retrograde signaling in response to defects in the electron transport chain.

ABI4 AND ITS FUNCTION IN PLASTID RETROGRADE SIGNALING DURING PLASTID DEVELOPMENT

Based on their functional implications, plastid retrograde signals have been divided into those related to plastid development and those involved in operational fine-tuning in response to environmental or metabolic fluctuations (Pogson et al., 2008). This classification is useful, but it is not absolute because diverse lines of evidence demonstrate that several of these pathways are interconnected and share various components. The transition from proplastid to chloroplast is probably one of the most critical moments during seedling establishment because autotrophic capabilities depend on this process. During this time, and in response to defects in the developmental process, at least three different pathways have been reported that produce particular signal(s) and regulate NEPPs involved in the photosynthetic pathway and in plastid maintenance. These pathways are known as the plastid gene expression (PGE), tetrapyrrole, and plastid protein import (Nott et al., 2006; Woodson and Chory, 2008; Inaba et al., 2011).

Independent analyses have reported the participation of ABI4 in the PGE and tetrapyrrole retrograde signaling pathways (**Figure 3**). PGE appears to be important in coordinating the NEPPs required for different plastid types in early development (Kanervo et al., 2008). In response to defects in plastid gene expression or translation, a down-regulation of the expression of multiple NEPPs such as *LHCB* was observed (Pesaresi et al., 2006; Koussevitzky et al., 2007). The PGE pathway has primarily been characterized with the use of inhibitors that impair organelle transcription (Rapp and Mullet, 1991) or translation, such as lincomycin (Sullivan and Gray, 1999). This pathway has also been analyzed with mutants that affect early organelle development (Hedtke et al., 1999; Pesaresi et al., 2001). Although various studies have reported that the PGE pathway functions predominantly during the first days after germination (Sullivan and Gray, 1999), the characterization of the effect of the *prors1* mutant in chloroplast translation suggests that this regulation persists in mature

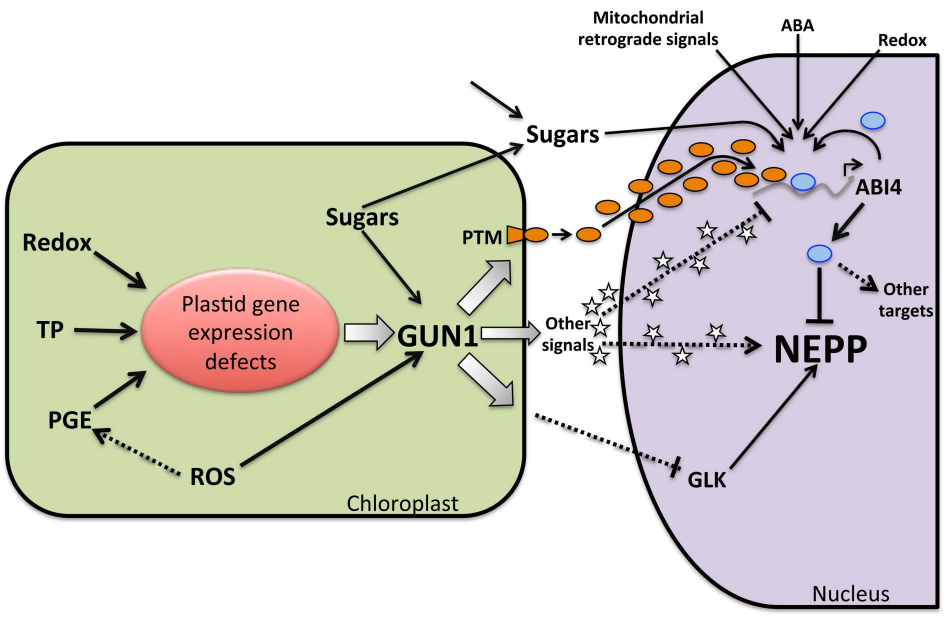

FIGURE 3 | Model of GUN1 and ABI4 function as integrators of NEPP regulation from several retrograde signaling pathways. Multiple conditions that alter plastid functionality, such as inhibition of plastid transcription or translation (PGE), tetrapyrrole biosynthesis inhibition (TB), altered redox status (Redox), and ROS production, result in defects in plastid gene expression. This model demonstrates how defects in plastid gene expression are capable of producing multiple signals, in close cooperation with GUN1, which acts as a convergent node. These signals can be positive or negative, resulting in the processing of the PTM factor in the plastid envelope and allowing its translocation to the nucleus (black circles), for example. In parallel, positive signals like heme (stars) generated by the plastid under normal conditions will decrease (represented by a smaller arrow). These events will lead to an increase in the level of the transcriptional regulator ABI4 (blue ovals) as a result of the induction of its transcription by factors such as PTM (orange ovals) or by the decrease of positive regulators. Elevated levels of ABI4 could also be the result of a reduction of its degradation. ABI4 acts as a repressor of photosynthetic nuclear genes and as an activator of other genes, such as those related to carbon catabolism. Positive signals such as heme (stars) could act by inhibiting the ABI4 expression or activating NEPPs. Defects in plastid gene expression mediated by GUN1 could modulate the levels of other factors such as GLKs that act as positive regulators of NEPPs. The final outcome in gene expression will depend on the levels of multiple positive and negative signals. ABI4 also responds to other signals such as the level of sugars produced inside the chloroplast or imported into the cell, ABA, redox status and retrograde signals from the mitochondria, which are all relevant for plastid function and modulate the NEPPs.

leaf tissues (Pesaresi et al., 2006). The signal(s) that initiates this pathway is still unknown, but recent data showed that changes in plastid gene expression in response to redox changes, could potentially trigger the PGE pathway. This establishes that the expression of the NEPPs is subject to physiological regulation by the redox status of the organelle. The recent characterization of the plastid redox-insensitive *prin2* mutant in *A. thaliana* supports this regulatory mechanism (Kindgren et al., 2012). PRIN2 is a plastid protein that localizes to the plastid transcriptionally active chromosome (pTAC) complex, and it enhances plastid transcription mediated by the plastid-encoded RNA polymerase (PEP). Consequently, in the *prin2* mutant, expression of plastid-encoded genes transcribed by the PEP is low, showing a similar profile to that observed in mutants with impaired PEP activity (Chateigner-Boutin et al., 2008; Arsova et al., 2010). Apparently, the low expression levels of plastid genes in the *prin2* mutant disrupt positive signals or induce negative signals that decrease the expression of NEPPs such as *LHCB* (**Figure 3**). Collectively, all these findings support the hypothesis that plastid gene expression mediated by PEP acts as a central integrator to initiate PGE retrograde signaling in response to developmental and metabolic cues.

One factor required in PGE signaling is GUN1, a plastid protein and member of the pentatricopeptide repeat (PPR) family. The *gun1* mutant is defective in the repression of NEPPs in response to lincomycin, and consequentially, *LHCB* expression is high in this mutant, a notable characteristic of the *gun* phenotype (Koussevitzky et al., 2007; Cottage et al., 2010; Sun et al., 2011). Interestingly, a weak *gun* phenotype was also observed in the *abi4* mutant in the presence of lincomycin, suggesting that this transcription factor plays a role in the PGE-dependent signaling pathway (**Figure 3**). Accordingly, overexpression of ABI4 suppresses the *gun* phenotype in the presence of lincomycin (Koussevitzky et al., 2007). However, the *gun* phenotype of the ABI4 mutant appears to be weaker than other *gun* mutants, and may be dependent on the high light conditions used during its analysis (Voigt et al., 2010; Kerchev et al., 2011), suggesting that other transcriptional regulators may also participate in the repression of NEPPs mediated by PGE (**Figure 3**).

Another retrograde signaling pathway involved in plastid development, which is probably the most extensively studied, is commonly referred to as the tetrapyrrole pathway. This pathway is associated with defects in the biosynthesis of chlorophyll (Nott et al., 2006; Woodson and Chory, 2008). In higher plants, the disruption of chloroplast development in response to photodamage caused by inhibitors of carotenoid biosynthesis such as norflurazon is associated with major changes in NEPP expression and the accumulation of intermediate tetrapyrrole compounds (Strand et al., 2003). Components of this signaling pathway were identified by isolating different *gun* mutants that no longer repressed NEPPs in the presence of norflurazon (Susek et al., 1993). Several of the characterized *gun* mutants affected different steps in porphyrin biosynthesis (Nott et al., 2006). These data led to the postulation that the tetrapyrrole intermediate Mg ProtoIX can be actively transported from the chloroplast to the cytosol and acts as a plastid signal (Mochizuki et al., 2001; Beck, 2005; Ankele et al., 2007). However, the role of the Mg ProtoIX as a signaling agent in this pathway has been questioned (Mochizuki et al., 2008; Moulin et al., 2008), and other molecules such as reactive oxygen species (ROS) and heme have been proposed to function as alternative signals (Mochizuki et al., 2008; Moulin et al., 2008; Woodson et al., 2011). The recent characterization of a new *gun* mutant (*gun6*) showed that excess accumulation of heme acts as an activator of the expression of photosynthetic genes. The role of heme as a signal that positively regulates NEPPs is particularly attractive not only because this molecule is known to be actively transported out of the plastids (Thomas and Weinstein, 1990) but also because heme functions as a signal in other organisms (Mense and Zhang, 2006; von Gromoff et al., 2008).

GUN1 is an essential factor in this signaling pathway and has been proposed to function as a node of convergence in the tetrapyrrole and PGE retrograde signaling pathways (Koussevitzky et al., 2007; Kakizaki et al., 2009). The function of the PPR protein GUN1 is still unclear, but very intriguing. PPR proteins have diverse functions, primarily related to organellar RNA metabolism (Schmitz-Linneweber and Small, 2008). Most of these proteins have specific RNA binding activity. Therefore, it has been speculated that a possible function for GUN1 is that it binds to a particular chloroplast transcript(s) that is essential for the generation of a chloroplast retrograde signal(s) (Woodson et al., 2012). GUN1 colocalizes with other PPR proteins such as pTAC2, a component of the pTAC that is involved in both transcription and post-transcriptional plastid processes (Ding et al., 2006; Pfalz et al., 2006). In addition to the PPR motifs, GUN1 and pTAC2, together with other five PPR proteins, share a "short mutS-related" domain that has been shown to have DNA-binding functions (Koussevitzky et al., 2007), indicating that these molecules maybe involved in the regulation of plastid transcription under certain conditions. Recently, Woodson et al. (2012) demonstrated that plastid transcription is a key element for the generation of at least two independent retrograde signals. Mutations in the sigma factors *sig2* and *sig6*, which are part of the PEP, result in the low expression of dozens of plastid-encoded and nuclear-encoded photosynthetic genes. Transcriptomic analysis demonstrated similarities in the expression pattern of these mutants compared to those of lincomycin- and norflurazon-treated plants. A key finding was that GUN1 is responsible for the defects observed in *sig2* and *sig6* mutants. Among the plastid genes with altered transcription levels in these *sig* mutants is $tRNA^{Glu}$, a key substrate of tetrapyrrole synthesis (Schon et al., 1986; Hanaoka et al., 2005). Accordingly, in *sig2* and *sig6* mutants, the levels of tetrapyrroles and heme are low. Increasing the levels of heme partially suppressed the expression defects only in the *sig2* mutant, supporting the role of this molecule as a positive regulator of nuclear gene expression (Woodson et al., 2012). These results add to the evidence of the role that plastid transcription plays in the generation of different signal(s) for PGE and tetrapyrrole retrograde pathways. One of such signals apparently originates directly from the transcription defects of the plastid genome. The other signal is related to the low levels of heme that result from the *sig* mutation. These results also position GUN1 as a strategic transmitter of these signals through a post-transcriptional regulatory mechanism by regulating the stability or the of plastid transcripts such as $tRNA^{Glu}$ (Woodson et al., 2012). Several lines of evidence support the idea that ABI4 is also important in the transmission of

tetrapyrrole pathway signals from the chloroplast to the nucleus. As in the *gun* mutants, the repression of the *LHCB* transcript in the *abi4* mutant is attenuated to approximately one-third that of the control plants after norflurazon treatment. Moreover, *gun1* has been shown to be epistatic to *abi4* because the expression of *LHCB* in the *gun1abi4* double mutant resembles that found in *gun1*. Similar to the PGE pathway, overexpression of ABI4 is capable of suppressing the misregulation of the *LHCB* gene observed in the *gun1* mutant (Koussevitzky et al., 2007). Finally, recent data showed that the expression of *ABI4* is induced by both lincomycin and norflurazon treatment (Sun et al., 2011), supporting a role for ABI4 in the retrograde responses of the PGE and tetrapyrrole pathways (**Figure 3**). However as previously mentioned, the fact that the expression level of genes such as *LHCB* in the *gun1* and *abi4* mutants never reaches that observed in control plants without treatment also suggests that additional factors or a more complex mechanism participate in NEPP repression caused by the disruption of chloroplast development.

ABI4 AND THE RETROGRADE OPERATIONAL CONTROL PATHWAYS

Changes in chloroplast function in response to high light or environmental fluctuations trigger different retrograde signaling responses classified as operational control pathways (Pogson et al., 2008). These pathways can adjust to changes in organelle status or initiate stress responses after organelle damage. Several of these pathways are triggered by specific ROS or by the redox status inherent to photosynthetic electron transfer (PET) and may be mostly related to chloroplasts (Foyer and Noctor, 2009; Galvez-Valdivieso and Mullineaux, 2010). Other pathways respond to the production of particular metabolites such as PAP (Estavillo et al., 2011) and MecPP (methylerythritol cyclodiphosphate; Xiao et al., 2012), which can potentially be produced by numerous plastid types.

Several lines of evidence support the concept that specific ROS species trigger independent signaling pathways, and these have been extensively reviewed (Pogson et al., 2008; Foyer and Noctor, 2009; Galvez-Valdivieso and Mullineaux, 2010; Mittler et al., 2011). The presence of high light levels damages chloroplasts and results in high levels of singlet oxygen ($^1O_2$), leading to a rapid inhibition of plant growth, the induction of plant cell death and the differential regulation of specific sets of nuclear genes (op den Camp et al., 2003). The characterization of the *flu* mutants that hyperaccumulate photosensitive compounds that generate $^1O_2$ supported the hypothesis that this ROS elicits a specific retrograde signaling pathway that is active during embryogenesis and impacts on plastid differentiation during germination (op den Camp et al., 2003; Lee et al., 2007; Kim et al., 2009). Recent data indicate that the $^1O_2$ pathway is also active under moderate light stress conditions, causing limited cell death that may be part of the acclimation response in plants that enhances stress resistance (Kim et al., 2012). Interestingly, the production of high $^1O_2$ levels has also been reported during norflurazon and lincomycin treatments, and this molecule has been considered to be a putative signal for the modulation of NEPPs in response to these inhibitors. As previously described, this regulation is no longer observed in mutants of GUN1 and ABI4, supporting a link between $^1O_2$ and these transcription factors (Moulin et al., 2008).

A second class of ROS that has been shown to elicit specific gene expression responses is hydrogen peroxide (H_2O_2; Cruz de Carvalho, 2008). Various stresses, including photoreduction of O_2 at photosystem I, high light, and herbicides such as paraquat, induce H_2O_2 production. Under these conditions, the expression of many genes related to biotic and abiotic stresses, such as ascorbate peroxidase and the nuclear transcription factors ZAT10 and ZAT12, are induced (Rossel et al., 2007; Maruta et al., 2012). Activation of a specific MAP protein kinase cascade is required for signal transduction (Nakagami et al., 2006; Pitzschke and Hirt, 2009). Mutations in the *GUN1* and *ABI4* genes also affect the induction of *ZAT10* and *ZAT12*. These findings have been taken as evidence of the participation of ABI4 and GUN1 in ROS-mediated retrograde pathways (Koussevitzky et al., 2007; Moulin et al., 2008). A key question that is still unanswered is which specific ROS molecule "converges" at GUN1 and consequently at ABI4, given that high light treatment can induce the production of free radicals (superoxide anion, O_2^- and hydroxyl radical, $^-$OH) and non-radical molecules ($^1O_2$, and H_2O_2).

Subtle changes in temperature, light quality, and intensity have tremendous effects on the chloroplasts' redox state. These changes are closely linked to the function of PET. Changes in the redox status of the plastoquinone (PQ) pool and thioredoxin proteins permit long-term adjustments that result in changes in the accumulation of photosynthetic components such as the NEPPs (Kleine et al., 2007; Wagner et al., 2008; Brautigam et al., 2009). Thioredoxins are also major redox transmitters that modulate the activity of many plastidial enzymes and regulatory proteins (Arsova et al., 2010; Pesaresi et al., 2010; Dietz and Pfannschmidt, 2011). The characterization of a novel plastidial thioredoxin isoform (TRX z) links these proteins to plastid gene expression and possibly also with retrograde signaling (Arsova et al., 2010). TRX z regulates the activity of PEP through the action of two nuclear-encoded kinases related to fructokinases (FLN1 and FLN2). These changes in plastid gene expression in response to the redox state could potentially trigger PGE-mediated retrograde signaling during early seedling development, establishing physiological regulation of NEPPs by the redox status of the organelle. As mentioned above, the low plastid gene expression levels in the *prin2* mutant disrupt positive signals or induce negative signals that decrease the expression of NEPPs (Kindgren et al., 2012). Collectively, these findings support the concept that plastid gene expression mediated by PEP functions as a central integrator to initiate retrograde signaling in response to developmental and metabolic cues. At this point, it is still an open question whether this redox-mediated regulation depends on GUN1 and ABI4.

ABI4 AS A REGULATOR OF NUCLEAR GENE EXPRESSION

Analysis of the expression patterns of the *abi4* mutant (Koussevitzky et al., 2007; Kerchev et al., 2012) or transgenic plants overexpressing ABI4 (Reeves et al., 2011) has demonstrated that ABI4 modulates the expression of a significant number of genes. Among its potential targets are genes involved in seed development and maturation, genes involved in metabolism, genes related to stress and defense and, finally, several transcription factors. These analyses have also revealed interesting overlaps in the

expression profiles of other mutants including *gun1* (Koussevitzky et al., 2007) and the ascorbate-deficient mutants *vtc1* and *vtc2* (Kerchev et al., 2012).

In *in vitro* and transient assays, ABI4 has been shown to bind to the CE1-like element CACCG, which is present in the promoters of its putative target genes in *A. thaliana* (Finkelstein et al., 1998; Niu et al., 2002; Sakuma et al., 2002; Acevedo-Hernandez et al., 2005; Koussevitzky et al., 2007; Bossi et al., 2009; Giraud et al., 2009; Yang et al., 2011; Lee et al., 2012) and maize (Hu et al., 2012). Binding to this sequence results in the activation or repression of target genes, including ABI4 itself (Acevedo-Hernandez et al., 2005; Rook et al., 2006b; Bossi et al., 2009). The dual function of this factor as a repressor or an activator apparently depends on the context of its binding site in conjunction with the binding site of essential activators (**Figures 4A,B**). In several repressed genes from different species such as *LHCB* and *RBCS* (**Figure 4B**), the ABI4 binding site overlaps with a G-box element (CACGTG), which is essential for high levels of expression in many light-regulated genes (Acevedo-Hernandez et al., 2005; Koussevitzky et al., 2007). In these two cases, the CE1-like element is present in a different orientation than in the activated genes (**Figure 4A**). It has been proposed that ABI4 competition for binding with activators such as G-box binding factors (GBFs) results in ABI4-mediated reduction of gene expression (**Figure 4C**; Acevedo-Hernandez et al., 2005; Rook et al., 2006b). Consistent with this arrangement for the repressed genes, most of the ABI4-specific activated targets identified by Reeves et al. (2011) do not contain the CE1-like element (GCCAC) that overlapped with a putative G-box in either orientation. Moreover, the GCCACGTG or CACGTGGC sequences in which a putative CE1-like element overlaps with a putative G-box, have been found enriched in promoters of photosyntheyic genes, which could be potential targets for repression by ABI4 (Joung et al., 2009). Finally, studies based on transcriptomic analysis of the *abi4* mutants or plants ectopically expressing ABI4 support that ABI4 positively or negatively regulates the expression of a significant number of genes involved in photosynthesis, hormone signaling and defense, among others (Foyer et al., 2007; Koussevitzky et al., 2007; Reeves et al., 2011). From these analyses, it was also suggested that ABI4 might have additional alternative binding sites, including a shorter version of the CE1-like motif (CCAC) or a motif that overlaps with ABRE sequences (Koussevitzky et al., 2007; Reeves et al., 2011).

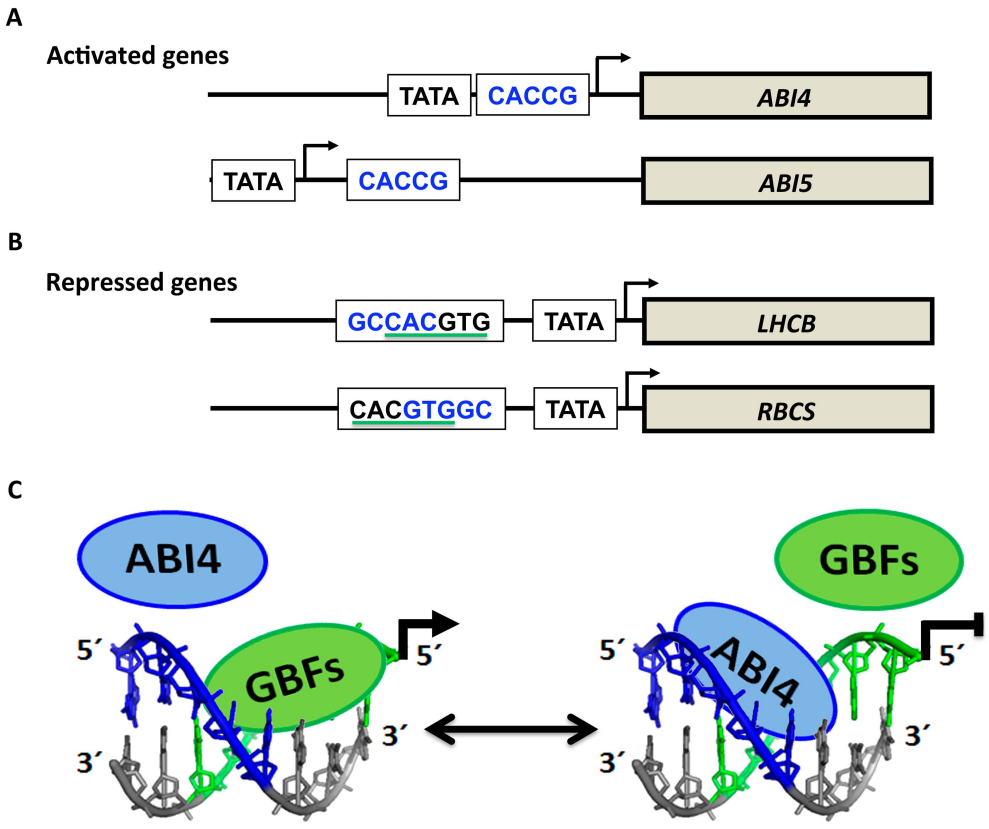

FIGURE 4 | Target genes of ABI4. (A) Genes activated by ABI4 generally contain the CE1-like sequence (CACCG; in blue) identified by Niu et al. (2002). In contrast, repressed genes contain the CE1-like element in the reverse orientation (GCCAC) and overlap with the G-box element (underlined in green; **B**). The proposed model of repression by ABI4 is depicted in **(C)**. Competition for the binding site between ABI4 and GBF (G-box binding factor) results in non-activation of GBF target genes represented by the line in **(C)**. For ease of interpretation, the G-box is shown on the complementary-sense strand (green), whereas the CE1-like element (in blue) is depicted on the direct sense-strand. The GCCACGTG sequence was modeled by 3D-DART (Van Dijk and Bonvin, 2009) and visualized with PyMOL (http://www.pymol.org/).

ABI4, AN ELUSIVE REGULATORY FACTOR

Despite support for the role of ABI4 as an important regulator in many processes, the mechanism through which this factor integrates different signals remains unknown. An important limitation to experimental investigation of this protein is that the ABI4 protein has been extremely difficult to detect. Most of our present knowledge about ABI4 comes from its analysis at the transcriptional level. The expression pattern of *ABI4* has been inferred mostly following the activity of the GUS marker fused to the upstream regulatory ABI4 sequences at different stages of plant development. Using this assay, various studies have found that under normal growing conditions, the expression of ABI4 is restricted to specific stages of development (Soderman et al., 2000; Penfield et al., 2006; Bossi et al., 2009; Cui et al., 2012). Transcription of *ABI4* is detected in the embryo during most stages of seed development, but its expression is undetectable in dry seeds. Shortly after seed imbibition (24 h), the *ABI4* transcript accumulates again in most of the germinating seedling, and its expression continues through the first days of the seedling emergence. In these stages, *ABI4* is expressed in the cotyledons, the hypocotyls, and the root tips, but it is barely detectable in the true leaves (Soderman et al., 2000; Bossi et al., 2009; Cui et al., 2012). The expression of *ABI4* in later developmental stages was reported only in the anthers (Soderman et al., 2000). However, the lack of ABI4 expression in later plant developmental stages is difficult to reconcile with the participation of this factor during processes that operate in later developmental stages, such as lateral root development or the retrograde regulation responses expected to be active in true leaves. Two recent studies have reported the expression of *ABI4* in the vascular tissue of true leaves, phloem, companion cells and parenchyma of 11-day-old roots (Shkolnik-Inbar and Bar-Zvi, 2010, 2011). The differences in these expression patterns may reflect the promoter fragments used in each case: 3 or 2.6 kb in the initial studies versus 2 kb in the more recent ones. A possible explanation of these results is that some regulatory elements required for tissue-specific regulation (repressors) were excluded in the 2 kb fragment. Available data support this possibility; in the glucose-insensitive mutant *gin6*, the defects associated with altered *ABI4* expression in normal conditions or in the presence of sugars are a direct consequence of a T-DNA insertion 2 kb upstream of the ABI4 translation initiation site (Arenas-Huertero et al., 2000). Additionally, a recent analysis demonstrated that the SCARECROW (SCR) regulator represses the expression of *ABI4* through direct binding to the ABI4 promoter between −2.3 and −2.6 kb from its transcription initiation site (Cui et al., 2012). These results demonstrate that ABI4 can be expressed in later developmental stages but in response to particular signals or the action of particular regulators.

FACTORS THAT REGULATE ABI4

The expression of *ABI4* is regulated by various factors, including ABI4 itself, which is an essential activator of its own expression during early seedling development (Arroyo et al., 2003; Bossi et al., 2009). As stated above, the plant-specific transcriptional regulator SCR has been found to repress *ABI4* expression in roots (Cui et al., 2012). SCR is required for the specification of the root endodermis, but recent data showed that SCR is also an important regulator in leaves (Dhondt et al., 2010). Additionally, recent evidence demonstrated that in the absence of the plant hormone ABA, the transcriptional regulator WRKY40 also represses *ABI4* expression (Shang et al., 2010). Similar to ABI4, WRKY40 has been implicated in plant defense responses, and this effect could be mediated, at least in part, by ABI4 (Shang et al., 2010; Kerchev et al., 2011). All these data demonstrate that the transcription of *ABI4* is tightly regulated by the action of different transcription factors.

A central question is whether it is possible that any of these regulators can transmit retrograde signals. One of the most interesting findings that potentially links ABI4 and retrograde chloroplast signaling is the recent identification of the transcriptional regulator PTM, which directly activates *ABI4* gene expression (Sun et al., 2011). PTM is a chloroplast membrane-bound protein that is conserved among plants that contain a homeodomain and localizes in the plastid envelope (Sun et al., 2011). Sun et al. (2011) demonstrated that in response to treatments that initiate retrograde signals such as norflurazon, lincomycin, and high light, PTM is processed by an unidentified intramembrane peptidase and released from the plastid envelope to the cytoplasm. The processed PTM accumulates in the nucleus, where it directly activates *ABI4* gene expression. Accordingly, in the *ptm* mutant, the expression of *ABI4* is reduced. Similar to ABI4, PTM is required in various retrograde signaling pathways (**Figure 3**). In the *ptm* mutant, treatments such as lincomycin and norflurazon do not repress *LHCB* expression. Interestingly, the function of PTM during *ABI4* expression appears to be related to histone modification in the ABI4 promoter, a regulatory mechanism that still has not been analyzed. This finding directly links plastid retrograde signals with the expression of *ABI4*, which in turn impacts on NEPPs. To be more confident in this conclusion, the endopeptidase responsible for PTM activation must be identified and the conditions that regulate its activity defined. It is also important to demonstrate whether *ABI4* induction mediated by PTM or other regulators alters active ABI4 protein levels because nuclear gene expression depends on the presence of an active protein.

ABI4 is tightly regulated at the post-transcriptional level (Finkelstein et al., 2011). Part of this regulation depends on the rapid turnover of the protein, which is mediated by the 26S proteasome (Finkelstein et al., 2011; Gregorio et al., unpublished data). Interestingly, ABI4 stability does not appear to be affected by ABA levels, unlike the ABI5 signaling factor (Lopez-Molina et al., 2003; Finkelstein et al., 2011). Thus, one of the major challenges in understanding the various functions of the ABI4 transcriptional regulator will be its analysis at the protein level. For example, binding of ABI4 to the CE1-like element does not appear to require additional factors, but this may not be the case with other alternative binding sites. Multifactor binding is an attractive alternative because it could provide the capacity to ABI4 to modulate NEPP in response to different signals, including the ability to affect different retrograde communication pathways (Koussevitzky et al., 2007;Reeves et al., 2011). For example, overexpression of the transcription factor ASR1 (abscisic acid stress ripening 1) results in *abi* and *gin* phenotypes. These phenotypes apparently are the result of displacement of ABI4 by high ASR1 levels because the binding

sites of both factors overlap in some target genes (Shkolnik and Bar-Zvi, 2008).

In addition to the well-conserved APETALA 2 (AP2) DNA-binding domain (Okamuro et al., 1997; Shigyo et al., 2006), ABI4 has other conserved regions, including a serine/threonine-rich domain of unknown function that is a putative target of phosphorylation and a putative protein–protein interaction domain at its C-terminus, likely required for transcriptional activation (Finkelstein et al., 1998; Soderman et al., 2000). Thus, ABI4 could potentially associate with other factors to modulate its own activity in response to different signals. Preliminary data using a yeast one-hybrid assay demonstrated synergisms between ABI4 and other transcription factors in the transcriptional activation of some genes (Finkelstein et al., 2011). However, until now, no interacting proteins of ABI4 have been identified. This is an important subject that merits future investigation.

In summary, although the participation of ABI4 in different retrograde signaling pathways has been observed in independent analyses, the mechanism by which this factor perceives these signals probably involves not only regulation at the expression level but also at the level of protein activity, through currently unknown post-translational regulatory mechanisms that need to be identified.

ADDITIONAL TRANSCRIPTION FACTORS

Although ABI4 has emerged as an important integrator of various retrograde signals, there are additional factors regulating these pathways. For example, in the *abi4* mutant, the expression of *LHCB* after norflurazon or lincomycin treatment is not reduced to the level of the wild-type, but the levels are still lower than without treatment (Koussevitzky et al., 2007; Sun et al., 2011). Some factors that have been shown to participate in retrograde signaling pathways include two related proteins GLK1 and GLK2 (Waters et al., 2009). These proteins are members of the GARP superfamily (Riechmann et al., 2000) and directly activate the expression of genes involved in chlorophyll biosynthesis, light harvesting, and electron transport (Waters et al., 2009). The GLK proteins were initially identified in maize, but related proteins exist in most plants (Fitter et al., 2002; Waters et al., 2009; Wang et al., 2012). These proteins are partially redundant and are required for normal chloroplast development. The *glk1*/*glk2* double mutant in maize displays a pale green phenotype with small, partially differentiated chloroplasts. GLKs have been implicated in retrograde signaling, specifically in the plastid protein import pathway (Kakizaki et al., 2009), because in the *glk1*/*glk2* double mutant, the expression of some retrograde signaling marker genes such as *LHCB*, *RBCS*, or carbonic anhydrase (*CA1*) are less sensitive to norflurazon or lincomycin treatment than wild-type plants, resulting in a weak GUN phenotype similar to that observed in ABI4 mutant (Waters et al., 2009). This result indicates that these regulatory factors may participate in the PGE and tetrapyrrole signaling pathways. In contrast to ABI4, GLKs interact with GBFs and positively regulate the expression of NEPPs (Tamai et al., 2002). In response to alterations in plastid function (photodamage, transcription, or protein import), the level of GLKs decreases and the level of ABI4 increases, resulting in massive changes in gene expression. The participation of two independent factors might provide a more versatile regulatory mechanism (**Figure 3**).

Transcription factors that exhibit dual subcellular localization are also good candidates for components of retrograde signaling mechanisms. In addition to PTM, additional factors that exhibit dual localization have been described (Krause et al., 2012). One example is pTAC12 (HEMERA), which participates in phytochrome signaling (Chen et al., 2010) and has also been detected as part of the pTAC (Pfalz et al., 2006). It has been proposed that this factor can directly modulate the expression of plastid and nuclear genes, but this function has not yet been demonstrated. Another example is the transcriptional regulator WHIRLY1, which localizes to the plastids and the nucleus of tobacco plants (Isemer et al., 2012). In plastids, this factor is also associated with the pTAC and is translocated to the nucleus through an unknown mechanism, where it activates the expression of genes related to pathogenesis. The possible participation of these dual-localized factors in retrograde signaling responses is required to be addressed.

CONCLUDING REMARKS

ABI4 has emerged as a central integrator of essential environmental signals such as light, carbon status, ABA, redox and organelle status, facilitating the coordination of development and central metabolic processes such as photosynthesis. Although our present understanding of the mode of action of this central regulator has advanced, there are still major questions that need to be addressed in the near future, including the impact that the transcriptional regulation of ABI4 has on the levels of its protein. An aspect which is essential to understanding the function of ABI4 as a regulatory node of different signaling pathways, including plastid retrograde signaling, is how it is regulated post-transcriptionally in addition to identifying possible interaction partners. It is still an open question whether different signals can modulate the stability or activity of ABI4 either by protein modification or through direct interaction.

After a period of research that was primarily dominated by the description of independent retrograde signaling pathways, recent findings provide compelling evidence that many of those pathways converge into common integrators. Our understanding of retrograde signaling regulation is evolving into a more dynamic process in which multiple signals are produced simultaneously. These signals can affect the expression of nuclear genes in opposing ways through the participation of convergent transcriptional factors such as ABI4. This could be a very powerful strategy to respond to subtle changes in plastid functionality. The current challenges include understanding the molecular mechanism that generates signals during plastid transcription and the molecular nature of these signals. Identification of the direct targets of GUN1 could provide important insights. Although GUN1 is the only PPR protein that has been found to be required in retrograde signaling to date, the function of other related PPRs should be evaluated.

Finally, an aspect that has to be taken into consideration is that even in the *gun1* and *abi4* mutants, NEPPs repression is not completely lost. This result supports the evidence of the existence of an independent *gun1* and *abi4* retrograde signaling pathway that modulates NEPPs expression that requires future investigation.

ACKNOWLEDGMENTS

We would like to thank Dr. Virginia Walbot and Dr. Mari Salmi for their helpful comments and suggestions. This work was supported by Consejo Nacional de Ciencia y Tecnología (127546) and Dirección General de Asuntos para el Personal Académico-UNAM (IN208211-3) grants.

REFERENCES

Acevedo-Hernandez, G. J., Leon, P., and Herrera-Estrella, L. R. (2005). Sugar and ABA responsiveness of a minimal RBCS light-responsive unit is mediated by direct binding of ABI4. *Plant J.* 43, 506–519.

Ankele, E., Kindgren, P., Pesquet, E., and Strand, A. (2007). *In vivo* visualization of Mg-protoporphyrin IX, a coordinator of photosynthetic gene expression in the nucleus and the chloroplast. *Plant Cell* 19, 1964–1979.

Arenas-Huertero, F., Arroyo, A., Zhou, L., Sheen, J., and Leon, P. (2000). Analysis of Arabidopsis glucose insensitive mutants, gin5 and gin6, reveals a central role of the plant hormone ABA in the regulation of plant vegetative development by sugar. *Genes Dev.* 14, 2085–2096.

Arroyo, A., Bossi, F., Finkelstein, R. R., and Leon, P. (2003). Three genes that affect sugar sensing (abscisic acid insensitive 4, abscisic acid insensitive 5, and constitutive triple response 1) are differentially regulated by glucose in Arabidopsis. *Plant Physiol.* 133, 231–242.

Arsova, B., Hoja, U., Wimmelbacher, M., Greiner, E., Ustun, S., Melzer, M., et al. (2010). Plastidial thioredoxin z interacts with two fructokinase-like proteins in a thiol-dependent manner: evidence for an essential role in chloroplast development in *Arabidopsis* and *Nicotiana benthamiana*. *Plant Cell* 22, 1498–1515.

Baier, M., and Dietz, K. J. (2005). Chloroplasts as source and target of cellular redox regulation: a discussion on chloroplast redox signals in the context of plant physiology. *J. Exp. Bot.* 56, 1449–1462.

Beck, C. F. (2005). Signaling pathways from the chloroplast to the nucleus. *Planta* 222, 743–756.

Bossi, F., Cordoba, E., Dupre, P., Mendoza, M. S., Roman, C. S., and Leon, P. (2009). The Arabidopsis ABA-INSENSITIVE (ABI) 4 factor acts as a central transcription activator of the expression of its own gene, and for the induction of ABI5 and SBE2.2 genes during sugar signaling. *Plant J.* 59, 359–374.

Bradbeer, J. W., Atkinson, Y., Börner, T., and Hagemann, R. (1979). Cytoplasmic synthesis of plastid polypeptides may be controlled by plastid-synthesised RNA. *Nature* 279, 816–817.

Brautigam, K., Dietzel, L., Kleine, T., Stroher, E., Wormuth, D., Dietz, K. J., et al. (2009). Dynamic plastid redox signals integrate gene expression and metabolism to induce distinct metabolic states in photosynthetic acclimation in Arabidopsis. *Plant Cell* 21, 2715–2732.

Chan, K. X., Crisp, P. A., Estavillo, G. M., and Pogson, B. J. (2010). Chloroplast-to-nucleus communication: current knowledge, experimental strategies and relationship to drought stress signaling. *Plant Signal. Behav.* 5, 1575–1582.

Chateigner-Boutin, A. L., Ramos-Vega, M., Guevara-Garcia, A., Andres, C., and De La Luz Gutierrez-Nava, M. (2008). CLB19, a pentatricopeptide repeat protein required for editing of rpoA and clpP chloroplast transcripts. *Plant J.* 56, 590–602.

Chen, M., Galvao, R. M., Li, M., Burger, B., Bugea, J., Bolado, J., et al. (2010). Arabidopsis HEMERA/pTAC12 initiates photomorphogenesis by phytochromes. *Cell* 141, 1230–1240.

Cottage, A., Mott, E. K., Kempster, J. A., and Gray, J. C. (2010). The Arabidopsis plastid-signalling mutant gun1 (genomes uncoupled1) shows altered sensitivity to sucrose and abscisic acid and alterations in early seedling development. *J. Exp. Bot.* 61, 3773–3786.

Cruz de Carvalho, M. H. (2008). Drought stress and reactive oxygen species: production, scavenging and signaling. *Plant Signal. Behav.* 3, 156–165.

Cui, H., Hao, Y., and Kong, D. (2012). SCARECROW has a SHORT-ROOT-independent role in modulating the sugar response. *Plant Physiol.* 158, 1769–1778.

Dekkers, B. J., Schuurmans, J. A., and Smeekens, S. C. (2008). Interaction between sugar and abscisic acid signalling during early seedling development in Arabidopsis. *Plant Mol. Biol.* 67, 151–167.

Dhondt, S., Coppens, F., De Winter, F., Swarup, K., Merks, R. M., Inze, D., et al. (2010). SHORT-ROOT and SCARECROW regulate leaf growth in Arabidopsis by stimulating S-phase progression of the cell cycle. *Plant Physiol.* 154, 1183–1195.

Dichtl, B., Stevens, A., and Tollervey, D. (1997). Lithium toxicity in yeast is due to the inhibition of RNA processing enzymes. *EMBO J.* 16, 7184–7195.

Dietz, K. J., and Pfannschmidt, T. (2011). Novel regulators in photosynthetic redox control of plant metabolism and gene expression. *Plant Physiol.* 155, 1477–1485.

Dietz, K. J., Vogel, M. O., and Viehhauser, A. (2010). AP2/EREBP transcription factors are part of gene regulatory networks and integrate metabolic, hormonal and environmental signals in stress acclimation and retrograde signalling. *Protoplasma* 245, 3–14.

Ding, Y. H., Liu, N. Y., Tang, Z. S., Liu, J., and Yang, W. C. (2006). Arabidopsis GLUTAMINE-RICH PROTEIN23 is essential for early embryogenesis and encodes a novel nuclear PPR motif protein that interacts with RNA polymerase II subunit III. *Plant Cell* 18, 815–830.

Estavillo, G. M., Crisp, P. A., Pornsiriwong, W., Wirtz, M., Collinge, D., Carrie, C., et al. (2011). Evidence for a SAL1-PAP chloroplast retrograde pathway that functions in drought and high light signaling in Arabidopsis. *Plant Cell* 23, 3992–4012.

Finkelstein, R., Lynch, T., Reeves, W., Petitfils, M., and Mostachetti, M. (2011). Accumulation of the transcription factor ABA-insensitive (ABI)4 is tightly regulated post-transcriptionally. *J. Exp. Bot.* 62, 3971–3979.

Finkelstein, R. R., Wang, M. L., Lynch, T. J., Rao, S., and Goodman, H. M. (1998). The Arabidopsis abscicic acid response locus ABI4 encodes an APETALA2 domain protein. *Plant Cell* 10, 1043–1054.

Fitter, D. W., Martin, D. J., Copley, M. J., Scotland, R. W., and Langdale, J. A. (2002). GLK gene pairs regulate chloroplast development in diverse plant species. *Plant J.* 31, 713–727.

Foyer, C. H., Kerchev, P. I., and Hancock, R. D. (2012). The ABA-INSENSITIVE-4 (ABI4) transcription factor links redox, hormone and sugar signaling pathways. *Plant Signal. Behav.* 7, 276–281.

Foyer, C. H., Kiddle, G., and Verrier, P. (2007). Transcriptional profiling approaches to understanding how plants regulate growth and defence: a case study illustrated by analysis of the role of vitamin C. *EXS* 97, 55–86.

Foyer, C. H., and Noctor, G. (2009). Redox regulation in photosynthetic organisms: signaling, acclimation, and practical implications. *Antioxid. Redox Signal.* 11, 861–905.

Galvez-Valdivieso, G., and Mullineaux, P. M. (2010). The role of reactive oxygen species in signalling from chloroplasts to the nucleus. *Physiol. Plant* 138, 430–439.

Giraud, E., Van Aken, O., Ho, L. H., and Whelan, J. (2009). The transcription factor ABI4 is a regulator of mitochondrial retrograde expression of ALTERNATIVE OXIDASE1a. *Plant Physiol.* 150, 1286–1296.

Gould, S. B., Waller, R. F., and Mcfadden, G. I. (2008). Plastid evolution. *Annu. Rev. Plant Biol.* 59, 491–517.

Hanaoka, M., Kanamaru, K., Fujiwara, M., Takahashi, H., and Tanaka, K. (2005). Glutamyl-tRNA mediates a switch in RNA polymerase use during chloroplast biogenesis. *EMBO Rep.* 6, 545–550.

Hedtke, B., Wagner, I., Borner, T., and Hess, W. R. (1999). Inter-organellar crosstalk in higher plants: impaired chloroplast development affects mitochondrial gene and transcript levels. *Plant J.* 19, 635–643.

Hu, Y. F., Li, Y. P., Zhang, J., Liu, H., Tian, M., and Huang, Y. (2012). Binding of ABI4 to a CACCG motif mediates the ABA-induced expression of the ZmSSI gene in maize (*Zea mays* L.) endosperm. *J. Exp. Bot.* 63, 5979–5989.

Huijser, C., Kortstee, A., Pego, J., Weisbeek, P., Wisman, E., and Smeekens, S. (2000). The Arabidopsis SUCROSE UNCOUPLED-6 gene is identical to ABSCISIC ACID INSENSITIVE-4: involvement of abscisic acid in sugar responses. *Plant J.* 23, 577–585.

Inaba, T., Yazu, F., Ito-Inaba, Y., Kakizaki, T., and Nakayama, K. (2011). Retrograde signaling pathway from plastid to nucleus. *Int. Rev. Cell Mol. Biol.* 290, 167–204.

Isemer, R., Mulisch, M., Schafer, A., Kirchner, S., Koop, H. U., and Krupinska, K. (2012). Recombinant Whirly1 translocates from transplastomic chloroplasts to the nucleus. *FEBS Lett.* 586, 85–88.

Jakab, G., Ton, J., Flors, V., Zimmerli, L., Metraux, J. P., and Mauch-Mani, B. (2005). Enhancing Arabidopsis salt and drought stress tolerance by chemical priming for its abscisic acid responses. *Plant Physiol.* 139, 267–274.

Janska, H., Kwasniak, M., and Szczepanowska, J. (2012). Protein quality control in organelles – AAA/

FtsH story. *Biochim. Biophys. Acta.* doi: 10.1016/j.bbamcr. 2012.03.016 [Epub ahead of print].

Joung, J. G., Corbett, A. M., Fellman, S. M., Tieman, D. M., Klee, H. J., Giovannoni, J. J., et al. (2009). Plant MetGenMAP: an integrative analysis system for plant systems biology. *Plant Physiol.* 151, 1758–1768.

Joyard, J., Ferro, M., Masselon, C., Seigneurin-Berny, D., Salvi, D., Garin, J., et al. (2009). Chloroplast proteomics and the compartmentation of plastidial isoprenoid biosynthetic pathways. *Mol. Plant* 2, 1154–1180.

Kakizaki, T., Matsumura, H., Nakayama, K., Che, F. S., Terauchi, R., and Inaba, T. (2009). Coordination of plastid protein import and nuclear gene expression by plastid-to-nucleus retrograde signaling. *Plant Physiol.* 151, 1339–1353.

Kaliff, M., Staal, J., Myrenas, M., and Dixelius, C. (2007). ABA is required for Leptosphaeria maculans resistance via ABI1- and ABI4-dependent signaling. *Mol. Plant Microbe Interact.* 20, 335–345.

Kanervo, E., Singh, M., Suorsa, M., Paakkarinen, V., Aro, E., Battchikova, N., et al. (2008). Expression of protein complexes and individual proteins upon transition of etioplasts to chloroplasts in pea (*Pisum sativum*). *Plant Cell Physiol.* 49, 396–410.

Katagiri, T., Ishiyama, K., Kato, T., Tabata, S., Kobayashi, M., and Shinozaki, K. (2005). An important role of phosphatidic acid in ABA signaling during germination in *Arabidopsis thaliana. Plant J.* 43, 107–117.

Kerchev, P. I., Fenton, B., Foyer, C. H., and Hancock, R. D. (2012). Infestation of potato (*Solanum tuberosum* L.) by the peach-potato aphid (*Myzus persicae* Sulzer) alters cellular redox status and is influenced by ascorbate. *Plant Cell Environ.* 35, 430–440.

Kerchev, P. I., Pellny, T. K., Vivancos, P. D., Kiddle, G., Hedden, P., Driscoll, S., et al. (2011). The transcription factor ABI4 Is required for the ascorbic acid-dependent regulation of growth and regulation of jasmonate-dependent defense signaling pathways in Arabidopsis. *Plant Cell* 23, 3319–3334.

Kim, C., Lee, K. P., Baruah, A., Nater, M., Gobel, C., Feussner, I., et al. (2009). (1)O_2-mediated retrograde signaling during late embryogenesis predetermines plastid differentiation in seedlings by recruiting abscisic acid. *Proc. Natl. Acad. Sci. U.S.A.* 106, 9920–9924.

Kim, C., Meskauskiene, R., Zhang, S., Lee, K. P., Lakshmanan Ashok, M., Blajecka, K., et al. (2012). Chloroplasts of Arabidopsis are the source and a primary target of a plant-specific programmed cell death signaling pathway. *Plant Cell* 24, 3026–3039.

Kindgren, P., Kremnev, D., Blanco, N. E., De Dios Barajas Lopez, J., Fernandez, A. P., Tellgren-Roth, C., et al. (2012). The plastid redox insensitive 2 mutant of Arabidopsis is impaired in PEP activity and high light-dependent plastid redox signalling to the nucleus. *Plant J.* 70, 279–291.

Kleine, T., Kindgren, P., Benedict, C., Hendrickson, L., and Strand, A. (2007). Genome-wide gene expression analysis reveals a critical role for CRYPTOCHROME1 in the response of Arabidopsis to high irradiance. *Plant Physiol.* 144, 1391–1406.

Koussevitzky, S., Nott, A., Mockler, T. C., Hong, F., Sachetto-Martins, G., Surpin, M., et al. (2007). Signals from chloroplasts converge to regulate nuclear gene expression. *Science* 316, 715–719.

Kovacs-Bogdan, E., Soll, J., and Bolter, B. (2010). Protein import into chloroplasts: the Tic complex and its regulation. *Biochim. Biophys. Acta* 1803, 740–747.

Krause, K., Oetke, S., and Krupinska, K. (2012). Dual targeting and retrograde translocation: regulators of plant nuclear gene expression can be sequestered by plastids. *Int. J. Mol. Sci.* 13, 11085–11101.

Laby, R. J., Kim, D., and Gibson, S. I. (2001). The ram1 mutant of Arabidopsis exhibits severely decreased beta-amylase activity. *Plant Physiol.* 127, 1798–1807.

Lee, K. P., Kim, C., Landgraf, F., and Apel, K. (2007). EXECUTER1- and EXECUTER2-dependent transfer of stress-related signals from the plastid to the nucleus of Arabidopsis thaliana. *Proc. Natl. Acad. Sci. U.S.A.* 104, 10270–10275.

Lee, S. A., Yoon, E. K., Heo, J. O., Lee, M. H., Hwang, I., Cheong, H., et al. (2012). Analysis of Arabidopsis glucose insensitive growth mutants reveals the involvement of the plastidial copper transporter PAA1 in glucose-induced intracellular signaling. *Plant Physiol.* 159, 1001–1012.

Leister, D. (2012). Retrograde signaling in plants: from simple to complex scenarios. *Front. Plant Sci.* 3:135. doi: 10.3389/fpls.2012.00135

Leister, D., Wang, X., Haberer, G., Mayer, K. F., and Kleine, T. (2011). Intracompartmental and intercompartmental transcriptional networks coordinate the expression of genes for organellar functions. *Plant Physiol.* 157, 386–404.

León, P., and Sheen, J. (2003). Sugar and hormone connections. *Trends Plant Sci.* 8, 110–116.

Li, H. M., and Chiu, C. C. (2010). Protein transport into chloroplasts. *Annu. Rev. Plant Biol.* 61, 157–180.

López-Juez, E. (2009). Steering the solar panel: plastids influence development. *New Phytol.* 182, 287–290.

Lopez-Molina, L., Mongrand, S., Kinoshita, N., and Chua, N. H. (2003). AFP is a novel negative regulator of ABA signaling that promotes ABI5 protein degradation. *Genes Dev.* 17, 410–418.

Margulis, L. (1971). Symbiosis and evolution. *Sci. Am.* 225, 48–57.

Maruta, T., Noshi, M., Tanouchi, A., Tamoi, M., Yabuta, Y., Yoshimura, K., et al. (2012). H_2O_2-triggered retrograde signaling from chloroplasts to nucleus plays specific role in response to stress. *J. Biol. Chem.* 287, 11717–11729.

Mense, S. M., and Zhang, L. (2006). Heme: a versatile signaling molecule controlling the activities of diverse regulators ranging from transcription factors to MAP kinases. *Cell Res.* 16, 681–692.

Mittler, R., Vanderauwera, S., Suzuki, N., Miller, G., Tognetti, V. B., Vandepoele, K., et al. (2011). ROS signaling: the new wave? *Trends Plant. Sci.* 16, 300–309.

Mizoi, J., Shinozaki, K., and Yamaguchi-Shinozaki, K. (2012). AP2/ERF family transcription factors in plant abiotic stress responses. *Biochim. Biophys. Acta* 1819, 86–96.

Mochizuki, N., Brusslan, J. A., Larkin, R., Nagatani, A., and Chory, J. (2001). Arabidopsis genomes uncoupled 5 (GUN5) mutant reveals the involvement of Mg-chelatase H subunit in plastid-to-nucleus signal transduction. *Proc. Natl. Acad. Sci. U.S.A.* 98, 2053–2058.

Mochizuki, N., Tanaka, R., Tanaka, A., Masuda, T., and Nagatani, A. (2008). The steady-state level of Mg-protoporphyrin IX is not a determinant of plastid-to-nucleus signaling in Arabidopsis. *Proc. Natl. Acad. Sci. U.S.A.* 105, 15184–15189.

Moulin, M., Mccormac, A. C., Terry, M. J., and Smith, A. G. (2008). Tetrapyrrole profiling in Arabidopsis seedlings reveals that retrograde plastid nuclear signaling is not due to Mg-protoporphyrin IX accumulation. *Proc. Natl. Acad. Sci. U.S.A.* 105, 15178–15183.

Mullineaux, P., and Karpinski, S. (2002). Signal transduction in response to excess light: getting out of the chloroplast. *Curr. Opin. Plant Biol.* 5, 43–48.

Nakagami, H., Soukupova, H., Schikora, A., Zarsky, V., and Hirt, H. (2006). A Mitogen-activated protein kinase kinase kinase mediates reactive oxygen species homeostasis in Arabidopsis. *J. Biol. Chem.* 281, 38697–38704.

Neuhaus, H. E., and Emes, M. J. (2000). Nonphotosynthetic metabolism in plastids. *Annu. Rev. Plant Physiol. Plant Mol. Biol.* 51, 111–140.

Niu, X., Helentjaris, T., and Bate, N. J. (2002). Maize ABI4 binds coupling element1 in abscisic acid and sugar response genes. *Plant Cell* 14, 2565–2575.

Nott, A., Jung, H. S., Koussevitzky, S., and Chory, J. (2006). Plastid-to-nucleus retrograde signaling. *Annu. Rev. Plant Biol.* 57, 739–759.

Okamuro, J. K., Caster, B., Villarroel, R., Montagu, V. M., and Jofuku, K. D. (1997). The AP2 domain of APETALA2 defines a large new family of DNA binding proteins in Arabidopsis. *Proc. Natl. Acad. Sci. U.S.A.* 94, 7076–7081.

Olinares, P. D., Kim, J., Davis, J. I., and Van Wijk, K. J. (2011). Subunit stoichiometry, evolution, and functional implications of an asymmetric plant plastid ClpP/R protease complex in Arabidopsis. *Plant Cell* 23, 2348–2361.

Olinares, P. D., Ponnala, L., and Van Wijk, K. J. (2010). Megadalton complexes in the chloroplast stroma of *Arabidopsis thaliana* characterized by size exclusion chromatography, mass spectrometry, and hierarchical clustering. *Mol. Cell. Proteomics* 9, 1594–1615.

op den Camp, R. G., Przybyla, D., Ochsenbein, C., Laloi, C., Kim, C., Danon, A., et al. (2003). Rapid induction of distinct stress responses after the release of singlet oxygen in Arabidopsis. *Plant Cell* 15, 2320–2332.

Penfield, S., Li, Y., Gilday, A. D., Graham, S., and Graham, I. A. (2006). Arabidopsis ABA INSENSITIVE4 regulates lipid mobilization in the embryo and reveals repression of seed germination by the endosperm. *Plant Cell* 18, 1887–1899.

Pesaresi, P., Hertle, A., Pribi, M., Schneider, A., Kleine, T., and Leister, D. (2010). Optimizing photosynthesis under fluctuating light: the role of

the Arabidopsis STN7 kinase. *Plant Signal. Behav.* 5, 21–25.

Pesaresi, P., Masiero, S., Eubel, H., Braun, H. P., Bhushan, S., Glaser, E., et al. (2006). Nuclear photosynthetic gene expression is synergistically modulated by rates of protein synthesis in chloroplasts and mitochondria. *Plant Cell* 18, 970–991.

Pesaresi, P., Schneider, A., Kleine, T., and Leister, D. (2007). Interorganellar communication. *Curr. Opin. Plant Biol.* 10, 600–606.

Pesaresi, P., Varotto, C., Meurer, J., Jahns, P., Salamini, F., and Leister, D. (2001). Knock-out of the plastid ribosomal protein L11 in Arabidopsis: effects on mRNA translation and photosynthesis. *Plant J.* 27, 179–189.

Pfalz, J., Liere, K., Kandlbinder, A., Dietz, K. J., and Oelmuller, R. (2006). pTAC2, -6, and -12 are components of the transcriptionally active plastid chromosome that are required for plastid gene expression. *Plant Cell* 18, 176–197.

Pitzschke, A., and Hirt, H. (2009). Disentangling the complexity of mitogen-activated protein kinases and reactive oxygen species signaling. *Plant Physiol.* 149, 606–615.

Pogson, B. J., Woo, N. S., Forster, B., and Small, I. D. (2008). Plastid signalling to the nucleus and beyond. *Trends Plant Sci.* 13, 602–609.

Rapp, J. C., and Mullet, J. E. (1991). Chloroplast transcription is required to express the nuclear genes rbcS and cab: plastid DNA copy number is regulated independently. *Plant Mol. Biol.* 17, 813–823.

Reeves, W. M., Lynch, T. J., Mobin, R., and Finkelstein, R. R. (2011). Direct targets of the transcription factors ABA-insensitive(ABI)4 and ABI5 reveal synergistic action by ABI4 and several bZIP ABA response factors. *Plant Mol. Biol.* 75, 347–363.

Rhoads, D. M., and Subbaiah, C. C. (2007). Mitochondrial retrograde regulation in plants. *Mitochondrion* 7, 177–194.

Rhoads, D. M., Umbach, A. L., Subbaiah, C. C., and Siedow, J. N. (2006). Mitochondrial reactive oxygen species. Contribution to oxidative stress and interorganellar signaling. *Plant Physiol.* 141, 357–366.

Richly, E., Dietzmann, A., Biehl, A., Kurth, J., Laloi, C., Apel, K., et al. (2003). Covariations in the nuclear chloroplast transcriptome reveal a regulatory master-switch. *EMBO Rep.* 4, 491–498.

Richly, E., and Leister, D. (2004). An improved prediction of chloroplast proteins reveals diversities and commonalities in the chloroplast proteomes of Arabidopsis and rice. *Gene* 329, 11–16.

Riechmann, J. L., Heard, J., Martin, G., Reuber, L., Jiang, C., Keddie, J., et al. (2000). Arabidopsis transcription factors: genome-wide comparative analysis among eukaryotes. *Science* 290, 2105–2110.

Rochaix, J. D. (2011). Assembly of the photosynthetic apparatus. *Plant Physiol.* 155, 1493–1500.

Rolland, F., Baena-Gonzalez, E., and Sheen, J. (2006). Sugar sensing and signaling in plants: conserved and novel mechanisms. *Annu. Rev. Plant Biol.* 57, 675–709.

Rook, F., Corke, F., Baier, M., Holman, R., May, A. G., and Bevan, M. W. (2006a). Impaired sucrose induction1 encodes a conserved plant-specific protein that couples carbohydrate availability to gene expression and plant growth. *Plant J.* 46, 1045–1058.

Rook, F., Corke, F., Card, R., Munz, G., Smith, C., and Bevan, M. W. (2001). Impaired sucrose-induction mutants reveal the modulation of sugar-induced starch biosynthetic gene expression by abscisic acid signalling. *Plant J.* 26, 421–433.

Rook, F., Hadingham, S. A., Li, Y., and Bevan, M. W. (2006b). Sugar and ABA response pathways and the control of gene expression. *Plant Cell Environ.* 29, 426–434.

Rossel, J. B., Wilson, P. B., Hussain, D., Woo, N. S., Gordon, M. J., Mewett, O. P., et al. (2007). Systemic and intracellular responses to photooxidative stress in Arabidopsis. *Plant Cell* 19, 4091–4110.

Sakuma, Y., Liu, Q., Dubouzet, J. G., Abe, H., Shinozaki, K., and Yamaguchi-Shinozaki, K. (2002). DNA-binding specificity of the ERF/AP2 domain of Arabidopsis DREBs, transcription factors involved in dehydration- and cold-inducible gene expression. *Biochem. Biophys. Res. Commun.* 290, 998–1009.

Schmitz-Linneweber, C., and Small, I. (2008). Pentatricopeptide repeat proteins: a socket set for organelle gene expression. *Trends Plant Sci.* 13, 663–670.

Schon, A., Krupp, G., Gough, S., Berry-Lowe, S., Kannangara, C. G., and Soll, D. (1986). The RNA required in the first step of chlorophyll biosynthesis is a chloroplast glutamate tRNA. *Nature* 322, 281–284.

Shang, Y., Yan, L., Liu, Z. Q., Cao, Z., Mei, C., Xin, Q., et al. (2010). The Mg-chelatase H subunit of Arabidopsis antagonizes a group of WRKY transcription repressors to relieve ABA-responsive genes of inhibition. *Plant Cell* 22, 1909–1935.

Shigyo, M., Hasebe, M., and Ito, M. (2006). Molecular evolution of the AP2 subfamily. *Gene* 366, 256–265.

Shkolnik, D., and Bar-Zvi, D. (2008). Tomato ASR1 abrogates the response to abscisic acid and glucose in Arabidopsis by competing with ABI4 for DNA binding. *Plant Biotechnol. J.* 6, 368–378.

Shkolnik-Inbar, D., and Bar-Zvi, D. (2010). ABI4 mediates abscisic acid and cytokinin inhibition of lateral root formation by reducing polar auxin transport in Arabidopsis. *Plant Cell* 22, 3560–3573.

Shkolnik-Inbar, D., and Bar-Zvi, D. (2011). Expression of ABSCISIC ACID INSENSITIVE 4 (ABI4) in developing Arabidopsis seedlings. *Plant Signal. Behav.* 6, 694–696.

Signora, L., De Smet, I., Foyer, C. H., and Zhang, H. (2001). ABA plays a central role in mediating the regulatory effects of nitrate on root branching in Arabidopsis. *Plant J.* 28, 655–662.

Soderman, E. M., Brocard, I. M., Lynch, T. J., and Finkelstein, R. R. (2000). Regulation and function of the Arabidopsis ABA-insensitive4 gene in seed and abscisic acid response signaling networks. *Plant Physiol.* 124, 1752–1765.

Stern, D. B., Goldschmidt-Clermont, M., and Hanson, M. R. (2010). Chloroplast RNA metabolism. *Annu. Rev. Plant Biol.* 61, 125–155.

Strand, A., Asami, T., Alonso, J., Ecker, J. R., and Chory, J. (2003). Chloroplast to nucleus communication triggered by accumulation of Mg-protoporphyrin IX. *Nature* 421, 79–83.

Sullivan, J. A., and Gray, J. C. (1999). Plastid translation is required for the expression of nuclear photosynthesis genes in the dark and in roots of the pea lip1 mutant. *Plant Cell* 11, 901–910.

Sun, X., Feng, P., Xu, X., Guo, H., Ma, J., Chi, W., et al. (2011). A chloroplast envelope-bound PHD transcription factor mediates chloroplast signals to the nucleus. *Nat. Commun.* 2, 477.

Susek, R., Ausubel, F., and Chory, J. (1993). Signal transduction mutants of Arabidopsis uncouple nuclar CAB and RBCS gene expression from chloroplast development. *Cell* 74, 787–799.

Tamai, H., Iwabuchi, M., and Meshi, T. (2002). Arabidopsis GARP transcriptional activators interact with the Pro-rich activation domain shared by G-box-binding bZIP factors. *Plant Cell Physiol.* 43, 99–107.

Thomas, J., and Weinstein, J. D. (1990). Measurement of heme efflux and heme content in isolated developing chloroplasts. *Plant Physiol.* 94, 1414–1423.

Van Dijk, M., and Bonvin, A. M. (2009). 3D-DART: a DNA structure modelling server. *Nucleic Acids Res.* 37, W235–W239.

Voigt, C., Oster, U., Bornke, F., Jahns, P., Dietz, K.J., Leister, D., et al. (2010). In-depth analysis of the distinctive effects of norflurazon implies that tetrapyrrole biosynthesis, organellar gene expression and ABA cooperate in the GUN-type of plastid signalling. *Physiol. Plant* 138, 503–519.

von Gromoff, E. D., Alawady, A., Meinecke, L., Grimm, B., and Beck, C. F. (2008). Heme, a plastid-derived regulator of nuclear gene expression in *Chlamydomonas*. *Plant Cell* 20, 552–567.

Vothknecht, U. C., and Westhoff, P. (2001). Biogenesis and origin of thylakoid membranes. *Biochem. Biophys. Acta* 1541, 91–101.

Wagner, R., Dietzel, L., Brautigam, K., Fischer, W., and Pfannschmidt, T. (2008). The long-term response to fluctuating light quality is an important and distinct light acclimation mechanism that supports survival of *Arabidopsis thaliana* under low light conditions. *Planta* 228, 573–587.

Wang, P., Fouracre, J., Kelly, S., Karki, S., Gowik, U., Aubry, S., et al. (2012). Evolution of GOLDEN2-LIKE gene function in C(3) and C (4) plants. *Planta*. doi: 10.1007/s00425-012-1754-3 [Epub ahead of print].

Waters, M. T., Wang, P., Korkaric, M., Capper, R. G., Saunders, N. J., and Langdale, J. A. (2009). GLK transcription factors coordinate expression of the photosynthetic apparatus in Arabidopsis. *Plant Cell* 21, 1109–1128.

Woodson, J. D., and Chory, J. (2008). Coordination of gene expression between organellar and nuclear genomes. *Nat. Rev. Genet.* 9, 383–395.

Woodson, J. D., Perez-Ruiz, J. M., and Chory, J. (2011). Heme synthesis by plastid ferrochelatase I regulates nuclear gene expression in plants. *Curr. Biol.* 21, 897–903.

Woodson, J. D., Perez-Ruiz, J. M., Schmitz, R. J., Ecker, J. R., and Chory, J. (2012). Sigma factor mediated plastid retrograde signals control nuclear gene expression. *Plant J.*

doi: 10.1111/tpj.12011 [Epub ahead of print].

Xiao, Y., Savchenko, T., Baidoo, E. E., Chehab, W. E., Hayden, D. M., Tolstikov, V., et al. (2012). Retrograde signaling by the plastidial metabolite MEcPP regulates expression of nuclear stress-response genes. *Cell* 149, 1525–1535.

Yang, Y., Yu, X., Song, L., and An, C. (2011). ABI4 activates DGAT1 expression in Arabidopsis seedlings during nitrogen deficiency. *Plant Physiol.* 156, 873–883.

Zybailov, B., Rutschow, H., Friso, G., Rudella, A., Emanuelsson, O., Sun, Q., et al. (2008). Sorting signals, N-terminal modifications and abundance of the chloroplast proteome. *PLoS ONE* 3:e1994. doi: 10.1371/journal.pone.0001994

Conflict of Interest Statement: The authors declare that the research was conducted in the absence of any commercial or financial relationships that could be construed as a potential conflict of interest.

Received: 10 October 2012; accepted: 18 December 2012; published online: 10 January 2013.

*Citation: León P, Gregorio J and Cordoba E (2013) ABI4 and its role in chloroplast retrograde communication. Front. Plant Sci. **3**:304. doi: 10.3389/fpls.2012.00304*

This article was submitted to Frontiers in Plant Physiology, a specialty of Frontiers in Plant Science.

Copyright © 2013 León, Gregorio and Cordoba. This is an open-access article distributed under the terms of the Creative Commons Attribution License, which permits use, distribution and reproduction in other forums, provided the original authors and source are credited and subject to any copyright notices concerning any third-party graphics etc.

frontiers in
PLANT SCIENCE

ORIGINAL RESEARCH ARTICLE
published: 24 December 2012
doi: 10.3389/fpls.2012.00281

Comparison of transcriptional changes to chloroplast and mitochondrial perturbations reveals common and specific responses in Arabidopsis

Olivier Van Aken and James Whelan*

ARC Centre of Excellence in Plant Energy Biology, University of Western Australia, Crawley, WA, Australia

Edited by:
Tatjana Kleine,
Ludwig-Maximilians-Universität München, Germany

Reviewed by:
Rainer E. Häusler, University Cologne, Germany
Iris Finkemeier,
Ludwig-Maximilians-Universität München, Germany

***Correspondence:**
James Whelan, ARC Centre of Excellence in Plant Energy Biology, University of Western Australia, 35 Stirling Highway, 6009 Crawley, WA, Australia.
e-mail: jim.whelan@uwa.edu.au

Throughout the life of a plant, the biogenesis and fine-tuning of energy organelles is essential both under normal growth and stress conditions. Communication from organelle to nucleus is essential to adapt gene regulation and protein synthesis specifically to the current needs of the plant. This organelle-to-nuclear communication is termed retrograde signaling and has been studied extensively over the last decades. In this study we have used large-scale gene expression data sets relating to perturbations of chloroplast and mitochondrial function to gain further insights into plant retrograde signaling and how mitochondrial and chloroplast retrograde pathways interact and differ. Twenty seven studies were included that assess transcript profiles in response to chemical inhibition as well as genetic mutations of organellar proteins. The results show a highly significant overlap between gene expression changes triggered by chloroplast and mitochondrial perturbations. These overlapping gene expression changes appear to be common with general abiotic, biotic, and nutrient stresses. However, retrograde signaling pathways are capable of distinguishing the source of the perturbation as indicated by a statistical overrepresentation of changes in genes encoding proteins of the affected organelle. Organelle-specific overrepresented functional categories among others relate to energy metabolism and protein synthesis. Our analysis also suggests that WRKY transcription factors play a coordinating role on the interface of both organellar signaling pathways. Global comparison of the expression profiles for each experiment revealed that the recently identified chloroplast retrograde pathway using phospho-adenosine phosphate is possibly more related to mitochondrial than chloroplast perturbations. Furthermore, new marker genes have been identified that respond specifically to mitochondrial and/or chloroplast dysfunction.

Keywords: *Arabidopsis*, mitochondria, chloroplasts, retrograde, stress, microarray

INTRODUCTION

It is well established that the energy organelles chloroplasts and mitochondria communicate with the cellular nucleus to allow for optimal functioning through signaling processes generally termed retrograde signaling. One reason for this retrograde regulation is easily envisaged, as during evolution of eukaryotes the majority of genes encoding plastid or mitochondrial proteins have relocated to the nucleus (Bock and Timmis, 2008). Therefore, the organelles must feed back to the nucleus to induce or reduce transcription of organellar proteins depending on developmental cues and environmental conditions. Accordingly, several nuclear marker genes encoding organellar proteins have been used in the past to study retrograde signaling, including *LHCB2.4* for plastid retrograde (Koussevitzky et al., 2007) and *AOX1a* for mitochondrial retrograde signaling (Dojcinovic et al., 2005; Giraud et al., 2009). When looking at the co-expression of genes encoded in the nucleus and genes still encoded in the organellar genome, it was found that co-expression could be observed for nuclear and organellar genes encoding plastid proteins, but not mitochondrial proteins (Leister et al., 2011).

However, it is apparent from a number of studies that these retrograde signals do not just affect the expression of genes encoding proteins targeted to the specific organelle, but also other cellular compartments and functional groups (Van Aken et al., 2007; Estavillo et al., 2011; Giraud et al., 2012). Recent studies have indicated for instance that mitochondrial perturbations can significantly affect functional categories such as plant-pathogen interactions, protein synthesis, and photosynthetic light reactions (Schwarzlander et al., 2012). In the case of mitochondrial retrograde signaling, links, and overlaps have also been shown with stress-responses and resistance (Rhoads and Subbaiah, 2007; Van Aken et al., 2007). Other studies have suggested that many signaling pathways are overlapping and very hard to separate, resulting in a lack of marker genes encoding chloroplast or mitochondrial proteins that respond only to specific conditions (Leister et al., 2011).

Although some insight has been developed regarding the transcriptional responses ensuing retrograde signaling, very few transcriptional regulators have been identified. For mitochondrial retrograde signaling, so far only Abscisic acid Insensitive 4 has

been identified as a regulator, and interestingly ABI4 had also been identified as an important regulator of chloroplast retrograde signaling (Koussevitzky et al., 2007; Giraud et al., 2009). Other proteins involved in chloroplast retrograde signaling contain the Genomes Uncoupled (GUN) proteins that act during early development of chloroplast function termed biogenic control (Susek et al., 1993; Koussevitzky et al., 2007) but are very divergent types of proteins ranging from pentatricopeptide repeat (PPR) protein GUN1 to Mg-chelatase H (Mochizuki et al., 2001; Koussevitzky et al., 2007). The actual molecules that may be messenger of GUN signals are controversial, with some groups suggesting Mg-protoporphyrin IX and other groups contesting this (Mochizuki et al., 2008; Moulin et al., 2008).

Once functional chloroplasts have been established, other retrograde pathways have been identified that regulate chloroplast function termed operational control. For example, during drought and high-light conditions a signaling pathway is active via SAL1, involved in dephosphorylation of phospho-adenosine phosphate (PAP), and XRN-type exoribonucleases that are inhibited by PAP concentrations (Chen et al., 2011; Estavillo et al., 2011). Another class of likely signals for chloroplast and probably mitochondrial retrograde signaling are reactive oxygen species (ROS). ROS are readily produced in metabolically active cells both in chloroplasts and mitochondria (among other subcellular sites), with the four common forms of ROS generated being singlet oxygen ($^1O_2$), the superoxide anion (O_2^-), hydrogen peroxide (H_2O_2), and the hydroxyl radical (HO•). ROS formation has also been long recognized as a common signal in all kinds of biotic and abiotic stresses, malnutrition, and hormone signaling. The most broadly studied type of ROS is probably H_2O_2, and it is a good candidate for involvement in retrograde signaling as it is a relatively stable molecule and could potentially travel from the chloroplasts or mitochondria to the cytosol or nucleus (Chan et al., 2010). Also singlet oxygen is thought to play a role in chloroplast retrograde signaling, as evidenced in the *fluorescent* (*flu*) mutant that accumulates protochlorophyllide in the chloroplasts during dark periods, and subsequently generates singlet oxygen once illuminated resulting in genome-wide expression changes and eventually cell death (Meskauskiene et al., 2001; Lee et al., 2007). Elimination of the Executer 1 protein is able to suppress these cell death signals in the *flu* mutant. Nevertheless, given the short life-span of ROS and the myriad of processes that can increase their presence, they are difficult to study specifically in the context of retrograde signaling.

To gain more detailed insight into the transcriptional effects that are common and different between chloroplast and mitochondrial retrograde signaling pathways we collected a series of microarray experiments that examined perturbations in either system. Most studies have employed chemical inhibitions using inhibitors such as norflurazon, lincomycin for chloroplasts and rotenone, oligomycin, and antimycin A for mitochondria. These compounds are known to have indirect side-effects that make interpretation more complicated. Therefore, several mutants in specifically chloroplast of mitochondrial proteins were examined. Furthermore, the expression of genes that responded significantly to these organellar perturbations was examined across a wide variety of developmental and stress-related microarray experiments to allow a better picture of how retrograde responses are situated within the lifecycle of a plant.

MATERIALS AND METHODS

GENERATION OF ORGANELLE-SPECIFIC GENE LISTS

Genes encoding chloroplast, mitochondrial or peroxisome proteins were selected based on publicly available information based on mass-spectrometry, Green Fluorescent Protein-targeting assays, and subcellular localization prediction algorithms. The list for mitochondria was taken from a previous study (Law et al., 2012). For chloroplasts, the *Arabidopsis* subcellular database SUBA (Heazlewood et al., 2007) was used as basis and genes for which either experimental (GFP targeting or more than half of mass-spectrometry identifications) or predicted (five or more of the 10 prediction algorithms) localization in chloroplasts was evidenced were selected. Furthermore, this list was expanded with the plant proteomics database PPDB (Sun et al., 2009) and was further expanded with chloroplast protein identifications published by (Yu et al., 2008). In this way 2384 genes were selected and in total 2183 probe sets represented genes in this list on the Affymetrix ATH1 GeneChip microarrays. Similarly, SUBA was used as a starting point for peroxisomal proteins and genes for which predicted (two or more of the 10 prediction algorithms) localization in peroxisomes was evidenced were selected. Proteins reported by several proteomic studies were also included (Reumann et al., 2007, 2009; Eubel et al., 2008; Lingner et al., 2011), as well as the Peroxisomes 2010[1] list of confirmed peroxisomal proteins. In total 306 genes encoding peroxisomal proteins were selected and in total 287 probe sets represented genes in this list on the Affymetrix ATH1 GeneChip. The list of transcription factors was based on their presence in at least two of the four *Arabidopsis* transcription factor databases RARTF, AGRIS, PlnTFDB, and DATF (Mitsuda and Ohme-Takagi, 2009), and as such 1983 genes encoding putative transcription factors. In total 1661 probe sets represented genes in this list on the Affymetrix ATH1 GeneChip. All gene lists are shown in Table S1 in Supplementary Material.

MICROARRAY DATA ANALYSIS

For the datasets related to chloroplast and mitochondrial perturbations CEL files were normalized using the MAS5.0 algorithm within the Avadis microarray analysis software package. Probe sets that were not called absent in at least half of the chips for one genotype or treatment were kept for further analysis. Statistical analysis was then performed using the CyberT Bayesian framework (Baldi and Long, 2001) and genes with average foldchange of more than twofold and PPDE ($<p$) > 0.95 were retained. If probe sets were called absent an expression value of fold change 1 was assigned for further analysis. Complete expression and statistical analysis results are available in Table S2 in Supplementary Material. CEL files for the additional microarray experiments related to stress, development, anatomy, nutrient availability etc. were also normalized using the MAS5.0 algorithm and probe sets that were not called absent in at least half of the chips for one timepoint, treatment or tissue type were kept for further analysis. If probe sets were

[1] http://www.peroxisome.msu.edu

called absent an expression value of fold change 1 was assigned for further analysis. Normalized expression data for all probes in all selected experiments are available in Table S3 in Supplementary Material. Visualization and hierarchical clustering of the microarray data were performed in the Multiexperiment Viewer MeV 4.8[2] using the Pearson correlation coefficient. Overrepresentation of functional categories was performed using the PageMan tool (Usadel et al., 2006). Functional categories with significant over- or underrepresentation ($p < 0.05$) and a ratio foldchange of twofold or more were retained. Complete PageMan outputs are shown in Table S4 in Supplementary Material.

PROMOTER MOTIF ANALYSIS

The 1 kb promoter regions of the selected marker genes were downloaded from TAIR[3]. The MEME suite was then used to discover overrepresented motifs in an unbiased search (Bailey et al., 2009). MEME parameters used were any number of motif repetitions per sequence, minimum motif width of five bases and maximum motif width of 50 bases. For analysis of known binding sites the Athena promoter analysis tool was used (O'Connor et al., 2005).

RESULTS

SELECTION OF MICROARRAY DATASETS

First, public repositories were searched for available microarray experiments that directly affect mitochondrial function in *Arabidopsis thaliana* (**Table 1**). For normalization purposes and comparability only datasets based on the Affymetrix ATH1 platform were selected, as this is by far the most widely used system for analysis of *A. thaliana* gene expression. Studies using mitochondrial inhibitor compounds included treatment with rotenone (Complex I inhibitor), oligomycin (ATP synthase inhibitor; Clifton et al., 2005), and antimycin A (Complex III inhibitor; Ng et al., 2012, GEO accession GSE36011). Additionally, several mutants in genes encoding mitochondrial proteins have been studied using microarrays. These include prohibitin *atphb3* (Van Aken et al., 2007), Complex I subunits *ndufs4*, and *ndufa1* (Meyer et al., 2009), alternative oxidase *aox1a* (Giraud et al., 2008), organellar RNA polymerase *rpotmp* (Kuhn et al., 2009), succinate dehydrogenase subunit *dsr1* (Gleason et al., 2011), regulators of mitochondrial recombination *msh1 recA3* double mutant (Shedge et al., 2010), mitochondrial splicing factor *rug3* (Kuhn et al., 2011), mitochondrial inner membrane translocase subunit *Tim23-2* knockout and overexpressor (Wang et al., 2012) and mitochondrial translation factor double mutant *letm1(−/−) LETM2(+/−*; Zhang et al., 2012). In total these comprise 14 different perturbations of mitochondrial function.

Next a similar selection of microarray experiments directly affecting chloroplast function and chloroplast retrograde regulation was made (**Table 1**). These include inhibitor studies using chlorophyll synthesis inhibitor norflurazon (McCormac and Terry, 2004), photosystem II protein synthesis inhibitor lincomycin (Koussevitzky et al., 2007), photosystem II inhibitor PNO8 (Goda et al., 2008). In addition the *gun1*, *gun5*, and *abi4* mutants in chloroplast retrograde signaling were compared against Col-0 wild type plants after treatment with lincomycin (Koussevitzky et al., 2007). Finally a number of mutants in genes encoding chloroplast proteins were selected, including leaf-type ferredoxin-NADP+ oxidoreductase *fnr1* (Lintala et al., 2009), S-sulfocysteine synthase *cs26* (Bermudez et al., 2010), as well as three mutants in chloroplast proteins that display distinct responses under high-light conditions including triose-phosphate translocator *tpt-1* (Walters et al., 2004), the *flu* mutant that accumulates the photosensitizer protochlorophyllide in the dark, and the thylakoid ascorbate overexpressor *35S:tAPX* (Laloi et al., 2007). Lastly, the *sal1* mutant in a protein dual-targeted to plastids and mitochondria that is involved in dephosphorylation of PAP was included. Accumulated PAP in *sal1* can relocate from plastids to cytosol and nucleus and triggers a retrograde signaling pathway from chloroplast to nucleus, possibly through PAP-induced inactivation of XRN-type exoribonucleases. Both *sal1* and *xrn2 xrn3* mutants were included (Estavillo et al., 2011).

Thirdly, a collection of publicly available microarray datasets encompassing various aspects of *Arabidopsis* development and environmental responsiveness were put together. For anatomy and development these included the AtGenExpress development dataset with over 60 tissue-types and developmental stages from embryogenesis to senescence (Schmid et al., 2005), as well as the radial root cell-type specific expression dataset (Brady et al., 2007), germination timecourse (Narsai et al., 2011), 24 h diurnal expression (Arrayexpress experiment E-GEOD-6174) and cell cycle synchronization with aphidicolin, sucrose deprivation and subculturing (Menges et al., 2003). For hormone response the AtGenExpress hormone datasets for auxin, cytokinin, gibberellin, brassinosteroid, abscisic acid, jasmonate, and ethylene (Goda et al., 2008) was used in addition to salicylic acid treatment (Clifton et al., 2005). For abiotic stress the AtGenExpress datasets for heat, salt, UV, genotoxic stress, oxidative stress, and osmotic stress (Kilian et al., 2007) were collected in addition to hydrogen peroxide (Clifton et al., 2005), high-light (Kleine et al., 2007), and ozone (Short et al., 2012). For biotic stresses the AtGenExpress datasets for infection with *Botrytis cinerea*, *Phytophtora infestans*, *Erysiphe orontii*, and elicitor Flg22 were selected (Goda et al., 2008), as well as infection with *E. cichoracearum* (Nishimura et al., 2003), *Blumeria graminis* (Jensen et al., 2008), and elicitor EF-Tu (Zipfel et al., 2006). For nutrient deprivation the following experiments were selected: iron deficiency (Schuler et al., 2011), potassium deprivation (E-GEOD-6825), nitrogen deprivation (Rubin et al., 2009), phosphate starvation (Li et al., 2010), sulfur deprivation (Iyer-Pascuzzi et al., 2011), exogenous sucrose addition (E-NASC-29), and high CO_2 (E-GEOD-5637).

PERTURBATION OF MITOCHONDRIAL AND CHLOROPLAST FUNCTION TRIGGERS OVERLAPPING BUT TARGETED EXPRESSION CHANGES

To assess the transcriptional changes that are caused by directly perturbing mitochondrial or chloroplast function, the selected microarray datasets were normalized and statistically analyzed. Genes that were significantly changed [PPDE ($<p$) > 0.95] and had a fold change of more than two up or down were selected for each of the microarray experiments described above (**Table 2**). For the mitochondrial perturbations 720 probe sets were significantly

[2]www.tm4.org/mev
[3]www.arabidopsis.org

Table 1 | List of microarray experiments related to mitochondrial and chloroplast perturbations used in this study.

	Experimental conditions	Source
MITOCHONDRIAL PERTURBATIONS		
Rotenone	40 μM, cell culture, 3 h	Clifton et al. (2005)
Oligomycin	12.5 μM, cell culture, 3 h	Clifton et al. (2005)
Antimycin A	50 μM, 3-week-old leaves in light, long day, 3 h	Ng et al. (2012) GEO GSE36011
atphb3	*In vitro* seedlings growth stage 1.04	Van Aken et al. (2007)
ndufs4	Leaves harvested in middle of photoperiod	Meyer et al. (2009)
ndufa1	Leaves harvested in middle of photoperiod	Meyer et al. (2009)
aox1a	4-week-old soil-grown plants	Giraud et al. (2008)
rpotmp	4-week-old soil-grown plants	Kuhn et al. (2009)
dsr1	10 h after treatment with water (mock)	Gleason et al. (2011)
msh1 recA3	Above-ground parts of 8 week old plants	Shedge et al. (2010)
rug3	*In vitro* seedlings 7 days old	Kuhn et al. (2011)
tim23-2	16-day-old leaf tissue	Wang et al. (2012)
TIM23-2 OX	16-day-old leaf tissue	Wang et al. (2012)
letm1(−/−) *LETM2*(+/−)	10-day-old leaf tissue	Zhang et al. (2012)
CHLOROPLAST PERTURBATIONS		
Norflurazon (Col-0, *gun1 gun5*)	3-day-old *in vitro* seedlings 5 μm	E-GEOD-5726
Lincomycin (Col-0, *abi4-102, gun1 gun5*)	5-day-old *in vitro* seedlings	Koussevitzky et al. (2007)
PNO8	1 μM 7-day-old *in vitro* seedlings	Goda et al. (2008)
fnr1	31-day-old plants middle of photoperiod	Lintala et al. (2009)
cs26	3-week-old leaves, long day	Bermudez et al. (2010)
tpt-1	Leaves growth stage 3.7; 2 h into photoperiod, 400 μE	E-GEOD-5737
flu	3-week-old rosette leaves 2 h reillumination	Laloi et al. (2007)
35S:tAPX	3-week-old rosette leaves 2 h reillumination	Laloi et al. (2007)
sal1	Whole rosette from seedlings stage 1.10	Estavillo et al. (2011)
xrn2 xrn3	Whole rosette from seedlings stage 1.10	Estavillo et al. (2011)

Table 2 | Perturbation of mitochondrial and chloroplast function triggers overlapping but targeted expression changes.

(A)						
	Mitoch. perturb.	**Chloroplast perturb.**	**Observed overlap**	**Expected**	***p*-Value**	**Obs/exp**
Chloroplast and mitochondrial overlap	720	606	129	19	<0.001	6.74
(B)						
	Compartment	**Genome-wide**	**Observed**	**Expected**	***p*-Value**	**Obs/exp**
Chloroplast perturbations (606)	Chloroplasts	2198	177	58	<0.001	3.03
	Mitochondria	1178	31	31	>0.05	0.99
	Peroxisome	287	7	8	>0.05	0.92
	Transcription factors	1661	41	44	>0.05	0.93
Mitochondrial perturbations (720)	Chloroplasts	2198	81	70	>0.05	1.16
	Mitochondria	1178	88	38	<0.001	2.34
	Peroxisome	287	4	9	>0.05	0.44
	Transcription factors	1661	71	53	<0.01	1.34

(A) Chi-Squared statistical analysis of the number of overlapping probe sets changing in at least four experiments perturbing mitochondrial or chloroplast function. Observed and expected overlaps, Chi-squared p-value and ratio of observed overlap versus expected overlap (obs/exp) are shown. Abbreviations: mitoch, mitochondrial; perturb, perturbation. (B) Chi-squared statistical analysis of the number of probe sets per subcellular compartment and transcription factors responding to chloroplast and mitochondrial perturbations. Shown are the number of probes in the entire genome (genome-wide) per compartment, total number of probes responding to at least four chloroplast or mitochondrial perturbations (606 and 720 probe sets, respectively), observed and expected number of responsive probes per compartment, Chi-squared p-value and ratio of observed overlap versus expected overlap (obs/exp).

changed in four or more of the 14 mitochondrial perturbation conditions. For the treatments or mutations that affected chloroplast function or retrograde signaling 606 probe sets were altered significantly in four or more of 13 chloroplast perturbation conditions. When comparing the two datasets it was found that 129 probe sets were in common between mitochondrial and chloroplast perturbations. This indicates an early sevenfold overabundance of common genes compared to the expected 19 in a random distribution ($p < 0.001$) and shows that perturbation of chloroplast or mitochondrial function results in surprisingly similar transcriptional responses (**Figure 1**).

The next step was to assess whether a bias could be observed with respect to which energy organelle was being target by the expression changes. Therefore, comprehensive lists were made of genes encoding mitochondrial (1178), chloroplast (2198), or peroxisomal proteins (287) based on experimental and prediction information (see Materials and Methods). Also a list of 1661 *Arabidopsis* transcription factors was prepared. **Table 2** shows the observed and expected number of probe sets representing energy organelle proteins that were present in the mitochondrial (720 probe sets) and chloroplast (606) perturbation data sets. Interestingly, a statistically significant overrepresentation of probe sets was shown that specifically represent proteins of the organelle where the initial perturbation originated, but not the other energy organelles. In other words, mitochondrial perturbation triggered significantly more expression changes in genes encoding mitochondrial proteins than randomly expected ($p < 0.001$), but not in genes encoding chloroplast or peroxisome proteins ($p > 0.05$). Conversely, chloroplast perturbation triggered significantly more expression changes in genes encoding chloroplast proteins than randomly expected ($p < 0.001$), but not in genes encoding mitochondrial or peroxisome proteins ($p > 0.05$). Furthermore, mitochondrial perturbations triggered statistically more changes in expression of transcription factors than randomly expected ($p < 0.01$), indicating an extensive network of transcriptional regulation underlies these expression changes. In conclusion, this analysis revealed that despite the large overlap between expression changes triggered by mitochondrial and chloroplast dysfunction, retrograde signals coming from chloroplasts or mitochondria are able to at least partially distinguish the signal source and can effectuate a targeted response.

Subsequently, the responses to chloroplast or mitochondrial perturbations were analyzed in more detail with regards to overrepresentation of functional classes. Therefore, the PageMan analysis tool was used to analyze the genes that were changed in expression due to chloroplast or mitochondrial perturbations. The expression values of all probe sets that were significantly changed in at least four of the mitochondrial or chloroplast perturbations were selected, resulting in 720 and 606 probe sets, respectively. Functional categories that were significantly overrepresented or underrepresented with p-value below 0.05 and greater than twofold change compared to the control group are shown in **Table 3**. For mitochondrial perturbations, several overrepresented categories are mitochondria and carbohydrate metabolism-related, such as alternative oxidases and NADH dehydrogenases, ATP synthase, cytochrome c oxidase, as well as fermentation and prokaryotic-like (mitochondrial) ribosomal proteins.

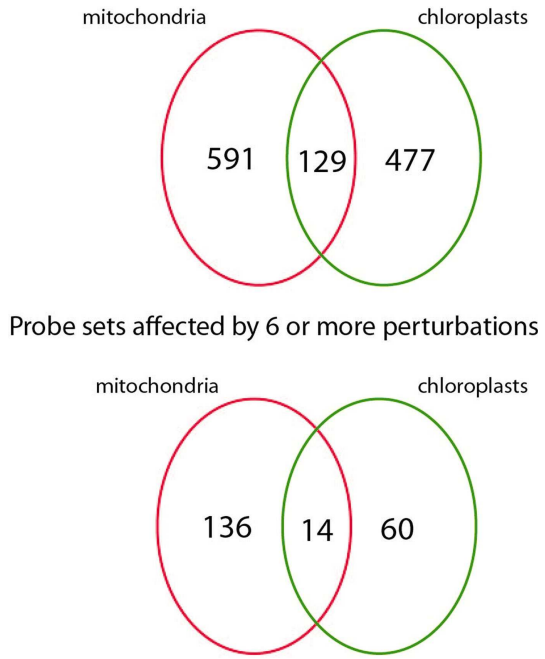

FIGURE 1 | Number ATH1 microarray probe sets responding to mitochondrial and chloroplast perturbations. Number of probe sets that were significantly altered in at least four (top) or six (bottom) microarray experiments relating to mitochondrial or chloroplast perturbations and their overlap.

Interestingly, in our study the photosynthesis functional category was underrepresented during mitochondrial perturbations, whereas another study found photosynthesis as being overrepresented (Schwarzlander et al., 2012). This difference may be caused by the use of different sets of microarray studies and a different analysis algorithm (Pageman versus Mapman). Abiotic and oxidative stress categories were also overrepresented, including heat stress, glutaredoxins, and glutathione *S*-transferases. Protein turnover was also present with AAA-type proteases, protein folding, and prokaryotic ribosomal proteins overrepresented, while ubiquitin-type degradation was underrepresented. Strikingly, auxin- and ethylene metabolism were statistically overrepresented, as well as several transcription factor classes including WRKY, pseudoresponse ARR, MYB, Constans, and pbf2.

For chloroplast perturbations, as expected photosynthesis-related categories were overrepresented including photosystems, Calvin cycle, photo-respiration, and tetrapyrrole (chlorophyll B and protochlorophyllide) synthesis. DNA synthesis category was downregulated, where it was upregulated in mitochondrial perturbations. Several similarities could also be observed between chloroplast and mitochondrial perturbations, mainly including redox (glutaredoxins, glutathione *S*-transferases), abiotic stress and protein turnover/degradation, but also metal handling, starch metabolism and cell wall structuring. The only overrepresented transcription factor family was the WRKY family, which interestingly was also overrepresented during mitochondrial

Table 3 | Significantly over- or underrepresented functional categories among probe sets commonly responding to mitochondrial (top) or chloroplast (bottom) dysfunction as determined by PageMan analysis.

BIN	Bin name	Counted	Genome	*p*-Value	Ratio
MITOCHONDRIAL PERTURBATIONS					
5.3	Fermentation.ADH	1	1	0.0320	31.25
25.1	C1-metabolism.formate dehydrogenase	1	1	0.0320	31.25
27.3.82	RNA.regulation of transcription.plant TF (pbf2)	1	1	0.0320	31.25
9.2.2	Mitochondrial electron transport/ATP synthesis.NADH-DH external	2	4	0.0059	15.62
9.4	Mitochondrial electron transport/ATP synthesis.alternative oxidase	2	5	0.0096	12.50
11.9.4.13	Lipidmetabolism.lipid degradation.beta-oxidation.acyl CoA reductase	2	6	0.0141	10.42
27.3.66	RNA.regulation of transcription.Pseudo ARR transcription factor family	2	8	0.0252	7.81
24.2	Biodegradation of Xenobiotics	2	10	0.0388	6.25
23.1.2	Nucleotide metabolism.synthesis.purine	3	15	0.0111	6.25
12	N-metabolism	4	24	0.0066	5.21
27.3.7	RNA.regulation of transcription, Constans-like zinc finger family	4	25	0.0077	5.00
21.4	Redox.glutaredoxins	5	33	0.0037	4.73
29.6	Protein.folding	9	62	0.0001	4.54
15.2	Metal handling.binding, chelation, and storage	6	44	0.0026	4.26
3.2	Minor CHO metabolism.trehalose	3	22	0.0320	4.26
9.9	Mitochondrial electron transport/ATP synthesis.F1-ATPase	3	22	0.0320	4.26
30.2.17	Signaling.receptor kinases.DUF 26	6	44	0.0026	4.26
26.9	Glutathione *S*-transferases	7	53	0.0014	4.13
28.1.3	DNA.synthesis/chromatin structure.histone	6	46	0.0033	4.08
9.7	Mitochondrial electron transport/ATP synthesis.cytochrome c oxidase	3	23	0.0359	4.08
23.1	Nucleotide metabolism.synthesis	4	32	0.0184	3.91
17.5.2	Hormone metabolism.ethylene	4	35	0.0248	3.57
9	Mitochondrial electron transport/ATP synthesis	14	124	0.0000	3.53
27.3.26	RNA.regulation of transcription.MYB-related transcription factor family	4	40	0.0383	3.12
29.5.9	Protein.degradation.AAA-type	4	41	0.0414	3.05
27.3.32	RNA.regulation of transcription.WRKY domain transcription factor family	6	62	0.0142	3.02
17.2	Hormone metabolism.auxin	14	152	0.0004	2.88
13.2	Amino acid metabolism.degradation (glutamate, GABA)	6	67	0.0202	2.80
2	Major CHO metabolism	8	99	0.0141	2.52
20.2.1	Stress.abiotic.heat	12	151	0.0034	2.48
29.2.1.1	Protein.synthesis.ribosomal protein.prokaryotic	10	127	0.0077	2.46
16.8	Secondary metabolism.flavonoids	6	82	0.0476	2.29
10	Cell wall	33	471	0.0000	2.19
34.16	Transport.ABC transporters and multidrug resistance systems	8	115	0.0315	2.17
29.5.11	Protein.degradation.ubiquitin	12	988	0.0001	0.38
1	PS photosystems	1	187	0.0336	0.17
CHLOROPLAST PERTUBATIONS					
19.16	Tetrapyrrole synthesis.chlorophyll b synthase	1	1	0.0266	37.54
16.8.2.1	Secondary metabolism.flavonoids.chalcones.naringenin-chalcone synthase	1	1	0.0266	37.54
13.2.2.2	Amino acid metabolism.degradation.glutamatefamily.proline	2	3	0.0021	25.02
19.14	Tetrapyrrole synthesis.protochlorophyllide reductase	2	3	0.0021	25.02
11.1.11	Lipid metabolism, FA synthesis, and FA elongation.fatty acid elongase	2	5	0.0067	15.01
1.1	PS.light reaction	49	136	0.0000	13.52
1	PS	59	187	0.0000	11.84
13.1.5.1	Amino acid metabolism.synthesis.serine-glycine-cysteine group.serine	2	7	0.0136	10.72
1.3	PS.calvincyle	7	31	0.0000	8.48
20.2.2	Stress.abiotic.cold	4	20	0.0017	7.51
21.4	Redox.glutaredoxins	6	33	0.0002	6.82
17.8	Hormone metabolism.salicylic acid	3	19	0.0133	5.93
33.1	Development.storage proteins	4	26	0.0047	5.77

(Continued)

Table 3 | Continued

BIN	Bin name	Counted	Genome	*p*-Value	Ratio
2.1.2	Major CHO metabolism.synthesis.starch	4	26	0.0047	5.77
14	S-assimilation	2	13	0.0455	5.77
1.2	PS.photo-respiration	3	20	0.0153	5.63
19	Tetrapyrrole synthesis	6	45	0.0012	5.00
21.2.1	Redox.ascorbate and glutathione.ascorbate	3	24	0.0251	4.69
33.2	Development.late embryogenesis abundant	3	26	0.0310	4.33
2.2.2	Major CHO metabolism.degradation.starch	3	26	0.0310	4.33
26.9	Misc.glutathione S-transferases	6	53	0.0028	4.25
29.2.1.1.1	Protein.synthesis.ribosomalprotein.prokaryotic.chloroplast	7	68	0.0022	3.86
17.5	Hormone metabolism.ethylene	9	93	0.0008	3.63
27.3.32	RNA.regulation of transcription.WRKY domain transcription factor family	6	62	0.0061	3.63
16.5.1	Secondary metabolism.sulfur-containing.glucosinolates	5	54	0.0143	3.48
17.3	Hormone metabolism.brassinosteroid	4	49	0.0412	3.06
29.6	Protein.folding	5	62	0.0246	3.03
17.1	Hormone metabolism.abscisic acid	4	50	0.0438	3.00
20.2.1	Stress.abiotic.heat	12	151	0.0007	2.98
15	Metal handling	5	64	0.0278	2.93
10.7	Cellwall.modification	5	66	0.0312	2.84
17.2	Hormone metabolism.auxin	11	152	0.0026	2.72
21	Redox	13	190	0.0018	2.57
26.1	Misc.cytochrome P450	13	199	0.0027	2.45
29.5.11	Protein.degradation.ubiquitin	13	988	0.0045	0.49
29.4	Protein.postranslational modification	6	668	0.0020	0.34
28.1	DNA.synthesis/chromatin structure	1	753	0.0000	0.05

Counted: number of members per functional category in specific probe list; Genome: number of members per functional category genome-wide; p-value: statistical significance; ratio: foldchange of number of members per functional category compared to the expected random distribution.

perturbation. Several hormone related categories were overrepresented including salicylic acid, auxins, ethylene, brassinosteroids, and abscisic acid.

COMPARISON OF MITOCHONDRIAL AND CHLOROPLAST PERTURBATIONS PROVIDES EVIDENCE FOR *sal*1 AND *xrn*2 *xrn*3-MEDIATED PAP PATHWAY IN MITOCHONDRIAL RETROGRADE REGULATION

Given the wide range of perturbations of mitochondrial and chloroplast function through mutation or chemical inhibition, it is of interest to examine which of these conditions show similarity with each other. Therefore, a hierarchical clustering method was applied on the expression values of a selection of the mitochondrial and chloroplast perturbation microarray experiments (**Figure 2**).

The expression values of all probe sets that were significantly changed in at least four of the mitochondrial or chloroplast perturbations were pooled, resulting in 1197 probe sets. The sample sets were hierarchically clustered using Pearson correlation with average linkage and visually represented as a phylogenetic tree (**Figure 2**). The clustering approach demonstrated the presence of three main groups of expression patterns. The co-clustering of specific perturbations appears to be mostly independent of tissue-types and ages used for the microarray experiments (**Table 1**). Looking at the samples present in each group revealed a number of expected patterns, but also some unexpected patterns were observed. Group I contains a number of mitochondrial mutants including *aox1a*, *tim23-2*, and Complex II subunit *sdh1*. These mitochondrial mutants clustered separately from the other mitochondrial mutants in Group II. Group II contained the remaining mutants in mitochondrial proteins with a variety of functions. Two subgroups were evident, one containing complex I subunit mutants *ndufa2* and *ndufs4*. The second subgroup contained splicing factor mutant *rug3*, *TIM23-2* overexpressor, and dual-targeted *RNA polymerase rpotmp*, all of which are known to be indirect Complex I mutants. The second subgroup also contained prohibitin mutant *atphb3*, mitochondrial genome recombination mutant *msh1 recA3*, mitochondrial mutant *letm1(−/−) Letm2(+/−)*, and chemical inhibitor of Complex III antimycin A. Surprisingly, this subgroup also contained the mutant in a recently described chloroplast retrograde pathway *sal1* revolving around PAP and the nuclear exoribonucleases *xrn2 xrn3* that are thought to be downstream effectors of this pathway (Estavillo et al., 2011). In fact, the expression changes triggered in the *xrn2 xrn3* mutants showed the highest similarity to antimycin A treatment, *atphb3* and *letm1(−/−) Letm2(+/−)* mutation, providing evidence for a role of PAP signaling in mitochondrial retrograde regulation. Msh1 was recently shown to be dual-targeted to mitochondria and chloroplasts, but based on the expression pattern the effects appear to be more similar to mitochondrial perturbations. This may be because RecA3 is thought to be specifically mitochondrial (Xu et al., 2012). Finally, Group III contained the mutations

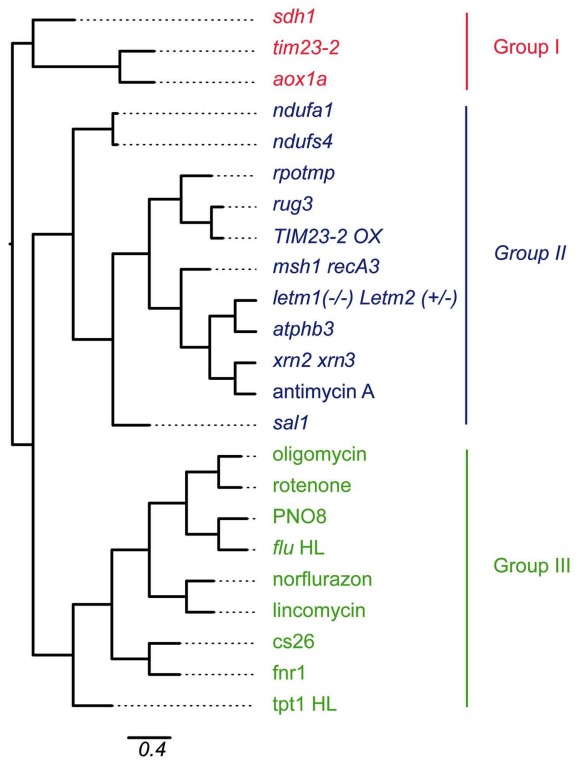

FIGURE 2 | Hierarchical clustering of microarray experiments relating to mitochondrial and chloroplast perturbations. Gene expression values of probe sets that were significantly altered in at least four of 13 experiments relating to mitochondrial or chloroplast perturbations were hierarchically clustered using Pearson correlation coefficient. Branch lengths indicate relative distance in expression patterns as indicated by the scale bar (percentage identity). Abbreviations: Cell cul, cell culture; Chloro Pert, chloroplast perturbation; Mito pert, mitochondrial perturbation.

or treatments that affect chloroplast function, such as inhibitors norflurazon and lincomycin which resulted in similar responses, as well as PSII inhibitor PNO8 and the *flu* mutant. The chloroplast mutants in S-sulfocysteine synthase *cs26*, ferredoxin NADH-oxidoreductase *fnr1* and triose-phosphate translocator *tpt-1* also clustered in Group III. Group III also contained the mitochondrial inhibitors oligomycin (ATP synthase) and rotenone (Complex I), suggesting that these inhibitors also inhibit chloroplast ATP synthase and a multi-subunit NADH dehydrogenase complex that has been characterized on the thylakoid membrane (Ifuku et al., 2011).

IDENTIFICATION OF MARKER GENES FOR ENERGY ORGANELLAR DYSFUNCTION

Next, genes that consistently respond to defects in mitochondrial and/or chloroplast functions were identified. Of 22810 ATH1 probe sets, 136 were significantly changed [twofold change with PPDE ($<p$) > 0.95] in at least six mitochondrial perturbations, while 60 probe sets were significantly changed in at least six chloroplast perturbations (Table S1 in Supplementary Material). Subsequently, 14 probe sets were identified that are changed in more than six mitochondrial and chloroplast perturbations and can thus be considered as general markers for mitochondrial and chloroplast dysfunction (**Table 4**). Conversely, a comparison was made to identify genes that strictly respond to either mitochondrial or chloroplast perturbation (significantly changed in seven or more mitochondrial and six or more chloroplast perturbations) but not the other (significantly changed in 0 or 1 perturbation). Twelve probe sets were identified that respond to mitochondrial but not chloroplast perturbation (**Table 4**), including *At5g09570* encoding a putative mitochondrial protein of unknown function that was significantly changed in 10 mitochondrial perturbations but in 0 chloroplast perturbations. Thus, *At5g09570* is an excellent marker gene to predict mitochondrial dysfunction. In contrast, 14 probe sets responded to chloroplast perturbations but not to mitochondrial stresses (**Table 4**), including a DNAJ heat shock protein that responded to seven chloroplast perturbations and only one mitochondrial perturbation (oligomycin), and a probe detecting Toll/Interleukin type receptors *At1g72910* and *At1g72930* responding to seven chloroplast but 0 mitochondrial perturbations.

The expression patterns of the genes most widely responsive to mitochondrial or chloroplast perturbations were also analyzed during a variety of environmental perturbations, including biotic and abiotic stresses, hormone treatments and nutrient deprivations, diurnal cycle, germination, cell cycle progression and plant developmental stages and tissue-types. Normalized expression values were hierarchically clustered to investigate expression patterns. Expression analysis of the genes responding to six or more mitochondrial perturbations revealed they were clearly divided into two main groups, with the largest group being induced not only by mitochondrial perturbations, but also by biotic and abiotic stresses, nutrient deficiencies, and in terms of hormone treatments mostly by salicylic acid (**Figure 3**).

This indicates that these genes are likely to be part of the general cellular stress signaling pathways. The 14 probe sets that respond to both mitochondrial and chloroplast perturbations are all part of the general stress-responsive cluster (**Figure 3**).

A second group of genes was far less responsive to external stress conditions and appeared to be most strongly altered by mitochondrial perturbations. Moreover, these genes showed a clear peak in expression shortly after the addition of sucrose or fresh nutrient media to stagnating suspension cells and under high CO_2 concentrations, linking these genes more directly with carbon availability and the basic energy-supply function of mitochondria. The genes in this second group showed clear induction in the later time points of stratification in the seed germination experiment and furthermore showed a dip in expression shortly after the start of daylight during the diurnal cycle. The expression patterns of the 12 genes that were responding to mitochondrial but not chloroplast stresses were varied and were spread over the generally stress-responsive and carbon availability responsive groups (**Figure 3**; **Figure A1** in Appendix). For instance the *At5g09570* gene showed very high foldchanges (e.g., 67 fold in the *atphb3* mutant) in response to mitochondrial perturbations, but was relatively stably expressed in all of the other tissues, developmental stages and showed only mild stress-inducible expression (sixfold during salt stress). Four of the other genes were strongly downregulated during the diurnal cycle with a low-point around the onset of day including circadian

Table 4 | Marker genes for mitochondrial and/or chloroplast perturbations.

Probe ID	Mitoch. perturb.	Chloropl. perturb.	AGI Code	Description	Loc.
260522_x_at	11	7	AT2G41730	Unknown protein	c
264042_at	10	7	AT2G03760	AtST1 sulfosteroid transferase	c
263402_at	10	6	AT2G04050	MATE efflux family protein	pm
263515_at	10	6	AT2G21640	UPOX	m
253046_at	9	6	AT4G37370	CYP81D8 cytochrome P450	er
247655_at	7	6	AT5G59820	ZAT12 transcription factor	n
263231_at	7	6	AT1G05680	UGT74E2 IBA UDP-glucosyl transferase	c
245038_at	6	7	AT2G26560	Phospholipase 2A PLP2	c
263403_at	6	7	AT2G04040	ATDTX1 MATE transporter	pm
246099_at	6	6	AT5G20230	AtBCB Blue-Copper binding protein	pm
247949_at	6	6	AT5G57220	CYP81F2 cytochrome P450	er
252131_at	6	6	AT3G50930	BCS1 AAA-type ATPase family protein	m
256376_s_at	6	6	AT1G66690;AT1G66700	SAM:carboxyl methyltransferase	c
259479_at	6	6	AT1G19020	Unknown protein	c
250515_at	10	0	AT5G09570	Unknown protein AtMSM1	p, m
253322_at	8	1	AT4G33980	Unknown protein	n
267036_at	8	1	AT2G38465	Unknown protein	pm
267364_at	8	0	AT2G40080	ELF4 (EARLY FLOWERING 4)	n
248709_at	7	0	AT5G48470	Unknown protein	n
252563_at	7	1	AT3G45970	Expansin ATEXLA1	ec
254208_at	7	0	AT4G24175	Unknown protein	p
256060_at	7	1	AT1G07050	CONSTANS-like protein	n
256252_at	7	0	AT3G11340	UGT76B1 glycosyltransferase	pm
263483_at	7	0	AT2G04030	Heat shock protein 90.5 kDa	p
267237_s_at	7	0	AT2G44040; AT3G59890	Dihydrodipicolinate reductase family	p, m
267474_at	7	0	AT2G02740	ATWHY3 transcription factor	p, m
256999_at	1	7	AT3G14200	DNAJ heat shock protein	n
262374_s_at	0	7	AT1G72910; AT1G72930	Disease resistance protein TIR-NBS	c
245876_at	1	6	AT1G26230	Chaperonin TCP-1	p
246313_at	1	6	AT1G31920	Pentatricopeptide (PPR) repeat- protein	c
246792_at	1	6	AT5G27290	Unknown protein	p
250054_at	1	6	AT5G17860	CAX7 calcium exchanger	pm
251218_at	1	6	AT3G62410	CP12-2	p
253104_at	1	6	AT4G36010	Pathogenesis-related thaumatin family	ec
253971_at	1	6	AT4G26530	Fructose-bisphosphate aldolase	p
256015_at	1	6	AT1G19150	LHCA6 PSI light-harvesting complex	p
260266_at	1	6	AT1G68520	Zinc finger (B-box type) family protein	n
261118_at	1	6	AT1G75460	ATP-dependent LON protease	p
264774_at	1	6	AT1G22890	Unknown protein	ec
266279_at	1	6	AT2G29290	Tropinone reductase	c

Top: list of probe sets that respond to at least six experiments affecting mitochondrial and chloroplast perturbations. Middle: list of probe sets that respond in at least six experiments affecting mitochondrial function but not chloroplast function. Bottom: list of probe sets that respond in at least six experiments that affect chloroplast function but not mitochondrial function. Abbreviations: Loc, subcellular location; p, plastid; m, mitochondrial; pm, plasma membrane; ec, extracellular; er, endoplasmic reticulum; n, nucleus; c, cytosol. Underlined locations indicated experimental evidence.

clock related *COL9* Constans-like protein and *Early Flowering 4*. A gene *At3g45970* encoding an expansin-like protein peaked at both day-night transition points, whereas the expression of five genes appeared to be linked with green tissues and are induced once light signals are received during germination (**Figure A1** in Appendix). In conclusion, it appears that the major trends for response to mitochondrial perturbation are induction of a general cell-wide stress response, and the induction of multiple genes that are induced by high carbon and carbohydrate supply.

Clustering of expression patterns for the genes responding to chloroplast perturbations revealed a similar division into two clusters (**Figure 4**). The largest cluster contained genes that were broadly induced by chloroplast perturbations, general stresses and nutrient deficiencies, and contain the genes that are in common

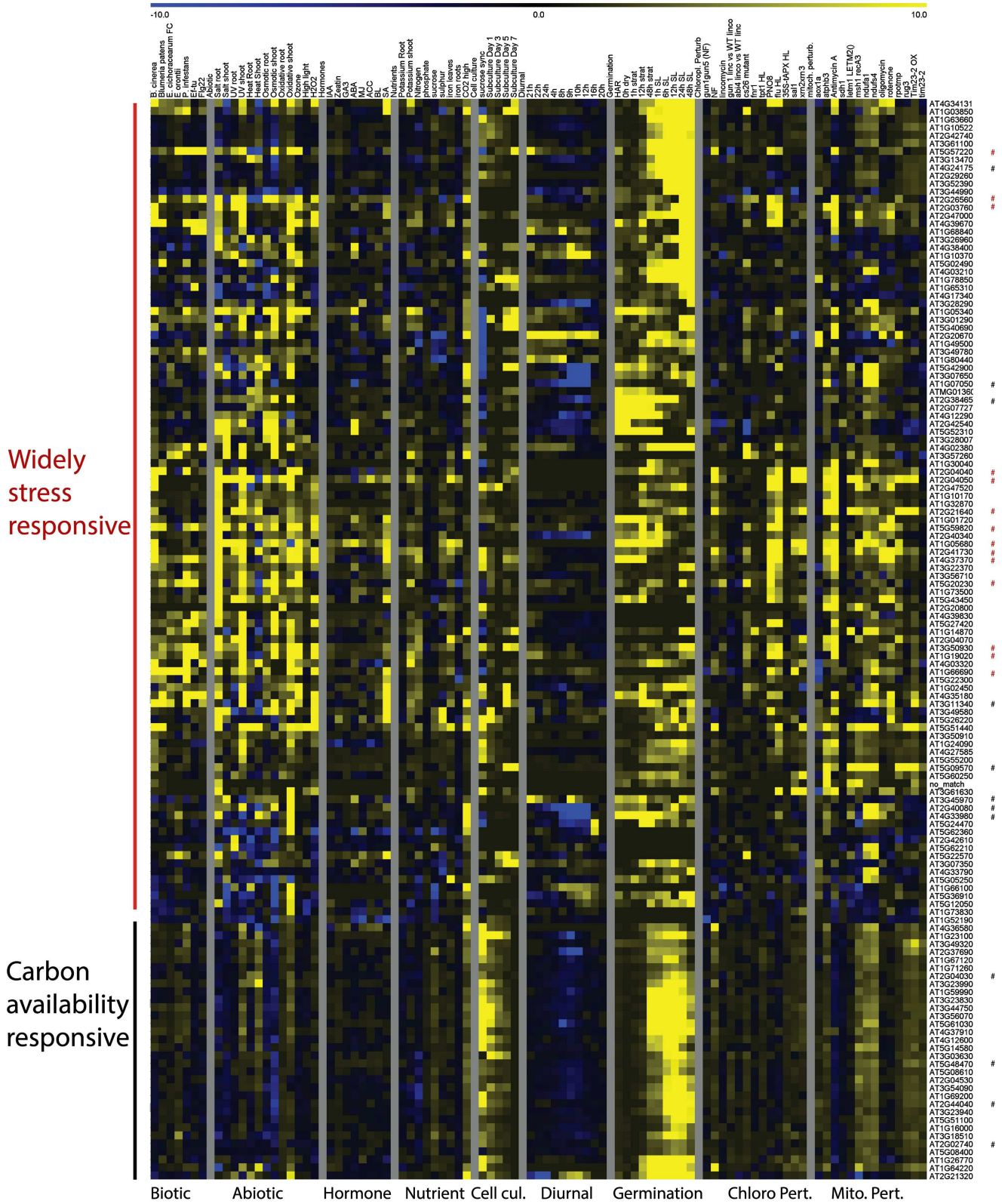

FIGURE 3 | Heat Map representing expression values of genes commonly responding to mitochondrial perturbations. Normalized expression values for genes responding to at least 6 of 13 experiments relating to mitochondrial perturbations in a variety of stress and development related microarray experiments. Red asterisks indicate probe sets that were also commonly altered by chloroplast perturbations, black asterisks indicate probe sets that were specifically responding to mitochondrial perturbations. Abbreviations: Cell cul, cell culture; Developm, development; Germin, germination; Chloro Pert, chloroplast perturbation; Mito pert, mitochondrial perturbation.

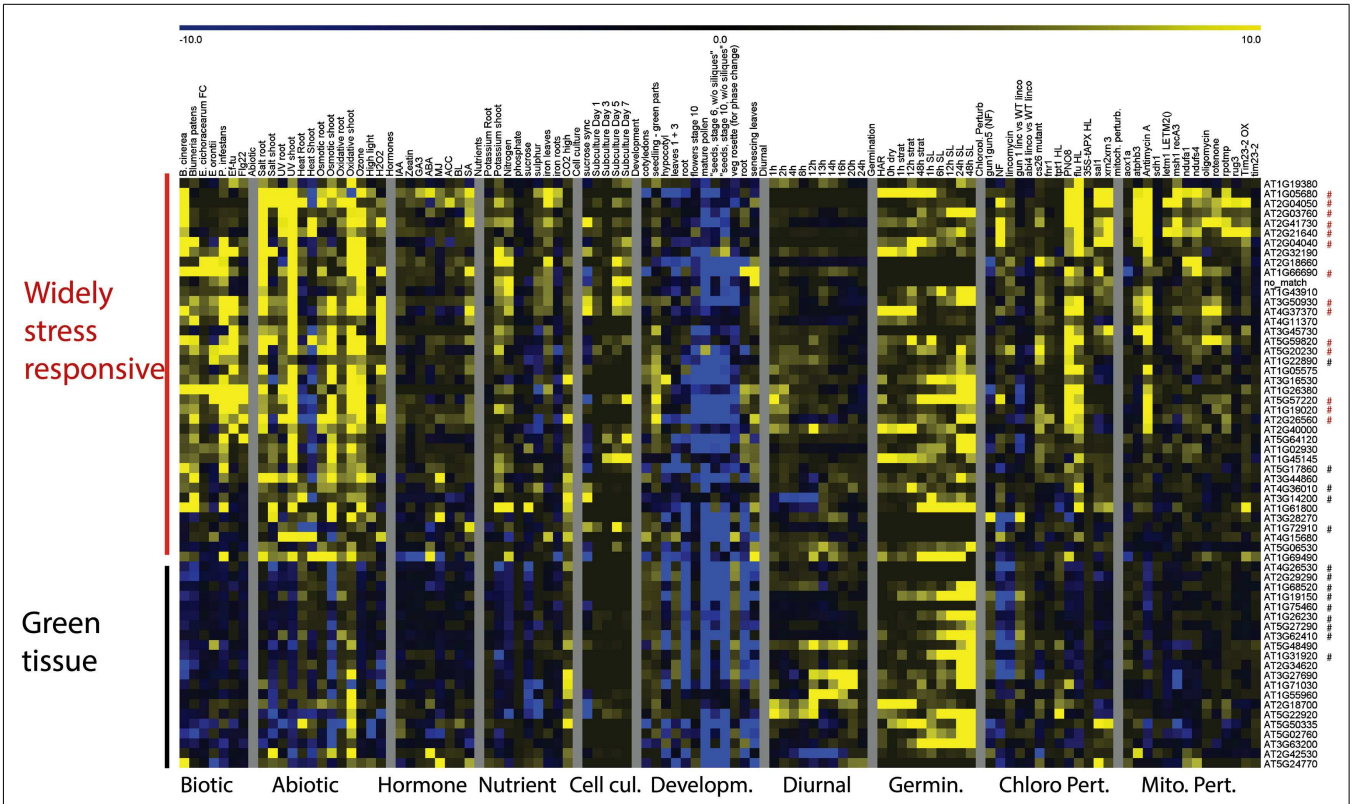

FIGURE 4 | Heat Map representing expression values of genes commonly responding to chloroplast perturbations. Normalized expression values for genes responding to at least 6 of 13 experiments relating to chloroplast perturbations in a variety of stress and development related microarray experiments. Red asterisks indicate probe sets that were also commonly altered by mitochondrial perturbations, black asterisks indicate probe sets that were specifically responding to chloroplast perturbations.

with mitochondrial perturbations. Conversely, the second group consist of genes of which the majority is downregulated by lincomycin and norflurazon, linking them with the classical GUN-mediated chloroplast retrograde pathways of chlorophyll synthesis inhibition (Koussevitzky et al., 2007). Interestingly, these genes tend to be downregulated by environmental stresses as well, as opposed to the first, stress-induced, cluster. When looking at their expression patterns during development and in different tissue-types, the genes of the second cluster are consistently expressed most highly in green tissues and less in roots, pollen, late flowers and seeds, and their expression usually increases during germination as soon as light signals are received. In contrast, the stress-induced cluster shows more random expression across tissues and development. Most of the genes that respond to chloroplast but not mitochondrial dysfunction belong to the second cluster containing genes that are downregulated during chlorophyll biosynthesis inhibition, general stresses and in non-green tissues. Therefore it seems that at least two types of chloroplast retrograde pathways are at play, one directly linked with the functioning of chloroplasts in photosynthetic conditions, and a second pathway which triggers a more general cellular stress response that is at least partly in common with mitochondrial perturbation signaling.

To obtain insight into the regulatory context of the identified marker genes, a promoter analysis was performed to identify the presence of known transcription factor binding motifs using the Athena promoter analysis tool (**Table 5**). Several statistically overrepresented motifs were found in the different marker categories. For marker genes responding to both mitochondrial and chloroplast perturbations overrepresentation was found for W-boxes (WRKY-binding site, p-value 0.0054; Yu et al., 2001), T-boxes (p-value 0.0137; Chan et al., 2001), and the CACGTG motif (G-box/ABA response element ABRE) which is known to bind both light responsive and ABA responsive transcription factors (p-value 0.0307; Guiltinan et al., 1990; Menkens and Cashmore, 1994). In the promoters of marker genes for mitochondrial perturbations putative MYB transcription factor binding sites (p-value 0.02530) and Evening Elements involved in circadian regulation (p-value 0.0357; Harmer et al., 2000) were overrepresented. Interestingly the three genes that contain the Evening Elements are strongly reduced in expression early in the day (**Figure 3**; **Figure A1** in Appendix). Thirdly, in the promoters of marker genes for chloroplast perturbations the I-box element involved in light signaling (p-value 0.0152; Giuliano et al., 1988), a GCCGCC motif responding to ethylene (p-value 0.0345; Solano et al., 1998) and also ABA response elements (p-value 0.0365) were overrepresented. Overall, it appears that WRKY transcription factors are involved in coordinating the common aspects of transcriptional responses to mitochondrial and chloroplast perturbations indicated by the

Table 5 | Occurrence of known transcription factor binding sites in marker genes.

MITOCHONDRIAL AND CHLOROPLAST PERTURBATIONS				
AGI Code	**Description**	**W-box**	**T-box**	**CACGTG**
AT2G41730	Unknown protein	3	1	
AT2G03760	AtST1 sulfosteroid transferase	2	1	
AT2G04050	MATE efflux family protein	1		1
AT2G21640	UPOX	2		1
AT4G37370	CYP81D8 cytochrome P450	3	2	1
AT5G59820	ZAT12 transcription factor	1	1	
AT1G05680	UGT74E2 IBA UDP-glucosyl transferase	1	1	1
AT2G26560	Phospholipase 2A PLP2	3	2	
AT2G04040	ATDTX1 MATE transporter	3	1	
AT5G20230	AtBCB Blue-Copper binding protein	1	1	
AT5G57220	CYP81F2 cytochrome P450	2	4	
AT3G50930	BCS1 AAA-type ATPase family protein	2	1	
AT1G66690	SAM:carboxylmethyl transferase		1	1
AT1G19020	Unknown protein	3		
MITOCHONDRIAL PERTURBATIONS				
AGI Code	**Description**	**Evening Element**	**MYB**	
AT5G09570	Unknown protein AtMSM1			
AT4G33980	Unknown protein	1		
AT2G38465	Unknown protein			
AT2G40080	ELF4 (EARLY FLOWERING 4)	1		
AT5G48470	Unknown protein			
AT3G45970	Expansin ATEXLA1		1	
AT4G24175	Unknown protein			
AT1G07050	CONSTANS-like protein	1	1	
AT3G11340	UGT76B1 glycosyltransferase			
AT2G04030	Heat shock protein 90.5 kDa		1	
AT2G44040	Dihydrodipicolinate reductase family		1	
AT2G02740	ATWHY3 transcription factor			
CHLOROPLAST PERTURBATIONS				
AGI Code	**Description**	**I-box**	**GCCGCC**	**ABRE**
AT3G14200	DNAJ heat shock protein		1	1
AT1G72910	Disease resistance protein TIR-NBS	1	1	
AT1G26230	Chaperonin TCP-1			
AT1G31920	Pentatricopeptide (PPR) repeat- protein	1		
AT5G27290	Unknown protein	1		
AT5G17860	CAX7 calcium exchanger			
AT3G62410	CP12-2	1		
AT4G36010	Pathogenesis-related thaumatin family		1	
AT4G26530	Fructose-bisphosphate aldolase	1		
AT1G19150	LHCA6 PSI light-harvesting complex			
AT1G68520	Zinc finger (B-box type) family protein	3		
AT1G75460	ATP-dependent LON protease	1		1
AT1G22890	Unknown protein	1		
AT2G29290	Tropinone reductase	1		

The 1 kb upstream promoter region of the marker genes for mitochondrial and/or chloroplast perturbations were searched for known transcription factor binding motifs. Statistically overrepresented motifs are shown for the different marker genes. The number of occurrences of each element per promoter are shown.

highly significant overrepresentation and wide occurrence of W-boxes. Also the overrepresentation and wide occurrence of the I-box involved in light signaling is likely to be important in the regulation of many of the chloroplast proteins.

Finally, the 1 kb upstream promoter regions of the top marker genes (**Table 4**) were analyzed for common sequence motifs using the MEME discovery suite (Bailey et al., 2009). A number of putative sequence motifs for each of the promoter sets were discovered and these are represented in **Figure 5**. Additional work will be required to validate their function in the regulation of retrograde responses, for instance using promoter reporter studies and identification of binding factors by yeast one-hybrid screens.

DISCUSSION

In this study we aimed to compare genome-wide transcriptional responses to perturbations of mitochondrial or chloroplast function. Retrograde signaling for both chloroplasts and mitochondria has classically been studied using chemical inhibitors such as norflurazone, lincomycin, rotenone, and antimycin A. To get a broader picture several mutants in specific mitochondrial or chloroplast proteins were also included in this study. One of the interesting outcomes of this study is the surprisingly high degree of similarity between mitochondrial and chloroplast retrograde responses to functional perturbations. In fact, over a quarter of the genes that regularly respond to chloroplast perturbations can also respond to mitochondrial perturbations. When looking at the functional categories that are common between the two, prominent categories are stress response, redox balance, transport, cell wall composition, starch metabolism but also auxin, brassinosteroid, and salicylic acid metabolism. In addition WRKY transcription factors appear to be on the interface between chloroplast and mitochondrial perturbations, making them interesting candidates for further characterization. In agreement, an overrepresentation of putative TTGAC WRKY-binding motifs was noted in the promoters of several highly stress-responsive genes encoding mitochondrial proteins (Van Aken et al., 2009). Differences between the two responses are related to the two basic functions of each organelle and their maintenance, namely photosynthesis and respiration. This is also reflected in the specific overrepresentation of genes encoding proteins that are targeted to the organelle that is primarily affected (**Table 2**), but not the other two energy organelles. In other words this analysis statistically demonstrates that organellar retrograde regulation 'works' in the sense that it is able to discriminate the source of the signal despite vastly overlapping signals.

The observation that the top overlapping genes are highly responsive to general abiotic and often biotic stresses raises the question whether this subset of stress-responsive genes is actually responding to organellar dysfunction. At least two scenarios can be envisaged, one in which general stresses and organellar dysfunction trigger the same signaling pathway resulting in the altered expression of these genes. In another scenario, the genes are directly responding to organelle function, and general stresses lead to impairment of these organelles, which thus results in changes in their expression. The fact that a set of 30 genes, almost all part of the top common responsive genes between chloroplast and mitochondrial perturbations, were previously reported to be uniquely altered in expression in an overexpression line of the mitochondrial protein AtPHB4, supports the second scenario (Van Aken et al., 2007, 2010). The observation that this gene set can be completely uncoupled from the general stress response suggests that a part of the response to mitochondrial, but also chloroplast dysfunction and general stress response is routed through the mitochondria. The exact signaling intermediates and transcription factors involved are thus far elusive. Another interesting finding from this study is that gene expression changes triggered by the recently uncovered chloroplast retrograde pathway involving PAP as a putative signaling molecule, PAP phosphatase SAL1 and the XRN-type exoribonucleases that are inhibited by PAP (Estavillo et al., 2011), shows highest similarity to mitochondrial perturbations. Similarity appears to be largest with the dataset for antimycin A and a number of mitochondrial mutants such as *atphb3*, *msh1 recA3*, and *letm1 LETM2(+/−)*. This leads to the hypothesis that the stress signal that is routed through the mitochondria might in fact be PAP, further corroborated by the fact that SAL1 is dual-targeted to chloroplasts and mitochondria.

Several marker genes have been identified in this study that may be useful for screening for organellar dysfunction (**Table 4**). In the marker genes that respond commonly to mitochondrial and chloroplast perturbations a number have been previously characterized to be involved in hormone metabolism: *UGT74E2* encodes an oxidative stress-responsive indole-butyric acid (IBA) glycosyltransferase involved in shoot branching and osmotic stress tolerance (Tognetti et al., 2010), and brassinosteroid sulfotransferase *AtST1* (Marsolais et al., 2007). Other genes also appear to be involved in enzymatic conversion or transport of chemicals: two cytochrome P450 oxygenating enzymes CYP81F2 and CYP81D8 belonging to the same family, methyltransferase PXMT1 that methylates 1,7-paraxanthine (or its homolog At1g66690) and 2 MATE-type efflux carrier proteins. Several proteins have also been reported to be involved in oxidative stress tolerance and cell death such as blue-copper binding protein AtBCB (Ezaki et al., 2005), UGT74E2 (Tognetti et al., 2010), and phospholipase PLP2 (La Camera et al., 2009). Also, the zinc finger transcription factor ZAT12 has been shown to be an important player in regulating the transcriptome in response to abiotic (e.g., cold), oxidative stresses (Rizhsky et al., 2004; Davletova et al., 2005; Vogel et al., 2005), and high-light (Iida et al., 2000), thus it will be of interest to investigate if ZAT12 is also involved in executing retrograde responses. Finally, a number of genes of unknown function that have previously been studied in other stress-related studies were retained including *UPOX*, *BCS1*, *At2g41730* (Gadjev et al., 2006; Ho et al., 2008; Van Aken et al., 2009), and *At1g19020*.

Looking at the 12 potential marker genes that respond uniquely to mitochondrial perturbations there is a striking number of genes encoding proteins of unknown function. The most interesting marker gene *At5g09570* responds to 10 of 14 mitochondrial experiments and no chloroplast experiments. It contains a CHCH (coiled coil – helix – coiled coil – helix) domain and shows homology with the COX19 protein from yeast that is important for post-translational processing of mitochondrial cytochrome c oxidase (Nobrega et al., 2002). *At5g09570* is also predicted to be mitochondrially targeted, so therefore we propose the name *AtMSM1* for *A. thaliana Mitochondrial Stress Marker 1*. *At4g24175* contains a domain found in bacterial protein of unknown function YjgA that co-migrates with the 50S ribosomal particle. Genes that have been

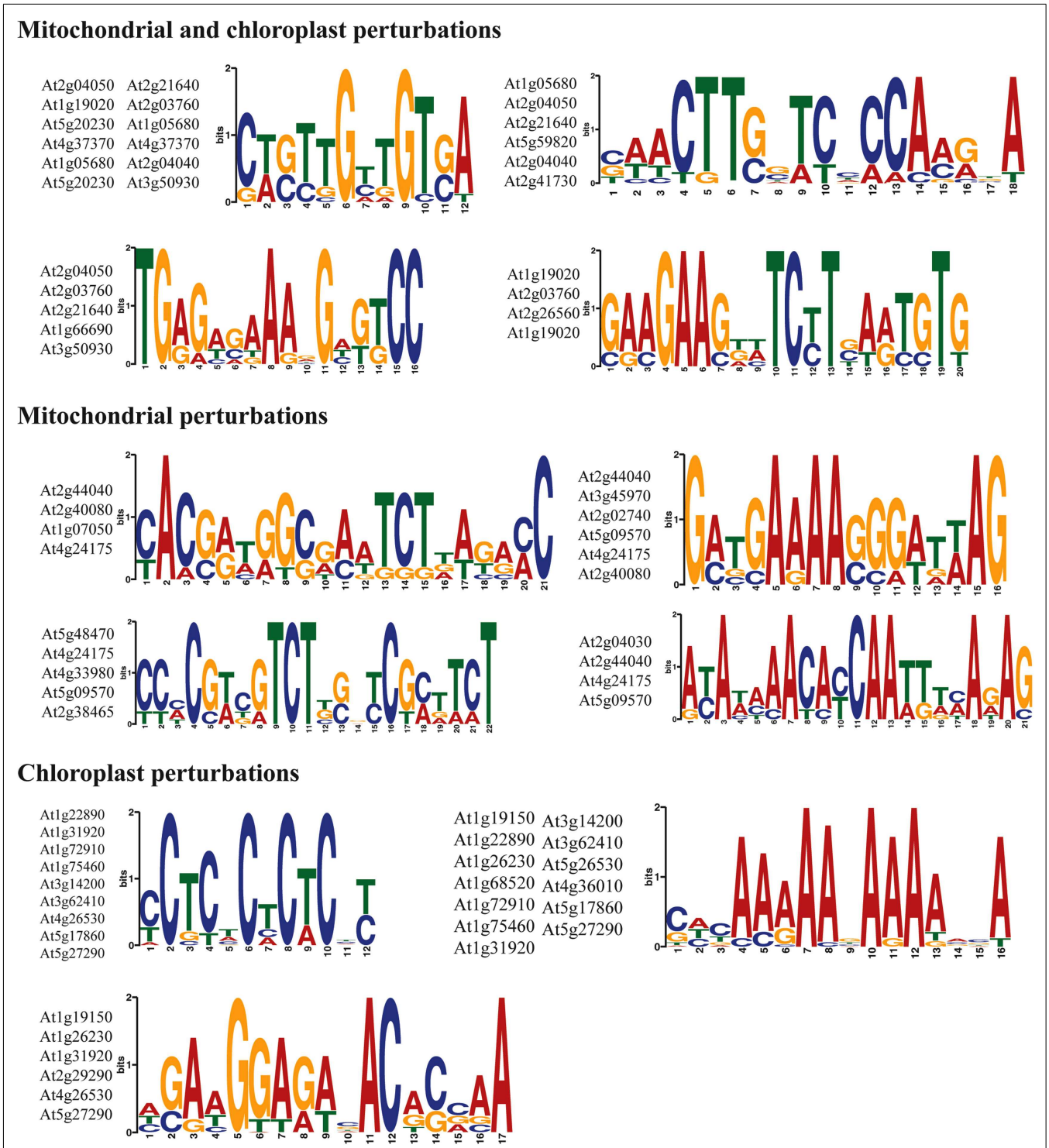

FIGURE 5 | Discovery of sequence motifs in the promoters of marker genes for retrograde regulation. The 1 kb upstream promoter regions were searched for common motifs using the MEME suite. Sequence consensus logos and the genes in which the promoter motifs occurred are shown.

characterized include *AtWHY3* encoding a DNA-binding protein that was shown to be involved in organellar genome stability (Marechal et al., 2009). Interestingly, AtWHY3 was shown to be located to plastids. AtWHY2 is active in the mitochondria and its transcript *At1g21760* also responds in six mitochondrial but none of the chloroplast perturbations, making it a good marker gene as well (**Figure 3**). The Whirly proteins bind ssDNA to promote accurate repair of DNA double-strand breaks (Cappadocia

et al., 2010). The isoleucine glycosyltransferase *UGT76B1* functions on the interface between SA and JA-mediated pathogen resistance (Von Saint Paul et al., 2011). Surprisingly, three genes encoding proteins closely related to circadian rhythm were responsive to mitochondrial perturbations, *Early Flowering 4* being a phytochrome-regulated negative regulator of the central clock oscillator (Kikis et al., 2005), a Constans-like gene *At1g07050* and *Expansin ATEXLA1*. It has previously been recognized that leaf expansion is affected by day and night transitions, possibly in relation to starch content. This may point toward a role of mitochondria and energy status in influencing the diurnal cycle (Pantin et al., 2011). Furthermore, a 90.5 kDa heat shock protein was identified that is targeted to plastids and has also been identified in mitochondria (Cao et al., 2003; Ito et al., 2006). In another study, TCP transcription factors were shown to link expression of genes encoding mitochondrial proteins with the diurnal cycle through the presence of site II promoter elements (Giraud et al., 2010). Together, these results suggest that mitochondrial function is regulated by the diurnal cycle and that in turn mitochondria may provide feedback, likely about energy status, to the central clock regulators.

Finally, a number of genes were identified that specifically respond to chloroplast perturbations but not mitochondrial perturbations (**Table 4**; **Figure 4**). The list contains several genes encoding plastid proteins: light-harvesting complex subunit *LHCA6*, chaperonin *TCP-1*, a LON protease, the CP12-2 stromal peptide found in protein complex with glyceraldehyde-3-phosphate dehydrogenase (GAPDH) and phosphoribulokinase (PRK) embedded in the Calvin cycle, an unknown protein *At5g27290* and fructose-bisphosphate aldolase *ATFBA5*. Hence, these genes might be useful markers for future chloroplast retrograde signaling studies. Several other genes encoding proteins with a variety of functions are present including a DNAJ chaperonin, a PPR protein *At1g31920*, calcium exchanger 7, NAD(P) tropinone oxidoreductase *At2g29290*, a pathogenesis-related thaumatin and a Toll/Interleukin-like receptor. Interestingly, an uncharacterized B-box Zinc Finger transcription factor is also specifically induced by chloroplast perturbations.

In conclusion, this meta-analysis of mitochondrial and chloroplast retrograde signaling has revealed novel insights into the strong similarities between the two pathways. To a large extent these overlapping signals are in common with more general abiotic and biotic stress-responses. Our results suggest that in the case of general stresses a subset of genes may indeed be responsive to functional perturbation of the energy organelles that are caused by the stress conditions. Nevertheless, specific responses can be found for each organelle and a number of novel marker genes have been identified for further functional characterization and use in screening methods. Furthermore, the results suggest that the recently identified chloroplast retrograde pathway involving PAP is likely to be closely linked to mitochondrial function as well and is a potential candidate for triggering the organelle-induced stress-responses in general. Future research will be required to fully understand the role of PAP and its associated proteins in retrograde signaling.

ACKNOWLEDGMENTS

The work was supported by an Australian Research Council Centre of Excellence grant to James Whelan (CEO561495). Olivier Van Aken was supported by Australian Research Council APD Discovery fellowship DP110102868. We thank Sophia Ng, Estelle Giraud and Aneta Ivanova for access to microarray data before publication.

SUPPLEMENTARY MATERIAL

The Supplementary Material for this article can be found online at http://www.frontiersin.org/Plant_Physiology/10.3389/fpls.2012.00281/abstract

REFERENCES

Bailey, T. L., Boden, M., Buske, F. A., Frith, M., Grant, C. E., Clementi, L., et al. (2009). MEME SUITE: tools for motif discovery and searching. *Nucleic Acids Res.* 37, W202–W208.

Baldi, P., and Long, A. D. (2001). A Bayesian framework for the analysis of microarray expression data: regularized t-test and statistical inferences of gene changes. *Bioinformatics* 17, 509–519.

Bermudez, M. A., Paez-Ochoa, M. A., Gotor, C., and Romero, L. C. (2010). Arabidopsis S-sulfocysteine synthase activity is essential for chloroplast function and long-day light-dependent redox control. *Plant Cell* 22, 403–416.

Bock, R., and Timmis, J. N. (2008). Reconstructing evolution: gene transfer from plastids to the nucleus. *BioEssays* 30, 556–566.

Brady, S. M., Orlando, D. A., Lee, J. Y., Wang, J. Y., Koch, J., Dinneny, J. R., et al. (2007). A high-resolution root spatiotemporal map reveals dominant expression patterns. *Science* 318, 801–806.

Cao, D., Froehlich, J. E., Zhang, H., and Cheng, C. L. (2003). The chlorate-resistant and photomorphogenesis-defective mutant cr88 encodes a chloroplast-targeted HSP90. *Plant J.* 33, 107–118.

Cappadocia, L., Marechal, A., Parent, J. S., Lepage, E., Sygusch, J., and Brisson, N. (2010). Crystal structures of DNA-Whirly complexes and their role in Arabidopsis organelle genome repair. *Plant Cell* 22, 1849–1867.

Chan, C. S., Guo, L., and Shih, M. C. (2001). Promoter analysis of the nuclear gene encoding the chloroplast glyceraldehyde-3-phosphate dehydrogenase B subunit of Arabidopsis thaliana. *Plant Mol. Biol.* 46, 131–141.

Chan, K. X., Crisp, P. A., Estavillo, G. M., and Pogson, B. J. (2010). Chloroplast-to-nucleus communication: current knowledge, experimental strategies and relationship to drought stress signaling. *Plant Signal. Behav.* 5, 1575–1582.

Chen, H., Zhang, B., Hicks, L. M., and Xiong, L. (2011). A nucleotide metabolite controls stress-responsive gene expression and plant development. *PLoS ONE* 6:e26661. doi:10.1371/journal.pone.0026661

Clifton, R., Lister, R., Parker, K. L., Sappl, P. G., Elhafez, D., Millar, A. H., et al. (2005). Stress-induced co-expression of alternative respiratory chain components in Arabidopsis thaliana. *Plant Mol. Biol.* 58, 193–212.

Davletova, S., Schlauch, K., Coutu, J., and Mittler, R. (2005). The zinc-finger protein Zat12 plays a central role in reactive oxygen and abiotic stress signaling in Arabidopsis. *Plant Physiol.* 139, 847–856.

Dojcinovic, D., Krosting, J., Harris, A. J., Wagner, D. J., and Rhoads, D. M. (2005). Identification of a region of the Arabidopsis AtAOX1a promoter necessary for mitochondrial retrograde regulation of expression. *Plant Mol. Biol.* 58, 159–175.

Estavillo, G. M., Crisp, P. A., Pornsiriwong, W., Wirtz, M., Collinge, D., Carrie, C., et al. (2011). Evidence for a SAL1-PAP chloroplast retrograde pathway that functions in drought and high light signaling in Arabidopsis. *Plant Cell* 23, 3992–4012.

Eubel, H., Meyer, E. H., Taylor, N. L., Bussell, J. D., O'toole, N., Heazlewood, J. L., et al. (2008). Novel proteins, putative membrane transporters, and an integrated metabolic network are revealed by quantitative proteomic analysis of Arabidopsis cell culture peroxisomes. *Plant Physiol.* 148, 1809–1829.

Ezaki, B., Sasaki, K., Matsumoto, H., and Nakashima, S. (2005). Functions of two genes in aluminium (Al) stress resistance: repression of oxidative damage by the AtBCB gene and promotion of efflux of Al ions by the NtGDI1 gene. *J. Exp. Bot.* 56, 2661–2671.

Gadjev, I., Vanderauwera, S., Gechev, T. S., Laloi, C., Minkov, I. N., Shulaev, V., et al. (2006). Transcriptomic footprints disclose specificity of reactive oxygen species signaling in Arabidopsis. *Plant Physiol.* 141, 436–445.

Giraud, E., Ho, L. H., Clifton, R., Carroll, A., Estavillo, G., Tan, Y. F., et al. (2008). The absence of ALTERNATIVE OXIDASE1a in Arabidopsis results in acute sensitivity to combined light and drought stress. *Plant Physiol.* 147, 595–610.

Giraud, E., Ng, S., Carrie, C., Duncan, O., Low, J., Lee, C. P., et al. (2010). TCP transcription factors link the regulation of genes encoding mitochondrial proteins with the circadian clock in Arabidopsis thaliana. *Plant Cell* 22, 3921–3934.

Giraud, E., Van Aken, O., Ho, L. H., and Whelan, J. (2009). The transcription factor ABI4 is a regulator of mitochondrial retrograde expression of ALTERNATIVE OXIDASE1a. *Plant Physiol.* 150, 1286–1296.

Giraud, E., Van Aken, O., Uggalla, V., and Whelan, J. (2012). REDOX regulation of mitochondrial function in plants. *Plant Cell Environ.* 35, 271–280.

Giuliano, G., Pichersky, E., Malik, V. S., Timko, M. P., Scolnik, P. A., and Cashmore, A. R. (1988). An evolutionarily conserved protein binding sequence upstream of a plant light-regulated gene. *Proc. Natl. Acad. Sci. U.S.A.* 85, 7089–7093.

Gleason, C., Huang, S., Thatcher, L. F., Foley, R. C., Anderson, C. R., Carroll, A. J., et al. (2011). Mitochondrial complex II has a key role in mitochondrial-derived reactive oxygen species influence on plant stress gene regulation and defense. *Proc. Natl. Acad. Sci. U.S.A.* 108, 10768–10773.

Goda, H., Sasaki, E., Akiyama, K., Maruyama-Nakashita, A., Nakabayashi, K., Li, W., et al. (2008). The AtGenExpress hormone and chemical treatment data set: experimental design, data evaluation, model data analysis and data access. *Plant J.* 55, 526–542.

Guiltinan, M. J., Marcotte, W. R. Jr., and Quatrano, R. S. (1990). A plant leucine zipper protein that recognizes an abscisic acid response element. *Science* 250, 267–271.

Harmer, S. L., Hogenesch, J. B., Straume, M., Chang, H. S., Han, B., Zhu, T., et al. (2000). Orchestrated transcription of key pathways in Arabidopsis by the circadian clock. *Science* 290, 2110–2113.

Heazlewood, J. L., Verboom, R. E., Tonti-Filippini, J., Small, I., and Millar, A. H. (2007). SUBA: the Arabidopsis subcellular database. *Nucleic Acids Res.* 35, D213–D218.

Ho, L. H., Giraud, E., Uggalla, V., Lister, R., Clifton, R., Glen, A., et al. (2008). Identification of regulatory pathways controlling gene expression of stress-responsive mitochondrial proteins in Arabidopsis. *Plant Physiol.* 147, 1858–1873.

Ifuku, K., Endo, T., Shikanai, T., and Aro, E. M. (2011). Structure of the chloroplast NADH dehydrogenase-like complex: nomenclature for nuclear-encoded subunits. *Plant Cell Physiol.* 52, 1560–1568.

Iida, A., Kazuoka, T., Torikai, S., Kikuchi, H., and Oeda, K. (2000). A zinc finger protein RHL41 mediates the light acclimatization response in Arabidopsis. *Plant J.* 24, 191–203.

Ito, J., Heazlewood, J. L., and Millar, A. H. (2006). Analysis of the soluble ATP-binding proteome of plant mitochondria identifies new proteins and nucleotide triphosphate interactions within the matrix. *J. Proteome Res.* 5, 3459–3469.

Iyer-Pascuzzi, A. S., Jackson, T., Cui, H., Petricka, J. J., Busch, W., Tsukagoshi, H., et al. (2011). Cell identity regulators link development and stress responses in the Arabidopsis root. *Dev. Cell* 21, 770–782.

Jensen, M. K., Hagedorn, P. H., De Torres-Zabala, M., Grant, M. R., Rung, J. H., Collinge, D. B., et al. (2008). Transcriptional regulation by an NAC (NAM-ATAF1,2-CUC2) transcription factor attenuates ABA signalling for efficient basal defence towards Blumeria graminis f. sp. hordei in Arabidopsis. *Plant J.* 56, 867–880.

Kikis, E. A., Khanna, R., and Quail, P. H. (2005). ELF4 is a phytochrome-regulated component of a negative-feedback loop involving the central oscillator components CCA1 and LHY. *Plant J.* 44, 300–313.

Kilian, J., Whitehead, D., Horak, J., Wanke, D., Weinl, S., Batistic, O., et al. (2007). The AtGenExpress global stress expression data set: protocols, evaluation and model data analysis of UV-B light, drought and cold stress responses. *Plant J.* 50, 347–363.

Kleine, T., Kindgren, P., Benedict, C., Hendrickson, L., and Strand, A. (2007). Genome-wide gene expression analysis reveals a critical role for CRYPTOCHROME1 in the response of Arabidopsis to high irradiance. *Plant Physiol.* 144, 1391–1406.

Koussevitzky, S., Nott, A., Mockler, T. C., Hong, F., Sachetto-Martins, G., Surpin, M., et al. (2007). Signals from chloroplasts converge to regulate nuclear gene expression. *Science* 316, 715–719.

Kuhn, K., Carrie, C., Giraud, E., Wang, Y., Meyer, E. H., Narsai, R., et al. (2011). The RCC1 family protein RUG3 is required for splicing of nad2 and complex I biogenesis in mitochondria of Arabidopsis thaliana. *Plant J.* 67, 1067–1080.

Kuhn, K., Richter, U., Meyer, E. H., Delannoy, E., De Longevialle, A. F., O'toole, N., et al. (2009). Phage-type RNA polymerase RPOTmp performs gene-specific transcription in mitochondria of Arabidopsis thaliana. *Plant Cell* 21, 2762–2779.

La Camera, S., Balague, C., Gobel, C., Geoffroy, P., Legrand, M., Feussner, I., et al. (2009). The Arabidopsis patatin-like protein 2 (PLP2) plays an essential role in cell death execution and differentially affects biosynthesis of oxylipins and resistance to pathogens. *Mol. Plant Microbe Interact.* 22, 469–481.

Laloi, C., Stachowiak, M., Pers-Kamczyc, E., Warzych, E., Murgia, I., and Apel, K. (2007). Cross-talk between singlet oxygen- and hydrogen peroxide-dependent signaling of stress responses in Arabidopsis thaliana. *Proc. Natl. Acad. Sci. U.S.A.* 104, 672–677.

Law, S. R., Narsai, R., Taylor, N. L., Delannoy, E., Carrie, C., Giraud, E., et al. (2012). Nucleotide and RNA metabolism prime translational initiation in the earliest events of mitochondrial biogenesis during Arabidopsis thaliana germination. *Plant Physiol.* 158, 1610–1627.

Lee, K. P., Kim, C., Landgraf, F., and Apel, K. (2007). EXECUTER1- and EXECUTER2-dependent transfer of stress-related signals from the plastid to the nucleus of Arabidopsis thaliana. *Proc. Natl. Acad. Sci. U.S.A.* 104, 10270–10275.

Leister, D., Wang, X., Haberer, G., Mayer, K. F., and Kleine, T. (2011). Intracompartmental and intercompartmental transcriptional networks coordinate the expression of genes for organellar functions. *Plant Physiol.* 157, 386–404.

Li, W. F., Perry, P. J., Prafulla, N. N., and Schmidt, W. (2010). Ubiquitin-specific protease 14 (UBP14) is involved in root responses to phosphate deficiency in Arabidopsis. *Mol Plant* 3, 212–223.

Lingner, T., Kataya, A. R., Antonicelli, G. E., Benichou, A., Nilssen, K., Chen, X. Y., et al. (2011). Identification of novel plant peroxisomal targeting signals by a combination of machine learning methods and in vivo subcellular targeting analyses. *Plant Cell* 23, 1556–1572.

Lintala, M., Allahverdiyeva, Y., Kangasjarvi, S., Lehtimaki, N., Keranen, M., Rintamaki, E., et al. (2009). Comparative analysis of leaf-type ferredoxin-NADP oxidoreductase isoforms in Arabidopsis thaliana. *Plant J.* 57, 1103–1115.

Marechal, A., Parent, J. S., Veronneau-Lafortune, F., Joyeux, A., Lang, B. F., and Brisson, N. (2009). Whirly proteins maintain plastid genome stability in Arabidopsis. *Proc. Natl. Acad. Sci. U.S.A.* 106, 14693–14698.

Marsolais, F., Boyd, J., Paredes, Y., Schinas, A. M., Garcia, M., Elzein, S., et al. (2007). Molecular and biochemical characterization of two brassinosteroid sulfotransferases from Arabidopsis, AtST4a (At2g14920) and AtST1 (At2g03760). *Planta* 225, 1233–1244.

McCormac, A. C., and Terry, M. J. (2004). The nuclear genes Lhcb and HEMA1 are differentially sensitive to plastid signals and suggest distinct roles for the GUN1 and GUN5 plastid-signalling pathways during de-etiolation. *Plant J.* 40, 672–685.

Menges, M., Hennig, L., Gruissem, W., and Murray, J. A. (2003). Genome-wide gene expression in an Arabidopsis cell suspension. *Plant Mol. Biol.* 53, 423–442.

Menkens, A. E., and Cashmore, A. R. (1994). Isolation and characterization of a fourth Arabidopsis thaliana G-box-binding factor, which has similarities to Fos oncoprotein. *Proc. Natl. Acad. Sci. U.S.A.* 91, 2522–2526.

Meskauskiene, R., Nater, M., Goslings, D., Kessler, F., Op Den Camp, R., and Apel, K. (2001). FLU: a negative regulator of chlorophyll biosynthesis in Arabidopsis thaliana. *Proc. Natl. Acad. Sci. U.S.A.* 98, 12826–12831.

Meyer, E. H., Tomaz, T., Carroll, A. J., Estavillo, G., Delannoy, E., Tanz, S. K., et al. (2009). Remodeled respiration in ndufs4 with low phosphorylation efficiency suppresses Arabidopsis germination and growth and alters control of metabolism at night. *Plant Physiol.* 151, 603–619.

Mitsuda, N., and Ohme-Takagi, M. (2009). Functional analysis of transcription factors in Arabidopsis. *Plant Cell Physiol.* 50, 1232–1248.

Mochizuki, N., Brusslan, J. A., Larkin, R., Nagatani, A., and Chory, J. (2001). Arabidopsis genomes uncoupled 5 (GUN5) mutant reveals the involvement of Mg-chelatase H

subunit in plastid-to-nucleus signal transduction. *Proc. Natl. Acad. Sci. U.S.A.* 98, 2053–2058.

Mochizuki, N., Tanaka, R., Tanaka, A., Masuda, T., and Nagatani, A. (2008). The steady-state level of Mg-protoporphyrin IX is not a determinant of plastid-to-nucleus signaling in Arabidopsis. *Proc. Natl. Acad. Sci. U.S.A.* 105, 15184–15189.

Moulin, M., Mccormac, A. C., Terry, M. J., and Smith, A. G. (2008). Tetrapyrrole profiling in Arabidopsis seedlings reveals that retrograde plastid nuclear signaling is not due to Mg-protoporphyrin IX accumulation. *Proc. Natl. Acad. Sci. U.S.A.* 105, 15178–15183.

Narsai, R., Law, S. R., Carrie, C., Xu, L., and Whelan, J. (2011). In-depth temporal transcriptome profiling reveals a crucial developmental switch with roles for RNA processing and organelle metabolism that are essential for germination in Arabidopsis. *Plant Physiol.* 157, 1342–1362.

Ng, S., Giraud, E., Duncan, O., Law, S. R., Wang, Y., Xu, L., et al. (2012). Cyclin-dependent kinase E;1 (CDKE;1) provides a cellular switch in plants between growth and stress responses. *J. Biol. Chem.* PMID:23229550 [Epub ahead of print].

Nishimura, M. T., Stein, M., Hou, B. H., Vogel, J. P., Edwards, H., and Somerville, S. C. (2003). Loss of a callose synthase results in salicylic acid-dependent disease resistance. *Science* 301, 969–972.

Nobrega, M. P., Bandeira, S. C., Beers, J., and Tzagoloff, A. (2002). Characterization of COX19, a widely distributed gene required for expression of mitochondrial cytochrome oxidase. *J. Biol. Chem.* 277, 40206–40211.

O'Connor, T. R., Dyreson, C., and Wyrick, J. J. (2005). Athena: a resource for rapid visualization and systematic analysis of Arabidopsis promoter sequences. *Bioinformatics* 21, 4411–4413.

Pantin, F., Simonneau, T., Rolland, G., Dauzat, M., and Muller, B. (2011). Control of leaf expansion: a developmental switch from metabolics to hydraulics. *Plant Physiol.* 156, 803–815.

Reumann, S., Babujee, L., Ma, C., Wienkoop, S., Siemsen, T., Antonicelli, G. E., et al. (2007). Proteome analysis of Arabidopsis leaf peroxisomes reveals novel targeting peptides, metabolic pathways, and defense mechanisms. *Plant Cell* 19, 3170–3193.

Reumann, S., Quan, S., Aung, K., Yang, P., Manandhar-Shrestha, K., Holbrook, D., et al. (2009). In-depth proteome analysis of Arabidopsis leaf peroxisomes combined with in vivo subcellular targeting verification indicates novel metabolic and regulatory functions of peroxisomes. *Plant Physiol.* 150, 125–143.

Rhoads, D. M., and Subbaiah, C. C. (2007). Mitochondrial retrograde regulation in plants. *Mitochondrion* 7, 177–194.

Rizhsky, L., Davletova, S., Liang, H., and Mittler, R. (2004). The zinc finger protein Zat12 is required for cytosolic ascorbate peroxidase 1 expression during oxidative stress in Arabidopsis. *J. Biol. Chem.* 279, 11736–11743.

Rubin, G., Tohge, T., Matsuda, F., Saito, K., and Scheible, W. R. (2009). Members of the LBD family of transcription factors repress anthocyanin synthesis and affect additional nitrogen responses in Arabidopsis. *Plant Cell* 21, 3567–3584.

Schmid, M., Davison, T. S., Henz, S. R., Pape, U. J., Demar, M., Vingron, M., et al. (2005). A gene expression map of Arabidopsis thaliana development. *Nat. Genet.* 37, 501–506.

Schuler, M., Keller, A., Backes, C., Philippar, K., Lenhof, H. P., and Bauer, P. (2011). Transcriptome analysis by GeneTrail revealed regulation of functional categories in response to alterations of iron homeostasis in Arabidopsis thaliana. *BMC Plant Biol.* 11:87. doi:10.1186/1471-2229-11-87

Schwarzlander, M., Konig, A. C., Sweetlove, L. J., and Finkemeier, I. (2012). The impact of impaired mitochondrial function on retrograde signalling: a meta-analysis of transcriptomic responses. *J. Exp. Bot.* 63, 1735–1750.

Shedge, V., Davila, J., Arrieta-Montiel, M. P., Mohammed, S., and Mackenzie, S. A. (2010). Extensive rearrangement of the Arabidopsis mitochondrial genome elicits cellular conditions for thermotolerance. *Plant Physiol.* 152, 1960–1970.

Short, E. F., North, K. A., Roberts, M. R., Hetherington, A. M., Shirras, A. D., and McAinsh, M. R. (2012). A stress-specific calcium signature regulating an ozone-responsive gene expression network in Arabidopsis. *Plant J.* 71, 948–961.

Solano, R., Stepanova, A., Chao, Q., and Ecker, J. R. (1998). Nuclear events in ethylene signaling: a transcriptional cascade mediated by ETHYLENE-INSENSITIVE3 and ETHYLENE-RESPONSE-FACTOR1. *Genes Dev.* 12, 3703–3714.

Sun, Q., Zybailov, B., Majeran, W., Friso, G., Olinares, P. D., and Van Wijk, K. J. (2009). PPDB, the plant proteomics database at Cornell. *Nucleic Acids Res.* 37, D969–D974.

Susek, R. E., Ausubel, F. M., and Chory, J. (1993). Signal transduction mutants of Arabidopsis uncouple nuclear CAB and RBCS gene expression from chloroplast development. *Cell* 74, 787–799.

Tognetti, V. B., Van Aken, O., Morreel, K., Vandenbroucke, K., Van De Cotte, B., De Clercq, I., et al. (2010). Perturbation of indole-3-butyric acid homeostasis by the UDP-glucosyltransferase UGT74E2 modulates Arabidopsis architecture and water stress tolerance. *Plant Cell* 22, 2660–2679.

Usadel, B., Nagel, A., Steinhauser, D., Gibon, Y., Blasing, O. E., Redestig, H., et al. (2006). PageMan: an interactive ontology tool to generate, display, and annotate overview graphs for profiling experiments. *BMC Bioinformatics* 7:535. doi:10.1186/1471-2105-7-535

Van Aken, O., Pecenkova, T., Van De Cotte, B., De Rycke, R., Eeckhout, D., Fromm, H., et al. (2007). Mitochondrial type-I prohibitins of Arabidopsis thaliana are required for supporting proficient meristem development. *Plant J.* 52, 850–864.

Van Aken, O., Whelan, J., and Van Breusegem, F. (2010). Prohibitins: mitochondrial partners in development and stress response. *Trends Plant Sci.* 15, 275–282.

Van Aken, O., Zhang, B., Carrie, C., Uggalla, V., Paynter, E., Giraud, E., et al. (2009). Defining the mitochondrial stress response in Arabidopsis thaliana. *Mol. Plant* 2, 1310–1324.

Vogel, J. T., Zarka, D. G., Van Buskirk, H. A., Fowler, S. G., and Thomashow, M. F. (2005). Roles of the CBF2 and ZAT12 transcription factors in configuring the low temperature transcriptome of Arabidopsis. *Plant J.* 41, 195–211.

Von Saint Paul, V., Zhang, W., Kanawati, B., Geist, B., Faus-Kessler, T., Schmitt-Kopplin, P., et al. (2011). The Arabidopsis glucosyltransferase UGT76B1 conjugates isoleucic acid and modulates plant defense and senescence. *Plant Cell* 23, 4124–4145.

Walters, R. G., Ibrahim, D. G., Horton, P., and Kruger, N. J. (2004). A mutant of Arabidopsis lacking the triose-phosphate/phosphate translocator reveals metabolic regulation of starch breakdown in the light. *Plant Physiol.* 135, 891–906.

Wang, Y., Carrie, C., Giraud, E., Elhafez, D., Narsai, R., Duncan, O., et al. (2012). Dual location of the mitochondrial preprotein transporters B14.7 and Tim23-2 in complex I and the TIM17:23 complex in Arabidopsis links mitochondrial activity and biogenesis. *Plant Cell* 24, 2675–2695.

Xu, Y. Z., Santamaria Rde, L., Virdi, K. S., Arrieta-Montiel, M. P., Razvi, F., Li, S., et al. (2012). The chloroplast triggers developmental reprogramming when mutS HOMOLOG1 is suppressed in plants. *Plant Physiol.* 159, 710–720.

Yu, D., Chen, C., and Chen, Z. (2001). Evidence for an important role of WRKY DNA binding proteins in the regulation of NPR1 gene expression. *Plant Cell* 13, 1527–1540.

Yu, Q. B., Li, G., Wang, G., Sun, J. C., Wang, P. C., Wang, C., et al. (2008). Construction of a chloroplast protein interaction network and functional mining of photosynthetic proteins in Arabidopsis thaliana. *Cell Res.* 18, 1007–1019.

Zhang, B., Carrie, C., Ivanova, A., Narsai, R., Murcha, M. W., Duncan, O., et al. (2012). LETM proteins play a role in the accumulation of mitochondrially encoded proteins in Arabidopsis thaliana and AtLETM2 displays parent of origin effects. *J. Biol. Chem.* PMID:23043101. [Epub ahead of print].

Zipfel, C., Kunze, G., Chinchilla, D., Caniard, A., Jones, J. D., Boller, T., et al. (2006). Perception of the bacterial PAMP EF-Tu by the receptor EFR restricts Agrobacterium-mediated transformation. *Cell* 125, 749–760.

Conflict of Interest Statement: The authors declare that the research was conducted in the absence of any commercial or financial relationships that could be construed as a potential conflict of interest.

Received: 20 November 2012; accepted: 26 November 2012; published online: 24 December 2012.

*Citation: Van Aken O and Whelan J (2012) Comparison of transcriptional changes to chloroplast and mitochondrial perturbations reveals common and specific responses in Arabidopsis. Front. Plant Sci. **3**:281. doi: 10.3389/fpls.2012.00281*

This article was submitted to Frontiers in Plant Physiology, a specialty of Frontiers in Plant Science.

Copyright © 2012 Van Aken and Whelan. This is an open-access article distributed under the terms of the Creative Commons Attribution License, which permits use, distribution and reproduction in other forums, provided the original authors and source are credited and subject to any copyright notices concerning any third-party graphics etc.

APPENDIX

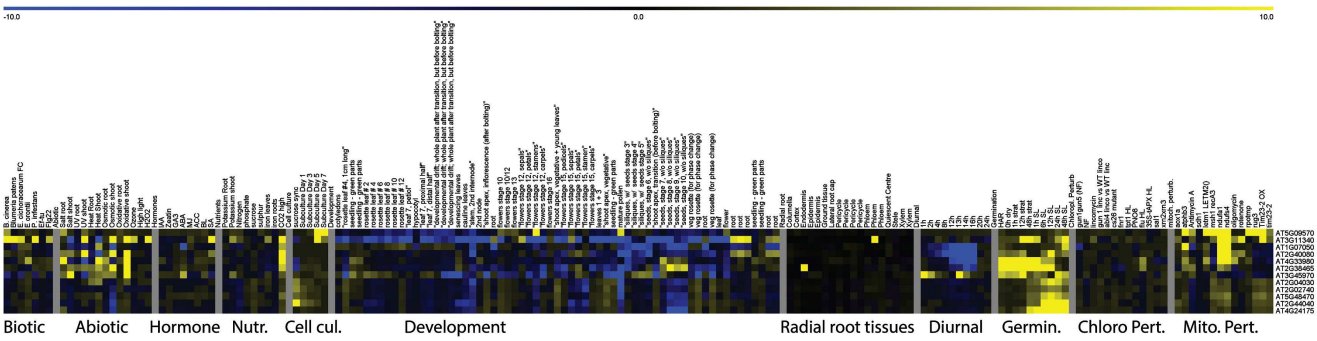

FIGURE A1 | Heat Map representing expression values of genes specifically responding to mitochondrial perturbations. Normalized expression values for genes responding to at least seven of 13 experiments relating to mitochondrial perturbations and 0 or 1 chloroplast perturbations in a variety of stress and development related microarray experiments.

frontiers in
PLANT SCIENCE

ORIGINAL RESEARCH ARTICLE
published: 24 December 2012
doi: 10.3389/fpls.2012.00283

Plastid located WHIRLY1 enhances the responsiveness of *Arabidopsis* seedlings toward abscisic acid

Rena Isemer[1], Kirsten Krause[2], Nils Grabe[1], Nobutaka Kitahata[3], Tadao Asami[3] and Karin Krupinska[1]*

[1] *Institute of Botany, Christian-Albrechts-University of Kiel, Kiel, Germany*
[2] *Department of Arctic and Marine Biology, University of Tromsø, Tromsø, Norway*
[3] *Department of Applied Biological Chemistry, The University of Tokyo, Tokyo, Japan*

Edited by:
Tatjana Kleine, Ludwig-Maximilians-Universität München, Germany

Reviewed by:
Mee-Len Chye, The University of Hong Kong, Hong Kong
Normand Brisson, Université de Montréal, Canada

***Correspondence:**
Karin Krupinska, Institute of Botany, Christian-Albrechts-University of Kiel, Olshausenstrasse 40, 24098 Kiel, Germany.
e-mail: kkrupinska@bot.uni-kiel.de

WHIRLY1 is a protein that can be translocated from the plastids to the nucleus, making it an ideal candidate for communicating information between these two compartments. Mutants of *Arabidopsis thaliana* lacking WHIRLY1 (*why1*) were shown to have a reduced sensitivity toward salicylic acid (SA) and abscisic acid (ABA) during germination. Germination assays in the presence of abamine, an inhibitor of ABA biosynthesis, revealed that the effect of SA on germination was in fact caused by a concomitant stimulation of ABA biosynthesis. In order to distinguish whether the plastid or the nuclear isoform of WHIRLY1 is adjusting the responsiveness toward ABA, sequences encoding either the complete WHIRLY1 protein or a truncated form lacking the plastid transit peptide were overexpressed in the *why1* mutant background. In plants overexpressing the full-length sequence, WHIRLY1 accumulated in both plastids and the nucleus, whereas in plants overexpressing the truncated sequence, WHIRLY1 accumulated exclusively in the nucleus. Seedlings containing recombinant WHIRLY1 in both compartments were hypersensitive toward ABA. In contrast, seedlings possessing only the nuclear form of WHIRLY1 were as insensitive toward ABA as the *why1* mutants. ABA was furthermore shown to lower the rate of germination of wildtype seeds even in the presence of abamine which is known to inhibit the formation of xanthoxin, the plastid located precursor of ABA. From this we conclude that plastid located WHIRLY1 enhances the responsiveness of seeds toward ABA even when ABA is supplied exogenously.

Keywords: abscisic acid, abamine, *Arabidopsis*, dual localization, *gun*, plastid signaling, salicylic acid, WHIRLY1

INTRODUCTION

WHIRLY1 is a DNA binding protein shown to be located both in chloroplasts and the nucleus and to have the same molecular weight in both compartments (Grabowski et al., 2008). After its synthesis on 80S ribosomes, WHIRLY1 is targeted to chloroplasts where it is processed by cleavage of an N-terminal plastid transit peptide (PTP). The functionality of the PTP has been shown before by subcellular detection of a WHIRLY1:GFP fusion protein and by import assays (Krause et al., 2005). Recently, it has been shown that recombinant hemagglutinin (HA)-tagged WHIRLY1 synthesized in plastids of transplastomic tobacco plants is translocated to the nucleus where it activates transcription of pathogen response (*PR*) genes (Isemer et al., 2012). This suggests that WHIRLY1 is sequestered in plastids before it gets translocated to the nucleus to adjust gene expression (Krause and Krupinska, 2009). Although the stimuli that lead to its translocation are still unknown, this feature makes WHIRLY1 an ideal candidate for transducing information from plastids to the nucleus.

The plastid and the nuclear isoforms of WHIRLY1 were shown to be responsible for diverse unique functions in the two compartments. Plastid located WHIRLY1 has been found in stroma fractions and additionally was shown to associate with plastid DNA (Pfalz et al., 2006; Majeran et al., 2012) and with plastid RNA (Prikryl et al., 2008; Melonek et al., 2010). WHIRLY1 from *Arabidopsis thaliana* has been implicated in plastid genome repair, assigning the protein an important role in maintaining plastid genome stability (Maréchal et al., 2009; Cappadocia et al., 2010). This plastid specific function of WHIRLY1 is also accomplished by WHIRLY3, the second member of the WHIRLY protein family that can be found in plastids (Maréchal et al., 2009; Cappadocia et al., 2010). Furthermore, WHIRLY1 was shown to promote the splicing of intron containing plastid encoded RNAs in maize and barley (Prikryl et al., 2008; Melonek et al., 2010). The nuclear form of WHIRLY1 has been implicated in PR reactions in potato as well as in *A. thaliana* (Desveaux et al., 2000, 2004, 2005). Transcriptional activation of *PR* genes by WHIRLY1 was reported to depend on salicylic acid (SA; Desveaux et al., 2000, 2004). SA is the only plant hormone which is completely and exclusively synthesized inside plastids (Wildermuth et al., 2001). Besides its well-known roles in pathogen defense signaling, it has many other functions in addition. For example, SA has been implicated in acclimation to high light and in regulation of the redox homeostasis (Mateo et al., 2006; Mühlenbock et al., 2008).

In recent years, plastids as sites of SA biosynthesis have also been implicated in perception of pathogens and in innate immunity (Padmanabhan and Dinesh-Kumar, 2010). For example, elicitors of the bacterial plant pathogen *Pseudomonas syringae* were predicted to localize to chloroplasts (Guttman et al., 2002). In tobacco

plants infected by tobacco mosaic virus (TMV) the chloroplast located protein N-receptor interacting protein 1 (NRIP1) was shown to mediate innate immunity. Even more interestingly, the chloroplast protein is recruited by a viral effector to the cytoplasm and nucleus (Caplan et al., 2008) indicating that redistribution of regulatory proteins from chloroplasts to the nucleus is involved in plant responses toward pathogens. Very recently, changes in the level of calcium within plastids and formation of singlet oxygen were shown to precede the stimulation of SA biosynthesis in response to pathogens (Nomura et al., 2012).

With regard to its formation inside plastids, SA could be the trigger inducing the translocation of WHIRLY1 from plastids to the nucleus. Such a mechanism would be in accordance with the model on WHIRLY1 activation during pathogen defense proposed by Brisson and co-workers (Desveaux et al., 2000, 2005). This model suggested that an inactive pool of WHIRLY1 is activated upon an increase in the level of SA and thus is able to bind to promoters of *PR* genes. It is feasible that the WHIRLY1 pool, which is inactive with regard to activation of the target genes, is identical with the subset of plastid located WHIRLY1.

Salicylic acid has also been found to be involved in regulation of plant development. In *Arabidopsis*, the level of SA is highly elevated during early seedling development (Preston et al., 2009) which might be related to the proposed role of SA in establishing defense mechanisms during germination (Rajjou et al., 2006). Application of SA was shown to inhibit germination and it has been proposed that this inhibitory effect is due to a concomitant increase in ABA (Rajjou et al., 2006) as measurements in wheat seedlings suggested (Shakirova et al., 2003). The stimulation of ABA synthesis might occur inside plastids, which harbor the key enzyme of ABA biosynthesis, 9-cis-epoxycarotenoid dioxygenase (NCED) that converts carotenoids into xanthoxin. Xanthoxin leaves the plastid and is converted to ABA in the cytosol (Cutler et al., 2010; Seo and Koshiba, 2011). Indeed, plants deficient in accumulation of SA were also shown to have lower levels of ABA making it difficult to analyze the effects of one or the other hormone originating from plastids separately (Abreu and Munné-Bosch, 2009). Accumulating evidence suggests that ABA is associated with plastid signaling. Indeed, ABA responsive *cis*-elements (ABREs) have been found in the promoters of many target genes of plastid signals (Rook et al., 2006; Koussevitzky et al., 2007). Moreover, the transcription factor ABI4, which was first described in connection with ABA insensitivity (Finkelstein, 1994), was shown to be common to different pathways of plastid signaling. Accordingly, the *abi4* mutant was found to be insensitive toward plastid signals produced during conditions of impaired chloroplast development (Koussevitzky et al., 2007).

In this study we analyzed the impact of WHIRLY1 on the responsiveness of seeds toward the plastid originating hormones SA and ABA during germination. *WHIRLY1* T-DNA insertion mutants (*why1*) of *Arabidopsis* were shown to be insensitive toward SA as well as ABA. When the biosynthesis of ABA was inhibited by abamine known to prevent formation of the ABA precursor xanthoxin, SA had no effect on germination. This showed that SA only indirectly affects seedling development by stimulation of ABA biosynthesis. Opposite to the mutants and to transgenic plants accumulating WHIRLY1 exclusively in the nucleus, transgenic plants accumulating WHIRLY1 in both plastids and the nucleus showed hypersensitivity toward ABA during germination. To conclude, our data indicate that WHIRLY1 enhances the responsiveness of seeds toward ABA only when it is located in the plastids. The plastid located precursor of ABA, xanthoxin, is not involved in this response, because germination was inhibited by external ABA also in the presence of the biosynthesis inhibitor abamine.

MATERIALS AND METHODS

PLANT MATERIAL AND GROWTH CONDITIONS

Plants of *A. thaliana*, ecotype Columbia, were grown under controlled conditions at 21°C with 13 h of illumination at a light intensity of 100 μmol photons s^{-1} m^{-2}. Under these conditions plants developed flowers within 8–9 weeks and mature seeds could be harvested after 12–14 weeks. T-DNA insertion lines Salk_023713 (*why1-1*) and Salk_147680 (*why1-2*) for *WHIRLY1* (At1g14410) were purchased from NASC and the positions of the T-DNA insertions were confirmed by PCR with the primers suggested by the T-DNA express tool of the SALK institute (http://signal.salk.edu/tdnaprimers.2.html). The absence of the initial ATG codon in the *WHIRLY1* mRNA of *why1-1* and *why1-2*, respectively, was shown by RT-PCR using the WHY1_fwd and WHY1_rvs primers. The *ACTIN2* gene was amplified to show equal amounts of templates. All primer sequences are listed in **Table A1** of the Appendix. The seeds of the *gun1-1* and *gun1-102* lines (Voigt et al., 2010) were a gift of Dario Leister. The seeds of the *gun5* line (Susek et al., 1993) were a gift of Bernhard Grimm.

GERMINATION ASSAYS

Arabidopsis seeds were surface sterilized as described before (Aronsson and Jarvis, 2011) and put on full-strength Murashige and Skoog (MS) medium (Duchefa, Haarlem, The Netherlands) containing 1.5% (w/v) sucrose and 1% (w/v) phyto agar (Duchefa, Haarlem, The Netherlands). After imbibition at 4°C in the dark over night, plates were exposed to controlled growth conditions at 21°C with 16 h of illumination at a light intensity of 60 μmol photons s^{-1} m^{-2} for germination assays in the presence of ABA. For germination assays in the presence of SA a neutral filter was used to eliminate UV radiation from the light spectra which reduced the light intensity to 30 μmol photons s^{-1} m^{-2}. Seeds of comparable age and storage conditions were used and the same amounts of medium were filled into the plates. To determine phenotypical differences during germination, sterile seeds were put on rectangular plates standing upright and photographed every day. The impact of phytohormones on germination was assayed as described (Choy et al., 2008). For preparation of stock solutions the sodium salt of SA (Sigma-Aldrich, Steinheim, Germany) was dissolved in sterile water to a final concentration of 1 M. ABA (6 cis-trans; Sigma A1049, Sigma-Aldrich, Steinheim, Germany) was first dissolved in 1 ml of 1 M NaOH and then diluted with sterile deionized water to a final stock concentration of 25 mM. Abamine (Han et al., 2004) was dissolved in dimethylsulfoxide to a final stock concentration of 130 mM. Twenty to 50 seeds each were plated on media containing the different compounds. Seven

days after imbibition the number of seeds, where emerging radicles could be observed with the naked eye, was determined.

CONSTRUCTION OF TRANSGENIC LINES OVEREXPRESSING *WHIRLY1*

The full-length coding sequence of *AtWHIRLY1* and the truncated *AtWHIRLY1* sequence lacking the first 141 bp encoding the plastid transit peptide (PTP) were amplified by PCR using the cDNA *U10139*, cloned into pENTR/TOPO gateway vector and sequenced to verify PCR product sequences. The HA tag was included in frame in the sequence of the reverse primer. After transfer of the two different *AtWHIRLY1* constructs into the binary destination vector pB2GW7.0 (Karimi et al., 2002), *why1-1* plants were transformed using *Agrobacterium tumefaciens* mediated flower transformation employing vacuum infiltration (Bechtold and Pelletier, 1998). Successfully transformed plants were selected by their resistance toward 0.1% (w/v) glufosinate ammonium (Basta, Bayer Crop Science, Germany) which was applied by spraying.

PREPARATION OF SUBCELLULAR FRACTIONS AND IMMUNOLOGICAL GEL BLOT ANALYSES

Chloroplasts were prepared from leaves of 7-week-old *Arabidopsis* plants and purified on percoll step gradients as described (Gruissem et al., 1986). Nuclear proteins were isolated from frozen leaves of 7-week-old *Arabidopsis* plants as described by Busk and Pagès (1997). Proteins were separated under denaturing conditions on 14% (w/v) acrylamide gels, transferred to nitrocellulose membranes and immunodecorated using standard protocols as described (Isemer et al., 2012). A monoclonal antibody directed toward the HA tag was purchased from Roche Diagnostics GmbH (Mannheim, Germany). Antibodies against the cytochrome b_{559} apoprotein A (Vallon et al., 1987) and RNA polymerase I (RNA POL-I; Agrisera, Vännäs, Sweden) respectively, were used to monitor the purity of the nuclear and chloroplast fractions.

RESULTS

CHARACTERIZATION OF TWO *WHIRLY1* MUTANTS OF *ARABIDOPSIS THALIANA*

Previously, functions of WHIRLY1 have been connected with the phytohormone SA (Desveaux et al., 2000, 2004, 2005; Xiong et al., 2009). Therefore, the initial aim of this study was to investigate whether WHIRLY1 (At1g14410) plays a role in SA induced inhibition of germination in *Arabidopsis*. For this purpose the two independent T-DNA insertion lines *why1-1* (Salk_023713) and *why1-2* (Salk_147680) were used. In the genomic DNA of mutant *why1-1* the T-DNA insertion was found to be located directly after the starting codon ATG, whereas in the *why1-2* line it was found to be located 25 base pairs further downstream (**Figure 1A**). Homozygosity of *why1-1* and *why1-2*, respectively, was shown by PCR (**Figure 1B**) with primers LP, RP, and LBa1 as suggested by the T-DNA express tool of the SALK institute (http://signal.salk.edu/tdnaprimers.2.html). In the mutants the LP-RP amplification product of the wildtype allele (approximately 1050 bp, see **Figure 1B**) was not visible. Only the smaller amplificate corresponding to the T-DNA insertion was visible, indicating that both mutant lines are indeed homozygous. The primers "fwd" and "rvs" spanning the AUG start codon, exon 1 and part of exon 2 (see **Figure 1A**) were used to probe for the presence of *WHIRLY1*

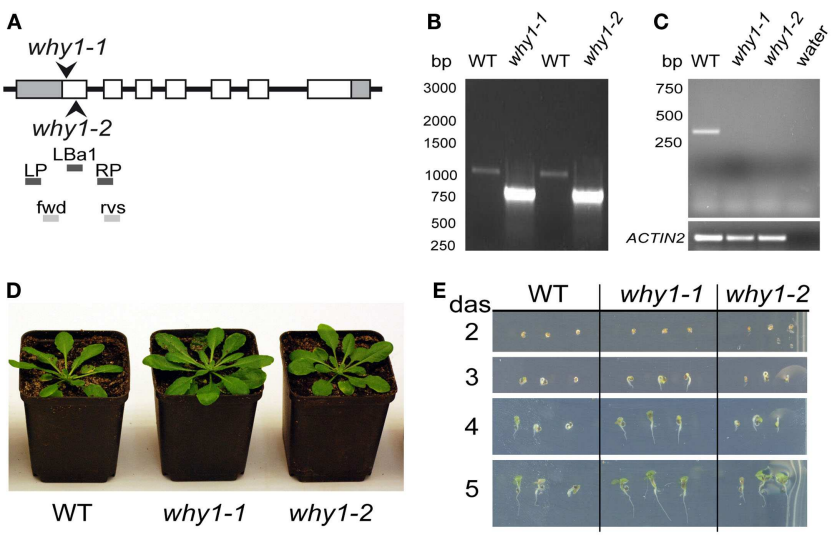

FIGURE 1 | Characterization of *why1* mutants. (A) Scheme showing the positions of T-DNA insertions in two independent mutant lines (*why1-1* and *why1-2*) for the *WHIRLY1* gene. The sites of the T-DNA insertions are indicated by arrowheads. Additionally, the positions of primers used for homozygous screening (LP, LBa1, RP) and verification of the presence of the initial start codon ATG in the *WHIRLY1* mRNA (fwd, rvs) are shown. **(B)** Genomic DNA derived from wildtype, *why1-1* and *why1-2* lines, respectively, was used to test for homozygosity of the mutants by use of the primers shown in **(A)**. **(C)** In order to detect the presence of *WHIRLY1* mRNA in the *why1-1* and *why1-2* lines, respectively, cDNA derived of the two mutant lines and wildtype (WT) and the primers shown in **(A)** were used in a RT-PCR. Primers specific for *ACTIN2* were used for loading controls. **(D)** Phenotype of the *why1-1* and *why1-2* mutants was compared to wildtype (WT) when grown under standard growth conditions. Six-week-old plants are shown. **(E)** Germination of *why1-1* and *why1-2* was compared to the wildtype (WT) under standard growth conditions. The phenotype of the seedlings was monitored 2–5 days after sowing (das).

mRNA. A 300-bp band corresponding to that region was detected only in wildtype plants whereas the control mRNA for ACTIN2 was detectable in wildtype as well as in mutants (**Figure 1C**). When cultivated under standard growth conditions the phenotypes of *why1-1* and *why1-2* mutants were indistinguishable from the wildtype (**Figures 1D,E**). This observation was true for mature plants (**Figure 1D**) as well as for young seedlings inspected at different times after germination on agar plates containing MS medium (**Figure 1E**). These findings are in accordance with previous results on the *why1-1* and *why1-2* mutant lines (formerly named KO-1 and KO-2; Yoo et al., 2007).

WHIRLY1 MUTANT SEEDS SHOW REDUCED RESPONSIVENESS TO SALICYLIC ACID AS WELL AS TO ABSCISIC ACID

Germination of *Arabidopsis* seeds is known to be inhibited by SA (Rajjou et al., 2006). In order to investigate whether this biological activity of SA is dependent on WHIRLY1, the two independent *WHIRLY1* T-DNA insertion mutants *why1-1* and *why1-2* were germinated on agar medium in the presence of different concentrations of SA ranging from 0.2 to 1 mM. For comparison, the same experiment was performed with wildtype seeds. The germination rate was scored 7 days after imbibition of seeds by assessing with the naked eye the number of seeds with emerged radicles. At concentrations ranging from 0.2 to 0.5 mM SA, germination of the *why1* mutant seeds was 10–15% more efficient than of wildtype seeds (**Figure 2A**). The most prominent alteration of germination was visible at a concentration of 1 mM, when the germination rate in the mutants was almost 40%, compared to an almost complete failure of the wildtype to germinate (**Figure 2A**).

External addition of SA to barley seeds was found to induce a transient increase in the level of abscisic acid (ABA; Shakirova et al., 2003), and the inhibitory effect of SA on germination of *Arabidopsis* seeds was assigned to the activity of ABA (Rajjou et al., 2006). Hence, it is possible that the tendentiously reduced sensitivity of the *why1* mutants toward SA might in fact be due to a reduced responsiveness toward ABA. Germination assays were therefore also performed in the presence of different concentrations of ABA ranging from 2 to 20 μM. Ten micromolars of ABA were sufficient to inhibit germination of almost 50% of the wildtype seeds. Twenty micromolars of ABA lowered the germination rate of the wildtype seeds to 40% whereas the germination rate in the mutant was on average twice as high (**Figure 2B**), illustrating that *why1* seeds are less sensitive to the inhibitory effect of ABA on germination.

THE INHIBITORY EFFECT OF SA ON GERMINATION IS ABOLISHED BY ABAMINE, AN INHIBITOR OF ABSCISIC ACID BIOSYNTHESIS

To investigate whether the inhibitory effect of SA on germination under the conditions employed here is indeed caused by a concomitant increase in the level of ABA, germination of wildtype seeds on SA containing agar plates during the first 7 days of development was assayed in the presence of abamine. Abamine is a specific inhibitor of the enzyme NCED preventing the formation of the ABA precursor xanthoxin (Han et al., 2004) which is the last intermediate of the ABA biosynthetic pathway being produced in the plastid (Seo and Koshiba, 2011). When wildtype seeds were treated with 0.5 mM SA, less than 20% of seeds were able to germinate in the first 2 days after imbibition (**Figure 3A**). The germination rate did not increase further after 4 days at which time it had reached 80% (**Figure 3A**). When wildtype seeds were exposed to SA in the presence of abamine, germination was observed to be as efficient as under control conditions without addition of SA (**Figure 3A**). When the same assays were done with seeds of the *why1-1* mutant line, no differences in germination efficiency were detectable between seeds treated either with only SA or with SA and abamine together, respectively, and the control setup (**Figure 3B**).

why1-, *gun1-*, AND *gun5* MUTANTS SHARE THE SAME INSENSITIVITY OF GERMINATION TOWARD SALICYLIC ACID AND ABSCISIC ACID

Germination assays revealed that *why1* mutants are insensitive toward SA and also to ABA. The responsiveness of *why1* observed in this study is in the same range as the responsiveness of the

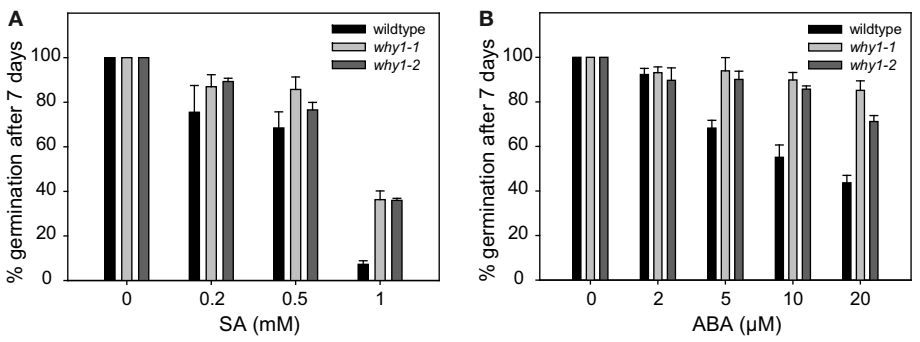

FIGURE 2 | Inhibition of germination by the phytohormones salicylic acid and abscisic acid. (A) In order to investigate the sensitivity of the two *why1* mutant lines (*why1-1* and *why1-2*) to the inhibitory effect of salicylic acid (SA) on germination, mutant, and wildtype seeds were grown on agar medium containing 0.2–1 mM SA. **(B)** The effect of abscisic acid (ABA) on germination of *why1* mutant seeds and wildtype seeds was scored by growth on agar medium containing 2–20 μM ABA. For germination assays in the presence of either SA or ABA, respectively, the percentage of seeds showing radicle emergence was scored after 7 days of growth at 21˚C in a 16-h light/dark regime. Values are the means ± SEM obtained from at least three independent experiments with 20–50 seeds each. The averaged percentage of germinated seeds in the control experiments without SA and ABA, respectively, was set to 100% and used as a reference to calculate the percentage of germination in the assays performed in the presence of SA or ABA.

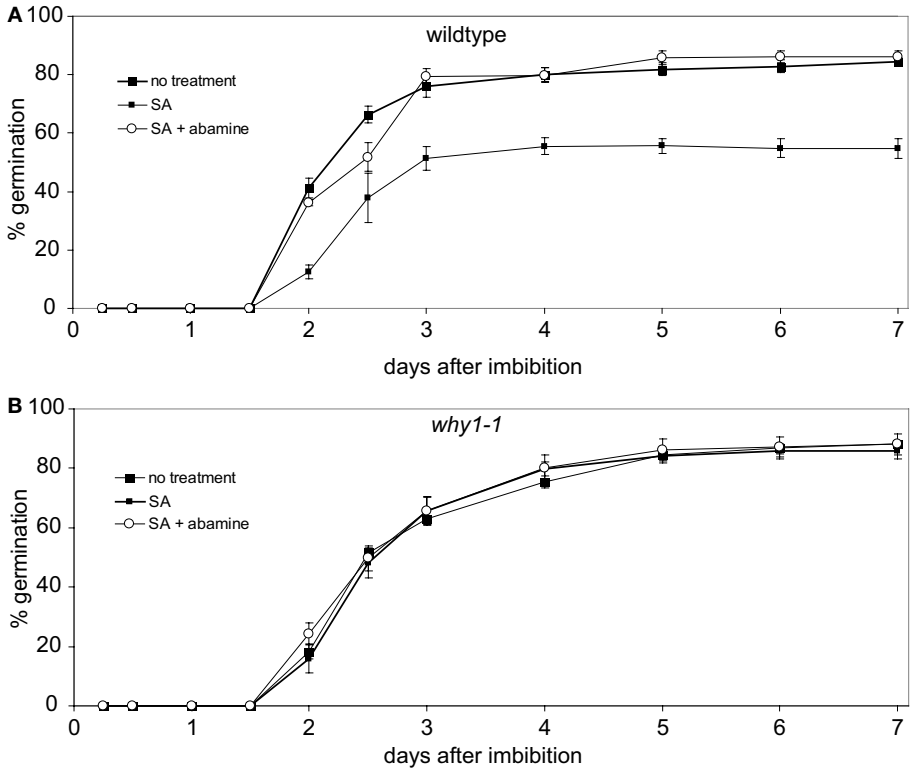

FIGURE 3 | Effects of abamine on salicylic acid mediated repression of germination. Wildtype seeds **(A)** and seeds of the *why1* mutant **(B)** were grown on agar medium containing 500 μM salicylic acid (SA) or 500 μM SA + 50 μM abamine, respectively. Germination rates of the two treatment conditions were compared to untreated seeds during the first 7 days after imbibition. Values are the means ± SEM obtained from five independent experiments with 20–50 seeds each.

abi1 mutant (Finkelstein and Somerville, 1990) indicating that WHIRLY1 might play a role in the ABA signaling pathway. Due to its dual localization in plastids and the nucleus, WHIRLY1 is an excellent candidate protein for transducing plastid signals to the nucleus. Interestingly, seeds of some *genomes uncoupled* (*gun*) mutants, that are characterized by impaired plastid-to-nucleus signaling, were likewise shown to be insensitive toward ABA (Choy et al., 2008; Cottage et al., 2010; Voigt et al., 2010; Kerchev et al., 2011). To investigate whether *why1* mutants are comparable to *gun* mutants with regard to ABA sensitivity of seeds, seeds of two *gun1* mutants (*gun1-1* and *gun1-102*), and one *gun5* mutant were subjected to the germination assay in the presence of different concentrations of ABA. At a concentration of 20 μM of ABA at which less than 20% of wildtype seeds were observed to germinate (**Figure 4A**), 60% of *gun1-102* seeds, and about 80% of *gun1-1* as well as *gun5* seeds showed germination (**Figure 4A**). This shows that the insensitivity of *gun1* and *gun5* mutants toward ABA is comparable to that of the *why1* mutants.

By application of the ABA inhibitor abamine it became obvious that the inhibitory effect of SA on germination is actually due to a concomitant increase in ABA content (**Figure 3**). Hence, mutants that are insensitive toward ABA during germination should also be insensitive toward SA. In order to investigate whether this is also true for the *gun* mutants, seeds of *gun1-1*, *gun1-102*, and *gun5* as well as wildtype seeds were placed on agar medium in the presence of different concentrations of SA ranging from 0.2 to 1 mM. While less than 70% of the wildtype seeds did germinate at a concentration of 0.5 mM SA, germination of the *gun* mutant seeds was only reduced by 20% by these concentrations (**Figure 4B**). The insensitivity of the *gun* mutants toward SA is in the same range as the insensitivity of the *why1* mutants (**Figure 2A**).

THE PLASTID ISOFORM OF WHIRLY1 ENHANCES THE RESPONSIVENESS OF SEEDLINGS TOWARD ABSCISIC ACID

Germination assays indicated that WHIRLY1 is enhancing the responsiveness of seeds toward ABA. To investigate whether either WHIRLY1 in plastids or WHIRLY1 in the nucleus or both isoforms are involved in the ABA response, the *WHIRLY1* gene was overexpressed under control of the *35S* promoter in the *why1-1* mutant background. Plants of a line accumulating an HA-tagged full-length protein (pnWHIRLY1:HA) were compared with a line accumulating a truncated protein lacking the PTP (nWHIRLY1:HA; **Figure 5A**). Both of the overexpression lines did not show any phenotypical difference when compared to wildtype (**Figures 5B** and **6A**).

The subcellular localization of the two recombinant proteins that is shown schematically in **Figure 5A** was confirmed by

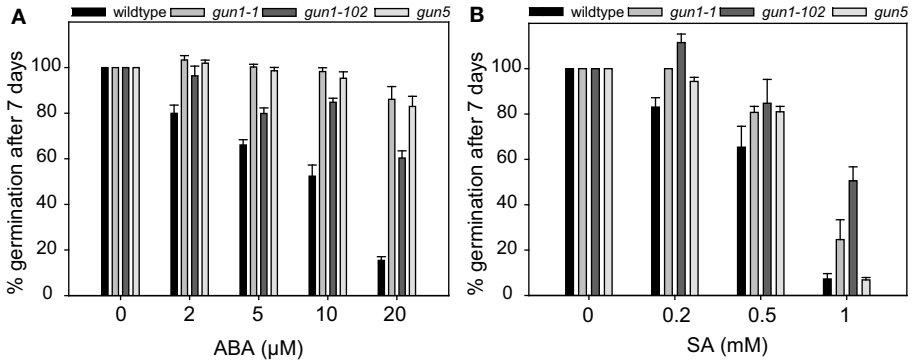

FIGURE 4 | Inhibition of germination by abscisic acid and salicylic acid in *gun* mutants. In order to investigate the germination of *gun* mutants in the presence of abscisic acid (ABA) **(A)** and salicylic acid (SA) **(B)**, respectively, seeds of the well described *gun* mutants *gun1-1*, *gun1-102*, and *gun5* were grown on agar medium containing 2–20 μM ABA or 0.2–1 mM SA. The percentage of seeds showing radicle emergence was scored after 7 days of growth at 21°C in a 16-h light/dark regime. Values are the means ± SEM obtained from at least three independent experiments with 20–50 seeds each. The average percentage of germination of seeds in the control experiments without ABA or SA, respectively, was set to 100% and used as a reference to calculate the percentage of germination in the germination assays done in the presence of ABA or SA.

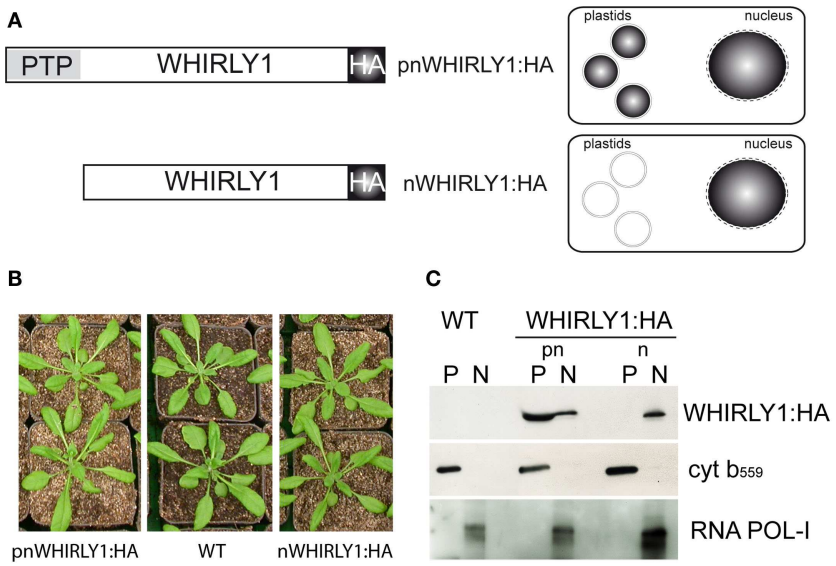

FIGURE 5 | Characterization of transgenic lines possessing HA-tagged versions of either the complete *WHIRLY1* gene (pnWHIRLY1:HA) or a truncated form lacking the plastid transit peptide (PTP) sequence (nWHIRLY1:HA). (A) Schematic drawings of constructs used for transformation and the expected subcellular distribution of the HA-tagged WHIRLY1. HA, hemagglutinin tag. **(B)** Phenotypes of the pnWHIRLY1:HA and nWHIRLY1:HA overexpression lines was compared to wildtype (WT) at 5 weeks after sowing. **(C)** Immunoblot analysis of protein extracts derived from chloroplasts (P) and nuclei (N) of the wildtype (WT) and transgenic lines overexpressing constructs for two HA-tagged versions of WHIRLY1 (pnWHIRLY1:HA and nWHIRLY1:HA). An antibody specific for the HA-tag was used to detect recombinant WHIRLY1 (WHIRLY1:HA). No HA-tag signal could be detected in wildtype (WT). Purity of the fractions was shown by immunodetection of cytochrome b_{559} (cyt b_{559}) as marker for chloroplasts and RNA polymerase I (RNA POL-I) as marker for the nucleus.

immunoblot analyses with protein extracts prepared from isolated chloroplasts and nuclei, respectively. In plants overexpressing the complete *WHIRLY1*-HA construct, the HA-tag was detectable in both compartments. In comparison, the protein arising from a construct devoid of the PTP accumulated exclusively in the nucleus (**Figure 5C**). Antibodies directed against cytochrome b_{559} as a marker for chloroplasts and against RNA POL-I as a marker for nuclear proteins, respectively, were used to monitor the purity of both fractions.

To investigate the responsiveness of the transgenic lines possessing WHIRLY1:HA toward ABA, germination assays were performed under the same conditions as used above for *why1* mutants. In the absence of ABA no differences in germination

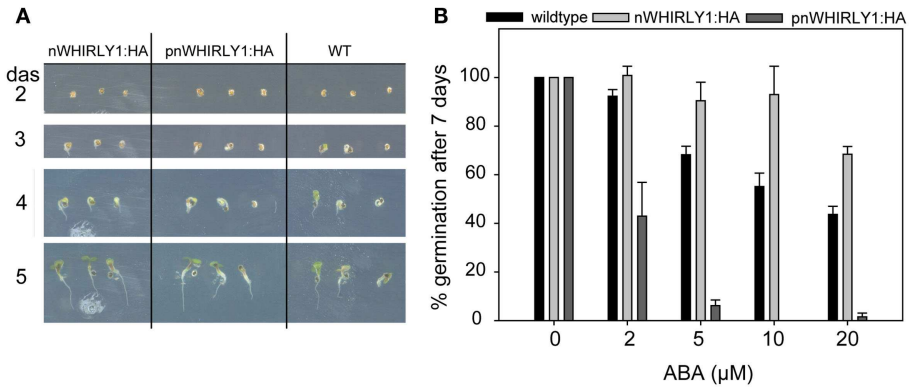

FIGURE 6 | Inhibition of germination by abscisic acid in transgenic lines overexpressing WHIRLY1. (A) Germination of pnWHIRLY1:HA and nWHIRLY1:HA overexpression lines was compared to the wildtype (WT) under standard growth conditions. The phenotype of the seedlings was monitored 2–5 days after sowing (das). **(B)** Transgenic lines overexpressing the sequences encoding the HA-tagged versions of WHIRLY1 were included in the abscisic acid (ABA) germination assay in order to show dose response of ABA inhibition of germination. The percentage of seeds showing radicle emergence was scored after 7 days of growth at 21˚C in a 16-h light/dark regime. Values are the means ± SEM obtained from at least three independent experiments with 20–50 seeds each. The averaged percentage of germinated seeds in the control experiments without ABA was set to 100% and used as a reference to calculate the percentage of germination in the assays performed in the presence of ABA.

were observed between wildtpye seeds and transgenic seeds (**Figure 6A**). When ABA was applied, seeds of plants accumulating WHIRLY1 in the nucleus only (nWHIRLY1:HA) were less sensitive to ABA than wildtype seeds (**Figure 6B**). They are hence comparable to the seeds of *why1* mutants (**Figure 2B**). Seeds of plants accumulating WHIRLY1, however, in both chloroplasts and nuclei (pnWHIRLY1:HA) displayed a much higher responsiveness to ABA than wildtype seeds (**Figure 6B**). At a concentration of 5 μM ABA less than 10% of the seeds were observed to germinate whereas more than 60% of wildtype seeds germinated (**Figure 6B**). With a second independent pnWHIRLY1:HA line similar results were obtained.

ABA INHIBITS GERMINATION IN THE PRESENCE OF ABAMINE

The results of the germination assays performed with seeds of transgenic lines overexpressing the full-length WHIRLY1:HA (pnWHIRLY1:HA) or a truncated version lacking the plastid transit peptide (nWHIRLY1:HA) indicated that the plastid located isoform of WHIRLY1 is enhancing the responsiveness of seeds toward ABA. This is surprising considering that ABA has been exogenously applied and even endogenous ABA is formed from xanthoxin outside of plastids (Cutler et al., 2010; Seo and Koshiba, 2011). In order to investigate whether the effect of ABA is mediated by changes in the level of xanthoxin inside plastids, the effect of ABA on germination of wildtype seeds was assayed in the presence of abamine which is known to inhibit the enzyme NCED catalyzing the formation of xanthoxin (Han et al., 2004). Addition of abamine enhanced the rate of germination indicating that the inhibitor indeed prevented the formation of ABA (**Figure 7**). When ABA was added alone the number of germinating seeds was reduced by 50% (**Figure 7**). When the same concentration of ABA was applied in the presence of abamine, the germination rate was the same as that determined in the presence of ABA only (**Figure 7**). This result shows that the exogenously applied ABA inhibits germination independent of the intrinsic production of the ABA precursor xanthoxin in plastids.

DISCUSSION

The WHIRLY1 protein was first discovered as a nuclear transcription factor implicated in *PR* and its function as a nuclear activator of *PR* genes was shown to depend on SA (Desveaux et al., 2000). Later, WHIRLY1 was found to be imported into plastids (Krause et al., 2005) whereas its potential to be translocated from the plastid to the nucleus was not known until recently (Isemer et al., 2012). SA is the only plant hormone completely synthesized in plastids (Wildermuth et al., 2001). It is hence possible that activation of WHIRLY1 in response to pathogens in fact occurs inside the organelle and not in the nucleus. This idea would be in accordance with the model presented by Brisson and co-workers on activation of an inactive pool of WHIRLY1 by SA (Desveaux et al., 2004, 2005). This would mean that plant responses toward pathogens mediated by SA would be under control of plastids as also recently suggested (Nomura et al., 2012).

The results obtained in this study suggested that WHIRLY1 is also involved in SA induced inhibition of germination. By simultaneous addition of SA and abamine, an inhibitor of the biosynthesis of ABA, it was, furthermore, demonstrated that the effect of SA on germination can be explained by its stimulatory effect on the biosynthesis of ABA. Although ABA is formed from xanthoxin in the cytoplasm, the enzymes limiting the level of its precursor are located inside chloroplasts (Seo and Koshiba, 2011). The crosstalk between ABA and SA was observed to be important in determining the outcome of plant pathogen interactions (Cao et al., 2011). The levels of both hormones and also that of jasmonic acid, another stress related hormone originating from plastids, were shown to depend on each other (Abreu and Munné-Bosch, 2009). It is likely that there is a crosstalk of the three stress related hormones completely or partially synthesized inside plastids which are the sites

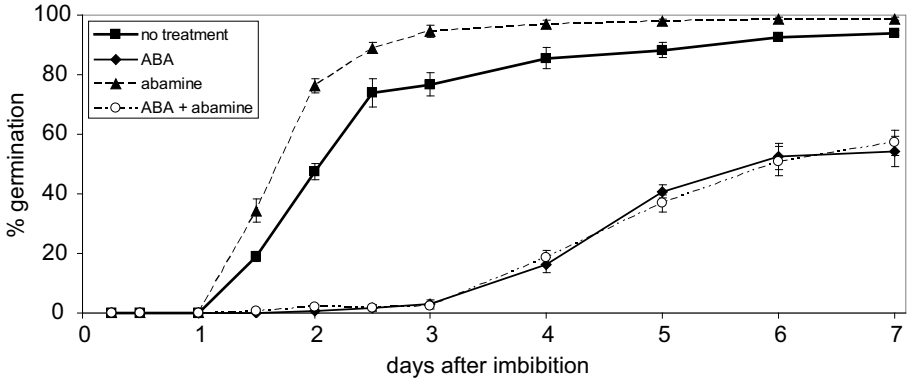

FIGURE 7 | Effect of abamine on abscisic acid mediated repression of germination. Wildtype seeds were grown on agar medium containing either no additive or 10 μM abscisic acid (ABA), 50 μM abamine or 10 μM ABA + 50 μM abamine, respectively. Germination rates were determined in the period from 1 to 7 days after imbibition. Values are the means ± SEM obtained from five independent experiments (20–50 seeds each).

where stress is primarily perceived in the plant cell (Bouvier et al., 2009).

The germination assays clearly demonstrated that WHIRLY1 is enhancing the responsiveness of germinating seeds toward ABA. Hence, the *why1* mutants also belong to the group of *aba insensitive* (*abi*) mutants. The previously identified *abi* mutants *1-5* were selected for their ability to germinate in the presence of 10 μmol ABA (Finkelstein, 1994), a concentration inhibiting germination of wildtype seeds. ABA responsiveness of the *why1* mutants is comparable to the *abi1* mutant (Finkelstein and Somerville, 1990) and even lower than the ABA sensitivity of the *abi4* and *abi5* mutants (Finkelstein, 1994). WHIRLY1 is found both in plastids and in the nucleus of the same cell (Grabowski et al., 2008). Germination assays with transgenic lines accumulating WHIRLY1 either in both plastids and the nucleus (pnWHIRLY) or only in the nucleus (nWHIRLY1) showed that it is the plastid localized WHIRLY1 that enhances the responsiveness of seedlings toward ABA. The inhibitory effect of ABA on germination was observed after external addition of ABA to the medium as well as after induction of its biosynthesis by addition of SA. It was shown before that WHIRLY1 as well as the other members of the WHIRLY protein family can form 24-mers in plastids, thereby building up a hollow oligomer which might store metabolites in order to protect the cell from possibly toxic compounds (Cappadocia et al., 2012). Such structures could also act as scaffolds binding specific proteins involved in signaling and thereby controlling the flow of signaling information (Zeke et al., 2009). Furthermore, the results obtained by use of the overexpression lines demonstrate an important function for the plastid in adjusting the activity of ABA.

Abscisic acid was recently reported to bind to plastid located magnesium-protoporphyrin IX chelatase which was proposed to function as a receptor of ABA (Shang et al., 2010). So far, it is not known whether ABA binds to the enzyme inside plastids or to a domain of the H subunit protruding into the cytoplasm (Shang et al., 2010). Both scenarios are possible because ABA can penetrate membranes in its protonated form and is known to diffuse inside the cell where it accumulates at sites of low pH (Seo and Koshiba, 2011).

ABA responsive *cis*-elements have been found in the promoters of many genes responding also to plastid signals. Multiple copies of ABRE (ACGT, CGTGTC) known to confer ABA responsiveness are in close proximity to G-boxes which are responsible for light-induced induction of the target genes. The transcription factor ABI4, which was first described in connection with ABA insensitivity (Finkelstein, 1994), was shown to be common to different pathways of plastid signaling (Koussevitzky et al., 2007). The *ABI4* gene encodes the apetala 2 transcription factor involved in transcriptional repression of photosynthesis associated nuclear genes when chloroplast development is blocked by addition of norflurazon (NF; Koussevitzky et al., 2007). NF blocks the production of chlorophyll due to its inhibitory effect on carotenoid biosynthesis and is commonly used as a herbicide (Sandmann and Böger, 1989). Alternatively, chloroplast development has been frequently blocked by treatment of seedlings with lincomycin, an inhibitor of plastid translation (Koussevitzky et al., 2007).

Mutants impaired in plastid signaling were named *gun*. Originally, five *gun* mutants (*gun1-5*) were identified in a screen for mutants that expressed photosynthesis associated nuclear genes when seedlings were grown in the presence of NF (Susek et al., 1993; Mochizuki et al., 2001). The *abi4* mutant shows derepression of *LHCB* gene expression levels after treatment of seedlings with lincomycin and is therefore also a *gun* mutant. In contrast, in the *abi1-3* and *abi5* mutants the expression of this gene was repressed to a similar extent as in the wildtype (Koussevitzky et al., 2007). This indicates that ABI4 is involved in plastid signaling and suggests that ABA itself is a plastid signal. Germination assays with *gun* mutants *gun1-1*, *gun1-102*, and *gun5* performed under the same conditions as with the *why1* mutant showed that these mutants have reduced sensitivity toward ABA during germination, furthermore indicating an important role for ABA during plastid retrograde signaling.

Most plastid signals so far described accumulate inside the plastid, e.g., reactive oxygen species, intermediates of tetrapyrrole biosynthesis or proteins such as GUN1 (Beck, 2005; Woodson and Chory, 2008; Leister, 2012). The ABA precursor xanthoxin is formed from carotenoids inside plastids but the last steps of ABA

biosynthesis take place in the cytoplasm (Seo and Koshiba, 2011). Germination assays in the presence of both ABA and abamine demonstrated that ABA itself and not the plastid located precursor xanthoxin inhibits germination. Earlier on it was deduced that ABA is unlikely to be a plastid signal because the ABA deficient mutant *aba1* failed to accumulate *LHCB* mRNA when grown in the presence of lincomycin (Koussevitzky et al., 2007). However, this conclusion is only relevant for plastid signaling induced by lincomycin and for only one of the many photosynthesis associated nuclear genes as target.

In fact, many more factors have been shown to affect plastid functionality and to change the expression of nuclear genes encoding chloroplast proteins (Leister, 2005). Plastid signals do not only control chloroplast development, but are also required for optimization of photosynthesis under changing environmental conditions to which mature plants are exposed (Pogson et al., 2008). Moreover, plastid signals were shown to affect processes not directly involving plastids such as the accumulation of anthocyanins (Ruckle and Larkin, 2009), the circadian clock (Hassidim et al., 2007), and pathogen response (Nomura et al., 2012). In fact, the entire development of plants seems to be controlled by plastids at least to some extent (Inaba and Ito-Inaba, 2010).

Taken together, the results of the studies on *why1* mutants and transgenic lines accumulating WHIRLY1 either in plastids and the nucleus or in the nucleus only suggest that the plastid located WHIRLY1 enhances the responsiveness of seeds toward ABA. Whether WHIRLY1 directly interacts with ABA and whether it is translocated from plastids to the nucleus in response to ABA remains to be investigated. In order to place WHIRLY1 within the network of plastid-to-nucleus signaling, nuclear gene expression in the *why1* mutants and in double mutants affected in addition in one of the well-known *gun* genes needs to be systematically analyzed in response to various treatments known to impair chloroplast development.

ACKNOWLEDGMENTS

Michela Zottini (University of Padova, Italy) is thanked for scientific advice. We thank Dario Leister (Ludwig Maximilians University Munich, Germany) for providing the *gun1-1* and *gun1-102* lines and Bernhard Grimm (Humboldt University Berlin, Germany) for providing the *gun5* line. Berit Haak (CAU Kiel, Germany) is thanked for technical assistance. This research was supported by a grant of the Deutsche Forschungsgemeinschaft (DFG: Kr1350/9-1).

REFERENCES

Abreu, M. E., and Munné-Bosch, S. (2009). Salicylic acid deficiency in *NahG* transgenic lines and *sid2* mutants increases seed yield in the annual plant *Arabidopsis thaliana*. *J. Exp. Bot.* 60, 1261–1271.

Aronsson, H., and Jarvis, R. P. (2011). "Rapid isolation of *Arabidopsis* chloroplasts and their use for in vitro protein import assays," in *Chloroplast Research in Arabidopsis: Methods and Protocols*, Vol. 1, ed. R. P. Jarvis (Springer Science+Business Media), 281–305.

Bechtold, N., and Pelletier, G. (1998). In planta *Agrobacterium*-mediated transformation of adult *Arabidopsis thaliana* plants by vacuum infiltration. *Methods Mol. Biol.* 82, 259–266.

Beck, C. F. (2005). Signaling pathways from the chloroplast to the nucleus. *Planta* 222, 743–756.

Bouvier, F., Mialoundama, A. S., and Camara, B. (2009). "A sentinel role for plastids," in *The Chloroplast*, eds A. S. Sandelius and H. Aronsson (Berlin: Springer), 267–292.

Busk, P. K., and Pagès, M. (1997). Microextraction of nuclear proteins from single maize embryos. *Plant Mol. Biol. Rep.* 15, 371–376.

Cao, F. Y., Yoshioka, K., and Desveaux, D. (2011). The roles of ABA in plant-pathogen interactions. *J. Plant Res.* 124, 489–499.

Caplan, J. L., Mamillapalli, P., Burch-Smith, T. M., Czymmek, K., and Dinesh-Kumar, S. P. (2008). Chloroplastic protein NRIP1 mediates innate immune receptor recognition of a viral effector. *Cell* 132, 449–462.

Cappadocia, L., Maréchal, A., Parent, J. S., Lépage, E., Sygusch, J., and Brisson, N. (2010). Crystal structures of DNA-Whirly complexes and their role in *Arabidopsis* organelle genome repair. *Plant Cell* 22, 1849–1867.

Cappadocia, L., Parent, J. S., Zampini, E., Lepage, E., Sygusch, J., and Brisson, N. (2012) A conserved lysine residue of plant Whirly proteins is necessary for higher order protein assembly and protection against DNA damage. *Nucleic Acids Res.* 40, 258–269.

Choy, M. K., Sullivan, J. A., Theobald, J. C., Davies, W. J., and Gray, J. C. (2008). An *Arabidopsis* mutant able to green after extended dark periods shows decreased transcripts of seed protein genes and altered sensitivity to abscisic acid. *J. Exp. Bot.* 59, 3869–3884.

Cottage, A., Mott, E. K., Kempster, J. A., and Gray, J. C. (2010). The *Arabidopsis* plastid-signalling mutant *gun1* (*genomes uncoupled1*) shows altered sensitivity to sucrose and abscisic acid and alterations in early seedling development. *J. Exp. Bot.* 61, 3773–3786.

Cutler, S. R., Rodriguez, P. L., Finkelstein, R. R., and Abrams, S. R. (2010). "Abscisic acid: emergence of a core signaling network," in *Annual Review of Plant Biology*, Vol. 61, eds S. Merchant, W. R. Briggs, and D. Ort (Palo Alto: Annula Reviews), 651–679.

Desveaux, D., Després, C., Joyeux, A., Subramaniam, R., and Brisson, N. (2000). PBF-2 is a novel single-stranded DNA binding factor implicated in *PR-10a* gene activation in potato. *Plant Cell* 12, 1477–1489.

Desveaux, D., Maréchal, A., and Brisson, N. (2005). Whirly transcription factors: defense gene regulation and beyond. *Trends Plant Sci.* 10, 95–102.

Desveaux, D., Subramanian, R., Després, C., Mess, J. N., Lévesque, C., Fobert, P. R., et al. (2004). A "Whirly" transcription factor is required for salicylic acid-dependent disease resistance in *Arabidopsis*. *Dev. Cell* 6, 229–240.

Finkelstein, R. R. (1994). Mutations at two new *Arabidopsis* ABA response loci are similar to the *abi3* mutations. *Plant J.* 5, 765–771.

Finkelstein, R. R., and Somerville, C. R. (1990). Three classes of abscisic acid (ABA)-insensitive mutations of *Arabidopsis* define genes that control overlapping subsets of ABA responses. *Plant Physiol.* 94, 1172–1179.

Grabowski, E., Miao, Y., Mulisch, M., and Krupinska, K. (2008). Single-stranded DNA-binding protein Whirly1 in barley leaves is located in plastids and the nucleus of the same cell. *Plant Physiol.* 147, 1800–1804.

Gruissem, W., Greenberg, B. M., Zurawski, G., and Hallick, R. B. (1986). Chloroplast gene expression and promoter identification in chloroplast extracts. *Methods Enzymol.* 118, 253–270.

Guttman, D. S., Vinatzer, B. A., Sarkar, S. F., Ranall, M. V., Kettler, G., and Greenberg, J. T. (2002). A functional screen for the type III (Hrp) secretome of the plant pathogen *Pseudomonas syringae*. *Science* 295, 1722–1726.

Han, S.-Y., Kitahata, N., Sekimata, K., Saito, T., Kobayashi, M., Nakashima, K., et al. (2004). A novel inhibitor of 9-cis-epoxycarotenoid dioxygenase in abscisic acid biosynthesis in higher plants. *Plant Physiol.* 135, 1574–1582.

Hassidim, M., Yakir, E., Fradkin, D., Hilman, D., Kron, I., Keren, N., et al. (2007). Mutations in CHLOROPLAST RNA BINDING provide evidence for the involvement of the chloroplast in the regulation of the circadian clock in *Arabidopsis*. *Plant J.* 51, 551–562.

Inaba, T., and Ito-Inaba, Y. (2010). Versatile roles of plastids in plant growth and development. *Plant Cell Physiol.* 51, 1847–1853.

Isemer, R., Mulisch, M., Schäfer, A., Kirchner, S., Koop, H. U., and Krupinska, K. (2012). Recombinant Whirly1 translocates from transplastomic chloroplasts to the nucleus. *FEBS Lett.* 586, 85–88.

Karimi, M., Inzé, D., and Depicker, A. (2002). GATEWAY vectors for *Agrobacterium*-mediated plant transformation. *Trends Plant Sci.* 7, 193–195.

Kerchev, P. I., Pellny, T. K., Vivancos, P. D., Kiddle, G., Hedden, P., Driscoll, S., et al. (2011). The transcription factor ABI-4 is required for the ascorbic acid-dependent regulation of growth and regulation of jasmonate-dependent defense signaling pathways in *Arabidopsis*. *Plant Cell* 23, 3319–3334.

Koussevitzky, S., Nott, A., Mockler, T. C., Hong, F., Sachetto-Martins, G., Surpin, M., et al. (2007). Signals from chloroplasts converge to regulate nuclear gene expression. *Science* 316, 715–719.

Krause, K., Kilbienski, I., Mulisch, M., Rödiger, A., Schäfer, A., and Krupinska, K. (2005). DNA-binding proteins of the Whirly family in *Arabidopsis thaliana* are targeted to the organelles. *FEBS Lett.* 579, 3707–3712.

Krause, K., and Krupinska, K. (2009). Nuclear regulators with a second home in organelles. *Trends Plant Sci.* 14, 194–199.

Leister, D. (2005). Genomics-based dissection of the cross-talk of chloroplasts with the nucleus and mitochondria in *Arabidopsis*. *Gene* 354, 110–116.

Leister, D. (2012). Retrograde signaling in plants: from complex to simple scenarios. *Front. Plant Sci.* 3:135. doi:10.3389/fpls.2012.00135

Majeran, W., Friso, G., Asakura, Y., Qu, X., Huang, M., Ponnala, L., et al. (2012). Nucleoid-enriched proteomes in developing plastids and chloroplasts from maize leaves: a new conceptual framework for nucleoid functions. *Plant Physiol.* 158, 156–189.

Maréchal, A., Parent, J. S., Véronneau-Lafortune, F., Joyeux, A., Lang, B. F., and Brisson, N. (2009). Whirly proteins maintain plastid genome stability in *Arabidopsis*. *Proc. Natl. Acad. Sci. U.S.A.* 106, 14693–14698.

Mateo, A., Funck, D., Mühlenbock, P., Kular, B., Mullineaux, P. M., and Karpinski, S. (2006). Controlled levels of salicylic acid are required for optimal photosynthesis and redox homeostasis. *J. Exp. Bot.* 57, 1795–1807.

Melonek, J., Mulisch, M., Schmitz-Linneweber, C., Grabowski, E., Hensel, G., and Krupinska, K. (2010). Whirly1 in chloroplasts associates with intron containing RNAs and rarely co-localizes with nucleoids. *Planta* 232, 471–481.

Mochizuki, N., Brusslan, J. A., Larkin, R., Nagatani, A., and Chory, J. (2001). *Arabidopsis* genomes uncoupled 5 (GUN5) mutant reveals the involvement of Mg-chelatase H subunit in plastid-to-nucleus signal transduction. *Proc. Natl. Acad. Sci. U.S.A.* 98, 2053–2058.

Mühlenbock, P., Szechyńska-Hebda, M., Plaszczyca, M., Baudo, M., Mateo, A., Mullineaux, P. M., et al. (2008). Chloroplast signaling and LESION SIMULATING DISEASE1 regulate crosstalk between light acclimation and immunity in *Arabidopsis*. *Plant Cell* 20, 2339–2356.

Nomura, H., Komori, T., Uemura, S., Kanda, Y., Shimotani, K., Nakai, K., et al. (2012). Chloroplast-mediated activation of plant immune signalling in *Arabidopsis*. *Nat. Commun.* 3, 926.

Padmanabhan, M. S., and Dinesh-Kumar, S. P. (2010). All hands on deck – the role of chloroplasts, endoplasmic reticulum, and the nucleus in driving plant innate immunity. *Mol. Plant Microbe Interact.* 23, 1368–1380.

Pfalz, J., Liere, K., Kandlbinder, A., Dietz, K.-J., and Oelmüller, R. (2006). pTAC2, -6, and -12 are components of the transcriptionally active plastid chromosome that are required for plastid gene expression. *Plant Cell* 18, 176–197.

Pogson, B. J., Woo, N. S., Förster, B., and Small, I. D. (2008). Plastid signalling to the nucleus and beyond. *Trends Plant Sci.* 13, 602–609.

Preston, J., Tatematsu, K., Kanno, Y., Hobo, T., Kimura, M., Jikumaru, Y., et al. (2009). Temporal expression patterns of hormone metabolism genes during imbibition of *Arabidopsis thaliana* seeds: a comparative study on dormant and non-dormant accessions. *Plant Cell Physiol.* 50, 1786–1800.

Prikryl, J., Watkins, K. P., Friso, G., van Wijk, K. J., and Barkan, A. (2008). A member of the Whirly family is a multifunctional RNA- and DNA-binding protein that is essential for chloroplast biogenesis. *Nucleic Acids Res.* 36, 5152–5165.

Rajjou, L., Belghazi, M., Huguet, R., Robin, C., Moreau, A., Job, C., et al. (2006). Proteomic investigation of the effect of salicylic acid on *Arabidopsis* seed germination and establishment of early defense mechanisms. *Plant Physiol.* 141, 910–923.

Rook, F., Hadingham, S. A., Li, Y., and Bevan, M. W. (2006). Sugar and ABA response pathways and the control of gene expression. *Plant Cell Environ.* 29, 426–434.

Ruckle, M. E., and Larkin, R. M. (2009). Plastid signals that affect photomorphogenesis in *Arabidopsis thaliana* are dependent on GENOMES UNCOUPLED 1 and cryptochrome 1. *New Phytol.* 182, 367–379.

Sandmann, G., and Böger, P. (1989). "Inhibition of carotenoid biosynthesis by herbicides," in *Target Sites of Herbicide Action*, ed. S. G. Böger (Boca Raton, FL: CRC Press), 25–44.

Seo, M., and Koshiba, T. (2011). Transport of ABA from the site of biosynthesis to the site of action. *J. Plant Res.* 124, 501–507.

Shakirova, F. M., Sakhabutdinova, A. R., Bezrukova, M. V., Fatkhutdinova, R. A., and Fatkhutdinova, D. R. (2003). Changes in the hormonal status of wheat seedlings induced by salicylic acid and salinity. *Plant Sci.* 164, 317–322.

Shang, Y., Yan, L., Liu, Z.-Q., Cao, Z., Mei, C., Xin, Q., et al. (2010). The Mg-chelatase H subunit of *Arabidopsis* antagonizes a group of WRKY transcription repressors to relieve ABA-responsive genes of inhibition. *Plant Cell* 22, 1909–1935.

Susek, R. E., Ausubel, F. M., and Chory, J. (1993). Signal transduction mutants of *Arabidopsis* uncouple nuclear CAB and RBCS gene expression from chloroplast development. *Cell* 74, 787–799.

Vallon, O., Hoyer-Hansen, G., and Simpson, D. J. (1987). Photosystem II and cytochrome b559 in the stroma lamellae of barley chloroplasts. *Carlsberg Res. Commun.* 52, 405–421.

Voigt, C., Oster, U., Börnke, F., Jahns, P., Dietz, K.-J., Leister, D., et al. (2010). In-depth analysis of the distinctive effects of norflurazon implies that tetrapyrrole biosynthesis, organellar gene expression and ABA cooperate in the GUN-type of plastid signalling. *Physiol. Plant* 138, 503–519.

Wildermuth, M. C., Dewdney, J., Wu, G., and Ausubel, F. M. (2001). Isochorismate synthase is required to synthesize salicylic acid for plant defence. *Nature* 414, 562–565.

Woodson, J. D., and Chory, J. (2008). Coordination of gene expression between organellar and nuclear genomes. *Nat. Rev. Genet.* 9, 383–395.

Xiong, J. Y., Lai, C. X., Qu, Z., Yang, X. Y., Qin, X. H., and Liu, G. Q. (2009). Recruitment of AtWHY1 and AtWHY3 by a distal element upstream of the kinesin gene AtKP1 to mediate transcriptional repression. *Plant Mol. Biol.* 71, 437–449.

Yoo, H. H., Kwon, C., Lee, M. M., and Chung, I. K. (2007). Single-stranded DNA binding factor AtWHY1 modulates telomere length homeostasis in *Arabidopsis*. *Plant J.* 49, 442–451.

Zeke, A., Lukàcs, M., and Lim, A. (2009). Scaffolds: interaction platforms for cellular signalling circuits. *Trends Cell Biol.* 19, 364–374.

Conflict of Interest Statement: The authors declare that the research was conducted in the absence of any commercial or financial relationships that could be construed as a potential conflict of interest.

Received: 17 September 2012; accepted: 30 November 2012; published online: 24 December 2012.

Citation: Isemer R, Krause K, Grabe N, Kitahata N, Asami T and Krupinska K (2012) Plastid located WHIRLY1 enhances the responsiveness of Arabidopsis seedlings toward abscisic acid. Front. Plant Sci. ***3****:283. doi: 10.3389/fpls.2012.00283*

This article was submitted to Frontiers in Plant Physiology, a specialty of Frontiers in Plant Science.

Copyright © 2012 Isemer, Krause, Grabe, Kitahata, Asami and Krupinska. This is an open-access article distributed under the terms of the Creative Commons Attribution License, which permits use, distribution and reproduction in other forums, provided the original authors and source are credited and subject to any copyright notices concerning any third-party graphics etc.

APPENDIX

Table A1 | Gene specific primers that were used in this study.

Gene name	Accession no.	Primer name	Sequence
WHIRLY1	At1g14410	LP	5′-TGACCAACAAACTGTTGATGG-3′
		RP	5′-TCGAATGACCCACGTAAAATC-3′
		WHY1_fwd	5′-AGGGAACAAACACAAAGCGA-3′
		WHY1_rvs	5′-CAGACTGATGTTTTGAGATACAACC-3′
Left border primer for T-DNA		LBa1	5′-TGGTTCACGTAGTGGGCCATCG-3′
ACTIN2	At3g18780	ACTIN2_for	5′-CTAAGCTCTCAAGATCAAAGGC-3′
		ACTIN2_rev	5′-AACATTGCAAAGAGTTTCAAGG-3′

frontiers in
PLANT SCIENCE

MINI REVIEW ARTICLE
published: 25 September 2012
doi: 10.3389/fpls.2012.00221

Dual localized mitochondrial and nuclear proteins as gene expression regulators in plants?

Anne-Marie Duchêne and Philippe Giegé*

Institut de Biologie Moléculaire des Plantes du Centre National de la Recherche Scientifique, University of Strasbourg, Strasbourg, France

Edited by:
Dario Leister, Ludwig-Maximilians-University Munich, Germany

Reviewed by:
Jim Whelan, Plant Energy Biology, The University of Western Australia, Australia
Elzbieta Glaser, Stockholm University, Sweden

***Correspondence:**
Philippe Giegé, Institut de Biologie Moléculaire des Plantes du Centre National de la Recherche Scientifique, University of Strasbourg, 12 Rue du General Zimmer, 67084 Strasbourg, France.
e-mail: giege@unistra.fr

Mitochondria heavily depend on the coordinated expression of both mitochondrial and nuclear genomes because some of their most significant activities are held by multi-subunit complexes composed of both mitochondrial and nuclear encoded proteins. Thus, precise communication and signaling pathways are believed to exist between the two compartments. Proteins dual localized to both mitochondria and the nucleus make excellent candidates for a potential involvement in the envisaged communication. Here, we review the identified instances of dual localized nucleo-mitochondrial proteins with an emphasis on plant proteins and discuss their functions, which are seemingly mostly related to gene expression regulation. We discuss whether dual localization could be achieved by dual targeting and/or by re-localization and try to apprehend the signals required for the respective processes. Finally, we propose that in some instances, dual localized mitochondrial and nuclear proteins might act as retrograde signaling molecules for mitochondrial biogenesis.

Keywords: mitochondria, nucleus, gene expression regulation, retrograde signaling, dual targeting, re-localization

INTRODUCTION

Mitochondria have arisen from the symbiosis of an α-proteobacteria with the archeal-like ancestor of eukaryotes (Gray, 1992; Lang et al., 1997; Gross and Bhattacharya, 2009). During evolution, massive gene transfer has occurred from the symbiont to its host cell (Gray, 1999). However, reverse genetic material transfer has also taken place as exemplified by the presence of nuclear originating retrotransposon-like sequences in mitochondrial genomes of higher plants (Unseld et al., 1997). Nevertheless, modern mitochondrial genomes are all extremely reduced as compared to their bacterial ancestor. They only encode approximately between 10 and 100 protein coding genes (Burger et al., 2003), thus merely a small fraction of the mitochondrial proteome, e.g., composed of an estimated 2000–3000 proteins in higher plants (Millar et al., 2005). Most of mitochondrial proteins are thus encoded in the nucleus, expressed in the cytosol and imported into mitochondria by a number of established pathways (Lithgow and Schneider, 2010). As a power station in eukaryotic cells, mitochondria perform key metabolic processes, in particular oxidative phosphorylation implemented by respiratory complexes. Interestingly, these essential multi-subunit complexes are composed of both mitochondrial encoded and nuclear encoded mitochondrial proteins. It is thus evident that precise gene expression coordination and communication pathways from mitochondria to the nucleus must exist to allow the biogenesis of respiratory complexes and proper cell function. In plants, retrograde regulatory pathways from chloroplasts to the nucleus have been well documented. They include control by epistasy of synthesis and a pathway involving tetrapyrroles and plastid gene expression (Pogson et al., 2008). In mitochondria, considerably less information is available, although it has been suggested that reactive oxygen species might be involved in retrograde signaling to the nucleus (Rhoads and Subbaiah, 2007). Nonetheless, proteins that would be localized to both mitochondria and the nucleus would also make very good candidates for an involvement is such communication pathways (Krause and Krupinska, 2009). It is now becoming increasingly evident that organellar protein multi-localization is a much more widespread phenomenon than previously thought. It has in particular been very often found for proteins dual targeted to both mitochondria and chloroplasts (Carrie et al., 2009a). For some protein families this dual targeting even seems to be the normal situation (Duchêne et al., 2005). However, it is also emerging that dual localization often takes place as well between organellar proteins and the nucleus (Krause and Krupinska, 2009), in particular as exemplified by the growing list of proteins found in both plant mitochondria and the nucleus. Here, we discuss the function of the identified nucleo-mitochondrial proteins and examine possible dual localization mechanisms and signaling pathways.

DUAL TARGETING IS WIDESPREAD IN PLANTS

Dual-targeted proteins are defined as proteins encoded by a single gene and localized in two cellular compartments. In consequence, the two isoforms have identical sequences in most of their length but can slightly differ in their extremities, due to the presence of targeting sequences. In plant cells, the first dual-targeted protein was identified in 1995. It is a pea glutathione reductase found in both mitochondria and chloroplasts. Since this discovery, numerous proteins were identified to be dual targeted. The vast majority, about one hundred of them, are plastidial and mitochondrial proteins (Carrie and Small, 2012). A dozen are mitochondrial and peroxisomal (Michaud and Duchêne, 2012), and an additional 10 proteins are nuclear and plastidial (Krause and Krupinska, 2009). Finally, some proteins have been found in mitochondria and

plasma membrane, in mitochondria and endoplasmic reticulum (ER), in plastids and ER, or even in mitochondria, chloroplasts, and the cytosol (Michaud and Duchêne, 2012).

The mechanisms allowing dual localization are multiple. Most of the dual mitochondrial–plastidial proteins have ambiguous targeting signals in their N-terminal extremities that are recognized by both mitochondrial and chloroplastic import apparatus. In contrast, distinct sorting sequences were identified in some mitochondria–peroxisome proteins, i.e., a N-terminal mitochondrial targeting sequence (MTS) and a C-terminal peroxisomal targeting signal, respectively (Michalecka et al., 2003; Carrie et al., 2009a). Post-translational modifications were also shown to allow dual targeting, e.g., farnesylation was proposed to control the localization of AtIPT3 to either plastids or the nucleus (Galichet et al., 2008). Re-localization mechanisms have also been suggested. For example, protein transport from the ER to plastids has been proposed for AtCaAH1, and post-translational modifications clearly influence CAH1 trafficking (Buren et al., 2011).

NUCLEO-MITOCHONDRIAL PROTEINS IN EUKARYOTES

The dual localization of proteins to mitochondria and the nucleus is also a common phenomenon and has been described in several instances. In many eukaryotes, it has become obvious that a higher as previously thought number of mitochondrial proteins have more than one localization. In particular, it has been shown that, up to one third of the mitochondrial proteome of yeast is composed of dual localized proteins (an estimated 316 out of 801 proteins; Ben-Menachem et al., 2011). Among them, a significant proportion of proteins could be localized to both mitochondrial and the nucleus (Yogev and Pines, 2011). Examples of nucleo-mitochondrial proteins include LRPPRC, a protein belonging to the pentatricopeptide repeat protein family (Lurin et al., 2004; Schmitz-Linneweber and Small, 2008). In human, a mutation in this protein was found to be responsible for the French-Canadian type of Leigh syndrome (Mootha et al., 2003; Xu et al., 2004). In mitochondria, LRPPRC is necessary for polyadenylation and coordination of translation of mitochondrial messengers (Ruzzenente et al., 2012). However, this protein was first described as part of a ribonucleoprotein complex accountable for the shuttling of mRNAs from the nucleus to the cytosol (Mili and Pinol-Roma, 2003). In addition, LRPPRC has been suggested to be a cofactor of the eukaryotic translation initiation factor 4E (Topisirovic et al., 2009). Finally, in the nucleus, this protein was proposed to regulate the expression of nuclear genes involved in mitochondrial biogenesis (Cooper et al., 2006). Other instances of nucleo-mitochondrial proteins include, e.g., ELAC2, a protein responsible for RNase Z activity, that removes 3′ trailer sequences of tRNA precursors, in both mitochondria and the nucleus in human (Rossmanith, 2011). TERT, the catalytic subunit of telomerase in the nucleus is exported from the nucleus during oxidative stress and imported into mitochondria where it protects the mitochondrial genome from reactive oxygen species (Ahmed et al., 2008). Finally, the nuclear transcription factor p53 involved in apoptosis through the activation or repression of pro- or anti-apoptotic genes, respectively, localizes to mitochondria during stress conditions. In mitochondria it uses its DNA binding domain to form an inhibitory complex with BclXL and Bcl2 (Mihara et al., 2003). Interestingly, all these examples of proteins found in both mitochondria and the nucleus appear to be involved in the control of gene expression or in post-transcriptional processes.

OCCURRENCE OF NUCLEO-MITOCHONDRIAL PROTEINS IN PLANTS

Contrary to other eukaryotes such a yeast or human, very few instances of nucleo-mitochondrial proteins have been described in plants. Here we review the known examples of these dual localized proteins and examine their function (**Table 1**).

Similar to human, RNase Z is present in different copies in plants. Out of the four RNase Z proteins found in *Arabidopsis*, green fluorescent protein (GFP) fusion experiments showed that one of them has a localization restricted to mitochondria, whereas another one, AtTRZ3, appears to be dual localized to both mitochondria and the nucleus (Canino et al., 2009). This protein seems to be the only nuclear RNase Z in *Arabidopsis*. However, its

Table 1 | Proteins identified in both mitochondria and the nucleus in plants.

Protein	Mito loc	Nuc loc	Function in Mito	Function in Nuc	Reference
AtTRZ3	GFP	GFP	RNase Z	RNase Z	Canino et al. (2009)
AtLigI	GFP	GFP	DNA repair?	DNA repair	Sunderland et al. (2006)
PsTrxoI	GFP, W, IG	GFP, W, IG	Thioredoxin	Oxidation protection of DNA?	Marti et al. (2009)
DHFR	IG, Act	IG?	Dihydrofolate reductase	Unknown	Luo et al. (1997)
AtAPL	GFP	GFP	Unknown	Transcription factor	Carrie et al. (2009b)
AtPNMI	GFP, W, IG	GFP, W, IG, IC	Translation?	Gene expression negative regulator	Hammani et al. (2011a)

At and Ps represent proteins identified in Arabidopis thaliana and Pisum sativum, respectively. "Mito loc" and "Nuc loc" indicate the methods used to localize proteins in mitochondria and the nucleus, respectively. GFP stands for green fluorescent protein fusion visualized by confocal microscopy; W stands for western blot analysis on purified cell fractions; IG stands for immunogold labeling; Act stands for activity assays with purified cell fractions, and IC stand for immunocytology. Envisaged or characterized functions in mitochondria and the nucleus are indicated. Question marks represent speculative location or functions in the respective compartments. It should be noted that many of the dual localizations described here were based on GFP fusion experiments. This technology sometimes leads to unspecific nuclear localizations when the fusion proteins are not large enough to be excluded from passive diffusion through nuclear pores (Seibel et al., 2007). Thus, occurrences of dual localizations of small proteins that were not confirmed by independent methods should be considered with caution.

gene was found to be non-essential. This hints that dual nuclear localization of other RNase Z isoforms in plants might have been overlooked.

Isoforms of the *Arabidopsis* DNA ligase 1 protein (AtLig1) have been found to localize to both mitochondria and the nucleus by GFP fusion experiments and confocal microscopy (Sunderland et al., 2006). In the two compartments, AtLig1 is expected to be involved in the final step of DNA repair processes (Tomkinson and Mackey, 1998). In the nucleus, this protein was indeed shown to play a crucial role in both DNA replication and excision repair pathways (Taylor et al., 1998). However, in mitochondria its precise molecular function has not yet been confirmed.

PsTrxo1, an isoform of thioredoxin in pea, was found in both mitochondria and nuclei by western blot analysis on purified cellular fractions, immunogold labeling as well as GFP fusions experiments (Marti et al., 2009). Thioredoxins are ubiquitous small proteins involved in the reduction of disulfide bonds of proteins. In mitochondria, PsTrxo1 is able to activate AOX and is proposed to reduce a number of predicted mitochondrial targets (Marti et al., 2009). Contrary to some mammalian thioredoxins that accumulate in the nucleus under stress conditions (Wei et al., 2000), PsTrxo1 is found in the nucleus in normal conditions (Marti et al., 2009). Its function at this location could be related to transcriptional regulation through oxidation protection of heterochromatin as proposed for the mammalian PRDX5 (Kropotov et al., 2006).

The plant mitochondrial dihydrofolate reductase (also found in plastids) was proposed to be present in plant nuclei as well because it was detected in the nucleolus of carrot by immunogold labeling (Luo et al., 1997; Krause and Krupinska, 2009). However, other studies in pea leaves clearly fail to identify dihydrofolate reductase activity in the nucleus (Neuburger et al., 1996). The occurrence of this protein as a nucleo-mitochondrial protein thus remains uncertain.

In *Arabidopsis*, the "altered phloem development" (AtAPL) transcription factor was found dual localized to mitochondria and the nucleus by a high throughput GFP fusion approach (Carrie et al., 2009b). This MYB coiled-coil type transcription factor was shown to regulate vascular tissue identity in *Arabidopsis* through the regulation of nuclear genes (Bonke et al., 2003), whereas its mitochondrial function is unknown.

Finally, AtPNM1, an *Arabidopsis* pentatricopeptide repeat protein, was identified in both mitochondria and the nucleus by immunodetections on purified cell fractions, by immunocytology, by immunogold labeling, and by GFP fusion experiments (Hammani et al., 2011a). The function of this protein in mitochondria is unclear although it could be related to translation because PNM1 is associated with mitochondrial polysomes. In the nucleus, it interacts with a nucleosome assembly protein as well as with a TCP transcription factor (Hammani et al., 2011a). This class of protein was proposed (Welchen and Gonzalez, 2006) and shown (Giraud et al., 2010) to be involved in the coordinated expression of nuclear encoded mitochondrial proteins. Hence, mutants expressing a version of PNM1 unable to localize to the nucleus revealed that some nuclear genes encoding mitochondrial proteins had increased mRNA levels in the absence of PNM1. This has thus suggested that in the nucleus, PNM1 might act as a negative regulator for the expression of nuclear encoded mitochondrial proteins (Hammani et al., 2011a,b).

Nevertheless, it appears that most plant nucleo-mitochondrial proteins, similar to their other eukaryotic counterparts, seem to be involved in the control of gene expression. These proteins therefore make very good candidates for the regulation of gene expression coordination between mitochondria and the nucleus (Giegé et al., 2005; Giraud et al., 2010) required for mitochondrial biogenesis.

HOW IS NUCLEO-MITOCHONDRIAL DUAL LOCALIZATION ACHIEVED?

For AtTRZ3, AtLig1, PsTrxo1, AtAPL, and AtPNM1, the dual nucleo-mitochondrial localization appears to be clearly established. These five proteins all have two distinct putative targeting signals, a MTS and a NLS. The two distinct sorting sequences MTS and NLS often compete with each other, leading to the dominance of one sorting signal over the second one. The main strategies for subcellular targeting appear to be the synthesis of proteins isoforms, either by alternative transcription start, alternative splicing, or alternative translation initiation.

Alternative splicing of AtAPL generates two transcripts with different 5′ extremities. Both encode protein isoforms with the MTS and NLS sequences (**Figure 1**). The first transcript codes for a protein of 293 aminoacids (aa) with a MTS at its N-terminal extremity. The second transcript codes for a larger protein (358 aa) with a N-terminal extension in front of its MTS sequence. Bonke et al. (2003) have demonstrated that GFP fused to the N-terminus of the larger protein is targeted to the nucleus. Carrie et al. (2009b) have shown that GFP fused to the C-terminus of the shorter protein is imported into mitochondria, and no signal is observed in the nucleus. Mitochondrial import appears dominant over nuclear targeting, suggesting that the MTS is dominant over the NLS. It has been proposed that the N-terminal extension in the larger protein masks the MTS, thus allowing targeting to nucleus.

For AtLig1, alternative transcription initiation yields three mRNA with different 5′ UTR. However, in that case, the coding sequence is identical for the three transcripts. Two in-frame AUG codons are present on these transcripts (**Figure 1**), and a mechanism of alternative translation initiation has been proposed. In a cell-free coupled transcription/translation system, translation initiation occurs at the first and the second AUG (half for each). Both the nucleotides context around the alternative start codons and the length of the 5′ UTR influence translation initiation efficiency (Sunderland et al., 2006). Fusions with GFP have revealed different targeting of the two protein isoforms. Translation initiation from the first start codon produces a mitochondrial isoform, on the other hand initiation from the second start codon produces a nuclear isoform. The larger protein contains both the MTS and NLS sequences, and the MTS appears dominant over the NLS. The smaller protein only containing the NLS is targeted to the nucleus.

Complementary approaches have indicated that the pea Trxo1 is dual localized in the nucleus and mitochondria (Marti et al., 2009). The molecular weight (MW) of the nuclear isoform is consistent with the MW of the pre-protein, and the MW of

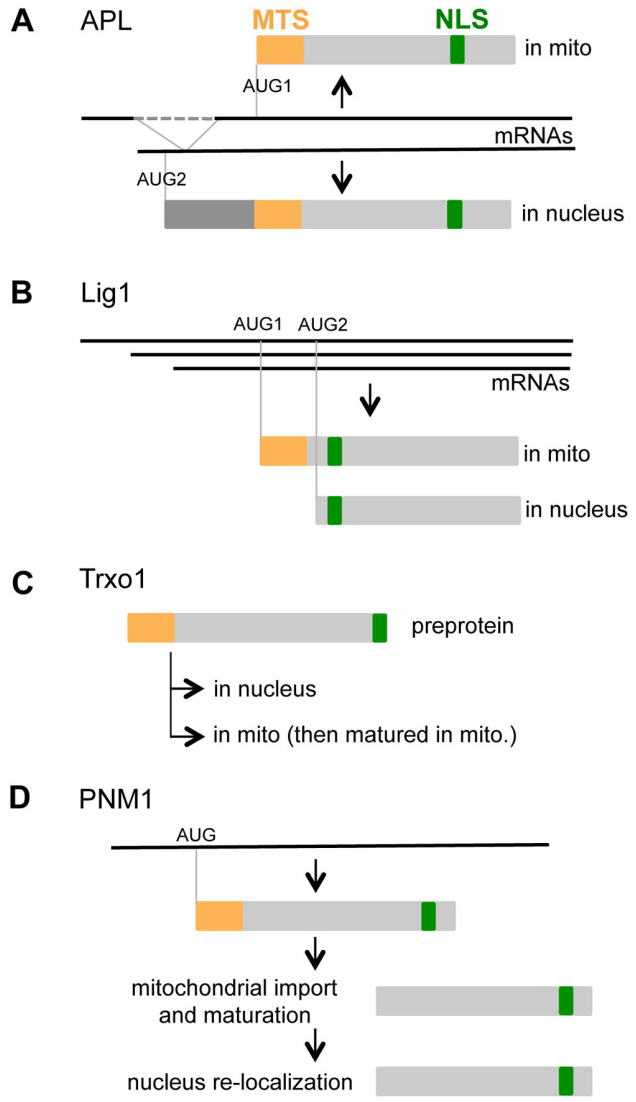

FIGURE 1 | Nucleo-mitochondrial dual targeting of proteins is controlled by different mechanisms. (A) Alternative splicing of APL generates two transcripts that code for different proteins. **(B)** Alternative initiation of transcription and of translation controls the balance of mitochondrial and nuclear Lig1. **(C)** The Trxo1 pre-protein is imported into both mitochondria and the nucleus, although the control of partition between the two organelles is not yet understood. **(D)** The nuclear localization of PNM1 can be explained by re-localization of the mitochondrial mature protein into the nucleus.

the mitochondrial isoform is in accordance with the maturation of the pre-protein after import. The pre-protein is thus imported into both mitochondria and nucleus, although the mechanism of partition between the two compartments is not known.

One unique transcript was detected for PNM1, and no in-frame AUG codon was found close to the initiation codon (Hammani et al., 2011a). Surprisingly, the isoforms of PNM1 detected in both compartments have a MW corresponding to the mature protein. As no alternative translation initiation is suspected, it is tempting to speculate that PNM1 is imported into mitochondria, matured, then partially re-localized into the nucleus (Hammani et al., 2011b). Such a mitochondria to nucleus shuttle had never been shown in plant but had been proposed for yeast fumarase (Singh and Gupta, 2006). Similarly, chloroplast to nucleus shuttling has been proposed for transcription factors such as pBrp or Tsip1 (Lagrange et al., 2003; Ham et al., 2006). It is thus imaginable that proteins such as PNM1 might relocate from the mitochondrial surface to the nucleus through a similar mechanism.

ENVISAGED NUCLEO-MITOCHONDRIAL SIGNALING PATHWAYS

Signaling pathways between mitochondria and the nucleus include both anterograde and retrograde regulations. Anterograde control of the nucleus over mitochondria is extensively documented with the incidence of the proteins responsible for mitochondrial gene expression, which are almost all encoded in the nucleus and subsequently targeted to mitochondria, thus enabling a precise control of the nucleus on mitochondrial function (Giegé and Brennicke, 2001).

On the other hand, little information is available on plant mitochondrial retrograde regulation (Pogson et al., 2008). Reactive oxygen species (ROS), that are often regarded as markers of mitochondrial oxidative stress, have been proposed to be involved in mitochondrial retrograde signaling to the nucleus (Rhoads and Subbaiah, 2007), similar to plastidial ones (Nott et al., 2006). In this process, sensors such as ROS scavenging proteins, could participate in the early steps of a signaling pathway that would ultimately lead to gene expression changes in the nucleus (Gray et al., 2004; Giegé, 2007). Other potential participants in mitochondrial retrograde regulation could be proteins belonging to "two-components" pathways. This type of signaling pathways that was until recently believed to be exclusively prokaryotic has been found in plants (Grefen and Harter, 2004). It implicates at least two proteins: a signal sensing histidine kinase and a response regulator that elicits the output response. ARR2, a response regulator protein primarily expressed in pollen is localized in the nucleus where it functions as a transcription factor, e.g., ARR2 regulates *in vivo* the promoter region of a mitochondrial complex I subunit nuclear gene (Lohrmann et al., 2001). Finally, the occurrence of proteins such as PNM1 that seem to be released from mitochondria in order to be re-localized to the nucleus suggests that some nucleo-mitochondrial proteins might act directly as retrograde signaling molecules for the coordination of gene expression in both mitochondria and the nucleus, as required for proper mitochondrial biogenesis.

CONCLUDING REMARKS

The growing list of proteins dual localized to mitochondria and the nucleus in plants, but also in other eukaryotes, shows that many of these proteins have a role in genome maintenance or in gene expression regulation, similar to what is also observed for nucleo-plastidial proteins (Desveaux et al., 2005). It has been hypothesized that the rationale for the occurrence of these proteins in two compartments might be for the sequestration of proteins in one compartment until specific environmental or developmental cues

require their function in the other (Krause and Krupinska, 2009). Alternatively, proteins might be dual targeted to mitochondria and the nucleus to perform the same functions for the respective genomes expression in the two compartments and thus to act as direct effectors of gene expression coordination. Nonetheless, it is also imaginable that some nucleo-mitochondrial proteins might act as signaling molecules from mitochondria to the nucleus. Overall the analysis of the identified instances of plant proteins localized to both mitochondria and the nucleus, suggests that these proteins have evolved different strategies to achieve dual localization, which enables them to act as regulators for the coordinated expression of the mitochondrial and nuclear genomes.

ACKNOWLEDGMENTS

This work was supported by the French "Centre National de la Recherche Scientifique." Philippe Giegé was supported by an ANR Blanc research grant "PRO-RNase P, ANR 11 BSV8 008 01." Philippe Giegé and Anne-Marie Duchêne were supported by the LabEx consortium "MitoCross."

REFERENCES

Ahmed, S., Passos, J. F., Birket, M. J., Beckmann, T., Brings, S., Peters, H., Birch-Machin, M. A., Von Zglinicki, T., and Saretzki, G. (2008). Telomerase does not counteract telomere shortening but protects mitochondrial function under oxidative stress. *J. Cell Sci.* 121, 1046–1053.

Ben-Menachem, R., Tal, M., Shadur, T., and Pines, O. (2011). A third of the yeast mitochondrial proteome is dual localized: a question of evolution. *Proteomics* 11, 4468–4476.

Bonke, M., Thitamadee, S., Mahonen, A. P., Hauser, M. T., and Helariutta, Y. (2003). APL regulates vascular tissue identity in *Arabidopsis*. *Nature* 426, 181–186.

Buren, S., Ortega-Villasante, C., Blanco-Rivero, A., Martinez-Bernardini, A., Shutova, T., Shevela, D., Messinger, J., Bako, L., Villarejo, A., and Samuelsson, G. (2011). Importance of post-translational modifications for functionality of a chloroplast-localized carbonic anhydrase (CAH1) in *Arabidopsis thaliana*. *PLoS ONE* 6, e21021. doi: 10.1371/journal.pone.0021021

Burger, G., Gray, M. W., and Lang, B. F. (2003). Mitochondrial genomes: anything goes. *Trends Genet.* 19, 709–716.

Canino, G., Bocian, E., Barbezier, N., Echeverria, M., Forner, J., Binder, S., and Marchfelder, A. (2009). *Arabidopsis* encodes four tRNase Z enzymes. *Plant Physiol.* 150, 1494–1502.

Carrie, C., Giraud, E., and Whelan, J. (2009a). Protein transport in organelles: dual targeting of proteins to mitochondria and chloroplasts. *FEBS J.* 276, 1187–1195.

Carrie, C., Kuhn, K., Murcha, M. W., Duncan, O., Small, I. D., O'Toole, N., and Whelan, J. (2009b). Approaches to defining dual-targeted proteins in *Arabidopsis*. *Plant J.* 57, 1128–1139.

Carrie, C., and Small, I. (2012). A reevaluation of dual-targeting of proteins to mitochondria and chloroplasts. *Biochim. Biophys. Acta.*

Cooper, M. P., Qu, L., Rohas, L. M., Lin, J., Yang, W., Erdjument-Bromage, H., Tempst, P., and Spiegelman, B. M. (2006). Defects in energy homeostasis in Leigh syndrome French Canadian variant through PGC-1alpha/LRP130 complex. *Genes Dev.* 20, 2996–3009.

Desveaux, D., Marechal, A., and Brisson, N. (2005). Whirly transcription factors: defense gene regulation and beyond. *Trends Plant Sci.* 10, 95–102.

Duchêne, A. M., Giritch, A., Hoffmann, B., Cognat, V., Lancelin, D., Peeters, N. M., Zaepfel, M., Maréchal-Drouard, L., and Small, I. D. (2005). Dual targeting is the rule for organellar aminoacyl-tRNA synthetases in *Arabidopsis thaliana*. *Proc. Natl. Acad. Sci. U.S.A.* 102, 16484–16489.

Galichet, A., Hoyerova, K., Kaminek, M., and Gruissem, W. (2008). Farnesylation directs AtIPT3 subcellular localization and modulates cytokinin biosynthesis in *Arabidopsis*. *Plant Physiol.* 146, 1155–1164.

Giegé, P. (2007). "Mitochondrial respiratory complexes biogenesis: communication, gene expression and assembly mechanisms," in *Plant Mitochondria*, ed. L. David (Oxford: Blackwell), 141–170.

Giegé, P., and Brennicke, A. (2001). From gene to protein in higher plant mitochondria. *C. R. Acad. Sci. III* 324, 209–217.

Giegé, P., Sweetlove, L. J., Cognat, V., and Leaver, C. J. (2005). Coordination of nuclear and mitochondrial genome expression during mitochondrial biogenesis in *Arabidopsis*. *Plant Cell* 17, 1497–1512.

Giraud, E., Ng, S., Carrie, C., Duncan, O., Low, J., Lee, C. P., Van Aken, O., Millar, A. H., Murcha, M., and Whelan, J. (2010). TCP transcription factors link the regulation of genes encoding mitochondrial proteins with the circadian clock in *Arabidopsis thaliana*. *Plant Cell* 22, 3921–3934.

Gray, M. W. (1992). The endosymbiont hypothesis revisited. *Int. Rev. Cytol.* 141, 233–357.

Gray, M. W. (1999). Evolution of organellar genomes. *Curr. Opin. Genet. Dev.* 9, 678–687.

Gray, G. R., Maxwell, D. P., Villarimo, A. R., and Mcintosh, L. (2004). Mitochondria/nuclear signaling of alternative oxidase gene expression occurs through distinct pathways involving organic acids and reactive oxygen species. *Plant Cell Rep.* 23, 497–503.

Grefen, C., and Harter, K. (2004). Plant two-component systems: principles, functions, complexity and cross talk. *Planta* 219, 733–742.

Gross, J., and Bhattacharya, D. (2009). Mitochondrial and plastid evolution in eukaryotes: an outsiders' perspective. *Nat. Rev. Genet.* 10, 495–505.

Ham, B. K., Park, J. M., Lee, S. B., Kim, M. J., Lee, I. J., Kim, K. J., Kwon, C. S., and Paek, K. H. (2006). Tobacco Tsip1, a DnaJ-type Zn finger protein, is recruited to and potentiates Tsi1-mediated transcriptional activation. *Plant Cell* 18, 2005–2020.

Hammani, K., Gobert, A., Hleibieh, K., Choulier, L., Small, I., and Giegé, P. (2011a). An *Arabidopsis* dual-localized pentatricopeptide repeat protein interacts with nuclear proteins involved in gene expression regulation. *Plant Cell* 23, 730–740.

Hammani, K., Gobert, A., Small, I., and Giegé, P. (2011b). A PPR protein involved in regulating nuclear genes encoding mitochondrial proteins? *Plant Signal. Behav.* 6, 748–750.

Krause, K., and Krupinska, K. (2009). Nuclear regulators with a second home in organelles. *Trends Plant Sci.* 14, 194–199.

Kropotov, A., Serikov, V., Suh, J., Smirnova, A., Bashkirov, V., Zhivotovsky, B., and Tomilin, N. (2006). Constitutive expression of the human peroxiredoxin V gene contributes to protection of the genome from oxidative DNA lesions and to suppression of transcription of noncoding DNA. *FEBS J.* 273, 2607–2617.

Lagrange, T., Hakimi, M. A., Pontier, D., Courtois, F., Alcaraz, J. P., Grunwald, D., Lam, E., and Lerbs-Mache, S. (2003). Transcription factor IIB (TFIIB)-related protein (pBrp), a plant-specific member of the TFIIB-related protein family. *Mol. Cell. Biol.* 23, 3274–3286.

Lang, B. F., Burger, G., O'Kelly, C. J., Cedergren, R., Golding, G. B., Lemieux, C., Sankoff, D., Turmel, M., and Gray, M. W. (1997). An ancestral mitochondrial DNA resembling a eubacterial genome in miniature. *Nature* 387, 493–496.

Lithgow, T., and Schneider, A. (2010). Evolution of macromolecular import pathways in mitochondria, hydrogenosomes and mitosomes. *Philos. Trans. R. Soc. Lond. B Biol. Sci.* 365, 799–817.

Lohrmann, J., Sweere, U., Zabaleta, E., Baurle, I., Keitel, C., Kozma-Bognar, L., Brennicke, A., Schafer, E., Kudla, J., and Harter, K. (2001). The response regulator ARR2: a pollen-specific transcription factor involved in the expression of nuclear genes for components of mitochondrial complex I in *Arabidopsis*. *Mol. Genet. Genomics* 265, 2–13.

Luo, M., Orsi, R., Patrucco, E., Pancaldi, S., and Cella, R. (1997). Multiple transcription start sites of the carrot dihydrofolate reductase-thymidylate synthase gene, and sub-cellular localization of the bifunctional protein. *Plant Mol. Biol.* 33, 709–722.

Lurin, C., Andres, C., Aubourg, S., Bellaoui, M., Bitton, F., Bruyere, C., Caboche, M., Debast, C., Gualberto, J., Hoffmann, B., Lecharny, A., Le Ret, M., Martin-Magniette, M. L., Mireau, H., Peeters, N., Renou, J. P., Szurek, B., Taconnat, L., and Small, I. (2004). Genome-wide analysis of *Arabidopsis* pentatricopeptide repeat proteins reveals their essential role in organelle biogenesis. *Plant Cell* 16, 2089–2103.

Marti, M. C., Olmos, E., Calvete, J. J., Diaz, I., Barranco-Medina, S., Whelan, J., Lazaro, J. J., Sevilla, F., and Jimenez, A. (2009). Mitochondrial and nuclear localization of a novel pea thioredoxin: identification of its mitochondrial target proteins. *Plant Physiol.* 150, 646–657.

Michalecka, A. M., Svensson, A. S., Johansson, F. I., Agius, S. C., Johanson, U., Brennicke, A., Binder, S., and

Rasmusson, A. G. (2003). *Arabidopsis* genes encoding mitochondrial type II NAD(P)H dehydrogenases have different evolutionary origin and show distinct responses to light. *Plant Physiol.* 133, 642–652.

Michaud, M., and Duchêne, A. M. (2012). "Macromolecular trafficking to plant mitochondria," in *Advances in Botanical Research*, Vol. 63, *Mitochondrial Genome Evolution*, ed. L. Maréchal-Drouard (Oxford: Elsevier), 347–421.

Mihara, M., Erster, S., Zaika, A., Petrenko, O., Chittenden, T., Pancoska, P., and Moll, U. M. (2003). p53 has a direct apoptogenic role at the mitochondria. *Mol. Cell* 11, 577–590.

Mili, S., and Pinol-Roma, S. (2003). LRP130, a pentatricopeptide motif protein with a noncanonical RNA-binding domain, is bound in vivo to mitochondrial and nuclear RNAs. *Mol. Cell. Biol.* 23, 4972–4982.

Millar, A. H., Heazlewood, J. L., Kristensen, B. K., Braun, H. P., and Moller, I. M. (2005). The plant mitochondrial proteome. *Trends Plant Sci.* 10, 36–43.

Mootha, V. K., Lepage, P., Miller, K., Bunkenborg, J., Reich, M., Hjerrild, M., Delmonte, T., Villeneuve, A., Sladek, R., Xu, F., Mitchell, G. A., Morin, C., Mann, M., Hudson, T. J., Robinson, B., Rioux, J. D., and Lander, E. S. (2003). Identification of a gene causing human cytochrome c oxidase deficiency by integrative genomics. *Proc. Natl. Acad. Sci. U.S.A.* 100, 605–610.

Neuburger, M., Rebeille, F., Jourdain, A., Nakamura, S., and Douce, R. (1996). Mitochondria are a major site for folate and thymidylate synthesis in plants. *J. Biol. Chem.* 271, 9466–9472.

Nott, A., Jung, H. S., Koussevitzky, S., and Chory, J. (2006). Plastid-to-nucleus retrograde signaling. *Annu. Rev. Plant Biol.* 57, 739–759.

Pogson, B. J., Woo, N. S., Forster, B., and Small, I. D. (2008). Plastid signalling to the nucleus and beyond. *Trends Plant Sci.* 13, 602–609.

Rhoads, D. M., and Subbaiah, C. C. (2007). Mitochondrial retrograde regulation in plants. *Mitochondrion* 7, 177–194.

Rossmanith, W. (2011). Localization of human RNase Z isoforms: dual nuclear/mitochondrial targeting of the ELAC2 gene product by alternative translation initiation. *PLoS ONE* 6, e19152. doi: 10.1371/journal.pone.0019152

Ruzzenente, B., Metodiev, M. D., Wredenberg, A., Bratic, A., Park, C. B., Camara, Y., Milenkovic, D., Zickermann, V., Wibom, R., Hultenby, K., Erdjument-Bromage, H., Tempst, P., Brandt, U., Stewart, J. B., Gustafsson, C. M., and Larsson, N. G. (2012). LRPPRC is necessary for polyadenylation and coordination of translation of mitochondrial mRNAs. *EMBO J.* 31, 443–456.

Schmitz-Linneweber, C., and Small, I. (2008). Pentatricopeptide repeat proteins: a socket set for organelle gene expression. *Trends Plant Sci.* 13, 663–670.

Seibel, N. M., Eljouni, J., Nalaskowski, M. M., and Hampe, W. (2007). Nuclear localization of enhanced green fluorescent protein homomultimers. *Anal. Biochem.* 368, 95–99.

Singh, B., and Gupta, R. S. (2006). Mitochondrial import of human and yeast fumarase in live mammalian cells: retrograde translocation of the yeast enzyme is mainly caused by its poor targeting sequence. *Biochem. Biophys. Res. Commun.* 346, 911–918.

Sunderland, P. A., West, C. E., Waterworth, W. M., and Bray, C. M. (2006). An evolutionarily conserved translation initiation mechanism regulates nuclear or mitochondrial targeting of DNA ligase 1 in *Arabidopsis thaliana*. *Plant J.* 47, 356–367.

Taylor, R. M., Hamer, M. J., Rosamond, J., and Bray, C. M. (1998). Molecular cloning and functional analysis of the *Arabidopsis thaliana* DNA ligase I homologue. *Plant J.* 14, 75–81.

Tomkinson, A. E., and Mackey, Z. B. (1998). Structure and function of mammalian DNA ligases. *Mutat. Res.* 407, 1–9.

Topisirovic, I., Siddiqui, N., Lapointe, V. L., Trost, M., Thibault, P., Bangeranye, C., Pinol-Roma, S., and Borden, K. L. (2009). Molecular dissection of the eukaryotic initiation factor 4E (eIF4E) export-competent RNP. *EMBO J.* 28, 1087–1098.

Unseld, M., Marienfeld, J. R., Brandt, P., and Brennicke, A. (1997). The mitochondrial genome of *Arabidopsis thaliana* contains 57 genes in 366,924 nucleotides. *Nat. Genet.* 15, 57–61.

Wei, S. J., Botero, A., Hirota, K., Bradbury, C. M., Markovina, S., Laszlo, A., Spitz, D. R., Goswami, P. C., Yodoi, J., and Gius, D. (2000). Thioredoxin nuclear translocation and interaction with redox factor-1 activates the activator protein-1 transcription factor in response to ionizing radiation. *Cancer Res.* 60, 6688–6695.

Welchen, E., and Gonzalez, D. H. (2006). Overrepresentation of elements recognized by TCP-domain transcription factors in the upstream regions of nuclear genes encoding components of the mitochondrial oxidative phosphorylation Machinery. *Plant Physiol.* 141, 540–545.

Xu, F., Morin, C., Mitchell, G., Ackerley, C., and Robinson, B. H. (2004). The role of the LRPPRC (leucine-rich pentatricopeptide repeat cassette) gene in cytochrome oxidase assembly: mutation causes lowered levels of COX (cytochrome c oxidase) I and COX III mRNA. *Biochem. J.* 382, 331–336.

Yogev, O., and Pines, O. (2011). Dual targeting of mitochondrial proteins: mechanism, regulation and function. *Biochim. Biophys. Acta* 1808, 1012–1020.

Conflict of Interest Statement: The authors declare that the research was conducted in the absence of any commercial or financial relationships that could be construed as a potential conflict of interest.

Received: 07 August 2012; paper pending published: 29 August 2012; accepted: 10 September 2012; published online: 25 September 2012.

*Citation: Duchêne A-M and Giegé P (2012) Dual localized mitochondrial and nuclear proteins as gene expression regulators in plants? Front. Plant Sci. **3**:221. doi: 10.3389/fpls.2012.00221*

This article was submitted to Frontiers in Plant Physiology, a specialty of Frontiers in Plant Science.

Copyright © 2012 Duchêne and Giegé. This is an open-access article distributed under the terms of the Creative Commons Attribution License, which permits use, distribution and reproduction in other forums, provided the original authors and source are credited and subject to any copyright notices concerning any third-party graphics etc.

frontiers in
PLANT SCIENCE

ORIGINAL RESEARCH ARTICLE
published: 09 November 2012
doi: 10.3389/fpls.2012.00247

The membrane-tethered transcription factor ANAC089 serves as redox-dependent suppressor of stromal ascorbate peroxidase gene expression

Peter Klein, Thorsten Seidel, Benedikt Stöcker and Karl-Josef Dietz*

Biochemistry and Physiology of Plants, W5-134, Faculty of Biology and CeBiTec, Bielefeld University, Bielefeld, Germany

Edited by:
Tatjana Kleine, Ludwig-Maximilians-Universität München, Germany

Reviewed by:
Wataru Sakamoto, Okayama University, Japan
Stanislaw Karpinski, Warsaw University of Life Sciences, Poland

***Correspondence:**
Karl-Josef Dietz, Biochemistry and Physiology of Plants, W5-134, Faculty of Biology and CeBiTec, Bielefeld University, 33501 Bielefeld, Germany.
e-mail: karl-josef.dietz@uni-bielefeld.de

The stromal ascorbate peroxidase (sAPX) functions as central element of the chloroplast antioxidant defense system. Its expression is under retrograde control of chloroplast signals including redox- and reactive oxygen species-linked cues. The sAPX promoter of *Arabidopsis thaliana* was dissected in transient reporter assays using mesophyll protoplasts. The study revealed regulatory elements up to −1868 upstream of the start codon. By yeast-one-hybrid screening, the transcription factor ANAC089 was identified to bind to the promoter fragment 2 (−1262 to −1646 bp upstream of translational initiation). Upon mutation of the *cis*-acting element CACG, binding of ANAC089 was abolished. Expression of a fused fluorescent protein version and comparison with known endomembrane markers localized ANAC089 to the *trans*-Golgi network and the ER. The transcription factor was released upon treatment with reducing agents and targeted to the nucleus. Transactivation assays using wild type and mutated versions of the promoter showed a partial suppression of reporter expression. The data indicate that ANAC089 functions in a negative retrograde loop, lowering sAPX expression if the cell encounters a highly reducing condition. This conclusion was supported by reciprocal transcript accumulation of ANAC089 and sAPX during acclimation to low, normal, and high light conditions.

Keywords: ascorbate peroxidase, gene expression, redox regulation, retrograde signaling, transcription factor

INTRODUCTION

Photosynthetic metabolism involves light driven electron transfer reactions, production of metabolic intermediates with high reducing potential and the generation of reactive oxygen species (ROS). The photosynthesizing chloroplast is equipped with an intricate redox sensory system, a multilayered antioxidant defense and diverse repair mechanisms to minimize ROS-dependent damage. On the one hand, appropriate sensing allows for using redox and ROS information to adjust photosynthetic metabolism and tune gene expression in the plastids but also in the nuclear genome by retrograde signal transfer from the chloroplast to the nucleus (Baier and Dietz, 2005). Pogson et al. (2008) distinguished retrograde signaling in developmental and operational control. Operational control coordinates nuclear gene expression with the actual needs of photosynthetic metabolism. Analyses of transcriptional dynamics in response to environmental or pharmacological perturbations and elaborated mutant screenings have allowed researchers to pinpoint to signaling cues triggering retrograde signaling in operational control (Leister, 2012). Accumulation of singlet oxygen, changes in redox state of intersystem electron transport chain, redox state of metabolites or proteins as for example thioredoxin downstream of photosystem I, intermediates of chlorophyll synthesis and hormone precursors such as for abscisic acid are linked to specific changes in transcript abundance of nuclear encoded chloroplast proteins (Pfannschmidt, 2010). While ROS generation in the illuminated chloroplast is mostly governed by primary light reactions and counteracted by mechanisms that quench excess excitation energy (Li et al., 2009), ROS are decomposed by high capacity antioxidant systems (Asada, 1999; Dietz et al., 2006).

Superoxide is dismutated by CuZn- and Fe-SOD, and hydrogen peroxide decomposed by thylakoid-bound and stromal ascorbate peroxidase (tAPX, sAPX; Nakano and Asada, 1981) or thiol-dependent peroxidases (Dietz, 2011). It has been estimated that thiol-dependent peroxidase activity reaches about 40% and ascorbate-dependent activity about 60% of total hydrogen peroxide decomposition activity in chloroplasts (Dietz et al., 2006). Both systems are prone to inhibition and thus are subjected to turnover, sAPX and tAPX in particular if ascorbate concentrations are low (Miyake and Asada, 1996). Their expression in the nucleus must be under retrograde control to cope with demand for antioxidant capacity (Oelze et al., 2012).

sAPX and tAPX are encoded by separate nuclear genes in *Arabidopsis thaliana*. Complete deletion of sAPX and tAPX is compensated in *A. thaliana* under regular growth conditions (Kangasjärvi et al., 2008). Symptoms of oxidative stress in these plants develop in stressful environment and in particular during early seedling development. *sAPX* and *tAPX* transcript levels

Abbreviations: 3-AT, 3-amino-1,2,4-triazol; DTT, dithiothreitol; CFP, (enhanced) cyan fluorescent protein; EMSA, electrophoretic mobility shift assay; FRET, Förster/fluorescence resonance energy transfer; MTTF, membrane-tethered transcription factors; ROS, reactive oxygen species; sAPX, stromal ascorbate peroxidase; SOD, superoxide dismutase; TF, transcription factor; YFP, (enhanced) yellow fluorescent protein.

are regulated in dependence on developmental state of the leaves (Pena-Ahumada et al., 2006) and environmental cues, such as light intensity (Oelze et al., 2012). After transfer of low or normal light acclimated *A. thaliana* to 100- or 10-fold higher light intensity, respectively, *sAPX*-mRNA levels start to increase after 30 min and reach a maximum at 3–6 h after transfer to high light (Oelze et al., 2012). In contrast to transcript regulation, sAPX and tAPX protein levels respond much less.

Signaling pathways often innervate transcription factors that modulate target gene expression in response to environmental stimuli (Golldack et al., 2011). However despite the importance of chloroplast ascorbate peroxidases in antioxidant defense, transcription factors involved in their regulation have not been described. Based on transcript regulation it can be assumed, that redox and ROS signals might be involved in regulating *tapx* and *sapx* gene expression. Transcriptome analyses have differentiated $O_2^{\cdot-}$/H_2O_2-dependent regulation from singlet oxygen-dependent regulation (op den Camp et al., 2003). *sAPX* was not among the significantly regulated transcripts responding to methylviologen or to illumination of protochlorophyllide accumulating *flu* mutants (op den Camp et al., 2003). Compensatory retrograde regulation is apparent from knock down lines of *A. thaliana* deficient in the alternative H_2O_2-detoxifying 2-Cys peroxiredoxin (Baier et al., 2000) where *sAPX* and *tAPX* transcripts were up-regulated, and in double knock out of tAPX and sAPX (Kangasjärvi et al., 2008) where 2-Cys peroxiredoxin protein levels were increased. Apparently there is a delicate feedback from the chloroplast antioxidant defense system to nuclear gene expression.

The aim of the study was to approach a better and mechanistic understanding of *sapx* gene expression regulation. The promoter was analyzed for regulatory regions. The transcription factor ANAC089 identified in a yeast-one-hybrid (Y1H) screening was subjected to a more detailed inspection for binding site and regulatory properties. The specific promoter region *sapx2*-1 proved to be responsive to oxidative versus reductive cues by ANAC089. The obtained data indicate a role of ANAC089 as repressor of sapx gene activity under highly reducing conditions where the need for sAPX expression or sAPX turnover might be low.

MATERIALS AND METHODS

PLANT GROWTH AND LIGHT TREATMENT

Arabidopsis thaliana was grown in a growth chamber at a photoperiod of 10 h with 80 µmol quanta m^{-2} s^{-1} and 21°C, and a dark phase of 14 h at 18°C, both at 50% relative humidity. The pots contained Spezialsubstrat (Stender AG, Schermbeck, Germany), Osmocote Start as fertilizer (Scotts Australia PTY Ltd, Bella Vista, Australia), and one tablet of Lizetan (Bayer, Leverkusen, Germany) per L soil. Three week old plants were either transferred to 8 µmol quanta m^{-2} s^{-1} (low light, L-light) or kept at 80 µmol quanta m^{-2} s^{-1} (normal light, N-light) for another 10 days. Then the 4.5 week old plants were exposed to high light (H-light, 800 µmol quanta m^{-2} s^{-1}) 1 h after onset of light (9 am). Control plants were kept in L- or N-light. At 3 p.m. complete rosettes of 4–12 plants from the four treatments were harvested, frozen in liquid nitrogen, and stored at −80°C until further processing.

TRANSCRIPT ANALYSIS

RNA isolation, cDNA synthesis, and semi-quantitative RT-PCR analysis were performed according to Wormuth et al. (2006) using primers as described in **Table 1**. Equal loading of cDNA was adjusted with *ACTIN2* amplificate. Annealing temperatures and amplification cycle numbers were optimized for each target transcript (Oelze et al., 2012).

GENERATION OF YEAST-ONE-HYBRID LIBRARY AND SCREENING

cDNA synthesis, construction of Y1H library and screening were performed using the Clontech Matchmaker system as described in Klein and Dietz (2010). To achieve a wide coverage of conditionally expressed transcripts, RNA was isolated from a set of differentially stress-treated *A. thaliana* seedlings. The treatments were as follows: (1) Control: 1 h at 120 µmol quanta m^{-2} s^{-1}; (2) combined oxidative and high light stress: 1 h at 5 mM H_2O_2 and 1140 µmol quanta m^{-2} s^{-1}; (3) drought stress and high light: 1 h drought and 1140 µmol quanta m^{-2} s^{-1}; (4) heat stress: 1 h at 40°C and 84 µmol quanta m^{-2} s^{-1}; (5) cold and darkness: 1 h at 4°C in darkness; (6) cold in light: 1 h at 4°C and 32 µmol quanta m^{-2} s^{-1}; (7) UV-illumination: 3 × UV for 10 s each with regeneration for 30 min at 120 µmol quanta m^{-2} s^{-1}; (8) dark-light transition: 1 h darkness followed by 30 min 120 µmol quanta m^{-2} s^{-1}; (9) high light: 1 h at about 1100 µmol quanta m^{-2} s^{-1}; and (10) low salt: 1 h at 5 mM NaCl and 1100 µmol quanta m^{-2} s^{-1}. The bait DNA sequence was cloned into the pHis2 vector using the *Sma*I and *Sac*I endonucleases, while the pGADT7-Rec2 was used as the prey vector. Both vectors were cotransformed into yeast strain Y187. Interaction between fusion protein and DNA-sequence was scored on SD medium supplemented with the appropriate amino acids, i.e., SD/-His/-Leu/-Trp. To suppress leaky His3 activity, 3-amino-1,2,4-triazol (3-AT) was added, for the promoter fragments

Table 1 | Oligonucleotide primers used for (a) cloning of the sAPX promotor fragments into the p35SYFP vector using *Bam*HI and *Nco*I restriction sites and (b) transcript analysis.

	Sequence
Promoter fragment	
sAPX-1-for	5′-AAAAAGGATCCTTTCGGACCTGGAGAG-3′
sAPX-2-for	5′-AAAAAGGATCCGCACGTCTAGTGAAAGATCC-3′
sAPX-2-mut-for	5′-AAAAAGGATCCGAAAATCTAGTGAAAGATCC-3′
sAPX-3-for	5′-AAAAAGGATCCTGTCAACCAAGTCGCCTTG-3′
sAPX-5-for	5′-AAAAAGGATCCCCCGTCACCATTACCATC-3′
sAPX-6-for	5′-AAAAAGGATCCCTCTATGGACTTTATTGG-3′
sAPX-rev	5′-AAAAACCCATGGTTCTGAGGGGTATAATAGTAAT-3′
Transcript analysis	
ANAC089-for	5′-ATGGACACGAAGGCGGTT-3′
ANAC089-DB-rev	5′-CAATCAGACGGGCTCCCTG-3′
sAPX-for	5′-ATGCTGCTAACGCTGGTCTT-3′
sAPX-rev	5′-CCTAACGTGTGAGCACCAGA-3′
Actin-2-for (At3g18780)	5′-TTGGTAGGCCAAGACATCAT-3′
Actin-2-rev	5′-GGAGCCTCGGTAAGAAGAAC-3′

sapx2-1 and *sapx2-1$_{mut}$*, the 3-AT concentration was adjusted to 15 mM.

AMPLIFICATION OF *sapx* PROMOTER FRAGMENTS

sapx (At4g08390) promoter fragments were amplified by polymerase chain reaction using the primers listed in **Table 1**. Amplification products were separated by agarose gel electrophoresis, eluted and used for cloning. For transient reporter assays they were fused to EYFP as described in Shaikhali et al. (2008). As reference construct, CFP was fused downstream of the p35S-promoter (Shaikhali et al., 2008). Correctness of constructs was confirmed by DNA sequencing (MWG Biotech, Eberswalde or CeBiTec, Bielefeld, Germany).

RECOMBINANT PRODUCTION OF ANAC089 PROTEIN AND ELECTROPHORETIC MOBILITY SHIFT ASSAY

The *anac089* coding sequence was amplified using forward (ANAC089-for: 5′-AAAAAAGGATCCATGGACACGAAGGCGGTTG-3′) and reverse primers (ANAC089-rev: 5′-AAAAACTCGAGTTCTAGATAAAACAACATTG-3′) and directionally cloned into pET28a vector using *Bam*HI and *Xho*I restriction sites. The vector was transformed into BL21 (DE3) pLysS *Escherichia coli* cells. Following inoculation with preculture the main culture was grown to OD = 0.6, induced with 400 μM isopropyl-β-D-thiogalactopyranoside and further incubated for 4 h. Cells were sedimented, frozen, and thawn, resuspended in lysis buffer (50 mM Na-phosphate buffer, pH 8, 300 mM NaCl, 10 mM imidazole, 1 mg/ml lysozyme), sonified, incubated and cell debris sedimented by centrifugation. The His_6-tagged ANAC089 protein was purified by Ni-nitrilotriacetic acid chromatography (Qiagen, Hilden, Germany). Following washing of loosely bound proteins, ANAC089 protein was eluted with elution buffer (50 mM Na-phosphate buffer, pH 8, 300 mM NaCl, 250 mM imidazole). Recombinant protein was dialyzed against 40 mM K-phosphate buffer, pH 7, using dialysis tubing with 10 kDa cutoff. Protein was quantified with BioRad reagent (BioRad Laboratories, München, Germany) with bovine serum albumin as standard. An electrophoretic mobility shift assay (EMSA) was performed with the DIG Gel Shift Kit (2nd generation, Roche, Mannheim, Germany): target DNA was the sAPX promoter fragment 2-1 at an amount of 8 ng per lane. As indicated unlabeled competitor DNA was added at 2 μg concentration and ANAC089 protein at 100 ng. An additional label free EMSA was performed as well. Here recombinant ANAC089 protein equivalent to 360 μM concentration was incubated with 25 ng promotor fragment *sapx-2* (or *sapx-2$_{mut}$*) in 20 μl EMSA buffer (100 mM HEPES, pH 7.5, 500 mM KCl, 25% glycerol, 5 mM dithiothreitol) at 22°C for 30 min. The assay mix was subsequently loaded on 4% agarose gels and the DNA separated by electrophoresis at 80 V. DNA was visualized by ethidium bromide staining and documented.

CONSTRUCTS FOR FLUORESCENCE MICROSCOPY

ANAC089 was fused to fluorescent proteins for various cell imaging experiments. In each case the enhanced variants of CFP and YFP (ECFP, EYFP) were used for the construction of the vectors. In the following, the short versions CFP and YFP are used in the text. In the transactivation analysis of **Figure 7**, mCherry was fused to ANAC089 (Seidel et al., 2010). The constructs were p35S:CFP:ANAC089, p35S:YFP:ANAC089, p35S:ANAC089:CFP, p35S:ANAC089:YFP, p35S:YFP:ANAC089:CFP, and p35S:mCherry:ANAC089. The cloning strategy included the insertion of the *anac089* gene upstream of the fluorophore gene into the p35S:CFP-NOST and the p35S:YFP-NOST vector using the ANAC089-for (5′-AAAAAAGGATCCAATGGACACGAAGGCGGTTG-3′) and ANAC089-rev (5′-AAAAAACCGGTTCTAGATAAAACAACATTGC-3′) primers for gene amplification. The *anac089* gene was then fused to the vector utilizing the *Bam*HI and *Age*I endonucleases. The p35S:CFP:ANAC089 and p35S:YFP:ANAC089 constructs were created using the ANAC089-for (5′-AAAAAGCGGCCGCATGGACACGAAGGCGGTT-3′) and ANAC089-rev (5′-AAAAAGAATTCTTATTCTAGATAAAACAACA-3′) primers for the gene amplification which was inserted into the vector using the *Not*I and *Eco*RI endonucleases. The generation of the p35S:YFP:ANAC089:CFP construct was performed in two steps. First the *anac089:cfp* hybrid gene was amplified using the p35S:ANAC089:CFP vector as DNA template. The ANAC089-for (5′-AAAAAAGCGGCCGCATGGACACGAAGGCGGTT-3′) and CFP-rev primer (5′-AAAAAGAATTCTTACTTGTACAGCTCGTC-3′) allowed to insert the amplified hybrid gene into the *Not*I and *Eco*RI restriction sites of the p35S:YFP-C vector, resulting in the p35S:YFP:ANAC089:CFP construct. The various p*sAPX*-YFP promoter fragments were generated using the primer combinations from **Table 1**. The deletion fragments were finally cloned into the pEYFP vector. Gos12 was cloned into 35S-CFP-Nost using the oligonucleotides Gos12-*Bam*HI-for (5′-AAAAGGATCCAATGACAGAATCGAGTCTGGAT-3′) and Gos12-*Age*I-rev (5′-AAAAACCGGTGATTTTGAGAGCCAGTAGATGAT-3′). Sar1 (Sar1-*Bam*HI-for 5′-AAAAGGATCCAATGTTCCTGGTGGATTGG-3′; Sar1-*Age*I-rev 5′-TTTTACCGGTCCGTCGATATATTGAGA-3′), and Clathrin light chain (ClathrinLC-*Bam*HI-for 5′-AAAAGGATCCAATGTCGTCAACCTTGAGC-3′; ClathrinLC-*Age*I-rev 5′-TTTTACCGGTCCCAACTTCTCTGTAAC-3′) were cloned into 35S-CFP-NosT and 35S-YFP-NosT using *Bam*HI and *Age*I restriction sites and plasma membrane ATPase AHA1 (AHA1-*Bam*HI-For 5′-AAAAGCGGCCGCATGTCAGGTCTCGAAGAT-3′; AHA1-*Eco*RI-rev 5′-TTTTTGAATTCTACACAGTGTAGTGATG-3′) was cloned into 35S-CFP-C and 35S-YFP-C, respectively, using *Not*I and *Eco*RI restriction sites. Emissions of fused fluorescent protein in cotransfection or transactivation experiments were quantified in the appropriate detector channel of the confocal laser scanning microscope as described in Shaikhali et al. (2008).

REDOX REGULATION OF THE sAPX PROMOTER

Protoplasts were prepared from At7 cell suspension culture of *A. thaliana* (Seidel et al., 2010). Five days after passage to new medium, cells were sedimented, washed in 50 ml 240 mM $CaCl_2$, digested and transfected with *sapx*:YFP promoter constructs as described in Seidel et al. (2004). After incubation at 26°C in darkness for 16 h the different batches were adjusted to the final H_2O_2 concentration of 5 mM and DTT of 10 mM, respectively, or left as controls and incubated for further 2 h in darkness at 26°C for 16 h. The relative YFP and CFP emission intensities were measured using the confocal laser scanning microscope (Leica SP2

Heidelberg, Germany). Finally, out of those three different samples the YFP/CFP was calculated.

CELL IMAGING OF SUBCELLULAR ANAC089 LOCALIZATION AND PROCESSING

Protoplasts prepared from the At7 cell suspension culture were transfected either with the construct combination 35S:ANAC089:CFP and 35S:ANAC089:YFP or 35S:CFP:ANAC089 and 35S:YFP:ANAC089. Homodimerization of ANAC089 *in vivo* was analyzed by Förster resonance energy transfer (FRET; Seidel et al., 2005). Fluorescence of single protoplasts was imaged with a confocal laser scanning microscope (Leica SP2, Heidelberg, Germany). Calculation of FRET efficiency was done as described in Seidel et al. (2005).

BIOINFORMATIC ANALYSIS OF PROMOTER SEQUENCES AND AMINO ACID SEQUENCES

sapx promoter sequences were searched for the presence of putative *cis*-elements with the program Matinspector[1]. The promoters of 27416 *A. thaliana* genes with a length of 3000 bp were downloaded from TAIR[2] and screened for the ATGCACGTC motif allowing for 1 bp mismatch with the program CLC Main Workbench[3]. Search for transcripts co-expressed with *sAPX* was performed using the online tool offered at http://www.arabidopsis.leeds.ac.uk/act/coexpanalyser.php. Cleavage site prediction of ANAC089 was performed with ProP1.0[4] and resulted in two hits, a peculiar Arg/Lys-specific site at amino acid position 163 and a second site at position 297 just close to the membrane spanning α-helix based on prediction from mammalian protease processing sites.

RESULTS

The promoter region of *sapx* was cloned as assumed full length or truncated form and fused to enhanced yellow fluorescent protein (YFP) as reporter gene. The selected *sapx1* DNA sequence started from −1868 bp upstream of the translational initiation site down to −1, *sapx3* from −1321 to −1, *sapx5* from −691 to −1 and *sapx6* from −263 to −1. At7-protoplasts were co-transfected with these EYFP reporter constructs simultaneously with a p35S:CFP construct as reference to correct for variable expression levels. The normalized ratios of YFP/CFP were calculated and plotted against the DNA fragment length (**Figure 1**). Transcriptional enhancers were present in all segments since reporter activity decreased with each truncation. H_2O_2 stimulated expression driven by each fragment significantly.

Since the data of **Figure 1** did not reveal a clear and restricted redox regulation site, the *sapx* promoter was fragmented into five overlapping segments (**Figure 2**) and used for a Y1H screening. 3-AT concentrations to suppress for leaky *His3*-expression without transactivator were adjusted for each construct and were within recommended concentration range for *sapx1* and *sapx2* with 15–20 mM, and already quite high for *sapx3* and *sapx4* (80 and

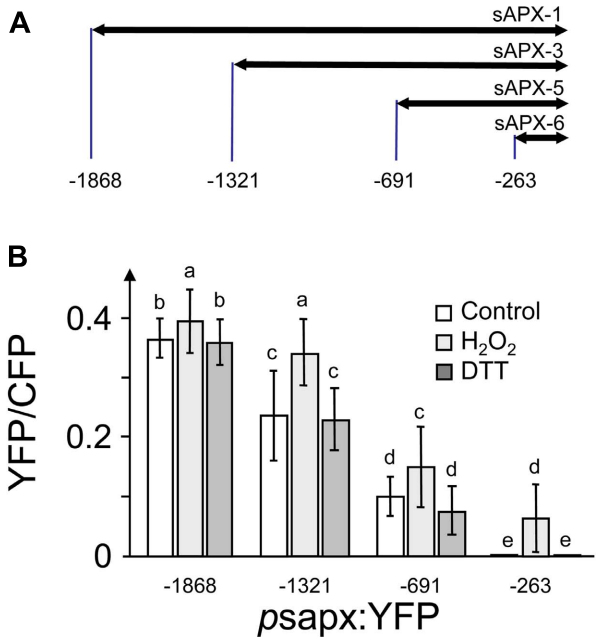

FIGURE 1 | Deletion fragments of the *sapx* promoter constructed for promoter activation assay in *A. thaliana* protoplasts. (A) Schematics of the *sapx* promoter fragments. **(B)** Expression of the YFP reporter gene fused downstream to the *sapx* promoter deletion fragments under control, oxidizing (5 mM H_2O_2) and reducing conditions (10 mM DTT) normalized to CFP accumulation under control of the 35S promoter. (1) Promoter fragment p*sapx1*; (2) promoter fragment p*sapx3*; (3) promoter fragment p*sapx5*; and (4) promoter fragment p*sapx6*. Intensities of CFP and YFP were quantified in the respective emission channels of the CLSM (Shaikhali et al., 2008). The results are means ± SD of 60–80 protoplasts. Different letters mark groups of significant difference with $p < 0.05$ (Student's *t*-test).

110 mM, respectively). The *sapx5* fragment remained leaky even at >120 mM 3-AT. This may explain why reliable and specific binding of promising candidates could not be observed for *sapx3* to *5*. Among the many positive clones only the gene encoding ANAC089 (At5g22290) which was identified as activator of *sapx2* fragment driven reporter expression in yeast appeared promising for further analysis. Retransformation of yeast cells with isolated bait and prey vectors reproduced the interaction between ANAC089 and *sapx2*. Bioinformatic analysis identified two potential binding sites for NAC transcription factors in *sapx2* (sequence position −1646 till −1431, original sequence: GCACGTCTAGTGAAAGATCC, mutated sequence: GAAAATCTAGTGAAAGATCC; second possible binding site was the motive CATCCC at −1627 till −1622). Subcloning confined the transactivation to the *sapx2-1* fragment of 216 bp length (**Figure 2B**, C1) and mutation of the upstream located CACG motif to AAAA (position −1645 to −1642) abolished transactivation of *HIS3* reporter in the *sapx2-1*$_{mut}$:*HIS3* reporter construct after cotransfection with ANAC089 (**Figure 2**, C3).

Analysis of the *in silico* translated cDNA allowed the identification of the N-terminal NAC domain and a putative C-terminal membrane anchor (**Figure 3A**). ANAC089 protein was recombinantly expressed in *E. coli* as His_6-tagged protein and purified by Ni-affinity chromatography (**Figure 3B**). Binding of

[1]http://www.genomatix.de

[2]ftp://ftp.arabidopsis.org

[3]http://www.clcbio.com/

[4]http://www.cbs.dtu.dk/services/ProP/

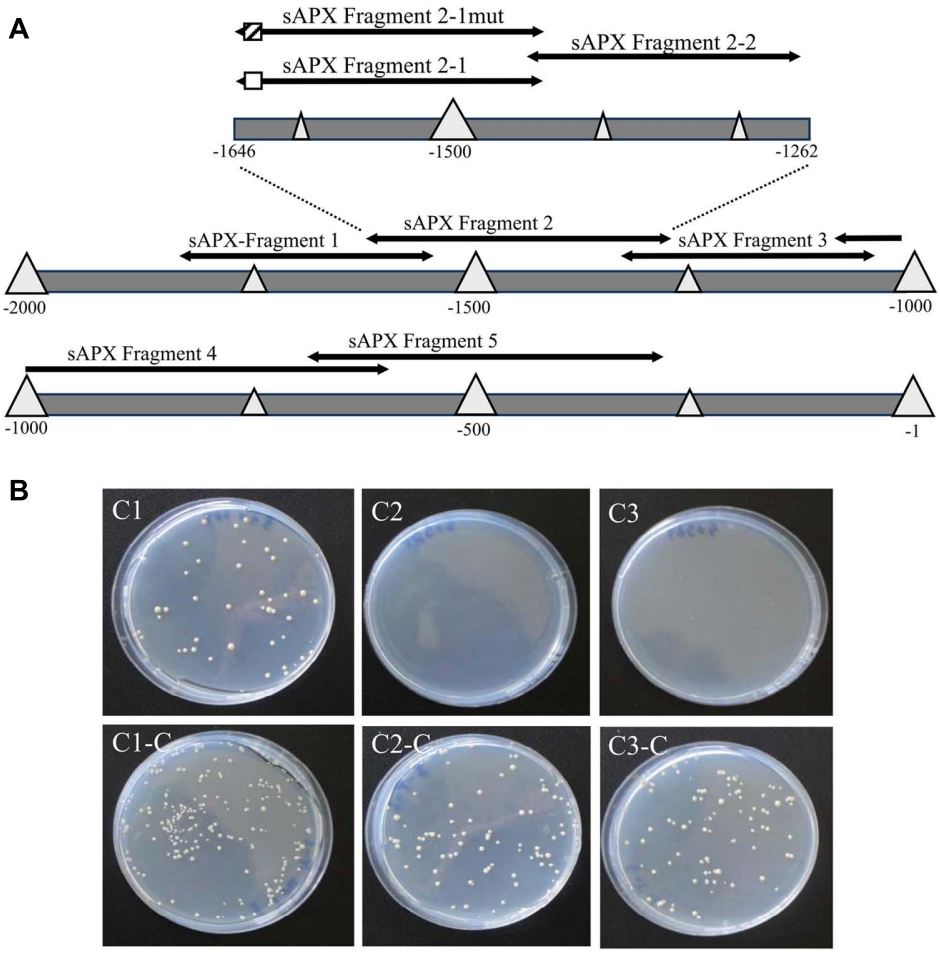

FIGURE 2 | Schematics of the promoter of *sapx* used for yeast-one-hybrid screening and binding to the specific *cis*-element. **(A)** Fragment p*sapx1* (−1563 to −1868 bp); p*sapx2* (−1262 to −1646 bp); p*sapx3* (−954 to −1321 bp); p*sapx4* (−609 to −1018 bp); p*sapx5* (−246 to −691 bp); p*sapx6* (−1 to −263 bp). Division of p*sapx2* for localization of the ANAC-binding *cis*-element: pHis2:*sapx2*-1/mut (−1432 bis −1646), pHis2:*sapx2*-2 (−1432 bis −1451). The potential target element for binding of ANAC089 is marked as hatched and the mutagenized region in white box. **(B)** Experimental identification of the binding site of ANAC089 within promoter segment pHis2:*sapx2* using the Y1H system on SD/-Trp/-His/-Leu/+3 AT selective medium (C1, C2, C3) and for control on SD/-Trp/-Leu selective medium (C1-C, C2-C, C3-C). (C1) p His2:*sapx2*-1; (C2) pHis2:*sapx2*-1mut; and (C3) p His2:*sapx2*-2. All cells grew under non-stringent selection showing their viability, while under stringent conditions only the cells grew that were harboring the wild type sapx2-1 fragment and expressing ANAC089.

His_6-ANAC089 to *sapx2-1* promoter fragment *in vitro* was studied using the EMSA (**Figure 3C**). A shift was seen upon addition ANAC089 protein and the shift was abolished upon addition of 250-fold excess competitor DNA. Mutation of the binding site abolished the ANAC089-dependent gel shift (not shown).

At7 protoplasts were transfected with constructs of p35S:ANAC089:CFP and p35S:ANAC089:YFP (**Figure 4**). Both constructs were co-expressed and the reporter fluorescence was observed in the plasma membrane and membrane vesicles (**Figures 4B,C**). Analysis for protein–protein interaction by FRET between the CFP- and YFP-fused ANAC089 revealed homooligomer formation (**Figure 4G**). FRET efficiency was significantly above the threshold which was defined as 10% from transfection results with free CFP and YFP (Seidel et al., 2005). FRET was higher if CFP and YFP were fused to the N-terminus of ANAC089. In this case, the fluorophore must have rested in the cytosol. Apparently, also the membrane-associated transcription factor is able to oligomerize. FRET between CFP:ANAC089 and YFP:ANAC089 was at about 28%, whereas the fusion the CFP and YFP fluorophores to the C-terminus of the ANAC089 resulted in 14% FRET efficiency, a value also above the threshold. Lower FRET might be explained by steric constraints, higher distance, or less stable interaction at the C-terminus of ANAC089 and cannot be distinguished by this *in vivo* method.

ABI5, a transcription factor with established localization in the nucleus (Lopez-Molina et al., 2003), was used as a control (**Figure 4F**) and accumulated at a site distinct to ANAC089. Analysis of the coding region with the program TMHMM Server v. 2.0 at http://www.cbs.dtu.dk/services/TMHMM-2.0/ allowed for the identification of a putative transmembrane domain at the C-terminus (**Figure 4H**, see also **Figure 3A**). ANAC089 has been reported before to be a member of a subgroup within the family of

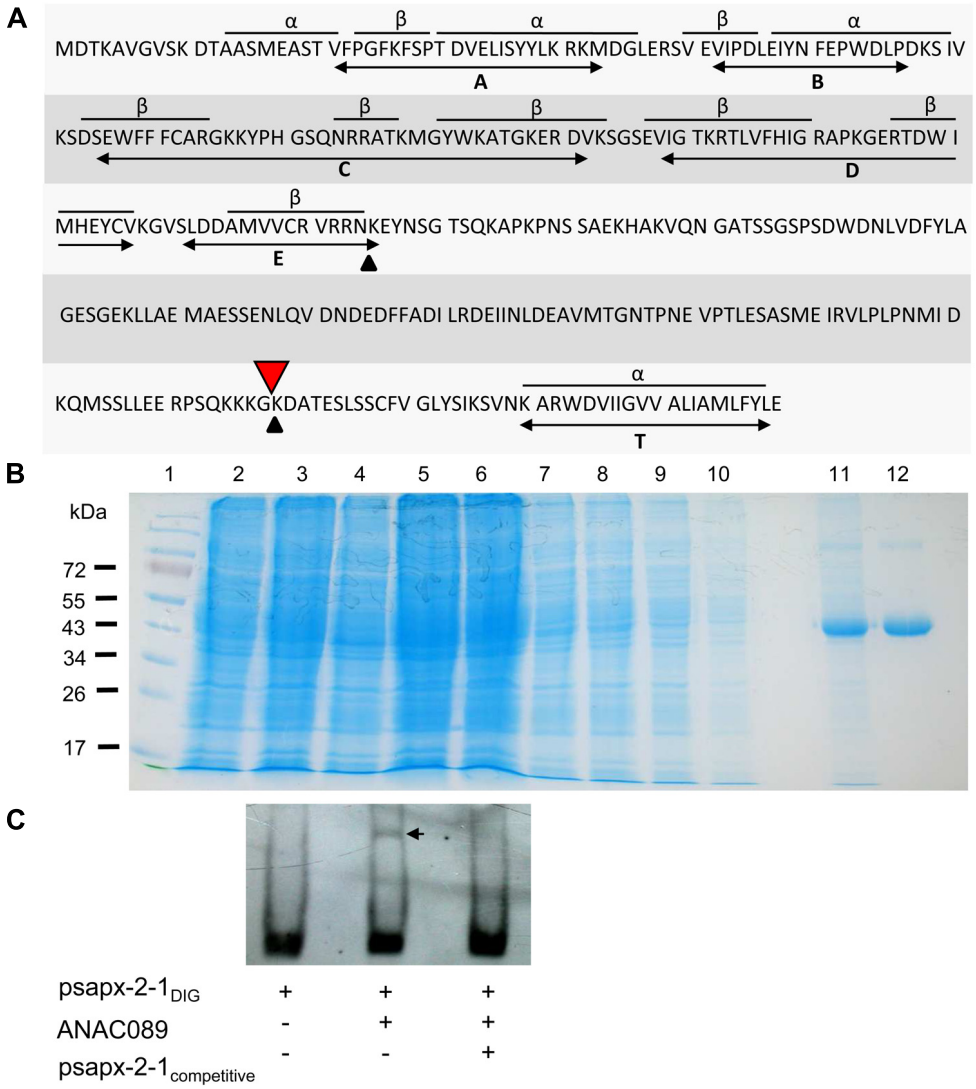

FIGURE 3 | Structure of ANAC089, generation of recombinant His_6-ANAC089 and EMSA. (A) Primary structure of the ANAC089 transcription factor. The N-terminal ANAC domain consists of three α-helices and eight β-sheets in conserved arrangement (A–E). The bioinformatically predicted transmembrane α-helix (T) of the ANAC089 protein is localized at amino acid position 319–339. Putative protein cleavage sites are indicated with arrows. His_6-ANAC089 was expressed in *E. coli* and purified by Ni-NTA affinity chromatography. **(B)** Heterologous expression and purification of His6-tagged ANAC089. The recombinant ANAC089 protein was expressed in BL21 (DE3) pLysS *E. coli* cells which were induced with 400 μM isopropyl-β-D-thiogalactopyranoside for 4 h. By SDS PAGE the time-dependent expression of the recombinant ANAC089 protein, as well as the purification process was analyzed. (1) Prestained protein ladder (Fermentas); (2) 0 h after IPTG induction; (3) 2 h after IPTG induction; (4) 4 h after IPTG induction; (5) cell extract; (6) cell pellet; (7–10) column wash fractions; (11) first fraction of ANAC089 elution; and (12) second fraction of ANAC089 elution. **(C)** Electrophoretic mobility shift assay: ANAC089 promoter fragment interaction *in vitro* using the DIG Gel Shift Kit (2nd generation, Roche). Verification of the specificity of ANAC089 binding to the *cis*-element within the sAPX promoter fragment 2-1. Promoter fragment psapx2-1 was loaded at 8 ng DNA. The amount of unlabeled competitor was 2 μg DNA. ANAC089 protein was added at 100 ng. The arrow head marks the shifted band.

NAC transcription factors which is tethered to membranes (Kim et al., 2007). Incubation of transfected protoplasts with dithiothreitol (10 mM) showed time-dependent release of ANAC089 from the membrane and translocation to the nucleus when the fluorophore was fused to the N-terminus of the transcription factor (**Figures 5A–F**). ANAC089 lacking the C-terminal membrane domain localized to the nucleus similar to the nuclear transcription factor ABI5 (**Figures 5G–I**). ANAC089 remained tethered to the membrane under oxidizing conditions established by addition of 10 mM H_2O_2 to the protoplast suspension (**Figures 5K–M**). The next experiment addressed the question whether the carboxyterminus rests at the peripheral membranes after cleavage. The protoplasts were transfected with the triple fusion construct YFP:ANAC089:CFP (**Figures 5N–P**). Following treatment with DTT, the released YFP:ANAC protein accumulated in the nucleus, while the CFP fused to the carboxyterminus of ANAC stayed at the membrane despite the reductive treatment of the protoplasts.

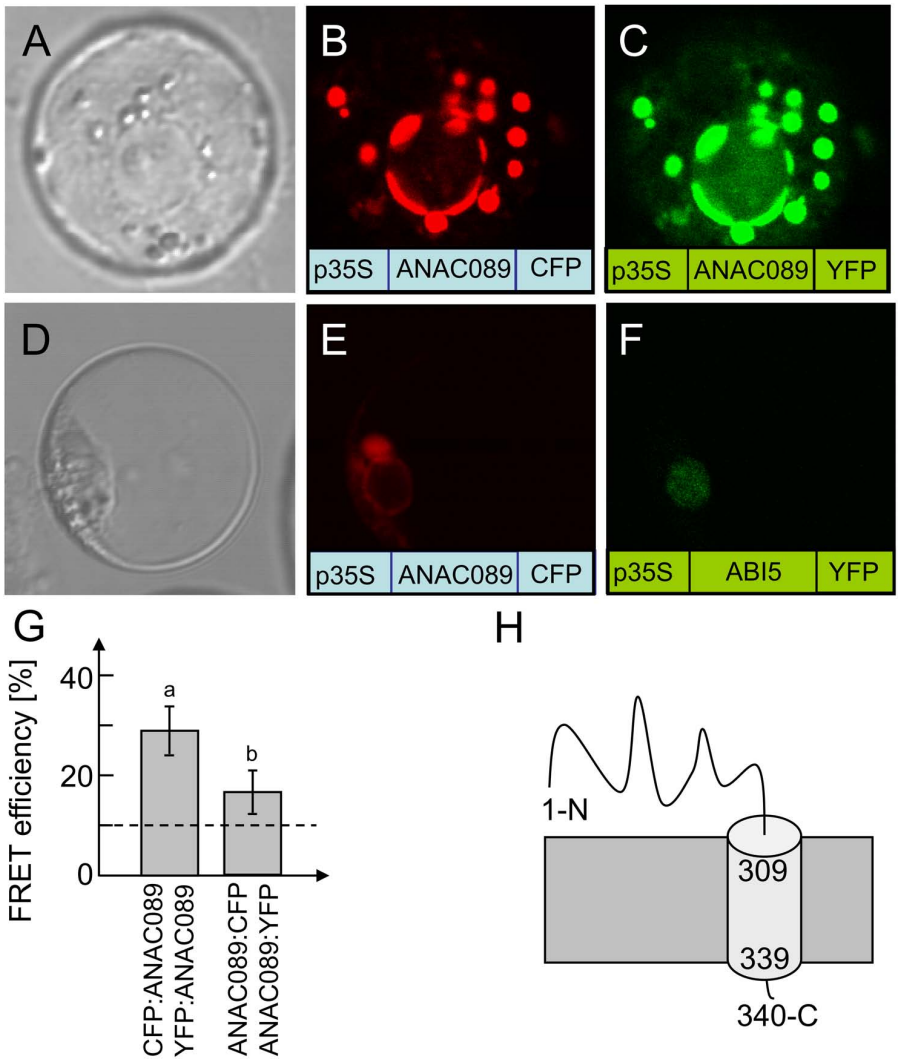

FIGURE 4 | Subcellular localization of ANAC089 in *A. thaliana* protoplasts. (A) Protoplast in bright field. Fluorescence image of a protoplast expressing the C-terminally CFP-tagged ANAC089 **(B)** or the C-terminally YFP-tagged ANAC089 **(C)**. Comparative localization of ANAC089 und ABI5 with C-terminally fused fluorophores in *A. thaliana* protoplasts. **(D)** Bright field control picture. **(E)** ANAC089-CFP-signal detected in vesicles, endoplasmic reticulum, and plasmamembrane. **(F)** ABI5-YFP-signal in cell nucleus. **(G)** Dimerization detection by FRET analysis: protoplasts were co-transfected with either CFP:ANAC089 and YFP:ANAC089:YFP (left column) or ANAC089:CFP and ANAC089:YFP (right). In both cases significant FRET above the threshold of co-expressed free CFP and YFP could be detected (mean ± SD, $n > 60$ protoplasts, three transfections). **(H)** Putative topology of ANAC089 in the membrane.

The membrane localization of the membrane-anchored ANAC089 was investigated in more detail in protoplasts co-transfected with a set of marker proteins for compartments of the secretory pathway (Uemura et al., 2004; Hanton et al., 2008; Neubert et al., 2008; Seidel et al., 2008; Hwang and Robinson, 2009; **Figure 6**). No co-localization was seen with the plasmamembrane H^+-ATPase and the Golgi SNARE Gos 12 (**Figures 6A–C,Q–S**), while VHA-e and Vma21a (**Figures 6G–I**) showed a high degree of co-localization with ANAC089, respectively (**Figures 6D–F**). All other marker proteins, the light chain of Clathrin (CLAT; **Figures 6K–M**) and Sar1 (**Figures 6N–P**) showed only partial co-localization. The data are consistent with a preferred localization of ANAC089 in the *trans*-Golgi network and in the ER.

The regulatory effect of ANAC089 on *sapx* gene expression was studied in transactivation assays (**Figure 7**). *A. thaliana* mesophyll protoplasts were transfected with (i) a reference constructs expressing CFP under the control of the 35S-promoter, (ii) the *yfp* gene placed under control of the *psap2-1* and *psap2-1*$_{mut}$ promoter sequences as transactivation reporter, and (iii) and the construct ANAC089:mCherry as transcriptional modifier. mCherry was fused to the C-terminus of the ANAC089 to check for expression of the *anac089*-gene in transfected protoplasts. The ratio of YFP to CFP was constant in protoplasts transfected with all combinations except for the cells containing the wild type *psap2-1* promoter and expressing ANAC089. Here a significant suppression of YFP reporter intensity by 25% was observed. This suppression was not

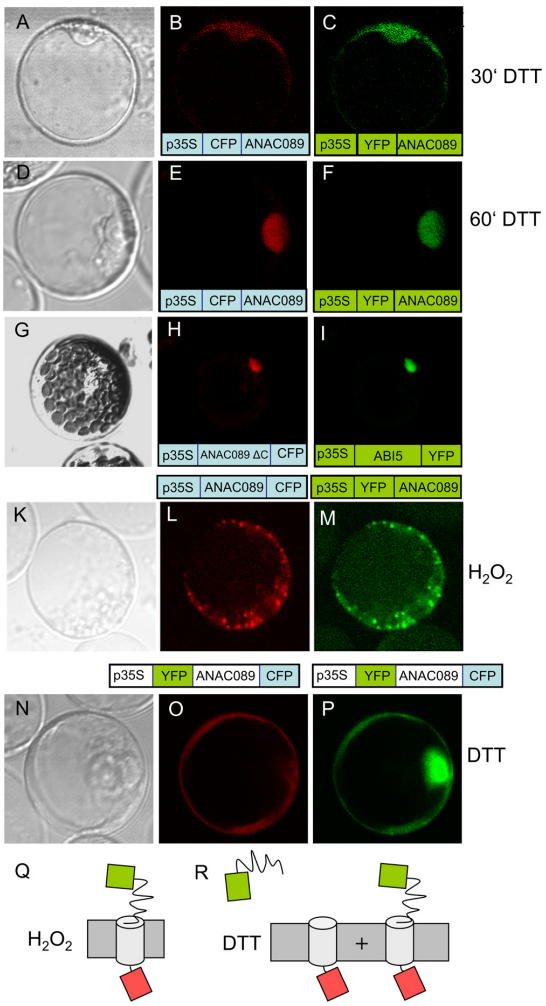

FIGURE 5 | Redox-dependent dynamics of ANAC089 localization. (A–F) Time-dependent localization of ANAC089 was documented following a treatment with dithiothreitol (10 mM DTT). Images were taken at $t = 30$ min **(A–C)** and $t = 60$ min **(D–F)**. **(A, D)** Bright field image. **(B, E)** Fluorescence signal of N-terminally fused CFP (ANAC089-CFP). **(C, F)** Fluorescence signal of N-terminally fused YFP (ANAC089-YFP). **(G–I)** Nuclear accumulation of ANAC089 lacking the transmembrane domain. Protoplasts were transformed with the 3′-truncated ANAC089 coding for a variant that lacks the C-terminal membrane domain (total remaining length 298 aa, see **Figure 3A**, red arrow). In parallel the protoplasts were transformed with ABI5 expression construct. Both fluorophore-fused proteins localized to the nucleus. **(K–M)** Localization of N-terminally fused fluorophores in response to H_2O_2. Protoplasts of *A. thaliana* were treated with 5 mM H_2O_2 for $t = 60$ min. **(K)** Bright field. **(L)** ANAC089:CFP-signal. **(M)** ANAC089:YFP-signal. **(N–P)** Translocation of ANAC089 to the nucleus following reductive activation with 10 mM DTT for 60 min. In this case a double fusion was used, namely YFP:ANAC089:CFP under control of the p35S. **(N)** Bright field image. **(O)** CFP signal of the membrane-associated domain. **(P)** YFP signal of the cleaved N-terminal domain of the ANAC089-YFP in the nucleus. The transfection experiments were repeated three times with 70–90% of the successfully transformed protoplasts showing the same result. **(Q,R)** Schematics of underlying model explaining release of YFP to the nucleus following cleavage: CFP in each case rests at the membrane due to its fusion to the membrane-residing helix. The N-terminally fused YFP also rests at the membrane under oxidizing conditions **(M)**, or is partially or fully released with time under reducing conditions which cause cleavage of the ANAC089 domain from the membrane anchor **(P)**.

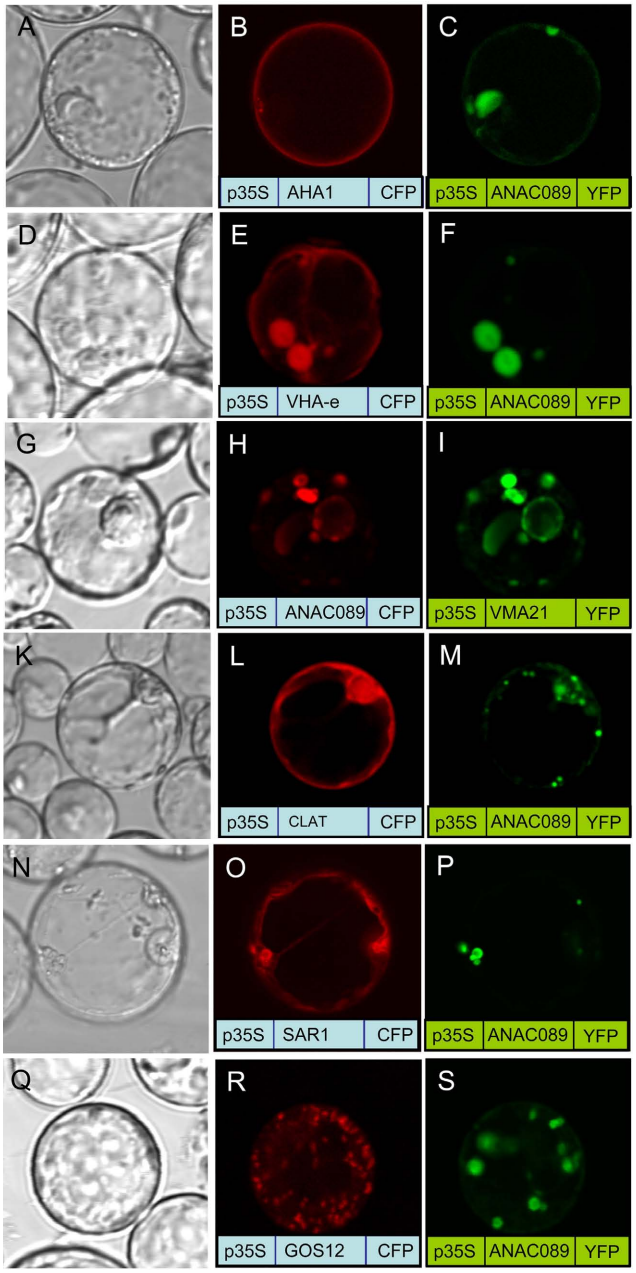

FIGURE 6 | Co-localization of fluorophore-fused ANAC089 with marker proteins. Protoplasts were co-transfected with ANAC089 fused to either CFP or YFP as indicated and a marker protein as follows: **(A–C)** AHA1, the plasmamembrane H^+-ATPase, **(D–F)** VHA-e, a subunit of the V_0 domain of V-ATPase that localizes to TGN/EE, **(G–I)** VMA21a, an ER-resident assembly factor of the V-ATPas, **(K–M)** Clathrin, the light chain of the clathrin coat, **(N–P)** Sar1, the small GTPase of COP II vesicle transport anterograde transport between ER and Golgi, and **(Q–S)** GOS12, a Golgi SNARE.

detected in protoplasts transfected with the mutated promoter proving the importance of the CACG-element in the suppressive regulation. The same suppressive effect was detected when using the full length *sapx* promoter in the absence or presence of co-expressed ANAC089 (**Figure 7B**).

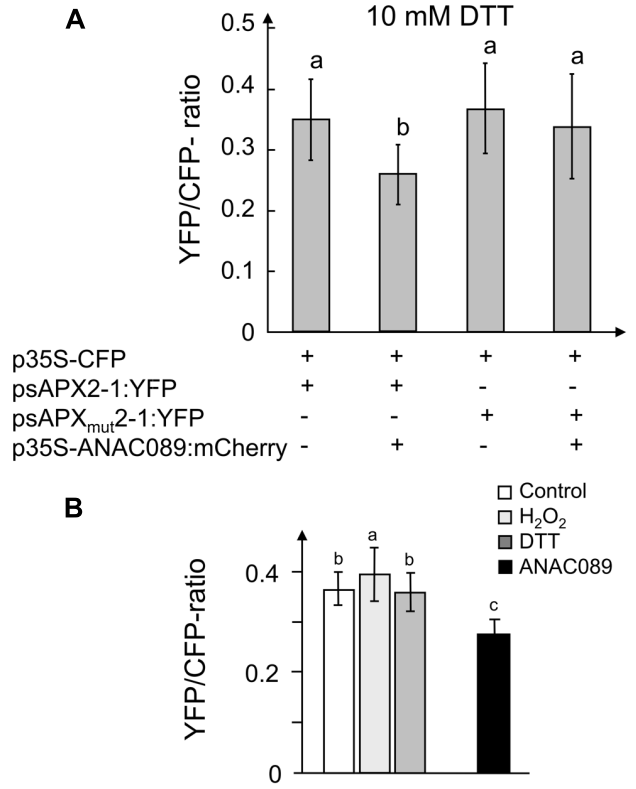

FIGURE 7 | Effect of overexpressed ANAC089 on reporter gene expression and confirmation of involved *cis*-element CACG. (A) (1st bar) Co-transformation of fragment p*sapx2*-1:YFP with 35S-CFP. (2nd bar) Co-transformation of p*sapx2*-1:YFP with 35S-ANAC089-mCherry and 35S-CFP. (3rd bar) Co-transformation of p*sapx2*-1mut:YFP with 35S-CFP. (4th bar) Co-transformation of p*sapx2*-1mut with 35S-ANAC089-mCherry and 35S-CFP. Prior to the measurement protoplasts were incubated with 10 mM DTT for 2 h. The result represent means ± SD from two experiments with a total $n > 30$ protoplasts per construct. **(B)** A similar effect was seen if the full length promoter (−1 to −1868) was used. The first three columns are as in **Figure 1** (expression in control, H_2O_2, or DTT-treated protoplasts), the set of three columns on the left hand side represent reporter strength under control conditions, in the presence of H_2O_2 and DTT, respectively, the fourth column shows the result with co-expressed p35S:ANAC089. The data are means ± SD from 68, 56, 56, 72, 74, and 83 protoplasts (from left to right column). Different letters indicate significant difference at $p < 0.05$ (Student's *t*-test).

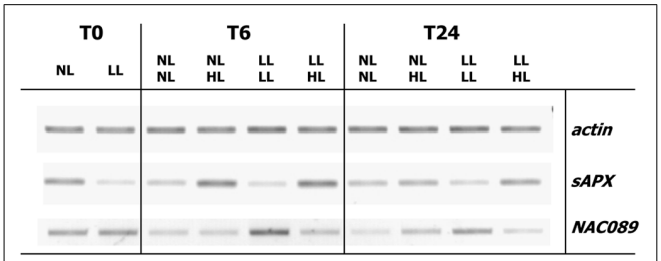

FIGURE 8 | Regulation of sAPX and ANAC089 transcript amounts in a light shift experiment. *A. thaliana* were grown for 3 weeks in normal light, either maintained under this condition for another 10 days (80 μmol quanta m^{-2} s^{-1}, N-light) or acclimated to very low light (8 μmol quanta·m^{-2} s^{-1}, L-light) for 10 days. The plants were transferred to high light (800 μmol quanta m^{-2} s^{-1}, H-light). Rosettes were harvested at $t = 0$, after 6 or 24 h. RNA was isolated and processed as described by Oelze et al. (2012). Semiquantitative RT-PCR was performed following cDNA synthesis. DNA products were separated by agarose gel electrophoresis and visualized by ethidium bromide staining. Band intensity indicates relative abundance of transcripts.

Finally the relationship between *anac089* and *sapx* gene expression was studied in *A. thaliana* rosettes subjected to a light shift treatment similar to the experiment described in Oelze et al. (2012). Plants fully acclimated to a shady growth condition for 10 days (8 μmol quanta·m^{-2} s^{-1}) or grown under normal growth conditions (80 μmol quanta·m^{-2} s^{-1}) were transferred to high light (800 μmol quanta·m^{-2} s^{-1}) for 6 h. This treatment is known to induce strong regulation of *sAPX* transcript amounts (Oelze et al., 2012). *sAPX* and *ANAC089* transcript amounts were semiquantified and normalized to *ACTIN2* transcript amounts (**Figure 8**). While *sAPX*-mRNA levels were higher in normal light grown plants than in low light acclimated ones, they increased upon transfer to high light. The response was stronger 6 h after transfer than after 24 h. *ANAC089* mRNA levels behaved in a roughly inverse manner. They were high when *sAPX* transcript levels were low and *vice versa*.

In the last step, the presence of the *cis*-element binding ANAC089 in sAPX promoter was searched in the whole *A. thaliana* genome. To this end the frequency of the putative ANAC *cis*-element ATGCACGTC identified by Matinspector with a score of 0.979 was investigated in the whole *A. thaliana* genome. The promoters of 27416 *A. thaliana* genes with a length of 3000 bp were downloaded from TAIR[5] and screened for the ATGCACGTC motif with the program CLC Main Workbench[6]. The fully conserved ATGCACGTC motif was found in 196 promoters, either in forward or reverse orientation. In 6903 promoters the motif was present with a single nucleotide exchange. *sAPX* co-expression was analyzed at http://www.arabidopsis.leeds.ac.uk/act/coexpanalyser.php and the 1400 most co-expressed genes were compared with the identified ANAC *cis*-element containing promoters. The obtained list contains candidate genes that might be partially co-regulated with sAPX based on the presence of the ATGCACGTC motif (**Table 2**). Among the genes containing the ATGCACGTC motif (one mismatch allowed) with a co-expression *p*-value > 0.5 are many candidates that show a functional link to stress acclimation and redox metabolism like glutathione reductase, flavonoid biosynthesis enzymes or mitochondrial function.

DISCUSSION

This work identified and describes the transcription factor ANAC089 as a negative regulator of *sapx* expression (**Figure 7**). The *A. thaliana* genome encodes close to 2,000 putative transcription factors (Iida et al., 2005). The plant-specific NAC transcription factor family comprises about 110 genes in *A. thaliana*. Their usually N-terminally conserved NAC domain of about 60 amino acids was first identified in the three representatives named NAM (no apical meristem), ATAF1/2 and CUC2 (cup shaped cotyledon;

[5]ftp://ftp.arabidopsis.org

[6]http://www.clcbio.com/

Table 2 | Bioinformatic identification of genes that carry the ATGCACGTC motif in their promoter and co-expressed with *sAPX*.

Identifier	*p*-value	*r*-value	Function
AT4G33520	0.628337	$8.9e^{-37}$	Metal-transporting P-type ATPase
AT3G29200	0.611953	$1.8e^{-34}$	Chorismate mutase, chloroplast (CM1)
AT3G55120	0.594613	$3.6e^{-32}$	Chalcone–flavanone isomerase
AT3G24170	0.592559	$6.6e^{-32}$	Glutathione reductase, putative
AT2G45440	0.585632	$4.9e^{-31}$	Dihydrodipicolinate synthase 2 (DHDPS2)
AT1G63290	0.569233	$4.8e^{-29}$	Ribulose-phosphate 3-epimerase, cytosolic, putative
AT4G16265	0.560068	$5.5e^{-28}$	DNA-directed RNA polymerase II, putative
AT1G18320	0.559598	$6.3e^{-28}$	Mitochondrial import inner membrane translocase subunit Tim17
AT3G17609	0.551960	$4.5e^{-27}$	bZIP transcription factor/HY5-like protein (HYH)
AT3G06680	0.544932	$2.7e^{-26}$	60S ribosomal protein L29 (RPL29B)
AT3G49180	0.530617	$8.8e^{-25}$	Transducin family protein/WD-40 repeat family
AT5G44160	0.528320	$1.5e^{-24}$	Zinc finger (C2H2 type) family protein
AT2G20450	0.523633	$4.5e^{-24}$	60S ribosomal protein L14 (RPL14A)
AT2G26380	0.522760	$5.6e^{-24}$	Disease resistance protein-related/LRR protein
AT5G59850	0.519257	$1.3e^{-23}$	40S ribosomal protein S15A
AT3G10530	0.519230	$1.3e^{-23}$	Transducin family protein/WD-40 repeat family
AT5G20600	0.514334	$3.8e^{-23}$	Expressed protein
AT5G50810	0.513390	$4.7e^{-23}$	Mitochondrial import inner membrane translocase TIM8
AT5G15910	0.512829	$5.4e^{-23}$	NAD(P)-dependent steroid dehydrogenase, related
AT2G23350	0.512790	$5.4e^{-23}$	Polyadenylate-binding protein, putative/PABP, putative
AT2G17270	0.510441	$9.2e^{-23}$	Mitochondrial substrate carrier family protein
AT4G36020	0.508859	$1.3e^{-22}$	Cold-shock DNA-binding family
AT1G60850	0.507399	$1.8e^{-22}$	DNA-directed RNA polymerase, putative

Following a genome-wide search with the ATGCACGTC motif, the hits were compared with the promoters of sAPX-co-regulated transcripts. The list gives the results with a p-value >0.5.

Jensen et al., 2010). The NAC domain contains the DNA binding domain, dimerization domain and nuclear localization sequence (Ernst et al., 2004). ANAC089 possesses all these features in its N-terminus.

NAC transcription factors have been shown to be involved in developmental processes, hormonal signaling and responses to abiotic and biotic stresses (Hu et al., 2010). Interestingly, several members of the NAC transcription factor family possess transmembrane anchors. They belong to the membrane-tethered transcription factors (MTTFs). The membrane-associated form is inactive by immobilization. Their proteolytic processing releases the functional TF. The transcript level of *NAC-MTTFs* often is up-regulated under conditions of abiotic stress or in the presence of hormones (Kim et al., 2006). Here it is shown that ANAC089 fusion protein localizes to vesicle-like structures and peripheral membranes. This is in line with the report by Li et al. (2010) showing similar localization. Upon its reductive release from the membrane ANAC089 localized to the nucleus (**Figure 5**). Thus our experiments provide evidence for a signaling cue that triggers its release and gives evidence for process dynamics. The almost exclusive nuclear localization after 60 min in this study was identical to images recorded after expressing a C-terminally truncated variant, ANAC089ΔC containing amino acids 1 to 310 (Li et al., 2010) and could be confirmed in our cell system after expressing a C-terminally truncated version of ANAC089 lacking the transmembrane domain. Our data indicate that a reductive stimulus is involved in release of the functional TF.

A critical element in the proposed signaling pathway is the protease that releases ANAC089 from the membrane. Conditional proteolysis which is hypothetical at present would allow for rapid transcriptional response to a changing environmental or developmental cue. Up to now, the molecular entities shedding the TFs from their membrane in plants are unknown. In the case of another NAC-MTTF named NTM1, the calpain inhibitor ALLN prevented cleavage from the membrane. Since ALLN specificity is not high, the precise nature of the involved protease remains to be established (Kim et al., 2006). The ANAC089 sequence contains two predicted cleavage sites; a peculiar Arg/Lys-specific site at amino acid position 163 (VVCRVRR|NK) with a high probability and a second site with lower score at position 297 (RPSQKKK|GK) just close to the membrane spanning α-helix based on mammalian protease processing sites (**Figure 3**). About 3% of all *A. thaliana* genes code for proteases (Garcia-Lorenzo et al., 2006) most of which have not been analyzed in any detail. The chloroplast serine

Deg1 protease is activated under reductive conditions. It is suggested to localize to the thylakoid membrane and contains many Cys residue, e.g., 10 Cys in *A. thaliana* (Ströher and Dietz, 2008). Deg proteases function as ATP-independent serine endopeptidases and are found in different organelles and the nucleolus (Deg9) but not in the cytosol or at the endomembranes (Schuhmann and Adamska, 2012). Thus they may serve as examples of principle but unlikely are involved in releasing ANAC089 from their endomembrane attachment site. Three *Arabidopsis* Cys proteases have been shown to be inhibited by binding to protein disulfide isomerase and activated *in vitro* after addition of DTT. The active Cys proteases are involved in cell type-specific programmed cell death in the endothelium of developing seeds (Ondzighi et al., 2008). Thus in addition to the more frequently described oxidative activation of proteases, the given examples reveal that reductive activation of specific proteases as hypothesized here occurs *in planta* as well. The cleavage sites in ANAC089 are predicted for serine proteases of the furin type which are also found in plants. In addition to redox-dependent activation of the protease by disulfide reduction or release from binding partners, a third type of redox regulation might be achieved by burying the cleavage domain of the substrate protein ANAC089 either by conformational changes or posttranslational modifications, e.g., by glutathionylation. ANAC089 contains four Cys residues which may be involved in such a mechanism (**Figure 3A**).

Recently, ANAC089 was linked to sugar sensing in a screen for fructose-insensitive *A. thaliana* mutants. One of the selected mutants *FSQ6* carries an *anac089* allele with premature translational stop in the third exon which enabled growth in the presence of 6.5% (w/v) fructose (Li et al., 2011). This C-terminally truncated ANAC089 in *FSQ6* lacks the membrane spanning helix, thus is not tethered to membranes and immediately translocates to the nucleus upon its synthesis. The expressed ANAC089 variant in *FSQ6* is considered as gain-of function mutation with constitutive ANAC089-dependent target gene expression (Li et al., 2011). Our results demonstrate release of the N-terminus of ANAC089 upon treatment with reductant (**Figure 5**). In their comprehensive search and cataloguing of NAC transcription factors in the rice and *A. thaliana* genomes Ooka et al. (2003) sorted ANAC089 in the group of OsNAC08-related NACs together with ANAC060 and ANAC040. Membrane-tethering of at least 13 ANACs was reported by Kim et al. (2007) the transcript levels of which were often up-regulated under cold, salinity, or heat stress. This contrasts expression of ANAC089. Its mRNA level was high at the end of the dark phase and under low light conditions (**Figure 8**) and down-regulated under high light. High light exposure of normal or low light grown plants imposes excess excitation energy stress and induces a profound transcriptional acclimation response (Khandelwal et al., 2008; Oelze et al., 2012 and unpublished). High light induces oxidative stress and ROS-related signaling (Bechtold et al., 2008). Thus *ANAC089* showed a regulation tentatively reciprocal to the ROS level.

First reports have described cues that lead to the release of membrane-tethered NAC transcription factor. Cytokinin-dependent signaling involves the membrane-anchored ANAC transcription factor NTM1 which regulates cell division (Kim et al., 2006). The MTTF-NAC (At3g49530) mediates part of the cold stress response. Cold temperatures lead to release of the functional NAC-TF from the plasmamembrane over a long time period between 0.5 and 15 h (Seo et al., 2010). In neither of these cases a biochemical cue could be proposed that triggers the shedding. Thus the here reported redox-dependent release offers a first mechanistic interpretation of the processing by intracellular redox signals.

ANAC089 has been shown to be expressed in cotyledons, germinating seedlings, in the vasculature of hypocotyls, roots, rosette and cauline leaves, but also in the interveinal region of the rosette leaves (Li et al., 2010). ANAC089 overexpression delayed flowering time possibly by affecting expression of flower regulatory genes such as CONSTANS (CO) and FLOWERING LOCUS T (FT) whose transcript was suppressed and FLOWERING LOCUS C (FLC) whose transcript accumulation was enhanced (Li et al., 2010). Apparently ANAC089 has multiple functions.

This study assigns an additional and novel role to ANAC089, namely in regulating the expression of sAPX, an important player of the chloroplast antioxidant system. The chloroplast antioxidant system in photosynthesizing cells is expressed at a high level under most conditions (Foyer and Noctor, 2005). This realizes a strong antioxidant defense in a variable environment. However leaves may encounter environmental conditions that prevent photosynthesis-related oxidative stress. Such a reduced state of the glutathione system (Noctor and Foyer, 1998) and the thiol-disulfide redox regulatory network (Dietz, 2008) are likely established if leaves are permanently shaded (Oelze et al., 2012). Then down-regulation of the defense system might save resources for other important synthetic activities. Shedding of ANAC089 from the cytosol-facing side of endomembranes by a thiol redox-regulated process may then allow for translocation of the released functional ANAC089-protein to the nucleus and will subsequently lower *sapx* gene expression. Comparing protein amounts and transcript levels in *A. thaliana* plants acclimated to low, normal, and high light indicates that low levels of *sAPX* transcript are sufficient to maintain high sAPX protein amounts under such conditions probably due to reduced turnover. Such a role of ANAC089 is tentatively supported by the antiparallel transcript regulation of *ANAC089* and *sAPX* in rosettes acclimated and maintained in low and normal light or subsequently transferred to high light (**Figure 8**). According to this scenario, ANAC089 functions in a negative retrograde loop, lowering sAPX expression if the cell encounters highly reducing conditions. In this case the retrograde signal would be a thiol-disulfide redox cue. The putative binding site ATGCACGTC of ANAC089 in the *sapx* promoter is present in many genes tentatively co-expressed with *sAPX*. It will be interesting to investigate the effect of ANAC089 on the expression of these candidate targets including *sapx* by use of transgenic *A. thaliana* lacking or overexpressing ANAC089.

ACKNOWLEDGMENTS

We gratefully acknowledge support by Prof. Margarete Baier (FU Berlin, Germany) in the very early phase of the project particularly in the Y1H-library construction. This work was conducted within the framework of the FOR804 on retrograde signaling (Di346) funded by the Deutsche Forschungsgemeinschaft.

REFERENCES

Asada, K. (1999). The water–water cycle in chloroplasts: scavenging of active oxygens and dissipation of excess photons. *Annu. Rev. Plant Physiol. Plant Mol. Biol.* 50, 601–639.

Baier, M., and Dietz, K. J. (2005). Chloroplasts as source and target of cellular redox regulation: a discussion on chloroplast redox signals in the context of plant physiology. *J. Exp. Bot.* 56, 1449–1462.

Baier, M., Noctor, G., Foyer, C. H., and Dietz, K. J. (2000). Antisense suppression of 2-Cys peroxiredoxin in *Arabidopsis thaliana* specifically enhances the activities and expression of enzymes associated with ascorbate metabolism, but not glutathione metabolism. *Plant Physiol.* 124, 823–832.

Bechtold, U., Richard, O., Zamboni, A., Gapper, C., Geisler, M., Pogson, B. J., et al. (2008). Impact of chloroplastic- and extracellular-sourced ROS on high light-responsive gene expression in *Arabidopsis*. *J. Exp. Bot.* 59, 121–133.

Dietz, K. J. (2008). Redox signal integration: from stimulus to networks and genes. *Physiol. Plant.* 133, 459–468.

Dietz, K. J. (2011). Peroxiredoxins in plants and cyanobacteria. *Antioxid. Redox Signal.* 15, 1129–1159.

Dietz, K. J., Jacob, S., Oelze, M. L., Laxa, M., Tognetti, V., de Miranda, S. M. N., et al. (2006). The function of peroxiredoxins in plant organelle redox metabolism. *J. Exp. Bot.* 57, 1697–1709.

Ernst, H. A., Olsen, A. N., Larsen, S., and Lo Leggio, L. (2004). Structure of the conserved domain of ANAC, a member of the NAC family of transcription factors. *EMBO Rep.* 5, 297–303.

Foyer, C. H., and Noctor, G. (2005). Oxidant and antioxidant signalling in plants: a re-evaluation of the concept of oxidative stress in a physiological context. *Plant Cell Physiol.* 28, 1056–1071.

Garcia-Lorenzo, M., Sjödin, A., Jansson, S., and Funk, C. (2006). Protease gene families in *Populus* and *Arabidopsis*. *BMC Plant Biol.* 6, 30. doi: 10.1186/1471-2229-6-30

Golldack, D., Lüking, I., and Yang, O. (2011). Plant tolerance to drought and salinity: stress regulating transcription factors and their functional significance in the cellular transcriptional network. *Plant Cell Rep.* 30, 1383–1391.

Hanton, S. L., Chatre, L., Matheson, L. A., Rossi, M., Held, M. A., and Brandizzi, F. (2008). Plant Sar1 isoforms with near-identical protein sequences exhibit different localizations and effects on secretion. *Plant Mol. Biol.* 67, 283–294.

Hu, R., Qi, G., Kong, Y., Kong, D., Gao, Q., and Zhou, G. (2010). Comprehensive analysis of NAC domain transcription factor gene family in *Populus trichocarpa*. *BMC Plant Biol.* 10, 145. doi: 10.1186/1471-2229-10-145

Hwang, I., and Robinson, D. G. (2009). Transport vesicle formation in plant cells. *Curr. Opin. Plant Biol.* 12, 660–669

Iida, K., Seki, M., Sakurai, T., Satou, M., Akiyama, K., Toyoda, T., et al. (2005). RARTF: database and tools for complete sets of *Arabidopsis* transcription factors. *DNA Res.* 12, 247–256.

Jensen, M. K., Kjaersgaard, T., Nielsen, M. M., Galberg, P., Petersen, K., O'Shea, C., et al. (2010). The *Arabidopsis thaliana* NAC transcription factor family: structure–function relationships and determinants of ANAC019 stress signalling. *Biochem. J.* 426, 183–196.

Kangasjärvi, S., Lepisto, A., Hannikainen, K., Piippo, M., Luomala, E. M., Aro, E. M., et al. (2008). Diverse roles for chloroplast stromal and thylakoid-bound ascorbate peroxidases in plant stress responses. *Biochem. J.* 412, 275–285.

Khandelwal, A., Elvitigala, T., Ghosh, B., and Quatrano, R. S. (2008). *Arabidopsis* transcriptome reveals control circuits regulating redox homeostasis and the role of an AP2 transcription factor. *Plant Physiol.* 148, 2050–2058.

Kim, S. Y., Kim, S. G., Kim, Y. S., Seo, P. J., Bae, M., Yoon, H. K., et al. (2007). Exploring membrane-associated NAC transcription factors in *Arabidopsis*: implications of membrane biology in genome regulation. *Nucleic Acid Res.* 35, 203–213.

Kim, Y. S., Kim, S. G., Park, J. E., Park, H. Y., Lim, M. H., Chua, N. H., et al. (2006). A membrane-bound NAC transcription factor regulates cell division in *Arabidopsis*. *Plant Cell* 18, 3132–3144.

Klein, P., and Dietz, K. J. (2010). Identification of DNA-binding proteins and protein–protein interactions by yeast one-hybrid and yeast two-hybrid screen. *Methods Mol. Biol.* 639, 171–192.

Leister, D. (2012). Retrograde signaling in plants: from simple to complex scenarios. *Front. Plant Sci.* 3: 135. doi: 10.3389/fpls.2012.00135

Li, J. Q., Zhang, J. A., Wang, X. C., and Chen, J. (2010). A membrane-tethered transcription factor ANAC089 negatively regulates floral initiation in *Arabidopsis thaliana*. *Sci. China Life Sci.* 53, 1299–1306.

Li, P., Wind, J. J., Shi, X., Zhang, H., Hanson, J., and Smeekens, S. C. (2011). Fructose sensitivity is suppressed in *Arabidopsis* by the transcription factor ANAC089 lacking the membrane-bound domain. *Proc. Natl. Acad. Sci. U.S.A.* 108, 3436–3441.

Li, Z. R., Wakao, S., Fischer, B. B., and Niyogi, K. K. (2009). Sensing and responding to excess light. *Annu. Rev. Plant Biol.* 60, 239–260.

Lopez-Molina, L., Mongrand, S., Kinoshita, N., and Chua, N.-H. (2003). AFP is a novel negative regulator of ABA signalling that promotes ABI5 protein degradation. *Genes Dev.* 17, 410–418.

Miyake, C., and Asada, K. (1996). Inactivation mechanism of ascorbate peroxidase at low concentrations of ascorbate; hydrogen peroxide decomposes compound I of ascorbate peroxidase. *Plant Cell Physiol.* 37, 423–430.

Nakano, Y., and Asada, K. (1981). Hydrogen peroxide is scavenged by ascorbate specific peroxidase in spinach chloroplasts. *Plant Cell Physiol.* 22, 867–880.

Neubert, C., Graham, L., Black-Maier, E. W., Liu, T. Y., Stierhof, Y. D., Seidel, T., et al. (2008). *Arabidopsis* has two functional orthologs of the yeast V-ATPase assembly factor Vma21p. *Traffic* 9, 1618–1628.

Noctor, G., and Foyer, C. H. (1998). Ascorbate and glutathione: keeping active oxygen under control. *Annu. Rev. Plant Physiol. Plant Mol. Biol.* 49, 249–279.

Oelze, M. L., Vogel, M. O., Alsharafa, K., Kahmann, U., Viehhauser, A., Maurino, V. G., et al. (2012). Efficient acclimation of the chloroplast antioxidant defence of *Arabidopsis thaliana* leaves in response to a 10- or 100-fold light increment and the possible involvement of retrograde signals. *J. Exp. Bot.* 63, 1297–1313.

Ondzighi, C. A., Christopher, D. A., Cho, E. J., Chang, S. C., and Staehelin, L. A. (2008). *Arabidopsis* protein disulfide isomerase-5 inhibits cysteine proteases during trafficking to vacuoles before programmed cell death of the endothelium in developing seeds. *Plant Cell* 20, 2205–2220.

Ooka, H., Satoh, K., Doi, K., Nagata, T., Otomo, Y., Murakami, K., et al. (2003). Comprehensive analysis of NAC family genes in *Oryza sativa* and *Arabidopsis thaliana*. *DNA Res.* 10, 239–247.

op den Camp, R. G. L., Przybyla, D., Ochsenbein, C., Laloi, C., Kim, C., Danon, A., et al. (2003). Rapid induction of distinct stress responses after the release of singlet oxygen in *Arabidopsis*. *Plant Cell* 15, 2320–2332.

Pena-Ahumada, A., Kahmann, U., Dietz, K. J., and Baier, M. (2006). Regulation of peroxiredoxin expression versus expression of Halliwell-Asada-Cycle enzymes during early seedling development of *Arabidopsis thaliana*. *Photosynth. Res.* 89, 99–112.

Pfannschmidt, T. (2010). Plastidial retrograde signaling – a true "plastid factor" or just metabolite signatures? *Trends Plant Sci.* 15, 427–435.

Pogson, B. J., Nick, S. W., Förster, B., and Small, I. (2008). Plastid signaling to the nucleus and beyond. *Trends Plant Sci.* 13, 602–609.

Schuhmann, H., and Adamska, I. (2012). Deg proteases and their role in protein quality control and processing in different subcellular compartments of the plant cell. *Physiol. Plant.* 145, 224–234.

Seidel, T., Golldack, D., and Dietz, K. J. (2005). Mapping of C-termini of V-ATPase subunits by in vivo-FRET measurements. *FEBS Lett.* 579, 4374–4382.

Seidel, T., Kluge, C., Hanitzsch, M., Ross, J., Sauer, M., Dietz, K. J., et al. (2004). Colocalization and FRET-analysis of subunits c and a of the vacuolar H+-ATPase in living plant cells. *J. Biotechnol.* 112, 165–175.

Seidel, T., Schnitzer, D., Golldack, D., and Dietz, K. J. (2008). Organelle-specific isoenzymes of plant V-ATPase as revealed by in vivo-FRET analysis. *BMC Cell Biol.* 9, 28. doi: 10.1186/1471-2121-9-28

Seidel, T., Seefeldt, B., Sauer, M., and Dietz, K. J. (2010) In vivo analysis of the 2-Cys peroxiredoxin oligomeric state by two-step FRET. *J. Biotechnol.* 149, 272–279.

Seo, P. J., Kim, M. J., Song, J. S., Kim, Y. S., Kim, H. J., and Park, C. M. (2010). Proteolytic processing of an *Arabidopsis* membrane-bound NAC transcription factor is triggered by cold-induced changes in membrane fluidity. *Biochem. J.* 427, 359–367.

Shaikhali, J., Heiber, I., Seidel, T., Ströher, E., Hiltscher, H., Birkmann, S., et al. (2008). The redox-sensitive transcription factor Rap2.4a controls nuclear expression of 2-Cys peroxiredoxin A and other chloroplast antioxidant enzymes. *BMC Plant Biol.* 8, 48. doi: 10.1186/1471-2229-8-48

Ströher, E., and Dietz, K. J. (2008). The dynamic thiol-disulphide redox proteome of the *Arabidopsis thaliana* chloroplast as revealed by differential

electrophoretic mobility. *Physiol. Plant.* 133, 566–583.

Uemura, T., Ueda, T., Ohniwa, R. L., Nakano, A., Takeyasu, K., and Sato, M. H. (2004). Systematic analysis of SNARE molecules in *Arabidopsis*: dissection of the post-Golgi Network in plant cells. *Cell Struct. Funct.* 29, 49–65

Wormuth, D., Baier, M., Kandlbinder, A., Scheibe, R., Hartung, W., and Dietz, K. J. (2006). Regulation of nuclear and chloroplast transcript levels by photosynthetic signals triggered through modified CO2 availability. *BMC Plant Biol.* 6, 15. doi: 10.1186/1471-2229-6-15

Conflict of Interest Statement: The authors declare that the research was conducted in the absence of any commercial or financial relationships that could be construed as a potential conflict of interest.

Received: 10 August 2012; paper pending published: 03 September 2012; accepted: 19 October 2012; published online: 09 November 2012.

Citation: Klein P, Seidel T, Stöcker B and Dietz K-J (2012) The membrane-tethered transcription factor ANAC089 serves as redox-dependent suppressor of stromal ascorbate peroxidase gene expression. Front. Plant Sci. ***3****:247. doi: 10.3389/fpls.2012.00247*

This article was submitted to Frontiers in Plant Physiology, a specialty of Frontiers in Plant Science.

Copyright © 2012 Klein, Seidel, Stöcker and Dietz. This is an open-access article distributed under the terms of the Creative Commons Attribution License, which permits use, distribution and reproduction in other forums, provided the original authors and source are credited and subject to any copyright notices concerning any third-party graphics etc.

frontiers in
PLANT SCIENCE

PERSPECTIVE ARTICLE
published: 05 December 2012
doi: 10.3389/fpls.2012.00267

Unraveling retrograde signaling pathways: finding candidate signaling molecules via metabolomics and systems biology driven approaches

Camila Caldana[1], Alisdair R. Fernie[2], Lothar Willmitzer[2] and Dirk Steinhauser[2]*

[1] Brazilian Bioethanol Science and Technology Laboratory (Brazilian Center of Research in Energy and Materials), Campinas, Brazil
[2] Department of Molecular Physiology, Max Planck Institute of Molecular Plant Physiology, Potsdam-Golm, Germany

Edited by:
Dario Leister, Ludwig-Maximilians-Universität München, Germany

Reviewed by:
Frederik Börnke, Friedrich-Alexander-University Erlangen-Nürnberg, Germany
Peter Geigenberger, Ludwig-Maximilians-Universität München, Germany

***Correspondence:**
Dirk Steinhauser, Department of Molecular Physiology, Max Planck Institute of Molecular Plant Physiology, Am Mühlenberg 1, 14476 Potsdam-Golm, Germany. e-mail: steinhauser@mpimp-golm.mpg.de

A tight coordination of biological processes between cellular compartments and organelles is crucial for the survival of any eukaryotic organism. According to cellular requirements, signals can be generated within organelles, such as chloroplasts and mitochondria, modulating the nuclear gene expression in a process called retrograde signaling. Whilst many research efforts have been focused on dissecting retrograde signaling pathways using biochemical and genetics approaches, metabolomics and systems biology driven studies have illustrated their great potential for hypotheses generation and for dissecting signaling networks in a rather unbiased or untargeted fashion. Recently, integrative genomics approaches, in which correlation analysis has been applied on transcript and metabolite profiling data of *Arabidopsis thaliana*, revealed the identification of metabolites which are putatively acting as mediators of nuclear gene expression. Complimentary, the continuous technological developments in the field of metabolomics *per se* has further demonstrated its potential as a very suitable readout to unravel metabolite-mediated signaling processes. As foundation for these studies here we outline and discuss recent advances in elucidating retrograde signaling molecules and pathways with an emphasis on metabolomics and systems biology driven approaches.

Keywords: retrograde signaling, metabolic signals, systems biology, metabolomics, sub-cellular metabolomics

INTRODUCTION

Biological systems rely on complex interactions of heterogeneous small- and macro-molecules to execute cellular functions required for their growth, survival, and propagation (Smeekens et al., 2010). To maintain cellular homeostasis the interactions of and among these heterogeneous molecules need to be strictly regulated and coordinately modified to respond appropriately to external and internal stimuli. This fundamental process, which is common to all organisms, is broadly termed signal transduction. Generally, it involves the sensing of a stimulus or signal, the integration of information within and between different systems levels and finally, the execution of regulatory events resulting in a cellular response (Keurentjes et al., 2011; Baldazzi et al., 2012). While on a first glance signal transduction seems to be unidirectional with respect to information processing, a continuous sensing and control of the regulated function is required for fine-tuning.

In contrast to bacteria, the eukaryotic cell comprises a large number of diverse subcellular compartments and organelles which are usually delineated by a lipid bilayer to maintain specific microenvironments (Pogson et al., 2008; Krueger et al., 2011). Along with this many physiological processes and metabolic reactions are either solely localized in a single compartment or partitioned between them (Martinoia et al., 2007; Weber and Fischer, 2007; Linka and Weber, 2010). Although these compartments are physically and biochemically distinct, a tight coordination of processes between them is essential to maintain the biological functionality of the eukaryotic cell (Lunn, 2007).

While the different subcellular compartments are involved in storage, detoxification, and synthesis of a variety of specific and important compounds (Paris et al., 1996; Dyall et al., 2004; Becker, 2007), plastids and mitochondria in particular play also an essential role in integrating environmental cues into metabolic responses assisting in the adjustments of growth and development (Leon et al., 1998; Yang et al., 2008; Kessler and Schnell, 2009). However and in spite of the broad range of functions housed in, e.g., the plastids, only 5% of its proteome is encoded and synthesized by the plastids themselves (Abdallah et al., 2000). Chloroplasts and mitochondria are believed to have originated by endosymbiosis of free-living bacterial ancestors by a pre-eukaryotic cell, but contain (in comparison to their closest free-living relatives) only a strongly reduced portion of the ancestral genome with the majority of genes having been either lost or transferred to the nucleus (Andersson et al., 2003; Dyall et al., 2004). Given that many components of the energy transduction cascades are encoded by both the organelle and the nuclear genome, a tight coordination of gene expression in two or more cellular compartments is required to ensure the correct concentrations of organelle proteins, independent of their genesis, and thus to maintain organelle functions (Pogson et al., 2008; Kleine et al., 2009). Such genome-coordination mechanisms are achieved by bidirectional signaling that controls the information flux from

the nucleus to the organelles (anterograde signaling; Sardiello et al., 2005) and by signals from the organelles to the nucleus (retrograde signaling; Biehl et al., 2005; Nott et al., 2006; Pesaresi et al., 2007; Jung and Chory, 2010). Retrograde signaling discloses the functional and developmental state of the organelles to the nucleus, which can then modulate anterograde control and cellular metabolism, as a result of environmental changes and signals perceived by the organelles (Woodson and Chory, 2008). Tight regulation of such signaling establishes the proper balance of gene expression and regulation in response to a fluctuating environment and thus, is fundamental for the survival of any organism. The intracellular communication between various organelles is quite complex and interdependent (Leister, 2005; Koussevitzky, 2007; Pesaresi et al., 2007; Jung and Chory, 2010). In photosynthetic eukaryotes, this scenario is even more complex owing the cross-talk between chloroplasts and mitochondria (Woodson and Chory, 2008).

TARGETED AND BOTTOM-UP APPROACHES FOR SIGNAL MOLECULE VALIDATION

To date, an increasing but still small number of candidate signaling molecules and their respective pathways have been identified. So far, the putative sources of retrograde signals are thought to derive from (i) components of tetrapyrrole biosynthetic pathway intermediates (Mochizuki et al., 2001; Strand et al., 2003), (ii) reactive oxygen species levels in plastid (op den Camp et al., 2003; Wagner et al., 2004; Laloi et al., 2006; Lee et al., 2007), (iii) the redox state of organelles (Bonardi et al., 2005; Piippo et al., 2006; Pesaresi et al., 2007), and (iv) protein synthesis (Koussevitzky, 2007; for recent reviews, see Leister, 2005, 2012; Nott et al., 2006; Koussevitzky, 2007; Pesaresi et al., 2007; Pogson et al., 2008; Kleine et al., 2009; Chan et al., 2010; Jung and Chory, 2010; Pfannschmidt, 2010; Leister et al., 2011). However, most of the research on retrograde signaling has targeted isolated pathways under artificial and/or pleiotropic conditions (Kleine et al., 2009). One of the best-studied chloroplast retrograde signaling pathways, the tetrapyrrole pathway provides an example of the complexity involved in unequivocally identifying a retrograde signal. Photo-oxidative damage of undeveloped chloroplasts leads to the accumulation of Mg-proto, an intermediate metabolite of chlorophyll biosynthesis, which represses nuclear genes encoding for photosynthesis-related proteins (Strand et al., 2003). Genetic screenings associated to microarray analysis in *Arabidopsis* have resulted in identifying the *genomes uncoupled* (*gun*) mutants, which block Mg-proto mediated retrograde signaling by affecting its accumulation (Mochizuki et al., 2001; Strand et al., 2003; Koussevitzky, 2007). Those earlier studies have found a direct correlation of nuclear gene expression and total cellular levels of Mg-proto IX estimated using fluorescence spectrometry (Mochizuki et al., 2001). However, later studies that employed a more sensitive and reproducible HPLC methodology revealed the absence of any correlation between Mg-proto IX and nuclear gene expression levels (Mochizuki et al., 2008). These finding argues against the proposed model for Mg-proto IX as a retrograde signal. Thus, further investigations using alternative analytical approaches together with subcellular localization estimation might be necessary to unambiguously accept or reject the involvement of Mg-proto IX in retrograde signaling. Therefore, the unambiguous experimental validation of a compound as a signaling molecule is an extremely laborious task and so far, arguably no "true" signaling molecule leaving the plastid has been identified (Pfannschmidt, 2010). Innovative biochemical and genetic screenings, such as inducible expression or inducible RNA interference (RNAi) are supposed to aid in further identifying proteins and signals in these pathways (Woodson and Chory, 2008). As the function of a cellular constitute might also be context-dependent, more holistic 'omics-like approaches might be helpful in elucidating the specificity of a candidate signaling molecule.

IDENTIFICATION AND VALIDATION OF NOVEL SIGNALING CANDIDATES VIA METABOLOMICS

Whilst much research efforts have been focused on dissecting signaling pathways using biochemical and genetics approaches, the number of yet discovered mechanisms of retrograde signaling are likely not sufficient to explain the tight regulation and interdependence of organelle functions. For instance, the cellular metabolism is tightly correlated with processes occurring in chloroplasts and mitochondria. It is widely believed that changes in the concentration of metabolites triggered by the organelles are likely sensed in the cytosol and thus, might regulate nuclear gene expression (Kleine et al., 2009). Therefore, metabolites are thought to be the most likely candidates for retrograde signaling molecules, since the metabolites exported from the organelles into the cytosol are likely reflective of the organellar metabolic state (Leister, 2012). A consequence of this view is that fluxes of metabolites between, e.g., the chloroplast and the cytosol can mediate information on the chloroplast redox stage and therefore, acting as potential intracellular signals (Kleine et al., 2009). For instance, trehalose 6-phosphate (T6P) promotes thioredoxin-mediated redox transfer to AGPase in response to cytosolic sugar levels, reporting on the metabolic status between the cytosol and the chloroplast (Kolbe et al., 2005). Another example of alteration in the cellular redox status has been reported for malate in tomato fruits (Centeno et al., 2011).

Over the past decades a number of analytical methods, such as gas chromatography (GC), liquid chromatography (LC), capillary electrophoresis (CE) coupled to mass spectrometry (MS) or nuclear magnetic resonance (NMR), have been developed and improved to accurately and sensitively analyze small molecules from complex sample mixtures (Kopka et al., 2004; Lisec et al., 2008; Lei et al., 2011). As these technologies enable the simultaneous detection of several hundred to several thousand metabolites, a more holistic view of cellular functions can be gathered since metabolites are considered to directly reflect the physiological status of a cell. Therefore, metabolite profiling has been considered as a powerful tool for the unbiased ability to characterize and differentiate genotypes and phenotypes (Hirai et al., 2005; Kusano et al., 2007; Hannah et al., 2010; Caldana et al., 2011) and provides also an excellent readout for the dissection of novel signaling pathways. Unfortunately, the measurement of all metabolites using a single analytical technology is yet not feasible due to the vast number of compounds which on top differ widely in their chemical properties, such as size, polarity, stability, and quantity, as well as in their immense dynamic concentration ranges (Kopka et al., 2004;

Lisec et al., 2008; Lei et al., 2011). The optimal selection of a technology will thus largely depend on the study aim and is usually a compromise of selectivity, speed, and throughput (Lei et al., 2011; Krueger et al., 2012). Therefore, orthogonal analytical technologies in conjunction with targeted and untargeted data analyses will support a broader compound coverage as the chemical properties and also the structure of molecules involved in signaling might not be known to date. Nonetheless, some metabolites might still not be precisely captured using a particular analytical 'omics technology or their combinations, thus requiring targeted biochemical assays either simultaneously applied or used for verification.

Several lines of evidence suggested that the development of target methods with high accuracy is very informative in elucidating the role of candidate signals. One successful example of the use of metabolic profiling for elucidating retrograde signals in plants is the identification of methylerythritol cyclodiphosphate (MEcPP; Xiao et al., 2012). Using a genetic approach the authors identified the retrograde signaling *ceh1* mutant, which displayed changes in expression of stress-related genes associated to salicylic acid response and resistance to the pathogen *Pseudomonas*. *Ceh1* is caused by a mutation in the *HDS* gene responsible for the conversion of MEcPP to hydroxymethylbutenyl diphosphate (HMBPP) in the methylerythritol phosphate (MEP) pathway. Metabolite profile analysis of MEP pathway intermediates by LC-MS revealed an accumulation of the intermediate metabolite MEcPP in *ceh1*. MEcPP is a specific and critical retrograde signaling metabolite that acts as a stress sensor by triggering the expression of specific stress-responsive nuclear encoded plastidial proteins (Xiao et al., 2012).

IDENTIFICATION AND VALIDATION OF NOVEL SIGNALING CANDIDATES VIA SUB-/CELLULAR METABOLOMICS

Despite the great potential of metabolomics in identifying novel signals, the majority of studies rely on the entire set of metabolic reactions that can take place within different tissues, but do not consider the type of tissue or the subcellular specificity and localization of metabolites. Taking this observation into account, only metabolites whose changes are readily transferable between compartments represent promising retrograde signals (Kleine et al., 2009; Leister, 2012). Thus, unraveling the subcellular localization of metabolites and their dynamics are crucial for identifying small molecules within organelles that potentially trigger retrograde signaling. The main challenge of such analysis is the fast conversion and reallocation of metabolites out of organelles. To date, several methods have been developed to monitor the spatial distribution of metabolites within the different cell types and cellular compartments (for a review, see Krueger et al., 2012).

Protoplast fractionation has been widely used to quantify metabolite levels in purified organelles such as chloroplasts, mitochondria, and the vacuole, respectively (e.g., Robinson and Walker, 1980; Stitt et al., 1983; Gerhardt and Heldt, 1984; Dancer et al., 1990; Martinoia et al., 1991; Gardestrom, 1993; Abdallah et al., 2000; Tohge et al., 2011). However, the procedure is very time-consuming as it includes several centrifugation steps, therefore causing a disturbance of the physiological and biochemical system (Krueger et al., 2012). Consequently, such artificial system may not accurately reflect the *in planta* situation. Recently, protoplast fractionation was used to detect the subcellular levels of 3′-Phosphoadenosine 5′-phosphate (PAP) and confirm its role as a retrograde signal (Estavillo et al., 2011). PAP was found to accumulate in response to drought and high light and is regulated by the enzyme SAL1, which is present in chloroplasts and mitochondria (Estavillo et al., 2011). The cellular levels of PAP correlated well with the nuclear gene expression. Interestingly, transgenic targeting of SAL1 to either the nucleus or chloroplast of *sal1* mutants reduced the total PAP levels (Estavillo et al., 2011). However, except for the chloroplast, the subcellular quantification of PAP fractions has failed due to technical reasons (Estavillo et al., 2011; Leister, 2012).

A more accurate technique to monitor spatial and temporal metabolic changes in cellular compartments of intact tissues is the use of genetically encoded metabolite nanosensors. The fluorescence resonance energy transfer (FRET) nanosensor makes use of a recognition element (a protein that binds with the metabolite of interest) fused to a report element (a fluorophore pair). Changes in protein conformation triggered by ligand (metabolite)-recognition element binding leads to the emission of fluorescent light via the report element (for review, see Frommer et al., 2009). In *Arabidopsis*, FRET-based glucose and sucrose sensors have been used to successfully monitor sucrose and glucose transport in root tips (Chaudhuri et al., 2008, 2011). To follow the dynamic changes of a given metabolite with subcellular resolution, the FRET sensor has to be flanked with a signal sequence recognized by the organelle (e.g., nuclear or ER signal sequence) to enable the proper import of the sensor into the organelle (Hou et al., 2011). As each metabolite however requires its own sensor, it remains an arduous task to engineer sensors for various potential signaling molecules. Thus, only small molecules with previous strong evidence of being a putative signal can likely be considered in such an approach.

The probably most promising strategy to analyze subcellular metabolite distribution is the non-aqueous fractionation method which separates cellular compartments under conditions where metabolite translocation and conversion are completely arrested (Gerhardt and Heldt, 1984; Riens et al., 1991). It has a proven record especially in plant science (Gerhardt et al., 1987; Riens et al., 1991; Winter et al., 1993; Fettke et al., 2005; Krueger et al., 2009) and routinely facilitates the separation of three distinct compartments from each other, namely the cytosol, the plastids, and the vacuole (Gerhardt et al., 1987; Farre et al., 2001; Krueger et al., 2009, 2011). Although NAF produces continuous metabolite distributions of organelles and a successful separation of mitochondria is not yet reported, the entire cellular content and thus its metabolites are represented in the gradient which can be considered as an advantage for identifying signaling molecules (Jung and Chory, 2010). As the collected NAF fractions can be analyzed with modern high-throughput metabolite profiling techniques several hundred molecules from different broad compound classes can be measured simultaneously (Krueger et al., 2011) and finally assigned into compartments using improved statistical tools (Klie et al., 2011). Thus, the impact of environmental changes on cellular and subcellular metabolism and the cell's state can be analyzed with high spatial resolution providing the

necessary basis to discover novel signaling molecules. Recently, non-aqueous fractionation (NAF) in conjunction with orthogonal metabolite profiling technologies was applied to unravel the subcellular localization of primary and secondary metabolites as well as lipids (Krueger et al., 2011). While this study depicts the subcellular localization for a large number of chemically diverse metabolites, it also illustrates that there is the potential to further increase the compartmental resolution as various metabolites could not be unambiguously assigned into one of the three resolved compartments.

SYSTEMS BIOLOGY APPROACHES IN RETROGRADE SIGNALING

The complexity and interdependence of the pathways involved in intracellular communication have a dramatic impact on cellular levels. To understand how plants adjust their biochemical machineries on several levels of biological information, a more holistic approach such as systems biology is required. Recent advances of high-throughput technologies and analytical methods, such as transcriptomics and metabolomics, have supported multilevel phenotyping and can help to understand many complex biological processes by generation of hypothesis about the dynamic system (Jung and Chory, 2010). Application of such systems-orientated analyses in retrograde control may provide novel means to unravel intracellular communication and corresponding signaling molecules.

Gene expression profiling has been widely used to study retrograde control. The classical approach to identify a set of nuclear genes under retrograde control is based on transcriptomics analysis of mutants defective in retrograde pathways (for examples, see the reviews of Jung and Chory, 2010). However, to avoid biased results caused by pleiotropic effects of a single experiment, it is highly recommended to use expression profile data of multiple experimental conditions. As an example, meta-analysis of 11 microarray experiments from mutants (e.g., *aox1a* and *msd1*-RNAi, among others) and short-term chemical treatments (e.g., antimycin A and rotenone) involved in plant mitochondrial dysfunction has been carried out to identify targets and pathways involved in mitochondrial retrograde signaling (Schwarzlander et al., 2012). Regardless of the level of severity of these mitochondrial impairments, three main retrograde signaling targets were identified, namely protein synthesis, photosynthetic light reactions, and plant–pathogen interactions (Schwarzlander et al., 2012). A similar approach has been performed to unravel intra- and inter-compartmental transcriptional networks coordinate the expression of genes for organellar functions (Leister et al., 2011).

Another recent study investigated the time-dependent impact of redox signals at both transcriptome and metabolome levels of *Arabidopsis thaliana* growing under either PSI or PSII light (Brautigam et al., 2009). The authors showed rapid and dynamic changes in nuclear transcript accumulation, which resulted in differential expression pattern for genes associated with photosynthesis and metabolism (Brautigam et al., 2009). This work proposed that photosynthesis acts as an environmental sensor, producing redox signals that perform a fine-tuning not only for photosynthesis but also for metabolic reactions (Brautigam et al., 2009).

Integration of high-throughput transcript and metabolite data has facilitated the identification of small molecules as potential mediators of gene expression (Hannah et al., 2010). Extensive analysis of transcript and metabolite correlations across a wide ranging of environmental conditions revealed single, highly-connected metabolites which correlated with several hundred to thousand transcripts. Among the candidates, compounds derived from carotenoid metabolism such as cryptoxanthin, zeaxanthin, and lutein were found to significantly correlate with a large number of transcripts. Interestingly, those metabolites displayed a significant overlap between positively correlated genes and those repressed by norflurazon, a known inhibitor of phytoene desaturase in the carotenoid biosynthesis (Hannah et al., 2010).

Another important issue for the identification of signals is to distinguish between "true" primary targets from tertiary targets (Pfannschmidt, 2010). Several lines of evidence demonstrated that retrograde signal may affect nuclear gene expression in a fast and dynamic range. Therefore, a combination of high resolution kinetic analysis combined with inducible systems and subcellular metabolite flux would allow setting a signal at a given time point. A recent example of this is that of *O*-acetylserine (OAS) which has been recently identified as a regulator of the sulfur status in *Arabidopsis* using computational analysis of time-series experiments and inducible transgenic plants revealing conditional increased OAS levels (Hubberten et al., 2012). However, it is important to note that OAS can be synthesized in multiple subcellular compartments. So, it is highly unlikely to represent a retrograde signal since such signals should confer organelle specific information. This is a crucial aspect of retrograde signaling which due to the extensive compartmentation (and three genomes) of the plant cell renders the identification of non-redundant signals highly complex. However, it would appear likely that the spatial-temporal resolution of metabolite levels and metabolite exchange between organelles will greatly aid in the detection and ultimately the mechanistic understanding of retrograde and anterograde signaling orchestrating plant organellar and nuclear gene expression.

REFERENCES

Abdallah, F., Salamini, F., and Leister, D. (2000). A prediction of the size and evolutionary origin of the proteome of chloroplasts of *Arabidopsis*. *Trends Plant Sci.* 5, 141–142.

Andersson, G. E., Karlberg, O., Canbäck, B., and Kurland, C. G. (2003). On the origin of mitochondria: a genomics perspective. *Philos. Trans. R. Soc. Lond. B Biol. Sci.* 358, 165–179.

Baldazzi, V., Bertin, N., De Jong, H., and Génard, M. (2012). Towards multiscale plant models: integrating cellular networks. *Trends Plant Sci.* doi: 10.1016/j.tplants.2012.06.012 [Epub ahead of print].

Becker, B. (2007). Function and evolution of the vacuolar compartment in green algae and land plants (Viridiplantae). *Int. Rev. Cytol.* 264, 1–24.

Biehl, A., Richly, E., Noutsos, C., Salamini, F., and Leister, D. (2005). Analysis of 101 nuclear transcriptomes reveals 23 distinct regulons and their relationship to metabolism, chromosomal gene distribution and co-ordination of nuclear and plastid gene expression. *Gene* 344, 33–41.

Bonardi, V., Pesaresi, P., Becker, T., Schleiff, E., Wagner, R., Pfannschmidt, T., et al. (2005). Photosystem II core phosphorylation and photosynthetic acclimation require two different protein kinases. *Nature* 437, 1179–1182.

Brautigam, K., Dietzel, L., Kleine, T., Stroher, E., Wormuth, D., Dietz, K. J., et al. (2009). Dynamic plastid redox signals integrate gene expression and metabolism to induce distinct metabolic states in photosynthetic acclimation in *Arabidopsis*. *Plant Cell* 21, 2715–2732.

Caldana, C., Degenkolbe, T., Cuadros-Inostroza, A., Klie, S., Sulpice, R., Leisse, A., et al. (2011). High-density kinetic analysis of the metabolomic and transcriptomic response of *Arabidopsis* to eight environmental conditions. *Plant J.* 67, 869–884.

Centeno, D. C., Osorio, S., Nunes-Nesi, A., Bertolo, A. L. F., Carneiro, R. T., Araujo, W. L., et al. (2011). Malate plays a crucial role in starch metabolism, ripening, and soluble solid content of tomato fruit and affects postharvest softening. *Plant Cell* 23, 162–184.

Chan, K. X., Crisp, P. A., Estavillo, G. M., and Pogson, B. J. (2010). Chloroplast-to-nucleus communication: current knowledge, experimental strategies and relationship to drought stress signaling. *Plant Signal. Behav.* 5, 1575–1582.

Chaudhuri, B., Hörmann, F., and Frommer, W. B. (2011). Dynamic imaging of glucose flux impedance using FRET sensors in wild-type *Arabidopsis* plants. *J. Exp. Bot.* 62, 2411–2417.

Chaudhuri, B., Hörmann, F., Lalonde, S., Brady, S. M., Orlando, D. A., Benfey, P., et al. (2008). Protonophore- and pH-insensitive glucose and sucrose accumulation detected by FRET nanosensors in *Arabidopsis* root tips. *Plant J.* 56, 948–962.

Dancer, J., Neuhaus, H. E., and Stitt, M. (1990). Subcellular compartmentation of uridine nucleotides and nucleoside-5′-diphosphate kinase in leaves. *Plant Physiol.* 92, 637–641.

Dyall, S. D., Brown, M. T., and Johnson, P. J. (2004). Ancient invasions: from endosymbionts to organelles. *Science* 304, 253–257.

Estavillo, G. M., Crisp, P. A., Pornsiriwong, W., Wirtz, M., Collinge, D., Carrie, C., et al. (2011). Evidence for a SAL1-PAP chloroplast retrograde pathway that functions in drought and high light signaling in *Arabidopsis*. *Plant Cell* 23, 3992–4012.

Farre, E. M., Tiessen, A., Roessner, U., Geigenberger, P., Trethewey, R. N., and Willmitzer, L. (2001). Analysis of the compartmentation of glycolytic intermediates, nucleotides, sugars, organic acids, amino acids, and sugar alcohols in potato tubers using a non-aqueous fractionation method. *Plant Physiol.* 127, 685–700.

Fettke, J., Eckermann, N., Tiessen, A., Geigenberger, P., and Steup, M. (2005). Identification, subcellular localization and biochemical characterization of water-soluble heteroglycans (SHG) in leaves of *Arabidopsis thaliana* L.: distinct SHG reside in the cytosol and in the apoplast. *Plant J.* 43, 568–585.

Frommer, W. B., Davidson, M. W., and Campbell, R. E. (2009). Genetically encoded biosensors based on engineered fluorescent proteins. *Chem. Soc. Rev.* 38, 2833–2841.

Gardestrom, P. (1993). Metabolite levels in the chrloroplast and extrachloroplast compartments of barley leaf protoplasts during the initial phase of photosynthetic induction. *Biochim. Biophys. Acta* 1183, 327–332.

Gerhardt, R., and Heldt, H. W. (1984). Measurement of subcellular metabolite levels in leaves by fractionation of freeze-stopped material in non-aqueous media. *Plant Physiol.* 75, 542–547.

Gerhardt, R., Stitt, M., and Heldt, H. W. (1987). Subcellular metabolite levels in spinach leaves – regulation of sucrose synthesis during diurnal alterations in photosynthetic partitioning. *Plant Physiol.* 83, 399–407.

Hannah, M. A., Caldana, C., Steinhauser, D., Balbo, I., Fernie, A. R., and Willmitzer, L. (2010). Combined transcript and metabolite profiling of *Arabidopsis* grown under widely variant growth conditions facilitates the identification of novel metabolite mediated regulation of gene expression. *Plant Physiol.* 152, 2120–2129.

Hirai, M. Y., Klein, M., Fujikawa, Y., Yano, M., Goodenowe, D. B., Yamazaki, Y., et al. (2005). Elucidation of gene-to-gene and metabolite-to-gene networks in Arabidopsis by integration of metabolomics and transcriptomics. *J. Biol. Chem.* 280, 25590–25595.

Hou, B. H., Takanaga, H., Grossmann, G., Chen, L. Q., Qu, X. Q., Jones, A. M., et al. (2011). Optical sensors for monitoring dynamic changes of intracellular metabolite levels in mammalian cells. *Nat. Protoc.* 6, 1818–1833.

Hubberten, H.-M., Klie, S., Caldana, C., Degenkolbe, T., Willmitzer, L., and Hoefgen, R. (2012). Additional role of *O*-acetylserine as a sulfur status-independent regulator during plant growth. *Plant J.* 70, 666–677.

Jung, H. S., and Chory, J. (2010). Signaling between chloroplasts and the nucleus: can a systems biology approach bring clarity to a complex and highly regulated pathway? *Plant Physiol.* 152, 453–459.

Kessler, F., and Schnell, D. (2009). Chloroplast biogenesis: diversity and regulation of the protein import apparatus. *Curr. Opin. Cell Biol.* 21, 494–500.

Keurentjes, J. J. B., Angenent, G. C., Dicke, M., Santos, V. A. P. M. D., Molenaar, J., Van Der Putten, W. H., et al. (2011). Redefining plant systems biology: from cell to ecosystem. *Trends Plant Sci.* 16, 183–190.

Kleine, T., Voigt, C., and Leister, D. (2009). Plastid signalling to the nucleus: messengers still lost in the mists? *Trends Genet.* 25, 185–190.

Klie, S., Krueger, S., Krall, L., Giavalisco, P., Flügge, U.-I., Willmitzer, L., et al. (2011). Analysis of the compartmentalized metabolome – a validation of the non-aqueous fractionation technique. *Front. Plant Sci.* 2:55. doi: 10.3389/fpls.2011.00055

Kolbe, A., Tiessen, A., Schluepmann, H., Paul, M., Ulrich, S., and Geigenberger, P. (2005). Trehalose 6-phosphate regulates starch synthesis via posttranslational redox activation of ADP-glucose pyrophosphorylase. *Proc. Natl. Acad. Sci. U.S.A.* 102, 11118–11123.

Kopka, J., Fernie, A., Weckwerth, W., Gibon, Y., and Stitt, M. (2004). Metabolite profiling in plant biology: platforms and destinations. *Genome Biol.* 5, 109.

Koussevitzky, S. (2007). Signals from chloroplasts converge to regulate nuclear gene expression. *Science* 316, 715–719.

Krueger, S., Giavalisco, P., Krall, L., Steinhauser, M. C., Bussis, D., Usadel, B., et al. (2011). A topological map of the compartmentalized *Arabidopsis thaliana* leaf metabolome. *PLoS ONE* 6:e17806. doi: 10.1371/journal.pone.0017806

Krueger, S., Niehl, A., Martin, M. C., Steinhauser, D., Donath, A., Hildebrandt, T., et al. (2009). Analysis of cytosolic and plastidic serine acetyltransferase mutants and subcellular metabolite distributions suggests interplay of the cellular compartments for cysteine biosynthesis in *Arabidopsis*. *Plant Cell Environ.* 32, 349–367.

Krueger, S., Steinhauser, D., Willmitzer, L., and Giavalisco, P. (2012). High-resolution plant metabolomics: from mass spectral features to metabolites and from whole-cell analysis to subcellular metabolite distributions. *Plant J.* 70, 39–50.

Kusano, M., Fukushima, A., Arita, M., Jonsson, P., Moritz, T., Kobayashi, M., et al. (2007). Unbiased characterization of genotype-dependent metabolic regulations by metabolomic approach in *Arabidopsis thaliana*. *BMC Syst. Biol.* 1:53. doi: 10.1186/1752-0509-1-53

Laloi, C., Przybyla, D., and Apel, K. (2006). A genetic approach towards elucidating the biological activity of different reactive oxygen species in *Arabidopsis thaliana*. *J. Exp. Bot.* 57, 1719–1724.

Lee, K. P., Kim, C., Landgraf, F., and Apel, K. (2007). EXECUTER1- and EXECUTER2-dependent transfer of stress-related signals from the plastid to the nucleus of *Arabidopsis thaliana*. *Proc. Natl. Acad. Sci. U.S.A.* 104, 10270–10275.

Lei, Z. T., Huhman, D. V., and Sumner, L. W. (2011). Mass spectrometry strategies in metabolomics. *J. Biol. Chem.* 286, 25435–25442.

Leister, D. (2005). Genomics-based dissection of the cross-talk of chloroplasts with the nucleus and mitochondria in *Arabidopsis*. *Gene* 354, 110–116.

Leister, D. (2012). Retrograde signalling in plants: from simple to complex scenarios. *Front. Plant Sci.* 3:135. doi: 10.3389/fpls.2012.00135

Leister, D., Wang, X., Haberer, G., Mayer, K. F. X., and Kleine, T. (2011). Intracompartmental and intercompartmental transcriptional networks coordinate the expression of genes for organellar functions. *Plant Physiol.* 157, 386–404.

Leon, P., Arroyo, A., and Mackenzie, S. (1998). Nuclear control of plastid and mitochondrial development in higher plants. *Annu. Rev. Plant Physiol. Plant Mol. Biol.* 49, 453–480.

Linka, N., and Weber, A. P. M. (2010). Intracellular metabolite transporters in plants. *Mol. Plant* 3, 21–53.

Lisec, J., Meyer, R. C., Steinfath, M., Redestig, H., Becher, M., Witucka-Wall, H., et al. (2008). Identification of metabolic and biomass QTL in *Arabidopsis thaliana* in a parallel analysis of RIL and IL populations. *Plant J.* 53, 960–972.

Lunn, J. E. (2007). Compartmentation in plant metabolism. *J. Exp. Bot.* 58, 35–47.

Martinoia, E., Maeshima, M., and Neuhaus, H. E. (2007). Vacuolar transporters and their essential role in plant metabolism. *J. Exp. Bot.* 58, 83–102.

Martinoia, E., Vogt, E., Rentsch, D., and Amrhein, N. (1991). Functional reconstitution of the malate carrier of barley mesophyll vacuoles in liposomes. *Biochim. Biophys. Acta* 1062, 271–278.

Mochizuki, N., Brusslan, J. A., Larkin, R., Nagatani, A., and Chory, J. (2001). Arabidopsis genomes uncoupled 5

(GUN5) mutant reveals the involvement of Mg-chelatase H subunit in plastid-to-nucleus signal transduction. *Proc. Natl. Acad. Sci. U.S.A.* 98, 2053–2058.

Mochizuki, N., Tanaka, R., Tanaka, A., Masuda, T., and Nagatani, A. (2008). The steady-state level of Mg-protoporphyrin IX is not a determinant of plastid-to-nucleus signaling in *Arabidopsis*. *Proc. Natl. Acad. Sci. U.S.A.* 105, 15184–15189.

Nott, A., Jung, H.-S., Koussevitzky, S., and Chory, J. (2006). Plastid-to-nucleus retrograde signaling. *Annu. Rev. Plant Biol.* 57, 739–759.

op den Camp, R. G. L., Przybyla, D., Ochsenbein, C., Laloi, C., Kim, C. H., Danon, A., et al. (2003). Rapid induction of distinct stress responses after the release of singlet oxygen in *Arabidopsis*. *Plant Cell* 15, 2320–2332.

Paris, N., Stanley, C. M., Jones, R. L., and Rogers, J. C. (1996). Plant cells contain two functionally distinct vacuolar compartments. *Cell* 85, 563–572.

Pesaresi, P., Schneider, A., Kleine, T., and Leister, D. (2007). Interorganellar communication. *Curr. Opin. Plant Biol.* 10, 600–606.

Pfannschmidt, T. (2010). Plastidial retrograde signalling – a true "plastid factor" or just metabolite signatures? *Trends Plant Sci.* 15, 427–435.

Piippo, M., Allahverdiyeva, Y., Paakkarinen, V., Suoranta, U. M., Battchikova, N., and Aro, E. M. (2006). Chloroplast-mediated regulation of nuclear genes in *Arabidopsis thaliana* in the absence of light stress. *Physiol. Genomics* 25, 142–152.

Pogson, B. J., Woo, N. S., Forster, B., and Small, I. D. (2008). Plastid signalling to the nucleus and beyond. *Trends Plant Sci.* 13, 602–609.

Riens, B., Lohaus, G., Heineke, D., and Heldt, H. W. (1991). Amino-acid and sucrose content determined in the cytosolic, chloroplastic, and vacuolar compartments and in the phloem sap of spinach leaves. *Plant Physiol.* 97, 227–233.

Robinson, S. P., and Walker, D. A. (1980). Distribution of metabolites between chloroplast and cytoplasm during the induction-phase of photosynthesis in leaf protoplasts. *Plant Physiol.* 65, 902–905.

Sardiello, M., Tripoli, G., Romito, A., Minervini, C., Viggiano, L., Caggese, C., et al. (2005). Energy biogenesis: one key for coordinating two genomes. *Trends Genet.* 21, 12–16.

Schwarzlander, M., Konig, A. C., Sweetlove, L. J., and Finkemeier, I. (2012). The impact of impaired mitochondrial function on retrograde signalling: a meta-analysis of transcriptomic responses. *J. Exp. Bot.* 63, 1735–1750.

Smeekens, S., Ma, J., Hanson, J., and Rolland, F. (2010). Sugar signals and molecular networks controlling plant growth. *Curr. Opin. Plant Biol.* 13, 273–278.

Stitt, M., Gerhardt, R., Kurzel, B., and Heldt, H. W. (1983). A role for fructose 2,6-biphosphate in the regulation of sucrose synthesis in spinach leaves. *Plant Physiol.* 72, 1139–1141.

Strand, A., Asami, T., Alonso, J., Ecker, J. R., and Chory, J. (2003). Chloroplast to nucleus communication triggered by accumulation of Mg-protoporphyrin IX. *Nature* 421, 79–83.

Tohge, T., Ramos, M. S., Nunes-Nesi, A., Mutwil, M., Giavalisco, P., Steinhauser, D., et al. (2011). Toward the storage metabolome: profiling the barley vacuole. *Plant Physiol.* 157, 1469–1482.

Wagner, D., Przybyla, D., Camp, R. O. D., Kim, C., Landgraf, F., Lee, K. P., et al. (2004). The genetic basis of singlet oxygen-induced stress responses of *Arabidopsis thaliana*. *Science* 306, 1183–1185.

Weber, A. P. M., and Fischer, K. (2007). Making the connections – the crucial role of metabolite transporters at the interface between chloroplast and cytosol. *FEBS Lett.* 581, 2215–2222.

Winter, H., Robinson, D. G., and Heldt, H. W. (1993). Subcellular volumes and metabolite concentrations in barley leaves. *Planta* 191, 180–190.

Woodson, J. D., and Chory, J. (2008). Coordination of gene expression between organellar and nuclear genomes. *Nat. Rev. Genet.* 9, 383–395.

Xiao, Y. M., Savchenko, T., Baidoo, E. E. K., Chehab, W. E., Hayden, D. M., Tolstikov, V., et al. (2012). Retrograde signaling by the plastidial metabolite MEcPP regulates expression of nuclear stress-response genes. *Cell* 149, 1525–1535.

Yang, J., Zhang, M., and Yu, J. (2008). Mitochondrial retrograde regulation tuning fork in nuclear genes expressions of higher plants. *J. Genet. Genomics* 35, 65–71.

Conflict of Interest Statement: The authors declare that the research was conducted in the absence of any commercial or financial relationships that could be construed as a potential conflict of interest.

Received: 14 September 2012; accepted: 14 November 2012; published online: 05 December 2012.

*Citation: Caldana C, Fernie AR, Willmitzer L and Steinhauser D (2012) Unraveling retrograde signaling pathways: finding candidate signaling molecules via metabolomics and systems biology driven approaches. Front. Plant Sci. **3**:267. doi: 10.3389/fpls.2012.00267*

This article was submitted to Frontiers in Plant Physiology, a specialty of Frontiers in Plant Science.

Copyright © 2012 Caldana, Fernie, Willmitzer and Steinhauser. This is an open-access article distributed under the terms of the Creative Commons Attribution License, which permits use, distribution and reproduction in other forums, provided the original authors and source are credited and subject to any copyright notices concerning any third-party graphics etc.

frontiers in
PLANT SCIENCE

HYPOTHESIS AND THEORY ARTICLE
published: 19 June 2012
doi: 10.3389/fpls.2012.00135

Retrograde signaling in plants: from simple to complex scenarios

Dario Leister*

Plant Molecular Biology (Botany), Department Biology I, Ludwig Maximilians University, Munich, Germany

Edited by:
Tatjana Kleine, Ludwig-Maximilians-Universität München, Germany

Reviewed by:
Shan Lu, Nanjing University, China
Karl-Josef Dietz, Universität Bielefeld, Germany

***Correspondence:**
Dario Leister, Plant Molecular Biology (Botany), Department Biology I, Ludwig Maximilians University Munich, Großhaderner Str. 2, D-82152 Planegg-Martinsried, Germany. e-mail: leister@lmu.de

The concept of retrograde signaling posits that signals originating from chloroplasts or mitochondria modulate the expression of nuclear genes. A popular scenario assumes that signaling factors are generated in, and exported from the organelles, then traverse the cytosol, and act in the nucleus. In this scenario, which is probably over-simplistic, it is tacitly assumed that the signal is transferred by passive diffusion and consequently that changes in nuclear gene expression (NGE) directly reflect changes in the total cellular abundance of putative retrograde signaling factors. Here, this notion is critically discussed, in particular in light of an alternative scenario in which a signaling factor is actively exported from the organelle. In this scenario, NGE can be altered without altering the total concentration of the signaling molecule in the cell as a whole. Moreover, the active transport scenario would include an additional level of complexity, because the rate of the export of the signaling molecule has to be controlled by another signal, which might be considered as the real retrograde signal. Additional alternative scenarios for retrograde signaling pathways are presented, in which the signaling molecules generated in the organelle and the factors that trigger NGE are not necessarily identical. Finally, the diverse consequences of signal integration within the organelle or at the level of NGE are discussed. Overall, regulation of NGE at the nuclear level by independent retrograde signals appears to allow for more complex regulation of NGE than signal integration within the organelle.

Keywords: retrograde signaling, plastid signaling, nuclear gene expression, signal integration

WHAT IS A RETROGRADE SIGNAL?

Changes in the developmental or metabolic state of chloroplasts or mitochondria can have profound effects on the rest of the plant cell and involve massive changes in the transcript profiles of nuclear genes. The concept of retrograde signaling therefore posits that signals originating in chloroplasts and/or mitochondria modulate nuclear gene expression (NGE). In the classical case, the retrograde signal is generated in the organelle(s), exported, and traverses the cytosol to act in the nucleus. Several such classical retrograde signals have been tentatively identified. However, messenger roles have also been proposed for factors which display some, but not all, of the characteristics attributed to classical retrograde signals.

THE SPECTRUM OF PUTATIVE RETROGRADE SIGNALS – A CURRENT INVENTORY

Several candidate signaling pathways and signaling molecules have been identified during the last three decades, and their number continues to increase. However, unambiguous experimental verification of a compound as a signaling molecule is an extremely difficult task, and in no case is the status of a candidate as a signaling molecule yet secure. Therefore, instead of presenting a detailed and exhaustive description of individual candidate signaling pathways/molecules (for recent reviews see Baier and Dietz, 2005; Beck, 2005; Nott et al., 2006; Pesaresi et al., 2007; Pogson et al., 2008; Kleine et al., 2009a; Chan et al., 2010; Pfannschmidt, 2010; Inaba et al., 2011), I wish to concentrate here on some basic aspects of retrograde signaling mechanisms and their impact on the character of the response.

The pertinent retrograde signals are thought to derive from various sources, including the tetrapyrrole pathway, organellar gene expression (OGE), reactive oxygen species (ROS), or the redox state of the organelle (**Table 1**). Conversely, one can ask which of the principal types of biomolecules produced in organelles have the potential to act as a retrograde signal, i.e., encode sufficient information on the state of the organelle to trigger an appropriate response in the nucleus. Nucleic acids can efficiently store and transfer information, and their relocation from organelle to nucleus over evolutionary time is well established (reviewed in Kleine et al., 2009b). Hence, more than three decades ago, it was hypothesized that organelle-derived RNAs might regulate cytoplasmic protein synthesis (Bradbeer et al., 1979), but experimental support for this idea has not yet been forthcoming. ROS are by-products of several organellar processes and their accumulation is associated with changes in NGE (Apel and Hirt, 2004). However, their suitability as classical retrograde signals has been questioned, either because they are probably too short-lived to reach the nucleus [in the case of singlet oxygen ($^1O_2$)] or too unspecific (H_2O_2) to act as information carriers (reviewed in Møller and Sweetlove, 2010). Although specific transporters for the export of chloroplast proteins, in particular transcription factors, have yet to be identified, evidence is accumulating that chloroplast-located transcription factors can be conveyed to the nucleus (Sun et al., 2011; Isemer et al., 2012). Nevertheless, metabolites still appear to

Table 1 | Overview of different classes of putative retrograde signaling molecules.

Putative retrograde signaling molecule	Examples	Reference
RNA		Bradbeer et al. (1979)
Protein: transcription factor	Whirly 1	Isemer et al. (2012)
	PTM	Sun et al. (2011)
	ABI4	Koussevitzky et al. (2007)
Protein: degradation products		Reviewed in Møller and Sweetlove (2010)
Reactive oxygen species	$^1O_2$	Reviewed in Apel and Hirt (2004)
	H_2O_2	Reviewed in Apel and Hirt (2004)
Metabolite	Mg-proto IX	Strand et al. (2003)
	Heme	Woodson et al. (2011)
	ABA	reviewed in Baier and Dietz (2005)
	PAP	Estavillo et al. (2011)
	β-Cyclocitral	Ramel et al. (2012)
Unknown	Organellar gene expression	Reviewed in Gray et al. (2003)
	Thylakoid redox state	Reviewed in Pfannschmidt (2003); Pfannschmidt et al. (2003)

be the most likely candidates for retrograde signaling molecules. This is because (i) the profile of metabolites exported from an organelle to the cytosol does indeed reflect the metabolic state of the organelle and (ii) numerous transporters exist that facilitate the controlled exchange of metabolites between organelles and the cytosol. Therefore, changes in the metabolic profile of the cytosol triggered by the organelle might well be used by the cell to adjust NGE, either by using a metabolite directly as a signaling molecule or by converting an appropriate metabolite into an active signaling molecule during its sojourn in the cytosol.

WHAT SORTS OF NUCLEAR GENES ARE REGULATED BY RETROGRADE SIGNALING?

Frequently used marker genes for the analysis of retrograde signaling or the identification of putative signaling mutants are *LHCB1*, *2CPA*, and *APX2* (Oelmüller and Mohr, 1986; Karpinski et al., 1997; Heiber et al., 2007), which code for a photosynthetic antenna protein, a chloroplast peroxidase and a cytosolic ascorbate peroxidase, respectively. Transcriptomics-based studies in *Arabidopsis thaliana* have identified large sets of nuclear genes as possible targets of retrograde signaling by employing either putative signaling mutants and/or conditions thought to trigger retrograde signaling. Thus, nuclear genes coding for chloroplast proteins have been associated with GUN signaling (Strand et al., 2003) and a subsequent study showed that the ACGT motif, the core of both the light-responsive G box (CACGTG) and the abscisic acid (ABA) response element (ABRE), was over-represented in putative target genes of GUN signaling (Koussevitzky et al., 2007). Analysis of the time-dependent impact of redox signals showed rapid and dynamic changes in nuclear transcript accumulation, resulting in differential and specific expression patterns for genes associated with photosynthesis and metabolism (Bräutigam et al., 2009). Another study analyzed the overlap between the differential gene expression profiles of several mutants affected in photosynthetic acclimation. The identified 56 nuclear genes could represent either nuclear target genes of photosynthesis-relevant retrograde signaling or genes that are differentially expressed to compensate for the effects of suppression of retrograde signaling (Pesaresi et al., 2009). Interestingly, genes involved in many different processes, including stress responses, post-transcriptional, translational and post-translational regulation of gene expression, as well as metabolism, were represented in this set; however, few of them appeared to be directly involved in the photosynthetic process (Pesaresi et al., 2009). ROS-responsive genes were also identified and it was possible to discriminate between H_2O_2- and $^1O_2$-responsive genes (op den Camp et al., 2003). Interestingly, nuclear genes coding for chloroplast proteins generally seem to be co-regulated to a certain degree irrespective of their biochemical function (Richly et al., 2003; Biehl et al., 2005; Leister et al., 2011), prompting the postulate that a transcriptional master switch might exist (Richly et al., 2003). Nuclear photosynthesis-associated genes, including genes coding for photosystem subunits, display a distinct regulation pattern, which is independent of the master switch, highlighting the unique role of photosynthesis as representing both stimulus and target of retrograde regulation (Biehl et al., 2005). The large-scale analysis of the transcript profiles of chloroplast- and mitochondrion-relevant genes in *A. thaliana* confirmed that the activity of gene sets involved in organellar energy production (OEP) or OGE in each of the organelles and in the nucleus is highly coordinated (Leister et al., 2011). Moreover, the same analysis indicated that dynamic inter- and intracompartmental transcriptional networks for OEP and OGE genes adjust the activity of organelles in response to the cellular energy state and environmental stresses (Leister et al., 2011).

Taken together, these studies suggest that large numbers of genes respond to retrograde signaling, but in most cases it remains unclear whether they are directly targeted by retrograde signaling or are regulated indirectly as part of broader adjustments that compensate for the original stimulus (in most cases mutations). The use of transient stimuli and kinetic analysis of transcriptional responses, as practiced by Bräutigam et al. (2009), seems the most appropriate way to address this question.

THE SIMPLEST SCENARIO: THE CLASSICAL RETROGRADE SIGNAL

As outlined above, classical signaling molecules are assumed to be generated in the organelle and make their way to the nucleus, where they modify NGE by either inducing or repressing the expression of specific genes (**Figure 1A**). Therefore, when gene expression patterns in retrograde signaling mutants are compared

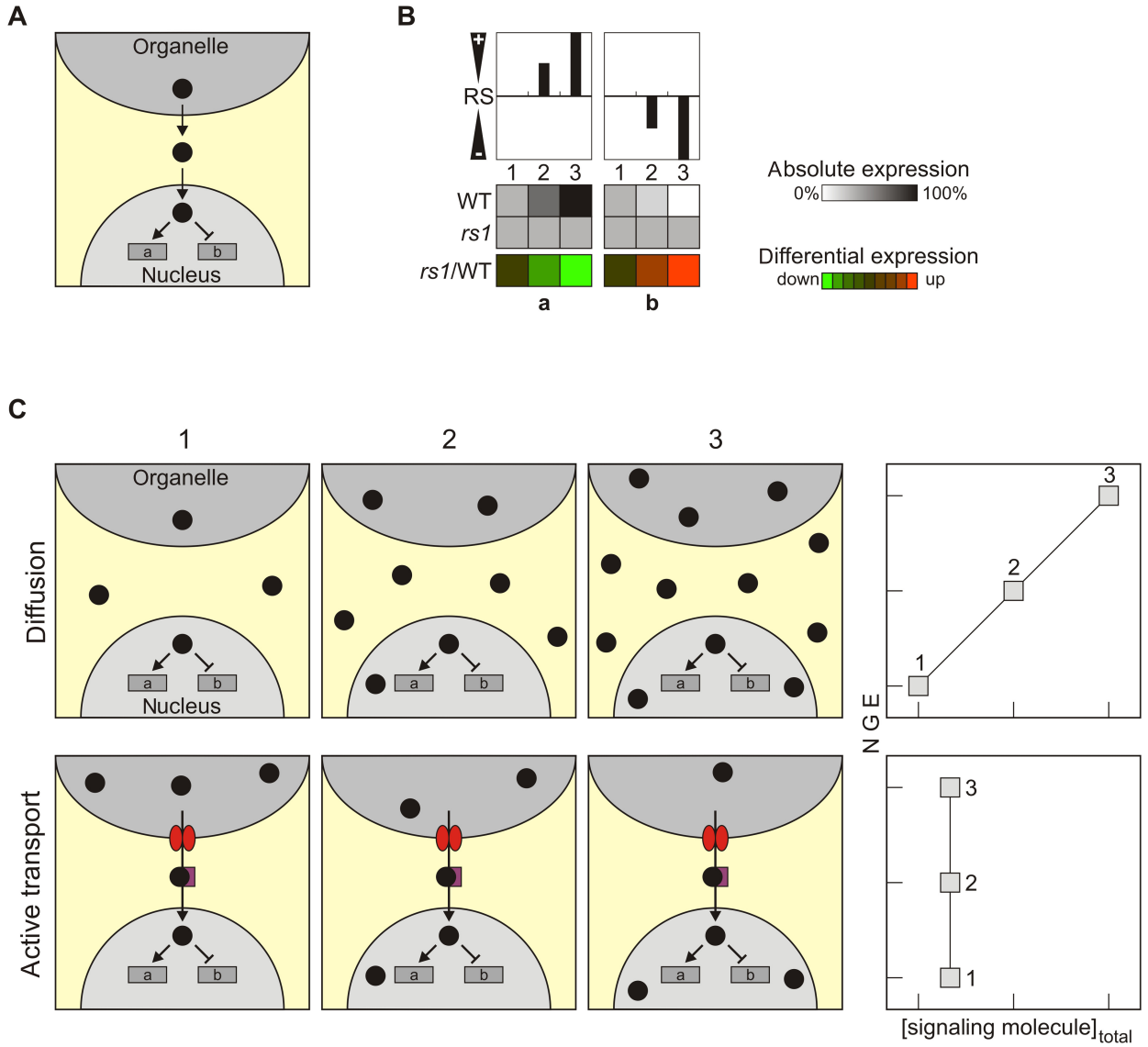

FIGURE 1 | Characteristics and transport of classical retrograde signals. **(A)** Schematic overview of the mode of operation of the simplest scenario for retrograde signaling, the case of a classical retrograde signal. **(B)** Overview of how changes in the relative abundance of the retrograde signal (RS) in the nucleus might affect NGE. Relative levels of the RS increase from state 1 (0%), state 2 (50%) to state 3 (100%), resulting in either induction (gene a) or repression (gene b) of the expression of a nuclear reporter gene (indicated in grayscale). The repressive effect of the RS is symbolized in the top panel by negative values ("−"), the inducing effect by positive values ("+"). In a signaling mutant *rs*, no expression changes occur and therefore differential expression (*rs1*/WT) in terms of down-regulation (gene a) or up-regulation (gene b) is observed (shown in color scale). **(C)** Passive diffusion versus active transport of RS. If the signaling molecule is disseminated by diffusion (upper panels, "Diffusion"), the total concentration of the signaling molecule in all cellular components increases during the transition from state 1 to state 3, leading to changes in NGE. In this case, a linear correlation between the total concentration of the signaling molecule and NGE is expected. If the signaling molecule is actively transported into the nucleus (lower panel, "Active transport"), NGE can be altered by specifically changing the abundance of the signaling molecule in the nucleus – without altering its total concentration in the cell as a whole. In consequence, analyses of total cell extracts would fail to identify any correlation between the overall abundance of the signaling molecule and NGE. The tetrapyrrole Mg-protoporphyrin IX, for which total cellular levels fail to correlate with changes in NGE, might represent such a signal. Note that the "active transport scenario" would require regulation of the activity of the transport by another signal. In fact, in such a scenario the signal that up-regulates export might be considered as the real signal, and the transported compound as second messenger.

with the profile in wild-type (WT) plants, differential expression of the regulated genes will be observed (**Figure 1B**). Two principal modes of transfer of retrograde signaling molecules present themselves: transfer by passive diffusion or active transport involving specific transporters (**Figure 1C**). In principle, the latter mode of transfer would include already an additional level of complexity, because the rate of the export of the signaling molecule has to be controlled by another signal, which might be considered as the real retrograde signal (**Figure 1C**). Here, three putative classical retrograde signaling

molecules are discussed in the context of these alternative modes of relocation: (i) the phosphonucleotide 3′-phosphoadenosine 5′-phosphate (PAP) and (ii) β-cyclocitral (β-CC), an oxidation product of β-carotene, both of which might be relocated by diffusion; and (iii) the tetrapyrrole Mg-protoporphyrin IX (Mg-proto IX).

PAP AND β-CYCLOCITRAL – TWO NOVEL CANDIDATE CLASSICAL SIGNALS

3′-Phosphoadenosine 5′-phosphate accumulates in *A. thaliana* in response to drought and high light (HL) stress (Estavillo et al., 2011). The enzyme SAL1, which is found in both mitochondria and chloroplasts, regulates PAP levels by dephosphorylating PAP to AMP; therefore, in *sal1* mutants PAP accumulates 20-fold (Estavillo et al., 2011). Moreover, *sal1* mutants display constitutive upregulation of many HL-regulated genes (Wilson et al., 2009). Except in the case of chloroplasts, where PAP could be detected by HPLC, attempts to identify PAP in subcellular fractions have failed for technical reasons (Estavillo et al., 2011). However, targeting of SAL1 to either the nucleus or chloroplasts in *sal1* mutants reduces total PAP levels and decreases expression of the nuclear marker gene *APX2*, indirectly demonstrating that PAP must be able to move between cellular compartments (**Table 2**). Because total cellular levels of PAP and nuclear marker gene expression correlate well (Estavillo et al., 2011), a plausible mechanism for the effects of PAP on NGE is the "free diffusion" scenario (**Figure 1C**). In this scenario, the total concentration of the signaling molecule in the organelle must reach a certain level to enable diffusion into the nucleus to supply sufficient amounts to its putative site of action. Consequently, PAP seems to represent a classical signaling molecule which is synthesized in organelles of a given type, leaves that organelle and reaches the nucleus by passive diffusion. Moreover, the physiological relevance of PAP as a possible retrograde signal is strongly supported by the fact that PAP levels increase in response to at least two abiotic stresses.

Oxidation products of β-carotene, like β-CC, have been suggested to act as "downstream" messengers or proxies for rising $^1O_2$ levels (Ramel et al., 2012; see below). β-CC is volatile; therefore, it should be capable of traversing the cytosol to regulate gene expression in the nucleus. β-CC is generated under physiological conditions, following exposure to excess light which promotes generation of $^1O_2$, which in turn oxidizes β-carotene. Moreover, treatment of plants with exogenous β-CC induces changes in the expression of many $^1O_2$-responsive genes. Therefore, it is tempting to speculate that β-CC represents a classical retrograde signal which is disseminated by diffusion. Because this HL-induced signaling pathway may involve at least two signaling molecules, $^1O_2$ and β-CC, this instance of retrograde signaling is discussed further in the next section.

IS Mg-PROTO IX A CLASSICAL RETROGRADE SIGNALING MOLECULE OR PART OF A MORE COMPLEX PATHWAY?

When it became clear that most *gun* mutants were affected in chloroplast tetrapyrrole biosynthesis (Mochizuki et al., 2001), the obvious next step was to test whether an intermediate in tetrapyrrole biosynthesis might be responsible for changes in NGE. Therefore, the possibility that the concentrations of various tetrapyrroles might be correlated with the expression of nuclear marker genes in *A. thaliana* was analyzed in several studies with conflicting results (Mochizuki et al., 2001, 2008; Strand et al., 2003; Moulin et al., 2008). Strand et al. (2003) claimed to have found a direct correlation between changes in the total cellular level of Mg-proto IX and NGE, although an earlier study by the same group had come to a different conclusion (Mochizuki et al., 2001). Later investigations employing more precise and reproducible tests, as well as additional genotypes, confirmed that no correlation exists between total Mg-proto IX levels and NGE (Mochizuki et al., 2008; Moulin et al., 2008). However, lack of correlation between changes in the total concentration of Mg-proto IX in plant leaves and alterations in the expression profiles of certain nuclear marker genes does not suffice to rule out the possibility that Mg-proto IX acts as a classical plastid signal. The finding simply argues against diffusion as a transport mechanism for the signal. It does not exclude the possibility that the signaling molecule is *actively* transported from its source to the nucleus. If the signaling

Table 2 | Characteristics of putative retrograde signaling molecules.

Putative signaling molecule	Localization			Physiological stimulus	Reference
	Organelle	Cytosol	Nucleus		
$^1O_2$	cp	Unclear	Unclear	Excess light	Apel and Hirt (2004), Fischer et al. (2007)
H_2O_2	cp + mt + per	Yes	Likely	Multiple	Apel and Hirt (2004), Mubarakshina et al. (2010)
Mg-Proto IX	cp	Unclear	Unclear	Unclear	Strand et al. (2003)
Heme	cp	Yes	Unclear	Unclear	Thomas and Weinstein (1990), Woodson et al. (2011)
PAP	cp + mt	Likely	Indirect evidence	Drought and excess light	Estavillo et al. (2011)
β-Cyclocitral	cp	Likely	Likely	Excess light	Ramel et al. (2012)
ABA	Precursor present in cp	Yes	Candidate receptor identified	Excess light	Wasilewska et al. (2008)

cp, chloroplast; mt, mitochondria; per, peroxisomes.

molecule is actively transported into the nucleus, its concentration there could still increase (with corresponding effects on NGE), while the total cellular concentration of the signaling molecule remained unchanged (**Figure 1C**). Whether or not this scenario holds for Mg-proto IX remains to be clarified; as a phototoxic molecule, it seems rather unlikely to act as a signaling molecule (Mochizuki et al., 2010). Heme is a somewhat better candidate retrograde signaling molecule deriving from the tetrapyrrole biosynthesis pathway (Woodson et al., 2011), but levels of total heme and *LHCB1* mRNA also fail to correlate (Voigt et al., 2010; Woodson et al., 2011).

Nevertheless, a correlation between perturbations in chloroplast tetrapyrrole biosynthesis and NGE changes undoubtedly exists, and future research has to clarify what retrograde signaling mechanisms mediate this relationship.

MORE COMPLEX SCENARIOS OF RETROGRADE SIGNALING

The classical scenario for a retrograde signaling molecule, in which the molecule that is generated in the organelle itself relays information to the nucleus, might be true for the phosphonucleotide PAP during drought and HL stress and for β-CC after HL stress (**Table 2**), but need not be valid for other retrograde signals. Thus, ABA, which has been proposed as a putative plastid signal, is generated in the cytosol but derives from a precursor (xanthoxin) which is synthesized in the chloroplast (reviewed in Baier and Dietz, 2005; **Figure 2A**). Alternatively, the original metabolite triggering retrograde signaling might not even leave the organelle (**Figure 2B**). For instance, singlet oxygen ($^1O_2$) is generated in chloroplasts and regulates the expression of a set of nuclear genes, although it is thought to be largely restricted to plastids with little, if any, leakage to the cytosol (Apel and Hirt, 2004; Fischer et al., 2007). In consequence, an unidentified second messenger should exist which relays the information from the plastid to the nucleus, and the two chloroplast proteins Executer 1 and 2 (reviewed in Kim et al., 2008), as well as ABA (Kim et al., 2009), seem to be involved in this retrograde signaling pathway. More recently, β-CC was suggested to act as a "downstream" messenger of $^1O_2$ (Ramel et al., 2012), possibly representing a classical retrograde signal which traverses the cytosol to regulate gene expression in the nucleus (see above).

So far, proteins that specifically transport signaling molecules from the organelle to the nucleus have not been identified. In an extreme case, the signaling molecules could be delivered directly to its target if organelle and nucleus were physically connected. In fact, stromules might represent such connection points between plastids and the nucleus (**Figure 2C**). Stromules are stroma-filled tubules that extend from the surface of plastids, are extremely variable in length and are highly dynamic structures (reviewed in Hanson and Sattarzadeh, 2008). Interestingly, stromules are induced by stress treatments, including drought and salt stress, and application of ABA (Gray et al., 2012) – conditions which are also thought to be associated with retrograde signaling.

INTEGRATION OF MULTIPLE SIGNALS

The existence of multiple candidate signaling molecules, including those discussed above, ABA, $^1O_2$ (and its tentative downstream signal β-CC), Mg-Proto IX and PAP, suggests that it is very likely that more than one retrograde signaling pathway exists. Moreover, the generation of signaling molecules in the organelle will itself be affected by multiple factors. Two model cases that take account of this complexity are discussed here. In scenario 1, each of two retrograde signals (RS1 and RS2) can act independently to activate or repress NGE. In scenario 2, only one retrograde signal (RS) operates, but its formation is controlled by two organellar factors (O1 and O2) that can act synergistically or in opposite senses (**Figure 3A**). To simulate the effects on NGE of the two retrograde signals in scenario 1 and the two organellar factors in scenario 2, three discrete doses for each retrograde signal or organellar factor were considered: 0, 50, and 100%. If both retrograde signals or organellar factors are assumed to act in the same sense, i.e., both stimulate (or repress) gene expression or generation of the retrograde signal, the two scenarios result in identical effects on NGE in WT plants (**Figures 3B,C**). Furthermore, where mutants for the two retrograde signaling pathways or organellar factors are available, the differential expression patterns determined in the two scenarios will be identical. Therefore,

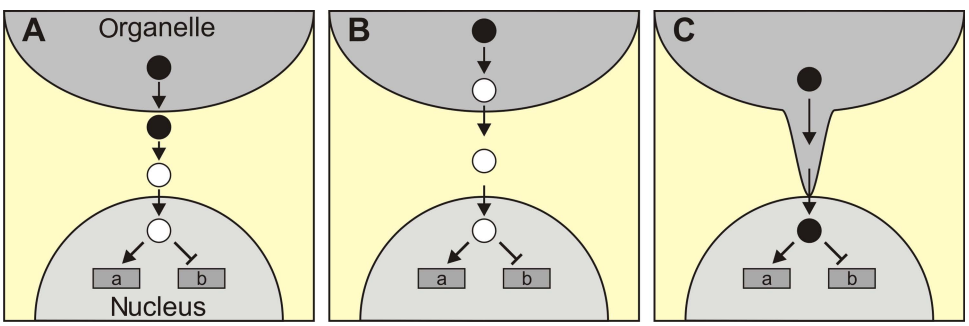

FIGURE 2 | More complex scenarios for retrograde signaling. (A) The signaling molecule generated in and exported from the organelle (filled circles), and the signaling molecule that enters the nucleus (open circles) might not be identical. ABA, which is synthesized in the cytosol from a chloroplast precursor, is a possible example. **(B)** The signaling molecule generated in the organelle might not even leave the organelle. $^1O_2$ serves here as an example, as it could, in principle, generate volatile oxidation products of carotenoids that serve as "downstream" messengers. **(C)** Direct delivery of the signaling molecule to the nucleus via stromules.

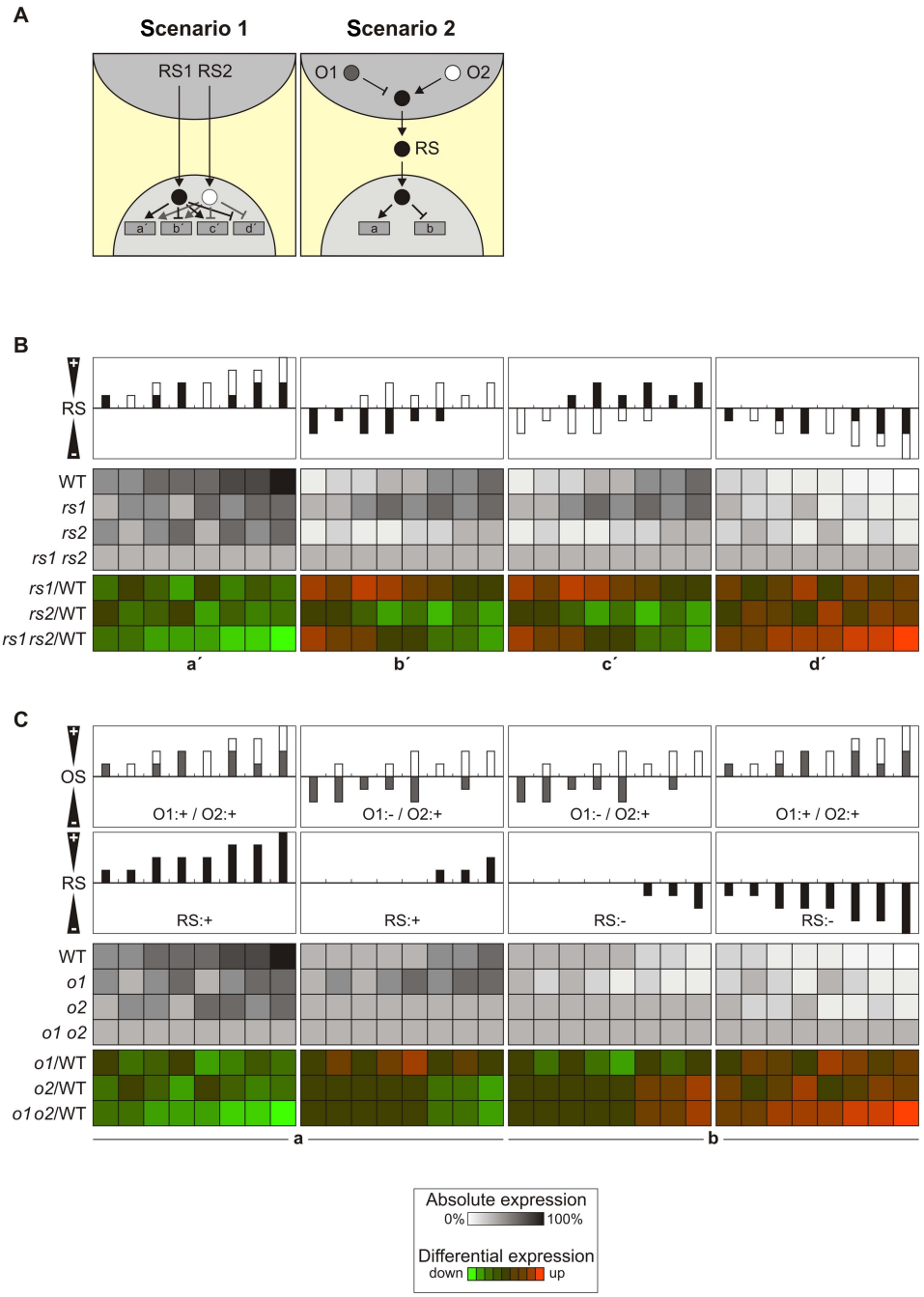

FIGURE 3 | Signal integration. (A) Schematic overview of the integration of two retrograde signals (RS1 and RS2) in the nucleus (left panel) or in the organelle (right panel). O1 and O2 refer to signals acting within the organelle. Activating signals are indicated by arrows, repressing signals by blunt-ended lines. Left panel (two retrograde signals, integration in the nucleus): gene a′, induced by RS1 and RS2; gene b′, repressed by RS1 and induced by RS2; gene c′, induced by RS1 and repressed by RS2; gene d′, repressed by RS1 and RS2. Right panel (two organellar signals, integration in the organelle): RS induces gene a and represses gene b as in **Figure 1A**. **(B)** Signal integration at the gene level. In this model each of the two retrograde signals can accumulate to 0, 50, or 100% [depicted as black (RS1) or white (RS2) bars], analogous to the three states discussed in **Figures 1B,C**, resulting in nine different combinations, of which eight are shown in the top panels (the combination RS1: 0%/RS2: 0% is not shown). The effects on NGE are shown in WT and corresponding single (*rs1* and *rs2*) and double (*rs1 rs2*) signaling mutants in grayscale. In color scale, effects on differential gene expression (mutant versus WT) are shown. In the left/right panel, the expected impact of additive inducing/repressing effects of the retrograde signals on genes a′ and d′ is shown. In the middle panel (b′/c′), the two retrograde signals act antagonistically and the outcome for the expression of genes b′ and c′ is very similar. **(C)** As in **(B)**, the two organellar signals can act additively with the same polarity (O1:+/O2:+) or act antagonistically (O1:−/O2:+; O1:+/O2:−; upper panel). The net effect of OS1 and OS2 on RS is shown in the second uppermost panel and can either induce gene expression (the two left panels, gene a) or repress gene expression (the two right panels, gene b). The resulting effects on NGE are again shown in grayscale for absolute expression and in color scale for differential expression (mutant versus WT).

it will not be possible to discriminate between the two scenarios on the basis of expression data from WT and mutant plants defective in signaling under conditions in which both retrograde signaling factors or both organellar signaling factors act additively.

In contrast, under conditions where the two retrograde signals or organellar factors act in opposite senses, differences in differential expression between signaling mutants and WT plants will emerge. In the case of two retrograde signals whose effects are integrated in the nucleus, differential up-regulation for one signaling mutant but down-regulation for the other signaling mutant will be observed (**Figure 3B**). On the other hand, where signal integration occurs already in the organelle, opposite regulation of the two organellar signals will essentially neutralize their effects on the generation of the retrograde signal (**Figure 3C**). In the model presented here, five out of eight conditions fail to produce a retrograde signal in the WT, and opposite differential regulation in signaling mutants is found only in one condition.

Overall, regulation of NGE by two independent retrograde signals appears to allow for more complex regulation of NGE, and this should be detectable by opposite regulation of NGE in corresponding signaling mutants under appropriate conditions. Of course, the crucial question is whether such complex regulatory scenarios are actually realized and whether sufficient expression data are available to decide whether signal integration occurs in the organelle or the nucleus. In fact, two instances of synergistic effects of two signaling mutants on NGE have been described so far. The first example concerns the *gun* mutants and the second involves mutants defective in OGE. The *gun* phenotype was originally defined as derepressed *LHCB1* expression after treatment with norflurazon (NF). Then the double mutants *gun1 gun4* and *gun1 gun5* were shown to exhibit higher levels of *LHCB1* mRNA after NF treatment than did the individual single mutants, indicating that GUN1 affects a separate pathway from GUN4 and GUN5 (Mochizuki et al., 2001). However, the same group showed in a later publication that the synergy between *gun1* and *gun5* does not extend to the *gun1–9* allele (Koussevitzky et al., 2007). Nevertheless, the available data are not sufficient to decide whether signal integration occurs in the chloroplast or at the nuclear level.

Changes in OGE affect the expression of nuclear genes, in particular genes coding for photosynthetic proteins (reviewed in Pesaresi et al., 2007). Pesaresi et al. (2006) showed that simultaneous perturbation of OGE in both mitochondria and chloroplasts down-regulates nuclear photosynthetic genes much more drastically than do treatments that affect OGE in only the one or the other. For this study, mutations affecting mitochondrial or chloroplast ribosomes, as well as mutations affecting a dual-targeted tRNA synthetase were analyzed. For all nuclear photosynthesis genes studied, the double mutant *prpl11 mrpl11*, in which ribosomal function was impaired in both types of organelles, always produced fewer transcripts than either of the single mutants *prpl11* and *mrpl11*, indicating that both plastid OGE and mitochondrial OGE stimulate NGE under the growth conditions employed in the study. In this case also, it is not possible to discriminate between signal integration in the organelle and the nucleus based on the expression profiles. However, because the two mutations affect separate organelles it is tempting to speculate that signal integration occurs in the cytosol or in the nucleus as outlined in **Figure 3B**.

CONCLUDING REMARKS: SOLID CRITERIA TO DEFINE A RETROGRADE SIGNAL

How can a candidate signaling molecule be unambiguously confirmed to be a real signal? In light of the different retrograde signaling scenarios outlined above, it is not possible to draw up a universal list of characteristics and experiments that could unequivocally decide whether a putative retrograde signal is a true retrograde signal. Nevertheless, a number of conclusions can be drawn from the considerations set out above. A classical retrograde signal should be detectable in all relevant compartments (organelle, cytosol and nucleus), assuming that passage through the cytosol is not rendered superfluous by the use of stromules. So far, no putative classical signal has been unambiguously detected in all relevant compartments (**Table 2**). Secondly, for a signal which follows the free diffusion scenario a correlation between overall signal level and NGE should exist, opening the way for systematic approaches involving LC–MS or GC–MS analyses. Finally, how can one show that a signaling molecule is not only required but also sufficient to trigger NGE? Feeding experiments in which PAP (the candidate most likely to conform to the "free diffusion" scenario) was supplied via the roots have so far failed to confirm a signaling role for it (Estavillo et al., 2011), whereas Mg-proto IX was reported to repress *LHCB* expression when fed to protoplasts for 5 h at relatively high concentrations (Strand et al., 2003). These two examples highlight the dilemma of feeding experiments. On the one hand, a negative result cannot conclusively disqualify a candidate retrograde signal, unless one can monitor the accumulation of the added molecule at its destination. Conversely, a positive result is only valid if the feeding assays truly mimic physiological conditions. Nevertheless, feeding experiments and *in vitro* assays with subcellular fractions (in which target nuclear genes are directly exposed to the signaling molecules), together with the transient activation of retrograde signaling pathways by inducible gene expression systems, are certainly needed to clarify the role of putative signaling molecules.

Finally, the reconstruction of signaling networks and of the synergistic and antagonistic integration of diverse retrograde inputs will be necessary for the knowledge-based modification of retrograde signaling. Studies, like the one of gene regulatory networks involving AP2/EREB transcription factors (Dietz et al., 2010), might serve as prototypes for systematic genome analysis of retrograde signaling, demonstrating that the examples provided here (see **Figure 3**) certainly represent simplifications of a much more complex phenomenon.

ACKNOWLEDGMENTS

We are grateful to the Deutsche Forschungsgemeinschaft for funding (grant FOR 804) and Paul Hardy for critical reading of the manuscript.

REFERENCES

Apel, K., and Hirt, H. (2004). Reactive oxygen species: metabolism, oxidative stress, and signal transduction. *Annu. Rev. Plant Biol.* 55, 373–399.

Baier, M., and Dietz, K. J. (2005). Chloroplasts as source and target of cellular redox regulation: a discussion on chloroplast redox signals in the context of plant physiology. *J. Exp. Bot.* 56, 1449–1462.

Beck, C. F. (2005). Signaling pathways from the chloroplast to the nucleus. *Planta* 222, 743–756.

Biehl, A., Richly, E., Noutsos, C., Salamini, F., and Leister, D. (2005). Analysis of 101 nuclear transcriptomes reveals 23 distinct regulons and their relationship to metabolism, chromosomal gene distribution and co-ordination of nuclear and plastid gene expression. *Gene* 344, 33–41.

Bradbeer, J. W., Atkinson, Y. E., Börner, T., and Hagemann, R. (1979). Cytoplasmic synthesis of plastid polypeptides may be controlled by plastid-synthesized RNA. *Nature* 279, 816–817.

Bräutigam, K., Dietzel, L., Kleine, T., Ströher, E., Wormuth, D., Dietz, K. J., Radke, D., Wirtz, M., Hell, R., Dörmann, P., Nunes-Nesi, A., Schauer, N., Fernie, A. R., Oliver, S. N., Geigenberger, P., Leister, D., and Pfannschmidt, T. (2009). Dynamic plastid redox signals integrate gene expression and metabolism to induce distinct metabolic states in photosynthetic acclimation in *Arabidopsis*. *Plant Cell* 21, 2715–2732.

Chan, K. X., Crisp, P. A., Estavillo, G. M., and Pogson, B. J. (2010). Chloroplast-to-nucleus communication: current knowledge, experimental strategies and relationship to drought stress signaling. *Plant Signal. Behav.* 5, 1575–1582.

Dietz, K. J., Vogel, M. O., and Viehhauser, A. (2010). AP2/EREBP transcription factors are part of gene regulatory networks and integrate metabolic, hormonal and environmental signals in stress acclimation and retrograde signalling. *Protoplasma* 245, 3–14.

Estavillo, G. M., Crisp, P. A., Pornsiriwong, W., Wirtz, M., Collinge, D., Carrie, C., Giraud, E., Whelan, J., David, P., Javot, H., Brearley, C., Hell, R., Marin, E., and Pogson, B. J. (2011). Evidence for a SAL1-PAP chloroplast retrograde pathway that functions in drought and high light signaling in *Arabidopsis*. *Plant Cell* 23, 3992–4012.

Fischer, B. B., Krieger-Liszkay, A., Hideg, E., Snyrychova, I., Wiesendanger, M., and Eggen, R. I. (2007). Role of singlet oxygen in chloroplast to nucleus retrograde signaling in *Chlamydomonas reinhardtii*. *FEBS Lett.* 581, 5555–5560.

Gray, J. C., Hansen, M. R., Shaw, D. J., Graham, K., Dale, R., Smallman, P., Natesan, S. K., and Newell, C. A. (2012). Plastid stromules are induced by stress treatments acting through abscisic acid. *Plant J.* 69, 387–398.

Gray, J. C., Sullivan, J. A., Wang, J. H., Jerome, C. A., and Maclean, D. (2003). Coordination of plastid and nuclear gene expression. *Philos. Trans. R. Soc. Lond. B Biol. Sci.* 358, 135–144; discussion 144–145.

Hanson, M. R., and Sattarzadeh, A. (2008). Dynamic morphology of plastids and stromules in angiosperm plants. *Plant Cell Environ.* 31, 646–657.

Heiber, I., Ströher, E., Raatz, B., Busse, I., Kahmann, U., Bevan, M. W., Dietz, K. J., and Baier, M. (2007). The redox imbalanced mutants of *Arabidopsis* differentiate signaling pathways for redox regulation of chloroplast antioxidant enzymes. *Plant Physiol.* 143, 1774–1788.

Inaba, T., Yazu, F., Ito-Inaba, Y., Kakizaki, T., and Nakayama, K. (2011). Retrograde signaling pathway from plastid to nucleus. *Int. Rev. Cell Mol. Biol.* 290, 167–204.

Isemer, R., Mulisch, M., Schäfer, A., Kirchner, S., Koop, H. U., and Krupinska, K. (2012). Recombinant Whirly1 translocates from transplastomic chloroplasts to the nucleus. *FEBS Lett.* 586, 85–88.

Karpinski, S., Escobar, C., Karpinska, B., Creissen, G., and Mullineaux, P. M. (1997). Photosynthetic electron transport regulates the expression of cytosolic ascorbate peroxidase genes in *Arabidopsis* during excess light stress. *Plant Cell* 9, 627–640.

Kim, C., Lee, K. P., Baruah, A., Nater, M., Gobel, C., Feussner, I., and Apel, K. (2009). $^1O_2$-mediated retrograde signaling during late embryogenesis predetermines plastid differentiation in seedlings by recruiting abscisic acid. *Proc. Natl. Acad. Sci. U.S.A.* 106, 9920–9924.

Kim, C., Meskauskiene, R., Apel, K., and Laloi, C. (2008). No single way to understand singlet oxygen signalling in plants. *EMBO Rep.* 9, 435–439.

Kleine, T., Voigt, C., and Leister, D. (2009a). Plastid signalling to the nucleus: messengers still lost in the mists? *Trends Genet.* 25, 185–192.

Kleine, T., Maier, U. G., and Leister, D. (2009b). DNA transfer from organelles to the nucleus: the idiosyncratic genetics of endosymbiosis. *Annu. Rev. Plant Biol.* 60, 115–138.

Koussevitzky, S., Nott, A., Mockler, T. C., Hong, F., Sachetto-Martins, G., Surpin, M., Lim, J., Mittler, R., and Chory, J. (2007). Signals from chloroplasts converge to regulate nuclear gene expression. *Science* 316, 715–719.

Leister, D., Wang, X., Haberer, G., Mayer, K. F., and Kleine, T. (2011). Intracompartmental and intercompartmental transcriptional networks coordinate the expression of genes for organellar functions. *Plant Physiol.* 157, 386–404.

Mochizuki, N., Brusslan, J. A., Larkin, R., Nagatani, A., and Chory, J. (2001). *Arabidopsis* genomes uncoupled 5 (GUN5) mutant reveals the involvement of Mg-chelatase H subunit in plastid-to-nucleus signal transduction. *Proc. Natl. Acad. Sci. U.S.A.* 98, 2053–2058.

Mochizuki, N., Tanaka, R., Grimm, B., Masuda, T., Moulin, M., Smith, A. G., Tanaka, A., and Terry, M. J. (2010). The cell biology of tetrapyrroles: a life and death struggle. *Trends Plant Sci.* 15, 488–498.

Mochizuki, N., Tanaka, R., Tanaka, A., Masuda, T., and Nagatani, A. (2008). The steady-state level of Mg-protoporphyrin IX is not a determinant of plastid-to-nucleus signaling in *Arabidopsis*. *Proc. Natl. Acad. Sci. U.S.A.* 105, 15184–15189.

Møller, I. M., and Sweetlove, L. J. (2010). ROS signalling – specificity is required. *Trends Plant Sci.* 15, 370–374.

Moulin, M., McCormac, A. C., Terry, M. J., and Smith, A. G. (2008). Tetrapyrrole profiling in *Arabidopsis* seedlings reveals that retrograde plastid nuclear signaling is not due to Mg-protoporphyrin IX accumulation. *Proc. Natl. Acad. Sci. U.S.A.* 105, 15178–15183.

Mubarakshina, M. M., Ivanov, B. N., Naydov, I. A., Hillier, W., Badger, M. R., and Krieger-Liszkay, A. (2010). Production and diffusion of chloroplastic H_2O_2 and its implication to signalling. *J. Exp. Bot.* 61, 3577–3587.

Nott, A., Jung, H. S., Koussevitzky, S., and Chory, J. (2006). Plastid-to-nucleus retrograde signaling. *Annu. Rev. Plant Biol.* 57, 739–759.

Oelmüller, R., and Mohr, H. (1986). Photooxidative destruction of chloroplasts and its consequences for expression of nuclear genes. *Planta* 167, 106–113.

op den Camp, R. G., Przybyla, D., Ochsenbein, C., Laloi, C., Kim, C., Danon, A., Wagner, D., Hideg, E., Gobel, C., Feussner, I., Nater, M., and Apel, K. (2003). Rapid induction of distinct stress responses after the release of singlet oxygen in *Arabidopsis*. *Plant Cell* 15, 2320–2332.

Pesaresi, P., Hertle, A., Pribil, M., Kleine, T., Wagner, R., Strissel, H., Ihnatowicz, A., Bonardi, V., Scharfenberg, M., Schneider, A., Pfannschmidt, T., and Leister, D. (2009). *Arabidopsis* STN7 kinase provides a link between short- and long-term photosynthetic acclimation. *Plant Cell* 21, 2402–2423.

Pesaresi, P., Masiero, S., Eubel, H., Braun, H. P., Bhushan, S., Glaser, E., Salamini, F., and Leister, D. (2006). Nuclear photosynthetic gene expression is synergistically modulated by rates of protein synthesis in chloroplasts and mitochondria. *Plant Cell* 18, 970–991.

Pesaresi, P., Schneider, A., Kleine, T., and Leister, D. (2007). Interorganellar communication. *Curr. Opin. Plant Biol.* 10, 600–606.

Pfannschmidt, T. (2003). Chloroplast redox signals: how photosynthesis controls its own genes. *Trends Plant Sci.* 8, 33–41.

Pfannschmidt, T. (2010). Plastidial retrograde signalling – a true "plastid factor" or just metabolite signatures? *Trends Plant Sci.* 15, 427–435.

Pfannschmidt, T., Schütze, K., Fey, V., Sherameti, I., and Oelmüller, R. (2003). Chloroplast redox control of nuclear gene expression – a new class of plastid signals in interorganellar communication. *Antioxid. Redox Signal.* 5, 95–101.

Pogson, B. J., Woo, N. S., Forster, B., and Small, I. D. (2008). Plastid signalling to the nucleus and beyond. *Trends Plant Sci.* 13, 602–609.

Ramel, F., Birtic, S., Ginies, C., Soubigou-Taconnat, L., Triantaphylides, C., and Havaux, M. (2012). Carotenoid oxidation products are stress signals that mediate gene responses to singlet oxygen in plants. *Proc. Natl. Acad. Sci. U.S.A.* 109, 5535–5540.

Richly, E., Dietzmann, A., Biehl, A., Kurth, J., Laloi, C., Apel, K., Salamini, F., and Leister, D. (2003). Covariations in the nuclear chloroplast transcriptome reveal a regulatory master-switch. *EMBO Rep.* 4, 491–498.

Strand, A., Asami, T., Alonso, J., Ecker, J. R., and Chory, J. (2003). Chloroplast to nucleus communication triggered by accumulation of Mg-protoporphyrinIX. *Nature* 421, 79–83.

Sun, X., Feng, P., Xu, X., Guo, H., Ma, J., Chi, W., Lin, R., Lu, C., and Zhang, L. (2011). A chloroplast envelope-bound PHD transcription factor mediates chloroplast signals to the nucleus. *Nat. Commun.* 2, 477.

Thomas, J., and Weinstein, J. D. (1990). Measurement of heme efflux and heme content in isolated developing chloroplasts. *Plant Physiol.* 94, 1414–1423.

Voigt, C., Oster, U., Börnke, F., Jahns, P., Dietz, K. J., Leister, D., and Kleine, T. (2010). In-depth analysis of the distinctive effects of norflurazon implies that tetrapyrrole biosynthesis, organellar gene expression and ABA cooperate in the GUN-type of plastid signalling. *Physiol. Plant.* 138, 503–519.

Wasilewska, A., Vlad, F., Sirichandra, C., Redko, Y., Jammes, F., Valon, C., Frei Dit Frey, N., and Leung, J. (2008). An update on abscisic acid signaling in plants and more. *Mol. Plant* 1, 198–217.

Wilson, P. B., Estavillo, G. M., Field, K. J., Pornsiriwong, W., Carroll, A. J., Howell, K. A., Woo, N. S., Lake, J. A., Smith, S. M., Millar, H. A., Von Caemmerer, S., and Pogson, B. J. (2009). The nucleotidase/phosphatase SAL1 is a negative regulator of drought tolerance in *Arabidopsis*. *Plant J.* 58, 299–317.

Woodson, J. D., Perez-Ruiz, J. M., and Chory, J. (2011). Heme synthesis by plastid ferrochelatase I regulates nuclear gene expression in plants. *Curr. Biol.* 21, 897–903.

Conflict of Interest Statement: The author declares that the research was conducted in the absence of any commercial or financial relationships that could be construed as a potential conflict of interest.

Received: 25 May 2012; accepted: 05 June 2012; published online: 19 June 2012.

Citation: Leister D (2012) Retrograde signaling in plants: from simple to complex scenarios. Front. Plant Sci. ***3****:135. doi: 10.3389/fpls.2012.00135*

This article was submitted to Frontiers in Plant Physiology, a specialty of Frontiers in Plant Science.

Copyright © 2012 Leister. This is an open-access article distributed under the terms of the Creative Commons Attribution Non Commercial License, which permits non-commercial use, distribution, and reproduction in other forums, provided the original authors and source are credited.